VOLUME 26 / NUMBER 15
AUGUST 8, 1988
ACC. NOS. N88-22003 TO N88-22854

STAR

AN ABSTRACT JOURNAL

Scientific and Technical Aerospace Reports

PRODUCED BY THE
SCIENTIFIC AND TECHNICAL
INFORMATION
DIVISION

NASA

NATIONAL AERONAUTICS AND SPACE ADMINISTRATION

WHAT YOU CAN DO FOR *STAR*

All users of this abstract service are urged to forward reports to be considered for announcement in *STAR*. This will aid NASA in its efforts to provide the fullest possible coverage of all scientific and technical publications that might support aeronautics and space research and development. If you have prepared relevant reports (other than those that you will transmit to NASA, DoD, or DOE through the usual contract- or grant-reporting channels), please send them for consideration to the NASA Scientific and Technical Information Facility, P.O. Box 8757, B.W.I. Airport, Maryland 21240.

Reprints of journal articles, book chapters, and conference papers are also welcome. These will be considered for announcement in *STAR's* companion journal, *International Aerospace Abstracts*.

You may specify a particular source to be included in a report announcement if you wish; otherwise the report will be placed on public sale at the National Technical Information Service. Copyrighted publications will be announced but not distributed or sold.

PURCHASE OF *STAR*

The semimonthly issues are available for sale by the Superintendent of Documents, U.S. Government Printing Office, Washington, D.C. 20402.

PUBLISHED BY:

UNITED STATES GOVERNMENT
NATIONAL AERONAUTICS AND SPACE ADMINISTRATION
SCIENTIFIC AND TECHNICAL INFORMATION DIVISION
Scientific and Technical Aerospace Reports, Volume 26, is prepared by the NASA Scientific and Technical Information Facility operated for the National Aeronautics and Space Administration by RMS Associates.

The Administrator of the National Aeronautics and Space Administration has determined that the publication of this periodical is necessary in the transaction of the public business required by law of this Agency. Use of funds for printing this periodical has been approved by the Director of the Office of Management and Budget through March 22, 1989.

US ISSN 0036-8741

INTRODUCTION

Scientific and Technical Aerospace Reports (STAR) is a major component of a comprehensive National Aeronautics and Space Administration information system covering aeronautics, space, and supporting disciplines. *STAR* is issued on the 8th and 23rd of each month and announces current publications of the following types:

- NASA, NASA contractor, and NASA grantee reports
- Reports issued by other U.S. Government Agencies, domestic and foreign institutions, universities, and private firms
- Translations in report form
- NASA-owned patents and patent applications
- Dissertations and theses

Journal, book, and conference literature, cover-to-cover journal translations, and certain foreign dissertations are announced in a companion journal, *International Aerospace Abstracts (IAA)*, available on subscription from the American Institute of Aeronautics and Astronautics, Technical Information Service, 555 West 57th Street, 12th Floor, New York, New York 10019.

SUBJECT SCOPE

Subject scope of *STAR*, and *IAA* includes all aspects of aeronautics and space research and development, supporting basic and applied research, and applications. Aerospace aspects of earth resources, energy development, conservation, oceanography, environmental protection, urban transportation, and other topics of high national priority are also covered.

OTHER NASA PUBLICATIONS

Other NASA publications and information services are described in the publication, *The NASA Scientific and Technical Information System ... and How to Use It*, available without charge from the NASA Scientific and Technical Information Facility, P.O. Box 8757, B.W.I. Airport, Maryland 21240.

HOW TO USE *STAR* SUBJECT CATEGORIES

STAR is categorized by 10 major subject divisions divided into 76 specific subject categories and one general category/division. The major subject divisions are listed in the Table of Contents, together with a note for each that defines its scope and provides any cross-references. For example:

AERONAUTICS

Includes aeronautics (general); aerodynamics; air transportation and safety; aircraft communications and navigation; aircraft design, testing and performance; aircraft instrumentation; aircraft propulsion and power; aircraft stability and control; and research and support facilities (air).

For related information see also *Astronautics*.

Each major division is further divided into as many as nine specific categories, which are identified by category numbers.

Abstracts in *STAR* are grouped by specific category, the categories appearing in sequential order. Category breaks in the abstract section are identified by the category number and title, and a scope note. Cross-references to other categories are provided as appropriate. For example:

02 AERODYNAMICS

Includes aerodynamics of bodies, combinations, wings, rotors, and control surfaces; and internal flow in ducts and turbomachinery.

For related information see also *34 Fluid Mechanics and Heat Transfer.*

CROSS-REFERENCES

Individual *STAR* abstracts are not ordinarily cross-referenced, except for certain conference reports or book translations that have had separate abstracts written for their component papers or chapters. Citations and abstracts of the components follow immediately after those of the parent document. When the subject content of a component differs sufficiently from the general content of the parent, a cross-reference citation also is printed at the end of the category to which it normally would have been assigned if it were independent.

DOCUMENTS ON MICROFICHE

Documents on microfiche[1] are designated by a pound sign (#) following the accession number. The pound sign is used without regard to the source or quality of the microfiche.

AVAILABILITIES

One or more sources from which a document announced in *STAR* is available to the public is given in each citation. The most commonly indicated sources and their acronyms or abbreviations are listed below. If the publication is available from a source other than those listed, the publisher and his address will be displayed on the availability line or in combination with the corporate source line.

Avail: NTIS. Sold by the National Technical Information Service. Prices for hard copy (HC) and microfiche (MF) are indicated by a price code following the letters HC or MF in the *STAR* citation. Current values for the price codes are given in the tables on page vii.

Initially distributed microfiche under the NTIS SRIM (Selected Research in Microfiche) is available at greatly reduced unit prices. For this service and for information concerning subscription to NASA printed reports, consult the NTIS Subscription Section, Springfield, Va. 22161.

NOTE ON ORDERING DOCUMENTS: When ordering NASA publications (those followed by the * symbol), use the N accession number. NASA patent applications (only the specifications are offered) should be ordered by the US-Patent-Appl-SN number. Non-NASA publications (no asterisk) should be ordered by the AD, PB, or other *report number* shown on the last line of the citation, not by the N accession number. It is also advisable to cite the title and other bibliographic identification.

Avail: SOD (or GPO). Sold by the Superintendent of Documents, U.S. Government Printing Office, in hard copy. The current price and order number are given following the availability line. (NTIS will fill microfiche requests, as indicated above, for those documents identified by a # symbol.)

(1) A microfiche is a transparent sheet of film, 105 by 148 mm in size, containing as many as 60 to 98 pages of information reduced to micro images (not to exceed 26:1 reduction).

Avail: BLL (formerly NLL): British Library Lending Division, Boston Spa, Wetherby, Yorkshire, England. Photocopies available from this organization at the price shown. (If none is given, inquiry should be addressed to the BLL.)

Avail: DOE Depository Libraries. Organizations in U.S. cities and abroad that maintain collections of Department of Energy reports, usually in microfiche form, are listed in *Energy Research Abstracts*. Services available from the DOE and its depositories are described in a booklet, *DOE Technical Information Center - Its Functions and Services* (TID-4660), which may be obtained without charge from the DOE Technical Information Center.

Avail: ESDU. Pricing information on specific data, computer programs, and details on ESDU topic categories can be obtained from ESDU International Ltd. Requesters in North America should use the Virginia address while all other requesters should use the London address, both of which are on page vi.

Avail: Fachinformationszentrum, Karlsruhe. Sold by the Fachinformationszentrum Energie, Physik, Mathematik GMBH, Eggenstein Leopoldshafen, Federal Republic of Germany, at the price shown in deutschmarks (DM).

Avail: HMSO. Publications of Her Majesty's Stationery Office are sold in the U.S. by Pendragon House, Inc. (PHI), Redwood City, California. The U.S. price (including a service and mailing charge) is given, or a conversion table may be obtained from PHI.

Avail: NASA Public Document Rooms. Documents so indicated may be examined at or purchased from the National Aeronautics and Space Administration, Public Documents Room (Room 126), 600 Independence Ave., S.W., Washington, D.C. 20546, or public document rooms located at each of the NASA research centers, the NASA Space Technology Laboratories, and the NASA Pasadena Office at the Jet Propulsion Laboratory.

Avail: Univ. Microfilms. Documents so indicated are dissertations selected from *Dissertation Abstracts* and are sold by University Microfilms as xerographic copy (HC) and microfilm. All requests should cite the author and the Order Number as they appear in the citation.

Avail: US Patent and Trademark Office. Sold by Commissioner of Patents and Trademarks, U.S. Patent and Trademark Office, at the standard price of $1.50 each, postage free. (See discussion of NASA patents and patent applications below.)

Avail: (US Sales Only). These foreign documents are available to users within the United States from the National Technical Information Service (NTIS). They are available to users outside the United States through the International Nuclear Information Service (INIS) representative in their country, or by applying directly to the issuing organization.

Avail: USGS. Originals of many reports from the U.S. Geological Survey, which may contain color illustrations, or otherwise may not have the quality of illustrations preserved in the microfiche or facsimile reproduction, may be examined by the public at the libraries of the USGS field offices whose addresses are listed in this Introduction. The libraries may be queried concerning the availability of specific documents and the possible utilization of local copying services, such as color reproduction.

Avail: Issuing Activity, or Corporate Author, or no indication of availability. Inquiries as to the availability of these documents should be addressed to the organization shown in the citation as the corporate author of the document.

NASA PATENTS AND PATENT APPLICATIONS

Patents and patent applications owned by NASA are announced in *STAR* under appropriate subject categories and are referenced in the *STAR* indexes. In the Report/Accession Number Index, patents are indexed by the NASA Case Number (which appears in lieu of the report number in other indexes), the U.S. Patent Number, the U.S. Patent Application Serial Number, and the U.S. Patent Class. Patent applications for which patents have not yet been issued are indexed by the NASA Case Number and the U.S. Patent Application Serial Number.

NASA *patent application specifications* are sold in paper copy by the National Technical Information Service at price code A02. Microfiche are sold at price code A01. The US-Patent-Appl-SN- number should be used in ordering either paper copy or microfiche from NTIS. Printed copies of *patents* (which are not microfiched) are available for purchase at $1.50 per copy from:

Commissioner of Patents and Trademarks
U.S. Patent and Trademark Office
Washington, D.C. 20231

When ordering patents, the U.S. Patent Number should be used, and payment must be remitted in advance, preferably by money order or check payable to the Commissioner of Patents and Trademarks. Prepaid purchase coupons for ordering are also available from the Patent and Trademark Office. The patents and patent applications announced in *STAR* are owned by NASA and are available for royalty-free licensing. Requests for licensing terms and further information should be addressed to:

Associate General Counsel for Intellectual Property/Code GP
National Aeronautics and Space Administration
Washington, D.C. 20546

ELIGIBILITY AND REGISTRATION FOR NASA INFORMATION PRODUCTS AND SERVICES

A variety of services is available to organizations of the following types that have registered with NASA to receive specific services or products:

1. NASA offices, research centers, contractors, subcontractors, grantees, and consultants;
2. Other U.S. Government agencies and their contractors;
3. Libraries in the United States that have arrangements with NASA to maintain collections of NASA documents for public reference;
4. Other organizations in the United States having a need for NASA documents in work related to aeronautics and space research;
5. Organizations abroad that have established reciprocal document exchange arrangements with NASA.

Only the central service points or central points of document acquisition and control within qualified organizations are eligible to register for NASA products and services. Domestic organizations that may be eligible to receive various classes of NASA publications and services should address their requests for registration or for further information to:

NASA Scientific and Technical Information Facility
ATTN: Registration Activity
P.O. Box 8757
B.W.I. Airport, Maryland 21240

Organizations abroad should direct requests to the same address, but to the attention of: International Exchange Program.

AVAILABILITY OF *STAR* ABSTRACTS ON MICROFICHE

Microfiche of the abstract sections of this issue and other issues of *STAR* are available on annual subscription from NTIS as PB88-911300, Attn: Subscriptions, 5285 Port Royal Road, Springfield, Virginia 22161. Annual subscription rates are $70.00 North America; $140.00 foreign. Abstract sections for previous years retroactive to 1964 are available at the current rates. Microfiche for individual *STAR* issue abstract sections are not available.

PUBLIC COLLECTIONS OF NASA DOCUMENTS

DOMESTIC: NASA and NASA-sponsored documents and a large number of aerospace publications are available to the public for reference purposes at the library maintained by the American Institute of Aeronautics and Astronautics, Technical Information Service, 555 West 57th Street, 12th Floor, New York, New York 10019

EUROPEAN: An extensive collection of NASA and NASA-sponsored publications is maintained by the British Library Lending Division, Boston Spa, Wetherby, Yorkshire, England for public access. The British Library Lending Division also has available many of the non-NASA publications cited in *STAR*. European requesters may purchase facsimile copy or microfiche of NASA and NASA-sponsored documents, those identified by both the symbols # and * from ESA - Information Retrieval Service European Space Agency, 8-10 rue Mario-Nikis, 75738 Paris CEDEX 15, France.

FEDERAL DEPOSITORY LIBRARY PROGRAM

In order to provide the general public with greater access to U.S. Government publications, Congress established the Federal Depository Library Program under the Government Printing Office (GPO), with 50 regional depositories responsible for permanent retention of material, inter-library loan, and reference services. At least one copy of nearly every NASA and NASA-sponsored publication, either in printed or microfiche format, is received and retained by the 50 regional depositories. A list of the regional GPO libraries, arranged alphabetically by state, appears on the inside back cover. These libraries are *not* sales outlets. A local library can contact a Regional Depository to help locate specific reports, or direct contact may be made by an individual.

ADDRESSES OF ORGANIZATIONS

American Institute of Aeronautics and Astronautics
Technical Information Service
555 West 57th Street, 12th Floor
New York, New York 10019

British Library Lending Division,
Boston Spa, Wetherby, Yorkshire,
England

Commissioner of Patents and Trademarks
U.S. Patent and Trademark Office
Washington, D.C. 20231

Department of Energy
Technical Information Center
P.O. Box 62
Oak Ridge, Tennessee 37830

ESA-Information Retrieval Service
ESRIN
Via Galileo Galilei
00044 Frascati (Rome) Italy

ESDU International, Ltd.
1495 Chain Bridge Road
McLean, Virginia 22101

ESDU International, Ltd.
251-259 Regent Street
London, W1R 7AD, England

Fachinformationszentrum Energie, Physik, Mathematik GMBH
7514 Eggenstein Leopoldshafen
Federal Republic of Germany

Her Majesty's Stationery Office
P.O. Box 569, S.E. 1
London, England

NASA Scientific and Technical Information Facility
P.O. Box 8757
B.W.I. Airport, Maryland 21240

National Aeronautics and Space Administration
Scientific and Technical Information Division (NTT-1)
Washington, D.C. 20546

National Technical Information Service
5285 Port Royal Road
Springfield, Virginia 22161

Pendragon House, Inc.
899 Broadway Avenue
Redwood City, California 94063

Superintendent of Documents
U.S. Government Printing Office
Washington, D.C. 20402

University Microfilms
A Xerox Company
300 North Zeeb Road
Ann Arbor, Michigan 48106

University Microfilms, Ltd.
Tylers Green
London, England

U.S. Geological Survey Library
National Center - MS 950
12201 Sunrise Valley Drive
Reston, Virginia 22092

U.S. Geological Survey Library
2255 North Gemini Drive
Flagstaff, Arizona 86001

U.S. Geological Survey
345 Middlefield Road
Menlo Park, California 94025

U.S. Geological Survey Library
Box 25046
Denver Federal Center, MS914
Denver, Colorado 80225

NTIS PRICE SCHEDULES

(Effective January 1, 1988)

Schedule A
STANDARD PRICE DOCUMENTS AND MICROFICHE

PRICE CODE	NORTH AMERICAN PRICE	FOREIGN PRICE
A01	$ 6.95	$13.90
A02	9.95	19.90
A03	12.95	25.90
A04-A05	14.95	29.90
A06-A09	19.95	39.90
A10-A13	25.95	51.90
A14-A17	32.95	65.90
A18-A21	38.95	77.90
A22-A25	44.95	89.90
A99	*	*
NO1	49.50	89.90
NO2	48.00	80.00

Schedule E
EXCEPTION PRICE DOCUMENTS AND MICROFICHE

PRICE CODE	NORTH AMERICAN PRICE	FOREIGN PRICE
E01	$ 8.50	17.00
E02	11.00	22.00
E03	12.00	24.00
E04	14.50	29.00
E05	16.50	33.00
E06	19.00	38.00
E07	21.50	43.00
E08	24.00	48.00
E09	26.50	53.00
E10	29.00	58.00
E11	31.50	63.00
E12	34.00	68.00
E13	36.50	73.00
E14	39.50	79.00
E15	43.00	86.00
E16	47.00	94.00
E17	51.00	102.00
E18	55.00	110.00
E19	61.00	122.00
E20	71.00	142.00
E99	*	*

* Contact NTIS for price quote.

IMPORTANT NOTICE

NTIS Shipping and Handling Charges
U.S., Canada, Mexico — ADD $3.00 per TOTAL ORDER
All Other Countries — ADD $4.00 per TOTAL ORDER

Exceptions — Does NOT apply to:
ORDERS REQUESTING NTIS RUSH HANDLING
ORDERS FOR SUBSCRIPTION OR STANDING ORDER PRODUCTS *ONLY*

NOTE: Each additional delivery address on an order requires a separate shipping and handling charge.

VOLUME 26 NUMBER 15 / AUGUST 8, 1988

TABLE OF CONTENTS

AERONAUTICS

Includes aeronautics (general); aerodynamics; air transportation and safety; aircraft communications and navigation; aircraft design, testing and performance; aircraft instrumentation; aircraft propulsion and power; aircraft stability and control; and research and support facilities (air).

For related information see also *Astronautics.*

01 AERONAUTICS (GENERAL) 2013

02 AERODYNAMICS 2013

Includes aerodynamics of bodies, combinations, wings, rotors, and control surfaces; and internal flow in ducts and turbomachinery.

For related information see also *34 Fluid Mechanics and Heat Transfer*

03 AIR TRANSPORTATION AND SAFETY 2016

Includes passenger and cargo air transport operations; and aircraft accidents.

For related information see also *16 Space Transportation* and *85 Urban Technology and Transportation.*

04 AIRCRAFT COMMUNICATIONS AND NAVIGATION N.A.

Includes digital and voice communication with aircraft; air navigation systems (satellite and ground based); and air traffic control.

For related information see also *17 Space Communications, Spacecraft Communications, Command and Tracking* and *32 Communications and Radar.*

05 AIRCRAFT DESIGN, TESTING AND PERFORMANCE 2016

Includes aircraft simulation technology.

For related information see also *18 Spacecraft Design, Testing and Performance* and *39 Structural Mechanics.* For land transportation vehicles see *85 Urban Technology and Transportation.*

06 AIRCRAFT INSTRUMENTATION N.A.

Includes cockpit and cabin display devices; and flight instruments.

For related information see also *19 Spacecraft Instrumentation* and *35 Instrumentation and Photography.*

07 AIRCRAFT PROPULSION AND POWER 2019

Includes prime propulsion systems and systems components, e.g., gas turbine engines and compressors; and onboard auxiliary power plants for aircraft.

For related information see also *20 Spacecraft Propulsion and Power, 28 Propellants and Fuels,* and *44 Energy Production and Conversion.*

08 AIRCRAFT STABILITY AND CONTROL 2020

Includes aircraft handling qualities; piloting; flight controls; and autopilots.

For related information see also *05 Aircraft Design, Testing and Performance.*

09 RESEARCH AND SUPPORT FACILITIES (AIR) 2021

Includes airports, hangars and runways; aircraft repair and overhaul facilities; wind tunnels; shock tubes; and aircraft engine test stands.

For related information see also *14 Ground Support Systems and Facilities (Space).*

ASTRONAUTICS

Includes astronautics (general); astrodynamics; ground support systems and facilities (space); launch vehicles and space vehicles; space transportation; space communications, spacecraft communications, command and tracking; spacecraft design, testing and performance; spacecraft instrumentation; and spacecraft propulsion and power.

For related information see also *Aeronautics*

12 ASTRONAUTICS (GENERAL) N.A.

For extraterrestrial exploration see *91 Lunar and Planetary Exploration.*

13 ASTRODYNAMICS 2022

Includes powered and free-flight trajectories; and orbital and launching dynamics.

14 GROUND SUPPORT SYSTEMS AND FACILITIES (SPACE) 2023

Includes launch complexes, research and production facilities; ground support equipment, e.g., mobile transporters; and simulators.

For related information see also *09 Research and Support Facilities (Air).*

15 LAUNCH VEHICLES AND SPACE VEHICLES N.A.

Includes boosters; operating problems of launch/space vehicle systems; and reusable vehicles.

For related information see also *20 Spacecraft Propulsion and Power.*

16 SPACE TRANSPORTATION 2024

Includes passenger and cargo space transportation, e.g., shuttle operations; and space rescue techniques.

For related information see also *03 Air Transportation and Safety* and *18 Spacecraft Design, Testing and Performance.* For space suits see *54 Man/System Technology and Life Support.*

17 SPACE COMMUNICATIONS, SPACECRAFT COMMUNICATIONS, COMMAND AND TRACKING N.A.

Includes telemetry; space communications networks; astronavigation and guidance; and radio blackout.

For related information see also *04 Aircraft Communications and Navigation* and *32 Communications and Radar.*

18 SPACECRAFT DESIGN, TESTING AND PERFORMANCE 2024

Includes satellites; space platforms; space stations; spacecraft systems and components such as thermal and environmental controls; and attitude controls.

For life support systems see *54 Man/System Technology and Life Support.* For related information see also *05 Aircraft Design, Testing and Performance, 39 Structural Mechanics,* and *16 Space Transportation.*

19 SPACECRAFT INSTRUMENTATION N.A.

For related information see also *06 Aircraft Instrumentation* and *35 Instrumentation and Photography.*

20 SPACECRAFT PROPULSION AND POWER 2027

Includes main propulsion systems and components, e.g. rocket engines; and spacecraft auxiliary power sources.

For related information see also *07 Aircraft Propulsion and Power, 28 Propellants and Fuels, 44 Energy Production and Conversion,* and *15 Launch Vehicles and Space Vehicles.*

CHEMISTRY AND MATERIALS

Includes chemistry and materials (general); composite materials; inorganic and physical chemistry; metallic materials; nonmetallic materials; propellants and fuels; and materials processing.

23 CHEMISTRY AND MATERIALS (GENERAL) 2028

24 COMPOSITE MATERIALS 2028

Includes physical, chemical, and mechanical properties of laminates and other composite materials.

For ceramic materials see *27 Nonmetallic Materials.*

25 INORGANIC AND PHYSICAL CHEMISTRY 2032

Includes chemical analysis, e.g., chromatography; combustion theory; electrochemistry; and photochemistry.

For related information see also *77 Thermodynamics and Statistical Physics.*

26 METALLIC MATERIALS 2037

Includes physical, chemical, and mechanical properties of metals, e.g., corrosion; and metallurgy.

27 NONMETALLIC MATERIALS 2042

Includes physical, chemical, and mechanical properties of plastics, elastomers, lubricants, polymers, textiles, adhesives, and ceramic materials.

For composite materials see *24 Composite Materials.*

28 PROPELLANTS AND FUELS 2048

Includes rocket propellants, igniters and oxidizers; their storage and handling procedures; and aircraft fuels.

For related information see also *07 Aircraft Propulsion and Power, 20 Spacecraft Propulsion and Power,* and *44 Energy Production and Conversion.*

29 MATERIALS PROCESSING 2049

Includes space-based development of products and processes for commercial application.

For biological materials see *55 Space Biology.*

ENGINEERING

Includes engineering (general); communications and radar; electronics and electrical engineering; fluid mechanics and heat transfer; instrumentation and photography; lasers and masers; mechanical engineering; quality assurance and reliability; and structural mechanics.

For related information see also *Physics.*

31 ENGINEERING (GENERAL) 2050

Includes vacuum technology; control engineering; display engineering; cryogenics; and fire prevention.

32 COMMUNICATIONS AND RADAR 2055

Includes radar; land and global communications; communications theory; and optical communications.

For related information see also *04 Aircraft Communications and Navigation* and *17 Space Communications, Spacecraft Communications, Command and Tracking.* For search and rescue see *03 Air Transportation and Safety,* and *16 Space Transportation.*

33 ELECTRONICS AND ELECTRICAL ENGINEERING 2058

Includes test equipment and maintainability; components, e.g., tunnel diodes and transistors; microminiaturization; and integrated circuitry.

For related information see also *60 Computer Operations and Hardware* and *76 Solid-State Physics.*

34 FLUID MECHANICS AND HEAT TRANSFER 2061

Includes boundary layers; hydrodynamics; fluidics; mass transfer and ablation cooling.

For related information see also *02 Aerodynamics* and *77 Thermodynamics and Statistical Physics.*

35 INSTRUMENTATION AND PHOTOGRAPHY 2068

Includes remote sensors; measuring instruments and gages; detectors; cameras and photographic supplies; and holography.

For aerial photography see *43 Earth Resources and Remote Sensing.* For related information see also *06 Aircraft Instrumentation* and *19 Spacecraft Instrumentation.*

36 LASERS AND MASERS 2070

Includes parametric amplifiers.

For related information see also *76 Solid-State Physics.*

37 MECHANICAL ENGINEERING 2073

Includes auxiliary systems (nonpower); machine elements and processes; and mechanical equipment.

38 QUALITY ASSURANCE AND RELIABILITY 2074

Includes product sampling procedures and techniques; and quality control.

39 STRUCTURAL MECHANICS 2075

Includes structural element design and weight analysis; fatigue; and thermal stress.

For applications see *05 Aircraft Design, Testing and Performance* and *18 Spacecraft Design, Testing and Performance.*

GEOSCIENCES

Includes geosciences (general); earth resources and remote sensing; energy production and conversion; environment pollution; geophysics; meteorology and climatology; and oceanography.

For related information see also *Space Sciences.*

42 GEOSCIENCES (GENERAL) N.A.

43 EARTH RESOURCES AND REMOTE SENSING 2089

Includes remote sensing of earth resources by aircraft and spacecraft; photogrammetry; and aerial photography.

For instrumentation see *35 Instrumentation and Photography.*

44 ENERGY PRODUCTION AND CONVERSION 2090

Includes specific energy conversion systems, e.g., fuel cells; global sources of energy; geophysical conversion; and windpower.

For related information see also *07 Aircraft Propulsion and Power, 20 Spacecraft Propulsion and Power,* and *28 Propellants and Fuels.*

45 ENVIRONMENT POLLUTION 2092

Includes atmospheric, noise, thermal, and water pollution.

46 GEOPHYSICS 2093

Includes aeronomy; upper and lower atmosphere studies; ionospheric and magnetospheric physics; and geomagnetism.

For space radiation see *93 Space Radiation.*

47 METEOROLOGY AND CLIMATOLOGY 2097

Includes weather forecasting and modification.

48 OCEANOGRAPHY 2099

Includes biological, dynamic, and physical oceanography; and marine resources.

For related information see also *43 Earth Resources and Remote Sensing.*

LIFE SCIENCES

Includes life sciences (general); aerospace medicine; behavioral sciences; man/system technology and life support; and space biology.

51 LIFE SCIENCES (GENERAL) 2100

52 AEROSPACE MEDICINE 2101

Includes physiological factors; biological effects of radiation; and effects of weightlessness on man and animals.

53 BEHAVIORAL SCIENCES 2104

Includes psychological factors; individual and group behavior; crew training and evaluation; and psychiatric research.

54 MAN/SYSTEM TECHNOLOGY AND LIFE SUPPORT 2104

Includes human engineering; biotechnology; and space suits and protective clothing.

For related information see also *16 Space Transportation.*

55 SPACE BIOLOGY N.A.

Includes exobiology; planetary biology; and extraterrestrial life.

MATHEMATICAL AND COMPUTER SCIENCES

Includes mathematical and computer sciences (general); computer operations and hardware; computer programming and software; computer systems; cybernetics; numerical analysis; statistics and probability; systems analysis; and theoretical mathematics.

59 MATHEMATICAL AND COMPUTER SCIENCES (GENERAL) 2105

60 COMPUTER OPERATIONS AND HARDWARE 2106

Includes hardware for computer graphics, firmware, and data processing.

For components see *33 Electronics and Electrical Engineering.*

61 COMPUTER PROGRAMMING AND SOFTWARE 2107

Includes computer programs, routines, algorithms, and specific applications, e.g., CAD/CAM.

62 COMPUTER SYSTEMS 2114

Includes computer networks and special application computer systems.

63 CYBERNETICS 2116

Includes feedback and control theory, artificial intelligence, robotics and expert systems.

For related information see also *54 Man/System Technology and Life Support.*

64 NUMERICAL ANALYSIS 2118

Includes iteration, difference equations, and numerical approximation.

65 STATISTICS AND PROBABILITY 2123

Includes data sampling and smoothing; Monte Carlo method; and stochastic processes.

66 SYSTEMS ANALYSIS 2126

Includes mathematical modeling; network analysis; and operations research.

67 THEORETICAL MATHEMATICS 2126

Includes topology and number theory.

PHYSICS

Includes physics (general); acoustics; atomic and molecular physics; nuclear and high-energy physics; optics; plasma physics; solid-state physics; and thermodynamics and statistical physics.

For related information see also *Engineering.*

70 PHYSICS (GENERAL) 2128

For precision time and time interval (PTTI) see *35 Instrumentation and Photography;* for geophysics, astrophysics or solar physics see *46 Geophysics, 90 Astrophysics,* or *92 Solar Physics.*

71 ACOUSTICS 2129
Includes sound generation, transmission, and attenuation.
For noise pollution see *45 Environment Pollution.*

72 ATOMIC AND MOLECULAR PHYSICS 2131
Includes atomic structure, electron properties, and molecular spectra.

73 NUCLEAR AND HIGH-ENERGY PHYSICS 2132
Includes elementary and nuclear particles; and reactor theory.
For space radiation see *93 Space Radiation.*

74 OPTICS 2133
Includes light phenomena and optical devices.
For lasers see *36 Lasers and Masers.*

75 PLASMA PHYSICS 2134
Includes magnetohydrodynamics and plasma fusion.
For ionospheric plasmas see *46 Geophysics.* For space plasmas see *90 Astrophysics.*

76 SOLID-STATE PHYSICS 2139
Includes superconductivity.
For related information see also *33 Electronics and Electrical Engineering* and *36 Lasers and Masers.*

77 THERMODYNAMICS AND STATISTICAL PHYSICS 2146
Includes quantum mechanics; theoretical physics; and Bose and Fermi statistics.
For related information see also *25 Inorganic and Physical Chemistry* and *34 Fluid Mechanics and Heat Transfer.*

SOCIAL SCIENCES

Includes social sciences (general); administration and management; documentation and information science; economics and cost analysis; law, political science, and space policy; and urban technology and transportation.

80 SOCIAL SCIENCES (GENERAL) N.A.
Includes educational matters.

81 ADMINISTRATION AND MANAGEMENT 2147
Includes management planning and research.

82 DOCUMENTATION AND INFORMATION SCIENCE 2148
Includes information management; information storage and retrieval technology; technical writing; graphic arts; and micrography.
For computer documentation see *61 Computer Programming and Software.*

83 ECONOMICS AND COST ANALYSIS N.A.
Includes cost effectiveness studies.

84 LAW, POLITICAL SCIENCE AND SPACE POLICY N.A.
Includes NASA appropriation hearings; aviation law; space law and policy; international law; international cooperation; and patent policy.

85 URBAN TECHNOLOGY AND TRANSPORTATION 2150
Includes applications of space technology to urban problems; technology transfer; technology assessment; and surface and mass transportation.
For related information see *03 Air Transportation and Safety, 16 Space Transportation,* and *44 Energy Production and Conversion.*

SPACE SCIENCES

Includes space sciences (general); astronomy; astrophysics; lunar and planetary exploration; solar physics; and space radiation.
For related information see also *Geosciences.*

88 SPACE SCIENCES (GENERAL) N.A.

89 ASTRONOMY 2150
Includes radio, gamma-ray, and infrared astronomy; and astrometry.

90 ASTROPHYSICS 2151
Includes cosmology; celestial mechanics; space plasmas; and interstellar and interplanetary gases and dust.
For related information see also *75 Plasma Physics.*

91 LUNAR AND PLANETARY EXPLORATION 2152
Includes planetology; and manned and unmanned flights.
For spacecraft design or space stations see *18 Spacecraft Design, Testing and Performance.*

92 SOLAR PHYSICS 2152
Includes solar activity, solar flares, solar radiation and sunspots.
For related information see *93 Space Radiation.*

93 SPACE RADIATION 2152
Includes cosmic radiation; and inner and outer earth's radiation belts.
For biological effects of radiation see *52 Aerospace Medicine.* For theory see *73 Nuclear and High-Energy Physics.*

GENERAL

Includes aeronautical, astronautical, and space science related histories, biographies, and pertinent reports too broad for categorization; histories or broad overviews of NASA programs.

99 GENERAL 2153

Note: N.A. means that no abstracts were assigned to this category for this issue.

SUBJECT INDEX I-1
PERSONAL AUTHOR INDEX I-55
CORPORATE SOURCE INDEX I-63
CONTRACT NUMBER INDEX I-75
REPORT/ACCESSION NUMBER INDEX I-79

TYPICAL CITATION AND ABSTRACT

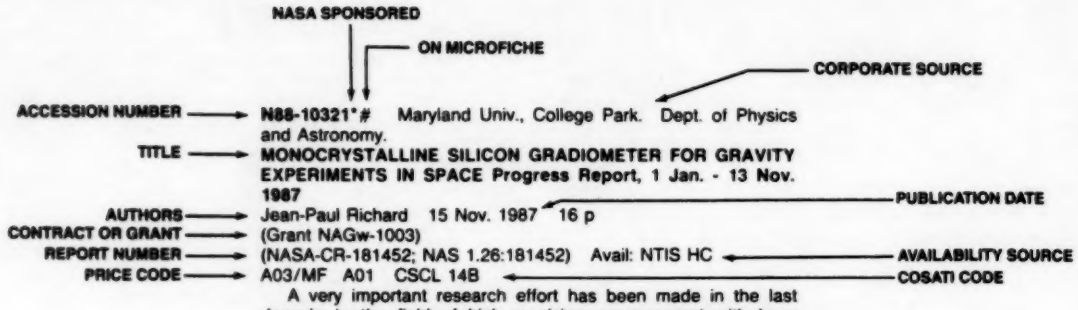

A very important research effort has been made in the last decade in the field of high precision measurement with laser instrumentation. The development of a space borne gradiometer operating at a high sensitivity level using laser measurement of the distance between proof mass over a short base line of order one meter is discussed. Two aspects of laser technology make it a promising tool for gradiometry measurements: quantum limited accuracy and absolute distance measurements. The quantum limit associated with laser instrumentation was formulated. The relevant quantum and classical sources of errors in laser measurements were reviewed and corresponding laser performance requirements for gradient measurements were evaluated. Some mechanical quality factor measurements were made on simple resonant monocrystalline silicon suspensions. It was discovered that the use of zero derivative restoring forces to position the gradiometer test masses will dramatically reduce the gradiometer temperature control requirements. A laser beam side injection scheme was discovered which permits rejection of common mode accelerations. These concepts are briefly discussed. Author

VOLUME 26 NUMBER 15 / AUGUST 8, 1988

Scientific and Technical Aerospace Reports

A Semimonthly Publication of the National Aeronautics and Space Administration

01 AERONAUTICS (GENERAL)

N88-22003# Transportation Systems Center, Cambridge, Mass.
GENERAL AVIATION ACTIVITY AND AVIONICS SURVEY: 1986 DATA Annual Summary Report
Dec. 1987 290 p
(AD-A189986; DOT-TSC-FAA-87-5; FAA-MS-87-5) Avail: NTIS HC A13/MF A01 CSCL 01C

This report presents the results and description of the 1986 General Aviation Activity and Avionics Survey. The survey was conducted during 1987 by the FAA to obtain information on the activity and avionics of the United States registered general aviation aircraft fleet, the dominant component of civil aviation in the U.S. The survey was based on a statistically selected sample of about 10.5 percent of the general aviation fleet. A response rate of 54.6 percent was obtained. Survey results are based upon responses but are expanded upward to represent the total population. Survey results revealed that during 1986 an estimated 34.4 million hours of flying time were logged and 95.1 million operations were performed by the 220,044 active general aviation aircraft in the U.S. fleet. The mean annual flight time per aircraft was 148.9 hours. The active aircraft represented about 81.9 percent of the registered general aviation fleet. The report contains breakdowns of these and other statistics by manufacturer/model group, aircraft type, state and region of based aircraft, and primary use. Also included are fuel consumption, lifetime airframe hours, avionics, engine hours, and miles flown estimates, tables for detailed analysis of the avionics capabilities of the general aviation fleet, estimates of the number of landings, IFR hours flown, and the cost and grade of fuel consumed by a GA fleet. GRA

02 AERODYNAMICS

Includes aerodynamics of bodies, combinations, wings, rotors, and control surfaces; and internal flow in ducts and turbomachinery.

For related information see also *34 Fluid Mechanics and Heat Transfer.*

N88-22004# Air Force Systems Command, Wright-Patterson AFB, Ohio. Foreign Technology Div.
CONTROL OF LAMINAR FLOW AROUND OF THE WING IN FREE-AIR CONDITIONS
V. B. Zozulya and O. R. Cheranovskiy 4 Dec. 1987 16 p Transl. into ENGLISH from Collection of Hydromechanics (USSR), issue 20, 1972 p 37
(AD-A187479; FTD-ID(RS)T-1042-87) Avail: NTIS HC A03/MF A01 CSCL 01A

The effect of the initial turbulence of flow on the distribution of the speed of suction from the boundary layer of the penetrated plate with the ideally smooth surface is examined. However, it is known that the initial turbulence of the atmosphere is considerably less than the corrected values. As the investigations, carried out by Shaubauer and Skramstad showed, with the sufficiently low turbulence level (order 0.08 percent) there is so-called upper critical Reynolds number. Therefore, the experimental confirmation of this face under the conditions of free atmosphere is of interest, and also the explanation of the minimally necessary suction intensity under such conditions. The decrease of initial turbulence in comparison with the value of turbulence in the duct by an order must lead to the noticeable increase in the extent of laminar section, which, however, under the conditions of the atmosphere must be limited by the value of the upper critical Reynolds number. In connection with this the value of suction intensity, necessary for the laminar flow, can be lowered approximately doubly in comparison with the values of intensity, obtained in the duct when epsilon = 0.2 percent. Author

N88-22005# Naval Postgraduate School, Monterey, Calif.
HIGH REYNOLDS NUMBER, LOW MACH NUMBER, STEADY FLOW FIELD CALCULATIONS OVER A NACA 0012 AIRFOIL USING NAVIER-STOKES AND INTERACTIVE BOUNDARY LAYER THEORY M.S. Thesis
Lisa J. Cowles Dec. 1987 118 p
(AD-A189871) Avail: NTIS HC A06/MF A01 CSCL 20D

A Navier-Stokes code, developed by N. L. Sankar, and an Interactive Boundary Layer code, developed by Tuncer Cebeci, are implemented for high Reynolds number, low Mach flows over a NACA 0012 airfoil. Upper surface pressure distribution, coefficients of lift, coefficients of friction, and velocity profiles obtained from the Navier-Stokes code are compared to results obtained from the Cebeci Interactive Boundary Layer code for steady flow. The steady state cases investigated are at .3 Mach and Reynolds numbers of 1 to 5 million and at .12 Mach and a Reynolds number of 1.5 million. GRA

N88-22006# Flow Research, Inc., Kent, Wash.
UNSTEADY AERODYNAMICS OF A WORTMANN FX-63-137 WING IN A FLUCTUATING WIND FIELD Final Report, 15 Sep. 1983 - 15 Sep. 1987
H.-T. Liu Nov. 1987 61 p
(Contract N00014-83-C-0694)
(AD-A190128; FLOW-RR-431) Avail: NTIS HC A04/MF A01 CSCL 01A

An environmental aerodynamic test (EATS) was designed and assembled to investigate the effects of gust and turbulence on the performance of a full-scale Wortmann FX-63-137 wing. Experiments were conducted in the atmospheric boundary layer by directing the elevated wing into the prevailing wind for a range of Reynolds numbers from 80,000 to 450,000. The unsteady wind field, in essence, introduces significant and favorable effects on the aerodynamics in terms of lift overshoot, stall delay, reduction of drag at small angles of attack, and endurance enhancement. Further analysis of the field data was conducted to investigate the unsteady aerodynamic phenomena, such as the hysteresis loops and the spectra of the aerodynamic forces and the relation to the ambient wind conditions. GRA

N88-22007# Arizona Univ., Tucson.
EXPERIMENTAL INVESTIGATION OF A SPANWISE FORCED MIXING LAYER Annual Report, 1 Jul. 1986 - 30 Jun. 1987
A. Glezer, I. J. Wygnanski, and T. F. Balsa 7 Nov. 1987 39 p
(Grant AF-AFOSR-0324-86)
(AD-A190136; AFOSR-87-1903TR) Avail: NTIS HC A03/MF A01 CSCL 20D

The occurrence of three-dimensional motion within a plane mixing layer results in a significant increase of the internal

mixedness (mixing transition). The three-dimensional motion necessary for mixing is induced by streamwise, counter-rotating vortex pairs superimposed on the primary spanwise vortices. While their appearance in the plane mixing layer has been established, their origin and their evolution with increasing streamwise distance remains an enigma. Stability considerations indicate that an instability in the spanwise direction may lead to the generation of streamwise vorticity. This suggests that the flow may be susceptible to low level spanwise periodic forcing. Previous experiments have demonstrated that forcing allows the enhancement of individual instability modes and is an essential step towards understanding the evolution of the natural flow. Furthermore, application of forcing to the flow provides a powerful tool of considerable practical significance for the control of the downstream evolution. We have begun an experimental investigation of a plane mixing layer which is forced independently in the spanwise and streamwise directions. Our objective is to study the evolution of spanwise instability.

GRA

N88-22008# Douglas Aircraft Co., Inc., Long Beach, Calif.
OSCILLATING AIRFOILS: ACHIEVEMENTS AND CONJECTURES Final Report, Oct. 1986 - Sep. 1987
Tuncer Cebeci Sep. 1987 31 p
(Contract F49620-87-C-0004)
(AD-A190490; MDC-K0535; AFOSR-87-1779TR) Avail: NTIS HC A03/MF A01 CSCL 20D

Recent developments and applications of an interactive boundary layer procedure for unsteady flows are reviewed. The emphasis is on a model problem corresponding to an oscillating thin airfoil in laminar flows and results are reported for different amplitudes and frequencies of oscillation. The use of the characteristic box scheme, with its stability criterion, are shown to allow the accurate calculation of reverse flows and the interaction procedure removes the singularity to allow calculation through regions of separated flow. Although the current focus of the interactive boundary layer procedure has been on the leading edge region, it has general applicability and, together with models for transition and turbulent flows, it can provide the basis for a method to deal with oscillation airfoils and wings and the rapid movement of fixed wing arrangements at angles of attack up to and beyond those of dynamic stall. Calculations at high angles of attack show that the behavior of the unsteady separated leading edge flow has similarities to steady flows down-stream of surface corrugations. The use of linear stability theory in the latter case shows that the locations of the onset of transition moves upstream with severity of corrugation and can move inside the separation bubble. In practice this means that the bubbles will be shortened and analogy with unsteady flows suggests that transition may play an important role.

GRA

N88-22009*# National Aeronautics and Space Administration. Ames Research Center, Moffett Field, Calif.
COMPUTATIONAL FLUID DYNAMICS DRAG PREDICTION: RESULTS FROM THE VISCOUS TRANSONIC AIRFOIL WORKSHOP
Terry L. Holst Apr. 1988 15 p Workshop held Jan. 1987
(NASA-TM-100095; A-88142; NAS 1.15:100095) Avail: NTIS HC A03/MF A01 CSCL 01A

Results from the Viscous Transonic Airfoil Workshop are compared with each other and with experimental data. Test cases used include attached and separated transonic flows for the NACA 0012 airfoil. A total of 23 sets of numerical results from 15 different author groups are included. The numerical method used vary widely and include: 16 Navier-Stokes methods, 2 Euler boundary layer methods, and 5 potential boundary layer methods. The results indicate a high degree of sophistication among the numerical methods with generally good agreement between the various computed and experimental results for attached or moderately separated cases. The agreement for cases with larger separation is only fair and suggests additional work is required in this area.

Author

N88-22010*# National Aeronautics and Space Administration. Ames Research Center, Moffett Field, Calif.
TRANSONIC NAVIER-STOKES COMPUTATIONS OF STRAKE-GENERATED VORTEX INTERACTIONS FOR A FIGHTER-LIKE CONFIGURATION
Steve Reznick Feb. 1988 117 p
(NASA-TM-100009; A-87288; NAS 1.15:100009) Avail: NTIS HC A06/MF A01 CSCL 01A

Transonic Euler/Navier-Stokes computations are accomplished for wing-body flow fields using a computer program called Transonic Navier-Stokes (TNS). The wing-body grids are generated using a program called ZONER, which subdivides a coarse grid about a fighter-like aircraft configuration into smaller zones, which are tailored to local grid requirements. These zones can be either finely clustered for capture of viscous effects, or coarsely clustered for inviscid portions of the flow field. Different equation sets may be solved in the different zone types. This modular approach also affords the opportunity to modify a local region of the grid without recomputing the global grid. This capability speeds up the design optimization process when quick modifications to the geometry definition are desired. The solution algorithm embodied in TNS is implicit, and is capable of capturing pressure gradients associated with shocks. The algebraic turbulence model employed has proven adequate for viscous interactions with moderate separation. Results confirm that the TNS program can successfully be used to simulate transonic viscous flows about complicated 3-D geometries.

Author

N88-22011*# University of Southern California, Los Angeles. Dept. of Aerospace Engineering.
PRESSURE MEASUREMENTS OF IMPINGING JET WITH ASYMMETRIC NOZZLE Progress Report
Chih-Ming Ho May 1988 24 p
(Grant NAG1-819)
(NASA-CR-182759; NAS 1.26:182759) Avail: NTIS HC A03/MF A01 CSCL 01A

For modern aircraft, impinging surfaces are commonly used as a device for obtaining vector thrust from engine exhaust. The nature of dynamic loading is important to understand for design purposes. In this study, the frequency, mode, and level of pressure fluctuations generated by an elliptic jet are examined. The elliptic jet is used because it has several operational advantages over a circular jet.

Author

N88-22012*# National Aeronautics and Space Administration. Langley Research Center, Hampton, Va.
LASER VELOCIMETER MEASUREMENTS IN A WING-FUSELAGE TYPE JUNCTURE
J. Scheiman and L. R. Kubendran (Analytical Services and Materials, Inc., Hampton, Va.) Apr. 1988 9 p Presented at the IEEE 11th International Congress on Instrumentation in Aerospace Simulation Facilities, Stanford, Calif., 26-28 Aug. 1985
(NASA-TM-100588; NAS 1.15:100588) Avail: NTIS HC A02/MF A01 CSCL 01A

A single axis, five beam, three component laser velocimeter system was used in a juncture flow experiment. A description of the seeding system developed for and used in this experiment is given. The performanace of the LV system was evaluated, and some of the problems associated with it were identified. Satisfactory results were obtained in the juncture flow experiments using this LV system.

Author

N88-22013*# National Aeronautics and Space Administration. Ames Research Center, Moffett Field, Calif.
BOUNDARY-LAYER AND WAKE MEASUREMENTS ON A SWEPT, CIRCULATION-CONTROL WING
Frank W. Spaid (McDonnell-Douglas Research Labs., St. Louis, Mo.) and Earl R. Keener Dec. 1987 91 p Previously announced in IAA as A87-22449
(NASA-TM-89426; A-87098; NAS 1.15:89426) Avail: NTIS HC A05/MF A01 CSCL 01A

Wind-tunnel measurements of boundary-layer and wake velocity profiles and surface static pressure distributions are presented for

a swept, circulation-control wing. The model is an aspect-ratio-four semispan wing mounted on the tunnel side wall at a sweep angle of 45 deg. A full-span, tangential, rearward blowing, circulation-control slot is located ahead of the trailing edge on the upper surface. Flow surveys were obtained at mid-semispan at freestream Mach numbers of 0.425 and 0.70. Boundary-layer profiles measured on the forward portions of the wing are approximately streamwise and two dimensional. The flow in the vicinity of the jet exit and in the near wake is highly three dimensional. The jet flow near the slot on the Coanda surface is directed normal to the slot. Near-wake surveys show large outboard flows at the center of the wake. At Mach 0.425 and a 5-deg angle of attack, a range of jet-blowing rates was found for which an abrupt transition from incipient separation to attached flow occurs in the boundary layer upstream of the slot. The variation in the lower-surface separation location with blowing rate was determined from boundary-layer measurements at Mach 0.425.
Author

N88-22014*# National Aeronautics and Space Administration. Ames Research Center, Moffett Field, Calif.
BIFURCATIONS IN UNSTEADY AERODYNAMICS-IMPLICATIONS FOR TESTING
Gary T. Chapman and Murray Tobak Mar. 1988 20 p
(NASA-TM-100083; A-88076; NAS 1.15:100083) Avail: NTIS HC A03/MF A01 CSCL 01A

The various forms of bifurcations that can occur between steady and unsteady aerodynamic flows are reviewed. Examples are provided to illustrate the various ways in which bifurcations may intervene to influence the outcome of dynamics tests involving unsteady aerodynamics. The presence of bifurcation phenomena in such tests must be taken into consideration to ensure the proper interpretation of results, and some recommendations are made to that end.
Author

N88-22015*# National Aeronautics and Space Administration. Langley Research Center, Hampton, Va.
INFLOW MEASUREMENT MADE WITH A LASER VELOCIMETER ON A HELICOPTER MODEL IN FORWARD FLIGHT. VOLUME 3: RECTANGULAR PLANFORM BLADES AT AN ADVANCE RATIO OF 0.30
Joe W. Elliott, Susan L. Althoff, and Richard H. Sailey (PRC Kentron, Inc., Hampton, Va.) Apr. 1988 390 p
(NASA-TM-100543; NAS 1.15:100543; AVSCOM-TM-88-B-006) Avail: NTIS HC A17/MF A01 CSCL 01A

An experimental investigation was conducted in the 14- by 22-Foot Subsonic Tunnel at NASA Langley Research Center to measure the inflow into a scale model helicopter rotor in forward flight (micron sub infinity = 0.30). The measurements were made with a two component Laser Velocimeter (LV) one chord above the plane formed by the path of the rotor tips (tip path plane). A conditional sampling technique was employed to determine the azimuthal position of the rotor at the time that each velocity measurement was made so that the azimuthal fluctuations in velocity could be determined. Measurements were made at a total of 180 separate locations in order to clearly define the inflow character. These data are presented without analysis.
Author

N88-22016*# National Aeronautics and Space Administration. Langley Research Center, Hampton, Va.
PROCEDURES AND REQUIREMENTS FOR TESTING IN THE LANGLEY RESEARCH CENTER UNITARY PLAN WIND TUNNEL
Donald L. Wassum and Curtis E. Hyman, Jr. (PRC Kentron, Inc., Hampton, Va.) Feb. 1988 53 p
(NASA-TM-100529; NAS 1.15:100529) Avail: NTIS HC A04/MF A01 CSCL 01A

Information is presented to assist those interested in conducting wind-tunnel testing within the Langley Unitary Plan Wind Tunnel. Procedures, requirements, forms and examples necessary for tunnel entry are included.
Author

N88-22017# National Aerospace Lab., Amsterdam (Netherlands). Informatics Div.
TRENDS IN COMPUTATIONAL FLUID DYNAMICS (CFD) FOR AERONAUTICAL 3D STEADY APPLICATIONS: THE DUTCH SITUATION
J. W. Boerstoel, A. E. P. Veldman, J. vanderVooren, and A. J. vanderWees 28 Jul. 1986 21 p Presented at the 25th Working Group on Computational Fluid Dynamics Meeting, Delft, The Netherlands, 20 Oct. 1986
(NLR-MP-86074-U; B8731726; ETN-88-92225) Avail: NTIS HC A03/MF A01

Developments in computational 3-D steady aerodynamics software focusing on the efficient aerodynamic design of the next generation of transport aircraft, are surveyed. The major aerodynamic problem areas accessible to computational aerodynamics are discussed. The coherence in computational methods development is explained by showing how the methods cover a growing part of the aircraft operating range. The development of the most advanced methods, based on the Euler and Reynolds-average Navier-Stokes equations, is outlined. Computing aspects are reviewed.
ESA

N88-22018*# Southampton Univ. (England). Dept. of Aeronautics and Astronautics.
FLEXIWALL 3 SO: A SECOND ORDER PREDICTIVE STRATEGY FOR RAPID WALL ADJUSTMENT IN TWO-DIMENSIONAL COMPRESSIBLE FLOW
M. J. Goodyer and Michael Judd Jul. 1981 59 p
(Grant NsG7-172)
(NASA-CR-181662; NAS 1.26:181662) Avail: NTIS HC A04/MF A01 CSCL 01A

An improvement is presented for the 2-D strategies for adjustment of the flexible top and bottom walls of an Adaptive (Wind Tunnel) Wall Test Section (AWTS). This adjustment is part of the wall adaptation process to eliminate top and bottom wall interference at the source. The improvements to account for second order effects are described in mathematical detail. It is intended that these improvements should further minimize the necessary iterations in the wall adaptation process. An associated computer program written in BASIC is presented and several test cases run with this program are discussed. The strategy performs well for a theoretical test case but when applied to experimental AWTS data some discrepancies in the adapted wall shapes are found.
Author

N88-22019*# National Aeronautics and Space Administration. Lewis Research Center, Cleveland, Ohio.
POROUS WIND TUNNEL CORRECTIONS FOR COUNTERROTATION PROPELLER TESTING
George L. Stefko and Robert J. Jeracki [1988] 18 p Presented at the 15th Aerodynamic Testing Conference, San Diego, Calif., 18-20 May 1988; sponsored by AIAA
(NASA-TM-100873; E-4099; NAS 1.15:100873) Avail: NTIS HC A03/MF A01 CSCL 01B

Wind tunnel interference corrections have direct impact on measured propeller efficiency. A systematic series of wind tunnel tests was done in the porous-wall NASA Lewis 8- by 6-Foot Wind Tunnel to determine the wind tunnel interference corrections to the NASA Lewis counterrotation propeller test data. The test results were compared with calculations from a potential flow code to determine the interference corrections. At a Mach number of 0.8, the interference corrections resulted in a -0.008 Mach number correction which reduced the counterrotation propeller net efficiency data by 0.46 percent at the reduced Mach number. Additional wind tunnel tests were done to measure the effect of propeller thrust on wind tunnel wall interference. No wall interference corrections due to propeller thrust were found necessary for the high speed counterrotation propeller data obtained in the porous wall NASA Lewis 8- by 6-Foot Wind Tunnel.
Author

N88-22241# Joint Publications Research Service, Arlington, Va.
INVESTIGATION OF SIDE-WALL EFFECTS IN WIND TUNNEL WITH SUPERCRITICAL AIRFOIL TESTING Abstract Only
Chao Gao *In its* JPRS Report: Science and Technology. China 11 Dec. 1987 p 50 Transl. into ENGLISH from Lixue Xuebao (Beijing, Peoples Republic of China), v. 19, no. 4, Jul. 1987 p 381-386 (For primary document see N88-22233 15-31)
Avail: NTIS HC A06/MF A01

N88-22243# Joint Publications Research Service, Arlington, Va.
THEORETICAL MODEL AND NUMERICAL SOLUTION FOR COMPRESSIBLE VISCOUS VORTEX CORES Abstract Only
Bingqiu Lin *In its* JPRS Report: Science and Technology. China 11 Dec. 1987 p 59 Transl. into ENGLISH from Kongqidonglixue Xuebao (Mianyang, Peoples Republic of China), v. 5, no. 3, Sep. 1987 p 235-243 Original language document was announced in IAA as A88-14016 (For primary document see N88-22233 15-31)
Avail: NTIS HC A06/MF A01

N88-22244# Joint Publications Research Service, Arlington, Va.
MIXED DIRECT-INVERSE PROBLEM OF TRANSONIC CASCADE Abstract Only
Wei Liu and Mengyu Shen *In its* JPRS Report: Science and Technology. China 11 Dec. 1987 p 60 Transl. into ENGLISH from Kongqidonglixue Xuebao (Mianyang, Peoples Republic of China), v. 5, no. 3, Sep. 1987 p 244-250 Original language document was announced in IAA as A88-14017 (For primary document see N88-22233 15-31)
Avail: NTIS HC A06/MF A01

N88-22246# Joint Publications Research Service, Arlington, Va.
ZERO-LIFT DRAG PREDICTIONS IN SUPERSONIC FLOW FOR COMPLEX CONFIGURATIONS Abstract Only
Qide Yang *In its* JPRS Report: Science and Technology. China 11 Dec. 1987 p 63 Transl. into ENGLISH from Kongqidonglixue Xuebao (Mianyang, Peoples Republic of China), v. 5, no. 3, Sep. 1987 p 293-297 Original language document was announced in IAA as A88-14021 (For primary document see N88-22233 15-31)
Avail: NTIS HC A06/MF A01

03 AIR TRANSPORTATION AND SAFETY

Includes passenger and cargo air transport operations; and aircraft accidents.

For related information see also *16 Space Transportation* and *85 Urban Technology and Transportation.*

N88-22020# National Transportation Safety Board, Washington, D. C. Bureau of Field Operations.
AIRCRAFT ACCIDENT REPORTS, BRIEF FORMAT, US CIVIL AND FOREIGN AVIATION, ISSUE NUMBER 10 OF 1986 ACCIDENTS
31 Dec. 1987 421 p
(PB87-916912; NTSB/AAB-87/12) Avail: NTIS HC A01/MF A01; also available on subscription, North American Continent HC $185.00/year; all others write for quote CSCL 01C

The publication contains selected aircraft accident reports in Brief Format ocurring in U.S. civil and foreign aviation operations during Calendar Year 1986. Approximately 200 General Aviation and Air Carrier accidents contained in the publication represent a random selection. The publication is issued irregularly, normally eighteen times each year. The Brief Format represents the facts, conditions, circumstances, and probable cause(s) for each accident. GRA

N88-22021# National Transportation Safety Board, Washington, D. C. Bureau of Accident Investigation.
AIRCRAFT ACCIDENT REPORT: NORTH STAR AVIATION, INC., PA-32 RT-300, N39614 AND ALAMEDA AERO CLUB CESSNA 172, N75584, OAKLAND, CALIFORNIA, MARCH 31, 1987
27 Oct. 1987 46 p
(PB87-910412; NTSB/AAR-87/09) Avail: NTIS HC A03/MF A01; also available on subscription, North American Continent HC $60.00/year; all others write for quote CSCL 01C

The National Transportation Safety Board determines that the probable cause of the accident was the failure of each pilot-in-command to see and avoid the other aircraft, and the failure of the local controller to perceive the traffic conflict and issue traffic advisories. Contributing to the accident was the reduction in airspace separation between arriving and departing aircraft at Oakland's north field runways caused by the failure of the FAA to exercise its authority over airspace management. GRA

04 AIRCRAFT COMMUNICATIONS AND NAVIGATION

Includes digital and voice communication with aircraft; air navigation systems (satellite and ground based); and air traffic control.

For related information see also *17 Space Communications, Spacecraft Communications, Command and Tracking* and *Communications and Radar.*

No abstracts in this category.

05 AIRCRAFT DESIGN, TESTING AND PERFORMANCE

Includes aircraft simulation technology.

For related information see also *18 Spacecraft Design, Testing and Performance* and *39 Structural Mechanics.*For land transportation vehicles see *85 Urban Technology and Transportation.*

N88-22022# Air Force Inst. of Tech., Wright-Patterson AFB, Ohio.
MODEL SELECTION FOR THE MULTIPLE MODEL ADAPTIVE ALGORITHM FOR IN-FLIGHT SIMULATION M.S. Thesis
James R. Mathes, Jr. Dec. 1987 241 p
(AD-A189715; AFIT/GE/ENG/87D-40) Avail: NTIS HC A11/MF A01 CSCL 01A

This thesis extends the research accomplished by Capt Pineiro and Lt Berens in the area of adaptive algorithm implementation. Specifically, this thesis explores the performance characteristics of the multiple model estimation algorithm and how they influence the selection of aircraft models to allow the parameter adaptive control system to maintain tracking performance over a portion of the flight envelope. The aircraft dynamic equations used are those of the AFTI/F-16 and the control law design is based on the method developed by Professor Porter. After selecting a set of aircraft models that results in the best overall system response, the effect of adjusting the control law gains on the performance of the multiple model estimation algorithm is evaluated. By assuming that all states are accessible, sensor noise is then added to each of the longitudinal states to study how noise impacts model selection. A set of models that produces acceptable tracking performance over the desired flight envelope and the most immunity to sensor noise is then selected. GRA

N88-22023# Naval Postgraduate School, Monterey, Calif.
THE EFFECTS OF TORQUE RESPONSE AND TIME DELAY ON ROTORCRAFT VERTICAL AXIS HANDLING QUALITIES M.S. Thesis
Peter A. Fyles Dec. 1987 54 p
(AD-A189873) Avail: NTIS HC A04/MF A01 CSCL 01C

Research was conducted in support of updating the U.S. military handling qualities specification, MIL-H-8501A. The effects of torque response and time delay on rotorcraft vertical axis handling qualities were investigated with the use of a CH-47B variable stability helicopter and a fixed base simulator. The frequency response of displayed torque dynamics was found to be an important factor in vertical axis handling qualities. This finding has caused a revision to the update of the MIL-H-8501A. GRA

N88-22024# Lockheed-California Co., Burbank.
KRASH PARAMETRIC SENSITIVITY STUDY: TRANSPORT CATEGORY AIRPLANES Final Report, Oct. 1985 - Jun. 1986
Gil Wittlin and W. L. LaBarge Dec. 1987 169 p
(Contract DTFA03-84-C-0004)
(AD-A189962; LR-31114; DOT/FAA/CT-87/13) Avail: NTIS HC A08/MF A01 CSCL 01C

The FAA/NASA jointly sponsored Controlled Impact Demonstration (CID) test was conducted. The CID test was a major milestone in a series of inter-related analyses and test prescribed in the FAA Crash Dynamics program. Prior to the CID test, several section and impact tests including analyses were performed. Subsequent to the CID test, correlation between KRASH pretest analyses and actual test data was evaluated. The actual CID test resulted in an unsymmetrical impact which was modeled and the results compared with the recorded test data. Analyses are performed for air-to-ground, ground-to-ground, and longitudinal-only impacts. The results are presented in the form of triangular pulses with definition of the peak amplitude, base time duration and pulse change of velocity. The analytically obtained data are integrated with the full-scale aircraft and section test data to formulate crash design velocity envelopes. The results of the study are used to suggest seat dynamic test conditions. GRA

N88-22025# Boeing Military Airplane Development, Seattle, Wash.
DEVELOPMENT AND EVALUATION OF AN AIRPLANE FUEL TANK ULLAGE COMPOSITION MODEL. VOLUME 2: EXPERIMENTAL DETERMINATION OF AIRPLANE FUEL TANK ULLAGE COMPOSITIONS Final Report, Nov. 1985 - Dec. 1986
A. J. Roth Oct. 1987 118 p
(Contract F33615-84-C-2431)
(AD-A190408; D180-30344-2-Vol-2; AFWAL-TR-87-2060-Vol-2)
Avail: NTIS HC A06/MF A01 CSCL 21D

The development and evaluation of a computer model designed to predict the composition of airplane fuel tank ullage spaces is documented in two volumes. Volume 1, Airplane Fuel Tank Ullage Computer Model: A detailed mathematical description of the model as it relates to the physical processes governing the ullage of an airplane fuel tank is included, along with user instructions and examples. Extensive comparisons of computer model predictions to experimental data are included. The model is interactive and can be used on a variety of computers including personal computers. Volume 2, Experimental Determination of Airplane Fuel Tank Ullage Compositions: Experimental work conducted using a fuel tank simulator to investigate the composition of airplane fuel tank ullage spaces is described. The investigations include ullage mixing by diffusion and convection, oxygen evolution during simulated climbs and refueling and complete mission simulations. GRA

N88-22026# Texas Univ., Austin. Dept. of Aerospace Engineering and Engineering Mechanics.
ADVANCED GUIDANCE ALGORITHMS FOR HOMING MISSILES WITH BEARINGS-ONLY MEASUREMENTS Final Technical Report
Jason L. Speyer and David G. Hull Nov. 1987 87 p
(Grant AF-AFOSR-0371-84)
(AD-A190435; AFOSR-87-1962TR) Avail: NTIS HC A05/MF A01 CSCL 17G

Homing missile guidance is formulated as an optimal stochastic control problem where the special nonlinear structure of the missile-target engagement is exploited. Since this stochastic control problem assumes a nested information pattern, the filter structure can be developed independently of the guidance scheme. However, the guidance scheme is dependent on and affects filter performance. Significant progress is being made on both the estimation problem and the guidance problem. Investigation of the nonlinear estimators especially tailored to the homing missile problem has produced not only a good deal of insight but responsive and mechanizable schemes. Although these schemes are applicable to active sensors, our emphasis has been on the more difficult passive sensor case where only angles are available. Recently-developed schemes based on coordinate transformations and on a assumed probability density function perform well, but the modified-gain extended Kalman filter has been used as the basis of a stochastic adaptive flight control scheme. Two important current efforts in missile guidance with bearings-only information are in development of the guidance schemes that enhance an information measure by trajectory modulation and in target acceleration detection. GRA

N88-22027# Air Force Inst. of Tech., Wright-Patterson AFB, Ohio. School of Engineering.
PERFORMANCE OPTIMIZATION OF A CRUISE MISSILE USING DYNAMIC-STALL INDUCED LIFT AUGMENTATION M.S. Thesis
William J. Dardis, III Sep. 1987 153 p
(AD-A190497; AFIT/GAE/AA/87S-1) Avail: NTIS HC A08/MF A01 CSCL 16B

An investigation was conducted to study the possible performance benefits of using the augmented lift produced by dynamic stall-type airfoil motions to a cruise-missile-type aircraft in terms of range, climb capability, and susceptibility to threat. A baseline cruise-missile-type aircraft is defined and compared to three modified versions with augmented lift capability. The wings for the three dynamic-lift vehicles are sized to produce the same maximum lift coefficient, while operating dynamically, as the maximum usable lift aircraft. By resizing the wing through chord reduction, increases in straight-and-level range of 20 to 25 percent are found along with improvements in climb, pull over terrain, and pull up from a dive, capability. Moderate improvements in performance are found for the same aspect ratio vehicle. The vehicle resized by span reduction consistently under-performed all vehicles except in some examples of pull out to level flight. Two typical cruise missile-type missions were chosen and the trajectories of the four vehicles were modeled. minimum time above a reference altitude was determined for the two missions as a representative measure of susceptability to threat. GRA

N88-22028# Air Force Inst. of Tech., Wright-Patterson AFB, Ohio. School of Engineering.
MODIFICATION OF THE BLUEMAX 2 TERRAIN FOLLOWING MODEL TO INCORPORATE RADAR DETECTION M.S. Thesis
Jeffrey D. Hearrell Mar. 1988 94 p
(AD-A190594; AFIT/GST/ENS/88M-5) Avail: NTIS HC A05/MF A01 CSCL 17I

The objective of this thesis was to show that introducing radar detection characteristics into one of the post-processors to BLUEMAX 2, a terrain following/terrain avoidance model, would decrease the number of detections by radar against a target. Additionally, it sought to decrease computer (CPU) run time. The objectives were met through the writing and implementation of two programs. DETECT and MAXMIN. A third program, TFTAEXP, was modified. The radar parameters used in program DETECT approximate the parameters of a tracking radar; the radar cross section values and the flight path that was used were provided by ASD/ENSSE. Results of several runs were compared to a base model that is currently in use at the Air Force Studies and

Analysis Office. Washington, D.C. and by ASD/ENSSE, Wright-Patterson AFB, Ohio. GRA

N88-22029# Army Aviation Engineering Flight Activity, Edwards AFB, Calif.
PRELIMINARY AIRWORTHINESS EVALUATION OF THE UH-60A EQUIPPED WITH THE XM-139 VOLCANO MINE DISPENSING SYSTEM Final Report
Thomas L. Reynolds, John I. Nagata, Randall W. Cason, and Daumants Belte Aug. 1987 125 p
(AD-A190604) Avail: NTIS HC A06/MF A01 CSCL 15F

Preliminary airworthiness flight tests totalling 22.4 hr were conducted at West Palm Beach, Fla., (elevation 28 feet). The tests were conducted to determine handling qualities and performance of the UH-60A in the VOLCANO system configuration at an average mission gross weight of 20,500 pounds and a longitudinal center of gravity at fuselage station 351.0. The handling qualities of the UH-60A with the VOLCANO system installed were similar to the normal utility UH-60A. Three shortcomings were noted in this configuration: (1) the increased frequency and magnitude of tail shake with the VOLCANO installed; (2) the position error for the ship's airspeed system was increased by approximately 8 knots at higher speeds (120 KCAS) due to the installation of the VOLCANO mine dispensing system; and (3) Stability Augmentation System (SAS) OFF dynamic response, not attributed to the VOLCANO installation, was aperiodic and divergent. The UH-60A helicopter with VOLCANO failed to meet two requirements of the Prime Item Development Specification; however, these noncompliances were not significant. Recommendations were made to incorporate data into the applicable portion of the VOLCANO operator's manual and to conduct additional testing. GRA

N88-22030# Army Aviation Engineering Flight Activity, Edwards AFB, Calif.
PRELIMINARY AIRWORTHINESS EVALUATION OF THE UH-60A WITH ADVANCED DIGITAL OPTICAL CONTROL SYSTEM (ADOCS) Final Report
Gary L. Bender and Robert D. Robbins Aug. 1987 57 p
(AD-A190674) Avail: NTIS HC A04/MF A01 CSCL 01D

The (ADOCS) is being developed on a UH-60A helicopter by the Boeing Vertol Co. to demonstrate the feasibility of a digital optical control system. The U.S. Army Aviation Engineering Flight Activity conducted a Preliminary Airworthiness Evaluation of ADOCS installed on a UH-60A aircraft to evaluate the handling qualities and to provide data for issuance of an airworthiness release for a demonstration of the system to the Army aviation community through a guest pilot program. The ADOCS consists of a Primary Flight Control System, which incorporates limited-displacement side-arm controllers for pilot inputs (right-side pilot station only), and an Automatic Flight Control System (AFCS) which is used to augment the basic UH-60A stability. Displacement of the controllers is measured and transmitted optically to digital flight control processors where the control commands are summed with the AFCS commands and sent to the rotor control actuators. The evaluation was conducted at the BV Flight Test Center at Wilmington, Delaware between 25 March and 9 April, 1987 and consisted of 9 flights comprising 17.5 hours (14.9 productive hours). Tests included handling qualities, simulated system failures, and mission maneuvers. Three enhancing characteristics were found: (1) the ease in rolling to and maintaining a desired bank angle; (2) the capability to maintain hands-off stabilized hover with all selectable modes engaged, and; (3) the capability of the barometric altitude hold mode to maintain altitude during simulated instrument flight tasks. GRA

N88-22031*# National Aeronautics and Space Administration. Langley Research Center, Hampton, Va.
SHAPE SENSITIVITY ANALYSIS OF WING STATIC AEROELASTIC CHARACTERISTICS
Jean-Francois M. Barthelemy and Fred D. Bergen (Virginia Polytechnic Inst. and State Univ., Blacksburg.) May 1988 30 p
(NASA-TP-2808; L-16418; NAS 1.60:2808) Avail: NTIS HC A03/MF A01 CSCL 01C

A method is presented to calculate analytically the sensitivity derivatives of wing static aeroelastic characteristics with respect to wing shape parameters. The wing aerodynamic response under fixed total load is predicted with Weissinger's L-method; its structural response is obtained with Giles' equivalent plate method. The characteristics of interest include the spanwise distribution of lift, trim angle of attack, rolling and pitching moments, wind induced drag, as well as the divergence dynamic pressure. The shape parameters considered are the wing area, aspect ratio, taper ratio, sweep angle, and tip twist angle. Results of sensitivity studies indicate that: (1) approximations based on analytical sensitivity derivatives can be used over wide ranges of variations of the shape parameters considered, and (2) the analytical calculation of sensitivity derivatives is significantly less expensive than the conventional finite-difference alternative. Author

N88-22032# Aeronautical Research Inst. of Sweden, Stockholm. Structures Dept.
IN-SERVICE MEASUREMENTS OF SAAB SF-340 LANDING GEAR LOADS
Anders I. Gustavsson Oct. 1987 106 p
(Contract STU-84-4563)
(FFA-TN-1987-48; ETN-88-92199) Avail: NTIS HC A06/MF A01

Landing gear loads on a commuter airliner were continuously monitored for 6 months, including different load components, load cases, runway and weather conditions, and different pilots and ground personnel. The data are presented as cumulative excedances of longitudinal, transversal, and vertical loads obtained from the rainflow count analyses performed on-line during the measurements. It is emphasized that the nose gear is more severely strained in terms of ground reaction factors than the main gears. ESA

N88-22033*# National Aeronautics and Space Administration. Hugh L. Dryden Flight Research Center, Edwards, Calif.
EFFECTS OF UPDATE AND REFRESH RATES ON FLIGHT SIMULATION VISUAL DISPLAYS
Gary V. Kellogg and Charles A. Wagner May 1988 19 p
(NASA-TM-100415; H-1439; NAS 1.15:100415) Avail: NTIS HC A03/MF A01 CSCL 01C

An experiment was performed to study the effects of update and refresh rates on dynamic calligraphic CRT displays, particularly those used for visual displays in flight simulators. A moving horizontal line was generated on a CRT and observed at various velocities. Observations were made with both one and two refreshes per update. The data gathered from these observations are presented on plots of refresh-update rate as a function of display velocity. The display velocity where picture degradation occurs can be found by using these plots. These velocities are related to actual simulated aircraft angular and linear velocities. Results show that a visual display updated at 30 Hz and refreshed at 60 Hz degrades at very low simulated aircraft angular and linear velocities. These velocities at which degradation occurs can be significantly increased by increasing the update rate of the visual display. Only minor improvements are possible by refreshing the display twice for each uptake. To display rapidly changing flight scenery without degradation, the display update rate must be far in excess of 60 Hz, typically several hundred Hz. Author

N88-22245# Joint Publications Research Service, Arlington, Va.
INFLUENCE OF UNSTEADY AERODYNAMIC FORCES ON DYNAMIC RESPONSE OF VARIABLE SWEEP AIRCRAFT Abstract Only
Ming Yan and Chuanren Qiu *In its* JPRS Report: Science and Technology. China 11 Dec. 1987 p 62 Transl. into ENGLISH from Kongqidonglixue Xuebao (Mianyang, Peoples Republic of China), v. 5, no. 3, Sep. 1987 p 261-270 Original language document was announced in IAA as A88-14018 (For primary document see N88-22233 15-31)
Avail: NTIS HC A06/MF A01

06 AIRCRAFT INSTRUMENTATION

Includes cockpit and cabin display devices; and flight instruments.

For related information see also *19 Spacecraft Instrumentation* and *35 Instrumentation and Photography.*

No abstracts in this category.

07 AIRCRAFT PROPULSION AND POWER

Includes prime propulsion systems and systems components, e.g., gas turbine engines and compressors; and onboard auxilliary power plants for aircraft.

For related information see also *20 Spacecraft Propulsion and Power, 28 Propellants and Fuels,* and *44 Energy Production and Conversion.*

N88-22034# Naval Postgraduate School, Monterey, Calif.
HEAT TRANSFER MODELING OF JET VANE THRUST VECTOR CONTROL (TVC) SYSTEMS M.S. Thesis
Michael F. Dulke Dec. 1987 169 p
(AD-A190106) Avail: NTIS HC A08/MF A01 CSCL 21E

The research presented herein, analyzes two models of a jet vane Thrust Vector Control (TVC) System. Computational modeling was accomplished using the latest version of the PHEONICS computer code, designated PHEONICS-84. The vane configurations studies, consisted of a simple wedge and a blunt bodied vane, with a leading edge radius of 1.016 mm. (1/25 in.). These models were examined in a two dimensional, subsonic and supersonic, cold flow field, for both laminar and turbulent flow cases. Results consist of a numerical solution and a graphical representation of surface shear stress coefficient, Stanton number and convective heat transfer coefficient. GRA

N88-22035# Air Force Inst. of Tech., Wright-Patterson AFB, Ohio. School of Engineering.
LINEAR STATE SPACE MODELING OF A TURBOFAN ENGINE Final Report, May 1986 - Dec. 1987
Gregory L. Thelen Dec. 1987 84 p
(AD-A190110; AFIT/GA/AA/87D-10) Avail: NTIS HC A05/MF A01 CSCL 21E

The F101 turbofan engine, used on the B-1B bomber, will be used as the example with the linear state space models being derived from the non-linear F101 engine computer simulation model. The internal convergence logic of the F101 engine simulation will be used to derive the individual elements making up the linear state space models. The linear state space models will consist of both high speed and low speed rotor dynamics and turbine inlet temperature heat soak dynamics. State space inputs considered will be fuel flow and engine exit nozzle area. Also disussed in this paper will be linear analytic equations in state space format and their comparative accuracies to the models derived using the F101 non-linear computer simulation model. Based on the linear state space models developed in this paper, control systems will be designed and implemented into the F101 engine computer model. Transient performance will be compared between current engine control design and the control design based on the linear state space models. Final results will confirm the validity of the state space models derived by showing improvement over current engine transient performance. GRA

N88-22036# Purdue Univ., West Lafayette, Ind. Thermal Sciences and Propulsion Center.
RESEARCH AS PART OF THE AIR FORCE IN AERO PROPULSION TECHNOLOGY (AFRAPT) PROGRAM Annual Summary Report, Aug. 1986 - Aug. 1987
Sanford Fleeter Aug. 1987 5 p
(Grant AF-AFOSR-0305-86)
(AD-A190336; AFOSR-87-1763TR) Avail: NTIS HC A02/MF A01 CSCL 01C

Seven students participated in the Air Force Research in Aero Propulsion Technology (AFRAPT) program during the 1986 to 1987 academic year. During this year: one new Ph.D. candidate successfully completed his qualifying exams and initiated his thesis research; one continuing M.S.M.E. candidate has nearly completed his experimental thesis research; five new M.S.M.E. candidates have completed most of their course work and have initiated their thesis research. GRA

N88-22037*# National Aeronautics and Space Administration. Lewis Research Center, Cleveland, Ohio.
SMALL ENGINE COMPONENTS TEST FACILITY TURBINE TESTING CELL
Brent C. Nowlin and Vincent G. Verhoff [1988] 17 p Prepared for presentation at the 24th Joint Propulsion Conference, Boston, Mass., 11-13 Jul. 1988; sponsored in part by AIAA, ASEE, ASME, and SAE
(NASA-TM-100887; E-4120; NAS 1.15:100887; AIAA-88-2963)
Avail: NTIS HC A03/MF A01 CSCL 21E

NASA Lewis Research Center has designed and constructed a new state-of-the-art test facility. This facility, called the Small Engine Components Test Facility (SECTF), is used to test gas turbines and compressors at conditions similar to actual engine conditions. The SECTF is comprised of two separate facilities - a turbine test cell and a compressor test cell. The paper will describe the turbine test cell. The capabilities of the facility make it unique - no other facility of its kind is capable of combining its pressure, speed, and temperature ranges. Turbine inlet air ranges up to 9 atm (125 psig). The turbine exhaust pressure ranges from 0.15 atm (2 psia) to atmospheric pressure. Turbine inlet air temperatures range from ambient to 700 K (1260 deg R). The controllable speed of the turbine rotor ranges from 4000 to 60,000 rpm and the maximum power absorbed by the facility dynamometer is 1250 hp. The data acquisition system scans up to 2000 channels/sec. This paper will discuss in detail the capabilities of the facility, overall facility design, instrumentation used in the facility, and the data acquisition system. Actual research data is not discussed. Author

N88-22383*# National Aeronautics and Space Administration. Lewis Research Center, Cleveland, Ohio.
HIGH-TEMPERATURE COMBUSTOR LINER TESTS IN STRUCTURAL COMPONENT RESPONSE TEST FACILITY
Paul E. Moorhead *In its* Lewis Structures Technology, 1988. Volume 2: Structural Mechanics May 1988 p 5-13 (For primary document see N88-22382 15-39)
Avail: NTIS HC A14/MF A01 CSCL 21E

N88-22384*# National Aeronautics and Space Administration. Lewis Research Center, Cleveland, Ohio.
LIFE ASSESSMENT OF COMBUSTOR LINER USING UNIFIED CONSTITUTIVE MODELS
M. T. Tong (Sverdrup Technology, Inc., Cleveland, Ohio.) and R. L. Thompson *In its* Lewis Structures Technology, 1988. Volume 2: Structural Mechanics May 1988 p 15-25 (For primary document see N88-22382 15-39)
(Contract NAS3-24105)
Avail: NTIS HC A14/MF A01 CSCL 21E

N88-22390*# National Aeronautics and Space Administration. Lewis Research Center, Cleveland, Ohio.
THE COMPOSITE BLADE STRUCTURAL ANALYZER (COBSTRAN)
Robert A. Aiello *In its* Lewis Structures Technology, 1988. Volume 2: Structural Mechanics May 1988 p 83-97 (For primary document see N88-22382 15-39)
Avail: NTIS HC A14/MF A01 CSCL 21E

N88-22394*# MARC Analysis Research Corp., Palo Alto, Calif.
MHOST: AN EFFICIENT FINITE ELEMENT PROGRAM FOR INELASTIC ANALYSIS OF SOLIDS AND STRUCTURES
S. Nakazawa *In* NASA. Lewis Research Center, Lewis Structures Technology, 1988. Volume 2: Structural Mechanics May 1988 p 131-140 (For primary document see N88-22382 15-39)
(Contract NAS3-23698)
Avail: NTIS HC A14/MF A01 CSCL 21E

N88-22399*# National Aeronautics and Space Administration. Lewis Research Center, Cleveland, Ohio.
COMPUTATIONAL STRUCTURAL MECHANICS FOR ENGINE STRUCTURES
Christos C. Chamis *In its* Lewis Structures Technology, 1988. Volume 2: Structural Mechanics May 1988 p 189-203 (For primary document see N88-22382 15-39)
Avail: NTIS HC A14/MF A01 CSCL 21E

N88-22431*# National Aeronautics and Space Administration. Lewis Research Center, Cleveland, Ohio.
REVIEW AND ASSESSMENT OF THE HOST TURBINE HEAT TRANSFER PROGRAM
Herbert J. Gladden *In its* Lewis Structures Technology, 1988. Volume 3: Structural Integrity Fatigue and Fracture Wind Turbines HOST May 1988 p 349-367 (For primary document see N88-22408 15-39)
Avail: NTIS HC A16/MF A01 CSCL 21E

08 AIRCRAFT STABILITY AND CONTROL

Includes aircraft handling qualities; piloting; flight controls; and autopilots.

For related information see also *05 Aircraft Design, Testing and Performance.*

N88-22038# National Aerospace Lab., Amsterdam (Netherlands).
DESIGN OF AN INTEGRATED CONTROL SYSTEM FOR FLUTTER MARGIN AUGMENTATION AND GUST LOAD ALLEVIATION, TESTED ON A DYNAMIC WINDTUNNEL MODEL
P. A. vanGelder 12 May 1986 17 p Presented at the AIAA Guidance, Navigation and Control Conference, Williamsburg, Va., 18-20 Aug. 1986
(PB88-149885; NLR-MP-86034-U) Avail: NTIS HC A03/MF A01 CSCL 01C

The design method is described and some results are given from wind tunnel tests of a digitally implemented, integrated control system for both flutter augmentation and gust load alleviation. The control system was designed using optimization techniques applied to a reduced order output controller. Either the ailerons or the spoilers were used as control surfaces, while tailplanes and rudder were used additionally for rigid body mode control.
Author

N88-22039# Air Force Inst. of Tech., Wright-Patterson AFB, Ohio. School of Engineering.
APPLICATION OF EIGENSTRUCTURE ASSIGNMENT TECHNIQUES IN THE DESIGN OF A LONGITUDINAL FLIGHT CONTROL SYSTEM M.S. Thesis
Daniel G. Goddard Sep. 1987 121 p
(AD-A189644; AFIT/GAE/AA/87S-2) Avail: NTIS HC A06/MF A01 CSCL 01A

The use of eigenstructure assignment techniques has received wide attention as a tool for designing flight control systems for aircraft with multiple control surfaces. Development of a method for choosing the desired eigenstructure of the augmented, closed-loop system which would meet the handling qualities specifications was examined. This method consisted of forming an optimal plant matrix which possessed desirable dynamic characteristics and performing a spectral decomposition of this matrix. The resulting eigenstructure was used as the desired eigenvalues and eigenvectors during the full-state feedback, eigenstructure assignment process. The resulting feedback gain matrix was used in the control system. This process was performed on a model of the X-29A using the canard, flaperon, and strake flap control surfaces. The resulting augmented system was evaluated using the Neal-Smith pilot-model analysis and also using an X-29A man-in-the-loop simulation. The results show that the method is very promising, although care must be taken that all anticipated control system dynamics are considered when forming the optimal A matrix.
GRA

N88-22040# Air Force Inst. of Tech., Wright-Patterson AFB, Ohio. School of Engineering.
MULTIVARIABLE CONTROL LAW DESIGN FOR THE AFTI/F-16 WITH A FAILED CONTROL SURFACE USING A PARAMETER-ADAPTIVE CONTROLLER M.S. Thesis
Julio E. Velez Dec. 1987 183 p
(AD-A189848; AFIT/GE/ENG/87D-69) Avail: NTIS HC A09/MF A01 CSCL 01D

Multivariable control laws are designed for the Advanced Fighter Technology Integration F-16 (AFTI/F-16). Both fixed gain and adaptive Proportional plus Integral (PI) controllers are designed for a plant were the number of outputs are not equal to the number of inputs (rectangular plant). Simulations are conducted for a healthy and a failed aircraft model. The failure consists of reducing the left elevator by 50 percent. When the fixed gain controller is used for the flight control system, the simulation reveals the fact that the aircraft failure causes the output responses to diverge. If provided with a persistently exciting input the adaptive controller prevents the aircraft failure simulation from diverging and going unstable. However, additional testing and/or tuning of the adaptive controller is required to determine and enhance the stability of the adaptive controller.
GRA

N88-22041# Air Force Inst. of Tech., Wright-Patterson AFB, Ohio. School of Engineering.
KALMAN FILTER RESIDUAL EXPERT SYSTEM M.S. Thesis
Jeffrey D. Grimshaw Dec. 1987 189 p
(AD-A190520; AFIT/GCE/ENG/87D-4) Avail: NTIS HC A09/MF A01 CSCL 12E

The Pilot's Associate (PA) program has been initiated to help mitigate the extensive workload of the fighter pilot. To operate effectively, the PA system must have situation awareness: the status of important on-board and off-board systems. This knowledge is gained through sensor systems. The data from these systems must be fused together to present the PA with a coherent picture of the internal (on-board) and external (off-board) states. Although many types of information can be extracted from sensor data, this paper emphasizes those parameters that help determine target track. One common technique for fusing sensor data uses Kalman filters. In a multiple model adaptive filter (MMAF) system, the most appropriate Kalman filter is chosen. This filter provides the best estimates of the desired states. An operating MMAF system continually selects which filter to use as the basis for the state estimates. The overall accuracy of the system is closely related to how well the filters are selected. Previous filter selection techniques have proved useful, but limited. To overcome some of these limitations, an expert system, KREST, was developed so that expert rules could be used to select filters.
GRA

N88-22042# Air Force Inst. of Tech., Wright-Patterson AFB, Ohio. School of Engineering.
SUBHARMONIC ALIASING AND ITS EFFECTS ON THE AFTI/F-16 DIGITAL FLIGHT CONTROL SYSTEM M.S. Thesis
David M. Thomas Dec. 1987 114 p
(AD-A190614; AFIT/GE/ENG/87D-66) Avail: NTIS HC A06/MF A01 CSCL 01D

The purpose of this research is threefold. First, determine the cause of subharmonic aliasing, described by the AFTI/F-16 engineers as the creation of uncorrelated low frequencies whenever a subharmonic of the sample frequency is input into the system. Second, model the subharmonic aliasing effect, so that, by knowing

only input frequency and the system sample rate the output characteristics can be calculated. And third, demonstrate by simulation the effect of input and output filters on the subharmonic alias, and the effect of signals in the subharmonic range (omega(N)/10 less than omega(0) less than omega(S)/2) on the interchannel difference and the software rate limiter. The model determined that subharmonic aliasing is the result of imposter frequencies (much like aliasing) being introduced into the output signal by the sampling process. We defined subharmonic aliases occur due to: imposter frequencies and a phenomena known as apparent low frequency surge, which occurs when the input frequency is nearly an integer multiple (greater than 1) of the imposter frequency. GRA

09 RESEARCH AND SUPPORT FACILITIES (AIR)

Includes airports, hangars and runways; aircraft repair and overhaul facilities; wind tunnels; shock tubes; and aircraft engine test stands.

For related information see also *14 Ground Support Systems and Facilities (Space).*

N88-22043# Air Force Inst. of Tech., Wright-Patterson AFB, Ohio. School of Engineering.

GEOMETRIC MODELING OF FLIGHT INFORMATION FOR GRAPHICAL COCKPIT DISPLAY M.S. Thesis

Mark A. Kanko Dec. 1987 120 p Original contains color illustrations

(AD-A190484; AFIT/GCE/ENG/87D-6) Avail: NTIS HC A06/MF A01 CSCL 01D

The purpose of this thesis was to design and implement a graphics-based environment capable of modeling tactical situation arenas as viewed from the cockpit. The modeled region was composed of mountains, hostile threat envelopes, and a projected flightpath through the region. Resulting displays were to be used in the Microprocessor-Based Application of Graphics Interactive Communication (MAGIC) cockpit owned by the Crew Systems Development Branch within the USAF FDL at Wright-Patterson. This cockpit is used to prototype new graphical display formats that might be used in future aircraft. The individual 3-D objects used to represent threats and mountains in the model were generated by geometric procedural models. A strongly-parameterized procedural model would generate a three-dimensional surface of revolution composed of polygons from a 2-D profile input by the user. Once defined, each object could then be instantiated into the model representing the complete tactical situation. Positioning of objects in the model was accomplished via a mouse input device. The implemented data representation allowed the model to be easily modifiable. An overall goal was to allow the cockpit display researcher to create an entirely new tactical situation display model in less than one hour. GRA

N88-22044# Air Force Inst. of Tech., Wright-Patterson AFB, Ohio. School of Engineering.

MULTIPLE MODEL PARAMETER ADAPTIVE CONTROL FOR IN-FLIGHT SIMULATION M.S. Thesis

Thomas J. Berens Mar. 1988 88 p

(AD-A190568; AFIT/GE/ENG/88M-3) Avail: NTIS HC A05/MF A01 CSCL 01D

Adaptive control of aircraft model-following systems has shown promising results for in-flight simulation, but the computational expense and slow convergence of conventional parameter estimation techniques for higher order models inhibits their direct use for in-flight simulation. Computer simulations of adaptive systems usually assume some knowledge of model parameters in order to maintain tracking fidelity at a reasonable computational cost as parameters change. This thesis incorporates apriori information into a multiple-model estimation algorithm which assigns a probability weighting of each estimator within a bank of estimators. Final parameter estimates used in adaptive control are formed as a probabalistic weighted sum of individual estimates. Simulations of the system show excellent tracking performance throughout the flight envelope. A moving bank scheme for use over a wide range of flight conditions is recommended as a further area of study. GRA

N88-22045*# Stanford Univ., Calif. Joint Inst. for Aeronautics and Acoustics.

CONTRACTION DESIGN FOR SMALL LOW-SPEED WIND TUNNELS

James H. Bell and Rabindra D. Mehta Apr. 1988 37 p

(Contract NCC2-294)

(NASA-CR-182747; NAS 1.26:182747; JIAA-TR-84) Avail: NTIS HC A03/MF A01 CSCL 14B

An iterative design procedure was developed for 2- or 3-dimensional contractions installed on small, low speed wind tunnels. The procedure consists of first computing the potential flow field and hence the pressure distributions along the walls of a contraction of given size and shape using a 3-dimensional numerical panel method. The pressure or velocity distributions are then fed into 2-dimensional boundary layer codes to predict the behavior of the boundary layers along the walls. For small, low speed contractions, it is shown that the assumption of a laminar boundary layer originating from stagnation conditions at the contraction entry and remaining laminar throughout passage through the successful designs is justified. This hypothesis was confirmed by comparing the predicted boundary layer data at the contraction exit with measured data in existing wind tunnels. The measured boundary layer momentum thicknesses at the exit of four existing contractions, two of which were 3-D, were found to lie within 10 percent of the predicted values, with the predicted values generally lower. From the contraction wall shapes investigated, the one based on a 5th order polynomial was selected for newly designed mixing wind tunnel installation. Author

N88-22046# Oak Ridge National Lab., Tenn.

INVESTIGATION OF AEROACOUSTIC MECHANISMS BY REMOTE THERMAL IMAGING

A. J. Witten and G. E. Courville 1988 15 p Presented at the 10th Thermosense Conference, Orlando, Fla., 4 Apr. 1988

(Contract DE-AC05-84OR-21400)

(DE88-002612; CONF-880461-1) Avail: NTIS HC A03/MF A01

A hush house is a hangar-like structure designed to isolate, from the surrounding environment, the noise produced by extended aircraft engine operations during testing. While hush houses meet this intended need by suppressing audible noise, they do emit significant subaudible acoustic energy causing structural vibrations in nearby facilities. As a first step in mitigating the problems associated with hush house induced vibrations, it is necessary to identify the mechanism responsible for the low frequency acoustic emissions. It was hypothesized that the low frequency acoustic waves are a result of acoustic Cherenkov radiation. This radiation is in the form of a coherent wave produced by the engine exhaust gas flow. The speed of sound in the exhaust gas is quite high as a result of its elevated temperature. Therefore, the gas flow is sonic or subsonic relative to its own sound speed, but is supersonic relative to sound speed in the surrounding cooler air and, as a result, produces acoustic Cherenkov radiation. To confirm this hypothesis, thermographic surveys were conducted to image the thermal structure of the engine exhaust gas within the hush house. In the near field, these images revealed that the exhaust gases did not behave like a high Reynolds number turbulent jet, but rather, the transition to turbulence is delayed by a suppression in growth of the self-excited instability wave as a result of acoustic Cherenkov radiation. DOE

N88-22047*# National Aeronautics and Space Administration. Langley Research Center, Hampton, Va.

MODIFICATIONS TO THE LANGLEY 8-FOOT TRANSONIC PRESSURE TUNNEL FOR THE LAMINAR FLOW CONTROL EXPERIMENT

Charles D. Harris and Cuyler W. Brooks, Jr. May 1988 123 p

(NASA-TM-4032; L-16387; NAS 1.15:4032) Avail: NTIS HC A06/MF A01 CSCL 14B

Modifications to the NASA Langley 8 Foot Transonic Pressure Tunnel in support of the Lamina Flow Control (LFC) Experiment included the installation of a honeymoon and five screens in the settling chamber upstream of the test section 41-long test section liner that extended from the upstream end of the test section contraction region, through the best section, and into the diffuser. The honeycomb and screens were installed as permanent additions to the facility, and the liner was a temporary addition to be removed at the conclusion of the LFC Experiment. These modifications are briefly described. Author

N88-22048# National Bureau of Standards, Boulder, Colo. Electromagnetic Fields Div.

EMR (ELECTROMAGNETIC RADIATION) TEST FACILITIES EVALUATION OF REVERBERATING CHAMBER LOCATED AT RADC (ROME AIR DEVELOPMENT CENTER), GRIFFISS AFB (AIR FORCE BASE), ROME, NEW YORK

M. L. Crawford, G. H. Koepke, and J. M. Ladbury Dec. 1987 78 p Sponsored by RADC, Griffiss AFB, N.Y.

(PB88-178827; NBSIR-87/3080) Avail: NTIS HC A05/MF A01 CSCL 14B

The report describes measurement procedures and results obtained from evaluating the reverberating chamber facility located at the Rome Air Development Center (RADC), Griffiss Air Force Base, Rome, New York. The facility was developed by the RADC for use in measuring and analyzing the electromagnetic susceptibility/vulnerability (EMS/V) of weapon systems and the shielding effectiveness of enclosures and shielding materials. A brief description of the facility, including the instrumentation used for performing its evaluation and calibration by the National Bureau of Standards (NBS) is given. GRA

N88-22049# National Telecommunications and Information Administration, Boulder, Colo. Inst. for Telecommunication Sciences.

INVESTIGATIONS OF TEST METHODOLOGY FOR THE STRESS LOADING FACILITY

R. D. Jennings Sep. 1987 188 p Sponsored by Army Electronic Proving Ground, Fort Huachuca, Ariz.

(PB88-166095; NTIA-87-228) Avail: NTIS HC A09/MF A01 CSCL 14B

The U.S. Army Electronic Proving Ground (USAEPG) is planning the development of a new test facility to be known as the Stress Loading Facility (SLF). The facility is envisioned as an integrated and automated test capability that will generate a dense electromagnetic threat test environment and simultaneously monitor key performance parameters of a system being tested. The report reviews current test capabilities that are relevant to the SLF, both within and outside of USAEPG, and develops test methodologies for the SLF. GRA

N88-22050*# National Aeronautics and Space Administration. Ames Research Center, Moffett Field, Calif.

REAL-TIME FLIGHT TEST DATA DISTRIBUTION AND DISPLAY

Michael C. Nesel and Kevin R. Hammons May 1988 11 p Presented at the 4th Flight Test Conference, San Diego, Calif., 18-20 May 1988

(NASA-TM-100424; H-1454; NAS 1.15:100424; Rept-314-50; Rept-314-60; AIAA-88-2216) Avail: NTIS HC A03/MF A01 CSCL 14B

Enhancements to the real-time processing and display systems of the NASA Western Aeronautical Test Range are described. Display processing has been moved out of the telemetry and radar acquisition processing systems super-minicomputers into user/client interactive graphic workstations. Real-time data is provided to the workstations by way of Ethernet. Future enhancement plans include use of fiber optic cable to replace the Ethernet. Author

12 ASTRONAUTICS (GENERAL)

For extraterrestrial exploration see *91 Lunar and Planetary Exploration.*

N88-22234# Joint Publications Research Service, Arlington, Va.

CHRONOLOGY OF CHINA'S SUCCESSFUL SATELLITE LAUNCHINGS

In its JPRS Report: Science and Technology. China 11 Dec. 1987 p 1-3 Transl. into ENGLISH from Kexue Ribao (Beijing, Peoples Republic of China), 11 Aug. 1987 p 1 (For primary document see N88-22233 15-31)

Avail: NTIS HC A06/MF A01

13 ASTRODYNAMICS

Includes powered and free-flight trajectories; and orbital and launching dynamics.

N88-22051# Air Force Inst. of Tech., Wright-Patterson AFB, Ohio. School of Engineering.

PERIODIC ORBITS AROUND A SATELLITE MODELLED AS A TRIAXIAL ELLIPSOID M.S. Thesis

Rodney A. Werner Dec. 1987 45 p

(AD-A190592; AFIT/GA/AA/87D-8) Avail: NTIS HC A03/MF A01 CSCL 03C

There are planetary satellites, particularly Phobos, which can be modeled as triaxial ellipsoids. To study orbital dynamics of a mass near such a satellite, Hamilton's canonical equations are developed and used to numerically evaluate the existence of periodic orbits around the satellite. Calculations were also done to check the stability of these orbits by evaluating the Poincare exponents. For Phobos, periodic orbits were found in Phobos's orbital plane from near the surface to beyond Phobos's sphere of influence. None of these orbits were found to be stable. Discussion of these orbits includes a bifurcation region caused by nearby inclined orbits. These inclined orbits appear as Lissajous figures with frequency ratios of two. Though the inclined orbits are numeric solutions they all pass below Phobos's surface at the anti-Mars point and are of only academic interest. GRA

N88-22052*# Ohio State Univ., Columbus. Dept. of Geodetic Science and Surveying.

BASELINE ESTIMATION FROM SIMULTANEOUS SATELLITE LASER TRACKING

George C. Dedes Oct. 1987 204 p

(Grant NsG-5265)

(NASA-CR-182750; NAS 1.26:182750; OSU-384) Avail: NTIS HC A10/MF A01 CSCL 22A

Simultaneous Range Differences (SRDs) to Lageos are obtained by dividing the observing stations into pairs with quasi-simultaneous observations. For each of those pairs the station with the least number of observations is identified, and at its observing epochs interpolated ranges for the alternate station are generated. The SRD observables are obtained by subtracting the actually observed laser range of the station having the least number of observations from the interpolated ranges of the alternate station. On the basis of these observables semidynamic single baseline solutions were performed. The aim of these solutions is to further develop and implement the SRD method in the real data environment, to assess its accuracy, its advantages and disadvantages as related to the range dynamic mode methods, when the baselines are the only parameters of interest. Baselines, using simultaneous laser range observations to Lageos, were also estimated through the purely geometric method. These baselines formed the standards the standards of comparison in the accuracy assessment of the SRD method when compared to that of the range dynamic mode methods. On the basis of this comparison it was concluded that for baselines of regional extent the SRD method is very effective, efficient, and at least as accurate as the range dynamic mode methods, and that on the basis of a simple orbital modeling and a limited orbit adjustment. The SRD method is

insensitive to the inconsistencies affecting the terrestrial reference frame and simultaneous adjustment of the Earth Rotation Parameters (ERPs) is not necessary. Author

N88-22053# Instituto de Pesquisas Espaciais, Sao Jose dos Campos (Brazil).
NUMERICAL ORBIT PROPAGATION METHODS FOR EARTH ARTIFICIAL SATELLITES Ph.D. Thesis [METODOS NUMERICOS EM PROPAGACAO DE ORBITA DE SATELITES ARTIFICIAIS TERRESTRES]
Helio KugaKoiti Oct. 1987 57 p In PORTUGUESE; ENGLISH summary Submitted for publication
(INPE-4405-RPE/556) Avail: NTIS HC A04/MF A01

Numerical orbit propagation for earth artificial satellites is described. The main orbital perturbations are summarized. Several formulations of the differential equations of motion as well as essential aspects of the ordinary differential equation resolution algorithms are considered. Qualitative aspects of the usual orbit propagation methods are also reviewed. Finally, an analysis of research trends from the literature is included. Author

N88-22054 Centre National d'Etudes Spatiales, Toulouse (France).
SPACECRAFT TRAJECTORIES [TRAJECTOIRES SPATIALES]
O. Zarrouati Jan. 1987 523 p In FRENCH Previously announced in IAA as A87-26851
(ISBN-2-85-428166-7; ETN-88-91803) Avail: CEPADUES-Editions, 111 rue Nicolas Vauquelin, 31100 Toulouse, France

The development and theoretical analysis of space trajectory systems for practical applications including the tracking of spacecraft for programs such as HERMES are considered. Orbital parameters and Keplerian motion, and the gravitational and nongravitational mathematical modeling of the effects of perturbations on satellites, are first discussed. Inertial reference systems; instrumentation for the measurement of distances; Doppler effects and angles; and the geometric interpretation and evaluation of micromeasurements are then considered. Finally. a discussion is presented of algorithms including linear filter, least-square, Kalman filter, and inversion methods, and of the analysis of error and covariance, with special attention given to the case of geostationary satellite orbits. ESA

14 GROUND SUPPORT SYSTEMS AND FACILITIES (SPACE)

Includes launch complexes, research and production facilities; ground support equipment, e.g., mobile transporters; and simulators.

For related information see also *09 Research and Support Facilities (Air).*

N88-22055# Army Armament Research and Development Command, Watervliet, N. Y. Weapons Lab.
LAUNCHABILITY OF BASE-DRIVEN ELECTROMAGNETIC PROJECTILES Final Report
C. G. Homan and P. M. Vottis Dec. 1987 14 p
(AD-A189635; ARCCB-MR-87036) Avail: NTIS HC A03/MF A01 CSCL 19F

The launchability of penetrator projectiles at the velocities attainable in electromagnetic (EM) launch is examined. By assuming a base-driven model, theoretical expressions are derived for the ratio of projectile mass to the mass of the penetrator core (M sub T/M sub p) as a function of the ratio (lambda) of the length of the penetrator (l) to the unsupported length of the penetrator. This analysis relates the specific strengths and densities of the penetrator and sabot materials to lambda and M sub T/M sub p. It is shown that an electromagnetic projectile made from materials used in fielded penetrators and launched with a maximum acceleration of 150,000 G's can have an unsupported length of 5 to 7.2 cm dependent on the material yield criteria used. Using conservative design criteria similar to those used in the XM829 round, we show that a projectile of 2 kg mass having a 1 kg penetrator core may be launched in the base-driven mode without exceeding material properties. GRA

N88-22056# Sandia National Labs., Albuquerque, N. Mex.
CONTINUOUS MEASUREMENTS OF IN-BORE PROJECTILE VELOCITY
J. R. Asay, C. H. Konrad, C. A. Hall, M. Shahinpoor, and R. Hickman 1988 5 p Presented at the 4th Symposium on Electromagnetic Launch Technology, Austin, Tex., 12 Apr. 1988 Prepared in cooperation with New Mexico Univ., Albuquerque and Ktech Corp., Albuquerque, N. Mex.
(Contract DE-AC04-76DP-00789)
(DE88-006841; SAND-87-2315C; CONF-880478-3) Avail: NTIS HC A02/MF A01

The application of velocity interferometry to the continuous measurement of in-bore projectile velocity in a small-bore three-stage railgun is described. These measurements are useful for determining projectile acceleration and for evaluating gun performance. The launcher employed in these studies consists of a two-stage light gas gun used to inject projectiles into a railgun for additional acceleration. Results obtained for projectile velocities to 7.4 km/s with the two-stage injector are reported and potential improvements for railgun applications are discussed. DOE

N88-22057# New Mexico Univ., Albuquerque. Dept. of Mechanical Engineering.
ANALYTIC SOLUTIONS TO DYNAMIC EQUATIONS OF PLASMA ARMATURE RAILGUNS
M. Shahinpoor and R. S. Hawke 1988 16 p Presented at the 4th Symposium on Electromagnetic Launch Technology, Austin, Tex., 12 Apr. 1988 Prepared in cooperation with Lawrence Livermore National Lab., Calif.
(Contract DE-AC04-76DP-00789)
(DE88-006842; SAND-87-2316C; CONF-880478-1) Avail: NTIS HC A03/MF A01

General governing nonlinear differential equations pertaining to the dynamic behavior of a plasma armature electromagnetic railgun are first derived. Three different cases are then considered and the corresponding governing equations are then solved exactly by means of a set of nonlinear transformations. These cases correspond to: (1) no-ablation, (2) continuous-ablation, and (3) partial-ablation for which an ablation threshold velocity v(sub t) plays a fundamental role. Corresponding to each case, a nonlinear transformation is employed to reduce the nonlinear differential equations to their equivalent linear ones and subsequently allow solution of the pertinent linear differential equations, which are second order, by means of the transition matrix technique. It is concluded that in order to achieve very high projectile velocities the projectile should be injected into the railgun at velocities higher than the ablation threshold velocity. Thus, the ablation may be completely alleviated and the ensuing turbulent drag may be significantly diminished. It is shown that under these conditions one may typically accelerate projectiles up to 30 km/s or more while without hypervelocity injection, for the same railgun and typical operating conditions, one might severely limit the maximum projectile velocity. DOE

N88-22058# Sandia National Labs., Albuquerque, N. Mex.
STRUCTURAL CONSEQUENCES OF RAILGUN AUGMENTATION
G. W. Wellman and K. W. Schuler 1988 7 p Presented at the 4th Symposium on Electromagnetic Launch Technology, Austin, Tex., 12 Apr. 1988
(Contract DE-AC04-76DP-00789)
(DE88-007036; SAND-87-2123C; CONF-880478-4) Avail: NTIS HC A02/MF A01

An augmented railgun can provide the same driving force on a projectile at a lower plasma arc current and thus less potential erosion and barrel damage as an unaugmented railgun. However, there are structural consequences to railgun augmentation which must be overcome before the advantages of lower plasma arc currents can be realized. To investigate these consequences, a

bolted V-block supporting structure is considered with two cores; unaugmented (a single pair of conducting rails), and augmented (conducting rails augmented by a second tandem set of conductors). The mechanical load on the cores consist of the static bolt preload, the plasma pressure behind the projectile, and the magnetic pressure induced by currents flowing in the rails or augmenting conductors. Assuming no current diffusion into the conductors, the magnetic pressure distribution on the conductors is determined by solving the two-dimensional magnetostatic field equations using an analogy with heat transfer. These loads are then used in a dynamic finite element structural model. The maximum rail current is found at which the unaugmented railgun can be repetitively fired without detrimental gaps forming at the bore. For the augmented railgun, at the same projectile acceleration, large permanent deformations can occur. Thus successful implementation of rail gun augmentation will require improvement of the supporting structure. DOE

15 LAUNCH VEHICLES AND SPACE VEHICLES

Includes boosters; operating problems of launch/space vehicle systems; and reusable vehicles.

For related information see also *20 Spacecraft Propulsion and Power.*

No abstracts in this category.

16 SPACE TRANSPORTATION

Includes passenger and cargo space transportation, e.g., shuttle operations; and space rescue techniques.

For related information see also *03 Air Transportation and Safety* and *18 Spacecraft Design, Testing and Performance.* For space suits see *54 Man/System Technology and Life Support.*

N88-22059# General Accounting Office, Washington, D. C.
SPACE SHUTTLE ACCIDENT: NASA'S ACTIONS TO ADDRESS THE PRESIDENTIAL COMMISSION REPORT
Oct. 1987 45 p
(PB88-135306; GAO/NSIAD-88-30BR) Avail: NTIS HC A03/MF A01 CSCL 22B

This report contains a review of NASA's actions to address the recommendations presented in the Report of the Presidential Commission on the Space Shuttle Challenger Accident, dated 6 June, 1986. It presents information contained in a briefing to representatives of the subcommittee on Space Science and Applications as well as the results of additional audit work performed. Identified were 39 specific recommendations within the 9 categories of recommendations presented in the Presidential Commission report. NASA has taken or is taking actions to address the intent of all of them. Author

N88-22060*# Martin Marietta Corp., Bethesda, Md.
ORBITAL TRANSFER VEHICLE: CONCEPT DEFINITION AND SYSTEM ANALYSIS STUDY Final Review Report
9 Dec. 1987 403 p
(Contract NAS8-36108)
(NASA-CR-179315; NAS 1.26:179315; MCR-87-2600; DR-3)
Avail: NTIS HC A18/MF A01 CSCL 22B

Previous results, the initial Orbital Transfer Vehicle (OTV) program, advanced mission, safety issues, aeroassist summary, and program summary are presented and discussed. B.G.

N88-22061# Space Data Corp., Tempe, Ariz.
ENGINEERING SUPPORT OF SPACE SHUTTLE EXPERIMENT INTEGRATION Final Report, 11 Aug. 1983 - 11 Aug. 1987
Curt Schroeder 11 Nov. 1987 15 p
(Contract F19628-83-C-0156)
(AD-A190135; SDC-TM-3309; AFGL-TR-87-0253) Avail: NTIS HC A03/MF A01 CSCL 20F

SOW Contractor Tasks: (1) Assist the AFGL CIRRIS Program Manager in coordinating the CIRRIS integration efforts of AFGL, Utah State University (USU), USU subcontractors and the Space Vehicle Integrating Contractor (SVIC); (2) Calculate the CIRRIS mass properties and electrical power requirements; (3) Develop a CIRRIS experiment drawing tree and parts list for use during testing and integration; (4) Identify shuttle documentation requirements and assist the AFGL Program Manager in originating documentation required for successful CIRRIS shuttle integration; (5) Review shuttle and SVIC documentation and regulations; determine their applicability to this experiment; (6) As required by AFGL, originate detail test plans and procedures to evaluate component and systems performance; (7) Provide engineering test support at all test sites; (8) Provide engineering field support, as required, for experiment buildup, shuttle integration, prelaunch preparation, launch recovery; (9) As required, attend technical and working group meetings between AFGL, USU, and subcontractors; (10) Data and reports in accordance with Attachment 2, DD Form 1423, dated 83APR11. GRA

17 SPACE COMM., SPACECRAFT COMM., COMMAND & TRACKING

Includes telemetry; space communications networks; astronavigation and guidance; and radio blackout.

For related information see also *04 Aircraft Communications and Navigation* and *32 Communications and Radar.*

No abstracts in this category.

18 SPACECRAFT DESIGN, TESTING AND PERFORMANCE

Includes satellites; space platforms; space stations; spacecraft systems and components such as thermal and environmental controls; and attitude controls.

For life support systems see *54 Man/System Technology and Life Support.* For related information see also *05 Aircraft Design, Testing and Performance, 39 Structural Mechanics,* and *16 Space Transportation.*

N88-22062# Atmospheric and Environmental Research, Inc., Cambridge, Mass.
BASELINE OBSERVING SYSTEM EXPERIMENTS USING THE AFGL GLOBAL DATA ASSIMILATION SYSTEM
J. F. Louis, R. N. Hoffman, T. Nehrkorn, T. Baldwin, and M. Mickelson 18 Nov. 1987 66 p
(Contract F19628-86-C-0141)
(AD-A188861; AFGL-TR-87-0327; SR-3) Avail: NTIS HC A04/MF A01 CSCL 04B

Four observing system experiments each includes one week of data assimilation during each special observing period of the FGGE year, and 3 four day forecasts, starting from the 3rd, 5th and 7th day of the assimilation periods. The first experiment (STATSAT) provides a baseline for the others and uses all the available level II-B FGGE data, except surface observations. Comparisons with the NMC level III-A analyses show that the AFGL system performs adequately. In the 2nd experiment (NOSAT) all satellite data are removed from the data set. As expected the impact on the analysis is small in the Northern Hemisphere, and large in the Southern Hemisphere. This experiment provides a measure of the sensitivity that can be expected from future experiments in which different satellite retrieval techniques are tested. The 3rd experiment (NOCON) was designed to test the

degradation of the analyses when all conventional data are denied and only satellite data are used. Differences between this and the STATSAT experiment appear first over continental areas but propagate quickly over the oceans, especially in the winter.
GRA

N88-22063# California Univ., Berkeley. Lawrence Berkeley Lab.
SUPERCONDUCTING MAGNET TECHNIQUE FOR ASTROMAG ON THE SPACE STATION
M. A. Green Sep. 1987 24 p Presented at the International Forum on Scientific Uses of the Space Station, Venice, Italy, 4 Oct. 1987
(Contract DE-AC03-76SF-00098)
(DE88-004560; LBL-23993; CONF-8710241-11) Avail: NTIS HC A03/MF A01

This paper describes superconducting magnet systems which could be used as part of a Particle Astrophysics Experiment ASTROMAG on the space station. This report deals with issues of superconductor selection (should one consider the use of high critical temperature superconductor), magnet coil and cryostat design, and the cryogenic cooling system for the superconducting magnet.
DOE

N88-22064# Air Force Inst. of Tech., Wright-Patterson AFB, Ohio. School of Engineering.
A SYSTEMS ANALYSIS OF FIRE SUPPRESSION ALTERNATIVES FOR THE US SPACE STATION M.S. Thesis
Joseph G. Sheridan Dec. 1987 105 p
(AD-A189847; AFIT/GAE/AA/87D-5) Avail: NTIS HC A06/MF A01 CSCL 22B

NASA's front line defense against fire abroad manned spacecraft has been strict control of materials, construction, and operation. This will continue with Space Station, but the inclusion of laboratory facilities and crew comfort features combined with the increasing routine-ization of space operations will increase the risk of fire. A safe, effective fire suppression system must be included. Every previous manned U.S. spacecraft has had some type of fire supression capability, but these may not be the best for the station. For example, the Space Shuttle Orbiters carry both fixed and portable Halon 1301 systems. Because of the toxicity of compounds produced when Halon 1301 reacts at high temperature with combustion products, NASA policy is to terminate the shuttle mission if a fixed system is discharged, even if the fire is extinguished.
GRA

N88-22065# California Univ., Los Angeles. School of Engineering and Applied Science.
OPTIMAL CONTROL AND IDENTIFICATION OF SPACE STRUCTURES Final Report, 15 Aug. 1984 - 14 Dec. 1987
J. S. Gibson 21 Dec. 1987 84 p
(Grant AF-AFOSR-0309-84)
(AD-A190033; AFOSR-88-0173TR) Avail: NTIS HC A05/MF A01 CSCL 22B

The focus of this research was to develop theoretical and computational tools for optimal control and adaptive parameter identification and control and adaptive parameter systems, primarily large flexible space structures. Approximation results for optimal control of infinite-dimensional systems were drived along with numerical results. Also developed was an approximation theory for discrete-time optimal regulator problems, which included problems with flexible structures as a particular example.
GRA

N88-22066# WEA, Cambridge, Mass.
WAVE PROPAGATION AND DYNAMICS OF LATTICE STRUCTURES Final Report, 1 Sep. 1985 - 30 Sep. 1987
James H. Williams, Jr. 1 Oct. 1987 40 p
(Contract F49620-85-C-0148)
(AD-A190037; AFOSR-88-0062TR) Avail: NTIS HC A03/MF A01 CSCL 22B

One of the most attractive structural configurations for large space structures (LSS) for outer space applications is the repetitive lattice concept. Achieving the operational requirements of such structures will necessitate considerable knowledge of the dynamics, control, materials and nondestructive evaluation (NDE) of these structural systems. Wave propagation analyses provide potentially valuable perspectives from which to consider this broad range of analysis, design and synthesis issues. The theoretical and experimental results of a two-year research program on the wave propagation and dynamics of LSS are briefly reviewed. Potential benefits of wave propagation analyses in the vibration, parameter identification, dynamic failure, control and NDE of lattice structures have been identified and are summarized in this report.
GRA

N88-22067# TCS, Inc., San Diego, Calif.
REAL-TIME STRESSED CHANNEL SIMULATOR Final Report
10 Dec. 1987 74 p
(Contract N00014-87-C-0133)
(AD-A190223; TCS-TP-87-059) Avail: NTIS HC A04/MF A01 CSCL 15C

SDI research is directed at a number of system architecture options involving space, airborne, and terrestrial platforms. A major consideration in the system architecture is the resolution of the battle management (BM) concept. To resolve the many complex issues, the Strategic Defense Initiative Organization (SDIO) has recognized the need for communication, command, and control (C3) data links between the various platforms. The link or communication channel conditions are relatively benign during peacetime; however, in wartime situations, during pre-, trans-, and post-attack periods, the channel conditions degrade rapidly causing severe disruptions in C3. The approaches to battle management, as they are tailored to the various architecture options being considered, will depend heavily on communications link integrity. This research is significant and timely in that it relates to the National Test Bed (NTB), in support of the SDI full-state development decision process. The NTB program is presently being undertaken by major contractors and invloves the design, development, and installation of both experimental and simulation capabilities to form the NTB. The Phase 1 research takes a major step in configuring a Real-Time Stressed Channel Simulator (RTSCS) to evaluate BM/C3 concepts for the SDI program.
GRA

N88-22068# Department of the Air Force, Washington, D.C. Directorate of Studies and Analysis.
FEEDBACK CONTROL OF DISTRIBUTED PARAMETER SYSTEMS WITH APPLICATIONS TO LARGE SPACE STRUCTURES Final Progress Report, 28 Dec. 1983 - 1 Sep. 1987
Mark J. Balas 15 Oct. 1987 27 p
(Grant AF-AFOSR-0124-83)
(AD-A190536; AFOSR-87-2034TR) Avail: NTIS HC A03/MF A01 CSCL 22B

Large space structures exhibit distributed parameter behavior in their dynamics and thus must be described on infinite-dimensional state-spaces. However, the controller algorithm must be finite-dimensional to be implemented. The focus of this research has been to make finite-dimensional approximations of infinite-dimensional controllers which stabilize the distributed parameter system. The investigator has shown conditions under which Galerkin approximation schemes can yield finite-dimensional stabilizing controllers for linear distributed parameter systems.
GRA

N88-22069# WEA, Cambridge, Mass.
WAVE PROPAGATION AND DYNAMICS OF LATTICE STRUCTURES Final Report, 1 Sep. 1985 - 30 Sep. 1987
James H. Williams, Jr. 1 Oct. 1987 8 p
(Contract F49620-85-C-0148)
(AD-A190611; AFOSR-87-1777TR) Avail: NTIS HC A02/MF A01 CSCL 22B

One of the most attractive structural configurations for large space structures (LSS) for outer space applications is the repetitive lattice concept. Achieving the operational requirements of such structures will necessitate considerable knowledge of the dynamics, control, materials and nondestructive evaluation (NDE) of these

structural systems. Wave propagation analyses provide potentially valuable perspectives from which to consider this broad range of analysis, design and synthesis issues. The theoretical and experimental results of a two-year research program on the wave propagation and dynamics of LSS are briefly reviewed. Potential benefits to wave propagation analyses in the vibration, parameter identification, dynamic failure, control and NDE of lattice structures have been identified and are summarized in this report. GRA

N88-22070# Clarkson Univ., Potsdam, N.Y.
NONLINEAR ANALYSIS AND OPTIMAL DESIGN OF DYNAMIC MECHANICAL SYSTEMS FOR SPACECRAFT APPLICATION Final Technical Report, 1 Feb. 1984 - 31 Jul. 1987
K. D. Willmert and M. Sathyamoorthy Sep. 1987 103 p
(Grant AF-AFOSR-0076-84)
(AD-A190644; AFOSR-87-2008TR) Avail: NTIS HC A06/MF A01 CSCL 22B

Analysis and optimal design procedures for planar as well as spatial mechanisms frequently used in space structures are developed. A nonlinear finite element procedure, developed originally for planar mechanisms during the initial stages of this research, has been modified considerably to handle complex mechanisms with sliding masses and mechanisms operating at relatively high speeds. The analysis takes into account the effects of geometric and material nonlinearities, vibrational effects and coupling of deformations. Numerical results have been reported for certain mechanism examples. The effects of nonlinearities on the dynamic behavior of mechanisms are significant. Considerable progress has been made in developing a nonlinear finite element procedure for 3-D mechanisms. Numerical results obtained for some example problems show the validity of the current 3-D formulation. A new optimization algorithm has also been developed based on the Gauss method to handle various types of nonlinear constraints with the goal of reducing the number of analyses required to obtain and optimal design. Details of the nonlinear finite element procedures as well as the optimization technique are available in published papers, copies of which are included. goal of reducing the number of analyses required to obtain an optimal design. Complete details of the nonlinear finite element procedures as well as the optimization technique are available in published papers, copies of which are included here in the Appendix. GRA

N88-22071# Air Force Inst. of Tech., Wright-Patterson AFB, Ohio. School of Engineering.
MOVING-BANK MULTIPLE MODEL ADAPTIVE ESTIMATION APPLIED TO FLEXIBLE SPACESTRUCTURE CONTROL M.S. Thesis
Robert W. Lashlee, Jr. Dec. 1987 231 p
(AD-A190761; AFIT/GE/ENG/87D-36) Avail: NTIS HC A11/MF A01 CSCL 22D

This investigation focused on the use of moving-bank multiple model adaptive estimation and control (MMAE). Moving-bank MMAE reduces the computational burden of MMAE by implementing only a subset of the Kalman filters (9 filters versus 100 in this research) that are necessary to describe the system to be estimated/controlled. Important to the development of the moving-bank MMAE are the decision logics governing the selection of the subset of filters. The decision logics cover three situations: initial acquisition of unknown parameter values; tracking unknown parameter values; and reacquisition of the unknown parameters following a jump change in these parameter values. This thesis applied moving-bank MMAE to a rotating two bay truss model of a flexible spacestructure. The rotating two bay truss approximated a space structure that had a hub with appendages extending from the structure. The mass of the hub was large relative to the mass of the appendage. The mathematical model was developed using finite element analysis, transformed into modal formulation, and reduced using a method referred to as singular perturbations. Multiple models were developed by assuming that variation occurred in the mass and stiffness of the structure. GRA

N88-22072*# National Aeronautics and Space Administration. Langley Research Center, Hampton, Va.
INVESTIGATION OF SUPER*ZIP SEPARATION JOINT
Laurence J. Bement and Morry L. Schimmel (Schimmel Co., Saint Louis, Mo.) May 1988 35 p Presented at the 1987 Annual Meeting, Pyrotechnics and Explosive Applications Section, American Defense Preparedness Association, Pasadena, Calif. 20-22 Oct. 1987
(NASA-TM-4031; L-16398; NAS 1.15:4031) Avail: NTIS HC A03/MF A01 CSCL 22B

An investigation to determine the most likely cause of two failures of five tests on 79 inch diameter Lockheed Super*Zip spacecraft separation joints being used for the development of a Shuttle/Centaur propulsion system. This joint utilizes an explosively expanded tube to fracture surrounding prenotched aluminum plates to achieve planar separation. A test method was developed and more than 300 tests firings were made to provide an understanding of severance mechanisms and the functional performance effects of system variables. An approach for defining functional margin was developed, and specific recommendations were made for improving existing and future systems. Author

N88-22073# Office National d'Etudes et de Recherches Aerospatiales, Paris (France). Direction de la Physique Generale.
STUDY OF SURFACE DISCHARGES Final Report [ETUDE DES DECHARGES DE SURFACE]
J. P. Marque, E. Faure, M. P. Cals, J. P. Boyer, S. Larigaldie, and F. Boulanger Jul. 1987 101 p In FRENCH
(Contract DRET-86-001)
(ONERA-12/7236-PY; ETN-88-91989) Avail: NTIS HC A06/MF A01 CSCL 22B

The degeneration and propagation of surface discharges were studied including the very low pressure discharges appearing on synchronous orbit spacecraft and return wave discharges. In the first case, a model representing the discharge is presented and the means to measure the dielectric charge profiles are discussed. In the second case experimental results measuring the evolution of the return wave are presented. Capacitor sensors were used to study the space-time potential distribution in the return arc. It is shown that local geometry largely determines the threshold level. ESA

N88-22074# Centre National d'Etudes Spatiales, Toulouse (France). Centre Spatial.
IDENTIFICATION OF A STAR FIELD FROM A SPINNING SATELLITE [IDENTIFICATION D'UN CHAMP D'ETOILES A BORD D'UN SATELLITE EN ROTATION]
Marcel Lamboley Dec. 1987 67 p In FRENCH; ENGLISH summary
(CNES-NT-120; ETN-88-92026) Avail: NTIS HC A04/MF A01

An algorithm for star identification on board a spinning satellite is described and the resources necessary for its implementation are assessed. The means required are a star tracker, a star catalog, random access memory and a processing unit. The study is based on the SED12 star tracker. Simulations on ground computers are planned. The algorithm on board a spinning satellite could make it autonomous. ESA

N88-22224# Joint Publications Research Service, Arlington, Va.
JAPANESE SPACE STATION MODULE
Akira B. Sawaoka *In its* JPRS Report: Science and Technology. Japan 3 Mar. 1988 p 30-31 Transl. into ENGLISH from Ceramics Japan (Tokyo, Japan), Apr. 1987 p 297-302 (For primary document see N88-22218 15-31)
Avail: NTIS HC A05/MF A01

19 SPACECRAFT INSTRUMENTATION

For related information see also *06 Aircraft Instrumentation* and *35 Instrumentation and Photography.*

No abstracts in this category.

20 SPACECRAFT PROPULSION AND POWER

Includes main propulsion systems and components, e.g., rocket engines; and spacecraft auxilliary power sources.

For related information see also *07 Aircraft Propulsion and Power, 28 Propellants and Fuels, 44 Energy Production and Conversion,* and *15 Launch Vehicles and Space Vehicles.*

N88-22075# Oak Ridge National Lab., Tenn.
THERMAL ANALYSIS OF HEAT STORAGE CANISTERS FOR A SOLAR DYNAMIC, SPACE POWER SYSTEM
R. P. Wichner, A. D. Solomon, J. B. Drake, and P. T. Williams 1988 11 p Presented at the 10th Annual American Society of Mechanical Engineers Solar Energy Conference, Denver, Colo., 10 Apr. 1988
(Contract DE-AC05-84OR-21400)
(DE88-004199; CONF-880457-2) Avail: NTIS HC A03

A thermal analysis was performed of a thermal energy storage canister of a type suggested for use in a solar receiver for an orbiting Brayton cycle power system. Energy storage for the eclipse portion of the cycle is provided by the latent heat of a eutectic mixture of LiF and CaF2 contained in the canister. The chief motivation for the study is the prediction of vapor void effects on temperature profiles and the identification of possible differences between ground test data and projected behavior in microgravity. The first phase of this study is based on a two-dimensional, cylindrical coordinates model using an interim procedure for describing void behavior in 1-g and microgravity. The thermal analysis includes the effects of solidification front behavior, conduction in liquid/solid salt and canister materials, void growth and shrinkage, radiant heat transfer across the void, and convection in the melt due to Marangoni-induced flow and, in 1-g, flow due to density gradients. A number of significant differences between 1-g and 0-g behavior were found. This resulted from differences in void location relative to the maximum heat flux and a significantly smaller effective conductance in 0-g due to the absence of gravity-induced convection. DOE

N88-22076# Air Force Inst. of Tech., Wright-Patterson AFB, Ohio.
AN EXPERIMENTAL INVESTIGATION OF ROCKET RAMJET NOZZLE ASSEMBLY BASE PRESSURES M.S. Thesis
Timothy R. Wesling Dec. 1987 153 p
(AD-A189714; AFIT/GA/AA/87D-9) Avail: NTIS HC A08/MF A01 CSCL 21H

This study investigated base pressures of clustered rocket-ramjet nozzles under shrouded and unshrouded conditions. Twelve combinations of expansion ratios and shrouds for rocket-ramjet nozzle clusters in cold flow were investigated. Pressure measurements were made along the base of the rocket-ramjet cluster under simulated altitude conditions ranging up to 70,000 feet and flight Mach numbers to just over 3.0. Comparisons were made of the effects on nozzle base pressures of altitude, ramjet plenum pressure, nozzle geometry and shrouding. A potential increase in base pressure thrust of certain nozzle geometries is shown to be possible. As the ramjet nozzle exit distance from there centerline of the nozzle assembly increases for unshrouded cases, base pressure thrust also increases. This appears to be due to recirculation of exhaust gases. These appear to be variations in performance caused by changes in the distance of the shroud from the nozzle assembly centerline. Also, there is a pressure gradient between nozzles in the base region which is affected by configuration and which has an important effect on evaluating base pressures. GRA

N88-22077# Air Force Inst. of Tech., Wright-Patterson AFB, Ohio. School of Engineering.
EXPERIMENTAL INVESTIGATION OF TWO-DIMENSIONAL CONFINED JET THRUST VECTOR CONTROL M.S. Thesis
Timothy A. Talda Dec. 1987 135 p
(AD-A189845; AFIT/GAE/AA/87D-22) Avail: NTIS HC A07/MF A01 CSCL 21H

Different types of thrust vector control systems are described, and a comparison of present systems is presented. Confined jet thrust vector control is shown to be an effective alternative. A two-dimensional nozzle that operates as a confined jet thrust vector control nozzle is experimentally demonstrated. Effects of changing geometric variables and inputs on ease of vectoring and performance of vectored thrust are analyzed. Schlieren photographs and movies show flow characteristics. Predictions of performance of operable nozzles are made based on results found in the experiments. Recommendations for further study are made. GRA

N88-22078# Air Force Astrophysics Lab., Edwards AFB, Calif.
DURABILITY TESTING OF AN IRIDIUM-PLATED STORABLE ROCKET ENGINE INJECTOR Special Report, Sep. 1986 - Mar. 1987
Kevin R. Benson Sep. 1987 29 p
(AD-A190707; AFAL-TR-87-061) Avail: NTIS HC A03/MF A01 CSCL 21H

A series of hot firings were conducted at the Air Force Astronautics Lab. to evaluate the durability of an iridium plated, like-doublet, storable rocket engine injector. The injector was designed for N2O4/MMH propellants and a chamber pressure of 1500 psia. Iridium plating failed to protect the injector face; however, valuable insights into the attack mechanism were gained. This report presents the results of AFAL's testing, including the analysis and evaluation of the injector orifice corrosion/erosion. GRA

N88-22079# Ogden Air Logistics Center, Hill AFB, Utah. Propellant Analysis Lab.
LGM-30B STAGE 2 DISECTED MOTOR TEST REPORT
Oct. 1987 114 p
(AD-A190771; MAQCP-NR-528(87)) Avail: NTIS HC A06/MF A01 CSCL 21I

Data in this report represent the second testing of Motor 0022687 with conditioning. Additional unconditioned specimens were tested so that data could be related to previously tested unconditioned specimens. Data points are shown on multi-motor plots previously published. These plots are for visual reference only. Effects of conditioning are noticeable in almost all tests and relationship to other test periods shows marked differences. No effort has been made to evaluate statistical significance. GRA

N88-22080*# National Aeronautics and Space Administration. Lewis Research Center, Cleveland, Ohio.
RAY TRACING OPTICAL ANALYSIS OF OFFSET SOLAR COLLECTOR FOR SPACE STATION SOLAR DYNAMIC SYSTEM
Kent S. Jefferies [1988] 20 p Prepared for presentation at the 23rd Intersociety Energy Conversion Engineering Conference, Denver, Colo., 31 Jul. - 5 Aug. 1988; sponsored in part by ASME, AIAA, ANS, SAE, IEEE, ACS, and AIChE
(NASA-TM-100853; E-4056; NAS 1.15:100853) Avail: NTIS HC A03/MF A01 CSCL 10A

OFFSET, a detailed ray tracing computer code, was developed at NASA Lewis Research Center to model the offset solar collector for the Space Station solar dynamic electric power system. This model traces rays from 50 points on the face of the Sun to 10 points on each of the 456 collector facets. The triangular facets are modeled with spherical, parabolic, or toroidal reflective surface contour and surface slope errors. The rays are then traced through the receiver aperture to the walls of the receiver. Images of the

collector and of the Sun within the receiver produced by this code provide insight into the collector receiver interface. Flux distribution on the receiver walls, plotted by this code, is improved by a combination of changes to aperture location and receiver tilt angle. Power loss by spillage at the receiver aperture is computed and is considerably reduced by using toroidal facets. Author

N88-22242# Joint Publications Research Service, Arlington, Va.
SPLIT-COEFFICIENT MATRIX SOLUTION AND EXPERIMENTAL STUDY OF AXISYMMETRIC UNDEREXPANDED EXHAUST PLUMES Abstract Only
Zuyuan Xie *In its* JPRS Report: Science and Technology. China 11 Dec. 1987 p 58 Transl. into ENGLISH from Kongqidonglixue Xuebao (Mianyang, Peoples Republic of China), v. 5, no. 3, Sep. 1987 p 226-234 Original language document was announced in IAA as A88-14015 (For primary document see N88-22233 15-31)
Avail: NTIS HC A06/MF A01

N88-22398*# Sverdrup Technology, Inc., Cleveland, Ohio.
STRUCTURAL TAILORING OF HIGH-SPEED TURBINE BLADES (SSME/STAEBL)
Robert Rubinstein *In* NASA. Lewis Research Center, Lewis Structures Technology, 1988. Volume 2: Structural Mechanics May 1988 p 183-188 (For primary document see N88-22382 15-39)
Avail: NTIS HC A14/MF A01 CSCL 21H

N88-22404*# National Aeronautics and Space Administration. Lewis Research Center, Cleveland, Ohio.
THERMAL-STRUCTURAL ANALYSES OF SPACE SHUTTLE MAIN ENGINE (SSME) HOT SECTION COMPONENTS
Ali Abdul-Aziz (Sverdrup Technology, Inc., Cleveland, Ohio.) and Robert L. Thompson *In its* Lewis Structures Technology, 1988. Volume 2: Structural Mechanics May 1988 p 255-264 (For primary document see N88-22382 15-39)
Avail: NTIS HC A14/MF A01 CSCL 21H

23 CHEMISTRY AND MATERIALS (GENERAL)

N88-22081# Atomic Energy Research Establishment, Harwell (England). Materials Engineering Centre.
HIGH TEMPERATURE MATERIALS: WHAT'S AVAILABLE
D. M. Dawson May 1987 22 p
(AERE-R-12632; HL87/1155) Avail: NTIS HC A03/MF A01

Over the last 10 years there was an enormous increase in the number of new and improved engineering materials coming onto the market place. The currently available materials systems are identified and compared. Their capabilities for applications at elevated temperatures (taken, for the purpose of this presentation, to be above 200 C) are illustrated. An overview of the strength of the categories of materials are provided as a function of temperature. A brief indication of the areas where developments can be expected in the near future is also indicated. Author

N88-22082# California Univ., Berkeley. Lawrence Berkeley Lab.
THE CONTRIBUTION OF ELECTRON MICROSCOPY OF MATERIALS SCIENCE TO SOCIETY
G. Thomas Aug. 1987 26 p Presented at the Philips Symposium, Eindhoven, Netherlands, 24 Sep. 1987
(Contract DE-AC03-76SF-00098)
(DE88-006341; LBL-24049; CONF-8709239-1) Avail: NTIS HC A03

The examples discussed are just a few of very many that could be used to illustrate the impact of electron microscopy in materials upon society. Electron microscopy, materials science and engineering represent classic examples of demanding and interdisciplinary team efforts. While in its early days, electron microscopy was mainly used as a sort of forensic tool to understand existing problems, it is now becoming more and more used in the development and design of new or improved materials required for advanced systems - to conserve energy and materials. Over a century ago, H. C. Sorby was the first scientist to develop the use of thin sections of minerals for optical microscopy. Today we use 1000 times thinner sections in order to resolve the atomic arrangements in powerful electron microscopes, at the surfaces, interfaces and inside crystal grains. Materials science and engineering cannot progress without the electron microscope.
DOE

24 COMPOSITE MATERIALS

Includes physical, chemical, and mechanical properties of laminates and other composite materials.
For ceramic materials see *27 Nonmetallic Materials.*

N88-22083# Illinois Univ., Urbana. Dept. of Civil Engineering.
CEMENT PASTE MATRIX COMPOSITE MATERIALS CENTER Annual Report No. 1, 29 Oct. 1986 - 29 Oct. 1987
J. F. Young and R. L. Berger Oct. 1987 16 p
(Contract F49620-87-C-0023)
(AD-A188657; AFOSR-87-1902TR) Avail: NTIS HC A03/MF A01 CSCL 11D

The report describes the first year implementation of the Center for Excellence on Cement Paste Matrix Composite Materials. Topics include organization and administration, equipment acquisitions, personnel and the development of a comprehensive research program. Preliminary results on projects involving processing of MDF cements and the electrical properties of DSP cements are presented. GRA

N88-22084# Lawrence Livermore National Lab., Calif.
THE COMBUSTION SYNTHESIS OF BORIDE COMPOSITES
D. C. Halverson, B. Y. Lum, and Z. A. Munir Oct. 1987 11 p Presented at the Symposium on High-Temperature Materials Chemistry, Honolulu, Hawaii, 18 Oct. 1987 Prepared in cooperation with California Univ., Davis.
(Contract W-7405-eng-48)
(DE88-005474; UCRL-96861; CONF-8710216-3) Avail: NTIS HC A03/MF A01

We have investigated the combustion synthesis process as a means of producing hard, tough, lightweight B sub 4 C/TiB sub 2 composites. We based our experimental program on thermodynamic calculations. Adiabatic temperatures and product compositions were determined on the basis of the stoichiometry and initial temperature of the reactants. For lightweight products the composition must be relatively rich in the B sub 4 C component. We found that B sub 4 C-rich composites could only be obtained by increasing the initial temperature of the reactants. The product is a hard, porous material whose toughness should be enhanced by filling the pores with aluminum using a liquid-metal infiltration process. DOE

N88-22085# Michigan Univ., Ann Arbor. Dept. of Materials Science and Engineering.
SUPERPLASTIC FLOW OF MULLITE-ZIRCONIA COMPOSITES
C. K. Yoon and I.-Wei Chen 1987 14 p Presented at the 1st International Workshop on Mullite, Tokyo, Japan, 9 Nov. 1987
(Contract DE-FG02-87ER-45302)
(DE88-005905; CONF-871189-2) Avail: NTIS HC A03/MF A01

Mullite-zirconia composites containing up to 50 v/o mullite have been superplastically deformed to large strains at relatively low temperatures and stresses. These composites can be sintered at 1400 C and have very fine grain sizes. At 1350 C, the flow stress of a composite containing 50 v/o mullite was 62 MPa at a strain rate of 0.001/s. The strain rate sensitivity is higher than 0.6 in the regime 2 and the grain size sensitivity is 3. The mullite grains behave like hard inclusions in a superplastic Y-TZP matrix. While a threshold stress was found at lower strain rates in regime 1,

regime 3 behavior was not apparent up to the highest strain rate tested of 0.007/s. DOE

N88-22086# Edgerton, Germeshausen and Grier, Inc., Idaho Falls, Idaho.
MICROPLASTICITY PHENOMENA IN GRAPHITE/MAGNESIUM METAL MATRIX COMPOSITES
J. S. Epstein, S. Rawal, and M. Misra 1987 7 p Presented at the SPIE International Conference on Photomechanics and Speckle Metrology, San Diego, Calif., 17 Aug. 1987 Prepared in cooperation with Martin Marietta Aerospace, Denver, Colo.
(Contract DE-AC07-76ID-01570)
(DE88-006772; EGG-M-02087; CONF-8708213-2) Avail: NTIS HC A02/MF A01

This paper discusses localized matrix plasticity in a Pitch 55 graphite/magnesium (Gr/Mg) metal matrix composite (MMC) due to damping/hysteresis effects in bending. It was found that for this material system, chosen mainly for its damping ability, plasticity or permanent deformation occurs in the matrix material of the composite from relatively small structural deformations. Hysteresis loops were determined on a local level in the diffusion bond region between adjacent graphite fiber bundles as well as on the free edge of the magnesium face sheet of the composite. Moire interferometry was combined with research on the microstructure of this particular material system to yield these subtle results. DOE

N88-22087# Army Lab. Command, Watertown, Mass. Material Technology Lab.
STRUCTURE AND SURFACE CHARACTERIZATIONS OF HIGH STRENGTH CARBON FIBERS Final Report
Sin S. Lin and Pearl W. Yip Sep. 1987 21 p
(AD-A189642; MTL-TR-87-49) Avail: NTIS HC A03/MF A01 CSCL 11D

Six commercial carbon fibers are characterized by X-ray diffraction, scanning electron microscopy (SEM) and X-ray photoelectron spectroscopy (XPS), or Electron Spectroscopy for Chemical Analysis (ESCA). Physical, structural, and surface parameters required to describe major properties of carbon fibers are examined and discussed. The correlation of these parameters is essential for developing optimizing and desired carbon composite materials. GRA

N88-22088# Texas A&M Univ., College Station. Mechanics and Materials Center.
DAMAGE MODELS FOR DELAMINATION AND TRANSVERSE FRACTURE Final Technical Report, 15 Feb. 1984 - 14 Jun. 1987
Richard A. Schapery, Douglas P. Goetz, and Mark J. Lamborn Aug. 1987 85 p
(Grant AF-AFOSR-0068-84)
(AD-A189652; MM-5034-87-11; AFOSR-88-0129TR) Avail: NTIS HC A05/MF A01 CSCL 11D

Theoretical and experimental work on the deformation and fracture of fibrous composites with distributed damage is described. Emphasis is on establishing the existence of potentials analogous to strain energy and on using these so called work potentials in deformation and fracture studies. The difference between changing damage and constant damage processes is accounted for by using multivalued work potentials. Discussed first are investigations of flat rectangular bar specimens and thin walled tubes under axial and torsional loading. The limited amount of experimental data presently available on angle ply laminates confirms the existence of a potential even when there are large increases in microcracking. Next, path independence of the J integral is discussed. A study is then described in which the J integral is used to determine fracture energy for delamination in double-cantilevered beam specimens, some of which have a large percentage of off-axis fibers; the results are compared with fracture energies found by standard methods (which do not account for effects of distributed damage). GRA

N88-22089# Air Force Inst. of Tech., Wright-Patterson AFB, Ohio. School of Engineering.
FRACTURE TOUGHNESS TESTING OF A CERAMIC MATRIX COMPOSITE M.S. Thesis
Robert P. Vozzola Dec. 1987 105 p
(AD-A189846; AFIT/GAE/AA/87D-24) Avail: NTIS HC A06/MF A01 CSCL 11B

The need for an accurate fracture toughness testing technique for fiber reinforced ceramic composites was identified. A technique was developed to measure small crack mouth displacements over small gauge lengths of small glass-ceramic composite specimens during loading. The technique was applied to Mode 2 crack propagation. A loading fixture capable of exerting and measuring small loads was developed. A technique to measure compliances in small composite specimens was perfected. The validity of using a laser based interferometric technique to determine the instant of crack initiation was studied. Finally, the Mode 2 critical strain energy release rate of interlaminar delamination growth was evaluated. Sample results for a 1723 glass matrix, silicon carbide fiber composite are included and recommendations for further study are described. GRA

N88-22090# Utah Univ., Salt Lake City. Dept. of Mechanical and Industrial Engineering.
AN INVESTIGATION OF THE FAILURE RESPONSE OF LAMINATES UNDER BIAXIAL STRESS Final Report, 1 Apr. 1986 - 31 Mar. 1987
Stephen R. Swanson Sep. 1987 34 p
(Grant AF AFOSR-0115-86)
(AD-A190039; AFOSR-88-0194TR) Avail: NTIS HC A03/MF A01 CSCL 11D

Advanced fiber composites are often used in laminate form in strength critical applications. However the ultimate strength of laminates is very poorly understood, primarily because of a lack of valid experimental data. A biaxial test specimen for laminates based on a tubular geometry was developed and used to determine the failure mechanics of two laminates. The results showed a failure process that includes matrix cracking, but this matrix cracking does not appear to directly affect fiber failure. Fiber failure in the laminate studied determines ultimate strength, and can be predicted based on either a maximum fiber stress of fiber strain criterion applied on a ply level. GRA

N88-22091# Army Lab. Command, Watertown, Mass. Material Technology Lab.
DRILLING METAL MATRIX COMPOSITES Final Report
William S. Ricci, Stacy E. Swider, and Thomas J. Moores Jan. 1988 21 p
(AD-A190480; MTL-TR-11-1) Avail: NTIS HC A03/MF A01 CSCL 11D

Polycrystalline diamond (PCD) tipped twist and spade drills, diamond plated twist and core drills, and the abrasive waterjet hole cutting process were evaluated for drilling aluminum metal matrix composites reinforced with SiC fibers or particulates. The diamond tipped twist drills outperformed all other drills. Core drills were found to be viable alternatives for the production of larger holes in high volume fraction composites. Plated twist drills were viable alternatives for low volume fraction particulate reinforced composites. Spade drills failed due to low edge strength. Abrasive waterjet hole cutting was successful for rough, large diameter hole cutting. Recommended drilling parameters are listed for all of the above techniques. The failure of diamond coated drills used on metal matrix composites was found to have been due to diamond glazing by the hard and abrasive reinforcement material and loading by the soft metallic matrix. It was determined that the machinability cutting rate of metal matrix composites can be predicted by using the rule of mixtures and machinability data for the individual components of a composite. GRA

N88-22092# Air Force Inst. of Tech., Wright-Patterson AFB, Ohio. School of Engineering.
A STUDY OF DAMAGE TOLERANCE IN CURVED COMPOSITE PANELS M.S. Thesis

Brendan L. Wilder Mar. 1988 152 p
(AD-A190617; AFIT/GA/AA/88M-3) Avail: NTIS HC A08/MF A01 CSCL 11D

As more and more composite materials are used in modern aircraft construction, the understanding of the damage tolerance of this relatively stiff, brittle, anisotropic material becomes important to designers. The behavior of a cylindrical composite panel made of AS4/3501-6 graphite/epoxy with ply orientations is investigated. Abrasion and burn surface damage was physically modeled in the panels. The panels were then tested by compressively loading them and a comparison was made to buckling predictions obtained. These tests indicated that panels which have suffered minor surface damage do not deviate significantly from buckling predictions. Composite laminates subjected to a low speed impact, such as a dropped tool or a manufacturing load, often develop an internal delamination. Since curved panels are 3-dimensional, and buckling is a non-linear phenomenon, the compressive load which will cause curved panels to become unstable is extremely hard to predict analytically. A technique whereby the local buckling loads at the delamination may be predicted using a 2-D model with a plane strain correction is presented. GRA

N88-22093# Michigan State Univ., East Lansing. Coll. of Engineering.
INTERFACIAL STRUCTURE-PROPERTY RELATIONSHIPS AT THE FIBER-MATRIX INTERPHASE IN ADVANCED COMPOSITES Final Report, 1 Sep. 1986 - 30 Sep. 1987
Lawrence T. Drzal 30 Sep. 1987 7 p
(Grant AF-AFOSR-0286-86)
(AD-A190649; AFOSR-87-1780TR) Avail: NTIS HC A02/MF A01 CSCL 11D

Interfacial structure property relationships at the fiber matrix interphase in advanced composite materials are discussed. This grant approved under the DOD University Research Instrumentation Grant Program was used to partially fund the purchase of surface spectroscopy equipment. The report contains the listings and descriptions of equipment actually acquired, a summary of research projects on which the equipment will be used, and other research work of interest to DOD for which this equipment will be used. GRA

N88-22094# Pacific Northwest Labs., Richland, Wash.
SPECIMEN PREPARATION TECHNIQUES FOR THE EXAMINATION OF CERAMIC AND METAL-MATRIX COMPOSITES
N. T. Saenz, D. H. Parks, C. A. Lavender, and M. T. Smith Sep. 1987 13 p Presented at the ASM International Composite Session, Cincinnati, Ohio, 13 Oct. 1987
(Contract DE-AC06-76RL-01830)
(DE88-005157; PNL-SA-15115; CONF-8710253-1) Avail: NTIS HC A03/MF A01

The need for stronger and lighter materials in industry and government has opened the door for many material applications of composite materials. With the emergence of ceramic and metal-matrix composites, new specimen preparation techniques are required to address the problems of polishing materials with varying mechanical and physical properties. Concerns about edge retention, interfacial flatness between microstructural constituents, polishing deformities or artifacts must be handled appropriately for an accurate microstructural analysis to be possible. The techniques developed specifically for composite materials will show differences in specimen preparation and polishing procedures, and illustrate how these adjustments have been successful in alleviating the problems mentioned. With the use of light optical microscopy in conjunction with other analytical methods, such as scanning electron microscopy and/or electron microprobe, a more complete picture of material analysis can be performed. DOE

N88-22095# Los Alamos National Lab., N. Mex.
MICROWAVE SINTERING OF ALUMINA-SIC COMPOSITES AT 2.45 AND 60 GHz
J. D. Katz, R. D. Blake, and J. J. Petrovic 1988 24 p Presented at the Conference on Composite Materials and Structures, Cocoa Beach, Fla., 20 Jan. 1988
(Contract W-7405-eng-36)
(DE88-006455; LA-UR-88-597; CONF-880118-2) Avail: NTIS HC A03

Composites of alumina-10 vol percent silicon carbide whiskers were sintered to 70 percent of theoretical density using both 2.45 and 60 GHz microwave radiation. Further densification was inhibited by formation of a constrained network of whiskers. Alumina-10 vol percent silicon carbide platelet composites were sintered to 94 percent of theoretical density with 2.45 GHz microwaves in less than 20 minutes. DOE

N88-22096*# Utah Univ., Salt Lake City.
FRACTOGRAPHY OF COMPOSITE DELAMINATION Progress Report, 1 Oct. 1987 - 15 Apr. 1988
23 May 1988 18 p
(Grant NAG1-705)
(NASA-CR-182757; NAS 1.26:182757) Avail: NTIS HC A03/MF A01 CSCL 11D

Studies were made of the fractography of mode 2 delamination and the impact damage of carbon fiber reinforced polymer composites. Laminates fractured under mode 2 loading were potted in a clear epoxy polymer, sectioned and polished and examined using transmission and reflection light microscopy. There were only occasional fibers bridging the mode 2 cracks. These cracks were not always visible probably because the crack opening displacement was too small as to be resolved using light microscopy. A study was made of the effect of repetitive impacts on laminates of AS4/3501-6 and IM6/3501-6. Plots of cumulative impact energy vs cumulative absorbed energy exhibited a sharp change in slope which corresponded to the damage area reaching the edges of the specimen. The initial slope was highly reproducible for both composite materials. On the other hand, the intersection point between the two slopes, where the damage area reaches the specimen edges, was highly variable between specimens. This variability is tentatively ascribed to differences in laminate quality. Author

N88-22097*# National Aeronautics and Space Administration. Langley Research Center, Hampton, Va.
INTERLAMINAR FRACTURE TOUGHNESS OF THERMOPLASTIC COMPOSITES
J. A. Hinkley, N. J. Johnston, and T. K. OBrien Feb. 1988 33 p
(NASA-TM-100532; NAS 1.15:100532; USAAVSCOM-TM-88-B-002) Avail: NTIS HC A03/MF A01 CSCL 11D

Edge delamination tension and double cantilever beam tests were used to characterize the interlaminar fracture toughness of continuous graphite-fiber composites made from experimental thermoplastic polyimides and a model thermoplastic. Residual thermal stresses, known to be significant in materials processed at high temperatures, were included in the edge delamination calculations. In the model thermoplastic system (polycarbonate matrix), surface properties of the graphite fiber were shown to be significant. Critical strain energy release rates for two different fibers having similar nominal tensile properties differed by 30 to 60 percent. The reason for the difference is not clear. Interlaminar toughness values for the thermoplastic polyimide composites (LARC-TPI and polyimidesulfone) were 3 to 4 in-lb/sq in. Scanning electron micrographs of the EDT fracture surfaces suggest poor fiber/matrix bonding. Residual thermal stresses account for up to 32 percent of the strain energy release in composites made from these high-temperature resins. Author

N88-22098*# California Inst. of Tech., Pasadena. Flight Sciences Lab.
POSTBUCKLING DELAMINATION OF A STIFFENED COMPOSITE PANEL USING FINITE ELEMENT METHODS
S. Natsiavas, C. D. Babcock, and W. G. Knauss Aug. 1987 20 p
(Grant NsG-1483)

(NASA-CR-182803; NAS 1.26:182803; GALCIT-SM-87-19) Avail: NTIS HC A03/MF A01 CSCL 11D

A combined numerical and experimental study is carried out for the postbuckling behavior of a stiffened composite panel. The panel is rectangular and is subjected to static in-plane compression on two opposite edges to the collapse level. Nonlinear (large deflection) plate theory is employed, together with an experimentally based failure criterion. It is found that the stiffened composite panel can exhibit significant postbuckling strength. Author

N88-22099*# National Aeronautics and Space Administration, Washington, D.C.

THERMAL EXPANSION BEHAVIOR OF RANDOMLY ORIENTED SHORT CARBON FIBER REINFORCED COPPER COMPOSITES

Keiichi Kuniya, Hideo Arakawa, and Takashi Namekawa May 1988 14 p Transl. into ENGLISH from Nippon Kinzoku Gakkaishi (Japan), v. 49, no. 12, 1985 p 1137-1141 Transl. by Scientific Translation Service, Santa Barbara

(Contract NASw-4307)

(NASA-TT-20175; NAS 1.77:20175) Avail: NTIS HC A03/MF A01 CSCL 11D

Several experiments were carried out on Cu composites with random orientation of short C fibers. The composite with random orientation of short C fibers swelled due to the elastic deformation of the fiber skeleton above 573 K. In a 3-D isotropic composite, the Cu matrix softened above 573 K and was fractured by the repulsive force of C fibers which were elastically deformed and released during heating. Swelling of the composite occurred when the fiber content was greater than or = 20 volume percent or the fiber length exceeded 0.5 millimeters. The addition of carbide-forming elements such as Ti was effective in preventing the swelling. Author

N88-22100*# National Aeronautics and Space Administration, Washington, D.C.

RECIPROCATING SLIDING WEAR CHARACTERISTICS OF COPPER-CARBON FIBER COMPOSITES

Keiichi Kuniya, Hideo Arakawa, and Takashi Namekawa May 1988 17 p Transl. into ENGLISH from Nippon Kinzoku Gakkaishi (Japan), v. 50, no. 1, 1986 p 119-125 Transl. by Scientific Translation Service, Santa Barbara, Calif.

(Contract NASw-4307)

(NASA-TT-20176; NAS 1.77:20176) Avail: NTIS HC A03/MF A01 CSCL 11D

The effect of fiber orientation and alloy composition on the reciprocating sliding wear behavior of Cu-C fiber composite was studied. The wear volume was smaller than that of Cu alloys. The wear volume increased with increasing sliding load and volume fraction of C fibers above 30 volume percent. The effectiveness of fiber orientation in decreasing the wear volume was the highest for random orientation, medium in the direction perpendicular to the fiber direction, and lowest in the fiber direction. The wear volume was decreased by the addition of Sn and Zr. However, the additions did not achieve isotropic wear characteristics of the composite. Isotropic wear was obtained by the addition of C powder. Isotropic and decreased composite wear were attained by adding Zr and C powder together. Author

N88-22101*# National Aeronautics and Space Administration, Washington, D.C.

APPLICATION OF COPPER-CARBON FIBER COMPOSITES TO POWER SEMICONDUCTOR DEVICES

Keiichi Kuniya, Hideo Arakawa, Tadashi Sakaue, Hitoshi Minorikawa, Kenji Akeyama, and Tatsuji Sakamoto May 1988 18 p Transl. into ENGLISH from Nippon Kinzoku Gakkaishi (Japan), v. 50, no. 6, 1986 p 583-589 Transl. by Scientific Translation Service, Santa Barbara, Calif.

(Contract NASw-4307)

(NASA-TT-20171; NAS 1.77:20171) Avail: NTIS HC A03/MF A01 CSCL 11D

Copper-carbon composite electrodes are used in a series of power semiconductor devices, i.e., resin molded diodes, button-type diodes, stud-type diodes, power modules, and integrated circuit igniter modules. The properties of these power semiconductor devices compare favorably with those conventional devices using Mo or W electrodes. In thermal fatigue tests, no degradation in the electrical and mechanical characteristics of these devices are observed. The new composite electrode with carbon fibers satisfies all of the major requirements for the electrodes in power semiconductor devices. Author

N88-22102*# National Aeronautics and Space Administration, Washington, D.C.

FIBER-REINFORCED PLASTIC COMPOSITES. POSSIBILITIES AND LIMITATIONS OF APPLICATIONS AS MACHINE-CONSTRUCTION MATERIALS

Lothar Ophey Apr. 1988 35 p Transl. into ENGLISH from Faser-Kunststoff Verbundwerkstoffe Einsatzmoeglichkeiten und -grenzen als Konstruktionswerkstoff im Maschinenbau, VDI-Z, (Federal Republic of Germany), v. 128, no. 20, Oct. 1986 p 817-824 Original language document was announced in IAA as A87-24125 Transl. by SCITRAN, Inc., Santa Barbara, Calif.

(Contract NASw-4307)

(NASA-TT-20159; NAS 1.77:20159) Avail: NTIS HC A03/MF A01 CSCL 11D

The use of fiber-reinforced composite structural materials in engineering applications is discussed in a survey of currently available technology and future prospects. The ongoing rapid growth in the use of these materials is described, and the criteria to be applied in selecting base materials, lamination schemes, fasteners, and processing methods are examined in detail and illustrated with graphs, diagrams, flow charts, and drawings. A description of a sample application (comparing the properties of steel, CFRP, SiC-reinforced Al, CFRP/steel, and CFRP/Al automobile piston rods) is included. Author

N88-22103# Office National d'Etudes et de Recherches Aerospatiales, Paris (France). Direction Scientifique de la Resistance des Structures.

A SYSTEM TO MEASURE DAMAGE IN COMPOSITE MATERIALS BY THE ULTRASONIC METHOD Final Report [CHAINE DE MESURE DE L'ENDOMMAGEMENT DES MATERIAUX COMPOSITES PAR LA METHODE DES ULTRA-SONS]

J. Renard and H. Kaczmarek Aug. 1987 25 p In FRENCH

(Contract STPA-85-95-004)

(ONERA-RT-2/7256-RY-061-R; ETN-88-91990) Avail: NTIS HC A03/MF A01

A nondestructive method to measure transversal breaking, delamination, and peeling of composite materials is presented. The laboratory procedure includes the automatic scanning of the specimen by the ultrasonic sensor. The design of a computer program to analyze multilevel amplitudes and geometrical correlations is described. ESA

N88-22104*# National Aeronautics and Space Administration, Washington, D.C.

JOINTS IN FIBER-REINFORCED ALUMINUM ALLOYS

K. Gerber and E. vanRensen Apr. 1988 22 p Transl. into ENGLISH of Fuegen Faserverstaerkter Aluminiumlegierungen presented at the 3rd Composites Meeting, 1974 p 359-376 Meeting held in Konstanz, Feb. Republic of Germany, 28-29 Mar. 1974 Original language document was announced in IAA as A75-21918 Transl. by Scientific Translation Service, Santa Barbara, Calif.

(Contract NASw-4307)

(NASA-TT-20160; NAS 1.77:20160) Avail: NTIS HC A03/MF A01 CSCL 11D

Problems of joining involving structural components made of aluminum alloys with boron-fiber reinforcements are discussed, giving attention to a diffusion-welding process. The tension characteristics and weight factors in the case of various types of welded joints are considered. Diffusion-welding equipment used in the experimental investigation is described. The strength

characteristics obtained in various cases of weld and component design are examined, taking into account static and dynamic stresses. IAA

N88-22387*# Akron Univ., Ohio.
UNIFIED CONSTITUTIVE MODEL DEVELOPMENT FOR METAL MATRIX COMPOSITES AT HIGH TEMPERATURE
D. N. Robinson *In* NASA. Lewis Research Center, Lewis Structures Technology, 1988. Volume 2: Structural Mechanics May 1988 p 49-56 (For primary document see N88-22382 15-39)
(Grant NAG3-379)
Avail: NTIS HC A14/MF A01 CSCL 11D

N88-22391*# National Aeronautics and Space Administration. Lewis Research Center, Cleveland, Ohio.
FEATURES AND APPLICATIONS OF THE INTEGRATED COMPOSITES ANALYZER (ICAN) CODE
Carol A. Ginty *In its* Lewis Structures Technology, 1988. Volume 2: Structural Mechanics May 1988 p 99-112 Previously announced as N87-16880 (For primary document see N88-22382 15-39)
Avail: NTIS HC A14/MF A01 CSCL 11D

N88-22395*# National Aeronautics and Space Administration. Lewis Research Center, Cleveland, Ohio.
METCAN: THE METAL MATRIX COMPOSITE ANALYZER
Dale A. Hopkins and Pappu L. N. Murthy (Cleveland State Univ., Ohio.) *In its* Lewis Structures Technology, 1988. Volume 2: Structural Mechanics May 1988 p 141-156 (For primary document see N88-22382 15-39)
(Grant NAG3-550)
Avail: NTIS HC A14/MF A01 CSCL 11D

N88-22396*# Cleveland State Univ., Ohio.
COMPUTATIONAL SIMULATION METHODS FOR COMPOSITE FRACTURE MECHANICS
Pappu L. N. Murthy *In* NASA. Lewis Research Center, Lewis Structures Technology, 1988. Volume 2: Structural Mechanics May 1988 p 157-169 (For primary document see N88-22382 15-39)
Avail: NTIS HC A14/MF A01 CSCL 11D

N88-22402*# National Aeronautics and Space Administration. Lewis Research Center, Cleveland, Ohio.
IMPACT DAMAGE IN COMPOSITE LAMINATES
Joseph E. Grady *In its* Lewis Structures Technology, 1988. Volume 2: Structural Mechanics May 1988 p 235-243 (For primary document see N88-22382 15-39)
Avail: NTIS HC A14/MF A01 CSCL 11D

N88-22405*# Sverdrup Technology, Inc., Cleveland, Ohio.
STRUCTURAL ANALYSES OF ENGINE WALL COOLING CONCEPTS AND MATERIALS
Albert Kaufman *In* NASA. Lewis Research Center, Lewis Structures Technology, 1988. Volume 2: Structural Mechanics May 1988 p 265-280 (For primary document see N88-22382 15-39)
Avail: NTIS HC A14/MF A01 CSCL 11D

25 INORGANIC AND PHYSICAL CHEMISTRY

Includes chemical analysis, e.g., chromatography; combustion theory; electrochemistry; and photochemistry.

For related information see also *77 Thermodynamics and Statistical Physics.*.

N88-22105# TRW Space Technology Labs., Redondo Beach, Calif. Engineering Sciences Lab.
BASIC RESEARCH ON FLAME RADIATION Annual Report, Aug. 1986 - Aug. 1987
L. D. Bergerson, G. F. Carrier, F. E. Fendell, F. L. Hetzel, and C. T. Hsu 1987 42 p
(Contract GRI-5086-260-1415)
(PB88-168372; TRW-S/N-48027; GRI-88/0003) Avail: NTIS HC A03/MF A01 CSCL 21B

Enhanced radiative transfer from natural-gas/air diffusion flames would be useful in many industrial contexts. Control of the formation and growth of the carbonaceous-particulate field is sought as a means of achieving this enhancement; soot-burn-up control is also sought, so that no emissions penalty is incurred. For predictive capability in design, a semiempirical model of soot inception, growth, aggregation, and oxidation is to be developed. The tentative formulation of the rates of the soot-associated processes in a model of engineering utility, together with the preliminary validation of the proposed rates, is pursued from data obtained in two laboratory experiments: (1) the steady 1-D counterflowing of two streams at slow speed, to permit ready intrusive measurement (via expanded spatial scale) of sooting phenomena, and (2) the unsteady, spatially homogeneous evolution of the soot-related fields in a novel light-gas gun. The project concentrates on the design, construction, instrumentation, check out, and utilization of the gun; the counterflow is being pursued simultaneously under an independent project. Author

N88-22106# Bhabha Atomic Research Centre, Bombay (India).
COMPUTER PROGRAM IN BASIC LANGUAGE FOR COMPUTATION OF SPECTROCHEMICAL ANALYTICAL DATA
R. Rajachandrasekar, P. G. Kulkarni, and M. V. Joshi 1986 32 p
(DE88-701229; BARC-1344) Avail: NTIS (US Sales Only) HC A03/MF A01

The spectrochemical computations of transforming optical density data into concentrations, hitherto done on Respektra calculating boards are time consuming. In order to speed up these calculations, a computer program has been devised in HI-BASIC language which can be used in HP-9845B desktop computer (Hewlett Packard, USA). The programs carry out the tasks of the emulsion calibration, background correction, intensity ratio calculation, plotting of working curves, printout of results of individual elements, working curves (on option) and collective results of all elements in a given sample. DOE

N88-22107# Argonne National Lab., Ill.
MASS TRANSFER MECHANISMS FOR WATER ADSORBED ON SILICA GEL
A. V. Fraioli 1987 8 p Presented at the ASME Winter Meeting, Boston, Mass., 13 Dec. 1987
(Contract W-31109-eng-38)
(DE88-005993; CONF-871234-13) Avail: NTIS HC A02

Water adsorption measurements were carried out on a commercial silica gel desiccant in humidistat tubes employing saturated salt solutions to maintain controlled final equilibrium partial pressures of water vapor over the adsorbent samples. The humidistat designs permitted measurement of adsorption in the air-saturated mode, or in the evacuated mode, where the vapor pressure of the water reestablished by the wet salt slurry was the total gas pressure of the system. Evaluation of the water adsorption data on silica gel obtained under both humidistat conditions disclosed a novel solid-side mass transport mechanism not previously considered in desiccant system modelling. It is proposed that at or about 40 percent relative humidity, pore flooding on the external surface creates a meniscal force imbalance with respect to the menisci adjacent to unfilled voids within the interior of the particle. At this point and beyond to saturation, fluid flow in a manner analogous to wicking saturates the particle, and appears to be responsible for the appearance of the second knee in the observed classical BET Type IV isotherm. DOE

N88-22108# Chicago Univ., Ill. Dept. of Geophysical Sciences.
ADVANCES IN GEOCHEMISTRY AND COSMOCHEMISTRY: TRACE ELEMENT MICRODISTRIBUTIONS WITH THE SYNCHROTRON X-RAY FLUORESCENCE MICROPROBE
S. R. Sutton, M. L. Rivers, J. V. Smith, and K. W. Jones 1987 6 p Presented at the Symposium on X-ray Microscopy, Upton,

N.Y., 31 Aug. 1987 Prepared in cooperation with BNL, Upton, N.Y.
(Contract DE-AC02-76CH-00016)
(DE88-006355; BNL-40762; CONF-8708180-8) Avail: NTIS HC A02/MF A01

Synchrotron radiation induced X-ray fluorescence analysis offers several advantages for chemical analyses of geological specimens over conventional geochemical techniques, such as electron microprobe and neutron activation analysis. Most important, high spatial resolution coupled with high elemental sensitivity allows analyses of trace elements on individual crystals, as opposed to bulk rocks or mineral separates, and the essential ability to avoid commonly occurring inclusions within these grains. The capability for detailed trace element mapping of geological specimens opens up new areas of studies. For example, laboratory studies of geochemical behavior can be performed under pressure, temperature and geochemical conditions which approximate geological environments more closely than ever before. The non-destructive nature of the analysis leaves specimens available for study by complementary techniques. The present microprobe uses continuum radiation from an arc magnet as the excitation source and an energy dispersive detector (30 sq mm Si(Li)). With this apparatus, minimum detection limits are typically several ppM for 20 micrometer spots. The initial results of the geochemistry and cosmochemistry experiments performed on this instrument through collaborations between BNL staff scientists and geoscientists from universities and industry are summarized.
DOE

N88-22109# Brookhaven National Lab., Upton, N. Y.
VARIABLE-ENERGY POSITRON STUDIES ON LIQUIDS AND LIQUID-SOLID INTERFACES
J. Throwe, K. G. Lynn, E. Gramsch, and I. Kanazawa 1987 17 p Presented at the International Symposium on Positron Annihilation Studies of Fluids, Arlington, Tex., 8 Jun. 1987
(Contract DE-AC02-76CH-00016)
(DE88-006356; BNL-40744; CONF-8706277-1) Avail: NTIS HC A03/MF A01

A variable energy (less than 25 keV) magnetically guided positron beam is being constructed for the study of liquid surfaces and solid-liquid phase transitions and interfaces. Positron beam design is discussed, with emphasis on special features necessary for the study of liquid and other high vapor pressure samples. Previous results are discussed, including measurements on amorphous metals and amorphous overlayers as well as measurements on bulk liquids. Experiments planned for the new beam will be presented.
DOE

N88-22110# Kentucky Univ., Lexington. Dept. of Chemistry.
LASER SPECTROSCOPY AND DYNAMICS OF COMBUSTION INTERMEDIATES Progress Report, 1 Jun. 1987 - 31 May 1988
Dennis J. Clouthier Jan. 1988 4 p
(Contract DE-FG05-86ER-13544)
(DE88-006541; DOE/ER-13544/T1) Avail: NTIS HC A02/MF A01

Collision-free single rotational fluorescence lifetimes have been measured for thioformaldehyde at very low pressures. Measurements are being conducted on the jet-cooled spectra of thioformaldehyde using a heated supersonic jet. Supersonic jet spectra of the S sub 1 (reverse arrow) S sub 0 spectrum of the transient species S2O have been recorded using the heterogeneous chemical reaction SOCl2 + Ag2S yields S2O + 2AgCl before the jet. The precursor C3OS has been flash photolyzed, and the spectrum expected of C2S was observed.
DOE

N88-22111# National Lab. for High Energy Physics, Oho (Japan).
SPECTROGRAPHIC DETECTION OF NITROGEN IMPURITY IN HELIUM
Katsuhiro Mimori and Masayoshi Wake Jul. 1987 16 p In JAPANESE; ENGLISH summary
(DE88-752301; KEK-87-6) Avail: NTIS (US Sales Only) HC A03/MF A01

A device to observe a very small amount of nitrogen impurity in helium gas was developed for a helium liquefaction system. The principle of detection is based on the optical spectroscopy of the discharge arc in the helium gas. The new detector uses 427.8 nm spectral line as the detection light source while the previous works in this type of detectors used 391.4 nm spectral line. The advantage of the newly introduced spectral line is that there is no strong helium spectral line in the neighbor of the observed line. As a result, it became possible to build a simple and reliable impurity detector which can continuously observe a very small amount of nitrogen in helium.
DOE

N88-22112# Rice Univ., Houston, Tex.
INFRARED ABSORPTION SPECTROSCOPY AND CHEMICAL KINETICS OF FREE RADICALS Progress Report, 1 Mar. 1985 - 1 Feb. 1987
R. F. Curl and G. P. Glass 1987 8 p
(Contract DE-FG05-85ER-13439)
(DE88-006536; DOE/ER-13439/3) Avail: NTIS HC A02/MF A01

Infrared kinetic spectroscopy using excimer laser flash photolysis and color center laser probing has been used to measure the branching ratio of the deNOx reaction: NH2 + NO yields HN2(?) + OH or N2 + H2O. The amidogen radical, NH2, was produced by ArF photolysis of NH3. Infrared absorptions of OH and H2O were measured to determine the absolute contributions of the OH and H2O product channels. Using color center laser kinetic spectroscopy to follow the time decay of C2H transient absorption, the rate constants for the reactions of C2H with H2, O2, C2H2, and NO have been measured. The C2H was produced by ArF excimer (193 nm) flash photolysis of trifluoropropyne for the H2, O2, and NO reactions. In the case of the C2H2 reaction, C2H was produced by flash photolysis of acetylene. An investigation to determine the identify of the products of the reaction between C2H and O2 has been initiated. Also, electronic transitions of C2H and C2D have been studied. New bands have been identified and rotationally analyzed.
DOE

N88-22113# Colorado Univ., Boulder. Dept. of Chemistry.
LASER PHOTOELECTRON SPECTROSCOPY OF IONS Annual Technical Progress Report
1988 3 p
(Contract DE-FG02-87ER-13695)
(DE88-006860; DOE/ER-13695) Avail: NTIS HC A02/MF A01

Equipment developments include new ion source, position sensitive detector, photoionization mass spectrometer, etc. The ions BH3(-) and BD3(-) were prepared and their spectra studied; their electron affinities are 0.044 and 0.030 + or - 0.011 eV.
DOE

N88-22114# Sandia National Labs., Albuquerque, N. Mex.
STRUCTURE OF SOL-GEL SILICA
C. J. Brinker, R. K. Brow, D. R. Tallant, and R. J. Kirkpatrick 1987 6 p Presented at the Fall Meeting of the Materials Research Society, Boston, Mass., 30 Nov. 1987 Prepared in cooperation with Illinois Univ., Urbana
(Contract DE-AC04-76DP-00789)
(DE88-006870; SAND-87-1503C; CONF-871124-93) Avail: NTIS HC A02/MF A01

Combined Raman, Si-29 NMR and reactivity studies of silica gels indicate that dehydroxylation of the silica surface results in cyclotrisiloxane species with reduced Si-O-Si bond angles and altered acid/base characteristics. XPS experiments indicate that the expected 0.35 eV shifts in Si2p and O1s binding energies due to the reduced bond angles are hidden within broad peaks due to the remaining hydroxyls. Additional Si2P, O1s, and C1s peaks are also observed and are postulated to result from preferential adsorption of extrinsic C-containing species on sites with enhanced acid/base properties.
DOE

N88-22115# Stanford Univ., Calif. High Temperature Gasdynamics Lab.
TURBULENT REACTING FLOWS AND SUPERSONIC COMBUSTION Annual Report, 15 Sep. 1986 - 30 Sep. 1987
C. T. Bowman, R. K. Hanson, M. G. Mungal, and W. C. Reynolds 30 Sep. 1987 28 p Original contains color illustrations
(Contract F49620-86-K-0022)
(AD-A189690; AFOSR-87-1899TR) Avail: NTIS HC A03/MF A01 CSCL 21B

An experimental and computational investigation of supersonic combustion flows is in progress. The principal objective of the research is to gain a more fundamental understanding of mixing and chemical reaction in supersonic flows. The research effort comprises three inter-related elements: (1) an experimental study of mixing and combustion in a supersonic plane mixing layer; (2) development of laser-induced fluorescence techniques for time-resolved two-dimensional imaging of species concentration, temperature, velocity and pressure; and, (3) numerical simulations of compressible reacting flows. The design of the supersonic plane mixing layer was completed and the high-pressure gas storage system was installed. The pulsed lasers and camera systems, to be used for two-dimensional flow field imaging, were installed and initial performance evaluations are in progress. This work has focussed on development of appropriate numerical methods for performing full-turbulence simulations of high-speed compressible flows and on the application of these methods to temporally and spatially developing compressible mixing layers. The effort to date has identified several promising numerical methods for compressible flow problems. In addition, a code was developed for compressible mixing layers, and initial simulation using this code shows interesting features, such as imbedded shock waves, in high-speed mixing layers. GRA

N88-22116# Massachusetts Inst. of Tech., Cambridge.
NUMERICAL SIMULATION OF TURBULENT FLAMES USING VORTEX METHODS Annual Report No. 3, 1 Sep. 1986 - 31 Aug. 1987
Ahmed F. Ghoniem 5 Oct. 1987 126 p
(Grant AF-AFOSR-0356-84)
(AD-A189813; AFOSR-87-1853TR) Avail: NTIS HC A07/MF A01 CSCL 21B

The vortex element method and the transport element method are developed for the numerical simulation of the Navier-Stokes equations and the energy and species conservation equations, accurate simulation of the governing equations at high Reynolds and Peclet numbers, without resorting to turbulence modelling. Finite rate chemical reactions, finite compressibility and finite heat release rates are also considered in the formulations of the numerical schemes. To validate these methods, we are obtaining solutions for reacting shear layers, both homogenous and heterogeneous, under various idealizations, and comparing the numerical results with experimental data. The solutions are also analyzed to investigate the mechanisms of turbulence combustion interactions. GRA

N88-22117# Stanford Univ., Calif. Dept. of Mechanical Engineering.
AN INVESTIGATION OF FLOW STRUCTURE, MIXING AND CHEMICAL REACTION IN COMBUSTING TURBULENT FLOWS Annual Technical Report, 1 Sep. 1986 - 31 Aug. 1987
Craig T. Bowman and Brian J. Cantwell 31 Aug. 1987 7 p
(Grant AF-AFOSR-0373-84)
(AD-A189980; AFOSR-87-1890TR) Avail: NTIS HC A02/MF A01 CSCL 21B

An experimental investigation of the relationship between flow structure and chemical reaction in turbulent reacting flows is in progress. The principal objective of the research is to examine the spatial structure of the unsteady reaction process as it relates to the unsteady velocity field. The configuration chosen for study is a co-flowing, non-premixed jet flame. A small perturbation in the fuel jet velocity, produced acoustically, is used to create a very periodic and controllable flame, suitable for conditional sampling. Initial measurements of the unsteady velocity field in the flame have been obtained using laser anemometry. In addition, flow visualization experiments have been conducted using direct and schlieren photography and Mie scattering from the seed particles introduced into the flow. Planar laser-induced fluorescence images of the OH radical, which provide spatially and temporally resolved information on the instantaneous location of the reaction zone, have been obtained. A particle tracking technique to facilitate acquisition of velocity field data has been developed, and is being used to provide velocity field data to be overlaid on the reaction field data to reveal the flame-flow interaction. GRA

N88-22118# Columbia Univ., New York, N.Y.
MOLECULAR DYNAMICS OF MATERIALS POSSESSING HIGH ENERGY CONTENT Final Report, 1 Nov. 1985 - 31 Oct. 1987
Nicholas J. Turro 26 Jan. 1988 17 p
(Grant AF-AFOSR-0040-84)
(AD-A190034; AFOSR-88-0168TR) Avail: NTIS HC A03/MF A01 CSCL 07C

The accomplished research has centered about the construction of new instrumentation for the investigation of transient high energy materials and the exploration of how the chemistry of transient high energy materials and the dynamics of these species respond to systematic variations in structure, environments, and experimental variables. Particular emphasis has been given to reactions in microheterogeneous environments and interfaces provided by micelles, polymers and porous solids, using resonance Raman spectroscopy, nuclear magnetic resonance spectroscopy, electron spin resonance spectroscopy, optical absorption and optical emission. The use of external magnetic fields on the reactivity of carbenes, of radical pairs and of biradicals, and of adsorption of reactive intermediates at interfaces has been explored as methods which may be capable of extending the lifetimes of these transient species. GRA

N88-22119# Colorado Univ., Boulder.
ELECTRONIC ENERGY TRANSFER PROCESSES IN THE ALKALI/ALKALINE EARTH METAL VAPORS Final Report, 5 Aug. 1984 - 15 Jan. 1988
Stephen R. Leone and Alan C. Gallagher 15 Jan. 1988 20 p
(Grant AF-AFOSR-0272-84)
(AD-A190035; AFOSR-88-0167TR) Avail: NTIS HC A03/MF A01 CSCL 20E

Collisional energy transfer rates from highly excited 1P states to nearby 3P, 1D, 3D, and F states of Ca and Sr and fine-structure mixing within the metastable 3P state of Sr have been studied. Several collisional and stimulated population-transfers between the lowest 1P, 3P, 1D, and 3D, states Sr have been isolated, and energy-pooling in collisions between pairs of these energy storage states has been studied. These processes interconnect the excited-state populations and produce energy leakage during high energy density storage in these metastable states. During the course of these studies, several multiphoton excitation and stimulated Raman population processes have been discovered. Studies have also been carried out to measure the effects of p orbital alignment on the cross sections for electronic state-changing collision. Large and remarkably selective alignment effects have been observed for energy transfer processes in both calcium and strontium upon collisions with rare gases and with some molecules revealing a new level of detail about the precise curve crossings and electronic potentials. GRA

N88-22120# Massachusetts Inst. of Tech., Cambridge.
BASIC INSTABILITY MECHANISMS IN CHEMICALLY REACTING SUBSONIC AND SUPERSONIC FLOWS Annual Technical Report, 30 Sep. 1986 - 29 Sep. 1987
Tau-Yi Toong 23 Oct. 1987 30 p
(Grant AF AFOSR-0373-83)
(AD-A190101; AFOSR-87-1889TR) Avail: NTIS HC A03/MF A01 CSCL 21B

The nature of turbulence-combustion interactions was examined by the use of simultaneous dual-thermocouple velocity and LDV-thermocouple measurements, which showed that the presence of the high-frequency velocity (in a direction normal to the flame

brush) and temperature fluctuations within slowly drifting turbulent premixed V-flames was associated with changes in the flame shapes, thicknesses, and propagation speeds. Unlike the RMS normal-velocity fluctuations which assumed maximum values within the reaction zone, the RMS tangential-velocity fluctuations remained almost constant, implying that the flame-generated turbulence was in the normal direction. Furthermore, cross-correlation coefficients of simultaneous velocity and temperature fluctuations remained positive within the flame, with values involving normal velocities higher than those involving tangential components. GRA

N88-22121# California Inst. of Tech., Pasadena.
INVESTIGATION OF COMBUSTION IN LARGE VORTICES Annual Technical Report, Sep. 1986 - Sep. 1987
Frank E. Marble 12 Oct. 1987 22 p
(Grant AF AFOSR-0286-84)
(AD-A190406) Avail: NTIS HC A03/MF A01 CSCL 21B

The investigations of non-steady and unstable combustion in a dump combustor have been completed. The large amplitude driving mechanism centers on the periodic formation and combustion of a large vortex, the phase of heat release being governed by both gas dynamic and chemical delay times. This mechanism is now very well understood, both in principle and in quantitative detail. These results make it a prime candidate for investigations into active control of unstable combustion. The unsteady combustion facility is now being modified to study the details of combustion processes in large vortices utilizing a CID image intensified camera and an LDV for velocity measurements in the hot gas. This study constitutes an essential element in a larger study of shock enhancement for combustion of hydrogen in supersonic burners. GRA

N88-22122# Stanford Univ., Calif. High Temperature Gasdynamics Lab.
ADVANCED DIAGNOSTICS FOR REACTING FLOWS Annual Report, 1 Oct. 1986 - 30 Sep. 1987
R. K. Hanson 30 Oct. 1987 53 p
(Grant AF-AFOSR-0056-87)
(AD-A190485; AFOSR-87-1830TR) Avail: NTIS HC A04/MF A01 CSCL 07D

Progress is reported for the past year of an interdisciplinary program to establish advanced optical diagnostic techniques applicable to combustion and plasma flows. The primary effort is on digital flowfield imaging techniques, which offer significant potential for a wide range of spatially resolved 2-d and 3-d measurements. The imaging is accomplished by recording light scattered from a planar laser-illuminated region using a modern solid-state camera. The scattering process is generally laser-induced fluorescence, though Mie scattering is also used in connection with sizing particles. Activities reported herein include: (1) single-photon fluorescence imaging of molecular oxygen; (2) two-photon fluorescence imaging of CO and H2O; (3) photofragmentation-based fluorescence imaging; (4) mutiple particle sizing by imaging of Mie-scattered light; (5) fluorescence-based velocity and pressure imaging; (6) 3-d imaging; (7) laser and solid-state camera development; and (8) processing/display of image data using a specialized image computer. Other diagnostics topics discussed in this report include research on laser wavelength modulation spectroscopy and development of plasma diagnostics based on laser-induced fluorescence and Stark broadening. GRA

N88-22123# Princeton Univ., N. J. Dept. of Mechanical and Aerospace Engineering.
AFRAPT (AIR FORCE RESEARCH IN AERO PROPULSION TECHNOLOGY) TRAINEE PROGRAM Annual Report, 1 Sep. 1986 - 30 Aug. 1987
Irvin Glassman 21 Sep. 1987 3 p
(Grant AF-AFOSR-0292-85)
(AD-A190525; AFOSR-87-1766TR) Avail: NTIS HC A02/MF A01 CSCL 21B

Three AFRAPT trainees were in residence as graduate students at Princeton during the period 1 Sept. 1986 to 30 Aug. 1987. These students spent their summers working at General Electric-Cincinnati, Pratt and Whitney-East Hartford and United Technologies Research Center. All three students have worked in problems related to combustion. One recently completed a M.S.E. thesis and accepted a position at AVCO-Lycoming to continue working in the aircraft jet engine field. Mr. Konopka is now directing his research attention to complex chemical kinetic mechanisms of combustion processes. Mr. Emdee's research topic is the oxidation of aromatic fuels. Mr. Kappelmeier accepted a position at AVCO-Lycoming in Connecticut and will be working on gas turbines. Mr. Robert J. Lawson will work on combustion of heavy fuels. GRA

N88-22124# Northwestern Univ., Evanston, Ill. Dept. of Chemistry.
THE SPECTROSCOPY AND REACTION KINETICS OF COORDINATIVELY UNSATURATED METAL CARBONYLS Final Technical Report, Oct. 1983 - Oct. 1987
Eric Weitz 24 Oct. 1987 17 p
(Grant AF-AFOSR-0372-83)
(AD-A190533; AFOSR-87-1785TR) Avail: NTIS HC A03/MF A01 CSCL 07C

A program involving the investigation and characterization of reactions of coordinatively unsaturated organometallic species is described. The program emphasizes the measurement of rates of reaction of photolytically produced coordinatively unsaturated species with the parent and rates for cluster formation. Experimental measurements are performed using a time resolved transient absorption apparatus which uses a line turnable carbon monoxide (CO) laser and a diode laser to record spectral and kinetic information by means of probing absorptions in the CO stretch region of the infrared. Systems that have been investigated include coordinatively unsaturated species generated from the Fe(CO)5, Cr(CO)6 and Mn2(CO)10 parents. The results of experiments with these systems are discussed. GRA

N88-22125# Illinois Univ., Urbana. Dept. of Chemistry.
FLUIDS, GELS AND GLASSES UNDER EXTREME CONDITIONS OF PRESSURE AND TEMPERATURE Final Technical Report, 1 Oct. 1986 - 30 Sep. 1987
Jiri Jonas 22 Jan. 1988 18 p
(Grant AF-AFOSR-0045-87)
(AD-A190655; AFOSR-88-0158TR) Avail: NTIS HC A03/MF A01 CSCL 20E

A multi-nuclear, high resolution, high field NMR spectrometer system equipped with wide-bore (89 mm) 7.05 Tesla superconducting magnet, and accessories for high resolution solid state work and an NMR data station were funded under this instrumentation grant. The basic system, a General Electric GN-300, was installed in September, 1986. The necessary accessories for high resolution NMR work on solids were installed during the week of February 23 to 28, 1987. The new Nicolet 1280 NMR data system, delivered in October 1986, is currently being used to control a recently built specialized NMR spectrometer using a wide bore 4.2 Tesla superconducting magnet made by Oxford Instruments. GRA

N88-22126# New Mexico Univ., Albuquerque.
MOLECULAR REACTION AND ENERGY TRANSFER RATE ESTIMATION FOR CHEMICAL-LASER ANALYSIS Final Report, May - Oct. 1984
J. C. Bellum and C. L. Beckel Dec. 1987 31 p
(Contract F29601-84-K-0038)
(AD-A190664; AFWL-TR-85-57) Avail: NTIS HC A03/MF A01 CSCL 20E

This report presents the results of an investigation of methods for estimation of reaction and energy transfer rates for collisions between electronically excited atoms and molecules of the sort typically present in energetic gases such as electronic-transition chemical laser media. The research specifically dealt with ground and excited-state electronic structure and energies of molecular collision complexes. The primary result of the investigation is a

systematic method, within the context of electronic-structure theory, for estimation of potential energy surfaces for molecules in electronically excited states. GRA

N88-22127# Naval Research Lab., Washington, D.C.
DIODE LASER SPECTROSCOPY OF CHEMICAL MOIETIES AT SURFACES Technical Report, Oct. 1986 - Sep. 1987
J. E. Butler, V. M. Bermudez, and R. L. Rubinovitz 15 Oct. 1987 7 p
(AD-A190710) Avail: NTIS HC A02/MF A01 CSCL 07D

The use of tunable infrared lead salt diode lasers as spectrally bright light sources for infrared reflection absorption spectroscopy (IRRAS) at interfaces will be presented. This new spectroscopy permits in situ, non-intrusive optical probing of the vibrational fingerprint spectrum (500 to 2000/cm) with sub-monolayer sensitivity at metal interfaces and can work through any moderately transmissive ambient. Recent results and instrumental developments will be presented. GRA

N88-22128# Rensselaer Polytechnic Inst., Troy, N.Y.
ADVANCED B AND Al COMBUSTION KINETICS OVER WIDE TEMPERATURE RANGES Annual Report, 1 Dec. 1986 - 31 Nov. 1987
Arthur Fontijn 17 Dec. 1987 13 p
(Grant AF-AFOSR-0019-86)
(AD-A190752; AFOSR-88-0170TR) Avail: NTIS HC A03/MF A01 CSCL 21B

Current ability to improve the combustion efficiency of B and Al solid propellants and slurries is hampered by a lack of understanding and knowledge of the kinetics of the individual reactions involved and the ways and manner by which temperature affects the rate coefficients and product channels. While the simple Arrhenius-type equation k(T) = AT(to the 1/2 power) exp(-E(A)/RT) has over limited temperature ranges been of great value, when applied to wide temperature ranges it is often not obeyed. Particularly for exothermic and slightly endothermic reactions, order of magnitude errors can be made by extrapolations based on the Arrhenius equation. It is the goal of this program to provide an insight in the kinetic behavior of B and Al radical oxidation reactions as influenced by temperature. To this end measurements are made in high-temperature fast-flow reactors (HTFFR). These unique tools provide measurements on isolated elementary reactions in a heat bath. GRA

N88-22129# Swedish Inst. for Materials Testing, Boras.
DENSITY MEASUREMENTS ON SOLIDS AND LIQUIDS
L. Pendrill and K. Mattiasson 1987 34 p
(PB88-164934; SP-RAPP-187-21; ISBN-91-7848-062-0) Avail: NTIS HC A03/MF A01 CSCL 07D

A measurement apparatus has been constructed for the accurate determination of the densities of liquids and solids. A ball to a roller-bearing, made of stainless steel, is weighted in air and, hydrostatically, in a liquid of interest, using an electronic, single pan balance. Measurements have been performed with pure water, and with kerosene. Extensive experiments have concentrated on the effects of surface tension on the hydrostatic weighing. Several choices of materials for the suspension wire have been invesitgated. Attempts to reduce the surface tension through application of an additive to the water are also reported. GRA

N88-22130*# National Aeronautics and Space Administration, Washington, D.C.
MEASUREMENT OF EMISSIVITY OF INDUSTRIAL SURFACES USING A SIMPLE METHOD
H. Dallmeyer Apr. 1988 18 p Transl. into ENGLISH from Chemie Ingenieur Technik (Fed. Republic of Germany), v. 41, no. 5-6, 1969 p 323-328 Transl. by Scientific Translation Service, Santa Barbara, Calif.
(Contract NASw-4307)
(NASA-TT-20165; NAS 1.77:20165) Avail: NTIS HC A03/MF A01 CSCL 07D

To detect emissivity, the drop in temperature of the sample undergoing radiation exchange with the wall in an evacuated space is measured over a given period. In this manner, emissivities of various synthetic resin lacquers, metals, and metallic coatings were measured. Once the emissivity is known, the same method can be used to detect specific heat and the head condition of gases. Author

N88-22131# Institut d'Aeronomie Spatiale de Belgique, Brussels.
ROTATIONAL STRUCTURE AND ABSORPTION CROSS SECTIONS FROM 300 TO 190 K OF THE SCHUMANN-RUNGE BANDS
M. Nicolet, S. Cieslik, and R. Kennes 1987 386 p Sponsored in cooperation with the Commission of the European Communities and the ONR
(Contract FC-85-563)
(Aeronomica-Acta-A-318-1987; ISSN-0065-3713; ETN-88-92210) Avail: NTIS HC A17/MF A01

Tables and figures of calculated absorption cross sections are given for molecular oxygen as a function of wave number over the spectral interval 49,000 to 57,000 cm sup -1 for temperatures between 1980 and 300 K. The spectrum corresponding to the domain of the rotation lines of the various bands of the B sup 3 sigma (-) sub u to X sup 3 Sigma (-) sub g Schumann-Runge system with their underlying continua is presented for the range of the (0-0) to (19-0) bands in 32 intervals of 25 cm sup -1. Calculated absorption cross sections were determined for each band after a comparison with laboratory measurements made at 300 K. The calculations required knowledge of the line wavenumbers of the (0-0) to (19-0) and (2-1) to (19-1) bands with their mean oscillator strengths and determination of the associated equivalent linewidths of the rotation lines with their underlying continuum. ESA

N88-22132# Institut d'Aeronomie Spatiale de Belgique, Brussels.
ULTRAVIOLET ABSORPTION CROSS SECTIONS OF METHYLBROMIDE AT STRATOSPHERIC TEMPERATURES
D. Gillotay and P. C. Simon 1987 20 p Submitted for publication
(Aeronomica-Acta-A-320-1987; ISSN-0065-3713; ETN-88-92212) Avail: NTIS HC A03/MF A01

The absorption cross sections of methyl bromide were measured in laboratory between 180 and 260 nm at temperatures of 295, 255, 227, and 209 K. A parametrical formula to compute the absorption cross sections for wavelengths between 200 and 260 nm and for temperatures between 210 and 300 K is proposed. ESA

N88-22133*# Brown Univ., Providence, R. I. Dept. of Engineering and Physics.
THEORETICAL STUDIES OF RESONANCE ENHANCED STIMULATED RAMAN SCATTERING (RESRS) OF FREQUENCY-DOUBLED ALEXANDRITE LASER WAVELENGTH IN CESIUM VAPOR Progress Report, Jan. - Jun. 1987
Nabil M. Lawandy 1987 56 p
(Grant NAG5-526)
(NASA-CR-182870; NAS 1.26:182870) Avail: NTIS HC A04/MF A01 CSCL 07D

The solutions for the imaginary susceptibility of the Raman field transition with arbitrary relaxation rates and field strengths are examined for three different sets of relaxation rates. These rates correspond to: (1) Far Infrared (FIR) Raman lasers in the diabatic collision regime without consideration of coupled population decay in a closed system, (2) Raman FIR lasers in the diabatic collision regime with coupled population conserving decay, and (3) IR Raman gain in cesium vapor. The model is further expanded to include Doppler broadening and used to predict the peak gain as a function of detuning for a frequency doubled Alexandrite laser-pumped cesium vapor gain cell. Author

N88-22134*# National Aeronautics and Space Administration, Washington, D.C.
NUCLEATION IN SUPER-SATURATED PRODUCTS
M. Volmer and A. Weber May 1988 30 p Transl. into ENGLISH from Zeitschrift fuer Physikalische Chemie (Fed. Republic of Germany), v. 119, 1926 p 277-301 Transl. by Scientific Translation Service, Santa Barbara, Calif.
(Contract NASw-4307)
(NASA-TT-20275; NAS 1.77:20275) Avail: NTIS HC A03/MF A01 CSCL 07D

The procedure used is based on theories of W. Gibbs. The formation of the liquid phase from a supersaturated vapor of a pure substance is first considered. A comparison is made with experience in the area of nucleation. Generally known facts and experiments are mentioned. Liquid nuclei and crystal nuclei are examined. Author

N88-22135*# National Aeronautics and Space Administration, Washington, D.C.
ON COPPER PEROXIDE
L. Moser Apr. 1988 12 p Transl. into ENGLISH from Zeitschrift fuer Anorganische und Allgemeine Chemie (Fed. Republic of Germany), v. 86, 1914 p 380-388 Transl. by Scientific Translation Service, Santa Barbara, Calif.
(Contract NASw-4307)
(NASA-TT-20263; NAS 1.77:20263) Avail: NTIS HC A03/MF A01 CSCL 07D

The action of hydrogen superoxide on copper salts in alcoholic solutions is studied. The action of hydrogen peroxide on copper hydroxide in alcoholic suspensions, and the action of ethereal hydrogen peroxide on copper hydroxide are discussed. It is concluded that using the procedure proposed excludes almost entirely the harmful effect of hydrolysis. Author

26 METALLIC MATERIALS

Includes physical, chemical, and mechanical properties of metals, e.g., corrosion; and metallurgy.

N88-22136# Massachusetts Inst. of Tech., Cambridge.
PROCESSING, MICROSTRUCTURE, AND MECHANICAL PROPERTIES OF SILICON CARBIDE PARTICULATE REINFORCED ALUMINUM ALLOYS Final Report, 10 Sep. 1984 - 31 Oct. 1987
Chikara Fujiwara, Joseph Blucher, and James A. Cornie 14 Jan. 1988 67 p
(Contract DAAG29-84-K-0174)
(AD-A188981; ARO-21530.1-MS) Avail: NTIS HC A04/MF A01 CSCL 11F

SiC particulate reinforced Al-2 percent Mg composites were produced at volume fractions 0.1, 0.2, and 0.3 by inert atmosphere ball milling followed by Hot Isostatic Pressing consolidation and extrusion. The SiC particulate sizes evaluated were 5 microns, 1 micron, and 0.2 microns. The processing sequences were carefully controlled to minimize oxygen contamination. The resulting microstructures of the as-extruded materials showed a very uniform distribution of particulates within the matrix. Ultimate strength, 0.2 percent yield strength, and modulus of elasticity increased with decreasing SiC particulate size: 1 micron SiC-Al matrix showed the highest elongation. Fractures originated at inclusions rich in iron, chromium, and nickel. These contaminants seemed to come from the mill chamber and/or the hardened steel balls during ball milling. GRA

N88-22137# Groningen Rijksuniversiteit (Netherlands). Solid State Physics Lab.
ELECTRICAL RESISTIVITIES OF SOME COMPOUND FORMING LIQUID METAL ALLOYS
C. vandetMarel, A. B. vanOosten, J. A. Meijer, G. J. B. Vinke, and W. vanderLugt 1987 27 p
(PB88-145172) Avail: NTIS HC A03/MF A01 CSCL 11F

A number of alloy systems which exhibit marked effects of compound formation were investigated. In the systems considered, one component is always an alkali metal, while the other is a Group 4B or a Group 3B element. The authors present resistivity data for the alloy systems Li-Pb, Na-Pb, K-Pb, Rb-Pb, Cs-Pb, Li-Sn, Na-Sn, N-In and K-In. These data are shown in graphical and tabulated form. Author

N88-22138# Gosudarstvennyi Komitet po Ispolzovaniyu Atomnoi Energii, Moscow (USSR). Inst. Atomnoj Ehnergii.
USE OF LONG-DISTANCE PAIR POTENTIALS IN CALCULATIONS OF DEFECT CHARACTERISTICS IN METALS
V. G. Kapinos and Yu. N. Osetskij 1986 16 p In RUSSIAN
(TI88-701039; IAE-4376/11) Avail: NTIS HC A03/MF A01

Dependence of monovacancy formation energy in sodium, alpha-iron and copper from interatomic potential cutting radius was investigated by the method of static simulation. Investigational results permitted to develop a calculation technique of radiation-induced defects in metals using pair potentials obtained from pseudopotential theory. The technique has been tested in calculations of self-interstitial formation energy in alpha-iron and vacancy complexes in alpha-iron and copper. DOE

N88-22139# Pakistan Inst. of Nuclear Science and Technology, Islamabad. Nuclear Physics Div.
SEGREGATION EFFECTS IN WELDED STAINLESS STEELS
J. I. Akhter, K. A. Shoaid, M. Ahmed, and A. Q. Malik 1987 16 p
(DE88-701224; PINSTECH/NPD-121) Avail: NTIS (US Sales Only) HC A03/MF A01

Welding of steels causes changes in the microstructure and chemical composition which could adversely affect the mechanical and corrosion properties. The report describes the experimental results of an investigation of segregation effects in welded austenitic stainless steels of AISI Type 304, 304L, 316 and 316L using the techniques of scanning electron microscopy and electron probe microanalysis. Considerable enhancement of chromium and carbon has been observed in certain well-defined zones on the parent metal and on composition, particularly in the parent metal, is attributed to the formation of (M(sub 23)C(sub 6)) precipitates. The formation of geometrically well-defined segregation zones is explained on the basis of the time-temperature-precipitation curve of (M(sub 23)C(sub 6)). DOE

N88-22140# Japan Atomic Energy Research Inst., Tokyo.
EFFECT OF STRAIN RATE ON HIGH-TEMPERATURE LOW-CYCLE FATIGUE BEHAVIOR OF HASTELLOY X AND HASTELLOY XR
Hirokazu Tsuji and Tatsuo Kondo Sep. 1987 43 p In JAPANESE; ENGLISH summary
(DE88-752302; JAERI-M-87-152) Avail: NTIS (US Sales Only) HC A03/MF A01

A series of strain controlled low-cycle fatigue tests at 900 C in the simulated HTGR helium environment were conducted on Hastelloy X and its modified version, Hastelloy XR, and the effect of strain rate on high-temperature low-cycle fatigue behavior was investigated. The results of this study provide the following conclusions: (1) decreasing the strain rate led to notable reductions in the fatigue life, (2) trends of strain softening and cyclic softening were observed at lower strain rates of 1 x 10 sup -4 s sup -1 and 2 x 10 sup -5 s sup -1, (3) both fracture modes of the transgranular and the intergranular were recognized on the fracture surfaces, with the former mode being predominant at a comparatively high strain rate of 1 x 10 sup -3 s sup -1. The intergranular fracture mode, however, became predominant at lower strain rates, 1 x 10 sup -4 s sup -1 and 2 x 10 sup -5 s sup -1, (4) the cumulative damage rule predicted an excessively conservative value for creep damage, (5) the data obtained lay on the straight line plots when the frequency modified fatigue life method was applied. No significant difference in fatigue behavior was resolved between Hastelloy X and Hastelloy XR under the test conditions employed. DOE

N88-22141# Stanford Univ., Calif. Dept. of Mechanical Engineering.
THE THERMAL RADIATIVE PROPERTIES OF METALS AT HIGH TEMPERATURE Annual Report, 20 Oct. 1986 - 30 Sep. 1987
S. A. Self 1987 26 p
(Contract W-7405-eng-48)
(DE88-006625; UCRL-21021) Avail: NTIS HC A03/MF A01

The principal aims of this research program are two-fold. The first is to develop apparatus and techniques for the detailed and reliable measurement of the optical constants of molten metals under highly controlled and documented surface conditions. The second is to make such measurements on a number of metals of technical interest to LLNL which will allow reliable radiative heat transfer calculations to be made in several applications of interest to LLNL. Measuring methods of optical properties and emissivity, along with instrument design, are discussed. DOE

N88-22142# Massachusetts Inst. of Tech., Cambridge. Dept. of Materials Science and Engineering.
ON ROTATING SPHERE-ON-A-PLATE EXPERIMENTS AND THE QUESTIONS OF WHETHER HIGH ANGLE GRAIN BOUNDARIES MELT BELOW BULK MELTING TEMPERATURES
R. W. Balluffi and R. Maurer 15 Jan. 1988 6 p Prepared in cooperation with Max-Planck-Inst. fuer Metallforschung, Stuttgart, Fed. Republic of Germany
(Contract DE-FG02-87ER-45310)
(DE88-006627; DOE/ER-45310/6) Avail: NTIS HC A02/MF A01

A study on the melting of grain boundaries of rotating copper and silver spheres-on-a-plate was conducted in order to test whether metals undergo complete melting at temperatures below melting temperatures. Essentially all the boundaries in the experiments at 0.96 T/sub M/ and 0.99 T/sub M/ could not have been completely melted. Instead, it appears that they remained crystalline and that the rotations occurred because of the dependence of their energy on crystal misorientation. Possible situations include a variety of cases where the boundary is considerably disordered but where the atomic positions are still highly correlated with the atomic positions in the two grains adjoining the boundary slab. This conclusion is consistent with numerous previous interpretations of these experiments. DOE

N88-22143# Edgerton, Germeshausen and Grier, Inc., Idaho Falls, Idaho.
GRAIN GROWTH BEHAVIOR OF EXTRUSION CONSOLIDATED CENTRIFUGALLY ATOMIZED TYPE 304 STAINLESS STEEL POWDER
J. E. Flinn, R. N. Wright, and G. E. Korth Nov. 1987 59 p
(Contract DE-AC07-76ID-01570)
(DE88-006788; EGG-SCM-7219) Avail: NTIS HC A04/MF A01

A study was performed to assess the role of entrapped helium in stabilizing the microstructure. Type 304 stainless steel powders produced by centrifugal atomization (CA) were consolidated by hot extrusion. The powders contain approx. 7 appM He which was retained during extrusion. Isothermal heat treatments were performed on the CA 304 SS extruded powder as well as on the attached wrought ingot metallurgy (I/M) can and a filler plug of Type 304 SS for comparisons. Compared with the wrought I/M Type 304 SS, the CA Type 304 SS extruded powder exhibited considerable grain growth retardation. Grain growth was shown to be independent of the means used for powder consolidation, including hot isostatic pressing and dynamic consolidation. Also, other CA consolidated alloy powders exhibited grain growth resistance equal to the CA Type 304 SS extruded powder. Results indicate that the entrapped helium in the CA consolidated powder materials plays a significant role in retarding grain growth. DOE

N88-22144# Tennessee Univ., Knoxville.
LASER ENHANCED ADHESION OF COPPER FILMS TO SAPPHIRE SUBSTRATES
A. J. Pedraza, M. J. Godbole, E. A. Kenik, D. H. Lowndes, and J. R. Thompson, Jr. 1987 17 p Presented at the 34th National Vacuum Symposium and Topical Conference, Anaheim, Calif., 2 Nov. 1987 Prepared in cooperation with Oak Ridge National Lab., Tenn.
(Contract DE-AC05-84OR-21400)
(DE88-006802; CONF-871125-22) Avail: NTIS HC A03/MF A01

Strongly adherent films of copper on sapphire can be grown by discrete and sequential sputter depositions alternating with pulsed laser treatment (PLT). In this work the influence of various processing parameters on the film adhesion and morphology are analyzed. Ultraviolet excimer lasers produce less damage to metallic films than do other visible or infrared pulsed lasers. However, the laser energy density must be carefully controlled in order to prevent excessive evaporation or film damage. Film damage and separation from the substrate is likely to occur during PLT if the initial copper films are thicker than 80 nm. Transmission Electron Microscopy reveals the formation of an intermediate copper/alumina compound in a 30 nm-thick film grown in two steps (10 nm + PLT = 20 nm + PLT). The regions of strong copper-sapphire bonding and good thermal contact that are established in the early stages of the sequential deposition process, and that are maintained during the subsequent process of building up a thick, adherent copper film, most probably consist of this intermediate compound. DOE

N88-22145# Maryland Univ., College Park. Dept. of Chemical and Nuclear Engineering.
FUNDAMENTAL STUDIES ON HIGH TEMPERATURE DEFORMATION RECRYSTALLIZATION, AND GRAIN GROWTH OF TWO-PHASE MATERIALS Interim Technical Report, 1 Dec. 1986 - 30 Nov. 1987
S. Ankem, G. Grewal, and M. N. Vijayshankar Jan. 1988 132 p
(Grant AF-AFOSR-0367-85)
(AD-A189725; AFOSR-88-0055TR) Avail: NTIS HC A07/MF A01 CSCL 11F

Two-phase materials are technologically important because optimum properties can be obtained by a proper combination of the two phases. Among these materials, two phase titanium alloys are of particular interest for high temperature aerospace applications. However, there is a lack of understanding in the areas of high temperature deformation, recrystallization and grain-growth behavior of two-phase alloys in terms of the properties of the component phases. Such an understanding is essential to develop new titanium alloys with greater high temperature strength and stability for high temperature applications. The lack of understanding is due to the complex deformation behavior of these two-phase materials. Whenever a material comprising two or more phases is subjected to stress, the component phases deform differently and this results in inhomogeneous strain and stress distributions. In addition, interaction stresses develop as a result of interactions between the deforming phases. For these reasons, the deformation behavior of two-phase materials cannot be explained by the simple law of mixture rule. GRA

N88-22146# Air Force Inst. of Tech., Wright-Patterson AFB, Ohio. School of Engineering.
THE EFFECTIVE FRACTURE TOUGHNESS OF ALUMINUM AT RAPID HEATING RATES M.S. Thesis
Joseph W. Nichols Dec. 1987 102 p
(AD-A189745; AFIT/GAE/AA/87D-14) Avail: NTIS HC A06/MF A01 CSCL 11F

The fracture of aluminum plates, at high temperatures and at rapid heating rates, was investigated using 6061 T-6 aluminum as the test material. Three heating rates were tried low (15 C/sec), medium (150 C/sec), and high (1500 C/sec). Rapid heating and room temperature tensile tests were performed to characterize the material as a function of temperature. Single edge notched specimen and center cracked panels were fabricated for use in fracture tests. A modified linear elastic fracture toughness, called the effective fracture toughness was used to quantify the relationship between fracture toughness and temperature. The Kc

was found to decrease as temperatures increased in the same manner as the strength. Heating rate, at least in the range tested, had little effect on either the strength or the fracture toughness. Further, it was found that the fracture behavior of 6061 T-6 aluminum under the tested conditions can be related to net-section yielding. A ductile fracture model was found to be useful in relating the critical crack size to critical stress. The test data from the present study showed good agreement with this model. GRA

N88-22147# Naval Postgraduate School, Monterey, Calif.
THE AGE HARDENING RESPONSE OF THERMOMECHANICALLY PROCESSED Al-Mg-Li ALLOYS M.S. Thesis
William F. Ferris Dec. 1987 85 p
(AD-A189870) Avail: NTIS HC A05/MF A01 CSCL 11F

Four Al-Mg-Li alloys of composition (weight percent) in the ranges 6 to 8 percent Mg, 0.5 to 2 percent Li, and 0.15 to 0.25 percent Zr were hot forged and warm rolled (thermo-mechanically processed) to achieve a microstructure suitable for superplasticity. They were then subjected to age-hardening studies at temperatures indicated by concurrent differential scanning calorimetry research. Optical and transmission electron microscopy techniques were used to relate microstructure to mechanical properties. Only the 6 percent Mg to 2 percent Li alloy showed significant age hardening response. However, concurrent research demonstrated excellent superplastic response in the 6 percent Mg to 1 percent Li and 8 percent Mg to 1 percent Li alloys. GRA

N88-22148# Army Armament Research and Development Command, Watervliet, N. Y. Weapons Lab.
DETERMINATION OF AQUO-COMPLEXES OF CHROMIUM AND IRON IN CHROMIUM PLATING AND POLISHING SOLUTIONS BY ION CHROMATOGRAPHY Final Report
Samuel Sopok Nov. 1987 13 p
(AD-A190168; ARCCB-TR-87034) Avail: NTIS HC A03/MF A01 CSCL 07D

Aquo-complexes of chromium and iron in chromium plating and polishing solutions of individual concentration levels above 7.5 g/l results in a poor quality plate condition. An ion chromatographic procedure utilizing UV-visible and atomic absorption detection for determining 0.20 g/l concentration levels of these aquo-complexes is described. Since no derivatizations are necessary, matrix effects are much less common compared to previous chromatographic methods. The relative standard deviation is about two percent and sensitivity is about 1 ppm for these determinations. GRA

N88-22149# Research Triangle Inst., Research Triangle Park, N.C.
STUDY OF MEAN FREE PATH EFFECTS ON GROWTH OF ULTRAFINE METALLIC AEROSOLS Final Report, Jul. 1986 - Sep. 1987
Philip A. Lawless Nov. 1987 66 p
(Contract F49620-84-C-0017)
(AD-A190206; AFOSR-87-1740TR) Avail: NTIS HC A04/MF A01 CSCL 04A

This is the final report of activities on a study of metallic aerosol growth under reduced pressure conditions. The aersol produced is very complex in shape, and the use of fractal descriptors was investigated. The report details the kind of fractal analysis used. It shows that the particles have fractal characteristics describing stages of growth and that the pressure under which the particles are grown does influence the growth structure. At very low pressures, the particles fail to form because of chamber size limitations. The conclusions reached show some of the utility of fractal analysis for investigating irregular particle shapes, some of the pressure effects on formation of metallic aerosols of different compositions, and extrapolations of the growth conditions to lower pressures. GRA

N88-22150# Massachusetts Inst. of Tech., Cambridge. Dept. of Ocean Engineering.
CRACKING TENDENCIES OF RESTRAINED WELDS IN HIGH STRENGTH LOW ALLOY STEELS UNDER HYPERBARIC CONDITIONS M.S. Thesis
Randolph Ni Jun. 1987 118 p
(Contract N00228-85-G-3262)
(AD-A190255) Avail: NTIS HC A06/MF A01 CSCL 11F

The weld cracking tendencies of two newly developed controlled rolled and accelerated cooled high strength low alloy (HSLA) steels are compared with a standard normalized steel of approximately the same ultimate tensile strength (50 kg square millimeter). All steels were welded with the shielded metal arc welding process at 0, 100, and 200 psig. Welding was conducted in a hyperbaric chamber under conditions of 100 percent humidity, using the Lehigh self restraint weld cracking test. A literature and mail survey was conducted on current U.S. practices in underwater welding using the shielded metal arc process. Test plates were subjected to macrascopic examinations to determine the extent of any existent cracking. It was found that the low carbon equivalent HSLA steels exhibited an excellent resistance to cracking, even when welded without the use of preheat. The general tendency for cracking susceptibility to lower as the cracking susceptibility factor (Pw) lowers was validated, even under hyperbaric conditions. However, it was substantiated that the current theories used to determine cracking susceptibility may be too conservative in predicting cracking susceptibility for HSLA steels. GRA

N88-22151# Northwestern Univ., Evanston, Ill. Dept. of Materials Science and Engineering.
INVESTIGATION AND SYNTHESIS OF HIGH TEMPERATURE AND INCREASED STIFFNESS RSP ALUMINUM ALLOYS Annual Report, 1 Oct. 1986 - 30 Sep. 1987
Morris E. Fine and Julia R. Weertman Sep. 1987 21 p
(Grant AF-AFOSR-0337-85)
(AD-A190407) Avail: NTIS HC A03/MF A01 CSCL 11F

This objective of this research is to investigate two promising systems as the basis for high temperature aluminum alloys useful to 425 C (800 F). The first is metal matrix composite consisting of an aluminum magnesium alloy matrix reinforced by spinel (magnesium aluminate) particulate. The second system is tri aluminum (zirconium, vanadium) dispersed in aluminum matrix. Here the lattice parameter matches that of the matrix. Research on dilute alloys has shown a low coarsening rate for this intermetallic at 425 C. Study of more concentrated alloys is underway. A mechanical alloying liquid metal infiltration procedure for preparing specimens of the aluminum alloy matrix spinel composite has been worked out and specimens with 4 vol percent spinel have been prepared. Also, 4 vol percent alumina composite samples were prepared for comparison. Spinel particles were within the aluminum alloys grains in contrast to the alumina which was at grain boundaries. The spinel composite had much better creep resistance at 410 C. Extrusions containing 5 vol percent tri-aluminum (0.75 vanadium, 0.25 zirconium) were prepared for this research by Lockheed-Palo Alto from rapidly solidified foil. The measured creep rate at 425 C is much lower than in the current aluminum-iron-cerium alloy. An aluminum vanadium intermetallic compound, however, forms at grain boundaries leading to a precipitate free zone which grows slowly at 425 C. GRA

N88-22152# McDonnell-Douglas Research Labs., St. Louis, Mo.
GROWTH AND DEFORMATION MECHANISMS OF REFRACTORY ALLOY HYBRID MATERIALS Annual Report, 15 Sep. 1986 - 15 Sep. 1987
S. M. Sastry, D. M. Bowden, B. D. London, R. J. Lederich, and J. E. ONeal Dec. 1987 38 p
(Contract F49620-86-C-0108)
(AD-A190492; MDC-QA002; AFOSR-87-2040TR) Avail: NTIS HC A03/MF A01 CSCL 11F

Oxide-dispersion-strengthened and whisker/particulate reinforced titanium and niobium alloys produced by rapid solidification processing are being investigated with the objectives of understanding the mechanisms of formation and growth of the

secondary phases and how these factors determine strengthening mechanisms and thermal stability of Ti and Nb alloys. During the first year of the three-year program, titanium alloys containing aluminum, erbium, boron, and carbon, and Nb alloys containing tungsten, hafnium, lanthanum, B, and C were prepared by nonconsumable electrode arc melting and microstructures were characterized. The alloys were rapidly solidified by electron beam melting and splat quenching and the rapidly solidified flakes were characterized by X-ray diffraction, optical metallography, and electron microscopy. The mechanical properties of rapidly solidified Ti alloys containing Er, B, and C were determined by tensile testing of specimens prepared from electron-beam-melted and splat-quenched flakes. GRA

N88-22153# Rensselaer Polytechnic Inst., Troy, N.Y. Dept. of Mathematical Sciences.
LASER PHOTODEPOSITION AND ETCHING STUDY Final Report, 1 Jul. 1986 - 30 Jun. 1987
A. Novick-Cohen Jun. 1987 6 p
(Grant AF AFOSR-0179-86)
(AD-A190535; AFOSR-87-1765TR) Avail: NTIS HC A02/MF A01 CSCL 11F

The important result reported is that under a distinguished limit procedure an alternative to the Kuramoto-Sivashinsky equation is obtained when modelling the evolution of solidification fronts. Three papers are being prepared for publication. Solidification Fronts: Asymptotic equations are derived to model the evolution of the solid liquid interface which occurs in the directional solidification of binary alloys. In the limit where GD/VCo(g + fc) is small, the Kuramoto-Sivashinsky equation is obtained. Viscous Phase Transition: Two equations are derived and analyzed which model the dynamics of viscous first order phase transitions. GRA

N88-22154# Air Force Systems Command, Wright-Patterson AFB, Ohio. Foreign Technology Div.
CORROSION AND ELECTROCHEMICAL BEHAVIOR OF BINARY MAGNESIUM ALLOYS
I. Yu. Mukhina, M. A. Timonova, M. B. Altman, and T. I. Yershova 26 Jan. 1988 13 p Transl. into ENGLISH from Tekhnologiya Legk. Splavov. Nauch-Tekh. Byull. Vses. Inst. Legk, Splavov (USSR), no. 4, 1971 p 60-64
(AD-A190624; FTD-ID(RS)T-1384-87) Avail: NTIS HC A03/MF A01 CSCL 11F

A systematic investigation of the effect of 23 elements on the corrosion behavior of magnesium alloys in a 3 percent solution of Sodium Chloride (NaCl) and in a humid atmosphere was carried out. The values of the stationary potentials and the variation of the potentials through times are determined. The purpose of this work is to make a systematic investigation of the effect of alloying additives on the corrosion resistance and electrochemical characteristics of magnesium alloys. It is very interesting to study the corrosion behavior of binary systems, not only from the theoretical standpoint, but also from the practical one, since the selection of systems for developing corrosion resistant alloys would be essentially random without these data. Reports give data about the effect of some elements on the corrosion and electrochemical behavior of magnesium alloys. However, the information in the literature about the systematic investigation of the effect of alloying components on the corrosion characteristics of magnesium alloys is inadequate. GRA

N88-22155# Army Belvoir Research and Development Center, Fort Belvoir, Va.
GALVANIC CORROSION INITIATIVES Final Report, Jan. 1985 - Oct. 1987
Dario A. Emeric, Lisa R. Whiting, and Mark Burns Dec. 1987 31 p
(AD-A190658; BRDEC-2460) Avail: NTIS HC A03/MF A01 CSCL 11F

In the past, there have been a number of material failures in Army equipment. Many of these failures were caused by galvanic corrosion. This research was performed to determine the effect of galvanic reactions on the mechanical properties of high strength materials in aggressive environments. Aluminum alloys, steels, and a graphite-epoxy composite were exposed to various environments, then tested to indicate whether the galvanic corrosion exposed to various environments, then tested to indicate whether the galvanic corrosion which developed was cosmetic or if it had an effect on the mechanical properties of the material. By doing this, the number of failures in military equipment might be reduced. GRA

N88-22156# Pennsylvania State Univ., University Park. Dept. of Materials Science and Engineering.
HIGH TEMPERATURE OXIDATION AND ELECTROCHEMICAL STUDIES RELATED TO HOT CORROSION Annual Technical Report
D.-H. Kim, J. Patton, and G. Simkovich Dec. 1987 26 p
(Contract N00014-86-K-0133)
(AD-A190699) Avail: NTIS HC A03/MF A01 CSCL 07D

This report covers some of the results attained during the past year concerning attempts to elucidating the mechanism(s) at hot corrosion processes. AC impedance tests and Wagner-Hebb type polarization measurements on pure Na2SO4 at 900 C were performed as a function of Na2O activities. These results, to be published in an Electrochem. Soc. Proceedings showed that the conductivties of the pure Na2SO4 were of the order of .257/ohm-cm and varied only slightly with Na2O activity changes. From the Wagner-Hebb type polarization measurements on the pure Na2SO4 it was found that electron conductivity was much higher than electron hole conductivity. Additional tests were conducted to determine: (1) the effect of height of Na2SO4 melts, (2) the effect of electronic short circuiting the Na2SO4 melts with gold wires, and (3) the effect of presaturating the salt melt with corrosion products in the hot corrosion process. However, the amount of Na2SO4 present, which is directly proportional to the height of the melt, does affect the rate of corrosion. This was demonstrated by the decrease in rate observed when the melt was presaturated with the corrosion products. GRA

N88-22157# Lawrence Livermore National Lab., Calif.
DIRECTED-ENERGY ELECTRON-BEAM PROCESSING OF A HYPOEUTECTIC Cr90Ta10 ALLOY
J. S. Huang and E. N. Kaufmann Sep. 1987 13 p Presented at the Meeting on Solidification Processing of Eutectic Alloys, Cincinnati, Ohio, 10 Oct. 1987
(Contract W-7405-eng-48)
(DE88-005621; UCRL-96370; CONF-8710288-1) Avail: NTIS HC A03/MF A01

A hypoeutectic Cr90Ta10 alloy was processed using a directed-energy electron-beam surface melting and resolidification technique to study its microstructure evolution during rapid solidification. The power of the electron beam was 2500 W and the scan speed ranged from 0.13 to 2.0 m/sec. Microstructure characteristics such as transitions from planar front to dendritic growth, and from cellular to dendritic growth were observed. At low solidification rate, the interdendritic regions are characterized by the Cr/Cr2Ta eutectic, and at high solidification rate the intercellular regions are characterized by a Cr2Ta phase. For the latter, the distribution of Ta-solute across the interior of a cell is very uniform. In a given sample, the primary cell spacing increases as the solidification front moves from the substrate/regrowth interface toward the surface. The solidification parameters, i.e., temperature gradient and growth velocity, were determined with finite-element heat flow analyses. The observed microstructure characteristics were correlated to these parameters using available theoretical models. DOE

N88-22158# Sandia National Labs., Albuquerque, N. Mex.
EFFECT OF P IMPLANTATION ON THE CORROSION BEHAVIOR OF Fe-Cr ALLOYS
N. R. Sorensen, R. B. Diegle, S. T. Picraux, and G. C. Nelson 1987 13 p Presented at the 172nd Meeting of the Electrochemical Society, Honolulu, Hawaii, 18 Oct. 1987
(Contract DE-AC04-76DP-00789)
(DE88-005732; SAND-87-1196C; CONF-871027-45) Avail: NTIS HC A03/MF A01

Ion implantation is used to study the corrosion/passivation behavior of glassy metals. The implantation process allows us to alter both the structure and composition of the surface. We are investigating P implantation (100 keV) into Fe-Cr alloys at fluences ranging from 2.3 x 10 to the 16th to 2.5 x 10 to the 17th P/sq cm, which induces a crystalline to amorphous structural transition. We are studying the passivation of implanted and unimplanted Fe-Cr alloys in 0.1N H2SO4 with small (0 to 500 ppM) additions of NaCl. At low Cr (6 at%) concentrations, P implantation improves passivity at applied passive potentials in the Cl-free electrolyte, but it induces pitting when chlorides are present. The improvement in passivity is manifested as an increase in the passivation rate and an increase in the quality of the film, which resists breakdown by Cl ions if they are added after the equilibrium passive film is established. At high Cr concentrations (18 at%) there is little benefit of implanting P because the base alloy is able to form a protective film by virtue of the high Cr content. At intermediate Cr concentrations, P implantation to produce an amorphous surface results in a decrease in current density of four orders of magnitude. For an Fe-10Cr alloy, increasing the P concentration causes a progressive change in corrosion morphology from general attack, through pitting, to passivation. During general attack the corrosion film is unprotective and permits uniform corrosion. In the P range where pitting is observed, a three-dimensional oxide film is present that thickens when passivity is observed. DOE

N88-22159# Oak Ridge National Lab., Tenn.
RESPONSE OF ALUMINUM ALLOYS TO EROSIVE PARTICLE IMPACTS
J. R. Keiser, R. S. Heidersbach, D. L. Dobbs, and W. C. Oliver 1988 12 p Presented at the National Association of Corrosion Engineers Meeting, St. Louis, Mo., 21 Mar. 1988
(Contract DE-AC05-84OR-21400)
(DE88-005910; CONF-880314-2) Avail: NTIS HC A03/MF A01

Erosive particle impacts can result in the high-strain-rate deposition of an appreciable amount of energy into the deformed volume of the target material. This energy likely causes local heating; softening or even melting was observed in many materials. Hardening caused by the high-strain-rate deformation has also been reported for strain-hardenable materials. The effect of individual impacts on the surface of selected aluminum alloys was determined both analytically using theoretical considerations and experimentally using 343 meter diameter tungsten carbide balls impacting at about 30 m/s and 30° incidence angle. After impact a mechanical properties microprobe was used to measure the hardness of both the crater bottom and material just below the original surface. Strain hardening, but no evidence of softening, was observed for two aluminum alloys. DOE

N88-22160# Minnesota Univ., Minneapolis.
CORROSION RESEARCH CENTER, UNIVERSITY OF MINNESOTA Final Report, 1 Sep. 1985 - 31 Oct. 1987
R. A. Oriani Feb. 1988 56 p
(Contract DE-FG02-84ER-45173)
(DE88-006681; DOE/ER-45173/4) Avail: NTIS HC A04/MF A01

Research projects have included investigation of stresses and their relaxation during high-temperature oxidation, hot corrosion, basic studies of the plasma spray process, application of many-body theory to corrosion phenomena, electrochemical passivation, electrochemical modeling, photoelectrochemistry of oxides, electronically conducting polymers, microelectrodes, and investigation of the electrode/electrolyte interface. DOE

N88-22161# Rhode Island Univ., Kingston.
SUMMARY OF THE 1987 GORDON RESEARCH CONFERENCE ON CORROSION Final Report, 19-24 Jul. 1987
G. H. Meier 24 Jul. 1987 15 p Conference held in New London, N.H., 20-24 Jul. 1987
(Grant AF-AFOSR-0314-87)
(AD-A189737; AFOSR-87-1732TR) Avail: NTIS HC A03/MF A01 CSCL 07B

The 1987 Gordon Research Conference on Corrosion covered a cross section of important areas in the field of high temperature corrosion: transport in oxide films, microchemical analysis of oxide films, stresses in oxide films and film adherence, effects of erosion and applied stresses on oxidation, hot corrosion, oxidation of titanium and the refractory metals, and oxidation of silicon and silicon-containing alloys. In addition to the lectures a significant number of papers was also presented. GRA

N88-22162# Edgerton, Germeshausen and Grier, Inc., Idaho Falls, Idaho.
CHARACTERIZATION OF AN EXPLOSIVELY CONSOLIDATED RAPIDLY SOLIDIFIED Fe-16Ni-9Cr-5Mo-2Cu ALLOY POWDER
G. E. Korth, J. E. Flinn, and R. N. Wright 1988 6 p Presented at the 2nd International Conference of Rapidly Solidified Materials, San Diego, Calif., 7 Mar. 1988
(Contract DE-AC07-76ID-01570)
(DE88-006733; EGG-M-12587; CONF-880358-1) Avail: NTIS HC A02/MF A01

Vacuum gas atomized Fe-16Ni-9Cr-4Mo-2Cu alloy powder was dynamically consolidated using explosive techniques. The microstructure and tensile properties were evaluated in the as-shocked condition and after various heat treatments. Results showed the product to be fully dense and in a shock-hardened condition after consolidation. Low bulk temperatures from the dynamic consolidation process allowed retention of the rapidly solidified microstructure of the powder except for the thin interparticle areas where metallurgical bonding (melting) has occurred. Thermal treatments resulted in decreasing strength as ductility increased. Microstructural observations and X-ray line broadening analysis were consistent with the changes in tensile properties. DOE

N88-22163# Centre d'Essais Aeronautique Toulouse (France).
INFLUENCE OF TEMPERATURE ON THE TENSILE STRENGTH AND TOUGHNESS CHARACTERISTICS. MATERIAL 35NCD16 ESR. TEST REPORT M5-521800 [INFLUENCE DE LA TEMPERATURE SUR LES CARACTERISTIQUES DE TRACTION ET DE TENACITE. MATIERE 35NCD16 ESR. PROCES VERBAL M5-521800]
M. Marquier 25 Aug. 1987 42 p In FRENCH
(M5-521800; ETN-88-91991) Avail: NTIS HC A03/MF A01

The mechanical performance of the 35NCD16 ESR steel treated to 1800 to 2000 MPa strength was studied in the temperature interval from -60 to +40C. Toughness drops by 30 percent while the other tensile characteristics are not sensitive to temperature effects. ESA

N88-22164# Centre d'Essais Aeronautique Toulouse (France).
CHARACTERIZATION OF HYTUF STEEL. SEMIFINISHED PRODUCT: 160 mm DIA FORGING BLOCK. PROCESSOR: C3f. TEST REPORT M3-434600 [CARACTERISATION DE L'ACIER HYTUF. DEMI-PRODUIT: BLOC FORGE 160 MM DIA. ELABORATEUR: C3F. PROCES VERBAL M3-434600]
M. Notton 19 May 1987 47 p In FRENCH
(Contract STPA-198/CO)
(M3-434600; ETN-88-91992) Avail: NTIS HC A03/MF A01

The HYTUF high temperature steel was investigated. A thermal treatment was performed to obtain a strength of 1600 MPa. The results obtained are in general very good, in toughness and tensile tests, and show a low anisotropy characteristic. The tenacity is also characterized by relatively high values. ESA

N88-22165# Helsinki Univ. of Technology, Espoo (Finland). Inst. of Process Metallurgy.
ACTIVITIES OF As, Sb, Bi AND Pb IN COPPER MATTES AND THEIR EFFECTS ON IMPURITY ELIMINATION Ph.D. Thesis
Antti Roine 1988 62 p Sponsored by Outokumpu Co. Foundation, Finland
(TKK-V-A10(1988); ISBN-9-51-754289-5; ISSN-0784-3577; ETN-88-92216) Avail: NTIS HC A04/MF A01

The Raoultian activity coefficients of As, Sb, Bi, and Pb were determined as a function of sulfur and oxygen partial pressures over copper mattes at 1200 C. Sulfur pressure has an extremely

significant effect on the activity coefficients, whereas the effect of the oxygen pressure is much smaller. When the sulfur-to-metal ratio of the matte (sulfur pressure) increases from the metal saturation region (0.000001 atm) to the high sulfur pressure region (0.1 atm), the experimental activity coefficients are: As = 0.05 to 38, Sb = 0.34 to 82, Bi = 75 to 3.4, and Pb = 20 to 0.079. The effects of Ni and Co on the activity coefficients are to decrease the activity coefficients of As and Sb at low sulfur pressures, but have no effect at higher pressures. Theory suggests that as can be eliminated by sulfidizing purge gas evaporation; Sb, Bi, and Pb can be eliminated by a combination of the sulfidizing purge gas treatment and chlorination; impurities can be more effectively eliminated from the matte than from the copper using vacuum evaporation; and As and Sb removal by an iron silicate slag can be slightly improved using sulfidation treatment. ESA

N88-22166# Helsinki Univ. of Technology, Espoo (Finland). Lab. of Metal Working and Heat Treatment.
STUDIES ON HOT-DIP ZINC-ALUMINUM COATED SHEET STEELS Ph.D. Thesis
Simo J. Makimattila 1987 108 p Sponsored by the Outokumpu Co. Foundation, Finland and Rasmet Co., Finland
(ETN-88-92217) Avail: NTIS HC A06/MF A01

A hot dip galvanizing technique for production of Zn-Al-alloy coated deep-drawable steel sheet was evaluated by laboratory and industrial experiments. The method, based on the quenching of an extra-low carbon steel strip with liquid eutectic zinc alloy after continuous annealing at 850 C provides a way for the production of deep-drawing quality hot dip galvanized sheet steel. The mechanical properties of the steels are close to those reported for other continuous annealing and quenching processes for cold-rolled, uncoated steels. The high cooling efficiency of the liquid metal bath gives a high supersaturation of carbon in ferrite and thus makes possible the use of a rapid, in-line over-aging process. The structure of the eutectic Zn-5 percent Al coating is different from the same coating produced by conventional hot dip galvanizing practices. The high immersion temperature of the strip enhances formation of a thicker than normal intermetallic layer at the steel surface. The use of the zinc quenching process requires a specially designed heat exchanger and mixing system for the stabilization of the bath temperature during continuous operation. ESA

N88-22167# Helsinki Univ. of Technology, Espoo (Finland). Lab. of Metal Working and Heat Treatment.
STRUCTURE AND PROPERTIES OF TITANIUM NITRIDE AND ZIRCONIUM NITRIDE THIN FILMS PREPARED BY REACTIVE ION PLATING Ph.D. Thesis
Jyrki M. Molarius 1987 83 p Sponsored by the Outokompu Co. Foundation, Finland; Academy of Finland; and the Technology Development Center, Finland
(ETN-88-92218) Avail: NTIS HC A05/MF A01

The performance of triode ion-plated nitride coatings in turning with high speed steel inserts was determined. Coatings studied include NbN, TiN, (Ti, Al) N, and ZrN. The turning tests were carried out without any lubrication. The work material corresponded to AISI 4140 but was calcium-treated for improved machinibility. Taylor curves corresponding to different coatings were compared. The best coating is ZrN. The second is the best variant of the (Ti, Al) N-family containing 33 at. percent Ti, 17 at. percent Al, and 50 at. percent N. The performance of a standard stoichiometric TiN can be improved by increasing the Al-content up to 17 at. percent. At higher contents, the performance decreases. Stoichiometric TiN is the third best coating, and NbN the worst. Although NbN improves tool life, it is not comparable with the other coatings. ESA

N88-22168*# National Aeronautics and Space Administration. Lewis Research Center, Cleveland, Ohio.
BITHERMAL FATIGUE OF A NICKEL-BASE SUPERALLOY SINGLE CRYSTAL
Michael J. Verrilli May 1988 15 p
(NASA-TM-100885; E-4118; NAS 1.15:100885) Avail: NTIS HC A03/MF A01 CSCL 11F

The thermomechanical fatigue behavior of a nickel-base superalloy single crystal was investigated using a bithermal test technique. The bithermal fatigue test was used as a simple alternative to the more complex thermomechanical fatigue test. Both in-phase and out-of-phase bithermal tests were performed on (100)-oriented coated and bare Rene N4 single crystals. In out-of-plane bithermal tests, the tensile and compressive halves of the cycle were applied isothermally at 760 and 982 C, respectively, while for the in-phase bithermal tests the temperature-loading sequence was reversed. The bithermal fatigue lives of bare specimens were shorter than the isothermal fatigue lives at either temperature extreme when compared on an inelastic strain basis. Both in-phase and out-of-phase bithermal fatigue life curves converged in the large strain regime and diverged in the small strain regime, out-of-phase resulting in the shortest lives. The coating had no effect on life for specimens cycled in-phase; however, the coating was detrimental for isothermal fatigue at 760 C and for out-of-phase fatigue under large strains. Author

N88-22217# Joint Publications Research Service, Arlington, Va.
MATERIAL SURFACE IMPROVEMENT BY LASER
Hiromichi Kawasumi *In its* JPRS Report: Science and Technology. Japan 11 Mar. 1988 p 71-89 Transl. into ENGLISH from Kino Zairyo (Tokyo, Japan), v. 7, Aug. 1987 p 59-70 (For primary document see N88-22210 15-31)
Avail: NTIS HC A05/MF A01

N88-22248# Joint Publications Research Service, Arlington, Va.
EVAPORATION CHARACTERISTICS OF ELEMENTS DURING VACUUM ARC REMELTING OF ALLOY A-286
Jie Fu, Yaohe Hu, Junhua Zhao, Yucai Zhao, and Jainzhong Zhu *In its* JPRS Report: Science and Technology. China 11 Dec. 1987 p 67-75 Transl. into ENGLISH from Jinshu Xuebao (Beijing, Peoples Republic of China), v. 22, no. 3, 18 Jun. 1986 p B97-B104 (For primary document see N88-22233 15-31)
Avail: NTIS HC A06/MF A01

N88-22427*# Pratt and Whitney Aircraft, East Hartford, Conn.
FATIGUE DAMAGE MODELING FOR COATED SINGLE CRYSTAL SUPERALLOYS
David M. Nissley *In* NASA. Lewis Research Center, Lewis Structures Technology, 1988. Volume 3: Structural Integrity Fatigue and Fracture Wind Turbines HOST May 1988 p 259-270 (For primary document see N88-22408 15-39)
(Contract NAS3-23939)
Avail: NTIS HC A16/MF A01 CSCL 11F

27 NONMETALLIC MATERIALS

Includes physical, chemical, and mechanical properties of plastics, elastomers, lubricants, polymers, textiles, adhesives, and ceramic materials.

For composite materials see *24 Composite Materials.*

N88-22169# Oak Ridge National Lab., Tenn.
THERMAL CONDUCTIVITY OF OXIDE CERAMICS
R. K. Williams, R. S. Graves, and D. W. Yarbrough 1987 6 p Presented at the 25th Automotive Technology Development Contractor's Coordination Meeting, Dearborn, Mich., 26 Oct. 1987
(Contract DE-AC05-84OR-21400)
(DE88-005842; CONF-8710116-6) Avail: NTIS HC A02

The phonon thermal conductivity of solids depends on temperature, grain size, solute content and the presence of conduction electrons. A study of these effects is reported, the materials studied included Al2O3-base ceramics and bcc Fe-base alloys. For ceramics, the effect of grain size is larger than expected from standard theory. This is not true for metals and also for ceramics at high temperatures. The magnitude of the grain size contribution can be quantitatively predicted by a new theory. The

variation with temperature is as expected from theory and the effect of solute content is almost entirely due to the solute-solvent mass difference. DOE

N88-22170# Allied Bendix Aerospace, Kansas City, Mo.
NMR ANALYSIS OF A FLUOROCARBON COPOLYMER
R. E. Smith and C. H. Smith Oct. 1987 13 p Presented at the 46th Society of Plastics Engineers Annual Technical Conference, Atlanta, Ga., 18 Apr. 1988
(Contract DE-AC04-76DP-00613)
(DE88-002364; BDX-613-3804; CONF-880445-1) Avail: NTIS HC A03/MF A01

Vinylidene fluoride (VF2) can be copolymerized with chlorotrifluoroethylene (CTFE) in an aqueous emulsion using a peroxide chain initiator. The physical properties of the resulting fluorocarbon polymer depend on the ratio of VF2 to CTFE and the randomness of the copolymerization. When CTFE and VF are polymerized in an approximately 3:1 mole ratio, the resulting polymer is soluble in acetone (and other solvents) at room temperature. Using proton and fluorine-19 NMR, the mole ratio of CTFE to VF2, the emulsifier (perfluorodecanoate) concentration, and the randomness of copolymerization can be determined. A trifluorotoluene internal standard is added to a d-acetone solution of the fluoropolymer. Proton NMR is used to determine the amount of VF2. Fluorine-19 NMR is used to measure the amount of emulsifier and the randomness of copolymerization. Each analysis requires about 5 minutes, and is quite precise, with relative standard deviations from 3 to 10 percent (10 replicates analyzed). In addition, the results from NMR analyses agree well with wet chemical analyses. DOE

N88-22171# Sandia National Labs., Albuquerque, N. Mex.
SINGLET OXYGEN BEHAVIOR IN SOLID POLYMER MATRICES
R. L. Clough, Kai-Kong lu, M. P. Dillon, and P. R. Ogilby 1987 10 p Presented at the Symposium on Polymer Photochemistry, Toronto, Ontario, 5 Jun. 1987 Prepared in cooperation with New Mexico Univ., Albuquerque
(Contract DE-AC04-76DP-00789)
(DE88-005171; SAND-87-2319C; CONF-8706276-1) Avail: NTIS HC A02/MF A01

Excited states of dye molecules are efficiently quenched by molecular oxygen. This can give rise to an excited state of the oxygen molecule: singlet oxygen. Singlet oxygen has been most extensively studied in liquid organic solvents and in the gas phase. However, since oxygen is very soluble in most polymers, whenever air is present singlet oxygen could be an important participant in the photophysics and photochemistry of polymeric materials. We are studying the kinetics of both singlet oxygen and its triplet organic dye precursor in aerated, dye-containing polymers. In this report we examine differences in photophysical behavior in glassy and rubbery matrices. DOE

N88-22172# Edgerton, Germeshausen and Grier, Inc., Idaho Falls, Idaho.
FRACTURE TOUGHNESS OF SILICON NITRIDE-SILICON NITRIDE JOINTS BONDED WITH OXYNITRIDE GLASS
D. N. Coon, R. M. Neilson, Jr., J. C. Mittl, and R. L. Tallman 1987 30 p Presented at the Annual Meeting of the American Ceramic Society, Chicago, Ill., 29 Apr. 1987
(Contract DE-AC07-76ID-01570)
(DE88-005548; EGG-M-06086; CONF-8704271-1) Avail: NTIS HC A03/MF A01

An investigation into the feasibility of using oxynitride glass as the bonding material to join silicon nitride was undertaken. Two characteristics of these glasses were the basis for their selection. First, their compatibility with silicon nitride as evidenced by their existence as a grain boundary phase. Second, property changes with nitrogen additions suggest higher temperature capabilities with respect to oxide glass. This communication reports the room temperature fracture toughness of silicon nitride joined with oxynitride glass. DOE

N88-22173# Oak Ridge National Lab., Tenn.
ULTRASONIC CHARACTERIZATION OF CERAMIC JOINTS
W. A. Simpson, Jr. and R. W. McClung 1987 27 p Presented at the International Forum on Joining of Structural Ceramics, Pittsburgh, Pa., 26 Apr. 1987
(Contract DE-AC05-84OR-21400)
(DE88-005844; CONF-8704270-1) Avail: NTIS HC A03/MF A01

We describe the development of ultrasonic techniques for the characterization of ceramic joints, including the ability to determine which face of a 50-micron-thick layer of braze filler metal is unbonded, thus providing information about the integrity of the ceramic-filler metal bond. We also describe the development of a rapid technique using Lamb waves to probe the bond between alumina coupons in flexature-strength specimens, which geometry makes conventional ultrasonic evaluation of the bond difficult. Also described are techniques for the detection of cracking under sessile drops on alumina disks and the determination of the extent and profile of cracks produced in the bond of flexture-strength specimens subjected to three-point bending. DOE

N88-22174# Texas Univ., Austin. Dept. of Chemical Engineering.
SYNTHESIS AND ANALYSIS OF NOVEL POLYMERS WITH POTENTIAL FOR PROVIDING BOTH HIGH PERMSELECTIVITY AND PERMEABILITY IN GAS SEPARATION APPLICATIONS
Progress Report, 20 Dec. 1986 - 20 Dec. 1987
W. J. Koros and D. R. Paul 29 Dec. 1987 9 p
(Contract DE-FG05-86ER-13507)
(DE88-006533; DOE/ER-13507/2) Avail: NTIS HC A02/MF A01

Optimum materials for gas separation membrane applications are being investigated. Permeation, sorption and diffusion characterization of polycarbonates, polysulfones and polyimides has been completed. The chemical structure and permselectivity data for a series of polycarbonates is presented. DOE

N88-22175# Lawrence Livermore National Lab., Calif.
OXIDE OPTICAL COATINGS PREPARED BY METAL-ORGANIC VAPOR DEPOSITION
R. Brusasco 26 Jan. 1988 17 p Presented at the Boulder Damage Symposium, Boulder, Colo., 26 Oct. 1987
(Contract W-7405-eng-48)
(DE88-006809; UCRL-97399; CONF-8710165-10) Avail: NTIS HC A03/MF A01

We prepared films of alumina, zirconia and hafnia by chemical vapor deposition (CVD) for evaluation as high refractive index optical components for high power laser applications. Films with high index of refraction (1.89 to 1.63) but with rather low single shot laser damage thresholds (4 to 10 J/sq cm) were prepared by high temperature (400 C) thermal decomposition. Lower temperature deposition with chemical assist improves some optical properties and laser damage thresholds at the expense of a lower index of refraction. DOE

N88-22176# United Technologies Research Center, East Hartford, Conn.
INVESTIGATION OF LASER DIAGNOSTICS OF PACVD PROCESSES FOR DEPOSITING HARD FACE COATINGS
Performance Report, 1 Feb. 1987 - 31 Jan. 1988
W. C. Roman Feb. 1988 5 p
(Contract DE-FG02-86ER-13560)
(DE88-007083; DOE/ER-13560/2) Avail: NTIS HC A02/MF A01

The objective is to improve the understanding of the mechanisms which govern the nonequilibrium reactive plasma atomistic or molecular deposition of hard face coatings for erosion resistant applications. The goal is to provide a predictive capability that is severely lacking in the present science base of plasma activated chemical vapor deposition (PACVD) processing for depositing hard face coatings. Advanced laser diagnostics will be used to probe the plasma for improving process control. DOE

N88-22177# SpecTran Corp., Sturbridge, Mass.
HERMETIC COATING OF OPTICAL FIBERS Final Report, Oct. 1984 - Jun. 1986
S. Raychaudhuri, Philip S. Levin, and Ray Sierra Nov. 1987 46 p
(Contract F30602-84-C-0199)
(AD-A189886; RADC-TR-87-200) Avail: NTIS HC A03/MF A01 CSCL 20F

Hermetically coated graded index silica fibers were to exhibit proof test levels greater than 200 Kpsi over one kilometer length. Fiber was to exhibit a stress corrosion factor N greater than 100. The dielectric coating materials were to include, but not be limited to diamond-like carbon and boron nitride. Techniques using a hollow cathode discharge coater produced coated fiber with N value less than 26. Severe arcing problems were faced with this technique resulting in large cracks on the coater anodes. An RF plasma coater was built and operated to deposit amorphous hydrogenated carbon (a - C:H) films on bulk deposition fiber samples. Fibers were drawn under a number of conditions to determine the role such factors as vacuum chamber alignment, tension plasma conditions play in the strength of the fiber. A stress corrosion susceptibility factor N = 26 was obtained. In only preliminary experiments with the deposition of silicon nitride coating on the fiber, N values up to 70 were achieved. Keywords: Fiber optics, Protective coating, Hermetic sealing, High strength fiber. GRA

N88-22178# Maine Univ., Orono. Lab. for Surface Science and Technology.
VAPOR PHASE DEPOSITION AND GROWTH OF POLYIMIDE FILMS ON COPPER
M. Grunze, J. P. Baxter, C. W. Kong, R. N. Lamb, and W. N. Unertl 10 Nov. 1987 23 p
(Contract N00014-85-K-0641)
(AD-A189969; TR-4) Avail: NTIS HC A03/MF A01 CSCL 11I

The formation of thin ploylmide films from vapor phase deposited 4,4 Oxydianiline (ODA) and Pyromellitic Dianhydride (PMDA) was studied by X-ray photoelectron spectroscopy and vibrational spectroscopies. Codeposition of ODA and PMDA onto polycrystalline copper substrates at room temperature, followed by heating in vacuum, led to polymerization and the formation of thermally stable polyimide films. Films with thickness ranging from ultra-thin (12 to 30 A) to several hundred nanometers thick were prepared by this method. Adhesion of the polymer to the surface involve chemical bonding to fragments of PMDA and ODA initially chemisorbed on the clean metal surface. GRA

N88-22179# Florida Univ., Gainesville. Center for Macromolecular Science.
DONOR ACCEPTOR POLYMERIZATION CHEMISTRY AS A VEHICLE TO LOW ENERGY CURE MATRIX RESINS Interim Report, Feb. 1986 - Apr. 1987
K. B. Wagener, Choon H. Do, Mike Johnson, and Mark A. Smith Nov. 1987 51 p
(Contract F33615-85-C-5093)
(AD-A190119; AFWAL-TR-87-4093) Avail: NTIS HC A04/MF A01 CSCL 07F

A recent study conducted by the National Materials Advisory Board has identified a need for matrix resins that can be prepared at ambient or near ambient room temperatures for onsite airfoil repair. This research project focuses on this problem through the synthesis of network polymers using donor/acceptor polymerization chemistry. The di and tetrafunctional donors used in this study are based on vinyl ether chemistry, and di and tetrafunctional maleimides are the acceptors. The first objective has been the synthesis of necessary donor and acceptor monomers and a variety of synthetic approaches is studied to create these needed compounds. In the case of donor monomers palladium-assisted vinyl exchange reaction is selected as the best route. Using this chemistry 15 monomers were successfully prepared based on vinyl ether chemistry. An equal number of maleimides were synthesized using a conventional synthetic chemistry, i.e., the reaction of maleic anhydride with amine, followed by condensation of the maleic acid to the maleimide itself. This chemistry requires a great deal of patience, yet if done properly, yields the necessary monomers in high purity. GRA

N88-22180# Honeywell, Inc., Bloomington, Minn. Physical Sciences Center.
RESEARCH ON STABLE PROCESSIBLE CONDUCTING POLYMERS FOR ELECTRONIC APPLICATIONS Final Report, 1 Sep. 1984 - 21 Sep. 1987
Samson A. Jenekhe and Stephen T. Wellinghoff 21 Dec. 1987 9 p
(Contract N00014-84-C-0699)
(AD-A190246) Avail: NTIS HC A02/MF A01 CSCL 20C

The primary objective of this three-year research project was to develop environmentally stable and processible electronically conductive polymers for potential applications in electronics, electro optics, and sensors. Our general approach was to synthesize and characterize several new heteroaromatic polymers and tailor their electronic, optical, and traditional polymer properties for these applications. A further objective was to understand the structure/electronic property relationships in electronically conducting heteroaromatic polymers. Many new electronically conducting polymers containing carbazole in the main chain were synthesized by a variety of synthetic techniques, characterized, and shown to be solution-processible and stable in air with room temperature d.c. conductivities as high as 1 to 10/ohm/cm. The mechanism of electronic conduction in 3,6-linked polycarbazoles was shown to be interchain and intrachain motions of radical cations delocalized over a dimeric unit of the polymer. Several other new conducting polymers were synthesized and characterized, including polydiphenylamines, methylene-bridged polythiophenes, polypyrroles, and polyfurans. The three different classes of conducting polymers, polycarbazoles, polydiphenylamines, and methylene bridged poly hetereocycles prepared in this research effort, provided diverse materials to conduct a comparative study of the conduction mechanisms, electronic structures, and chemical, optical, electrical, and physical properties. GRA

N88-22181# Southern Research Inst., Birmingham, Ala.
DEVELOPMENT OF POLYMERIC FILMS WITH PIEZOELECTRICAL PROPERTIES FROM POLYPEPTIDES; LOW, ODD NYLONS; OR POLYUREAS Final Report, 15 Sep. 1984 - 14 Jun. 1987
James P. English, David P. Vanderbilt, and Gerald W. McNeely Sep. 1987 89 p
(Contract N62269-84-C-0268; DA Proj. RS3-4-A-52; DA Proj. F61-543)
(AD-A190301; SORI-EAS-87-554) Avail: NTIS HC A05/MF A01 CSCL 11I

A 33-month project was undertaken to study piezoelectricity in low, odd nylons; odd, odd nylons; polyureas; and polypeptides. The commercially available polypeptides poly(L alanine), poly(L valine), and poly(L asparagine) were apparently not of sufficiently high molecular weight to provide usable films for piezoelectric testing. Likewise, the polyureas synthesized -poly(trimethyleneurea), poly(pentamethyleneurea), and poly(1,2-propylene diisocynate) were also poor film-forming materials. Consequently, most of the efforts were devoted to synthesizing film-forming nylons. High molecular-weight nylon 5 was prepared via anionic ring-opening polymerization of piperidone. Films of high quality were solvent cast from trifluoroethanol, and these films were poled in the presence and absence of a plasticizer (2-ethyl-1,3-hexanediol). The highest values of the piezoelectric strain (d31) and stress (e31) constants obtained were for plasticized nylon 5 to 1.3 pC/N and 2.8 mC/m2 respectively. GRA

N88-22182# North Carolina Univ., Chapel Hill. Dept. of Chemistry.
TEMPERATURE-DEPENDENT CONDUCTIVITY OF OXYGEN-DEPLETED YBCO CERAMICS
J. H. Miller, Jr., B. Liu, W. J. Riley, A. N. DiBianca, and S. L. Holder 9 Jan. 1988 11 p

(Contracts N00014-76-C-0816; N00014-86-K-0608)
(AD-A190340; TR-29) Avail: NTIS HC A03/MF A01 CSCL 11B

The electrical conductivity of the oxygen depleted material YBa2Cu3O6.4 has been determined as a function of temperature. The conductance is more accurately described as variable range hopping between localized states than as activated conductivity characteristic of a semiconductor. GRA

N88-22183# Rockwell International Corp., Thousand Oaks, Calif. Science Center.
TRANSFORMATION TOUGHENING OF CERAMICS Annual Report No. 2, 1 Sep. 1986 - 31 Aug. 1987
D. B. Marshall Oct. 1987 124 p
(Contract F49620-85-C-0143)
(AD-A190399; SC5444.AR; AFOSR-87-1854TR) Avail: NTIS HC A06/MF A01 CSCL 11B

The mechanical properties of high toughness magnesia partially stabilized zirconia were found to be severely degraded by a single cooling cycle between room temperature and 196 C. In situ Raman spectroscopy and optical interference measurements, and room temperature X-ray diffraction were used to correlate the changes in mechanical properties with structural changes; cooling to temperatures below approximately -100 C caused transformation of most of the tetragonal precipitates that are responsible for toughening to a new phase was stable with heating to 300 C, but at 400 C it transformed back to the tetragonal structure. After heating to 400 C the original high toughness mechanical properties were also restored. A new approach for measuring the nature and distribution of strains within transformation zones surrounding cracks in transformation toughened materials was demonstrated, using Mg-PSZ. The method involves measuring out-of-plane distortions adjacent to a surface-breaking crack and comparing the measurements with computed displacements. The fraction of transformation was found to be a strongly varying function of distance from the crack plane. GRA

N88-22184# Northrop Services, Inc., Dayton, Ohio. Environmental Sciences.
EVALUATION OF THE ACUTE TOXICITY OF A SYNTHETIC POLYALPHAOLEFIN-BASED HYDRAULIC FLUID Technical Report, Jun. 1986 - May 1987
E. R. Kinkead, B. T. Culpepper, S. S. Henry, D. L. Pollard, and E. C. Kimmel Nov. 1987 37 p
(Contract F33615-85-C-0532)
(AD-A190412; AAMRL-TR-87-053; NMRI-87-55) Avail: NTIS HC A03/MF A01 CSCL 06K

In contingency planning for alternative hydraulic fluids in the event that critical shortages should occur in the supply of petroleum based fluids, the U.S. Navy has investigated various synthetic compounds including polyalphaolefins. Earlier toxicity assessments (1983) on five formulations of polyalphaolefin hydraulic fluids and a base fluid indicated that one formation (N501) was toxic via inhalation. This material was reformulated (now designated B85-174) and retested along with its base polyalphaolefin (R-1061-3). The LC50 values for the reformulated hydraulic fluid B85-174 were 1.60 and 1.37 mg/L for male and female rats, respectively. Nor was the material irritating to the skin or eyes treated of treated rabbits. Similar results were obtained from tests on the base polyalphaolefin used for comparison. In contrast, the previous base material demonstrates con inhalation toxicity. The 1983 and 1986 polyalphaolefin base materials were obtained from different suppliers and infrared analysis demonstrated compositional differences. GRA

N88-22185# Texas Univ., Arlington. Dept. of Chemistry.
ELECTRONIC AND IONIC TRANSPORT IN POLYMERS Quarterly Technical Report No. 4, 1 Oct. - 31 Dec. 1987
Martin Pomerantz, John R. Reynolds, Krishnan Rajeshwar, Dennis S. Marynick, and Timothy D. Shaffer 31 Dec. 1987 7 p
(Contract N00014-86-K-0769)
(AD-A190434) Avail: NTIS HC A02/MF A01 CSCL 07F

Ethylmercapto-substituted polythiophenes have been studied and the results have been compared to theoretically derived band structure and oligomer conformation. The quartz crystal microbalance has been shown to be an effective tool for studying ion exchange in doped conjugated polymers. Electrochemical studies of anion exchange in free standing polypyrrole tosylate membranes has been completed. The luminescence modulation of an interfacial probe during redox switching of polypyrrole has been shown to reflect the conductivity. PRDDO and ab initio spin density calculations have been correlated with the ability of a heteroaromatic monomer to be polymerized electrochemically. Similarly, conductivities have been correlated to both electronic structure and conformation of the polymer. Poly(azomerthine) ethers have been prepared with a variety of (CH2)n spacer groups and these have been studied for their liquid crystalline properties. GRA

N88-22186# Texas Christian Univ., Fort Worth. Dept. of Chemistry.
NEW PHOSPHORUS BASED POLYMER SYSTEMS Final Report, Jun. 1984 - Sep. 1987
Robert H. Neilson 25 Jan. 1988 5 p
(Contract N00014-79-C-0632)
(AD-A190457) Avail: NTIS HC A02/MF A01 CSCL 07F

This report summarizes the results obtained on this contract during the period 6/84 to 9/87 dealing with the synthesis, characterization, and reactivity of new phosphorus based polymers and their precursors. Some results in a new area of boron-nitrogen chemistry are also reported. Lists of personnel working on the contract and the publications arising from it are included. GRA

N88-22187# National Bureau of Standards, Gaithersburg, Md. Ceramics Div.
STRESS CORROSION OF CERAMIC MATERIALS Annual Report, 1 Oct. 1985 - 30 Sep. 1986
S. W. Freiman, G. S. White, T. L. Baker, S. M. Wiederhorn, and T. D. Coyle Nov. 1987 64 p
(Contract N00014-86-F-0022)
(AD-A190501) Avail: NTIS HC A04/MF A01 CSCL 11B

Environmentally enhanced crack growth data was obtained on Gallium Arsenide in water and methanol. No effect of ammonia was observed. Strains in the liquid encapsulated Czochralski (LEC)/GaAs crystals were mapped using X-ray topography. Critical fracture toughness and dynamic fatigue data were obtained on capacitor ceramics of varying composition and microstructure. A wide range of values for KIC and crack growth exponent, N, were observed. Collaborative work with Draper Labs and North American Phillips was performed in an effort to develop a non-destructive crack detection procedure. GRA

N88-22188# Durham Univ. (England). Dept. of Chemistry.
A NEW APPROACH TO HIGHLY FLUORINATED LUBRICANTS Final Report, 1 Sep. 1982 - 31 Aug. 1987
Richard D. Chambers, Peter T. Telford, and Michael W. West 30 Oct. 1987 33 p
(Grant AF-AFOSR-0084-82)
(AD-A190523; AFOSR-87-1762TR) Avail: NTIS HC A03/MF A01 CSCL 11H

Perfluorinated polyethers constitute an important class of materials that demonstrate exceptional chemical and thermal stability, amongst organic liquids, and some of these materials show good lubricant properties. Consequently, such materials are of special interest to the U.S.A.F. as lubricants in agressive environments and, particularly, as potential liquid lubricants for high temperature/high efficiency aero engines. The aim of this project is to explore new approaches to the synthesis of perfluorinated ethers because the main problem that limits the wider application of industrially available materials is their high cost, which is an inevitable consequence of the limited methodology available. GRA

N88-22189# SRI International Corp., Menlo Park, Calif.
THE CORROSION RESISTANCE OF AN ALUMINUM ALLOY COATED WITH POLYSILAZANE DERIVED CERAMICS Technical Report No. 11, May 1986 - May 1987
S. J. Lenhart, Y. D. Blum, and R. M. Laine 20 Dec. 1987 15 p
(Contracts N00014-84-C-0392; N00014-85-C-0668)
(AD-A190703) Avail: NTIS HC A03/MF A01 CSCL 11F

Aluminum plates were dip coated in a poly N methylsilazane, solution. Heating process at 400 C transformed the inorganic polymer into coatings that exhibited good corrosion resistance characteristics in a marine environment relative to the bare metal as measured and interpreted by electrochemical methods. The corrosion rate was inhibited by almost one order of magnitude. No microscopic degradation of the coatings was observed after 21 days of measurement, which confirms the stability of the coatings as determined by the electrochemical technique. GRA

N88-22190# Cincinnati Univ., Ohio. Dept. of Chemistry.
HIGH-PERFORMANCE POLYMERIC MATERIALS Final Report, 1 Nov. 1982 - 31 Oct. 1987
J. E. Mark 7 Dec. 1987 233 p
(Grant AF-AFOSR-0027-83)
(AD-A190708; AFOSR-87-2011TR) Avail: NTIS HC A11/MF A01 CSCL 07F

A variety of theoretical methods were used to elucidate the structure and properties of rigid rodlike polymer chains which are of interest as high-performance polymeric materials. Semi-empirical molecular mechanics methods were used to calculate the intramolecular and intermolecular energies pertinent to conformational flexibility and chain packing effects. Also, geometry optimized CNDO/2 molecular orbital calculations were carried out to investigate the structure and conformational characteristics of the rodlike polymers, in both the unprotonated and protonated states. Electronic band gap calculations within the extended Huckel approximation were carried out to elucidate the packing and electronic properties of these chains in the crystalline state. GRA

N88-22191# National Bureau of Standards, Gaithersburg, Md. Ceramics Div.
STRENGTH AND MICROSTRUCTURE OF CERAMICS Annual Report, 1 Oct. 1986 - 30 Sep. 1987
Brian R. Lawn, Peter L. Swanson, Carolyn J. Fairbanks, Bernard J. Hockey, and Yiu-Wing Mai Nov. 1987 38 p
(Contract AFOSR-ISSA-87-0034; AF Proj. 2306)
(AD-A190712; AFOSR-87-2041TR) Avail: NTIS HC A03/MF A01 CSCL 11B

Our goal in this program continues to be the understanding of the role of microstructure in the strength properties of ceramics. It is becoming increasingly apparent to the brittle fracture community that the toughness characteristics and flaw distributions of structural ceramics can be very much influenced, sometimes with great sensitivity, by small details in the microstructural makeup. For instance, the addition of less than 1 percent glassy phase to the grain boundaries of alumina polycrystals can alter the fracture properties dramatically, giving rise to significant improvements in strength. GRA

N88-22192# Sandia National Labs., Albuquerque, N. Mex.
A THREE-DIMENSIONAL MODEL FOR THE ELASTIC PROPERTIES OF A FOAM
W. E. Warren and A. M. Kraynik 1988 5 p Presented at the 7th International Conference on Deformation, Yield and Fracture of Polymers, Cambridge, United Kingdom, 11 Apr. 1988
(Contract DE-AC04-76DP-00789)
(DE88-006197; SAND-87-3065C; CONF-880475-1) Avail: NTIS HC A02/MF A01

A strain energy function that describes the nonlinear elastic response of a 3-D open-cell foam is developed. A tetrahedral unit cell containing four half-struts that join at equal angles represents essential features of foam microstructure. The deformation of a strut is expressed by compliances for bending and stretching, which are the primary mechanisms for small and large distortion, respectively, of a low-density foam. Higher-order contributions to the strain energy are determined by assuming that the structure is effectively pin jointed. DOE

N88-22193# Pittsburgh Univ., Pa. Dept. of Materials Science and Engineering.
HIGH TEMPERATURE CORROSION OF CERAMICS Final Report
J. R. Blachere and F. S. Pettit 30 Dec. 1987 113 p
(Contract DE-FG02-84ER-45117)
(DE88-006567; DOE/ER-45117/3) Avail: NTIS HC A06/MF A01

Materials investigated were silica, alumina, silicon nitride and silicon carbide. In addition to the purer single crystals or CVD materials, typical engineering materials of various purities were included except for the silica which was vitreous. The corrosion conditions were hot corrosion in which gaseous corrosion was enhanced by Na2SO4 deposits. Some gaseous corrosion and oxidation experiments were also performed. The hot corrosion was studied at 1000 C and at lower temperatures, in presence of pure oxygen and oxygen containing SO2 and SO3 (usually 1 percent SO2 in 1 atm O2 at room temperature). In general the extent of the degradation was small and weight changes were negligible or very small. The changes in morphology of the surfaces were observed in the scanning electron microscope. This instrument and the related X-ray microanalysis were the major tools of this research. A method of measurement of oxide thickness in the electron microprobe was developed for the experiments on silicon nitride and silicon carbide. The hot corrosion was strongly influenced by the impurity content of the aluminas, silicon nitrides and silicon carbides. The environmental conditions and the impurities affect the wetting (and corrosion) of the substrates by the sulfate. Bulk silica degrades in presence of Na2SO4 by devitrification and spalling. Alumina corroded more under acidic conditions. The morphologies of the corroded silicon nitrides and silicon carbides were studied in detail. DOE

N88-22194*# Utah Univ., Salt Lake City. Dept. of Materials Science and Engineering.
A TEST FOR INTERFACIAL EFFECTS AND STRESS TRANSFER IN CERAMIC MATRIX COMPOSITES Progress Report, 1 Sep. 1987 - 1 Apr. 1988
23 May 1988 25 p
(Grant NAG2-444)
(NASA-CR-182758; NAS 1.26:182758) Avail: NTIS HC A03/MF A01 CSCL 11C

A test specimen was devised for measuring stress transfer between a high modulus fiber and a ceramic matrix. Single filaments of SiC were embedded in chemically vapor deposited SiC on a thin plate of molybdenum. The CVD overcoating which encapsulated the fiber was continuous with a coating of SiC on the molybdenum. When placed in a microtensile test device and loaded in the fiber direction, the fiber fracture characteristics provide information on the fiber/matrix adhesion and stress transfer. Problems were encountered due to the formation of a weak boundary between the SiC and the molybdenum which obviated any meaningful tensile tests. Also, the high CVD temperature used in fabricating these specimens restrict the fiber, matrix (and substrate) to materials having similar thermal coefficients of expansion in order to minimize thermal stresses. Author

N88-22195# Swedish Inst. for Materials Testing, Boras.
CONTINUAL CAPILLARY VISCOSIMETRY USING EXTRUSIOGRAPH TECHNIQUES
J. Hetenyi, C. Lagerquist, and B. Sjoeblom 1987 29 p
(PB88-166293; SP-RAPP-1987:19; ISBN-91-7848-060-4) Avail: NTIS HC A03/MF A01 CSCL 11B

The report is intended to provide means of determining the rheological properties of molten polymers, such as thermoplastic elastomers over a range of temperatures by continual capillary viscosimetry with Extrusiograph techniques. GRA

N88-22196# Technische Hogeschool, Eindhoven (Netherlands).
MECHANICAL BEHAVIOUR OF PARTICLE FILLED THERMOPLASTICS Ph.D. Thesis
P. H. T. Vollenberg 29 Sep. 1987 130 p
(PB88-169297) Avail: NTIS HC A07/MF A01 CSCL 11B

An investigation of the mechanical behavior of composite materials under load is reported. The composites consist of a dispersion of inorganic fillers in a polymer matrix. A model is described that makes it possible to calculate the stress at which the loss of contact between the filler and polymer occurs. The model is extensively experimentally tested, under variation of a number of parameters. The kind and the shape of the filler particles have a noticeable influence on the modulus. In addition, adding fillers to polymers has a generally decreasing effect on the fracture behavior of the materials. GRA

N88-22197*# Illinois Univ., Urbana-Champaign. Dept. of Materials Science and Engineering.
HAFNIA-RICH MIXED OXIDE CERAMICS OF THE SYSTEM HfO2-ZrO2-TiO2 FOR HEATERS AND HEAT EXCHANGERS IN ELECTROTHERMAL THRUSTERS: THE EFFECTS OF TITANIA ON SELECTED ELECTRICAL AND MECHANICAL PROPERTIES OF HAFNIA-RICH MIXED OXIDES IN THE SYSTEM HAFNIA-ZIRCONIA-TITANIA, VOLUME 1
Paul Russell Staszak, G. P. Wirtz, M. Berg, and S. D. Brown May 1988 146 p
(Grant NAG3-495)
(NASA-CR-182800-Vol-1; NAS 1.26:182800-Vol-1) Avail: NTIS HC A07/MF A01 CSCL 11B

A study of the effects of titania on selected properties of hafnia-rich mixed oxides in the system hafnia-zirconia-titania (HZT) was made in the region 5 to 20 mol percent titania. The studied properties included electrical conductivity, thermal expansion, and fracture strength and toughness. The effects of titania on the properties were studied for the reduced state as well as the oxidized state of the sintered mixed oxides. X-ray analysis showed that the materials were not always single phase. The oxidized compositions went from being monoclinic solid solutions at low titania additions to having three phases (two monoclinic and a titanate phase) at high additions of titania. The reduced compositions showed an increasing cubic phase presence mixed with the monoclinic phase as titania was added. The electrical conductivity increased with temperature at approximately 0.1 mhos/cm at 1700 C for all compositions. The thermal expansion coefficient decreased with increasing titania as did the monoclinic to tetragonal transformation temperature. The fracture strength of the oxidized bars tended to decrease with the addition of titania owing to the presence of the second phase titania. The fracture strength of the reduced bars exhibited a minimum corresponding to a two-phase region of monoclinic and cubic phases. When the second phases were suppressed, the titania tended to increase the fracture strength slightly in both the oxidized and reduced states. The fracture toughness followed similar trends. Author

N88-22198# Pacific Northwest Labs., Richland, Wash.
GAMMA-RAY DENSITOMETRY: NONDESTRUCTIVE ANALYSIS OF DENSITY EVOLUTION DURING CERAMIC POWDER PROCESSING
C. H. Schilling, G. L. Graff, W. D. Samuels, and I. A. Aksay Feb. 1988 14 p Presented at the Conference on Atomic and Molecular Processing of Electronic and Ceramic Materials: Preparation, Characterization and Properties, Seattle, Wash., 31 Aug. 1987 Prepared in cooperation with Washington Univ., Seattle
(Contract DE-AC06-76RL-01830)
(DE88-006671; PNL-SA-15179; CONF-870878-5) Avail: NTIS HC A03

Gamma-ray attenuation measurements enable nondestructive analysis of density heterogeneities which evolve during the processing of ceramics and ceramic composites by powder consolidation methods. A densitometer apparatus has been constructed at the Pacific Northwest Laboratory for in situ measurement of porosity and composition as a function of time and position during powder compaction and sintering. Attenuation experiments were performed with aqueous suspensions of colloidal alpha-Al2O3 to evaluate the sensitivity of the gamma-ray densitometer and also to investigate the role of pH on compaction processes during sedimentation. One of the concerns with this technique is whether gamma radiation degrades sample solvents or dispersing agents; no evidence of radiation damage was revealed in aqueous polymer solutions, based on analysis with gas chromatography, ion chromatography, and nuclear magnetic resonance spectroscopy. DOE

N88-22199# Sandia National Labs., Albuquerque, N. Mex.
MELT PROCESSING CERAMIC YBa2Cu3O(SUB 6.9)
R. J. Baughman, D. S. Ginley, J. F. Kwak, B. Morosin, and E. L. Venturini 1988 8 p Presented at the Spring Meeting of the Materials Research Society, Reno, Nev., 4 Apr. 1988
(Contract DE-AC04-76DP-00789)
(DE88-007039; SAND-88-0486C; CONF-880408-2) Avail: NTIS HC A02/MF A01

The practical utilization of high T(sub c) superconductors will depend on achieving materials properties optimized for the particular application. Properties crucial for almost all applications are critical current density, mechanical properties, processibility, and environmental stability. The best way to achieve these in anisotropic YBa2Cu3O(sub 6.9) is to have completely dense, aligned oxygenated material with minimal grain boundary disruption of the lattice. This paper presents preliminary work on the melt processing of YBa2Cu3O(sub 6.9) under high oxygen overpressures. The material obtained to date is very close to theoretical density, essentially single phase, superconducting and mechanically robust. DOE

N88-22212# Joint Publications Research Service, Arlington, Va.
COMPOUND CERAMIC PROCESSING
Mamoru Okutomi *In its* JPRS Report: Science and Technology. Japan 11 Mar. 1988 p 8-25 Transl. into ENGLISH from Kino Zairyo (Tokyo, Japan), v. 7, Aug. 1987 p 11-24 (For primary document see N88-22210 15-31)
Avail: NTIS HC A05/MF A01

N88-22214# Joint Publications Research Service, Arlington, Va.
FINE GRAIN DEVELOPMENT BY LASER CVD
Kiyoshi Sawano *In its* JPRS Report: Science and Technology. Japan 11 Mar. 1988 p 36-46 Transl. into ENGLISH from Kino Zairyo (Tokyo, Japan), v. 7, Aug. 1987 p 33-39 (For primary document see N88-22210 15-31)
Avail: NTIS HC A05/MF A01

N88-22215# Joint Publications Research Service, Arlington, Va.
SUPERFINE GRAIN DEVELOPMENT BY LASER
Akira Matsunawa *In its* JPRS Report: Science and Technology. Japan 11 Mar. 1988 p 46-59 Transl. into ENGLISH from Kino Zairyo (Tokyo, Japan), v. 7, Aug. 1987 p 40-49 (For primary document see N88-22210 15-31)
Avail: NTIS HC A05/MF A01

N88-22216# Joint Publications Research Service, Arlington, Va.
HARD CERAMIC FILM BY LASER PVD
Shinei Mineda and Nobuo Yasunaga *In its* JPRS Report: Science and Technology. Japan 11 Mar. 1988 p 59-70 Transl. into ENGLISH from Kino Zairyo (Tokyo, Japan), v. 7, Aug. 1987 p 50-58 (For primary document see N88-22210 15-31)
Avail: NTIS HC A05/MF A01

N88-22227# Joint Publications Research Service, Arlington, Va.
FUNCTION OF JAPAN FINE CERAMICS CENTER DESCRIBED
In its JPRS Report: Science and Technology. Japan 3 Mar. 1988 p 82-85 Transl. into ENGLISH from Nikko Materials (Tokyo, Japan), Sep. 1987 p 3-7 (For primary document see N88-22218 15-31)
Avail: NTIS HC A05/MF A01

N88-22229# Joint Publications Research Service, Arlington, Va.
DEVELOPMENTS IN CERAMIC SUPERCONDUCTING MATERIALS

Eizo Yamaka *In its* JPRS Report: Science and Technology. Japan 27 Oct. 1987 p 1-6 Transl. into ENGLISH from Nikko Materials (Tokyo, Japan), Jul. 1987 p 12 (For primary document see N88-22228 15-31)
Avail: NTIS HC A07/MF A01

N88-22409*# National Aeronautics and Space Administration. Lewis Research Center, Cleveland, Ohio.
MONOLITHIC CERAMIC ANALYSIS USING THE SCARE PROGRAM
Jane M. Manderscheid *In its* Lewis Structures Technology, 1988. Volume 3: Structural Integrity Fatigue and Fracture Wind Turbines HOST May 1988 p 5-20 (For primary document see N88-22408 15-39)
Avail: NTIS HC A16/MF A01 CSCL 11B

N88-22410*# Cleveland State Univ., Ohio.
WHISKER-REINFORCED CERAMIC COMPOSITES FOR HEAT ENGINE COMPONENTS
Stephen F. Duffy *In* NASA. Lewis Research Center, Lewis Structures Technology, 1988. Volume 3: Structural Integrity Fatigue and Fracture Wind Turbines HOST May 1988 p 21-40 (For primary document see N88-22408 15-39)
(Contract NCC3-81)
Avail: NTIS HC A16/MF A01 CSCL 11B

N88-22411*# Cleveland State Univ., Ohio.
CONTINUOUS FIBER CERAMIC MATRIX COMPOSITES FOR HEAT ENGINE COMPONENTS
David E. Tripp *In* NASA. Lewis Research Center, Lewis Structures Technology, 1988. Volume 3: Structural Integrity Fatigue and Fracture Wind Turbines HOST May 1988 p 41-61 (For primary document see N88-22408 15-39)
(Contract NCC3-81)
Avail: NTIS HC A16/MF A01 CSCL 11B

28 PROPELLANTS AND FUELS

Includes rocket propellants, igniters, and oxidizers; their storage and handling procedures; and aircraft fuels.

For related information see also *07 Aircraft Propulsion and Power, 20 Spacecraft Propulsion and Power,* and *44 Energy Production and Conversion.*

N88-22200# Wayne State Univ., Detroit, Mich. Center for Automotive Research.
CETANE SCALE EVALUATION AND POSSIBLE MODIFICATION Final Report, 1 Sep. 1984 - 31 Aug. 1987
Naeim A. Henein 23 Dec. 1987 118 p
(Contract DAAG29-84-K-0164)
(AD-A189730; ARO-21397.2-EG) Avail: NTIS HC A06/MF A01 CSCL 21D

An evaluation is made of the validity and accuracy of the cetane scale in rating fuels used in diesel engines. Six problems have been identified, analyzed and possible solutions have been proposed. Three of the problems are intrinsic to the scale and are related to its inability to rate low ignition quality fuels, instability of the ignition delay meter and the inconformity of the Cooperative Fuels Research (CFR) combustion system with actual diesel systems. The other three problems are related to fuels and engines. These are the invalidity of C.N. in correlating the ignition delay data, its inaccuracy in ranking overall engine performance and emissions and its inability in rating the cold startability of engines on different fuels. The cold startability problem is investigated in two engines, under steady and actual starting conditions in a cold room. Also, a mathematical model is developed to predict the startability of the engine. These investigations indicate very clearly that the cetane rating is a hot engine, high temperature test and is unable to rate the cold startability of diesel engines. Cetane number; Diesel fuels. GRA

N88-22201# Virginia Polytechnic Inst. and State Univ., Blacksburg. Dept. of Engineering Science and Mechanics.
CRACK OPENING AND EXTENSION IN INERT SOLID PROPELLANT. AN EXPERIMENTAL STUDY Final Report, 30 Sep. 1985 - 31 Mar. 1987
D. Post, C. W. Smith, and R. Czarnek Sep. 1987 121 p
(Contract F04611-85-C-0098)
(AD-A189808; AFAL-TR-87-043) Avail: NTIS HC A06/MF A01 CSCL 21I

When cracks occur in rocket motor grains, they may significantly alter the subsequent motor performance. Consequently as performance requirements are advanced, it becomes critical to incorporate fracture control concepts into the evaluation of the structural integrity of motor grains. While most such concepts are typically based on two-dimensional analysis, the motor geometry and conditions of use suggest the presence of significant three-dimensional effects. Over the past decade, attempts have been made to develop mathematical models for predicting fracture behavior in rocket motors but model validation has been inhibited by lack of an extensive data base for validating three-dimensional effects. Moreover, certain such effects have only recently been identified, and have not been evaluated for rocket propellant. In particular, the near tip behavior of cracks in solid propellant material during opening and extension of the crack needs to be quantified experimentally. GRA

N88-22202# Naval Surface Weapons Center, Silver Spring, Md.
EFFECT OF MOISTURE LEVEL IN PBXW-109(E) (PLASTIC-BONDED EXPLOSIVE) MIXES ON THE AGING OF THE CURED EXPLOSIVE Final Report
Rolf H. Renner Feb. 1987 49 p
(AD-A190200; NSWC/TR-86-104) Avail: NTIS HC A03/MF A01 CSCL 19A

Initial water content in PBXW-109(E) explosive was varied from 0.01 to 0.75 percent in order to determine the limit at which the explosive formulation would still meet all specification requirements. The above objective could not be accomplished. Irrespective of initial water content, at each end of cycle, the mix was found to be dry (0.01 percent water). This was caused by water being evaporated as a result of the vacuum pulled during mixing. Data are presented on the variations in end-of-mix viscosity, pot-life and cure time. It appears that variations in these properties are due to the effect of water on the catalyst and binder ingredients during initial cycles of the mixing procedures. GRA

N88-22203# Southwest Research Inst., San Antonio, Tex.
DEVELOPMENT OF A LABORATORY TEST FOR MULTIPORT INJECTOR DEPOSITS: APPROACHES 1 AND 2 Final Report
L. L. Stavinoha, R. M. Estefan, and H. W. Marbach, Jr. Sep. 1987 56 p
(Contract DAAK70-85-E-0054)
(AD-A190697; SwRI-4765/1) Avail: NTIS HC A04/MF A01 CSCL 21D

A novel approach for measuring MPFI (Multiport Fuel Injectors) injector deposit-forming tendencies of fuel is evaluated. By slowly coating a cylindrical metal surface with a thin film of gasoline and applying sufficient amounts of heat in alternate cycles of coating and soaking, two critical requirements of deposit formation were used. The deposit generated from a known injector-fouling fuel (fuel A) were measured gravimetrically and compared to a relatively clean fuel (fuel C). Significantly greater concentrations of deposits were measured from fuel A when compared to fuel C. Fuel A was treated with 2 different types of additives (polymeric and amine) form 4 different manufactures at high, clean-up levels and low, keep-clean concentrations and evaluated by the Bomb Method. Very few deposits were measured by any of the additive-treated fuels at high or low treatment levels. Greatly reduced levels of each additive in fuel A were tested for additive response by measuring deposit formation of as a function of additive concentration. Several additives appeared to begin losing their efficacy at lower concentrations in fuel A. With improved design of the delivery system and optimization of experimental parameters,

the Bomb Method promises to be a viable bench test method for measuring the deposit-forming tendencies of fuel. GRA

N88-22204# Mobil Research and Development Corp., Paulsboro, N.J.
EVALUATION OF DIRECT METHANE CONVERSION TO HIGHER HYDROCARBONS AND OXYGENATES Final Report
J. C. W. Kuo Aug. 1987 218 p
(Contract DE-AC22-86PC-90009)
(DE88-003812; DOE/PC-90009/3) Avail: NTIS HC A10/MF A01

This report describes evaluation studies on processes that directly convert methane to higher hydrocarbons and oxygenates (without formation of H2 and CO as intermediates). The direct methane conversion processes were first screened through preliminary evaluations, including thermochemical calculations, some scoping calculations of the thermal and carbon efficiencies, and summary of the advantages, disadvantages, and recommendations of each direct conversion process. Two processes were then selected for more detailed evaluation. As a standard of process comparison, two cases of a conventional Natural Gas-to-Methanol via Steam Reforming process were established. The detailed evaluation included designs of a base case and several sensitivity cases, heat and material balance calculations, and calculations of the thermal and carbon efficiencies and the process duties (the heat transfer, and gas compression and expansion). With high methanol selectivities (greater than 80 percent) and reasonable conversions (greater than 7.5 percent), the Direct Partial Oxidation route was far superior to the standard indirect conversion route, particularly in the heat transfer duties. The process scheme was simple because of simple products and easy product separation. Recommendations for future work are given, including a thorough evaluation of the potential advantages of emerging indirect conversion technologies. DOE

N88-22205# Oak Ridge National Lab., Tenn.
TECHNICAL HIGHLIGHTS OF THE ALTERNATIVE FUELS UTILIZATION PROGRAM
R. L. Graves 1987 7 p Presented at the 25th Automotive Technology Development Contractor's Coordination Meeting, Dearborn, Mich., 26 Oct. 1987
(Contract DE-AC05-84OR-21400)
(DE88-005064; CONF-8710116-7) Avail: NTIS HC A02/MF A01

The Alternative Fuels Utilization Program currently encompasses two significant projects in alternative transportation fuels: (1) the Alternative Fuels Utilization Project, a long-range activity of applied research and development, (2) The Federal Methanol Fleet Project, an effort initiated by Congress to introduce methanol vehicles into the fleet of federally-owned vehicles. The overall objectives and summaries of activities are described in this paper. DOE

N88-22206# Sandia National Labs., Albuquerque, N. Mex.
STABILITY OF THE HIGH-TEMPERATURE G-16 PRIMER COMPOSITION
N. A. Durand, R. R. Weinmaster, T. A. Massis, and W. Fleming 1988 7 p Presented at the American Defense Preparedness Association Compatibility Symposium, New Orleans, La., 18 Apr. 1988 Prepared in cooperation with Unidynamics, Phoenix, Ariz.
(Contract DE-AC04-76DP-00789)
(DE88-006201; SAND-87-2191C; CONF-880473-1) Avail: NTIS HC A02/MF A01

The stability of the G-16 pyrotechnic primer mixture of antimony sulfide, calcium silicide, and potassium chlorate was studied at temperatures up to 200 C in sealed and open environments. Data have shown that this mixture is stable in open environments at 200 C for up to 48 hours. However, in sealed, limited volume environments, the mixture completely decomposes within 24 hours at 200 C. In sealed environments, the mixture shows stability with copper present. Both functional testing and chemical analysis were used to evaluate the primer composition after temperature exposure. The degree of degradation of the mixture was determined from the concentration of final reaction products (sulfate and chloride ions), using ion chromatography. When copper was present, the intermediate reaction products were scavenged by the copper, and the degradation was reduced. The role of copper in the reaction was verified with differential scanning calorimetry and surface analysis. DOE

29 MATERIALS PROCESSING

Includes space-based development of products and processes for commercial applications.
For biological materials see *55 Space Biology.*

N88-22207*# Worcester Polytechnic Inst., Mass. Dept. of Mechanical Engineering.
PRELIMINARY MARKET ANALYSIS FOR LARGE ZEOLITE CRYSTALS B.S. Thesis
Thomas Doblmaier, Paul Grafing, and Kim Knight 19 Oct. 1987 109 p
(Grant NAG8-619)
(NASA-CR-182882; NAS 1.26:182882) Avail: NTIS HC A06/MF A01 CSCL 12A

Zeolite crystals are used in the manufacture of countless products today, which utilize their properties of absorption, ion exchange, and catalysis. It was determined that zeolites grown in space could be much larger in size than any of those currently available on Earth. The objective was to identify and examine some of the potential uses for these larger crystals. Of the several industries examined, the medical and nuclear industries offer the greatest potential. Author

N88-22219# Joint Publications Research Service, Arlington, Va.
SPACE UTILIZATION PLANS
Tetsuhisa Shirakawa *In its* JPRS Report: Science and Technology. Japan 3 Mar. 1988 p 1-5 Transl. into ENGLISH from Ceramics Japan (Tokyo, Japan), Apr. 1987 p 262-268 (For primary document see N88-22218 15-31)
Avail: NTIS HC A05/MF A01

N88-22220# Joint Publications Research Service, Arlington, Va.
SPACE EXPERIMENT PLAN FMPT
Toshihiko Kikuyama *In its* JPRS Report: Science and Technology. Japan 3 Mar. 1988 p 5-9 Transl. into ENGLISH from Ceramics Japan (Tokyo, Japan), Apr. 1987 p 269-276 (For primary document see N88-22218 15-31)
Avail: NTIS HC A05/MF A01

N88-22221# Joint Publications Research Service, Arlington, Va.
AMORPHOUS SEMICONDUCTORS MADE IN SPACE
Yoshihiro Hamakawa *In its* JPRS Report: Science and Technology. Japan 3 Mar. 1988 p 9-19 Transl. into ENGLISH from Ceramics Japan (Tokyo, Japan), Apr. 1987 p 277-285 (For primary document see N88-22218 15-31)
Avail: NTIS HC A05/MF A01

N88-22222# Joint Publications Research Service, Arlington, Va.
CONTAINERLESS GLASS MELTING
Toru Komiyama, Junji Hayakawa, and Misaki Makihara *In its* JPRS Report: Science and Technology. Japan 3 Mar. 1988 p 19-23 Transl. into ENGLISH from Ceramics Japan (Tokyo, Japan), Apr. 1987 p 286-290 (For primary document see N88-22218 15-31)
Avail: NTIS HC A05/MF A01

N88-22223# Joint Publications Research Service, Arlington, Va.
Pb(1-x)Sn(x)Te CRYSTAL GROWTH IN SPACE
Tomoaki Yamada *In its* JPRS Report: Science and Technology. Japan 3 Mar. 1988 p 23-30 Transl. into ENGLISH from Ceramics Japan (Tokyo, Japan), Apr. 1987 p 291-296 (For primary document see N88-22218 15-31)
Avail: NTIS HC A05/MF A01

31 ENGINEERING (GENERAL)

Includes vacuum technology; control engineering; display engineering; cryogenics; and fire prevention.

N88-22208# Rutgers - The State Univ., New Brunswick, N. J. Dept. of Mechanical and Aerospace Engineering.
HEAT TRANSFER FROM A NEGATIVELY BUOYANT WALL JET
K. Kapoor and Y. Jaluria Feb. 1988 45 p
(Grant NB83NADA4047)
(NBS-GCR-88-541) Avail: NTIS HC A03/MF A01

An experimental investigation is conducted on the heat transfer characteristics of a turbulent, negatively bouyant, 2-D wall jet. A jet of hot air is discharged adjacent to a water-cooled, isothermal surface in an extensive environment. The heat transfer to the surface from the elevated temperature jet is measured along the isothermal surface for several values of wall, jet and ambient temperatures. Wide ranges of Grashof (Gr) and Reynolds number (Re) are investigated. It is found that the total heat transfer rate to the isothermal vertical surface decreases with an increase in Gr/Re squared. The effect of the surface temperature T sub s on the downward penetration of the jet and on the heat transfer rate is also investigated. Correlating equations are derived from the experimental data to characterize the dependence of the surface heat transfer rate on the various physical parameters governing the transport process. An interesting flow circumstance arises when the surface temperature is higher than the ambient temperature but lower than the jet discharge temperature, since the downward wall jet flow interacts with an upward buoyancy induced flow adjacent to the wall. The heat transfer mechanisms are investigated in detail for this flow. Author

N88-22209# Academy of Sciences of the Armenian SSR, Erivan.
DILUTION REFRIGERATOR WITH NON-VALVE ADSORPTION SYSTEM OF sup 3/He CIRCULATION
A. A. Aroyan, M. A. Arutyunyan, R. T. Mina, S. T. Boldarev, V. M. Mishachev, and R. G. Amamchyan 1986 16 p In RUSSIAN; ENGLISH summary
(DE88-700974; EFI-937(88)-86) Avail: NTIS (US Sales Only) HC A03/MF A01

For the first time a two stage continuous action dilution refrigerator was constructed based on a nonvalve adsorption system of sup 3 He pumping, as an upper stage. The minimum temperature of the lower (dilutional) stage was approximately 0.2 K. The interrelation of the lower and upper refrigerator stages at different sup 3 He circulation rates in the lower was studied. Some essential characteristics of the condensation pump dependence on temperature of still and mixing chamber were calculated and the ways to refrigerator development were determined. The presence of transfer over the superfluid sup 4 He film in dilution refrigerators with condensation pumping and its influence on the parameters of refrigerator were discussed. DOE

N88-22210# Joint Publications Research Service, Arlington, Va.
JPRS REPORT: SCIENCE AND TECHNOLOGY. JAPAN
11 Mar. 1988 92 p Transl. into ENGLISH from various Japanese articles
(JPRS-JST-88-002) Avail: NTIS HC A05/MF A01

Translations are presented of scientific and technological articles from Japanese journals and books. This issue is devoted entirely to lasers, sensors, and optics. More specifically the articles are about laser applications. For individual titles, see N88-22211 through N88-22217.

N88-22211# Joint Publications Research Service, Arlington, Va.
LASER PROCESSING-STATUS, PERSPECTIVES **c36**
Hiromichi Kawasumi *In its* JPRS Report: Science and Technology. Japan 11 Mar. 1988 p 1-8 Transl. into ENGLISH from Kino Zairyo (Tokyo, Japan), v. 7, Aug. 1987 p 6-10 (For primary document see N88-22210 15-31)
Avail: NTIS HC A05/MF A01

A brief history of the development and use of lasers is given. Lasers are classified into four categories and uses for each category is given. Features of functional material making method using lasers are discussed, including synthesis of ceramics, thin film making and processing for surface properties reforming. E.R.

N88-22212# Joint Publications Research Service, Arlington, Va.
COMPOUND CERAMIC PROCESSING **c27**
Mamoru Okutomi *In its* JPRS Report: Science and Technology. Japan 11 Mar. 1988 p 8-25 Transl. into ENGLISH from Kino Zairyo (Tokyo, Japan), v. 7, Aug. 1987 p 11-24 (For primary document see N88-22210 15-31)
Avail: NTIS HC A05/MF A01

The synthesis of a number of kinds of oxides having melting temperatures higher than 2000 C using laser sintering methods are discussed as part of the effort to develop ceramic lasers having high strength and toughness using CO2 lasers. Also discussed is the results of the synthesis of Al2O3-WO3 system ceramics, which were created with the lasers being melted under nonequilibrium condition and then by being put to a steep cooling process for solidifying the melted lasers. Regarding the Al2O3-WO3 system ceramics thus synthesized, new kinds of compounds and monocrystals were recognized within the ceramics. Research was conducted to clarify the microstructures of those compounds and crystals and to study the phase changes and mechanical strength of them. Author

N88-22213# Joint Publications Research Service, Arlington, Va.
SINGLE CRYSTAL GROWTH BY LASER CVD **c76**
Shigeyuki Hayashi *In its* JPRS Report: Science and Technology. Japan 11 Mar. 1988 p 25-36 Transl. into ENGLISH from Kino Zairyo (Tokyo, Japan), v. 7, Aug. 1987 p 25-32 (For primary document see N88-22210 15-31)
Avail: NTIS HC A05/MF A01

CO2 gas lasers prove to be a superb heat source for use in various applications. Using the lasers, thin monocrystals with a diameter of less than 1 mm were grown. The processes are discussed for creation of the crystals, including a report on related work done by a U.S. research group. CO2 lasers can be used with various kinds of substances, and in the future it could be used for the growth and synthesis of thin films, fibers, and fine particles of various materials. Author

N88-22214# Joint Publications Research Service, Arlington, Va.
FINE GRAIN DEVELOPMENT BY LASER CVD **c27**
Kiyoshi Sawano *In its* JPRS Report: Science and Technology. Japan 11 Mar. 1988 p 36-46 Transl. into ENGLISH from Kino Zairyo (Tokyo, Japan), v. 7, Aug. 1987 p 33-39 (For primary document see N88-22210 15-31)
Avail: NTIS HC A05/MF A01

Demands for superfine grains of various materials have been increasing, and they have been put into practical industrial applications in various fields. Laser CVD is one of the methods for producing such grains, and the method is attracting industry attention. The principles and features of CVD method and a laser CVD system are introduced. In addition, the properties of the grains produced, the synthesizing mechanism and the examples of application of the grains to practical usages are described. Author

N88-22215# Joint Publications Research Service, Arlington, Va.
SUPERFINE GRAIN DEVELOPMENT BY LASER **c27**
Akira Matsunawa *In its* JPRS Report: Science and Technology. Japan 11 Mar. 1988 p 46-59 Transl. into ENGLISH from Kino Zairyo (Tokyo, Japan), v. 7, Aug. 1987 p 40-49 (For primary document see N88-22210 15-31)
Avail: NTIS HC A05/MF A01

Among existing means for providing practical heat sources, lasers are attracting attention as a powerful heat source, which can deliver a power density which is nearly the same or higher than that of an electron beam. By bombarding with such a high density beam, it is possible to evaporate any kind of material instantly. Recent developments in the production of superfine grains

of a number of kinds of substances using lasers, including the features of high power, high density lasers, the evaporation characteristics of irradiated materials, the condensation process of evaporated atoms, and the feature of produced power gains, are discussed. Author

N88-22216# Joint Publications Research Service, Arlington, Va.
HARD CERAMIC FILM BY LASER PVD **c27**
Shinei Mineda and Nobuo Yasunaga *In its* JPRS Report: Science and Technology. Japan 11 Mar. 1988 p 59-70 Transl. into ENGLISH from Kino Zairyo (Tokyo, Japan), v. 7, Aug. 1987 p 50-58 (For primary document see N88-22210 15-31)
Avail: NTIS HC A05/MF A01

A new laser PVD method was developed to deposit the film of vaporized ceramics on the surface of a substrate, by evaporating a ceramic body in revolution, by irradiating the body surface with a CO2 laser beam from a direction of the tangential line. This method enables forming various kinds of dense and very hard ceramic film on the surface of a substrate efficiency. By introducing N ions, a superhard film on cBN can be formed on a substrate. The laser PVD method could be used to make products which have good anti-wear, anti-heat, and anti-corrosion capabilities. In addition, the method could also be used to form a film having good electrical insulation. Author

N88-22217# Joint Publications Research Service, Arlington, Va.
MATERIAL SURFACE IMPROVEMENT BY LASER **c26**
Hiromichi Kawasumi *In its* JPRS Report: Science and Technology. Japan 11 Mar. 1988 p 71-89 Transl. into ENGLISH from Kino Zairyo (Tokyo, Japan), v. 7, Aug. 1987 p 59-70 (For primary document see N88-22210 15-31)
Avail: NTIS HC A05/MF A01

The methods for reforming the surface of industrial materials can be classified by the processing conditions roughly into thermal processing method, compound processing method, and light excitation processing method. The surface reform technology of steel is examined, which is currently used in the steel and automobile manufacturing industries as a mass production technology, from a viewpoint of thermal conduction and metallurgical technology. Also examined is what must be taken into account in introducing the reform technology into practical applications, and problems encountered in the applications. Author

N88-22218# Joint Publications Research Service, Arlington, Va.
JPRS REPORT: SCIENCE AND TECHNOLOGY. JAPAN
3 Mar. 1988 91 p Transl. into ENGLISH from various Japanese articles
(JPRS-JST-88-001) Avail: NTIS HC A05/MF A01

Topics addressed include: civil aviation, aerospace engineering, advanced materials, computers, biotechnology, defense industries, science and technology policy, nuclear developments, and microelectronics. For individual titles, see N88-22219 through N88-22227.

N88-22219# Joint Publications Research Service, Arlington, Va.
SPACE UTILIZATION PLANS **c29**
Tetsuhisa Shirakawa *In its* JPRS Report: Science and Technology. Japan 3 Mar. 1988 p 1-5 Transl. into ENGLISH from Ceramics Japan (Tokyo, Japan), Apr. 1987 p 262-268 (For primary document see N88-22218 15-31)
Avail: NTIS HC A05/MF A01

Space utilization used to be an issue in fields such as communications, broadcasting, and meteorology. Such space utilization counts on the high altitudes of artificial satellites. Recently, the additional interest was shown in the utilization of such aspects of the space environment as microgravity and high vacuum. More concretely, interest is present regarding the possibility of material development, e.g., crystal growth, in a microgravitational environment where there is little difference in gravity between different materials and where no thermal convection is caused. Movements in that direction are already active in the United States and Europe. In Japan, space environment utilization is being tackled, regarding it as a field of space utilization, coming after rockets and artificial satellites. The present status of the Japanese space utilization programs is discussed. Author

N88-22220# Joint Publications Research Service, Arlington, Va.
SPACE EXPERIMENT PLAN FMPT **c29**
Toshihiko Kikuyama *In its* JPRS Report: Science and Technology. Japan 3 Mar. 1988 p 5-9 Transl. into ENGLISH from Ceramics Japan (Tokyo, Japan), Apr. 1987 p 269-276 (For primary document see N88-22218 15-31)
Avail: NTIS HC A05/MF A01

In Japan, the National Space Development Agency is playing a central role in promoting the planning of space experiments to be conducted utilizing the Space Shuttle/Spacelab. The plan being promoted is called the First Material Processing Test (FMPT). According to the plan, Japan is to install its experiment apparatus in the Spacelab, occupying abount half the space available there, with the experiments conducted by a Japanese astronaut. A flow chart of the FMPT plan is presented from experiment subject selection to experiment apparatus fabrication, astronaut screening and training, Space Shuttle launching, space experiment, and experiment result analysis. Author

N88-22221# Joint Publications Research Service, Arlington, Va.
AMORPHOUS SEMICONDUCTORS MADE IN SPACE **c29**
Yoshihiro Hamakawa *In its* JPRS Report: Science and Technology. Japan 3 Mar. 1988 p 9-19 Transl. into ENGLISH from Ceramics Japan (Tokyo, Japan), Apr. 1987 p 277-285 (For primary document see N88-22218 15-31)
Avail: NTIS HC A05/MF A01

The reason why the Si-As-Ti semiconductor is regarded as a dream semiconductor is explained based on the results of preliminary ground experiments already conducted. The experiment is outlined using the TT-500A rocket, and the results introduced. The problems regarding the First Material Processing Test (FMPT) are described. Author

N88-22222# Joint Publications Research Service, Arlington, Va.
CONTAINERLESS GLASS MELTING **c29**
Toru Komiyama, Junji Hayakawa, and Misaki Makihara *In its* JPRS Report: Science and Technology. Japan 3 Mar. 1988 p 19-23 Transl. into ENGLISH from Ceramics Japan (Tokyo, Japan), Apr. 1987 p 286-290 (For primary document see N88-22218 15-31)
Avail: NTIS HC A05/MF A01

The First Material Processing Test (FMPT), scheduled to be carried out in 1991, is the first full-scale space experiment ever planned by Japan. Among the research subjects proposed for the FMPT is research involving invisible-region optical material proposed by the Government Industrial Research Institute, Osaka. This subject aims at test-manufacturing high-purity glass with a superior infrared ray transmission characteristic in a microgravity environment. Preparations are being made for the experiment. The preparations include ground experiments, apparatus development, and glass melting experiments in a microgravity environment obtained by making a trajectory aircraft flight. These preparations are outlined. Author

N88-22223# Joint Publications Research Service, Arlington, Va.
Pb(1-x)Sn(x)Te CRYSTAL GROWTH IN SPACE **c29**
Tomoaki Yamada *In its* JPRS Report: Science and Technology. Japan 3 Mar. 1988 p 23-30 Transl. into ENGLISH from Ceramics Japan (Tokyo, Japan), Apr. 1987 p 291-296 (For primary document see N88-22218 15-31)
Avail: NTIS HC A05/MF A01

An experiment titled crystal growth of narrow bandgap ternary compound semiconductor Pb(1-x)Sn(n)Te under microgravity is being planned as the part of the First Material Processing Test (FMPT) to be carried out in May 1991 utilizing the Space Shuttle. The experiment was suggested by the idea that a microgravity environment where no thermal convection occurs may enable the

growing of quality crystals. The significance of the experiment and the preparations for it are discussed. Author

N88-22224# Joint Publications Research Service, Arlington, Va.
JAPANESE SPACE STATION MODULE **c18**
Akira B. Sawaoka *In its* JPRS Report: Science and Technology. Japan 3 Mar. 1988 p 30-31 Transl. into ENGLISH from Ceramics Japan (Tokyo, Japan), Apr. 1987 p 297-302 (For primary document see N88-22218 15-31)
Avail: NTIS HC A05/MF A01

Japan is scheduled to build a space station in the 1990s. It will not be a whole space station, but a space station module to be docked with the NASA space station. The module to be build by Japan is comprised of a space laboratory called JEM (Japanese Experiment Module). The total cost of JEM, including the cost of experimental apparatus to be installed and the expenses for operation in the initial stage, will amount to well over Y300 billion. The JEM will measure about 4 m in diameter and 18 m in length. A total of four modules, including JEM, are scheduled to be docked with the space station proper. The design of the JEM and the goals of the Japanese Space Program are discussed. Author

N88-22225# Joint Publications Research Service, Arlington, Va.
SOLAR CELL COVER GLASSES FOR SATELLITES **c44**
Tokio Kimura *In its* JPRS Report: Science and Technology. Japan 3 Mar. 1988 p 31-37 Transl. into ENGLISH from Ceramics Japan (Tokyo, Japan), Apr. 1987 p 303-308 (For primary document see N88-22218 15-31)
Avail: NTIS HC A05/MF A01

Since the world's first artificial satellite, Vostok 1, was launched in October 1957, many artificial satellites were launched for many purposes. It is not generally known that such satellites incorporate glass parts which play important roles. Such glass parts include the cover glasses for solar cell systems attached to satellites and the thermal control mirrors for the satellite proper. These glass parts are used to protect satellites from radiation and heat, enabling them to function properly in space where environmental severity is beyond the imagination. Cover glasses will be examined. First, the space environment will be described in connection with the use of cover glasses. Then, the purposes of using cover glasses and the functions required of them covered. Finally, the actual cover glasses are described and the cover glass reliability management explained. Author

N88-22226# Joint Publications Research Service, Arlington, Va.
CHARACTERISTICS OF LSI-WIRING EXPERT SYSTEM DISCUSSED **c33**
T. Goto *In its* JPRS Report: Science and Technology. Japan 3 Mar. 1988 p 54-58 Transl. into ENGLISH from Denshi Zairyo (Tokyo, Japan), Sep. 1987 p 132-135 (For primary document see N88-22218 15-31)
Avail: NTIS HC A05/MF A01

This system is mainly applied to wiring between terminals, which was not accomplished by the LSI automatic wiring program. The Intellectual processing portion is written in PROLOG, and the procedure processing portion is written in FORTRAN, in an attempt to shorten the calculation time and reduce the necessary memory capacity. The program for procedure processing has an advantage in that conventional programs can be applied to this program without any changes or modifications. Even for nonexperts in the area of wiring design, this system enables the achievement of good quality designs in a short time. For instance, it usually takes more than 2 hours for a specialist to complete the wiring design of a gate array LSI with 2,100 gates. However, this same design can be done within a half hour by a nonspecialist when using this system. Author

N88-22227# Joint Publications Research Service, Arlington, Va.
FUNCTION OF JAPAN FINE CERAMICS CENTER DESCRIBED **c27**
In its JPRS Report: Science and Technology. Japan 3 Mar. 1988 p 82-85 Transl. into ENGLISH from Nikko Materials (Tokyo, Japan), Sep. 1987 p 3-7 (For primary document see N88-22218 15-31)
Avail: NTIS HC A05/MF A01

Prospects for overall market expansion are examined. The Japan Fine Ceramics Center was created to develop the future potential and utility of fine ceramics. The Center conducts research on structural chemistry, structural characteristics, and superconducting materials. Author

N88-22228# Joint Publications Research Service, Arlington, Va.
JPRS REPORT: SCIENCE AND TECHNOLOGY. JAPAN
27 Oct. 1987 128 p Transl. into ENGLISH from various Japanese articles
(JPRS-JST-87-029) Avail: NTIS HC A07/MF A01

Topics addressed include: computers; advanced materials; civil aviation; aerospace engineering; energy technology; defense industries; laser applications; optics; and science and technology policy. For individual titles, see N88-22229 through N88-22232.

N88-22229# Joint Publications Research Service, Arlington, Va.
DEVELOPMENTS IN CERAMIC SUPERCONDUCTING MATERIALS **c27**
Eizo Yamaka *In its* JPRS Report: Science and Technology. Japan 27 Oct. 1987 p 1-6 Transl. into ENGLISH from Nikko Materials (Tokyo, Japan), Jul. 1987 p 12 (For primary document see N88-22228 15-31)
Avail: NTIS HC A07/MF A01

The energy gap of a ceramic superconducting material was measured. The material used for measurement was a ceramic of yttrium, barium, and copper. The result reveals that a very large energy gap exists. High transition-temperature substances, and the mechanism responsible for the substance's superconductivity were also investigated. This research will involve the preparation of high quality Y-Ba-Cu-O powder, the creation of the mono-crystal, the determination of the structure, a phase-diagram analysis, and measurements of the physical properties. B.G.

N88-22230# Joint Publications Research Service, Arlington, Va.
SIGMA SYSTEM: OVERVIEW, PROSPECTS **c61**
Masaki Nakayama *In its* JPRS Report: Science and Technology. Japan 27 Oct. 1987 p 19-32 Transl. into ENGLISH from Denshi Kogyo Geppo (Tokyo, Japan), no. 6, 1987 p 27-36 (For primary document see N88-22228 15-31)
Avail: NTIS HC A07/MF A01

The Sigma System is a software production and industrialization system developed for the purpose of improving the fundamental environment for software development in Japan. The Sigma System Construction Project is achieving most of its objectives. Prototype Sigma work stations are now operational, and work is going ahead on the Sigma network, Sigma utilities, and Sigma Center according to the development schedule set forth in the basic plans. Studies are also being made on the implementation specifics, operating guidelines, implementation plan, scheduling, and other factors involved in implementing the monitor tests scheduled for the second half of this fiscal year. Manufacturers of Sigma work stations have begun to move into the product creation stage, and are poised to take the first step toward concrete system embodiment. B.G.

N88-22231# Joint Publications Research Service, Arlington, Va.
OVERVIEW OF 1987 MOONLIGHT PROJECT **c44**
In its JPRS Report: Science and Technology. Japan 27 Oct. 1987 p 48-54 Transl. into ENGLISH from Jita Nyusu (Tokyo, Japan), Mar. 1987 p 11-13 (For primary document see N88-22228 15-31)
Avail: NTIS HC A07/MF A01

The Moonlight Project was established in FY78 to promote the comprehensive and planned research and development of energy-conservation technologies encompassing the industry, academia, and national research institutes. So far, the research and development have produced a number of concrete results including an absorption heat pump system and a waste-heat recycling system that is used in factories, both domestic and

overseas. The individual projects for FY87 are briefly described. B.G.

N88-22232# Joint Publications Research Service, Arlington, Va.
MERIT OF HADAMARD TRANSFORM ACTIVE ABSORPTION SPECTROMETER DESCRIBED **c35**
Nobuo Sugimoto *In its* JPRS Report: Science and Technology. Japan 27 Oct. 1987 p 55-71 Transl. into ENGLISH from Ibaraki Bunko Kenkyu (Tokyo, Japan), v. 36, no. 2, Feb. 1987 p 112-122 (For primary document see N88-22228 15-31)
Avail: NTIS HC A07/MF A01

The merit of the Hadamard transfrom active long-path absorption spectrometer was demonstrated by laboratory experiments. The dependence of measurement errors on modulation codes was investigated. The spectral resolution of a spectrometer system and the deformation of the spectrum was tested. The sensitivity of the NO3 measurement in the 660 nm region was estimated for a system using high intensity LEDs and a room temperature photodiode array. The effect of the ghost of the Hadamard transform due to the nonlinearity of the detector and a method to correct the ghost are discussed. Author

N88-22233# Joint Publications Research Service, Arlington, Va.
JPRS REPORT: SCIENCE AND TECHNOLOGY. CHINA
11 Dec. 1987 122 p Transl. into ENGLISH from various Chinese articles
(JPRS-CST-87-043) Avail: NTIS HC A06/MF A01

Translated scientific and technological articles from Chinese journals and books are presented. The areas of concern are: aerospace; applied sciences; environmental quality; life sciences; and national developments. For individual titles, see N88-22234 through N88-22249.

N88-22234# Joint Publications Research Service, Arlington, Va.
CHRONOLOGY OF CHINA'S SUCCESSFUL SATELLITE LAUNCHINGS **c12**
In its JPRS Report: Science and Technology. China 11 Dec. 1987 p 1-3 Transl. into ENGLISH from Kexue Ribao (Beijing, Peoples Republic of China), 11 Aug. 1987 p 1 (For primary document see N88-22233 15-31)
Avail: NTIS HC A06/MF A01

A chronology is given of China's successful satellite launchings. Included is the name of the satellite, date of launch and certain specifications such as weight, orbit time, etc. E.R.

N88-22235# Joint Publications Research Service, Arlington, Va.
SMOOTHING TECHNIQUE TO RESOLVE X-RAY SPECTRA IN LASER NUCLEAR FUSION **c75**
Chenghai Liu and Zhengqiang Lu *In its* JPRS Report: Science and Technology. China 11 Dec. 1987 p 4-15 Transl. into ENGLISH from Jisuan Wuli (Beijing, Peoples Republic of China), v. 2, no. 2, Sep. 1985 p 313-320 (For primary document see N88-22233 15-31)
Avail: NTIS HC A06/MF A01

A finite amplitude iteration method with periodic smoothing which has been used in resolving X-ray energy spectra in laser nuclear fusion is provided. By constructing a smoothed weighted function and using this weighted function to do smoothing treatment of iteration spectra in iteration processes, the X-ray energy spectrum numerical structures produced in iteration processes are eliminated, iteration convergence is improved, and the spectrum resolution level is increased. The physical basis of smoothing is discussed, and a theoretical analysis is provided along with experimental results concerning the smoothing parameter as well as weighted function width selection. Author

N88-22236# Joint Publications Research Service, Arlington, Va.
MAGIC LIGHT HIGH-POWER LASER PASSES STATE CERTIFICATION Abstract Only **c36**
Ganchang Wang, Daheng Wang, Min Yu, Nunkuan Chen, Kaijia Cheng, and Fuxi Gan *In its* JPRS Report: Science and Technology. China 11 Dec. 1987 p 16 Transl. ino ENGLISH from Yingyong Jiguang (Shanghai, Peoples Republic of China), v. 7, no. 4, Aug. 1987 p 159 (For primary document see N88-22233 15-31)
Avail: NTIS HC A06/MF A01

China has developed a Magic Light high powered laser and it was certified on 26 and 27 of June. The system consists of two parallel branches of lasers, each branch has a number of amplifiers, isolators and spatial filters. In the 100 meters of optical path, the two laser beams are synchronized to an accuracy of better than 3 mm. The use of the Magic Light laser will be for conducting basic research in laser fusion, high temperature high pressure and high density plasma physics, highly ionized atomic physics research, laser particle accelerator, and material states under extreme physical conditions. E.R.

N88-22237# Joint Publications Research Service, Arlington, Va.
PROTECTION AGAINST LASER DAMAGE TO HUMAN BODY REVIEWED **c52**
Bingyu Yan *In its* JPRS Report: Science and Technology. China 11 Dec. 1987 p 17-23 Transl. into ENGLISH from Yingyong Jiguang (Shanghai, Peoples Republic of China), v. 7, no. 4, Aug. 1987 p 172-176 (For primary document see N88-22233 15-31)
Avail: NTIS HC A06/MF A01

Lasers can cause damage to the human eye. The main points of protection against laser damage are described. The proper use of lasers is given along with the protection against bodily damage. E.R.

N88-22238# Joint Publications Research Service, Arlington, Va.
NUMERICAL AND EXPERIMENTAL RESEARCH ON PROPAGATION OF ELASTIC STRESS WAVES IN CONICAL SHELL UNDER AXIAL IMPULSIVE LOADING Abstract Only **c39**
Yuze Chen *In its* JPRS Report: Science and Technology. China 11 Dec. 1987 p 45 Transl. into ENGLISH from Lixue Xuebao (Beijing, Peoples Republic of China), v. 19, no. 2. Mar. 1987 p 146-155 (For primary document see N88-22233 15-31)
Avail: NTIS HC A06/MF A01

The propagation of elastic stress waves in a conical shell subjected to axial impulsive loading was studied by means of the finite element method and model experiment. Based on these results, it is shown that there are two axisymmetrical stress waves propagating with different velocities. One, produced by the membrane strain, is called the longitudinal wave, the other, produced by bending deformation, is called the bending wave. Their attenuation along the surface of the shell is discussed. It can be found that the longitudinal wave and bending wave generated by reflection are coupled when a longitudinal wave impinges on the fixed boundary of the shell, and the two reflected waves will continue propagating with corresponding velocities separately in the structure. Author

N88-22239# Joint Publications Research Service, Arlington, Va.
CUBIC SPLINE SOLUTION OF SYMMETRIC BUCKLING PROBLEMS OF CLAMPED SHALLOW SPHERICAL SHELLS Abstract Only **c39**
Shuxian Gu *In its* JPRS Report: Science and Technology. China 11 Dec. 1987 p 46 Transl. into ENGLISH from Lixue Xuebao (Beijing, Peoples Republic of China), v. 19, no. 2, Mar. 1987 p 179-185 (For primary document see N88-22233 15-31)
Avail: NTIS HC A06/MF A01

Cubic B-spline approximations and iterative techniques were used in computing highly nonlinear deflections of clamped shallow spherical shells under successive increments of uniformly distributed loads. It was found that for shells with certain geometric parameters, the slopes (load central deflection) curves may reach infinity (and become negative) before snap-through buckling loads have been attained. A special algorithm which alternately uses the increments of central deflection and load as iterative parameters was developed to cope with this situation. This algorithm gives fairly good convergence rates for values of lambda as high as 46, and the buckling loads obtained for lambda less than 20 are

comparible with those computed by Budiansky and Archer using entirely different methods. Author

N88-22240# Joint Publications Research Service, Arlington, Va.
EFFIC!ENT METHOD FOR STRUCTURAL OPTIMIZATION Abstract Only **c64**
Renwei Xia *In its* JPRS Report: Science and Technology. China 11 Dec. 1987 p 48 Transl. into ENGLISH from Lixue Xuebao (Beijing, Peoples Republic of China), v. 19, no. 3, May 1987 p 246-257 (For primary document see N88-22233 15-31)
Avail: NTIS HC A06/MF A01

Based on the dual theory of a nonlinear programming method and the second order Taylor series expansions of functions, an efficient method for structural optimization is derived, which can be used to solve large scale structural system problems with various kinds of behavioral constraints and can identify the set of critical constraints automatically at the optimum point. The formulas for computing the first and second derivatives of behavioral parameters expressed through element stress are also given. The expressions of the second derivatives and Hessian matrix can be significantly simplified using Saint-Venant's principle, and the efficiency of the optimization procedures can be further improved. Computational results for several typical examples show that the method present performs satisfactorily in comparison with other computing techniques. Author

N88-22241# Joint Publications Research Service, Arlington, Va.
INVESTIGATION OF SIDE-WALL EFFECTS IN WIND TUNNEL WITH SUPERCRITICAL AIRFOIL TESTING Abstract Only **c02**
Chao Gao *In its* JPRS Report: Science and Technology. China 11 Dec. 1987 p 50 Transl. into ENGLISH from Lixue Xuebao (Beijing, Peoples Republic of China), v. 19, no. 4, Jul. 1987 p 381-386 (For primary document see N88-22233 15-31)
Avail: NTIS HC A06/MF A01

An investigation is presented of the side-wall effect in a two dimensional transonic wind tunnel with side-wall boundary layer suction around the model. The span of the airfoil model used in the experiments is larger than the width of the test section. Therefore, the model can be shifted laterally and the streamwise pressure distribution for different spanwise sections can be obtained. The test results show that, for supercritical flow, the application of side-wall suction will result in an improvement of spanwise uniformity of aerodynamics and a downstream movement of the shock wave. Author

N88-22242# Joint Publications Research Service, Arlington, Va.
SPLIT-COEFFICIENT MATRIX SOLUTION AND EXPERIMENTAL STUDY OF AXISYMMETRIC UNDEREXPANDED EXHAUST PLUMES Abstract Only **c20**
Zuyuan Xie *In its* JPRS Report: Science and Technology. China 11 Dec. 1987 p 58 Transl. into ENGLISH from Kongqidonglixue Xuebao (Mianyang, Peoples Republic of China), v. 5, no. 3, Sep. 1987 p 226-234 Original language document was announced in IAA as A88-14015 (For primary document see N88-22233 15-31)
Avail: NTIS HC A06/MF A01

The space marching split coefficient matrix method for solving the axisymmetric underexpanded exhaust plume flow field was developed and tested, and the viscous/inviscid split method is used to treat viscous flow. The color Schlieren photographs taken from experiments clearly show all the details of the flow field. The numerical experiments reveal that the split coefficient matrix method is much more stable and accurate than the central difference scheme, since the shock and contact discontinuities can be captured correctly with little smearing or oscillation. Author

N88-22243# Joint Publications Research Service, Arlington, Va.
THEORETICAL MODEL AND NUMERICAL SOLUTION FOR COMPRESSIBLE VISCOUS VORTEX CORES Abstract Only **c02**
Bingqiu Lin *In its* JPRS Report: Science and Technology. China 11 Dec. 1987 p 59 Transl. into ENGLISH from Kongqidonglixue Xuebao (Mianyang, Peoples Republic of China), v. 5, no. 3, Sep. 1987 p 235-243 Original language document was announced in IAA as A88-14016 (For primary document see N88-22233 15-31)
Avail: NTIS HC A06/MF A01

Based on the dimensional analysis, the parabolic equation of a compressible viscous vortex core was derived. A simpler numerical method described can be used to calculate the subsonic, transonic, and supersonic vortex motions. Numerical results for two examples are also shown, one for the expanding motion of the stable vortex and the other for the contracting motion of the stable vortex. Author

N88-22244# Joint Publications Research Service, Arlington, Va.
MIXED DIRECT-INVERSE PROBLEM OF TRANSONIC CASCADE Abstract Only **c02**
Wei Liu and Mengyu Shen *In its* JPRS Report: Science and Technology. China 11 Dec. 1987 p 60 Transl. into ENGLISH from Kongqidonglixue Xuebao (Mianyang, Peoples Republic of China), v. 5, no. 3, Sep. 1987 p 244-250 Original language document was announced in IAA as A88-14017 (For primary document see N88-22233 15-31)
Avail: NTIS HC A06/MF A01

A computational method is used to solve the mixed direct-inverse problem of a transonic plane cascade. It is based on the finite volume method and solves Euler equations directly. In effect the flow field in which shocks exist can be studied. The present method can be used in a wider range then the transonic relaxation method. E.R.

N88-22245# Joint Publications Research Service, Arlington, Va.
INFLUENCE OF UNSTEADY AERODYNAMIC FORCES ON DYNAMIC RESPONSE OF VARIABLE SWEEP AIRCRAFT Abstract Only **c05**
Ming Yan and Chuanren Qiu *In its* JPRS Report: Science and Technology. China 11 Dec. 1987 p 62 Transl. into ENGLISH from Kongqidonglixue Xuebao (Mianyang, Peoples Republic of China), v. 5, no. 3, Sep. 1987 p 261-270 Original language document was announced in IAA as A88-14018 (For primary document see N88-22233 15-31)
Avail: NTIS HC A06/MF A01

A numerical method to obtain a complete solution for the dynamic response of a variable sweep wing aircraft while changing the angle of sweep is presented. Both aerodynamic and trajectory computations are included. During the flight of the sweptback angle variation, the aerodynamic forces acting on the aircraft are obviously unsteady, therefore, methods for computing these forces and accompanying responses of aircraft are also presented. Author

N88-22246# Joint Publications Research Service, Arlington, Va.
ZERO-LIFT DRAG PREDICTIONS IN SUPERSONIC FLOW FOR COMPLEX CONFIGURATIONS Abstract Only **c02**
Qide Yang *In its* JPRS Report: Science and Technology. China 11 Dec. 1987 p 63 Transl. into ENGLISH from Kongqidonglixue Xuebao (Mianyang, Peoples Republic of China), v. 5, no. 3, Sep. 1987 p 293-297 Original language document was announced in IAA as A88-14021 (For primary document see N88-22233 15-31)
Avail: NTIS HC A06/MF A01

A supersonic zero lift drag computer program was developed for complex missile-like body shapes. A mixed method was developed for wave drag prediction. Van Dyke's second order perturbation theory is used to compute the pressure distribution and resulting wave drag of the main body. The wave drag of the complete configuration is obtained via the product of the wave drag of the main body and the interference factors. E.R.

N88-22247# Joint Publications Research Service, Arlington, Va.
RELATIONSHIP BETWEEN OPTICAL TRANSFER FUNCTION AND NATURAL LIGHT FIELD IN SEA OR ATMOSPHERE Abstract Only **c46**
Zhishen Liu and Zhiming Zhang *In its* JPRS Report: Science

and Technology. China 11 Dec. 1987 p 66 Transl. into ENGLISH from Guangxue Xuebao (Shanghai, Peoples Republic of China), v. 7, no. 8, Aug. 1987 p 707-713 (For primary document see N88-22233 15-31)
Avail: NTIS HC A06/MF A01

The relationship between the optical transfer function of seawater and the distribution of the natural radiance field in the sea is simply and directly determined based on the transform model of the sea radiance transfer. The variance of the angle spectrum of the sea radiance field is analyzed. A new simple method for estimating the distribution of the sea radiance field and measuring the optical transfer function of the seawater is proposed. The method is appropriate for the atmospheric circumstances. Author

N88-22248# Joint Publications Research Service, Arlington, Va.
EVAPORATION CHARACTERISTICS OF ELEMENTS DURING VACUUM ARC REMELTING OF ALLOY A-286 **c26**
Jie Fu, Yaohe Hu, Junhua Zhao, Yucai Zhao, and Jainzhong Zhu *In its* JPRS Report: Science and Technology. China 11 Dec. 1987 p 67-75 Transl. into ENGLISH from Jinshu Xuebao (Beijing, Peoples Republic of China), v. 22, no. 3, 18 Jun. 1986 p B97-B104 (For primary document see N88-22233 15-31)
Avail: NTIS HC A06/MF A01

The melting characteristics and the Mn distribution at the electrode tip during the vacuum arc remelting of a 410 mm diameter consumable alloy A-286 electrode are investigated. It was discovered that Mn evaporation occurred primarily during the droplet formation stage at the tip. The distribution of Mn in the liquid phase is uniform and the content is close to the equilibrium level during evaporation. At the interface, the Mn content increases linearly from the liquid film to the electrode itself. It is believed that Mn evaporation is controlled by the migration rate of Mn in the liquid-solid two phase region. An expression is given for the Mn content in the remelted ingot. Author

N88-22249# Joint Publications Research Service, Arlington, Va.
RAINBOW HOLOGRAPHIC IMAGE RECONSTRUCTED BY SPATIALLY EXTENDED WHITE LIGHT SOURCE Abstract Only **c35**
Luzhong Cai and Youwen Zhang *In its* JPRS Report: Science and Technology. China 11 Dec. 1987 p 76 Transl. into ENGLISH from Guangxue Xuebao (Shanghai, Peoples Republic of China), v. 7, no. 8, Aug. 1987 p 721-728 (For primary document see N88-22233 15-31)
Avail: NTIS HC A06/MF A01

It is well known that rainbow holograms can be reconstructed by a spatially extended white light source. A new concept is proposed, the effective width of extended source, that can explain this fact. The effective width comes from two limiting apertures, the skut and the viewer's pupil. These two apertures make a rainbow hologram different from other holograms. The effects of spatial and spectral extensions on the image point of the rainbow hologram were studied and proved to be approximately equivalent whether they existed separately or simultaneously. The resolution of the rainbow hologram image is derived for the spatial and spectral extended reconstruction source. Some reasonable conclusions are given. Author

32 COMMUNICATIONS AND RADAR

Includes radar; land and global communications; communications theory; and optical communications.

For related information see also *04 Aircraft Communications and Navigation* and *17 Space Communications, Spacecraft Communications, Command and Tracking.* For search and rescue see *03 Air Transportation and Safety,* and *16 Space Transportation.*

N88-22250# Naval Postgraduate School, Monterey, Calif.
OPTIMUM SIGNAL PROCESSING IN DISTRIBUTED SENSOR SYSTEMS Ph.D. Thesis
Abdel-Aziz M. Al-Bassiouni Dec. 1987 143 p
(AD-A189443) Avail: NTIS HC A07/MF A01 CSCL 17H

We consider the problem of detection of known signals in noise using quantized, discrete sensor observations. Optimal design of the quantizers at the sensor sites as well as the global fusion of the quantized observations is presented. Also the equivalence between a team of two sensors and their fusion center and another team of a primary decision maker and a second opinion is shown. Since the fusion of information is a main pillar of the thesis, an early chapter is devoted to the optimum fusion policy. Extension of the results to the case of vector sensor observations is also considered. GRA

N88-22251# Texas Univ., Austin. Inst. for Fusion Studies.
WAVE ENERGY FLOW CONSERVATION FOR PROPAGATION IN INHOMOGENEOUS VLASOV-MAXWELL EQUILIBRIA
H. J. Kull, H. L. Berk, and P. J. Morrison Feb. 1988 19 p
(Contract DE-FG05-80ET-53088)
(DE88-006705; DOE/ET-53088/309; IFSR-309) Avail: NTIS HC A03/MF A01

Wave energy flow conservation is demonstrated for Hermitian differential operators that arise in the Vlasov-Maxwell theory for propagation perpendicular to a magnetic field. The energy flow can be related to the bilinear concomitant, for a solution and its complex conjugate, by using the Lagrange identity of the operator. This bilinear form obeys a conservation law and is shown to describe the usual WKB energy flow for asymptotically homogeneous regions. The additivity and uniqueness of the energy flow expression is discussed for a general superposition of waves with real and complex wave numbers. Furthermore, a global energy conservation theorem is demonstrated for an inhomogeneity in one-dimension and generalized reflection and transmission coefficients are thereby obtained. DOE

N88-22252# Pennsylvania Univ., Philadelphia. School of Electrical Engineering.
CONFORMAL MICROSTRIP SLOT ANTENNA AND ANTENNA ARRAY Final Report, Dec. 1983 - Sep. 1987
Moshe Kisliuk, Bernard Steinberg, and William Whistler Nov. 1987 102 p
(Contract F19628-84-K-0021)
(AD-A189623; RADC-TR-87-209) Avail: NTIS HC A06/MF A01 CSCL 09A

This final report covers the investigation of two microstrip antenna types, the microstrip slot radiator and the microstrip dual folded dipole. The slot dipole is a wide bandwidth (20 percent), low efficiency (20 percent) radiator suitable for use in for use in serial slot arrays, and is subject to beam steering with frequency. Array tests showed 20 dB sidelobes, and methods of varying slot susceptance are discussed. The dual folded dipole (DFD) is a 10 percent bandwidth designed on dual dielectric substrates; the lower substrate can be a high-K dielectric useful for MMIC front-end designs. A noncontacting coupling is made to the DFD radiator. Tests show a tested gain of + 7.3 dBi. GRA

N88-22253# Science Applications International Corp., San Diego, Calif.
PERFORMANCE OF DATA COMPRESSION CODES IN CHANNELS WITH ERRORS Final Report, Oct. 1986 - Jan. 1987
Oct. 1987 13 p
(Contract N66001-85-D-0029; DA Proj. CM5-1)
(AD-A189667; NOSC/TD-1166) Avail: NTIS HC A03/MF A01 CSCL 25E

Huffman codes, comma-free codes, and block codes with shift indicators are important candidate message compression codes for improving the efficiency of communications systems. This study was undertaken to determine if these codes could be used to increase the thruput of the fixed very low frequency (FVLF) communication system. This application involves the use of compression codes in a channel with errors. GRA

N88-22254# Air Force Inst. of Tech., Wright-Patterson AFB, Ohio. School of Engineering.
HIGH SPEED, BANDPASS SAMPLING OF DIGITAL COMMUNICATIONS WAVEFORMS M.S. Thesis
Tommy E. Keith Dec. 1987 102 p
(AD-A189842; AFIT/GE/ENG/87D-31) Avail: NTIS HC A06/MF A01 CSCL 14B

The purpose of this thesis is to investigate and analyze bandpass sampling techniques. Bandpass sampling theory is shown to be an extension of the Shannon low-pass sampling theory. Five bandpass sampling techniques are investigated; direct sampling (also called first-order sampling), pth-order sampling (in particular second-order sampling where p=2), conventional quadrature sampling, quadrature sampling, and complex sampling (also called Hilbert transform sampling). Direct sampling is a single channel approach to bandpass sampling while the other approaches require two channels. The two channel techniques offer a sampling rate reduction of up to one half over direct sampling, but there are trade-offs to consider when choosing a two channel technique. It is shown that the effects of random phase error can render the conventional quadrature sampling approach useless. Timing is critical with quadrature sampling. Reconstruction error, due to hardware timing errors, is shown to be directly proportional to the center frequency and is a function of the bandwidth of the signal. GRA

N88-22255# Naval Postgraduate School, Monterey, Calif.
STRATEGIES IN THE TOPOLOGICAL APPROACH TO ELECTROMAGNETIC INTERFERENCE CONTROL M.S. Thesis
Vernon D. Ingram Dec. 1987 77 p
(AD-A189874; NPS-62-88-009) Avail: NTIS HC A05/MF A01 CSCL 17B

The ability of standard commercial equipment cabinets to be used to provide a electromagnetic interference is explored. The internal to external, and external to internal, electromagnetic isolation provided by various configurations of cabinet-penetrating conductors was measured at frequencies from 20 Hz to 20 MHz. Excellent isolation was obtained over the entire frequency range when penetrating conductors (coaxial cables, grounds buses, power conductor green-wires, and power conductor black and white wires) were installed in accord with barrier principles. Little or no isolation was obtained with the direct penetration of the cabinet by conductors. These results were confirmed by laboratory and field measurements (at operating CDAA sites). GRA

N88-22256# Naval Postgraduate School, Monterey, Calif.
DIRECT BIT DETECTION RECEIVER NOISE PERFORMANCE ANALYSIS FOR 32-PSK AND 64-PSK MODULATED SIGNALS M.S. Thesis
Iftikhar Ahmed Dec. 1987 90 p
(AD-A190009) Avail: NTIS HC A05/MF A01 CSCL 25E

Simple two channel receivers for 32-PSK and 64-PSK modulated signals have been proposed which allow digital data (namely bits), to be recovered directly instead of the traditional approach of symbol detection followed by symbol to bit mappings. This allows for binary rather than M-ary receiver decisions, reduces the amount of signal processing operations and permits parallel recovery of the bits. The noise performance of these receivers quantified by the Bit Error Rate (BER) assuming an Additive White Gaussian Noise interference model is evaluated as a function of Eb/No, the signal to noise ratio, and transmitted phase angles of the signals. The performance results of the direct bit detection receivers (DBDR) when compared to that of convectional phase measurement receivers demonstrate that DBDR's are optimum in BER sense. The simplicity of the receiver implementations and the BER of the delivered data make DBDR's attractive for high speed, spectrally efficient digital communication systems. GRA

N88-22257# Naval Postgraduate School, Monterey, Calif.
EFFECT OF FRICTION AND CONTROL PARAMETERS ON THE TRACKING ACCURACY OF A TARGET SEEKER M.S. Thesis
Joseph K. Chan Dec. 1987 75 p
(AD-A190010) Avail: NTIS HC A04/MF A01 CSCL 17K

The Tracking accuracy of a missile target seeker depends on many variables. For a target seeker using a gimbaled platform, an important variable is the friction induced by the preloaded bearings, and by the short wires which connect the target detector with the rest of the seeker's electronics. This friction force is nonlinear and sufficiently large enough such that accurate position tracking of a target, whether stationary or moving, is difficult. Conventional control methods such as P.D. (proportional plus derivative) or P.I.D. (proportional plus derivative plus integral) control action can not satisfactorily meet the error criteria. To overcome the deficiency of these two methods, a model-reference method has been synthesized, relying on idealized predictor corrector control to improve the tracking accuracy of the missile seeker. Computer simulations using the Dynamic Simulation Language have demonstrated the superior performance expected from this method. GRA

N88-22258# Naval Postgraduate School, Monterey, Calif.
THE 2 FSK/QPSK (FREQUENCY SHIFT KEYING/QUADRATURE PHASE SHIFT KEYING) TRANSMITTER AND RECEIVER: DESIGN AND PERFORMANCE M.S. Thesis
Nels A. Frostenson and Michael D. Sonnefeld Dec. 1987 106 p
(AD-A190028) Avail: NTIS HC A06/MF A01 CSCL 12I

This research considers a particular form of M-ary signaling called 2 FSK/QPSK. It is a unique way of combining two modulation methods to produce an 8-ary signaling technique whose noise performance is shown to be significantly better than 8-PSK. A transmitter and receiver for 2 FSK/QPSK is designed, built tested and analyzed. Theoretical and experimental results are compared using a plot of probability of bit error versus signal-to-noise ratio (SNR). Known theoretical performance of 8-PSK is used for comparison. Results show a 5 dB theoretical improvement in SNR and a 3 dB experimental improvement of 2 FSK/QPSK relative to 8-PSK. GRA

N88-22259# Ohio State Univ., Columbus. Electrosciences Lab.
POLARIMETRIC ISAR IMAGING USING EITHER MEASURED OR CALCULATED TRANSIENT SIGNATURES
Guelbin Dural and Jonathan D. Young Oct. 1987 52 p Original contains color illustrations
(Contract N00014-86-K-0202)
(AD-A190077; ESL-718048-6) Avail: NTIS HC A04/MF A01 CSCL 17I

An approximation to generate ISAR images from electromagnetic scattering data is illustrated. An imaging algorithm which combines 1-D filtered time domain signals with aspect angle information is used to substitute for the 2-D Fourier transform. Polarimetric scattering characteristics of the targets are investigated. Images of the targets with different linear polarizations are generated and compared. Different sets of colors are assigned to different polarizations to illustrate the polarization dependence of the targets. Both measured and simulated data based on UTD are used with the same frequency window. Different scattering mechanisms observed on the measured and calculated images are discussed. Frequency scaling techniques are applied to combine measured data to widen the bandwidth. The work has concentrated on both geometrically simple and more complicated targets. Polarization is shown to be a useful tool in target identification with imaging. GRA

N88-22260# SRI International Corp., Menlo Park, Calif.
ELECTROMAGNETIC SENSOR ARRAYS FOR NONDESTRUCTIVE EVALUATION AND ROBOT CONTROL Final Annual Report, 1 Sep. 1986 - 31 Aug. 1987
A. J. Bahr and A. Rosengreen Oct. 1987 43 p
(Contract F49620-84-K-0011)
(AD-A190210; AFOSR-87-1752TR) Avail: NTIS HC A03/MF A01 CSCL 17K

The objective of this research program was to develop the theoretical models, design methodology, and technology needed for optimally applying near field electromagnetic sensor arrays to

nondestructive evaluation (NDE) and robot control. This program was a collaborative effort by SRI International and Stanford University. This report summarizes SRI's contribution to the program's third-year research activities. SRI's work on this study has shown that small printed circuit single turn loops exhibit good sensitivity when used as sensors. This technology allows ready fabrication of high resolution arrays. By addressing different elements in the array and suitably processing the resulting signals, different sensing functions can be realized with the same array. In particular, SRI has demonstrated the use of such arrays for edge tracking and ranging (proximity sensing). GRA

N88-22261# Naval Research Lab., Washington, D.C.
MODELS FOR ELECTROMAGNETIC SCATTERING FROM THE SEA AT EXTREMELY LOW GRAZING ANGLES
Lewis B. Wetzel 31 Dec. 1987 85 p
(AD-A190472; NRL-MR-6098) Avail: NTIS HC A05/MF A01 CSCL 17I

The present state of understanding in the field of low-grazing-angle sea scatter is reviewed and extended. The important concept of shadowing is approached from the point of view of diffraction theory, and limits in wind speed and radar frequency are found for the application of shadowing theories based on geometrical optics. The implications of shadowing function based on illumination thresholding are shown to compare favorably with a variety of experimental results. Scattering from the exposed surface peaks is treated by a composite-surface Bragg model, and by wedge models using both physical optics and the method of equivalent currents. Curiously, the scattering levels predicted by these widely different approximations are all in fairly good agreement with experimental values for moderately low grazing angles (about 5 deg), with the physical optics wedge model being superior at 1 deg. A new scattering feature, the slosh, is introduced, with scattering behavior that resembles the temporal and polarization dependence of observed low angle returns from calm water. The plume model of scattering from breaking waves (from earlier work) is discussed as a source of high-intensity Sea Spikes. It is emphasized that the prediction of low angle scattering from the sea will require considerably more information about the shape, size, and distribution of the actual scattering features. GRA

N88-22262# Air Force Inst. of Tech., Wright-Patterson AFB, Ohio.
SYNTHETIC-APERTURE RADARS VIEWED AS INTERFEROMETERS WITH MATCHED FILTER PROCESSING OF THE COLLECTED DATA Final Report, Oct. - Nov. 1986
Edwin B. Champagne May 1987 74 p
(AD-A190608; AFWAL-TR-86-1160) Avail: NTIS HC A04/MF A01 CSCL 17I

This report attempts to characterize a synthetic aperture radar in its most basic physical form and to illustrate the characteristics of various engineering approaches to the implementation of a working system. Much of the present activity in the SAR area centers on data forms, and we have illustrated that these are processing or implementation concerns and not basic radar concerns. Thus, there may be preferred ways to implement processing schemes to achieve some end, but there are probably alternatives which will achieve the same end. Perhaps this separation of the fundamentals and the engineering aspects will afford the opportunity for more approaches to be proposed and may provide a better understanding of SAR. Introductory sections are devoted to the interferometer and matched filter concepts basic to SAR. Secondary sections provide a description of traditional range azimuth formatting approaches to matched filtering, and go on to describe the polar formatting process conceived to alleviate the shortcoming of the range-azimuth format. The final sections deal with various digital and optical implementations which are being, or can be used, to perform the final reduction of polar formatted residue data. This process is basically a 2-D Fourier-Transform process. Topics covered include the Fast Fourier transform, interpolation, and back projection processing. GRA

N88-22263# Air Force Inst. of Tech., Wright-Patterson AFB, Ohio. School of Engineering.
A MULTIPLE MODEL ADAPTIVE TRACKING ALGORITHM AGAINST AIRBORNE TARGETS M.S. Thesis
Thomas A. Leeney Dec. 1987 323 p
(AD-A190619; AFIT/GE/ENG/87D-37) Avail: NTIS HC A14/MF A01 CSCL 17E

The AFIT research directed towards replacing a standard correlation tracker with a Kalman filter bank/enhanced correlation tracker in a high energy laser weapon system is discussed. Airborne targets are tracked by a Bayesian multiple model adaptive filtering (MMAF) algorithm, which utilizes an array of infrared sensing detectors as the measurement information for 2-D position data. Two target dynamics models are exercised: a linear, Gauss-Markov acceleration model, and a nonlinear, constant turn-rate model. Performance analyses are accomplished via Monte Carlo simulation techniques. Extending the adaptive potential of the tracking algorithm is of primary emphasis. The effects of bending and vibration of a large space structure on the FLIR's ability to resolve target position is analyzed. Also, a performance comparison/simulation time tradeoff is conducted with the tracking algorithm operating at both 30 Hz and 50 Hz. Sensitivity studies of adaptive responsiveness to varying target trajectories, various filter-assumed correlation times, range to pixel size relationships, and pixel size to filter driving white noise strength relationships are performed. The robustness of the multiple model algorithm is demonstrated. size relationships, and pixel size to filter driving white noise strength relationships are performed. The robustness of the multiple model algorithm is demonstrated by its ability to adapt to scenarios which it had not been previously tuned. GRA

N88-22264# Technische Hogeschool, Delft (Netherlands). Afd. der Elektrotechniek.
ELECTROMAGNETIC COMPATABILITY: AN INTRODUCTION TO THE THEORY OF INTERFERENCE AND SHIELDING, 3RD REVISED EDITION
A. T. deHoop, D. Quak, and B. L. Michielsen Sep. 1987 44 p
(PB88-165410; Rept-1987-23) Avail: NTIS HC A03/MF A01 CSCL 20N

General aspects of the theory of electromagnetic interference and shielding are presented. In particular, the properties of two one-port systems interacting-at-a-distance are discussed, including the influence of the presence of a shielding domain. Next, the properties of a passive one-port immersed in an arbitrary interfering electromagnetic field are expressed in terms of an equivalent one-port system with internal sources. Finally, the electromagnetic fields emitted by known current distributions in patterns of thin conductors are discussed, while in two examples the influence of a shield will be illustrated. GRA

N88-22265# National Telecommunications and Information Administration, Boulder, Colo. Inst. for Telecommunication Sciences.
PERFORMANCE OF SINGLE AND MULTIPLE SYSTEM AM STEREO DECODER RECEIVERS
J. E. Adams, E. J. Haakinson, V. M. ODay, B. L. Bedford, and B. Riddle Aug. 1987 276 p
(PB88-168307; NTIA-87-223) Avail: NTIS HC A13/MF A01 CSCL 17B

To determine the feasibility of multiple system decoders for AM stereo receivers, the Institute for Telecommunication Sciences made a series of laboratory and field tests on certain commercially available AM stereo receivers. In analyzing the data, the authors compared distortion, signal-to-noise ratio, and stereo detection capabilities of the receivers. These data were measured over a full range of audio frequencies from 50 to 10000 Hz, both without any interfering signal, and with interference. The interference was at both lower and upper adjacent channel frequencies and precisely offset from the desired carrier frequency by 15 and 25 Hz. They measured receiver performance, and obtained data for 3 levels of desired carrier amplitude and 3 levels of modulation. GRA

N88-22266# Centre National d'Etudes Spatiales, Toulouse (France). Centre Spatial.
SHORT EXPERIMENT STUDY OF FOUR-WIRE HELICAL ANTENNAS (HALF TURN HALF WAVE) [BREVE ETUDE EXPERIMENTALE SUR LES ANTENNES HELICES QUADRIFILAIRES COURTES (1/2 TOUR - 1/2 ONDE)]
A. Auriol 16 Oct. 1986 69 p In FRENCH; ENGLISH summary
(CNES-CT/DRT/TIT/AN-249-T; ETN-88-92024) Avail: NTIS HC A04/MF A01

The resonance frequency, the analysis of radiation patterns as a function of frequency and technology, the determination of the differential front to back gain ratio, and the study of the effect of top antenna in the case of dual frequency superimposed antennas are discussed. ESA

N88-22267# Centre National d'Etudes Spatiales, Toulouse (France). Centre Spatial.
DEFINITION AND IMPLEMENTATION STUDY FOR THE VARAN-S RADAR [ETUDE DE DEFINITION ET DE MISE EN OEUVRE DU RADAR VARAN-S]
N. Lannelongue and D. Vaillant 1 Aug. 1985 178 p In FRENCH
(CNES-CT/DRT/TIT/RL-143-T; ETN-88-92030) Avail: NTIS HC A09/MF A01

The Varan-S side looking radar was developed to implement high resolution imagery for oceanographic applications. It works as a synthetic aperture radar. The technical parameters required for oceanographic utilization and the onboard equipment necessary to implement the radar system are described. The ground-based data processing is also discussed. The specifications are given. ESA

N88-22268# Centre National d'Etudes Spatiales, Toulouse (France). Centre Spatial.
DEGRADATION OF DOWNLINK DISTANCE MEASUREMENT INDEXES BY THE ADDITION OF A THIRD TONE [DEGRADATION DES INDICES DE MESURE DE DISTANCE EN LIAISON DESCENDANTE PAR L'ADJONCTION D'UN TON SUPPLEMENTAIRE]
P. Savary 25 Jun. 1985 13 p In FRENCH; ENGLISH summary
(CNES-CT/DRT/TIT/TR-122-T; ETN-88-92031) Avail: NTIS HC A03/MF A01

The computation of downlink indexes when three tones and noise are present on the link is described. The case arises usually in failure cases, when three tones are simultaneously sent. The mathematical analysis shows the possibility to establish the modulation indexes associated to each tone once the signal to noise ratios are determined. ESA

N88-22269# Research Inst. of National Defence, Linkoeping (Sweden).
SOFT DECODING OF RECORDED HF DATA
Gunnar Hedby and Mats Sloglund Oct. 1987 21 p Sponsored by the Swedish Material Administration of the Armed Forces Air Material Dept.
(FOA-C-30473-3.3; ISSN-0347-3708; ETN-88-92206) Avail: NTIS HC A03/MF A01; Research Inst. of National Defense, Box 1165, S-581 11 Linkoping, Sweden, 50 Swedish crowns

The performance of and an estimation of the complexity of decoding schemes for concatenated codes that take advantage of channel measurement information are shown. The main purpose is to improve the performance of a frequency hopping system on the HF-channel. The work is done by simulations on a computer using recorded data from measurements with this system. It is possible to obtain a resultant bit error rate of 0.00001 when the bit error rate before decoding is below 5.1 percent by use of a concateneted code and soft information with a coding rate of 0.3. ESA

33 ELECTRONICS AND ELECTRICAL ENGINEERING

Includes test equipment and maintainability; components, e.g., tunnel diodes and transistors; microminiaturization; and integrated circuitry.

For related information see also *60 Computer Operations and Hardware* and *76 Solid-State Physics.*

N88-22270# Gosudarstvennyi Komitet po Ispolzovaniyu Atomnoi Energii, Moscow (USSR). Inst. Teoreticheskoj i Ehksperimental'noj
HIGH-VOLTAGE INVERSE-SQUARE FUNCTION GENERATOR
O. V. Belovolov, A. E. Bolshakov, I. V. Dubinin, V. I. Nikolaev, and A. L. Semenov 1987 20 p In RUSSIAN
(DE88-701109; ITEF-24(1987)) Avail: NTIS (US Sales Only) HC A03/MF A01

Calculation and block-diagram of a high-voltage inverse-square-law function generator for using as a functional unit of an electrodynamic analyzer mass spectrometric system are given. The generator comprises a pulse shaping unit, a high-voltage fast switch, a control unit of transient process parameters and several RC circuits with code-controlled capacitors. Sufficiently high amplitude, fast response and pulse generation accuracy as well as a wide dynamic range make the generator useful for analysis of energy distributions of laser plasma ion components in a wide range of masses and energies. DOE

N88-22271# Edgerton, Germeshausen and Grier, Inc., Idaho Falls, Idaho.
STATUS OF ELECTRIC VEHICLE SIMULATION PROGRAMS AT THE INEL: SUMMER 1987
A. F. Burke Dec. 1987 83 p
(Contract DE-AC07-76ID-01570)
(DE88-006745; EGG-EP-7946) Avail: NTIS HC A05/MF A01

This is an interim status report of efforts at the Idaho National Engineering Laboratory to implement and improve several electric vehicle simulation programs. A qualitative assessment of the ELVEC, HEAVY, HYVEC, DIANE, and MARVEL computer codes is given. The report focuses on the two programs, ELVEC and HEAVY. The status of these programs as they exist August 1987, is discussed. Results of verification and validation testing on these programs are discussed. Range and energy economy predictions are compared with dynamometer test data for various vehicle/battery combinations. The predictions and data are found to agree to within 10 percent in most instances where test data are available. Second by second comparisons of battery power, current and voltage are made. Possible improvements and enhancements to ELVEC and HEAVY are suggested. An appendix includes typical input and output files for HEAVY and ELVEC. DOE

N88-22272# Edgerton, Germeshausen and Grier, Inc., Idaho Falls, Idaho.
GTE BATTERY MANAGEMENT SYSTEM: STATE OF CHARGE INDICATOR EVALUATION
T. L. Bennett, A. F. Burke, J. E. Hardin, and G. L. Hunt Dec. 1987 97 p
(Contract DE-AC07-76ID-01570)
(DE88-006800; EGG-EP-7780) Avail: NTIS HC A05/MF A01

This report gives a description of the battery management system (BMS), its history, components and function. The testing of two BMSs at GTE Laboratories is summarized. Certainly the bulk of this report is devoted to the INEL testing of the most troublesome component of the BMS, the Gould state of charge indicator (SCI). The SCI does track the battery state of charge but does not meet the requirement of +0, -20 percent. The limitations of the Gould SCI appears to be two things: (1) the 10 kW discharge rate used to predict the remaining energy, and (2) high current peaks are not taken into account in calculating battery capacity. Software implementation of the Gould SCI is recommended for future work. DOE

N88-22273# Grenoble-1 Univ. (France). Techniques de llnformatique, des Mathematiques, de la Microelectronique et de la Microscopie Quantit

FRENCH MULTIPROJECT CHIP (MPC) ACTIVITY REPORT, 1986

C. Antonio, H. Delori, A. Guyot, and J. F. Paillotin Mar. 1987 62 p

(RR-650-I; ETN-88-92281) Avail: NTIS HC A04/MF A01

Operations performed in the development of NMOS and CMOS chips are summarized. Masks, fabrication of chip elements, and assembly and tests are covered. ESA

N88-22274# Air Force Inst. of Tech., Wright-Patterson AFB, Ohio. School of Engineering.

AN EXPERT SYSTEM FOR DISCRETE COMPONENT DIGITAL CIRCUIT DESIGN M.S. Thesis

Steven M. Wagner Dec. 1987 132 p

(AD-A189680; AFIT/GCS/ENG/87D-28) Avail: NTIS HC A07/MF A01 CSCL 09A

The design of digital circuits is cumbersome and prone to errors. Current estimates show that a circuit designed with 5 integrated circuits has less than a 50 percent chance of working, due to wiring errors, when power is first applied. As the complexity increases, the probability of the circuit working on the first try decreases rapidly. Design errors fall into two categories: wiring or logic errors. Wiring errors consist of improperly connected gates, missing connections, and violations of fanout, or race conditions. Logic errors, which are more complex to detect, require knowledge of intended circuit function. This thesis designs, develops, and tests an expert system which decomposes digital circuits into subproblems described by database technology in order to detect wiring errors. Information needed to connect chips together is viewed as knowledge base information for the expert system. Information such as number of pins, value of each pin (input, output), type of chip, etc., are represented in a database. GRA

N88-22275# North Carolina State Univ., Raleigh. Dept. of Electrical and Computer Engineering.

INSTRUMENTATION FOR THE CHARACTERIZATION AND DEVELOPMENT OF MILLIMETER WAVE COMPONENTS COMPATIBLE WITH MONOLITHIC INTEGRATION Final Report, Aug. 1986 - Nov. 1987

R. J. Trew 22 Jan. 1988 33 p

(Grant AF-AFOSR-0262-86)

(AD-A189724; AFOSR-88-0033TR) Avail: NTIS HC A03/MF A01 CSCL 09A

This report describes the design and development of a W-band (75 to 110 GHz) vector automatic network analyzer. The system was funded under the DOD sponsored University Research Instrumentation Program. The W-band system will be located in the Microwave Laboratory located in the Electrical and Computer Engineering Department of North Carolina State University. The equipment funded under this program will interface with an existing Hewlett-Packard 8510A automatic network analyzer and will extend the operating frequency range of this instrument to the millimeter-wave bands. Currently, the system is limited to an upper frequency of 26.5 GHz. The enhanced system will permit research to be performed in the area of millimeter-wave characterization of solid-state devices. In particular, we are interested in performing S-parameter measurements on experimental mm-wave devices in order to determine ultimate frequency and performance limitations. It is anticipated that information of this type will contribute to research directed towards developing optimized solid-state devices for mm-wave applications. GRA

N88-22276# Hughes Aircraft Co., El Segundo, Calif.

ADVANCED CAPACITOR DEVELOPMENT Interim Report, Oct. 1984 - Apr. 1986

Robert S. Buritz 1987 158 p

(Contract F33615-84-C-2424)

(AD-A189985; AFWAL-TR-86-2073) Avail: NTIS HC A08/MF A01 CSCL 09A

This document describes the technical approach taken by Hughes Aircraft Company for the development and testing of ac filter capacitors for airborne applications which will have a higher operating temperature than presently available. This program will result in improved lightweight, highly reliable filter capacitors operating at ambient temperatures exceeding 200 C, which will significantly advance the state of the art in capacitor technology. Two problems faced in achieving higher operating temperatures are the temperature limitation of the dielectric materials and thermal management of the heat generated. Failures are usually caused by the dissipation of relatively large amounts of power in a poorly cooled volume. These failures can take the form of thermal runaway, insulation failure because of very great local hot-spot temperatures, and excessive thermal expansion. Because the thermal properties of films available for capacitor use range from about 115 to more than 450 C, operating temperatures up to 300 to 400 C appear to be feasible. Since these numbers far exceed operating temperatures reported in the literature, the question arises as to the reason for the large difference. than 450 C, operating temperatures up to 300 to 400 C appear to be feasible. Since these numbers far exceed operating temperatures reported in the literature, the question arises as to the reason for the large difference. GRA

N88-22277# Naval Postgraduate School, Monterey, Calif.

THEORETICAL MODEL OF THE CATHODE SPOT ON A UNIPOLAR ARC M.S. Thesis

Dwayne H. Curtiss Dec. 1987 99 p

(AD-A190109) Avail: NTIS HC A05/MF A01 CSCL 20C

A theoretical study and computer analysis of the cathode spot of a unipolar arc was conducted. The underlying theories of plasma physics, space charge effects, and electron emission needed for an understanding of cathode phenomena are presented. Two models of unipolar arcing are reviewed and an analysis of the cathode spot is begun. A stationary model of the cathode spot is formulated with a system of equations that is not closed. A method of solution, using the Steenbeck Minimum Principle, is used and a computer program developed to determine the cathode spot parameters. Results of the analysis are presented for arc currents of 100, 150, 175, 200, 300, and 400 Amperes. It is found that for copper, stable arcs occur only for arc currents greater than 200 amperes. GRA

N88-22278# Texas Univ., Austin. Microwave Lab.

MONOLITHIC PHASE SHIFTER STUDY Annual Technical Report, Nov. 1986 - Oct. 1987

D. P. Neikirk and T. Itoh 25 Nov. 1987 30 p

(Grant AF-AFOSR-0036-86)

(AD-A190213; MW-87-P-10; AFOSR-87-1739TR) Avail: NTIS HC A03/MF A01 CSCL 09A

Modeling and preliminary testing of a monolithic coplanar waveguide (CPW) phase shifter using both optical and Schottky-contact control techniques has been performed. Simulation work on a periodically illuminated structure has been completed, showing that some improvement in performance may be possible, although with a reduction in frequency bandwidth. CPW transmission lines have been fabricated on semi-insulating GaAs, on heavily doped epi GaAs, and on an AlGaAs/GaAs heterostructure, and initial electrical characterization has been performed. Optically controlled phase shift has been obtained with the heterostructure device, and Schottky-bias controlled behavior has been seen with the epi sample. GRA

N88-22279# Wisconsin Univ., Madison.

VORTICES IN LONG JOSEPHSON JUNCTIONS Annual Report, 16 Nov. 1986 - 14 Nov. 1987

James E. Nordman and James B. Beyer Nov. 1987 9 p

(Grant AF-AFOSR-0025-86)

(AD-A190338; AFOSR-87-2042TR) Avail: NTIS HC A02/MF A01 CSCL 09A

Research during the second year of this grant extended the studies begun during the first year on fabrication and modeling of long Josephson junction structures. The Nb-Pb technology, although reliable, is not versatile enough for proposed multilayer

structures and considerable effort was expended in the development of an all Nb and a parallel all NbN technology. This effort is not over but recently we were able to demonstrate an all NbN vortex flow transistor possessing superior properties to the Nb-Pb version. Progress was made toward solution of the problems of high frequency testing of the very low impedance vortex flow transistor and towards determination of its potential for high frequency applications. It was demonstrated that the device exhibits active behavior in the form of a measurable transresistance out of frequencies of about 10 percent of the theoretical transit time cutoff frequency. Capability of higher frequency testing was developed with the design of novel new impedance matching structures. A new type of distributed amplifier was also proposed and modeled. Modeling of spatially nonuniform long junction structures resistance was necessary in order to obtain realistic simulations. GRA

N88-22280# Army Construction Engineering Research Lab., Champaign, Ill.
ECP (ELECTRICAL CIRCUITRY PROGRAM): A PROPOSED PROGRAM FOR ELECTRICAL CIRCUITRY ANALYSIS Final Report
Cynthia K. Barton and Anthony J. Williams Feb. 1988 28 p
(AD-A190494; CERL-TR-E-88/03) Avail: NTIS HC A03/MF A01 CSCL 09A

This research analyzed and proposed development of the computerized Electrical Circuitry Program (ECP). ECP is proposed to assist U.S. Army Corps of Engineers (USACE) in-house electrical engineers in performing the required analysis during facilities concept design phase. The program would include features which allow the user to design a thorough power system with minimum effort. The program would also allow the user to graphically determine outlet locations for luminaries, establish receptacle locations and types, select switch locations and types, lay out wiring diagrams for the system, and locate and describe the features of the panelboards. ECP would be equipped to perform voltage drop, short circuit, and wire length calculations to insure the system design's efficiency. Using the information entered into the program, ECP would create summary reports and panel schedules to be submitted with design documents. GRA

N88-22281# Clarkson Univ., Potsdam, N.Y. Div. of Research.
NONDESTRUCTIVE MOISTURE MEASUREMENT IN MICROELECTRONICS Final Report, Sep. 1985 - Aug. 1986
Didier Kane and Henry Domingos Dec. 1987 54 p
(Contract F30602-81-C-0206)
(AD-A190515; RADC-TR-87-210) Avail: NTIS HC A04/MF A01 CSCL 14B

This project was aimed at understanding moisture induced effects on materials used in microelectronic device manufacture. The approach chosen has been the use of state-of-the-art interdigitated surface conductivity test structures for characterizing the responses of microelectronic materials to ambient and condensed moisture, by performing nondestructive moisture measurements on both hermetically sealed and delidded packages. A test chamber and an appropriate electrical test setup have been developed for assessing the specificity, reproducibility and sensitivity of these effects. GRA

N88-22282# Air Force Inst. of Tech., Wright-Patterson AFB, Ohio. School of Engineering.
FABRICATION AND ELECTRICAL CHARACTERIZATION OF MULTILEVEL ALUMINUM INTERCONNECTS USED TO ACHIEVE SILICON-HYBRID WAFER-SCALE INTEGRATION M.S. Thesis
Grant L. Takahashi Dec. 1987 182 p
(AD-A190519; AFIT/GE/ENG/87D-65) Avail: NTIS HC A09/MF A01 CSCL 09A

The purpose of this research was to develop, fabricate, and electrically characterize a wafer-scale process developed for use with the 272-point Prime Factor Algorithm (PFA) processor. This process integrates a discrete integrated circuit die in a planarized wafer package. The entire wafer surface was coated with photosensitive polyimide, which was patterned with vias for the interconnect contacts. The two die were electrically interconnected with printed aluminum interconnects using conventional silicon processing equipment. The original goals of this research included a system test to evaluate the interconnect network. However, difficulties in the processing environment only allowed a single interconnect to be parametrically evaluated up to 10 MHz. The aluminum interconnect was 26 microns wide and 1.2 microns thick. This interconnect exhibited no distinguishable propagation delay and attenuation for a one centimeter path length. GRA

N88-22283# Massachusetts Inst. of Tech., Cambridge. Artificial Intelligence Lab.
A FULLY ABSTRACT SEMANTICS FOR EVENT-BASED SIMULATION
Robert J. Hall May 1987 19 p
(Contract N00014-85-K-0124)
(AD-A190560; AI-M-966) Avail: NTIS HC A03/MF A01 CSCL 05H

Event-based simulation is a popular technique for predicting the behavior of, among other things, digital circuits. On the other hand, applicative denotational formalisms, in which circuits are represented by functional equations with an explicit time variable, are becoming popular for other reasoning tasks. Before a system is to be used questions of semantic equivalence must be addressed. In particular, if two circuits are equivalent in one formalism, will they be equivalent in the other? What modeling restrictions are needed to bring this about? This paper shows that, provided circuits have no zero-delay loops, a tight relationship, full abstraction, exists between a natural event-based operational semantics for circuits and a natural denotational semantics for circuits based on causal functions on value timelines. The paper also discusses what goes wrong if zero-delay loops are allowed, and illustrates the application of this semantic relationship to modeling questions. GRA

N88-22284# Air Force Inst. of Tech., Wright-Patterson AFB, Ohio. School of Engineering.
AN IMPROVED METHOD FOR CALCULATING POWER DENSITY IN THE FRESNEL REGION OF CIRCULAR PARABOLIC REFLECTOR ANTENNAS M.S. Thesis
Johnnie E. Mize Mar. 1988 97 p
(AD-A190569; AFIT/GE/ENG/88M-8) Avail: NTIS HC A05/MF A01 CSCL 09A

A computer program is presented which calculates power density in the Fresnel region of circular parabolic reflector antennas. The aperture illumination model is the one-parameter circular distribution developed by Hansen. The program is applicable to the analysis of electrically large, center-fed (or Cassegrain) paraboloids with linearly polarized feeds. The scalar Kirchoff diffraction integral is solved numerically by Romberg integration for points both on and perpendicular to the antenna boresight. Axial results cannot be directly compared to any others obtained with this illumination model, but they are consistent with what is expected in the Fresnel region where a quadratic must be added to the linear phase term of the integral expression. Graphical results are presented for uniform illumination and for cases where the first sidelobe ratio is 20, 25, 30, and 35 dB. GRA

N88-22285# Army Armament Research and Development Command, Dover, N. J. Fire Supp Ort Armament Center.
DETERMINATION OF THE COMMUTATION AND ANGLE AND LOAD RESPONSE FOR A CONTINUOUS-CURRENT, SINGLE PHASE CONTROLLED RECTIFIER Final Report, Jan. - May 1987
John A. Pappas and Joseph E. Beno Mar. 1988 39 p
(AD-A190602; ARFSD-TR-87010) Avail: NTIS HC A03/MF A01 CSCL 09A

A method has been developed to quantitatively determine the commutation angle and load response for a continuous-current, single-phase controlled rectifier. An analytical model was developed and solved numerically. The results, in the form of load current plots, predict the commutation time and the shape and magnitude

of the response. The underlying assumptions used in the development of the model, the limitations of the model, and the interpretation of the results are discussed. GRA

N88-22286# Naval Research Lab., Washington, D.C.
ANALYSIS OF ANOMALOUS RESISTIVITY DURING THE CONDUCTION PHASE OF THE PLASMA EROSION OPENING SWITCH Interim Report
R. Kulsrud, P. F. Ottinger, and J. M. Grossmann 2 Feb. 1988 30 p
(Contract DE-AI08-79DP-40092)
(DE88-006382; NRL-MR-6149) Avail: NTIS HC A03/MF A01

During the conduction phase of the plasma erosion opening switch, the current channel width in the body of the plasma away from the electrodes has been observed to be many times wider than the collisionless skin depth. Anomalous collisions have been invoked to explain this discrepancy. Here the problem is analyzed using an electrostatic Vlasov approach and an unstable ion acoustic mode is identified. The derived growth rate is fast enough and the nonlinear saturation level is high enough to explain the observed magnetic field penetration. DOE

N88-22287# Eltech Systems, Inc., Fairport Harbor, Ohio. Research and Development Center.
ALUMINUM-AIR BATTERY DEVELOPMENT Final Report
20 Nov. 1987 223 p
(Contract W-7405-eng-48)
(DE88-006620; UCRL-21018-Vol-1) Avail: NTIS HC A10/MF A01

This volume covers air cathode development. DOE

N88-22288# General Electric Co., Schenectady, N.Y. Corporate Research and Development Center.
A HIGH PERFORMANCE INVERTER-FED DRIVE SYSTEM OF AN INTERIOR PERMANENT MAGNET SYNCHRONOUS MACHINE
B. K. Bose 1987 39 p Presented at the 22nd IEEE/IAS Annual Meeting, Atlanta, Ga., 19 Oct. 1987
(Contract DE-AC07-76ID-01570)
(DE88-006753; EGG-M-04787; CONF-871065-2) Avail: NTIS HC A03/MF A01

A high performance fully operational four-quadrant control scheme of an interior permanent magnet synchronous machine is described. The machine operates smoothly with full performance in constant-torque region, as well as in flux-weakening constant-power region in both directions of motion. The transition between constant-torque region and constant-power region is very smooth at all conditions of operation. The control in constant-torque region is based on vector or field-oriented technique with the direct-axis aligned to the total stator flux, whereas the constant-power region control is implemented by orientation of torque angle of the impressed square-wave voltage through the feedforward vector rotator. The control system is implemented digitally using distributed microcomputer system and all the essential feedback signals, such as torque, flux, etc., are estimated with precision. The control has been described with an outer torque control loop primarily for traction type applications, but speed and position control loops can be easily added to extend its application to other industrial drives. A 70 hp drive system using a Neodymium-Iron-Boron PM machine and transistor PWM inverter has been designed and extensively tested in laboratory on a dynamometer, and performances are found to be excellent. DOE

N88-22289# Oak Ridge Gaseous Diffusion Plant, Tenn.
PERFORMANCE TEST RESULTS: AXIAL-GAP, PERMANENT MAGNET COMPRESSOR MOTOR
R. A. Hawsey, C. E. Leonard, C. P. White, C. W. Sohns, and J. M. Bailey Feb. 1988 45 p Prepared in cooperation with ORNL, Tenn. and Tennessee Univ., Knoxville
(Contract DE-AC05-84OT-21400)
(DE88-006857; K/ETAC-51) Avail: NTIS HC A03/MF A01

A 30-hp, 15,000-rpm, axial-gap, permanent magnet motor and adjustable-speed drive were designed, constructed, and tested. The direct-drive motor had 72 slots and used a full-pitch winding. The rotor consisted of eight, 2.8-in.-diam NdFeB magnets which provided for high air gap flux densities over a large range of air gaps. The drive system was simplified to eliminate phase-lock-loop control and used three Hall probes to permit output switching of the bridge inverter. Dynamometer measurements confirmed the equivalent circuit developed using a cylindrical rotor model when saliency effects may be neglected. DOE

N88-22226# Joint Publications Research Service, Arlington, Va.
CHARACTERISTICS OF LSI-WIRING EXPERT SYSTEM DISCUSSED
T. Goto *In its* JPRS Report: Science and Technology. Japan 3 Mar. 1988 p 54-58 Transl. into ENGLISH from Denshi Zairyo (Tokyo, Japan), Sep. 1987 p 132-135 (For primary document see N88-22218 15-31)
Avail: NTIS HC A05/MF A01

34 FLUID MECHANICS AND HEAT TRANSFER

Includes boundary layers; hydrodynamics; fluidics; mass transfer; and ablation cooling.

For related information see also *02 Aerodynamics* and *77 Thermodynamics and Statistical Physics.*

N88-22290# Instituto Nacional de Tecnica Aeroespacial, Esteban Terradas, Torrejon de Ardoz (Spain). Dept. de Aerodinamica y Navegabilidad.
A PANEL METHOD BASED ON VELOCITY POTENTIAL TO COMPUTE HARMONICALLY OSCILLATING LIFT SURFACE SYSTEMS [METODO DE PANELES BASADO EN EL POTENCIAL DE VELOCIDADES PARA EL CALCULO DE SISTEMAS DE SUPERFICIES SUSTENTADORAS OSCILANTES ARMONICAMENTE]
Luis P. RuizCalavera 1987 13 p In SPANISH; ENGLISH summary Presented at the 5th International Congress on Numerical Methods in Laminar and Turbulent Flow, Montreal, Quebec, 6-10 Jul. 1987
(ETN-88-91886) Avail: NTIS HC A03/MF A01

A numerical method to calculate unsteady pressure distributions on systems of interferring lifting surfaces harmonically oscillating in incompressible flow was developed. Unlike the conventional approach to this kind of problem which use Prandtl's acceleration potential, this method is based on the velocity potential, whose simplicity allows to take into account thickness effects. Special attention is paid to the treatment of the wake influence, by far the most difficult problem in this type of method. The linearized version shows excellent agreement with techniques based on acceleration potential. ESA

N88-22291# Japan Atomic Energy Research Inst., Tokyo. Dept. of High Temperature Engineering.
BASIC CHARACTERISTICS OF HEAT-EXCHANGER-TYPE STEAM REFORMER HEATED BY HIGH-TEMPERATURE HELIUM GAS (2). ANALYSIS BY SIMULATION MODEL (2)
K. Okuyama Feb. 1987 106 p In JAPANESE; ENGLISH summary
(DE87-702962; JAERI-M-87-007) Avail: NTIS (US Sales Only) HC A06/MF A01

A computer-simulation model was developed to analyze the basic characteristics of a heat-exchanger-type steam-methane reformer, which is the key component to produce hydrogen using the nuclear process heat from a high-temperature gas-cooled reactor. This model is based on the one-dimensional one taking account of heat transfer and reaction kinetics. In a previous report, the analytical model and the solution procedure are described, and an example of calculation results were shown compared with the experimental data. This report describes simulation results of the dependencies of the characteristic quantities such as heat

flux, reaction rates, and hydrogen production rate in the reformer tube on selected parameters, namely, the operating conditions (inlet gas temperatures, pressure, and flow rates), the activities of the catalyst, the heat-transfer rate and the dimensions of the reaction tube. DOE

N88-22292# Sandia National Labs., Albuquerque, N. Mex.
THE NUMERICAL SIMULATION OF VISCOUS FLOWS WITH CHANGE OF PHASE AND CHEMICAL REACTION
D. K. Gartling 1988 5 p Presented at the International Conference on Computational Engineering Science, Atlanta, Ga., 10 Apr. 1988
(Contract DE-AC04-76DP-00789)
(DE88-003204; SAND-87-0611C; CONF-880438-2) Avail: NTIS HC A02/MF A01

A computational procedure, based on the finite element method, is developed to study the fluid dynamics of a chemically reacting system. Specifically, the problem involves the phase change (gelation) of an incompressible liquid due to an exothermic chemical reaction. Typical thermosetting materials are considered under conditions of both buoyancy-driven and forced flow. The focus of the present article is on the development of a robust numerical algorithm to handle the complexities of this class of flow problems. DOE

N88-22293# Edgerton, Germeshausen and Grier, Inc., Idaho Falls, Idaho.
APPLICATION AND TECHNOLOGY REQUIREMENTS FOR HEAT PUMPS AT THE PROCESS INDUSTRIES
S. Priebe and R. Chappell 1987 8 p Presented at the 9th Annual Industrial Energy Technical Conference, Houston, Tex., 16 Sep. 1987 Prepared in cooperation with DOE, Idaho Falls, Idaho
(Contract DE-AC07-76ID-01570)
(DE88-006740; EGG-M-26787; CONF-8709248-1) Avail: NTIS HC A02/MF A01

There are basically three categories of equipment used to manage heat energy flows in an industrial process. First, heat exchangers are used to move heat through the process down the temperature gradient. Second, heat pumps are used to move heat through the process up the temperature gradient. Third, heat engines are used to convert heat to shaft power or electricity. The subject here is heat pumps, and they will be discussed relative to their potential for heat energy conservation in industrial processes. The large categories of applications in refrigeration and space heating are not addressed. DOE

N88-22294# Gosudarstvennyi Komitet po Ispolzovaniyu Atomnoi Energii, Obninsk (USSR).
DETECTING THE GAS BUBBLES IN A LIQUID METAL COOLANT BY MEANS OF MAGNETIC FLOWMETERS [DETEKTIROVANIE PUZYRKOV GAZA V ZHIDKOMETALLICHESKOM TEPLONOSITELE S POMOSHCHYU MAGNITNYKH RASKHODOMEROV]
A. I. Mogilner, S. A. Morozov, S. O. Zakharov, and A. Yu. Uralets 1987 24 p In RUSSIAN
(TI88-701427; FEI-1820) Avail: NTIS (US Sales Only) HC A03/MF A01

Solution of some problems of control and diagnosis of circuits with a liquid-metal coolant (LMC) often requires the detection of gas bubbles penetrating the circulation loop. The sources of gas intake can be presented by failed fuel elements in reactor core, failed heat-exchange surfaces in sodium-water steam generators in the secondary circuits, gas capture by circulating coolant from gas circuits. Sometimes the gas is especially injected into circulating coolant to study the dynamics of accumulation and extraction of gas bubbles and to solve research problems related to simulations of emergency situations. The most commonly used methods for gas bubble detection include methods based on measuring coolant electric conductivity. A method for detecting gas bubbles in LMC, based on revealing the change of its electric conductivity is considered. Magnetic flowmeter is used as a detecting element of these changes. Approximate theory for describing spectral and energy noises in signals of a magnetic flowmeter, controlling the flow rate of LMC with gas bubbles is suggested. A new method for signal reading is suggested. Experimental results illustrating the possibility of using the method for measuring the rate of bubble movement and studying the dependence of gas bubble volume on the flow rate of injected gas are presented. DOE

N88-22295*# North Carolina State Univ., Raleigh. Dept. of Mechanical and Aerospace Engineering.
ENHANCED VISCOUS FLOW DRAG REDUCTION USING ACOUSTIC EXCITATION Final Report
R. T. Nagel [1988] 114 p
(Grant NAG1-654)
(NASA-CR-182734; NAS 1.26:182734) Avail: NTIS HC A06/MF A01 CSCL 20D

Large eddy break up devices (LEBUs) constitute a promising method of obtaining drag reduction in a turbulent boundary layer. Enhancement of the LEBU effectiveness by exciting its trailing edge with acoustic waves phase locked to the large scale structure influencing the momentum transfer to the wall is sought. An initial estimate of the required sound pressure level for an effective pulse was obtained by considering the magnitude of the pressure perturbations at the near wake of a thin plate in inviscid flow. Detailed skin friction measurments were obtained in the flow region downstream of a LEBU excited with acoustic waves. The data are compared with skin friction measurements of a simply manipulated flow, without acoustic excitation and with a plain flow configuration. The properties and the scales of motion in the flow regime downstream of the acoustically excited LEBU are studied. A parametric study based upon the characteristics of the acoustic input was pursued in addition to the careful mapping of the drag reduction phenomenon within the acoustically manipulated boundary layer. This study of boundary layer manipulation has lead to improved skin friction drag reduction and further understanding of the turbulent boundary layer. Author

N88-22296*# Lockheed Missiles and Space Co., Huntsville, Ala. Engineering Center.
DUCT FLOW NONUNIFORMITIES: EFFECT OF STRUTS IN SSME HGM II(+) Interim Report
Roger Burke 25 Jan. 1988 36 p
(Contract NAS8-37359)
(NASA-CR-179285; NAS 1.26:179285; LMSC-HEC-TR-F225800) Avail: NTIS HC A03/MF A01 CSCL 20D

A numerical study, using the INS3D flow solver, of laminar and turbulent flow around a two dimensional strut, and three dimensional flow around a strut in an annulus is presented. A multi-block procedure was used to calculate two dimensional laminar flow around two struts in parallel, with each strut represented by one computational block. Single block calculations were performed for turbulent flow around a two dimensional strut, using a Baldwin-Lomax turbulence model to parameterize the turbulent shear stresses. A modified Baldwin-Lomax model was applied to the case of a three dimensional strut in an annulus. The results displayed the essential features of wing-body flows, including the presence of a horseshoe vortex system at the junction of the strut and the lower annulus surface. A similar system was observed at the upper annulus surface. The test geometries discussed were useful in developing the capability to perform multiblock calculations, and to simulate turbulent flow around obstructions located between curved walls. Both of these skills will be necessary to model the three dimensional flow in the strut assembly of the SSME. Work is now in progress on performing a three dimensional two block turbulent calculation of the flow in the turnaround duct (TAD) and strut/fuel bowl juncture region. Author

N88-22297# Army Cold Regions Research and Engineering Lab., Hanover, N.H.
THERMAL INSTABILITY AND HEAT TRANSFER CHARACTERISTICS IN WATER/ICE SYSTEMS
Yin-Chao Yen Nov. 1987 51 p
(AD-A189627; CRREL-87-22) Avail: NTIS HC A04/MF A01 CSCL 08C

This review discusses problems associated with the anomalous temperature-density relations of water. It covers: (1) onset of convection, (2) temperature structure and natural convective heat transfer, and (3) laminar forced convective heat transfer in the water/ice system. The onset of convection in a water/ice system was found dependent on thermal boundary conditions, not a constant value as in the classical fluids that have a monotonic temperature-density relationship. The water/ice system also exhibits a unique temperature distribution in the melt layer immediately after the critical Rayleigh number is exceeded and soon after it establishes a more or less constant temperature region progressively deepening as the melt layer grows. The constant temperature is approximately 3.2 C for water layers formed from above but varies for melt layers from below. The heat flux across the water/ice interface was found to be a weak power function and to increase linearly with temperature for melted layers from above and below, respectively. GRA

N88-22298# Naval Postgraduate School, Monterey, Calif.
UNSTEADY FLOW FIELD MEASUREMENTS USING LDV (LASER DOPPLER VELOCIMETRY) M.S. Thesis
Steven D. Hedrick Dec. 1987 73 p
(AD-A189907) Avail: NTIS HC A04/MF A01 CSCL 20D

The primary goal of this thesis was the development of an experimental technique, and supporting software, for the acquisition and analysis of unsteady velocity data generated by an oscillating airfoil. This research was in support of a major investigation of the compressibility effects on dynamic stall. The experimental procedure involved schlieren flow visualization for comparison of steady and unsteady flow fields, and for determination of parameters for further study. Laser Doppler velocimetry was employed for obtaining velocity data in the airfoil wake. For unsteady data, the airfoil was oscillated in pitch about its quarter chord. The data analysis produced wake profile plots representing the flow field distributed by the airfoil. Results were obtained for steady and unsteady conditions. GRA

N88-22299# Technion - Israel Inst. of Tech., Haifa.
VISUALIZATION OF FLOWS IN TURBOMACHINERY Final Report
J. Bindon, D. Alder, and I. Ianovici Dec. 1987 70 p
(Grant AF-AFOSR-0308-85)
(AD-A189927) Avail: NTIS HC A04/MF A01 CSCL 20D

The basic flow mechanisms are presented for leakage and boundary layer flows at the tips of axial turbine rotors. Various methods for visualization the flows near a rotating turbine tip are assessed. These include smoke injection, spark tracers, pulsed lasers and fluorescent traces. Experimental results are presented for flow visualization by seeding with fluorescent droplets. GRA

N88-22300# Technion - Israel Inst. of Tech., Haifa.
VISUALISATION OF THE FLOW AT THE TIP OF A HIGH SPEED AXIAL FLOW TURBINE ROTOR Final Report
J. Bindon, D. Alder, and I. Ianovici Nov. 1987 60 p
(Grant AF-AFOSR-0308-85)
(AD-A189928) Avail: NTIS HC A04/MF A01 CSCL 20D

The previous work having relevance to the flow in the region of an unshrouded turbine rotor blade tip was examined. It was found that, although extensive information is available on the effect of leakage flow on the loss mechanisms on the suction side of the blade, an almost complete dearth of detailed information exists on the flow structure and mechanisms in the pressure side corner and tip gap regions which are considered important with respect to blade cooling. It would thus seem essential to lay a foundation of understanding from simple models and ending with the complex full speed situation. A logical qualitative prediction of the expected flows is presented. Apart from being complex with various zones of flow behaving almost independently from each other, the effect of upstream tangential unsymmetry (nozzle wakes) was shown to complicate the flow visualization technique and render the normal type of continuous tracer injection of no use. Thus either an experimental rig is required which has tangentially uniform flow upstream of the rotor or a new type of pulse trace technique is needed. It is suggested that both of these requirements be adopted. GRA

N88-22301# Technion - Israel Inst. of Tech., Haifa.
VISUALISATION OF THE FLOW AT THE TIP OF A HIGH SPEED AXIAL FLOW TURBINE ROTOR: AN ASSESSMENT OF FLOW VISUALISATION TECHNIQUES AND THE REQUIREMENT OF THE EXPERIMENTAL TURBINE Final Report
J. Bindon, D. Alder, and I. Ianovici Nov. 1987 69 p
(Grant AF-AFOSR-0308-85)
(AD-A189929) Avail: NTIS HC A04/MF A01 CSCL 20D

The field of flow visualization has been reviewed and its application to the study of the flow near the tip of an unshrouded axial turbine rotor discussed in detail. The logical conceptualization of experiments which could lead to a final understanding of the flow structure was developed and how this leads to test turbine design philosophy is suggested. The rotor periodicity shed by the stator requires that particle of pulse tracing is needed rather than the more universal continuous streamline trace which arises from a continuous tracer injection at a point in a flow. While the whole field of flow visualization at a rotor tip is demanding because of its very nature, pulse tracking will place a greater demand on the development of new skills and techniques. Since streamline tracking is somewhat more standard, these demands will not be as great. A fundamental choice does however need to be made between the two methods. The suggested experimental turbine should thus, always with the facility of infinitely variable Mach number, model the following: (1) Stationary annular cascade with tip clearance inside a stationary outer endwall; (2) Stationary annular cascade with tip clearance inside a moving endwall; (3) The transfer of flow visualization techniques developed into the rotating frame; (4) Fully rotating rotor with no inlet periodicity; (5) Fully rotating rotor with inlet periodicity. GRA

N88-22302# State Univ. of New York, Albany. Research Foundation.
ENHANCEMENT OF DATA ACQUISITION AND NUMERICAL COMPUTATION CAPABILITIES FOR UNSTEADY FLUID DYNAMICS Final Report, 26 May 1986 - 25 May 1987
William K. George 20 Oct. 1987 4 p
(Grant AF-AFOSR-0209-86)
(AD-A190115; AFOSR-87-1788TR) Avail: NTIS HC A02/MF A01 CSCL 14B

A significant improvement in the data acquisition and numerical computation capabilities of the Turbulence Research Laboratory was achieved by: (1) the upgrading of the data acquisition system to a PDP 11/84, (2) the addition of a micro VAX work station, and (3) the upgrading of the central computing array processor. All facilities are linked with Ethernet thereby providing for very high speed data links from the laboratory to the VAX Cluster and Array Processor. Also, the facilities are linked by NYSERNET (59k baud) to the NSF supercomputer network. GRA

N88-22303# Johns Hopkins Univ., Baltimore, Md.
RANDOM PROCESSES, TURBULENCE AND DISORDERING FIELDS Technical Report, Jan. 1986 - Jan. 1987
G. Domokos, S. Kovesi-Domokos, and C. K. Zoltani Oct. 1987 26 p
(DA Proj. 1L1-61102-AH-43)
(AD-A190123; BRL-TR-2861) Avail: NTIS HC A03/MF A01 CSCL 12C

There are many classical, nonlinear systems exhibiting some kind of chaotic behavior. Examples include the turbulent flow of a fluid, usually described by means of the Navier-Stokes equations, and the behavior of liquids, gases or antiferromagnets above the critical point, etc. In this paper, we reexamine and further develop an approach to the description of such systems. The statistical theory of random process is cast into a Lagrangian form. The formalism requires the existence of an arbitrarily weak random stirring force, playing the role of a disordering field. In scale invariant

systems the coupling strength of the weak stirring force can be scaled out and it disappears from the theory. GRA

N88-22304# Wisconsin Univ., Madison. Dept. of Engineering Mechanics.
A NEW METHOD OF MEASURING MULTIGRADE OIL SHEAR ELASTICITY AND VISCOSITY AT HIGH SHEAR RATES
Arthur S. Lodge 1987 20 p
(Contract DAAG29-84-K-0046)
(AD-A190145; ARO-20815.7-EG) Avail: NTIS HC A03/MF A01 CSCL 11H

Recent journal bearing oil film thickness data strongly suggest that, in order to develop minimum-viscosity multigrade oils for maximizing fuel economy, it is not enough to examine viscosity eta alone, it is essential also to examine a certain kind of shear elasticity, of which one measure is the first normal stress difference N1 in shear flow. Within a group of isoviscous multigrade oils, N1 values can differ significantly; for 10W-40 and 15W-40 oils, an average of 75 percent of the minimum oil film thickness can be attributed to N1. GRA

N88-22305# Grumman Aerospace Corp., Bethpage, N.Y. Corporate Research Center.
ON THE PREDICTION OF HIGHLY VORTICAL FLOWS USING AN EULER EQUATION MODEL, PART 2 Final Report, 31 Jul. 1985 - 31 Jul. 1987
Frank Marconi 30 Oct. 1987 137 p
(Contract F49620-85-C-0115)
(AD-A190245; AFOSR-87-1910TR-Pt-2) Avail: NTIS HC A07/MF A01 CSCL 20D

An investigation of the power of the Euler equations in the prediction of conical separated flows is presented. These equations are solved numerically for the highly vortical supersonic flow about simple bodies. Two sources of vorticity are studied: the first is the flow field shock system and the second is the vorticity shed into the flow field from a separating boundary layer. Both sources of vorticity are found to produce separation and vortices. In the case of shed vorticity, the surface point from which the vorticity is shed (i.e., separation point) is determined empirically. At very high angles of attack the only stable separated solution is found to be asymmetric. Solutions obtained with both sources of vorticity are studied in detail, compared with each other and with potential calculations and experimental data. GRA

N88-22306# Massachusetts Inst. of Tech., Cambridge. Dept. of Ocean Engineering.
COMPARISON OF ENTROPY GENERATION AND CONVENTIONAL DESIGN METHODS FOR HEAT EXCHANGERS M.S. Thesis
David S. Herbein Jun. 1987 65 p
(Contract N00228-85-G-3262)
(AD-A190256) Avail: NTIS HC A04/MF A01 CSCL 13J

The design of heat exchangers traditionally focuses on the known constraints of the problem such as inlet and outlet temperatures, flow rates, and pressure drops. This leads mainly to a sizing problem where the designer must select surfaces, flow configuration, and materials to meet the minimum design objectives. An alternate approach based on an acceptable level of thermodynamic irreversibility (entropy generation) has been proposed. When the entropy generation level has been set, the geometric parameters of the heat exchanger can be determined. The design of a plate-fin type, gas-to-gas recuperator for a regenerative open Brayton cycle has been used as a demonstrative device. The resulting heat exchanger designs are then examined to determine what caused the differences and why either method should be preferred over the other. GRA

N88-22307# Michigan Univ., Ann Arbor. Dept. of Aerospace Engineering.
DENSE-SPRAY STRUCTURE AND PHENOMENA. PART 2: PRESSURE-ATOMIZED SPRAYS Annual Report, 15 Jul. 1986 - 14 Jul. 1987
G. A. Ruff and G. M. Faeth 15 Aug. 1987 69 p
(Grant AF-AFOSR-0244-85)
(AD-A190312; AFOSR-87-2009TR-Pt-2) Avail: NTIS HC A04/MF A01 CSCL 20D

A theoretical and experimental study of the dense-spray region of pressure-atomized nonevaporating sprays is described, emphasizing operation in the wind-induced and atomization breakup regimes. Experiments involved large-scale (9.5 and 19.1 mm injector diameters) water jets in still air. The flows were visualized using flash photography. In addition, the following measurements were made: mean and fluctuating streamwise velocities at the injector exit, mean liquid volume fraction distributions, and mean entertainment rates. The new measurements were used to assess predictions of flow structure based on the locally-homogeneous-flow approximation, i.e., assuming that interphase transport rates are infinitely fast so that relative velocities between the phases are negligible. GRA

N88-22308# Massachusetts Inst. of Tech., Cambridge. Acoustics and Vibration Lab.
BODIES IN UNSTEADY FLOW Final Report, 1 Sep. 1978 - 31 Aug. 1985
Patrick Leehey 30 Dec. 1987 6 p
(Contract N00014-78-C-0696)
(AD-A190416; Rept-87144-2) Avail: NTIS HC A02/MF A01 CSCL 20D

Research accomplished on vortex shedding from a cylinder, development of a floating element gauge for measuring shear stress, axisymmetric towed hydrophone housing, and experimental study of a thick axisymmetric turbulent boundary layer is discussed. GRA

N88-22309# Pennsylvania State Univ., University Park. Applied Research Lab.
THE SENSITIVITY OF BOUNDARY LAYER INSTABILITY GROWTH RATES TO COMPLIANT WALL PROPERTIES M.S. Thesis
R. D. Joslin and Philip J. Morris Dec. 1987 102 p
(Contract N00024-85-C-6041)
(AD-A190433; ARL/PSU/TR-87-014) Avail: NTIS HC A06/MF A01 CSCL 20D

A spatial stability analysis is performed for the boundary layer over a non-isotropic compliant surface. A spectral approximation is used to obtain a solution of the equations governing the normal velocity component of a small disturbance. The streamwise wavenumber becomes the eigenvalue in the nonlinear eigenvalue problem formed. The resulting solution spectrum contains values which indicate the growth rates of the Tollmien-Schlichting and flow-induced surface instabilities. It is shown that the Tollmien-Schlichting instability is most sensitive to changes in the surface properties. It is shown that varying the surface properties can reduce the growth rate of the Tollmien Schlichting instability but has little effect on the flow-induced surface instability. The surface properties are optimized using a minimization algorithm. It is found that appropriate surface properties lead to a decrease in the growth rates of the flow instability. The simple mechanical model for the compliant surface is an elastic plate over spring-rigid supports. The functional relationship between the flexural rigidity, thickness, and modulus of elasticity of the plate provides a means to vary the properties and determine the effect on the instabilities. It is found that by keeping the flexural rigidity essentially constant and simultaneously increasing the plate thickness and decreasing the modulus of elasticity a decrease in the growth rate of the Tollmien-Schlichting instability is obtained. GRA

N88-22310# Air Force Inst. of Tech., Wright-Patterson AFB, Ohio. School of Engineering.
INTERACTION OF A TWO-DIMENSIONAL BLUFF BODY AND INCOMPRESSIBLE JET AND ANNULUS FLOWS M.S. Thesis
Christopher A. Boedicker Dec. 1987 165 p
(AD-A190503; AFIT/GAE/AA/87D-2) Avail: NTIS HC A08/MF A01 CSCL 20D

A particular interaction of bluff body and jet flows was studied using two dimensional slot jet (aspect ratio = 50) surrounded by

a two dimensional bluff body. The coflowing system used air in the annulus and nitrogen in the jet. Flow visualization identified flow patterns containing large vortex structures. These were observed as jet velocities changed. Laser Doppler Anenometry measurements of instantaneous velocities were examined to characterize the flowfield details, and high speed movies provided qualitative insight into flow dynamics. The concept of jet and annulus fields is introduced. The jet field is the region above the bluff body that extends six or seven slot widths downstream, and the annulus field is the region above the jet field. The annulus flow dictates the flowfield dynamics in the annulus field up to jet-to-annulus velocity ratios of 1.45. The jet is responsible for the formation of the large-scale structures and dominates the flow in the jet field. Jet domination of the entire flowfield is seen at velocity ratios of 1.45 and above. Mie scattering was used to determine shedding frequencies of the large structures. GRA

N88-22311# National Bureau of Standards, Gaithersburg, Md. Center for Fire Research.
CHEMICALLY REACTING TURBULENT FLOW Final Report, 1 Oct. 1982 - 30 Sep. 1986
William H. Pitts and Takashi Kashiwagi 14 Apr. 1987 69 p
(Grants AF-AFOSR-ISSA-00008-86; AF-AFOSR-ISSA-00012-85)
(AD-A190522; AFOSR-87-1761TR) Avail: NTIS HC A04/MF A01 CSCL 20D

This report summarizes the research findings of a project which has been jointly funded by the Air Force Office of Scientific Research and the National Bureau of Standards. The goal of the research was to improve the fundamental understanding of chemically reacting turbulent flow. The approach which was taken was to investigate mixing in variable density flows in order to better understand the role of local density fluctuations (which result from chemical heat release) on the turbulent mixing behavior. The development of new experimental diagnostics having excellent spatial and temporal resolution is described. These techniques have been utilized to investigate a wide range of mixing properties in variable density flows. These results are summarized along with a discussion of their importance to an improved understanding of chemically reacting flow. GRA

N88-22312# Stanford Univ., Calif. Dept. of Mechanical Engineering.
INSTRUMENTS FOR USE IN EXPERIMENTAL STUDIES OF COMPLEX TURBULENT SHEAR FLOW: THREE COMPONENT LDVs Final Report, 1 Aug. 1986 - 31 Jul. 1987
James P. Johnston 12 Nov. 1987 4 p
(Grant AF-AFOSR-0276-86)
(AD-A190526; AFOSR-87-1770TR) Avail: NTIS HC A02/MF A01 CSCL 20D

The goal of the grant was to enhance the capability of our laboratory to acquire detailed, quantitative, fluid velocity data in three orthogonal directions simultaneously in our two low speed water flow channels. These facilities are being used to study the turbulence structure of boundary and free mixing layers perturbed by the effects of longitudinal curvature and high levels of free stream turbulence. GRA

N88-22313# Massachusetts Inst. of Tech., Cambridge. Artificial Intelligence Lab.
COMPARATIVE ANALYSIS
Daniel S. Weld Nov. 1987 49 p
(Contract N00014-85-K-0124)
(AD-A190556; AI-M-951) Avail: NTIS HC A03/MF A01 CSCL 12I

Comparative analysis involves the problem of predicting how a system will react to perturbations in its parameters, and why. For example, comparative analysis could be asked to explain why the period of an oscillating spring/block system would increase if the mass of the block were larger. This paper formalizes the problem of comparative analysis and presents a technique, differential qualitative (DQ) analysis, which solves the task, providing explanation based generalization. DQ analysis uses inference rules to deduce qualitative information about the relative change of system parameters. Multiple perspectives are used to represent relative change values over intervals of time. Differential analysis has been implemented, tested on a dozen examples, and proven sound. Unfortunately, the technique is incomplete; it always terminates, but does not always return an answer. GRA

N88-22314# Air Force Inst. of Tech., Wright-Patterson AFB, Ohio. School of Engineering.
INVESTIGATION OF BOUNDARY LAYER DISTURBANCES CAUSED BY PERIODIC HEATING OF A THIN RIBBON M.S. Thesis
Brenda Haven Mar. 1988 112 p
(AD-A190572; AFIT/GAE/AA/88M-2) Avail: NTIS HC A06/MF A01 CSCL 20D

Wind tunnel experiments were conducted to investigate the use of a periodically heated Nichrome ribbon as a boundary layer control device. The specific items of interest were: (1) the physical parameters governing the ribbon behavior, (2) the consequence of the ribbon on the downstream development of the laminar boundary layer, and (3) the controllability of the ribbon to produce the desired consequence. The disturbances detected in the boundary layer immediately downstream of the vibrating ribbon exhibited the same frequency characteristics as the ribbon. The evolution of these disturbances in the boundary layer was studied by positioning a hot wire anemometer boundary layer probe at different locations behind the ribbon. The selective amplification and damping of the disturbance frequencies agreed with the predictions of linear Tollmien-Schlichting stability theory. GRA

N88-22315# Michigan Univ., Ann Arbor. Gas Dynamics Labs.
DENSE-SPRAY STRUCTURE AND PHENOMENA. PART 1. TURBULENCE/DISPERSED-PHASE INTERACTIONS Annual Report, 15 Jul. 1986 - 14 Jul. 1987
R. N. Parthasarathy and G. M. Faeth 15 Aug. 1987 81 p
(AF Proj. 2308)
(AD-A190606; AFOSR-87-1758TR-Pt-1) Avail: NTIS HC A05/MF A01 CSCL 20D

This report describes one aspect of an investigation of dense-spray processes: namely turbulence/dispersed-phase interactions. The work was divided into two phases: measurements of particle-laden jets injected into a still liquid; and homogenous particle flows, consisting of particles falling in a still (in the mean) liquid bath. The structure of turbulent, dilute, particle-laden water jets, submerged in still water, was studied both experimentally and theoretically. Nonintrusive measurements were made of mean and fluctuating phase velocities and particle number fluxes. Analysis was used to help interpret the measurements, considering three limiting cases, as follows: (1) locally-homogenous flow, where relative velocities between the phases are ignored; (2) deterministic separated flow, where relative velocities are considered, but particle/turbulence interactions are ignored; and (3) stochastic separated flow, where both phenomena are considered using random-walk methods. The locally-homogenous flow approximation was more effective than for past work involving larger density ratios between the phases; nevertheless, stochastic analysis yielded best agreement with measurements. GRA

N88-22316# Air Force Inst. of Tech., Wright-Patterson AFB, Ohio. School of Engineering.
EFFECT OF FREESTREAM TURBULENCE ON A TWO DIMENSIONAL CASCADE, WITH DIFFERENT SURFACE ROUGHNESS, AT HIGH REYNOLDS NUMBER M.S. Thesis
Salman Absar Mar. 1988 283 p
(AD-A190615; AFIT/GAE/AA/88M-1) Avail: NTIS HC A13/MF A01 CSCL 20D

The present study shows the effects of high freestream turbulence on the performance of a two dimensional cascade. The cascade consisted of seven NACA 65-A506 airfoils with two inches chord. Experiments were carried out at flow Reynolds number per foot in excess of two and a half million. Flow turbulence intensity of 7 percent was generated upstream of the cascade. Blades with three different categories of surface roughness were studied. High freestream turbulence results in a decrease in total

pressure loss coefficient in the cascade and an increase in the total pressure loss coefficient in the wake. The results also show an increase in pressure coefficient, over the suction surface, independent of the amount of surface roughness. The boundary layer thickness, after 50 percent chord, increases substantially, with an increase in freestream turbulence. This effect is aggravated with higher surface roughness. The effects of high freestream turbulence on boundary layer edge velocity are sensitive to local surface roughness. With low surface roughness, the boundary layer edge velocity increases with freestream turbulence. The results indicate an opposite effect when local surface roughness is increased. GRA

N88-22317# Air Force Systems Command, Wright-Patterson AFB, Ohio. Foreign Technology Div.

EXPERIMENTAL DETERMINATION OF THE COEFFICIENTS OF THE HYDRAULIC RESISTANCE OF APERTURES IN THE ROTARY DISKS

I. T. Shvets, Ye. P. Dyban, G. F. Selyavin, and M. V. Stradomskiy 22 Jan. 1988 27 p Transl. into ENGLISH from Izvestiya Vysshikh Uchebnykh Zavedeniy Energetika (USSR), no. 2, Mar. 1960 p 89-99

(AD-A190627; FTD-ID(RS)T-1334-87) Avail: NTIS HC A03/MF A01 CSCL 20D

Following are some conclusions reached in the determination of the haydraulic resistance of apertures in rotary disks: (1) rotation of disk exerts a substantial influence on condition of course of air through apertures. In the large ratios of the velocity of the rotation of the mean flow rate in the aperture (order u/c = 2.5) the value of the coefficient of flow rate for the apertures with the sharp entering edges decreases approximately 6 times; (2) with sufficient high u/c (more than 4) effect of form of entering edges it is possible not to consider; (3) rounding of trailing edges virtually does not have effect on conditions of air flow through apertures in rotary disks; (4) coefficient of flow rate of apertures of square form investigated in work is close to coefficient of expenditure of cylindrical channels (with identical hydraulic radii); (5) relative depth of aperture in the range of relations 0.96 less than l/d less than 6.04 virtually does not have effect on dependence of value of coefficient of flow rate from rotation; (6) on the basis of analysis of experimental data in work empirical dependence of coefficients of flow rate and hydraulic resistance on parameters K and K, are obtained. The ratios indicated are valid for the disk, which rotates in the housing with the value relative to the axial clearance between the disk and the housing of more than 1.5. GRA

N88-22318# Pennsylvania State Univ., University Park. Applied Research Lab.

CAVITATION INCEPTION IN RECTANGULAR TWO-DIMENSIONAL SLOTS M.S. Thesis

W. G. Blair and J. M. Cimbala Dec. 1987 140 p

(Contract N00024-85-C-6041)

(AD-A190677; ARL/PSU/TR-87-013) Avail: NTIS HC A07/MF A01 CSCL 20D

The two dimensional fluid mechanics of flow over a rectangular slot along a flat wall were studied in air. A thick (greater than slot width) turbulent boundary layer was established at the slot entrance location. The flow field within and at the slot entrance was studied as the slot geometry was varied for depth-to-width ratios (aspects ratios) ranging from 0.5 to 3.0. Flow visualization inside the slot describes the internal flow field of the slot and reveals the highly unsteady nature of the vortex-like structure(s) that develop. Flow visualization as well as direct pressure measurements inside the slot document vortex location as a function of aspect ratio. The minimum pressure in the slot, found at the primary vortex center, is also documented as a function of aspect ratio. The measured pressure coefficients inside the slot are an order of magnitude lower than those of which cavitation has been observed in previous water tunnel experiments. These measurements therefore lead to question the interpretation of the previous water tunnel slot cavitation experiments. Specifically, it is likely that the previously reported cavitation was partially gaseous rather than purely vaporous cavitation, as had been assumed. GRA

N88-22319# Ballistic Research Labs., Aberdeen Proving Ground, Md.

FLUID MOTION IN A SPINNING, CONING CYLINDER VIA SPATIAL EIGENFUNCTION EXPANSION

Philip Hall, Raymond Sedney, and Nathan Gerber Aug. 1987 58 p Supersedes BRL-IMR-886

(AD-A190758; BRL-TR-2813; BRL-IMR-886) Avail: NTIS HC A04/MF A01 CSCL 20D

The first attempts to explain the motion of a liquid-filled projectile were confined to the limit Reynolds Number = Re approaches infinity and linear theory. Recently, the need became apparent for the limit Re approaches 0 for which the spatial eigenvalue method was developed; it is not restricted in Re, however. The eigenvalue problem is defined by ordinary differential equations in the radial direction. The eigenvalues are determined by an iterative process for which sufficiently accurate initial estimates are required. The flow variables are expanded in a eigenfunction series with coefficients determined by satisfying the boundary conditions; a least squares method and collocation method are used for this purpose. The pressure and shear stress so determined give the pressure coefficient and overturning moment. The accuracy of the calculation is discussed. Results are given over a range of Re, aspect ratio, and nutational frequency. The CPU time required on the VAX 8600 varies from 10 seconds at Re = 10 to 30 minutes at Re = 1,000. Results are compared with experimental measurements. Comparisons are also made with results from the large scale finite difference program of Strikwerda. GRA

N88-22320# Illinois Univ., Urbana. Dept. of Mechanical and Industrial Engineering.

NUMERICAL AND EXPERIMENTAL INVESTIGATION OF MULTIPLE SHOCK WAVE/TURBULENT BOUNDARY LAYER INTERACTIONS IN A RECTANGULAR DUCT Final Technical Report, 1 Jul. 1985 - 31 Dec. 1987

J. C. Dutton and B. F. Carroll 6 Jan. 1988 115 p

(Contract N00014-85-K-0665)

(AD-A190772; UILU-ENG-88-4001) Avail: NTIS HC A06/MF A01 CSCL 20D

Multiple shock wave/turbulent boundary layer interactions in constant or nearly constant area supersonic duct flows occur in a variety of devices including scramjet inlets, gas ejectors, and supersonic wind tunnels. For sufficiently high duct exit pressures, a multiple shock wave/turbulent boundary layer interaction or shock train may form in the duct and cause a highly nonuniform, and possibly unsteady, flow at the duct exit. In this report, the mean flow characteristics of two shock train interactions, one with an initial Mach number of 2.5 the other at Mach 1.6, are investigated using spark Schlieren photography, surface oil flow visualization, and mean wall pressure measurements. The Mach 2.5 interaction was oblique and asymmetric in nature. A large separation occurs after the first oblique shock. The top and bottom wall boundary layer separation has been investigated, revealing that the shape of the reattachment lines and surface flow patterns for the two separation regions are quite different. This oblique shock flow pattern occurs in a neurally stable fashion with each type of opposing separation region alternately existing on either the top or bottom wall during the course of a run. A small scale unsteadiness in the shock train location, with movement on the order of a boundary layer thickness, is also observed. GRA

N88-22321# Boeing Aerospace Co., Seattle, Wash.

FLOSIN: A FLUID LOOP ANALYZER FOR SINDA

Steven M. Lunde [1988] 11 p Presented at the SAE 18th Intersociety Conference on Environment Systems

Avail: NTIS HC A03/MF A01

High-power heat transport systems for large space platforms require the use of complex fluid loops to effectively and efficiently move waste heat energy from source to sink. In particular, use of two-phase heat acquisition and transport systems offers significant advantages such as reduction of pump power, automation of control systems, constant sink temperatures at the load, and flexible load placement. Analytical tools are needed for design analysis and

performance prediction of these systems. Moreover, environmental considerations and insulation systems need to be taken into account, especially when subcooling and superheating become important parameters in the overall design. The development and use of FLOSIN, a system-level, two-phase fluid loop analyzer, are discussed. Explained are the modeling approach for systems utilizing Rotary Fluid Management Device (RFMD), Back Pressure Regulating Valve (BPRV), and cavitating venturis. Described are the unique components and special subroutines for processing input and output, for handling flow splits, and for generating Systems Improved Numerical Differencing Analyzer (SINDA) thermal networks. Author

N88-22322*# Minnesota Univ., Minneapolis.
A SURVEY OF OSCILLATING FLOW IN STIRLING ENGINE HEAT EXCHANGERS Annual Contractor Report
Terrence W. Simon and Jorge R. Seume Mar. 1988 133 p
(Grant NAG3-598)
(NASA-CR-182108; NAS 1.26:182108) Avail: NTIS HC A07/MF A01 CSCL 20D

Similarity parameters for characterizing the effect of flow oscillation on wall shear stress, viscous dissipation, pressure drop and heat transfer rates are proposed. They are based on physical agruments and are derived by normalizing the governing equations. The literature on oscillating duct flows, regenerator and porous media flows is surveyed. The operating characteristics of the heat exchanger of eleven Stirling engines are discribed in terms of the similarity parameters. Previous experimental and analytical results are discussed in terms of these parameters and used to estimate the nature of the oscillating flow under engine operating conditions. The operating points for many of the modern Stirling engines are in or near the laminar to turbulent transition region. In several engines, working fluid does not pass entirely through heat exchangers during a cycle. Questions that need to be addressed by further research are identified. Author

N88-22323# Southwest Research Inst., San Antonio, Tex.
EXPERIMENTS ON DENSELY-LOADED NON-NEWTONIAN SLURRIES IN LAMINAR AND TURBULENT PIPE FLOWS Quarterly Progress Report No. 5
J. T. Park, R. J. Mannheimer, T. A. Grimley, and T. B. Morrow 23 Feb. 1988 47 p
(Contract DE-FG22-86PC-90962)
(DE88-006209; DOE/PC-90962/T5) Avail: NTIS HC A03/MF A01

An experimental description of the flow structure of non-Newtonian slurries in the laminar, transitional, and full turbulent pipe flow regimes is the primary objective of this research. Measurements include rheological characterization of the fluid and local fluid velocity measurements with a laser Doppler velocimeter (LDV). Optical access to the flow is gained through a test section and model slurry which are both transparent. The model slurry is formulated from silica gel particles and hydrocarbon liquid mixture whose indices of refraction are matched so that light is not scattered from the particles. Experiments are being conducted in a large-scale pipe slurry flow facility with an inside pipe diameter of 51 mm (2 inches). Detailed flow measurements including turbulence quantities such as Reynolds stress were measured with a two-component two-color LDV. The present research indicates that non-Newtonian slurries are possible with concentrations of a few percent by weight of small particles whose sizes are one micron or less. A non-Newtonian slurry from small particles could maintain large particles (100 micron size) at high concentrations in suspension almost indefinitely. Such a slurry would prevent particle fallout and its associated problems. Velocity profiles were acquired by the LDV in the laminar, transitional, and turbulent flow regimes. The velocity profile for laminar flow was in agreement with theory. The range of the transition region was 21 percent of the transition velocity in comparison to 50 percent for a Newtonian fluid. DOE

N88-22324# Sandia National Labs., Albuquerque, N. Mex.
TRANSIENT COMPRESSIBLE FLOW IN POROUS MATERIALS
J. E. Shepherd and D. R. Begeal Jan. 1988 63 p
(Contract DE-AC04-76DP-00789)
(DE88-006685; SAND-83-1788) Avail: NTIS HC A04/MF A01

An experimental investigation of transient compressible flow in porous materials is reported. Two types of experiments have been carried out to verify the simplified models of compressible flow that have been developed by other investigators over the last decade and to extend the drag coefficient measurements to high Reynolds numbers. Results are reported for packed beds constructed from glass beads and three types of granular explosives: CP, HMX, and HNS. DOE

N88-22325*# National Aeronautics and Space Administration. Langley Research Center, Hampton, Va.
AEROTHERMAL TESTS OF QUILTED DOME MODELS ON A FLAT PLATE AT A MACH NUMBER OF 6.5
Christopher E. Glass and L. Roane Hunt May 1988 72 p
(NASA-TP-2804; L-16346; NAS 1.60:2804) Avail: NTIS HC A04/MF A01 CSCL 20D

Aerothermal tests were conducted in the NASA Langley 8 Foot High Temperature Tunnel (8'HTT) at a Mach number of 6.5 on simulated arrays of thermally bowed metallic thermal protection system (TPS) tiles at an angle of attack of 5 deg. Detailed surface pressures and heating rates were obtained for arrays aligned with the flow and skewed 45 deg diagonally to the flow with nominal bowed heights of 0.1, 0.2, and 0.4 inch submerged in both laminar and turbulent boundary layers. Aerothermal tests were made at a nominal total temperature of 3300 R, a total pressure of 400 psia, a total enthalpy of 950 Btu/lbm, a dynamic pressure of 2.7 psi, and a unit Reynolds number of 400,000 per foot. The experimental results form a data base that can be used to help protect aerothermal load increases from bowed arrays of TPS tiles. Author

N88-22326*# National Aeronautics and Space Administration, Washington, D.C.
DESIGNS OF PROFILES FOR CASCADES
L. Goettsching Apr. 1988 30 p Transl. into ENGLISH from Thermodynamic and Flow Mechanical Problems in Aircraft and Spacecraft Drives (Fed. Republic of Germany, Stuttgart Univ.), Apr. 1986 p 243-267 Transl. by Scientific Translation Service, Santa Barbara, Calif. Original language document was announced as N87-14340
(Contract NASw-4307)
(NASA-TT-20161; NAS 1.77:20161; ETN-87-98751) Avail: NTIS HC A03/MF A01 CSCL 20D

Optimized cascade profiles for arbitrary applications were designed. The influence of Mach number, Reynolds number, and degree of turbulence were taken into account. The optimization aimed at maximum pressure increase, minimum pressure loss, low Reynolds number dependence, or large angle-of-attack range. Starting from the boundary layer form parameter distribution (by which transition point and separation point can be controlled) the velocity distribution and the contour were calculated. The profile characteristics were tested off-design and were improved. Interferometric measurements were performed in the transonic cascade channel. Author

N88-22327# Massachusetts Univ., Amherst. Dept. of Chemical Engineering.
MIXING: STRETCHING, BREAKUP AND CHAOS
J. M. Ottino 1987 9 p Presented at the 1st Symposium on Energy Engineering Sciences, Argonne, Ill., 17 Jun. 1987
(Contract DE-FG02-85ER-13333)
(DE88-006699; CONF-8706187-1) Avail: NTIS HC A02/MF A01

In spite of its universality and practical implications, the understanding of fluid mixing remains largely empirical and little theoretical foundation exists at the present time. In this paper some recent work in this area is briefly summarized. Two closely related matters are discussed: (1) theoretical and experimental investigations of the conditions that determine the onset of chaos in deterministic two dimensional flows, and (2) studies of the

dynamics of stretching and breakup of small droplets in such flows. Thus, (1) focuses on a global scale whereas (2) is a local analysis focusing on deformation and breakup in Lagrangian (linear) time dependent flows. The breakup depends in a complicated way on the balance between elongation and vorticity at small scales; on the other hand, the dispersion is effective if the large scale flow is chaotic. Much work remains to mesh the two levels; in this paper we elaborate on both aspects and indicate possible lines of attack for future studies. DOE

N88-22328# Babcock and Wilcox Co., Lynchburg, Va. Lynchburg Research Center.
AN EVALUATION OF NONDESTRUCTIVE METHODS FOR CERAMIC HEAT EXCHANGER APPLICATIONS
J. R. Bower and T. Powers 1987 17 p Presented at the Conference on Nondestructive Testing of High Performance Ceramics, Boston, Mass., 25 Aug. 1987
(Contract DE-AC07-76ID-01570)
(DE88-006731; EGG-M-08687; CONF-870856-4) Avail: NTIS HC A03/MF A01

For both seeded defects and naturally occurring defects, there is little correlation between test results for small defects. This is because X-ray is sensitive to density variations and ultrasonics and scanning laser acoustic microscopy (SLAM) are sensitive to acoustic impedance variations. The grain boundaries and microporosity of the material produce a high scattering background for the acoustic methods, masking small inclusions. X-ray is insensitive to grain boundary effects and the uniform microporosity averages out over the material thickness. If minor inclusions are to be detected, X-ray must be used. Ultrasonics and SLAM are sensitive only to the presence of an open crack, not its width. If cracks are to be detected, ultrasonics or SLAM must be used. SLAM is by far the fastest method of scanning for OD cracks, but only ultrasonics will find ID cracks. Results of this first phase study give four guidelines to tube design. First, surface irregularities are a major limitation to testing. The eventual tests will be much more sensitive if surface finish can be improved. Second, porosity is another major limit to testing. Pores are not generally strength limiting in this material, but pores scatter ultrasound very badly and produce irregular densities on X-ray film, in both cases obscuring more important defect indications. Third, the dimple shape of the closed end is essentially untestable. The fourth design guideline is provided by the fractography results. In some cases, failure was initiated in or near clusters of large grains. Defect sizing depends upon the detection methods. DOE

N88-22329# Erlangen-Nuremberg Univ. (West Germany). Lehrstuhl fuer Stroemungsmechanik.
PISTON-DRIVEN, UNSTEADY SEPARATION AT A SUDDEN EXPANSION IN A TUBE: FLOW VISUALIZATION AND LASER DOPPLER ANEMOMETER (LDA) MEASUREMENTS
F. Durst, T. Maxworthy (University of Southern California, Los Angeles.), and J. C. F. Pereira 1987 56 p Sponsored in cooperation with Forschungsvereinigung-Verbrennungskraftmaschinen, Federal Republic of Germany and The Alexander von Humbolt Foundation.
(Contract DFG-DU-101/7-1,2)
(ETN-88-92104) Avail: NTIS HC A04/MF A01

Flow visualization studies and measurements were performed of the flow field generated at a sudden expansion in a cylindrical pipe during the intake stroke of a piston. Piston Reynolds numbers investigated were 18 to 125 and covered the laminar and transition-to-turbulence regimes. A study of the parameters influencing the structure of the flow, i.e., the clearance volume and the piston velocity, is presented, and the mechanism for the creation of flow instabilities at low Reynolds numbers is outlined. The effect of flow Reynolds number is found to be small while the magnitude of the initial clearance volume is very important and controls the qualitative features of the flow in the otherwise invariant geometry. Qualitative comparisons of the streamline patterns found from the flow visualization studies and from integration of the experimental velocity field measured by laser Doppler anemometry are given. The data can be used to compare computational schemes proposed to numerically study problems of this type. ESA

N88-22330# Deutsche Forschungs- und Versuchsanstalt fuer Luft- und Raumfahrt, Goettingen (West Germany). Inst. fuer Theoretische Stroemungsmechanik.
THEORETICAL INVESTIGATION OF SECONDARY INSTABILITY OF THREE-DIMENSIONAL BOUNDARY-LAYER FLOWS WITH APPLICATION TO THE DFVLR-F5 MODEL WING
Thomas M. Fischer and Uwe Dallmann Sep. 1987 64 p
(DFVLR-FB-87-44; ISSN-0171-1342; ETN-88-92113) Avail: NTIS HC A04/MF A01; DFVLR, VB-PL-DO, 90 60 58, 5000 Cologne, Federal Republic of Germany, 20.50 deutsche marks

The transition of a laminar three-dimensional boundary-layer flow to a turbulent flow was studied. The transition is governed by nonlinear interactions between stationary vortex structures and instationary disturbances. In order to incorporate such interactions into a transition model, the boundary layer flow being primarily disturbed by the stationary so-called crossflow vortices was investigated locally for secondary instability. Results for the boundary layer of a swept model wing show the importance of waves traveling preferably oblique to the direction of the external inviscid flow. ESA

35 INSTRUMENTATION AND PHOTOGRAPHY

Includes remote sensors; measuring instruments and gages; detectors; cameras and photographic supplies; and holography.

For aerial photography see *43 Earth Resources and Remote Sensing.* For related information see also *06 Aircraft Instrumentation,* and *19 Spacecraft Instrumentation.*

N88-22331*# RCA Aerospace and Defense, Camden, N.J. Government Communications Systems Div.
UARS SPACECRAFT RECORDER Final Report
23 Jul. 1987 32 p
(Contract NAS5-29186)
(NASA-CR-180768; NAS 1.26:180768) Avail: NTIS HC A03/MF A01 CSCL 14C

The objective was the design, development, and fabrication of UARS spacecraft recorders. The UARS recorder is a tailored configuration of the RCA Standard Tape recorder STR-108. The specifications and requirements are reviewed. B.G.

N88-22332# Gosudarstvennyi Komitet po Ispolzovaniyu Atomnoi Energii, Moscow (USSR). Inst. Teoreticheskoj i Ehksperimental'noj.
MIG-1 ON-LINE MEASURING HOLOGRAPHIC MICROSCOPE
Yu. D. Aleshin, V. A. Goncharov, and T. D. Karlov 1987 12 p In RUSSIAN
(TI88-701103; ITEF-4(1987)) Avail: NTIS (US Sales Only) HC A03/MF A01

Design and main technical parameters of MIG-1 automated holographic microscope are described. Microscope permits the measurement of elementary particles detected and holographically reconstructed. The design takes into account peculiarities of focuced image extra-axial holography. Microscope control is automated by Ehlectronica-60 computer. MIG-1 is designed on the basis of UIM-23 instrumental microscope mounted on a 2000 x 1000 mm bench plate with film-pulling mechanism and laser. Specially developed third measuring carriage with vertical movement is added to UIM-23 two horizontal measuring carriages. DOE

N88-22333# Gosudarstvennyi Komitet po Ispolzovaniyu Atomnoi Energii, Moscow (USSR). Inst. Teoreticheskoj i ehksperimental'noj.
FOCUSED IMAGE HOLOGRAPHY ABBERATIONS

I. A. Melnichenko 1987 20 p In RUSSIAN
(TI88-701105; ITEF-12(1987)) Avail: NTIS (US Sales Only) HC A03/MF A01

At present for operation at new constructing tevatron-accelerators holographic recording methods are developed for 15-foot Fermilab chamber, for BEBC chamber in CERN, for one-meter holographic bubble chamber of Tokyo University. Theoretical and experimental study of focused image holography (FIH) aberrations is carried out, the values of admissible parameters of restoration, in which range aberrations do not deteriorate resolution on reconstructed image of the object, are determined. It is shown that in FIH diagram aberrations are absent at reconstructed image, if while recording reconstructing beam wave length is equal to that of reference beam, and the first beam is equal to the second conjugated. FIH lenses aberrations may be insignificant if reconstruction parameters in certain limits are equal to that of recording process. DOE

N88-22334# Arizona State Univ., Tempe.
SUMMARY AND CONCLUSIONS ON ELECTROOPTICAL STREAK CAMERA PROJECT
B. Welch 1988 28 p
(Contract W-7405-eng-48)
(DE88-006616; UCRL-21017) Avail: NTIS HC A03

Two modifications to the evaluation set-up which would provide increased insight into the performance of the crystal streak camera are proposed. The first was tested with the results included in this report. The simple RC ramp circuit was modified by placing a diode across the output capacitance which shorts out the over-shoot which could depolarize the crystal. A pulser was added between the Stanford Research logic pulse generator and the Bragg cell modulator. This pulser is gated on and off to produce several laser pulses during the ramp. The concept was to be able to observe directly the resolvability of individual laser pulses beginning with 1 pulse on then two pulses on during the ramp, then increasing the number of pulses until the individual pulses are no longer resolvable. This can be converted into CTF (contrast transfer function) plotted against LPM (line pairs per millimeter) used in the evaluation of streak cameras. The second modification proposed is to place the crystal in a liquid environment which will enable the application of voltages between 10 and 20 kV across the 1.3 mm crystal. A suitable liquid has been identified and ordered, Fluorinert, manufactured by 3M, with a break-down strength of about 21 kV per 1.3 mm. This should enable a deflection of about 250 pixels (at 16.25 kilo-volts) with the present optics or 500 pixels with a mirror causing two passes through the crystal. DOE

N88-22335# Ballistic Research Labs., Aberdeen Proving Ground, Md.
A 150,000 POUNDS PER SQUARE INCH DYNAMIC PRESSURE CALIBRATOR
Arpad A. Juhasz, Donald H. Newhall, Charles D. Bullock, James O. Pilcher, and Melinda B. Krummerich Oct. 1987 28 p
(AD-A190659; BRL-TR-2856) Avail: NTIS HC A03/MF A01 CSCL 09A

A positive step pressure generator suitable for the dynamic calibration of ballistic pressure transducers is described. The device uses a hydraulic system to generate pressures up to 150,000 pounds per square inch and is capable of delivering pressure steps in one millisecond or less. Final pressure step values can be traced to conventional deadweight calibration figures with an accuracy of 0.2 percent by using a transfer standard (static reference gage). Among the uses for the device are examining transducer response characteristics to rapid positive pressure steps and comparing the relative response behavior of several transducers to a common pressure step. GRA

N88-22336*# National Aeronautics and Space Administration. Ames Research Center, Moffett Field, Calif.
DEVELOPMENT OF SUBMINIATURE MULTI-SENSOR HOT-WIRE PROBES
Russell V. Westphal, Phillip M. Ligrani (Naval Postgraduate School, Monterey, Calif.), and Fred R. Lemos Mar. 1988 33 p
(NASA-TM-100052; A-88045; NAS 1.15:100052) Avail: NTIS HC A03/MF A01 CSCL 14B

Limitations on the spatial resolution of multisensor hot wire probes have precluded accurate measurements of Reynolds stresses very near solid surfaces in wind tunnels and in many practical aerodynamic flows. The fabrication, calibration and qualification testing of very small single horizontal and X-array hot-wire probes which are intended to be used near solid boundaries in turbulent flows where length scales are particularly small, is described. Details of the sensor fabrication procedure are reported, along with information needed to successfully operate the probes. As compared with conventional probes, manufacture of the subminiature probes is more complex, requiring special equipment and careful handling. The subminiature probes tested were more fragile and shorter lived than conventional probes; they obeyed the same calibration laws but with slightly larger experimental uncertainty. In spite of these disadvantages, measurements of mean statistical quantities and spectra demonstrate the ability of the subminiature sensors to provide the measurements in the near wall region of turbulent boundary layers that are more accurate than conventional sized probes. Author

N88-22337*# National Aeronautics and Space Administration. Ames Research Center, Moffett Field, Calif.
A METHOD OF ATMOSPHERIC DENSITY MEASUREMENTS DURING SPACE SHUTTLE ENTRY USING ULTRAVIOLET-LASER RAYLEIGH SCATTERING
Robert L. McKenzie Mar. 1988 37 p
(NASA-TM-100056; A-88058; NAS 1.15:100056) Avail: NTIS HC A03/MF A01 CSCL 14B

An analytical study and its experimental verification are described which show the performance capabilities and the hardware requirements of a method for measuring atmospheric density along the Space Shuttle flightpath during entry. Using onboard instrumentation, the technique relies on Rayleigh scattering of light from a pulsed ArF excimer laser operating at a wavelength of 193 nm. The method is shown to be capable of providing density measurements with an uncertainty of less than 1 percent and with a spatial resolution along the flightpath of 1 km, over an altitude range from 50 to 90 km. Experimental verification of the signal linearity and the expected signal-to-noise ratios is demonstrated in a simulation facility at conditions that duplicate the signal levels of the flight environment. Author

N88-22338# Institut Franco-Allemand de Recherches, St. Louis (France).
A REVIEW ON HOLOGRAPHY, ITS PRINCIPLES AND APPLICATIONS [VUE D'ENSEMBLE SUR L'HOLOGRAPHIE, SES PRINCIPES ET SES APPLICATIONS]
H. Royer 7 Nov. 1986 36 p In FRENCH Presented at the Musee de l'Holographie, Paris, France, 17-21 Mar. 1986
(ISL-CO-242/86; ETN-88-92016) Avail: NTIS HC A03/MF A01

The laws describing light interference and diffraction phenomena are discussed to introduce holography as a technique related to those concepts. The main holographic technologies are described including Denisyuk, Gabor and separate reference assemblies, double exposure holographic interferometry, time integration interferometry, and real time interferometry. ESA

N88-22232# Joint Publications Research Service, Arlington, Va.
MERIT OF HADAMARD TRANSFORM ACTIVE ABSORPTION SPECTROMETER DESCRIBED
Nobuo Sugimoto *In its* JPRS Report: Science and Technology. Japan 27 Oct. 1987 p 55-71 Transl. into ENGLISH from Ibaraki Bunko Kenkyu (Tokyo, Japan), v. 36, no. 2, Feb. 1987 p 112-122 (For primary document see N88-22228 15-31)
Avail: NTIS HC A07/MF A01

N88-22249# Joint Publications Research Service, Arlington, Va.
RAINBOW HOLOGRAPHIC IMAGE RECONSTRUCTED BY SPATIALLY EXTENDED WHITE LIGHT SOURCE Abstract Only

Luzhong Cai and Youwen Zhang *In its* JPRS Report: Science and Technology. China 11 Dec. 1987 p 76 Transl. into ENGLISH from Guangxue Xuebao (Shanghai, Peoples Republic of China), v. 7, no. 8, Aug. 1987 p 721-728 (For primary document see N88-22233 15-31)
Avail: NTIS HC A06/MF A01

N88-22430*# National Aeronautics and Space Administration. Lewis Research Center, Cleveland, Ohio.
RESEARCH SENSORS
David R. Englund *In its* Lewis Structures Technology, 1988. Volume 3: Structural Integrity Fatigue and Fracture Wind Turbines HOST May 1988 p 323-335 (For primary document see N88-22408 15-39)
Avail: NTIS HC A16/MF A01 CSCL 14B

36 LASERS AND MASERS

Includes parametric amplifiers.
For related information see also *76 Solid-State Physics*.

N88-22339# Los Alamos National Lab., N. Mex.
DISCHARGE EXCITATION OF THE XeF C TO A TRANSITION
R. C. Sze, D. P. Greene, I. J. Bigio, T. M. Shay, A. W. McCown, J. F. Figueira, P. Smith, M. Vannini, R. Sauerbrey, and F. K. Tittel 1987 5 p Presented at Lasers '87, Lake Tahoe, Nev., 7 Dec. 1987 Prepared in cooperation with Saint Andrews Univ., United Kingdom, Consiglio Nazionale delle Ricerche, Florence, Italy and Rice Univ., Houston, Tex.
(Contract W-7405-eng-36)
(DE88-006448; LA-UR-88-656; CONF-871254-4) Avail: NTIS HC A02/MF A01

Recent success in high efficiency and high energy laser extraction of tunable radiation in the blue-green C-A transition of XeF under intense, short-pulse electron beam excitation has renewed interest in the possibility of similar performance in avalanche discharges. We present preliminary results of discharge excited fluorescence studies in a variety of devices having different degrees of energy loading. DOE

N88-22340# Los Alamos National Lab., N. Mex.
FUNDAMENTAL NOISE PROCESSES IN A LASER EXCITED OPTICAL FILTER
E. C. Apel, T. R. Gosnell, T. M. Shay, and R. Samadani 1987 7 p Presented at Lasers '87, Lake Tahoe, Nev., 7 Dec. 1987
(Contract W-7405-eng-36)
(DE88-006460; LA-UR-88-573; CONF-871254-6) Avail: NTIS HC A02/MF A01

A rubidium narrow bandwidth optical filter is being investigated as a device for detecting weak narrow bandwidth radiation. In our configuration, the optical filter is actively pumped (or laser excited, i.e., LEOF). This configuration has a major inherent advantage over a passive optical filter, namely, wavelength versatility. One possible limitation to the Rb LEOF is due to an intrinsic noise source caused by the energy pooling of Rb 5p atoms which are produced by the pump laser. This process, i.e., Rb (5p) + Rb (5p) yields Rb (5d) + (Rb(5s)) yields Rb (6p), produces Rb atoms in the 6p state which subsequently emit radiation within the bandwidth of the detection channel (420-323 nm). Hence, this constitutes a noise process since photons are produced at the detector in the absence of narrow bandwidth signal radiation. Herein, we present preliminary results on kinetic studies of the energy pooling process with the ultimate goal of quantifying the process (rate constant determination) and thus assessing its implications. DOE

N88-22341# Los Alamos National Lab., N. Mex.
EXTENSION OF FREE-ELECTRON LASERS INTO THE EXTREME ULTRAVIOLET
B. E. Newman 1988 22 p Presented at the Free-Electron Laser: Critical Review of Technology, Los Angeles, Calif., 11 Jan. 1988
(Contract W-7405-eng-36)
(DE88-005373; LA-UR-88-51; CONF-880164-1) Avail: NTIS HC A03/MF A01

Encouraged by experimental operation of free-electron lasers in the visible to far-infrared, several research centers are now designing and/or building devices to extend into the vacuum-ultraviolet and soft X-ray regions below 100 nm, collectively referred to as the extreme ultraviolet. Here the peak- and average-power output of FEL oscillators and amplifiers should surpass the capabilities of any existing, continuously tunable photon sources by many orders of magnitude. These devices are certain to greatly enhance the future research capabilities of a number of scientific disciplines and industrial applications beyond those possible with synchrotron light sources. We review the features and output parameters of several of these active or proposed programs and the technological challenges that must be met to guarantee their success. DOE

N88-22342# Kansas State Univ., Manhattan. Dept. of Chemistry.
REACTIONS OF N2(A SUP 3 SIGMA SUP + SUB u) CANDIDATES FOR SHORT WAVELENGTH LASERS Report, 1 Jun. 1986 - 31 May 1987
D. W. Setser Dec. 1987 70 p
(Contract W-7405-eng-48)
(DE88-007018; UCRL-21009-Pt-3) Avail: NTIS HC A04/MF A01

Experiments are proposed to provide data about kinetic systems which have relevance for development of short wavelength lasers based on excitation-transfer reactions of N2(A) or other metastable energy carriers. Pulsed laser excitation techniques will be used to study important aspects of the electronic quenching and vibrational relaxation kinetics of the SO(A (sup 3) pi (sub 0, 1, 2)) molecule. Pulsed laser excitation techniques will be developed to study the spectroscopy and relaxation kinetics of the PF(A (sup 3) pi (sub 0, 1, 2)) molecule. Experiments will be done to develop sources of the PF(X) molecule for kinetic studies. Such experiments also may involve the first two singlet states of PF. DOE

N88-22343# Los Alamos National Lab., N. Mex.
CONSTELLATION SIZING FOR MODEST DIRECTED ENERGY PLATFORMS
G. H. Canavan and J. H. Hammond Apr. 1988 24 p
(Contract W-7405-eng-36)
(DE88-007033; LA-11238-MS) Avail: NTIS HC A03/MF A01

Discussions of boost phase directed energy constellation scaling have concentrated on tradeoffs for large lasers and mirrors, which require development. This report explores more modest lasers that could be deployed sooner, finding that for anticipated threats, performance and effectiveness are adequate. DOE

N88-22344# Nauchno-Issledovatelskij Inst. Ehlekt- Rofizicheskoj Apparatury, Leningrad (USSR).
NUMERICAL MODELLING SPECIFIC ENERGY CHARCTERISTICS OF EXCIMER KrF LASERS WITH ELECTRON BEAM EXCITATION [CHISLENNOE MODELIROVANIE UDELNYKH EHNERGETICHESKIKH KHARAKTERISTIK EHKSIMERNYKH KRF-LAZEROV S EHLEKTRONNO-PUCHKOVYM VOZBUZHDENIEM]
V. A. Burtsev, A. G. Grad, V. S. Kuznetsov, and R. P. Fidelskaya 1986 18 p In RUSSIAN
(DE88-701525; NIIEFA-P-K-0733) Avail: NTIS HC A03/MF A01

Kinetics of excimer KrF laser active medium formation in Ar:Kr:F sub 2 gaseous mixture is considered. The mixture is excited by an electron beam. A computing program allowing one to calculate the main parameters of the active medium and laser output characteristics is developed. Laser internal efficiency dependences on the pulse duration, power and full excitation energy are calculated. DOE

N88-22345# United Technologies Research Center, East Hartford, Conn.
COUPLED HIGH POWER WAVEGUIDE LASER RESEARCH Final Report, 1 Jul. 1986 - 30 Jun. 1987
A. J. Cantor, R. A. Hart, J. T. Kennedy, and L. A. Newman 30 Sep. 1987 48 p
(Contract F49620-85-C-0106)
(AD-A189800; UTRC/R87-927184; AFOSR-87-1747TR) Avail: NTIS HC A03/MF A01 CSCL 09C

The experimental and theoretical progress that has been made in the coupled high power waveguide laser research program is reported. A problem has been encountered with the hollow-bore ridge waveguide laser array approach in which multimode operation occurs when the array is increased to above three elements. Alternative waveguide geometries were explored with the objective of achieving both phase locked operation and mode discrimination for an array size of 5 elements. Three new waveguide geometries were investigated. Of these new geometries, a modified hollow-bore ridge waveguide, utilizing a staggered ridge, has been used successfully to obtain single mode operation. This array, with a gain volume equivalent to six waveguide lasers, produced an output of 68 watts. The theoretical effort has resulted in the development of a theoretical method for calculating the modes and frequencies of two coupled rectangular waveguides separated by an infinitely thin partition with a gap in it. GRA

N88-22346# Rockwell International Corp., Thousand Oaks, Calif.
LASER EVAPORATION STUDIES Final Report, 1 Sep. 1984 - 31 Aug. 1987
H. O. Sankur Oct. 1987 64 p
(Contract F49620-84-C-0091)
(AD-A189815; SC5411.FR; AFOSR-87-1928TR) Avail: NTIS HC A04/MF A01 CSCL 20L

The physics of vaporization of matter under pulsed CO2 laser evaporation was studied. Analysis of the nature of the vapor plume in several materials indicated the presence of numerous excited species, neutral as well as ionized species, and ions with high kinetic energies. High quality films of refractory metal oxides and epitaxial films of Ge were deposited. The oxide materials were dense and crystalline and had high refractive index values, even when deposited on room temperature substrates. Ge films were epitaxial and single crystalline when deposited on Si substrates at 300 C. Study of the relationship of deposition conditions and film properties clearly indicated the beneficial role of the energetic ions in the film deposition. Special emphasis was given to the solution of the problem of particulates in the films. GRA

N88-22347# Krug International, San Antonio, Tex. Technology Services Div.
A PRELIMINARY COMPARISON OF THE TRANSIENT EFFECTS OF SINGLE VERSUS MULTIPLE q-SWITCHED DOUBLED-NEODYMIUM LASER PULSES Final Report, Jul. - Nov. 1986
Fred H. Previc Sep. 1987 14 p
(Contract F33615-84-C-0600)
(AD-A189855; USAFSAM-TR-87-15) Avail: NTIS HC A03/MF A01 CSCL 06G

A comparison between the effects of single and multiple laser pulse-trains of equivalent energy was performed. Visual evoked potentials (VEPS) recorded bipolarly from the visual cortex of two rhesus monkeys in response to a counterphasing grating were used to assess the magnitude of the visual loss following four types of exposures: single and multiple pulses with total energies equal to 50 and 500 percent of the maximum permissible exposure (MPE) standard for humans. The results showed that the effects of a series of laser flashes presented within 200 ms are similar to those of a single laser flash whose energy is equivalent to the cumulative energy of the multiple-pulse exposure. GRA

N88-22348# Arizona State Univ., Tempe. Dept. of Mechanical and Aerospace Engineering.
RESEARCH ON CERTAIN ASPECTS OF LASER DIFFRACTION PARTICLE SIZING RELEVANT TO AUTONOMOUS SELF-DIAGNOSING INSTRUMENTATION Annual Report, 1 Oct. 1986 - 1 Oct. 1987
E. D. Hirleman, Paul A. Dellenback, and Joseph H. Koo Oct. 1987 8 p
(Grant AF-AFOSR-0187-84)
(AD-A190220; AFOSR-87-1896TR) Avail: NTIS HC A02/MF A01 CSCL 17E

The fundamental scientific deficiencies impeding the integration of laser diffraction particle sizing techniques into intelligent sensors for next generation propulsion systems have been identified. The research addressed three relevant areas: inverse scattering algorithms; multiple scattering; and the problems of laser beam deflections due to refractive index gradients in hostile propulsion environments. A generalized eigenfunction approach to the inverse Fraunhofer diffraction particle sizing problem has been developed. Based on an analysis of the eigenvalue spectrum, scaling laws for optimal configuration of the system are proposed. The results are in agreement with an independent analysis of the system based on condition number analysis of the linear system produced by numerical quadrature as reported in a previous annual report. The formulation and scaling laws provide a scheme for determining the optimal number and location of the scattering sensors and the maximum number of pieces of independent information on the particle size distribution which can be reliably extracted from the inversion. Finally, a new concept involving programmable (real time) detector configuration at the transform plane has been demonstrated. GRA

N88-22349# Boston Univ., Mass. Coll. of Engineering.
ADVANCED PROGRAMMING AND CONTROL TECHNIQUES FOR COMPLEX MECHANICAL SYSTEMS Final Report, 30 Jul. 1986 - 29 Jul. 1987
John Baillieul 30 Oct. 1987 15 p
(Grant AF-AFOSR-0273-86)
(AD-A190238; AFOSR-87-1796TR) Avail: NTIS HC A03/MF A01 CSCL 09C

The purpose of this report was to evaluate spectral protective characteristics of a revised prototype polycarbonate laser protective filter submitted to the Army by the American Optical (AO) Corporation as a material for the ballistic/laser protective spectacles (B/LPS) and to make recommendations necessary to assure the adequacy of the filter for protection of personnel using the B/LPS around Lambda 2 laser filter systems. GRA

N88-22350# Iowa Univ., Iowa City.
ALKALI METAL DIFFUSE BAND LASERS Final Technical Report, 1 Jun. 1986 - 31 May 1987
William C. Stwalley 12 Aug. 1987 19 p
(Grant AF AFOSR-0178-84)
(AD-A190244; IADBL/3; AFOSR-87-1736TR) Avail: NTIS HC A03/MF A01 CSCL 09C

Progress is described on study of a new class of potential excimer lasers based on diffuse bands of the alkali metal vapors. In particular, the violet diffuse bands of sodium vapor and the yellow diffuse bands of potassium vapor have been shown by detailed modeling of single vibrational-rotational level emission to be each composed of overlapping singlet and triplet excimer emission continua of the diatomic molecule. The gain and low absorption loss previously found in the violet and yellow with laser optical pumping of sodium vapor and potassium vapor, respectively, have been quantitatively examined. Prospects for laser oscillation appear to be good at low pressures where quenching is not dominant. Free-bound-free spectra (which include only the triplet portion of the diffuse bands) have been produced and analyzed in sodium, potassium, rubidium and cesium. GRA

N88-22351# Old Dominion Univ., Norfolk, Va. Dept. of Physics.
SDIO/IST ULTRASHORT WAVELENGTH LASER: NOVEL EXPERIMENTAL SCHEMES FOR OBSERVING THE MOSSBAUER EFFECT IN LONG-LIVED NUCLEAR LEVELS Final Report, for period ending 31 Mar. 1987
Gilbert R. Hoy Jul. 1987 26 p
(Contract N00014-86-C-2356)
(AD-A190275; PTR-87-6) Avail: NTIS HC A03/MF A01 CSCL 09C

The development of gamma-ray lasers (GRASERS) will, in all probability, depend on the utilization of recoillessly emitted gamma-rays from nuclear transitions, i.e., the Mossbauer Effect (ME). Past research in Mossbauer spectroscopy which relates to GRASERS is briefly reviewed. The nuclear lifetimes, required from practical considerations, may have to be on the order of seconds, if storage and transfer processes prove infeasible. It is not clear that the ME has been observed in such long-lived states. Even if such long-lived states are not needed directly for GRASERS, successful observation of the ME in such a system will answer important questions of line broadening due to field inhomogeneities in single crystals. We propose some novel experimental schemes to observe the ME in Ag-109 whose relevant lifetime is about 40 seconds. The techniques proposed are: coincidence Mossbauer spectroscopy, conversion-electron Mossbauer spectroscopy, gravitational line sweeping, and gamma-ray self absorption. Preliminary results using the last technique are presented. Possible future, relevant ME research is discussed. GRA

N88-22352# Old Dominion Univ., Norfolk, Va.
SDIO/IST ULTRASHORT WAVELENGTH LASER. MOSSBAUER EFFECT IN GAMMA-RAY LASERS Interim Report, period ending 28 Feb. 1987
Gilbert R. Hoy and R. D. Taylor Mar. 1987 26 p
(Contract N00014-86-C-2356)
(AD-A190306) Avail: NTIS HC A03/MF A01 CSCL 09C

In order to gain some perspective on the relationship of the Mossbauer effect to the possible development of gamma-ray lasers, it is useful to review the Mossbauer effect literature. These results show that: (1) Rayleigh and nuclear resonant diffraction by scattering are coherent, (2) one can obtain pure nuclear resonant diffraction by scattering from a sample for which the structure factor for Rayleigh scattering is small, (3) nuclear anomalous dispersion occurs, (4) interference can occur between nuclear hyperfine components in nuclear resonant diffraction, (5) in nuclear resonant Bragg scattering, processes having different final nuclear spin projections are incoherent, and (6) there can be anomalously deep penetration and high reflectivity using single crystals as a result of the suppression of inelastic channels. GRA

N88-22353# Thermo Electron Corp., Waltham, Mass.
PROGRAM TO RESEARCH LASER-DRIVEN THERMIONIC ELECTRON SOURCES FOR FREE ELECTRON LASERS Final Report
Jan. 1988 38 p
(Contract N00014-83-C-0333)
(AD-A190473; TE4327-20-88) Avail: NTIS HC A03/MF A01 CSCL 09C

This is the Final Report on the research and development of high brightness pulse laser driven thermionic electron sources. Enhanced coupling of electron beam energies to radiative fields in accelerator-driven free-electron lasers requires injector cathodes of higher brightness than is possible with conventional dispenser cathodes or plasma-forming field emitters. Cesiated refractory surfaces and dispenser cathodes which are pulse laser heated may offer such an increase in brightness, by the emission of monoenergetic beams of electrons at high current densities. The studies were designed to investigate the emission characteristics of both of these types of thermionic cathodes. GRA

N88-22354# Florida Univ., Gainesville. Space Astronomy Lab.
THE INTERACTION OF SMALL PARTICLES WITH LASER BEAMS Annual Report, 10 Oct. 1986 - 9 Oct. 1987
N. Y. Misconi, K. F. Ratcliff, and E. T. Rusk 17 Dec. 1987 42 p
(Contract F49620-85-C-0117)
(AD-A190716; AFOSR-87-2043TR) Avail: NTIS HC A03/MF A01 CSCL 20F

This report summarizes our research under Award/Contract F49620-85-C-0117 which deals with light scattering measurements of levitated spherical and irregular particles in an Argon laser beam (effective wavelength, 514.5 nm) of highly transparent silica. The particles range in size from 25 to 55 microns in diameter. Comparisons between the measurements for scattering angles theta = 27 to 162 deg and computed theoretical Mie scattering curves are made. Preliminary results on rotating irregular particles are included. GRA

N88-22355# Los Alamos National Lab., N. Mex.
SOLID HOSTS FOR DYE LASER RODS. PART 1: CRITERIA FOR CHOOSING A HOST MATERIAL
G. F. Erickson 1987 5 p Presented at Lasers '87, Lake Tahoe, Nev., 7 Dec. 1987
(Contract W-7405-eng-36)
(DE88-006478; LA-UR-88-414-Pt-1; CONF-871254-5-Pt-1) Avail: NTIS HC A02/MF A01

This paper will attempt to provide selection criteria for polymers as hosts for flashlamp-pumped dye laser rods. The properties of transparent polymer materials are compared with typical inorganic crystal and glass hosts. DOE

N88-22356# Mound Lab., Miamisburg, Ohio.
REDUCED THERMAL INPUT BY PROPER SELECTION OF YAG LASER WELDING PARAMETERS
W. H. Jones 1987 4 p Presented at the International Conference on Applications of Electron and Laser Beam Welding, Hartford, Conn., 16 Sep. 1987
(Contract DE-AC04-76DP-00053)
(DE88-000730; MLM-3456(OP); CONF-8709178-1) Avail: NTIS HC A02/MF A01

This paper presents a case history to illustrate the importance of properly selected YAG laser welding parameters to control thermal input to temperature sensitive components. One of the assembly operations in the production of a small detonator is the attachment of a 304 stainless steel charge holder to the 304 stainless steel header body by laser welding. A high percentage of these assemblies were failing the final helium leak test. To locate production operations that tended to cause leakers, a comprehensive study was conducted on a lot of 333 detonators. The results of this study showed that the laser welding operation was causing a 23 percent leak reject rate. This assembly had been in production about four years with varying degrees of helium leak test problems. The original requirements for the circumferential weld was that it sealed the joint and held the components in relative position. When the parameters were developed in 1978, we knew much less about the laser welding process than in 1982 when this work was completed. Little concern had been given to the total heat input required to produce the weld. A study was initiated to determine how much thermal input could be reduced before weld integrity was affected. DOE

N88-22357# Instituto de Pesquisas Espaciais, Sao Jose dos Campos (Brazil).
FABRICATION AND CHARACTERIZATION OF SEMICONDUCTOR LASERS OF Pb(1-x)Sn(x)Te
Eduardo Abramof, Sukarno OlavoFerreira, and Iraja NewtonBandeira Jul. 1987 8 p Submitted for publication
(INPE-4253-PRE/1126) Avail: NTIS HC A02/MF A01

The fabrication and characterization of PbTe homostructure diode lasers are described. The threshold current density is in the range between 2.5 and 10 KA/sq cm and the factors leading to device degradation are discussed. Author

N88-22358# Helsinki Univ. of Technology, Espoo (Finland). Dept. of Technical Physics.
THE DEVELOPMENT OF HIGH POWER KrF LASER SYSTEMS FOR PLASMA RESEARCH BY THE APPLICATION OF STIMULATED RAMAN SCATTERING Ph.D. Thesis
Jouni P. Partanen 1987 24 p Sponsored by the Academy of Finland; the Osk. Huttunen Foundation, Finland; The Heikki and Hilma Honkanen Foundation, Finland; and the British Council, United Kingdom
(ETN-88-92220) Avail: NTIS HC A03/MF A01

The X-ray emission from KrF laser-produced plasmas; high-power forward Raman amplifiers employing low-pressure gases in light guides; threshold measurements of stimulated Raman scattering in gases using picosecond KrF laser pulses; a multipass grating interferometer applied to line narrowing in excimer lasers; and a single mode KrF laser are discussed. ESA

N88-22211# Joint Publications Research Service, Arlington, Va.
LASER PROCESSING-STATUS, PERSPECTIVES
Hiromichi Kawasumi *In its* JPRS Report: Science and Technology. Japan 11 Mar. 1988 p 1-8 Transl. into ENGLISH from Kino Zairyo (Tokyo, Japan), v. 7, Aug. 1987 p 6-10 (For primary document see N88-22210 15-31)
Avail: NTIS HC A05/MF A01

N88-22236# Joint Publications Research Service, Arlington, Va.
MAGIC LIGHT HIGH-POWER LASER PASSES STATE CERTIFICATION Abstract Only
Ganchang Wang, Daheng Wang, Min Yu, Nunkuan Chen, Kaijia Cheng, and Fuxi Gan *In its* JPRS Report: Science and Technology. China 11 Dec. 1987 p 16 Transl. ino ENGLISH from Yingyong Jiguang (Shanghai, Peoples Republic of China), v. 7, no. 4, Aug. 1987 p 159 (For primary document see N88-22233 15-31)
Avail: NTIS HC A06/MF A01

37 MECHANICAL ENGINEERING

Includes auxiliary systems (nonpower); machine elements and processes; and mechanical equipment.

N88-22359# MRC Bearings-SKF Aerospace, King of Prussia, Pa.
TRACTION MODEL DEVELOPMENT Final Report, 28 Sep. 1984 - 31 Mar. 1987
John I. McCool Sep. 1987 162 p
(Contract F33615-84-C-5028)
(AD-A188450; AFWAL-TR-87-4079) Avail: NTIS HC A08/MF A01 CSCL 13I

The theoretical background, the numerical procedures and a comparison with test results for a PC-based computer program for computing traction force components and torque in an elastohydrodynamically lubricated contact are discussed. The program provides a comprehensive tribological assessment of a general lubricated, concentrated contact under combined rolling, spinning and sliding. The joint effect of 34 input variables can be considered in the descriptive characteristics of the contact.
Author

N88-22360# Oak Ridge National Lab., Tenn.
RANGE IMAGE SEGMENTATION AND SURFACE PARAMETER EXTRACTION FOR A MOBILE ROBOT
M. Goldstein, F. G. Pin, and C. R. Weisbin 1987 27 p Presented at the IEEE International Conference on Robotics and Automation, Philadelphia, Pa., 25 Apr. 1988
(Contract DE-AC05-84OR-21400)
(DE87-013877; CONF-880424-4) Avail: NTIS HC A03/MF A01

This paper presents a methodology for a concise representation of the 3-D world model for a mobile robot, using range data. The process starts with the segmentation of the scene into objects that are given a unique label, based on principles of range continuity. Then the external surface of each object is partitioned into homogeneous surface patches. Contours of surface patches in 3-D space are identified by estimating the normal and curvature associated with each pixel. The resulting surface patches are then classified as planar, convex or concave. Since the world model uses a volumetric representation for the 3-D environment, planar surfaces are represented by thin volumetric polyhedra. Spherical and clindrical surfaces are extracted and represented by appropriate volumetric primitives. All other surfaces are represented using the boolean union of spherical volumes (as described in a separate paper by the same authors). The result is a general, concise representation of the external 3-D world, which allows for efficient and robust 3-D object recognition. DOE

N88-22361# Pennsylvania State Univ., University Park. Dept. of Mathematics.
STABILIZATION AND CONTROL PROBLEMS IN STRUCTURAL DYNAMICS Final Report, 1 Sep. 1985 - 31 Aug. 1986
Goong Chen 10 Sep. 1987 21 p
(Grant AF-AFOSR-0253-85)
(AD-A190197; AFOSR-87-1799TR) Avail: NTIS HC A03/MF A01 CSCL 13M

The most significant research progress and accomplishment in our project is on the modelling, analysis and designs of stabilizing joints for coupled structures. In a series of papers, we have studied second order dynamic structures modelling vibrating strings and cables, and fourth order dynamic structures modelling vibrating beams. We are able to classify all linear dissipative joints into types. Dr. H. H. West of the Civil Engineering Department of the Pennsylvania State University has collaborated with us and completed mechanical designs for all of them. Numerical and experimental verification have also been carried out. Dr. Chen's Ph.D. student M. P. Coleman is now using the Cyber 205 supercomputer to compute eigen frequencies of a damped plate. Experiments were conducted at the MIPAC Facility of the University of Wisconsin in collaboration with Dr. D. L. Russell. GRA

N88-22362# Sandia National Labs., Albuquerque, N. Mex.
FINITE ELEMENT SIMULATION OF PERFORATION OF ALUMINUM PLATES
E. P. Chen 1988 10 p Presented at the International Conference on Computational Engineering Science, Atlanta, Ga., 10 Apr. 1988
(Contract DE-AC04-76DP-00789)
(DE88-002092; SAND-87-0988C; CONF-880438-1) Avail: NTIS HC A02/MF A01

Perforation of aluminum plates by steel penetrators is the subject of discussion in the present investigation. Specifically, laboratory scale experiments were simulated using the transient dynamic finite element code PRONTO 2D. For the range of impact velocities considered in this study, the penetrator experiences little deformation while the target exhibits ductile hole-growth behavior. Thus, both the penetrator and the target are taken as elastic/plastic hardening materials in the finite element model. Detailed numerical treatment of the perforation process is discussed. Comparison between calculated results and experimental data show good agreements. DOE

N88-22363# New Mexico Univ., Albuquerque.
TELEROBOTIC OPERATION OF CONVENTIONAL ROBOT MANIPULATORS
P. T. Boissiere and R. W. Harrigan 1988 9 p Presented at the IEEE International Conference on Robotics and Automation, Philadelphia, Pa., 25 Apr. 1988 Prepared in cooperation with Sandia National Labs., Albuquerque, N. Mex.
(Contract DE-AC04-76DP-00789)
(DE88-005718; SAND-87-1835C; CONF-880424-8) Avail: NTIS HC A02/MF A01

This paper discusses a new telerobotic control concept and its implementation using a PUMA-560 robot manipulator. The control concept couples human supervisory commands with computer reasoning. The control system is responsive and accomplishes an operator's commands while providing obstacle avoidance and controlled interactions with the environment where

desired. This provides a system which not only assists the operator in accomplishing tasks but modifies inappropriate operator commands which can result in safety hazards and/or equipment damage. DOE

N88-22364# Electrotechnical Lab., Ibaraki (Japan).
STUDY ON SHAFT SEALS FOR POTASSIUM TURBINE
Sadayoshi Korenaga, Hiroyuki Imai, Tadashi Koga, Hiroo Tanoue, Shigeru Matsumoto, and Hiroshi Takata Jan. 1988 134 p In JAPANESE; ENGLISH summary
(EL-891; ISSN-0366-9106) Avail: NTIS HC A07/MF A01

Shaft seals for a potassium turbine using potassium vapor as a working fluid is described. The potassium turbine is one of the components in the Rankine cycle which is operated in the temperature range from 450 to 900 C. When this turbine is used together with a steam turbine as a binary vapor cycle, very high efficiency can be expected. It is extremely important that the outward leak of potassium from the turbine through the shaft seals at high vapor pressure to the atmosphere be prevented because of potassium's caustic chemical properties. Furthermore, the inward leaking of the gases to the turbine at low vapor pressure also must be prevented to avoid a decrease in turbine efficiency. Therefore it is necessary to develop a highly reliable seal system to achieve the successful operation of a potassium turbine. One of the main objectives of the study is the development of the shaft seal system for a small potassium turbine in test facilities, and the other is the design of a seal system for large scale turbines in commercial power plants. Author

38 QUALITY ASSURANCE AND RELIABILITY

Includes product sampling procedures and techniques; and quality control.

N88-22365# Naval Surface Weapons Center, Silver Spring, Md.
EDDY CURRENT NONDESTRUCTIVE INSPECTION OF GRAPHITE EPOXY USING FERRITE CUP CORE PROBES Final Report
Susan N. Vernon Sep. 1987 70 p
(AD-A189823; NSWC/TR-87-148) Avail: NTIS HC A04/MF A01 CSCL 11D

This report summarizes the results of a three year project to develop the eddy current technical base for the detection and measurement of broken fiber damage in graphite epoxy using eddy current. Since graphite epoxy components are frequently made of panels having only one accessible surface, a single sided technique using a probe coil was required. Parameters of ferrite pot core probes which affect the defect sensitivity of the probe were identified and evaluated in terms of the coil efficiency factor or coupling coefficient. As a result of this investigation, it is possible to optimize eddy current probes for the single sided inspection of graphite epoxy and other high resistivity materials. GRA

N88-22366# Northwestern Univ., Evanston, Ill.
MONTE CARLO RELIABILITY ANALYSIS Annual Report, 1 Sep. 1986 - 31 Aug. 1987
E. E. Lewis 1 Oct. 1987 11 p
(Grant AF-AFOSR-0340-84)
(AD-A189972) Avail: NTIS HC A03/MF A01 CSCL 12A

The work carried out is summarized. The Monte Carlo simulation methods are generalized to treat nonMarkovian systems and applied to problems with time and batch replacement maintenance policies. Trimodular redundant systems with reconfigurable spares are also simulated. A new graphical technique is developed for the presentation of Monte Carlo results. Finally, an investigation of the reliability behavior of brittle solids is initiated. GRA

N88-22367# Center for Naval Analyses, Alexandria, Va. Naval Planning Manpower and Logistics Div.
MODELING FAILURES OF INTERMITTENTLY USED MACHINES Final Report
Dean A. Follmann Jul. 1987 37 p
(Contract N00014-87-C-0001)
(AD-A190298; CRM-87-111) Avail: NTIS HC A03/MF A01 CSCL 12D

This research memorandum presents methodology for analyzing failures of machines that are repeatedly turned on and off. Because a machine can fail both when it is on and off, different parametric models for failure are used for each of these periods. An important issue addressed for such machines is how the intermittent use itself affects failure. Because the models can predict the chance of failure under different usage patterns, less harmful usage patterns can be recommended. As an example, the models are applied to a radar system, and both the immediate and cumulative effects of on-off cycling are demonstrated. GRA

N88-22368# Technical Research Centre of Finland, Espoo. Metals Lab.
MANUFACTURING OF ULTRASONIC FOCUSED PROBES
Jorma Pitkanen and Kari Lahdenpera Jun. 1987 33 p In FINNISH; ENGLISH summary Sponsored by the Technology Developing Center, Finland
(VTT-RR-487; ISBN-9-51-382912-X; ISSN-0358-5077; ETN-88-92213) Avail: NTIS HC A03/MF A01; Government Printing Center, P.O. Box 516, SF-00101 Helsinki, Finland 40 finmarks

Factors affecting the design, manufacturing, and assembly of focused probes are discussed. The probes consist of a conical polycarbonate lens, a plexishoe, and an ultrasonic probe with circular crystal (50 mm diam). Focused probes were tested on thick steel specimens (150 to 200 mm dia) containing defects. The diameter of the focused sound field is 5 mm at the focal position. The estimation of the defect size with the 6 dB drop method shown that focused probes are better than unfocused probes when the sizes of the flat bottom holes used for calibration purposes are less than 10 mm dia and the sound paths exceed 100 mm. ESA

N88-22369# National Aerospace Lab., Amsterdam (Netherlands). Informatics Div.
RELIABILITY ANALYSIS WITHIN A COMPUTER AIDED ENGINEERING (CAE) INFRASTRUCTURE
P. J. H. M. Manders and D. W. v.d.Kwaak 30 Sep. 1986 11 p Presented at the Reliability and Maintainability Symposium, Philadelphia, Penn., Jan. 1987
(NLR-MP-86059-U; B8733100; ETN-88-92223) Avail: NTIS HC A03/MF A01

A computer aided engineering (CAE) infrastructure for supporting the development of electronic systems, and the evaluation, and introduction, of software packages for reliability analysis of electronic systems under development is described. Prior conditions, functional requirements, performance characteristics, and implementation aspects of the CAE infrastructure as well as the reliability analysis software package are presented. The importance of a standard for common design information in the CAE infrastructure through all projects stages is discussed, and the influence of the CAE infrastructure on the requirement for reliability analysis is assessed. ESA

N88-22412*# National Aeronautics and Space Administration. Lewis Research Center, Cleveland, Ohio.
NONDESTRUCTIVE EVALUATION BY ACOUSTO-ULTRASONICS
Harold E. Kautz *In its* Lewis Structures Technology, 1988. Volume 3: Structural Integrity Fatigue and Fracture Wind Turbines HOST May 1988 p 67-77 (For primary document see N88-22408 15-39)
Avail: NTIS HC A16/MF A01 CSCL 14D

N88-22413*# National Aeronautics and Space Administration. Lewis Research Center, Cleveland, Ohio.
CHARACTERIZATION OF SINTERED SiC BY USING NDE
George Y. Baaklini *In its* Lewis Structures Technology, 1988. Volume 3: Structural Integrity Fatigue and Fracture Wind Turbines

HOST May 1988 p 79-91 (For primary document see N88-22408 15-39)
Avail: NTIS HC A16/MF A01 CSCL 14D

N88-22414*# National Aeronautics and Space Administration. Lewis Research Center, Cleveland, Ohio.
SYSTEMS FOR ULTRASONIC SCANNING, ANALYSIS AND IMAGERY
David B. Stang, Edward R. Generazio, and Steve Abe (Cleveland State Univ., Ohio.) *In its* Lewis Structures Technology, 1988. Volume 3: Structural Integrity Fatigue and Fracture Wind Turbines HOST May 1988 p 93-105 (For primary document see N88-22408 15-39)
(Contracts NAS3-2410S; NCC3-24)
Avail: NTIS HC A16/MF A01 CSCL 14D

N88-22415*# National Aeronautics and Space Administration. Lewis Research Center, Cleveland, Ohio.
FLAW CHARACTERIZATION IN STRUCTURAL CERAMICS USING SCANNING LASER ACOUSTIC MICROSCOPY
Don J. Roth *In its* Lewis Structures Technology, 1988. Volume 3: Structural Integrity Fatigue and Fracture Wind Turbines HOST May 1988 p 107-122 (For primary document see N88-22408 15-39)
Avail: NTIS HC A16/MF A01 CSCL 14D

N88-22416*# National Aeronautics and Space Administration. Lewis Research Center, Cleveland, Ohio.
NONDESTRUCTIVE EVALUATION OF SINTERED CERAMICS
George Y. Baaklini, Stanley J. Klima, and William A. Sanders *In its* Lewis Structures Technology, 1988. Volume 3: Structural Integrity Fatigue and Fracture Wind Turbines HOST May 1988 p 123-133 (For primary document see N88-22408 15-39)
Avail: NTIS HC A16/MF A01 CSCL 14D

N88-22425*# National Aeronautics and Space Administration. Lewis Research Center, Cleveland, Ohio.
LIFE PREDICTION MODELING BASED ON STRAINRANGE PARTITIONING
Gary R. Halford *In its* Lewis Structures Technology, 1988. Volume 3: Structural Integrity Fatigue and Fracture Wind Turbines HOST May 1988 p 231-244 (For primary document see N88-22408 15-39)
Avail: NTIS HC A16/MF A01 CSCL 14D

N88-22426*# Pratt and Whitney Aircraft, East Hartford, Conn.
LIFE PREDICTION MODELING BASED ON CYCLIC DAMAGE ACCUMULATION
Richard S. Nelson *In* NASA. Lewis Research Center, Lewis Structures Technology, 1988. Volume 3: Structural Integrity Fatigue and Fracture Wind Turbines HOST May 1988 p 245-257 (For primary document see N88-22408 15-39)
(Contract NAS3-23288)
Avail: NTIS HC A16/MF A01 CSCL 14D

N88-22428*# National Aeronautics and Space Administration. Lewis Research Center, Cleveland, Ohio.
LIFE AND RELIABILITY OF ROTATING DISKS
Erwin V. Zaretsky, Todd E. Smith, and Richard August (Sverdrup Technology, Inc., Cleveland, Ohio.) *In its* Lewis Structures Technology, 1988. Volume 3: Structural Integrity Fatigue and Fracture Wind Turbines HOST May 1988 p 271-284 (For primary document see N88-22408 15-39)
(Contract NAS3-24105)
Avail: NTIS HC A16/MF A01 CSCL 14D

39 STRUCTURAL MECHANICS

Includes structural element design and weight analysis; fatigue; and thermal stress.

For applications see *05 Aircraft Design, Testing and Performance* and *18 Spacecraft Design, Testing and Performance.*

N88-22370# Bhabha Atomic Research Centre, Bombay (India). Reactor Engineering Div.
DEVELOPMENT OF A COMPUTER CODE CRACK FOR ELASTIC AND ELASTOPLASTIC FRACTURE MECHANICS ANALYSIS OF 2-D STRUCTURES BY FINITE ELEMENT TECHNIQUE
B. K. Dutta, A. Kakodkar, and S. K. Maiti 1986 11 p
(DE88-701231; BARC-1346) Avail: NTIS (US Sales Only) HC A03/MF A01

The fracture mechanics analysis of nuclear components is required to ensure prevention of sudden failure due to dynamic loadings. The linear elastic analysis near to a crack tip shows presence of stress singularity at the crack tip. The simulation of this singularity in numerical methods enhance convergence capability. In finite element technique this can be achieved by placing mid nodes of 8 noded or 6 noded isoparametric elements, at one fourth distance from crack tip. This characteristic of finite element is detailed, as is the implementation of this element in a code CRACK, implementation of J integral to compute stress intensity factor and solution of number of cases for elastic and elastoplastic fracture mechanics analysis. DOE

N88-22371# Midwest Research Inst., Golden, Colo. Solar Energy Research Inst.
FLAP (FORCE AND LOADS ANALYSIS PROGRAM) CODE DEVELOPMENT AND VALIDATION
A. D. Wright, M. L. Buhl, and R. W. Thresher Jan. 1988 330 p
(Contract DE-AC02-83CH-10093)
(DE88-001131; SERI/TR-217-3125) Avail: NTIS HC A15/MF A01

The Force and Loads Analysis Program (FLAP) has been refined to include the teetering degree of freedom (without delta-3). This report describes these refinements, as well as comparisons of predicted blade-bending moments to test measurements. Wind-tunnel data for a 1/20-scale model of the Boeing MOD-2 machine were used to compare FLAP predictions for the cyclic flap-bending moments at the 33 percent spanwise station for three different wind speeds. The comparisons were made for both rigid- and teetering-hub cases. The code was written in FORTRAN 77 to be especially useful on the IBM PC family of computers. A special effort was made to make the program user friendly and readable. This report can be used as a user's guide; it includes a program description, a method of preparing input files, and information on the correct method of executing the code. A method of correctly preparing blade input data from a structural-dynamics viewpoint is also described. The code and this report are now available for public use. DOE

N88-22372# Sandia National Labs., Albuquerque, N. Mex.
ELASTO-PLASTIC ANALYSIS USING A STRESS-BASED FINITE ELEMENT METHOD AND AN ENDOCHRONIC THEORY OF PLASTICITY
S. W. Attaway 1988 7 p Presented at the International Conference on Computational Engineering Science, Atlanta, Ga., 10 Apr. 1988
(Contract DE-AC04-76DP-00789)
(DE88-003001; SAND-87-1218C; CONF-880438-3) Avail: NTIS HC A02/MF A01

A stress-based finite element methodology that uses the endochronic theory to model elasto-plastic structural behavior is presented. The methodology is implemented through a tangent stiffness formulation using a discretization of four-fields consisting of: (1) stress, (2) displacement, (3) magnitude of plastic strain, and (4) hydrostatic stress. The four-field approach allows elastically incompressible materials and materials that become incompressible due to plastic flow to be modeled. The stress-based element has

been demonstrated to give more accurate solutions for displacements and stresses than conventional displacement models. DOE

N88-22373# Sandia National Labs., Albuquerque, N. Mex.
A 3-D SOLID RENDERING OF NDT DATA
C. Little 1988 5 p Presented at the 30th Meeting of the Weapons Agencies Nondestructive Testing Organization (WANTO), Largo, Fla., 12 Jan. 1988
(Contract DE-AC04-76DP-00789)
(DE88-006199; SAND-88-0378C; CONF-880160-3) Avail: NTIS HC A02/MF A01

The Non-Destructive Testing division at Sandia Labs in Albuquerque is working on a solid rendering project to view volumetric data. Thresholding of the intensity levels within the volumetric data is used to determine the surfaces to be rendered. We are looking for a graphics system to display the surfaces with shading, lighting, rotation, translation, clipping, and hidden surface removal calculations performed in the graphics system. It should also allow the user to interactively modify the viewing position and lighting, and redraw the new view as quickly as possible, real time being ideal. DOE

N88-22374# Air Force Inst. of Tech., Wright-Patterson AFB, Ohio. School of Engineering.
THE BUCKLING AND VIBRATION OF COMPOSITE PLATES USING THE LEVY METHOD CONSIDERING SHEAR DEFORMATION AND ROTARY INERTIA M.S. Thesis
Real F. Palardy Dec. 1987 119 p
(AD-A189743; AFIT/GAE/AA/87D-16) Avail: NTIS HC A06/MF A01 CSCL 11D

An analytical study is conducted to determine the stability and free vibration characteristics of laminated anisotropic plates using the Levy approach. Included in the plate model are the effects of shear deformation and rotary inertia. Six different boundary conditions in the y direction are analyzed in conjunction with simply-supported boundaries in the x direction. The y directed boundaries considered are simple-simple, clamped-clamped, simple-clamped, simple-free, clamped-free, and free-free. Solutions are presented for the buckling loads and natural frequencies of rectangular, graphite-epoxy symmetric plates. The results indicate the importance of including shear effects and rotary inertia in a plate's mathematical model. The overall importance of these equation parameters is definitely a function of the boundary condition and a general statement cannot be made. In addition, the effectiveness of the Levy technique, in studying laminated problems, becomes apparent in handling the more complicated boundaries as compared to the Galerkin or Rayleigh-Ritz techniques. GRA

N88-22375# Wisconsin Univ., Madison.
INSTRUMENTATION TO PROVIDE AN ACTIVE CONTROL CAPABILITY FOR DISTRIBUTED PARAMETER SYSTEMS Final Report, 30 Jul. 1986 - 27 Oct. 1987
David Russell 4 Feb. 1988 5 p
(Grant AF-AFOSR-0254-86)
(AD-A190043; AFOSR-88-0164TR) Avail: NTIS HC A02/MF A01 CSCL 20K

This final report describes the purpose and details of the equipment purchased under a University Research Instrumentation Program (URIP) grant. Equipment includes instruments for remote sensing of vibrations, for modal analysis of vibrating structures, and for active vibration suppression of viscoelastic beams. GRA

N88-22376# Ballistic Research Labs., Aberdeen Proving Ground, Md.
BUCKLING OF BLAST LOADED CYLINDER Final Report, 1985 - 1986
Joseph M. Santiago, Michael H. Klaus, and Henry L. Wisniewski Oct. 1987 52 p
(AD-A190124; BRL-TR-2863) Avail: NTIS HC A04/MF A01 CSCL 20K

The transient response of a thin-walled aluminum cylinder subjected to an enveloping shock wave has been simulated with the ADINA finite element program and the results have been compared with counterpart experimental data. The analysis employed the ADINA 16-noded rectangular curved shell. Using linear analysis, the computed strain histories at gage locations were found to correlate reasonably well with test records for the first four milliseconds, but some strain records rapidly diverged thereafter. A subsequent nonlinear analysis showed dynamic buckling to be the principal cause of this discrepancy. The non-linear calculations and test results were found to generally agree in the number of buckling nodes, the magnitude of the deformation, and frequencies excited, although buckling sensitivity to imperfections prevented an exact coincidence of circumferential modes. GRA

N88-22377# Lehigh Univ., Bethlehem, Pa. Inst. of Fracture and Solid Mechanics.
ENVIRONMENTALLY ASSISTED CRACK GROWTH IN STRUCTURAL ALLOYS: PERSPECTIVES AND NEW DIRECTIONS Technical Report, 1 Jan. - 31 Dec. 1987
Robert P. Wei and Richard P. Gangloff Dec. 1987 63 p
(Contract N00014-83-K-0107)
(AD-A190137; ISFM-87-148) Avail: NTIS HC A04/MF A01 CSCL 11F

Environmentally assisted crack growth (namely, stress corrosion cracking and corrosion fatigue) in alloys is one of the principal determining factors for durability and reliability of engineering structures. Over the past 20 years, activities in this area have transformed from principally that of screening and qualitative characterizations of the phenomena, to that of quantitative assessment and scientific understanding. This work has enabled the recent development of life prediction procedures. In this paper, the contributions of fracture mechanics in this transformation are reviewed. Current mechanistic understanding and environmentally assisted crack growth by hydrogen embrittlement is summarized and placed in perspective. Applications to mitigate stress corrosion and corrosion fatigue cracking in marine environments are summarized. Some outstanding issues and new directions for research are discussed. GRA

N88-22378# Weidlinger Associates, New York, N.Y.
VIBRATIONS OF STRUCTURES WITH PARAMETRIC UNCERTAINTIES Final Report, Jan. 1984 - Sep. 1987
Haym Benaroya 31 Oct. 1987 75 p
(Contract F49620-84-C-0009)
(AD-A190400; AFOSR-87-1734TR) Avail: NTIS HC A04/MF A01 CSCL 22A

The focus of this research effort has been the study of structural dynamics with parameter and environmental uncertainties. The motivation for this study rests with the need to understand the dynamics and control of large space structures. Stochastic stability and output stationarity are also studied. GRA

N88-22379# Portsmouth Polytechnic (England). Mechanical Behaviour of Materials Lab.
THE GROWTH OF CORNER CRACKS UNDER THE CONJOINT ACTION OF HIGH AND LOW CYCLE FATIGUE Final Report, Jun. 1985 - Jun. 1987
B. E. Powell, I. Henderson, and R. F. Hall Feb. 1988 98 p
(Contract F49620-85-C-0116)
(AD-A190510; AFWAL-TR-87-4130) Avail: NTIS HC A05/MF A01 CSCL 11F

Fatigue crack propagation rates have been measured for Ti-6Al-4V and Ti-5331S aeroengine disc materials using compact tension and corner notched tensile test-pieces. The loadings used simulate both the start-stop operations of aeroengines which lead to low cycle fatigue and the in-flight vibrations which may cause high cycle fatigue. It is suggested that the different fatigue crack growth behavior of Ti-5331S, relative to that of Ti-6Al-4V, arises largely from the greater proportion of crack closure and short crack growth occurring in this alloy. GRA

N88-22380# Army Cold Regions Research and Engineering Lab., Hanover, N.H.
THE CRREL (COLD REGIONS RESEARCH AND ENGINEERING LABORATORY) HOPKINSON BAR APPARATUS
Piyush K. Dutta, Dennis Farrell, and John Kalafut Dec. 1987 38 p
(AD-A190599; CRREL-SR-87-24) Avail: NTIS HC A03/MF A01 CSCL 11G

Most materials at low temperatures change their modulus and tend to become brittle. When using these materials in structural components that are likely to be subjected to impact it is important to understand their behavior at low temperatures under dynamic loading. The CRREL split Hopkinson Test Bar was designed and set up to conduct compressive strain rate tests (up to 1000 strains/s, i.e., in./in. per s) at low temperatures (down to -100 C). The results provide dynamic stress strain relationships of materials at low temperatures by considering the transmission of the stress wave through a test specimen sandwiched between two elastic bars. The specimen is contained in a liquid nitrogen cooling environment. During the test an elastic striker impacts the bar; as a result a stress wave passes down the bar. At the specimen a part of the wave is reflected and the rest is transmitted to the second bar. Strain gauges mounted on the bars record the wave shapes, which are analyzed to obtain the dynamic stress-strain relationships. The test bars are 1-1/2 in. in diameter and each is 8 ft long. The apparatus is suitable for testing light metals, plastics, composites, rocks, ice, and frozen soil. The data acquisition and analysis system are completely automatic, using software developed at CRREL, so the system provides for a rapid and low-cost method for high strain rate behavior studies of materials. GRA

N88-22381# Battelle Pacific Northwest Labs., Richland, Wash.
EVOLUTION OF HARDENING AND DAMAGE DURING VISCOPLASTIC DEFORMATION Final Report, 1 Dec. 1986 - 30 Aug. 1987
R. E. Williford 15 Oct. 1987 70 p
(Contract F49620-87-C-0031)
(AD-A190714; Rept-23111-07367; AFOSR-87-2007TR) Avail: NTIS HC A04/MF A01 CSCL 20K

Although theories of nonlocal mechanics were developed to address the role of hardening and damage microstructures in heterogeneous engineering materials, these theories frequently require additional, but unavailable, information concerning the concentrations or size distributions of the microstructures to compute the internal stresses. An objective of this work was to develop generalized equations for the size distributions of hardening and damage microstructures as functions of the stress, strain rate, and the scale of observation, and thus, to reduce the above information requirements. The two approaches employed addressed incompressible and compressible materials. Limitations identified from the incompressible formulation were employed to construct a variational integral for compressible materials. Definition of the variables in this integral was completed except for a strain rate scale factor. The associated Euler Lagrange equations are expected to provide the desired microstructure evolution equations. GRA

N88-22382*# National Aeronautics and Space Administration. Lewis Research Center, Cleveland, Ohio.
LEWIS STRUCTURES TECHNOLOGY, 1988. VOLUME 2: STRUCTURAL MECHANICS
May 1988 307 p Symposium held in Cleveland, Ohio, 24-25 May 1988
(NASA-CP-3003-Vol-2; E-3970-Vol-2; NAS 1.55:3003-Vol-2)
Avail: NTIS HC A14/MF A01 CSCL 20K

Lewis Structures Div. performs and disseminates results of research conducted in support of aerospace engine structures. These results have a wide range of applicability to practitioners of structural engineering mechanics beyond the aerospace arena. The engineering community was familiarized with the depth and range of research performed by the division and its academic and industrial partners. Sessions covered vibration control, fracture mechanics, ceramic component reliability, parallel computing, nondestructive evaluation, constitutive models and experimental capabilities, dynamic systems, fatigue and damage, wind turbines, hot section technology (HOST), aeroelasticity, structural mechanics codes, computational methods for dynamics, structural optimization, and applications of structural dynamics, and structural mechanics computer codes. For individual titles, see N88-22383 through N88-22407.

N88-22383*# National Aeronautics and Space Administration. Lewis Research Center, Cleveland, Ohio.
HIGH-TEMPERATURE COMBUSTOR LINER TESTS IN STRUCTURAL COMPONENT RESPONSE TEST FACILITY **c07**
Paul E. Moorhead *In its* Lewis Structures Technology, 1988. Volume 2: Structural Mechanics May 1988 p 5-13 (For primary document see N88-22382 15-39)
Avail: NTIS HC A14/MF A01 CSCL 21E

Jet engine combustor liners were tested in the structural component response facility at NASA Lewis. In this facility combustor liners were thermally cycled to simulate a flight envelope of takeoff, cruise, and return to idle. Temperatures were measured with both thermocouples and an infrared thermal imaging system. A conventional stacked-ring louvered combustor liner developed a crack at 1603 cycles. This test was discontinued after 1728 cycles because of distortion of the liner. A segmented or float wall combustor liner tested at the same heat flux showed no significant change after 1600 cycles. Changes are being made in the facility to allow higher temperatures. Author

N88-22384*# National Aeronautics and Space Administration. Lewis Research Center, Cleveland, Ohio.
LIFE ASSESSMENT OF COMBUSTOR LINER USING UNIFIED CONSTITUTIVE MODELS **c07**
M. T. Tong (Sverdrup Technology, Inc., Cleveland, Ohio.) and R. L. Thompson *In its* Lewis Structures Technology, 1988. Volume 2: Structural Mechanics May 1988 p 15-25 (For primary document see N88-22382 15-39)
(Contract NAS3-24105)
Avail: NTIS HC A14/MF A01 CSCL 21E

Hot section components of gas turbine engines are subject to severe thermomechanical loads during each mission cycle. Inelastic deformation can be induced in localized regions leading to eventual fatigue cracking. Assessment of durability requires reasonably accurate calculation of the structural response at the critical location for crack initiation. In recent years nonlinear finite element computer codes have become available for calculating inelastic structural response under cyclic loading. NASA-Lewis sponsored the development of unified constitutive material models and their implementation in nonlinear finite element computer codes for the structural analysis of hot section components. These unified models were evaluated with regard to their effect on the life prediction of a hot section component. The component considered was a gas turbine engine combustor liner. A typical engine mission cycle was used for the thermal and structural analyses. The analyses were performed on a CRAY computer using the MARC finite element code. The results were compared with laboratory test results, in terms of crack initiation lives. Author

N88-22385*# National Aeronautics and Space Administration. Lewis Research Center, Cleveland, Ohio.
EXPERIMENTS INVESTIGATING ADVANCED MATERIALS UNDER THERMOMECHANICAL LOADING
Paul A. Bartolotta *In its* Lewis Structures Technology, 1988. Volume 2: Structural Mechanics May 1988 p 27-35 (For primary document see N88-22382 15-39)
Avail: NTIS HC A14/MF A01 CSCL 20K

Many high temperature aircraft and rocket engine components experience large mechanical loads as well as severe thermal gradients and transients. These nonisothermal conditions are often large enough to cause inelastic deformations, which are the ultimate cause for failure in those parts. A way to alleviate this problem is through improved engine designs based on better predictions of thermomechanical material behavior. To address this concern, an

experimental effort was recently initiated within the Hot Section Technology (HOST) program at Lewis. As part of this effort, two new test systems were added to the Fatigue and Structures Lab., which allowed thermomechanical tests to be conducted under closely controlled conditions. These systems are now being used for thermomechanical testing for the Space Station Receiver program, and will be used to support development of metal matrix composites. Author

N88-22386*# National Aeronautics and Space Administration. Lewis Research Center, Cleveland, Ohio.
BIAXIAL EXPERIMENTS SUPPORTING THE DEVELOPMENT OF CONSTITUTIVE THEORIES FOR ADVANCED HIGH-TEMPERATURE MATERIALS
J. R. Ellis *In its* Lewis Structures Technology, 1988. Volume 2: Structural Mechanics May 1988 p 37-48 (For primary document see N88-22382 15-39)
Avail: NTIS HC A14/MF A01 CSCL 20K

Complex states of stress and strain are introduced into components during service in engineering applications. It follows that analysis of such components requires material descriptions, or constitutive theories, which reflect the tensorial nature of stress and strain. For applications involving stress levels above yield, the situation is more complex in that material response is both nonlinear and history dependent. This has led to the development of viscoplastic constitutive theories which introduce time by expressing the flow and evolutionary equation in the form of time derivatives. Models were developed here which can be used to analyze high temperature components manufactured from advanced composite materials. In parallel with these studies, effort was directed at developing multiaxial testing techniques to verify the various theories. Recent progress in the development of constitutive theories from both the theoretical and experimental viewpoints are outlined. One important aspect is that material descriptions for advanced composite materials which can be implemented in general purpose finite element codes and used for practical design are verified. Author

N88-22387*# Akron Univ., Ohio.
UNIFIED CONSTITUTIVE MODEL DEVELOPMENT FOR METAL MATRIX COMPOSITES AT HIGH TEMPERATURE **c24**
D. N. Robinson *In* NASA. Lewis Research Center, Lewis Structures Technology, 1988. Volume 2: Structural Mechanics May 1988 p 49-56 (For primary document see N88-22382 15-39) (Grant NAG3-379)
Avail: NTIS HC A14/MF A01 CSCL 11D

Structural alloys used in high temperature applications exhibit complex thermomechanical behavior that is time dependent and hereditary. Recent attention is being focused on metal matrix composite materials for high temperature applications where they exhibit all the complexities of conventional alloys and their strong anisotropy adds further complexities. Here, a proven constitutive model for isotropic materials in which the inelastic strain rate and internal state are expressible as gradients of a dissipation potential is taken to depend on invariants that reflect local transverse isotropy. Applications illustrate the capability of the theory of representing the time dependent, hereditary, anisotropic behavior typical of these materials at high temperature. Author

N88-22388*# Engineering Science Software, Inc., Smithfield, R.I.
UNIFIED CONSTITUTIVE MODEL FOR SINGLE CRYSTAL DEFORMATION BEHAVIOR WITH APPLICATIONS
K. P. Walker, T. G. Meyer, and E. H. Jordan (Connecticut Univ., Storrs.) *In* NASA. Lewis Research Center, Lewis Structures Technology, 1988. Volume 2: Structural Mechanics May 1988 p 57-71 (For primary document see N88-22382 15-39) (Contract NAS3-23939; Grant NAG3-512)
Avail: NTIS HC A14/MF A01 CSCL 20K

Single crystal materials are being used in gas turbine airfoils and are candidates for other hot section components because of their increased temperature capabilities and resistance to thermal fatigue. Development of a constitutive model which assesses the inelastic behavior of these materials has been studied in 2 NASA programs: Life Prediction and Constitutive Models for Engine Hot Section Anisotropic Materials and Biaxial Constitutive Equation Development for Single Crystals. The model has been fit to a large body of constitutive data for single crystal PWA 1480 material. The model uses a unified approach for computing total inelastic strains (creep plus plasticity) on crystallographic slip systems reproducing observed directional and strain rate effects as a natural consequence of the summed slip system quantities. The model includes several of the effects that have been reported to influence deformation in single crystal materials, such as shear stress, latent hardening, and cross slip. The model is operational in a commercial Finite Element code and is being installed in a Boundary Element Method code. Author

N88-22389*# National Aeronautics and Space Administration. Lewis Research Center, Cleveland, Ohio.
FINITE ELEMENT (MARC) SOLUTION TECHNOLOGIES FOR VISCOPLASTIC ANALYSES
V. K. Arya (National Academy of Sciences - National Research Council, Washington, D. C.) and Robert L. Thompson *In its* Lewis Structures Technology, 1988. Volume 2: Structural Mechanics May 1988 p 73-79 (For primary document see N88-22382 15-39)
Avail: NTIS HC A14/MF A01 CSCL 20K

A need for development of realistic constitutive models for structural components operating at high temperatures, accompanied by appropriate solution technologies for stress/life analyses of these components is studied. Viscoplastic models provide a better description of inelastic behavior of materials, but their mathematical structure is very complex. The highly nonlinear and stiff nature of the constitutive equations makes analytical solutions difficult. Therefore, suitable solution, finite element or other numerical, technologies must be developed to make these models adaptable for better and rational designs of components. NASA-Lewis has developed several solution technologies and successfully applied them to the solution of a number of uniaxial and multiaxial problems. Some of these solution technologies are described along with the models and representative results. The solution technologies developed and presented encompass a wide range of models, such as, isotropic, anisotropic, metal matrix composites, and single crystal models. Author

N88-22390*# National Aeronautics and Space Administration. Lewis Research Center, Cleveland, Ohio.
THE COMPOSITE BLADE STRUCTURAL ANALYZER (COBSTRAN) **c07**
Robert A. Aiello *In its* Lewis Structures Technology, 1988. Volume 2: Structural Mechanics May 1988 p 83-97 (For primary document see N88-22382 15-39)
Avail: NTIS HC A14/MF A01 CSCL 21E

The use and application of the COBSTRAN (COmposite Blade STRuctural ANalyzer) computer code is presented. COBSTRAN was developed at NASA-Lewis and is currently being used for the design and analysis of aircraft engine ducted and unducted fan blades. The features of COBSTRAN are demonstrated for the modeling and analysis of a scaled down wind tunnel model propfan blade made from fiber composites. Comparison of analytical and experimental mode shapes and frequencies are shown, verifying the model development and analysis techniques used. The methodologies and programs developed for this analysis are directly applicable to other propfan blades. Author

N88-22391*# National Aeronautics and Space Administration. Lewis Research Center, Cleveland, Ohio.
FEATURES AND APPLICATIONS OF THE INTEGRATED COMPOSITES ANALYZER (ICAN) CODE **c24**
Carol A. Ginty *In its* Lewis Structures Technology, 1988. Volume 2: Structural Mechanics May 1988 p 99-112 Previously announced as N87-16880 (For primary document see N88-22382 15-39)
Avail: NTIS HC A14/MF A01 CSCL 11D

The thermal behavior of composite spacecraft antenna

reflectors was investigated with the Integrated Composites Analyzer (ICAN) computer code. Parametric studies were conducted on the face sheets and honeycomb core which constitute the sandwich-type structures. Selected thermal and mechanical properties of the composite faces and sandwich structures are presented graphically as functions of varying fiber volume ratio, laminate configuration, fabrication factors, and environmental conditions. Author

N88-22392*# Sverdrup Technology, Inc., Cleveland, Ohio.
THREE-DIMENSIONAL INELASTIC APPROXIMATE ANALYSIS CODE (MOMM)
Jeffrey P. Meister *In* NASA. Lewis Research Center, Lewis Structures Technology, 1988. Volume 2: Structural Mechanics May 1988 p 113-122 (For primary document see N88-22382 15-39)
Avail: NTIS HC A14/MF A01 CSCL 20K

The Mechanics of Materials Model (MOMM) is one of a series of new stand-alone three dimensional nonlinear structural analysis codes. Incorporation of a general purpose finite element computer code into the hot section design process was severely limited by the high costs involved. MOMM is a stiffness method finite element code that uses an internally generated network of beams to characterize hot section component behavior. The method was proposed as a fast, easy to use, computationally efficient tool for approximate analyses. MOMM incorporates a wide variety of analysis capabilities, material models, and load type specifiers instrumental for the analysis of hot section components. Author

N88-22393*# Sverdrup Technology, Inc., Cleveland, Ohio.
SPECIALTY THREE-DIMENSIONAL FINITE ELEMENT ANALYSIS CODES
Joseph J. Lackney *In* NASA. Lewis Research Center, Lewis Structures Technology, 1988. Volume 2: Structural Mechanics May 1988 p 123-129 (For primary document see N88-22382 15-39)
Avail: NTIS HC A14/MF A01 CSCL 20K

General purpose finite element computer codes that can model inelastic material behavior have been available for more than a decade. However, these codes have not been accurate enough for use in analyzing hot section engine components. To correct this problem, General Electric developed a series of nine new stand-alone computer codes for NASA. Because of the large temperature excursions associated with hot section engine components, these codes have been designed to accommodate broad variations in material behavior, including plasticity and creep. The capabilities of these computer codes are summarized. Author

N88-22394*# MARC Analysis Research Corp., Palo Alto, Calif.
MHOST: AN EFFICIENT FINITE ELEMENT PROGRAM FOR INELASTIC ANALYSIS OF SOLIDS AND STRUCTURES **c07**
S. Nakazawa *In* NASA. Lewis Research Center, Lewis Structures Technology, 1988. Volume 2: Structural Mechanics May 1988 p 131-140 (For primary document see N88-22382 15-39)
(Contract NAS3-23698)
Avail: NTIS HC A14/MF A01 CSCL 21E

An efficient finite element program for 3-D inelastic analysis of gas turbine hot section components was constructed and validated. A novel mixed iterative solution strategy is derived from the augmented Hu-Washizu variational principle in order to nodally interpolate coordinates, displacements, deformation, strains, stresses and material properties. A series of increasingly sophisticated material models incorporated in MHOST include elasticity, secant plasticity, infinitesimal and finite deformation plasticity, creep and unified viscoplastic constitutive model proposed by Walker. A library of high performance elements is built into this computer program utilizing the concepts of selective reduced integrations and independent strain interpolations. A family of efficient solution algorithms is implemented in MHOST for linear and nonlinear equation solution including the classical Newton-Raphson, modified, quasi and secant Newton methods with optional line search and the conjugate gradient method. Author

N88-22395*# National Aeronautics and Space Administration. Lewis Research Center, Cleveland, Ohio.
METCAN: THE METAL MATRIX COMPOSITE ANALYZER **c24**
Dale A. Hopkins and Pappu L. N. Murthy (Cleveland State Univ., Ohio.) *In its* Lewis Structures Technology, 1988. Volume 2: Structural Mechanics May 1988 p 141-156 (For primary document see N88-22382 15-39)
(Grant NAG3-550)
Avail: NTIS HC A14/MF A01 CSCL 11D

Metal matrix composites (MMC) are the subject of intensive study and are receiving serious consideration for critical structural applications in advanced aerospace systems. MMC structural analysis and design methodologies are studied. Predicting the mechanical and thermal behavior and the structural response of components fabricated from MMC requires the use of a variety of mathematical models. These models relate stresses to applied forces, stress intensities at the tips of cracks to nominal stresses, buckling resistance to applied force, or vibration response to excitation forces. The extensive research in computational mechanics methods for predicting the nonlinear behavior of MMC are described. This research has culminated in the development of the METCAN (METal Matrix Composite ANalyzer) computer code. Author

N88-22396*# Cleveland State Univ., Ohio.
COMPUTATIONAL SIMULATION METHODS FOR COMPOSITE FRACTURE MECHANICS **c24**
Pappu L. N. Murthy *In* NASA. Lewis Research Center, Lewis Structures Technology, 1988. Volume 2: Structural Mechanics May 1988 p 157-169 (For primary document see N88-22382 15-39)
Avail: NTIS HC A14/MF A01 CSCL 11D

Structural integrity, durability, and damage tolerance of advanced composites are assessed by studying damage initiation at various scales (micro, macro, and global) and accumulation and growth leading to global failure, quantitatively and qualitatively. In addition, various fracture toughness parameters associated with a typical damage and its growth must be determined. Computational structural analysis codes to aid the composite design engineer in performing these tasks were developed. CODSTRAN (COmposite Durability STRuctural ANalysis) is used to qualitatively and quantitatively assess the progressive damage occurring in composite structures due to mechanical and environmental loads. Next, methods are covered that are currently being developed and used at Lewis to predict interlaminar fracture toughness and related parameters of fiber composites given a prescribed damage. The general purpose finite element code MSC/NASTRAN was used to simulate the interlaminar fracture and the associated individual as well as mixed-mode strain energy release rates in fiber composites. Author

N88-22397*# Sverdrup Technology, Inc., Cleveland, Ohio.
PROBABILISTIC STRUCTURAL ANALYSIS COMPUTER CODE (NESSUS)
Michael C. Shiao *In* NASA. Lewis Research Center, Lewis Structures Technology, 1988. Volume 2: Structural Mechanics May 1988 p 173-181 (For primary document see N88-22382 15-39)
(Grant NAG3-24105)
Avail: NTIS HC A14/MF A01 CSCL 20K

Probabilistic structural analysis has been developed to analyze the effects of fluctuating loads, variable material properties, and uncertain analytical models especially for high performance structures such as SSME turbopump blades. The computer code NESSUS (Numerical Evaluation of Stochastic Structure Under Stress) was developed to serve as a primary computation tool for the characterization of the probabilistic structural response due to the stochastic environments by statistical description. The code consists of three major modules NESSUS/PRE, NESSUS/FEM, and NESSUS/FPI. NESSUS/PRE is a preprocessor which

decomposes the spatially correlated random variables into a set of uncorrelated random variables using a modal analysis method. NESSUS/FEM is a finite element module which provides structural sensitivities to all the random variables considered. NESSUS/FPI is Fast Probability Integration method by which a cumulative distribution function or a probability density function is calculated. Author

N88-22398*# Sverdrup Technology, Inc., Cleveland, Ohio.
STRUCTURAL TAILORING OF HIGH-SPEED TURBINE BLADES (SSME/STAEBL) **c20**
Robert Rubinstein *In* NASA. Lewis Research Center, Lewis Structures Technology, 1988. Volume 2: Structural Mechanics May 1988 p 183-188 (For primary document see N88-22382 15-39)
Avail: NTIS HC A14/MF A01 CSCL 21H

Space shuttle main engine (SSME) blades are subject to severe thermal, pressure, and forced vibration environments. Structural optimization provides an automated alternative to time consuming iterations. Any number of analyses, design variables, and constraints can be incorporated in a structural optimization computer code. This idea was applied to develop the code SSME/STAEBL, which is a stand alone code suitable for automated design of SSME turbopump blades. Additions and modifications of STAEBL included in SSME/STAEBL include the following: (1) thermal stress analysis, (2) gas dynamic (pressure) loads, (3) temperature-dependent material and thermal properties, (4) forced vibrations, (5) tip displacement constraints, (6) single crystal material analysis, (7) blade cross-section stacking offsets, and (8) direct time integration algorithm for transient dynamic response. Author

N88-22399*# National Aeronautics and Space Administration. Lewis Research Center, Cleveland, Ohio.
COMPUTATIONAL STRUCTURAL MECHANICS FOR ENGINE STRUCTURES **c07**
Christos C. Chamis *In its* Lewis Structures Technology, 1988. Volume 2: Structural Mechanics May 1988 p 189-203 (For primary document see N88-22382 15-39)
Avail: NTIS HC A14/MF A01 CSCL 21E

The computational structural mechanics (CSM) program at Lewis encompasses the formulation and solution of structural mechanics problems and the development of integrated software systems to computationally simulate the performance, durability, and life of engine structures. It is structured to supplement, complement, and, whenever possible, replace costly experimental efforts. Specific objectives are to investigate unique advantages of parallel and multiprocessing for reformulating and solving structural mechanics and formulating and solving multidisciplinary mechanics and to develop integrated structural system computational simulators for predicting structural performance, evaluating newly developed methods, and identifying and prioritizing improved or missing methods. Author

N88-22400*# National Aeronautics and Space Administration. Lewis Research Center, Cleveland, Ohio.
STRUCTURAL TAILORING OF ADVANCED TURBOPROPS
K. W. Brown (Pratt and Whitney Aircraft, East Hartford, Conn.) and Dale A. Hopkins *In its* Lewis Structures Technology, 1988. Volume 2: Structural Mechanics May 1988 p 205-217 (For primary document see N88-22382 15-39)
(Contract NAS3-23941)
Avail: NTIS HC A14/MF A01 CSCL 20K

The Structural Tailoring of Advanced Turboprops (STAT) computer program was developed to perform numerical optimization on highly swept propfan blades. The optimization procedure seeks to minimize an objective function defined as either: (1) direct operating cost of full scale blade or, (2) aeroelastic differences between a blade and its scaled model, by tuning internal and external geometry variables that must satisfy realistic blade design constraints. The STAT analysis system includes an aerodynamic efficiency evaluation, a finite element stress and vibration analysis, an acoustic analysis, a flutter analysis, and a once-per-revolution forced response life prediction capability. STAT includes all relevant propfan design constraints. Author

N88-22401*# Sverdrup Technology, Inc., Cleveland, Ohio.
ADVANCED PROBABILISTIC METHODS FOR QUANTIFYING THE EFFECTS OF VARIOUS UNCERTAINTIES IN STRUCTURAL RESPONSE
Vinod K. Nagpal *In* NASA. Lewis Research Center, Lewis Structures Technology, 1988. Volume 2: Structural Mechanics May 1988 p 219-232 Sponsored by NASA, Lewis Research Center, Cleveland, Ohio (For primary document see N88-22382 15-39)
Avail: NTIS HC A14/MF A01 CSCL 20K

The effects of actual variations, also called uncertainties, in geometry and material properties on the structural response of a space shuttle main engine turbopump blade are evaluated. A normal distribution was assumed to represent the uncertainties statistically. Uncertainties were assumed to be totally random, partially correlated, and fully correlated. The magnitude of these uncertainties were represented in terms of mean and variance. Blade responses, recorded in terms of displacements, natural frequencies, and maximum stress, was evaluated and plotted in the form of probabilistic distributions under combined uncertainties. These distributions provide an estimate of the range of magnitudes of the response and probability of occurrence of a given response. Most importantly, these distributions provide the information needed to estimate quantitatively the risk in a structural design. Author

N88-22402*# National Aeronautics and Space Administration. Lewis Research Center, Cleveland, Ohio.
IMPACT DAMAGE IN COMPOSITE LAMINATES **c24**
Joseph E. Grady *In its* Lewis Structures Technology, 1988. Volume 2: Structural Mechanics May 1988 p 235-243 (For primary document see N88-22382 15-39)
Avail: NTIS HC A14/MF A01 CSCL 11D

Damage tolerance requirements have become an important consideration in the design and fabrication of composite structural components for modern aircraft. The ability of a component to contain a flaw of a given size without serious loss of its structural integrity is of prime concern. Composite laminates are particularly susceptible to damage caused by transverse impact loading. The ongoing program described is aimed at developing experimental and analytical methods that can be used to assess damage tolerance capabilities in composite structures subjected to impulsive loading. Some significant results of this work and the methodology used to obtain them are outlined. Author

N88-22403*# National Aeronautics and Space Administration. Lewis Research Center, Cleveland, Ohio.
THERMOSTRUCTURAL ANALYSIS OF SIMULATED COWL LIPS
Matthew E. Melis *In its* Lewis Structures Technology, 1988. Volume 2: Structural Mechanics May 1988 p 245-254 (For primary document see N88-22382 15-39)
Avail: NTIS HC A14/MF A01 CSCL 20K

Three dimensional finite element analyses using MSC/NASTRAN and MARC are performed to predict the thermal and structural response of various cooling schemes under high heat loads. Steady state heat transfer analyses and elastic stress analyses are performed using MSC/NASTRAN. Elastic/plastic analyses are done using MARC. To help verify these analyses experimentally, a hydrogen-oxygen rocket engine was modified to use the exhaust stream as a high enthalpy, high heat flux source to evaluate various actively cooled, simulated cowl lip (leading edges) segments as well as flat structural segments. Cross flow and parallel flow cooling configurations were tested and analyzed using cooling fluids of water and gaseous hydrogen. In addition, various material types, including high conductivity copper, nickel, and a copper and graphite metal matrix composite were tested and compared. Author

N88-22404*# National Aeronautics and Space Administration. Lewis Research Center, Cleveland, Ohio.
THERMAL-STRUCTURAL ANALYSES OF SPACE SHUTTLE MAIN ENGINE (SSME) HOT SECTION COMPONENTS c20
Ali Abdul-Aziz (Sverdrup Technology, Inc., Cleveland, Ohio.) and Robert L. Thompson *In its* Lewis Structures Technology, 1988. Volume 2: Structural Mechanics May 1988 p 255-264 (For primary document see N88-22382 15-39)
Avail: NTIS HC A14/MF A01 CSCL 21H

Three dimensional nonlinear finite element heat transfer and structural analyses were performed for the first stage high pressure fuel turbopump (HPFTP) blade of the space shuttle main engine (SSME). Directionally solidified (DS) MAR-M 246 and single crystal (SC) PWA-1480 material properties were used for the analyses. Analytical conditions were based on a typical test stand engine cycle. Blade temperature and stress strain histories were calculated by using the MARC finite element computer code. The structural response of an SSME turbine blade was assessed and a greater understanding of blade damage mechanisms, convective cooling effects, and thermal mechanical effects was gained. Author

N88-22405*# Sverdrup Technology, Inc., Cleveland, Ohio.
STRUCTURAL ANALYSES OF ENGINE WALL COOLING CONCEPTS AND MATERIALS c24
Albert Kaufman *In* NASA. Lewis Research Center, Lewis Structures Technology, 1988. Volume 2: Structural Mechanics May 1988 p 265-280 (For primary document see N88-22382 15-39)
Avail: NTIS HC A14/MF A01 CSCL 11D

The severe thermal environments under which hypersonic aircraft such as the National Aerospace Plane (NASP) will operate require cooling of the engine walls, especially in the combustor. A preliminary assessment is made of some candidate materials based on structural analyses for a number of convective cooling configurations. Three materials were studied: graphite/copper and tungsten/copper composite alloys with 50 percent fiber volume fractions and a wrought cobalt-base superalloy, Haynes 188. Anisotropic mechanical and thermal properties for the composites were obtained from a computer code, ICAN, which determines the composite material properties from the individual properties of the fiber and matrix materials. The structural analyses were performed by using the MARC nonlinear finite element code. Heat transfer analyses were conducted to calculate the metal temperature distributions. Author

N88-22406*# National Aeronautics and Space Administration. Lewis Research Center, Cleveland, Ohio.
STRUCTURAL ASSESSMENT OF A SPACE STATION SOLAR DYNAMIC HEAT RECEIVER THERMAL ENERGY STORAGE CANISTER
R. L. Thompson, T. W. Kerslake, and M. T. Tong (Sverdrup Technology, Inc., Cleveland, Ohio.) *In its* Lewis Structures Technology, 1988. Volume 2: Structural Mechanics May 1988 p 281-294 Previously announced in IAA as N88-31396 (For primary document see N88-22382 15-39)
Avail: NTIS HC A14/MF A01 CSCL 20K

The structural performance of a space station thermal energy storage (TES) canister subject to orbital solar flux variation and engine cold start up operating conditions was assessed. The impact of working fluid temperature and salt-void distribution on the canister structure are assessed. Both analytical and experimental studies were conducted to determine the temperature distribution of the canister. Subsequent finite element structural analyses of the canister were performed using both analytically and experimentally obtained temperatures. The Arrhenius creep law was incorporated into the procedure, using secondary creep data for the canister material, Haynes 188 alloy. The predicted cyclic creep strain accumulations at the hot spot were used to assess the structural performance of the canister. In addition, the structural performance of the canister based on the analytically determined temperature was compared with that based on the experimentally measured temperature data. Author

N88-22407*# National Aeronautics and Space Administration. Lewis Research Center, Cleveland, Ohio.
AN EFFICIENT MINDLIN FINITE STRIP PLATE ELEMENT BASED ON ASSUMED STRAIN DISTRIBUTION
Abhisak Chulya (Case Western Reserve Univ., Cleveland, Ohio.) and Robert L. Thompson *In its* Lewis Structures Technology, 1988. Volume 2: Structural Mechanics May 1988 p 295-306 (For primary document see N88-22382 15-39)
Avail: NTIS HC A14/MF A01 CSCL 20K

A simple two node, linear, finite strip plate bending element based on Mindlin-Reissner plate theory for the analysis of very thin to thick bridges, plates, and axisymmetric shells is presented. The new transverse shear strains are assumed for constant distribution in the two node linear strip. The important aspect is the choice of the points that relate the nodal displacements and rotations through the locking transverse shear strains. The element stiffness matrix is explicitly formulated for efficient computation and ease in computer implementation. Numerical results showing the efficiency and predictive capability of the element for analyzing plates with different supports, loading conditions, and a wide range of thicknesses are given. The results show no sign of the shear locking phenomenon. Author

N88-22408*# National Aeronautics and Space Administration. Lewis Research Center, Cleveland, Ohio.
LEWIS STRUCTURES TECHNOLOGY, 1988. VOLUME 3: STRUCTURAL INTEGRITY FATIGUE AND FRACTURE WIND TURBINES HOST
May 1988 366 p Symposium held in Cleveland, Ohio, 24-25 May 1988
(NASA-CP-3003-Vol-3; E-3970-Vol-3; NAS 1.55:3003-Vol-3)
Avail: NTIS HC A16/MF A01 CSCL 20K

The charter of the Structures Division is to perform and disseminate results of research conducted in support of aerospace engine structures. These results have a wide range of applicability to practioners of structural engineering mechanics beyond the aerospace arena. The specific purpose of the symposium was to familiarize the engineering structures community with the depth and range of research performed by the division and its academic and industrial partners. Sessions covered vibration control, fracture mechanics, ceramic component reliability, parallel computing, nondestructive evaluation, constitutive models and experimental capabilities, dynamic systems, fatigue and damage, wind turbines, hot section technology (HOST), aeroelasticity, structural mechanics codes, computational methods for dynamics, structural optimization, and applications of structural dynamics, and structural mechanics computer codes. For individual titles, see N88-22409 through N88-22431.

N88-22409*# National Aeronautics and Space Administration. Lewis Research Center, Cleveland, Ohio.
MONOLITHIC CERAMIC ANALYSIS USING THE SCARE PROGRAM c27
Jane M. Manderscheid *In its* Lewis Structures Technology, 1988. Volume 3: Structural Integrity Fatigue and Fracture Wind Turbines HOST May 1988 p 5-20 (For primary document see N88-22408 15-39)
Avail: NTIS HC A16/MF A01 CSCL 11B

The Structural Ceramics Analysis and Reliability Evaluation (SCARE) computer program calculates the fast fracture reliability of monolithic ceramic components. The code is a post-processor to the MSC/NASTRAN general purpose finite element program. The SCARE program automatically accepts the MSC/NASTRAN output necessary to compute reliability. This includes element stresses, temperatures, volumes, and areas. The SCARE program computes two-parameter Weibull strength distributions from input fracture data for both volume and surface flaws. The distributions can then be used to calculate the reliability of geometrically complex components subjected to multiaxial stress states. Several fracture criteria and flaw types are available for selection by the user, including out-of-plane crack extension theories. The theoretical basis for the reliability calculations was proposed by Batdorf. These models combine linear elastic fracture mechanics (LEFM) with

Weibull statistics to provide a mechanistic failure criterion. Other fracture theories included in SCARE are the normal stress averaging technique and the principle of independent action. The objective of this presentation is to summarize these theories, including their limitations and advantages, and to provide a general description of the SCARE program, along with example problems.
Author

N88-22410*# Cleveland State Univ., Ohio.
WHISKER-REINFORCED CERAMIC COMPOSITES FOR HEAT ENGINE COMPONENTS **c27**
Stephen F. Duffy *In* NASA. Lewis Research Center, Lewis Structures Technology, 1988. Volume 3: Structural Integrity Fatigue and Fracture Wind Turbines HOST May 1988 p 21-40 (For primary document see N88-22408 15-39)
(Contract NCC3-81)
Avail: NTIS HC A16/MF A01 CSCL 11B

Much work was undertaken to develop techniques of incorporating SiC whiskers into either a Si3N4 or SiC matrix. The result was the fabrication of ceramic composites with ever-increasing fracture toughness and strength. To complement this research effort, the fracture behavior of whisker-reinforced ceramics is studied so as to develop methodologies for the analysis of structural components fabricated from this toughened material. The results, outlined herein, focus on the following areas: the use of micromechanics to predict thermoelastic properties, theoretical aspects of fracture behavior, and reliability analysis. Author

N88-22411*# Cleveland State Univ., Ohio.
CONTINUOUS FIBER CERAMIC MATRIX COMPOSITES FOR HEAT ENGINE COMPONENTS **c27**
David E. Tripp *In* NASA. Lewis Research Center, Lewis Structures Technology, 1988. Volume 3: Structural Integrity Fatigue and Fracture Wind Turbines HOST May 1988 p 41-61 (For primary document see N88-22408 15-39)
(Contract NCC3-81)
Avail: NTIS HC A16/MF A01 CSCL 11B

High strength at elevated temperatures, low density, resistance to wear, and abundance of nonstrategic raw materials make structural ceramics attractive for advanced heat engine applications. Unfortunately, ceramics have a low fracture toughness and fail catastrophically because of overload, impact, and contact stresses. Ceramic matrix composites provide the means to achieve improved fracture toughness while retaining desirable characteristics, such as high strength and low density. Materials scientists and engineers are trying to develop the ideal fibers and matrices to achieve the optimum ceramic matrix composite properties. A need exists for the development of failure models for the design of ceramic matrix composite heat engine components. Phenomenological failure models are currently the most frequently used in industry, but they are deterministic and do not adequately describe ceramic matrix composite behavior. Semi-empirical models were proposed, which relate the failure of notched composite laminates to the stress a characteristic distance away from the notch. Shear lag models describe composite failure modes at the micromechanics level. The enhanced matrix cracking stress occurs at the same applied stress level predicted by the two models of steady state cracking. Finally, statistical models take into consideration the distribution in composite failure strength. The intent is to develop these models into computer algorithms for the failure analysis of ceramic matrix composites under monotonically increasing loads. The algorithms will be included in a postprocessor to general purpose finite element programs.
Author

N88-22412*# National Aeronautics and Space Administration. Lewis Research Center, Cleveland, Ohio.
NONDESTRUCTIVE EVALUATION BY ACOUSTO-ULTRASONICS **c38**
Harold E. Kautz *In its* Lewis Structures Technology, 1988. Volume 3: Structural Integrity Fatigue and Fracture Wind Turbines HOST May 1988 p 67-77 (For primary document see N88-22408 15-39)
Avail: NTIS HC A16/MF A01 CSCL 14D

Acousto-ultrasonics is an ultrasonic technique that was originally devised to cope with the particular problems associated with nondestructive evaluation (NDE) of fiber/polymer composite structures. The fiber/polymer composites are more attenuating to ultrasound than any other material presently of interest. This limits the applicability of high-frequency ultrasonics. A common use of ultrasound is the imaging of flaws internal to a structure by scattering from the interface with the flaw. However, structural features of composites can scatter ultrasound internally, thus obscuring the flaws. A need relative to composites is to be able to nondestructively measure the strength of laminar boundaries in order to assess the integrity of a structure. Acousto-ultrasonics has exhibited the ability to use the internal scattering to provide information for determining the strength of laminar boundaries. Analysis of acousto-ultrasonic signals by the wave ray paths that compose it leads to waveform partitioning that enhances the sensitivity to mechanical strength parameters. Author

N88-22413*# National Aeronautics and Space Administration. Lewis Research Center, Cleveland, Ohio.
CHARACTERIZATION OF SINTERED SiC BY USING NDE **c38**
George Y. Baaklini *In its* Lewis Structures Technology, 1988. Volume 3: Structural Integrity Fatigue and Fracture Wind Turbines HOST May 1988 p 79-91 (For primary document see N88-22408 15-39)
Avail: NTIS HC A16/MF A01 CSCL 14D

Capabilities of projection microfocus X-radiography and of ultrasonic velocity and attenuation for characterizing silicon carbide specimens were assessed. Silicon carbide batches covered a range of densities and different microstructural characteristics. Room-temperature, four-point flexural strength tests were conducted. Fractography was used to identify types, sizes, and locations of fracture origins. Fracture toughness values were calculated from fracture strength and flaw characterization data. Detection capabilities of radiography for fracture-causing flaws were evaluated. Applicability of ultrasonics for verifying material strength and toughness was examined. Radiography proved useful in detecting high-density inclusions and isolated voids, but failed in detecting surface and subsurface agglomerates and large grains as fracture origins. Ultrasonic velocity dependency on density was evident. Attenuation dependency on density and mean pore size was clearly demonstrated. Understanding attenuation as a function of toughness was limited by shortcomings in K sub IC determination. Author

N88-22414*# National Aeronautics and Space Administration. Lewis Research Center, Cleveland, Ohio.
SYSTEMS FOR ULTRASONIC SCANNING, ANALYSIS AND IMAGERY **c38**
David B. Stang, Edward R. Generazio, and Steve Abe (Cleveland State Univ., Ohio.) *In its* Lewis Structures Technology, 1988. Volume 3: Structural Integrity Fatigue and Fracture Wind Turbines HOST May 1988 p 93-105 (For primary document see N88-22408 15-39)
(Contracts NAS3-2410S; NCC3-24)
Avail: NTIS HC A16/MF A01 CSCL 14D

A variety of ultrasonic scanning and imagery techniques are used to investigate various aspects of materials and microstructures. Two ultrasonic scanning systems are in use by the Lewis Research Center's Structural Integrity Branch: an immersion scanner and a contact scanning system. The basic principles of scanning are reviewed, examples of images are presented, and structural features suggested by these images are discussed. Both of these systems are custom designed; their capabilities, advantages, and disadvantages are highlighted.
Author

N88-22415*# National Aeronautics and Space Administration. Lewis Research Center, Cleveland, Ohio.
FLAW CHARACTERIZATION IN STRUCTURAL CERAMICS USING SCANNING LASER ACOUSTIC MICROSCOPY **c38**

Don J. Roth *In its* Lewis Structures Technology, 1988. Volume 3: Structural Integrity Fatigue and Fracture Wind Turbines HOST May 1988 p 107-122 (For primary document see N88-22408 15-39)
Avail: NTIS HC A16/MF A01 CSCL 14D

The ability of scanning laser acoustic microscopy (SLAM) to characterize artifically seeded voids in sintered silicon nitride structural ceramic specimens was investigated. The voids ranged from 20 to 430 microns in diameter and were embedded up to 2 mm beneath the surface of the specimens. Probability of detection was determined as a function of void depth and size. Trigonometric relationships and Airy's diffraction theory were used to obtain predictions of void depth and size from acoustic diffraction patterns produced by the voids. Agreement was observed between actual and predicted void depths. However, predicted void diameters were generally much greater than actual diameters. Precise diameter predictions are difficult to obtain because of measurement uncertainty and the limitations of the 100 MHz SLAM applied to typical ceramic specimens. Author

N88-22416*# National Aeronautics and Space Administration. Lewis Research Center, Cleveland, Ohio.
NONDESTRUCTIVE EVALUATION OF SINTERED CERAMICS
c38
George Y. Baaklini, Stanley J. Klima, and William A. Sanders *In its* Lewis Structures Technology, 1988. Volume 3: Structural Integrity Fatigue and Fracture Wind Turbines HOST May 1988 p 123-133 (For primary document see N88-22408 15-39)
Avail: NTIS HC A16/MF A01 CSCL 14D

Radiography and several acoustic and thermoacoustic microscopy techniques are investigated for application to structural ceramics for advanced heat engines. A comparison is made of the results obtained from the use of scanning acoustic microscopy (SAM), scanning laser acoustic microscopy (SLAM), and thermoacoustic microscopy (TAM). These techniques are evaluated on research samples of green and sintered monolithic silicon nitrides and silicon carbides in the form of modulus-of-rupture (MOR) bars containing deliberately introduced flaws. Strengths and limitations of the techniques are described, with the emphasis being on statistics of detectability of flaws that constitute potential fracture origins. Further, it is shown that radiographic evaluation and guidance helped develop uniform high-density Si3N4 MOR bars with improved four-point flexural strength (875, 544, and 462 MPa at room temperature, 1200 C, 1370 C, respectively) and reduced scatter in bend strength. Author

N88-22417*# National Aeronautics and Space Administration. Lewis Research Center, Cleveland, Ohio.
FRACTURE TECHNOLOGY FOR BRITTLE MATERIALS
Jonathan A. Salem *In its* Lewis Structures Technology, 1988. Volume 3: Structural Integrity Fatigue and Fracture Wind Turbines HOST May 1988 p 141-148 (For primary document see N88-22408 15-39)
Avail: NTIS HC A16/MF A01 CSCL 20K

Ceramics materials have the potential for use in high-temperature, fuel-efficient engines. However, because these materials are brittle, their fracture characteristics must be well documented prior to their application. Thus Lewis is working to understand the fracture and strength properties of brittle ceramic and ceramic matrix materials. An understanding of fracture properties aids both designers who are attempting to design high-temperature structures and materials scientists who seek to design more temperature-resistant materials. Both analytical and experimental approaches to fracture analysis are being taken. Methods for testing fracture toughness, crack growth resistance, and strength are being developed. The failure mechanisms at both room and elevated temperatures are also being investigated. Such investigations aid materials scientists in developing better high-temperature materials. Of concern is the anisotropy of ceramic materials and the experimental verification of ceramic design codes that will allow brittle material behavior to be accurately predicted at high temperature. Author

N88-22418*# National Aeronautics and Space Administration. Lewis Research Center, Cleveland, Ohio.
MODE 2 FRACTURE MECHANICS
Robert J. Buzzard and Louis Ghosn (Cleveland State Univ., Ohio.) *In its* Lewis Structures Technology, 1988. Volume 3: Structural Integrity Fatigue and Fracture Wind Turbines HOST May 1988 p 149-159 (For primary document see N88-22408 15-39)
(Contract NCC3-46)
Avail: NTIS HC A16/MF A01 CSCL 20K

Current development of high-performance rolling element bearings for aircraft engines (up to 3 million DN, where DN is the product of shaft diameter in millimeters and speed in revolutions per minute) has aroused concern about fatigue crack growth in the inner bearing race that leads to catastrophic failure of the bearing and the engine. A failure sequence was postulated by Srawley, and an analytical program was undertaken to simulate fatigue crack propagation in the inner raceway of such a bearing. A fatigue specimen was developed at NASA by which fatigue data may be obtained relative to the cracking problems. The specimen may be used to obtain either mode 2 data alone or a combination of mixed-mode (1 and 2) data as well and was calibrated in this regard. Mixed-mode fracture data for M-50 bearing steel are presented, and a method for performing reversed-loading tests is described. Author

N88-22419*# National Aeronautics and Space Administration. Lewis Research Center, Cleveland, Ohio.
IN SITU FATIGUE LOADING STAGE INSIDE SCANNING ELECTRON MICROSCOPE
Jack Telesman, Peter Kantzos, and David Brewer (Army Propulsion Lab., Cleveland, Ohio.) *In its* Lewis Structures Technology, 1988. Volume 3: Structural Integrity Fatigue and Fracture Wind Turbines HOST May 1988 p 161-172 (For primary document see N88-22408 15-39)
Avail: NTIS HC A16/MF A01 CSCL 20K

A fatigue loading stage inside a scanning electron microscopy (SEM) was developed. The stage allows dynamic and static high-magnification and high-resolution viewing of the fatigue crack initiation and crack propagation processes. The loading stage is controlled by a closed-loop servohydraulic system. Maximum load is 1000 lb (4450 N) with test frequencies ranging up to 30 Hz. The stage accommodates specimens up to 2 inches (50 mm) in length and tolerates substantial specimen translation to view the propagating crack. At room temperature, acceptable working resolution is obtainable for magnifications ranging up to 10,000X. The system is equipped with a high-temperature setup designed for temperatures up to 2000 F (1100 C). The signal can be videotaped for further analysis of the pertinent fatigue damage mechanisms. The design allows for quick and easy interchange and conversion of the SEM from a loading stage configuration to its normal operational configuration and vice versa. Tests are performed entirely in the in-situ mode. In contrast to other designs, the NASA design has greatly extended the life of the loading stage by not exposing the bellows to cyclic loading. The loading stage was used to investigate the fatigue crack growth mechanisms in the (100)-oriented PWA 1480 single-crystal, nickel-based supperalloy. The high-magnification observations revealed the details of the crack growth processes. Author

N88-22420*# Syracuse Univ., N. Y.
GRAIN BOUNDARY OXIDATION AND LOW-CYCLE FATIGUE AT ELEVATED TEMPERATURES
H. W. Liu and Y. Oshida *In* NASA. Lewis Research Center, Lewis Structures Technology, 1988. Volume 3: Structural Integrity Fatigue and Fracture Wind Turbines HOST May 1988 p 173-185 (For primary document see N88-22408 15-39)
(Grant NAG3-348)
Avail: NTIS HC A16/MF A01 CSCL 20K

Fatigue life consists of fatigue crack nucleation and propagation periods. In order to predict fatigue life accurately, a methodology for the quantitative assessment of these two fatigue damage processes had to be devised. Grain boundary oxidation penetrates faster than does oxidation within a grain. This faster oxidation

penetration causes intergranular fatigue failures at elevated temperatures. Grain boundary oxidation accelerates both crack nucleation and propagation. Grain boundary oxidation kinetics and the statistical distribution of grain boundary oxide penetration depth were measured. Quantitative applications of the grain boundary oxidation kinetics to fatigue crack nucleation and propagation were analyzed. A method, based on the Weibull distribution, of extrapolating the laboratory oxidation data measured with small samples to large engineering structures is presented. Author

N88-22421*# General Electric Co., Evendale, Ohio.
ELEVATED TEMPERATURE CRACK GROWTH
K. S. Kim, R. H. VanStone, S. N. Malik, and J. H. Laflen *In* NASA. Lewis Research Center, Lewis Structures Technology, 1988. Volume 3: Structural Integrity Fatigue and Fracture Wind Turbines HOST May 1988 p 187-198 (For primary document see N88-22408 15-39)
(Contract NAS3-23940)
Avail: NTIS HC A16/MF A01 CSCL 20K

The problem of crack growth in hot path components such as combustor liners is complicated by several practical and theoretical considerations. The loading environment of such components involves high temperature levels and gradients that lead to considerations such as thermal stresses, crack closure, hold time, inelastic strains (both time dependent and independent), and Thermal Mechanical Fatigue (TMF). In general, a good understanding of the influence of these factors on crack growth was not obtained. At the same time, several nonlinear fracture mechanics parameters were suggested for such applications; however, most of the proposed methods were not tested for broad applications such as required for hot section components. It was the purpose of this program to evaluate proposed nonlinear methods by performing a thorough experimental and analytical study. The results illustrated that much progress was made in developing nonlinear methods. Author

N88-22422*# National Aeronautics and Space Administration. Lewis Research Center, Cleveland, Ohio.
CUMULATIVE FATIGUE DAMAGE MODELS
Michael A. McGaw *In its* Lewis Structures Technology, 1988. Volume 3: Structural Integrity Fatigue and Fracture Wind Turbines HOST May 1988 p 201-212 (For primary document see N88-22408 15-39)
Avail: NTIS HC A16/MF A01 CSCL 20K

The problem of calculating expected component life under fatigue loading conditions is complicated by the fact that component loading histories contain, in many cases, cyclic loads of widely varying amplitudes. In such a case a cumulative damage model is required, in addition to a fatigue damage criterion, or life relationship, in order to compute the expected fatigue life. The traditional cumulative damage model used in design is the linear damage rule. This model, while being simple to use, can yield grossly unconservative results under certain loading conditions. Research at the NASA Lewis Research Center has led to the development of a nonlinear cumulative damage model, named the double damage curve approach (DDCA), that has greatly improved predictive capability. This model, which considers the life (or loading) level dependence of damage evolution, was applied successfully to two polycrystalline materials, 316 stainless steel and Haynes 188. The cumulative fatigue behavior of the PWA 1480 single-crystal material is currently being measured to determine the applicability of the DDCA for this material. Author

N88-22423*# Illinois Univ., Urbana-Champaign. Dept. of Mechanical and Industrial Engineering.
FATIGUE DAMAGE MAPPING
Darrell Socie *In* NASA. Lewis Research Center, Lewis Structures Technology, 1988. Volume 3: Structural Integrity Fatigue and Fracture Wind Turbines HOST May 1988 p 213-220 (For primary document see N88-22408 15-39)
(Grant NAG3-465)
Avail: NTIS HC A16/MF A01 CSCL 20K

Observations of fatigue crack nucleation and early growth are presented. The state of stress/strain was shown to play a significant role in this process. Early growth occurs on planes experiencing the largest range of shear strain (Mode 2) or normal strain (Mode 1) depending on the stress state, strain amplitude, and microstructure. These observations were summarized in a fatigue map for each material. These maps provide regions where one fatigue failure mode dominates the behavior. Each failure mechanism results in a different failure mode. Once the expected failure mode is identified, bulk deformation models based on the cyclic stresses and strains can be used to obtain reliable estimates of fatigue lives for complex loading situations. Author

N88-22424*# National Aeronautics and Space Administration. Lewis Research Center, Cleveland, Ohio.
BITHERMAL FATIGUE: A SIMPLIFIED ALTERNATIVE TO THERMOMECHANICAL FATIGUE
Michael J. Verrilli *In its* Lewis Structures Technology, 1988. Volume 3: Structural Integrity Fatigue and Fracture Wind Turbines HOST May 1988 p 221-230 (For primary document see N88-22408 15-39)
Avail: NTIS HC A16/MF A01 CSCL 20K

A bithermal fatigue test technique was proposed as a simplified alternative to the thermomechanical fatigue test. Both the thermomechanical cycle and the bithermal technique can be used to study nonisothermal fatigue behavior. The difference between the two cycles is that in a conventional thermomechanical fatigue cycle the temperature is continuously varied concurrently with the applied mechanical strains, but in the bithermal fatigue cycle the specimen is held at zero load during the temperature excursions and all the loads are applied at the two extreme temperatures of the cycle. Experimentally, the bithermal fatigue test technique offers advantages such as ease in synchronizing the temperature and mechanical strain waveforms, in minimizing temperature gradients in the specimen gauge length, and in reducing and interpreting thermal fatigue such as the influence of alternate high and low temperatures on the cyclic stress-strain response characteristics, the effects of thermal state, and the possibility of introducing high- and low-temperature deformation mechanisms within the same cycle. The bithermal technique was used to study nonisothermal fatigue behavior of alloys such as single-crystal PWA 1480, single-crystal Rene N4, cast B1900+Hf, and wrought Haynes 188. Author

N88-22425*# National Aeronautics and Space Administration. Lewis Research Center, Cleveland, Ohio.
LIFE PREDICTION MODELING BASED ON STRAINRANGE PARTITIONING **c38**
Gary R. Halford *In its* Lewis Structures Technology, 1988. Volume 3: Structural Integrity Fatigue and Fracture Wind Turbines HOST May 1988 p 231-244 (For primary document see N88-22408 15-39)
Avail: NTIS HC A16/MF A01 CSCL 14D

Strainrange partitioning (SRP) is an integrated low-cycle-fatigue life predicting system. It was created specifically for calculating cyclic crack initiation life under severe high-temperature fatigue conditions. The key feature of the SRP system is its recognition of the interacting mechanisms of cyclic inelastic deformation that govern cyclic life at high temperatures. The SRP system bridges the gap between the mechanistic level of understanding that breeds new and better materials and the phenomenological level wherein workable engineering life prediction methods are in great demand. The system was recently expanded to address engineering fatigue problems in the low-strain, long-life, nominally elastic regime. This breakthrough, along with other advances in material behavior and testing technology, has permitted the system to also encompass low-strain thermomechanical loading conditions. Other important refinements of the originally proposed method include procedures for dealing with life-reducing effects of multiaxial loading, ratcheting, mean stresses, nonrepetitive (cumulative loading) loading, and environmental and long-time exposure. Procedure were also developed for partitioning creep and plastic strain and for estimating strainrange versus life relations from tensile and creep rupture properties. Each of the important engineering features of the SRP

system are discussed and examples shown of how they help toward predicting high-temperature fatigue life under practical, although complex, loading conditions. Author

N88-22426*# Pratt and Whitney Aircraft, East Hartford, Conn.
LIFE PREDICTION MODELING BASED ON CYCLIC DAMAGE ACCUMULATION **c38**
Richard S. Nelson *In* NASA. Lewis Research Center, Lewis Structures Technology, 1988. Volume 3: Structural Integrity Fatigue and Fracture Wind Turbines HOST May 1988 p 245-257 (For primary document see N88-22408 15-39)
(Contract NAS3-23288)
Avail: NTIS HC A16/MF A01 CSCL 14D

A high temperature, low cycle fatigue life prediction method was developed. This method, Cyclic Damage Accumulation (CDA), was developed for use in predicting the crack initiation lifetime of gas turbine engine materials, where initiation was defined as a 0.030 inch surface length crack. A principal engineering feature of the CDA method is the minimum data base required for implementation. Model constants can be evaluated through a few simple specimen tests such as monotonic loading and rapic cycle fatigue. The method was expanded to account for the effects on creep-fatigue life of complex loadings such as thermomechanical fatigue, hold periods, waveshapes, mean stresses, multiaxiality, cumulative damage, coatings, and environmental attack. A significant data base was generated on the behavior of the cast nickel-base superalloy B1900+Hf, including hundreds of specimen tests under such loading conditions. This information is being used to refine and extend the CDA life prediction model, which is now nearing completion. The model is also being verified using additional specimen tests on wrought INCO 718, and the final version of the model is expected to be adaptable to most any high-temperature alloy. The model is currently available in the form of equations and related constants. A proposed contract addition will make the model available in the near future in the form of a computer code to potential users. Author

N88-22427*# Pratt and Whitney Aircraft, East Hartford, Conn.
FATIGUE DAMAGE MODELING FOR COATED SINGLE CRYSTAL SUPERALLOYS **c26**
David M. Nissley *In* NASA. Lewis Research Center, Lewis Structures Technology, 1988. Volume 3: Structural Integrity Fatigue and Fracture Wind Turbines HOST May 1988 p 259-270 (For primary document see N88-22408 15-39)
(Contract NAS3-23939)
Avail: NTIS HC A16/MF A01 CSCL 11F

A high temperature, low-cycle fatigue life prediction method for coated single crystal nickel-base superalloys is being developed. The method is being developed for use in predicting crack initiation life of coated single crystal turbine airfoils. Although the models are being developed using coated single crystal PWA 1480, they should be readily adaptable to other coated nickel-base single crystal materials. The coatings choosen for this effort were of two generic types: a low pressure plasma sprayed NiCoCrAlY overlay, designated PWA 286, and an aluminide diffusion, designated PWA 273. In order to predict the useful crack initiation life of airfoils, the constitutive and failure behavior of the coating/substrate combination must be taken into account. Coatings alter the airfoil surface microstructure and are a primary source from which cracks originate. The adopted life prediction approach addresses this complexity by separating the coating and single crystal crack initiation regimes. This provides a flexible means for using different life model formulations for the coating and single crystal materials. At the completion of this program, all constitutive and life model formulations will be available in equation form and as software. The software will use the MARC general purpose finite element code to drive the constitutive models and calculate life parameters. Author

N88-22428*# National Aeronautics and Space Administration. Lewis Research Center, Cleveland, Ohio.
LIFE AND RELIABILITY OF ROTATING DISKS **c38**
Erwin V. Zaretsky, Todd E. Smith, and Richard August (Sverdrup Technology, Inc., Cleveland, Ohio.) *In its* Lewis Structures Technology, 1988. Volume 3: Structural Integrity Fatigue and Fracture Wind Turbines HOST May 1988 p 271-284 (For primary document see N88-22408 15-39)
(Contract NAS3-24105)
Avail: NTIS HC A16/MF A01 CSCL 14D

In aerospace applications, an engineer must be especially cognizant of size and weight constraints which affect design decisions. Although designing at or below the material fatigue limit may be desirable in most industrial applications, in aerospace application it is almost mandatory to design certain components for a finite life at an acceptable probability of survival. Zaretsky outlined such a methodology based in part on the work of W. Weibull (1939, 1951) and G. Lundberg and A. Palmgren (1947a, 1947b, 1952). It is the objective of this work to apply the method of Zaretsky (1987) to statistically predict the life of a generic solid disk with and without bolt holes; determine the effect of disk design variables, thermal loads, and speed on relative life; and develop a generalized equation for determining disk life by incorporating only these variables. Author

N88-22429*# National Aeronautics and Space Administration. Lewis Research Center, Cleveland, Ohio.
LARGE-SCALE WIND TURBINE STRUCTURES **c44**
David A. Spera *In its* Lewis Structures Technology, 1988. Volume 3: Structural Integrity Fatigue and Fracture Wind Turbines HOST May 1988 p 285-297 (For primary document see N88-22408 15-39)
Avail: NTIS HC A16/MF A01 CSCL 10A

The purpose of this presentation is to show how structural technology was applied in the design of modern wind turbines, which were recently brought to an advanced stage of development as sources of renewable power. Wind turbine structures present many difficult problems because they are relatively slender and flexible; subject to vibration and aeroelastic instabilities; acted upon by loads which are often nondeterministic; operated continuously with little maintenance in all weather; and dominated by life-cycle cost considerations. Progress in horizontal-axis wind turbines (HAWT) development was paced by progress in the understanding of structural loads, modeling of structural dynamic response, and designing of innovative structural response. During the past 15 years a series of large HAWTs was developed. This has culminated in the recent completion of the world's largest operating wind turbine, the 3.2 MW Mod-5B power plane installed on the island of Oahu, Hawaii. Some of the applications of structures technology to wind turbine will be illustrated by referring to the Mod-5B design. First, a video overview will be presented to provide familiarization with the Mod-5B project and the important components of the wind turbine system. Next, the structural requirements for large-scale wind turbines will be discussed, emphasizing the difficult fatigue-life requirements. Finally, the procedures used to design the structure will be presented, including the use of the fracture mechanics approach for determining allowable fatigue stresses. Author

N88-22430*# National Aeronautics and Space Administration. Lewis Research Center, Cleveland, Ohio.
RESEARCH SENSORS **c35**
David R. Englund *In its* Lewis Structures Technology, 1988. Volume 3: Structural Integrity Fatigue and Fracture Wind Turbines HOST May 1988 p 323-335 (For primary document see N88-22408 15-39)
Avail: NTIS HC A16/MF A01 CSCL 14B

The work described is part of a program (Englund and Seasholtz, 1988) to develop sensors and sensing techniques for research applications on aircraft turbine engines. In general, the sensors are used to measure the environment at a given location within a turbine engine or to measure the response of an engine component to the imposed environment. Locations of concern are generally in the gas path and, for the most part, are within the hot section. Specific parameters of concern are dynamic gas temperature, heat flux, airfoil surface temperature, and strain on airfoils and combustor liners. To minimize the intrusiveness of surface-mounted sensors,

a considerable effort was expended to develop thin-film sensors for surface temperature, strain, and heat flux measurements. In addition, an optical system for viewing the interior of an operating combustor was developed. Most of the work described is sufficiently advanced that the sensors were used and useful data were obtained. The notable exception is the work to develop a high-temperature static strain measuring capability; the work is still in progress. Author

N88-22431*# National Aeronautics and Space Administration. Lewis Research Center, Cleveland, Ohio.
REVIEW AND ASSESSMENT OF THE HOST TURBINE HEAT TRANSFER PROGRAM **c07**
Herbert J. Gladden *In its* Lewis Structures Technology, 1988. Volume 3: Structural Integrity Fatigue and Fracture Wind Turbines HOST May 1988 p 349-367 (For primary document see N88-22408 15-39)
Avail: NTIS HC A16/MF A01 CSCL 21E

The objectives of the HOST Turbine Heat Transfer subproject were to obtain a better understanding of the physics of the aerothermodynamic phenomena occurring in high-performance gas turbine engines and to assess and improve the analytical methods used to predict the fluid dynamics and heat transfer phenomena. At the time the HOST project was initiated, an across-the-board improvement in turbine design technology was needed. Therefore, a building-block approach was utilized, with research ranging from the study of fundamental phenomena and analytical modeling to experiments in simulated real-engine environments. Experimental research accounted for 75 percent of the project, and analytical efforts accounted for approximately 25 percent. Extensive experimental datasets were created depicting the three-dimensional flow field, high free-stream turbulence, boundary-layer transition, blade tip region heat transfer, film cooling effects in a simulated engine environment, rough-wall cooling enhancement in a rotating passage, and rotor-stator interaction effects. In addition, analytical modeling of these phenomena was initiated using boundary-layer assumptions as well as Navier-Stokes solutions. Author

N88-22432# Lawrence Livermore National Lab., Calif.
THE CONCEPT OF AN IMPACT RESONANCE DIAGRAM FOR CHARACTERIZING THE NONLINEAR RESPONSE OF IMPACT VIBRATION
T. O. Dalrymple Jan. 1988 17 p Presented at the 2nd International Symposium on Transport Phenomena, Dynamics and Design of Rotating Machinery, Honolulu, Hawaii, 3 Apr. 1988
(Contract W-7405-eng-48)
(DE88-005475; UCRL-97240; CONF-880469-1) Avail: NTIS HC A03/MF A01

Due to part tolerances or tolerances that allow for assembly, a closed component assembly may be thought of as a closed system of independent rigid bodies, such as a system of nestled shells where a gap exists between each pair of shells. When the assembly is subjected to vertical forced excitations, such as harmonic or random vibration, the individual components will separate and move independently once the level of excitation has overcome the local gravity field. The separated bodies will move independently of one another until impact occurs, then resume independent motion with new initial velocities until the next impact, etc. By defining resonance for a closed impacting system as being the region of harmonic driving frequency and magnitude that causes the most severe impacting we are well on the way to constructing a resonance diagram for that system. Thus, the impact resonance diagram is a graphical tool that consists of plotting the response of an impacting system in terms of impact severity against the two independent variables of excitation frequency and excitation magnitude. The purpose of the impact resonance diagram is to have a graphical tool to quickly identify regions of excitation frequency and magnitude that will be detrimental to the system. DOE

N88-22433# Sandia National Labs., Albuquerque, N. Mex.
OSCILLATION DAMPED MOVEMENT OF SUSPENDED OBJECTS
J. F. Jones and B. J. Petterson 1988 7 p Presented at the IEEE International Conference on Robotics and Automation, Philadelphia, Pa., 25 Apr. 1988
(Contract DE-AC04-76DP-00789)
(DE88-005715; SAND-87-2192C; CONF-880424-9) Avail: NTIS HC A02/MF A01

Transportation of objects using overhead cranes or manipulators can induce pendulum motion of the object. Residual oscillation from transportation typically must be damped or allowed to decay before the next process can take place. By properly programming the acceleration of the transporting device (e.g., crane) an oscillation damped transport and swing free stop is obtainable. This paper reviews the theory associated with oscillation damped trajectories for simply suspended objects and describes a particular implementation using a CIMCORP XR 6100 gantry robot. DOE

N88-22434*# National Aeronautics and Space Administration. Langley Research Center, Hampton, Va.
IMPROVEMENTS TO TILT ROTOR PERFORMANCE THROUGH PASSIVE BLADE TWIST CONTROL
Mark W. Nixon (Army Aviation Systems Command, St. Louis, Mo.) Apr. 1988 11 p
(NASA-TM-100583; NAS 1.15:100583; AVSCOM-TM-88-B-010)
Avail: NTIS HC A03/MF A01 CSCL 20K

A passive blade twist control is presented in which the twist distribution of a tilt rotor blade is elastically changed as a function of rotor speed. The elastic twist deformation is used to achieve two different blade twist distributions corresponding to the two rotor speeds used on conventional tilt rotors in hover and forward flight. By changing the blade twist distribution, the aerodynamic performance can be improved in both modes of flight. The concept presented obtains a change in twist distribution with extension-twist-coupled composite blade structure. This investigation first determines the linear twists which are optimum for each flight mode. Based on the optimum linear twist distributions, three extension-twist-coupled blade designs are developed using coupled-beam and laminate analyses integrated with an optimization analysis. The designs are optimized for maximum twist deformation subject to material strength limitations. The aerodynamic performances of the final designs are determined which show that the passive blade twist control concept is viable, and can enhance conventional tilt rotor performance. Author

N88-22435*# National Aeronautics and Space Administration. Langley Research Center, Hampton, Va.
COUPLED BENDING-TORSION STEADY-STATE RESPONSE OF PRETWISTED, NONUNIFORM ROTATING BEAMS USING A TRANSFER-MATRIX METHOD
Carl E. Gray, Jr. Mar. 1988 98 p
(NASA-TM-100596; NAS 1.15:100596) Avail: NTIS HC A05/MF A01 CSCL 20K

Using the Newtonian method, the equations of motion are developed for the coupled bending-torsion steady-state response of beams rotating at constant angular velocity in a fixed plane. The resulting equations are valid to first order strain-displacement relationships for a long beam with all other nonlinear terms retained. In addition, the equations are valid for beams with the mass centroidal axis offset (eccentric) from the elastic axis, nonuniform mass and section properties, and variable twist. The solution of these coupled, nonlinear, nonhomogeneous, differential equations is obtained by modifying a Hunter linear second-order transfer-matrix solution procedure to solve the nonlinear differential equations and programming the solution for a desk-top personal computer. The modified transfer-matrix method was verified by comparing the solution for a rotating beam with a geometric, nonlinear, finite-element computer code solution; and for a simple rotating beam problem, the modified method demonstrated a significant advantage over the finite-element solution in accuracy, ease of solution, and actual computer processing time required to effect a solution. Author

N88-22436# Technische Hogeschool, Eindhoven (Netherlands).
EXPERIMENTAL DESIGN AND STRUCTURAL OPTIMIZATION Ph.D. Thesis
A. J. G. Schoofs 1987 153 p
(PB88-169255; ISBN-90-71382-19-2) Avail: NTIS HC A08/MF A01 CSCL 20K

Structural optimization problems are almost always essentially nonlinear, demanding an iterative solution method; the structure is analyzed and, subsequently, improved values for the design variables are estimated. The process is repeated until, in general, a local optimum has been achieved. Here, the author's main interest is the final result; afterwards, the intermediate iteration steps are of little importance. GRA

N88-22437# Edgerton, Germeshausen and Grier, Inc., Idaho Falls, Idaho.
MEASUREMENT OF THE ELASTIC-PLASTIC SURFACE FLAW BACK SURFACE TOPOLOGY AND ITS RELATION TO CONSTRAINT
J. S. Epstein, W. R. Lloyd, and W. G. Reuter 1987 9 p Presented at the SPIE International Conference on Photomechanics and Speckle Metrology, San Diego, Calif., 17 Aug. 1987
(Contract DE-AC07-76ID-01570)
(DE88-006765; EGG-M-02287; CONF-8708213-3) Avail: NTIS HC A02/MF A01

This investigation concerns the identification of physical conditions by which the transition from constrained elastic-plastic fracture to unconstrained fully plastic fracture occurs. The geometry under investigation is the surface flaw under tension in ASTM A-710 steel. Two physical aspects associated with surface flaw constraint will be discussed: first, the out-of-plane back surface dimple and second, the in-plane back surface displacement. Shadow moire is used to map the out-of-plane displacements. Amplitude moire is used to map in-plane displacements. DOE

N88-22438*# National Aeronautics and Space Administration. Langley Research Center, Hampton, Va.
THERMAL STRESS IN HIGH TEMPERATURE CYLINDRICAL FASTENERS
Max L. Blosser May 1988 13 p Presented at the 29th SDM Conference, Williamsburg, Va., 18-22 Apr. 1988
(NASA-TM-100611; NAS 1.15:100611) Avail: NTIS HC A03/MF A01 CSCL 20K

Uninsulated structures fabricated from carbon or silicon-based materials, which are allowed to become hot during flight, are attractive for the design of some components of hypersonic vehicles. They have the potential to reduce weight and increase vehicle efficiency. Because of manufacturing contraints, these structures will consist of parts which must be fastened together. The thermal expansion mismatch between conventional metal fasteners and carbon or silicon-based structural materials may make it difficult to design a structural joint which is tight over the operational temperature range without exceeding allowable stress limits. In this study, algebraic, closed-form solutions for calculating the thermal stresses resulting from radial thermal expansion mismatch around a cylindrical fastener are developed. These solutions permit a designer to quickly evaluate many combinations of materials for the fastener and the structure. Using the algebraic equations developed, material properties and joint geometry were varied to determine their effect on thermal stresses. Finite element analyses were used to verify that the closed-form solutions derived give the correct thermal stress distribution around a cylindrical fastener and to investigate the effect of some of the simplifying assumptions made in developing the closed-form solutions for thermal stresses. Author

N88-22439*# National Aeronautics and Space Administration. Langley Research Center, Hampton, Va.
THE ANALYSIS OF NON-LINEAR DYNAMIC BEHAVIOR (INCLUDING SNAP-THROUGH) OF POSTBUCKLED PLATES BY SIMPLE ANALYTICAL SOLUTION
C. F. Ng Apr. 1988 31 p Presented at the Symposium on Non-Linear Vibrations, Stability and Dynamics of Structures and Mechanisms, Blacksburg, Va., 23-25 Mar. 1987
(NASA-TM-89165; NAS 1.15:89165) Avail: NTIS HC A03/MF A01 CSCL 20K

Static postbuckling and nonlinear dynamic analysis of plates are usually accomplished by multimode analyses, although the methods are complicated and do not give straightforward understanding of the nonlinear behavior. Assuming single-mode transverse displacement, a simple formula is derived for the transverse load displacement relationship of a plate under in-plane compression. The formula is used to derive a simple analytical expression for the static postbuckling displacement and nonlinear dynamic responses of postbuckled plates under sinusoidal or random excitation. Regions with softening and hardening spring behavior are identified. Also, the highly nonlinear motion of snap-through and its effects on the overall dynamic response can be easily interpreted using the single-mode formula. Theoretical results are compared with experimental results obtained using a buckled aluminum panel, using discrete frequency and broadband point excitation. Some important effects of the snap-through motion on the dynamic response of the postbuckled plates are found. Author

N88-22440# California Univ., San Diego, La Jolla. Dept. of Applied Mechanics and Engineering Sciences.
PHENOMENOLOGICAL MODELLING OF RATE-DEPENDENT PLASTICITY FOR HIGH STRAIN RATE PROBLEMS
D. T. Chung, S. Nemat-Nasser, and L. M. Taylor 14 Jan. 1988 5 p Presented at the International Conference on Computational Engineering Science, Atlanta, Ga., 10 Apr. 1988 Prepared in cooperation with Sandia National Labs., Albuquerque, N. Mex.
(Contract DE-AC04-76DP-00789)
(DE88-006647; SAND-88-0240C; CONF-880438-5) Avail: NTIS HC A02/MF A01

The results of two related theoretical investigations for large-scale computations of elasto-plastic deformations at ultrahigh strain rates are summarized in this paper. The first effort concerns the development of a phenomenological constitutive model for finite deformation elastoplasticity which includes the effects of thermal softening, strain hardening and rate-dependency, and the incorporation of this model in the large-scale explicit finite-element code PRONTO 2D. The second effort involves the investigation of localized deformations and shear banding at high strain rates. It is shown that the constitutive model considered, together with standard quadrilateral finite elements with one point integration (piece-wise constant strain and stress fields), can nicely produce the observed intense localized deformations without recourse to any special elements. The results are illustrated in terms of the shear localization observed in uniaxial extension and the void collapse in uniaxial compression. In addition, the effect of noncoaxiality of the plastic strain rate and the stress tensor is included in the model, and its influence on strain localization at high strain rates is investigated. DOE

N88-22441# Fraunhofer Inst. fuer Werkstoffmechanik, Freiburg (West Germany).
PROCESSING DEFECTS AND STRENGTH OF ALUMINA SUBSTRATES
Wilma Berweiler, James R. Varner, Hermann Riedel, Friedrich Harbach, and Ludwig Weiler (Brown, Boveri und Cie, A.G., Heidelberg, West Germany) Sep. 1987 25 p Presented at the International Symposium on Ceramic Substrates and Packages, Denver, Colo., 18-21 Oct. 1987
(Contract BMFT-03-M-2008-5)
(W-10/87; ETN-88-92101) Avail: NTIS HC A03/MF A01

Two sets of commercial alpha-alumina plates with a mean grain size of 1 to 2 microns were tested using the concentric-ring test. All specimens were taken from the same batch of material. The two sets of specimens had different plate diameters such that for the smaller of the specimens, linear plate bending theory was applicable, while the larger ones experienced so large deflections that geometric nonlinearities reduced the local stresses by 30 percent. The parameters of the Weibull distribution including their confidence intervals were evaluated. Fractographic examinations

helped to identify the fracture origins with great certainty. This knowledge can be used to optimize the materials by avoiding the introduction of critical defects during processing. The strengths of the specimens are related to the sizes of their critical defects by a fracture-mechanical relation. ESA

N88-22442# Aeronautical Research Inst. of Sweden, Stockholm. Structures Dept.
INCREASING STRENGTH OF GRAPHITE/EPOXY BOLTED JOINTS BY INTRODUCING AN ADHESIVELY BONDED METALLIC INSERT
Soren Nilsson Oct. 1987 20 p Sponsored by the Swedish Material Administration of the Armed Forces Air Material Dept.
(FFA-TN-1987-45; ETN-88-92198) Avail: NTIS HC A03/MF A01

A method to increase the failure load in graphite/epoxy bolted joints where the failure mode is bearing strength is proposed by bonding a metallic insert in the hole. In order to design test specimens with significantly reduced compressive stresses at the hole boundary, finite element (FE) analyses were performed. The FE-analyses reveal the possibility to reduce the compressive stresses at the hole boundary in quasi-isotropic laminate by 50 percent, if a 10 mm hole is enlarged to 14 mm and a 2 mm thick metallic insert is adhesively bonded in the hole. Experiment results show an increase in failure load of up to 55 percent when using an aluminum insert and of 30 percent when using steel insert, the steel insert also giving a 13 percent stiffer joint. The adhesively bonded insert alters the failure mode to failure in the adhesive combined with net tension failure of the composite member. Studies of FE-results explain the difference in failure load when using a steel or aluminum insert respectively by the fact that the stiffer steel insert causes higher tension stresses in the adhesive, which lead to a primary tension failure in the adhesive. ESA

N88-22443# Technical Research Centre of Finland, Espoo. Metals Lab.
SPECTRUM FATIGUE TESTING FOR MATERIALS CHARACTERIZATION
Jussi Solin Oct. 1987 34 p Sponsored by the Finnish Federation of Metal and Engineering Industries; the Finnish Industry; Technical Research Centre of Finland, Espoo, Finland; the Lappeenranta Univ. of Tech., Finland; and the Nordic Industry Foundation
(VTT-RR-502; ISBN-9-51-382988-X; ISSN-0358-5077; ETN-88-92214) Avail: NTIS HC A03/MF A01; Government Printing Center, P.O. Box 516, SF-00101 Helsinki, Finland, 40 finmarks

An algorithm for calculation of an equivalent constant amplitude loading is proposed. The derivation of the applicable equations is presented. The developed analysis methods give realistic results closely comparable to the constant amplitude test results. The proposed equivalent loading parameters are physically justified and represent the weighted average amplitudes or ranges. The virtual fatigue damages per cycle are used as weight factors when making the average. Improvement in the respect that more complex fatigue equations can be treated is achieved. ESA

N88-22444# Technical Research Centre of Finland, Espoo. Metals Lab.
A SIMPLIFIED KEY-CURVE APPROACH FOR J-R-CURVE TESTING OF CT SPECIMENS
Kim Wallin Oct. 1987 26 p Sponsored by the Finnish Ministry of Trade and Industry
(VTT-RR-503; ISBN-9-51-382645-7; ISSN-0358-5077; ETN-88-92215) Avail: NTIS HC A03/MF A01; Government Printing Center, P.O. Box 516, SF-00101 Helsinki, Finland, 40 finmarks

A key-curve based procedure for crack length measurement on CT-specimens is compared with other testing methods for three different pressure vessel steels. The procedure is shown to yield accurate enough results for normal J-R-curve testing. Causes affecting the accuracy of the method are discussed. ESA

N88-22445*# National Aeronautics and Space Administration. Langley Research Center, Hampton, Va.
STRESS-INTENSITY FACTORS FOR SMALL SURFACE AND CORNER CRACKS IN PLATES
I. S. Raju, S. N. Atluri (Georgia Inst. of Tech., Atlanta.), and J. C. Newman, Jr. Apr. 1988 45 p
(NASA-TM-100599; NAS 1.15:100599) Avail: NTIS HC A03/MF A01 CSCL 20K

Three-dimensional finite-element and finite-alternating methods were used to obtain the stress-intensity factors for small surface and corner cracked plates subjected to remote tension and bending loads. The crack-depth-to-crack-length ratios (a/c) ranged from 0.2 to 1 and the crack-depth-to-plate-thickness ratios (a/t) ranged from 0.05 to 0.2. The performance of the finite-element alternating method was studied on these crack configurations. A study of the computational effort involved in the finite-element alternating method showed that several crack configurations could be analyzed with a single rectangular mesh idealization, whereas the conventional finite-element method requires a different mesh for each configuration. The stress-intensity factors obtained with the finite-element-alternating method agreed well (within 5 percent) with those calculated from the finite-element method with singularity elements. Author

N88-22446*# National Aeronautics and Space Administration. Lewis Research Center, Cleveland, Ohio.
STRUCTURAL DYNAMICS BRANCH RESEARCH AND ACCOMPLISHMENTS FOR FISCAL YEAR 1987
May 1988 34 p
(NASA-TM-100279; E-3920; NAS 1.15:100279) Avail: NTIS HC A03/MF A01 CSCL 20K

This publication contains a collection of fiscal year 1987 research highlights from the Structural Dynamics Branch at NASA Lewis Research Center. Highlights from the branch's four major work areas, Aeroelasticity, Vibration Control, Dynamic Systems, and Computational Structural Methods, are included in the report as well as a complete listing of the FY87 branch publications. Author

N88-22238# Joint Publications Research Service, Arlington, Va.
NUMERICAL AND EXPERIMENTAL RESEARCH ON PROPAGATION OF ELASTIC STRESS WAVES IN CONICAL SHELL UNDER AXIAL IMPULSIVE LOADING Abstract Only
Yuze Chen *In its* JPRS Report: Science and Technology. China 11 Dec. 1987 p 45 Transl. into ENGLISH from Lixue Xuebao (Beijing, Peoples Republic of China), v. 19, no. 2. Mar. 1987 p 146-155 (For primary document see N88-22233 15-31)
Avail: NTIS HC A06/MF A01

N88-22239# Joint Publications Research Service, Arlington, Va.
CUBIC SPLINE SOLUTION OF SYMMETRIC BUCKLING PROBLEMS OF CLAMPED SHALLOW SPHERICAL SHELLS Abstract Only
Shuxian Gu *In its* JPRS Report: Science and Technology. China 11 Dec. 1987 p 46 Transl. into ENGLISH from Lixue Xuebao (Beijing, Peoples Republic of China), v. 19, no. 2, Mar. 1987 p 179-185 (For primary document see N88-22233 15-31)
Avail: NTIS HC A06/MF A01

42 GEOSCIENCES (GENERAL)

No abstracts in this category.

43 EARTH RESOURCES AND REMOTE SENSING

Includes remote sensing of earth resources by aircraft and spacecraft; photogrammetry; and aerial photography.

For instrumentation see *35 Instrumentation and Photography.*

N88-22447*# Bohan (Walter A.) Co., Park Ridge, Ill.
NIMBUS-7 CZCS. COASTAL ZONE COLOR SCANNER IMAGERY FOR SELECTED COASTAL REGIONS. NORTH AMERICA - EUROPE. SOUTH AMERICA - AFRICA - ANTARCTICA. LEVEL 2 PHOTOGRAPHIC PRODUCT
[1984] 99 p Original contains color illustrations
(Contract NAS5-29079)
(NASA-CR-180755; NAS 1.26:180755) Avail: NTIS HC A05/MF A01 CSCL 08B

The Nimbus-7 Coastal Zone Color Scanner (CZCS) is the first spacecraft instrument devoted to the measurement of ocean color. Although instruments on other satellites have sensed ocean color, their spectral bands, spatial resolution, and dynamic range were optimized for geographical or meteorological use. In the CZCS, every parameter is optimized for use over water to the exclusion of any other type of sensing. The signal-to-noise ratios in the spectral channels sensing reflected solar radiance are higher than those required in the past. These ratios need to be high because the ocean is such a poor reflecting surface that the majority of the signal seen by the reflected energy channels at spacecraft altitudes is backscattered solar radiation from the atmosphere rather than reflected solar energy from the ocean. The CZCS is a conventional multichannel scanning radiometer utilizing a rotating plane mirror at a 45 deg angle to the optic axis of a Cassegrain telescope. The mirror scans 360 deg; however, only 80 deg of data centered on the spacecraft nadir is collected for ocean color measurements. Spatial resolution at spacecraft nadir is 825x825 m with some degradation at the edges of the scan swath. The useful swath width from a spacecraft altitude of 955 km is 1600 km. Author

N88-22448# Environmental Protection Agency, Research Triangle Park, N.C. Atmospheric Sciences Research Lab.
ASSESSMENT OF CROP LOSS FROM AIR POLLUTANTS: METEOROLOGY-ATMOSPHERIC CHEMISTRY AND LONG RANGE TRANSPORT
A. P. Altshuller Dec. 1987 49 p
(PB88-146857; EPA-600/D-87-366) Avail: NTIS HC A03/MF A01 CSCL 02C

The scales of intermediate and longer range transport influencing the atmospheric distribution of O3 are discussed. Atmospheric concentrations of O3 can vary substantially during each day, from day to day, and with the season of the year as well as with geographical location. In contrast to ozone, sulfur dioxide is a primary pollutant. Both the sources of SO2 and its mechanisms of removal can be much different than for ozone. Sulfur dioxide exposures tend to be of concern on a local rather than a regional scale. Author

N88-22449# Massachusetts Inst. of Tech., Cambridge. Artificial Intelligence Lab.
RELATIVE ORIENTATION
Berthold K. Horn Sep. 1987 32 p
(Contracts N00014-85-K-0124; DACA76-85-C-0100)
(AD-A190385; AD-E801598; AI-M-994) Avail: NTIS HC A03/MF A01 CSCL 08B

Before corresponding points in images taken with two cameras can be used to recover distances to objects in a scene, one has to determine the position and orientation of one camera relative to the other. This is the classic photogrammetric problem of relative orientation, central to the interpretation of binocular stereo information. Iterative methods for determining relative orientation were developed long ago; without them we would not have most of the topographic maps we do today. Relative orientation is also of importance in the recovery of motion and shape from an image sequence when successive frames are widely separated in time. Workers in motion vision are rediscovering some of the methods of photogrammetry. Described here is a particularly simple iterative scheme of recovering relative orientation that, unlike existing methods, does not require a good initial guess for the baseline and the rotation. The data required is a set of pairs of corresponding rays from the two projection centers to points in the scene. It is well known that at least five pairs of rays are needed. Less appears to be known about the existence of multiple solutions and their interpretation. These issues are discussed here in detail. GRA

N88-22450# Northwest Research Associates, Inc., Bellevue, Wash.
GEOMETRIC RESTORATION OF SATELLITE IMAGE DATA Scientific Report No. 3, 20 Feb. - 30 Sep. 1987
R. D. Lucas and Robert E. Robins 15 Oct. 1987 31 p
(Contract F19628-87-C-0003)
(AD-A190462; NWRA-CR-R019; AFGL-TR-87-0270) Avail: NTIS HC A03/MF A01 CSCL 08B

We describe an approach for projecting satellite image data onto arbitrary map coordinates. This transformation removes distortions caused by the basic geometry of cross-track scanners and by spacecraft pitch, roll, and yaw. Geometrically restored images are useful for morphological analyses and correlative studies involving concurrent data from multiple sensors. It is possible, for example, to present AIRS passes from distinct receivers, all-sky camera images, radar data, and other relevant spatial measurements on one map in geographic coordinates. Out approach is rigorous in that arbitrary satellite motions are accounted for and exact principles of geometry are used throughout. The floating-point intensive geometry calculations are performed on an arbitrary (adjustable) reference grid, which can be coarse for quick-look purposes, or fine for highest accuracy. Concurrent images for distinct wavelengths can be efficiently projected without redundant geometry calculations. An IBM PC/AT compatible implementation for Polar BEAR AIRS image data is described. Results are presented for two data sets representing moderate and severe platform motions. GRA

N88-22451# Northwest Research Associates, Inc., Bellevue, Wash.
SATELLITE UV IMAGE PROCESSING Scientific Report No. 4, 1 Jul. - 10 Sep. 1987
Norman Rosenberg 9 Oct. 1987 56 p
(Contract F19628-87-C-0003)
(AD-A190466; NWRA-CR-87-R016; AFGL-TR-87-0271) Avail: NTIS HC A04/MF A01 CSCL 17E

The overall objective of the computer program is the photometric and geometric processing of UV satellite images. The data source is the AIRS scanning UV spectrometer aboard the POLAR BEAR satellite. The processing is designed to provide geographic-mapped images which describe the spatial and temporal variability of airglow and aurora of emitting species. The AIRS data stream provided simultaneous records from 3 detectors received at several ground stations from several passes per day. These total about 1500 useful images from launch to Feb. 1987. The major progress during the report period has been development of programs to accomplish the following: (1) Statistical filtering of low-count images to provide meaningful brightness estimates; (2) Use of observed limb locations to provide attitude correction in daylit images and attitude estimation in night images to provide accurate ground positions; (3) Normalization of airglow based on column path length and solar flux which allows separation of aurora from airglow portions of the images; (4) Multi-band presentation of auroral features which clearly define differences between the location of emitting species. GRA

N88-22452*# Alabama A & M Univ., Huntsville. Center for Application of Remote Sensing.
DEVELOPMENT OF REMOTE SENSING TECHNIQUES CAPABLE OF DELINEATING SOILS AS AN AID TO SOIL SURVEY Final Report, 1 Oct. 1984 - 1 Mar. 1986
T. L. Coleman and O. L. Montgomery 12 Apr. 1988 28 p

(Grant NAG13-3)
(NASA-CR-182610; NAS 1.26:182610; ACARS-123187) Avail: NTIS HC A03/MF A01 CSCL 08M

Eighty-one benchmark soils from Alabama, Georgia, Florida, Tennessee, and Mississippi were evaluated to determine the feasibility of spectrally differentiating among soil categories. Relationships among spectral properties that occur between soils and within soils were examined, using discriminant analysis. Soil spectral data were obtained from air-dried samples using an Exotech Model 20C field spectroradiometer (0.37 to 2.36 microns). Differentiating among the orders, suborders, great groups, and subgroups using reflectance spectra achieved varying percentages of accuracy. Six distinct reflectance curve forms were developed from the air-dried samples based on the shape and presence or absence of adsorption bands. Iron oxide and organic matter content were the dominant soil parameters affecting the spectral characteristics for differentiating among and between these soils. Author

N88-22453# Instituto de Pesquisas Espaciais, Sao Jose dos Campos (Brazil).
UPDATING OF THE MUNICIPAL OFFICIAL REGISTER OF REAL ESTATE THROUGH A GEOGRAPHICAL INFORMATION SYSTEM [ATUALIZACAO DO CADASTRO IMOBILIARIO MUNICIPAL ATRAVES DE UM SISTEMA DE INFORMACOES GEOGRAFICAS]
Adriana Abrahao and Moacir GodoyJunior Dec. 1987 18 p In PORTUGUESE; ENGLISH summary Presented at the 1st National Meeting on Applied Remote Sensing for Municipal Planning, 22-23 Oct. 1987
(INPE-4459-PRE/1238) Avail: NTIS HC A03/MF A01

The objective of this work is to demonstrate the feasibility of automating the municipal land register by using the geographical information system now being developed at INPE. The test area was Jambeiro city located in the Vale do Paraiba region, Sao Paulo state. The pilot program to update maps and taxes were devoloped with the municipal land register in mind. Author

N88-22454# Instituto de Pesquisas Espaciais, Sao Jose dos Campos (Brazil).
METHOD FOR RESTORATION AND RESAMPLING OF TM SENSOR IMAGERY [METODO PARA RESTAURACAO E REAMOSTRAGEM DE IMAGENS DO SENSOR TM]
Leila Maria GarciaFonseca and Nelson DelfinodAvilaMascarenhas Mar. 1988 16 p In PORTUGUESE; ENGLISH summary Presented at the 2nd Latin American Symposium on Remote Sensing, Bogota, Colombia, Nov. 1987
(INPE-4491-PRE/1255) Avail: NTIS HC A03/MF A01

Some results obtained with the restoration for resampling TM images using techniques designed in the Fourier domain and implemented in the spatial domain are presented. The main idea is to obtain a good approximation for the original image over a finer grid, by substituting conventional interpolation techniques by the restoration technique. Therefore, image data with slightly better spatial and radiometric quality than the raw data can be synthesized with the resampling process. The work involves the design of a linear restoration filter with input and output defined on different sampling grids. The filter is designed in the Fourier domain by using the technique of compensation of the transfer function. Subsequently, a linear operator in the spatial domain is derived to be applied in the image restoration process. The restoration filter is applied to resample images from the TM sensor of the LANDSAT-5 on a 15 m sampling grid. These restored images are compared to the images that were resampled with the parametric cubic convolution. The comparison is made in visual terms, through the radiometric profile along on image line, through the difference between the images and through statistical measures, indicating better results with the proposed method. Author

N88-22455# Instituto de Pesquisas Espaciais, Sao Jose dos Campos (Brazil).
PROJECT CODEAMA/FUNCATE (TEST-AREA OF BARREIRINHA-AM): FIELD REPORT
Tomoyuki Ohara, Paulo Roberto Martini, Sergio dosAnjosFerreiraPinto, and Nelio NogueiradoNascimento Mar. 1988 55 p In PORTUGUESE; ENGLISH summary
(INPE-4500-RPE/563) Avail: NTIS HC A04/MF A01

The places studied during the multidisciplinary survey realized in the test-area of Barreirinha - Amazon State (CODEAMA Project), with the purpose of testing the use of MSS/LANDSAT images and checking the accuracy of the information obtained and incorporated in geomorphological and hydrical system (inundation areas) maps, in the scale of 1:100,000 are described. The multidisciplinary survey was carried out from January 30 to February 14, 1985, investigating nearly 360 kilometers of fluvial and/or terrestrial survey, from which 64 places were described. The Appendix presents the map of localization of the places studied, in the scale of 1:250,000, which holds all the studied places. Author

N88-22456# Instituto de Pesquisas Espaciais, Sao Jose dos Campos (Brazil).
COMPARATIVE UTILIZATION OF ANALOG AND DIGITAL PROCESSES IN THE TREATMENT OF MSS-LANDSAT DATA FOR STUDYING THE NATIONAL PARKS OF BRAZIL M.S. Thesis
Joaquim Henrique DuranPinto Oct. 1986 184 p In PORTUGUESE; ENGLISH summary Original contains color illustrations
(INPE-4011-TDL/240) Avail: NTIS HC A09/MF A01

Three MSS-LANDSAT data interpretation methods are presented in a comparative form: visual interpretation using multispectral images of channel 5 and 7 at the 1:250,000 scale; visual interpretation using positive transparencies of the four channels at the 1:3,704,000 scale through a Color Additive Viewer; and digital analysis of compatible computer tapes (CCT) by means of the Image-100 System. The study areas comprise three modules of 400 sq km in the regions of Araguaia, Emas, and Iguacu National Parks. Qualitative, quantitative, and cost evaluations were made in the comparison of the three methods. This work also presents an analysis of land use in the regions around the parks. The results of this comparative study led to the following conclusions: the utilization of the color composite obtained by the Color Additive Viewer presented the best visualization of the classes, with clearly defined limits; visual interpretation through a Color Additive Viewer presented the lowest cost per square kilometer mapped, but it was the most-time consuming; on the other hand, the sophisticated digital analysis was the fastest with the highest cost, and generally, the resulted maps of the three interpretative methods showed that there was no significant differences in terms of area, form, and classes spatial distribution, when compared to ground information. Author

44 ENERGY PRODUCTION AND CONVERSION

Includes specific energy conversion systems, e.g., fuel cells; global sources of energy; geophysical conversion; and windpower.

For related information see also *07 Aircraft Propulsion and Power, 20 Spacecraft Propulsion and Power,* and *28 Propellants and Fuels.*

N88-22457# Sandia National Labs., Albuquerque, N. Mex.
TODAY'S PHOTOVOLTAIC SYSTEMS: AN EVALUATION OF THEIR PERFORMANCE
D. F. Menicucci and A. V. Poore 1987 31 p
(Contract DE-AC04-76DP-00789)
(DE88-006926; SAND-87-2585) Avail: NTIS HC A03/MF A01

Photovoltaic systems offer the potential to provide a viable and important source of energy both for today and tomorrow. A key factor in verifying this potential is assessing the satisfactory field performance of the systems, together with their maintenance cost and requirements. Recognizing this need, the National Photovoltaic Program instituted a systems evaluation group nearly

a decade ago. Since then, numerous systems, large and small, have been evaluated, and industry has used the results to perfect the technology. The result of this government/industry partnership is a photovoltaic system technology of which to be proud. The systems evaluations, results of which are reported, have verified the technical viability of the technology. Long-term operation and maintenance goals set by the national program have been met, certainly an enviable record. DOE

N88-22458*# National Aeronautics and Space Administration. Lewis Research Center, Cleveland, Ohio.
DEVELOPMENT OF AN INTEGRATED HEAT PIPE-THERMAL STORAGE SYSTEM FOR A SOLAR RECEIVER
E. S. Keddy, J. T. Sena, M. A. Merrigan, G. Heidenreich (Sundstrand Advanced Technology Group, Rockford, Ill.), and S. Johnson 1987 10 p Presented at the Thermophysics Conference, San Antonio, Tex., 27 Jun. 1987
(Contract W-7405-eng-36)
(NASA-TM-101099; NAS 1.15:101099; DE88-003153; LA-UR-87-3950; CONF-8706254-1) Avail: NTIS HC A02/MF A01 CSCL 10A

The Organic Rankine Cycle (ORC) Solar Dynamic Power System (SDPS) is one of the candidates for Space Station prime power application. In the low Earth orbit of the Space Station approximately 34 minutes of the 94-minute orbital period is spent in eclipse with no solar energy input to the power system. For this period the SDPS will use thermal energy storage (TES) material to provide a constant power output. An integrated heat-pipe thermal storage receiver system is being developed as part of the ORC-SDPS solar receiver. This system incorporates potassium heat pipe elements to absorb and transfer the solar energy within the receiver cavity. The heat pipes contain the TES canisters within the potassium vapor space with the toluene heater tube used as the condenser region of the heat pipe. During the insolation period of the Earth orbit, solar energy is delivered to the heat pipe in the ORC-SDPS receiver cavity. The heat pipe transforms the non-uniform solar flux incident in the heat pipe surface within the receiver cavity to an essentially uniform flux at the potassium vapor condensation interface in the heat pipe. During solar insolation, part of the thermal energy is delivered to the heater tube and the balance is stored in the TES units. During the eclipse period of the orbit, the balance stored in the TES units is transferred by the potassium vapor to the toluene heater tube. DOE

N88-22459# Department of Energy, Washington, D. C. Assistant Secretary for Conservation and Renewable Energy.
ENERGY FROM THE WIND
Jul. 1987 16 p
(DE88-006897; DOE/CE-0189) Avail: NTIS HC A03/MF A01

This document provides a brief description of the use of wind power. Windmills from the 18th century are described. Modern wind turbines and wind turbine arrays are discussed. Present and future applications of wind power in the U.S. are explained. DOE

N88-22460# Astrosystems International, Inc., Newark, Del. Astro Power Div.
HIGH-EFFICIENCY THIN-FILM SILICON-ON-GaP SOLAR CELL FOR IMPROVED RADIATION RESISTANCE Final Report, Jul. 1986 - Feb. 1987
Jerome S. Culik Sep. 1987 28 p
(Contract F33615-86-C-2658)
(AD-A190268; AFWAL-TR-87-2070) Avail: NTIS HC A03/MF A01 CSCL 10B

The ultimate high efficiency silicon solar cell is a light trapping thin film silicon structure epitaxially grown on an oxide overcoated substrate such as silicon or gallium phosphide (GaP). In addition to high performance, this thin-base silicon device is more tolerant of radiation effects than a thick-base solar cell because this structure is less sensitive to reductions in minority-carrier diffusion length. The oxide overcoating layer, an integral part of this design, will serve as a dielectric back surface reflector leading to light trapping, and it will also eliminate dangling bonds in the overgrown silicon layer, effectively passivating the silicon-oxide interface and reducing back surface recombination. GRA

N88-22461# Sandia National Labs., Albuquerque, N. Mex.
PERFORMANCE EVALUATION OF MOLTEN SALT THERMAL STORAGE SYSTEMS
G. J. Kolb and U. Nikolai Sep. 1987 15 p Presented at the Testing and Measurement in Solar Energy Systems, Denver, Colo., 10 Apr. 1988 Prepared in cooperation with Deutsche Forschungs- und Versuchsanstalt fuer Luft- und Raumfahrt e.V., Cologne, Fed. Republic of Germany
(Contract DE-AC04-76DP-00789)
(DE87-014645; SAND-87-1497C; CONF-880420-1) Avail: NTIS HC A03/MF A01

The molton salt thermal storage system located at the Central Receiver Test Facility (CRTF) was recently subjected to thermal performance tests. The system is composed of a hot storage tank containing molten nitrate salt at a temperature of 1050 F and a cold tank containing 550 F salt with associated valves and controls. It is rated at 7 MWht and was designed and installed by Martin Marietta Corporation in 1982. The results of these tests were used to accomplish four objectives: (1) to compare the current thermal performance of the system with the performance of the system soon after it was installed, (2) to validate a dynamic computer model of the system, (3) to obtain an estimate of an annual system efficiency for a hypothetical commercial scale 1200 MWht system and (4) to compare the performance of the CRTF system with thermal storage systems developed by the European solar community. DOE

N88-22462# Sandia National Labs., Albuquerque, N. Mex.
RECENT ADVANCES IN PHOTOVOLTAIC CONCENTRATOR TECHNOLOGY
A. B. Maish and E. C. Boes 1988 8 p Presented at the 10th Annual American Society of Mechanical Engineers Solar Energy Conference, Denver, Colo., 10 Apr. 1988
(Contract DE-AC04-76DP-00789)
(DE88-003948; SAND-87-3078C; CONF-880457-1) Avail: NTIS HC A02/MF A01

Photovoltaic concentrator technology is experiencing rapid, significant advances in efficiency, cost and reliability, making it a leading candidate to add to the nation's electrical generating capacity in the next decade. This paper reviews the development path being pursued by the Department of Energy program to achieve its near-term energy cost goals and to transfer this technology to the private sector. The paper summarizes the research status of concentrator cells, components, modules and arrays. System reliability is also discussed in the context of a new reliability program. DOE

N88-22463# Los Alamos National Lab., N. Mex.
ADVANCED GEOTHERMAL TECHNOLOGIES
J. T. Whetten, H. D. Murphy, R. J. Hanold, C. W. Myers, and J. C. Dunn 1988 16 p Presented at the 15th Annual Energy Technology Conference and Exposition, Washington, D.C., 17 Feb. 1988 Prepared in cooperation with Sandia National Labs., Albuquerque, N. Mex.
(Contract W-7405-eng-36)
(DE88-004307; LA-UR-87-4125; CONF-880212-4) Avail: NTIS HC A03/MF A01

Research and development in advanced technologies for geothermal energy production continue to increase the energy production options for the Nation. The high-risk investment over the past few years by the U.S. Department of Energy in geopressured, hot dry rock, and magma energy resources is producing new means to lower production costs and to take advantage of these resources. The Nation has far larger and more regionally extensive geothermal resources than heretofore realized. At the end of a short 30-day closed-loop flow test, the manmade hot dry rock reservoir at Fenton Hill, New Mexico was producing 10 MW thermal, and still climbing, proving the technical feasibility of this new technology. The scientific feasibility of magma energy extraction was demonstrated, and new field tests to evaluate this

technology are planned. Analysis and field tests confirm the viability of geopressured-geothermal energy and the prospect that many dry-hole or depleted petroleum wells can be turned into producing geopressured-geothermal wells. Technological advances achieved through hot dry rock, magma, geopressured, and other geothermal research are making these resources and conventional hydrothermal resources more competitive. DOE

N88-22464# Los Alamos National Lab., N. Mex.
RECENT ADVANCES IN SOLID POLYMER ELECTROLYTE FUEL CELL TECHNOLOGY
E. A. Ticianelli, S. Srinivasan, and E. R. Gonzalez 1988 15 p Presented at the 6th Brazilian Symposium on Electrochemistry and Electroanalytical Chemistry, Sao Paulo, Brazil, 1 Apr. 1988 Prepared in cooperation with Sao Paulo Univ., Sao Carlos, Brazil
(Contract W-7405-eng-36)
(DE88-005380; LA-UR-88-100; CONF-880468-1) Avail: NTIS HC A03/MF A01

With methods used to advance solid polymer electrolyte fuel cell technology, we are close to obtaining the goal of 1 A/sq cm at 0.7. Higher power densities have been reported (2 A/sq cm at 0.5 V) but only with high catalyst loading electrodes (2 mg/sq cm and 4 mg/sq cm at anode and cathode, respectively) and using a Dow membrane with a better conductivity and water retention characteristics. Work is in progress to ascertain performances of cells with Dow membrane impregnated electrodes and Dow membrane electrolytes. DOE

N88-22225# Joint Publications Research Service, Arlington, Va.
SOLAR CELL COVER GLASSES FOR SATELLITES
Tokio Kimura *In its* JPRS Report: Science and Technology. Japan 3 Mar. 1988 p 31-37 Transl. into ENGLISH from Ceramics Japan (Tokyo, Japan), Apr. 1987 p 303-308 (For primary document see N88-22218 15-31)
Avail: NTIS HC A05/MF A01

N88-22231# Joint Publications Research Service, Arlington, Va.
OVERVIEW OF 1987 MOONLIGHT PROJECT
In its JPRS Report: Science and Technology. Japan 27 Oct. 1987 p 48-54 Transl. into ENGLISH from Jita Nyusu (Tokyo, Japan), Mar. 1987 p 11-13 (For primary document see N88-22228 15-31)
Avail: NTIS HC A07/MF A01

N88-22429*# National Aeronautics and Space Administration. Lewis Research Center, Cleveland, Ohio.
LARGE-SCALE WIND TURBINE STRUCTURES
David A. Spera *In its* Lewis Structures Technology, 1988. Volume 3: Structural Integrity Fatigue and Fracture Wind Turbines HOST May 1988 p 285-297 (For primary document see N88-22408 15-39)
Avail: NTIS HC A16/MF A01 CSCL 10A

45 ENVIRONMENT POLLUTION

Includes atmospheric, noise, thermal, and water pollution.

N88-22465# Oak Ridge National Lab., Tenn.
ATMOSPHERIC CARBON DIOXIDE AND THE GLOBAL CARBON CYCLE: THE KEY UNCERTAINTIES
T. H. Peng, W. M. Post, D. L. DeAngelis, V. H. Dale, and M. P. Farrell 1987 21 p Presented at the 8th Miami International Conference on Alternative Energy Sources, Miami Beach, Fla., 14 Dec. 1987
(Contract DE-AC05-84OR-21400)
(DE88-005059; CONF-871204-4) Avail: NTIS HC A03

The biogeochemical cycling of carbon between its sources and sinks determines the rate of increase in atmospheric CO2 concentrations. The observed increase in atmospheric CO2 content is less than the estimated release from fossil fuel consumption and deforestation. This discrepancy can be explained by interactions between the atmosphere and other global carbon reservoirs such as the oceans, and the terrestrial biosphere including soils. Undoubtedly, the oceans have been the most important sinks for CO2 produced by man. But, the physical, chemical, and biological processes of oceans are complex and, therefore, credible estimates of CO2 uptake can probably only come from mathematical models. Unfortunately, one- and two-dimensional ocean models do not allow for enough CO2 uptake to accurately account for known releases. Thus, they produce higher concentrations of atmospheric CO2 than was historically the case. More complex three-dimensional models, while currently being developed, may make better use of existing tracer data than do one- and two-dimensional models and will also incorporate climate feedback effects to provide a more realistic view of ocean dynamics and CO2 fluxes. The instability of current models to estimate accurately oceanic uptake of CO2 creates one of the key uncertainties in predictions of atmospheric CO2 increases and climate responses over the next 100 to 200 years. DOE

N88-22466# Dornier-Werke G.m.b.H., Friedrichshafen (West Germany).
FEASIBILITY STUDY FOR A 2ND GENERATION SYSTEM FOR AIRBORNE MARITIME POLLUTION SURVEILLANCE Final Report, 12 Dec. 1987
Joerg Koepp and Josef Schober Bonn, Federal Republic of Germany BMFT 30 Apr. 1987 739 p Partly in ENGLISH and GERMAN Sponsored by BMFT
(ETN-88-92108) Copyright Avail: NTIS HC A99/MF E03

The feasibility of a sensor system for maritime pollution monitoring was established. Operational requirements for a sensor system, the technical description of possible mission equipment, and proposals for an optimal sensor-package are presented. Planning data for development and costs are given. ESA

N88-22467# Lawrence Livermore National Lab., Calif.
A SURVEY OF DENSER-THAN-AIR ATMOSPHERIC DISPERSION MODELS
D. L. Ermak, H. C. Rodean, R. Lange, and S. T. Chan Feb. 1988 49 p
(Contract W-7405-eng-48)
(DE88-006626; UCRL-21024) Avail: NTIS HC A03/MF A01

This survey of denser-than-air atmospheric dispersion models has been conducted by the Lawrence Livermore National Laboratory for the U.S. Air Force Engineering and Services Center, Tyndall AFB as part of their effort to update their atmospheric dispersion modeling capability. The goal of this LLNL study is to identify the more recent denser-than-air atmospheric dispersion models proposed in the literature and to provide brief descriptions of current models. For the purposes of this survey, more recent is defined as the year 1980 and later. Furthermore, we do not describe every model found in this category; rather we consider only those models that appear to have been actively used and further developed during the 1980's and are therefore judged to be current. DOE

N88-22468# Instituto de Pesquisas Espaciais, Sao Jose dos Campos (Brazil).
RADON-222 IN THE ANTARCTIC PENINSULA
Enio B. Pereira, Alberto W. Setzer, and Iracema F. A. Cavalcanti Mar. 1988 15 p Presented at the 2nd Encontro Regional de Geofisica, Salvador, Brazil, 25-27 Nov. 1987, and at the 4th International Symposium on the Natural Radiation Environment, Lisbon, Portugal, 7-11 Dec. 1987
(Contract FINEP-537/CT; Grants CIRM-PROANTAR-9586; CIRM-PROANTAR-9618; CIRM-PROANTAR-9503)
(INPE-4486-PRE/1251) Avail: NTIS HC A03/MF A01

Radon-222 was continuously measured at the Brazilian Antarctic Station (62 deg S, 58 deg W) during 1986. Baseline radon concentration averaged 0.7 pCi/cu m with surges peaking at 15 pCi/cu m. The data exhibited an irregular rhythm of about 25 days and a strong positive association with short term fluctuations of atmospheric temperature. No seasonal variations of radon were observed. Interpretation of the radon surges with reference to synoptic charts and weather satellite pictures showed that the

continental influence of radon at the Antarctic Peninsula is probably very small and comes only from the tip of the southern tip of South America. Author

N88-22469# Instituto de Pesquisas Espaciais, Sao Jose dos Campos (Brazil).
SURFACE CO RESULTS FROM THE ABLE-2B EXPEDITION TO AMAZONIA
V. W. J. H. Kirchhoff and E. V. A. Marinho Mar. 1988 21 p Presented at the Spring AGU Meeting, Baltimore, Md., 16-20 May 1988
(Contract FINEP-537/CT)
(INPE-4501-PRE/1258) Avail: NTIS HC A03/MF A01

The first carbon monoxide (CO) measurements performed directly in the Amazonian rainforests from air samples collected near the surface are presented. The CO mixing ratios from air grab samples were measured several times a day, at several sites, during 36 consecutive days in the Amazonian wet season. A sensitive instrument using chromatographic separation followed by mercury vapor detection was installed in the middle of the Amazonian rainforest, at Ducke forest preserve, 30 km north of Manaus (3 deg S, 60 deg W). The average background concentration of surface CO was about 100 ppbv. This is three to four times smaller than values measured by other groups during the dry season, implying a large seasonal (dry x wet) variation. During the first half of the experiment there was considerable variability in the CO data with daily averages showing large error bars. Only small variability was observed during the last half of the experiment, probably owing to local meteorological conditions. Comparisons of samples from the clearing, representing air masses from above the canopy, with samples taken inside the forest, under the canopy, gave consistently larger concentrations within the forest. Author

46 GEOPHYSICS

Includes aeronomy; upper and lower atmosphere studies; ionospheric and magnetospheric physics; and geomagnetism.

For space radiation see *93 Space Radiation.*

N88-22470# Gosudarstvennyi Komitet po Ispolzovaniyu Atomnoi Energii, Moscow (USSR). Inst. Teoreticheskoj i Ehksperimental'noj.
SPIN PRECESSION IN STATIONARY GRAVITATIONAL FIELDS
N. A. Voronov 1987 22 p In RUSSIAN
(TI88-701107; ITEF-15(1987)) Avail: NTIS (US Sales Only) HC A03/MF A01

The Lorentz references obtained from the laboratory one by the Lorentz transformation without rotation are derived explicitly for the Schwarzschild and Reissner-Nordstroem spaces. Due to this fact it becomes possible to calculate exactly the frequency of spin procession of a trial particle during its longitudinal motion. The coordinate transformation leading the Reissner-Nordstroem metrics to the isotropic view was found. DOE

N88-22471# Bhabha Atomic Research Centre, Bombay (India). Seismology Section.
EARTHQUAKES FROM PENINSULAR INDIA: DATA FROM THE GAURIBIDANUR SEISMIC ARRAY
B. K. Gangrade, A. G. V. Prasad, and R. D. Sharma 1987 32 p
(DE88-701232; BARC-1347) Avail: NTIS (US Sales Only) HC A03/MF A01

Arrival times of the P and S wave signals recorded at the Gauribidanur seismic array from earthquakes in the neighboring areas in peninsular India were analysed to estimate their locations (latitudes and longitudes of the epicenters), magnitudes and origin times. Considering typical inaccuracies in the observed data, uncertainties in the estimated epicentral parameters were illustrated. Using a crustal model, which was specifically derived for the region around the array, expected arrival times of these signals at other important seismic stations (Kodaikanal, Hyderabad, Poona, New Delhi and Shillong) have been computed for identifying events at these stations in order to determine accurate arrival times at these stations. Due to a higher signal detection capability of the Gauribidanur array, the number of events given in this catalogue is much greater than that detected by these stations. The M sub S magnitude estimates of events detected at the Hyderabad station have been used to obtain a magnitude scale for Gauribidanur. Origin times, epicentral locations and magnitudes of these events are listed. DOE

N88-22472# Bhabha Atomic Research Centre, Bombay (India).
CHARACTERISTICS OF SEISMIC SOURCES OF SOME ASIAN EARTHQUAKES AND SOVIET UNDERGROUND EXPLOSIONS FROM GAURIBIDANUR ARRAY RECORDS
T. K. Basu and S. K. Arora 1987 33 p
(DE88-701233; BARC-1348) Avail: NTIS (US Sales Only) HC A03/MF A01

Among one hundred sixty-five shallow-focus earthquakes which occurred over a six-year period (1980 to 1985) in thirty-five different Asian provinces, Gauribidanur array (GBA) P-wave seismograms of all of them and P sub c P seismograms of thirty-one of them from fourteen regions were processed to deduce temporal and spectral characteristics of their sources. These were compared with the corresponding features deduced earlier (Basu and Arora ; 1985, 1986) from eighty-eight known and presumed Soviet underground explosions. The identifiers that yielded wider separation between earthquakes and explosions included among others: (1) cube root of signal complexity per unit TMF (third moment of frequency: CTMF parameter), (2) spectral energy ratio of P sub c P in two distinct frequency passbands (SENR parameters), and (3) normalized time-window energy ratio (NTENR parameter) and normalized spectral energy ratio (NSENR parameter) of P and P sub c P signals. The last two of these particularly helped to accentuate the main phase and the relative high-frequency content in the P sub c P record, which considerably increased the efficacy of the P sub c P discriminant. DOE

N88-22473# Department of Energy, Washington, D. C. Office of Policy, Planning and Analysis.
NORTHERN LIGHTS: THE ECONOMIC AND PRACTICAL POTENTIAL OF IMPORTED POWER FROM CANADA
Dec. 1987 265 p
(DE88-006026; DOE/PE-0079) Avail: NTIS HC A12/MF A01

This document contains ten appendices with extensive tables and charts on the electric power potential of Canada and that portion now supplied to the United States. The executive summary is written for the non-specialist and provides an evaluation of the data contained in the appendicies. DOE

N88-22474# Air Force Geophysics Lab., Hanscom AFB, Mass.
RESULTS OF THE INTERNATIONAL COMPARISON OF ABSOLUTE GRAVIMETERS (2ND) HELD IN SEVRES, FRANCE IN JUNE-JULY 1985
Yu. Boulanger, J. Faller, E. Groten, G. Arnautow, and M. Becker 8 Apr. 1987 33 p Conference held in Sevres, France, Jun.-Jul. 1985
(AD-A189869; AFGL-TR-87-0114) Avail: NTIS HC A03/MF A01 CSCL 08E

The second International Comparison of Absolute Gravimeters was carried out with six instruments, from five countries occupying pre-assigned sites at the Bureau of Weights and Measures (BIPM). The objective was to learn of possible systematic errors associated with these instruments and also to learn of the different approaches used by other experimenters in the field of absolute gravimetry. GRA

N88-22475# Israel Oceanographic and Limnological Research Ltd., Haifa.
DERIVATION OF CONSISTENT SURFACE FIXED FIELDS FOR USE IN A GLOBAL NWP MODEL Interim Report, 1 Oct. 1986 - 30 Sep. 1987
Stephen Brenner 30 Nov. 1987 18 p

(Grant AF AFOSR-0066-87)
(AD-A190131; SR-1) Avail: NTIS HC A03/MF A01 CSCL 04B

This report describes a method for generating a consistent set of surface fixed fields for use in a global NWP model. These fields include orography, the land sea mask and the sea surface temperature. The method is based on two principles. First, the interpolation from the higher resolution data grid to the coarser resolution model grid is done with a local filtering or analysis technique. Second, the three analyzed fields are kept consistent by using the same method and filter parameters for each field. The basic orographic data set is the 1 X 1 degree Sripps data. This is used to produce the model grid values of orography and the land sea mask. The basic data for the sea surface temperature consists of monthly mean values on the 2.5 X 2.5 degree grid used by NMC. For the orography and land sea mask, we first use the basic data to generate values on the 2.5 X 2.5 degree grid. Then all three fields are interpolated to the model grid. The resulting land sea mask also allows for fractional land coverage at model grid points. GRA

N88-22476# Northwest Research Associates, Inc., Bellevue, Wash.
SUPPORT FOR FY87 MIDLATITUDE ELECTRON-DENSITY CALIBRATION CAMPAIGN Scientific Report No. 5, 4 Jun. - 15 Oct. 1987
John M. Lansinger 15 Oct. 1987 14 p
(Contract F19628-87-C-0003)
(AD-A190174; NWRA-CR-87-R018; AFGL-TR-87-0299) Avail: NTIS HC A03/MF A01 CSCL 04A

One of the applications of data from AFGL's Auroral and Ionospheric Remote Sensor (AIRS) aboard the Polar BEAR Satellite is an attempt to produce electron-density profiles from remote passive topside sensing. Development of this procedure required real-time acquisition of AIRS data simultaneously and closely co-located with data from the Millstone Hill incoherent-scatter radar. The field procedure to accomplish this objective involved utilization of the DNA Rover ground station deployed in the vicinity of Westford, MA to receive AIRS and other support data from Polar BEAR while the satellite overflew the radar. The radar provided ground-truth information on ionospheric electron-density profiles and measurements of electron and ion temperature, plasma drift, and the thermospheric neutral wind during selected satellite passes between 1 July and 11 August, 1987. This report describes the field operations in support of the stated objective and some observations related to attitude determination for the Polar BEAR Satellite. ultraviolet, Remote sensing. GRA

N88-22477# Pittsburgh Univ., Pa.
EFFECT OF VIBRATIONAL EXCITATION ON RATE PARAMETERS OF ATMOSPHERIC REACTIONS Final Report, 3 Nov. 1983 - 2 May 1987
Michael F. Golde 23 Sep. 1987 35 p
(Contract F19628-84-K-0005)
(AD-A190464; AFGL-TR-87-0262) Avail: NTIS HC A03/MF A01 CSCL 04A

In the Earth's thermosphere, under conditions of low pressure and high solar flux, metastable atomic and molecular species acquire increased importance, particularly under conditions of natural or artificial perturbation. For molecules, the excitation can be either electronic or vibrational, and it is estimated that approx 40 percent of thermospheric solar UV energy is channeled through metastables. The effect of vibrational excitation on the reactivity of a given species is poorly understood at present. The purpose of this project was to obtain relevant data, both for direct input to models of perturbated atmospheres, and to yield new insight into the effects of vibrational excitation. This study has concentrated on the reactions of the lowest electronically excited state of N2, the metastable N2 A3 Sigma sub u+ state, in its lowest seven vibrational levels. The reagents O2, NO, CO, N2O and C2H4 were chosen for their atmospheric relevance, but also exhibit an interesting variety of properties. The study was extended to include two inefficient electronic quenchers, CH4 and CF4, which are shown to deactivate N2(A) principally via vibrational relaxation. Preliminary data on two other inefficient quenchers, H2 and D2, are also included in this report, as are results on product analysis of the related reaction of N2(A) with O(3p) atoms. GRA

N88-22478# Manchester Univ. (England). Inst. of Science and Technology.
THE GROWTH POTENTIAL OF CORONA DISCHARGES FROM AIRCRAFT FLYING IN PRECIPITATION Final Scientific Report, 1 Jan. 1983 - 31 Dec. 1985
J. A. Bicknell 12 Nov. 1987 149 p
(Grant AF-AFOSR-0083-83)
(AD-A190507; AFOSR-87-1781TR) Avail: NTIS HC A07/MF A01 CSCL 04A

The behavior of positive streamers in fields near and above the stability field was studied in quasi-uniform fields of up to 18 cm in extent with the aim of producing a model of the behavior so that predictions can be made for much greater distances. In particular the evolution in air of free charge produced by the propagation has been monitored and the effect of pressure and propagation distance on this evolution studied. A frequency gamma or coefficient gamma has been defined and measured which characterizes the growth of free charge. The Schockley-Ramo theorem has been used to analyze the data which not only provides values for other relevant parameters such as attachment coefficient and streamer velocity but also provides a novel way of observing prebreakdown streamer modes. A model has been constructed which adequately accounts for the observed behavior in small gaps but which predicts unrealistically large amounts of free charge in large gaps (greater than 1 m). This suggests that some other mechanism might predominate in this case; an increase in electron density leading to channel thermalization is suggested as a possibility. GRA

N88-22479# Rome Air Development Center, Griffiss AFB, N.Y.
STELLAR SCINTILLOMETER ATMOSPHERIC OPTICAL TURBULENCE PROFILING EXPERIMENT: A QUALITATIVE COMPARISON OF TWO IDENTICAL INSTRUMENTS AT AMOS (AIR FORCE MAUI OPTICAL STATION), 1985
N. Chonacky Nov. 1987 79 p
(AD-A190589; RADC-TR-87-245) Avail: NTIS HC A05/MF A01 CSCL 04A

Two identical atmospheric optical turbulence profiling instruments were operated. The daily average results of looking along common lines-of-sight, through identical atmospheres, show systematic differences at lower altitudes and near agreement at higher altitudes. Systematic biases from background noise can significantly affect the turbulence values measured, especially at lower altitudes, and may be responsible for part of the instruments' disagreement there. But other, non-noise biases, due to nonequivalent light geometries combined with spatially non-uniform PMT photocathode responses, likely also contribute to systematic biases. The average results of looking along two different lines-of-sight, through different regions of the atmosphere, show systematic differences at higher altitudes which we interpret as horizontal structure in the distribution of atmospheric optical turbulence above the 10 km level. GRA

N88-22480# Oak Ridge National Lab., Tenn.
A HARDWARE/SOFTWARE SYSTEM FOR IMPLEMENTING GEOPHYSICAL DIFFRACTION TOMOGRAPHY
A. J. Witten and W. C. King 1988 15 p Presented at the SPIE's Technical Symposium on Optics, Electro-optic and Sensors, Orlando, Fla., 4 Apr. 1988 Prepared in cooperation with Tennessee Univ., Knoxville
(Contract DE-AC05-84OR-21400)
(DE88-006411; CONF-880462-3) Avail: NTIS HC A03/MF A01

Geophysical diffraction tomography is a technique for high resolution, quantitative imaging of subsurface cross-sections. The method is based upon an imaging process known as filtered backpropagation. In backpropagation, an image of spatial variations in refractive index is formed by backpropagating data received along an array of detectors, by means of the reduced wave

equation, from the array into the support volume of the host medium. While there has been considerable development in theory of backpropagation, less effort has been devoted to problems associated with its implementation. Problems of practical importance that must be considered include: (1) the development of a data acquisition system capable of resolving the necessary wave characteristics; (2) quantification of the incident field in a homogeneous host matrix; and (3) in-field, real-time signal processing. This paper describes a microprocessor-based data acquisition system specifically designed and fabricated for geophysical diffraction tomography, discusses signal processing algorithms which are implemented on the system and presents results of several field studies. DOE

N88-22481# Sandia National Labs., Albuquerque, N. Mex.
DESCRIPTION OF GROUND MOTION DATA PROCESSING CODES, VOLUME 2
M. L. Sanders Feb. 1988 422 p
(Contract DE-AC04-76DP-00789)
(DE88-007137; SAND-87-1176-Vol-2) Avail: NTIS HC A18/MF A01

Data processing codes developed to process ground motion at the Nevada Test Site for the Weapons Test Seismic Investigations Project are used today as part of the program to process ground motion records for the Nevada Nuclear Waste Investigations Project. The work contained in this report documents and lists these codes and verifies the PSRV code. Volume 1, which contains the program specifications for the scientific and engineering software, consists of the following programs: SPECTRA calculates the power density spectrum of digitized time histories from underground nuclear explosions (UNEs); FILTER designs optimum finite impulse response filters and then filters UNE ground motion data; and PSRV calculates the pseudo-relative velocity response spectrum for UNE ground motions. Volume 2 contains the following program specifications for the auxiliary software. ACCESS allows the user to scan, update, delete, or add records contained in the Weapons Test Seismic Investigations data base. SCAN produces an inventory of the time histories contained in a large data file. PLOT plots the data files: ROTATE converts data in the horizontal plane into a UNE specific coordinate system; and VECTOR calculates the magnitude versus time of the 2-D (horizontal components) and 3-D (vertical and horizontal components) vectors. Volume 3 comprises the users' manuals for each of the programs described in Volumes 1 and 2. DOE

N88-22482# Instituto de Pesquisas Espaciais, Sao Jose dos Campos (Brazil).
IN-SITU PLASMA BUBBLE OBSERVATIONS ASSOCIATED WITH EQUATORIAL SPREAD-F OVER NATAL
P. Muralikrishna and M. A. Abdu Mar. 1988 19 p Presented at the 2nd Encontro Regional de Geofisica, Salvador-BA, 25-27 Nov. 1987
(Contract FINEP-539/CT)
(INPE-4488-PRE/1252) Avail: NTIS HC A03/MF A01

On 11 December, 1985, at 2030 hrs local time, a Sonda III rocket, carrying a Langmuir Probe (LP) and a High Frequency Capacitance Probe (HFC) was launched from Natal to study the phenomenon of equatorial Spread-F associated with plasma bubble formation. As expected, the rocket passed through regions of depleted electron density, known as plasma bubbles, which under certain ambient physical conditions are known to be responsible for the generation of plasma irregularities giving rise to spread-F traces on the ionograms. Both LP and HFC data showed the presence of two dominant plasma bubbles centered around the altitudes of about 370 and 420 km. These plasma bubbles had vertical scale sizes of about 30 to 40 km. Their observation, though with reduced amplitudes, even during the rocket descent, indicates the large (a few hundred km) horizontal scale sizes of these bubbles. The general implications of these observations in the light of existing theories on bubble formation and development are reviewed and discussed. Author

N88-22483# Instituto de Pesquisas Espaciais, Sao Jose dos Campos (Brazil).
STRATOSPHERIC ELECTRIC FIELD AND CONDUCTIVITY MEASUREMENTS OVER ELECTRIFIED CONVECTIVE CLOUDS IN THE SOUTH AMERICAN REGION, REVISED
I. R. C. A. Pinto, O. Pinto, Jr., W. D. Gonzalez, S. L. G. Dutra, J. Wygant, and F. S. Mozer Nov. 1986 19 p Submitted for publication Revised Dec. 1987
(Contract FINEP 537/CT; Grant NSF ATM-80-02097)
(INPE-4046-PRE/1012-Rev-3) Avail: NTIS HC A03/MF A01

Stratospheric dc electric fields and conductivity measurements, associated with electrified convective clouds identified by satellite infrared imagery, are presented. These measurements were obtained at an altitude of 26 km by a balloon-borne double-probe detector, launched from Cachoeira Paulista (geographic coordinates 23 deg 40 min S, 45 deg W) on April 2, 1980. The electric fields are found to correspond to electrified convective clouds with charges of the order of a few coulombs. The conductivity measurements show variations by over a factor of 2 around the average value of 4 x 10 to the minus 12th mho/m. Such variations, which merit more investigation, did not show an apparent relation with the simultaneous electric field measurements. Using the vertical electric field and conductivity measurements, a current density is also estimated. Furthermore, a detailed original discussion on conductivity measurements in the atmosphere as well as a suggestion for estimating distances from the detector to the cloud, using the ratio between the magnitude of the measured vertical and horizontal electric fields, is included. Author

N88-22484# Instituto de Pesquisas Espaciais, Sao Jose dos Campos (Brazil).
SURFACE OZONE AND OZONESOUNDING RESULTS FROM THE ABLE-2B EXPEDITION TO AMAZONIA
V. W. J. H. Kirchhoff and I. M. O. daSilva May 1988 25 p Presented at the Spring AGU Meeting, Baltimore, Md., 16-20 May 1988
(Contract FINEP-537/CT)
(INPE-4523-PRE/1275) Avail: NTIS HC A03/MF A01

Surface ozone mixing ratios at several levels above the surface were obtained during the period of about 45 days in the Amazonian wet season. In addition, 20 ozonesondes of the ECC type were launched gathering ozone data in the troposphere and stratosphere. The ozone concentrations considered low in the 1985 dry season, were even lower during this 1987 wet season. At the surface, daytime maxima averaged only abour 6 ppbv, about half of the dry season average. The magnitudes under the forest canopy were even smaller, about 3 ppbv. In comparison to the previous dry season results, the O3 mixing ratio was smaller by about 40 percent in the whole troposphere. The ozone mixing ratio gradient between the surface and 500 mb is 40 percent less than that during the dry season. Above 200 mb there is no difference between the dry-wet seasons. Below 100 mb the tropospheric O3 content equals 24 DU in the wet season against 28.7 DU in the dry season. Author

N88-22485# Instituto de Pesquisas Espaciais, Sao Jose dos Campos (Brazil).
CALIBRATION AND PROCESSING OF AVHRR DATA FOR TEMPERATURE ESTIMATION [CALIBRACAO E PROCESSAMENTO DOS DADOS DE AVHRR PARA ESTIMATIVA DE TEMPERATURA]
Keiko Tanaka, Carlos Ho Shih Ning, Yoshihiro Yamazaki, and Valder MatosdeMedeiros Mar. 1988 25 p In PORTUGUESE; ENGLISH summary Presented at the SELPER/86, Gramado/RS, Brazil, 10-15 Aug. 1986
(INPE-4493-PRE/1257) Avail: NTIS HC A03/MF A01

The results of a quantitative analysis of the thermal channels of the NOAA-9 satellite Advanced Very High Resolution Radiometer (AVHRR) scanning radiometer digital data, recorded on a CCT magnetic tape, are presented. The calibration coefficients derived from the reference parameters contain information on the following telemetry data: the energy levels detected by the AVHRR sensor during space view and the internal calibration target for each

thermal channel and each scanning. The linearization functions are found by taking, for each channel, the radiometric mean of 10 samples of space view and internal target data. The linear radiance was produced by taking the average of 50 scan data. These linear functions give the sensor radiance variations for each target scanned, and were used to convert the digital image data into radiance, and consequently, into temperature values using the inverse Planck function. The main results of the April 18th, 1986 image processed, applying the navigation system, for an area of 256 x 256 pixels are presented. Author

N88-22486# Instituto de Pesquisas Espaciais, Sao Jose dos Campos (Brazil).
A STUDY ON ELECTRIC FIELDS AND CONDUCTIVITY ASSOCIATED WITH ELECTRIFIED CLOUDS IN THE REGION OF SOUTH AMERICA Ph.D. Thesis, 17 Dec. 1987 [ESTUDOS SOBRE CAMPOS ELETRICOS E CONDUTIVIDADE ASSOCIADOS A NUVENS ELETRIFICADAS NA REGIAO DA AMERICA DO SUL]
I. R. C. A. Pinto Mar. 1988 144 p In PORTUGUESE; ENGLISH summary
(INPE-4487-TDL/325) Avail: NTIS HC A07/MF A01

A study of quasi-static electric field and electric conductivity in the Earth's atmosphere, in association with tropospheric electrified clouds is presented. Electric field and conductivity data, obtained by a double-probe balloon-borne detector launched from Cachoeira Paulista, Brazil on April 2, 1980, together with radiosonde balloon, meteorological radar and infrared data, all by a sensor on board the SMS-2 meteorolodial satellite, all measured simultaneously for the first time at the South Hemisphere, are discussed. A theory regarding the calculations of the electric field at the stratosphere due to an electrified cloud is presented. An application of this theory for estimating the distance between a detector and an electrified cloud, using the ratio between the horizontal and the vertical electric fields, is suggested. An analytic theory about atmospheric conductivity measurements by using electric field probes is developed. The analysis of the electric field data showed that they are associated with electrified clouds near the detector, with charges of the order of a few coulombs and without a shielding layer. The analysis of the conductivity measurements showed variations by a factor of two. Such variations, which can be regarded as one of the first evidences that the global atmospheric electric circuit is not static, could play an important role in the study of time variations in this circuit, mainly if it is considered that they occur in a region where the thunderstorm activity is very intense, such as in the South American region. Author

N88-22487# Max-Planck-Inst. fuer Aeronomie, Katlenburg-Lindau (West Germany).
COORDINATED AURORAL EXPERIMENTS USING SCATTER AND ROCKET INVESTIGATIONS (CAESAR INVESTIGATIONS)
K. Wilhelm, K. Rinnert, K. Schlegel, H. Kohl, N. Kloecker, H. Luehr, W. Oelschlaegel, G. Dehmel, M. P. Gough (Uppsala Ionospheric Observatory, Sweden), and B. Holback et al. Apr. 1987 113 p Sponsored by the Bundesministerium fuer Forschung und Technologie, Bonn, Federal Republic of Germany Original contains color illustrations
(MPAE-W-47-87-13; ETN-88-92083) Avail: NTIS HC A06/MF A01

The CAESAR project investigated the interaction of the magnetosphere with the ionospheric plasma during discrete auroral arc displays at high geomagnetic latitudes. It observed energetic charged particle distributions and electromagnetic, magnetic and electrostatic fields, and measured the important plasma parameters on the sounding rocket payloads and with EISCAT, to define the electrodynamics in relation to this geophysical condition in adequate detail in order to make the step from a phenomelogical to a physical description of the situation. On the last day of the launch window, a stable arc appeared near the projected measuring location of the payload and since EISCAT indicated strong signals, it was decided to launch the payload despite the cloud coverage of 50 percent of the sky. During the flight, auroral activity developed, but it is extremely difficult to determine the exact arc configuration. This, together with the fact that the payload trajectory flew 10 deg westward of the planned flight azimuth and hence no good match with the preschedule EISCAT was obtained, will require some assumptions made on the spatial distribution of the electric fields and the precipitation regions. ESA

N88-22488# Kiruna Geophysical Inst. (Sweden). Swedish Inst. of Space Physics.
ON THE ACCELERATION OF ELECTRONS AND POSITIVE IONS IN THE SAME DIRECTION ALONG MAGNETIC FIELD LINES BY PARALLEL ELECTRIC FIELDS
Bengt Hultqvist Nov. 1987 25 p
(IRF-Preprint-103; ISSN-0284-1711; ETN-88-92197) Avail: NTIS HC A03/MF A01

It is demonstrated that the simultaneous observations on Swedish Viking satellite of upward field aligned fluxes of energetic ions and electrons of energies in the same range may be due to acceleration in field aligned electric fields, the ions in an upward directed parallel dc field and the electrons in a downward parallel field which is fluctuating but appears as quasistatic for the electrons as long as they are in the acceleration region. Most of the upward accelerated electrons leave the limited acceleration region in an effective half period of the fluctuating field when it points downward. The fluctuating field has only a small effect on the ions. ESA

N88-22489# Instituto de Pesquisas Espaciais, Sao Jose dos Campos (Brazil).
ROCKET MEASUREMENTS OF IONOSPHERIC ELECTRON TEMPERATURE OVER NATAL
I. J. Kantor, P. Muralikrishna, and M. A. Abdu Mar. 1988 18 p In PORTUGUESE; ENGLISH summary Presented at the 2nd Regional Meeting of Geophysics, 25-27 Nov. 1987, Salvador, Brazil
(Contract FINEP-537/CT)
(INPE-4485-PRE/1250) Avail: NTIS HC A03/MF A01

A Sonda 3 rocket was launched from Natal on December 11, 1985, at 21:30 LT, with a Langmuir probe that measured the kinetic electron temperature in the ionosphere. The rocket reached approximately 524 km giving information on the E and F regions of the equatorial ionosphere over Natal. Two electron temperature determination processes are possible: derivation of the current versus voltage characteristics of the Langmuir probe and detection of the space potential. Both processes are utilized with the available data. Problems encountered for the electronic temperature measurements with Langmuir probe are discussed and suggestions for future improvements are presented. Author

N88-22490*# National Aeronautics and Space Administration, Washington, D.C.
BILATERAL SYMMETRY ELEMENTS OF THE ZHAMANSHIN IMPACT CRATER
V. L. Masaytis May 1988 11 p Transl. into ENGLISH from Meteoritika, Akademiya Nauk SSSR (USSR), issue 46, 1987 p 119-123 Transl. by Scientific Translation Service, Santa Barbara, Calif.
(Contract NASw-4307)
(NASA-TT-20288; NAS 1.77:20288) Avail: NTIS HC A03/MF A01 CSCL 08G

The internal structure of the Zhamanshin impact structure and the nature of rocks developed within it are studied to establish the impact structure parameters. It is found that the diameter of the visible crater is about 13 km. The small annular structures observed are found to not be secondary craters, and no correlation is found between the asymmetrical distribution of ejecta material and the arrangement of these annular forms. Author

N88-22247# Joint Publications Research Service, Arlington, Va.
RELATIONSHIP BETWEEN OPTICAL TRANSFER FUNCTION AND NATURAL LIGHT FIELD IN SEA OR ATMOSPHERE Abstract Only
Zhishen Liu and Zhiming Zhang *In its* JPRS Report: Science and Technology. China 11 Dec. 1987 p 66 Transl. into

ENGLISH from Guangxue Xuebao (Shanghai, Peoples Republic of China), v. 7, no. 8, Aug. 1987 p 707-713 (For primary document see N88-22233 15-31)
Avail: NTIS HC A06/MF A01

47 METEOROLOGY AND CLIMATOLOGY

Includes weather forecasting and modification.

N88-22491*# Illinois State Water Survey, Champaign. Climate and Meteorology Section.
A MULTIVARIATE VARIATIONAL OBJECTIVE ANALYSIS-ASSIMILATION METHOD. PART 1: DEVELOPMENT OF THE BASIC MODEL
Gary L. Achtemeier and Harry T. Ochs, III 14 Apr. 1988 43 p
(Grant NAG8-059)
(NASA-CR-182651; NAS 1.26:182651) Avail: NTIS HC A03/MF A01 CSCL 04B

The variational method of undetermined multipliers is used to derive a multivariate model for objective analysis. The model is intended for the assimilation of 3-D fields of rawinsonde height, temperature and wind, and mean level temperature observed by satellite into a dynamically consistent data set. Relative measurement errors are taken into account. The dynamic equations are the two nonlinear horizontal momentum equations, the hydrostatic equation, and an integrated continuity equation. The model Euler-Lagrange equations are eleven linear and/or nonlinear partial differential and/or algebraic equations. A cyclical solution sequence is described. Other model features include a nonlinear terrain-following vertical coordinate that eliminates truncation error in the pressure gradient terms of the horizontal momentum equations and easily accommodates satellite observed mean layer temperatures in the middle and upper troposphere. A projection of the pressure gradient onto equivalent pressure surfaces removes most of the adverse impacts of the lower coordinate surface on the variational adjustment. Author

N88-22492*# Illinois State Water Survey, Champaign. Climate and Meteorology Section.
A MULTIVARIATE VARIATIONAL OBJECTIVE ANALYSIS-ASSIMILATION METHOD. PART 2: CASE STUDY RESULTS WITH AND WITHOUT SATELLITE DATA
Gary L. Achtemeier, Stanley Q. Kidder, and Robert W. Scott 14 Apr. 1988 57 p
(Grant NAG8-059)
(NASA-CR-182653; NAS 1.26:182653) Avail: NTIS HC A04/MF A01 CSCL 04B

The variational multivariate assimilation method described in a companion paper by Achtemeier and Ochs is applied to conventional and conventional plus satellite data. Ground-based and space-based meteorological data are weighted according to the respective measurement errors and blended into a data set that is a solution of numerical forms of the two nonlinear horizontal momentum equations, the hydrostatic equation, and an integrated continuity equation for a dry atmosphere. The analyses serve first, to evaluate the accuracy of the model, and second to contrast the analyses with and without satellite data. Evaluation criteria measure the extent to which: (1) the assimilated fields satisfy the dynamical constraints, (2) the assimilated fields depart from the observations, and (3) the assimilated fields are judged to be realistic through pattern analysis. The last criterion requires that the signs, magnitudes, and patterns of the hypersensitive vertical velocity and local tendencies of the horizontal velocity components be physically consistent with respect to the larger scale weather systems. Author

N88-22493# Naval Postgraduate School, Monterey, Calif.
PARAMETERIZATION OF HORIZONTAL WIND VELOCITY VARIABILITY M.S. Thesis
Timothy J. Dowding Dec. 1987 153 p
(AD-A190107) Avail: NTIS HC A08/MF A01 CSCL 04B

Longitudinal and transverse horizontal wind velocity variability of parameterized based on data collected for the Bureau of Land Management (BLM) between 1980 and 1982. The BLM data sets were used to derive horizontal wind velocity components and standard deviations of these components in the longitudinal (downwind; u, sigma u) and transverse (crosswind; v, sigma v) directions for various time averages. The standard deviations were plotted versus wind speed so that trends in the change of values could be determined. A methodology was used to develop a theoretical algorithm to account for turbulence production mechanisms due to shear, buoyancy and mesoscale processes. Empirical fits were determined for both the u and v wind directions over four different time averages. The results were related to puff growth in the x, y directions and form the basis for improving a puff dispersion model for near-coast overwater regions. GRA

N88-22494# Army Cold Regions Research and Engineering Lab., Hanover, N.H.
SPECTRAL MEASUREMENTS IN A DISTURBED BOUNDARY LAYER OVER SNOW
Edgar L. Andreas Nov. 1987 49 p
(AD-A190217; CRREL-87-21) Avail: NTIS HC A03/MF A01 CSCL 04B

The author measured time series of longitudinal (u) and vertical (w) velocity and temperature (t) and humidity (q) fluctuations with fast-responding sensors in the near-neutrally stable surface layer over a snow-covered field. These series yielded individual spectra and u-w, w-t, w-q and t-q cospectra, phase spectra and coherence spectra for nondimensional frequencies (fz/U) from roughly 0.001 to 10. With the exception of the u-w cospectra, all the spectra and cospectra displayed the expected dependence on frequency in an inertial or inertial-convective subrange. All, however, contained significantly more energy at low frequency than the Kansas neutral-stability spectra and cospectra. This excess low-frequency energy and the erratic behavior of the u-w cospectra imply that forested hills bordering the site on two sides were producing disturbances in the flow field at scales roughly equal to the height of the hills, 100 m. The phase and coherence spectra suggest that internal gravity waves were also frequently present, since the atmospheric boundary layer generally had slightly stable stratification. Consequently, at this complex site, turbulence alone determines the spectra and cospectra at high frequency; at low frequency the spectra and cospectra reflect a combination of topographically generated turbulence and internal waves. From the measured temperature and humidity spectra and the t-q cospectra, the author computed refractive index spectra for light of 0.55 microns and millimeter wavelengths. The refractive index spectra has shapes like the other scalar spectra: excess energy at low frequencies and an inertial-convective subrange at high frequencies. GRA

N88-22495# Wisconsin Univ., Madison. Space Science and Engineering Center.
THE COLLECTION OF STATISTICS ON THE FREQUENCY OF CLOUD COVER OVER NORTH AMERICA Annual Letter Report, FY87
Edwin W. Eloranta and Donald P. Wylie 1987 12 p
(Contract N00014-87-K-0436)
(AD-A190456) Avail: NTIS HC A03/MF A01 CSCL 04B

Statistics of cloud characteristics over North America have been calculated for the past two years. The frequency of cloud cover with the associated heights and infrared attenuation were charted using the CO2 channel radiometric data from the geostationary VISSR Atmospheric Sounder (VAS). Cloud top pressure was determined from the ratio of VAS CO2 channel radiances in a radiative transfer equation formulation. Cloud emissivities were then calculated from infrared window channel observations. CO2 techniques derived height and emissivity assignments have been found to be reliable in all cloud types, including thin cirrus clouds where other techniques have been inconsistent. Observations since 1985 revealed that 25 to 35 percent of the United States was covered with thin clouds (radiative attenuation was less than 95 percent), 45 percent was covered with thick opaque clouds, and 20 to 30 percent had clear sky conditions. Geographical distribution

of cloud cover shows a latitudinal dependence mainly over the Pacific Ocean. Moderate seasonal and diurnal changes were also found. GRA

N88-22496# Air Force Inst. of Tech., Wright-Patterson AFB, Ohio. School of Engineering.
EXPERIMENTAL COMPARISON OF LIGHTNING SIMULATION TECHNIQUES TO CV-580 AIRBORNE LIGHTNING STRIKE MEASUREMENTS M.S. Thesis
Rudy M. Braza Dec. 1987 132 p
(AD-A190576; AFIT/GE/ENG/87D-5) Avail: NTIS HC A07/MF A01 CSCL 04A

Experimental tests on the Lightning Test Cylinder, which further investigated the assessment of lightning simulation techniques conducted by Butters et al., included swept frequency continuous wave (SFCW), current pulse, and shock-excitation. Designed to model the fuselage of an aircraft, the aluminum test cylinder is over ten meters long with a one meter diameter. To test the effects of various aircraft construction materials, the cylinder was constructed with an aperture where various composite and metal panels can be mounted. The research involved determination of the electrical field and magnetic field response transfer functions for each simulation test technique. With these transfer functions, analysis and comparison of the external and internal field responses between the SFCW, current pulse, and shock-excitation tests were made. A major portion of the research was to examine the validity of the linear model for the current pulse simulation technique. In this investigation, transfer functions were derived for various current pulse waveforms. The current waveforms injected into the test cylinder included a 20 kA unipolar, double-exponential pulse and two oscillatory waveforms with peak amplitudes of 20 kA and 100 kA. GRA

N88-22497# SRI International Corp., Menlo Park, Calif.
INFRARED DIFFERENTIAL ABSORPTION LIDAR FOR VAPOR DETECTION Contractor Report, 1983 - 1984
J. P. Carrico, K. R. Phelps, J. vanderLaan, E. E. Uthe, and P. L. Holland Feb. 1988 37 p
(Contract DAAK11-82-C-0158)
(AD-A190600; CRDEC-CR-88039) Avail: NTIS HC A03/MF A01 CSCL 17I

Ground-mobile and airborne carbon dioxide laser systems were developed to measure vapor clouds using differential absorption lidar (DIAL) techniques. Field testing with the ground-mobile lidar detected a vapor cloud at 7 km using the return signal from a topographic target at a range of 8.5 km. Range-resolved detection enabled mapping of vapor cloud concentration to a range of at least 1 km. The airborne lidar mapped vertically integrated, cross-cloud gas concentrations at 3 km and detected vapor clouds 7 km downwind from the vapor source. GRA

N88-22498# Air Force Systems Command, Wright-Patterson AFB, Ohio. Foreign Technology Div.
STUDY OF LIGHTNING AND LIGHTNING PROTECTION (SELECTED PAGES)
I. S. Stekolnikov 18 Feb. 1988 27 p Transl. into ENGLISH from Izucheniye Molnii i Grozozashchitta (Moscow, USSR), 1955 p 101-112; 158-159
(AD-A190623; FTD-ID(RS)T-0004-88) Avail: NTIS HC A03/MF A01 CSCL 20C

This Russian translations deals primarily with ball lightning including laboratory methods for making ball lightning. Brief sections discuss luminous clouds and Black lightning. A table of contents for the entire book is also included. GRA

N88-22499# Lawrence Livermore National Lab., Calif.
PROCEEDINGS OF THE LIGHTNING THREAT WARNING WORKSHOP
1987 114 p Workshop held in Cocoa Beach, Fla., 15 Sep. 1987
(Contract W-7405-eng-48)
(DE88-006607; CONF-8709162-Summ) Avail: NTIS HC A06

This volume contains the proceedings of a workshop on lightning detection and warning. Papers from government and private industry researchers are presented. The topics of the papers cover electric field sensors, mathematical models of thunderclouds, lightning damage mechanisms, and future warning systems. Briefings are included which summarize each participant's involvement with lightning threats. Papers are indexed separately. DOE

N88-22500# Colorado State Univ., Fort Collins. Dept. of Atmospheric Science.
FORECAST OF ATLANTIC SEASONAL HURRICANE ACTIVITY FOR 1988
William M. Gray 26 May 1988 40 p Sponsored by National Science Foundation, Washington, D.C.
Avail: NTIS HC A03/MF A01

Discussed is the amount of tropical cyclone activity which might be expected in the Atlantic Ocean region (including the Caribbean and the Gulf of Mexico) in 1988. This forecast is based on previous and current research, which relates seasonal amount of Atlantic tropical cyclone activity to four factors: (1) the El Nino; (2) the Quasi-Biennial Oscillation of equatorial stratospheric wind; (3) Gulf of Mexico and Caribbean Basin Sea-Level Pressure Anomaly; and (4) lower latitude Caribbean Basin 200 mb zonal wind anomaly. Information received up to 26 May 1988 indicates that the 1988 hurricane season can be expected to have about 7 hurricanes, 11 total named storms of both hurricane and tropical storm intensity, and about 30 hurricane days. This means that the 1988 Atlantic hurricane season will likely be above average by the standards of the last 18 years and particularly so as regards to the last 6 seasons. The probability is also high that this season will have a few more intense hurricanes than have occurred during the last few seasons. The Hurricane Destruction Potential (or HDP) of hurricanes in 1988 should be higher than in any previous season since 1981 except for the active season of 1985. Author

N88-22501# Instituto de Pesquisas Espaciais, Sao Jose dos Campos (Brazil).
AERODYNAMIC ASPECTS OF THE AMAZON FOREST M.D. Thesis [ASPECTOS AERODINAMICOS DE UMA FLORESTA AMAZONICA]
Antonio OcimarManzi Dec. 1987 133 p In PORTUGUESE; ENGLISH summary
(INPE-4445-TDL/313) Avail: NTIS HC A07/MF A01

Some results of the micrometeorological parameters over the Amazon Forest of the Terra Firme are presented. Two hundred and forty two mean hourly profiles of wind, temperature, and humidity for a wide range of stability conditions were analyzed in the context of the Monin-Obukhov similarity theory. The zero plane displacement for momentum was d = 0.08 h and the roughness parameter z = 0.09 h in conditions of neutrality. The parameters Ri and zeta have shown significant differences in unstable conditions when the effect of water vapor is included in the calculations. The Richardson number Ri is approximately equal to 0.1 when zeta tends to infinity. Values of Ri increased with increasing height. The parameters phi sub m, phi sub h, and phi sub e are presented as functions of Ri and zeta. For the first layer in neutral conditions the values of phi sub m, phi sub h, and phi sub e, were approximately 1.6, 0.35, and 0.4, respectively, and for the second layer 2.0, 0.8, and 0.9, respectively. Values of the ratios of diffusivities K sub h/K sub m and K sub e/K sub m were much greater than one for all stability conditions. The ratio K sub e/K sub h is more than one for inversion conditions and less than one for lapse conditions. These results differ with those obtained over plane areas having small parameters. Author

N88-22502# Instituto de Pesquisas Espaciais, Sao Jose dos Campos (Brazil).
TROPICAL CIRCULATIONS AND THE ASSOCIATED RAINFALL ANOMALIES DURING TWO CONTRASTING YEARS
Mary Toshie Kayano, V. B. Rao, and Antonio DivinoMoura Apr. 1988 26 p Submitted for publication Revised version
(INPE-4506-PRE/1261-Rev) Avail: NTIS HC A03/MF A01

The severe drought conditions observed during 1983 over large

extensions of the tropical lands were associated with the 1982 to 1983 El Nino event. In contrast, during 1984, above normal rainfall was observed over these areas. The tropical circulations were examined for these two contrasting years. The intensity and location of the rising and sinking motions were consistent with the rainfall anomalies and also with the outgoing long wave radiation anomalies. It was found that the north-south migration of the tropical trough played an important role in modulating the tropical rainfall during these two years. In the context of the currently acceptable theoretical notions of the tropical circulation, it was found that some of the observed characteristics could be explained in terms of an atmospheric response to tropical heat sources. The results suggest that seasonal changes were involved in the 1982 to 1983 El Nino collapse. Author

N88-22503*# National Aeronautics and Space Administration. Goddard Space Flight Center, Greenbelt, Md.
MONTHLY MEAN GLOBAL CLIMATOLOGY OF TEMPERATURE, WIND, GEOPOTENTIAL HEIGHT, AND PRESSURE FOR 0 - 120 KM
Eric L. Fleming, Sushil Chandra, Mark R. Schoeberl, and John J. Barnett (Oxford Univ., England) Feb. 1988 91 p
(NASA-TM-100697; Rept-88B0092; NAS 1.15:100697) Avail: NTIS HC A05/MF A01 CSCL 04B

A monthly mean climatology is presented of temperature, wind, and geopotential height with nearly pole-to-pole coverage (80 S to 80 N) for 0 to 210 km, which can be used as a function of altitude and pressure. The purpose is to provide a reference for various atmospheric research and analysis activities. Data sources and methods of computation are described; in general, hydrostatic and thermal wind balance are maintained at all levels and latitudes. As observed in a series of cross-sectional plots, this climatology accurately reproduces most of the characteristic features of the atmosphere such as equatorial wind and the general structure of the tropopause, stratopause, and mesopause. A series of zonal wind profiles is also represented comparing this climatological wind with monthly mean climatological direct wind measurements in the upper mesosphere and lower thermosphere. The temperature and zonal wind climatology at stratospheric levels is compared with corresponding data from the National Meteorological Center, and general agreement is observed between the two data sets. Tables of the climatological values as a function of latitude and height for each month are contained in Appendix B, and are also available in floppy disk. Author

48 OCEANOGRAPHY

Includes biological, dynamic, and physical oceanography; and marine resources.

For related information see also *43 Earth Resources and Remote Sensing.*

N88-22504# Pacific Northwest Labs., Richland, Wash.
OCEAN GENERAL CIRCULATION MODELS: REPORT ON PROCEEDINGS OF A MEETING OF OCEAN AND CLIMATE MODELERS
C. R. Sherwood and J. P. Downing Jan. 1988 101 p Presented at the Meeting on Ocean and Climate Modelers: Ocean General Circulation Models, Sequim, Wash., 30 Jul. 1987
(Contract DE-AC06-76RL-01830)
(DE88-005530; PNL-SA-15557; CONF-8707147-Summ) Avail: NTIS HC A06/MF A01

The proceedings of a meeting of ocean general circulation modelers and oceanographers are summarized. New developments in coupling ocean general circulation models and atmospheric general circulation models, improvements in the representation of mixed layer and sea ice processes, optimization of model codes for parallel processing on the next generation of supercomputers and ocean data sets and their limitations are among the topics discussed. Author

N88-22505# University of South Florida, St. Petersburg. Dept. of Marine Science.
SIMULATION ANALYSIS OF MOORED FLUOROMETER TIME SERIES FROM THE MID-ATLANTIC BIGHT Progress Report, 1986-1987
J. J. Walsh 1987 4 p
(Contract DE-FG05-85ER-60285)
(DE88-006066; DOE/ER-60285/T1) Avail: NTIS HC A02/MF A01

During FY86-87, a great deal of effort was devoted to synthesis of the results from the SEEP-I field experiment, conducted in 1983 to 1984, south of Martha's Vineyard and Long Island. As guest editor of a special SEEP-I volume of Continental Shelf Research, 20 manuscripts were reviewed and accepted for publication, of which three were written by the author. In summary, the component of the multidisciplinary SEEP-I program found from the 1984 time series of moored instruments that a seaward export of perhaps 0.20 mg chl/cu/m/day evidently occur red at depths of 75 to 81 m, between the 80- and 120-m isobaths during February to April 1984. Using a C/chl ratio of 45/1, such a horizontal loss of algal carbon over the lower third of the water column would be 19 to 67 percent of the March through April 1984 primary production within the overlying euphotic zone. DOE

N88-22506# Naval Postgraduate School, Monterey, Calif.
HYDROGRAPHIC DATA FROM THE OPTOMA (OCEAN PREDICTION THROUGH OBSERVATION, MODELING AND ANALYSIS) PROGRAM: OPTOMA 23, 9-19 NOVEMBER 1986 Progress Report, Nov. 1986 - Sep. 1987
J. E. Johnson, Paul A. Wittmann, and Christopher N. Mooers 8 Jan. 1988 95 p
(AD-A189868; NPS-68-88-001) Avail: NTIS HC A05/MF A01 CSCL 08C

The OPTOMA (Ocean Prediction Through Observation, Modeling and Analysis) program, seeks to understand the mesoscale (fronts, eddies, and jets) variability and dynamics of the California Current System (CCS) and to determine the scientific limits to practical mesoscale ocean forecasting. OPTOMA 23 is the last of the OPTOMA surveys and it is unique in that this was the first effort to integrate concurrent satellite, drifting buoy, ship, and aircraft data in a comprehensive oceanographic, meteorological, and acoustical study of the CCS. Specific goals of the airborne surveys were to: provide synoptic data for objective analysis of various parameters (e.g., SST from AXBT and PRT-5, mixed layer depth, thermal structure); provide initialization, boundary condition updating, and verification fields for dynamical model forecasts; and coordinate the observational strategy of the R/V POINT SUR by using near real time analyses to vector the ship into areas of interesting mesoscale activity. GRA

N88-22507# Oregon State Univ., Corvallis. Coll. of Oceanography.
PHYSICAL, CHEMICAL AND CTD (CONDUCTIVITY/TEMPERATURE/DEPTH) DATA FROM THE MARATHON 2 EXPEDITION
Margie Martin, Lynne D. Talley, and Roland A. DeSzoeke May 1987 214 p
(Contract N00014-84-C-0218; Grant NSF OCE-83-16930)
(AD-A189930) Avail: NTIS HC A10/MF A01 CSCL 08H

Hydrographic and CTD measurements were taken from ninety-eight stations between Honolulu, Hawaii and Kodiak, Alaska, from 4 May to 4 June 1984 on the second leg of the Marathon Expedition. This report consists of the cruise track, vertical sections, listings of all discrete hydrographic data, a subsample of the CTD data, plots of temperature and salinity as a function of pressure and plots of potential temperature as a function of salinity. GRA

N88-22508# Woods Hole Oceanographic Institution, Mass.
REAL-TIME ENVIRONMENTAL ARCTIC MONITORING (R-TEAM) Interim Technical Report
Alessandro Bocconcelli Nov. 1987 83 p
(Contract N00014-86-C-0135)

(AD-A189948; WHOI-87-50) Avail: NTIS HC A05/MF A01 CSCL 08C

The R-TEAM mooring is designed to collect oceanic environmental data in Arctic regions and to transmit these data to shore on a daily basis via ARGOS satellite telemetry. An ascent module comes to the surface once a day and transmits directly to ARGOS (ice free surface). When not transmitting the module remains in its rest position most of the time, well away from the surface, thus diminishing the risks of damage at the ice interface. The R-TEAM's design life is one year in situ. The mooring must be capable of deployment in depths of up to 4500 and must be able to withstand a maximum current speed of 2 knots at the surface. At an early stage two different transit options were considered. The variable ballast elevator seemed more directly compatible with our existing capabilities. UHF and MF transmitters, antennae, and associated electronic were designed and built to system specifications. The prototype mooring was deployed at 2700 m at 39 deg N, 30 deg W on June 2, 1987 and entirely recovered 62 days later. By and large this experimental deployment was very successful but the test also revealed two deficiencies which need to be corrected. GRA

N88-22509# Naval Postgraduate School, Monterey, Calif.
THE PHYSICAL OCEANOGRAPHY OF THE NORTHERN BAFFIN BAY-NARES STRAIT REGION M.S. Thesis
Victor C. Addison, Jr. Dec. 1987 110 p
(AD-A190015; NPS-68-87-008) Avail: NTIS HC A06/MF A01 CSCL 08C

A dense network of conductivity-temperature-depth measurements was conducted from Baffin Bay northward to 82 deg 09 min N at the entrance to the Lincoln Sea, in the most comprehensive physical oceanographic survey ever performed in the northern Baffin Bay-Nares Strait region. These data indicate Nares Strait Atlantic Intermediate Water and Arctic Basin Polar Water to be derived from Arctic Basin waters via the Canadian Archipelago, whereas the West Greenland Current (WGC) is the source of the comparatively dilute West Greenland Current Atlantic Intermediate Water and West Greenland Current Polar Water fractions. Baffin Bay Surface Water is found seasonally throughout northern Baffin Bay. Recurvature of component branches of the WGC, which attains a maximum baroclinic transport of 0.7 Sv, occurs primarily in Melville Bay (0.2 Sv), south of the Carey Islands (0.1 Sv) and ultimately in Smith Sound (0.2 Sv). The Baffin Current originates as an ice-edge jet in Smith Sound and is augmented by net outflow from Smith, Jones and Lancaster Sounds at rates of 0.3 Sv, 0.3 Sv and 1.1 Sv, respectively. Circulation in Smith, Jones and Lancaster Sounds can be described in terms of the Geostrophic Estuarine Circulation Model. The North Water is caused by the combined influences of near-surface layer enthalpy and mechanical ice removal. GRA

N88-22510# Naval Postgraduate School, Monterey, Calif.
CHANGES IN THE CALIFORNIA CURRENT SYSTEM OBSERVED OFF NORTHERN CALIFORNIA DURING JULY-AUGUST 1986 M.S. Thesis
Michael E. Beasley, Mary L. Batteen, and Christopher N. Mooers Dec. 1987 73 p
(AD-A190027; NPS-68-88-002) Avail: NTIS HC A04/MF A01 CSCL 08C

Changes in the flow pattern of the California Current System (CCS) in a relatively short time period (approx. one week) are investigated. The offshore flow pattern changed orientation from southwestward to southward on a cool filament seen previously was no longer discernible. The nearshore flow pattern changed from a predominantly southward to a northward flow. The changes occurred between two OPTOMA cruises conducted in the summer of 1986. Two possible causes are investigated for these changes: (1) a change in a poleward undercurrent of the CCS, and (2) a change in the coastal winds. Analysis of cross sections of the poleward undercurrent indicate that it remained subsurface throughout the cruises. Analysis of wind data indicate that southward winds were the dominant wind pattern throughout the first cruise. Wind data from a moored buoy off Point Arena indicate northward winds (i.e., wind reversals) following the first cruise, which could be associated with the changes in the flow patterns of the CCS. GRA

N88-22511# Naval Postgraduate School, Monterey, Calif.
THE EFFECTS OF TIME-DEPENDENT WINDS AND OCEAN EDDIES ON ICE MOTION IN A MARGINAL ICE ZONE M.S. Thesis
Jeffrey L. Barker Dec. 1987 53 p
(AD-A190105) Avail: NTIS HC A04/MF A01 CSCL 08L

Observations made during the MIZEX program indicate the presence of mesoscale eddies in the ocean front at the marginal ice edge in the East Greenland Current. The eddies ranged in scale from 5 to 80 km. Barotropic and baroclinic instability may be the physical mechanisms responsible for the existance of such eddies. The observations also indicate transient wind reversals (3 to 10 m/s) with a frequency of several days. Here the effect of time-dependent winds and ocean eddies on ice motion in a marginal ice zone is studied. Results are obtained with a two-layer, nonlinear, primitive equation ocean model and a coupled free-drift ice model. THe results indicate that ocean eddy signature in the ice edge is sensitive to cross-ice-edge motion induced by the winds and is shown to be dependent on magnitude, direction, and duration of the wind. GRA

51 LIFE SCIENCES (GENERAL)

N88-22512# Pennsylvania Univ., Philadelphia. Dept. of Bioengineering.
MICROWAVE DISPERSION AND ABSORPTION IN TISSUES: MOLECULAR MECHANISMS Final Report, 1 Jan. 1978 - 28 Feb. 1986
Kenneth R. Foster 10 Dec. 1987 13 p
(Contract N00014-78-C-0392; Proj. RR0-4108)
(AD-A190118) Avail: NTIS HC A03/MF A01 CSCL 06G

We measured the dielectric properties of materials (tissues, aqueous protein solutions, microemulsions, macroscopic suspensions) from 0.1 to 18 GHz. These properties are determined over this frequency range by the dielectric properties of water and by ionic effects. Analysis of the data shows that the dielectric properties of the suspending water differ from those of the pure liquid, presumably due to interfacial effects. Similar effects are seen in diverse transport properties and even in nonaqueous systems. The results suggest that water within a couple of monolayers from surfaces have motional correlation times that are tenfold or so longer than those of the bulk liquid. We suggest that this motional restriction is a physical effect due to the presence of relatively immobile surfaces, rather than from chemically specific binding. This study has led to an improved understanding of the mechanisms of absorption of microwave energy in tissues, and shown the usefulness of comparative studies of transport processes in complex suspensions. GRA

N88-22513# Pacific Northwest Labs., Richland, Wash.
CHARACTERIZATION OF SPACE RADIATION ENVIRONMENT IN TERMS OF THE ENERGY DEPOSITION IN FUNCTIONALLY IMPORTANT VOLUMES
L. A. Braby, N. F. Metting, W. E. Wilson, and C. A. Ratcliffe Jan. 1988 10 p Presented at the Conference on High Energy Radiation Background in Space, Sanibel Island, Fla., 3 Nov. 1987
(Contract DE-AC06-76RL-01830)
(DE88-005627; PNL-SA-15056; CONF-8711149-1) Avail: NTIS HC A02/MF A01

Since the damage which initiates detrimental effects occurs in a small site (semiconductor junctions, or biological cell nuclei), these differences in spatial distribution of ionization maybe the relevant factor controlling the effectiveness of different radiations. Again, when the appropriate cross section data are available Monte Carlo methods can be used to simulate the positions of all ionizations and excitations produced by a typical charged particle.

This calculated track structure must interact with the biological or electronic entity in which it occurs to produce the effect. However, we do not know the mechanisms of this interaction and thus cannot specify which characteristics of the charged particle track are responsible for the relevant damage. From track structure we can obtain the spectrum of energy deposition in small volumes which may be relevant to the processes of concern. This has led to a new approach to dosimetry, one which emphasizes the stochastic nature of energy deposition in small sites, known as microdosimetry. DOE

N88-22514# Rochester Univ., N. Y. Medical Center.
STUDIES OF MOLECULAR BIOLOGY Final Report
1988 24 p
(Contract DE-FG02-85ER-60281)
(DE88-005906; DOE/ER-60281/3) Avail: NTIS HC A03/MF A01

This report is the annual summary for the Studies on Molecular Biology Program of the Biophysics Department of the University of Rochester, Medical Center. Brief summaries of five studies are provided. Each individual study was also abstracted and indexed for the Energy Data Base. DOE

N88-22515*# Lockheed Engineering and Management Services Co., Inc., Washington, D.C.
USSR SPACE LIFE SCIENCES DIGEST, ISSUE 16
Lydia Razran Hooke, ed., Ronald Teeter, ed., Bette Siegel, ed., P. Lynn Donaldson, ed., Lauren B. Leveton, ed., and Joseph Rowe, ed. (Library of Congress, Washington, D. C.) Apr. 1988 124 p
(Contract NASw-4292)
(NASA-CR-3922(19); NAS 1.26:3922(19)) Avail: NTIS HC A06/MF A01 CSCL 06C

This is the sixteenth issue of NASA's USSR Life Sciences Digest. It contains abstracts of 57 papers published in Russian language periodicals or presented at conferences and of 2 new Soviet monographs. Selected abstracts are illustrated with figures and tables from the original. An additional feature is the review of a book concerned with metabolic response to the stress of space flight. The abstracts included in this issue are relevant to 33 areas of space biology and medicine. These areas are: adaptation, biological rhythms, bionics, biospherics, body fluids, botany, cardiovascular and respiratory systems, developmental biology, endocrinology, enzymology, exobiology, gastrointestinal system, genetics, gravitational biology, habitability and environmental effects, hematology, human performance, immunology, life support systems, man-machine systems, mathematical modeling, metabolism, microbiology, musculoskeletal system, neurophysiology, nutrition, operational medicine, perception, personnel selection, psychology, radiobiology, reproductive biology, and space biology. Author

52 AEROSPACE MEDICINE

Includes physiological factors; biological effects of radiation; and effects of weightlessness on man and animals.

N88-22516# Tracer Technologies, Inc., Somerville, Mass.
A LASER-BASED PHOTOACOUSTIC SPECTROMETER FOR DIRECT BREATH C-13O2/C-12O2 MEASUREMENT Final Report
F. Walsh Aug. 1987 38 p
(Contract DE-FG02-85ER-60344)
(DE88-004915; DOE/ER-60344/1) Avail: NTIS HC A03/MF A01

The use of C-13 enriched tracers in health care settings has been limited despite repeated scientific validation and practical application advantages. One limitation has been the absence of a low-cost, operator-easy instrument for the measurement of the extent of C-13 enrichment of samples obtained after ingestion or injection of C-13 enriched tracers. Under DOE Contract DE-AC02-82ER-60063, tracer demonstrated that a laser-based photoacoustic spectrometer could be used to accurately measure CO2 content in gases. The objective of the present program was to test whether such an instrument could be used to accurately measure C-13 enrichment in CO2 in breath samples. Under the present program, tracer designed and made a dual-chamber resonant spectrophone coupled with a computer-based data acquisition and analysis system. The laser used to drive the spectrophone was a rf-modulated CO2 laser with C-13O2 fill. The data obtained under the program demonstrated that the laser-based photoacoustic spectrophone is capable of accurate measurement of breath samples; however, the precision in the measurement of specific samples is not sufficient to warrant the use of this instrument in health care settings. DOE

N88-22517# Nevada Univ., Las Vegas.
EVALUATION OF EXISTING TOTAL HUMAN EXPOSURE MODELS
M. D. Pandian Dec. 1987 94 p
(Grant EPA-R-812189)
(PB88-146840; EPA-600/4-87-044) Avail: NTIS HC A05/MF A01 CSCL 06P

A special class of models is examined and several existing formulations are compared. These models use pollutant concentration distributions and human time-activity patterns, methods of matching concentrations and activities, the number of pollutants that can be handled, accommodation of short-term and long-term exposures, treatment of uncertainties and errors in modeling techniques. Models are also compared to ascertain whether the computer program itself is well written. Author

N88-22518# Air Force Inst. of Tech., Wright-Patterson AFB, Ohio. School of Engineering.
MOTION SICKNESS: QUANTITATIVE, ALGORITHMIC MALAISE INDICATION IN REAL TIME M.S. Thesis
Edward L. Fix Dec. 1987 109 p
(AD-A189674; AFIT/GE/ENG/87D-18) Avail: NTIS HC A06/MF A01 CSCL 06J

Physiological data were collected on human volunteers to study the effects of motion sickness. Data were analyzed and correlated using least squares curve fitting and other statistical methods that are described. An equation is developed that relates five separate physiological signals to subjective motion sickness. A computer program is presented and described which takes the physiological signals in real time and computes the motion sickness. A pattern recognition type of approach which uses a neural net is presented and discussed as an alternative to the equation model. The two models are compared. This disorder is characterized by a variety of symptoms; the most prevalent are nausea, pallor, sweating, and vomiting. Other possible symptoms include salivation, feeling of warmth, light-headedness, depression or apathy, yawning and drowsiness, belching or flatulence, headache, and occasionally hyperventilation. They are brought on by unusual or provocative motion stimulus, either real or perceived. The leading theory about the mechanism of motion sickness is the sensory conflict theory. It says that when there is a conflict between different parts of the balance system, motion sickness can result. GRA

N88-22519# Krug International, San Antonio, Tex. Technology Services Div.
A COMPARISON OF VISUAL EVOKED POTENTIAL AND BEHAVIORAL MEASURES OF FLASHBLINDNESS IN HUMANS Final Report, Sep. 1985 - Oct. 1986
Fred H. Previc and Ralph G. Allen Sep. 1987 17 p
(Contract F33615-84-C-0600)
(AD-A189757; USAFSAM-TR-87-21) Avail: NTIS HC A03/MF A01 CSCL 06J

A comparison between visual evoked potential (VEP) and behavioral measures of flashblindness following exposure to intense but eyesafe xenon flashes was performed. The purpose was to further validate the animal model of laser flashblindness based on VEP recordings in anesthetized rhesus monkeys. Monopolar VEPs were recorded from the posterior scalp of six human subjects in response to square-wave gratings of three differential spatial frequencies. The VEPs were recorded prior and

subsequent to the presentation of a 125-ms, 7, 3 log td-s xenon flash. The results showed that the moment of initial post-flash visibility of the grating as assessed by the VEP's recovery above its baseline was highly comparable to that measured behaviorally. This comparison was demonstrated more clearly in the group data than in data obtained from individual subjects, suggesting that the predictive ability of the VEP depends in part on its signal-to-noise ratio. In general, the the assumptions underlying the animal flashblindness model are largely supported by the high correlations between predicted and obtained recovery estimates in this study and previous monkey studies. GRA

N88-22520# Wisconsin Univ., Milwaukee. Dept. of Psychology.
MECHANISMS MEDIATING PERCEPTION OF COMPLEX ACOUSTIC PATTERNS Final Report, 1 Aug. 1986 - 30 Jul. 1987
Richard M. Warren 20 Nov. 1987 4 p
(Grant AF-AFOSR-0304-86)
(AD-A189765; AFOSR-87-1636TR) Avail: NTIS HC A02/MF A01 CSCL 05H

Five items of equipment were acquired under this instrumentation grant: a filter system for audio waveforms, a two channel audio synthesizer, a two track recorder, a two channel Fast Fourier Transformation (FFT) system, and a sound spectrograph. All are used in a laboratory devoted to the relationship between acoustic features and auditory perception. GRA

N88-22521# Brigham and Women's Hospital, Boston, Mass.
A PROGRAM FOR THE STUDY OF SKELETAL MUSCLE CATABOLISM FOLLOWING PHYSICAL TRAUMA Annual Report, Sep. 1982 - Sep. 1984
Douglas W. Wilmore 6 Dec. 1987 42 p
(Contract DAMD17-81-C-1201)
(AD-A189771) Avail: NTIS HC A03/MF A01 CSCL 06O

The purpose of this work was to attenuate skeletal muscle proteolysis in the post-traumatic period. In the initial study, amino acid solutions were administered with or without glutamine supplementation. Amino Acid administration at the dose of 0.624 grams nitrogen kg hour was associated with near nitrogen balance, maintenance of skeletal muscle intracellular stores, and attenuation of hind-quarter nitrogen loss. In additional studies, adrenergic blockade was achieved by administering phentolamine and propranolol or utilizing high epidural anesthesia. While blockade did not reduce nitrogen excretion in the posttraumatic period, nitrogen efflux from the hind-quarter was markedly attenuated. This is the first demonstration of a relationship between the adrenergic nervous system and accelerated proteolysis. The significance of these findings is discussed. GRA

N88-22522# Yale Univ., New Haven, Conn. School of Medicine.
LABORATORY EQUIPMENT UPDATE Final Report, 1 Sep. 1986 - 31 Aug. 1987
Joy Hirsch 31 Oct. 1987 14 p
(Grant AF-AFOSR-0308-86)
(AD-A189781; AFOSR-87-1728TR) Avail: NTIS HC A03/MF A01 CSCL 06D

We have digitized the cone centers of a primate and a human photoreceptor lattice and have determined that the Nyquist limit predicts visual resolution out to nearly two degrees of retinal eccentricity. Beyond 2 degrees lattice disorder appears to have a deleterious factor between cone density and aperture size. A developing model of lattice structure and design strategies reflects complex principles involved in the evolution of human spatial vision. We are currently exploring a bottom up model of human vision where sampling limitations are propagated along the spatial vision processing hierarchy. The observations that this model addresses include a new class of two dimensional spatial discriminated more accurately than the bisection of two points of comparable separation. This discovery has led to the development of two additional lines of research, area discrimination and dot density discrimination. We have identified a fundamental similarity between spatial frequency discrimination and vernier acuity that demonstrates that Weber's Law applied similarity to both tasks. Further, we have shown that two-dot vernier discrimination falls off within two degrees of retinal eccentricity similarly to changes in retinal sampling. These findings contribute to a model of spatial discriminations that includes limits imposed at the sampling level of the visual process. GRA

N88-22523# Loyola Univ., Chicago, Ill. Hearing Inst.
COMPLEX SOUND PROCESSING: AN INTERDISCIPLINARY APPROACH Final Report, 1 Oct. 1986 - 1 Oct. 1987
William A. Yost, Richard R. Fay, and William Shofner 10 Nov. 1987 4 p
(Grant AF-AFOSR-0054-87)
(AD-A189782; AFOSR-87-1931TR) Avail: NTIS HC A02/MF A01 CSCL 06D

Complex sounds describe most of the sounds that are perceived in our everyday life. However, most of our present knowledge is about the neural process of simple sounds. More knowledge is required about the neural processing of complex signals and about how animals process similar complex sounds. This proposal was to purchase two real-time, high-speed data acquisition computers similar to the one used for the human perception research at the Parmly Hearing Institute. These computers, MASSCOMPs, will be used to generate stimuli and to analyze behavioral and neurophysiological response. The research in these projects involves the human perception of complex stimuli, and combined animal behavior and neurophysiological measures of some of these stimuli, and combined animal behavior and neurophysiological measures of some of these stimuli. The physiological studies include measurements within the eighth nerve and at the level of the cochlear nucleus of the auditory system. In order to relate these measures to the animal's ability to process these stimuli a series of animal behavioral studies are described. The addition of these computer was essential for the full benefit of a multidisciplinary study of the processing of complex sounds. GRA

N88-22524# Indiana Univ., Bloomington. Bloomington Hearing and Communication Lab.
PERCEPTION OF COMPLEX AUDITORY PATTERNS Final Report, 1 Sep. 1984 - 31 Aug. 1987
Charles S. Watson 2 Nov. 1987 45 p
(Grant AF AFOSR-0337-84)
(AD-A190218; AFOSR-87-1781TR) Avail: NTIS HC A03/MF A01 CSCL 06D

This project continued and extended a series of experiments on the discrimination and identification of complex auditory patterns. The general purpose of this work is to determine the limits of human listeners' abilities to extract information from complex sounds including, but not limited to, those with temporal and spectral properties approximating speech. Experiments used criterion-controlled psychophysical methods in which listeners were trained until approaching asymptotic performance in various discrimination and identification tasks. Advances were made in the following areas: (1) the spectral and temporal range of selective auditory attention; (2) the time course of auditory perceptual learning; (3) informational limits on pattern discrimination; (4) listeners' abilities to learn to attend to multi-tone targets within longer patterns; (5) individual differences in auditory sensitivity, and (6) the perception of spectrally complex sound, including speech and non-speech sounds. GRA

N88-22525# Naval Health Research Center, San Diego, Calif.
NAPPING AND HUMAN FUNCTIONING DURING PROLONGED WORK Interim Report
Paul Naitoh and Robert G. Angus 30 Apr. 1987 41 p
(AD-A190228; NHRC-87-21) Avail: NTIS HC A03/MF A01 CSCL 06J

In prolonged work periods, men and women often forego satisfying their sleep need to complete their assigned jobs, resulting in an accumulation of performance/mood degrading sleep loss and fatigue. Sleep need can be satisfied only by a slow process

of sleeping for an average of 7 to 8 consecutive hours per 24 hour period, i.e., a long period of time-out. However, sleep management suggests that recovery from fatigue and sleepiness during a prolonged work period can be accomplished by short or ultra-short sleep (naps) taken during a prolonged work period. Naps are shown not only to refresh and restore human functioning, but also to maintain performance and mood during a prolonged work period. In this paper, naps power as a counter-degradation measure are described first through the literature review, and then through critical evaluation of studies conducted at the Defense and Civil Institute of Environmental Medicine, Canada and the Naval Health Research Center. GRA

N88-22526# Naval Health Research Center, San Diego, Calif.
PREDICTION OF PHYSICAL FITNESS: ESTIMATED PERCENT BODY FAT USING BODY CIRCUMFERENCES VERSUS WEIGHT-HEIGHT MEASURES Interim Report
Keith A. Peterson, Terry A. Cronan, and Terry L. Conway 30 Jun. 1987 17 p
(AD-A190233; NHRC-87-25) Avail: NTIS HC A03/MF A01 CSCL 06D

Weight-height indices with an estimate of percent body fat based on a few circumference measurements are compared. The utility of alternative obesity/overfatness measures was assessed by comparing the strength of their associations with several measures of physical fitness, including a 1.5-mile run/walk, 2-minute sit-ups test, sit-reach flexibility test, and an average fitness score. Study participants included 5710 Navy men and 477 Navy women. For men, percent body fat estimated from circumference measures predicted all the components of physical fitness significantly better than any of the weight-height indices. For women, estimated percent body fat was a significantly better predictor of two of the four fitness measures. Overall, the pattern of associations between physical fitness and both the estimated percent body fat and the weight-height measures was similar for men and women; however, the correlations between the percent fat and the fitness measures were stronger for men. These findings suggest that the Navy's procedure for estimating fatness using circumference measures provides a better screen for physical fitness than would any of the commonly used indices. GRA

N88-22527# Naval Health Research Center, San Diego, Calif.
DIETARY FACTORS RELATED TO PHYSICAL FITNESS Interim Report
Linda J. Dutton and Terry L. Conway 30 Sep. 1987 33 p
(AD-A190272; NHRC-87-28) Avail: NTIS HC A03/MF A01 CSCL 06H

This study examined the relationship between habitual dietary practices and performance on the physical readiness test required of all activity duty Navy personnel (OPNAV6110.1B). Participants were 1013 men (mean age =26.2 years) stationed aboard 9 Navy ships. The men completed a self report survey of lifestyle and dietary habits and were evaluated on four tests of physical fitness: 1.5-mile run, situps, sit-reach, and percent body fat. A standardized overall fitness score was also computed for each person. Results indicated that the participants tend to skip breakfast, ingest moderate amounts of caffeine, and favor a high-fat, low-fiber diet. Fitness scores were associated with a number of dietary variables, including caffeine intake, between-meal snacking, and overeating (all negatively related to fitness), and having a general nutrition orientation (positively related to fitness). Diet was a significant predictor of fitness, even after controlling for age, exercise, and smoking. GRA

N88-22528# Defence Research Establishment, Ottawa. (Ontario).
ANTHROPOMORPHIC PHANTOM RADIATION DOSIMETRY AT THE NATO STANDARD REFERENCE POINT AT ABERDEEN PROVING GROUND
T. Cousins and L. P. Rushton Apr. 1987 30 p
(AD-A190508; DREO-968) Avail: NTIS HC A03/MF A01 CSCL 06G

As part of the NATO Dosimetry Intercomparison Project, a series of experiments were conducted at Aberdeen Proving Ground in September 1986 in order to determine neutron and gamma-ray doses delivered to various internal and external locations on an anthropomorphic phantom from a fission source. Thus, the effect of such parameters as self-shielding by the body on dosimeter reading may be determined. The results will be used eventually to validate computer simulations of the Aberdeen environment in order to understand completely the correlation between dosimeter reading and bone marrow dose, or other parameters relating to performance decrement. GRA

N88-22529# Central Inst. for the Deaf, St. Louis, Mo.
AUDITORY PERCEPTION OF COMPLEX SOUNDS Final Technical Report, 1 Sep. 1984 - 31 Aug. 1987
Hirsh, Ira J. 30 Oct. 1987 18 p
(Grant AF-AFOSR-0335-84)
(AD-A190528; AFOSR-87-1772TR) Avail: NTIS HC A03/MF A01 CSCL 06D

The studies summarized in this report concern auditory perceptual processes that underlie aspects of complex pattern recognition, whether, of speech, of music, or of environmental sounds. These patterns differ from each other according to the characteristics of individual sound events and also characteristics of the pattern sequences themselves. Among the sound characteristics, the focus is on pitch, quality and duration. It is found that spectral properties of complex tones can be changed to yield changes in both apparent pitch and quality, that individuals differ with respect to relative performance on those dimensions, and that both pitch and quality or timbre can play similar grouping roles in auditory systems. Most of the experimental work has concerned timing of successive sounds in sequences. It is found that at slow rates, listeners detect equally well small temporal offsets or jitters at different positions in the sequence. Increasing the frequency of one of the tones, or increasing the duration of one or two of the successive intervals produces changes in performance at or near the changes. Some of these timing effects are also manifest in the rhythmic aspects of spoken sentences. GRA

N88-22530# Rutgers - The State Univ., New Brunswick, N. J.
SELECTIVE MECHANISMS IN AUDITORY AND BIMODAL SIGNAL PROCESSING Final Scientific Report, 15 Jul. 1983 - 31 May 1987
E. Kowler, S. Sternberg, and R. M. Mulligan 27 Oct. 1987 36 p
(Grant AF-AFOSR-0206-83)
(AD-A190529; AFOSR-87-1773TR) Avail: NTIS HC A03/MF A01 CSCL 05B

The purpose of this research program was the investigation of mechanisms of attention in auditory and bimodal information processing. The manner in which division of attention influences three stages of information processing, stimulus coding, decision making, and response selection, was described previously by the principle investigator in a general, quantitative theory of attention. Previous work had shown that, within the framework of this theory, the effects of division of attention on the first two stages could be separately identified. As in the earlier research, the work reported here has focused on two key issues: what are the decision processes involved in combining information from two or more sources, and what division of attention degrades the information obtained from each source (i.e., does it result in losses of information at the coding stage). GRA

N88-22531# Federal Aviation Administration, Washington, D.C. Office of Aviation Medicine.
AGE, ALCOHOL, AND SIMULATED ALTITUDE: EFFECTS ON PERFORMANCE AND BREATHALYZER SCORES
William E. Collins and Henry W. Mertens Jan. 1988 20 p
(AD-A190642; DOT/FAA/AM-88/2) Avail: NTIS HC A03/MF A01 CSCL 06K

Trained men in two groups, 30 to 39 (n=12) and 60 to 69 (n=13), each performed at the Multiple Task Performance Battery (MTPB) in four separate full-day sessions with and without alcohol

(2.2 mL of 100-proof vodka per kg of body weight) at ground level and at a simulated altitude of 12,500 ft (3810 m). Subjects breathed appropriate gas mixtures through oxygen masks at both ground level and altitude. Mean breathalyzer readings peaked near 88 mg percent and did not differ between age groups or altitude conditions. Younger subjects performed better than older subjects; performance of both age groups was significantly impaired by alcohol, but these adverse effects were greater for the older subjects. No significant effects on performance were obtained due to altitude or to the interaction of altitude with alcohol. These results and those from several other studies suggest that prevalent views regarding the nature of the combined effects of alcohol and altitude on blood levels and on performance need to be redefined. GRA

N88-22532# Technische Hogeschool, Eindhoven (Netherlands).
METHODS OF MEASUREMENT FOR THE EVALUATION OF MONOLAYER PROPERTIES. DEVELOPMENT AND APPLICATIONS Ph.D. Thesis
Paulus Maria Corneli Gieles 1987 175 p
(ETN-88-92229) Avail: NTIS HC A08/MF A01

In order to understand the role of lung surfactant and its components, and in order to develop criteria for an artificial surfactant or for the maturity of lung surfactant, methods of measurement were studied. Four methods, concerned with the physico-chemical properties of surfactant, and which establish the interfacial tension to surface area relation (sigma-A) are described: the Langmuir-Wilhelmy method; asymmetric method; Benjamins-de Feijter method; and oscillating bubble method. It is argued that drawing conclusions about the in-vivo behavior of lung surfactant from sigma-A measurements is not justified. ESA

N88-22237# Joint Publications Research Service, Arlington, Va.
PROTECTION AGAINST LASER DAMAGE TO HUMAN BODY REVIEWED
Bingyu Yan *In its* JPRS Report: Science and Technology. China 11 Dec. 1987 p 17-23 Transl. into ENGLISH from Yingyong Jiguang (Shanghai, Peoples Republic of China), v. 7, no. 4, Aug. 1987 p 172-176 (For primary document see N88-22233 15-31)
Avail: NTIS HC A06/MF A01

53 BEHAVIORAL SCIENCES

Includes psychological factors; individual and group behavior; crew training and evaluation; and psychiatric research.

N88-22533# Massachusetts Univ., Amherst.
ADAPTIVE NEURAL NETWORK ARCHITECTURE Final Report, 1 Aug. 1986 - 31 Jul. 1987
Andrew Barto 28 Oct. 1987 4 p
(Grant AF-AFOSR-0260-86)
(AD-A190114; AFOSR-87-1789TR) Avail: NTIS HC A02/MF A01 CSCL 05I

Sun microsystems computer equipment acquired through Grant AFOSR-86-0260 is being used for research directed toward developing learning methods and architectures for artificial neural networks, or connectionist networks. The equipment is being used to simulate artificial neural networks implementing a variety of learning methods, including the Associative Reward-Penalty method and the Adaptive Critic Algorithm, as well as the error backpropagation method, and various combinations of these learning methods. GRA

N88-22534# Purdue Univ., West Lafayette, Ind. Dept. of Psychological Sciences.
AUDITORY PATTERN MEMORY: MECHANISMS OF TONAL SEQUENCE DISCRIMINATION BY HUMAN OBSERVERS Final Report, 1 Sep. 1984 - 31 Aug. 1987
Robert D. Sorkin 30 Sep. 1987 46 p
(Grant AF AFOSR-0302-84)
(AD-A190337; AFOSR-87-1775TR) Avail: NTIS HC A03/MF A01 CSCL 12F

A two-process model of pattern discrimination was developed to describe how tonal sequences are processed, stored, and discriminated by the human auditory system. The model was tested in tasks in which subjects were required to discriminate between the frequency patterns encoded in two sequences of tones. The experimental results strongly supported the assumptions of a trace and context coding mechanism and indicated that the trace mechanism is relatively insensitive to temporal transformations made to the stimulus. An attempt to model the pattern discrimination mechanism with specific computational algorithms was less successful. A technique was developed to assess the manner in which information is accumulated from elements of an auditory or visual stimulus. Results indicate that the technique may be useful in the design of display systems. GRA

N88-22535# Aerospace Medical Research Labs., Wright-Patterson AFB, Ohio.
CONFLICT RESOLUTION IN COOPERATIVE SYSTEMS Final Report, Oct. 1985 - Oct. 1987
Daniel E. Snyder and Michael D. McNeese Oct. 1987 93 p
(AD-A190351; AD-E500947; AAMRL-TR-87-066) Avail: NTIS HC A05/MF A01 CSCL 12I

An integrated conflict resolution methodology is described in terms of its potential to reduce cognitive conflicts within cooperating human-intelligent systems environments. Three specific components of this methodology are presented. The first component, The Description/Depiction of Total Knowledge Concepts, explains a representational schema for depicting and isolating conflicting processes/states. The second component, Resolution Processes within Total Knowledge Concepts, proposes a baseline conflict resolver along with a review of theoretical positions regarding the processes of conflict resolution. This stage also describes the requirements for integrating human and non-human intelligent systems through the use of the human intelligence perspective. The result of this union is the creation of an intelligent architecture of resolution. The role of blackboard and processing models is outlined for such an architecture. The third component, Experimentation in Human Conflict Resolution, suggests direction that conflict resolution research must go to make significant contributions. The report's emphasis is on human cognitive analogs that provide examples for the modeling of conflict resolution processes. GRA

54 MAN/SYSTEM TECHNOLOGY AND LIFE SUPPORT

Includes human engineering; biotechnology; and space suits and protective clothing.

For related information see also *16 Space Transportation.*

N88-22536# Transportation Systems Center, Cambridge, Mass.
ANALYSIS OF HEAD RESPONSE TO TORSO ACCELERATION. VOLUME 2: DESCRIPTION OF DATA RETRIEVAL, ANALYSIS AND DISPLAY SOFTWARE Final Report, Dec. 1982 - Jul. 1986
C. H. Spenny Dec. 1987 152 p Sponsored by National Highway Traffic Safety Administration, Washington, D.C.
(PB88-156765; DOT-TSC-NHTSA-86-6-Vol-2; DOT-HS-807-158-Vol-2) Avail: NTIS HC A08/MF A01 CSCL 05H

The data retrieval, analysis and display software described here consists of a general purpose data manipulation program, the Data Retrieval and Display (DRD) program, and a pair of specialized analysis programs, HEAD and NECK. The DRD program is user friendly and is designed to quickly and efficiently retrieve and graphically display data on head and neck response. HEAD and NECK are programs written for use in the analysis of head and neck response. Author

N88-22537# Applied Technologies, Inc., Boulder, Colo.
ULTRASONIC OXYGEN SENSOR Final Report, May 1986 - Aug. 1987
W. R. Dagle Dec. 1987 28 p
(Contract F33615-86-C-4503)
(AD-A189723; USAFSAM-TR-87-31) Avail: NTIS HC A03/MF A01 CSCL 14B

The respirable gases generated by an on board oxygen generation system (OBOGS) are comprised of a mixture of oxygen, argon, and nitrogen. This gas mixture can be measured ultrasonically to determine the concentration of oxygen within the mixture. This final report describes an ultrasonic measurement system that has been successfully tested to a simulated altitude of 20,000 ft. The concentration of oxygen calculated from ultrasonic data is accurate to approximately 1 percent over the range of 21 to 95 percent. In addition to measuring the concentration of oxygen, the ultrasonic oxygen sensor can also measure the flow rate of the respirable gases produced by an OBOGS accurate to approximately 1.6 L/min. GRA

N88-22538# Federal Aviation Administration, Washington, D.C. Office of Aviation Medicine.
AN EVALUATION OF THE EFFECTS OF HIGH VISUAL TASKLOAD ON THE SEPARATE BEHAVIORS INVOLVED IN COMPLEX MONITORING PERFORMANCE
Richard I. Thackray and R. M. Touchstone Jan. 1988 16 p
(AD-A190641; DOT/FAA/AM-88/1) Avail: NTIS HC A03/MF A01 CSCL 05H

Operational monitoring situations, in contrast to typical laboratory vigilance tasks, generally involve more than just stimulus detection and recognition. They frequently involve complex multidimensional discriminations, interpretations of significance, decisions as to appropriate action, implementation of action, and evaluation of consequences. A simulated air traffic control (ATC) task was developed to study the effects of prolonged monitoring on a number of such behaviors. All subjects performed the task under relatively high visual taskload conditions for a single 120-min session. Time to detect aircraft at the same altitude increased significantly over the monitoring period as did omission errors for this type of event. Detection time for the more readily detectible alphanumeric changes involving loss of altitude information showed no evidence of impairment, nor was any impairment found for any of the other task behaviors that were measured. The findings are discussed with reference to previous studies suggesting that complex monitoring primarily effects attentional processes and that the rate of decline in attention appears to be related to the degree of information processing required for event detection. GRA

N88-22539# Air Force Human Resources Lab., Brooks AFB, Tex.
RELATIONSHIP OF ENCODING SPEED AND MEMORY TESTS TO FLIGHT TRAINING PERFORMANCE Interim Report, Sep. 1983 - Dec. 1986
Thomas R. Carretta Mar. 1988 24 p
(AD-A190670; AFHRL-TP-87-49) Avail: NTIS HC A03/MF A01 CSCL 05H

The demands on the cognitive/perceptual abilities of military pilots have increased steadily as aircraft have become more sophisticated. The ability to encode and classify signals and to retrieve information from short-term memory are two of the several cognitive/perceptual abilities that have been linked to flying performance. Two tests, Encoding Speed (encoding and classification ability) and Immediate/Delayed Memory (short-term memory retrieval), were administered to 2,219 United States Air Force pilot candidates prior to entry into Undergraduate Pilot Training (UPT). Performance on the Encoding Speed test was related to successful completion of UPT, in-flight performance measures, and advanced training assignment. However, scores on the Immediate/Delayed memory test were not related to training performance. Pilot candidates who made quick or accurate responses on the Encoding Speed test were more likely to perform well on in-flight performance measures and be recommended for post-UPT training in a fast-jet (Fighter-Attack-Reconnaissance) aircraft. Implications for pilot selection and classification are discussed. GRA

N88-22540*# Stanford Univ., Calif. Center for Design Research.
DESIGN, DEVELOPMENT AND EVALUATION OF STANFORD/AMES EVA PREHENSORS Final Report
Larry J. Leifer, J. Aldrich, M. LeBlanc, E. Sabelman, and D. Schwandt May 1988 10 p
(Contract NCC2-295)
(NASA-CR-182688; NAS 1.26:182688) Avail: NTIS HC A02/MF A01 CSCL 05H

Space Station operations and maintenance are expected to make unprecedented demands on astronaut EVA. With Space Station expected to operate with an 8 to 10 psi atmosphere (4 psi for Shuttle operations), the effectivness of pressurized gloves is called into doubt at the same time that EVA activity levels are to be increased. To address the need for more frequent and complex EVA missions and also to extend the dexterity, duration, and safety of EVA astronauts, NASA Ames and Stanford University have an ongoing cooperative agreement to explore and compare alternatives. This is the final Stanford/Ames report on manually powered Prehensors, each of which consists of a shroud forming a pressure enclosure around the astronaut's hand, and a linkage system to transfer the motions and forces of the hand to mechanical digits attached to the shroud. All prehensors are intended for attachment to a standard wrist coupling, as found on the AX-5 hard suit prototype, so that realistic tests can be performed under normal and reduced gravity as simulated by water flotation. Author

55 SPACE BIOLOGY

Includes exobiology; planetary biology; and extraterrestrial life.

No abstracts in this category.

59 MATHEMATICAL AND COMPUTER SCIENCES (GENERAL)

N88-22541*# National Aeronautics and Space Administration. Langley Research Center, Hampton, Va.
BOUNDARY SHAPE IDENTIFICATION PROBLEMS IN TWO-DIMENSIONAL DOMAINS RELATED TO THERMAL TESTING OF MATERIALS Final Report
H. T. Banks and Fumio Kojima Mar. 1988 33 p Submitted for publication
(Contract NAS1-18107)
(NASA-CR-181654; ICASE-88-23; NAS 1.26:181654) Avail: NTIS HC A03/MF A01 CSCL 12A

The identification of the geometrical structure of the system boundary for a two-dimensional diffusion system is reported. The domain identification problem treated here is converted into an optimization problem based on a fit-to-data criterion and theoretical convergence results for approximate identification techniques are discussed. Results of numerical experiments to demonstrate the efficacy of the theoretical ideas are reported. Author

60 COMPUTER OPERATIONS AND HARDWARE

Includes hardware for computer graphics, firmware, and data processing.

For components see *33 Electronics and Electrical Engineering.*

N88-22542# Los Alamos National Lab., N. Mex.
MONITORING THE USAGE OF A COMPUTER SYSTEM
D. J. Bailey Nov. 1987 14 p Presented at the IEEE Symposium on Security and Privacy, Oakland, Calif., 1 Apr. 1988
(Contract W-7405-eng-36)
(DE88-004310; LA-UR-87-4103; CONF-880456-1) Avail: NTIS HC A03/MF A01

Controlling the usage of computer systems particularly those operated for the Federal government, is an important topic today. Audit requirements have grown to the point where they can be a significant burden to the proprietors of the system. The paper briefly mentions several proposals for responding to increased audit requirements and for monitoring a system to detect unauthorized activity. A technique is proposed for situations where the proscribed or the intended activity can be characterized in terms of program or system performance parameters. The design of a usage monitoring system is outlined. The design is based on enhancing the audit data provided by the monitored system, capturing the audit data in a separate system to protect it from user access, and implementing one of the audit trail analysis systems currently under development. DOE

N88-22543# Gosudarstvennyi Komitet po Ispolzovaniyu Atomnoi Energii, Moscow (USSR). Inst. Teoreticheskoj i Ehksperimentalnoj.
FAST ANALOG-TO-DIGITAL CONVERTER [BYSTRODEJSTVUYUSHCHIJ ANALOGO-TSIFROVOJ PREOBRAZOVATEL]
A. P. Semenov and O. V. Sokolova 1987 11 p In RUSSIAN
(TI88-701488; ITEF-59(1987)) Avail: NTIS (US Sales Only) HC A03/MF A01

A fast analog-to-digital device for data acquisition and processing is described. Two analog-to-digital converters (ADC), an analog buffer, a clock pulse generator and an interface unit are its main elements. The fast ADC unit is constructed using large integrated circuits. The frequency of input channel digitation equals 20 MHz, ADC digit is 6 bit. The maximum duration of the signal processed is approx. 20 microsec. DOE

N88-22544# Gosudarstvennyi Komitet po Ispolzovaniyu Atomnoi Energii, Moscow (USSR). Inst. Teoreticheskoj i Ehksperimentalnoj.
APPLICATION OF STATIC MEMORY FOR DATA ACQUISITION AND TRANSMISSION INTO A COMPUTER [ISPOLZOVANIE STATICHESKOJ PAMYATI DLYA NAKOPLENIYA DANNYKH I PEREDACHI IKH V EHVM]
I. N. Borodina, G. K. Bysheva, L. N. Gusev, and V. P. Chernyshev 1987 11 p In RUSSIAN
(TI88-701491; ITEF-156(1987)) Avail: NTIS (US Sales Only) HC A03/MF A01

A bloc diagram and principle of operation of the data acquisition and transmission system using multiwire detectors is described. There are two static memory units based on integrated circuits in the system. The volume of the static memory is 2 banks at 2048 bytes each. Time for filling of a data bank is 10 ms. The total time of data transmission from one bank is 5 ms. The system speeds up by approx. 5 times the acquisition of data and its transmission into a computer. DOE

N88-22545# Grenoble-1 Univ. (France). Techniques de lInformatique, des Mathematiques, de la Microelectronique et de la Microscopie Quantit
SELF-CHECKING LOGIC ARRAYS
M. Nicolaidis and B. Courtois Apr. 1987 26 p
(RR-656-I; ETN-88-92285) Avail: NTIS HC A03/MF A01

Schemes ensuring the concurrent error detection for programmable logic arrays, ROMs, and RAMs and for a realistic fault model are presented. The schemes are checked by simple codes and necessitate low area overhead. The solutions proposed may be chosen according to criteria such as the area overhead, fault coverage, or automatic design and optimization. ESA

N88-22546# National Computing Centre Ltd., Manchester (England).
Ada (TRADEMARK) COMPILER VALIDATION SUMMARY REPORT. ALSYS: AlsyCOMP-013, V2.0 HOST: IBM PC AT. TARGET: IBM 370 3084Q
30 Apr. 1987 61 p
(AD-A189640) Avail: NTIS HC A04/MF A01 CSCL 12E

This Validation Summary Report (VSR) summarizes the results and conclusions of validation testing performed on the AlsyCOMP-013, V2.0 using Version 1.8 of the Ada Compiler Validation Capability (ACVC). The AlsyCOMP-013 V2.0, is hosted on a IBM PC AT operating under PC/DOS, V3.1. Programs processed by this compiler may be executed on a IBM 370 3084Q operating under MVS, V3.2. GRA

N88-22547# Pittsburgh Univ., Pa. Dept. of Computer Science.
PARALLEL MEMORY ADDRESSING USING COINCIDENT OPTICAL PULSES
Donald Chirulli, Rami Melhem, and Steve Levitan Dec. 1987 21 p
(AD-A189767) Avail: NTIS HC A03/MF A01 CSCL 12F

The common computer bus, shared memory, multiprocessors are the most widely used parallel processing architectures. Unfortunately, such systems suffer from a memory/bus bandwidth limitation problem. For the designer of a hybrid optical/electronic supercomputer, an immediate temptation is to replace the shared electronic bus with an optical analog of higher bandwidth. To make that replacement is only a partial solution. The true bottleneck in such systems is in the address decoding circuits of shared memory units. In this paper we propose a new memory structure which provides for parallel access in a multiprocessor environment. The proposed system has two advantages. First, it distributes the address decoding circuitry to each of the requesting units on a common bus, thus eliminating the bottleneck of centralized decoding of encoded memory addresses. Second, it allows for parallel fetches of memory data with a level of parallelism limited only by the ratios of optical to electronic bus bandwidths and the dimensionality of the memory array. GRA

N88-22548# BDM Corp., McLean, Va.
APPLICATIONS OF OPTICAL COMPUTING TO PROBLEMS WITH SYMBOLIC COMPUTATIONS Quarterly Report No. 7, 1 Aug. 1986 - 1 Nov. 1987
Brian G. Kushner 31 Oct. 1987 5 p
(Contract F49620-86-C-0030)
(AD-A189772; AFOSR-87-1743TR) Avail: NTIS HC A02/MF A01 CSCL 20F

This report, experimentally demonstrates digital all-optical Compare and Energy circuits based on our original designs. The circuits use ZnS bistable optical devices in novel operational modes such as bidirectional and latching logic. These modes are central to the low complexity of the implementation. In addition, the experimental demonstration utilizes polarization multiplexing and filtering to reduce crosstalk, losses and feedback in the optical system. The capabilities of optical interconnection networks are generally useful in parallel processing and specifically useful in sorting. GRA

N88-22549# Boston Univ., Mass. Center for Adaptive Systems.
INSTRUMENTATION FOR SCIENTIFIC COMPUTING IN NEURAL NETWORKS, INFORMATION SCIENCE, ARTIFICIAL INTELLIGENCE AND APPLIED MATHEMATICS Final Progress Report, 30 Jul. 1986 - 29 Jul. 1987
Stephen Grossberg Oct. 1987 5 p
(Grant AF-AFOSR-0282-86)

(AD-A189981; AFOSR-87-1966TR) Avail: NTIS HC A02/MF A01 CSCL 12I

This was an instrumentation grant to purchase equipment of support of research in neural networks, information science, artificial intelligence, and applied mathematics. Computer lab equipment, motor control and robotics lab equipment, speech analysis equipment and computational vision equipment were purchased. GRA

N88-22550# VERAC, Inc., San Diego, Calif.
OPTICAL CONCEPTUAL COMPUTING AND ASSOCIATIVE MEMORY (OCCAM) Final Report, 1 Jun. 1986 - 1 Jun. 1987
Sep. 1987 36 p
(Contract F49620-86-C-0070)
(AD-A190030; R-088-87; AFOSR-88-0148TR) Avail: NTIS HC A03/MF A01 CSCL 09E

The Optical Conceptual Computing and Associative Memory (OCCAM) program applied the techniques of neural-network dynamical systems analysis and fuzzy theory to problems in conceptual computing. Key contributions are detailed in the ten technical papers included in the Appendix. Three fundamental results were: the development of bidirectional associative memories (BAMs), a fuzzy knowledge combination scheme that allows arbitrarily many neural (casual) network expert systems from experts with arbitrary credibility to be naturally synthesized into a single, representative associative knowledge network, and the development of pure fuzzy associative memories (FAMs). UCSD focused on the theory and application of optical neurocomputing. Four fundamental research strategies were: the design and implementation of optical neural networks, especially optical BAMs, the investigation of physical properties important to neural network implementations, the application of optics to fuzzy knowledge processing and to fuzzy computing (approximate reasoning) in general, and the application of neural netwrok principles to optical pattern recognition. Holographic and nonholographic BAM systems were devised, with emphasis on volume holography. A backpropagation (hierarchial supervised learning) network was taught to perform rotation-invariant pattern recognition. GRA

N88-22551# Illinois Univ., Urbana.
SUPERCOMPUTER ENVIRONMENT Annual Technical Report, 1 Oct. 1986 - 30 Sep. 1987
30 Oct. 1987 7 p
(Contract F49620-86-C-0136)
(AD-A190633; AFOSR-87-1968TR) Avail: NTIS HC A02/MF A01 CSCL 12E

This summary covers goals and first year accomplishments of the Faust project, a research effort to develop a software engineering environment of supercomputer application development. The goal of Faust is to provide a user-friendly workstation of integrated development tools that caters to a broad range of user expertise. Faust comprises individual efforts in the area of user interface tools, expert systems, parallel program debugging, performance evaluation, symbolic processing, error analysis, and graphics. The Faust project is additionally supporting efforts in the areas of fluid and structural dynamics. Overall project goals are outlined, followed by a summary of the first contract year's accomplishments presented to the Faust project review team on August 6, 1987. GRA

61 COMPUTER PROGRAMMING AND SOFTWARE

Includes computer programs, routines, alogorithms, and specific applications, e.g., CAD/CAM.

N88-22552*# Tennessee Space Labs., Inc., Manchester.
INVESTIGATION INTO THE DEVELOPMENT OF COMPUTER AIDED DESIGN SOFTWARE FOR SPACE BASED SENSORS Final Report
C. W. Pender and W. L. Clark 31 Aug. 1987 79 p
(Contract NAS5-30061)
(NASA-CR-180772; NAS 1.26:180772) Avail: NTIS HC A05/MF A01 CSCL 09B

The described effort is phase one of the development of a Computer Aided Design (CAD) software to be used to perform radiometric sensor design. The software package will be referred to as SCAD and is directed toward the preliminary phase of the design of space based sensor system. The approach being followed is to develop a modern, graphic intensive, user friendly software package using existing software as building blocks. The emphasis will be directed toward the development of a shell containing menus, smart defaults, and interfaces, which can accommodate a wide variety of existing application software packages. The shell will offer expected utilities such as graphics, tailored menus, and a variety of drivers for I/O devices. Following the development of the shell, the development of SCAD is planned as chiefly selection and integration of appropriate building blocks. The phase one development activities have included: the selection of hardware which will be used with SCAD; the determination of the scope of SCAD; the preliminary evaluation of a number of software packages for applicability to SCAD; determination of a method for achieving required capabilities where voids exist; and then establishing a strategy for binding the software modules into an easy to use tool kit. Author

N88-22553# Rochester Univ., N. Y. Dept. of Computer Science.
A PROBABILISTIC APPROACH TO LOW-LEVEL VISION
David B. Sher Oct. 1987 215 p
(Contracts N00014-82-K-0193; DACA76-85-C-0001)
(AD-A189041; TR-232) Avail: NTIS HC A10/MF A01 CSCL 23C

A probabilistic approach to low-level vision algorithms results in algorithms that are easy to tune for a particular application and modules that can be used for many applications. Several routines that return likelihoods can be combined into a single more robust routine. Thus it is easy to construct specialized yet robust low-level vision systems out of algorithms that calculate likelihoods. This dissertation studies algorithms that generate and use likelihoods. Probabilities derive from likelihoods using Bayes' rule. Thus vision algorithms that return likelihoods also generate probabilities. Likelihoods are used by Markov Random Field algorithms. This approach yields facet model boundary pixel detectors that return likelihoods. Experiments show that the detectors designed for the step edge model are on par with the best edge detectors reported in the literature. Algorithms are represented here that use the generalized Hough transform to calculate likelihoods for object recognition. Evidence, represented as likelihoods, from several detectors that view the same data with different models are combined here. The likelihoods that result are used to build robust detectors out of several specialized ones. Results are shown here for combining boundary detectors that assume several levels of noise and combining detectors of several sizes. GRA

N88-22554# Bhabha Atomic Research Centre, Bombay (India).
PROJECT MONITORING PACKAGE (PMP): A PACKAGE FOR PROJECT ACTIVITY MONITORING
K. N. Vyas, A. Kannan, R. Susandhi, and S. Basu 1987 6 p
(DE88-701234; BARC-1349) Avail: NTIS (US Sales Only) HC A02/MF A01

A package for preparing PERT/CPM network diagrams has been written for PDP-11/34. The program uses PLOT-10 library calls for device interfacing. The package is essentially non-interactive in nature, and reads input data in the form of activity description and duration. It calculates the critical path time and performs time scaling of the events. The report gives a brief outline of the logic used, a sample plot and tabular output for reference. An additional facility for performing project activity monitoring has also been implemented. Activity monitoring generally requires various reports such as feed back reports from various group co-ordinators, information report for project co-ordinator and brief periodical reports for management. A package DATATRIEVE (DTR) on PDP-11/34 system is utilized for generating the above

mentioned reports. As DTR can also use normal sequential files, an interfacing program has been written which reformats the files accepted by PERT program acceptable to DTR. Various types of reports as generated by DTR are included. However this part of the package is not transportable and can be implemented only on systems having DTR. DOE

N88-22555# Bhabha Atomic Research Centre, Bombay (India).
COMESH: A CORNER MESH FINITE DIFFERENCE CODE TO SOLVE MULTIGROUP DIFFUSION EQUATIONS IN MULTIDIMENSIONS
V. Jagannathan, A. K. Kulkarni, and R. P. Jain 1987 42 p
(DE88-701248; BARC-1367) Avail: NTIS (US Sales Only) HC A03/MF A01

A code called COMESH based on corner mesh finite difference scheme has been developed to solve multigroup diffusion theory equations. One can solve 1-D, 2-D or 3-D problems in Cartesian geometry and 1-D (r) or 2-D (r-z) problem in cylindrical geometry. On external boundary one can use either homogeneous Dirichlet (theta-specified) or Neumann (nablatheta specified) type boundary conditions or a linear combination of the two. Internal boundaries for control absorber simulations are also tackled by COMESH. Many an acceleration schemes like successive line over-relaxation, two parameter Chebyschev acceleration for fission source, generalised coarse mesh rebalancing etc., render the code COMESH a very fast one for estimating eigenvalue and flux/power profiles in any type of reactor core configuration. DOE

N88-22556# Louisiana State Univ., Baton Rouge. Dept. of Computer Science.
THE VISIT PROBLEM: VISIBILITY GRAPH-BASED SOLUTION
N. S. V. Rao, S. S. Iyengar, and G. deSaussure 1987 30 p Presented at the IEEE International Conference on Robotics and Automation, Philadelphia, Pa., 25 Apr. 1988 Prepared in cooperation with Oak Ridge National Lab., Tenn.
(Contract DE-AC05-84OR-21400)
(DE88-000343; CONF-880424-2) Avail: NTIS HC A03/MF A01

The visit problem is defined as follows: a circular body R is located at point d sub 0 in a finite-sized two-dimensional terrain populated by a finite number of polygonal obstacles; each obstacle has a finite number of vertices. The R is equipped with a sensor system capable of detecting all vertices and edges seen from it's present location. A computing device with storage capability is also housed on R. Initially, the R is located at a point d sub 0, and no terrain model is available to R. The R is capable of translational motion. The R is required to execute a navigational mission which involves visiting a sequence of the destination points, namely d sub 1, d sub 2,...,d sub M, in the specified order. We present the algorithm LNAV that navigates R from d sub i to d sub i + 1. We prove the correctness of this algorithm, and also estimate its performance in terms of the number of scan operations, the distance traversed and the computational complexity. We then present the algorithm GNAV that executes the navigational mission. It uses LNAV in traversing in between successive destination points in the mission, and builds a global visibility graph of the terrain by integrating the sensor information obtained, over a period of time, as R keeps navigating. DOE

N88-22557# Massachusetts Univ., Amherst.
COMPUTER GRAPHICS TOOLS FOR THE STUDY OF MINIMAL SURFACES
M. Callahan, D. Hoffman, and J. T. Hoffman Aug. 1987 39 p
(Contract DE-FG02-86ER-25015)
(DE88-006421; DOE/ER-25015/2) Avail: NTIS HC A03/MF A01

This paper discusses the use of computer graphics to represent the mathematical concepts of minimal surfaces. Analysis and examples of minimal surfaces are given. DOE

N88-22558# Bhabha Atomic Research Centre, Bombay (India).
PLOT3D (VERSION-5): A COMPUTER CODE FOR DRAWING THREE DIMENSIONAL GRAPHS, MAPS AND HISTOGRAMS, IN SINGLE OR MULTIPLE COLOURS, FOR MONO OR STEREOSCOPIC VIEWING
Balhans Jayaswal 1987 70 p
(DE88-701410; BARC-1369) Avail: NTIS (US Sales Only) HC A04/MF A01

PLOT3D series of graphic codes (version 1 to 5) were developed for drawing three dimensional graphs, maps, histograms and simple layout diagrams on monochrome or color raster graphic terminal and plotter. Of these, PLOT3D Version-5 is an advanced code, equipped with several features that make it specially suitable for drawing 3D maps, multicolor 3D and contour graphs, and 3D layout diagrams, in axonometric or perspective projection. Prior to drawing, graphic parameters that define orientation, magnification, smoothening, shading, color-map, etc., of the figure can be selected interactively by means of simple commands on the user terminal, or by reading those commands from an input data file. This code requires linking with any one of three supporting libraries: PLOT 10 TCS, PLOT 10 IGL, and CALCOMP, and the figure can be plotted in single color, or displayed in single or multiple colours depending upon the type of library support and output device. Furthermore, this code can also be used to plot left and right eye view projections of 3D figure for composing a stereoscopic image from them with the aid of a viewer. DOE

N88-22559# Bhabha Atomic Research Centre, Bombay (India).
OUTPUT FORMATTING IN APPLE-SOFT BASIC
A. S. Navale 1987 14 p
(DE88-701413; BARC-1374) Avail: NTIS (US Sales Only) HC A03/MF A01

Personal computers are being used extensively in various fields. BASIC is a very popular and widely used language in personal computers. Apple computer is one of the popular machines used for scientific and engineering applications. Presenting output from computers in a neat and easy to read form is very important. Languages like FORTRAN have utility command FORMAT which takes care of the formatting of the output in user-defined form. In some versions of BASIC a PRINT USING facility is available but it is not as powerful as the FORTRAN statement FORMAT. Apple-soft BASIC does not have even this PRINT USING command. Programmers have to write their own program segments to handle output formatting in Apple-soft BASIC. Generally, such user written programs are of limited use as they cannot be used easily with other programs. A general purpose and easily transportable subroutine in Apple-soft BASIC is presented here for handling output formatting in user-defined structure. The subroutine is nearly as powerful as the FORMAT statement in FORTRAN. It can also be used in other versions of BASIC with very little modifications. DOE

N88-22560 National Physical Lab., Teddington (England). Div. of Materials Applications.
COMPUTER GRADING OF EXTENSOMETERS (BS 3846)
Steven E. Booth Dec. 1987 24 p
(NPL-DMA(A)-152; ISSN-0143-7313; ETN-88-92076) Copyright Avail: National Physics Laboratory, Teddington, Middlesex, TW11 OLW, United Kingdom

A computer program to analyze and grade extensometers and transducers for creep and tensile testing machines, in accordance with British Standard 3846 is presented. The program runs on an IBM PC AT microcomputer, using DOS version 3.2 and IBM Disk BASIC and includes automatic printout of the calibration certificate. ESA

N88-22561 Politecnico di Milano (Italy). Dipt. di Elettronica.
MULTIPLE-TRANSFORM PIPELINES FOR IMAGE CODING
Anna Antola 1987 36 p
(Rept-87-038; ETN-88-92272) Avail: Politecnico di Milano, Piazza Leonardo da Vinci 32, 20133 Milan, Italy

Definition of pipelined VLSI/WSI architectures supporting image coding transforms, such as the Fourier transform, the discrete

cosine transform, and the discrete sine transform is considered. The structures were derived by considering a common algorithmic kernel of the transforms. The pipelines are composed by a basic pipeline performing the common kernel of computation and by transform-dependent input and output stages. Three different pipelines were defined and figures of merit, such as silicon area occupation and throughput, were evaluated for architecture comparisons. ESA

N88-22562 Politecnico di Milano (Italy). Dipt. di Elettronica.
AN INTELLIGENT SIMULATION MODEL GENERATOR
G. Guariso, M. Hitz, and H. Werthner 1987 16 p Spondored by Rank Xerox
(Rept-87-053; ETN-88-92273) Avail: Politecnico di Milano, Piazza Leonardo da Vinci 32, 20133 Milan, Italy

The conceptual design and a prototype implementation of an intelligent interactive generator of simulation models is presented. The system manages a model base, a knowledge base, and a data base. Integration of the model and the knowledge base is emphasized. Connection of numeric and knowledge representation components is one of the main advantages of the approach. The prototype was implemented on a XEROX 1186 workstation and takes advantage of the presence of two processors: a LISP processor managing the logical description, selection, and maintenance of models as well as the overall control of the system and the user interface, and an 8088 processor to run the simulation programs that are written in classical programming languages. The system is designed to free scientists from details about computer science and to let them concentrate on simulation problems. ESA

N88-22563# Grenoble-1 Univ. (France). Lab. dInformatique Fondamentale et dIntelligence Artificielle.
ON THE GEOMETRIC INTERPRETATION OF IMAGE CONTOURS
Radu Horaud and Michael Brady Mar. 1987 26 p Submitted for publication
(RR-647-I-IMAG-57-LIFIA; ETN-88-92279) Avail: NTIS HC A03/MF A01

A computational model for the 3D interpretation of a 2D view based on contour classification and contour interpretation is suggested. Contours arising from discontinuities in surface orientation are stressed. A generic surface description well suited for visual tasks is combined with a model of the image formation process in order to derive image contour configurations that are likely to be interpreted in terms of surface contours. A computer algorithm to interpret image contours is described. An image analysis process produces a description in terms of contours and relationships between them. Among these contours, those which form a desired configuration are selected, and the selected contours are combined with constraints available with the image formation process in order to be interpreted in terms of discontinuities in surface orientation. As a consequence, there is a dramatic reduction in the number of possible orientations of the associated scene surfaces. ESA

N88-22564# Grenoble-1 Univ. (France). Techniques de lInformatique, des Mathematiques, de la Microelectronique et de la Microscopie Quantit
CONSISTENT ESTIMATES OF AUTOREGRESSIVE PARAMETERS FOR AUTOREGRESSIVE MOVING AVERAGE MODELS
Pham Dinh Tuan May 1987 26 p
(RR-663-I; ETN-88-92286) Avail: NTIS HC A03/MF A01

A quick algorithm for estimating autoregressive parameters for an autoregressive moving average model is presented. The algorithm is recursive in the order, and can be used for model selection, by providing a criterion and a two-way table of certain partial covariances. Consistency and asymptotic normality of the estimate are shown. ESA

N88-22565# Air Force Inst. of Tech., Wright-Patterson AFB, Ohio. School of Engineering.
A UNIX-BASED INTERACTIVE VHDL (HARDWARE DESCRIPTION LANGUAGE) SIMULATOR M.S. Thesis
Harvey H. Kodama 7 Dec. 1987 79 p
(AD-A189749; AFIT/GE/ENG/87D-33) Avail: NTIS HC A05/MF A01 CSCL 12E

This thesis effort investigated and implemented a UNIX-based VHDL subset interactive simulator. The simulator was written in the C programming language. The simulator is capable of handling many of the VHDL operators, sequential assignment statements, and concurrent statements. Although the simulator is a subset, the data structures were designed to incorporate the features of the complete VHDL version 7.2. GRA

N88-22566# California Univ., Berkeley. Dept. of Electrical Engineering and Computer Science.
SimPL: A SIMULATOR FOR PARALLEL LISP Technical Report, 7 Aug. 1984 - 6 Aug. 1987
Lisa Penninger 2 Jun. 1987 76 p
(Contract N00039-84-C-0087; ARPA Order 4871)
(AD-A189831) Avail: NTIS HC A05/MF A01 CSCL 12G

In spite of the great interest in speeding up programs by using parallelism, few convenient parallel machines are available, and those may not have the types of parallelism of greatest benefit. This paper describes a simulator, written in Common LISP, that provides a method for experimenting with varying amounts of explicit (programmer-specified) parallelism, and gathering information about the efficiency of such programs if they were to be run on a parallel processor. The system chosen for simulation is Multilisp. Its parallel constructs are quite simple, and rely heavily on the programmer to decide on their efficient and correct use. Multilisp is explained in a later section of this paper; however, a working knowledge of some dialect of LISP is assumed. GRA

N88-22567# Air Force Inst. of Tech., Wright-Patterson AFB, Ohio. School of Engineering.
IMPLEMENTATION OF A DISTRIBUTED ADAPTIVE ROUTING ALGORITHM ON THE INTEL iPSC (INTEL PERSONAL SUPER-COMPUTER) M.S. Thesis
Tommy C. Farinelli Dec. 1987 103 p
(AD-A189849; AFIT/GCS/ENG/87D-11) Avail: NTIS HC A06/MF A01 CSCL 12E

The use of distributed adaptive routing algorithms on concurrent class computers is examined. The implemented routing algorithm allowed each node to select the next node based on two criteria: the fewest number of hops; and the smallest delay time. This study was limited to the comparison of a distributed adaptive routing algorithm, implemented at the applications layer, with the current static routing and with a simulation of the current routing implemented at the applications layer. The comparison with the simulated current static routing provides a measure of the possible performance gain had the adaptive routing algorithm been implemented at the network layer. Each of three configuration was comprised of four processes: a Host Process, a Routing Process, a Ring Control Process, and a Network Loading Process. The Host Process controlled the loading of the processes onto the iPSC, the Routing Process controlled the message routing, the Ring Control Process provided the baseline message passing, while the Network Loading Process provided communications congestion on selected links. The metric used to compare the Routing Process performance was the average delay time for passing a message around the ring. congestion on selected links. The metric used to compare the Routing Process performance was the average delay time for passing a message around the ring. GRA

N88-22568# Naval Postgraduate School, Monterey, Calif.
TUTORIAL ON GAMS (GENERALIZED ALGEBRAIC MODELING SYSTEM): A MODELING LANGUAGE FOR OPTIMIZATION
Richard E. Rosenthal Jan. 1988 39 p

(AD-A189867; NPS55-88-001) Avail: NTIS HC A03/MF A01 CSCL 12E

The Generalized Algebraic Modeling System (GAMS), developed by Alexander Meeraus, Anthony Brooke et al., is a language for expressing mathematical models in a form that is both easily understandable to a modeler and processible by a computer. For practitioners and researchers, it can greatly reduce the time required for formulating, documenting, solving and analyzing large, complex linear, nonlinear and integer programs. For teachers and students, it is a valuable tool for learning advanced modeling. This paper is a tutorial for the beginning GAMS user. GRA

N88-22569# Naval Postgraduate School, Monterey, Calif.
MEMORY EFFICIENT EVALUATIONS OF NONLINEAR STOCHASTIC EQUATIONS AND C3 APPLICATIONS M.S. Thesis
John C. Connell, Jr. Dec. 1987 70 p
(AD-A189872) Avail: NTIS HC A04/MF A01 CSCL 25E

The Statistical Mechanical Neural Computer (SMNC) developed in this thesis utilizes a Statistical Mechanical Nonlinear Algorithm (SMNA) to determine the long-time probability distribution of highly nonlinear stochastic systems. The use of the SMNA and a novel mesoscopic scaling technique help provide the SMNC with the capabilities of neural computers without the drawbacks of huge connection matrices and their attendant computational requirements. In this thesis, the SMNC is initially used to verify the ability of the SMNA to duplicate relatively simple, single variable path integral solutions to nonlinear Fokker-Planck equations. After the fundamental algorithms are validated, the SMNC's ability to simulate a two-variable, multicellular problem by modeling a portion of the neocortex consisting of 100,000 neural units is discussed. There are many important applications of the SMNC and its unique SMNA to C3 systems including radar, sonar and electronic signals processing, missile guidance systems and an integrated battle management system. Such C3 systems will benefit from the SMNC's potential to efficiently filter large amounts of data, recognize patterns and anticipate, with some degree of uncertainty, the future state of highly nonlinear stochastic systems. GRA

N88-22570# Washington Univ., Seattle. Dept. of Computer Science.
AN ANALYSIS OF MULTIPLE GRAIN CHIP ARCHITECTURES Final Report, 15 Apr. 1985 - 30 Sep. 1986
Lawrence Snyder 28 Feb. 1987 11 p
(Contract N00014-85-K-0328)
(AD-A189942) Avail: NTIS HC A03/MF A01 CSCL 12F

The major accomplishments of the Blue CHiP Project Multigrain Architecture Research are described in the areas of theory, algorithms, architecture software and VLSI. A multigauge architecture is a design for a standard von Neumann machine that permits the data path to be partitioned into subunits that can execute concurrently when the data values are small. Thus, it is a method of achieving parallelism within the arithmetic/logic unit of a computer that is applicable to both stand alone serial processors and to the processor elements of highly parallel computers. Its advantages are the twin benefits of parallelism for narrow data and the ability to use the processor in its regular mode under programmer control when full precision is necessary. There is the added benefit that multigauging is available with minimal added hardware in certain cases, but this is simply a benefit, not the justification for the architecture. GRA

N88-22571# Science Applications International Corp., San Diego, Calif.
METHODOLOGY FOR SOFTWARE RELIABILITY PREDICTION, VOLUME 1 Final Report, Jun. 1983 - May 1987
J. McCall, W. Randall, C. Bowen, N. McKelvey, and R. Senn Nov. 1987 204 p
(Contract F30602-83-C-0118)
(AD-A190018; RADC-TR-87-171-Vol-1) Avail: NTIS HC A10/MF A01 CSCL 12E

The variation in fault density on Air Force programs in enormous: the worst programs are 390 times more error-prone than the best. Obviously, there are some critical differences in these programs that cause more errors to be introduced or left undetected. If we could solve the problem of what these differences are and how to control them, then we would have learned something fundamental about the occurrence of errors in software and how to avoid them. This report describes the results of a research and development effort to develop a methodology for predicting and estimating software reliability. A software Reliability Measurement Framework was established which spans the life cycle of a software reliability. Data from 59 systems, representing over 5 million lines of code, were analyzed and generally applicable observations about software reliability were made. A detailed approach to the collection and analysis of reliability data is also presented. GRA

N88-22572# Science Applications International Corp., San Diego, Calif.
METHODOLOGY FOR SOFTWARE RELIABILITY PREDICTION, VOLUME 3 Final Report, Jun. 1983 - May 1987
J. McCall, W. Randall, C. Bowen, N. McKelvey, and R. Senn Nov. 1987 174 p
(Contract F30602-83-C-0118)
(AD-A190019; RADC-TR-87-171-Vol-2) Avail: NTIS HC A08/MF A01 CSCL 12E

The Guidebook provides detailed procedures for the preparation of software reliability predictions and estimations on DOD projects. In developing the Guidebook, 59 software systems were examined and 19 key variables were identified that affected the software reliability of those systems. Procedures to measure these variables were developed to account for the type of application, development, environment, various software characteristics (such as modularity and complexity), test technique, test effort and test coverage. A methodology was also provided to use these measures to predict software fault density and software failure rates. The Guidebook could be applied by an Air Force acquisition office to help plan for adequate software reliability early in a project's life, specify achievable software reliability goals in a RFP, evaluate progress toward those goals at key project milestones and decide when to release the software. The Guidebook could also be used by the technical staff to establish thresholds for critical measures such as complexity. In addition the Guidebook also contains Quality Review and Standards Review Checklists that can be used in conjunction with the software reliability prediction and estimation methodology. The Quality Review Checklists are used to assess the quality of the requirements and design representation of the software while the Standards Review Checklist would be applied to software code. The checklists provide good guidance for ensuring that quality is built into the software. GRA

N88-22573# Yale Univ., New Haven, Conn.
RAPID FEATURE EXTRACTION VIA THE RADON TRANSFORM Final Report, 1 Oct. 1985 - 1 Dec. 1987
Arthur F. Gmitro and Gene R. Gindi 1 Feb. 1988 33 p
(Grant AF AFOSR-0344-85)
(AD-A190032; AFOSR-88-0172TR) Avail: NTIS HC A03/MF A01 CSCL 12I

The area of neural-net associative memories and their optical implementations is explored. The problem of organizing an associative memory to reflect known structure in the pattern is addressed; because the structure is encoded as a model in the memory, the memory differs considerably from simple pattern matchers where an iconic version of the pattern is stored. Early work concentrated on encoding a compositional hierarchy within the memory. Though this worked well, the theory was inadequate to explain the behavior of the memory. An optimization approach was adopted in which the goal of the computation could be stated in a mathematical objective function. The ideas of compositional and inheritance hierarchies were encoded directly into the objective function. A simulator was completed demonstrating these ideas. Optical implementation was concerned with the problem of implementing ever more general interconnect patterns. The investigators began with the construction of a system that computed

Radon Transforms of the input object. This demonstrated the necessary first step of an optical connection scheme to transform objects to parameter spaces. A more complex system was built demonstrating discrete space-invariant connection patterns. This worked satisfactorily. The current work involves designs for holographic space-variant connection patterns. GRA

N88-22574# Stanford Univ., Calif. Center for Reliable Computing.
EXHAUSTIVE AND PSEUDO-EXHAUSTIVE TESTING
Edward J. McCluskey Jul. 1987 88 p
(Contract N00014-85-K-0600)
(AD-A190140; CRC-TR-87-13; CSL-TN-87-331) Avail: NTIS HC A05/MF A01 CSCL 12F

This chapter discusses an approach to test pattern generation for functional testing of combinational digital integrated circuits. The techniques to be presented apply all possible input patterns either to the entire circuit under test or to portions of the circuit under test. For some circuits, exhaustive testing is economically practical; all possible input combinations are applied to the entire circuit. An exhaustive test is a complete functional test and no assumptions about the internal structure of the circuit under test are required. When the number of inputs is so large that an exhaustive test is impractical, it is still possible to retain many of the advantages of exhaustive testing by using a pseudo-exhaustive test technique, which requires that some details of the internal circuit structure either be known or assumed. A disadvantage of exhaustive and pseudo-exhaustive testing is the size of the test sets, they can be substantially larger than minimum-length test sets. The major advantages of exhaustive and pseudo-exhaustive tests are the extremely high fault coverage, the generality of the fault model, and the absence of a requirement to do fault simulation. Another advantage of output function verification is the ease of generating the test set. Segmentation and determination of the corresponding test sets requires more computation. GRA

N88-22575*# Jet Propulsion Lab., California Inst. of Tech., Pasadena.
EXTENSION OF COMPUTER BASED ALGORITHMS BY OPERATOR ANALYSTS Final Report
Michael W. Rennie (Mathematical Analysis Research Corp., Claremont, Calif.) 28 Apr. 1987 7 p
(Contract NAS7-918)
(NASA-CR-182798; JPL-D-4624; NAS 1.26:182798; AD-A190173; ALGO-Pub-0097; TM-27) Avail: NTIS HC A02/MF A01 CSCL 09B

Algorithm development should have two phases. The computer portion and the portion to be incorporated in operator analyst training. A knowledgeable operator analyst should be able to perform analysis beyond the means of any particular computerized algorithm available to that analyst. This follows from the fact that humans can understand the consequences of the limitations of particular computer implementations and correct, in part, for them. Computer based algorithm limitations may have different causes: (1) the algorithms may be based on incomplete or inaccurate models; (2) the algorithms may not be flexible enough to adapt to the need for changes in analysis criteria; (3) the algorithms may take shortcuts because of limitations in computer storage or speed; (4) there may be refinements in the analysis which could be computed but are not because they depend on parameters which are insufficiently well known; and (5) computer output formats may be restrictive. GRA

N88-22576# Indiana Univ., Bloomington. Dept. of Computer Science.
TRANSFORMATIONS OF CONCURRENT ALGORITHMS FOR HIGHLY PARALLEL SYSTEMS: A ONE YEAR PROJECT SUMMARY REPORT Final Report, period ending 1 Oct. 1987
Dennis Gannon Oct. 1987 6 p
(Grant AF AFOSR-0147-86)
(AD-A190236; AFOSR-87-1737TR) Avail: NTIS HC A02/MF A01 CSCL 12F

It has become a certainty that Multiple Instruction Stream, Multiple Data Stream (MIMD) parallel architectures are going to play a major role in all aspects of high speed computer design for the foreseeable future. What is not clear is whether we will be able to devise a means to design algorithms and software for these machines that transcends our current ad hoc, nonportable techniques. In this research project the author has focused on the portability issue from the perspective of parallel algorithm design and how it effects the internal organization of advanced compilers. The eventual goal of the project is to produce an expert system that can help users transform large, complex applications from one highly parallel machine to another. The basic strategy has been to follow the following plan: (1) build an experimental research laboratory for parallel computation; (2) design and experimental program of research that would shed light on the problems involved with restructuring parallel programs for different machines; (3) attempt to provide a mathematical characterization of the properties of the machines and how algorithms must be restructured to run on them; and (4) attmept to design a model of machine architecture that can be embedded into the inference engine or knowledge base of an expert system for program restructuring. GRA

N88-22577# JAYCOR, Vienna, Va.
CK-LOG SYSTEM CONVERSION (USER'S MANUAL AND USER INTERFACE)
16 Jun. 1987 7 p
(Contract N00014-86-C-2352)
(AD-A190273) Avail: NTIS HC A02/MF A01 CSCL 12F

The CK-LOG code written in TOPS-20 ELISP has been converted to Common LISP, and is running on the LMI Lambda. This required both across-the-board syntactic changes in functions as well as entire rewriting of functions. There was no need to change any domain data, as the domain was rebuilt from scratch in Common LISP. A user interface/display for Oplan-Consultant was created. It uses both CK-LOG routines and LMI windowing facilities. There are two categories of information that can be displayed: the lattice of time events and the lattice of class information. Time events are markers in the CK-LOG domain (database of information, or world state) which indicate that some change has occurred at a particular time. The change could be an addition to the domain, a deletion, or a change in a pre-existing condition. CK-LOG is unique in that it associates a time with these changes, thereby allowing for logical reasoning about the feasibility of assertions made to the domain. The time lattice displays event numbers, representing events in time, in a bottom-up tree. GRA

N88-22578# Massachusetts Inst. of Tech., Cambridge. Lab. for Computer Science.
ARGUS REFERENCE MANUAL
Barbara Liskov, Mark Day, Maurice Herlihy, Paul Johnson, and Gary Leavens Nov. 1987 160 p
(Contract N00014-83-K-0125; Grant NSF DCR-85-03662)
(AD-A190382; AD-E801598; MIT/LCS/TR-400) Avail: NTIS HC A08/MF A01 CSCL 12E

Argus is an experimental language/system designed to support the construction and execution of distributed programs. Argus is intended to support only a subset of the applications that could benefit from being implemented by a distributed program. Two properties distinguish these applications: they make use of on-line data that must remain consistent in spite of concurrency and hardware failures, and they provide services under real-time constraints that are not severe. Examples of such applications are office automation systems and banking systems. Argus is based on CLU. It is largely an extension of CLU, but there are differences. Like CLU, Argus provides procedures for procedural abstraction, iterators for control abstraction, and clusters for data abstraction. In addition, Argus provides guardians that encapsulate and control access to one or more resources. Argus also provides equate modules as a convenient way to refer to constants. As in CLU, modules may be parameterized, so that a single module can define a class of related abstractions. GRA

N88-22579# Massachusetts Inst. of Tech., Cambridge. Artificial Intelligence Lab.
SOFTWARE STRUCTURING PRINCIPLES FOR VLSI CAD
Jacob Katzenelson and Richard Zippel 3 Dec. 1987 19 p
(Contracts N00014-86-K-0180; N00014-80-C-0622)
(AD-A190386; AD-E801598; AI-M-1008) Avail: NTIS HC
A03/MF A01 CSCL 12E

VLSI CAD systems are typically large and undergo frequent changes. A frustrating aspect of these changes is that so little of the old available programs can be reused. The reason is that it takes too much time and effort to find the reuseable pieces and recast them for the new use. We believe that such systems should be designed for reusability by anticipating change. Our thesis is that this goal can be achieved by designing the software as layers of problem oriented languages, which are implemented by suitably extending a base language. A language layer rarely needs to be adapted to changes, only the application (i.e., algorithm) needs to be changed. We illustrate this methodology with respect to VLSI CAD programs and a particular language layer: a language for handling networks. A concept shared by many CAD programs is that of networks consisting of components and their interconnects. We capture this common part by providing a language for handling network problems. Such a language consists of our base language (EC or Lisp) plus data types, operations and control structures that are relevant to network problems. GRA

N88-22580# Air Force Inst. of Tech., Wright-Patterson AFB, Ohio. School of Engineering.
DESIGN AND IMPLEMENTATION OF VLSI PRIME FACTOR ALGORITHM PROCESSOR M.S. Thesis
Robert S. Hauser Dec. 1987 168 p
(AD-A190483; AFIT/GCE/ENG/87D-5) Avail: NTIS HC
A08/MF A01 CSCL 12F

High-speed digital signal processing has a wide range of applications including, radar, sonar, image processing, and target acquisition. The calculations of the Discrete Fourier Transform (DFT) used in these applications has long been a significant bottleneck for high-speed processing. Previous AFIT students have adopted a Prime Factor Algorithm (PFA) method using Winograd Fourier Transform (WFT) processors. Three WFT processors are pipelined into a system capable of computing a 4080-point DFT on complex data approximately every 120 microseconds when operating with a 70 MHz clock. This thesis effort addressed the design and implementation of PFA controller chip and interconnecting memory modules between the WFT processors. The PFA controller is an application specific processor to control the flow of information in the pipeline, interface to the WFT processors, monitor pipeline status, and take corrective action in the presence of faults. The interconnecting memory modules buffer the data coming out of a WFT processor and going into another allowing concurrent reading and writing. GRA

N88-22581# Air Force Inst. of Tech., Wright-Patterson AFB, Ohio. School of Engineering.
DESIGN OF AN ALGORITHM TO TRANSLATE NESTED RELATIONAL ALGEBRA QUERIES TO GENESIS TRACE MANAGER COMMANDS M.S. Thesis
Alan F. Hartman Dec. 1987 98 p
(AD-A190502; AFIT/GCS/ENG/87D-13) Avail: NTIS HC
A05/MF A01 CSCL 12E

This thesis describes an algorithm to convert nested relational queries into GENESIS Trace Manager commands. Nested relational algebra is an extension to traditional relational algebra to include multivalued (i.e., nested) attributes. The GENESIS Trace Manager is part of the GENESIS database management system being developed at the University of Texas at Austin, Texas. The GENESIS Trace Manager is used to manipulate fields in a record that has been read into a buffer in memory. The algorithm consists of two phases. The first phase of the algorithm is the development of an intermediate data structure to represent the various constructs of the nested relational algebra query. The second phase of the algorithm is the conversion of the intermediate data structure into GENESIS Trace Manager commands. This phase consists of dividing the translation into a number of sub-tasks and providing an algorithm to perform each of these sub-tasks. The GENESIS Trace Manager is limited to working with fields in a record located in a buffer in primary memory. It does not include facilities for reading records from a data base into memory, writing records from memory to a database, or presenting the user with a formated output of the result of the query. Because the GENESIS Trace Manager does not include these facilities, the algorithm does not produce GENESIS commands to perform these functions. GRA

N88-22582# Air Force Inst. of Tech., Wright-Patterson AFB, Ohio. School of Engineering.
SOFTWARE VERIFICATION USING PARTITION ANALYSIS M.S. Thesis
Robert P. Graham, Jr. Mar. 1988 68 p
(AD-A190570; AFIT/GCS/MA/88M-02) Avail: NTIS HC
A04/MF A01 CSCL 12E

Software verification is the process of determining whether a piece of software is reliable, whether it performs as it is supposed to. As traditionally performed, program verification can account for 40 percent or more of the development time and cost of a software product. In spite of this fact, released software is notorious for its unreliability. These two facts, the expense of our attempts at program verification and our limited success, have sustained a great deal of research interest directed at finding more effective methods. This thesis develops extensions to a promising new verification technique called Partition Analysis, developed by Debra J. Richardson (1981). Partition Analysis appears to be a powerful approach for identifying program faults, but in its current state can only be applied to single program modules that produce no side effects, including input or output. This thesis extends the applicability of Partition Analysis by permitting the use of procedure and function calls, thereby allowing complete programs to be analyzed. The result is a set of techniques for handling regular, nonrecursive procedure and function calls, separate methods for the analysis of recursive procedures and functions, and an approach to the larger problem of analyzing entire programs. GRA

N88-22583# Air Force Inst. of Tech., Wright-Patterson AFB, Ohio. School of Engineering.
SEARCH: AN INTERACTIVE COMPUTER PROGRAM FOR OPTIMIZING TWO-VARIABLE, UNCONSTRAINED EXPERIMENTS OR SIMULATION M.S. Thesis
Billy G. Ploetner Mar. 1988 70 p
(AD-A190593; AFIT/GST/ENS/88M-9) Avail: NTIS HC
A04/MF A01 CSCL 12A

The purpose of this study was to develop a computer program that incorporates efficient techniques for solving optimization of experimental test or simulation models. The program is interactive and user-friendly. The program is written in FORTRAN but can be attached to any simulation model or experiment. The program is limited to two independent variables and one dependent variable. The study compared several gradient methods and found 2-k factorial the most efficient. The study also concluded that Davies, Swann, and Campey (DSC) - Powell was the most useful line search. The study uses an improvement by Faix to the PARTAN method to eliminate the final linear search. The program is designed to efficiently solve second-order equations and less efficiently higher order equations. GRA

N88-22584# Air Force Inst. of Tech., Wright-Patterson AFB, Ohio. School of Engineering.
A GRAPHICS EDITOR FOR STRUCTURED ANALYSIS WITH A DATA DICTIONARY M.S. Thesis
Steven E. Johnson Dec. 1987 173 p
(AD-A190618; AFIT/GE/ENG/87D-28) Avail: NTIS HC
A08/MF A01 CSCL 12E

A computer tool was designed and implemented that integrated two approaches for documenting software requirements analysis, structured analysis (SA) diagrams and data dictionaries. The tool provides the requirements analyst with an environment for creating the SA diagrams and entering parts of the data dictionary. The

tool derives the remaining data dictionary information from the diagram. Background information is provided on existing structured analysis techniques, data dictionary uses, and on human computer interface design issues. A graphic SA syntax was derived from existing SA techniques and the data dictionary formats were specified by previous work at AFIT. Requirements for the human computer interface as well as the functional aspects of the tool are discussed. A summary of the design decisions made are also presented. The tool was used and evaluated by more than 35 graduate level software engineering students. The students evaluated the tool using a standard questionnaire developed at AFIT for this purpose. The responses were compiled and analyzed using statistical methods and are also presented. Author (GRA)

N88-22585# Massachusetts Univ., Amherst.
THE ELLIPTIC SINH-GORDON EQUATION AND THE CONSTRUCTION OF TOROIDAL SOAP BUBBLES
J. Spruck Oct. 1987 37 p
(Contract DE-FG02-86ER-25015)
(DE88-006426; DOE/ER-25015/6) Avail: NTIS HC A03/MF A01

In this paper we study all positive solutions to the nonlinear eigenvalue problem delta u + lambda sinh u = 0 on a symmetric domain D. We characterize the limit solution as lambda tends to zero. For a rectangle we prove that the solutions are unique and have a hidden additional symmetry property. This equation figures prominently in recent work on the construction of compact soap bubbles of genus 1. DOE

N88-22586# North Carolina State Univ., Raleigh.
CHOLESKY DOWNDATING ON A HYPERCUBE
C. S. Henkel, M. T. Heath, and R. J. Plemmons 1988 7 p Presented at the 3rd Conference on Hypercube Concurrent Computers and Applications, Pasadena, Calif., 19 Jan. 1988 Prepared in cooperation with ORNL, Tenn.
(Contract DE-AC05-84OR-21400)
(DE88-006780; CONF-880117-1) Avail: NTIS HC A02/MF A01

Least squares modifications associated with the addition or deletion of data often involve updating or downdating the Cholesky factor of the observation matrix. We describe and compare parallel implementations for the hypercube of three methods for downdating the Cholesky factor: an orthogonal scheme, a hyperbolic scheme, and a hybrid scheme combining the first two. The computational complexities of these algorithms vary significantly, but the parallel implementations of all three are similar in communication complexity to solving triangular systems. In computational tests on an Intel iPSC hypercube, the algorithms performed similarly, suggesting a preference for the orthogonal method based on stability considerations. The methods we describe can be adapted to the parallel computation of general orthogonal factorizations, but our discussion is motivated by applications in signal processing using windowed recursive least squares filtering for near real-time computations. DOE

N88-22587# Institut Franco-Allemand de Recherches, St. Louis (France).
CONTOUR INTERACTIVE EXTRACTION USING IMAGE NUMERICAL TREATMENT [EXTRACTION INTERACTIVE DE CONTOURS PAR TRAITEMENT NUMERIQUE D'IMAGES]
R. Scherrer 30 May 1986 37 p In FRENCH
(ISL-R-114/86; ETN-88-92014) Avail: NTIS HC A03/MF A01

A computer program is presented based on the median filter concept and the differentiation notion. The goal is the interactive extraction of a maximum likelihood contour, to obtain the contour points coordinates, which are saved in a file. It is shown that the proposed method is valuable, and several illustrations are included. ESA

N88-22588# Ecole Nationale Superieure des Telecommunications, Paris (France). Dept. Informatique.
USING COLORED STOCHASTIC PETRI NET (CS-PN) SOFTWARE FOR PROTOCOL SPECIFICATION, VALIDATION, AND EVALUATION
Alexandre Zenie and Jean-Pierre Luguern (Paris VI Univ., France) 1987 12 p Presented at the 4th Intern. Workshop on Software, Specification and Design, Monterey, Calif., 3-4 Apr. 1987; spons. by IEEE Computer Society; ACM SIGSOFT; ICRST, Japan; Alvey Directorate, United Kingdom; Agence de l'Informatique, France; AFCET, France
(ENST-87C004; ISSN-0751-1337; ETN-88-92172) Avail: NTIS HC A03/MF A01

The specification, verification, validation, and evaluation, which make up the different steps of the CS-PN software are outlined. The colored stochastic Petri net software is applied to a Wound/Wait protocol decomposable into two principal modules: request or couple (transaction, granule) treatment module and wound treatment module. Each module is specified, verified, validated, and then evaluated separately, to deduce a verification, validation and evaluation of the complete protocol. The colored stochastic Petri nets tool is shown to be a natural extension of the stochastic tool, adapted to distributed systems and protocols, because the color conveniently takes into account the numerous sites, transactions, granules and messages. ESA

N88-22589# Ecole Nationale Superieure des Telecommunications, Paris (France). Dept. Informatique.
THE COLORED STOCHASTIC PETRI NET (CS-PN) SOFTWARE: APPLICATION TO THE VALIDATION AND THE PERFORMANCE EVALUATION OF DISTRIBUTED SYSTEMS
Alexandre Zenie Sep. 1987 24 p
(ENST-87D005; ISSN-0751-1345; ETN-88-92175) Avail: NTIS HC A03/MF A01

Use of the colored stochastic Petri net software to analyze the parallelism between the different functions of a distributed system, to validate its operation, and to evaluate its performance is described. The performance analysis proceeds in four steps. (1) The description presents the model in a multivectorial and multifunctional form. (2) The algebraic aggregation constructs the list of states reachable from the initial state (they may be equivalent to one another). This list generates an aggregated state space which is characteristic of the dynamics of the model described. (3) The validation verifies the ergodicity of the model by analyzing the aggregated state space. (4) The performance evaluation is based on the prerequisite construction of the stochastic matrix. Given this matrix, it is possible, by solving a linear functional equation, to deduce the aggregated steady-state probability multivector. Several performance criteria can be computed at the same time, by solving mean-value algebraic equations. The software is applied to a distributed concurrency control model which manages cooperation between different sites. ESA

N88-22590# Instituto de Pesquisas Espaciais, Sao Jose dos Campos (Brazil).
INFERENCE ENGINE FOR EXPERT SYSTEMS Ph.D. Thesis
Edson Luiz FrancaSenne Jan. 1988 165 p In PORTUGUESE; ENGLISH summary
(INPE-4465-TDL/321) Avail: NTIS HC A08/MF A01

A kernel of a tool for building expert systems is proposed. In essence, a language is proposed to express decision rules that will be stored in the system's knowledge base and a meta-knowledge-controlled inference mechanism that uses forward as well as backward chaining and can be adapted to the characteristics of specific domains. The use of a semantic network is also proposed to store structured, well-established knowledge of a domain and to provide information in order to determine suitable contexts for decision rules application. In addition, an approach to inexact reasoning based on the Dempster-Shafer theory is proposed. Author

N88-22591*# National Aeronautics and Space Administration. Lewis Research Center, Cleveland, Ohio.
TWO-DIMENSIONAL GRAPHICS TOOLS FOR A TRANSPUTER BASED DISPLAY BOARD
Graham K. Ellis [1988] 16 p Presented at the Parallel Computing Workshop/OCCAM User Group Meeting, Portland, Oregon, 11-13 Apr. 1988; sponsored by OSU/OCATE and

INMOS
(NASA-TM-100820; E-4010; ICOMP-88-4; NAS 1.15:100820)
Avail: NTIS HC A03/MF A01 CSCL 09B

A package of 2-D graphics routines has been developed in an effort to standardize and simplify the user interface for a transputer based graphics display board. The routines available take advantage of the graphic board's capabilities while also presenting an intuitive approach for generating drawings. The routines allow a user to perform graphics rendering in a 2-D real-coordinate space without regard to the actual screen coordinates. Multiple windows, which can be placed arbitrarily on the screen as well as the ability to use double-buffering techniques for smooth animations are also supported. The routines are designed to be run on a transputer other than the graphics display board. The window and screen parameters are maintained locally. The conversion to device coordinates is also performed locally. The only data sent to the display board are control and device coordinate display commands. The routines available include: rotation translation, and scaling commands; absolute and relative point and line commands; circle, rectangle and polygon commands; and window and viewpoint definition commands. Author

N88-22230# Joint Publications Research Service, Arlington, Va.
SIGMA SYSTEM: OVERVIEW, PROSPECTS
Masaki Nakayama *In its* JPRS Report: Science and Technology. Japan 27 Oct. 1987 p 19-32 Transl. into ENGLISH from Denshi Kogyo Geppo (Tokyo, Japan), no. 6, 1987 p 27-36 (For primary document see N88-22228 15-31)
Avail: NTIS HC A07/MF A01

62 COMPUTER SYSTEMS

Includes computer networks and special application computer systems.

N88-22592# Illinois Univ., Urbana. Dept. of Computer Science.
LOGARITHMICALLY CONNECTED, REPETITIVE COMPUTER NETWORKS AND NUMERICAL APPLICATIONS
C. W. Gear Jan. 1988 19 p
(Contract DE-FG02-87ER-25026)
(DE88-006632; DOE/ER-25026/18; UILU-ENG-88-1706; UIUCDCS-R-88-1402) Avail: NTIS HC A03/MF A01

This note describes regular networks in Cartesian space which are such that any pair of nodes separated by a physical distance d have a connecting path which passes through no more than O(logd) intermediate nodes and yet which have no more than a bounded number of connections to any single node (as opposed to the hypercube, in which the number of connections increases logarithmically as the size of the network). The application of such networks to differential equations is discussed briefly. DOE

N88-22593# Grenoble-1 Univ. (France). Lab. Circuits et Systems.
MODELING A PARALLEL ARCHITECTURE FOR IMAGE PROCESSING
Pierre Houeix and Monique Becker Mar. 1987 25 p
(RR-646-I; ETN-88-92284) Avail: NTIS HC A03/MF A01

A parallel architecture for the management of an image database is described. In order to get the response time, a model of the system is made. An approximate solution is given: a fork-join with p processors and n arrivals (where n is different from p) is approximated by the join of the response times of a multiserver queue with bulk arrivals. The method is of general use. ESA

N88-22594# Air Force Inst. of Tech., Wright-Patterson AFB, Ohio. School of Engineering.
SIMULATION OF FAULT TOLERANCE IN A HYPERCUBE ARRANGEMENT OF DISCRETE PROCESSORS M.S. Thesis
Gil Zilberstein Dec. 1987 86 p
(AD-A189682; AFIT/GSO/ENG/87D-1) Avail: NTIS HC A05/MF A01 CSCL 12E

The purpose of this study was to implement a technique for fault-tolerant parallel computation on the Intel Corporation's Hypercube computer. This work was motivated by the recent progress in parallel computation and neural network techniques. This study focuses on the implementation of one particular type of parallel processing architecture on the Intel Hypercube. The architecture in question is known as the cube-connected cycle (CCC). This architecture is used as a basis for a reconfiguration scheme known as reconfigurable cube-connected cycles. The aim of this reconfiguration is to build a parallel computing system with fault tolerance capability. Implementation of this technique on the Intel Hypercube was by simulation. The loading of only part of the hypercube available nodes, holding the remaining nodes in reserve was accomplished, followed by a simulation of the replacement of a deactivated node with a spare node. Conclusions are reached regarding the suitability of the Intel machine for fault tolerance experiments versus the rapid computation for which it was designed. Recommendations are made regarding the next logical steps in continuation of the work presented in this study. GRA

N88-22595# Indiana Univ.-Purdue Univ., Indianapolis. School of Engineering and Technology.
A ZONAL APPROACH FOR THE SOLUTION OF COUPLED EULER AND POTENTIAL SOLUTIONS OF FLOWS WITH COMPLEX GEOMETRIES Final Report, 1 Jul. 1986 - 1 Jun. 1987
Akin Ecer 1 Feb. 1988 12 p
(Grant AF-AFOSR-0015-87)
(AD-A189752) Avail: NTIS HC A03/MF A01 CSCL 20D

A block structured solution scheme which was developed for the solution of three dimensional Euler equations was implemented on the Intel Hypercube computer. By using this scheme, a complex flow problem is divided into a series of blocks. Each block is stored on an individual processor of the system and solved. The boundary conditions between the neighboring blocks are iteratively calculated. The communication of the boundary conditions between neighboring blocks occur on individual I/O channels. GRA

N88-22596# Princeton Univ., N. J. Dept. of Chemistry.
MICROVAX NETWORKED COMPUTER SYSTEM Final Report
Herschel Rabitz Dec. 1987 6 p
(Grant AF-AFOSR-0021-87)
(AD-A190308; AFOSR-87-1958TR) Avail: NTIS HC A02/MF A01 CSCL 12G

This final report covers the action taken regarding equipment purchases for the purpose of establishing a network of Microwax computers for research in the area of chemical physics, particularly involving dynamics and kinetics phenomena. All original items were procured except the line printer and the IBM-PC terminals. These latter items were replaced with the purchase of the extra disk storage deemed important to attain maximal usage from the hardware. The overall system network is fully on-line and we are finding that the machines make a significant impact on our research. The design of the networked set of computers linked to the Departmental mainframe VAX is proving to be very effective. Additional experience will be needed to finally establish the optimal mode of system operation but we are already finding considerable speed-up in the rate that computations can be performed. The computers are being especially put to use for studying problems in gas-surface dynamics, molecular collisions and related problems in chemical kinetics. GRA

N88-22597# Massachusetts Inst. of Tech., Cambridge. Lab. for Computer Science.
MULTISCHEME: A PARALLEL PROCESSING SYSTEM BASED ON MIT (MASSACHUSETTS INSTITUTE OF TECHNOLOGY) SCHEME Ph.D. Thesis
James S. Miller Sep. 1987 247 p
(Contracts N00014-83-K-0125; N00014-84-K-0099)
(AD-A190383; AD-E801598; MIT/LCS/TR-402) Avail: NTIS HC A11/MF A01 CSCL 12F

MultiScheme is a fully operational parallel-programming system based on the Scheme dialect of Lisp. Like its Lisp ancestors,

MultiScheme provides a conducive environment for prototyping and testing new linguistic structures and programming methodologies. MultiScheme supports a diverse community of users who have a wide range of interests in parallel programming. MultiScheme's flexible support for system-based experiments in parallel processing has enabled it to serve as a development vehicle for university and industrial research. At the same time, MultiScheme is sufficiently robust, and supports a sufficiently wide range of parallel-processing applications, that it has become the base for a commercial product, the Butterfly Lisp System produced by BBN Advanced Computers, Inc. GRA

N88-22598# Duke Univ., Durham, N. C. Dept. of Computer Science.
COMPARATIVE ANALYSIS OF MULTISTAGE INTERCONNECTION NETWORKS Ph.D. Thesis. Final Report
James T. Blake Dec. 1987 207 p
(AD-A190436) Avail: NTIS HC A10/MF A01 CSCL 25E

A comparative analysis of various interconnection networks and multiprocessor systems is given. The Shuffle-Exchange multistage interconnection Network (SEN) and its variants are evaluated and compared. Comparison is based on reliability, composite measures of performance and reliability, and cost. Closed-form expressions for the computation of the available bandwidth for multiprocessor systems with a capability of graceful degradation are developed. The time dependent reliability of the SEN and three fault-tolerant schemes aimed at improving system reliability are examined. These schemes are the redundant network, the extra stage network, and the network augmented with intrastage links. Exact closed-form expressions for the time-dependent reliability of the N x N Shuffle-Exchange Network (SEN), the 8 x 8 and 16 x 16 SEN with an additional stage (SEN+), and the 4 X 4 and 8 X 8 Augmented SEN (ASEN) are derived. Upper and lower bounds useful for the analysis of larger SEN+ and ASEN networks are derived. Performability analysis of a complete multiprocessor system is conducted. GRA

N88-22599# Air Force Inst. of Tech., Wright-Patterson AFB, Ohio. School of Engineering.
THE MODELING, SIMULATION AND COMPARISON OF INTERCONNECTION NETWORKS FOR PARALLEL PROCESSING M.S. Thesis
Richard A. Raines Dec. 1987 117 p
(AD-A190571; AFIT/GCE/ENG/87D-8) Avail: NTIS HC A06/MF A01 CSCL 25E

This thesis extends existing modeling, analysis and comparison of interconnection networks for parallel processing systems. Simulation models are developed for the multistage cube network, the single stage cube network (hypercube), and the Illiac IV mesh-type network. They are then used to provide a comparison of three classes of interconnection networks which, until now, has not been performed. These models implemented using a commercially packaged simulation language provide for compact source code and ease of readability. The networks are modeled under a common set of operating assumptions and system environment. This allows for accurate comparisons of average network packet delays an memory requirements necessary to physically implement the chosen network at a given network operating load. It is concluded that, for the network sizes and operating conditions established, the multistage cube network performs better at a lower hardware cost than do the single stage cube and mesh networks. As a result, the designer of a parallel processing system is given additional insight for choosing an interconnection network which best suits the application needs. GRA

N88-22600# Air Force Inst. of Tech., Wright-Patterson AFB, Ohio. School of Engineering.
IMPLEMENTATION AND PERFORMANCE ANALYSIS OF PARALLEL ASSIGNMENT ALGORITHMS ON A HYPERCUBE COMPUTER M.S. Thesis
Barry A. Carpenter Dec. 1987 165 p
(AD-A190678; AFIT/GCE/ENG/87-2) Avail: NTIS HC A08/MF A01 CSCL 12G

The process of effectively coordinating and controlling resources during a military engagement is known as Battle Management/Command, Control, and Communications (BM/C3). One key task of BM/C3 is allocating weapons to destroy targets. The focus of this research is on developing parallel methods to achieve fast and cost effective assignment of weapons to targets. Using the sequential Hungarian method for solving the assignment problem as a basis, this report presents the development and relative performance comparison of four parallel assignment algorithms implemented on the Intel iPSC hypercube computer. The first approach partitions the problem space into smaller, independent subproblems and assigns each to a processing node in the hypercube. The second and third approaches also partition the problem space, but they assign each partition to a group of processing nodes. Each group is controlled by a separate node which further subdivides the partition among members of the group. In the second approach, the control node acts as an arbitrator to eliminate the redundant assignment of weapons to targets by idling redundantly allocated weapons. The third approach eliminates redundant weapon allocations by selecting the least costly redundant allocations and directing additional processing to reallocate the more costly weapons. The fourth approach is a parallel implementation of the Hungarian algorithm, where certain subtasks are performed in parallel. This approach produces an optimal assignment instead of the sub-optimal assignment generally obtained using either of the three heuristic approaches. GRA

N88-22601# Oak Ridge National Lab., Tenn.
DESIGN AND IMPLEMENTATION OF A PARALLEL COMPUTER FOR EXPERT SYSTEM APPLICATIONS
P. L. Butler, J. D. Allen, Jr., and D. W. Bouldin 1988 8 p Presented at the SPIE's Technical Symposium on Optics, Electro-optic and Sensors, Orlando, Fla., 4 Apr. 1988 Prepared in cooperation with Tennessee Univ., Knoxville
(Contract DE-AC05-84OR-21400)
(DE88-005288; CONF-880462-1) Avail: NTIS HC A02/MF A01

A parallel computer for high-speed execution of expert system programs has been designed and implemented at the Oak Ridge National Laboratory. Programs written in the popular OPS5 language for serial machines need not be modified by the programmer, since the compiler on this special-purpose machine automatically employs the parallelism inherent in the language. Performance improvements of a factor of 10 over serial machines have already been demonstrated. The initial hardware implementation of the parallel architecture consists of a host computer that broadcasts to 64 parallel rule processors over a transmit-only bus. The communication time is kept to a minimum by using direct-memory access and a memory-mapped addressing scheme that permit each of the parallel rule processors to receive the appropriate information simultaneously. A wired-OR completion flag signals the host whenever all of the parallel rule processors have finished their recognition tasks. The host then extracts information from those rule processors whose rules have been satisfied and, based on a global criterion, selects one of these rules. The host then carried out the actions dictated by this rule and broadcasts new information to the rule processors to begin another recognize-act cycle. Statistics detailing the activities of the host and all of the rule processors are collected and displayed in real time. Thus, the performance of the various aspects of the architecture can be readily analyzed. Also, the execution of the expert system program itself can be studied to detect situations that may be altered to permit additional speedup. DOE

N88-22602*# Alabama Univ., Tuscaloosa. Dept. of Electrical Engineering.
A DIRECT-EXECUTION PARALLEL ARCHITECTURE FOR THE ADVANCED CONTINUOUS SIMULATION LANGUAGE (ACSL)
Chester C. Carroll and Jeffrey E. Owen May 1988 137 p
(Grant NAG8-093)
(NASA-CR-182809; NAS 1.26:182809; BER-424-17) Avail: NTIS HC A07/MF A01 CSCL 09B

A direct-execution parallel architecture for the Advanced Continuous Simulation Language (ACSL) is presented which overcomes the traditional disadvantages of simulations executed on a digital computer. The incorporation of parallel processing allows the mapping of simulations into a digital computer to be done in the same inherently parallel manner as they are currently mapped onto an analog computer. The direct-execution format maximizes the efficiency of the executed code since the need for a high level language compiler is eliminated. Resolution is greatly increased over that which is available with an analog computer without the sacrifice in execution speed normally expected with digitial computer simulations. Although this report covers all aspects of the new architecture, key emphasis is placed on the processing element configuration and the microprogramming of the ACLS constructs. The execution times for all ACLS constructs are computed using a model of a processing element based on the AMD 29000 CPU and the AMD 29027 FPU. The increase in execution speed provided by parallel processing is exemplified by comparing the derived execution times of two ACSL programs with the execution times for the same programs executed on a similar sequential architecture. Author

63 CYBERNETICS

Includes feedback and control theory, artificial intelligence, robotics and expert systems.

For related information see also *54 Man/System Technology and Life Support.*

N88-22603# Lawrence Livermore National Lab., Calif.
ARTIFICIAL NEURAL NETWORKS: AN INTRODUCTION WITH AN ANNOTATED BIBLIOGRAPHY
V. Vemuri 27 Jan. 1988 32 p
(Contract W-7405-eng-48)
(DE88-007003; UCID-21313) Avail: NTIS HC A03/MF A01

Within the last decade tremendous progress has been made in the understanding of neurobiological models and the ability to fabricate optical and electronic circuits based on these models. These models are composed of numerous nonlinear computational elements fashioned as a network and operating in parallel. The prospect of using these networks to solve complex problems related to pattern recognition, image understanding and natural language understanding has never been brighter. With the recent spate of significant contributions from so many varied directions, leaders from both commercial and military sectors are placing heavy bets on the future of this emerging area. Although several bibliographies are available, there still is a need for a guide to help the novice walk through this area. This report is meant to fill this need. DOE

N88-22604# Naval Postgraduate School, Monterey, Calif.
A THREE DIMENSIONAL NON-SINGULAR MODELLING OF RIGID MANIPULATORS M.S. Thesis
Sadrettin Altinok Dec. 1987 105 p
(AD-A189707) Avail: NTIS HC A06/MF A01 CSCL 12I

There are several common approaches used to obtain the kinematic and dynamic equations which describe the motion of robot manipulators. However, a problem arises when these conventional body oriented robot arm kinematic equations are used to simulate the manipulator motion. In this case, the Jacobian matrix which relates the end effector motion to joint angle variations becomes singular when two successive arm links align. When the robot arm passes through these singular points, the Jacobian matrix is not invertible, and as a result, the motion cannot be simulated. This thesis investigates how this situation can be avoided by using a Newton Euler approach to variable definition, and using the equations interpreted in a fixed references frame. GRA

N88-22605# Alberta Univ., Edmonton. Dept. of Statistics and Applied Probability.
THE ADJOINT PROCESS IN STOCHASTIC OPTIMAL CONTROL Report, 30 Sep. 1986 - 30 Sep. 1987
Robert J. Elliott and Michael Kohlmann 11 Nov. 1987 17 p
(Grant AF-AFOSR-0332-86)
(AD-A189720; AFOSR-87-1846TR) Avail: NTIS HC A03/MF A01 CSCL 12C

The focus of this research is filtering jump processes. To investigate the filtering of manifold valued processes, their approximation by random walks and Markov chains was studied. The object was to approximate a signal process by a finite state jump process for which a finite dimensional filter is available. Four papers were published during the past year, including the existence of smooth densities for the prediction, filtering and smoothing problems and the partially observed stochastic minimum principle. Using stochastic flows a minimum principle is obtained when a diffusion is controlled using stochastic open loop controls. An equation for the adjoint process is then derived using an explicit formula for the integrand in a certain stochastic integral. GRA

N88-22606# Yale Univ., New Haven, Conn.
MEMORY-BASED EXPERT SYSTEMS Final Report, 15 Jan. 1982 - 29 Sep. 1985
R. Schank Jun. 1987 64 p
(Contract F49620-82-K-0010)
(AD-A190203; AFOSR-87-1745TR) Avail: NTIS HC A04/MF A01 CSCL 12E

There are three major areas of accomplishments in recent AFOSR sponsored Artificial Intelligence (AI) research at Yale. While case-based reasoning is simple in concept, there are of course many subtle and difficult design issues that have to be resolved to make it work. One major achievement in the past two years at Yale has been the development of an explicit structure for the case-based reasoning process, as shown in the slide containing the flowchart entitled Case-Based Reasoning. This process description summarizes results from the JUDGE (Bain 1986) AFOSR project, as well as from other projects such as CHEF (Hammond 1986) and COACH (Collins forthcoming). The flow of control in the process (represented by the arrows and boxes) is task-independent, while the particular knowledge bases (represented by the ovals) are task specific. The JUDGE program models the subjective assessment task of judicial sentencing. That is, given a description of an event, such as a fight between two people that ended in a death or serious injury, where someone has been convicted of a criminal act. GRA

N88-22607# Massachusetts Inst. of Tech., Cambridge. Artificial Intelligence Lab.
SYNAPSES THAT COMPUTE MOTION
Tomaso Poggio and Christof Koch Jun. 1987 14 p
(Contracts N00014-85-K-0124; DACA76-85-C-0010)
(AD-A190389; AD-E801598; AI-M-973) Avail: NTIS HC A03/MF A01 CSCL 06C

Biophysics of computation is a new field that attempts to characterize the role in information processing of the several biophysical mechanisms in neurons, synapses and membranes that have been uncovered in recent years. In this article, we review a synaptic mechanism, based on the interaction between excitation and silent inhibition, that implements a veto-like operation. Synapses of this type may underlie direction selectivity to direction of motion in the vertebrate retina. GRA

N88-22608# Illinois Univ., Urbana. Coll. of Engineering.
REPRESENTATION, ANALYSIS AND DESIGN OF MULTIRATE DISCRETE-TIME CONTROL SYSTEMS M.S. Thesis
Kevin L. Buescher Feb. 1988 88 p
(Contract N00014-84-C-0149)
(AD-A190499; UILU-ENG-88-2211; DC-101) Avail: NTIS HC A05/MF A01 CSCL 12D

Multirate discrete-time systems, systems in which sampling and discrete-time calculations are performed at two or more rates, arise in a variety of applications. The multirate character of the system may be intrinsic, due to digital subsystems operating at multiple rates. Alternately, the multirate nature of the system may be induced by the addition of sensors, actuators, and discrete-time

control structures at different rates for the purposes of economy or performance. GRA

N88-22609# Massachusetts Inst. of Tech., Cambridge. Artificial Intelligence Lab.
FINDING TEXTURE BOUNDARIES IN IMAGES M.S. Thesis
Harry Voorhees Jun. 1987 105 p
(Contracts N00014-85-K-0124; DACA76-85-C-0010)
(AD-A190554; AI-TR-968) Avail: NTIS HC A06/MF A01 CSCL 12E

Texture provides one cue for identifying the physical cause of an intensity edge, such as occlusion, shadow, surface orientation or reflectance change. Marr, Julesz, and others have proposed that texture is represented by small lines or blobs, called textons by Julesz (1981a), together with their attributes, such as orientation, elongation, and intensity. Psychophysical studies suggest that texture boundaries are perceived where distributions of attributes over neighborhoods of textons differ significantly. However, these studies, which deal with synthetic images, neglect to consider two important questions: How can these textons be extracted from images of natural scenes? And how, exactly, are texture boundaries then found? This thesis proposes answers to these questions by presenting an algorithm for computing blobs from natural images and a statistic for measuring the difference between two sample distributions of blob attributes. As part of the blob detection algorithm, methods for estimating image noise are presented, which are applicable to edge detection as well. GRA

N88-22610# Carnegie-Mellon Univ., Pittsburgh, Pa. Dept. of Electrical and Computer Engineering.
MULTI-DISCIPLINARY TECHNIQUES FOR UNDERSTANDING TIME-VARYING SPACE-BASED IMAGERY Report, May 1985 - Mar. 1987
David Casasent, Arthur Sanderson, Takeo Kanade, and B. V. VijayaKumar 29 Apr. 1987 154 p
(Grant AF-AFOSR-0239-84)
(AD-A190711; AFOSR-87-1756TR) Avail: NTIS HC A08/MF A01 CSCL 17K

This project combined pattern recognition, image understanding and artificial intelligence techniques for space-based image processing. A special feature of this effort is the attempt to use both optical and digital processing methods. Subpixel target detection and tracking algorithms are analyzed and conclusions are presented regarding their suitability for this application. We also present an adaptive subpixel delay estimation method using Group-Delay Functions. Image understanding techniques for three dimensional scene interpretation are also discussed. GRA

N88-22611# Sandia National Labs., Albuquerque, N. Mex.
INSERTIONS USING GEOMETRIC ANALYSIS AND HYBRID FORCE-POSITION CONTROL: METHOD AND ANALYSIS
D. R. Strip 14 Sep. 1987 16 p Presented at the IEEE International Conference on Robotics and Automation, Pittsburgh, Pa., 25 Apr. 1988
(Contract DE-AC04-76DP-00789)
(DE87-013652; SAND-87-1942C; CONF-880424-3) Avail: NTIS HC A03/MF A01

Automatic programming of insertions is an essential step in achieving a truly flexible manufacturing environment. We present techniques based on active compliance implemented with hybrid force position control which are capable of inserting a wide variety of shaped pegs. We analyze the forces encountered during the insertions to determine what classes of shapes these techniques will consistently insert. The analysis also gives guidance in selecting parameters of these techniques for specific shapes. These techniques provide a significant step towards an automatically programmed flexible manufacturing environment. Author

N88-22612# Los Alamos National Lab., N. Mex.
RAPID PROTOTYPING OF SIMULATIONS IN ARTIFICIAL INTELLIGENCE ENVIRONMENTS
R. Martinez 1988 8 p Presented at the Conference of the Society of Computer Simulation, Orlando, Fla., 18 Apr. 1988
(Contract W-7405-eng-36)
(DE88-004295; LA-UR-87-4255; CONF-880455-3) Avail: NTIS HC A02/MF A01

The benefits derived from rapidly constructing a prototypical simulation model for use in characterizing the scope of a project should not be underestimated. The initial period of contact with the end-user of a simulation will establish the ground-rules by which the project will progress. This paper describes some experiences in the application of an expert system shell in the development of knowledge-based discrete event simulations. This model development approach leverages the benefits of object-oriented programming, frames for representing the objects to be simulated, and the graphics capabilities inherent within many expert system shells. The user interface relies heavily upon the use of graphical active images for the modification of important object attributes prior to runtime. Having a functional knowledge-based simulation facilitates the process of accurately determining the needs of the client. DOE

N88-22613# Los Alamos National Lab., N. Mex.
DISCRETE EVENT SIMULATION IN THE ARTIFICIAL INTELLIGENCE ENVIRONMENT
H. W. Egdorf and D. J. Roberts 1987 8 p Presented at the Conference of the Society of Computer Simulation, Orlando, Fla., 18 Apr. 1988
(Contract W-7405-eng-36)
(DE88-004296; LA-UR-87-4256; CONF-880455-4) Avail: NTIS HC A02/MF A01

Discrete Event Simulations performed in an Artificial Intelligence (AI) environment provide benefits in two major areas. The productivity provided by Object Oriented Programming, Rule Based Programming, and AI development environments allows simulations to be developed and maintained more efficiently than conventional environments allow. Secondly, the use of AI techniques allows direct simulation of human decision making processes, command and control aspects of a system under study. An introduction to AI techniques is presented. Two discrete event simulations produced in these environments are described. Finally, a software engineering methodology is discussed that allows simulations to be designed for use in these environments. DOE

N88-22614# Oak Ridge National Lab., Tenn.
CONCURRENT ALGORITHMS FOR A MOBILE ROBOT VISION SYSTEM
J. P. Jones and R. C. Mann 1988 9 p Presented at the SPIE's Technical Symposium on Optics, Electro-optic and Sensors, Orlando, Fla., 4 Apr. 1988
(Contract DE-AC05-84OR-21400)
(DE88-005850; CONF-880462-2; CESAR-88/06) Avail: NTIS HC A02/MF A01

The application of computer vision to mobile robots has generally been hampered by insufficient on-board computing power. The advent of very large scale integration (VLSI) based general purpose concurrent multiprocessor systems promises to give mobile robots an increasing amount of on-board computing capability, and to allow computation intensive data analysis to be performed without high-bandwidth communication with a remote system. This paper describes the integration of robot vision algorithms on a 3-dimensional hypercube system on-board a mobile robot developed at Oak Ridge National Laboratory. The vision system is interfaced to navigation and robot control software, enabling the robot to maneuver in a laboratory environment, to find a known object of interest and to recognize the object's status based on visual sensing. We first present the robot system architecture and the principles followed in the vision system implementation. We then provide some benchmark timings for low-level image processing routines, describe a concurrent algorithm with load balancing for the Hough transform, a new algorithm for binary component labeling, and an algorithm for the concurrent extraction of region features from labeled images. This system analyzes a scene in less than 5 seconds and has proven to be a valuable experimental tool for research in mobile autonomous robots. DOE

64 NUMERICAL ANALYSIS

Includes iteration, difference equations, and numerical approximation.

N88-22615# China Nuclear Information Centre, Beijing.
MULTIGROUP FLUX-LIMITED ASYMPTOTIC DIFFUSION FOKKER-PLANCK EQUATION
Liu Chengan 1987 11 p In CHINESE; ENGLISH summary
(DE88-700958; CNIC-00047; IAPCM-0004) Avail: NTIS (US Sales Only) HC A03/MF A01

A more perfect flux-limited method is applied to combine with asymptotic diffusion theory of the radiation transport, and the high peaked component in the scattering angle is treated with Fokker-Planck methods, thus, the flux-limited asymptotic diffusion Fokker-Planck equation was founded. Since the equation is of diffusion form, it retains the simplity and the convenience of the classical diffusion theory, and improves precision in describing radiation transport problems. DOE

N88-22616# Hiroshima Univ., Takehara (Japan). Research Inst. for Theoretical Physics.
RECENT DEVELOPMENTS IN THE PATH INTEGRAL APPROACH TO ANOMALIES
K. Fujikawa Aug. 1986 24 p
(DE87-703032; RRK-86-32) Avail: NTIS (US Sales Only) HC A02/MF A01

After a brief summary of the path integral approach to anomalous identities, some of the recent developments in this approach are discussed. The topics discussed include construction of the effective action by means of the covariant current, Gauss law constraint in anomalous gauge theories, the path integral approach to anomalies in superconformal transformations, conformal and ghost number anomalies in string theory in analogy with the instant on calculation, and covariant local Lorentz anomaly and its connection with the mathematical construction of the consistent anomaly. DOE

N88-22617# Hiroshima Univ., Takehara (Japan). Research Inst. for Theoretical Physics.
REMARKS ON THE TIME TRANSFORMATION OF PATH-INTEGRAL MEASURES
R. Kubo Sep. 1986 9 p
(DE87-703040; RRK-86-40) Avail: NTIS (US Sales Only) HC A02/MF A01

By means of a time transformation of path-integral measures, we rewrite the usual Feynman path integral as a path integral of determininants with the Wiener measure. We derive a formula which is useful in evaluating path integrals. DOE

N88-22618# Massachusetts Univ., Amherst.
ALMOST-PERIODIC SOLUTIONS OF NONLINEAR PARABOLIC EQUATIONS
Yisong Yang Oct. 1987 13 p
(Contract DE-FG02-86ER-25015)
(DE88-006423; DOE/ER-25015/9) Avail: NTIS HC A03/MF A01

In this note the recent result of Corduneanu on almost periodicity of L sup 2 (G)-bounded solutions of nonlinear parabolic equations is extended to the case when the nonlinear growth rate is beyond the first eigenvalue of the associated elliptic boundary value problem. DOE

N88-22619# Massachusetts Univ., Amherst.
COMPLETE MINIMAL SURFACES IN R OF LOW TOTAL CURVATURE
E. L. Barbanel Sep. 1987 58 p
(Contract DE-FG02-86ER-25015)
(DE88-006425; DOE/ER-25015/7) Avail: NTIS HC A04/MF A01

In this paper we wish to determine all the complete minimal surfaces of genus zero and finite total curvature -8 pi in three-dimensional Euclidean space R^3. The surfaces are written down explicitly, using the Weierstrass representation. They are separated into parameter families of surfaces with the same number of ends and the same Gauss map. Pictures of representative members of each type are given. DOE

N88-22620# Massachusetts Univ., Amherst.
THE INVERSE POWER METHOD FOR SEMILINEAR ELLIPTIC EQUATIONS
A. Eydeland and J. Spruck Oct. 1987 22 p
(Contract DE-FG02-86ER-25015)
(DE88-006427; DOE/ER-25015/5) Avail: NTIS HC A03/MF A01

In this paper we develop globally convergent iterative algorithms for the solution of nonlinear eigenvalue problem delta u + lambda f (x,u) = 0 in bounded D. These algorithms are extremely useful in a wide variety of geometric and physical problems. DOE

N88-22621# Los Alamos National Lab., N. Mex.
NONLINEAR SIGNAL PROCESSING USING NEURAL NETWORKS: PREDICTION AND SYSTEM MODELLING
A. Lapedes and R. Farber Jun. 1987 52 p Presented at the 1st IEEE International Conference on Neural Networks, San Diego, Calif., 21 Jun. 1987
(Contract W-7405-eng-36)
(DE88-006479; LA-UR-87-2662; CONF-8706130-4) Avail: NTIS HC A04/MF A01

The backpropagation learning algorithm for neural networks is developed into a formalism for nonlinear signal processing. The method is illustrated by selecting two common topics in signal processing, prediction and system modelling, demonstrating that nonlinear applications can be handled extremely well by using neural networks. The formalism is a natural, nonlinear extension of the linear Least Mean Squares algorithm commonly used in adaptive signal processing. Simulations are presented that document the additional performance achieved by using nonlinear neural networks. First, it is demonstrated that the formalism may be used to predict points in a highly chaotic time series with orders of magnitude increase in accuracy over conventional methods including the Linear Predictive Method and the Gabor-Volterra-Weiner Polynomial Method. Deterministic chaos is thought to be involved in many physical situations including the onset of turbulence in fluids, chemical reactions and plasma physics. Secondly, the use of the formalism in nonlinear system modelling is demonstrated by providing a graphic example in which it is clear that the neural network has accurately modeled the nonlinear transfer function. It is interesting to note that the formalism provides explicit, analytic, global, approximations to the nonlinear maps underlying the various time series. Furthermore, the neural net seems to be extremely parsimonious in its requirements for data points from the time series. It is shown that the neural net is able to perform well because it globally approximates the relevant maps by performing a kind of generalized mode decomposition of the maps. DOE

N88-22622# Utah State Univ., Logan.
NUMERICAL SOLUTION OF NONLINEAR ALGEBRAIC EQUATIONS IN STIFF ODE SOLVING Technical Progress Report, 1987-1988
H. F. Walker 1988 6 p
(Contract DE-FG02-86ER-25018)
(DE88-006634; DOE/ER-25018/2) Avail: NTIS HC A02/MF A01

The primary objective of this project is to investigate numerical methods for solving particular systems of nonlinear algebraic equations, namely, those which arise in the implementation of implicit methods for stiff ODE initial-value problems. Many of the issues for these nonlinear systems also apply to more general nonlinear systems which share some of their characteristics, and during the last year this project has naturally come to involve a significant component of work directed toward more such general systems. Our model method for solving nonlinear systems is Newton's method, and this research has centered around two major variants of Newton's method which appear to offer special advantages in solving stiff ODE systems and similar systems. These

are quasi-Newton methods, which employ secant updates of an approximate Jacobian, and matrix-free implementations of Newton's method, in which Newton steps are determined by approximately solving linear systems using matrix-free iterative methods. The quasi-Newton methods are intended for applications in which full-matrix techniques are inadmissible, of interest primarily in the case of very large systems. DOE

N88-22623# Massachusetts Univ., Amherst.
GLOBAL SPATIAL PERIODIC SOLUTIONS TO THE GINZBURG-LANDAU EQUATIONS
Yisong Yang Oct. 1987 19 p
(Contract DE-FG02-86ER-25015)
(DE88-006424; DOE/ER-25015/8) Avail: NTIS HC A03

In this paper we study the global existence and nonexistence of spatially periodic solutions to the initial value problem of the Ginzburg-Landau equation. DOE

N88-22624# Grenoble-1 Univ. (France). Lab. dInformatique Fondamentale et dIntelligence Artificielle.
ABOUT DISEQUATIONS SIMPLIFICATION
H. Comon Feb. 1987 39 p
(RR-645-I-IMAG-55-LIFIA; ETN-88-92278) Avail: NTIS HC A03/MF A01

For t and t' being two terms in an algebra T sub sigma (X) an algorithm for finding the substitutions sigma such that sigma (t) and sigma (t') are not unifiable is presented. This is exactly the counterpart of the unification procedure: unification allows one to solve equations in such algebras, here disequations are solved, for particular cases, and the general case, extending results on disunification. Extensions such as solving disequations systems are given. A unification-like presentation of disunification is employed. ESA

N88-22625# Illinois Univ., Urbana. Coordinated Science Lab.
THE TOTAL INTERVAL OF A GRAPH Ph.D. Thesis
Thomas M. Kratzke Jan. 1988 124 p
(Contract N00014-85-K-0570)
(AD-A189648; UILU-ENG-88-2202; UILU-ACT-86) Avail: NTIS HC A06/MF A01 CSCL 12B

An interval representation (or simply representation) R of a graph G is a collection of finite sets(R(v): v Epsilon V(G) of closed bounded intervals so that u is equivalent to v if and only if there exist theta sub u epsilon R(u), theta sub v epsilon R(v) with theta sub u intersects theta sub v not equal to 0. The size of a representation is the number of intervals in the entire collection. The total interval number of G is the size of the smallest representation of G and denoted I(G). This thesis studies I(G) by proving best possible upper bounds for several classes of graphs. For some of the classes, the bounds are in terms of the number of vertices and for some of the classes, the bounds are in terms of the number of edges. The main result is that for planar graphs, I(G) is less than or = 2n(G) - 3. GRA

N88-22626# Alberta Univ., Edmonton. Dept. of Statistics and Applied Probability.
MARTINGALE REPRESENTATION AND THE MALLIAVIN CALCULUS Report, 30 Sep. 1986 - 30 Sep. 1987
Robert J. Elliott and Michael Kohlmann 11 Nov. 1987 13 p
(Grant AF-AFOSR-0332-86)
(AD-A189721; AFOSR-87-1845TR) Avail: NTIS HC A03/MF A01 CSCL 12C

Using the theory of stochastic flows the integrand in a stochastic integral is identified. After some rearrangement this integrand is itself written in terms of a martingale which can be expressed as a stochastic integral, and by recursively repeating the representation a homogeneous chaos expansion is obtained. Using the stochastic integral representation an integration by parts formula is then derived. If the inverse of the Malliavin matrix M belongs to all the spaces L superscript p (Omega) we show a random variable has a smooth density. The difficult questions concerning the relationship between Hoermander's conditions on the coefficient vector fields and the integrability of 1/M are not discussed, but, at least for Markov flows, the discussion below appears to be an elementary treatment of some ideas of the Malliavin calculus. GRA

N88-22627# Air Force Inst. of Tech., Wright-Patterson AFB, Ohio. School of Engineering.
HIGH SPEED TRANSCENDENTAL ELEMENTARY FUNCTION ARCHITECTURE IN SUPPORT OF THE VECTOR WAVE EQUATION (VWE) M.S. Thesis
Mickey J. Bailey Dec. 1987 93 p
(AD-A189746; AFIT/GE/ENG/87D-3) Avail: NTIS HC A05/MF A01 CSCL 12A

In support of a Very High Speed Integrated Circuit (VHSIC) class processor for computation of a set of equations known as the Vector Wave Equations (VWE), certain elementary functions including sine, cosine, and division are required. These elementary functions are the bottlenecks in the VWE processor. Floating point multipliers and adders comprise the remainder of the pipeline stages in the VWE processor. To speed up the computation of the elementary functions, pipelining within the functions is considered. To compute sine, cosine, and division, the CORDIC algorithm is presented. Another method for computation of sine and cosine is the expansion of the Chebyshev polynomials. The equations for the CORDIC processor are recursive and the resulting hardware is very simple, consisting of three adders, three shifters, and lookup table for some of the coefficients. The shifters replace the multiplies, because in binary, i right shifts is the same as multiplying by 2 to the 8th power. The expansion of the Chebyshev polynomials can be used to compute other trigonometric functions as well as the exponential and logarithmic functions. The expansion of the Chebyshev polynomials can be used as a mathematic coprocessor. GRA

N88-22628# Rensselaer Polytechnic Inst., Troy, N.Y. Dept. of Computer Science.
NUMERICAL METHODS FOR SINGULARLY PERTURBED DIFFERENTIAL EQUATIONS WITH APPLICATIONS Annual Report, 1 Jun. 1986 - 31 May 1987
Joseph E. Flaherty May 1987 12 p
(Grant AF-AFOSR-0156-85)
(AD-A189786; AFOSR-87-1828TR) Avail: NTIS HC A03/MF A01 CSCL 12B

Research was continued on the development and applications of adaptive numerical methods for singularly perturbed initial-boundary value problems for partial differential equations. Analysis is made of mesh moving schemes, examined local refinement methods, and developed a posteriori error estimation technique for none-and-two-dimensional hyperbolic and parabolic problems. Development has begun on parallel versions of some adaptive procedures. These methods are applied to several interesting physical problems, that arise in, e.g., elastic-plastic deformation, combustion, and fluid mechanics. GRA

N88-22629# Alberta Univ., Edmonton. Dept. of Statistics and Applied Probability.
THE EXISTENCE OF SMOOTH DENSITIES FOR THE PREDICTION FILTERING AND SMOOTHING PROBLEMS Report, 30 Sep. 1986 - 30 Sep. 1987
Robert J. Elliott Nov. 1987 28 p
(Grant AF-AFOSR-0332-86)
(AD-A189865; AFOSR-87-1847TR) Avail: NTIS HC A03/MF A01 CSCL 12C

Using a simple martingale representation result a conditional version of the Malliavin calculus is developed. Under Hormander's conditions on the coefficient vector fields the filtering, smoothing and prediction problems are shown to have C subscript infinity density solutions. GRA

N88-22630# Emory Univ., Atlanta, Ga.
NEW METHODS FOR NUMERICAL SOLUTION OF ONE CLASS OF STRONGLY NONLINEAR PARTIAL DIFFERENTIAL EQUATIONS WITH APPLICATIONS Final Technical Report
V. I. Oliker and P. Waltman Aug. 1987 8 p

(Grant AF-AFOSR-0285-84)
(AD-A189945; AFOSR-87-1729TR) Avail: NTIS HC A02/MF A01 CSCL 12A

The physical phenomena described by nonlinear partial differential equations have become at present the central theme of investigation by many researchers. A good understanding of most physical processes requires accounting for nonlinear effects and, consequently, methods for studying nonlinear equations have to be developed. Among nonlinear equations the Dirichlet problem for the Monge-Ampere equation is the model case for fully nonlinear equations. GRA

N88-22631# California Univ., Davis. School of Administration.
NUMERICAL METHODS FOR LINEAR AND NONLINEAR OPTIMIZATION Final Report, 1 Jul. 1986 - 30 Jun. 1987
David F. Shanno 16 Sep. 1987 9 p
(Grant AF-AFOSR-0170-86)
(AD-A190029; AFOSR-88-0174TR) Avail: NTIS HC A02/MF A01 CSCL 12D

Three major objectives were completed during the year. The first demonstrates how to directly use rank-one updates to a Cholesky factorization of the required inverse for Karmarkar projections while fully exploiting sparsity. This can significantly improve computational speed when only a few variables are changing significantly at each step. The second demonstrates a new method for adding new variables to a quasi-Newton Hessian approximation which preserves problem scale and positive definiteness of the Hessian. Numerical results show the method to be preferable to known methods. The third examines a variety of ways of implementing a sequential quadratic programming code, and uses numerical testing to indicate a suitable merit function and good algorithms for updating Lagrange multiplier and Hessian approximations. Recent new results for updating Hessians for unconstrained problems are currently being studied to determine if better Hessian approximations can be obtained. GRA

N88-22632# Pennsylvania State Univ., University Park. Dept. of Mathematics.
POINTWISE STABILIZATION FOR COUPLED QUASILINEAR AND LINEAR WAVE EQUATIONS Report, 1 Sep. 1985 - 31 Aug. 1986
Goong Chen and Han-Kun Wang 8 Jan. 1988 26 p
(Grant AF-AFOSR-0253-85)
(AD-A190031; AFOSR-88-0146TR) Avail: NTIS HC A03/MF A01 CSCL 13M

A large structure is formed by the coupling of simple structural elements. This paper considers the simplest type of such structures which is made up of two coupled strings modelled by quasilinear or linear wave equations. Two stabilizers are installed: one at the left boundary and one at an in-span point. The exponential stability property of this coupled dynamic structure is studied. The method of characteristics, and a frequency domain theorem due to F. L. Huang are used. For the quasilinear case, one can determine various parameters so that the system is exponentially stable for sufficiently small data. For the linear case, installing a stabilizer at a boundary point is robust for the exponential stability of the system. GRA

N88-22633# Washington Univ., St. Louis, Mo. Dept. of Systems Science and Mathematics.
DEVELOPMENT AND APPLICATION OF THE p-VERSION OF THE FINITE ELEMENT METHOD Final Report, 30 Sep. 1985 - 30 Sep. 1987
I. N. Katz, Barna A. Szabo, and A. P. Greensfelder 30 Dec. 1987 30 p
(Grant AF-AFOSR-0315-82)
(AD-A190036; AFOSR-88-0149TR) Avail: NTIS HC A03/MF A01 CSCL 12A

The p-version of the finite element method is a new, important, computationally efficient, approach to finite element analysis. It is more robust than the conventional h-version and its rate of convergence, for domains with corners and for other singularity problems, is twice that of the h-version. Hierarchic elements which implement the p-version efficiently have been formulated so as to enforce C superscript 0 or C superscript 1 continuity in the planar case, and so as to enforce C superscript 0 continuity in three dimensions. Recent research accomplishments include: (1) development of an algorithm that finds all roots of an analytic function in a finite domain, (2) preprocessing procedures to restrict the search in unbounded domains which contain roots to bounded domains, (3) a reliable numerical argument principle algorithm to compute number of zeros within a closed contour, (4) formulation of equations which determine the nature of stress singularity at a corner of a plate composed of n isotropic materials. All of the above are used in the extraction method for p-version finite element analysis of composite materials with corners. GRA

N88-22634# Massachusetts Inst. of Tech., Cambridge.
RESEARCH ON ALGEBRAIC MANIPULATION Final Report, 1 Sep. 1985 - 31 Aug. 1986
Joel Moses 15 Apr. 1987 3 p
(Grant AF-AFOSR-0264-85)
(AD-A190149; AFOSR-87-2039TR) Avail: NTIS HC A02/MF A01 CSCL 12A

The focus of this research was algebraic manipulation or symbolic computation as in MACSYMA. The dilogarithm function was studied to obtain methods for the integration of dilogs in closed form. The work points the way for a generalization of the concept of closed form solutions. GRA

N88-22635# University of Southern California, Los Angeles. Dept. of Electrical Engineering.
THE ALGEBRAIC STRUCTURE OF CONVOLUTIONAL CODES Final Report, 15 Jul. 1985 - 14 Jul. 1987
Irving S. Reed 25 Sep. 1987 46 p
(Grant AF-AFOSR-0259-85)
(AD-A190280; AFOSR-87-1738TR) Avail: NTIS HC A03/MF A01 CSCL 09A

A new pruned-trellis search algorithm for high-rate convolutional code is developed. The search time and memory size is significantly reduced from standard search techniques. Some new high-rate systematic optimum convolutional codes of rate up to 7/8 have been found by this new search technique, and with constraint length up to 15. These newly found high-rate convolutional codes can be efficiently decoded using pruned, error-trellis, syndrome decoding. The real advantage of the pruned error-trellis decoding over the conventional Viterbi decoding algorithm is the reduction of the memory size required. Simulation shows that the error trellis performance of pruned error-trellis decoding suffers only a 0.2 dB loss for some systematic high-rate convolutional codes compared with conventional, full trellis decoding. GRA

N88-22636# Army Armament Research and Development Command, Watervliet, N. Y. Weapons Lab.
A POSTERIOR ERROR ESTIMATION IN A FINITE ELEMENT METHOD FOR PARABOLIC PARTIAL DIFFERENTIAL EQUATIONS Final Report
J. M. Coyle and J. E. Flaherty Dec. 1987 29 p
(AD-A190296; ARCCB-TR-87037) Avail: NTIS HC A03/MF A01 CSCL 12A

Superconvergence properties and quadratic polynomials are used to derive a computationally inexpensive approximation to the spatial component of the error in a piecewise linear finite element method for one-dimensional parabolic partial differential equations. This technique is coupled with time integration schemes of successively higher orders to obtain an approximation of the temporal and total discretization errors. Computational results indicate that these approximations converge to the exact discretization errors as the mesh is refined. The approximate errors are used to control an adaptive mesh refinement strategy. GRA

N88-22637# North Carolina Univ., Chapel Hill. Center for Stochastic Processes.
NORMED BELLMAN EQUATION WITH DEGENERATE DIFFUSION COEFFICIENTS AND ITS APPLICATION TO DIFFERENTIAL EQUATIONS

Masatoshi Fujisaki Oct. 1987 35 p
(Contract F49620-85-C-0144)
(AD-A190319; TR-211; AFOSR-87-1817TR) Avail: NTIS HC A03/MF A01 CSCL 12C

The purpose of this paper is to prove the existence and uniqueness of generalized solution of the normed Bellman equation with degenerate diffusion coefficients and also to prove that this unique solution is the cost function of a stochastic control problem associated with the normed Bellman equation. We can apply these results to some interesting degenerate and nonlinear differential equations. GRA

N88-22638# North Carolina Univ., Chapel Hill. Center for Stochastic Processes.
SEQUENTIAL TESTS FOR THE DRIFT OF A WIENER PROCESS WITH A SMOOTH PRIOR AND THE HEAT EQUATION
Gordon Simon, Yi-Ching Yao, and Xizhi Wu Oct. 1987 18 p
(Contract F49620-85-C-0144)
(AD-A190322; TR-212; AFOSR-87-1878TR) Avail: NTIS HC A03/MF A01 CSCL 12A

Methods are described which permit one to work with continuous-time optimal stopping problems, using the heat equation, even when the prior placed on the drift parameter of a Wiener process is not normal. The details of the method are worked out for Chernoff's problem of testing the sign of the drift parameter when the prior is smooth. GRA

N88-22639# Pittsburgh Univ., Pa. Center for Multivariate Analysis.
SOME COMMENTS ON QUADRANT DEPENDENCE IN HIGHER DIMENSIONS
K. Subramanyam Sep. 1987 13 p
(Contract N00014-85-C-0008; AF Proj. 2304)
(AD-A190329; TR-87-32) Avail: NTIS HC A03/MF A01 CSCL 12B

An extreme point analysis has been performed on two natural definitions of positive quadrant dependence of three random variable. This analysis helps us to understand how much these two notions of dependence are different. GRA

N88-22640# Massachusetts Inst. of Tech., Cambridge. Artificial Intelligence Lab.
NON-RIGID MOTION AND REGGE CALCULUS
R. Jasinschi and A. Yuille Nov. 1987 35 p
(Contract N00014-85-K-0124)
(AD-A190387; AD-E801598; AI-M-996) Avail: NTIS HC A03/MF A01 CSCL 12A

This document studies the problem of recovering the structure from the motion of figures which are allowed to perform a controlled non-rigid motion. The authors use Regge Calculus to approximate a general surface by a net of triangles. The non-rigid flexing motion they deal with corresponds to keeping the triangles rigid and allowing bending only at the joints between triangles. Such motion has been studied by Koenderink and van Doorn (1986). It is shown that this motion keeps the Gaussian curvature of the surface constant but changes the principal curvatures. The authors show that depth information of the vertices of the triangles can be obtained by using a modified version of the Incremental Rigidity Scheme devised by Ullman (1984). In cases where the motion of the figure displays fundamentally different views at each frame presentation the algorithm works well, not only for strictly rigid motion (Ullman 1984, Grzwacz and Hildreth 1985) but also for a limited amount of bending deformation. This scheme is modified to allow for flexing motion (in the sense defined above). This version is called the Incremental Semirigidity Scheme. GRA

N88-22641# Maryland Univ., College Park.
HIGHER ORDER CROSSINGS Final Report, Jun. 1982 - 31 May 1987
B. Kedem May 1987 4 p
(Grant AF-AFOSR-0187-82)
(AD-A190489; AFOSR-87-1768TR) Avail: NTIS HC A02/MF A01 CSCL 12B

A graphical device that is useful as a diagnostic tool for higher order crossings was introduced. The graphical tool is also useful as a descriptive similarity measure for time series models. Higher order crossings analysis has been applied to real data, revealing several known periodicities as well as several previously undiscovered periodicities. The class of strictly oscillatory processes was introduced. GRA

N88-22642# Cornell Univ., Ithaca, N.Y. Center for Applied Mathematics.
SYMMETRY AND GLOBAL BIFURCATION IN NONLINEAR SOLID MECHANICS Final Report, 1 Aug. 1986 - 31 Jul. 1987
Timothy J. Healy 16 Nov. 1987 15 p
(Grant AF-AFOSR-0185-86)
(AD-A190521; AFOSR-87-1755TR) Avail: NTIS HC A03/MF A01 CSCL 12A

Applications of tools from group theory and nonlinear analysis to global bifurcation problems from solid mechanics are summarized. These include both topological and computational approaches for problems involving structural frameworks, strings, rods and 3-dimensional elastic bodies. GRA

N88-22643# Massachusetts Inst. of Tech., Cambridge. Artificial Intelligence Lab.
ONTIC: A KNOWLEDGE REPRESENTATION SYSTEM FOR MATHEMATICS Ph.D. Thesis
David A. McAllester 1987 386 p
(Contract N00014-86-K-0180)
(AD-A190553; AI-TR-979) Avail: NTIS HC A17/MF A01 CSCL 12E

ONTIC is an interactive system for developing and verifying mathematics. ONTIC's verification mechanism is capable of automatically finding and applying information from a library containing hundreds of mathematical facts. Starting with only the axioms of Zermelo-Fraenkel set theory, the ONTIC system has been used to build a data base of definitions and lemmas leading to a proof of the Stone representation theorem for Boolean lattices. The ONTIC system has been used to explore issues in knowledge representation, automated deduction, and the automatic use of large data bases. GRA

N88-22644# Massachusetts Inst. of Tech., Cambridge. Artificial Intelligence Lab.
EXPRESSING MATHEMATICAL SUBROUTINES CONSTRUCTIVELY
Gerald L. Roylance Nov. 1987 16 p
(Contracts N00014-86-K-0180; N00014-85-K-0124)
(AD-A190559; AI-M-999) Avail: NTIS HC A03/MF A01 CSCL 12E

The typical subroutines that compute sin(x) and exp(x) bear little resemblance to our mathematical knowledge of these functions: they are composed of concrete arithmetic expressions that include many mysterious numerical constants. Instead of programming these subroutines conventionally, we can express their construction using symbolic ideas such as periodicity and Taylor series. Such an approach has many advantages: the code is closer the mathematical basis of the function, less vulnerable to errors, and is trivially adaptable to various precisions. GRA

N88-22645# Air Force Inst. of Tech., Wright-Patterson AFB, Ohio. School of Engineering.
AN APPROXIMATION TECHNIQUE FOR SOLVING A SYSTEM OF FREDHOLM INTEGRAL EQUATIONS FOR ASYMMETRIC DETECTOR RESPONSE FUNCTIONS M.S. Thesis
Russell B. Daniel Mar. 1988 150 p
(AD-A190577; AFIT/GNE/ENG/88M-3) Avail: NTIS HC A07/MF A01 CSCL 12E

The purpose of this study was to develop the methodology to implement a computer program to approximate a solution to a system of Fredholm integral equations. The system of equations used in this study is representative of the equations formed during

the detection of pulsed radiation using a series of detectors with asymmetric response functions. Though general in nature and applicable to all systems of Fredholm integral equations, the equations studied are of importance to the Defense Nuclear Agency with regard to the measurement of radiation spectra during underground nuclear effects simulation testing. The deconvolution or solution technique consisted of representing the unfolded spectrum as a weighted sum of basis functions. This unfolded spectrum, the actual spectrum, and predicted spectrum were then used to form a chi square test statistic. By adjusting the parameters in the basic functions and their weights, chi square was minimized and the unfolded spectrum was corrected to approximate the actual spectrum. The methodology for this deconvolution technique was then converted into a general computer program. The validation cases conducted on the two types of spectra confirmed the reliability of the methodology and the computer program. GRA

N88-22646# Argonne National Lab., Ill.
TRUST REGIONS AND PROJECTED GRADIENTS
J. J. More Jan. 1988 16 p Presented at the 13th IFIP Conference on System Modelling and Optimization, Tokyo, Japan, 31 Aug. 1987
(Contract W-31-109-eng-38)
(DE88-005829; ANL/MCS-TM-107; CONF-8708220-1) Avail: NTIS HC A03/MF A01

The numerical solution of large scale linearly constrained problems by algorithms which use the gradient projection method is a promising research area. Algorithms based on the gradient projection method are able to drop and add many constraints at each iteration, and this ability gives them an important advantage in large scale problems. In this paper we show how the ideas from the gradient projection method combine with trust region methods, and we give an indication of the powerful convergence results that are available for algorithms of this type. DOE

N88-22647# Amsterdam Univ. (Netherlands). Dept. of Computer Science.
CONSTRUCTIVE VERSION OF THE APPROXIMATION INDUCTION PRINCIPLE
S. Mauw Apr. 1987 18 p
(PB88-165477; FVI-87-09) Avail: NTIS HC A03/MF A01 CSCL 12A

A constructive version of the Approximation Induction Principle is formulated, which states that equality of processes can be decided after observing the initial behavior of the processes. The principle is proved correct for the class of regular processes. The number of states of the processes determines the number of steps to be considered. This principle can be used to formulate a complete inference system for regular processes and algorithms to decide upon equality. GRA

N88-22648# Amsterdam Univ. (Netherlands). Dept. of Computer Science.
COMPLEXITY OF SOME PROBLEMS IN MODULE ALGEBRA
W. Kowalczyk Mar. 1987 18 p
(PB88-165386; FVI-87-07) Avail: NTIS HC A03/MF A01 CSCL 12A

The complexity of some relations on signatures and modules is established. The Signature Isomorphism Problem and the Module Isomorphism Problem are shown to be equivalent (with respect to polynomial time reductions) to the Graph Isomorphism Problem, whereas the Module Biinterpretation Problem and the Module Total Biinterpretation Problem are shown to be NP-complete. GRA

N88-22649# Helsinki Univ. of Technology, Espoo (Finland). Lab. of Electromechanics.
BOUNDARY ELEMENT METHOD FOR THREE-DIMENSIONAL MAGNETOSTATIC FIELDS IN TERMS OF VECTOR VARIABLES Ph.D. Thesis
Lixin Li 1988 62 p Sponsored by the State Education Commission of China and the Finnish Ministry of Education
(EL-61; ISBN-9-51-666253-6; ISSN-0001-6845; ETN-88-92219)
Avail: NTIS HC A04/MF A01

A boundary element method for three-dimensional magnetostatic problems, where analysis is performed in terms of the magnetic flux density or the magnetic vector potential, is developed. Uniqueness conditions for boundary value problems in magnetostatics are presented. A set of vector boundary integral equations is derived. The integral equations are approximated by applying the point matching of Galerkin method, and the formulations of isoparametric boundary element solution are developed for linear homogeneous problems. An interpolation method is introduced to take special features in magnetostatics into consideration, and a numerical scheme catering for the singularity in integral equations is described. The technique for homogeneous problems is extended for interface problems with modification. Numerical examples for homogeneous and interface problems are given. ESA

N88-22650*# National Aeronautics and Space Administration. Ames Research Center, Moffett Field, Calif.
NUMERICAL STUDY OF UNSTEADY VISCOUS HYPERSONIC BLUNT BODY FLOWS WITH AN IMPINGING SHOCK
G. H. Klopfer (Nielsen Engineering and Research, Inc., Mountain View, Calif.), H. C. Yee, and P. Kutler Apr. 1988 10 p
(NASA-TM-100096; A-88147; NAS 1.15:100096) Avail: NTIS HC A02/MF A01 CSCL 12A

A complex two-dimensional, unsteady, viscous hypersonic shock wave interaction is numerically simulated by a high-resolution, second-order fully implicit shock-capturing scheme. The physical model consists of a nonstationary oblique shock impinging on the bow shock of a blunt body. Studies indicated that the unsteady flow patterns are slightly different from their steady counterparts. However, for the sample cases investigated the peak surface pressures for the unsteady flows seem to occur at very different impingement locations than for the steady flow cases. Author

N88-22651*# National Aeronautics and Space Administration. Ames Research Center, Moffett Field, Calif.
HIGH-RESOLUTION SHOCK-CAPTURING SCHEMES FOR INVISCID AND VISCOUS HYPERSONIC FLOWS
H. C. Yee, G. H. Klopfer, and J.-L. Montagne (Office National d'Etudes et de Recherches Aeronautiques, Paris, France) Apr. 1988 36 p
(NASA-TM-100097; A-88148; NAS 1.15:100097) Avail: NTIS HC A03/MF A01 CSCL 12A

A class of implicit Total Variation Diminishing (TVD) type algorithms suitable for transonic and supersonic multidimensional Euler and Navier-Stokes equations was extended to hypersonic computations. The improved conservative shock-capturing schemes are spatially second- and third-order, and are fully implicit. They can be first- or second-order accurate in time and are suitable for either steady or unsteady calculations. Enhancement of stability and convergence rate for hypersonic flows is discussed. With the proper choice of the temporal discretization and suitable implicit linearization, these schemes are fairly efficient and accurate for very complex two-dimensional hypersonic inviscid and viscous shock interactions. This study is complimented by a variety of steady and unsteady viscous and inviscid hypersonic blunt-body flow computations. Due to the inherent stiffness of viscous flow problems, numerical experiments indicated that the convergence rate is in general slower for viscous flows than for inviscid steady flows. Author

N88-22652*# National Aeronautics and Space Administration. Lewis Research Center, Cleveland, Ohio.
A PHYSICALLY CONSISTENT MODEL FOR ARTIFICIAL DISSIPATION IN TRANSONIC POTENTIAL FLOW COMPUTATIONS
George S. Dulikravich, Karl W. Mortara, and Lionel Marraffa (Office National d'Etudes et de Recherches Aerospatiales, Paris, France) May 1988 14 p
(NASA-TM-100846; E-4040; ICOMP-88-6; NAS 1.15:100846)
Avail: NTIS HC A03/MF A01 CSCL 12A

The effect that artificial dissipation has on numerical solutions of the transonic Full Potential Equation (FPE) are investigated by

comparing the artificially dissipative FPE to a Physically Dissipative Potential (PDP) equation. Analytic expressions were derived from the variables C and M sub c that are used in the artificial density formulation. It was shown that these new values generate artificial dissipation which is equivalent to the physical dissipation existing in the PDP equation. The new expression for the variables C and M sub c can easily be incorporated into the existing full potential codes which are based either on the artificial density or on the artificial viscosity formulation. A comparison of Physically Dissipative Potential (PDP), Artificial Density or Viscosity (ADV), Artificial Mass Flux (AMF), and ADV with variable C and M sub c formulation (MCC) is also presented. Author

N88-22240# Joint Publications Research Service, Arlington, Va.
EFFICIENT METHOD FOR STRUCTURAL OPTIMIZATION Abstract Only
Renwei Xia *In its* JPRS Report: Science and Technology. China 11 Dec. 1987 p 48 Transl. into ENGLISH from Lixue Xuebao (Beijing, Peoples Republic of China), v. 19, no. 3, May 1987 p 246-257 (For primary document see N88-22233 15-31)
Avail: NTIS HC A06/MF A01

65 STATISTICS AND PROBABILITY

Includes data sampling and smoothing; Monte Carlo method; and stochastic processes.

N88-22653*# National Aeronautics and Space Administration. Langley Research Center, Hampton, Va.
ANALYSIS AND TESTING OF THE SURE PROGRAM
Kelly J. Dotson [1988] 1 p
(NASA-TP-2817; L-16413; NAS 1.60:2817) PREVIEW CSCL 12A

The results of an extensive effort to test the SURE (Semi-Markov Unreliability Range Evaluator) program are presented. The SURE program is a reliability analysis tool developed at NASA Langley Research Center that computes upper and lower bounds on the death-state probabilities of semi-Markov models. The intent of the program is to use the bounds to assess the reliability of fault tolerant computer systems modeled by semi-Markov processes. Testing was conducted in three phases. In the first phase, several simple semi-Markov models were solved analytically for the death-state probabilities; then, these solutions were compared to the corresponding bounds given by SURE. During the second phase, much larger and more realistic models of fault tolerant systems were examined. The SURE bounds for the unreliability of each of these models was compared with the unreliability estimates from other reliability analysis tools including CARE III (Computer Aided Reliability Estimation version 3), PAWS (Pade Approximation With Scaling), ARIES (Automated Reliability Interactive Estimation System), and STEM (Scaled Taylor Exponential Matrix). The final phase of testing consisted of an error analysis of the mathematical bounds. Author

N88-22654*# National Aeronautics and Space Administration. Lyndon B. Johnson Space Center, Houston, Tex.
RANDOM PROCESS SIMULATION FOR STOCHASTIC FATIGUE ANALYSIS Ph.D. Thesis - Rice Univ., Houston, Tex.
Curtis E. Larsen Mar. 1988 150 p
(NASA-TM-100464; S-576; NAS 1.15:100464) Avail: NTIS HC A07/MF A01 CSCL 12A

A simulation technique is described which directly synthesizes the extrema of a random process and is more efficient than the Gaussian simulation method. Such a technique is particularly useful in stochastic fatigue analysis because the required stress range moment E(R sup m), is a function only of the extrema of the random stress process. The family of autoregressive moving average (ARMA) models is reviewed and an autoregressive model is presented for modeling the extrema of any random process which has a unimodal power spectral density (psd). The proposed autoregressive technique is found to produce rainflow stress range moments which compare favorably with those computed by the Gaussian technique and to average 11.7 times faster than the Gaussian technique. The autoregressive technique is also adapted for processes having bimodal psd's. The adaptation involves using two autoregressive processes to simulate the extrema due to each mode and the superposition of these two extrema sequences. The proposed autoregressive superposition technique is 9 to 13 times faster than the Gaussian technique and produces comparable values for E(R sup m) for bimodal psd's having the frequency of one mode at least 2.5 times that of the other mode. Author

N88-22655 Politecnico di Milano (Italy). Dipt. di Elettronica.
NEAR OPTIMAL BLIND DECONVOLUTION
Sandro Bellini and Fabio Rocca 1987 34 p
(Rept-87-016; ETN-88-92271) Avail: Politecnico di Milano, Piazza Leonardo da Vinci 32, 20133 Milan, Italy

A solution for the blind deconvolution problem, i.e., the estimation of the impulse response of an unknown discrete time channel given the output data sequence and statistical information on the input sequence is proposed. The solution approaches the optimal one when the input sequence is independent and identically distributed and the channel distortion is small. The variance of the estimates is calculated and checked against the Cramer-Rao bound. In the case of a Gaussian input, the solution reduces to the classical spectral estimation. In the non-Gaussian case, the variance of the estimated amplitude spectrum is reduced, and the phase spectrum can be estimated too. The estimation is based on the use of a generalized crosscovariance between the output data sequence and a nonlinear function of the same data. Numerical results are given in the case of the optimal nonlinearity, which depends on the input probability density function, and in the case of the very simple sign nonlinearity. A comparison with polyspectral techniques is made. ESA

N88-22656# Alberta Univ., Edmonton. Dept. of Statistics and Applied Probability.
FILTERING OF JUMP PROCESSES Annual Report, 30 Sep. 1986 - 30 Sep. 1987
Robert J. Elliott 30 Oct. 1987 7 p
(Grant AF-AFOSR-0332-86)
(AD-A189701; AFOSR-87-1930TR) Avail: NTIS HC A02/MF A01 CSCL 12C

The focus of this research is the filtering jump processes. To investigate the filtering of manifold-valued processes, their approximation by random walks and Markov chains was studied. The object was to approximate a signal process by a finite-state jump process for which a finite-dimensional filter is available. GRA

N88-22657# Massachusetts Inst. of Tech., Cambridge. Lab. for Information and Decision Systems.
STRUCTURAL DECOMPOSITION OF MULTIPLE TIME SCALE MARKOV PROCESSES
J. R. Rohlicek and A. S. Willsky Oct. 1987 11 p
(Grant AF-AFOSR-0258-82)
(AD-A189739; LIDS-P-1711; AFOSR-87-1852TR) Avail: NTIS HC A03/MF A01 CSCL 12C

A straightforward algorithm for the multiple time scale decomposition of singularly perturbed Markov processes is presented. That algorithm provides a uniform approximation of the probability transition function over the interval t greater than or equal to 0 through the construction of a sequence of aggregate models valid at successively slower time scales. When only the structure of these models is desired, the algorithm can be expressed simply in terms of graphs associated with each of the aggregated models. The major computation then becomes computing shortest paths in these graphs. This representation of the algorithm furthermore allows analysis of more complex systems where there are multiple perturbation parameters with unknown relative orders of magnitude. GRA

N88-22658# Alberta Univ., Edmonton. Dept. of Statistics and Applied Probability.
THE PARTIALLY OBSERVED STOCHASTIC MINIMUM PRINCIPLE Report, 30 Sep. 1986 - 30 Sep. 1987
John Baras, Robert J. Elliott, and Michael Kohlmann 11 Nov. 1987 20 p
(Grant AF-AFOSR-0332-86)
(AD-A189787; AFOSR-87-1939TR) Avail: NTIS HC A03/MF A01 CSCL 12C

The focus of this research is the filtering jump processes. To investigate the filtering of manifold valued processes, their approximation by random walks and Markov chains was studied. The object was to approximate a signal process by a finite-state jump process for which a finite dimensional filter is available. The Partially Observed Stochastic Minimum Principle: A minimum principle for a partially observed diffusion can be obtained by differentiating the statement that a control u* is optimal. The results on stochastic flows enable us to compute in an easy and explicit way the change in the cost due to a strong variation of an optical control. The only technical difficulty is the justification of the differentiation. GRA

N88-22659# North Carolina Univ., Chapel Hill. Center for Stochastic Processes.
APPROXIMATIONS IN EXTREME VALUE THEORY Report, Sep. 1987 - Aug. 1988
Richard L. Smith Sep. 1987 35 p
(Contract F49620-85-C-0144)
(AD-A189817; TR-205; AFOSR-87-1848TR) Avail: NTIS HC A03/MF A01 CSCL 12C

Following a survey of rates of convergence in extreme value theory, a new class of approximations is developed and compared with existing approximations based on the extreme value distributions. Convergence in Hellinger distance is established, this distance measure being chosen because of its statistical applications. Numerical examples confirm the superiority of the new approximation. GRA

N88-22660# Center for Naval Analyses, Alexandria, Va. Marine Corps Operations Analysis Group.
PROPERTIES OF SOME BAYESIAN SCORING PROCEDURES FOR COMPUTERIZED ADAPTIVE TESTS
D. R. Divgi Aug. 1987 26 p
(Contract N00014-87-C-0001)
(AD-A189925; CRM-87-161) Avail: NTIS HC A03/MF A01 CSCL 08J

The computerized adaptive version of the Armed Services Vocational Aptitude Battery will use a Bayesian procedure for computing test scores. Properties of three common Bayesian procedures are examined in this research memorandum. The results show that the procedures are almost equally reliable and that reliability drops if item parameters change from paper-pencil to computerized administration. GRA

N88-22661# Pittsburgh Univ., Pa.
MULTIVARIATE ANALYSIS AND ITS APPLICATION Final Report, 1 Oct. 1984 - 30 Sep. 1987
P. R. Krishnaiah and C. R. Rao Sep. 1987 59 p
(Contract F49620-85-C-0008)
(AD-A189983; AFOSR-87-1967TR) Avail: NTIS HC A04/MF A01 CSCL 12C

Some important contribution by this project were made to several areas of multivariate analysis, with applications in manufacturing technology, signal processing, automation, expert systems, pattern recognition, and machine intelligence. GRA

N88-22662# University of Southern California, Los Angeles. Dept. of Mathematics.
APPROXIMATION METHODS FOR THE IDENTIFICATION AND CONTROL OF DISTRIBUTED PARAMETER SYSTEMS Final Technical Report, 1 Oct. 1984 - 30 Sep. 1987
I. G. Rosen 20 Nov. 1987 43 p
(Grant AF-AFOSR-0393-84)
(AD-A190201; AFOSR-87-1980TR) Avail: NTIS HC A03/MF A01 CSCL 12D

Efforts to develop computational methods for the identification and optimal control of linear and nonlinear systems governed by distributed parameter systems are reported. Specifically, approximation methods for determining Optimal LOG compensators (feedback control and estimator gains) and functional parameters in linear and nonlinear partial differential equations and hereditary systems were developed, analyzed and tested. The study included theoretical, experimental and numerical components. Covergence theories for spline-based and modal finite element schemes were established and extensive numerical studies on both conventional (serial) and vector supercomputers were carried out. A parameter estimation scheme was tested using experimental data taken from the RPL structure, a laboratory experiment designed to test control algorithms for the large angle slewing of spacecraft with flexible appendages, and other projects involving the identification of flexible structures based on experimental data were initiated. GRA

N88-22663# Stanford Univ., Calif. Dept. of Statistics.
DISTRIBUTIONS OF QUADRATIC FORMS
Mary E. Bock and Herbert Solomon 24 Nov. 1987 18 p
(Contract N00014-86-K-0156)
(AD-A190224; TR-398) Avail: NTIS HC A03/MF A01 CSCL 12C

For independent chi-square variables x squared sub m and x squared sub n with m and n degrees of freedom, respectively, we consider the quadratic form where the positive ci are distinct. This paper gives exact finite expressions for the distribution of Q in terms of available functions such as the distribution function of chi-square random variables, modified Bessel Functions, Dawson's integral. These formulas are useful for checking the accuracy of approximations and tables of the distribution of Q and provide a simple alternative in their absence. For large m and n, reasonable approximations to the distribution of Q are available. For the general quadratic form Williams (1984) compares algorithms for truncations of infinite series expansions of the distribution. GRA

N88-22664# North Carolina Univ., Chapel Hill. Center for Stochastic Processes.
STOPPING RULES AND OBSERVED SIGNIFICANCE LEVELS
John Bather Sep. 1987 14 p
(Contract F49620-85-C-0144)
(AD-A190320; TR-209; AFOSR-87-1013TR) Avail: NTIS HC A03/MF A01 CSCL 12C

It is well known how to combine the significance levels observed in a number of independent experiments. When this number is a random variable determined by a stopping rule, the observed significance level can still be calculated if there is an acceptable ordering of the points in the extended sample space. But what can be said if the stopping time is ill-defined? This paper obtains explicit lower bounds on the level of significance by considering orderings based on a family of alternative hypotheses. These bounds give some measure of the effect of failing to specify the stopping rule in advance. GRA

N88-22665# North Carolina Univ., Chapel Hill. Dept. of Statistics.
INFORMATION AND CODING CAPACITIES OF MISMATCHED GAUSSIAN CHANNELS
Charles R. Baker Sep. 1987 12 p
(Contract N00014-86-K-0039)
(AD-A190321; LISS-19) Avail: NTIS HC A03/MF A01 CSCL 12I

Recent results on coding capacity and information capacity for the mismatched Gaussian channel are discussed. Sufficient conditions for casual feedback to increase information capacity are given for the finite-dimensional discrete-time Gaussian channel. GRA

N88-22666# North Carolina Univ., Chapel Hill. Center for STochastic Processes.
ESTIMATION OF CONVOLUTION TAILS Technical Report, 1 Oct. 1986 - 30 Sep. 1987
Eric Willekens Sep. 1987 21 p
(Contract F49620-85-C-0144)
(AD-A190323; TR-206; AFOSR-87-1851TR) Avail: NTIS HC A03/MF A01 CSCL 12C

Several classes of distribution functions (d.f.) are originated by considering distributions whose tail functions satisfy special asymptotic relations. A large class sharing this property is provided by a certain subexponential class, in which case the asymptotic relation involves tails of convolution powers. This paper introduces a statistic which estimates the asymptotic behavior of convolution tails of a given d.f. and it is shown that this statistic is strongly consistent and asymptotically normal under appropriate conditions. Furthermore, the statistic can be used to test the hypothesis that a d.f. is in the exponential class being described. GRA

N88-22667# North Carolina Univ., Chapel Hill. Center for Stochastic Processes.
CONTINUITY OF SYMMETRIC STABLE PROCESSES Technical Report, 1 Oct. 1986 - 30 Sep. 1987
John P. Nolan Sep. 1987 19 p
(Contract F49620-85-C-0144)
(AD-A190324; TR-200; AFOSR-87-1955TR) Avail: NTIS HC A03/MF A01 CSCL 12C

The path continuity of a symmetric p-stable process is examined in terms of any stochastic integral representation for the process. When $0 < p < 1$, we give necessary and sufficient conditions for path continuity in terms of any (every) representation. When $1 < \text{or} = p < 2$, we extend the know sufficiency condition in terms of metric entropy and offer a conjecture as to the complete solution. Finally, necessary and sufficient conditions for path continuity are given in terms of continuity at a point for $0<p<2$. GRA

N88-22668# North Carolina Univ., Chapel Hill. Center for Stochastic Processes.
EXTREME VALUE FOR DEPENDENT SEQUENCES VIA THE STEIN-CHEN METHOD OF POISSON APPROXIMATION
Richard L. Smith Oct. 1987 19 p
(Contract F49620-85-C-0144)
(AD-A190325; TR-87-213; AFOSR-87-1876TR) Avail: NTIS HC A03/MF A01 CSCL 12C

In 1970 Stein introduced a new method for bounding the approximation error in central limit theory for dependent variables. This was subsequently developed by Chen for Poisson approximation and has proved very successful in the areas to which it has been applied. Here this document shows how the method can be applied to extreme value theory for dependent sequences, focussing particularly on the nonstationary case. The method gives new and shorter proofs of some known results, with explicit bounds for the approximation error. GRA

N88-22669# Pittsburgh Univ., Pa. Center for Multivariate Analysis.
ADMISSIBLE BAYES TESTS FOR STRUCTURAL RELATIONSHIP
Wei-Hsiung Shen and Bimal K. Sinha Sep. 1987 20 p
(Contract F49620-85-C-0008)
(AD-A190326; TR-87-31; AFOSR-87-1959TR) Avail: NTIS HC A03/MF A01 CSCL 12C

It is an open problem to construct a test for structural relationship among the mean vectors of several multivariate normal populations with known but unequal covariance matrices. In this paper, a class of admissible Bayes tests for the above problem is derived. As a byproduct, in the special case of known and equal covariance matrices, the likelihood ratio test of Rao(1973) is shown to be admissible Bayes. GRA

N88-22670# Pittsburgh Univ., Pa. Center for Multivariate Analysis.
EMPIRICAL AND HIERARCHICAL BAYES COMPETITORS OF PRELIMINARY TEST ESTIMATORS IN TWO SAMPLE PROBLEMS
Malay Ghosh and Bimal K. Sinha Sep. 1987 31 p
(Contract F49620-85-C-0008)
(AD-A190327; TR-87-34; AFOSR-87-1960TR) Avail: NTIS HC A03/MF A01 CSCL 12C

Suppose in a laboratory, say Laboratory I, a certain instrument is designed to measure several characteristics, and a number of vector-valued measurements is recorded. The objective is to estimate the unknown population mean. It is known, however, that a similar instrument is used in another laboratory, say Laboratory II for the same purpose, and a number of observations is recorded from the second instrument. It is also suspected that the two population means are equal, in which case, observations recorded in Laboratory II can possibly be used effectively together with those in Laboratory I for estimating the population mean of the first instrument. Thus, the question that naturally arises is whether one should use the sample mean from Laboratory I or the pooled mean from the two laboratories. In problems of this type what is normally sought is a compromise estimator which leans more towards the pooled sample mean when the null hypothesis of the equality of the two population means is accepted, and towards the sample mean from Laboratory I when such a hypothesis is rejected. A very popular way to achieve this compromise is to use a preliminary test estimator (PTE) which uses the pooled mean when the null hypothesis is accepted at a desired level of significance, and uses the sample mean from Laboratory I when opposite is the case. This paper proposes, instead, an empirical Bayes estimator which achieves the intended compromise. GRA

N88-22671# Pittsburgh Univ., Pa. Center for Multivariate Analysis.
DETECTION OF THE NUMBER, LOCATIONS AND MAGNITUDES OF JUMPS
Y. Q. Yin Aug. 1987 15 p
(Contract F49620-85-C-0008)
(AD-A190328; TR-87-27; AFOSR-87-1961TR) Avail: NTIS HC A03/MF A01 CSCL 12C

Consider a signal $x(t) = f(t) + w(t)$, $0 < \text{or} = 1$. Here the noise w(t) is an independent process, and f(t) is a function with only finitely many jumps, satisfies a Lipschitz' condition between any two consecutive jumps. This paper gives an algorithm to determine the number, locations and magnitudes of the jumps of f(t). The consistency and speeds of convergence are obtained. GRA

N88-22672*# Jet Propulsion Lab., California Inst. of Tech., Pasadena.
MATHEMATICS CLINIC PROBABILISTIC POSITION-FIXING Final Report
Ellis Cumberbatch Jun. 1987 70 p
(Contract NAS7-918)
(NASA-CR-182753; JPL-D-462; NAS 1.26:182753; AD-A190397; TM-29) Avail: NTIS HC A04/MF A01 CSCL 12C

The problem is to determine confidence regions for the location of objects or emitters on which bearings are taken from two or more sensors whose positions are known. This clinic studied the classical approach to determining such regions, which involved the assumption that an error of observation of the line of bearing displaces the line parallel to itself. By dropping this assumption, they found that the classical probability regions, which are ellipses, contained only 50 to 80 percent of the probability claimed. One goal of this year's clinic was to determine the reason for this very large discrepancy. As it turned out, the reason was neither the dropping of the parallel displacement assumption, nor computational errors in the clinic's work, but two equations in the original publication describing the classical approach were printed incorrectly. These errors are probably transcription errors, but no

corrections or references to them were found in a search of the relevant literature. GRA

N88-22673# Johns Hopkins Univ., Baltimore, Md. Dept. of Mathematical Sciences.
STATISTICAL INFERENCE FOR STOCHASTIC PROCESSES Final Report, 1 Jan. 1982 - 31 Dec. 1986
Alan F. Karr 15 Oct. 1987 40 p
(Grant AF-AFOSR-0029-82)
(AD-A190491; AFOSR-87-2016TR) Avail: NTIS HC A03/MF A01 CSCL 12C

Research under this grant resulted in 42 research papers and one book. Topics included state estimation for Cox processes, inferences for stationary point processes, inference for multiplicative intensity model, inference for thinned point processes, inference for 0 to 1 Markov processes, and inference for stationary random fields. GRA

N88-22674# Northwestern Univ., Evanston, Ill.
MARKOV PROCESSES APPLIED TO CONTROL, REPLACEMENT AND SIGNAL ANALYSIS Final Technical Report, 1 Jun. 1982 - 31 Jul. 1987
Mark A. Pinsky 30 Sep. 1987 5 p
(Grant AF-AFOSR-0189-82)
(AD-A190563; AFOSR-87-2015TR) Avail: NTIS HC A02/MF A01 CSCL 12C

The top Lyapunov exponent of a system of stochastic differential equations was investigated. Brownian motion paths on a Riemannian manifold were discussed and several theoretical results were obtained. A new asymptotic formula for the volume of a small extrinsic ball in a submanifold was obtained. Finally, an invariance principle for Lie groups was obtained. GRA

N88-22675# Purdue Univ., West Lafayette, Ind. Dept. of Statistics.
ON TWO-STAGE ALLOCATION PROCEDURES FOR SELECTION PROBLEMS
Shanti S. Gupta and TaChen Liang 8 Dec. 1987 16 p
(Contract N00014-84-C-0167; Grant NSF DMS-86-06964)
(AD-A190766; TR-87-53) Avail: NTIS HC A03/MF A01 CSCL 12C

This paper deals with the problem of deriving two-stage allocation procedures for selecting the best normal population. If the prior distribution is assumed to be known, an exact Bayes two-stage allocation procedure is obtained. If the prior distribution depends on some unknown parameter, an adaptive two-stage allocation procedure is proposed. Using the empirical Bayes formulation, we prove that the proposed adaptive two-stage allocation procedure has some asymptotic optimality property. GRA

66 SYSTEMS ANALYSIS

Includes mathematical modeling; network analysis; and operations research.

N88-22676*# Colorado Univ., Boulder. Center for Space and Geosciences Policy.
NASA AND THE CHALLENGE OF ISDN: THE ROLE OF SATELLITES IN AN ISDN WORLD Final Report
Radford Byerly, Frank Barnes, George Codding, and Jefferson Hofgard 25 May 1988 67 p
(Grant NAGw-1105)
(NASA-CR-182749; NAS 1.26:182749) Avail: NTIS HC A04/MF A01 CSCL 12B

To understand what role satellites may play in Integrated Services Digital Network (ISDN), it is necessary to understand the concept of ISDN, including key organizations involved, the current status of key standards recommendations, and domestic and international progress implementation of ISDN. Each of these areas are explained. A summary of the technical performance criteria for ISDN, current standards for satellites in ISDN, key players in the ISDN environment, and what steps can be taken to encourage application of satellites in ISDN are also covered. Author

67 THEORETICAL MATHEMATICS

Includes topology and number theory.

N88-22677# North Carolina Univ., Chapel Hill. Center for Stochastic Processes.
STOCHASTIC EVOLUTION EQUATIONS DRIVEN BY NUCLEAR SPACE VALUED MARTINGALES Technical Report, 1 Oct. 1986 - 30 Sep. 1987
G. Kallianpur and V. Perez-Abreu Sep. 1987 59 p
(Contract F49620-85-C-0144)
(AD-A189342; TR-204; AFOSR-87-1914TR) Avail: NTIS HC A04/MF A01 CSCL 12B

The paper presents a theory of stochastic evolution equations for nuclear space valued processes and provides a unified treatment of several examples from the field of applications. (C sub O,1) reversed evolution systems on countably Hilbertian nuclear spaces are also investigated. GRA

N88-22678# Joint Inst. for Nuclear Research, Dubna (USSR). Lab. of Theoretical Physics.
ADIABATIC REPRESENTATION OF THREE-BODY PROBLEM IN HYPERSPHERICAL COORDINATES. STATEMENT OF THE PROBLEM
S. I. Vinitskij and M. B. Kadomtsev 1986 18 p In RUSSIAN; ENGLISH summary
(TI88-701162; JINR-R-4-86-696) Avail: NTIS (US Sales Only) HC A03/MF A01

For a three body Coulomb problem a hyperspherical parameterization is given for independent variables on a five dimensional sphere S sup 5 with a hyperradius R sub H, the first linear invariant of the tensor of inertia of three particles. The hyperspherical adiabatic basis is defined as a complete set of eigenfunctions and eigenvalues of the Hamiltonian angular part on the sphere S sup 5 for every fixed value of the slow variable R sub H. The partial wave analysis in the total momentum J representation allows us to separate three Euler angles and to reduce the hyperspherical problem on S sup 5 to a system of (J+1) two dimensional problems. Classification is given of states of the hyperspherical adiabatic basis for small and large values of the hyperradius R sub H and the logarithmic Fock singularity at the point of three body collision is explicitly shown. The approach is assigned at computing the cross sections of mesic-atomic processes in the muon-catalysis problem. DOE

N88-22679# Massachusetts Univ., Amherst.
REGULARITY OF THE ALBANESE MAP FOR NONORIENTED SURFACES
W. H. Meeks, III Sep. 1987 17 p
(Contract DE-FG02-86ER-25015)
(DE88-006428; DOE/ER-25015/4) Avail: NTIS HC A03/MF A01

This paper contains a generalization of the Jacobi imbedding theorem in classical Riemann surface theory. The main theorem gives necessary and sufficient conditions for the Albanese map of a closed nonorientable Riemannian surface to be a regular embedding of the surface into its Albanese variety. DOE

N88-22680# Massachusetts Univ., Amherst.
EMBEDDED MINIMAL SUFACES WITH AN INFINITE NUMBER OF ENDS
M. Callahan, D. Hoffman, and W. H. Meeks, III Sep. 1987 71 p
(Contract DE-FG02-86ER-25015)
(DE88-006429; DOE/ER-25015/3) Avail: NTIS HC A04/MF A01

We prove the existence of an infinite family of periodic properly

embedded minimal surfaces with an infinite number of annular ends. DOE

N88-22681# Hiroshima Univ., Takehara (Japan). Research Inst. for Theoretical Physics.
SUPER VIRASORO ALGEBRA AND SOLVABLE SUPERSYMMETRIC QUANTUM FIELD THEORIES
Yamanaka, Itaru and Ryu Sasaki Sep. 1987 34 p
(DE88-752299; RRK-87-21) Avail: NTIS (US Sales Only) HC A03/MF A01

Interesting and deep relationships between super Virasoro algebras and super soliton systems (super KdV, super mKdV and super sine-Gordon equations) are investigated at both classical and quantum levels. An infinite set of conserved quantities responsible for solvability is characterized by super Virasoro algebras only. Several members of the infinite set of conserved quantities are derived explicitly. DOE

N88-22682# Texas Univ., Austin. Center for Particle Theory.
GEOMETRIC METHODS AND THE GAUGE STRUCTURE OF BERRY'S PHASE
B. F. Bednarz Dec. 1987 20 p
(Contract DE-FG05-85ER-40200)
(DE88-006538; DOE/ER-40200/127) Avail: NTIS HC A03/MF A01

The use of geometric methods to obtain the connection associated with Berry's phase is discussed. Failures and successes in past attempts at using only geometry are presented. It is argued that this approach is most useful for Hamiltonians rotated on the parameter space. DOE

N88-22683# Rome Univ. (Italy). Dipt. di Fisica.
ON NEW SOLVABLE MANY-BODY DYNAMICAL SYSTEMS WITH VELOCITY DEPENDENT FORCES
M. Bruschi and O. Ragnisco 7 Jan. 1987 8 p Sponsored in part by the Italian Ministry of Public Education
(Preprint-581; ETN-88-92270) Avail: NTIS HC A02/MF A01

Results on solvable many-body dynamical systems, strictly related to relativistic Ruijsenaars systems, are presented. ESA

N88-22684# California Univ., San Diego. Inst. for Pure and Applied Physical Sciences.
BAECKLUND TRANSFORMATION AND THE SCHWARZIAN DERIVATIVE Final Report, 1 Feb. 1986 - 31 Jul. 1987
John E. Weiss 1 Nov. 1987 9 p
(Grant AF-AFOSR-0068-86)
(AD-A190277; AFOSR-87-1795TR) Avail: NTIS HC A02/MF A01 CSCL 12A

We complete the discussion of the periodic fixed points of Backlund transformations for the Korteweg-de Vries equation. It will be shown that the systems of equations defined by the KdV periodic fixed points are equivalent to the periodic Kac-Van Moerbeke systems. As a consequence, for even order fixed points, the KdV systems are equivalent to the periodic Toda lattice. The periodic fixed points of the Backlund transformation for the Boussinesq equation are found to have a Hamiltonian structure. The integrals of these systems are found. GRA

N88-22685# North Carolina Univ., Chapel Hill. Dept. of Statistics.
CODING CAPACITY OF GENERALIZED ADDITIVE CHANNELS
Charles R. Baker Oct. 1987 15 p
(Contract N00014-86-K-0039)
(AD-A190315; LISS-20) Avail: NTIS HC A03/MF A01 CSCL 12D

The generalized additive channel was introduced. It is described by an additive noise process with sample functions inducing a measure on a linear topological vector space, and by a constraint which includes dimensionality. The coding capacity of the matched channel was analyzed, with an exact value obtained for the Gaussian channel and an upper bound for a class of nonGaussian channels. Bounds on the coding capacity for the mismatched Gaussian generalized channel were obtained. In this paper, the exact coding capacity of the mismatched Gaussian generalized channel is determined, along with an upper bound for a class of nonGaussian mismatched channels. The set of admissable constraints is also greatly increased over that considered. Although the treatment here is restricted to noise measures induced on a separable Hilbert space, it can readily be seen that the results extended immediately to the class of linear topological vector spaces considered. The results of the present paper are partly based on the Hilbert space results on information capacity given, for the extension of linear topological vector spaces, one would use the corresponding results given. The focus on Hilbert space is useful for application of the results given here to the discrete-time or continuous-time additive channel. GRA

N88-22686# North Carolina Univ., Chapel Hill. Dept. of Statistics.
INFORMATION CAPACITY OF GAUSSIAN CHANNELS
Charles R. Baker Dec. 1987 23 p
(Contract N00014-86-K-0039)
(AD-A190316; LISS-18) Avail: NTIS HC A03/MF A01 CSCL 12I

Information capacity of Gaussian channels is one of the basic problems of information theory. Shannon's results for white Gaussian channels and Fano's waterfilling analysis of stationary Gaussian channnels are two of the best-known works of early information theory. Results are given here which extend to a general framework these results and others due to Gallager and to Kadota, Zakai, and Ziv. The development applies to arbitrary Gaussian channels when the channel noise has sample paths in a separable Banach space, and to a large class of Gaussian channels when the noise has sample paths in a linear topological vector space. Solutions for the capacity are given for both matched and mismatched channels. GRA

N88-22687# North Carolina Univ., Chapel Hill. Dept. of Statistics.
CONDITIONS FOR INFORMATION CAPACITY OF THE DISCRETE-TIME GAUSSIAN CHANNEL TO BE INCREASED BY FEEDBACK
Charles R. Baker Dec. 1987 25 p
(Contract N00014-86-K-0039)
(AD-A190317; LISS-22) Avail: NTIS HC A03/MF A01 CSCL 12I

Sufficient conditions are given for optimal causal feedback to increase information capacity for the discrete-time additive Gaussian channel. The conditions are obtained by assuming linear feedback and reformulating the problem into an equivalent no feedback problem. GRA

N88-22688# North Carolina Univ., Chapel Hill. Dept. of Statistics.
CODING CAPACITY OF DISCRETE-TIME GAUSSIAN AND NONGAUSSIAN CHANNELS
Charles R. Baker Oct. 1987 34 p
(Contract N00014-86-K-0039)
(AD-A190318; LISS-21) Avail: NTIS HC A03/MF A01 CSCL 12I

Coding capacity is obtained for the discrete time Gaussian channel, and upper bounds on capacity are obtained for a class of nonGaussian channels. The results apply to channels with or without memory, stationary or nonstationary. An assumption is required in order to obtain these results; this assumption is appropriate for channels without memory using an average energy constraint and for a large class of channels with memory. GRA

N88-22689# Princeton Univ., N. J. Dept. of Mechanical and Aerospace Engineering.
LUMPED MODEL GENERATION AND EVALUATION: SENSITIVITY AND LIE ALGEBRAIC TECHNIQUES WITH APPLICATIONS TO COMBUSTION Annual Technical Report, 1 Sep. 1986 - 1 Oct. 1987
F. L. Dryer, H. Rabitz, and R. Yetter 1 Oct. 1987 170 p

(Grant AF-AFOSR-0346-85)
(AD-A190402; AFOSR-87-1891TR) Avail: NTIS HC A08/MF A01 CSCL 07D

This program dealt with the development and application of new approaches for producing and evaluating lumped parameter models of physical processes. Local and global sensitivity analysis procedures were studied for achieving this goal. Specifically, Lie group formalism was developed to address global parameter space mapping issues of temporal kinetics problems and extended to more complex reactive-diffusive problems. Furthermore, Lie group theoretical techniques were also used to gain analytic insight into the solution of nonlinear kinetic systems. Using local gradient methods, the lumpability (or model reduction) of hydrogen/oxygen and carbon monoxide/hydrogen/oxygen kinetic mechanisms were studied in various physical environments. It was found that the presence of strong scaling and self similarity in the sensitivities allowed for kinetic model simplification. Such scaling and similarity was found associated with strong thermal coupling in the systems. Lastly, a general analysis method for the exact lumping of chemical kinetic mechanisms was developed and illustrated. GRA

N88-22690# Stanford Univ., Calif. Systems Optimization Lab.
SUFFICIENT MATRICES AND THE LINEAR COMPLEMENTARITY PROBLEM
R. W. Cottle, J. S. Pang, and V. Venkateswaran Dec. 1987 22 p
(Contract N00014-85-K-0343; Grant NSF DMS-84-0623)
(AD-A190429; SU-SOL-87-15) Avail: NTIS HC A03/MF A01 CSCL 12D

This paper poses and answers two questions about solutions of the linear complementary problem (LCP). The first question is concerned with the conditions on a square matrix M which guarantee that for every vector q, the solutions of LCP (q, M) are identical to the Karush-Kuhn-Tucker points of the natural quadratic program associated with (q, M). In answering this question the authors introduce the class of row sufficient matrices. The transpose of such a matrix is what is called column sufficient. The latter matrices turn out to furnish the answer to the second question which asks for the conditions on M under which the solution set of (q, M) is convex for every q. In addition to these two main results, this paper discusses the connections of these two new matrix classes with other well-known matrix classes in linear complementarity theory. GRA

N88-22691# Rensselaer Polytechnic Inst., Troy, N.Y.
PROBLEMS IN NONLINEAR CONTINUUM DYNAMICS Final Progress Report
Marshall Slemrod 1987 9 p
(Grant AF AFOSR-0239-85)
(AD-A190538; AFOSR-87-1769TR) Avail: NTIS HC A02/MF A01 CSCL 20K

The focus of this research was primarily feedback stabilization of distributed parameter systems. The principal investigator derived feedback operators for a general class of distributed systems, which include flexible beams, under the constraint of bounded control. Six papers were published, including Feedback Stabilization in Hilbert Space. Feedback laws are found for control systems governed by partial differential equations. In particular those control systems which give the dynamics of aeroelastic systems have been of interest. GRA

70 PHYSICS (GENERAL)

For precision time and time interval (PTTI) see *35 Instrumentation and Photography;* for geophysics, astrophysics or solar physics see *46 Geophysics, 90 Astrophysics,* or *92 Solar Physics.*

N88-22692# Oak Ridge National Lab., Tenn.
DROPLET SIZE CHARACTERISTICS AND ENERGY INPUT REQUIREMENTS OF EMULSIONS FORMED USING HIGH-INTENSITY-PULSED ELECTRIC FIELDS
T. C. Scott and W. G. Sisson 1987 16 p Presented at the 5th Symposium on Separation Science and Technology for Energy Application, Knoxville, Tenn., 26 Oct. 1987
(Contract DE-AC05-84OR-21400)
(DE88-005912; CONF-871038-10) Avail: NTIS HC A03/MF A01

Experimental methods have been developed to measure droplet size characteristics and energy inputs associated with the rupture of aqueous droplets by high-intensity-pulsed electric fields. The combination of in situ microscope optics and high-speed video cameras allows reliable observation of liquid droplets down to 0.5 microns in size. Videotapes of electric-field-created emulsions reveal that average droplet sizes of less than 5 microns are easily obtained in such systems. Analysis of the energy inputs into the fluids indicates that the electric field method requires less than 1 percent of the energy required from mechanical agitation to create comparable droplet sizes. DOE

N88-22693# Xerox Corp., Palo Alto, Calif. Inst. for Research on Learning.
A QUALITATIVE APPROACH TO ELECTRICITY Technical Report, Jun. 1985 - Sep. 1986
Hermann Haertel 15 Sep. 1987 126 p
(Contract N00014-85-C-0688; DA Proj. RR0-4206)
(AD-A189854; IRL87-0001) Avail: NTIS HC A07/MF A01 CSCL 20C

In the teaching of physics, the study of electricity and magnetism typically follows the introduction of the basic concepts of mechanics. However, there are some new concepts associated with electromagnetic fields that seem at first to the student to be unrelated to, or even incompatible with, Newton's third law as learned in mechanics. Furthermore, the transition from electrostatics to studies of moving charges and associated magnetic phenomena seems to many thoughtful students not to be consistent with concepts learned earlier in the course. This report describes approaches to electrostatics, to elementary circuits, and to the effects of moving charges in a way carefully designed to be fully consistent throughout, so that the thoughtful student is not left with quandaries about the relationship of each set of basic concepts to the other sets in the course. GRA

N88-22694# Massachusetts Inst. of Tech., Cambridge. Artificial Intelligence Lab.
RIGIDITY AND SMOOTHNESS OF MOTION
Shimon Ullman and Alan Yuille Nov. 1987 29 p
(Contract N00014-85-K-0124)
(AD-A190555; AI-M-989) Avail: NTIS HC A03/MF A01 CSCL 12I

Many theories of structure from motion divide the process into two parts which are solved using different assumptions. Smoothness of the velocity field is often assumed to solve the motion correspondence problem and then rigidity is typically used to recover the 3D structure. We prove results showing that, in a statistical sense, smoothness of the velocity field follows from rigidity of the motion. GRA

N88-22695# Washington Univ., Seattle. Aerospace and Energetics Research Program.
A CHEMICAL METHOD FOR ACHIEVING ACCELERATION OF MACROPARTICLES TO ULTRAHIGH VELOCITIES Final Report, 1 Jun. 1985 - 30 Apr. 1987
A. Hertzberg, A. P. Bruckner, A. T. Mattick, D. W. Bogdanoff, D. C. Brackett, and K. A. McFall 1987 158 p
(Contract DE-FG06-85ER-13382)
(DE88-006377; DOE/ER-13382/T1) Avail: NTIS HC A08/MF A01

This report describes work performed for the Department of Energy over the time period 1 June 1985 to 30 April 1987. The main areas of investigation are computational studies of gas and high explosive driven ramjet-in-tube concepts over the velocity range 3 to 20 km/sec, linear velocity multiplication over the velocity range 7 to 100+ km/sec and radiation emitted from impacts at

closing velocities of 80 to 400 km/sec. This report presents the computational methods used, including benchmark proof tests of these methods, as well as results of the investigations. DOE

N88-22696# Ecole Polytechnique, Palaiseau (France). Groupement de Recherches Coordonnees Interaction Laser-Matiere.
[ACTIVITIES REPORT IN LASER-MATTER INTERACTION] Annual Report, 1986 [RAPPORT D'ACIVITE 1986]
J. Fournier, ed., D. Smadja, ed., and F. Angibault, ed. Sep. 1987 283 p In FRENCH
(ETN-88-92007) Avail: NTIS HC A13/MF A01

Inertial confinement, high density physics, plasma physics, atomic physics, and X-ray lasers are discussed. Laser particle acceleration, product processing by laser shock, X-ray sources, and microlithography are reviewed. A multibeam facility is described. ESA

N88-22697# Technische Hogeschool, Eindhoven (Netherlands). Dept. of Physics.
EXCITATIONS IN MAGNETIC LOW-DIMENSIONAL SYSTEMS: A SPECTROSCOPIC STUDY Ph.D. Thesis
Leon Antoon Bosch 1987 119 p Sponsored by the Stichting voor Fundamenteel Onderzoek der Materie
(ETN-88-92230) Avail: NTIS HC A06/MF A01

Electron spin resonance and far infrared spectroscopy were used to study low lying magnetic excitations of a two-dimensional magnetic system and two chain-like systems. Far infrared magnetic excitation spectrum of CoCl2 (Nc5H5)2; magnetic interactions in the ferromagnetic chain compound CuCl2 times TMSO studied by (anti) ferromagnetic resonance and magnetization measurements; and magnetic excitations in the Ising-like layer compound (Co (gamma-CH3-C5H4NO)6) (ClO4)2 are discussed. ESA

N88-22698*# National Aeronautics and Space Administration, Washington, D.C.
METHOD AND DEVICE FOR THE DETECTION AND IDENTIFICATION OF A HELICOPTER
Hans Siebecker May 1988 22 p Transl. into ENGLISH of German Patent no. DE2655520-C3 (8 Dec. 1986) 7 p Transl. by Scientific Translation Service, Santa Barbara, Calif.
(Contract NASw-4307)
(NASA-TT-20251; NAS 1.77:20251) Avail: NTIS HC A03/MF A01 CSCL 20C

The invention presents a method for detecting and identifying a helicopter based on its characteristic emission of energy in the visual and infrared regions as well as acoustic energy by employing a fire control computer with data storage and a device for targeting and observation. Author

71 ACOUSTICS

Includes sound generation, transmission and attenuation. For noise pollution see *45 Environmental Pollution.*

N88-22699# Argonne National Lab., Ill.
ULTRASONIC BEAM DISTORTION IN TRANSVERSELY ISOTROPIC MEDIA
R. A. Roberts and D. S. Kupperman Aug. 1987 9 p Presented at the Review of Progress in Quantitative NDE, Williamsburg, Va., 21 Jun. 1987
(Contract W-31109-eng-38)
(DE88-005937; CONF-870691-11) Avail: NTIS HC A02/MF A01

The distortion of beam profiles and skewing of beam energy observed in transmission of ultrasound into a transversely isotropic medium can lead to erroneous interpretations of NDE data for materials such as columnar-grain steels and fiber-reinforced composites. In this paper, results are presented for the numerical evaluation of the exact Fourier integral representation of transmission of an arbitrary incident field from an isotropic into a transversely isotropic half-space. The problem is fully three-dimensional, i.e., the symmetry axis of the transversely isotropic material is oriented arbitrarily relative to the half-space boundary and angles of incidence. The cases chosen for numerical study were selected from previously unexplained experimental data obtained from the study of propagation in columnar grain steels (welds), and from situations commonly encountered during the inspection of fiber-reinforced composites. Experimental results which give evidence to the numerically observed phenomena are presented. DOE

N88-22700# Duke Univ., Durham, N. C. Dept. of Psychology.
ON CATEGORIZING SOUNDS Final Technical Report, 1 Aug. 1985 - 31 Jul. 1987
Gregory R. Lockhead 17 Nov. 1987 19 p
(Grant AF-AFOSR-0302-85)
(AD-A189784; AFOSR-87-1912TR) Avail: NTIS HC A03/MF A01 CSCL 05H

Judgements of sounds depend on context. How a sound is labeled depends on the sounds that just occurred (sequence effects) and the sounds that might occur (set effects or range effects). These dependencies are sufficiently large that they sometimes predict performance better that the stimulus itself. This report summarizes studies of context conducted during two years of AFOSR support. These studies of sound classification evaluated features of a memory model constructed to account for univariate judgements. The data show how response variability depends on stimulus variability, and demonstrate the importance of experimental details such as whether feedback is given and whether an identification function is present. It is concluded that three variables are needed to describe the collection of results. These are the stimulus itself, the stimulus or response (depending on feedback) on the just prior trial, and an average (called a memory pool) of the stimuli on each of several earlier trials. GRA

N88-22701# Michigan Univ., Ann Arbor. Communications and Signal Processing Lab.
SPATIAL MATCHED PROCESSING FOR MULTIPATH PROPAGATION Technical Memo No. 121
Matthew A. Dzieciuch and T. G. Birdsall 16 Nov. 1987 40 p
(AD-A189790; Rept-080043-1-M; TM-121) Avail: NTIS HC A03/MF A01 CSCL 20A

Underwater acoustic propagation is characterized by multipath or multimode propagation. Ray theory and mode theory are not fully adequate for modeling physical reality. Impulse responses can be more accurately calculated using Gaussian beam theory. Signal processors can be designed to take advantage of the channel complexity if the propagation is actually known so that detectability is increased. The proposed technique, channel matched filtering, synthetically backpropagates the wave front to a hypothesized source location. Accurate passive estimates can be made without knowledge of signal characteristics. GB theory can easily accommodate a range-dependent deep water environment. GRA

N88-22702# Air Force Occupational and Environmental Health Lab., Brooks AFB, Tex.
NOISE ASSESSMENT OF UNSUPPRESSED TF-34-GE-100A ENGINE AT WARFIELD ANG, BALTIMORE, MARYLAND Final Report
Winston J. Shaffer, II and John C. Ellis, II Dec. 1987 50 p
(AD-A189966; USAFOEHL-87-164EH0441LNA) Avail: NTIS HC A03/MF A01 CSCL 20A

This report presents the results of noise data measurements of an unsuppressed TF34-GE-100A engine and a community noise survey of the local area around the engine. Three recommendations were made. A two barrier design should be installed as an interim noise control measure. Justification and installation of a noise suppressor, as a long term solution, should be pursued. Day-night sound levels should continue to be monitored until adequate characterization of the airport noise environment is obtained. GRA

N88-22703# Naval Postgraduate School, Monterey, Calif.
TARGET LOCALIZATION IN AN INHOMOGENEOUS MEDIUM M.S. Thesis
Michael D. Budney Dec. 1987 64 p
(AD-A190008) Avail: NTIS HC A04/MF A01 CSCL 17A

A computer algorithm was developed to determine if an acoustic transmitter can be localized based on estimates of local angles of arrival of acoustic signals incident upon a receive planar sonar array, knowledge of the deterministic effects of the ocean on sound propagation, and local sound-speed profiles of the ocean. The algorithm was designed to determine azimuthal and elevation/depression angles to the transmitter as well as computing the depth, range, cross range, and line-of-sight range separations between the transmitter and the receive array. The algorithm utilizes ray acoustics and model-based phase weights to determine the transmitter's location relative to the receive array's position. As written, the algorithm is capable of solving localization problems in which the transmitter and receiver are in the same gradient of the local sound-speed profile, provided that the range from transmitter to receiver is not so great that the acoustic signal passes through a turning point prior to reaching the receive array. The results indicate that the method proposed is viable for the class of problems for which it was designed, and accuracies on the order of 0.1 meters are obtained for line-of-sight ranges on the order of several kilometers. GRA

N88-22704# Naval Postgraduate School, Monterey, Calif.
A COMPUTERIZED INVESTIGATION USING THE METHOD OF IMAGES TO PREDICT THE SOUND FIELD IN A FLUID WEDGE OVERLYING A SLOW FLUID HALF-SPACE M.S. Thesis
Carolus Kaswandi Dec. 1987 86 p
(AD-A190013) Avail: NTIS HC A05/MF A01 CSCL 20A

Sound fields in wedge-shaped ocean layers, modeling conditions on the continental shelf, have been studied at the Naval Postgraduate School in the last few years using the method of images. These studies are carried further in the present work. This method is implemented in different environmental conditions. This thesis examines the influence of several parameters on the sound field for downslope propagation in a wedge-shaped fluid of speed of sound c2 overlying a slow bottom of speed of sound c1. GRA

N88-22705# Wisconsin Univ., Milwaukee. Dept. of Psychology.
MECHANISMS MEDIATING THE PERCEPTION OF COMPLEX ACOUSTIC PATTERNS Annual Progress Report, 1 Aug. 1986 - 30 Jul. 1987
Richard M. Warren 31 Aug. 1987 6 p
(Grant AF-AFOSR-0260-85)
(AD-A190112; AFOSR-87-1430TR) Avail: NTIS HC A02/MF A01 CSCL 06D

Three studies dealing with perception of acoustic repetition for long-duration complex sounds have been completed: (1) repetition of frozen Gaussian noise can be detected for infratonal repetition frequencies from 1 Hz through 20 Hz (repetition frequencies above 20 Hz are tonal). Infratonal repetition might be perceived either through the detection of the reoccurrence of singularities within the acoustic pattern, or through a holistic recognition of the entire pattern. This investigation indicated that a holistic recognition of the complex sound is normally responsible for detection of periodicity, (2) illusory continuity of interrupted tones (pulsation thresholds) have been used to study peripheral auditory mechanisms. The investigators found that illusory continuity also occurs in the infratonal range, requiring revision of the theories of basilar membrane mechanics based on the pulsation threshold paradigm, (3) the investigators demonstrated that frozen noises repeated at infratonal frequencies at one ear (silence at the other ear) are detected by some listeners with much greater clarity than when the other ear receives the signal. Ear advantages of this nature have not been observed with other types of complex sounds, and this finding has some interesting implications for auditory theory. GRA

N88-22706# Massachusetts Inst. of Tech., Cambridge. Dept. of Ocean Engineering.
DESCRIBING THE SOURCE CREATED BY TURBULENT FLOW OVER ORIFICES AND LOUVERS M.S. Thesis
Glenn E. Cann Jun. 1987 107 p
(Contract N00228-85-G-3262)
(AD-A190254) Avail: NTIS HC A06/MF A01 CSCL 20A

Orifice and louver sound power spectra are investigated, using an intensity probe, at various wind speeds in a low noise, semi-anechoic, subsonic wind tunnel for free stream velocities below 50 meters per second. The radiated noise is created by turbulent flow over various orifice and louver geometries which are flushed mounted into the wall of a long duct. Five orifice samples of rectangular shape and various transverse dimensions as well as four louver samples with multiple rectangular and circular orifices are tested. Also investigated is the effect of the leading and trailing edge angle on the radiated sound power. The scaling laws of the excitation frequencies and the speed/power laws are presented for ratios of the boundary layer thickness to the transverse orifice dimension from 1.01 to 4.29. A detailed theoretical model is developed for rectangular shaped aperture orifices and louvers based on the work by Ffowcs Williams, Nelson, and Corcos. GRA

N88-22707# Utah Univ., Salt Lake City. Dept. of Physics.
THE KINETICS OF CONTACT NOISE IN NaBETA ALUMINA Technical Report, 1987 - Jan 1988
Chu K. Kuo and James J. Brophy Jan. 1988 14 p
(Contract N00014-82-K-0603)
(AD-A190651; TR-15-ONR) Avail: NTIS HC A03/MF A01 CSCL 20A

The kinetics of interfacial chemical reaction noise at sodium amalgam and NaI propylene carbonate contacts to NaBeta Alumina are examined by determining the time and temperature dependence of the noise. The rate constant for the reaction noise is larger for amalgam contacts and increases with sodium concentration in both cases. The noise is thermally activated with an activation energy of 0.5eV, which is similar to that of bulk diffusion noise in NaBeta Alumina. GRA

N88-22708# Naval Underwater Systems Center, New London, Conn.
SPACE TIME PROCESSING, ENVIRONMENTAL-ACOUSTIC EFFECTS
William M. Carey and William B. Moseley 15 Aug. 1987 80 p
(AD-A190764; NUSC-TR-8077) Avail: NTIS HC A05/MF A01 CSCL 20A

This paper had as its focus the problem of ocean-acoustic measurements with line arrays. The space-time transforms were reviewed to demonstrate the analogy between spatial and temporal properties, to stress the importance of convolution and matched field processing. A criteria was presented by which the resolution of such measurements systems could be calculated. GRA

N88-22709*# National Aeronautics and Space Administration. Langley Research Center, Hampton, Va.
MODEL-SCALE SOUND PROPAGATION EXPERIMENT
William L. Willshire, Jr. Apr. 1988 32 p Presented at the 3rd Symposium on Long-Range Sound Propagation and Coupling Into the Ground, Jackson, Miss., 28-30 Mar. 1988
(NASA-TM-100602; NAS 1.15:100602) Avail: NTIS HC A03/MF A01 CSCL 20A

The results of a scale model propagation experiment to investigate grazing propagation above a finite impedance boundary are reported. In the experiment, a 20 x 25 ft ground plane was installed in an anechoic chamber. Propagation tests were performed over the plywood surface of the ground plane and with the ground plane covered with felt, styrofoam, and fiberboard. Tests were performed with discrete tones in the frequency range of 10 to 15 kHz. The acoustic source and microphones varied in height above the test surface from flush to 6 in. Microphones were located in a linear array up to 18 ft from the source. A preliminary experiment using the same ground plane, but only testing the plywood and

felt surfaces was performed. The results of this first experiment were encouraging, but data variability and repeatability were poor, particularly, for the felt surface, making comparisons with theoretical predictions difficult. In the main experiment the sound source, microphones, microphone positioning, data acquisition, quality of the anechoic chamber, and environmental control of the anechoic chamber were improved. High-quality, repeatable acoustic data were measured in the main experiment for all four test surfaces. Comparisons with predictions are good, but limited by uncertainties of the impedance values of the test surfaces. Author

N88-22710*# National Aeronautics and Space Administration. Langley Research Center, Hampton, Va.
ADVANCING-SIDE DIRECTIVITY AND RETREATING-SIDE INTERACTIONS OF MODEL ROTOR BLADE-VORTEX INTERACTION NOISE
R. M. Martin, W. R. Splettstoesser, J. W. Elliott, and K.-J. Schultz (Deutsche Forschungs- und Versuchsanstalt fuer Luft- und Raumfahrt, Brunswick, West Germany) May 1988 43 p
(NASA-TP-2784; L-16354; NAS 1.60:2784; AVSCOM-TR-87-B-3) Avail: NTIS HC A03/MF A01 CSCL 20A

Acoustic data are presented from a 40 percent scale model of the four-bladed BO-105 helicopter main rotor, tested in a large aerodynamic wind tunnel. Rotor blade-vortex interaction (BVI) noise data in the low-speed flight range were acquired using a traversing in-flow microphone array. Acoustic results presented are used to assess the acoustic far field of BVI noise, to map the directivity and temporal characteristics of BVI impulsive noise, and to show the existence of retreating-side BVI signals. The characterics of the acoustic radiation patterns, which can often be strongly focused, are found to be very dependent on rotor operating condition. The acoustic signals exhibit multiple blade-vortex interactions per blade with broad impulsive content at lower speeds, while at higher speeds, they exhibit fewer interactions per blade, with much sharper, higher amplitude acoustic signals. Moderate-amplitude BVI acoustic signals measured under the aft retreating quadrant of the rotor are shown to originate from the retreating side of the rotor. Author

N88-22711# Technische Hogeschool, Delft (Netherlands). Afd. der Elektrotechniek.
SEISMIC INVERSION BY A RMS (ROOT-MEAN-SQUARE) BORN APPROXIMATION IN THE SPACE-TIME DOMAIN
J. T. Fokkema and P. M. vandenBerg Nov. 1987 39 p
(PB88-165402; Rept-1987-26) Avail: NTIS HC A03/MF A01 CSCL 20A

A new approximate method to calculate the space-time acoustic wave motion generated by an impulsive point source in a horizonatally layered configuration is presented. The configuration consists of a stack of fluid layers between two acoustic half-spaces where the source and the receiver are located in the upper half-space. A distorted wave Born approximation is introduced; the important feature of the present method is the assumption of the presence of a background medium with vertical varying root-mean-square acoustic wave speed. In the inverse scheme the wave speed and mass density can be reconstructed within a single trace. Results of the inversion scheme applied to synthetic data were shown. GRA

N88-22712# Institut Franco-Allemand de Recherches, St. Louis (France).
EXPERIMENTAL STUDY ON THE INFLUENCE OF WIND ON ACOUSTIC PRESSURE SENSORS [ETUDE EXPERIMENTALE DE L'INFLUENCE DU VENT SUR LES CAPTEURS DE PRESSION ACOUSTIQUE]
G. Parmentier, J. Vermorel, E. Burde, and Ph. Rateau 26 Aug. 1986 40 p In FRENCH
(ISL-R-121/86; ETN-88-92015) Avail: NTIS HC A03/MF A01

Microphones were exposed to winds at varying velocities up to 9m/sec. Similar tests were carried out in laboratory, using a well defined air flow and placing the microphone on a rotating arm. Devices to protect the microphones from wind induced noise were tested, including polyurethane foam, aerodynamic profiles, and a combination of fabric screens and foam. The attenuations obtained are from 14.5 to 22 dB. ESA

N88-22713# Institut Franco-Allemand de Recherches, St. Louis (France).
ACOUSTIC PROPAGATION IN THE LOW ATMOSPHERE. EXPERIMENTAL STUDY AND MODELING BY THE RADIUS METHOD [PROPAGATION ACOUSTIQUE DANS LA BASSE ATMOSPHERE. ETUDE EXPERIMENTALE ET MODELISATION PAR LA METHODE DES RAYONS]
J. Vermorel and G. Parmentier 21 Nov. 1986 43 p In FRENCH; ENGLISH summary
(Contract DRET-85-053)
(ISL-CO-247/86; ETN-88-92018) Avail: NTIS HC A03/MF A01

Acoustic detection is studied with a focus on detection of helicopters. Sound propagation is analyzed as a function of soil and meteorological parameters. Acoustic sensors less sensitive to wind effects were also studied. Propagation calculations were developed, including three dimensional and unsteady computations. The results show the correlation of global acoustic pressure to meteorological parameters and the important perturbations produced by atmospheric turbulence. ESA

72 ATOMIC AND MOLECULAR PHYSICS

Includes atomic structure, electron properties, and molecular spectra.

N88-22714# Fondazione Ugo Bordoni, Rome (Italy).
COLLECTIVE ROTATION OF MOLECULES DRIVEN BY THE ANGULAR MOMENTUM OF LIGHT IN A NEMATIC FILM
Benedetto Daino, Marco Romagnoli, Marina Settembre, Enrico Santamato, and Yuen Ron Shen (California Univ., Berkeley.) Sep. 1986 6 p
(FUB-6-1986; ETN-88-91871) Copyright Avail: NTIS HC A02/MF A01

It is experimentally demonstrated that a circularly polarized laser beam normally incident on a homeotropically aligned nematic film can induce a collective precession of the molecules in the film if the laser intensity is above the threshold for the Freedericksz transition. The effect is shown to result from a transfer of angular momentum from the laser beam to the medium. ESA

N88-22715# California Univ., Berkeley. Lawrence Berkeley Lab.
STUDIES OF SURFACES USING OPTICAL SUM-FREQUENCY GENERATION Ph.D. Thesis
J. H. Hunt Jan. 1988 128 p
(Contract DE-AC03-76SF-00098)
(DE88-006334; LBL-24692) Avail: NTIS HC A07/MF A01

Sum-frequency generation (infrared-visible) was used as probe of molecular species at interfaces. The process being a second order non-linear optical process causes the technique to be surface-specific when used at an interface between two centrosymmetric media. The resonant enhancement of chi that occurs when the infrared input is tuned through a vibrational resonance allows one to determine the vibrational spectrum of the species adsorbed to the surface. The polarization dependence of the spectrum can be used to deduce the molecular orientations of the species at the interface. The laser system uses an amplified single pulse selected from the output train of a active/passive mode-locked Nd:YAG oscillator. The pulse contains sufficient energy to generate both an intense visible pulse via second-harmonic generation and an intense infrared pulse via optical parametric amplification. The first experiments were performed on a series of alcohols at an air-glass interface. These experiments demonstrated that the basic technique produced spectra several orders of magnitude above the bare glass background. Although the spectra did not extend far enough into the infrared to identify the adsorbed species, the spectra were

correlated with spectra taken in bulk samples. The technique was used to examine the spectra of a Langmuir film (air-water interface) of pentadecanoic acid at several surface densities. It was found that in the high density phase, the molecular hydrocarbon tails were fully extended and aligned nearly normal to the surface. At lower densities, the tail was free to bend and evidence of trans-gauche conformations was observed. The experiment makes use of the ability of sum-frequency generation to do in-situ spectral measurements not possible with other techniques. The use of difference-frequency generation was discussed. DOE

N88-22716# Rochester Univ., N. Y.
THEORY OF THE DISSOCIATION DYNAMICS OF SMALL MOLECULES ON METAL SURFACES: FINITE TEMPERATURE STUDIES Technical Progress Report
B. E. Jackson 1988 5 p
(Contract DE-FG02-87ER-13744)
(DE88-006495; DOE/ER-13744/2) Avail: NTIS HC A02/MF A01

The primary goal of this study is to develop realistic theoretical models for the dissociative adsorption of diatomics on metals. There are many detailed and beautiful experimental studies of dissociative sticking, an important first step in many catalytic processes. The theoretical studies, however, have been limited to simple classical trajectory simulations, and are often done at zero temperature. By taking advantage of modern time dependent scattering techniques, we wish to treat the dissociating molecule as quantum mechanically as possible, and to properly include coupling to the thermal fluctuations of the solid. In these scattering techniques, the wave function of the molecule is written in an explicitly time dependent fashion. It is then evolved in time via the Schroedinger equation, and scattered from or reacted with the surface. The final wave function is then used to compute all properties of interest. We have already made much progress in three major areas of emphasis. DOE

N88-22717# Rome Univ. (Italy). Dipt. di Fisica.
LATTICE QCD CALCULATION OF K YIELDS PI NONLEPTONIC WEAK TRANSITION AND OTHER HADRONIC WEAK PARAMETERS
M. B. Gavela, L. Maiani, G. Martinelli, O. Pene (Paris-Sud Univ., Orsay, France), and S. Petrarca 16 Dec. 1987 14 p Presented at the Symposium International sur la Theorie de Champs sur Reseau-Seillac, France, 28 Sep. - 2 Oct. 1987 Sponsored by the CNR and the Istituto Nazionale di Fisico Nucleare
(Preprint-580; ETN-88-92269) Avail: NTIS HC A03/MF A01

Results obtained on the K yields pi matrix elements of the weak nonleptonic Hamiltonian, computed in lattice QCD with Wilson fermions and in the quenched approximation are presented. Axial coupling and the B parameter of c q bar mesons were also calculated. ESA

N88-22718# Massachusetts Inst. of Tech., Cambridge. Dept. of Chemistry.
SEQUENTIAL EXCITATION PREPARATION OF MOLECULAR ENERGY LEVELS WITH SPECIAL STRUCTURAL AND CHEMICAL PROPERTIES Final Report, 1 Oct. 1984 - 31 Oct. 1987
Robert W. Field and James L. Kinsey 31 Dec. 1987 28 p
(Grant AF AFOSR-0381-85)
(AD-A190041; AFOSR-88-0166TR) Avail: NTIS HC A03/MF A01 CSCL 07D

The research objectives are: (1) to apply the stimulated emission pumping (SEP) technique to highly excited vibrational levels of H2CO and D2CO, (2) discover whether the rotation-vibration levels of H2CO/D2CO remain well organized at chemically significant levels of vibrational excitation, (3) develop new multiple resonance spectroscopic techniques capable of measuring rotational energy transfer rates (RET) in highly excited vibrational levels of H2CO, and (4) develop statistical diagnostics for quantum ergodicity which are applicable to real SEP spectra of H2CO/D2CO, are presented. GRA

73 NUCLEAR AND HIGH-ENERGY PHYSICS

Includes elementary and nuclear particles; and reactor theory.

For space radiation see *93 Space Radiation.*

N88-22719# Edgerton, Germeshausen and Grier, Inc., Idaho Falls, Idaho.
REQUIREMENTS AND COST CONSIDERATIONS FOR A COMBINED SPACE NUCLEAR REACTOR TEST FACILITY
E. A. Harvego, D. L. Park, J. H. Ramsthaler, W. C. Reed, J. F. Whitbeck, and B. B. Gillies 1987 31 p Presented at the 4th Symposium on Space Nuclear Power Systems, Albuquerque, N. Mex., 12 Jan. 1987 Prepared in cooperation with Rockwell International Corp., Canoga Park, Calif.
(Contract DE-AC07-76ID-01570)
(DE88-006763; EGG-M-25786; CONF-870102-32) Avail: NTIS HC A03/MF A01

A number of U.S. military programs are currently considering nuclear power systems for space propulsion and electric power applications. These space power systems will each require expensive ground testing of nuclear components and systems prior to deployment in space. In some cases, the ground test facility construction and operating costs can represent a major portion of the total program budget. To minimize the costs to individual programs, consideration is given to the potential for reducing total costs by constructing a single facility in which two or more test programs can be conducted simultaneously. This concept is referred to as a Combined Space Nuclear Reactor Test Facility. This paper presents the results of a study in which the requirements and costs associated with conducting two space nuclear reactor ground test programs separately and in combination were examined. The findings of this study were that, for all new construction, the costs associated with construction and operation of a combined Space Nuclear Reactor Test Facility were substantially less than those associated with constructing and operating separate facilities. However, if existing test support facilities can be used, the potential costs of the two options are comparable. DOE

N88-22720# International Atomic Energy Agency, Vienna (Austria).
SMALL AND MEDIUM POWER REACTORS 1987
Dec. 1987 113 p
(TI88-701435; IAEA-TECDOC-445) Avail: NTIS (US Sales Only) HC A06/MF A01

This TECDOC follows the publication of TECDOC-347: Small and Medium Power Reactors (SMPR) Project Initiation Study, Phase 1, published in 1985 and TECDOC-376: Small and Medium Power Reactors 1985 published in 1986. It is mainly intended for decision makers in Developing Member States interested in embarking on a nuclear power program. It consists of two parts: (1) guidelines for the introduction of small and medium power reactors in developing countries. These Guidelines were established during the Advisory Group Meeting held in Vienna from 11 to 15 May 1987. Their purpose is to review key aspects relating to the introduction of small and medium power reactors in developing countries; (2) up-dated information on SMPR Concepts Contributed by Supplier Industries. According to the recommendations of the Second Technical Committee Meeting on SMPRs held in Vienna in March 1985, this part contains the up-dated information formerly published in Annex 1 of the above mentioned TECDOC-347. DOE

N88-22721# Physical Sciences, Inc., Alexandria, Va.
PARTICLE BEAM ALIGNMENT SYSTEM FOR SINGLE EVENT UPSET-VAN DE GRAAF EXPERIMENTS Final Report
Michael R. Corson, Jack A. McKay, and James H. McDermott 1 Jun. 1987 24 p
(Contract N00014-83-C-2255)
(AD-A189695; PSI-9898; TR-683) Avail: NTIS HC A03/MF A01 CSCL 20G

This report documents the design and operation of the particle beam alignment system developed for single event upset - Van de Graaff experiments. This system is designed to provide a faster and more accurate optical alignment of the pinhole and the device under test. In this alignment system a laser beam is focused on the device under test, and the pinhole is then aligned with the laser beam using an electronic display. In this way the pinhole is aligned over the device under test. The alignment system consists of three main components: (1) a beam expander for the He-Ne laser which was previously used for pinhole alignment, and neutral density filters to attenuate the laser beam when necessary, (2) a new flange for the sample chamber incorporating a calibrated x-y translation stage for the pinhole, and a calibrated x-y translation stage carrying a quadrant photodiode, and (3) an amplifier and display module to display the output of the photodiode. GRA

74 OPTICS

Includes light phenomena; and optical devices.
For lasers see *36 Lasers and Masers.*

N88-22722# Rochester Univ., N. Y. Dept. of Computer Science.
ROVER: A PROTOTYPE ACTIVE VISION SYSTEM
David J. Coombs and Brian D. Marsh Aug. 1987 37 p
(Contract DACA76-85-C-0001; Grant NSF DCR-86-02958)
(AD-A189246; TR-219) Avail: NTIS HC A03/MF A01 CSCL 23C

The Roving Eyes project is an experiment in active vision. We present the design and implementation of a prototype that tracks colored balls in images from an on-line charge coupled device (CCD) camera. Rover is designed to keep up with its rapidly changing environment by handling best and average case conditions and ignoring the worst case. This allows Rover's techniques to be less sophisticated and consequently faster. Each of Rover's major functional units is relatively isolated from the others, and an executive which knows all the functional units directs the computation by deciding which jobs would be most effective to run. This organization is realized with a priority queue of jobs and their arguments. Rover's structure not only allows it to adapt its strategy to the environment, but also makes the system extensible. A capability can be added to the system by adding a functional module with a well defined interface and by modifying the executive to make use of the new module. The current implementation is discussed in the appendices. GRA

N88-22723# Drexel Univ., Philadelphia, Pa.
MULTIPLE SCATTERING FROM NONSPHERICAL TARGETS Contractor Report, Jun. 1984 - Jun. 1987
Leonard D. Cohen, Richard D. Haracz, and Ariel Cohen Nov. 1987 65 p
(Contract DAAK11-84-C-0010)
(AD-A189939; CRDEC-CR-88005) Avail: NTIS HC A04/MF A01 CSCL 20F

The Shifrin Acquista integral equation technique was modified to handle scattering from nonspherical, nonsymmetric particles, such as helices and toroids. This approach was applied to the analysis of an experiment on scattering by a helix with very good results. We also computed asymmetry factors for scattering from long cylinders. This result is useful in computing the average amount of light scattered in the forward direction from a collection of randomly oriented cylinders, such as a cloud of cylinders. GRA

N88-22724# Texas Technological Univ., Lubbock. Optical Systems Lab.
SPACE-VARIANT OPTICAL SYSTEMS Final Technical Report, 30 Sep. 1984 - 30 Sep. 1987
John F. Walkup and Thomas F. Krile Dec. 1987 24 p
(Grant AF-AFOSR-0382-84)
(AD-A189967; AFOSR-87-1860TR) Avail: NTIS HC A03/MF A01 CSCL 20F

Analytical and experimental investigations of 1-D and 2-D space-variant optical processors have been conducted. Areas investigated have included: (1) measures of the degree of invariance of linear optical system; (2) a real-time holographic charge-coupled device (CCD) recording technique for preserving phase information; (3) a fast, highly parallel architecture for optical multiplication; and (4) a complete analytical and experimental investigation of the bilinear transform and its applications. GRA

N88-22725# Purdue Univ., West Lafayette, Ind. Research Foundation.
THEORY OF INTERACTIONS OF INTENSE LIGHT WITH NONLINEAR, INHOMOGENEOUS AND PERIODIC STRUCTURES AND ITS APPLICATIONS TO OPTICAL BISTABILITY, OPTIC GYROSCOPES, NONLINEAR SPECTROSCOPY, RADIATION PROTECTION, X-RAY EMISSION AND RELATED FIELDS Final Report, 1 Nov. 1984 - 31 Aug. 1987
Alexander E. Kaplan Oct. 1987 14 p
(Grant AF-AFOSR-0006-85)
(AD-A190040; AFOSR-88-0162TR) Avail: NTIS HC A03/MF A01 CSCL 20F

During the grant period, a number of new theoretical results were obtained in the field of nonlinear optics and quantum electronics. Progress was made in the search of novel principles and effects in the field of superfast optical switching, optical bistability, new sources of X-ray radiation, optic gyroscopes, general nonlinear optics, as well as in the development of a new fundamental field of quantum and nonlinear optics of single particles. GRA

N88-22726# Pennsylvania State Univ., University Park. Dept. of Electrical Engineering.
STUDY OF MICROCOMPUTER-BASED REAL-TIME PROGRAMMABLE OPTICAL SIGNAL PROCESSOR AND APPLICATION Final Report, 1 Aug. 1986 - 30 Sep. 1987
Francis T. Yu 18 Nov. 1987 129 p
(Grant AF-AFOSR-0264-86)
(AD-A190076; AFOSR-87-1802TR) Avail: NTIS HC A07/MF A01 CSCL 12F

We have, in this period, developed a microcomputer-based optical linear transformation processing technique. The technique utilizes a systolic array processing method to perform various types of linear transformations, such as discrete Fourier transformation, discrete Hilbert transformation, discrete chirp-Z transformation and many others. By partially parallel addressing two magneto-optic spatial light modulators (MOSLM), this proposed system would offer high speed and parallel processing capability of optics and programmability of microcomputer. In this research, we have shown that a color liquid crystal television (LCTV) can be used for color pattern recognition. The grid structure of the display panel together with a specially designed color filter provides spatially isolated polychromatic spectra to enable polychromatic signal detection. We have found a serious drawback of the color LCTV which is the lack of space invariance, even after it has been immersed in a liquid gate. This drawback is primarily due to the inherent color filter in the liquid crystal display and the phase modulation by liquid crystal molecules. A quantitative investigation of space variance of the LCTV, especially the color LCTV, is currently being studied. GRA

N88-22727# Naval Ocean Systems Center, San Diego, Calif.
AMPLIFICATION OF SIGNALS IN FIBER OPTICS USING THE STIMULATED RAMAN EFFECT Interim Report, Oct. 1986 - Apr. 1987
S. D. Russell and T. Stamnitz Sep. 1987 46 p
(AD-A190281; NOSC/TR-1196) Avail: NTIS HC A03/MF A01 CSCL 09C

This report details phase 1 of an Independent Exploratory Development project designed to investigate the feasibility of developing nonlinear optical-transmission lines. The report gives a brief review of the theoretical basis and a description of the experimental design, prototype setup, and results. The appendices serve as a reference for future investigators. GRA

N88-22728# Naval Ocean Systems Center, San Diego, Calif.
A 104-km UNREPEATERED BIDIRECTIONAL FIBER OPTIC DEMONSTRATION LINK Research Report, Oct. 1985 - Aug. 1986
M. R. Brininstool Jun. 1987 29 p
(AD-A190282; NOSC/TR-1185) Avail: NTIS HC A03/MF A01 CSCL 25E

Experiments demonstrate that full-duplex, bidirectional data can be transmitted via optical fiber 100 km long without the use of optical repeaters. Two transmitter wavelengths were employed: 1.3 and 1.55 micron. Improvements planned for follow-on tests should extend the unrepeatered system length to 200 km. GRA

N88-22729# Massachusetts Inst. of Tech., Cambridge. Dept. of Electrical Engineering and Computer Science.
INFRARED-SENSITIVE SPATIAL LIGHT MODULATOR Final Report, 1 Jun. 1984 - 20 May 1987
Cardinal Warde Nov. 1987 30 p
(Contract F08635-84-K-0209)
(AD-A190391; AD-E801598; AFATL-TR-87-32) Avail: NTIS HC A03/MF A01 CSCL 17E

This final report summarizes a preliminary investigation of an infrared-sensitive spatial light modulator that is designed to respond to white light in the 3 to 5 micrometers wavelength range. The device can be read out with visible light and, as such, is intended to function simultaneously as an image wavelength upconverter and light modulator. The device design employs a thin-film InSb photoconductor that addresses a DKDP crystal which is cooled near the Curie temperature (-51 degrees centigrade) of DKDP. Preliminary results are reported on: thin flash-evaporated films on InSb; the development of the cooled DKDP substrates; design and fabrication of the modulator vacuum cell; and theoretical modelling of the device performance. GRA

N88-22730# Environmental Research Inst. of Michigan, Ann Arbor. Advanced Concepts Div.
OPTICAL SWITCHING AND CONTROL TECHNIQUES USING NONLINEAR OPTICAL WAVE MIXING Final Report, 15 Sep. 1985 - 15 Jun. 1987
Lauren M. Peterson Dec. 1987 95 p
(Contract F49620-84-C-0067; ARPA Order 4952)
(AD-A190467; ERIM-175900-12-F; AFOSR-88-0095TR) Avail: NTIS HC A05/MF A01 CSCL 20F

It is shown experimentally that thermooptically induced beam guides and phase grating structures can be used to efficiently switch an optical beam by redirecting its energy in times of 20 and 2 nsec, respectively. Beam guiding was achieved by passing a focused TEM at infinity laser pulse through an absorbing liquid to which an absorbing dye had been added. Heating of the liquid in the focal region by the Gaussian profile beam changed the refractive index to produce a long cylindrical volume analogous to a graded-index (GRIN) optical fiber. Radiation from a second laser beam not absorbed by the liquid could be coupled into the graded index real-time fiber and redirected by it with an efficiency as high as 90 percent. The switch-on time was 20 nsec and persisted without intervention for about 1 millisecond (i.e., optical memory). The rise and decay times are in good agreement with calculations using a simple thermal model which describes the process. The thermo-optically induced phase grating was generated by interfering two beams of laser radiation in an absorbing liquid. Heating of the liquid along the interference pattern produced a sinusoidally varying refractive pattern or phase grating. This real-time optically generated grating was used to switch (redirect by diffraction) a probing laser beam. For a small crossing angle of 7 deg, a switching time of 2 nsec was measured and was in good agreement with the thermal model. GRA

N88-22731# Lawrence Livermore National Lab., Calif.
CLINICAL MEASUREMENTS USING FIBER OPTIC SENSORS
J. N. Roe Sep. 1987 14 p Presented at the NATO Advanced Study Institute, Cape Sounion Beach, Greece, 20 Jun. 1987
(Contract W-7405-eng-48)
(DE88-005624; UCRL-97818; CONF-8706274-1) Avail: NTIS HC A03/MF A01

The use of fiber optics in clinical measurements for illumination and imaging is widespread, but a more advanced sensing concept can be realized. The attachment of species specific fiber terminations at the distal end of the fiber optic so that in-situ analysis can be made is discussed along with measurement instrumentation. These terminations are called optrodes (optical electrodes), and a group of optrodes are presently under development for the in-vivo and in-vitro identification and quantification of species of interest to the clinician. The current development includes pH, carbon dioxide, potassium, and anti-cancer drugs. DOE

N88-22732# Lawrence Livermore National Lab., Calif.
COMPUTING X-RAY EFFECTS IN OPTICS
C. E. Rhoades, Jr. Feb. 1988 16 p
(Contract W-7405-eng-48)
(DE88-006722; UCID-21340) Avail: NTIS HC A03/MF A01

In this paper, we discuss the physical phenomena that are important in understanding the behavior of optics exposed to X-ray fluences, and four computer programs that are commonly used to perform such calculations. We describe several model problems and spectra that we used to exercise the four computer codes. Finally, we close with a number of conclusions and recommendations for those who wish to use one or more of the codes to predict the response of optics to X-ray fluences. In particular, we find that multidimensional geometry issues must be carefully addressed and special care must be taken to insure that even the one dimensional calculations have converged. DOE

N88-22733# Lawrence Livermore National Lab., Calif.
PREPARING THE ALCATOR C BOLOMETER SYSTEM FOR USE ON MTX (MICROWAVE TOKAMAK EXPERIMENT)
Marty Marinak (California Univ., Berkeley.) Feb. 1988 19 p
(Contract W-7405-eng-48)
(DE88-006724; UCID-21140) Avail: NTIS HC A03/MF A01

The Alcator C bolometer array has been modified to be compatible with electron cyclotron heating on the Microwave Tokamak Experiment. Fine wire mesh screens are mounted on the front of the bolometer collimator tubes to attenuate microwave heating of the bolometers. Structural changes eliminate openings in the seams of the bolometer housing, which represent pathways for microwaves to enter the system. This paper outlines the operational principles of the bolometer system, discusses the measured and predicted performance characteristics of the bolometer array, and includes a concise guide to the operation of the bolometer controller. DOE

75 PLASMA PHYSICS

Includes magnetohydrodynamics and plasma fusion.
For ionospheric plasmas see *46 Geophysics*. For space plasmas see *90 Astrophysics*.

N88-22734# Academy of Sciences of the Armenian SSR, Erivan.
NONLINEAR EFFECTS IN PLASMA WAKE FIELD ACCELERATION
A. Ts. Amatuni, S. S. Elbakyan, and E. V. Sekhposyan 1986 22 p
(TI88-700972; EFI-935(86)-86) Avail: NTIS (US Sales Only) HC A03/MF A01

The possible use of the nonlinear wake waves excited by electron bunches passing through plasma for acceleration of charged particles is investigated. The expressions for nonlinear fields and wave lengths inside and behind the particle bunch are obtained. It is shown that when the bunch density approaches the half of the plasma electron equilibrium density the maximal wake field depends on the bunch gamma factor, and one can use it for charged particle acceleration. DOE

N88-22735# Japan Atomic Energy Research Inst., Tokyo.
ANALYSES AND EXPERIMENTS ON THE INTEGRITY AND LIFETIME PREDICTIONS OF PLASMA-FACING COMPONENTS IN FUSION REACTORS
T. Tone, M. Seki, A. Minato, Tomoyoshi Horie, Hiroshi Kawamura, Masuro Ogawa, Kaoru Fujimura, Tetsuaki Takeda, Kiyoshi Fukaya, and Hiromasa Iida et al. Jan. 1987 310 p In JAPANESE; ENGLISH summary
(DE87-702957; JAERI-M-86-176) Avail: NTIS HC A14/MF A01

Analyses and experiments on the integrity evaluation and lifetime predictions of plasma facing components in fusion reactors such as first walls, divertor plates and pumped limiter plates have been performed. Results of the following issues have been obtained: (1) examination of life limiting factors based on one-dimensional calculations; (2) plastic deformation impact based on two dimensional elastic-plastic analysis; (3) sputtering and redeposition analysis; (4) thermo-mechanical analysis of the first wall subjected to one-sided heating; (5) melting and evaporation experiments of solid walls subjected to intense heating; (6) melt layer stability; (7) thermal fatigue tests of tungsten copper duplex structures for divertor plates; (8) torsional fatigue tests of tungsten copper butt joints; (9) analysis of eddy current and dynamic electromagnetic force; (10) experiments on the dynamic deformation of ferritic and non-ferritic metal caused by electromagnetic force. DOE

N88-22736# Israel Atomic Energy Commission, Yavneh. Nuclear Research Center.
PLASMOR: A LASER-PLASMA SIMULATION CODE, PART 2
D. Salzman, A. D. Krumbein, and H. Szichman Jun. 1987 25 p
(DE88-701289; IA-1432-Pt-2) Avail: NTIS (US Sales Only) HC A03/MF A01

This report supplements a previous one which describes the PLASMOR hydrodynamics code. The present report documents the recent changes and additions made in the code. In particular described are two new subroutines for radiative preheat, a system of preprocessors which prepare the code before run, a list of postprocessors which simulate experimental setups, and the basic data sets required to run PLASMOR. In the Appendix a new computer-based manual which lists the main features of PLASMOR is reproduced. DOE

N88-22737# Israel Atomic Energy Commission, Yavneh. Nuclear Research Center.
PARTICLE ACCELERATION TO HIGH ENERGIES AND AMPLIFICATION OF COHERENT RADIATION BY ELECTROMAGNETIC INTERACTIONS IN PLASMAS Ph.D. Thesis
Abraham Loeb May 1986 123 p In HEBREW; ENGLISH summary
(TI88-701020; IA-1422) Avail: NTIS HC A06/MF A01

An Autoresonance Laser Acceleration (ALA) scheme permits the acceleration of charged particles, moving along an axisymmetric magnetic field, in the Doppler shifted cyclotron resonance with a rotating electromagnetic field. The radiation losses in a TeV accelerator are negligible. An Nd:glass laser with an intensity of 10 sup 18 W/sq cm is capable of accelerating a high current electron beam from 0.25 to 2.5 GeV over 1 m along a 100 kG guide magnetic field. Significant exponential amplification with a gain factor of several tenths of cm -1 for strong millimeter radiation, is obtained in a plasma accelerator with MeV electron beams with current densities of several kA/sq cm. In electron-positron plasmas the acceleration is based on a self-sustained cyclotron resonance between the particles and a homogeneous, luminous, linearly polarized laser radiation, propagating along an axial magnetic field. An electron (positron) which initially satisfies the cyclotron resonance condition, will be accelerated asymptotically, by using a linearly polarized laser field. DOE

N88-22738# Israel Atomic Energy Commission, Yavneh. Nuclear Research Center.
NEW METHODS OF CONFINEMENT AND HEATING OF PLASMA IN MAGNETIC FIELDS Ph.D. Thesis
Michael Kishinevsky May 1987 86 p In HEBREW; ENGLISH summary
(TI88-701021; IA-1424) Avail: NTIS (US Sales Only) HC A05/MF A01

In this work two new schemes of plasma magnetic trapping are proposed: Tandem Mirror and Toroidally Linked Mirrors. Calculation and analysis of plasma confinement were performed and a problem of stochastical diffusion losses were experimentally studied. This has shown that Tandem Mirror Trap does not have a classical energy gain limitation of the usual magnetic mirror and can eventually reach an ignition (Q = infinity). In the Toroidally Linked Mirrors the radial losses can be substantially reduced by using ICRF power and by localizing of the curvature region in high-magnetic field sections. Concerning the heating, an experimental and theoretical research was performed on negative hydrogen ion production mechanism for charge exchange plasma fueling and heating. Mechanism of secondary ion emission from metal surfaces was explained and experiment on hydrogen dynamics on the cathode surface have been carried out. DOE

N88-22739# Joint Inst. for Nuclear Research, Dubna (USSR). Lab. of Theoretical Physics.
PLASMA WAVE RADIATIVE DAMPING OF A NEW TYPE IN A RELATIVISTIC ONE-DIMENSIONAL PLASMA
N. N. Bogolyubov, P. A. Polyakov, and M. A. Tasev 1987 6 p In RUSSIAN; ENGLISH summary
(TI88-701191; JINR-R-17-87-128) Avail: NTIS (US Sales Only) HC A02/MF A01

The dispersion equation for plasma waves in a relativistic one-dimensional plasma is investigated taking into account radiative damping of charged particles. This kind of plasma oscillations is shown to undergo an additional attenuation in ultra-relativistic case due to radiative braking of charged particles in the collective field of the wave. This extra damping is proved to be less than one at nonrelativistic temperatures. DOE

N88-22740# Edgerton, Germeshausen and Grier, Inc., Idaho Falls, Idaho.
ENVIRONMENTAL ASSESSMENT FOR THE COMPACT IGNITION TOKAMAK
M. A. McKenzie-Carter and J. R. Stencel 1987 4 p Presented at the 12th Symposium on Fusion Engineering, Monterey, Calif., 12 Oct. 1987 Prepared in cooperation with Princeton Univ., N.J.
(Contract DE-AC07-76ID-01570)
(DE88-005633; EGG-M-33387; CONF-871007-86) Avail: NTIS HC A02/MF A01

The Compact Ignition Tokamak (CIT) is the proposed next step in the U.S. magnetic confinement fusion energy program. DOE has chosen the Princeton Plasma Physics Laboratory (PPPL) as the preferred location for this ignition research device. The site at PPPL is adjacent to the existing Tokamak Fusion Test Reactor (TFTR) test cell. One of the necessary early planning steps in the schedule for the project is compliance with the National Environmental Policy Act (NEPA). Projected environmental impacts of the CIT are minimal. The only unique nonradiological environmental aspect to the project will be releases of relatively large but innocuous amounts of nitrogen gas, as a result of passive liquid nitrogen cooling of the machine. Consequently, potential radiological impacts are of greatest interest. Estimates of releases of tritium and air activation products from the CIT, which may use up to 20 grams of tritium, have been made and consequential doses calculated. These preliminary dose calculations indicate that the routine operation design objective dose of 10 mrem/yr to the maximally exposed member of the public will be met. Potential accident scenarios have been developed and the potential effects summarized. DOE

N88-22741# Argonne National Lab., Ill.
ALEX RESULTS: A COMPARISON OF MEASUREMENTS FROM A ROUND AND A RECTANGULAR DUCT WITH 3-D CODE PREDICTIONS
C. B. Reed, B. F. Picologlou, T. Q. Hua, and J. S. Walker 1987 5 p Presented at the 12th Symposium on Fusion Engineering,

Monterey, Calif., 12 Oct. 1987 Prepared in cooperation with Illinois Univ., Urbana.
(Contract W-31109-eng-38)
(DE88-005947; CONF-871007-90) Avail: NTIS HC A02

Recent results of liquid-metal magnetohydrodynamic (MHD) measurements from a rectangular duct and earlier measurements from a round duct are reported. A fully three-dimensional numerical analysis of each test section in the fringing region of an applied magnetic field is briefly described. The results of the experiments and the 3-D code predictions are compared and discussed. Excellent agreement is obtained in both test section geometries for interaction parameters ranging from 500 less than or equal to N less than or equal to 1.25 x 10 to the 5th power. DOE

N88-22742# Oak Ridge National Lab., Tenn. Fusion Energy Div.
LONG-TIME IMPURITY CONFINEMENT AS A PRECURSOR TO DISRUPTIONS IN OHMICALLY HEATED TOKAMAKS
R. C. Isler and W. L. Rowan 1988 45 p Presented at the Meeting on Density Limits and Disruptions, Abingdon, United Kingdom, 26 Jan. 1988 Prepared in cooperation with Texas Univ., Austin
(Contract DE-AC05-84OR-21400)
(DE88-006183; CONF-880163-1-Vugraphs) Avail: NTIS HC A03

It has been observed in several tokamaks that the confinement of test impurities increases dramatically when operating near density limits. The characteristics of the working gas transport coefficients also change character under these conditions. These changes appear to be caused by a suppression of the anomalous transport mechanisms. This series of vugraphs investigates the role of these changes in initiating disruptions. DOE

N88-22743# Massachusetts Inst. of Tech., Cambridge. Plasma Fusion Center.
CURRENT-DRIVE ON THE VERSATOR-2 TOKAMAK WITH A SLOTTED-WAVEGUIDE FAST-WAVE COUPLER Ph.D. Thesis
J. A. Colborn Nov. 1987 104 p
(Contract DE-AC02-78ET-51013)
(DE88-006261; DOE/ET-51013/242; PFC/RR-87-20) Avail: NTIS HC A06/MF A01

A slotted-waveguide fast-wave coupler has been constructed, without dielectric, and used to drive current on the Versator-2 tokamak. Up to 35 kW of net microwave power at 2.45 GHz has been radiated into plasmas with 2 x 10 to the 12th/cu cm less than or equal to mean of n(sub e) less than or equal to 1.2 x 10 to the 13th/cu cm and B(sub tor) approx. = 1.0 T. The launched spectrum had a peak near N(sub parallel) = -2.0 and a larger peak near N(sub parallel) = 0.7. Radiating efficiency of the antenna was roughly independent of antenna position except when the antenna was at least 0.2 cm outside the limiter, in which case the radiating efficiency slightly improved as the antenna was moved farther outside. When the coupler was inside the limiter, radiating efficiency improved moderately with increased mean of n(sub e). Current-drive efficiency was comparable to that of the slow wave and was not affected when the antenna spectrum was reversed; however, no current was driven for mean of n(sub e) less than or equal to 2 x 10 to the 12th/cu cm. These results indicate the fast wave was launched, but a substantial part of the power may have been mode-converted to the slow wave, possible via a downshift in N(sub parallel), and these slow waves may have been responsible for most of the driven current. Relevant theory for waves in plasma, current-drive efficiency, and coupling of the slotted-waveguide is discussed, the antenna design method is explained, and future work, including the construction of a much-improved probe-fed antenna, is described. DOE

N88-22744# California Univ., Los Angeles. Inst. for Plasma and Fusion Research.
MAGNETIC FUSION ENERGY PLASMA INTERACTIVE AND HIGH HEAT FLUX COMPONENTS. VOLUME 5: TECHNICAL ASSESSMENT OF CRITICAL ISSUES IN THE STEADY STATE OPERATION OF FUSION CONFINEMENT DEVICES
Jan. 1988 201 p
(Contract DE-FG03-85ER-51069)
(DE88-006920; UCLA/PPG-1125-Vol-5) Avail: NTIS HC A10/MF A01

Critical issues for the steady state operation of plasma confinement devices exist in both the physics and technology fields of fusion research. Due to the wide range and number of these issues, this technical assessment has focused on the crucial issues associated with the plasma physics and the plasma interactive components. The document provides information on the problem areas that affect the design and operation of a steady state ETR or ITER type confinement device. It discusses both tokamaks and alternative concepts, and provides a survey of existing and planned confinement machines and laboratory facilities able to address the identified issues. A universal definition of steady state operation is difficult to obtain. From a physics point of view, steady state is generally achieved when the time derivatives approach zero and the operation time greatly exceeds the characteristic time constants of the device. Steady state operation for materials depends on whether thermal stress, creep, fatigue, radiation damage, or power removal are being discussed. For erosion issues, the fluence and availability of the machine for continuous operation are important, assuming that transient events such as disruptions do not limit the component lifetimes. The panel suggests, in general terms, that steady state requires plasma operation from 100 to 1000 seconds and an availability of more than a few percent, which is similar to the expectations for an ETR type device. The assessment of critical issues for steady state operation is divided into four sections: physics issues; technology issues; issues in alternative concepts; and devices and laboratory facilities that can address these problems. DOE

N88-22745# Wisconsin Univ., Madison. Dept. of Physics.
ELECTRICAL CIRCUIT MODELING OF REVERSED FIELD PINCHES
J. C. Sprott Feb. 1988 55 p
(Contract DE-FG02-85ER-53198)
(DE88-006942; DOE/ER-53198/117) Avail: NTIS HC A04/MF A01

Equations are proposed to describe the radial variation of the magnetic field and current density in a circular, cylindrical RFP. These equations are used to derive the electrical circuit parameters (inductance, resistance, and coupling coefficient) for an RFP discharge. The circuit parameters are used to evaluate the flux and energy consumption for various startup modes and for steady-state operation using oscillating field current drive. The results are applied to the MST device. DOE

N88-22746# Kyoto Univ., Uji (Japan). Plasma Physics Lab.
HEATING AND CONFINEMENT STUDIES OF ELECTRON CYCLOTRON RESONANCE HEATED PLASMAS IN HELIOTRON E
H. Zushi, M. Sato, and O. Motojima Jun. 1987 51 p
(DE88-752312; PPLK-R-15) Avail: NTIS (US Sales Only) HC A04/MF A01

Rf heating of currentless plasmas is performed at the fundamental and second harmonic cyclotron frequency. The effects of irradiation pattern on plasma heating are studied. In the fundamental heating experiments, the absorbed power profile is determined from the decay of the electron internal energy profile immediately after the rf pulse turned off. Measurements of absorbed power profile by varying the position of the cyclotron resonance layer are compared with the single-pass absorption profiles predicted by a ray tracing code. The profiles of electron temperature, density and ion temperature are studied as a function of the heating power, its profile, and the electron line averaged density. Finally, a scaling of the energy confinement time is obtained by using a regression analysis and compared with a scaling for neutral beam heated plasmas. DOE

N88-22747# Japan Atomic Energy Research Inst., Tokyo.
IMPROVEMENT OF PLASMA CONFINEMENT DUE TO ELECTRON LANDAU DAMPING IN TOKAMAKS

Kazuya Uehara Nov. 1987 28 p
(DE88-752339; JAERI-M-87-180) Avail: NTIS (US Sales Only) HC A03/MF A01

It is shown that the E vector sub rf x B vector sub 0 theta drift for resonant electrons in tokamaks does not cancel and forms an inward flux during rf heating with a travelling wave type spectrum when an exact treatment of Landau damping in the presence of the magnetic field is performed as an initial value problem, where E vector sub rf is rf electric field and B vector sub 0 theta is poloidal magnetic field. This effect could be the basis of the phenomenon that the plasma confinement is improved during low density lower-hybrid current drive in tokamaks. DOE

N88-22748# Academy of Sciences of the Ukrainian SSR, Kiev. Inst. Yadernykh Issledovanij.
PARAMETRIC INSTABILITIES OF INHOMOGENEOUS PLASMA NEAR THE LOWER-HYBRID RESONANCE
T. A. Davydova and V. S. Marchenko 1987 46 p In RUSSIAN; ENGLISH summary
(TI88-701201; KIYI-86-17) Avail: NTIS (US Sales Only) HC A03/MF A01

Parametric instabilities of inhomogeneous plasma near the lower-hybrid resonance taking account of linear transformation of the pump wave are analytically investigated. Corresponding threshold conditions, temporal growth rates, the structure and domain of localization of unstable modes are obtained. It is shown that at the linear stage of instability compression of localization domain of unstable modes takes place. This should result in fast dissipation of HF energy in the resonance region. By optimal choice of lower-hybrid wave power and other parameters these processes will result in the heating of a central region of plasma filament in tokamaks. DOE

N88-22749# Auburn Univ., Ala. Dept. of Physics.
THEORETICAL STUDIES OF THE HEATING OF TOROIDAL PLASMAS WITH RADIOFREQUENCY ELECTROMAGNETIC RADIATION Progress Report, 1 Jul. 1987 - 30 Jun. 1988
D. G. Swanson, J. M. Wersinger, and J. D. Hanson Feb. 1988 87 p
(Contract DE-FG05-85ER-53206)
(DE88-006913; DOE/ER-53206/10) Avail: NTIS HC A05/MF A01

Two main studies have been made since the beginning of this grant. First, Inho Park has obtained results for quasi-mode decay at lower hybrid geometric foci using an analytic model. Many lower hybrid rays have been traced to assess the wide occurrence of true geometric line foci. Three regimes for daughter wave amplification have been identified in three regions of the foci. The problem of obtaining realistic pump wave amplitudes is clearly defined and cannot be obtained from focusing. Second, a lower hybrid ray tracing code has been built for ETR, using a numerical equilibrium. The last details of coding up and graphics generation are being worked out. The goal is to study both current drive and the possibility to burn through the distribution functions to improve accessibility. For the remainder of this grant period we will start work on Ion Bernstein Wave Heating in collaboration with Oak Ridge. DOE

N88-22750# Bhabha Atomic Research Centre, Bombay (India).
RAYLEIGH-TAYLOR INSTABILITY IN INERTIAL CONFINEMENT FUSION
N. K. Gupta 1987 169 p
(TI88-701411; BARC-1372) Avail: NTIS (US Sales Only) HC A08/MF A01

Summarized are the results of theoretical analysis on the problem of Rayleigh-Taylor instability in inertial confinement fusion (ICF). This report covers four basic problems: (1) an analytical formulation to consider the effects of plasma density inhomogeneities on the growth of the instability in plane geometry is presented. It is concluded that, for minimizing the growth rate of the instability, it may be advantageous to use the driver laser beams of higher irradiance and an optimum wave length in an ICF experiment, (2) a new formulation for the analysis of the instability in curved (cylindrical and spherical) geometries is presented. A general eigenvalue equation for the growth rate of the instability which is applicable for both plane and curved geometries is derived. A comparative study is made between the plane, cylindrical and spherical geometries. Also analytical expressions for the growth rates are obtained in the cases of spherical and cylindrical shell targets and their variations with respect to the aspect ratios of the shells are discussed, (3) a semi-analysis of the instability where the growth rate is obtained by solving numerically a (2N-1)x(2N-1) determinant equation is presented. The semi-analysis developed is applicable for the study of the growth of the instability in the present day multi-structured spherical shell targets. Finally, a dynamic analysis of the growth of the instability for a representative spherical solid target driven by laser beams symmetrically from all the sides is carried out numerically using a computer code developed for this purpose. DOE

N88-22751# R and D Associates, Alexandria, Va.
MPD (MAGNETOPLASMADYNAMIC) THRUST CHAMBER FLOW DYNAMICS Annual Report, 1 Oct. 1986 - 30 Sep. 1987
29 Sep. 1987 60 p
(Contract F49620-86-C-0117)
(AD-A189940; RDA-TR-144200; AFOSR-87-1883TR) Avail: NTIS HC A04/MF A01 CSCL 21C

Performance characteristics of Magnetoplasmadynamic (MPD) arcjets depend on proper matching of electromagnetic and fluid mechanical constraints within the thrust chamber. Experimental measurements of internal flow conditions during MPD arcjet operation are needed to guide development of flow models and to assess the validity of theoretical predictions. Efforts are continuing in a corporative effort to apply an array of diagnostic techniques including time-, space-, and spectrally-resolved photography to examine MPD arcjet internal flows. Experimental elucidation of the internal flow structure is used to develop predictive models for optimal geometries and operating parameters. Probes have been used to map the current and voltage distributions within uniform height and flared annular channels. This work is concerned with the effect of thruster channel variations on the current conduction regions of the MPD internal flow. Other aspects of the internal flow structure that have been modeled involve the transition of the input mass flow from neutral gas to electrically-conducting plasma. Scale sizes for the transition region were estimated in terms of the electrical and thermodynamic properties of the propellant gas (e.g., argon). These estimates indicate that the electrical conductivity of the flow can be established in distances that are small compared to the characteristic dimension for current conduction near the entrance to the arcjet thrust chamber. GRA

N88-22752# California Univ., Irvine. Dept. of Physics.
HIGH POWER, HIGH FREQUENCY RADIATION FROM BEAM-PLASMA INTERACTIONS Annual Report, 15 Jun. 1982 - 14 Jun. 1987
Gregory Benford 14 Jun. 1987 44 p
(Grant AF-AFOSR-0233-82)
(AD-A190207; AFOSR-87-1829TR) Avail: NTIS HC A03/MF A01 CSCL 20I

A theory has been developed for the probability distribution of the electric field in a highly turbulent plasma environment. Experimental optical studies have been carried out to quantify the distribution function for electrical fields less than 10 kV/cm. Preliminary studies have been conducted of the anisotropy of microwave emission from beam plasma systems. GRA

N88-22753# Carnegie-Mellon Univ., Pittsburgh, Pa. Dept. of Mechanical Engineering.
FUNDAMENTAL STUDIES ON MPD THRUSTERS Final Progress Report, Apr. 1985 - Dec. 1986
J. L. Lawless 2 Sep. 1987 258 p
(Grant AF-AFOSR-0033-83)
(AD-A190307; Rept-1-52097; AFOSR-87-2012TR) Avail: NTIS HC A12/MF A01 CSCL 21C

A theory has been developed which predicts onset and erosion in MPD thrusters. The theory predicts onset currents which are in quantitative agreement with experiment. Erosion rates are predicted for a steady-state hot cathode thruster. This theory is the first to model the viscous and thermal electrode boundary layers in MPD thrusters. Stability criteria for diffuse-mode electrode current conduction have been found. GRA

N88-22754# Massachusetts Inst. of Tech., Cambridge. Space Systems Lab.
PHYSICAL FLUID MECHANICS IN MPD THRUSTERS Annual Report, 1 May 1986 - 30 Apr. 1987
Manuel Martinez-Sanchez 18 Sep. 1987 53 p
(Grant AF-AFOSR-0119-86)
(AD-A190309; AFOSR-87-1760TR) Avail: NTIS HC A04/MF A01 CSCL 21C

This report describes work done on three areas of MPD research: (1) a rigorous theoretical examination of the one dimensional flow of a self-field accelerated plasma, clarifying the roles of area change, sonic vs. magnetoacoustic chocking, and finite magnetic Reynolds number, (2) continued development of computational codes for axisymmetric MPD flows, and (3) results of a first test series on two channels designed to verify productions on the effects of area variation, showing ability to redistribute current by this means. GRA

N88-22755# Massachusetts Inst. of Tech., Cambridge. Plasma Fusion Center.
PLASMA-GAS INTERACTION STUDIES IN A HYBRID PLUME PLASMA ROCKET Annual Report, 1 Sep. 1986 - 30 Aug. 1987
F. R. Chang-Diaz and T. F. Yang 30 Sep. 1987 31 p
(Grant AF AFOSR-0190-84)
(AD-A190310; AFOSR-87-1759TR) Avail: NTIS HC A03/MF A01 CSCL 21C

This report discusses the progress in the fluid modeling of a hybrid plume plasma rocket and the heating of plasma in a tandem mirror device. In the theoretical area three tasks have been accomplished: (1) a major advance has been made in the development of a numerical method for solving the time dependent fluid equations for both ions and electrons in the plasma, (2) a mathematical model has been formulated for studying the radio frequency heating of the hot plasma in cylindrical geometry, (3) an analysis on the performance characteristics of the hybrid plume rocket has been carried out. Under the funding of the instrumentation program the component fabrication is on progress. The coils have been delivered. GRA

N88-22756# Argonne National Lab., Ill.
MPD (MAGNETOPLASMADYNAMIC) THRUSTER ADVANCED PUMPING SYSTEM CONCEPTS Final Report, Jun. 1985 - Aug. 1986
S. K. Bhattacharyya, L. W. Carlson, L. S. Chow, E. D. Doss, and H. Herman Dec. 1987 72 p
(AF Proj. 5730)
(AD-A190513; AFAL-TR-87-067; RPL-69005) Avail: NTIS HC A04/MF A01 CSCL 21C

Magnetoplasmadynamic (MPD) thrusters have a number of features that make them attractive for use in several intermediate term missions planned by the U.S. Air Force and NASA. Theoretical studies and laboratory scale pulsed tests performed to date have established the basic characteristics of MPD thrusters and have provided a basis for optimism regarding their eventual performance. The high (multimegawatt) power sources for space use currently being developed in the Strategic Defense Initiative can be adapted for use with MPD thrusters. Given these conditions, a major requirement for MPD thruster development is the availability of a suitable prototype test facility since successful development of multimegawatt MPD thrusters will depend, to a great extent, on testing them under realistic steady characteristics, life cycle expectancy, electrode erosion rates, and other data essential to the design of working thrusters. The major technical obstacle for ground testing of MPD thrusters in a space simulation facility is the inability of state-of-the-art vacuum systems to provide the tremendous pumping speeds that are required for multimegawatt MPD thrusters. This is true for other types of electric propulsion devices as well. GRA

N88-22757# Oak Ridge National Lab., Tenn.
TRANSPORT SIMULATIONS OF OHMIC IGNITION EXPERIMENT: IGNITEX
N. A. Uckan and H. C. Howe Dec. 1987 22 p Presented at the 12th Symposium on Fusion Engineering, Monterey, Calif., 12 Oct. 1987
(Contract DE-AC05-84OR-21400)
(DE88-006055; ORNL/TM-10617; CONF-871007-88) Avail: NTIS HC A03/MF A01

The IGNITEX device, proposed by Rosenbluth et al., is a compact, super-high-field, high-current, copper-coil tokamak envisioned to reach ignition with ohmic (OH) heating alone. Several simulations of IGNITEX were made with a 0-D global model and with the 1-D PROCTR transport code. It is shown that OH ignition is a sensitive function of the assumptions about density profile, wall reflectivity of synchrotron radiation, impurity radiation, plasma edge conditions, and additional anomalous losses. In IGNITEX, OH ignition is accessible with nearly all scalings based on favorable OH confinement (such as neo-Alcator). Also, OH ignition appears to be accessible for most (not all) L-mode scalings (such as Kaye-Goldston), provided that the density profile is not too broad (parabolic or more peaked profiles are needed), Z sub eff is not too large, and anomalous radiation and alpha losses and/or other enhanced transport losses (eta sub i modes, edge convective energy losses, etc.) are not present. In IGNITEX, because the figure-of-merit parameters are large, ignition can be accessed (either with OH heating alone or with the aid of a small amount of auxiliary power) at relatively low beta, far from stability limits. DOE

N88-22758# Instituto de Pesquisas Espaciais, Sao Jose dos Campos (Brazil).
VACUUM-ARC PLASMA CENTRIFUGE EXPERIMENT
Edson DelBosco, Renato Sergio Dallaqua, Jose Augusto Bittencourt, and Gerson Otto Ludwig May 1988 5 p Presented at the 13th International Symposium on Discharges and Electrical Insulation in Vacuum, Paris, France, 1988
(INPE-4509-PRE/1263) Avail: NTIS HC A02/MF A01

Vacuum-arc plasma centrifuges, for isotope and element enrichment, have been studied to some extent over the last ten years. This paper describes the vacuum-arc plasma centrifuge developed at INPE. The experiment is characterized by its relatively small dimensions. Angular rotation frequencies in the range of 1.9 x 10 to the 5th rad/s to 3.5 x 10 to the 5th rad/s, measured with Langmuir probes, are presented for a magnesium plasma. Enrichments of 15 percent for Mg-25 and 26 percent for Mg-26 were measured with a quadrupole mass spectrometer. The dependence of magnesium isotope enrichment on the magnetic field is also presented. Author

N88-22759# Institut d'Aeronomie Spatiale de Belgique, Brussels.
PLASMAPAUSE FORMATION
J. Lemaire 1987 36 p Presented at the 6th International Symposium on Solar-Terrestrial Relationships, Toulouse, France, 30 Jun. - 5 Jul. 1986 Previously announced in IAA as A88-20638 Submitted for publication Sponsored by the Belgian Fonds National de la Recherche Scientifique and the Belgian Ministere de l'Education Nationale
(Aeronomica-Acta-A-319-1987; ISSN-0065-3713; ETN-88-92211)
Avail: NTIS HC A03/MF A01

The theory of plasmapause formation is examined. Particular attention is given to the role of magnetospheric fields in the inner magnetosphere, the noon-midnight and dawn-dusk asymmetries, plasma density distribution in the plasmasphere, plasmapause positions in the nightside sector and the daytime LT sector, the LT distribution of detached plasma elements, the growth rate of interchange instability, the formation of new density knees at each

new enhancement in magnetospheric convection, and diagmagnetic and finite-temperature effects. The ideal MHD theory for the formation of the plasmapause is considered. ESA

N88-22235# Joint Publications Research Service, Arlington, Va.
SMOOTHING TECHNIQUE TO RESOLVE X-RAY SPECTRA IN LASER NUCLEAR FUSION
Chenghai Liu and Zhengqiang Lu *In its* JPRS Report: Science and Technology. China 11 Dec. 1987 p 4-15 Transl. into ENGLISH from Jisuan Wuli (Beijing, Peoples Republic of China), v. 2, no. 2, Sep. 1985 p 313-320 (For primary document see N88-22233 15-31)
Avail: NTIS HC A06/MF A01

76 SOLID-STATE PHYSICS

Includes superconductivity.

For related information, see also *33 Electronics and Electrical Engineering* and *36 Lasers and Masers.*

N88-22760# Atomic Energy Research Establishment, Harwell (England). Materials and Surface Science Group.
ANGULAR RESOLVED ENERGY ANALYSIS OF (69)Ga+ IONS FROM A GALLIUM LIQUID METAL ION SOURCE
P. Marriott May 1987 11 p Prepared in cooperation with Salford Univ., United Kingdom
(AERE-R-12649; HL87/1163) Avail: NTIS HC A03/MF A01

An analysis system was designed and built to characterize liquid metal ion source beams. Both mass and angular resolved energy distribution measurments can be made, from which both FWHM energy spreads and energy deficits can be obtained, thus making this system unique worldwide. The system is briefly described, and the first off-axis results taken with a gallium liquid metal ion source are presented and discussed. Author

N88-22761# Carnegie-Mellon Univ., Pittsburgh, Pa. Dept. of Computer Science.
TWO PAPERS ON A SYMBOLIC ANALYZER FOR MOS (METAL-OXIDE SEMICONDUCTORS) CIRCUITS Interim Report
R. E. Bryant Dec. 1987 73 p
(Contract F33615-84-K-1520)
(AD-A188617; CMU-CS-87-106; AFWAL-TR-87-1167) Avail: NTIS HC A04/MF A01 CSCL 12B

A network of switches controlled by Boolean variables can be represented as a system of Boolean equations. The solution of this system gives a symbolic description of the conducting paths in the network. Gaussian elimination provides an efficient technique for solving sparse systems of Boolean equations. For the class of networks that arise when analyzing digital metal-oxide semiconductor (MOS) circuits, a simple pivot selection rule guarantees that most a switch networks encountered in practice can be solved with O(s) operations. When represented by a directed acyclic graph, the set of Boolean formulas generated by the analysis has total size bounded by the number of operations required by the Gaussian elimination. This paper presents the mathematical basis for systems of Boolean equations, their solution by Gaussian elimination, data structures and algorithms for representing and manipulating Boolean formulas. GRA

N88-22762# Gosudarstvennyi Komitet po Ispolzovaniyu Atomnoi Energii, Moscow (USSR). Inst. Atmnoj Ehnergii.
DOES THE PIPE DIFFUSION OF SELF-INTERSTITIALS IN CRYSTALS UNDER STRESSES EXIST
V. V. Kolomytkin 1986 4 p In RUSSIAN
(TI88-701027; IAE-4324/11) Avail: NTIS (US Sales Only) HC A02/MF A01

Migration of self-interstitials (SI) along nucleus of edge disloation (100) (010) in uniaxially loaded (along Burgers vector) alpha iron cyrstallite has been investigated. Method of molecular dynamics with artificial energy dissipation was used to determine migration energies. No accelerated SI pipe diffusion either in the center or in a near-surface layer of a dislocation pipe up to 2.5 percent tensile deformation has been discovered. DOE

N88-22763# Israel Atomic Energy Commission, Yavneh. Nuclear Research Center.
GROWTH OF Pb/SUB 1-x/Eu/SUB x/Te EPITAXIAL LAYERS BY THE LIQUID PHASE EPITAXY TECHNIQUE Ph.D. Thesis
Avi Hacham Jun. 1987 68 p In HEBREW; ENGLISH summary
(TI88-701022; IA-1428) Avail: NTIS (US Sales Only) HC A04/MF A01

Lead salts are direct narrow-gap semiconductors useful for optoelectric devices - mainly, injection diode lasers. Pb sub 1-x Eu sub x Te is a new compound in this family. The incorporation of Eu into PbTe lattice causes a rapid increase of the energy gap, enabling the fabrication of devices operating at wavelengths shorter than 5 m in the infrared region. Diode lasers of this compound operate at higher temperatures than usually achieved. In this work, for the first time, we report the growth of (Pb,Eu)Te from solutions using Liquid Phase Epitaxy (LPE) technique. DOE

N88-22764# Lawrence Livermore National Lab., Calif.
SYNTHESIS OF METASTABLE SUPERCONDUCTORS BY HIGH DYNAMIC PRESSURE
W. J. Nellis, M. B. Maple, and T. H. Geballe Jan. 1988 10 p Presented at the SPIE O-E Lase 88: Optoelectronics and Laser Applications in Science and Engineering, Los Angeles, Calif., 10 Jan. 1988 Prepared in cooperation with California Univ., San Diego, La Jolla.; Stanford Univ., Calif.
(Contracts DE-FG03-86ER45230; W-7405-eng-48)
(DE88-005620; UCRL-98108; CONF-880110-22) Avail: NTIS HC A02

High dynamic pressure is used to synthesize metastable superconducting materials and to process superconductors into practical form. Specimens are subjected to shock pressures in the range 0.1 to 1 Mbar, temperatures up to several 1000 K and quenches at rates up to 10 to the 12th power bar/s and 10 to the 9th power K/s. Shock waves are generated by impact of projectiles accelerated up to 3.5 km/s by the LLNL two-stage light-gas gun. Recovered specimens are characterized for superconductivity and structural properties. The gas gun, specimen recovery fixture, and phenomenology of the technique are described. Results are reviewed and include a quenched solid-solid phase transition (A15 Nb3Si); amorphous, fine-grained, and multiphase materials produced by shock-induced melting of powders and subsequent rapid solidification; and the shock-compaction in a metal matrix of thin powder layers of high-T(sub c) oxides mixed with metal. The latter is a potential method for fabricating superconducting wire, which could be scaled to long lengths using explosives. DOE

N88-22765# Argonne National Lab., Ill.
RF PROPERTIES OF SUPERCONDUCTING Pb ELECTROPLATED ONTO Cu
J. R. Delayen 1987 25 p Presented at the 3rd Workshop on RF Superconductivity, Argonne, Ill., 14 Sep. 1987
(Contract W-31109-eng-38)
(DE88-005918; CONF-870955-4) Avail: NTIS HC A03

The properties of Pb as a superconducting material for high power rf applications are reviewed. The most common method of producing Pb superconducting resonators, which is by electrodeposition of a thin layer on a Cu substrate, is described. DOE

N88-22766# Georgia Univ., Athens. Dept. of Physics and Astronomy.
EFFECTIVE ELECTRON INTERACTIONS DUE TO VIRTUAL CHARGE AND SPIN EXCITATIONS IN AN EXTENDED HUBBARD MODEL FOR Cu-O SUPERCONDUCTORS
H. B. Schuettler and A. J. Fedro Nov. 1987 10 p Presented at the 32nd Conference on Magnetism and Magnetic Materials, Chicago, Ill., 9 Nov. 1987 Prepared in cooperation with Northern

Illinois Univ., Dekalb, Argonne National Lab., Ill.
(Contract W-31109-eng-38)
(DE88-005971; CONF-871126-11) Avail: NTIS HC A02

We have studied the effect of virtual Cu-O charge and spin fluctuations in the perovskite high-T(sub c) materials by applying a strong coupling expansion to an extended Hubbard model with hybridized Cu d-orbitals and O p-orbitals. Results for the charge and spin fluctuation-mediated effective interactions are derived and discussed. DOE

N88-22767# Argonne National Lab., Ill.
ION-BEAM MIXING AND AMORPHIZATION IN Au/Zr BILAYERS
Fu-Rong Ding, P. R. Okamoto, and L. E. Rehn Nov. 1987 7 p Presented at the Fall Meeting of the Materials Research Society, Boston, Mass., 30 Nov. 1987 Prepared in cooperation with Beijing Univ. (China)
(Contract W-31109-eng-38)
(DE88-005999; CONF-871124-92) Avail: NTIS HC A02/MF A01

Au/Zr bilayer films with inert-gas markers were produced by low energy (less than or equal to 4 keV) implantation. Mass transport was measured during ion-beam mixing with 1 MeV Kr at several temperatures between 330 and 540 K. Two distinct regimes of apparent Arrhenius behavior were found with activation enthalpies of 0.06 and 0.9 eV in the temperature range 330 to 440 K and 460 to 540 K, respectively. Microstructural changes during ion-beam mixing were studied in situ, in a high voltage electron microscope. Heterogeneous nucleation of an amorphous phase was observed during mixing. Results are compared with similar studies reported previously in Ni/Zr bilayer specimens. DOE

N88-22768# Argonne National Lab., Ill.
DYNAMICAL OPTIMIZATION TECHNIQUES FOR THE CALCULATION OF ELECTRONIC STRUCTURE IN SOLIDS
R. Benedek, B. I. Min, and J. Garner Aug. 1987 10 p Presented at the US-Japan Seminar on Electronic Structure and Lattice Defects in Alloys, Honolulu, Hawaii, 4 May 1987 Prepared in cooperation with Bradley Univ., Peoria, Ill.
(Contract W-31109-eng-38)
(DE88-006010; CONF-8705226-4) Avail: NTIS HC A02/MF A01

The method of dynamical simulated annealing, recently introduced by Car and Parrinello, provides a new tool for electronic structure computation as well as for molecular dynamics simulation. In this paper, we explore an optimization technique that is complementary to dynamical simulated annealing, the method of steepest descents (SD). As an illustration, SD is applied to calculate the total energy of diamond-Si, a system previously treated by Car and Parrinello. The adaptation of SD to treat metallic systems is discussed and a numerical application is presented. DOE

N88-22769# Michigan Univ., Ann Arbor. Dept. of Materials Science and Engineering.
SUPERCONDUCTIVITY AND THE TAILORING OF LATTICE PARAMETERS OF THE COMPOUND YBa2Cu3O(SUB x)
I-Wei Chen, S. Keating, C. Y. Keating, X. Wu, J. Xu, P. E. Reyes-Morel, and T. Y. Tien 1987 22 p Presented at the 89th Annual Meeting of the American Ceramic Society, Pittsburgh, Pa., 26 Apr. 1987
(Contract DE-FG02-87ER-45302)
(DE88-005904; CONF-870422-11) Avail: NTIS HC A03/MF A01

The compound YBa2Cu3O(x) was given various oxidation treatments over a range of oxygen pressures from 0.02 to 200 MPa and temperatures up to 1223K. A tetragonal to orthorhombic transition was observed. At higher oxygen content, the orthorhombic phase becomes superconducting below 93K. At lower oxygen content, the tetragonal phase was stable down to room temperature. Doping by alkaline cations favored the formation of the orthorhombic phase even in a less oxidizing atmosphere, simultaneously improving the sinterability. The orthorhombic unit cell parameters, i.e., volume, bond lengths, and axial distortions, were found to correlate with the superconducting transition temperatures. These correlations are rationalized in terms of the interrelationship of oxygen stoichiometry with the lattice parameters of the orthorhombic phase. DOE

N88-22770# Argonne National Lab., Ill.
THERMOCHEMISTRY AND HIGH TEMPERATURE THERMODYNAMIC PROPERTIES OF RARE EARTH-ALKALINE EARTH-COPPER OXIDE SUPERCONDUCTORS
L. R. Morss, D. C. Sonnenberger, and R. J. Thorn 1987 3 p Presented at the Symposium on High Temperature Superconductors, Boston, Mass., 30 Nov. 1987
(Contract W-31-109-eng-38)
(DE88-005976; CONF-8711114-5) Avail: NTIS HC A02/MF A01

Enthalpies of formation of the perovskite-related oxides, La sub 1.85 Srsub 0.15CuO4, YBa2Cu3O sub y, with y = 6.93, 6.62, and 6.41 have been determined at 298.15 K by perchloric acid solution calorimetry. Enthalpies of formation and reaction with air have been evaluated. The partial molar enthalpy of solution of oxygen in YBa2Cu3O sub y has been determined and compared with the value derived from measurements of the equilibrium partial vapor pressures of oxygen. The significance of the defect state thermochemistry in conductivity is identified. DOE

N88-22771# California Univ., Berkeley. Lawrence Berkeley Lab.
THE INFLUENCE OF CURRENT STRESSING ON THE STRUCTURE OF Ag CONTACTS TO GaAs
Z. Liliental-Weber, A. Miret-Goutier, N. Newman, C. Jou, W. E. Spicer, J. Washburn, and E. R. Weber Dec. 1987 6 p Presented at the Symposium on Epitoxy of Semiconductor Layered Structures, Boston, Mass., 1 Dec. 1987 Prepared in cooperation with Stanford Univ., Calif.
(Contract DE-AC03-76SF-00098)
(DE88-005988; LBL-24490; CONF-871273-1) Avail: NTIS HC A02/MF A01

The stability of Ag Schottky contacts on GaAs after voltage and current stressing has been investigated. The barrier height and its stability against voltage and current stressing were found to depend on the diode fabrication method (metal deposition onto either air-exposed or ultra-high vacuum cleaved (UHV) substrates). The barrier height of Ag diodes formed on air-exposed surfaces is 0.96 eV, and a significant decrease of 70 MeV was found upon exposure to voltage and current stressing. In contrast, the barrier height of Ag diode formed on UHV cleaved samples is 0.89 eV, and no significant change was found upon exposure to stressing. The structure of the contacts was studied by transmission electron microscopy. Ag deposited on UHV cleaved substrates shows an epitaxial relationship to GaAs and atomically flat interfaces. Exposure to air before the metal deposition led to nonuniform reactions and compound formation at the interface as compared to UHV samples. After current stressing, void formation and electromigration of Ag were observed in the air-exposed contacts. Ag contacts formed on UHV-cleaved GaAs (110) were stable during current stressing. DOE

N88-22772# California Univ., Berkeley. Lawrence Berkeley Lab.
ABSOLUTE PRESSURE DERIVATIVES OF DEEP LEVEL DEFECTS IN 3-5 SEMICONDUCTORS
D. D. Nolte, W. Walukiewicz, and E. E. Haller Nov. 1987 8 p Presented at the Fall Meeting of the Materials Research Society, Boston, Mass., 30 Nov. 1987 Prepared in cooperation with California Univ., Berkeley
(Contract DE-AC03-76SF-00098)
(DE88-006318; LBL-23599; CONF-871124-80) Avail: NTIS HC A02/MF A01

Based on transition metal reference levels, absolute pressure derivatives are presented for band-edges in GaAs and InP and defects in GaAs. The defect deformation potentials are directly related to the electron-lattice coupling which drives lattice relaxation

around the defects. An exceedingly large inward lattice relaxation of the EL2 defect is found in GaAs upon electron emission. DOE

N88-22773# California Univ., Berkeley. Lawrence Berkeley Lab.
FIRST-PRINCIPLES CALCULATIONS OF QUASIPARTICLE ENERGIES AT SURFACES AND INTERFACES: SEMICONDUCTOR SURFACE-STATE SPECTRA AND BAND OFFSETS
S. G. Louie Dec. 1987 7 p Presented at the Solvay Conference on Surface Science, Austin, Tex., 14 Dec. 1987
(Contract DE-AC03-76SF-00098)
(DE88-006340; LBL-24467; CONF-871266-1) Avail: NTIS HC A02/MF A01

The first-principles theory for calculating surface-state energies and semiconductor band offsets is described. Within a quasiparticle interpretation of excitation spectra, the approach provides well-founded energies which can be compared directly with sepctroscopy measurements. Results for the As-capped Si(111) and Ge(111) surfaces and for the GaAs-AlAs(001) heterojunction are discussed and compared with experiment. DOE

N88-22774# Texas Accelerator Center, The Woodlands.
MAGNET STRENGTH FLUCTUATIONS IN THE SSC (SUPERCONDUCTING SUPER COLLIDER) LATTICE. PART 2: FREQUENCY MODULATION
G. P. Goderre Jun. 1987 21 p
(Contract DE-FG05-87ER-40374)
(DE88-006491; DOE/ER-40374/4-Pt-2;
UH-IBPD-002-87(1987)-Pt-2) Avail: NTIS HC A03/MF A01

This is a continuation of SSC-N-305. SSC-N-305 examined the effects of field strength modulation, when the modulation frequency (f sub mod) was equal to zero (i.e., current offset). The objective of this study is to examine the effect of field strength modulation with modulation frequencies other than zero. To this end, the tracking routine TEAPOT is modified to simulate frequency modulation of the current output from the 10 main SSC magnet power supplies. The amplitude (A sub i) and phase (phi sub i) of the modulation for the i sup th power supply are chosen randomly. Effects of bore tube shielding are included only when studying 60 Hz modulation frequency. Bore tube shielding is due to the copper coating on the bore tube walls. This coating modifies the amplitude and phase of the modulation inside the bore tube. The bore tube is more effective at shielding the dipole field and it becomes most effective as the modulation frequency increases. DOE

N88-22775# California Univ., Berkeley. Lawrence Berkeley Lab.
OPTICAL CHARACTERIZATION OF MICROCRYSTALS
L. Davis, D. Eimerl, and S. Velsko 10 Dec. 1987 23 p Presented at the American Conference on Crystal Growth, Monterey, Calif., 13 Jul. 1987
(Contract W-7405-eng-48)
(DE88-006622; UCRL-96109; CONF-870799-5) Avail: NTIS HC A03/MF A01

A new method to optical characterization of microcrystals is described and illustrated with experimental results. Techniques for characterizing the linear and nonlinear parameters of new materials at early stages of crystal growth have been developed. The linear indices of refraction and their dispersion are determined using combined methods of spindle stage microscopy and refractometry. This method has been extended to measurements at nonvisible wavelengths. An SHG apparatus of novel design is used to evaluate the overall nonlinearity. Both methods are used to study materials with single crystal domains as small as 50 microns. DOE

N88-22776# Bhabha Atomic Research Centre, Bombay (India).
SUPERCONDUCTIVITY IN POWER ENGINEERING
P. Chaddah, Y. D. Dande, B. A. Dasannacharya, M. K. Malik, and R. V. Raghavan 1987 11 p
(DE88-701414; BARC-1376) Avail: NTIS (US Sales Only) HC A03/MF A01

The advantages of low power loss, high magnetic fields and compactness of size of superconducting magnets have generated world-wide interest in using them for MHD generators, Tokamak fusion reactors, energy storage systems etc. With a view to assess the feasibility of using the technology in power engineering in India, the status of the efforts in the country is reviewed and the areas of R and D required are indicated. DOE

N88-22777# Air Force Inst. of Tech., Wright-Patterson AFB, Ohio. School of Engineering.
CALCULATING DEPLETION REGION CARRIER CONCENTRATIONS WITH CAPACITANCE-VOLTAGE MEASUREMENTS AND ETCHING M.S. Thesis
Gordon H. Gainer, Jr. Dec. 1987 90 p
(AD-A189630; AFIT/GEP/ENP/87D-8) Avail: NTIS HC A05/MF A01 CSCL 20L

Methods were developed for finding the charge carrier concentrations within the initial depletion region of n-type semiconductors. These methods combine the capacitance-voltage (C-V) technique with the etching of layers from the semiconductor surface. After each etch, the depletion region is made to end at the same location within the semiconductor. This location is used as a common reference and is arbitrarily chosen at a distance deep below the original unetched surface. For each etch depth, the voltage which extends the depletion region to the common reference distance is found. The voltage drop from an etch depth to the deeper common reference distance is the same as it would be if the semiconductor was not etched. This voltage drop is the sum of the applied voltage and the built-in potential. The built-in potential depends on the barrier potential at the semiconductor surface and the concentration at the common reference distance. GRA

N88-22778# Air Force Inst. of Tech., Wright-Patterson AFB, Ohio. School of Engineering.
EXAMINATION OF TEMPERATURE EFFECTS ON GATE-TO-DRAIN AVALANCHE BREAKDOWN IN GaAs MESFETs (METAL-SEMICONDUCTOR FIELD EFFECT TRANSISTORS) BY MEASURING LIGHT EMISSION UNDER RF DRIVE M.S. Thesis
Roger E. Robb Dec. 1987 161 p
(AD-A189634; AFIT/GE/ENG/87D-73) Avail: NTIS HC A08/MF A01 CSCL 09A

This investigation examines temperature effects on avalanche breakdown in GaAs MESFETs to determine if this failure mechanism is accelerated by high temperature life tests. The specific objective is to assess whether the accelerated life test evaluations performed on a GaAs MESFET planned for use in future Defense Satellite Communications System (DSCS) spacecraft have adequately addressed the reliability issues concerning the gate-to-drain avalanche breakdown failure mechanism. This objective was accomplished by adapting an existing analytical model for temperature effects, and using it to predict the variation in avalanche multiplication activity with temperature. To verify this model, it was used to calculate the associated changes in light emissions over temperature which were experimentally validated on one device of the type planned for use by the DSCS program. Once validated, these models were used to evaluate the adequacy of the accelerated temperature life tests. The results of this evaluation indicate that the avalanche breakdown failure mechanism is decelerated with temperature, and therefore, the effects of avalanche breakdown on the reliability of GaAs MESFETs cannot be determined by accelerated temperature life testing. GRA

N88-22779# Arizona State Univ., Tempe. Semiconductor Materials Research Lab.
AUTONOMOUS CONTROL SYSTEM FOR CZOCHRALSKI GROWTH OF LEC GaAs Scientific Report, 1 Jul. - 30 Sep. 1987
G. H. Schwuttke, Karl Riedling, and Robert C. White 29 Dec. 1987 23 p

(Contract F49620-86-C-0012; ARPA Order 9099)
(AD-A189726; AFOSR-88-0193TR) Avail: NTIS HC A03/MF A01 CSCL 12I

The goals of this program include the establishment of autonomous liquid encapsulated Czochralski (LEC) crystal growth and its commercialization. This report provides a short description of the autonomous control system, a detailed description of the digital hardware developed for the control system and the multibus computer system and the computer-puller hardware of the growth system. Technical drawings for the signal processing box and the motor controller board are also given. During the first period (1 year) this system has grown 30 single GaAs crystals with a yield of better than 70 percent of single crystals. GRA

N88-22780# Office of the Deputy Under Secretary of Defense for Research and Development (Research and Advanced Technology), Washington, D.C.
THE DEPARTMENT OF DEFENSE SUPERCONDUCTIVITY RESEARCH AND DEVELOPMENT (DSRD) OPTIONS. A STUDY OF POSSIBLE DIRECTIONS FOR EXPLOITATION OF SUPERCONDUCTIVITY IN MILITARY APPLICATIONS
Jul. 1987 126 p
(AD-A189747) Avail: NTIS HC A07/MF A01 CSCL 20C

Although the technology associated with traditional low temperature superconductivity (LTS) materials is relatively mature, the scientific foundations for the newly discovered high temperature superconducting (HTS) materials are in a more rudimentary state, and the engineering parameters required for definition of possible realms of exploration are largely unknown. Within the limitations imposed by these unknown factors, this document sets forth a menu for a five-year Department of Defense Superconductivity Research and Development (DSRD) program. The goal of this program is to assure that the potential of HTS is realized at the earliest opportunity for military applications, including both small-and large scale applications. GRA

N88-22781# North Carolina Univ., Chapel Hill. Dept. of Geology.
AN INVESTIGATION OF THE CRYSTALCHEMISTRY AND THERMOCHEMISTRY OF SELECTED MINERAL SYSTEMS Final Report, 1 Feb. 1983 - 31 Oct. 1987
Robert R. Reeber 29 Oct. 1987 10 p
(Grant DAAG29-79-D-1002)
(AD-A189758; ARO-20010.5-MS) Avail: NTIS HC A02/MF A01 CSCL 07B

A computer-controlled travelling Laue X-ray camera and small rapid response furnace system was designed, constructed and operated for the study of phase transitions in solid state systems. The camera is capable of continuously monitoring crystallographic phase changes occurring in small single crystal samples over temperature range from 100 to 1000 K. Extensive studies of complex structural changes in natural crystals to tridymite were completed. Some preliminary experiments were also made with single crystals of CdS and CdTe. All materials were characterized with transmission electron microscopy. Defect and strain distributions in CdS and CdTe crystal were also examined with synchrotron white beam topography. This report gives a brief overview of results accomplished. It includes a list of papers and abstracts published during the course of the research. GRA

N88-22782# Colorado State Univ., Fort Collins. Dept. of Electrical Engineering.
GAS SOURCE MBE (MOLECULAR BEAM EPITAXY) Final Report, 1 Oct. 1986 - 10 Sep. 1987
Gary Y. Robinson Nov. 1987 12 p
(Grant AF-AFOSR-0028-87)
(AD-A189763; AFOSR-87-1742TR) Avail: NTIS HC A03/MF A01 CSCL 20L

This report describes the equipment acquired and the research performed under the DOD University Research Instrumentation Program grant for Gas Source MBE at Colorado State University. The objective of the research supported by the grant is to grow epitaxial 3-5 semiconductor films using gaseous materials for molecular beam epitaxy (MBE). The grant provided the critical equipment items needed to customize the existing commercial MBE system and allow growth of heteroepitaxial structures that can not be fabricated by other techniques. The resulting gas source MBE materials could provide the optoelectronic device technology required for the high data rate signal processing of the vast quantities of input data expected in future DOD space and ground-based sensing systems. GRA

N88-22783# Princeton Univ., N. J. Dept. of Physics.
EXPERIMENTAL STUDIES ON ELECTRONIC PROPERTIES OF HgTe/CdTe AND Hg SUB 1-z Cd SUB x Te/CdTe HETEROSTRUCTURES AND SUPERLATTICES Final Report, 1 Mar. 1984 - 30 Sep. 1987
Nai-Phuan Ong 10 Dec. 1987 3 p
(Contract DAAL03-86-K-0052; Grant DAAG29-84-K-0032)
(AD-A189826; ARO-23975.3-PH; ARO-21015.4-PH) Avail: NTIS HC A02/MF A01 CSCL 07B

The electronic properties of superlattices made of alternating layers of HgTe and CdTe are studied at low temperatures T (down to 0.5 K) and in high dc magnetic fields (up to 29 T.) There are two motivations for performing these studies: (1) whereas superlattices made from 3 to 5 materials such as Aluminum Gallium Arsenides and Indium Phosphide have been fabricated and shown to support very high mobility electrons in two-dimensional wells, similar studies had not been performed on the 2 to 6 compounds. In 1982, Dr. Jeff Cheung at Rockwell, Thousand Oaks, succeeded in fabricating superlattices of HgTe and CdTe using a novel laser flash evaporation technique. Initial studies at University of Southern California showed that prospects looked good for realizing excellent 2-D electronic devices despite the poor mobility of the early samples, (2) on the practical side, far-infrared (FIR) detectors made from the bulk alloy Hg(1-X)Cd(X)Te suffer from inhomogeneity problems which lead to spatial variations of the gap, especially in the 10-micrometer range. Following suggestions that the gap superlattice HgTe-CdTe can be tuned by changing the periodicity, the FIR capabilities in the Rockwell samples. GRA

N88-22784# Air Force Inst. of Tech., Wright-Patterson AFB, Ohio. School of Engineering.
A MODEL FOR NITROGEN ATOM RECOMBINATION ON A SILICON DIOXIDE SURFACE M.S. Thesis
Michael Newman Dec. 1987 192 p
(AD-A189843; AFIT/GE/ENG/87D-50) Avail: NTIS HC A09/MF A01 CSCL 07B

The heterogeneous recombination of particles (molecular and atomic) upon solid surfaces (metallic as well as nonmetallic) is, in theory, straightforward and understandable. The need to accurately characterize a surface, coupled with a better understanding of the heterogeneous recombination process are especially important with regard to Earth orbiting reentry vehicles such as the Space Shuttle Orbiter, the planned Aeroassisted Orbital Transfer Vehicle (AOTV), and the planned Space Plane. In fact, surface recombination rates are now known to play a major role in heating the surfaces of the Space Shuttle Orbiter. According to Scott, however, the initial design of the space shuttle completely ignored the effects of a catalytic surface, not to mention the resulting structure changes of the surface with temperature. GRA

N88-22785# Colorado State Univ., Fort Collins.
BEAM ASSISTED FABRICATION OF 3-5/Si MONOLITHIC DEVICES Annual Report, 9 Nov. 1986 - 9 Oct. 1987
Gary Y. Robinson 10 Sep. 1987 35 p
(Contract F49620-86-K-0021)
(AD-A189979) Avail: NTIS HC A03/MF A01 CSCL 09A

The objective of this research project is to explore two new methods for deposition of 3-5 semiconducting films on silicon substrates. Using gas-source molecular beam epitaxy (MBE) and photon-beam and electron-beam assisted metal-organic chemical vapor deposition (MOCVD), Gallium Arsenide and other 3-5 films with abrupt heterojunctions are being formed epitaxially on Si, and by means of optical and electrical characterization the suitability

of the resulting 3-5/Si structures are being examined for use in monolithic devices. GRA

N88-22786# Stanford Univ., Calif. Dept. of Materials Science and Engineering.
FUNDAMENTAL STUDIES OF THE MECHANICAL BEHAVIOR OF MICROELECTRONIC THIN FILM MATERIALS Annual Report, 1 Nov. 1986 - 31 Oct. 1987
William D. Nix Dec. 1987 37 p
(Grant AF-AFOSR-0051-86)
(AD-A190038; AFOSR-88-0161TR) Avail: NTIS HC A03/MF A01 CSCL 20L

A fundamental program of research on the mechanical properties of microelectronic thin film materials is underway at Stanford University. The work is being supported under AFOSR Grant No. 86-0051. In this interim Scientific Report, some of the progress made during the second year of the program is reviewed. We have made rapid progress since starting this development of new experimental techniques for measuring mechanical properties of thin films. That work led to several publications and to an equal number of invited oral presentations, both of which are listed at the end of this report. Now much of our work involves the use of these techniques to study mechanical properties of thin film materials of interest in microelectronics. GRA

N88-22787# California Univ., Los Angeles.
FUNDAMENTAL PROPERTIES AND DEVICES APPLICATIONS OF Ge(x)Si(1-x)/Si SUPERLATTICES Technical Report, 1 Aug. 1985 - 31 Jul. 1987
Kang L. Wang 1987 49 p
(Contract N00014-85-K-0555)
(AD-A190129) Avail: NTIS HC A03/MF A01 CSCL 20L

This progress report include the following: (1) growth and characterization of GexSi(1-x)/Si epitaxial films and superlattices, (2) study of power loss by two dimensional holes in coherently strained GexSi(1-x)/Si heterostructures, (3) theoretical prediction of resonances of intraband absorption, and (4) study of B2O3 as a low temperature p-type dopant. Initial stage of growth of GexSi(1-x)/Si films were studied using reflection high energy electron diffraction (RHEED) and the superlattice structures were characterized using TEM. In the study of magnetotransport of holes in GexSi(1-x)/Si SLS's, it was found that the power loss data can be well understood by taking into account the effects from the acoustic mode phonons by both the deformation potential and the piezoelectric coupling. The resonance nature of intraband absorption can be used for sensitive and tunable IR detector applications. The possibility of using B2O3 as an effective p-type doping source is demonstrated for providing abrupt doping profiles needed for GexSi(1-x)/Si superlattices. GRA

N88-22788# California Univ., San Diego.
RESEARCH ON MATERIALS AND COMPONENTS FOR OPTO-ELECTRONIC SIGNAL PROCESSING AND COMPUTING Interim Report, 1 Dec. 1986 - 30 Nov. 1987
William S. Chang, Shigern Nikki, Timothy VanEck, H. H. Wieder, and Andrew Williams 28 Sep. 1987 28 p
(Grant AF-AFOSR-0389-84)
(AD-A190130; AFOSR-87-1880TR) Avail: NTIS HC A03/MF A01 CSCL 19E

Electro-absorption and electro-refraction properties of strained multiple quantum-well structures (QW) in In(x)Ga(1-x)As/GaAs were investigated for spatial modulation applications. A new technique that will allow us to obtain large number of quantum well periods and large depth of modulation has been developed. Optical-optical interaction of a modulator-detector diode pair made form such QW structure had been demonstrated. Optimization of QW structure design has been investigated. GRA

N88-22789# Carnegie-Mellon Univ., Pittsburgh, Pa. Dept. of Electrical and Computer Engineerin G.
HIGH DENSITY ION IMPLANTED CONTIGUOUS DISK BUBBLE TECHNOLOGY Annual Scientific Report No. 1, 30 Sep. 1986 - 29 Sep. 1987
M. H. Kryder, D. W. Greve, A. Guzman, S. C. Jo, and M. Ramesh
31 Oct. 1987 267 p
(Grant AF-AFOSR-0341-84)
(AD-A190169; AFOSR-87-2044TR) Avail: NTIS HC A12/MF A01 CSCL 09A

During the past year we have advanced the state-of-tho-art in several areas of magnetic bubble technology. The main thrust of our research has been to advance ion implanted contiguous disk devices because these devices offer order of magnitude higher bit density than presently manufactured bubble devices. We succeeded in several regards. Noteworthy accomplishments include demonstration of bubble propagation in devices having 4 sq micron bit cells and exhibiting operating margins equal to those of today's manufactured devices. These devices were demonstrated to operate from 0 C to 120 C, the limits of our present testing capabilities. A major factor in this success was our development of new epitaxial garnet materials which exhibited isotropic magnetostrictive properties -- a feature previously not obtained. In addition to the work on bubble propagation we made significant progress on demonstrating a fully operational contiguous disk chip, complete with bubble generators, transfer gates and stretcher/detectors. All components have now been demonstrated to operate with good overlapping margins and a complete chip has been designed and fabricated. We are in the process of testing it. GRA

N88-22790# Maryland Univ., College Park. Dept. of Electrical Engineering.
REPETITIVE OPENING SWITCHES USING OPTICALLY ACTIVATED SEMICONDUCTORS Final Technical Report, 1 Sep. 1984 - 31 Aug. 1987
Chi H. Lee and Moon-Jhong Rhee 1 Oct. 1987 58 p
(Grant AF AFOSR-0359-84)
(AD-A190196; AFOSR-87-1995TR) Avail: NTIS HC A04/MF A01 CSCL 09E

This is the final technical report for a research program to study repetitive opening switches using optically activated semiconductors. This program was funded by the Air Force Office of Scientific Research for the period September 1, 1984 to August 31, 1987 under Grant No. AFOSR-84-0359. The goal of this research was to study opening switch characteristics of various semiconductors in conjunction with inductive energy storage systems. GRA

N88-22791# Wisconsin Univ., Madison. Dept. of Physics.
THIN SUPERCONDUCTING FILM CHARACTERIZATION BY SURFACE ACOUSTIC WAVES Annual Progress Report, 30 Sep. 1986 - 30 Sep. 1987
Moises Levy 30 Oct. 1987 15 p
(Grant AF-AFOSR-0350-84)
(AD-A190417; AFOSR-87-1897TR) Avail: NTIS HC A03/MF A01 CSCL 20M

A dilution refrigerator was installed, tested and modified. Several cryogenic probes were fabricated to measure resistivity, ac susceptibility and ultrasonic attenuation in high T superconductors. Ultrasonic attenuation measurements were performed on single crystals of UPt3 and URu2Si2. A maximum in attenuation was found below the superconducting transition temperature TC of URu2Si2. A magnetic field decreased this maximum. The temperature of the attenuation in the normal and superconducting states below Tc was measured in UPt3. The ratio of the attenuation follows a power law dependence indicative of an anisotropic superconducting energy gap. A peak in attenuation was found in the mixed state of UPt3, which may be associated with a phase transition of the flux line lattice. GRA

N88-22792# Air Force Inst. of Tech., Wright-Patterson AFB, Ohio. School of Engineering.
MODELING THE EFFECTS OF HEAVY CHARGED PARTICLES ON MOSFETS (METAL-OXIDE-SEMICONDUCTOR FIELD EFFECT TRANSISTORS) M.S. Thesis
Kevin M. Kattner Mar. 1988 49 p

(AD-A190575; AFIT/GEP/GNE/88M-4) Avail: NTIS HC A03/MF A01 CSCL 09A

A simple model to characterize the effects of heavy charged particles on metal-oxide semiconductor field-effect transistors (MOSFET) is presented. The model is applied to experimental results provided by the Air Force Weapons Laboratory, and an attempt made to simulate saturation phenomena observed in the threshold voltage change. The model assumes all trapped holes are within a few nanometers of the oxide-semiconductor interface, and takes into account the resultant counter electric field, and its effect on the fraction escaping recombination. An equation relating threshold voltage change as a function of dose is derived and used, but does not duplicate the saturation effect. This is because the charge trapped near the interface reduces the internal oxide electric field very little. However, similarities in p-channel and n-channel MOSFET damage sensitivities indicate considerable bulk charge trapping. This would modulate the internal electric field considerably. To determine whether this accounts for saturation will necessitate refinement of the model, taking hole transport and bulk trapping into account. GRA

N88-22793# North Carolina Univ., Chapel Hill. Dept. of Chemistry.

MAGNETIC ANOMALIES IN THE RARE EARTH OXIDE SUPERCONDUCTORS GdBa2Cu3O(7-x) AND YbBa2Cu3O(7-x)

William E. Hatfield, Brian R. Rohrs, Martin L. Kirk, Jeffrey H. Helms, and Hyekyeong Ro 9 Jan. 1988 12 p

(Contract N00014-76-C-0816)

(AD-A190713; TR-3) Avail: NTIS HC A03/MF A01 CSCL 20C

The magnetic properties of GdBa2Cu3O(7-x) and YBa2Cu3O(7-x) have been studied in low applied magnetic field by using pellet samples. The magnetic behavior may be explained by the occurrence of a spin-glass state due to a granular superconductor. The model assumes superconducting grains which are small compared to the penetration depth, and these are coupled into closed loops. Cooling in zero-field, followed by the application of a field at a fixed temperature produces a metastable state resulting in frustration and spin-glass behavior. GRA

N88-22794# Massachusetts Inst. of Tech., Cambridge. Research Lab. of Electronics.

INTERFACE FORMATION AND PRECURSORY DYNAMICS Annual Report, 15 Nov. 1986 - 15 Nov. 1987

John D. Poannopoulos 22 Dec. 1987 12 p

(Grant AF-AFOSR-0098-87)

(AD-A190741; AFOSR-88-0056TR) Avail: NTIS HC A03/MF A01 CSCL 09A

A completely ab initio investigation was made of the structure of a grain boundary in geranium. This was accomplished using a quantum molecular dynamics simulated annealing method. This method allows global minimization of the boundary energy to be achieved with respect to all electronic and ionic structural degrees of freedom using ab initio local pseudopotentials. The method has significant advantages in computational speed and storage requirements over traditional total energy techniques, especially when systems of low symmetry are involved or in which large relaxations take place. GRA

N88-22795# International Business Machines Corp., Yorktown Heights, N. Y. Research Center.

THE STRUCTURE OF THE BORON-HYDROGEN COMPLEX IN SILICON

A. D. Marwick, G. S. Oehrlein, J. H. Barrett, and N. M. Johnson 1987 7 p Presented at the Symposium on Defects in Electronic Materials, Boston, Mass., 30 Nov. 1987 Prepared in cooperation with ORNL, Tenn. and Xerox Palo Alto Research Center, Calif.

(Contract DE-AC05-84OR-21400)

(DE88-005433; CONF-8711157-1) Avail: NTIS HC A02/MF A01

Channeling and lattice location has been used to investigate the structure of the boron-hydrogen complex in crystalline silicon. The positions of both the boron and hydrogen atoms have been determined. Results are compared with Monte-Carlo simulations. The boron atom in the B-H pair is found to be displaced from a substitutional site by 0.28 + or - 0.03 A, while the hydrogen atom is predominantly at a bond-center site, with a small proportion in a back-bonded position. DOE

N88-22796# Argonne National Lab., Ill.

STATUS OF RF SUPERCONDUCTIVITY AT ARGONNE NATIONAL LABORATORY

P. M. Markovich, K. W. Shepard, and G. P. Zinkann 1987 13 p Presented at the 3rd Workshop on RF Superconductivity, Argonnne, Ill., 14 Sep. 1987

(Contract W-31-109-eng-38)

(DE88-005913; CONF-870955-3) Avail: NTIS HC A03/MF A01

This paper reports the status of hardware development for the linac portion of the Argonne tandem-linac accelerator system (ATLAS). The ATLAS superconducting linac consists of an independent-phased array of 45 superconducting niobium resonators of the split-ring type. The linac has been operating in its present form since 1985, on a 24-hours per day, 5 days per week schedule. An upgrade of the ATLAS system is currently under construction, the positive-ion injector (PII). The PII system will consist of an ECR positive-ion source mounted on a high-voltage platform injecting a very-low-velocity superconducting linac. The completed system will provide for the acceleration of beams of mass up to uranium, and will replace the tandem electrostatic accelerator as the injector for ATLAS. The status of resonator development for the superconducting linac is reported in this paper. Accelerating gradients in the existing ATLAS linac are currently limited by excessive heating and RF loss in the fast-tuning system associated with each superconducting resonator. Development of an upgraded fast tuning system is also reported. DOE

N88-22797# Northeastern Univ., Boston, Mass. Dept. of Physics.

ANNIHILATION MOMENTUM DENSITY OF POSITRONS TRAPPED AT VACANCY-TYPE DEFECTS IN METALS AND ALLOYS

A. Bansil, R. Prasad, and R. Benedek Jan. 1988 7 p Presented at the NATO Advanced Study Institute on Alloy Phase Stability, Crete, Greece, 14 Jun. 1987 Prepared in cooperation with Indian Inst. of Tech., Kanpur and Argonne National Lab., Ill.

(Contract W-31-109-eng-38)

(DE88-005936; CONF-8706103-7) Avail: NTIS HC A02

Positron annihilation, especially the angular correlation of annihilation radiation, is a powerful tool for investigating the electronic spectra of ordered as well as defected materials. The tendency of positrons to trap at vacancy-type defects should enable this technique to study the local environment of such defects. However, we need to develop a theoretical basis for calculating the two-photon annihilation momentum density rho/sub 2gamma/(p-vector). We have recently formulated and implemented a theory of rho/sub 2gamma/(p-vector) from vacancy-type defects in metals and alloys. This article gives an outline of our approach together with a few of our results. Section 2 summarizes the basic equations for evaluating rho/sub 2gamma/(p-vector). Our Green's function-based approach is nonperturbative and employs a realistic (one-particle) muffin-tin Hamiltonian for treating electrons and positrons. Section 3 presents and discusses rho/sub 2gamma/(p-vector) results for a mono-vacancy in Cu. We have neglected the effects of electron-positron correlations and of lattice distortion around the vacancy. Section 4 comments briefly on the question of treating defects such as divacancies and metal-impurity complexes in metals and alloys. Finally, in Section 5, we remark on the form of rho/sub 2gamma/(p-vector) for a mono-vacancy in jellium. DOE

N88-22798# Argonne National Lab., Ill.

HIGH-T(SUB c) SUPERCONDUCTING WIRE FABRICATION AND TESTING

D. W. Capone, II, J. T. Dusek, and K. C. Goretta Oct. 1987 12 p Presented at the 36th International Wire and Cable

Symposium, Arlington, Va., 17 Nov. 1987
(Contract W-31-109-eng-38)
(DE88-005989; CONF-871167-2) Avail: NTIS HC A03/MF A01

This paper describes the fabrication of ceramic fibers of the high-T sub c superconductor YBa2Cu3O7 and the testing procedures used to characterize these materials. The major factors important to the fabrication of these fibers are described in general terms including some of the issues relating to the strength and flexibility of the wires. Measurements of the three parameters which most easily characterize the superconducting properties of the fibers, T sub c, H sub c2, and J sub c, are described, particularly the critical current density, J sub c. DOE

N88-22799# Northwestern Univ., Evanston, Ill.
PREPARATION OF LARGE AREA NbN/AlN/NbN JOSEPHSON JUNCTIONS
S. N. Song, B. Y. Jin, H. Q. Yang, J. B. Ketterson, and I. K. Schuller Dec. 1987 3 p Presented at the 18th Conference on Low Temperature Physics, Kyoto, Japan, 20 Aug. 1987 Prepared in cooperation with Argonne National Lab., Ill.
(Contract W-31-109-eng-38)
(DE88-006074; CONF-870873-26) Avail: NTIS HC A02/MF A01

AlN has been used as a barrier material in large Josephson junctions. The chemical and structural compatibility of AlN with NbN make it possible to fabricate NbN/AlN/NbN junctions by sequential reactive sputtering in a common Ar and N2 atmosphere. In a junction with an area of about 1.0 x 1.0 sq mm, having a transition temperature of 14.5 K, the measured 1-5 and first derivative curves yield a sum gap value of about 3.0 MeV. DOE

N88-22800# Lawrence Livermore National Lab., Calif.
DISPERSION MEASUREMENTS OF MICROCRYSTALS IN THE NEAR ULTRAVIOLET AND INFRARED
L. E. Davis 10 Dec. 1987 19 p Presented at the 31st SPIE Annual International Technical Symposium on Optical and Optoelectronic Applied Science and Engineering, San Diego, Calif., 16 Aug. 1987
(Contract W-7405-eng-48)
(DE88-006234; UCRL-96102; CONF-8708110-32) Avail: NTIS HC A03/MF A01

A modified spindle stage refractometer is described for measuring the refractive indices of transparent materials. Determinations are made on small, single crystal fragments 50 microns in size and yield accurate data on the principal refractive indices over the spectra region 0.38 to 1.10 microns . The technique has been applied to study new harmonic generating crystals and the results used to predict phasematching properties and noncritical wavelengths. The spindle stage refractometer is especially useful for screening candidate materials, because accurate linear optical properties may be determined without requiring extensive crystal growth of each compound. DOE

N88-22801# California Univ., Berkeley. Lawrence Berkeley Lab.
FERMI LEVEL STABILIZATION IN SEMICONDUCTORS: IMPLICATIONS FOR IMPLANT ACTIVATION EFFICIENCY
W. Walukiewicz Nov. 1987 5 p Presented at the Fall Meeting of the Materials Research Society, Boston, Mass., 30 Nov. 1987
(Contract DE-AC03-76SF-00098)
(DE88-006332; LBL-23600; CONF-871124-89) Avail: NTIS HC A02/MF A01

We propose the existence of a Fermi level stabilization energy in 3-5 semiconductors which provides a reference level for the electronic part of defect annihilation energies. It is shown that the position of the stabilization energy with respect to the band edges determines the maximum free carrier concentration which can be obtained through doping. The proposed model accounts for previously unexplained trends in implant activation efficiency in 3-5 semiconductors. DOE

N88-22802# Du Pont de Nemours (E. I.) and Co., Wilmington, Del. Central Research and Development Dept.
HIGH TEMPERATURE SUPERCONDUCTORS IN THE La(SUB 1+x)Ba(SUB 2-x)Cu O(SUB y SYSTEM
E. M. McCarron, III, C. C. Torardi, J. P. Attfield, K. J. Morrissey, A. W. Sleight, D. E. Cox, R. K. Bordia, W. E. Farneth, R. B. Flippen, and M. A. Subramanian 1987 7 p Presented at the Fall Meeting of the Materials Research Society, Boston, Mass., 30 Nov. 1987 Prepared in cooperation with Brookhaven National Lab., Upton, N.Y. and Virginia Univ., Charlottesville
(Contract DE-AC02-76CH-00016)
(DE88-006367; BNL-40757; CONF-871124-85) Avail: NTIS HC A02/MF A01

In the La Ba Cu oxide system the La ions can substitute on the Ba sites due to a close match in the ionic radius of the two (as opposed to the Y Ba Cu oxide system). Thus it is possible to make a solid solution La sub 1+x Ba sub 2-x Cu2O sub y where O approx. x less than or equal to 0.5 and y approx. 7. Several compounds of this family have been made, and their synthesis and crystal structure are described. LaBa2Cu3O sub y can be made under high pressure O2. This phase is orthorhombic: as the La content increases. La substitutes on the Ba sites until for La sub 1.5 Ba sub 1.5 Cu2O sub 7.33, 1/4 of the Ba are replaced by La (disordered). This substitution changes the crystal symmetry from orthorhombic to tetragonal. The transition temperature and the critical current for various members of this series are presented. In particular, it will be shown that the midpoint in this series, La sub 1.25 Ba sub 1.75 Cu2O sub y. Is a tetragonal bulk superconductor. Effect of various heat treatments on the superconducting properties is also presented. DOE

N88-22803# Los Alamos National Lab., N. Mex.
REMARKS ON SOLID STATE AMORPHIZING TRANSFORMATIONS
R. B. Schwarz and W. L. Johnson 1987 14 p Presented at the Conference on Solid State Amorphizing Transformation, Los Alamos, N. Mex., 10 Aug. 1987 Prepared in cooperation with California Inst. of Tech., Pasadena
(Contract W-7405-eng-36)
(DE88-006452; LA-UR-88-588; CONF-8708104-7) Avail: NTIS HC A03/MF A01

Amorphous solids can now be produced through a variety of laboratory synthesis techniques as well as through many naturally occurring processes. In general, we can classify the methods of synthesis of amorphous solids as follows: (1) rapid solidification of melts or vapors; (2) atomic disordering of crystalline lattices; (3) solid state reactions between pure elements; (4) solid-state transformations from metastable crystalline states; and (5) deposition from electrolytes. We give a short summary of the historical development of methods (1)-(4) (method (5) is clearly outside the focus of this conference) and we discuss the basic physical principles behind the methods. DOE

N88-22804# Instituto de Pesquisas Espaciais, Sao Jose dos Campos (Brazil).
EQUILIBRIUM STABILITY OF STRAINED EPITAXIAL LAYERS ON A RIGID SUBSTRATE
Enzo Granato, J. M. Kosterlitz, and S. C. Ying (Brown Univ., Providence, R. I.) Jul. 1987 8 p Presented at the 3rd Escola Brasileira de Fisica de Semicondutores, Campinas, Brazil, 1987 Submitted for publication
(INPE-4254-PRE/1127) Avail: NTIS HC A02/MF A01

A simple theory of the equilibrium stability of a strained epitaxial layer on a rigid substrate is presented. The Frank-van der Merwe model of a single layer is generalized and N layers of adsorbate on a substrate considered. Continuum elasticity theory is used to describe each layer, but the coupling between layers is treated in a discrete fashion. This method interpolates between a few layers and the thick film limit of standard dislocation theory, and in this limit the standard results are obtained. In addition, a variational approach is developed which agrees well with exact calculations. The advantage of this method over previous ones is that it permits

the performance of the stability analyses of arbitrary supperlattice configurations. Author

N88-22805*# National Aeronautics and Space Administration. Lewis Research Center, Cleveland, Ohio.
SYNTHESIS AND CHARACTERIZATION OF HIGH-T(SUB c) SCREEN-PRINTED Y-Ba-Cu-O FILMS ON ALUMINA
Narottam P. Bansal, Rainee N. Simons, and D. E. Farrell (Case Western Reserve Univ., Cleveland, Ohio.) [1988] 11 p Presented at the 90th Annual Meeting of the American Ceramic Society, Cincinnati, Ohio, 1-5 May 1988
(NASA-TM-100860; E-4069; NAS 1.15:100860) Avail: NTIS HC A03/MF A01 CSCL 20L

Thick films of YBa2Cu3O(sub 7-x) have been deposited on highly polished alumina substrates by the screen printing technique. To optimize the post-printing heat treatment, the films were baked at various temperatures for different lengths of time and oxygen-annealed at a lower temperature. The resulting films were characterized by electrical resistivity measurements, x-ray diffraction, and optical and scanning electron microscopy. Properties of the films were found to be highly sensitive to the post-printing thermal treatment. Films baked for 15 min at 1000 C in oxygen were hard, adherent, near single phase, and superconducting with T(sub c)(onset) approx 96 K, T(sub c)(zero) approx 66 K and Delta T sub c (10 to 90 percent) approx 10 K. Author

N88-22213# Joint Publications Research Service, Arlington, Va.
SINGLE CRYSTAL GROWTH BY LASER CVD
Shigeyuki Hayashi *In its* JPRS Report: Science and Technology. Japan 11 Mar. 1988 p 25-36 Transl. into ENGLISH from Kino Zairyo (Tokyo, Japan), v. 7, Aug. 1987 p 25-32 (For primary document see N88-22210 15-31)
Avail: NTIS HC A05/MF A01

77 THERMODYNAMICS AND STATISTICAL PHYSICS

Includes quantum mechanics; theoretical physics; and Bose and Fermi statistics.

For related information see also *25 Inorganic and Physical Chemistry* and *34 Fluid Mechanics and Heat Transfer.*

N88-22806# Joint Inst. for Nuclear Research, Dubna (USSR).
SINGULAR LAGRANGIANS. CLASSICAL DYNAMICS AND QUANTIZATION. LECTURES FOR YOUNG SCIENTISTS
V. V. Nesterenko and A. M. Chervyakov 1986 101 p In RUSSIAN; ENGLISH summary
(TI88-701158; JINR-R-2-86-323) Avail: NTIS (US Sales Only) HC A06/MF A01

The lectures are devoted to the classical and quantum dynamics of the systems described by singular (or degenerate) Lagrangians. The complete set of the Hamiltonian constraints is constructed in the framework of the Lagrangian formalism. The equations of motion in the phase space are derived by taking into account all the constraints in the theory. It is proved that the dynamic on the physical submanifold of the phase space has the Hamiltonian form. On lectures the second Noether theorem is widely used. On its basis the properties of the Poisson brackets of the primary constraints are investigated and the invariance of the Lagrangian constraints during evolution is proved. The setting of the Cauchy problem in the theories with singular Lagrangians is discussed. The quantization of the systems with constraints is carried out by the functional integration in the phase space. There is considered the most general case of the first class and the second class constraints with an explicit time dependence. The gauge conditions may be noninvoluntary and time dependent. The material is illustrated by some examples (relativistic point particle, relativistic string, electromagnetic field, and Yang-Mills fields). DOE

N88-22807# Joint Inst. for Nuclear Research, Dubna (USSR). Lab. of Theoretical Physics.
TO THE FIELD THEORY WITH A FUNDAMENTAL MASS
R. M. Ibadov and V. G. Kadyshevskij 1986 19 p In RUSSIAN; ENGLISH summary
(TI88-701159; JINR-R-2-86-830) Avail: NTIS (US Sales Only) HC A03/MF A01

This paper is a continuation of the investigations along the lines of constructing a consistent field theory with fundamental mass M - a hypothetical universal scale in the ultrahigh energy region. Earlier, in the developed approach the key role was played by the de Sitter momentum space of radius M. In this paper a quantum version of this idea is worked out: p-space is assumed to be a de Sitter one like before; however, the four momentum is treated as a quantum mechanical operator. DOE

N88-22808# Hiroshima Univ., Takehara (Japan). Research Inst. for Theoretical Physics.
TEN DIMENSIONAL N = 1 SUPERGRAVITY COUPLED TO SUPERSYMMETRIC YANG-MILLS FIELDS IN SUPERSPACE
Masaru Takao Aug. 1986 35 p
(DE87-703033; RRK-86-33) Avail: NTIS (US Sales Only) HC A03/MF A01

We present the superspace approach to the ten dimensional supergravity theory coupled to supersymmetric Yang-Mills fields proposed by Chapline and Manton. By postulating maximal constraint equations on the system, we derive an on-shell supergravity as a consequence of the Biachi identities. DOE

N88-22809# Fermi National Accelerator Lab., Batavia, Ill.
EINSTEIN METRICS AND BRANS-DICKE SUPERFIELDS
S. Marques Jan. 1988 22 p
(Contract DE-AC02-76CH-03000)
(DE88-006992; FNAL/Pub-88/18-A) Avail: NTIS HC A03/MF A01

It is obtained here a space conformal to the Einstein space-time, making the transition from an internal bosonic space, constructed with the Majorana constant spinors in the Majorana representation, to a bosonic superspace, through the use of Einstein vierbeins. These spaces are related to a Grassmann space constructed with the Majorana spinors referred to above, where the metric is a function of internal bosonic coordinates. The conformal function is a scale factor in the zone of gravitational radiation. A conformal function dependent on space-time coordinates can be constructed in that region when we introduce Majorana spinors which are functions of those coordinates. With this we obtain a scalar field of Brans-Dicke type. DOE

N88-22810# Hiroshima Univ., Takehara (Japan). Research Inst. for Theoretical Physics.
PATH INTEGRAL, BRS SYMMETRY, AND STRING AND MEMBRANE THEORIES
Kazuo Fujikawa Sep. 1987 29 p
(DE88-752300; RRK-87-20) Avail: NTIS (US Sales Only) HC A03/MF A01

A unified treatment of quantum symmetries is attempted on the basis of the BRS symmetry appearing in the path integral. We first briefly review a systematic derivation of anomalous commutators and the fact that all the known non-trivial anomalous commutators are related to the anomaly. We next present a refined treatment of the reparameterization invariant path integral measure, which is then illustrated for the two-dimensional string theory. The critical dimension is shown to arise from the explicit or implicit gauge fixing of the Weyl freedom. We finally present a Faddeev-Popov-BRS treatment of the bosonic membrane. The narrow limit of the quantized closed membrane is shown to reproduce certain massless states of the closed string. DOE

N88-22811# Texas Univ., Austin. Dept. of Physics.
INVOLUTION-DEPENDENT CONSTANTS AND THE CANCELLATION OF DIVERGENCES IN THE 1-LOOP OPEN STRING AMPLITUDE
G. Nagao Dec. 1987 29 p

(Contract DE-FG05-85ER-40200)
(DE88-006537; DOE/ER-40200/126) Avail: NTIS HC A03/MF A01

We recalculate the bosonic 1-loop open string scattering amplitude using the results of the bosonic 1-loop closed string amplitude. The results show explicitly how the cancellation of divergences depends upon of a set of involution-dependent constants which relate the torus to the cylinder and Moebius strip. Such a set of involution-dependent constants exists at each loop level and thus provides a means with which to study the cancellation of divergences and the connection between the world-sheet and internal symmetries. DOE

N88-22812# Fermi National Accelerator Lab., Batavia, Ill. Dept. of Physics.
FINITE WIDTH CORRECTIONS TO THE NAMBU ACTION FOR THE NIELSEN-OLESEN STRING
K. Maeda and N. Turok Nov. 1987 12 p Prepared in cooperation with Tokyo Univ., Japan
(Contract DE-AC02-76CH-03000)
(DE88-006996; FNAL/Pub-87/209-A; UTAP-66/87) Avail: NTIS HC A03/MF A01

The finite width correction terms to the Nambu action for Nielsen-Olesen strings are calculated. They consist of an extrinsic curvature squared or rigidity term and a new twist term. The extrinsic curvature term prevents cusps forming, rounding them off with a curvature radius of the order of the string width. DOE

N88-22813# Joint Inst. for Nuclear Research, Dubna (USSR). Lab. of Theoretical Physics.
QUANTIZATION OF AXIAL ELECTRODYNAMICS
Nguen Suan Han and V. N. Pervushin 1987 7 p Presented at the International Conference on High Energy Physics, Sweden, 1987 Submitted for publication
(TI88-701498; JINR-E-2-87-279) Avail: NTIS (US Sales Only) HC A02/MF A01

The possibility of constructing the Hamiltonian quantization for axial electrodynamics with anomalies in a four-dimensional space is studied. It is shown that in this theory the Jacobi identity for operators of the Hamiltonian, of a time component of the current and of the very field is broken. The usual quantum theory is consistent only for a zero magnetic field. DOE

N88-22814# Joint Inst. for Nuclear Research, Dubna (USSR). Lab. of Theoretical Physics.
SECONDARY GAUGE CONDITIONS IN FIELD THEORY
N. B. Skachkov and O. Yu. Shevchenko 1987 18 p Submitted for publication
(TI88-701499; JINR-E-2-87-368) Avail: NTIS (US Sales Only) HC A03/MF A01

It is shown that upon imposing one gauge condition on the gauge fields the latter turn out to obey the secondary gauge condition that in QED has the form of a Lorentz gauge condition. A new class of gauge-invariant and part-dependent non-Abelian fields is introduced. It is shown that all of the QED relations, i.e., the equations of motion, the formulae of the connection with the strength tensor, the secondary gauge condition etc., take place for these new fields with only the substitution of the ordinary derivatives by the Mandelstam ones. DOE

N88-22815# Joint Inst. for Nuclear Research, Dubna (USSR). Lab. of Theoretical Physics.
HAMILTONIAN FORMALISM IN THE MODEL OF THE RELATIVISTIC STRING WITH RIGIDITY
V. V. Nesterenko and Nguen Suan Han 1987 16 p In RUSSIAN; ENGLISH summary Submitted for publication
(TI88-701503; JINR-R-2-87-363) Avail: NTIS (US Sales Only) HC A03/MF A01

The model of the bosonic string with the Nambu - Goto action extended by the term, proportional to the external curvature of the world sheet is explored. The external curvature of the world-sheet is determined by the second order derivatives of the string coordinates. Thus, the modified Lagrangian is a singular Lagrangian of second order. The canonical variables for this theory are introduced, constraints are found and Hamiltonian formulation of the classical dynamics in this theory is constructed. The transition to the quantum theory is briefly discussed. DOE

N88-22816# Air Force Inst. of Tech., Wright-Patterson AFB, Ohio. School of Engineering.
FILM COOLING EFFECTIVENESS ON A FLAT PLATE IN HIGH FREE-STREAM TURBULENCE USING A SINGLE ROW OF 30 DEG SLANT-HOLE INJECTORS M.S. Thesis
Geoffrey W. Jumper Dec. 1987 91 p
(AD-A190500; AFIT/GAE/AA/87D-7) Avail: NTIS HC A05/MF A01 CSCL 20M

In the continuing search to understand the mechanisms influencing film cooling effectiveness, this thesis examines film cooling effectiveness on a flat plate in high free-stream turbulence using a single row of 30 slant-hole injectors. The primary area of focus is the area within 42 diameters down-stream of injection. Of interest are blowing rates for optimum film cooling effectiveness within 10 diameters down-stream of injection, and the decay of film cooling effectiveness down the plate. Free-stream velocities from 50 to 175 fps and free-stream turbulence intensities from 13.5 - 18.5 percent were examined. Changes in Reynolds number or free-stream turbulence had little effect on blowing rates for optimum film cooling effectiveness. In comparison with tests conducted in low free-stream turbulence, around 5%, higher free-stream turbulence causes a faster decay in film cooling effectiveness down the plate. GRA

N88-22817# State Univ. of New York, Buffalo. Dept. of Chemistry.
ANOMALIES IN THE HEAT-CAPACITY SIGNATURES OF SUBMONOLAYER ADSORBATES WITH ATTRACTIVE LATERAL INTERACTIONS
Young Sik Kim, Franco Battaglia, and Thomas F. George Feb. 1988 40 p Submitted for publication
(Contract N00014-86-K-0043)
(AD-A190736; UBuffalo/DC/88/TR-63) Avail: NTIS HC A03/MF A01 CSCL 20M

The analytic closed form of the heat-capacity signatures previously derived for the McQuistan-Hock (MQH) model of a lattice gas is applied to various adsorbed systems for which the lateral interaction varies from a few MeV to about 300 MeV. It is shown that whenever the adsorption system can be described by a two-dimensional gas on which the substrate effects are less important than the adatom-adatom interactions, the computed temperatures at which the heat-capacity signatures display their maximum are in excellent agreement with the experimental measurements. GRA

80 SOCIAL SCIENCES (GENERAL)

Includes educational matters.

No abstracts in this category.

81 ADMINISTRATION AND MANAGEMENT

Includes management planning and research.

N88-22818# Naval Postgraduate School, Monterey, Calif.
THE IMPACT OF INDEPENDENT RESEARCH AND DEVELOPMENT REGULATIONS ON COMPANIES NOT REQUIRED TO NEGOTIATE ADVANCED INDEPENDENT RESEARCH AND DEVELOPMENT AGREEMENTS M.S. Thesis
Craig C. Drew Dec. 1987 105 p
(AD-A190007) Avail: NTIS HC A06/MF A01 CSCL 05A

This study was to determine the impact of Independent Research and Development (IR&D) regulations on companies not required to negotiate advanced IR&D agreements. The study used data gathered from a survey questionnaire. The questionnaire addressed the contract characteristics of these companies and the impact of the regulations in the areas of (1) cost allowability and allocability, (2) the IR&D ceiling formula and (3) the nature of IR&D costs and their incurrance. The responses to the survey showed that approximately 30 percent of the companies doing business with the Government were not involved in any significant IR&D efforts. A significant number of companies engaged in IR&D efforts expressed some dissatisfaction with the IR&D regulations. In general, however most companies indicated the present system was acceptable. GRA

N88-22819# Instituto de Pesquisas Espaciais, Sao Jose dos Campos (Brazil).
A FAULT TOLERANT SUPERVISION SYSTEM M.S. Thesis [UM SISTEMA DE SUPERVISAO TOLERANTE A FALHAS]
Maria deFatimaMattielloFrancisco Nov. 1987 152 p In PORTUGUESE; ENGLISH summary
(INPE-4419-TDL/307) Avail: NTIS HC A08/MF A01

This paper proposes the incorporation of fault tolerant techniques in a process control oriented real time system to be applied in activities of supervision. These techniques should provide a higher availability of the Supervision System if simple fault of the hardware should occur. A basic architecture with dual redundancy is proposed. With regard to the software the backward-error-recovery technique is explored by establishing recovery points under the control of the supervision applicatives. Author

N88-22820# Instituto de Pesquisas Espaciais, Sao Jose dos Campos (Brazil).
INPE POSITION PAPER ON THE CCSDS STANDARDIZED METHOD OF LINK BUDGET COMPUTATION
Pedro Manuel MartinsdeBarros, Janio Kono, Jose Antonio Rodrigues, and Pawel Rozenfeld May 1988 7 p Presented at the 4th Meeting at DFVLR, 5-9 Nov. 1984
(INPE-4533-NTE/279) Avail: NTIS HC A02/MF A01

This work contains the guidelines suggested by Brazil's INPE (Instituto de Pesquisas Espaciais) for the standardization of satellite link budget in the CCSDS context. Author

82 DOCUMENTATION AND INFORMATION SCIENCE

Includes information management; information storage and retrieval technology; technical writing; graphic arts; and micrography.

For computer documentation see *61 Computer Programming and Software.*

N88-22821# Aeritalia S.p.A., Turin (Italy). Gruppo Sistemi Avionica ed Equipaggiamenti.
INFORMATION SYSTEMS FOR QUALITY. EXPERIENCE AT THE NERVIANO AERITALIA PLANT. AVIONIC SYSTEMS AND EQUIPMENT GROUP [SISTEMA INFORMATIVO PER LA QUALITA': ESPERIENZE PRESSO LO STABILIMENTO DI NERVIANO DI AERITALIA]
G. Casati and R. Colombini 1987 10 p In ITALIAN Presented at Giornata di Studio Indicatori Qualita', Bologna, Italy, 20 Oct. 1987
(ETN-88-92274) Avail: NTIS HC A02/MF A01

The quality information system used at an aerospace industrial plant is described. The goals and the philosophy of the quality organization are discussed. Quality control and quality safety are distinguished. The quality indicators are classified in three categories: product quality indicators, process quality indicators, and project quality indicators. The structure of the quality reports is discussed, including the description of the different rates and indexes used in the report. ESA

N88-22822# Defense Technical Information Center, Alexandria, Va. Office of Information Systems and Technology.
THE SCIENTIFIC AND TECHNICAL INFORMATION NETWORK (STINET). FOUNDATION FOR EVOLUTION
Gladys A. Cotter Sep. 1987 33 p
(AD-A189750; DTIC/TR-88/5) Avail: NTIS HC A03/MF A01 CSCL 05B

This paper describes advances which are being made in information retrieval systems to assist end-users and information specialists to overcome the critical barriers which make it difficult for them to exploit the power of these systems. Technology which is being applied to allow users to interact with information retrieval systems with greater ease and more successful results is identified. To illustrate this process, the efforts of the U.S. Defense Technical Information Center to develop and implement an integrated, functional, scientific and technical information network are described. This network was purposefully designed to incorporate both end-users and their information management intermediaries in a complementary manner making them resolute partners in the work and its rewards. The uses of technology modules - artificial intelligence, expert systems, gateways, user-friendly interfaces - to overcome user barriers are described. GRA

N88-22823# Aerospace Structures Information and Analysis Center, Wright-Patterson AFB, Ohio.
APPLICATION OF NEW TECHNOLOGIES TO DTIC DOCUMENT PROCESSING Interim Report, Jun. - Aug. 1987
Steven G. Harris, R. L. Citerley, and David F. Cahn Aug. 1987 42 p
(Contract F33615-84-C-3216)
(AD-A189778; ASIAC-887.1A) Avail: NTIS HC A03/MF A01 CSCL 05B

The use of integrated optical character recognition (OCR) and database management technology to improve DTIC document input processing is examined. Significant near-term improvements in efficiency can be realized using commercially available components fused into an integrated system. An approach and system architecture are defined that will permit a staged implementation of this technology within the framework of the current DTIC work flow. While the emphasis of this report is on reducing labor-intensive manual keystroking operations presently in use, the proposed system provides an open ended approach which will interface easily with both existing and future DTIC operations. An in-depth review of current DTIC document processing was used to guide the definition of the pilot system architecture developed in this study, and the results of that review are presented and discussed. GRA

N88-22824# Army Construction Engineering Research Lab., Champaign, Ill.
SOURCES OF DIGITAL SPATIAL DATA FOR GEOGRAPHIC INFORMATION SYSTEMS Final Technical Report
Mark O. Johnson and William D. Goran Dec. 1987 36 p
(AD-A189788; CERL-TR-N-88/01) Avail: NTIS HC A03/MF A01 CSCL 05A

Several computer programs are available to help Army installations plan military training activities while ensuring environmental quality and protecting natural resources. One such system, the Geographic Resources Analysis Support System (GRASS), requires digital spatial information for developing area-specific databases. This information previously was available only on a limited basis. Today, many more digital spatial data sources have come into existence. Use of such sources, compared with generating new data, can usually save an installation a large amount of time and money. In addition, these sources ensure minimum standards for accuracy and quality. This report identifies digital data sources to help installations evaluate the feasibility of implementing systems such as GRASS. Included is a list of the following characteristics for each source: format, scale/resolution, coverage, media, costs, and a textual description. GRA

N88-22825# Air Force Inst. of Tech., Wright-Patterson AFB, Ohio. School of Engineering.
A METHODOLGY, BASED ON ANALYTICAL MODELING, FOR THE DESIGN OF PARALLEL AND DISTRIBUTED ARCHITECTURES FOR RELATIONAL DATABASE QUERY PROCESSORS Ph.D. Thesis
Timothy G. Kearns Dec. 1987 351 p
(AD-A189844; AFIT/DS/ENG/87-1) Avail: NTIS HC A16/MF A01 CSCL 12F

The design of faster relational database query processors to improve the data retrieval capability of a database was the goal of this research. The emphasis was on evaluating the potential of parallel implementations to allow use of multiprocessing. First, the theoretical properties of applying relational operations to distributed data were considered to provide an underlying data distribution and parallel processing environment model. Next, analytical models were constructed to evaluate various implementations of the select, project, and join relational operations and the update operations of addition, deletion, and modification for a range of data structures and architectural configurations. To simulate the performance of the query processor for all cases, the individual operator models needed to be extended for complex queries consisting of several relational operations. A solution to modeling multi-step queries was the use of a general normal form to express a query. This normal form query tree used combined operations to express relational algebra equivalent queries in a standard form. This standard tree form was then used to construct analytical models for multi-step queries. These models provide the capability to simulate the potential of different forms of parallelism in solving complex queries. The analysis of results of the analytical models presents a logical design for a multiprocessor query processor. GRA

N88-22826# Syracuse Univ., N. Y.
NEW GENERATION KNOWLEDGE PROCESSING, VOLUME 1 Final Report, Dec. 1983 - Jan. 1987
J. A. Robinson and Kevin J. Greene Oct. 1987 77 p
(Contract F30602-84-K-0001)
(AD-A190165; RADC-TR-87-165-Vol-1) Avail: NTIS HC A05/MF A01 CSCL 12E

The main goal of this project was to design a high-level programming system SUPER (Syracuse University Parallel Expression Reducer) with two parts: a language which would combine the functional (as in LISP, SASL, or ML) with the relational (as in PROLOG) programming concepts into a single new paradigm and a machine which would execute programs written in the language, using reduction and a multiprocessor architecture. The SUPER language is an extension of the basic lambda-calculus which we call lambda plus. It is formally a collection of expressions together with some rules and definitions which give them meaning and make it possible to do deductive reasoning and computation with them. The expressions of the SUPER language fall into three main syntactic categories: atoms, abstractions, and combinations. Volume 2 contains a detailed presentation of the single-processor software programming system LNF which was developed to serve as a test bed and simulation tool for the classical part of the SUPER system. Volume 3 presents the final, enhanced version of LNF. GRA

N88-22827# JAYCOR, Vienna, Va.
DATA BASE DESIGN AND IMPLEMENTATION
16 Jun. 1987 6 p
(Contract N00014-86-C-2352)
(AD-A190414) Avail: NTIS HC A02/MF A01 CSCL 05B

JAYCOR has determined that the Naval Center for Applied Research in Artificial Intelligence(NCARAI) Library requires a database for its holdings in order to make efficient use of both the Library and its resources. Bibliographic information contained in the database should conform to accepted Library procedures, namely Library of Congress classification and AACRII cataloging. The Online Computer Library Center (OCLC) database and LS2000 provide the necessary resources. OCLC promotes catalog standardization. OCLC was established in 1967 to develop a cooperative, computerized regional network for its 54 Ohio member college libraries. The system has expanded since to a database containing bibliographic information created by the cooperative cataloging efforts of over 3,500 participating libraries nationwide. OCLC's database is the largest machine-readable file of bibliographic information in the world and is continually growing. The LS2000 system is an integrated online system providing catalog access, bibliographic and circulation control. It was installed in the main NRL library in 1986 and obtained for the NCARAI Library by NRL at no cost. and is continually growing. LS2000 system is an integrated online system that provides catalog access, bibliographic control and circulation control. It was installed at the main NRL Library in 1986 and obtained for the NCARAI Library through NRL at no cost. The LS2000 system will provide access to the NCARAI catalog for all researchers at the Center via terminals. GRA

N88-22828# Du Pont de Nemours (E. I.) and Co., Aiken, S.C.
OCR VISION SYSTEM, AN ALTERNATIVE TO BAR CODE
D. R. Leader 2 Nov. 1987 7 p Presented at the I.D. Expo, Boston, Mass., 20 Apr. 1988
(Contract DE-AC09-76SR-00001)
(DE88-003761; DP-MS-87-132; CONF-880458-1) Avail: NTIS HC A02/MF A01

This report describes optical character reader system advantages and applications. Comparisons are made to bar code readers. DOE

N88-22829# Instituto de Pesquisas Espaciais, Sao Jose dos Campos (Brazil).
GEORELATIONAL DATA MODEL [MODELO DE DADOS GEO-RELACIONAL]
Guaraci Jose Erthal, Diogenes SalasAlves, and Gilberto CamaraNeto Mar. 1988 11 p In PORTUGUESE; ENGLISH summary Presented at the 2nd SELPER, Bogota, Colombia, Nov. 1987
(INPE-4490-PRE/1254) Avail: NTIS HC A03/MF A01

A model is presented for data organization in Geographic Information systems. The model is an extension of the relational data model incorporating spatial information. Treatment of a geographic area is organized within a Project. A project is composed of Information Planes (PI), grouping objects of the same type. A type is composed of spatial data of the same category, with attributes defined by a particular relation. The model incorporates six data categories: Thematic Maps (polygonal areas), Digital Elevation Models, Hydrography, Networks, Points and Images. Data within a PI can be stored in several different formats. The proposed model is being used in the development of INPE's Geographic Information System. Types can be arbitrarily defined by users. Author

N88-22830*# National Aeronautics and Space Administration, Washington, D.C.
NASA SCIENTIFIC AND TECHNICAL PUBLICATIONS: A CATALOG OF SPECIAL PUBLICATIONS, REFERENCE PUBLICATIONS, CONFERENCE PUBLICATIONS, AND TECHNICAL PAPERS, 1987
Mar. 1988 69 p
(NASA-SP-7063(02); NAS 1.21:7063(02)) Avail: NTIS HC free as PR-828; NASA Scientific and Technical Information Facility, P.O. Box 8757, BWI Airport, Md. 21240 HC free CSCL 05B

This catalog lists 239 citations of all NASA Special Publications, NASA Reference Publications, NASA Conference Publications, and NASA Technical Papers that were entered in the NASA scientific and technical information database during accession year 1987. The entries are grouped by subject category. Indexes of subject terms, personal authors, and NASA report numbers are provided. Author

83 ECONOMICS AND COST ANALYSIS

Includes cost effectiveness studies.

No abstracts in this category.

84 LAW, POLITICAL SCIENCE AND SPACE POLICY

Includes NASA appropriation hearings; aviation law; space law and policy; international law; international cooperation; and patent policy.

No abstracts in this category.

85 URBAN TECHNOLOGY AND TRANSPORTATION

Includes applications of space technology to urban problems; technology transfer; technology assessment; and surface and mass transportation.

For related information see also *03 Air Transportation and Safety, 16 Space Transportation,* and *44 Energy Production and Conversion.*

N88-22831# Naval Postgraduate School, Monterey, Calif.
A METHOD FOR ESTIMATING AND CONTROLLING THE COST OF EXTENDING TECHNOLOGY Final Report
Willis R. Greer, Jr. 10 Mar. 1988 116 p
(AD-A190717; NPS-54-88-002) Avail: NTIS HC A06/MF A01 CSCL 05C

Both the theoretical and practical aspects of costing extensions of technology are addressed. A method for measuring the level of technology embodied in a system is developed. The increment in technology represented by a development project is found to be highly correlated with development time. Development time is then broken down into normal and abnormal components, which are found to be correlated with development cost. Cost control methods are developed. GRA

N88-22832# Instituto de Pesquisas Espaciais, Sao Jose dos Campos (Brazil).
THE NECESSITY OF AUTOMATION IN BRAZIL [A NECESSIDADE DA AUTOMACAO NO BRASIL]
Atair RiosNeto Sep. 1987 20 p In PORTUGUESE; ENGLISH summary Presented at the 39th SBPC Multidisciplinary Symposium on Impact of the Informatization and Automation Submitted for publication
(INPE-4346-PRE/1183) Avail: NTIS HC A03/MF A01

The subject of automation is considered from a multidisciplinary point of view. Initially a general characterization of the field of automation is done. The need for automation is analyzed from the perspective of the dynamics of technological evolution. The conclusion that this need is a matter of historical destiny leads to the evaluation of the state of the Brazilian economy and its capacity to absorb the technology. Author

N88-22833# Instituto de Pesquisas Espaciais, Sao Jose dos Campos (Brazil).
ORBITAL REMOTE SENSING: AN INSTRUMENT FOR MONITORING URBAN GROWTH
Maria deLourdesN.O.Kurkdjian Apr. 1988 7 p In PORTUGUESE; ENGLISH summary Presented at the National Meeting of the Study on Urban Growth, 5-9 Oct. 1987, Recife, Brazil
(INPE-4456-PRE/1287) Avail: NTIS HC A02/MF A01

The principal advantages in using orbital remote sensing data as an auxiliary instrument for urban growth monitoring are examined. Author

88 SPACE SCIENCES (GENERAL)

No abstracts in this category.

89 ASTRONOMY

Includes radio, gamma-ray, and infrared astronomy, and astrometry.

N88-22834*# Martin Marietta Corp., Bethesda, Md. Manned Space Systems.
EXTERNAL TANK GAMMA RAY IMAGING TELESCOPE STUDY. FINAL REVIEW, PHASE 2
Feb. 1988 147 p
(Contract NAS8-36394)
(NASA-CR-179320; NAS 1.26:179320) Avail: NTIS HC A07/MF A01 CSCL 03A

Potential scientific uses of the external tanks were examined. An onorbit conversion of the external tank to a gamma ray telescope/spacecraft is feasible. The development time and cost are acceptable. The specific engineering research and development requirements are listed. Concepts for onorbit utilization of external tanks were developed. The tasks for phase three were summarized. B.G.

N88-22835# Instituto de Pesquisas Espaciais, Sao Jose dos Campos (Brazil).
MULTIPLE OBJECT REDSHIFT DETERMINATIONS IN CLUSTERS OF GALAXIES USING OCTOPUS
A. Mazure, D. Proust, L. Sodre, H. V. Capelato, and G. Lund (Nice Univ., France) Apr. 1988 7 p Previously announced in IAA as A87-47633 Submitted for publication
(INPE-4528-PRE/1278) Avail: NTIS HC A02/MF A01

The ESO multiobject facility, Octopus, was used to observe a sample of galaxy clusters such as SC2008-565 in an attempt to collect a large set of individual radial velocities. A dispersion of 114 A/mm was used, providing spectral coverage from 3800 to 5180 A. Octopus was found to be a well-adapted instrument for the rapid and simultaneous determination of redshifts in cataloged galaxy clusters. Author

N88-22836 Max-Planck-Inst. fuer Physik und Astrophysik, Garching (West Germany). Inst. fuer Extraterrestrische Physik.
DESIGN, CONSTRUCTION AND PERFORMANCE OF THE ROSAT HIGH RESOLUTION X-RAY MIRROR ASSEMBLY
Bernd Aschenbach Oct. 1987 38 p Presented at the 31st SPIE Annual International Symposium, San Diego, Calif., Aug. 1987 Previously announced in IAA as A88-35008 Submitted for publication
(MPE-Preprint-101; ETN-88-92086) Copyright Avail: Fachinformationszentrum Karlsruhe, 7514 Eggenstein-Leopoldshafen 2, Fed. Republic of Germany

A grazing incidence telescope has been developed for the X-ray astronomy satellite ROSAT including a verification and a flight model. The telescope consists of a four-fold nested Wolter type I mirror assembly of 84 cm front aperture and 240 cm focal length. Full aperture X-ray measurements performed in a 130 m long beam facility are presented and successfully compared with model predictions based on mirror metrology data. An energy independent angular resolution of 4 arcsec half-energy width for the encircled point spread function and a mirror surface microroughness of less than 3 A are achieved. Metrology of the

actual flight mirrors (although not yet assembled into a telescope) indicates an even better performance. ESA

90 ASTROPHYSICS

Includes cosmology; celestial mechanics; space plasmas; and interstellar and interplanetary gases and dust.
For related information see also *75 Plasma Physics*.

N88-22837# Gosudarstvennyi Komitet po Ispolzovaniyu Atomnoi Energii, Moscow (USSR). Inst.Teoreticheskoj i Ehksperimental'noj.
HYDRODYNAMICAL MODELS OF SUPERNOVA SN 1987 A IN THE LMC
E. K. Grassberg, V. S. Imshennik, D. K. Nadezhin, and V. P. Utrobin 1987 13 p
(TI88-701123; ITEP-57(1987)) Avail: NTIS (US Sales Only) HC A03/MF A01

It is shown that the properties of SN1987A in LMC can be described well by hydrodynamical models of explosions of compact massive stars. In accordance with these models, the mass of the expelled envelope the presupernova radius and the total energy of explosion E, are evaluated for SN1987A to be approx. 16M sub Sun, approx. 30R sub Sun, and approx. 3.10 sup 51 erg, respectively. The progenitor of supernova remnant Cas A may be considered as the prototype to the SN1987A in our own Galaxy. In other galaxies, this subtype of supernovae can be represented by SN1948B in NGC6946. If energy of explosion transfers from collapsed core of the star to the envelope within timescale less than 1 hour, then delay delta t approx. 3 hours between the neutrino pulse and the steep rise of optical luminosity of SN1987A does not contradict with scenario of explosions of compact massive stars. DOE

N88-22838# Hiroshima Univ., Takehara (Japan). Research Inst. for Theoretical Physics.
HYDRODYNAMICAL EQUATIONS FOR SPHERICAL GRAVITATIONAL COLLAPSE IN TERMS OF A GENERALIZED THEORY OF GRAVITATION WITH HIGHER DERIVATIVES
H. Nariai Jun. 1986 13 p
(DE87-703027; RRK-86-23) Avail: NTIA (US Sales Only) HC A02/MF A01

A formalism for the spherical gravitational collapse is presented on the basis of a generalized theory of gravitation in the sense of Utiyama-Dewitt. The resulting formalism is similar to that developed by the author in 1972 that was based on the scalar-tensor theory of gravity. DOE

N88-22839# Hiroshima Univ., Takehara (Japan). Research Inst. for Theoretical Physics.
GENERATION AND PROPAGATION OF SOUND WAVES IN A COLLAPSING OR ANTI-COLLAPSING STAR WITH UNIFORM DENSITY
H. Nariai Sep. 1986 12 p
(DE87-703034; RRK-86-34) Avail: NTIS (US Sales Only— HC A03/MF A01

The generation and propagation of sound waves on a collapsing or anti-collapsing star with uniform density are discussed. It seems that its contents do not lose their physical meaning even at the present time. DOE

N88-22840# Hiroshima Univ., Takehara (Japan). Research Inst. for Theoretical Physics.
DENSITY PERTURBATIONS IN A ROTATING UNIVERSE
H. Nariai Sep. 1986 13 p
(DE87-703036; RRK-86-36) Avail: NTIS (US Sales Only) HC A03/MF A01

Density perturbations in a rotating universe were worked out on the basis of Newtonian cosmology. This approach is comprehensive in such a way that it does not lose a physical meaning even at the present time. DOE

N88-22841# Fermi National Accelerator Lab., Batavia, Ill.
STRING DRIVEN INFLATION
N. Turok Nov. 1987 14 p
(Contract DE-AC02-76CH-03000)
(DE88-006994; FNAL/Pub-87/215-A) Avail: NTIS HC A03/MF A01

It is argued that, in fundamental string theories, as one traces the universe back in time a point is reached when the expansion rate is so fast that the rate of string creation due to quantum effects balances the dilution of the string density due to the expansion. One is therefore led into a phase of constant string density and an exponentially expanding universe. Fundamental strings therefore seem to lead naturally to inflation. DOE

N88-22842# Fermi National Accelerator Lab., Batavia, Ill.
COSMOLOGY FOR HIGH ENERGY PHYSICISTS
A. Albrecht Nov. 1987 40 p Presented at the Theoretical Advanced Summer Institute, Santa Fe, N. Mex., 6 Jul. 1987
(Contract DE-AC02-76CH-03000)
(DE88-005705; FNAL/C-87/206-A; CONF-8707141-4) Avail: NTIS HC A03/MF A01

The standard big bang model of cosmology is presented. Although not perfect, its many successes make it a good starting point for most discussions of cosmology. Places are indicated where well understood laboratory physics is incorporated into the big bang, leading to successful predictions. Much less established aspects of high energy physics and some of the new ideas they have introduced into the field of cosmology are discussed, such as string theory, inflation and monopoles. DOE

N88-22843*# Arizona Univ., Tucson.
SPECKLE INTERFEROMETRY OF ASTEROIDS Final Report, 1 Feb. 1987 - 31 Jan. 1988
Jack Drummond 31 May 1988 24 p
(Grant NAGw-867)
(NASA-CR-180438; NAS 1.26:180438) Avail: NTIS HC A03/MF A01 CSCL 03B

This final report for NASA Contract NAGw-867 consists of abstracts of the first three papers in a series of four appearing in Icarus that were funded by the preceding contract NAGw-224: (1) Speckle Interferometry of Asteroids I. 433 Eros; (2) Speckle Interferometry of Asteroids II. 532 Herculina; (3) Speckle Interferometry of Asteroids III. 511 Davida and its Photometry; and the fourth abstract attributed to NAGw-867, (4) Speckle Interferometry of Asteroids IV. Reconstructed images of 4 Vesta; and a review of the results from the asteroid interferometry program at Steward Observatory prepared for the Asteroids II book, (5) Speckle Interferometry of Asteroids. Two papers on asteroids, indirectly related to speckle interferometry, were written in part under NAGw-867. One is in press and its abstract is included here: Photometric Geodesy of Main-Belt Asteroids. II. Analysis of Lightcurves for Poles, Periods and Shapes; and the other paper, Triaxial Ellipsoid Dimensions and Rotational Pole of 2 Pallas from Two Stellar Occultations, is included in full. Author

N88-22844# Fermi National Accelerator Lab., Batavia, Ill.
PARTICLE COSMOLOGY COMES OF AGE
M. S. Turner Dec. 1987 26 p Presented at the International Symposium on Lepton and Photon Interactions at High Energies, Hamburg, Fed. Republic of Germany, 27 Jul. 1987 Prepared in cooperation with Chicago Univ., Ill.
(Contract DE-AC02-76CH-03000)
(DE88-006998; FNAL/C-87/228-A; CONF-870797-13) Avail: NTIS HC A03/MF A01

The application of modern ideas in particle physics to astrophysical and cosmological settings is a continuation of a fruitful tradition in astrophysics which began with the application of atomic physics, and then nuclear physics. In the past decade particle cosmology and particle astrophysics have been recognized as legitimate activities by both particle physicists and astrophysicists and astronomers. During this time there was a high level of theoretical activity producing much speculation about the earliest history of the Universe, as well as important and interesting

astrophysical and cosmological constraints to particle physics theories. This period of intense theoretical activity has produced a number of ideas most worthy of careful consideration and scrutiny, and even more importantly, amenable to experimental/observational test. Among the ideas which are likely to be tested in the next decade are: the cosmological bound to the number of neutrino flavors, inflation, relic WIMPs as the dark matter, and MSW neutrino oscillations as a solution to the solar neutrino problems. DOE

N88-22845# Instituto de Pesquisas Espaciais, Sao Jose dos Campos (Brazil).
NEW MEASUREMENTS OF RADIAL VELOCITIES IN CLUSTERS OF GALAXIES
D. Proust, A. Talavera, E. SalvadorSole, A. Mazure (Observatoire de Paris-Meudon, France), and H. V. Capelato Apr. 1988 7 p Previously announced in IAA as A87-28754 Submitted for publication
(INPE-4527-PRE/1277) Avail: NTIS HC A02/MF A01

Redshifts for 100 galaxies in 10 clusters of galaxies are presented based on data obtained between March 1984 and March 1985 from Calar Alto, La Palma, and ESO, and on data from Mauna Kea. Data for individual galaxies are given, and the accuracy of the velocities of the four instruments is discussed. Comparison with published data shows the present velocites to be shifted by +4.4 km/s on average, with a standard deviation in the difference of 89.7 km/s, consistent with the rms of redshift measurements which range from 50 to 100 km/s. Author

N88-22846# California Inst. of Tech., Pasadena.
NEAR-INFRARED OBSERVATIONS OF CEPHEIDS: THE DISTANCE TO M33
Barry F. Madore, Christopher W. McAlary, R. A. McLaren, D. L. Welch (Toronto Univ., Ontario), G. Neugebauer, and K. Matthews [1988] 26 p
Avail: NTIS HC A03/MF A01

H-band (1.65 micron) random-phase observations of 15 Cepheids in the Local Group Sc galaxy M33 are reported. Fitting to a composite infrared Period-Luminosity relation for the Galaxy and both of the Magellanic Clouds yields a distance modulus of 24.5 + or - 0.2 mag. A comparison with Sandage's observations of the Cepheids in the blue indicates E(B-V)= 0.25 mag and a reddening corrected distance modulus of 24.3 + or - 10.2 mag. Author

91 LUNAR AND PLANETARY EXPLORATION

Includes planetology; and manned and unmanned flights.

For spacecraft design or space stations see *18 Spacecraft Design, Testing and Performance.*

N88-22847*# University of Southern Illinois, Carbondale. Surficial Processes Research Group.
GROUNDWATER SAPPING VALLEYS: EXPERIMENTAL STUDIES, GEOLOGICAL CONTROLS AND IMPLICATIONS TO THE INTERPRETATION OF VALLEY NETWORKS ON MARS
Final Contractor's Report, 1 Feb. 1985 - 31 Jan. 1988
R. Craig Kochel 15 May 1988 77 p
(Grant NAGw-707)
(NASA-CR-182718; NAS 1.26:182718) Avail: NTIS HC A05/MF A01 CSCL 03B

An integrated approach using experimental laboratory models, field studies of terrestrial analogs, and remote studies of terrestrial field sites were applied to the goals of understanding the nature and morphology of valley networks formed by groundwater sapping. In spite of problems with scaling, the experimental studies provide valuable insights into concepts relating to the initiation, development, and evolution of valleys by groundwater sapping. These investigations are also aimed at developing geomorphic criteria for distinguishing valleys formed by surface runoff from those formed by groundwater sapping processes. Channels that were field classified as sapping vs. runoff were successfully distinguished using statistical analysis of their respective morphologies; therefore, it may be possible to use similar techniques to interpret channel genesis on Mars. The terrestrial and flume studies provide the ground truth dataset which can be used (and will be during the present year) to help interpret the genesis of valley networks on Mars. Author

N88-22848# Instituto de Pesquisas Espaciais, Sao Jose dos Campos (Brazil).
THE 1985 MUTUAL PHENOMENA OF JUPITER'S SATELLITES OBSERVED IN BRAZIL
J. Barroso, Jr., F. J. Jablonski, and G. R. Quast Apr. 1988 9 p Submitted for publication
(INPE-4526-PRE/1276) Avail: NTIS HC A02/MF A01

The results of the 1985 photoelectric photometry measurements on mutual phenomena among the satellites of Jupiter are presented. The data reduction method is explained and the results discussed. The orbital position of the satellites was obtained with an error of approximately 100 km. Author

92 SOLAR PHYSICS

Includes solar activity, solar flares, solar radiation and sunspots.

For related information see *93 Space Radiation.*

N88-22849# National Geophysical Data Center, Boulder, Colo.
SOLAR-GEOPHYSICAL DATA NUMBER 520, DECEMBER 1987. PART 2: (COMPREHENSIVE REPORTS). DATA FOR JUNE 1987 AND MISCELLANEA
Helen E. Coffey, ed. and John A. McKinnon, ed. Dec. 1987 30 p
(Contract N00014-86-F-0049)
(PB88-164207; SGD-520-Pt-2; ISSN-0038-0911; LC-79-640375)
Avail: NTIS HC A03/MF A01 CSCL 03B

The contents of Solar-Geophysical Data Report 520 are as follows: Detailed index for 1987; and Data for June 1987 (Meudon Carte Synoptique, Solar flares, Solar radio bursts at fixed frequencies, Solar X-ray radiation from GOES satellites, Mass ejections from the Sun, Active prominences and filaments). GRA

93 SPACE RADIATION

Includes cosmic radiation; and inner and outer earth's radiation belts.

For biological effects of radiation see *52 Aerospace Medicine.* For theory see *73 Nuclear and High-Energy Physics.*

N88-22850# Instituto de Pesquisas Espaciais, Sao Jose dos Campos (Brazil).
A MAP OF THE COSMIC BACKGROUND RADIATON AT 3 MILLIMETERS
P. Lubin, T. Villela, G. Epstein, and G. Smoot (California Univ., Berkeley.) Apr. 1988 9 p Previously announced in IAA as A86-14893 Submitted for publication
(INPE-4529-PRE/1279) Avail: NTIS HC A02/MF A01

Data from a series of balloon flights covering both the Northern and Southern Hemispheres, measuring the large angular scale anisotropy in the cosmic background radiation at 3.3 mm wavelength are presented. The data cover 85 percent of the sky to a limiting sensitivity of 0.7 mK per 7-deg field of view. The data show a 50-sigma (statistical error only) dipole anisotropy with an amplitude of 3.44 +/- 0.17 mK and a direction of alpha= 11.2 h +/- 0.1 h, and delta = -6.0 deg +/- 1.5 deg. A 90 percent confidence level upper limit of 0.00007 is obtained for the rms quadrupole amplitude. Flights separated by six months show the motion of Earth around the Sun. Galactic contamination is very small, with less than 0.1 mK contribution to the dipole

quadrupole terms. A map of the sky has been generated from the data. Author

99 GENERAL

N88-22851*# National Aeronautics and Space Administration. Lewis Research Center, Cleveland, Ohio.
RESEARCH AND TECHNOLOGY Annual Report, 1987
1987 103 p
(NASA-TM-100172; E-3740; NAS 1.15:100172) Avail: NTIS HC A06/MF A01 CSCL 05A

The NASA Lewis Research Center's research and technology accomplishments for fiscal year 1987 are summarized. It comprises approximately 100 short articles submitted by staff members of the technical directorates and is organized into four sections: aeronautics, aerospace technology (which includes space communications), space station systems, and computational support. A table of contents by subject was developed to assist the reader in finding articles of special interest. Author

N88-22852*# National Aeronautics and Space Administration. Marshall Space Flight Center, Huntsville, Ala.
MARSHALL SPACE FLIGHT CENTER 1960-1985: 25TH ANNIVERSARY REPORT
Jul. 1985 98 p Original contains color illustrations
(NASA-TM-100328; NAS 1.15:100328) Avail: NTIS HC A05/MF A01; also available SOD HC $6.00 as 033-000-00965-8 CSCL 05D

The Marshall Space FLight Center marks its 25th aniversary with a record of notable achievements. These accomplishments are the essence of the Marshall Center's history. Behind the scenes of the space launches and missions, however, lies the story of challenges faced and problems solved. The highlights of that story are presented. The story is organized not as a straight chronology but as three parallel reviews of the major assignments: propulsion systems and launch vehicles, space science research and technology, and manned space systems. The general goals were to reach space, to know and understand the space environment, and to inhabit and utilize space for the benefit of mankind. Also included is a chronology of major events, presented as a fold-out chart for ready reference. Author

N88-22853*# National Aeronautics and Space Administration. Langley Research Center, Hampton, Va.
LANGLEY AEROSPACE TEST HIGHLIGHTS, 1987
May 1988 114 p
(NASA-TM-100595; NAS 1.15:100595) Avail: NTIS HC A06/MF A01 CSCL 05D

The role of the Langley Research Center is to perform basic and applied research necessary for the advancement of aeronautics and space flight, to generate new and advanced concepts for the accomplishment of related national goals, and to provide research advice, technological support, and assistance to other NASA installations, other government agencies, and industry. Some of the significant tests which were performed during the calender year 1987 in Langley test facilites are illustrated. Both the broad range of the research and technology activities at Langley and the contributions of this work toward maintaining the U.S. leadership in aeronautic and space research are illustrated. Author

N88-22854*# National Aeronautics and Space Administration. Langley Research Center, Hampton, Va.
SPACE DIRECTORATE RESEARCH AND TECHNOLOGY ACCOMPLISHMENTS FOR FISCAL YEAR 1987
Don E. Avery May 1988 164 p
(NASA-TM-100607; NAS 1.15:100607) Avail: NTIS HC A08/MF A01 CSCL 05D

The major accomplishments and test highlights of the Space Directorate of NASA Langley Research Center for FY87 are presented. Accomplishments and test highlights are listed by Division and Branch. This information should be useful in coordinating programs with government organizations, universities, and industry in areas of mutual interest. Author

☆ U.S. GOVERNMENT PRINTING OFFICE: 1988— 202-150/80013

Typical Subject Index Listing

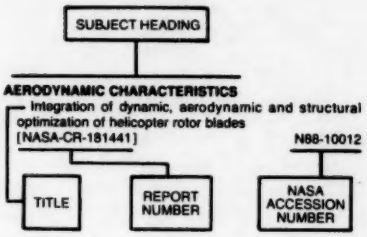

The subject heading is the key to the subject content of the document. Titles, report numbers, and accession numbers of pertinent documents are provided under each subject heading. When the title is insufficiently descriptive of the document content, a title extension has been added, separated from the title by three hyphens. The report number helps to indicate the type of document cited (e.g., NASA report, NASA translation, NASA contractor report). The NASA accession number is the number by which the document abstracts are arranged in this journal and by which the document is sold or requested. The titles, with title extensions if present, are arranged under each subject heading in ascending accession number order. The subject headings have been selected from the latest revision of the *NASA Thesaurus* (NASA SP-7053).

A

A STARS
Generation and propagation of sound waves in a collapsing or anti-collapsing star with uniform density
[DE87-703034] N88-22839

ABLATION
Analytic solutions to dynamic equations of plasma armature railguns
[DE88-006842] N88-22057

ABSORPTION
Determination of aquo-complexes of chromium and iron in chromium plating and polishing solutions by ion chromatography
[AD-A190168] N88-22148

ABSORPTION CROSS SECTIONS
Rotational structure and absorption cross sections from 300 to 190 K of the Schumann-Runge bands
[AERONOMICA-ACTA-A-318-1987] N88-22131

Ultraviolet absorption cross sections of methylbromide at stratospheric temperatures
[AERONOMICA-ACTA-A-320-1987] N88-22132

ABSORPTION SPECTROSCOPY
Infrared absorption spectroscopy and chemical kinetics of free radicals
[DE88-006536] N88-22112

Diode laser spectroscopy of chemical moieties at surfaces
[AD-A190710] N88-22127

Merit of Hadamard transform active absorption spectrometer described N88-22232

ACCELERATED LIFE TESTS
Examination of temperature effects on gate-to-drain avalanche breakdown in GaAs MESFETs (Metal-Semiconductor Field Effect Transistors) by measuring light emission under RF drive
[AD-A189634] N88-22778

ACCELERATION TOLERANCE
Analysis of head response to torso acceleration. Volume 2: Description of data retrieval, analysis and display software
[PB88-156765] N88-22536

ACCEPTOR MATERIALS
Donor acceptor polymerization chemistry as a vehicle to low energy cure matrix resins
[AD-A190119] N88-22179

ACCIDENT INVESTIGATION
Space shuttle accident: NASA's actions to address the Presidential Commission report
[PB88-135306] N88-22059

ACCOUNTING
Monitoring the usage of a computer system
[DE88-004310] N88-22542

ACCURACY
Density measurements on solids and liquids
[PB88-164934] N88-22129

Effect of friction and control parameters on the tracking accuracy of a target seeker
[AD-A190010] N88-22257

ACOUSTIC EXCITATION
Enhanced viscous flow drag reduction using acoustic excitation
[NASA-CR-182734] N88-22295

ACOUSTIC FREQUENCIES
Describing the source created by turbulent flow over orifices and louvers
[AD-A190254] N88-22706

ACOUSTIC MEASUREMENT
Space time processing, environmental-acoustic effects
[AD-A190764] N88-22708

Acoustic propagation in the low atmosphere. Experimental study and modeling by the radius method
[ISL-CO-247/86] N88-22713

ACOUSTIC PROPAGATION
Model-scale sound propagation experiment
[NASA-TM-100602] N88-22709

Acoustic propagation in the low atmosphere. Experimental study and modeling by the radius method
[ISL-CO-247/86] N88-22713

ACOUSTIC VELOCITY
Target localization in an inhomogeneous medium
[AD-A190008] N88-22703

ACOUSTICS
Nondestructive evaluation by acousto-ultrasonics N88-22412

Flaw characterization in structural ceramics using scanning laser acoustic microscopy N88-22415

Nondestructive evaluation of sintered ceramics N88-22416

Mechanisms mediating perception of complex acoustic patterns
[AD-A189765] N88-22520

Mechanisms mediating the perception of complex acoustic patterns
[AD-A190112] N88-22705

Space time processing, environmental-acoustic effects
[AD-A190764] N88-22708

Thin superconducting film characterization by surface acoustic waves
[AD-A190417] N88-22791

ACTIVE CONTROL
Instrumentation to provide an active control capability for distributed parameter systems
[AD-A190043] N88-22375

ADA (PROGRAMMING LANGUAGE)
Ada (Trademark) compiler validation summary report. ALSYS: AlsyCOMP-013, V2.0 HOST: IBM PC AT. Target: IBM 370 3084Q
[AD-A189640] N88-22546

ADAPTATION
A multiple model adaptive tracking algorithm against airborne targets
[AD-A190619] N88-22263

Adaptive neural network architecture
[AD-A190114] N88-22533

Implementation of a distributed adaptive routing algorithm on the Intel IPSC (Intel Personal Super-Computer)
[AD-A189849] N88-22567

ADAPTIVE CONTROL
Flexiwall 3 SO: A second order predictive strategy for rapid wall adjustment in two-dimensional compressible flow
[NASA-CR-181662] N88-22018

Model selection for the multiple model adaptive algorithm for in-flight simulation
[AD-A189715] N88-22022

Multivariable control law design for the AFTI/F-16 with a failed control surface using a parameter-adaptive controller
[AD-A189848] N88-22040

Multiple model parameter adaptive control for in-flight simulation
[AD-A190568] N88-22044

Optimal control and identification of space structures
[AD-A190033] N88-22065

Moving-bank multiple model adaptive estimation applied to flexible spacestructure control
[AD-A190761] N88-22071

ADDITIVES
Development of a laboratory test for multiport injector deposits: Approaches 1 and 2
[AD-A190697] N88-22203

ADHESION
Laser enhanced adhesion of copper films to sapphire substrates
[DE88-006802] N88-22144

Fracture toughness of silicon nitride-silicon nitride joints bonded with oxynitride glass
[DE88-005548] N88-22172

ADHESIVE BONDING
Increasing strength of graphite/epoxy bolted joints by introducing an adhesively bonded metallic insert
[FFA-TN-1987-45] N88-22442

ADIABATIC CONDITIONS
Adiabatic representation of three-body problem in hyperspherical coordinates. Statement of the problem
[TI88-701162] N88-22678

ADIPOSE TISSUES
Prediction of physical fitness: Estimated percent body fat using body circumferences versus weight-height measures
[AD-A190233] N88-22526

ADJOINTS
The adjoint process in stochastic optimal control
[AD-A189720] N88-22605

ADSORPTION
Mass transfer mechanisms for water adsorbed on silica gel
[DE88-005993] N88-22107

Molecular dynamics of materials posessing high energy content
[AD-A190034] N88-22118

Dilution refrigerator with non-valve adsorption system of sup 3/He circulation
[DE88-700974] N88-22209

Theory of the dissociation dynamics of small molecules on metal surfaces: Finite temperature studies
[DE88-006495] N88-22716

Anomalies in the heat-capacity signatures of submonolayer adsorbates with attractive lateral interactions
[AD-A190736] N88-22817

AERIAL RECONNAISSANCE
Hydrographic data from the OPTOMA (Ocean Prediction Through Observation, Modeling and Analysis) program: OPTOMA 23, 9-19 November 1986
[AD-A189868] N88-22506

AEROACOUSTICS
Investigation of aeroacoustic mechanisms by remote thermal imaging
[DE88-002612] N88-22046

AEROASSIST
Orbital transfer vehicle: Concept definition and system analysis study
[NASA-CR-179315] N88-22080

AERODYNAMIC CHARACTERISTICS
Oscillating airfoils: Achievements and conjectures
[AD-A190490] N88-22008

Improvements to tilt rotor performance through passive blade twist control
[NASA-TM-100563] N88-22434
AERODYNAMIC CONFIGURATIONS
Designs of profiles for cascades
[NASA-TT-20161] N88-22326
AERODYNAMIC DRAG
Computational fluid dynamics drag prediction: Results from the Viscous Transonic Airfoil Workshop
[NASA-TM-100095] N88-22009
Zero-lift drag predictions in supersonic flow for complex configurations N88-22246
AERODYNAMIC FORCES
Unsteady aerodynamics of a Wortmann FX-63-137 wing in a fluctuating wind field
[AD-A190128] N88-22006
Influence of unsteady aerodynamic forces on dynamic response of variable sweep aircraft N88-22245
AERODYNAMIC INTERFERENCE
Porous wind tunnel corrections for counterrotation propeller testing
[NASA-TM-100873] N88-22019
AERODYNAMIC STABILITY
Unsteady aerodynamics of a Wortmann FX-63-137 wing in a fluctuating wind field
[AD-A190128] N88-22006
Preliminary airworthiness evaluation of the UH-60A with Advanced Digital Optical Control System (ADOCS)
[AD-A190674] N88-22030
AERODYNAMIC STALLING
Performance optimization of a cruise missile using dynamic-stall induced lift augmentation
[AD-A190497] N88-22027
AEROELASTICITY
Shape sensitivity analysis of wing static aeroelastic characteristics
[NASA-TP-2808] N88-22031
AERONAUTICAL ENGINEERING
External tank gamma ray imaging telescope study. Final review, phase 2
[NASA-CR-179320] N88-22834
Research and technology
[NASA-TM-100172] N88-22851
AERONAUTICS
Langley aerospace test highlights, 1987
[NASA-TM-100595] N88-22853
AEROSOLS
Study of mean free path effects on growth of ultrafine metallic aerosols
[AD-A190206] N88-22149
AEROSPACE ENGINEERING
Wave propagation and dynamics of lattice structures
[AD-A190611] N88-22069
JPRS report: Science and technology. Japan
[JPRS-JST-88-001] N88-22218
JPRS report: Science and technology. Japan
[JPRS-JST-87-029] N88-22228
Life and reliability of rotating disks N88-22428
AEROSPACE ENVIRONMENTS
Space utilization plans N88-22219
AEROSPACE MEDICINE
USSR Space Life Sciences Digest, issue 16
[NASA-CR-3922(19)] N88-22515
AEROSPACE SCIENCES
USSR Space Life Sciences Digest, issue 16
[NASA-CR-3922(19)] N88-22515
NASA scientific and technical publications: A catalog of Special Publications, Reference Publications, Conference Publications, and Technical Papers, 1987
[NASA-SP-7063(02)] N88-22830
AEROSPACE TECHNOLOGY TRANSFER
Langley aerospace test highlights, 1987
[NASA-TM-100595] N88-22853
AEROTHERMODYNAMICS
Aerothermal tests of quilted dome models on a flat plate at a Mach number of 6.5
[NASA-TP-2804] N88-22325
Review and assessment of the HOST turbine heat transfer program N88-22431
AGE FACTOR
Age, alcohol, and simulated altitude: Effects on performance and breathalyzer scores
[AD-A190642] N88-22531
AGING (MATERIALS)
Effect of moisture level in PBXW-109(E) (plastic-bonded explosive) mixes on the aging of the cured explosive
[AD-A190200] N88-22202
AGREEMENTS
The impact of independent research and development regulations on companies not required to negotiate advanced independent research and development agreements
[AD-A190007] N88-22818
AGRICULTURE
Assessment of crop loss from air pollutants: Meteorology-atmospheric chemistry and long range transport
[PB88-146857] N88-22448
AIR POLLUTION
Assessment of crop loss from air pollutants: Meteorology-atmospheric chemistry and long range transport
[PB88-146857] N88-22448
AIR TRAFFIC CONTROL
Aircraft accident report: North Star Aviation, Inc., PA-32 RT-300, N39614 and Alameda Aero Club Cessna 172, N75584, Oakland, California, March 31, 1987
[PB87-910412] N88-22021
An evaluation of the effects of high visual taskload on the separate behaviors involved in complex monitoring performance
[AD-A190641] N88-22538
AIR WATER INTERACTIONS
Changes in the California current system observed off northern California during July-August 1986
[AD-A190027] N88-22510
AIRBORNE EQUIPMENT
Feasibility study for a 2nd generation system for airborne maritime pollution surveillance
[ETN-88-92108] N88-22486
AIRCRAFT ACCIDENT INVESTIGATION
Aircraft accident reports, brief format, US civil and foreign aviation, issue number 10 of 1986 accidents
[PB87-916912] N88-22020
Aircraft accident report: North Star Aviation, Inc., PA-32 RT-300, N39614 and Alameda Aero Club Cessna 172, N75584, Oakland, California, March 31, 1987
[PB87-910412] N88-22021
AIRCRAFT CONFIGURATIONS
Oscillating airfoils: Achievements and conjectures
[AD-A190490] N88-22008
Trends in Computational Fluid Dynamics (CFD) for aeronautical 3D steady applications: The Dutch situation
[NLR-MP-86074-U] N88-22017
AIRCRAFT CONSTRUCTION MATERIALS
Experimental comparison of lightning simulation techniques to CV-580 airborne lightning strike measurements
[AD-A190576] N88-22496
AIRCRAFT CONTROL
Design of an integrated control system for flutter margin augmentation and gust load alleviation, tested on a dynamic windtunnel model
[PB88-149885] N88-22038
AIRCRAFT DESIGN
Trends in Computational Fluid Dynamics (CFD) for aeronautical 3D steady applications: The Dutch situation
[NLR-MP-86074-U] N88-22017
AIRCRAFT ENGINES
Research as part of the Air Force in aero propulsion technology (AFRAPT) program
[AD-A190336] N88-22036
AFRAPT (Air Force Research in Aero Propulsion Technology) trainee program
[AD-A190525] N88-22123
Lewis Structures Technology, 1988. Volume 2: Structural Mechanics
[NASA-CP-3003-VOL-2] N88-22382
Structural analyses of engine wall cooling concepts and materials N88-22405
AIRCRAFT HAZARDS
Heat transfer from a negatively buoyant wall jet
[NBS-GCR-88-541] N88-22208
AIRCRAFT MODELS
Model selection for the multiple model adaptive algorithm for in-flight simulation
[AD-A189715] N88-22022
AIRCRAFT NOISE
Noise assessment of unsuppressed TF-34-GE-100A engine at Warfield ANG, Baltimore, Maryland
[AD-A189966] N88-22702
AIRCRAFT PILOTS
Relationship of encoding speed and memory tests to flight training performance
[AD-A190670] N88-22539
AIRCRAFT RELIABILITY
Preliminary airworthiness evaluation of the UH-60A equipped with the XM-139 VOLCANO mine dispensing system
[AD-A190604] N88-22029
Preliminary airworthiness evaluation of the UH-60A with Advanced Digital Optical Control System (ADOCS)
[AD-A190674] N88-22030
AIRCRAFT STABILITY
The effects of torque response and time delay on rotorcraft vertical axis handling qualities
[AD-A189873] N88-22023
Influence of unsteady aerodynamic forces on dynamic response of variable sweep aircraft N88-22245
AIRCRAFT STRUCTURES
A study of damage tolerance in curved composite panels
[AD-A190617] N88-22092
AIRFOIL OSCILLATIONS
Unsteady flow field measurements using LDV (Laser Doppler Velocimetry)
[AD-A189907] N88-22298
AIRFOIL PROFILES
High Reynolds number, low Mach number, steady flow field calculations over a NACA 0012 airfoil using Navier-Stokes and interactive boundary layer theory
[AD-A189871] N88-22005
Computational fluid dynamics drag prediction: Results from the Viscous Transonic Airfoil Workshop
[NASA-TM-100095] N88-22009
Designs of profiles for cascades
[NASA-TT-20161] N88-22326
AIRFOILS
High Reynolds number, low Mach number, steady flow field calculations over a NACA 0012 airfoil using Navier-Stokes and interactive boundary layer theory
[AD-A189871] N88-22005
Oscillating airfoils: Achievements and conjectures
[AD-A190490] N88-22008
AIRFRAMES
A study of damage tolerance in curved composite panels
[AD-A190617] N88-22092
AIRPORTS
Noise assessment of unsuppressed TF-34-GE-100A engine at Warfield ANG, Baltimore, Maryland
[AD-A189966] N88-22702
ALCOHOLS
Age, alcohol, and simulated altitude: Effects on performance and breathalyzer scores
[AD-A190642] N88-22531
ALERTNESS
An evaluation of the effects of high visual taskload on the separate behaviors involved in complex monitoring performance
[AD-A190641] N88-22538
ALGEBRA
Tutorial on GAMS (Generalized Algebraic Modeling System): A modeling language for optimization
[AD-A189867] N88-22568
Design of an algorithm to translate nested relational algebra queries to GENESIS trace manager commands
[AD-A190502] N88-22581
Numerical solution of nonlinear algebraic equations in stiff ODE solving
[DE88-006634] N88-22622
About disequations simplification
[RR-645-I-IMAG-55-LIFIA] N88-22624
Research on algebraic manipulation
[AD-A190149] N88-22634
The algebraic structure of convolutional codes
[AD-A190280] N88-22635
Complexity of some problems in module algebra
[PB88-165386] N88-22648
Super Virasoro algebra and solvable supersymmetric quantum field theories
[DE88-752299] N88-22681
ALGORITHMS
Model selection for the multiple model adaptive algorithm for in-flight simulation
[AD-A189715] N88-22022
Moving-bank multiple model adaptive estimation applied to flexible spacestructure control
[AD-A190761] N88-22071
Identification of a star field from a spinning satellite
[CNES-NT-120] N88-22074
A multiple model adaptive tracking algorithm against airborne targets
[AD-A190619] N88-22263
Motion sickness: Quantitative, algorithmic malaise indication in real time
[AD-A189674] N88-22518
The visit problem: Visibility graph-based solution
[DE88-000343] N88-22556
Consistent estimates of autoregressive parameters for autoregressive moving average models
[RR-663-I] N88-22564
Implementation of a distributed adaptive routing algorithm on the Intel iPSC (Intel Personal Super-Computer)
[AD-A189849] N88-22567
Memory efficient evaluations of nonlinear stochastic equations and C3 applications
[AD-A189872] N88-22569
An analysis of multiple grain CHiP architectures
[AD-A189942] N88-22570
Extension of computer based algorithms by operator analysts
[NASA-CR-182798] N88-22575

Transformations of concurrent algorithms for highly parallel systems: A one year project summary report
[AD-A190236] N88-22576
Design and implementation of VLSI prime factor algorithm processor
[AD-A190483] N88-22580
Design of an algorithm to translate nested relational algebra queries to GENESIS trace manager commands
[AD-A190502] N88-22581
SEARCH: An interactive computer program for optimizing two-variable, unconstrained experiments or simulation
[AD-A190593] N88-22583
Cholesky downdating on a hypercube
[DE88-006780] N88-22586
Implementation and performance analysis of parallel assignment algorithms on a hypercube computer
[AD-A190678] N88-22600
Finding texture boundaries in images
[AD-A190554] N88-22609
Multi-disciplinary techniques for understanding time-varying space-based imagery
[AD-A190711] N88-22610
Development and application of the p-version of the finite element method
[AD-A190036] N88-22633
The algebraic structure of convolutional codes
[AD-A190280] N88-22635
Non-rigid motion and Regge calculus
[AD-A190387] N88-22640
Trust regions and projected gradients
[DE88-005829] N88-22646
Structural decomposition of multiple time scale Markov processes
[AD-A189739] N88-22657
Approximation methods for the identification and control of distributed parameter systems
[AD-A190201] N88-22662
Target localization in an inhomogeneous medium
[AD-A190008] N88-22703

ALIGNMENT

Particle beam alignment system for single event upset-Van de Graaf experiments
[AD-A189695] N88-22721

ALKALINE EARTH METALS

Electronic energy transfer processes in the alkali/alkaline earth metal vapors
[AD-A190035] N88-22119
Thermochemistry and high temperature thermodynamic properties of rare earth-alkaline earth-copper oxide superconductors
[DE88-005976] N88-22770

ALKENES

Evaluation of the acute toxicity of a synthetic polyalphaolefin-based hydraulic fluid
[AD-A190412] N88-22184

ALKYLATION

Evaluation of direct methane conversion to higher hydrocarbons and oxygenates
[DE88-003812] N88-22204

ALLOCATIONS

On two-stage allocation procedures for selection problems
[AD-A190766] N88-22675

ALLOYS

Electrical resistivities of some compound forming liquid metal alloys
[PB88-145172] N88-22137
Bithermal fatigue: A simplified alternative to thermomechanical fatigue N88-22424

ALTERNATING CURRENT

Advanced capacitor development
[AD-A189985] N88-22276

ALTERNATIVES

A systems analysis of fire suppression alternatives for the US space station
[AD-A189847] N88-22064

ALTITUDE SIMULATION

Age, alcohol, and simulated altitude: Effects on performance and breathalyzer scores
[AD-A190642] N88-22531

ALUMINUM

Fabrication and electrical characterization of multilevel aluminum interconnects used to achieve silicon-hybrid wafer-scale integration
[AD-A190519] N88-22282

ALUMINUM ALLOYS

Joints in fiber-reinforced aluminum alloys
[NASA-TT-20160] N88-22104
Processing, microstructure, and mechanical properties of silicon carbide particulate reinforced aluminum alloys
[AD-A188981] N88-22136
The effective fracture toughness of aluminum at rapid heating rates
[AD-A189745] N88-22146
The age hardening response of thermomechanically processed Al-Mg-Li alloys
[AD-A189870] N88-22147
Investigation and synthesis of high temperature and increased stiffness RSP aluminum alloys
[AD-A190407] N88-22151
Response of aluminum alloys to erosive particle impacts
[DE88-005910] N88-22159
The corrosion resistance of an aluminum alloy coated with polysilazane derived ceramics
[AD-A190703] N88-22189
Aluminum-air battery development
[DE88-006620] N88-22287

ALUMINUM COATINGS

Studies on hot-dip zinc-aluminum coated sheet steels
[ETN-88-92217] N88-22166

ALUMINUM OXIDES

Microwave sintering of alumina-SiC composites at 2.45 and 60 GHz
[DE88-006455] N88-22095
Processing defects and strength of alumina substrates
[W-10/87] N88-22441
The kinetics of contact noise in NaBeta alumina
[AD-A190651] N88-22707
Synthesis and characterization of high-T(sub c) screen-printed Y-Ba-Cu-O films on alumina
[NASA-TM-100860] N88-22805

AMAZON REGION (SOUTH AMERICA)

Project CODEAMA/FUNCATE (test-area of Barreirinha-AM): Field report
[INPE-4500-RPE/563] N88-22455
Surface CO results from the ABLE-2B expedition to Amazonia
[INPE-4501-PRE/1258] N88-22469
Surface ozone and ozonesounding results from the ABLE-2B expedition to Amazonia
[INPE-4523-PRE/1275] N88-22484
Aerodynamic aspects of the Amazon Forest
[INPE-4445-TDL/313] N88-22501

AMINO ACIDS

A program for the study of skeletal muscle catabolism following physical trauma
[AD-A189771] N88-22521

AMPLIFICATION

Amplification of signals in fiber optics using the stimulated Raman effect
[AD-A190281] N88-22727

AMPLITUDE DISTRIBUTION ANALYSIS

Near optimal blind deconvolution
[REPT-87-016] N88-22655

AMPLITUDE MODULATION

Magnet strength fluctuations in the SSC (Superconducting Super Collider) lattice. Part 2: Frequency modulation
[DE88-006491] N88-22774

ANALOG TO DIGITAL CONVERTERS

Fast analog-to-digital converter
[TI88-701488] N88-22543

ANALYSIS (MATHEMATICS)

Nonlinear analysis and optimal design of dynamic mechanical systems for spacecraft application
[AD-A190644] N88-22070
The analysis of non-linear dynamic behavior (including snap-through) of postbuckled plates by simple analytical solution
[NASA-TM-89165] N88-22439
Symmetry and global bifurcation in nonlinear solid mechanics
[AD-A190521] N88-22642

ANALYZERS

Instrumentation for the characterization and development of millimeter wave components compatible with monolithic integration
[AD-A189724] N88-22275
FLOSIN: A fluid loop analyzer for SINDA N88-22321
Two papers on a symbolic analyzer for MOS (Metal-Oxide Semiconductors) circuits
[AD-A188617] N88-22761

ANGULAR DISTRIBUTION

Angular resolved energy analysis of (69)Ga+ ions from a gallium liquid metal ion source
[AERE-R-12649] N88-22760

ANGULAR MOMENTUM

Collective rotation of molecules driven by the angular momentum of light in a nematic film
[FUB-6-1986] N88-22714

ANISOTROPIC PLATES

The buckling and vibration of composite plates using the Levy method considering shear deformation and rotary inertia
[AD-A189743] N88-22374

ANISOTROPY

Improvements to tilt rotor performance through passive blade twist control
[NASA-TM-100583] N88-22434

ANNEALING

Dynamical optimization techniques for the calculation of electronic structure in solids
[DE88-006010] N88-22768

ANNIHILATION REACTIONS

Annihilation momentum density of positrons trapped at vacancy-type defects in metals and alloys
[DE88-005936] N88-22797

ANNULAR FLOW

Interaction of a two-dimensional bluff body and incompressible jet and annulus flows
[AD-A190503] N88-22310

ANNULI

Embedded minimal surfaces with an infinite number of ends
[DE88-006429] N88-22680

ANOMALIES

Aerodynamic aspects of the Amazon Forest
[INPE-4445-TDL/313] N88-22501
Tropical circulations and the associated rainfall anomalies during two contrasting years
[INPE-4506-PRE/1261-REV] N88-22502
Recent developments in the path integral approach to anomalies
[DE87-703032] N88-22618

ANTARCTIC REGIONS

Radon-222 in the Antarctic Peninsula
[INPE-4486-PRE/1251] N88-22468

ANTENNA ARRAYS

Conformal microstrip slot antenna and antenna array
[AD-A189623] N88-22252

ANTENNA COMPONENTS

Features and applications of the integrated composites analyzer (ICAN) code N88-22391

ANTENNA DESIGN

Short experiment study of four-wire helical antennas (half turn half wave)
[CNES-CT/DRT/TIT/AN-249-T] N88-22266

ANTENNA RADIATION PATTERNS

Short experiment study of four-wire helical antennas (half turn half wave)
[CNES-CT/DRT/TIT/AN-249-T] N88-22266

ANTIMISSILE DEFENSE

Real-time stressed channel simulator
[AD-A190223] N88-22067
Constellation sizing for modest directed energy platforms
[DE88-007033] N88-22343
MPD (magnetoplasmadynamic) thruster advanced pumping system concepts
[AD-A190513] N88-22756

ANTIMONY COMPOUNDS

Activities of As, Sb, Bi and Pb in copper mattes and their effects on impurity elimination
[TKK-V-A10(1988)] N88-22165

ANTIREFLECTION COATINGS

Oxide optical coatings prepared by metal-organic vapor deposition
[DE88-006809] N88-22175

APERTURES

Experimental determination of the coefficients of the hydraulic resistance of apertures in the rotary disks
[AD-A190627] N88-22317

APPLICATIONS PROGRAMS (COMPUTERS)

Monolithic ceramic analysis using the SCARE program N88-22409
Continuous fiber ceramic matrix composites for heat engine components N88-22411

APPROXIMATION

A posterior error estimation in a finite element method for parabolic partial differential equations
[AD-A190296] N88-22636
An approximation technique for solving a system of Fredholm integral equations for asymmetric detector response functions
[AD-A190577] N88-22645
Constructive version of the approximation induction principle
[PB88-165477] N88-22647
Approximations in extreme value theory
[AD-A189817] N88-22659
Approximation methods for the identification and control of distributed parameter systems
[AD-A190201] N88-22662
Extreme value for dependent sequences via the Stein-Chen method of poisson approximation
[AD-A190325] N88-22668

APTITUDE

Properties of some Bayesian scoring procedures for computerized adaptive tests
[AD-A189925] N88-22660

ARC DISCHARGES

Study of surface discharges
[ONERA-12/7236-PY] N88-22073

ARC JET ENGINES
MPD (magnetoplasmadynamic) thrust chamber flow dynamics
[AD-A189940] N88-22751
ARC MELTING
Growth and deformation mechanisms of refractory alloy hybrid materials
[AD-A190492] N88-22152
Evaporation characteristics of elements during vacuum arc remelting of alloy A-286 N88-22248
ARCHITECTURE
Real-time stressed channel simulator
[AD-A190223] N88-22067
A direct-execution parallel architecture for the Advanced Continuous Simulation Language (ACSL)
[NASA-CR-182609] N88-22602
ARCHITECTURE (COMPUTERS)
Adaptive neural network architecture
[AD-A190114] N88-22533
Parallel memory addressing using coincident optical pulses
[AD-A189767] N88-22547
Multiple-transform pipelines for image coding
[REPT-87-038] N88-22561
An analysis of multiple grain CHIP architectures
[AD-A189942] N88-22570
Transformations of concurrent algorithms for highly parallel systems: A one year project summary report
[AD-A190236] N88-22576
Inference engine for expert systems
[INPE-4465-TDL/321] N88-22590
Modeling a parallel architecture for image processing
[RR-646-I] N88-22593
Simulation of fault tolerance in a hypercube arrangement of discrete processors
[AD-A189682] N88-22594
The modeling, simulation and comparison of interconnection networks for parallel processing
[AD-A190571] N88-22599
Design and implementation of a parallel computer for expert system applications
[DE88-005288] N88-22601
Concurrent algorithms for a mobile robot vision system
[DE88-005850] N88-22614
High speed transcendental elementary function architecture in support of the Vector Wave Equation (VWE)
[AD-A189746] N88-22627
Space-variant optical systems
[AD-A189967] N88-22724
Application of new technologies to DTIC document processing
[AD-A189778] N88-22823
A methodolgy, based on analytical modeling, for the design of parallel and distributed architectures for relational database query processors
[AD-A189844] N88-22825
New generation knowledge processing, volume 1
[AD-A190165] N88-22826
ARCTIC REGIONS
Real-time environmental Arctic monitoring (R-TEAM)
[AD-A189948] N88-22508
ARGON LASERS
The interaction of small particles with laser beams
[AD-A190716] N88-22354
ARM (ANATOMY)
A three dimensional non-singular modelling of rigid manipulators
[AD-A189707] N88-22604
ARMATURES
Analytic solutions to dynamic equations of plasma armature railguns
[DE88-006842] N88-22057
ARRAYS
Electromagnetic sensor arrays for nondestructive evaluation and robot control
[AD-A190210] N88-22260
Coupled high power waveguide laser research
[AD-A189800] N88-22345
Today's photovoltaic systems: An evaluation of their performance
[DE88-006926] N88-22457
Self-checking logic arrays
[RR-656-I] N88-22545
ARSENIDES
Activities of As, Sb, Bi and Pb in copper mattes and their effects on impurity elimination
[TKK-V-A10(1988)] N88-22165
ARTIFICIAL INTELLIGENCE
Comparative analysis
[AD-A190556] N88-22313
Instrumentation for scientific computing in neural networks, information science, artificial intelligence and applied mathematics
[AD-A189981] N88-22549
A probabilistic approach to low-level vision
[AD-A189041] N88-22553
An intelligent simulation model generator
[REPT-87-053] N88-22562
Inference engine for expert systems
[INPE-4465-TDL/321] N88-22590
Memory-based expert systems
[AD-A190203] N88-22606
Synapses that compute motion
[AD-A190389] N88-22607
Multi-disciplinary techniques for understanding time-varying space-based imagery
[AD-A190711] N88-22610
Discrete event simulation in the artificial intelligence environment
[DE88-004296] N88-22613
Multivariate analysis and its application
[AD-A189983] N88-22661
Rigidity and smoothness of motion
[AD-A190555] N88-22694
ROVER: A prototype active vision system
[AD-A189246] N88-22722
Autonomous control system for Czochralski growth of LEC GaAs
[AD-A189726] N88-22779
The Scientific and Technical Information Network (STINET). Foundation for evolution
[AD-A189750] N88-22822
Data base design and implementation
[AD-A190414] N88-22827
ARTIFICIAL SATELLITES
Numerical orbit propagation methods for earth artificial satellites
[INPE-4405-RPE/556] N88-22053
Chronology of China's successful satellite launchings N88-22234
ASSOCIATIVE PROCESSING (COMPUTERS)
Optical Conceptual Computing and Associative Memory (OCCAM)
[AD-A190030] N88-22550
Rapid feature extraction via the radon transform
[AD-A190032] N88-22573
ASTEROIDS
Speckle interferometry of asteroids
[NASA-CR-180438] N88-22843
ASTRONAUTS
Design, development and evaluation of Stanford/Ames EVA prehensors
[NASA-CR-182688] N88-22540
ASTRONOMICAL SPECTROSCOPY
Multiple object redshift determinations in clusters of galaxies using OCTOPUS
[INPE-4528-PRE/1278] N88-22835
ASTROPHYSICS
Particle cosmology comes of age
[DE88-006998] N88-22844
ASYMMETRY
Multiple scattering from nonspherical targets
[AD-A189939] N88-22723
ASYMPTOTIC METHODS
Estimation of convolution tails
[AD-A190323] N88-22666
ATLANTIC OCEAN
Forecast of Atlantic seasonal hurricane activity for 1988 N88-22500
ATMOSPHERIC BOUNDARY LAYER
Unsteady aerodynamics of a Wortmann FX-63-137 wing in a fluctuating wind field
[AD-A190128] N88-22006
Spectral measurements in a disturbed boundary layer over snow
[AD-A190217] N88-22494
ATMOSPHERIC CHEMISTRY
Atmospheric carbon dioxide and the global carbon cycle: The key uncertainties
[DE88-005059] N88-22465
Effect of vibrational excitation on rate parameters of atmospheric reactions
[AD-A190464] N88-22477
Surface ozone and ozonesounding results from the ABLE-2B expedition to Amazonia
[INPE-4523-PRE/1275] N88-22484
ATMOSPHERIC CIRCULATION
Stellar scintillometer atmospheric optical turbulence profiling experiment: A qualitative comparison of two identical instruments at AMOS (Air Force Maui Optical Station), 1985
[AD-A190589] N88-22479
Aerodynamic aspects of the Amazon Forest
[INPE-4445-TDL/313] N88-22501
Tropical circulations and the associated rainfall anomalies during two contrasting years
[INPE-4506-PRE/1261-REV] N88-22502
Ocean general circulation models: Report on proceedings of a meeting of ocean and climate modelers
[DE88-005530] N88-22504
ATMOSPHERIC COMPOSITION
Assessment of crop loss from air pollutants: Meteorology-atmospheric chemistry and long range transport
[PB88-146857] N88-22448
Surface CO results from the ABLE-2B expedition to Amazonia
[INPE-4501-PRE/1258] N88-22469
ATMOSPHERIC DENSITY
A method of atmospheric density measurements during space shuttle entry using ultraviolet-laser Rayleigh scattering
[NASA-TM-100056] N88-22337
A survey of denser-than-air atmospheric dispersion models
[DE88-006626] N88-22467
ATMOSPHERIC ELECTRICITY
The growth potential of corona discharges from aircraft flying in precipitation
[AD-A190507] N88-22478
ATMOSPHERIC MODELS
Derivation of consistent surface fixed fields for use in a global NWP model
[AD-A190131] N88-22475
A study on electric fields and conductivity associated with electrified clouds in the region of South America
[INPE-4487-TDL/325] N88-22486
Ocean general circulation models: Report on proceedings of a meeting of ocean and climate modelers
[DE88-005530] N88-22504
ATMOSPHERIC PHYSICS
Plasmapause formation
[AERONOMICA-ACTA-A-319-1987] N88-22759
ATMOSPHERIC RADIATION
Radon-222 in the Antarctic Peninsula
[INPE-4486-PRE/1251] N88-22468
ATMOSPHERIC SOUNDING
Coordinated Auroral Experiments using Scatter And Rocket investigations (CAESAR investigations)
[MPAE-W-47-87-13] N88-22487
A multivariate variational objective analysis-assimilation method. Part 1: Development of the basic model
[NASA-CR-182651] N88-22491
ATMOSPHERIC TEMPERATURE
Ultraviolet absorption cross sections of methylbromide at stratospheric temperatures
[AERONOMICA-ACTA-A-320-1987] N88-22132
ATMOSPHERIC TURBULENCE
Stellar scintillometer atmospheric optical turbulence profiling experiment: A qualitative comparison of two identical instruments at AMOS (Air Force Maui Optical Station), 1985
[AD-A190589] N88-22479
ATOMIC ENERGY LEVELS
Electronic energy transfer processes in the alkali/alkaline earth metal vapors
[AD-A190035] N88-22119
ATOMIC STRUCTURE
Research on stable processible conducting polymers for electronic applications
[AD-A190246] N88-22180
Dynamical optimization techniques for the calculation of electronic structure in solids
[DE88-006010] N88-22768
First-principles calculations of quasiparticle energies at surfaces and interfaces: Semiconductor surface-state spectra and band offsets
[DE88-006340] N88-22773
Experimental studies on electronic properties of HgTe/CdTe and Hg sub 1-z Cd sub x Te/CdTe heterostructures and superlattices
[AD-A189826] N88-22783
ATTENTION
Selective mechanisms in auditory and bimodal signal processing
[AD-A190529] N88-22530
ATTITUDE CONTROL
Multivariable control law design for the AFTI/F-16 with a failed control surface using a parameter-adaptive controller
[AD-A189848] N88-22040
AUDIO FREQUENCIES
Performance of single and multiple system AM stereo decoder receivers
[PB88-168307] N88-22265
Auditory pattern memory: Mechanisms of tonal sequence discrimination by human observers
[AD-A190337] N88-22534

AUDITORY PERCEPTION
Mechanisms mediating perception of complex acoustic patterns
[AD-A189765] N88-22520
Complex sound processing: An interdisciplinary approach
[AD-A189782] N88-22523
Perception of complex auditory patterns
[AD-A190218] N88-22524
Auditory perception of complex sounds
[AD-A190528] N88-22529
Mechanisms mediating the perception of complex acoustic patterns
[AD-A190112] N88-22705
AUDITORY SIGNALS
Complex sound processing: An interdisciplinary approach
[AD-A189782] N88-22523
Auditory perception of complex sounds
[AD-A190528] N88-22529
Selective mechanisms in auditory and bimodal signal processing
[AD-A190529] N88-22530
Auditory pattern memory: Mechanisms of tonal sequence discrimination by human observers
[AD-A190337] N88-22534
AUDITORY STIMULI
Complex sound processing: An interdisciplinary approach
[AD-A189782] N88-22523
Auditory pattern memory: Mechanisms of tonal sequence discrimination by human observers
[AD-A190337] N88-22534
AUGMENTATION
Real-time flight test data distribution and display
[NASA-TM-100424] N88-22050
Theoretical studies of Resonance Enhanced Stimulated Raman Scattering (RESRS) of frequency-doubled Alexandrite laser wavelength in cesium vapor
[NASA-CR-182870] N88-22133
AURORAL ARCS
Coordinated Auroral Experiments using Scatter And Rocket investigations (CAESAR investigations)
[MPAE-W-47-87-13] N88-22487
AURORAL TEMPERATURE
Support for FY87 midlatitude electron-density calibration campaign
[AD-A190174] N88-22476
AURORAS
On the acceleration of electrons and positive ions in the same direction along magnetic field lines by parallel electric fields
[IRF-PREPRINT-103] N88-22488
AUTOMATIC CONTROL
Autonomous control system for Czochralski growth of LEC GaAs
[AD-A189726] N88-22779
The necessity of automation in Brazil
[INPE-4346-PRE/1183] N88-22832
AUTOMATIC FLIGHT CONTROL
Preliminary airworthiness evaluation of the UH-60A with Advanced Digital Optical Control System (ADOCS)
[AD-A190674] N88-22030
AUTOMOBILE FUELS
Technical highlights of the Alternative Fuels Utilization Program
[DE88-005064] N88-22205
AUTOREGRESSIVE PROCESSES
Consistent estimates of autoregressive parameters for autoregressive moving average models
[RR-663-I] N88-22564
AVALANCHE DIODES
Examination of temperature effects on gate-to-drain avalanche breakdown in GaAs MESFETs (Metal-Semiconductor Field Effect Transistors) by measuring light emission under RF drive
[AD-A189634] N88-22778
AVIONICS
General aviation activity and avionics survey: 1986 data
[AD-A189986] N88-22003
Reliability analysis within a Computer Aided Engineering (CAE) infrastructure
[NLR-MP-86059-U] N88-22369
Information systems for quality. Experience at the Nerviano Aeritalia plant. Avionic systems and equipment group
[ETN-88-92274] N88-22821
AXIAL FLOW TURBINES
Visualization of flows in turbomachinery
[AD-A189927] N88-22299
Visualisation of the flow at the tip of a high speed axial flow turbine rotor
[AD-A189928] N88-22300
Visualisation of the flow at the tip of a high speed axial flow turbine rotor: An assessment of flow visualisation techniques and the requirement of the experimental turbine
[AD-A189929] N88-22301
AXIAL LOADS
Damage models for delamination and transverse fracture
[AD-A189652] N88-22088
Numerical and experimental research on propagation of elastic stress waves in conical shell under axial impulsive loading N88-22238
AXIAL STRESS
An investigation of the failure response of laminates under biaxial stress
[AD-A190039] N88-22090
AXISYMMETRIC FLOW
Visualisation of the flow at the tip of a high speed axial flow turbine rotor
[AD-A189928] N88-22300

B

BACKGROUND NOISE
Stellar scintillometer atmospheric optical turbulence profiling experiment: A qualitative comparison of two identical instruments at AMOS (Air Force Maui Optical Station), 1985
[AD-A190589] N88-22479
BACKGROUND RADIATION
A map of the cosmic background radiaton at 3 millimeters
[INPE-4529-PRE/1279] N88-22850
BANDWIDTH
High speed, bandpass sampling of digital communications waveforms
[AD-A189842] N88-22254
Monolithic phase shifter study
[AD-A190213] N88-22278
BARIUM
Magnetic anomalies in the rare earth oxide superconductors GdBa2Cu3O(7-x) and YbBa2Cu3O(7-x)
[AD-A190713] N88-22793
Synthesis and characterization of high-T(sub c) screen-printed Y-Ba-Cu-O films on alumina
[NASA-TM-100860] N88-22805
BARIUM OXIDES
Melt processing ceramic YBa2Cu3O(sub 6.9)
[DE88-007039] N88-22199
Superconductivity and the tailoring of lattice parameters of the compound YBa2Cu3O(sub x)
[DE88-005904] N88-22769
High temperature superconductors in the La(sub 1+x)Ba(sub 2-x)Cu O(sub y system
[DE88-006367] N88-22802
BARRIER LAYERS
Calculating depletion region carrier concentrations with capacitance-voltage measurements and etching
[AD-A189630] N88-22777
BASE PRESSURE
An experimental investigation of rocket ramjet nozzle assembly base pressures
[AD-A189714] N88-22076
BASIC (PROGRAMMING LANGUAGE)
Computer program in BASIC language for computation of spectrochemical analytical data
[DE88-701229] N88-22106
BATTERY CHARGERS
GTE battery management system: State of charge indicator evaluation
[DE88-006800] N88-22272
BAYES THEOREM
Sequential tests for the drift of a Wiener process with a smooth prior and the heat equation
[AD-A190322] N88-22638
Properties of some Bayesian scoring procedures for computerized adaptive tests
[AD-A189925] N88-22660
Admissible Bayes tests for structural relationship
[AD-A190326] N88-22669
Empirical and hierarchical Bayes competitors of preliminary test estimators in two sample problems
[AD-A190327] N88-22670
On two-stage allocation procedures for selection problems
[AD-A190766] N88-22675
BAYS (STRUCTURAL UNITS)
Moving-bank multiple model adaptive estimation applied to flexible spacestructure control
[AD-A190761] N88-22071
BEAMS (RADIATION)
Variable-energy positron studies on liquids and liquid-solid interfaces
[DE88-006356] N88-22109
The interaction of small particles with laser beams
[AD-A190716] N88-22354
Ultrasonic beam distortion in transversely isotropic media
[DE88-005937] N88-22699
Optical switching and control techniques using nonlinear optical wave mixing
[AD-A190467] N88-22730
BEAMS (SUPPORTS)
Stabilization and control problems in structural dynamics
[AD-A190197] N88-22361
Coupled bending-torsion steady-state respcnse of pretwisted, nonuniform rotating beams using a transfer-matrix method
[NASA-TM-100596] N88-22435
BEARING (DIRECTION)
Relative orientation
[AD-A190365] N88-22449
BEARINGS
Mode 2 fracture mechanics N88-22418
BEHAVIOR
An evaluation of the effects of high visual taskload on the separate behaviors involved in complex monitoring performance
[AD-A190641] N88-22538
BELLMAN THEORY
Normed Bellman equation with degenerate diffusion coefficients and its application to differential equations
[AD-A190319] N88-22637
BENDING
An efficient Mindlin finite strip plate element based on assumed strain distribution N88-22407
Coupled bending-torsion steady-state response of pretwisted, nonuniform rotating beams using a transfer-matrix method
[NASA-TM-100596] N88-22435
Non-rigid motion and Regge calculus
[AD-A190387] N88-22640
BESSEL FUNCTIONS
Expressing mathematical subroutines constructively
[AD-A190559] N88-22644
Distributions of quadratic forms
[AD-A190224] N88-22663
BIBLIOGRAPHIES
Artificial neural networks: An introduction with an annotated bibliography
[DE88-007003] N88-22603
BINARY ALLOYS
Fundamental studies on high temperature deformation recrystallization, and grain growth of two-phase materials
[AD-A189725] N88-22145
Corrosion and electrochemical behavior of binary magnesium alloys
[AD-A190624] N88-22154
BINDERS (MATERIALS)
Effect of moisture level in PBXW-109(E) (plastic-bonded explosive) mixes on the aging of the cured explosive
[AD-A190200] N88-22202
BIOCONTROL SYSTEMS
Motion sickness: Quantitative, algorithmic malaise indication in real time
[AD-A189674] N88-22518
BIODYNAMICS
Analysis of head response to torso acceleration. Volume 2: Description of data retrieval, analysis and display software
[PB88-156765] N88-22536
BIOLOGICAL EFFECTS
Protection against laser damage to human body reviewed N88-22237
BIONICS
Complex sound processing: An interdisciplinary approach
[AD-A189782] N88-22523
BIOPHYSICS
Synapses that compute motion
[AD-A190389] N88-22607
BIOTECHNOLOGY
JPRS report: Science and technology. Japan
[JPRS-JST-88-001] N88-22218
BISMUTH SULFIDES
Activities of As, Sb, Bi and Pb in copper mattes and their effects on impurity elimination
[TKK-V-A10(1988)] N88-22165
BISTABLE CIRCUITS
Applications of optical computing to problems with symbolic computations
[AD-A189772] N88-22548
BIT ERROR RATE
Direct bit detection receiver noise performance analysis for 32-PSK and 64-PSK modulated signals
[AD-A190009] N88-22256

BITS
Direct bit detection receiver noise performance analysis for 32-PSK and 64-PSK modulated signals
[AD-A190009] N88-22256
BLADE-VORTEX INTERACTION
Advancing-side directivity and retreating-side interactions of model rotor blade-vortex interaction noise
[NASA-TP-2784] N88-22710
BLAST LOADS
Buckling of blast loaded cylinder
[AD-A190124] N88-22376
BLUFF BODIES
Interaction of a two-dimensional bluff body and incompressible jet and annulus flows
[AD-A190503] N88-22310
BLUNT BODIES
Interaction of a two-dimensional bluff body and incompressible jet and annulus flows
[AD-A190503] N88-22310
Numerical study of unsteady viscous hypersonic blunt body flows with an impinging shock
[NASA-TM-100096] N88-22650
High-resolution shock-capturing schemes for inviscid and viscous hypersonic flows
[NASA-TM-100097] N88-22651
BODY-WING CONFIGURATIONS
Transonic Navier-Stokes computations of strake-generated vortex interactions for a fighter-like configuration
[NASA-TM-100009] N88-22010
Laser velocimeter measurements in a wing-fuselage type juncture
[NASA-TM-100588] N88-22012
BOLOMETERS
Preparing the Alcator C bolometer system for use on MTX (Microwave Tokamak Experiment)
[DE88-006724] N88-22733
BOLTS
Increasing strength of graphite/epoxy bolted joints by introducing an adhesively bonded metallic insert
[FFA-TN-1987-45] N88-22442
BONDING
Fracture toughness of silicon nitride-silicon nitride joints bonded with oxynitride glass
[DE88-005548] N88-22172
BOOLEAN ALGEBRA
Two papers on a symbolic analyzer for MOS (Metal-Oxide Semiconductors) circuits
[AD-A188617] N88-22761
BORIDES
The combustion synthesis of boride composites
[DE88-005474] N88-22084
BORN APPROXIMATION
Seismic inversion by a RMS (Root-Mean-Square) Born approximation in the space-time domain
[PB88-165402] N88-22711
BORON
The structure of the boron-hydrogen complex in silicon
[DE88-005433] N88-22795
BORON CARBIDES
The combustion synthesis of boride composites
[DE88-005474] N88-22084
BORON CHLORIDES
Advanced B and Al combustion kinetics over wide temperature ranges
[AD-A190752] N88-22128
BORON NITRIDES
Hermetic coating of optical fibers
[AD-A189886] N88-22177
BORON REINFORCED MATERIALS
Joints in fiber-reinforced aluminum alloys
[NASA-TT-20160] N88-22104
BOSONS
Einstein metrics and Brans-Dicke superfields
[DE88-006992] N88-22809
Involution-dependent constants and the cancellation of divergences in the 1-loop open string amplitude
[DE88-006537] N88-22811
BOUNDARIES
Finding texture boundaries in images
[AD-A190554] N88-22609
BOUNDARY ELEMENT METHOD
Boundary element method for three-dimensional magnetostatic fields in terms of vector variables
[EL-61] N88-22649
BOUNDARY LAYER CONTROL
Control of laminar flow around of the wing in free-air conditions
[AD-A187479] N88-22004
Modifications to the Langley 8-foot transonic pressure tunnel for the laminar flow control experiment
[NASA-TM-4032] N88-22047
Investigation of boundary layer disturbances caused by periodic heating of a thin ribbon
[AD-A190572] N88-22314
BOUNDARY LAYER EQUATIONS
The sensitivity of boundary layer instability growth rates to compliant wall properties
[AD-A190433] N88-22309
BOUNDARY LAYER FLOW
Boundary-layer and wake measurements on a swept, circulation-control wing
[NASA-TM-89426] N88-22013
Visualization of flows in turbomachinery
[AD-A189927] N88-22299
Cavitation inception in rectangular two-dimensional slots
[AD-A190677] N88-22318
Theoretical investigation of secondary instability of three-dimensional boundary-layer flows with application to the DFVLR-F5 model wing
[DFVLR-FB-87-44] N88-22330
BOUNDARY LAYER PLASMAS
Fundamental studies on MPD thrusters
[AD-A190307] N88-22753
BOUNDARY LAYER STABILITY
Oscillating airfoils: Achievements and conjectures
[AD-A190490] N88-22008
The sensitivity of boundary layer instability growth rates to compliant wall properties
[AD-A190433] N88-22309
Investigation of boundary layer disturbances caused by periodic heating of a thin ribbon
[AD-A190572] N88-22314
Theoretical investigation of secondary instability of three-dimensional boundary-layer flows with application to the DFVLR-F5 model wing
[DFVLR-FB-87-44] N88-22330
Spectral measurements in a disturbed boundary layer over snow
[AD-A190217] N88-22494
BOUNDARY LAYER TRANSITION
Control of laminar flow around of the wing in free-air conditions
[AD-A187479] N88-22004
The sensitivity of boundary layer instability growth rates to compliant wall properties
[AD-A190433] N88-22309
Theoretical investigation of secondary instability of three-dimensional boundary-layer flows with application to the DFVLR-F5 model wing
[DFVLR-FB-87-44] N88-22330
BOUNDARY LAYERS
High Reynolds number, low Mach number, steady flow field calculations over a NACA 0012 airfoil using Navier-Stokes and interactive boundary layer theory
[AD-A189871] N88-22005
BOUNDARY VALUE PROBLEMS
Global spatial periodic solutions to the Ginzburg-Landau equations
[DE88-006424] N88-22623
Numerical methods for singularly perturbed differential equations with applications
[AD-A189786] N88-22628
Pointwise stabilization for coupled quasilinear and linear wave equations
[AD-A190031] N88-22632
Sequential tests for the drift of a Wiener process with a smooth prior and the heat equation
[AD-A190322] N88-22638
Stopping rules and observed significance levels
[AD-A190320] N88-22664
BRAGG ANGLE
Models for electromagnetic scattering from the sea at extremely low grazing angles
[AD-A190472] N88-22261
BRANCHING (MATHEMATICS)
Bifurcations in unsteady aerodynamics-implications for testing
[NASA-TM-100083] N88-22014
Symmetry and global bifurcation in nonlinear solid mechanics
[AD-A190521] N88-22642
BRAYTON CYCLE
Comparison of entropy generation and conventional design methods for heat exchangers
[AD-A190256] N88-22306
BRAZIL
Radon-222 in the Antarctic Peninsula
[INPE-4486-PRE/1251] N88-22468
The necessity of automation in Brazil
[INPE-4346-PRE/1183] N88-22832
The 1985 mutual phenomena of Jupiter's satellites observed in Brazil
[INPE-4526-PRE/1276] N88-22848
BRAZILIAN SPACE PROGRAM
INPE position paper on the CCSDS standardized method of link budget computation
[INPE-4533-NTE/279] N88-22820
BRITTLENESS
High-performance polymeric materials
[AD-A190708] N88-22190
Strength and microstructure of ceramics
[AD-A190712] N88-22191
Fracture technology for brittle materials N88-22417
BROMIDES
Ultraviolet absorption cross sections of methylbromide at stratospheric temperatures
[AERONOMICA-ACTA-A-320-1987] N88-22132
BROWNIAN MOVEMENTS
Filtering of jump processes
[AD-A189701] N88-22656
BUBBLE MEMORY DEVICES
High density ion implanted contiguous disk bubble technology
[AD-A190169] N88-22789
BUBBLE TECHNIQUE
High density ion implanted contiguous disk bubble technology
[AD-A190169] N88-22789
BUBBLES
Detecting the gas bubbles in a liquid metal coolant by means of magnetic flowmeters
[TI88-701427] N88-22294
The elliptic Sinh-Gordon equation and the construction of toroidal soap bubbles
[DE88-006426] N88-22585
BUCKLING
Postbuckling delamination of a stiffened composite panel using finite element methods
[NASA-CR-182803] N88-22098
Cubic spline solution of symmetric buckling problems of clamped shallow spherical shells N88-22239
The buckling and vibration of composite plates using the Levy method considering shear deformation and rotary inertia
[AD-A189743] N88-22374
Buckling of blast loaded cylinder
[AD-A190124] N88-22376
The analysis of non-linear dynamic behavior (including snap-through) of postbuckled plates by simple analytical solution
[NASA-TM-89165] N88-22439
BUDGETS
INPE position paper on the CCSDS standardized method of link budget computation
[INPE-4533-NTE/279] N88-22820
BUOYANCY
Heat transfer from a negatively buoyant wall jet
[NBS-GCR-88-541] N88-22208
BURNING RATE
Crack opening and extension in inert solid propellant. An experimental study
[AD-A189808] N88-22201

C

CALCULUS
Martingale representation and the Malliavin calculus
[AD-A189721] N88-22626
Non-rigid motion and Regge calculus
[AD-A190387] N88-22640
Filtering of jump processes
[AD-A189701] N88-22656
CALCULUS OF VARIATIONS
The inverse power method for semilinear elliptic equations
[DE88-006427] N88-22620
CALIBRATING
A 150,000 pounds per square inch dynamic pressure calibrator
[AD-A190659] N88-22335
Support for FY87 midlatitude electron-density calibration campaign
[AD-A190174] N88-22476
Stellar scintillometer atmospheric optical turbulence profiling experiment: A qualitative comparison of two identical instruments at AMOS (Air Force Maui Optical Station), 1985
[AD-A190589] N88-22479
Computer grading of extensometers (BS 3846)
[NPL-DMA(A)-152] N88-22560
CALIFORNIA
Hydrographic data from the OPTOMA (Ocean Prediction Through Observation, Modeling and Analysis) program: OPTOMA 23, 9-19 November 1986
[AD-A189868] N88-22506
CAMERAS
ROVER: A prototype active vision system
[AD-A189246] N88-22722
An investigation of the crystalchemistry and thermochemistry of selected mineral systems
[AD-A189758] N88-22781

CANADA
Northern lights: The economic and practical potential of imported power from Canada
[DE88-006026] N88-22473
CANOPIES (VEGETATION)
Surface CO results from the ABLE-2B expedition to Amazonia
[INPE-4501-PRE/1258] N88-22469
CAPACITANCE-VOLTAGE CHARACTERISTICS
Calculating depletion region carrier concentrations with capacitance-voltage measurements and etching
[AD-A189630] N88-22777
CAPACITORS
Advanced capacitor development
[AD-A189985] N88-22276
CAPILLARY FLOW
Continual capillary viscosimetry using extrusiograph techniques
[PB88-166293] N88-22195
CARBAZOLES
Research on stable processible conducting polymers for electronic applications
[AD-A190246] N88-22180
CARBON
Hermetic coating of optical fibers
[AD-A189886] N88-22177
CARBON CYCLE
Atmospheric carbon dioxide and the global carbon cycle: The key uncertainties
[DE88-005059] N88-22465
Simulation analysis of moored fluorometer time series from the Mid-Atlantic Bight
[DE88-006066] N88-22505
CARBON DIOXIDE
Atmospheric carbon dioxide and the global carbon cycle: The key uncertainties
[DE88-005059] N88-22465
A laser-based photoacoustic spectrometer for direct breath C-13O2/C-12O2 measurement
[DE88-004915] N88-22516
CARBON DIOXIDE CONCENTRATION
Atmospheric carbon dioxide and the global carbon cycle: The key uncertainties
[DE88-005059] N88-22465
Surface CO results from the ABLE-2B expedition to Amazonia
[INPE-4501-PRE/1258] N88-22469
CARBON DIOXIDE LASERS
Laser processing-status, perspectives N88-22211
Compound ceramic processing N88-22212
Single crystal growth by laser CVD N88-22213
Hard ceramic film by laser PVD N88-22216
Coupled high power waveguide laser research
[AD-A189800] N88-22345
Laser evaporation studies
[AD-A189815] N88-22348
CARBON FIBER REINFORCED PLASTICS
Fractography of composite delamination
[NASA-CR-182757] N88-22096
CARBON FIBERS
Structure and surface characterizations of high strength carbon fibers
[AD-A189642] N88-22087
Interfacial structure-property relationships at the fiber-matrix interphase in advanced composites
[AD-A190649] N88-22093
Thermal expansion behavior of randomly oriented short carbon fiber reinforced copper composites
[NASA-TT-20175] N88-22099
Reciprocating sliding wear characteristics of copper-carbon fiber composites
[NASA-TT-20176] N88-22100
Eddy current nondestructive inspection of graphite epoxy using ferrite cup core probes
[AD-A189823] N88-22365
CARBONYL COMPOUNDS
The spectroscopy and reaction kinetics of coordinatively unsaturated metal carbonyls
[AD-A190533] N88-22124
CARTESIAN COORDINATES
COMESH: A corner mesh finite difference code to solve multigroup diffusion equations in multidimensions
[DE88-701248] N88-22555
CASCADE FLOW
Mixed direct-inverse problem of transonic cascade N88-22244
Effect of freestream turbulence on a two dimensional cascade, with different surface roughness, at high Reynolds number
[AD-A190615] N88-22316
Designs of profiles for cascades
[NASA-TT-20161] N88-22326
CATABOLISM
A program for the study of skeletal muscle catabolism following physical trauma
[AD-A189771] N88-22521
CATALOGS (PUBLICATIONS)
NASA scientific and technical publications: A catalog of Special Publications, Reference Publications, Conference Publications, and Technical Papers, 1987
[NASA-SP-7063(02)] N88-22830
CATALYSIS
On copper peroxide
[NASA-TT-20263] N88-22135
CATALYSTS
Evaluation of direct methane conversion to higher hydrocarbons and oxygenates
[DE88-003812] N88-22204
CATHODES
Theoretical model of the cathode spot on a unipolar arc
[AD-A190109] N88-22277
Aluminum-air battery development
[DE88-006620] N88-22287
CAVITATION FLOW
Cavitation inception in rectangular two-dimensional slots
[AD-A190677] N88-22318
CAVITY RESONATORS
Status of RF superconductivity at Argonne National Laboratory
[DE88-005913] N88-22796
CELESTIAL MECHANICS
Periodic orbits around a satellite modelled as a triaxial ellipsoid
[AD-A190592] N88-22051
CEMENTS
Cement paste matrix composite materials center
[AD-A188657] N88-22083
CENTRIFUGES
Vacuum-arc plasma centrifuge experiment
[INPE-4509-PRE/1263] N88-22758
CEPHEID VARIABLES
Near-infrared observations of cepheids: The distance to M33 N88-22846
CERAMIC COATINGS
The corrosion resistance of an aluminum alloy coated with polysilazane derived ceramics
[AD-A190703] N88-22189
CERAMIC FIBERS
High-T(sub c) superconducting wire fabrication and testing
[DE88-005989] N88-22798
CERAMIC MATRIX COMPOSITES
Fracture toughness testing of a ceramic matrix composite
[AD-A189846] N88-22089
A test for interfacial effects and stress transfer in ceramic matrix composites
[NASA-CR-182758] N88-22194
Continuous fiber ceramic matrix composites for heat engine components N88-22411
Fracture technology for brittle materials N88-22417
CERAMICS
Interfacial structure-property relationships at the fiber-matrix interphase in advanced composites
[AD-A190649] N88-22093
Specimen preparation techniques for the examination of ceramic and metal-matrix composites
[DE88-005157] N88-22094
Thermal conductivity of oxide ceramics
[DE88-005842] N88-22169
Ultrasonic characterization of ceramic joints
[DE88-005844] N88-22173
Temperature-dependent conductivity of oxygen-depleted YBCO ceramics
[AD-A190340] N88-22182
Transformation toughening of ceramics
[AD-A190399] N88-22183
Stress corrosion of ceramic materials
[AD-A190501] N88-22187
High-performance polymeric materials
[AD-A190708] N88-22190
Strength and microstructure of ceramics
[AD-A190712] N88-22191
High temperature corrosion of ceramics
[DE88-006567] N88-22193
Hafnia-rich mixed oxide ceramics of the system HfO2-ZrO2-TiO2 for heaters and heat exchangers in electrothermal thrusters: The effects of titania on selected electrical and mechanical properties of Hafnia-rich mixed oxides in the system Hafnia-Zirconia-Titania, volume 1
[NASA-CR-182800-VOL-1] N88-22197
Gamma-ray densitometry: Nondestructive analysis of density evolution during ceramic powder processing
[DE88-006671] N88-22198
Melt processing ceramic YBa2Cu3O(sub 6.9)
[DE88-007039] N88-22199
JPRS report: Science and technology. Japan
[JPRS-JST-88-002] N88-22210
Compound ceramic processing N88-22212
Hard ceramic film by laser PVD N88-22216
Function of Japan Fine Ceramics Center described N88-22227
JPRS report: Science and technology. Japan
[JPRS-JST-87-029] N88-22228
Developments in ceramic superconducting materials N88-22229
An evaluation of nondestructive methods for ceramic heat exchanger applications
[DE88-006731] N88-22328
Monolithic ceramic analysis using the SCARE program N88-22409
Whisker-reinforced ceramic composites for heat engine components N88-22410
Nondestructive evaluation of sintered ceramics N88-22416
Magnetic anomalies in the rare earth oxide superconductors GdBa2Cu3O(7-x) and YbBa2Cu3O(7-x)
[AD-A190713] N88-22793
Synthesis and characterization of high-T(sub c) screen-printed Y-Ba-Cu-O films on alumina
[NASA-TM-100860] N88-22805
CETANE
Cetane scale evaluation and possible modification
[AD-A189730] N88-22200
CHALLENGER (ORBITER)
Space shuttle accident: NASA's actions to address the Presidential Commission report
[PB88-135306] N88-22059
CHANNEL CAPACITY
Information and coding capacities of mismatched Gaussian channels
[AD-A190321] N88-22665
Coding capacity of generalized additive channels
[AD-A190315] N88-22685
Information capacity of Gaussian channels
[AD-A190316] N88-22686
Conditions for information capacity of the discrete-time Gaussian channel to be increased by feedback
[AD-A190317] N88-22687
Coding capacity of discrete-time Gaussian and nonGaussian channels
[AD-A190318] N88-22688
CHANNEL NOISE
Information capacity of Gaussian channels
[AD-A190316] N88-22686
CHARACTER RECOGNITION
Application of new technologies to DTIC document processing
[AD-A189778] N88-22823
CHARACTERIZATION
Fabrication and characterization of semiconductor lasers of Pb(1-x)Sn(x)Te
[INPE-4253-PRE/1126] N88-22357
Spectrum fatigue testing for materials characterization
[VTT-RR-502] N88-22443
Synthesis and characterization of high-T(sub c) screen-printed Y-Ba-Cu-O films on alumina
[NASA-TM-100860] N88-22805
CHARGE CARRIERS
Calculating depletion region carrier concentrations with capacitance-voltage measurements and etching
[AD-A189630] N88-22777
CHARGE COUPLED DEVICES
ROVER: A prototype active vision system
[AD-A189246] N88-22722
Space-variant optical systems
[AD-A189967] N88-22724
CHARGED PARTICLES
Modeling the effects of heavy charged particles on MOSFETs (Metal-Oxide-Semiconductor Field Effect Transistors)
[AD-A190575] N88-22792
CHEMICAL ANALYSIS
Structure and surface characterizations of high strength carbon fibers
[AD-A189642] N88-22087
Spectrographic detection of nitrogen impurity in helium
[DE88-752301] N88-22111
On copper peroxide
[NASA-TT-20263] N88-22135
NMR analysis of a fluorocarbon copolymer
[DE88-002364] N88-22170
Simulation analysis of moored fluorometer time series from the Mid-Atlantic Bight
[DE88-006066] N88-22505
CHEMICAL BONDS
Vapor phase deposition and growth of polyimide films on copper
[AD-A189969] N88-22178
CHEMICAL COMPOSITION
Segregation effects in welded stainless steels
[DE88-701224] N88-22139
Stability of the high-temperature G-16 primer composition
[DE88-006201] N88-22206

CHEMICAL ENERGY
A chemical method for achieving acceleration of macroparticles to ultrahigh velocities
[DE88-006377] N88-22695
CHEMICAL PROPERTIES
Structure of sol-gel silica
[DE88-006870] N88-22114
Diode laser spectroscopy of chemical moieties at surfaces
[AD-A190710] N88-22127
CHEMICAL REACTIONS
Numerical simulation of turbulent flames using vortex methods
[AD-A189813] N88-22116
An investigation of flow structure, mixing and chemical reaction in combusting turbulent flows
[AD-A189980] N88-22117
Investigation of combustion in large vortices
[AD-A190406] N88-22121
AFRAPT (Air Force Research in Aero Propulsion Technology) trainee program
[AD-A190525] N88-22123
Evaluation of direct methane conversion to higher hydrocarbons and oxygenates
[DE88-003812] N88-22204
The numerical simulation of viscous flows with change of phase and chemical reaction
[DE88-003204] N88-22292
Chemically reacting turbulent flow
[AD-A190522] N88-22311
The kinetics of contact noise in NaBeta alumina
[AD-A190651] N88-22707
CHEMISORPTION
First-principles calculations of quasiparticle energies at surfaces and interfaces: Semiconductor surface-state spectra and band offsets
[DE88-006340] N88-22773
CHIPS (ELECTRONICS)
French Multiproject Chip (MPC) activity report, 1986
[RR-650-I] N88-22273
An expert system for discrete component digital circuit design
[AD-A189680] N88-22274
An analysis of multiple grain CHIP architectures
[AD-A189942] N88-22570
Design and implementation of VLSI prime factor algorithm processor
[AD-A190483] N88-22580
High density ion implanted contiguous disk bubble technology
[AD-A190169] N88-22789
CHOLESKY FACTORIZATION
Cholesky downdating on a hypercube
[DE88-006780] N88-22586
CHROMATOGRAPHY
Determination of aquo-complexes of chromium and iron in chromium plating and polishing solutions by ion chromatography
[AD-A190166] N88-22148
CHROMIUM ALLOYS
Effect of P implantation on the corrosion behavior of Fe-Cr alloys
[DE88-005732] N88-22158
Characterization of an explosively consolidated rapidly solidified Fe-16Ni-9Cr-5Mo-2Cu alloy powder
[DE88-006733] N88-22162
CHRONOLOGY
Marshall Space Flight Center 1960-1985: 25th anniversary report
[NASA-TM-100326] N88-22852
CIRCUIT DIAGRAMS
ECP (Electrical Circuitry Program): A proposed program for electrical circuitry analysis
[AD-A190494] N88-22280
CIRCUITS
ECP (Electrical Circuitry Program): A proposed program for electrical circuitry analysis
[AD-A190494] N88-22280
A fully abstract semantics for event-based simulation
[AD-A190560] N88-22283
Electrical circuit modeling of reversed field pinches
[DE88-006942] N88-22745
CIRCULATION CONTROL AIRFOILS
Boundary-layer and wake measurements on a swept, circulation-control wing
[NASA-TM-89426] N88-22013
CIRRUS CLOUDS
The collection of statistics on the frequency of cloud cover over North America
[AD-A190456] N88-22495
CIVIL AVIATION
General aviation activity and avionics survey: 1986 data
[AD-A189966] N88-22003
Aircraft accident reports, brief format, US civil and foreign aviation, issue number 10 of 1986 accidents
[PB87-916912] N88-22020
JPRS report: Science and technology. Japan
[JPRS-JST-88-001] N88-22218
CLASSICAL MECHANICS
Singular Lagrangians. Classical dynamics and quantization. Lectures for young scientists
[TI88-701158] N88-22806
CLASSIFICATIONS
High temperature materials: What's available
[AERE-R-12632] N88-22081
On categorizing sounds
[AD-A189784] N88-22700
CLIMATOLOGY
A multivariate variational objective analysis-assimilation method. Part 1: Development of the basic model
[NASA-CR-182651] N88-22491
Monthly mean global climatology of temperature, wind, geopotential height, and pressure for 0 - 120 km
[NASA-TM-100697] N88-22503
CLINICAL MEDICINE
Clinical measurements using fiber optic sensors
[DE88-005624] N88-22731
CLOUD COVER
The collection of statistics on the frequency of cloud cover over North America
[AD-A190456] N88-22495
CMOS
French Multiproject Chip (MPC) activity report, 1986
[RR-650-I] N88-22273
COASTAL WATER
Changes in the California current system observed off northern California during July-August 1986
[AD-A190027] N88-22510
COASTAL ZONE COLOR SCANNER
NIMBUS-7 CZCS. Coastal Zone Color Scanner imagery for selected coastal regions. North America - Europe. South America - Africa - Antarctica. Level 2 photographic product
[NASA-CR-180755] N88-22447
COATINGS
Fatigue damage modeling for coated single crystal superalloys N88-22427
COCKPITS
Geometric modeling of flight information for graphical cockpit display
[AD-A190484] N88-22043
CODING
Performance of data compression codes in channels with errors
[AD-A189667] N88-22253
Status of electric vehicle simulation programs at the INEL: Summer 1987
[DE88-006745] N88-22271
Selective mechanisms in auditory and bimodal signal processing
[AD-A190529] N88-22530
Multiple-transform pipelines for image coding
[REPT-87-038] N88-22561
The algebraic structure of convolutional codes
[AD-A190280] N88-22635
Information and coding capacities of mismatched Gaussian channels
[AD-A190321] N88-22665
Coding capacity of generalized additive channels
[AD-A190315] N88-22685
OCR vision system, an alternative to bar code
[DE88-003761] N88-22828
COEFFICIENTS
Experimental determination of the coefficients of the hydraulic resistance of apertures in the rotary disks
[AD-A190627] N88-22317
COGNITION
Conflict resolution in cooperative systems
[AD-A190351] N88-22535
Relationship of encoding speed and memory tests to flight training performance
[AD-A190670] N88-22539
COHERENT RADIATION
Particle acceleration to high energies and amplification of coherent radiation by electromagnetic interactions in plasmas
[TI88-701020] N88-22737
COLLAPSE
Generation and propagation of sound waves in a collapsing or anti-collapsing star with uniform density
[DE87-703034] N88-22839
COLLISIONS
Electronic energy transfer processes in the alkali/alkaline earth metal vapors
[AD-A190035] N88-22119
COLOR CENTERS
Infrared absorption spectroscopy and chemical kinetics of free radicals
[DE88-006536] N88-22112
COLOR CODING
Comparative utilization of analog and digital processes in the treatment of MSS-LANDSAT data for studying the national parks of Brazil
[INPE-4011-TDL/240] N88-22456
COMBUSTIBLE FLOW
An investigation of flow structure, mixing and chemical reaction in combusting turbulent flows
[AD-A189980] N88-22117
Advanced diagnostics for reacting flows
[AD-A190485] N88-22122
Chemically reacting turbulent flow
[AD-A190522] N88-22311
COMBUSTION
The combustion synthesis of boride composites
[DE88-005474] N88-22084
Cetane scale evaluation and possible modification
[AD-A189730] N88-22200
COMBUSTION CHAMBERS
High-temperature combustor liner tests in structural component response test facility N88-22383
Life assessment of combustor liner using unified constitutive models N88-22384
COMBUSTION CHEMISTRY
Laser spectroscopy and dynamics of combustion intermediates
[DE88-006541] N88-22110
COMBUSTION EFFICIENCY
Research as part of the Air Force in aero propulsion technology (AFRAPT) program
[AD-A190336] N88-22036
Advanced B and Al combustion kinetics over wide temperature ranges
[AD-A190752] N88-22128
COMBUSTION PHYSICS
Advanced B and Al combustion kinetics over wide temperature ranges
[AD-A190752] N88-22128
COMBUSTION STABILITY
Basic instability mechanisms in chemically reacting subsonic and supersonic flows
[AD-A190101] N88-22120
Investigation of combustion in large vortices
[AD-A190406] N88-22121
AFRAPT (Air Force Research in Aero Propulsion Technology) trainee program
[AD-A190525] N88-22123
COMMUNICATION
Research and technology
[NASA-TM-100172] N88-22851
COMMUNICATION NETWORKS
Real-time stressed channel simulator
[AD-A190223] N88-22067
NASA and the challenge of ISDN: The role of satellites in an ISDN world
[NASA-CR-182749] N88-22676
COMMUNICATION SATELLITES
NASA and the challenge of ISDN: The role of satellites in an ISDN world
[NASA-CR-182749] N88-22676
COMMUTATION
Determination of the commutation and angle and load response for a continuous-current, single phase controlled rectifier
[AD-A190602] N88-22285
COMPARISON
Stellar scintillometer atmospheric optical turbulence profiling experiment: A qualitative comparison of two identical instruments at AMOS (Air Force Maui Optical Station), 1985
[AD-A190589] N88-22479
Comparative analysis of multistage interconnection networks
[AD-A190436] N88-22598
Groundwater sapping valleys: Experimental studies, geological controls and implications to the interpretation of valley networks on Mars
[NASA-CR-182718] N88-22847
COMPILERS
Ada (Trademark) compiler validation summary report. ALSYS: AlsyCOMP-013, V2.0 HOST: IBM PC AT. Target: IBM 370 3084Q
[AD-A189640] N88-22546
ONTIC: A knowledge representation system for mathematics
[AD-A190553] N88-22643
COMPLEX COMPOUNDS
The structure of the boron-hydrogen complex in silicon
[DE88-005433] N88-22795
COMPONENT RELIABILITY
Monolithic ceramic analysis using the SCARE program N88-22409
Continuous fiber ceramic matrix composites for heat engine components N88-22411
Cumulative fatigue damage models N88-22422

Life and reliability of rotating disks N88-22428

COMPOSITE MATERIALS

Cement paste matrix composite materials center
[AD-A188657] N88-22083

The combustion synthesis of boride composites
[DE88-005474] N88-22084

Superplastic flow of mullite-zirconia composites
[DE88-005905] N88-22085

Microplasticity phenomena in graphite/magnesium metal matrix composites
[DE88-006772] N88-22086

Structure and surface characterizations of high strength carbon fibers
[AD-A189642] N88-22087

An investigation of the failure response of laminates under biaxial stress
[AD-A190039] N88-22090

A study of damage tolerance in curved composite panels
[AD-A190617] N88-22092

Microwave sintering of alumina-SiC composites at 2.45 and 60 GHz
[DE88-006455] N88-22095

Interlaminar fracture toughness of thermoplastic composites
[NASA-TM-100532] N88-22097

Application of copper-carbon fiber composites to power semiconductor devices
[NASA-TT-20171] N88-22101

Mechanical behaviour of particle filled thermoplastics
[PB88-169297] N88-22196

Eddy current nondestructive inspection of graphite epoxy using ferrite cup core probes
[AD-A189823] N88-22365

Biaxial experiments supporting the development of constitutive theories for advanced high-temperature materials N88-22386

Structural analyses of engine wall cooling concepts and materials N88-22405

Ultrasonic beam distortion in transversely isotropic media
[DE88-005937] N88-22699

COMPOSITE STRUCTURES

A study of damage tolerance in curved composite panels
[AD-A190617] N88-22092

Postbuckling delamination of a stiffened composite panel using finite element methods
[NASA-CR-182803] N88-22098

Features and applications of the integrated composites analyzer (ICAN) code N88-22391

Computational simulation methods for composite fracture mechanics N88-22396

Thermal stress in high temperature cylindrical fasteners
[NASA-TM-100611] N88-22438

Experimental comparison of lightning simulation techniques to CV-580 airborne lightning strike measurements
[AD-A190576] N88-22496

COMPRESSIBILITY

Unsteady flow field measurements using LDV (Laser Doppler Velocimetry)
[AD-A189907] N88-22298

COMPRESSIBLE FLOW

Flexiwall 3 SO: A second order predictive strategy for rapid wall adjustment in two-dimensional compressible flow
[NASA-CR-181662] N88-22018

Turbulent reacting flows and supersonic combustion
[AD-A189690] N88-22115

Theoretical model and numerical solution for compressible viscous vortex cores N88-22243

Transient compressible flow in porous materials
[DE88-006685] N88-22324

COMPUTATION

Calibration and processing of AVHRR data for temperature estimation
[INPE-4493-PRE/1257] N88-22485

Optical Conceptual Computing and Associative Memory (OCCAM)
[AD-A190030] N88-22550

Rapid feature extraction via the radon transform
[AD-A190032] N88-22573

Microvax networked computer system
[AD-A190308] N88-22596

High speed transcendental elementary function architecture in support of the Vector Wave Equation (VWE)
[AD-A189746] N88-22627

Numerical methods for linear and nonlinear optimization
[AD-A190029] N88-22631

Research on algebraic manipulation
[AD-A190149] N88-22634

A physically consistent model for artificial dissipation in transonic potential flow computations
[NASA-TM-100846] N88-22652

Interface formation and precursory dynamics
[AD-A190741] N88-22794

INPE position paper on the CCSDS standardized method of link budget computation
[INPE-4533-NTE/279] N88-22820

COMPUTATIONAL FLUID DYNAMICS

Computational fluid dynamics drag prediction: Results from the Viscous Transonic Airfoil Workshop
[NASA-TM-100095] N88-22009

Trends in Computational Fluid Dynamics (CFD) for aeronautical 3D steady applications: The Dutch situation
[NLR-MP-86074-U] N88-22017

Split-coefficient matrix solution and experimental study of axisymmetric underexpanded exhaust plumes N88-22242

Theoretical model and numerical solution for compressible viscous vortex cores N88-22243

Mixed direct-inverse problem of transonic cascade N88-22244

Zero-lift drag predictions in supersonic flow for complex configurations N88-22246

A panel method based on velocity potential to compute harmonically oscillating lift surface systems
[ETN-88-91886] N88-22290

Duct flow nonuniformities: Effect of struts in SSME HGM II(+)
[NASA-CR-179285] N88-22296

Theoretical investigation of secondary instability of three-dimensional boundary-layer flows with application to the DFVLR-F5 model wing
[DFVLR-FB-87-44] N88-22330

Numerical study of unsteady viscous hypersonic blunt body flows with an impinging shock
[NASA-TM-100096] N88-22650

High-resolution shock-capturing schemes for inviscid and viscous hypersonic flows
[NASA-TM-100097] N88-22651

COMPUTATIONAL GRIDS

COMESH: A corner mesh finite difference code to solve multigroup diffusion equations in multidimensions
[DE88-701248] N88-22555

COMPUTER AIDED DESIGN

Characteristics of LSI-wiring expert system discussed N88-22226

Reliability analysis within a Computer Aided Engineering (CAE) infrastructure
[NLR-MP-86059-U] N88-22369

Investigation into the development of computer aided design software for space based sensors
[NASA-CR-180772] N88-22552

Software structuring principles for VLSI CAD
[AD-A190386] N88-22579

A graphics editor for structured analysis with a data dictionary
[AD-A190618] N88-22584

High speed transcendental elementary function architecture in support of the Vector Wave Equation (VWE)
[AD-A189746] N88-22627

COMPUTER AIDED TOMOGRAPHY

A hardware/software system for implementing geophysical diffraction tomography
[DE88-006411] N88-22480

COMPUTER ASSISTED INSTRUCTION

Tutorial on GAMS (Generalized Algebraic Modeling System): A modeling language for optimization
[AD-A189867] N88-22568

COMPUTER DESIGN

Design and implementation of a parallel computer for expert system applications
[DE88-005288] N88-22601

COMPUTER GRAPHICS

Effects of update and refresh rates on flight simulation visual displays
[NASA-TM-100415] N88-22033

Geometric modeling of flight information for graphical cockpit display
[AD-A190484] N88-22043

Investigation into the development of computer aided design software for space based sensors
[NASA-CR-180772] N88-22552

The visit problem: Visibility graph-based solution
[DE88-000343] N88-22556

Computer graphics tools for the study of minimal surfaces
[DE88-006421] N88-22557

PLOT3D (version-5): A computer code for drawing three dimensional graphs, maps and histograms, in single or multiple colours, for mono or stereoscopic viewing
[DE88-701410] N88-22558

A graphics editor for structured analysis with a data dictionary
[AD-A190618] N88-22584

The elliptic Sinh-Gordon equation and the construction of toroidal soap bubbles
[DE88-006426] N88-22585

Two-dimensional graphics tools for a transputer based display board
[NASA-TM-100820] N88-22591

Rapid prototyping of simulations in artificial intelligence environments
[DE88-004295] N88-22612

Discrete event simulation in the artificial intelligence environment
[DE88-004296] N88-22613

Higher order crossings
[AD-A190489] N88-22641

COMPUTER INFORMATION SECURITY

Monitoring the usage of a computer system
[DE88-004310] N88-22542

COMPUTER NETWORKS

Sigma system: Overview, prospects N88-22230

Project Monitoring Package (PMP): A package for project activity monitoring
[DE88-701234] N88-22554

Logarithmically connected, repetitive computer networks and numerical applications
[DE88-006632] N88-22592

COMPUTER PROGRAM INTEGRITY

Methodology for software reliability prediction, volume 1
[AD-A190018] N88-22571

Methodology for software reliability prediction, volume 3
[AD-A190019] N88-22572

COMPUTER PROGRAMMING

Description of ground motion data processing codes, volume 2
[DE88-007137] N88-22481

Tutorial on GAMS (Generalized Algebraic Modeling System): A modeling language for optimization
[AD-A189867] N88-22568

Contour interactive extraction using image numerical treatment
[ISL-R-114/86] N88-22587

Inference engine for expert systems
[INPE-4465-TDL/321] N88-22590

Numerical methods for linear and nonlinear optimization
[AD-A190029] N88-22631

PLASMOR: A laser-plasma simulation code, part 2
[DE88-701289] N88-22736

New generation knowledge processing, volume 1
[AD-A190165] N88-22826

COMPUTER PROGRAMS

Basic research on flame radiation
[PB88-168372] N88-22105

Computer program in BASIC language for computation of spectrochemical analytical data
[DE88-701229] N88-22106

Status of electric vehicle simulation programs at the INEL: Summer 1987
[DE88-006745] N88-22271

An improved method for calculating power density in the Fresnel region of circular parabolic reflector antennas
[AD-A190569] N88-22284

Traction model development
[AD-A188450] N88-22359

Development of a computer code CRACK for elastic and elastoplastic fracture mechanics analysis of 2-D structures by finite element technique
[DE88-701231] N88-22370

The composite blade structural analyzer (COBSTRAN) N88-22390

Three-dimensional inelastic approximate analysis code (MOMM) N88-22392

Specialty three-dimensional finite element analysis codes N88-22393

MHOST: An efficient finite element program for inelastic analysis of solids and structures N88-22394

METCAN: The metal matrix composite analyzer N88-22395

Computational simulation methods for composite fracture mechanics N88-22396

Probabilistic structural analysis computer code (NESSUS) N88-22397

Structural tailoring of high-speed turbine blades (SSME/STAEBL) N88-22398

Computational structural mechanics for engine structures N88-22399

Structural tailoring of advanced turboprops N88-22400

Geometric restoration of satellite image data
[AD-A190462] N88-22450

Satellite UV image processing
[AD-A190466] N88-22451

Updating of the municipal official register of real estate through a geographical information system
[INPE-4459-PRE/1236] N88-22453
A survey of denser-than-air atmospheric dispersion models
[DE88-006626] N88-22467
A hardware/software system for implementing geophysical diffraction tomography
[DE88-006411] N88-22480
Motion sickness: Quantitative, algorithmic malaise indication in real time
[AD-A189674] N88-22518
Analysis of head response to torso acceleration. Volume 2: Description of data retrieval, analysis and display software
[PB88-156765] N88-22536
Project Monitoring Package (PMP): A package for project activity monitoring
[DE88-701234] N88-22554
COMESH: A corner mesh finite difference code to solve multigroup diffusion equations in multidimensions
[DE88-701248] N88-22555
PLOT3D (version-5): A computer code for drawing three dimensional graphs, maps and histograms, in single or multiple colours, for mono or stereoscopic viewing
[DE88-701410] N88-22558
Computer grading of extensometers (BS 3846)
[NPL-DMA(A)-152] N88-22560
Methodology for software reliability prediction, volume 1
[AD-A190018] N88-22571
Methodology for software reliability prediction, volume 3
[AD-A190019] N88-22572
Transformations of concurrent algorithms for highly parallel systems: A one year project summary report
[AD-A190236] N88-22576
CK-LOG system conversion (user's manual and user interface)
[AD-A190273] N88-22577
Software verification using partition analysis
[AD-A190570] N88-22582
Memory-based expert systems
[AD-A190203] N88-22606
ONTIC: A knowledge representation system for mathematics
[AD-A190553] N88-22643
An approximation technique for solving a system of Fredholm integral equations for asymmetric detector response functions
[AD-A190577] N88-22645
Analysis and testing of the SURE program
[NASA-TP-2817] N88-22653
A chemical method for achieving acceleration of macroparticles to ultrahigh velocities
[DE88-006377] N88-22695
Sources of digital spatial data for geographic information systems
[AD-A189788] N88-22824

COMPUTER STORAGE DEVICES
Application of static memory for data acquisition and transmission into a computer
[TI86-701491] N88-22544
Parallel memory addressing using coincident optical pulses
[AD-A189767] N88-22547
Memory efficient evaluations of nonlinear stochastic equations and C3 applications
[AD-A189872] N88-22569
Design of an algorithm to translate nested relational algebra queries to GENESIS trace manager commands
[AD-A190502] N88-22581
Microvax networked computer system
[AD-A190308] N88-22596
The modeling, simulation and comparison of interconnection networks for parallel processing
[AD-A190571] N88-22599
The algebraic structure of convolutional codes
[AD-A190280] N88-22635

COMPUTER SYSTEMS DESIGN
Sigma system: Overview, prospects N88-22230
An intelligent simulation model generator
[REPT-87-053] N88-22562
Transformations of concurrent algorithms for highly parallel systems: A one year project summary report
[AD-A190236] N88-22576

COMPUTER SYSTEMS PERFORMANCE
Methodology for software reliability prediction, volume 1
[AD-A190018] N88-22571
Methodology for software reliability prediction, volume 3
[AD-A190019] N88-22572
CK-LOG system conversion (user's manual and user interface)
[AD-A190273] N88-22577
The Colored Stochastic Petri Net (CS-PN) software: Application to the validation and the performance evaluation of distributed systems
[ENST-87D005] N88-22589
Implementation and performance analysis of parallel assignment algorithms on a hypercube computer
[AD-A190678] N88-22600

COMPUTER SYSTEMS PROGRAMS
Software structuring principles for VLSI CAD
[AD-A190386] N88-22579

COMPUTER TECHNIQUES
Exhaustive and pseudo-exhaustive testing
[AD-A190140] N88-22574
Argus reference manual
[AD-A190382] N88-22578
Simulation of fault tolerance in a hypercube arrangement of discrete processors
[AD-A189682] N88-22594
A zonal approach for the solution of coupled Euler and potential solutions of flows with complex geometries
[AD-A189752] N88-22595
MultiSchema: A parallel processing system based on MIT (Massachusetts Institute of Technology) scheme
[AD-A190383] N88-22597
Data base design and implementation
[AD-A190414] N88-22827

COMPUTER VISION
On the geometric interpretation of image contours
[RR-647-I-IMAG-57-LIFIA] N88-22563
Concurrent algorithms for a mobile robot vision system
[DE88-005850] N88-22614

COMPUTERIZED SIMULATION
Development and evaluation of an airplane fuel tank ullage composition model. Volume 2: Experimental determination of airplane fuel tank ullage compositions
[AD-A190408] N88-22025
Linear state space modeling of a turbofan engine
[AD-A190110] N88-22035
Moving-bank multiple model adaptive estimation applied to flexible spacestructure control
[AD-A190761] N88-22071
Status of electric vehicle simulation programs at the INEL: Summer 1987
[DE88-006745] N88-22271
Basic characteristics of heat-exchanger-type steam reformer heated by high-temperature helium gas (2). Analysis by simulation model (2)
[DE87-702962] N88-22291
Finite element simulation of perforation of aluminum plates
[DE88-002092] N88-22362
Computational simulation methods for composite fracture mechanics N88-22396
Performance evaluation of molten salt thermal storage systems
[DE87-014645] N88-22461
Advanced geothermal technologies
[DE88-004307] N88-22463
Anthropomorphic phantom radiation dosimetry at the NATO standard reference point at Aberdeen Proving Ground
[AD-A190508] N88-22528
An intelligent simulation model generator
[REPT-87-053] N88-22562
A UNIX-based interactive VHDL (hardware description language) simulator
[AD-A189749] N88-22565
Memory efficient evaluations of nonlinear stochastic equations and C3 applications
[AD-A189872] N88-22569
SEARCH: An interactive computer program for optimizing two-variable, unconstrained experiments or simulation
[AD-A190593] N88-22583
The modeling, simulation and comparison of interconnection networks for parallel processing
[AD-A190571] N88-22599
Rapid prototyping of simulations in artificial intelligence environments
[DE88-004295] N88-22612
Discrete event simulation in the artificial intelligence environment
[DE88-004296] N88-22613
Properties of some Bayesian scoring procedures for computerized adaptive tests
[AD-A189925] N88-22660
PLASMOR: A laser-plasma simulation code, part 2
[DE88-701289] N88-22736
Transport simulations of ohmic ignition experiment: IGNITEX
[DE88-006055] N88-22757
Interface formation and precursory dynamics
[AD-A190741] N88-22794

COMPUTERS
JPRS report: Science and technology. Japan
[JPRS-JST-88-001] N88-22218
JPRS report: Science and technology. Japan
[JPRS-JST-87-029] N88-22228
Complex sound processing: An interdisciplinary approach
[AD-A189782] N88-22523
Extension of computer based algorithms by operator analysts
[NASA-CR-182798] N88-22575

CONCENTRATION (COMPOSITION)
Ultrasonic oxygen sensor
[AD-A189723] N88-22537

CONCENTRATORS
Recent advances in photovoltaic concentrator technology
[DE88-003948] N88-22462

CONFERENCES
Summary of the 1987 Gordon Research Conference on Corrosion
[AD-A189737] N88-22161
Lewis Structures Technology, 1988. Volume 3: Structural Integrity Fatigue and Fracture Wind Turbines HOST
[NASA-CP-3003-VOL-3] N88-22408
Proceedings of the Lightning Threat Warning Workshop
[DE88-006607] N88-22499
Ocean general circulation models: Report on proceedings of a meeting of ocean and climate modelers
[DE88-005530] N88-22504
NASA scientific and technical publications: A catalog of Special Publications, Reference Publications, Conference Publications, and Technical Papers, 1987
[NASA-SP-7063(02)] N88-22830

CONFIDENCE LIMITS
Mathematics clinic probabilistic position-fixing
[NASA-CR-182753] N88-22672

CONFINEMENT
Experimental investigation of two-dimensional confined jet thrust vector control
[AD-A189845] N88-22077
Heating and confinement studies of electron cyclotron resonance heated plasmas in Heliotron E
[DE88-752312] N88-22746

CONICAL BODIES
Fluid motion in a spinning, coning cylinder via spatial eigenfunction expansion
[AD-A190758] N88-22319

CONICAL SHELLS
Numerical and experimental research on propagation of elastic stress waves in conical shell under axial impulsive loading N88-22238

CONNECTORS
Fabrication and electrical characterization of multilevel aluminum interconnects used to achieve silicon-hybrid wafer-scale integration
[AD-A190519] N88-22282

CONSERVATION LAWS
Super Virasoro algebra and solvable supersymmetric quantum field theories
[DE88-752299] N88-22681

CONSISTENCY
Derivation of consistent surface fixed fields for use in a global NWP model
[AD-A190131] N88-22475

CONSOLIDATION
Characterization of an explosively consolidated rapidly solidified Fe-16Ni-9Cr-5Mo-2Cu alloy powder
[DE88-006733] N88-22162

CONSTANTS
Involution-dependent constants and the cancellation of divergences in the 1-loop open string amplitude
[DE88-006537] N88-22811

CONSTITUTIVE EQUATIONS
Life assessment of combustor liner using unified constitutive models N88-22384
Biaxial experiments supporting the development of constitutive theories for advanced high-temperature materials N88-22386
Unified constitutive model development for metal matrix composites at high temperature N88-22387
Unified constitutive model for single crystal deformation behavior with applications N88-22388
Finite element (MARC) solution technologies for viscoplastic analyses N88-22389

CONSTRAINTS
Measurement of the elastic-plastic surface flaw back surface topology and its relation to constraint
[DE88-006765] N88-22437

CONTAINERLESS MELTS
Containerless glass melting N88-22222

CONTAMINATION
On copper peroxide
[NASA-TT-20263] N88-22135

CONTINENTAL SHELVES
Simulation analysis of moored fluorometer time series from the Mid-Atlantic Bight
[DE88-006066] N88-22505
A computerized investigation using the method of images to predict the sound field in a fluid wedge overlying a slow fluid half-space
[AD-A190013] N88-22704
CONTINUITY
Continuity of symmetric stable processes
[AD-A190324] N88-22667
CONTINUUM MECHANICS
Problems in nonlinear continuum dynamics
[AD-A190538] N88-22691
CONTOUR SENSORS
Contour interactive extraction using image numerical treatment
[ISL-R-114/86] N88-22587
CONTOURS
On the geometric interpretation of image contours
[RR-647-I-IMAG-57-LIFIA] N88-22563
CONTRACT NEGOTIATION
The impact of independent research and development regulations on companies not required to negotiate advanced independent research and development agreements
[AD-A190007] N88-22818
CONTRACTION
Contraction design for small low-speed wind tunnels
[NASA-CR-182747] N88-22045
CONTROL SIMULATION
Multiple model parameter adaptive control for in-flight simulation
[AD-A190568] N88-22044
CONTROL SURFACES
Multivariable control law design for the AFTI/F-16 with a failed control surface using a parameter-adaptive controller
[AD-A189848] N88-22040
CONTROL SYSTEMS DESIGN
Linear state space modeling of a turbofan engine
[AD-A190110] N88-22035
Design of an integrated control system for flutter margin augmentation and gust load alleviation, tested on a dynamic windtunnel model
[PB88-149685] N88-22038
Application of eigenstructure assignment techniques in the design of a longitudinal flight control system
[AD-A189644] N88-22039
Telerobotic operation of conventional robot manipulators
[DE88-005718] N88-22363
Representation, analysis and design of multirate discrete-time control systems
[AD-A190499] N88-22608
Optical switching and control techniques using nonlinear optical wave mixing
[AD-A190467] N88-22730
CONTROL THEORY
Model selection for the multiple model adaptive algorithm for in-flight simulation
[AD-A189715] N88-22022
Multivariable control law design for the AFTI/F-16 with a failed control surface using a parameter-adaptive controller
[AD-A189848] N88-22040
Wave propagation and dynamics of lattice structures
[AD-A190037] N88-22066
Telerobotic operation of conventional robot manipulators
[DE88-005718] N88-22363
Instrumentation for scientific computing in neural networks, information science, artificial intelligence and applied mathematics
[AD-A189981] N88-22549
Insertions using geometric analysis and hybrid force-position control: Method and analysis
[DE87-013652] N88-22611
Information capacity of Gaussian channels
[AD-A190316] N88-22686
CONTROLLABILITY
The effects of torque response and time delay on rotorcraft vertical axis handling qualities
[AD-A189873] N88-22023
Preliminary airworthiness evaluation of the UH-60A with Advanced Digital Optical Control System (ADOCS)
[AD-A190674] N88-22030
CONTROLLERS
Multivariable control law design for the AFTI/F-16 with a failed control surface using a parameter-adaptive controller
[AD-A189848] N88-22040
CONVECTION CLOUDS
Stratospheric electric field and conductivity measurements over electrified convective clouds in the South American region, revised
[INPE-4046-PRE/1012-REV-3] N88-22483
A study on electric fields and conductivity associated with electrified clouds in the region of South America
[INPE-4487-TDL/325] N88-22486
CONVECTIVE HEAT TRANSFER
Heat transfer modeling of jet vane Thrust Vector Control (TVC) systems
[AD-A190106] N88-22034
Heat transfer from a negatively buoyant wall jet
[NBS-GCR-88-541] N88-22208
Thermal instability and heat transfer characteristics in water/ice systems
[AD-A189627] N88-22297
CONVERGENCE
Development and application of the p-version of the finite element method
[AD-A190036] N88-22633
Trust regions and projected gradients
[DE88-005829] N88-22646
Detection of the number, locations and magnitudes of jumps
[AD-A190328] N88-22671
CONVOLUTION INTEGRALS
The algebraic structure of convolutional codes
[AD-A190280] N88-22635
Near optimal blind deconvolution
[REPT-87-016] N88-22655
COOLING
Structural analyses of engine wall cooling concepts and materials N88-22405
COOLING SYSTEMS
Superconducting magnet technique for ASTROMAG on the space station
[DE88-004560] N88-22063
COPOLYMERIZATION
NMR analysis of a fluorocarbon copolymer
[DE88-002364] N88-22170
COPOLYMERS
NMR analysis of a fluorocarbon copolymer
[DE88-002364] N88-22170
Singlet oxygen behavior in solid polymer matrices
[DE88-005171] N88-22171
Donor acceptor polymerization chemistry as a vehicle to low energy cure matrix resins
[AD-A190119] N88-22179
COPPER
Thermal expansion behavior of randomly oriented short carbon fiber reinforced copper composites
[NASA-TT-20175] N88-22099
Reciprocating sliding wear characteristics of copper-carbon fiber composites
[NASA-TT-20176] N88-22100
Application of copper-carbon fiber composites to power semiconductor devices
[NASA-TT-20171] N88-22101
Use of long-distance pair potentials in calculations of defect characteristics in metals
[TI88-701039] N88-22138
Laser enhanced adhesion of copper films to sapphire substrates
[DE88-006802] N88-22144
Vapor phase deposition and growth of polyimide films on copper
[AD-A189969] N88-22178
RF properties of superconducting Pb electroplated onto Cu
[DE88-005918] N88-22765
Magnetic anomalies in the rare earth oxide superconductors GdBa2Cu3O(7-x) and YbBa2Cu3O(7-x)
[AD-A190713] N88-22793
COPPER ALLOYS
Characterization of an explosively consolidated rapidly solidified Fe-16Ni-9Cr-5Mo-2Cu alloy powder
[DE88-006733] N88-22162
COPPER OXIDES
On copper peroxide
[NASA-TT-20263] N88-22135
Superconductivity and the tailoring of lattice parameters of the compound YBa2Cu3O(sub x)
[DE88-005904] N88-22769
Thermochemistry and high temperature thermodynamic properties of rare earth-alkaline earth-copper oxide superconductors
[DE88-005976] N88-22770
High temperature superconductors in the La(sub 1+x)Ba(sub 2-x)Cu O(sub y system
[DE88-006367] N88-22802
Synthesis and characterization of high-T(sub c) screen-printed Y-Ba-Cu-O films on alumina
[NASA-TM-100860] N88-22805
COPPER SULFIDES
Activities of As, Sb, Bi and Pb in copper mattes and their effects on impurity elimination
[TKK-V-A10(1988)] N88-22165
CORE FLOW
Theoretical model and numerical solution for compressible viscous vortex cores N88-22243
CORNER FLOW
Laser velocimeter measurements in a wing-fuselage type juncture
[NASA-TM-100588] N88-22012
CORROSION
Durability testing of an iridium-plated storable rocket engine injector
[AD-A190707] N88-22078
Galvanic corrosion initiatives
[AD-A190658] N88-22155
Effect of P implantation on the corrosion behavior of Fe-Cr alloys
[DE88-005732] N88-22158
Summary of the 1987 Gordon Research Conference on Corrosion
[AD-A189737] N88-22161
CORROSION RESISTANCE
Corrosion and electrochemical behavior of binary magnesium alloys
[AD-A190624] N88-22154
The corrosion resistance of an aluminum alloy coated with polysilazane derived ceramics
[AD-A190703] N88-22189
COSMIC RAYS
Hydrodynamical models of supernova SN 1987 A in the LMC
[TI88-701123] N88-22837
A map of the cosmic background radiaton at 3 millimeters
[INPE-4529-PRE/1279] N88-22850
COSMOCHEMISTRY
Advances in geochemistry and cosmochemistry: Trace element microdistributions with the synchrotron X-ray fluorescence microprobe
[DE88-006355] N88-22108
COSMOLOGY
Finite width corrections to the Nambu action for the Nielsen-Olesen string
[DE88-006996] N88-22812
Density perturbations in a rotating universe
[DE87-703036] N88-22840
String driven inflation
[DE88-006994] N88-22841
Cosmology for high energy physicists
[DE88-005705] N88-22842
Particle cosmology comes of age
[DE88-006998] N88-22844
COST ANALYSIS
Requirements and cost considerations for a Combined Space Nuclear Reactor Test Facility
[DE88-006763] N88-22719
A method for estimating and controlling the cost of extending technology
[AD-A190717] N88-22831
COST ESTIMATES
A method for estimating and controlling the cost of extending technology
[AD-A190717] N88-22831
COSTS
Sigma system: Overview, prospects N88-22230
Microvax networked computer system
[AD-A190308] N88-22596
A method for estimating and controlling the cost of extending technology
[AD-A190717] N88-22831
COUNTER ROTATION
Porous wind tunnel corrections for counterrotation propeller testing
[NASA-TM-100873] N88-22019
COUPLERS
Coupled high power waveguide laser research
[AD-A189800] N88-22345
Current-drive on the Versator-2 tokamak with a slotted-waveguide fast-wave coupler
[DE88-006261] N88-22743
COUPLING
Stabilization and control problems in structural dynamics
[AD-A190197] N88-22361
Coupled bending-torsion steady-state response of pretwisted, nonuniform rotating beams using a transfer-matrix method
[NASA-TM-100596] N88-22435
COVARIANCE
Mathematics clinic probabilistic position-fixing
[NASA-CR-182753] N88-22672

COVERINGS
An experimental investigation of rocket ramjet nozzle assembly base pressures
[AD-A189714] N88-22076
Solar cell cover glasses for satellites N88-22225
COWLINGS
Thermostructural analysis of simulated cowl lips N88-22403
CRACK INITIATION
Computational simulation methods for composite fracture mechanics N88-22396
In situ fatigue loading stage inside scanning electron microscope N88-22419
Grain boundary oxidation and low-cycle fatigue at elevated temperatures N88-22420
Fatigue damage mapping N88-22423
Life prediction modeling based on strainrange partitioning N88-22425
Life prediction modeling based on cyclic damage accumulation N88-22426
Fatigue damage modeling for coated single crystal superalloys N88-22427
CRACK PROPAGATION
Fracture toughness testing of a ceramic matrix composite
[AD-A189646] N88-22089
Fractography of composite delamination
[NASA-CR-182757] N88-22096
The effective fracture toughness of aluminum at rapid heating rates
[AD-A189745] N88-22146
Stress corrosion of ceramic materials
[AD-A190501] N88-22187
Crack opening and extension in inert solid propellant. An experimental study
[AD-A189606] N88-22201
Environmentally assisted crack growth in structural alloys: Perspectives and new directions
[AD-A190137] N88-22377
The growth of corner cracks under the conjoint action of high and low cycle fatigue
[AD-A190510] N88-22379
Mode 2 fracture mechanics N88-22418
In situ fatigue loading stage inside scanning electron microscope N88-22419
Grain boundary oxidation and low-cycle fatigue at elevated temperatures N88-22420
Elevated temperature crack growth N88-22421
Fatigue damage mapping N88-22423
A simplified key-curve approach for J-R-curve testing of CT specimens
[VTT-RR-503] N88-22444
CRACKING (FRACTURING)
Fracture toughness testing of a ceramic matrix composite
[AD-A189646] N88-22089
An investigation of the failure response of laminates under biaxial stress
[AD-A190039] N88-22090
Stress-intensity factors for small surface and corner cracks in plates
[NASA-TM-100599] N88-22445
CRACKS
Cracking tendencies of restrained welds in high strength low alloy steels under hyperbaric conditions
[AD-A190255] N88-22150
Ultrasonic characterization of ceramic joints
[DE88-005844] N88-22173
An evaluation of nondestructive methods for ceramic heat exchanger applications
[DE88-006731] N88-22328
CRANES
Oscillation damped movement of suspended objects
[DE88-005715] N88-22433
CRASHES
KRASH parametric sensitivity study: Transport category airplanes
[AD-A189962] N88-22024
CRATERS
Bilateral symmetry elements of the Zhamanshin impact crater
[NASA-TT-20288] N88-22490
CREEP PROPERTIES
Effect of strain rate on high-temperature low-cycle fatigue behavior of Hastelloy X and Hastelloy XR
[DE88-752302] N88-22140
CROP GROWTH
Assessment of crop loss from air pollutants: Meteorology-atmospheric chemistry and long range transport
[PB88-146857] N88-22448
CROSSINGS
Higher order crossings
[AD-A190469] N88-22641
CRUISE MISSILES
Performance optimization of a cruise missile using dynamic-stall induced lift augmentation
[AD-A190497] N88-22027
CRYOGENICS
Thin superconducting film characterization by surface acoustic waves
[AD-A190417] N88-22791
CRYSTAL DEFECTS
Absolute pressure derivatives of deep level defects in 3-5 semiconductors
[DE88-006318] N88-22772
The structure of the boron-hydrogen complex in silicon
[DE88-005433] N88-22795
Annihilation momentum density of positrons trapped at vacancy-type defects in metals and alloys
[DE88-005936] N88-22797
CRYSTAL GROWTH
Grain growth behavior of extrusion consolidated centrifugally atomized Type 304 stainless steel powder
[DE88-006788] N88-22143
Fundamental studies on high temperature deformation recrystallization, and grain growth of two-phase materials
[AD-A189725] N88-22145
JPRS report: Science and technology. Japan
[JPRS-JST-88-002] N88-22210
Single crystal growth by laser CVD N88-22213
Pb(1-x)Sn(x)Te crystal growth in space N88-22223
CRYSTAL LATTICES
Absolute pressure derivatives of deep level defects in 3-5 semiconductors
[DE88-006318] N88-22772
First-principles calculations of quasiparticle energies at surfaces and interfaces: Semiconductor surface-state spectra and band offsets
[DE88-006340] N88-22773
Fundamental properties and devices applications of Ge(x)Si(1-x)/Si superlattices
[AD-A190129] N88-22787
The structure of the boron-hydrogen complex in silicon
[DE88-005433] N88-22795
CRYSTAL STRUCTURE
Investigation and synthesis of high temperature and increased stiffness RSP aluminum alloys
[AD-A190407] N88-22151
Superconductivity and the tailoring of lattice parameters of the compound YBa2Cu3O(sub x)
[DE88-005904] N88-22769
CRYSTALS
Nucleation in super-saturated products
[NASA-TT-20275] N88-22134
On rotating sphere-on-a-plate experiments and the questions of whether high angle grain boundaries melt below bulk melting temperatures
[DE88-006627] N88-22142
High-performance polymeric materials
[AD-A190706] N88-22190
Does the pipe diffusion of self-interstitials in crystals under stresses exist
[TI88-701027] N88-22762
Optical characterization of microcrystals
[DE88-006622] N88-22775
CURING
Effect of moisture level in PBXW-109(E) (plastic-bonded explosive) mixes on the aging of the cured explosive
[AD-A190200] N88-22202
CURRENT DENSITY
Stratospheric electric field and conductivity measurements over electrified convective clouds in the South American region, revised
[INPE-4046-PRE/1012-REV-3] N88-22483
High-T(sub c) superconducting wire fabrication and testing
[DE88-005989] N88-22798
High temperature superconductors in the La(sub 1+x)Ba(sub 2-x)Cu O(sub y system
[DE88-006367] N88-22802
CURVATURE
Complete minimal surfaces in R³ of low total curvature
[DE88-006425] N88-22619
CURVE FITTING
Motion sickness: Quantitative, algorithmic malaise indication in real time
[AD-A189674] N88-22518
CURVED PANELS
A study of damage tolerance in curved composite panels
[AD-A190617] N88-22092
CUTTING
Drilling metal matrix composites
[AD-A190480] N88-22091
CYCLIC LOADS
The growth of corner cracks under the conjoint action of high and low cycle fatigue
[AD-A190510] N88-22379
High-temperature combustor liner tests in structural component response test facility N88-22383
Life assessment of combustor liner using unified constitutive models N88-22384
CYCLOTRON RADIATION
Heating and confinement studies of electron cyclotron resonance heated plasmas in Heliotron E
[DE88-752312] N88-22746
CYCLOTRON RESONANCE
Heating and confinement studies of electron cyclotron resonance heated plasmas in Heliotron E
[DE88-752312] N88-22746
Status of RF superconductivity at Argonne National Laboratory
[DE88-005913] N88-22796
CYLINDRICAL BODIES
A study of damage tolerance in curved composite panels
[AD-A190617] N88-22092
Bodies in unsteady flow
[AD-A190416] N88-22308
Experimental determination of the coefficients of the hydraulic resistance of apertures in the rotary disks
[AD-A190627] N88-22317
Buckling of blast loaded cylinder
[AD-A190124] N88-22376
Thermal stress in high temperature cylindrical fasteners
[NASA-TM-100611] N88-22438
Multiple scattering from nonspherical targets
[AD-A189939] N88-22723
CZOCHRALSKI METHOD
Stress corrosion of ceramic materials
[AD-A190501] N88-22187
Autonomous control system for Czochralski growth of LEC GaAs
[AD-A189726] N88-22779

D

DAMAGE
Structural consequences of railgun augmentation
[DE88-007036] N88-22058
A study of damage tolerance in curved composite panels
[AD-A190617] N88-22092
Buckling of blast loaded cylinder
[AD-A190124] N88-22376
Evolution of hardening and damage during viscoplastic deformation
[AD-A190714] N88-22381
DAMAGE ASSESSMENT
Damage models for delamination and transverse fracture
[AD-A189652] N88-22088
Oxide optical coatings prepared by metal-organic vapor deposition
[DE88-006809] N88-22175
Impact damage in composite laminates N88-22402
Life prediction modeling based on cyclic damage accumulation N88-22426
DAMPING
Oscillation damped movement of suspended objects
[DE88-005715] N88-22433
DATA ACQUISITION
Enhancement of data acquisition and numerical computation capabilities for unsteady fluid dynamics
[AD-A190115] N88-22302
Calibration and processing of AVHRR data for temperature estimation
[INPE-4493-PRE/1257] N88-22485
A multivariate variational objective analysis-assimilation method. Part 2: Case study results with and without satellite data
[NASA-CR-182653] N88-22492
Real-time environmental Arctic monitoring (R-TEAM)
[AD-A189948] N88-22508
Complex sound processing: An interdisciplinary approach
[AD-A189782] N88-22523
Fast analog-to-digital converter
[TI88-701488] N88-22543
Application of static memory for data acquisition and transmission into a computer
[TI88-701491] N88-22544
DATA BASE MANAGEMENT SYSTEMS
Design of an algorithm to translate nested relational algebra queries to GENESIS trace manager commands
[AD-A190502] N88-22581

A graphics editor for structured analysis with a data dictionary
[AD-A190618] N88-22584
Modeling a parallel architecture for image processing
[RR-646-I] N88-22593
Application of new technologies to DTIC document processing
[AD-A189778] N88-22823
Data base design and implementation
[AD-A190414] N88-22827
Georelational data model
[INPE-4490-PRE/1254] N88-22829

DATA BASES
LGM-30B stage 2 disected motor test report
[AD-A190771] N88-22079
An expert system for discrete component digital circuit design
[AD-A189680] N88-22274
Analysis of head response to torso acceleration. Volume 2: Description of data retrieval, analysis and display software
[PB88-156765] N88-22536
A UNIX-based interactive VHDL (hardware description language) simulator
[AD-A189749] N88-22565
ONTIC: A knowledge representation system for mathematics
[AD-A190553] N88-22643
Sources of digital spatial data for geographic information systems
[AD-A189786] N88-22824

DATA COMPRESSION
Performance of data compression codes in channels with errors
[AD-A189667] N88-22253

DATA LINKS
Degradation of downlink distance measurement indexes by the addition of a third tone — tone ranging
[CNES-CT/DRT/TIT/TR-122-T] N88-22268

DATA MANAGEMENT
Sigma system: Overview, prospects N88-22230
Synthetic-aperture radars viewed as interferometers with matched filter processing of the collected data
[AD-A190608] N88-22262

DATA PROCESSING
Real-time flight test data distribution and display
[NASA-TM-100424] N88-22050
Baseline observing system experiments using the AFGL global data assimilation system
[AD-A188861] N88-22062
Basic research on flame radiation
[PB88-168372] N88-22105
Fast analog-to-digital converter
[TI88-701488] N88-22543

DATA PROCESSING EQUIPMENT
A methodolgy, based on analytical modeling, for the design of parallel and distributed architectures for relational database query processors
[AD-A189844] N88-22825

DATA REDUCTION
A multivariate variational objective analysis-assimilation method. Part 2: Case study results with and without satellite data
[NASA-CR-182653] N88-22492

DATA RETRIEVAL
Basic research on flame radiation
[PB88-168372] N88-22105
Analysis of head response to torso acceleration. Volume 2: Description of data retrieval, analysis and display software
[PB88-156765] N88-22536

DATA SMOOTHING
Smoothing technique to resolve X-ray spectra in laser nuclear fusion N88-22235

DATA STORAGE
Method and device for the detection and identification of a helicopter
[NASA-TT-20251] N88-22698

DATA SYSTEMS
Baseline observing system experiments using the AFGL global data assimilation system
[AD-A188861] N88-22062

DATA TRANSMISSION
Application of static memory for data acquisition and transmission into a computer
[TI88-701491] N88-22544

DECISION MAKING
Selective mechanisms in auditory and bimodal signal processing
[AD-A190529] N88-22530
Conflict resolution in cooperative systems
[AD-A190351] N88-22535

DECODING
Performance of single and multiple system AM stereo decoder receivers
[PB88-168307] N88-22265
Soft decoding of recorded HF data
[FOA-C-30473-3.3] N88-22269
Parallel memory addressing using coincident optical pulses
[AD-A189767] N88-22547

DECOMPOSITION
Structural decomposition of multiple time scale Markov processes
[AD-A189739] N88-22657

DEFECTS
Use of long-distance pair potentials in calculations of defect characteristics in metals
[TI88-701039] N88-22138
Nondestructive evaluation of sintered ceramics N88-22416
Processing defects and strength of alumina substrates
[W-10/87] N88-22441

DEFENSE INDUSTRY
JPRS report: Science and technology. Japan
[JPRS-JST-88-001] N88-22218
JPRS report: Science and technology. Japan
[JPRS-JST-87-029] N88-22228

DEFLECTION
Cubic spline solution of symmetric buckling problems of clamped shallow spherical shells N88-22239

DEFORMATION
Fundamental studies on high temperature deformation recrystallization, and grain growth of two-phase materials
[AD-A189725] N88-22145
The buckling and vibration of composite plates using the Levy method considering shear deformation and rotary inertia
[AD-A189743] N88-22374
Evolution of hardening and damage during viscoplastic deformation
[AD-A190714] N88-22381
Unified constitutive model for single crystal deformation behavior with applications N88-22388
Fundamental properties and devices applications of Ge(x)Si(1-x)/Si superlattices
[AD-A190129] N88-22787

DEGREES OF FREEDOM
Distributions of quadratic forms
[AD-A190224] N88-22663

DELAMINATING
Damage models for delamination and transverse fracture
[AD-A189652] N88-22088
Fractography of composite delamination
[NASA-CR-182757] N88-22096
Postbuckling delamination of a stiffened composite panel using finite element methods
[NASA-CR-182803] N88-22098

DELAY
Investigation of combustion in large vortices
[AD-A190406] N88-22121

DENSIMETERS
Gamma-ray densitometry: Nondestructive analysis of density evolution during ceramic powder processing
[DE88-006671] N88-22198

DENSITY MEASUREMENT
Density measurements on solids and liquids
[PB88-164934] N88-22129
Gamma-ray densitometry: Nondestructive analysis of density evolution during ceramic powder processing
[DE88-006671] N88-22198
A method of atmospheric density measurements during space shuttle entry using ultraviolet-laser Rayleigh scattering
[NASA-TM-100056] N88-22337
Annihilation momentum density of positrons trapped at vacancy-type defects in metals and alloys
[DE88-005936] N88-22797

DEPLOYMENT
Real-time environmental Arctic monitoring (R-TEAM)
[AD-A189948] N88-22508

DEPOSITION
Laser photodeposition and etching study
[AD-A190535] N88-22153

DEPOSITS
Development of a laboratory test for multiport injector deposits: Approaches 1 and 2
[AD-A190697] N88-22203

DEPTH
Physical, chemical and CTD (Conductivity/Temperature/Depth) data from the Marathon 2 expedition
[AD-A189930] N88-22507

DERIVATION
Derivation of consistent surface fixed fields for use in a global NWP model
[AD-A190131] N88-22475
Absolute pressure derivatives of deep level defects in 3-5 semiconductors
[DE88-006318] N88-22772

DESICCANTS
Mass transfer mechanisms for water adsorbed on silica gel
[DE88-005993] N88-22107

DESIGN ANALYSIS
Comparison of entropy generation and conventional design methods for heat exchangers
[AD-A190256] N88-22306
FLOSIN: A fluid loop analyzer for SINDA N88-22321
Constellation sizing for modest directed energy platforms
[DE88-007033] N88-22343
Improvements to tilt rotor performance through passive blade twist control
[NASA-TM-100583] N88-22434

DETECTION
Spectrographic detection of nitrogen impurity in helium
[DE88-752301] N88-22111
Optimum signal processing in distributed sensor systems
[AD-A189443] N88-22250
A multiple model adaptive tracking algorithm against airborne targets
[AD-A190619] N88-22263
Detecting the gas bubbles in a liquid metal coolant by means of magnetic flowmeters
[TI88-701427] N88-22294
Infrared differential absorption lidar for vapor detection
[AD-A190600] N88-22497
Proceedings of the Lightning Threat Warning Workshop
[DE88-006607] N88-22499
An evaluation of the effects of high visual taskload on the separate behaviors involved in complex monitoring performance
[AD-A190641] N88-22538
Finding texture boundaries in images
[AD-A190554] N88-22609
Mechanisms mediating the perception of complex acoustic patterns
[AD-A190112] N88-22705

DIAGNOSIS
Clinical measurements using fiber optic sensors
[DE88-005624] N88-22731

DIAGRAMS
PLOT3D (version-5): A computer code for drawing three dimensional graphs, maps and histograms, in single or multiple colours, for mono or stereoscopic viewing
[DE88-701410] N88-22558

DIAMONDS
Drilling metal matrix composites
[AD-A190480] N88-22091

DIATOMIC MOLECULES
Theory of the dissociation dynamics of small molecules on metal surfaces: Finite temperature studies
[DE88-006495] N88-22716

DICTIONARIES
A graphics editor for structured analysis with a data dictionary
[AD-A190618] N88-22584

DIELECTRIC PROPERTIES
Microwave dispersion and absorption in tissues: Molecular mechanisms
[AD-A190118] N88-22512

DIESEL ENGINES
Cetane scale evaluation and possible modification
[AD-A189730] N88-22200

DIESEL FUELS
Cetane scale evaluation and possible modification
[AD-A189730] N88-22200

DIETS
Dietary factors related to physical fitness
[AD-A190272] N88-22527

DIFFERENTIAL EQUATIONS
Analytic solutions to dynamic equations of plasma armature railguns
[DE88-006842] N88-22057
Fluid motion in a spinning, coning cylinder via spatial eigenfunction expansion
[AD-A190758] N88-22319
Evolution of hardening and damage during viscoplastic deformation
[AD-A190714] N88-22381
Logarithmically connected, repetitive computer networks and numerical applications
[DE88-006632] N88-22592
A zonal approach for the solution of coupled Euler and potential solutions of flows with complex geometries
[AD-A189752] N88-22595
Numerical solution of nonlinear algebraic equations in stiff ODE solving
[DE88-006634] N88-22622
Numerical methods for singularly perturbed differential equations with applications
[AD-A189786] N88-22628

Normed Bellman equation with degenerate diffusion coefficients and its application to differential equations
[AD-A190319] N88-22637

DIFFRACTION
Research on certain aspects of laser diffraction particle sizing relevant to autonomous self-diagnosing instrumentation
[AD-A190220] N88-22348
A hardware/software system for implementing geophysical diffraction tomography
[DE88-006411] N88-22480

DIFFRACTION PATTERNS
A review on holography, its principles and applications
[ISL-CO-242/86] N88-22398

DIFFUSION COEFFICIENT
Normed Bellman equation with degenerate diffusion coefficients and its application to differential equations
[AD-A190319] N88-22637

DIFFUSION ELECTRODES
The kinetics of contact noise in NaBeta alumina
[AD-A190651] N88-22707

DIFFUSION LENGTH
Multigroup flux-limited asymptotic diffusion Fokker-Planck equation
[DE88-700958] N88-22615

DIFFUSION THEORY
COMESH: A corner mesh finite difference code to solve multigroup diffusion equations in multidimensions
[DE88-701248] N88-22555
Multigroup flux-limited asymptotic diffusion Fokker-Planck equation
[DE88-700958] N88-22615

DIFFUSION WELDING
Joints in fiber-reinforced aluminum alloys
[NASA-TT-20160] N88-22104

DIGITAL DATA
Direct bit detection receiver noise performance analysis for 32-PSK and 64-PSK modulated signals
[AD-A190009] N88-22256
Calibration and processing of AVHRR data for temperature estimation
[INPE-4493-PRE/1257] N88-22485
NASA and the challenge of ISDN: The role of satellites in an ISDN world
[NASA-CR-182749] N88-22676

DIGITAL SYSTEMS
Preliminary airworthiness evaluation of the UH-60A with Advanced Digital Optical Control System (ADOCS)
[AD-A190674] N88-22030
Subharmonic aliasing and its effects on the AFTI/F-16 digital flight control system
[AD-A190614] N88-22042
A fully abstract semantics for event-based simulation
[AD-A190560] N88-22283
Exhaustive and pseudo-exhaustive testing
[AD-A190140] N88-22574
Design and implementation of VLSI prime factor algorithm processor
[AD-A190483] N88-22580
Representation, analysis and design of multirate discrete-time control systems
[AD-A190499] N88-22608
Two papers on a symbolic analyzer for MOS (Metal-Oxide Semiconductors) circuits
[AD-A188617] N88-22761
Sources of digital spatial data for geographic information systems
[AD-A189788] N88-22824

DIGITAL TECHNIQUES
Comparative utilization of analog and digital processes in the treatment of MSS-LANDSAT data for studying the national parks of Brazil
[INPE-4011-TDL/240] N88-22456

DIPOLE ANTENNAS
An improved method for calculating power density in the Fresnel region of circular parabolic reflector antennas
[AD-A190569] N88-22284

DIPPING
Studies on hot-dip zinc-aluminum coated sheet steels
[ETN-88-92217] N88-22166

DISCONTINUITY
Detection of the number, locations and magnitudes of jumps
[AD-A190328] N88-22571

DISCRETE FUNCTIONS
Representation, analysis and design of multirate discrete-time control systems
[AD-A190499] N88-22608

DISCRIMINATION
Auditory pattern memory: Mechanisms of tonal sequence discrimination by human observers
[AD-A190337] N88-22534

DISPENSERS
Preliminary airworthiness evaluation of the UH-60A equipped with the XM-139 VOLCANO mine dispensing system
[AD-A190604] N88-22029

DISPERSING
Dense-spray structure and phenomena. Part 1. Turbulence/dispersed-phase interactions
[AD-A190606] N88-22315
Microwave dispersion and absorption in tissues: Molecular mechanisms
[AD-A190118] N88-22512

DISPERSIONS
A survey of denser-than-air atmospheric dispersion models
[DE88-006626] N88-22467

DISPLACEMENT
An efficient Mindlin finite strip plate element based on assumed strain distribution N88-22407

DISPLAY DEVICES
Effects of update and refresh rates on flight simulation visual displays
[NASA-TM-100415] N88-22033
Geometric modeling of flight information for graphical cockpit display
[AD-A190484] N88-22043
Real-time flight test data distribution and display
[NASA-TM-100424] N88-22050
Basic research on flame radiation
[PB88-168372] N88-22105
A 3-D solid rendering of NDT data
[DE88-006199] N88-22373
Auditory pattern memory: Mechanisms of tonal sequence discrimination by human observers
[AD-A190337] N88-22534
A graphics editor for structured analysis with a data dictionary
[AD-A190618] N88-22584
Two-dimensional graphics tools for a transputer based display board
[NASA-TM-100820] N88-22591

DISSIPATION
A physically consistent model for artificial dissipation in transonic potential flow computations
[NASA-TM-100846] N88-22652

DISSOCIATION
Theory of the dissociation dynamics of small molecules on metal surfaces: Finite temperature studies
[DE88-006495] N88-22718

DISTANCE MEASURING EQUIPMENT
Degradation of downlink distance measurement indexes by the addition of a third tone — tone ranging
[CNES-CT/DRT/TIT/TR-122-T] N88-22268

DISTORTION
Ultrasonic beam distortion in transversely isotropic media
[DE88-005937] N88-22699

DISTRIBUTED PARAMETER SYSTEMS
Feedback control of distributed parameter systems with applications to large space structures
[AD-A190536] N88-22068
Instrumentation to provide an active control capability for distributed parameter systems
[AD-A190043] N88-22375
Boundary shape identification problems in two-dimensional domains related to thermal testing of materials
[NASA-CR-181654] N88-22541
The Colored Stochastic Petri Net (CS-PN) software: Application to the validation and the performance evaluation of distributed systems
[ENST-87D005] N88-22589
Approximation methods for the identification and control of distributed parameter systems
[AD-A190201] N88-22662

DISTRIBUTED PROCESSING
Argus reference manual
[AD-A190382] N88-22578
The Colored Stochastic Petri Net (CS-PN) software: Application to the validation and the performance evaluation of distributed systems
[ENST-87D005] N88-22589
A methodolgy, based on analytical modeling, for the design of parallel and distributed architectures for relational database query processors
[AD-A189844] N88-22825

DISTRIBUTION (PROPERTY)
Assessment of crop loss from air pollutants: Meteorology-atmospheric chemistry and long range transport
[PB88-146857] N88-22448

DISTRIBUTION FUNCTIONS
Distributions of quadratic forms
[AD-A190224] N88-22663
Estimation of convolution tails
[AD-A190323] N88-22666

DIVERGENCE
Involution-dependent constants and the cancellation of divergences in the 1-loop open string amplitude
[DE88-006537] N88-22611

DOCUMENTATION
NASA scientific and technical publications: A catalog of Special Publications, Reference Publications, Conference Publications, and Technical Papers, 1987
[NASA-SP-7063(02)] N88-22830

DOCUMENTS
Application of new technologies to DTIC document processing
[AD-A189778] N88-22823

DOMAINS
Boundary shape identification problems in two-dimensional domains related to thermal testing of materials
[NASA-CR-181654] N88-22541

DOPED CRYSTALS
Singlet oxygen behavior in solid polymer matrices
[DE88-005171] N88-22171
Superconductivity and the tailoring of lattice parameters of the compound YBa2Cu3O(sub x)
[DE88-005904] N88-22769

DOSIMETERS
Characterization of space radiation environment in terms of the energy deposition in functionally important volumes
[DE88-005627] N88-22513
Anthropomorphic phantom radiation dosimetry at the NATO standard reference point at Aberdeen Proving Ground
[AD-A190508] N88-22528

DOWNLINKING
INPE position paper on the CCSDS standardized method of link budget computation
[INPE-4533-NTE/279] N88-22820

DRAG REDUCTION
Control of laminar flow around of the wing in free-air conditions
[AD-A187479] N88-22004
Enhanced viscous flow drag reduction using acoustic excitation
[NASA-CR-182734] N88-22295

DRAWINGS
PLOT3D (version-5): A computer code for drawing three dimensional graphs, maps and histograms, in single or multiple colours, for mono or stereoscopic viewing
[DE88-701410] N88-22558

DRILLING
Drilling metal matrix composites
[AD-A190480] N88-22091

DROP SIZE
Droplet size characteristics and energy input requirements of emulsions formed using high-intensity-pulsed electric fields
[DE88-005912] N88-22692

DUCTED FLOW
A survey of oscillating flow in Stirling engine heat exchangers
[NASA-CR-182108] N88-22322

DUCTED ROCKET ENGINES
An experimental investigation of rocket ramjet nozzle assembly base pressures
[AD-A189714] N88-22076

DUCTILITY
The effective fracture toughness of aluminum at rapid heating rates
[AD-A189745] N88-22146

DUCTS
Numerical and experimental investigation of multiple shock wave/turbulent boundary layer interactions in a rectangular duct
[AD-A190772] N88-22320
ALEX results: A comparison of measurements from a round and a rectangular duct with 3-D code predictions
[DE88-005947] N88-22741

DUMMIES
Anthropomorphic phantom radiation dosimetry at the NATO standard reference point at Aberdeen Proving Ground
[AD-A190508] N88-22528

DURABILITY
Durability testing of an iridium-plated storable rocket engine injector
[AD-A190707] N88-22078
Computational structural mechanics for engine structures N88-22399

DYE LASERS
Solid hosts for dye laser rods. Part 1: Criteria for choosing a host material
[DE88-006478] N88-22355

DYNAMIC CHARACTERISTICS
The effects of torque response and time delay on rotorcraft vertical axis handling qualities
[AD-A189873] N88-22023

KRASH parametric sensitivity study: Transport category airplanes
[AD-A189962] N88-22024
Nonlinear analysis and optimal design of dynamic mechanical systems for spacecraft application
[AD-A190644] N88-22070
Molecular dynamics of materials possessing high energy content
[AD-A190034] N88-22118
Unsteady flow field measurements using LDV (Laser Doppler Velocimetry)
[AD-A189907] N88-22298
The CRREL (Cold Regions Research and Engineering Laboratory) Hopkinson bar apparatus
[AD-A190599] N88-22380

DYNAMIC CONTROL
Linear state space modeling of a turbofan engine
[AD-A190110] N88-22035
Feedback control of distributed parameter systems with applications to large space structures
[AD-A190536] N88-22068
Effect of friction and control parameters on the tracking accuracy of a target seeker
[AD-A190010] N88-22257
Problems in nonlinear continuum dynamics
[AD-A190538] N88-22691

DYNAMIC LOADS
Pressure measurements of impinging jet with asymmetric nozzle
[NASA-CR-182759] N88-22011
Development of a computer code CRACK for elastic and elastoplastic fracture mechanics analysis of 2-D structures by finite element technique
[DE88-701231] N88-22370
FLAP (Force and Loads Analysis Program) code development and validation
[DE88-001131] N88-22371
The CRREL (Cold Regions Research and Engineering Laboratory) Hopkinson bar apparatus
[AD-A190599] N88-22380

DYNAMIC MODELS
Laser photodeposition and etching study
[AD-A190535] N88-22153

DYNAMIC PRESSURE
A 150,000 pounds per square inch dynamic pressure calibrator
[AD-A190659] N88-22335
Synthesis of metastable superconductors by high dynamic pressure
[DE88-005620] N88-22764

DYNAMIC RESPONSE
Shape sensitivity analysis of wing static aeroelastic characteristics
[NASA-TP-2808] N88-22031
Feedback control of distributed parameter systems with applications to large space structures
[AD-A190536] N88-22068
Galvanic corrosion initiatives
[AD-A190658] N88-22155
Influence of unsteady aerodynamic forces on dynamic response of variable sweep aircraft N88-22245
The concept of an impact resonance diagram for characterizing the nonlinear response of impact vibration
[DE88-005475] N88-22432
Coupled bending-torsion steady-state response of pretwisted, nonuniform rotating beams using a transfer-matrix method
[NASA-TM-100596] N88-22435
The analysis of non-linear dynamic behavior (including snap-through) of postbuckled plates by simple analytical solution
[NASA-TM-89165] N88-22439

DYNAMIC STABILITY
Vibrations of structures with parametric uncertainties
[AD-A190400] N88-22378

DYNAMIC STRUCTURAL ANALYSIS
Wave propagation and dynamics of lattice structures
[AD-A190037] N88-22066
Wave propagation and dynamics of lattice structures
[AD-A190611] N88-22069
Nonlinear analysis and optimal design of dynamic mechanical systems for spacecraft application
[AD-A190644] N88-22070
Stabilization and control problems in structural dynamics
[AD-A190197] N88-22361
FLAP (Force and Loads Analysis Program) code development and validation
[DE88-001131] N88-22371
Lewis Structures Technology, 1988. Volume 2: Structural Mechanics
[NASA-CP-3003-VOL-2] N88-22382
Lewis Structures Technology, 1988. Volume 3: Structural Integrity Fatigue and Fracture Wind Turbines HOST
[NASA-CP-3003-VOL-3] N88-22408
Structural dynamics branch research and accomplishments for fiscal year 1987
[NASA-TM-100279] N88-22446

DYNAMIC TESTS
KRASH parametric sensitivity study: Transport category airplanes
[AD-A189962] N88-22024

DYNAMICAL SYSTEMS
Laser spectroscopy and dynamics of combustion intermediates
[DE88-006541] N88-22110
On new solvable many-body dynamical systems with velocity dependent forces
[PREPRINT-581] N88-22683

E

E REGION
Rocket measurements of ionospheric electron temperature over Natal
[INPE-4485-PRE/1250] N88-22489

EARTH MOVEMENTS
Description of ground motion data processing codes, volume 2
[DE88-007137] N88-22481

EARTHQUAKES
Earthquakes from peninsular India: Data from the Gauribidanur seismic array
[DE88-701232] N88-22471
Characteristics of seismic sources of some Asian earthquakes and Soviet underground explosions from Gauribidanur array records
[DE88-701233] N88-22472

ECONOMIC ANALYSIS
Northern lights: The economic and practical potential of imported power from Canada
[DE88-006026] N88-22473

EDDY CURRENTS
Eddy current nondestructive inspection of graphite epoxy using ferrite cup core probes
[AD-A189823] N88-22365

EDGES
Finding texture boundaries in images
[AD-A190554] N88-22609

EFFECTIVENESS
Film cooling effectiveness on a flat plate in high free-stream turbulence using a single row of 30 deg slant-hole injectors
[AD-A190500] N88-22816

EIGENVALUES
Application of eigenstructure assignment techniques in the design of a longitudinal flight control system
[AD-A189644] N88-22039
Fluid motion in a spinning, coning cylinder via spatial eigenfunction expansion
[AD-A190758] N88-22319

EIGENVECTORS
Application of eigenstructure assignment techniques in the design of a longitudinal flight control system
[AD-A189644] N88-22039
Fluid motion in a spinning, coning cylinder via spatial eigenfunction expansion
[AD-A190758] N88-22319

EISCAT RADAR SYSTEM (EUROPE)
Coordinated Auroral Experiments using Scatter And Rocket investigations (CAESAR investigations)
[MPAE-W-47-87-13] N88-22487

EJECTA
Bilateral symmetry elements of the Zhamanshin impact crater
[NASA-TT-20288] N88-22490

EJECTORS
Numerical and experimental investigation of multiple shock wave/turbulent boundary layer interactions in a rectangular duct
[AD-A190772] N88-22320

ELASTIC DEFORMATION
Phenomenological modelling of rate-dependent plasticity for high strain rate problems
[DE88-006647] N88-22440

ELASTIC PROPERTIES
High-performance polymeric materials
[AD-A190708] N88-22190
A three-dimensional model for the elastic properties of a foam
[DE88-006197] N88-22192
A new method of measuring multigrade oil shear elasticity and viscosity at high shear rates
[AD-A190145] N88-22304
The CRREL (Cold Regions Research and Engineering Laboratory) Hopkinson bar apparatus
[AD-A190599] N88-22380
Measurement of the elastic-plastic surface flaw back surface topology and its relation to constraint
[DE88-006765] N88-22437

ELASTOMERS
High-performance polymeric materials
[AD-A190708] N88-22190

ELASTOPLASTICITY
Development of a computer code CRACK for elastic and elastoplastic fracture mechanics analysis of 2-D structures by finite element technique
[DE88-701231] N88-22370

ELECTRIC ARCS
Theoretical model of the cathode spot on a unipolar arc
[AD-A190109] N88-22277

ELECTRIC BATTERIES
GTE battery management system: State of charge indicator evaluation
[DE88-006800] N88-22272

ELECTRIC CONDUCTORS
Strategies in the topological approach to electromagnetic interference control
[AD-A189874] N88-22255

ELECTRIC CONTACTS
The kinetics of contact noise in NaBeta alumina
[AD-A190651] N88-22707
The influence of current stressing on the structure of Ag contacts to GaAs
[DE88-005988] N88-22771

ELECTRIC CORONA
The growth potential of corona discharges from aircraft flying in precipitation
[AD-A190507] N88-22478

ELECTRIC DISCHARGES
The growth potential of corona discharges from aircraft flying in precipitation
[AD-A190507] N88-22478

ELECTRIC FIELDS
Stratospheric electric field and conductivity measurements over electrified convective clouds in the South American region, revised
[INPE-4046-PRE/1012-REV-3] N88-22483
A study on electric fields and conductivity associated with electrified clouds in the region of South America
[INPE-4487-TDL/325] N88-22486
On the acceleration of electrons and positive ions in the same direction along magnetic field lines by parallel electric fields
[IRF-PREPRINT-103] N88-22488
Experimental comparison of lightning simulation techniques to CV-580 airborne lightning strike measurements
[AD-A190576] N88-22496
Droplet size characteristics and energy input requirements of emulsions formed using high-intensity-pulsed electric fields
[DE88-005912] N88-22692
Parametric instabilities of inhomogeneous plasma near the lower-hybrid resonance
[TI88-701201] N88-22748
High power, high frequency radiation from beam-plasma interactions
[AD-A190207] N88-22752

ELECTRIC GENERATORS
Superconductivity in power engineering
[DE88-701414] N88-22776

ELECTRIC MOTOR VEHICLES
Status of electric vehicle simulation programs at the INEL: Summer 1987
[DE88-006745] N88-22271

ELECTRIC NETWORKS
ECP (Electrical Circuitry Program): A proposed program for electrical circuitry analysis
[AD-A190494] N88-22280

ELECTRIC POTENTIAL
Modeling the effects of heavy charged particles on MOSFETs (Metal-Oxide-Semiconductor Field Effect Transistors)
[AD-A190575] N88-22792

ELECTRIC POWER TRANSMISSION
Northern lights: The economic and practical potential of imported power from Canada
[DE88-006026] N88-22473

ELECTRIC PROPULSION
Physical fluid mechanics in MPD thrusters
[AD-A190309] N88-22754

ELECTRICAL MEASUREMENT
Calculating depletion region carrier concentrations with capacitance-voltage measurements and etching
[AD-A189630] N88-22777

ELECTRICAL PROPERTIES
Electrical circuit modeling of reversed field pinches
[DE88-006942] N88-22745
Preparation of large area NbN/AlN/NbN Josephson junctions
[DE88-006074] N88-22799

ELECTRICAL RESISTIVITY
Electrical resistivities of some compound forming liquid metal alloys
[PB88-145172] N88-22137
Research on stable processible conducting polymers for electronic applications
[AD-A190246] N88-22180
Temperature-dependent conductivity of oxygen-depleted YBCO ceramics
[AD-A190340] N88-22182
Analysis of anomalous resistivity during the conduction phase of the plasma erosion opening switch
[DE88-006382] N88-22286
Stratospheric electric field and conductivity measurements over electrified convective clouds in the South American region, revised
[INPE-4046-PRE/1012-REV-3] N88-22483
A study on electric fields and conductivity associated with electrified clouds in the region of South America
[INPE-4487-TDL/325] N88-22486
Physical, chemical and CTD (Conductivity/Temperature/Depth) data from the Marathon 2 expedition
[AD-A189930] N88-22507
ELECTRICITY
Northern lights: The economic and practical potential of imported power from Canada
[DE88-006026] N88-22473
A qualitative approach to electricity
[AD-A189654] N88-22693
ELECTRO-OPTICS
Summary and conclusions on electrooptical streak camera project
[DE88-006616] N88-22334
Collective rotation of molecules driven by the angular momentum of light in a nematic film
[FUB-6-1986] N88-22714
Gas source MBE (Molecular Beam Epitaxy)
[AD-A189763] N88-22782
Research on materials and components for opto-electronic signal processing and computing
[AD-A190130] N88-22788
ELECTROCHEMICAL CORROSION
Corrosion and electrochemical behavior of binary magnesium alloys
[AD-A190624] N88-22154
Galvanic corrosion initiatives
[AD-A190658] N88-22155
High temperature oxidation and electrochemical studies related to hot corrosion
[AD-A190699] N88-22156
Corrosion Research Center, University of Minnesota
[DE88-006681] N88-22160
ELECTROCHEMICAL OXIDATION
High temperature oxidation and electrochemical studies related to hot corrosion
[AD-A190699] N88-22156
ELECTROCHEMISTRY
Electronic and ionic transport in polymers
[AD-A190434] N88-22185
ELECTRODES
Application of copper-carbon fiber composites to power semiconductor devices
[NASA-TT-20171] N88-22101
Growth and deformation mechanisms of refractory alloy hybrid materials
[AD-A190492] N88-22152
Evaporation characteristics of elements during vacuum arc remelting of alloy A-286 N88-22248
ELECTROLYTIC CELLS
Recent advances in solid polymer electrolyte fuel cell technology
[DE88-005380] N88-22484
ELECTROMAGNETIC ABSORPTION
Microwave dispersion and absorption in tissues: Molecular mechanisms
[AD-A190118] N88-22512
Research on materials and components for opto-electronic signal processing and computing
[AD-A190130] N88-22788
ELECTROMAGNETIC COMPATIBILITY
Strategies in the topological approach to electromagnetic interference control
[AD-A189874] N88-22255
Electromagnetic compatability: An introduction to the theory of interference and shielding, 3rd revised edition
[PB88-165410] N88-22264
ELECTROMAGNETIC FIELDS
A qualitative approach to electricity
[AD-A189654] N88-22693
ELECTROMAGNETIC INTERACTIONS
Particle acceleration to high energies and amplification of coherent radiation by electromagnetic interactions in plasmas
[TI86-701020] N88-22737
ELECTROMAGNETIC INTERFERENCE
Strategies in the topological approach to electromagnetic interference control
[AD-A189874] N88-22255
Electromagnetic compatability: An introduction to the theory of interference and shielding, 3rd revised edition
[PB88-165410] N88-22264
ELECTROMAGNETIC PULSES
EMR (Electromagnetic Radiation) test facilities evaluation of reverberating chamber located at RADC (Rome Air Development Center), Griffiss AFB (Air Force Base), Rome, New York
[PB88-178827] N88-22048
Investigations of test methodology for the stress loading facility
[PB88-166095] N88-22049
Parallel memory addressing using coincident optical pulses
[AD-A189767] N88-22547
ELECTROMAGNETIC RADIATION
Strategies in the topological approach to electromagnetic interference control
[AD-A189874] N88-22255
Electromagnetic sensor arrays for nondestructive evaluation and robot control
[AD-A190210] N88-22260
Theoretical studies of the heating of toroidal plasmas with radiofrequency electromagnetic radiation
[DE88-006913] N88-22749
ELECTROMAGNETIC SCATTERING
Polarimetric ISAR imaging using either measured or calculated transient signatures
[AD-A190077] N88-22259
Models for electromagnetic scattering from the sea at extremely low grazing angles
[AD-A190472] N88-22261
ELECTROMAGNETIC SHIELDING
Strategies in the topological approach to electromagnetic interference control
[AD-A189874] N88-22255
Electromagnetic compatability: An introduction to the theory of interference and shielding, 3rd revised edition
[PB88-165410] N88-22264
ELECTROMAGNETIC WAVE TRANSMISSION
High speed transcendental elementary function architecture in support of the Vector Wave Equation (VWE)
[AD-A189746] N88-22627
Parametric instabilities of inhomogeneous plasma near the lower-hybrid resonance
[TI88-701201] N88-22748
ELECTROMAGNETISM
Launchability of base-driven electromagnetic projectiles
[AD-A189635] N88-22055
ELECTRON BEAMS
Growth and deformation mechanisms of refractory alloy hybrid materials
[AD-A190492] N88-22152
Directed-energy electron-beam processing of a hypoeutectic Cr90Ta10 alloy
[DE88-005621] N88-22157
Discharge excitation of the XeF C to A transition
[DE88-006448] N88-22339
Numerical modelling specific energy charcteristics of excimer KrF lasers with electron beam excitation
[DE88-701525] N88-22344
Nonlinear effects in plasma wake field acceleration
[TI88-700972] N88-22734
High power, high frequency radiation from beam-plasma interactions
[AD-A190207] N88-22752
ELECTRON CYCLOTRON HEATING
Preparing the Alcator C bolometer system for use on MTX (Microwave Tokamak Experiment)
[DE88-006724] N88-22733
ELECTRON DENSITY PROFILES
Support for FY87 midlatitude electron-density calibration campaign
[AD-A190174] N88-22476
ELECTRON DIFFRACTION
Fundamental properties and devices applications of Ge(x)Si(1-x)/Si superlattices
[AD-A190129] N88-22787
ELECTRON EMISSION
Theoretical model of the cathode spot on a unipolar arc
[AD-A190109] N88-22277
ELECTRON ENERGY
Rocket measurements of ionospheric electron temperature over Natal
[INPE-4485-PRE/1250] N88-22489
ELECTRON MICROSCOPES
The contribution of electron microscopy of materials science to society
[DE88-006341] N88-22082
In situ fatigue loading stage inside scanning electron microscope N88-22419
ELECTRON MICROSCOPY
The contribution of electron microscopy of materials science to society
[DE88-006341] N88-22082
An investigation of the crystalchemistry and thermochemistry of selected mineral systems
[AD-A189758] N88-22781
ELECTRON PARAMAGNETIC RESONANCE
Excitations in magnetic low-dimensional systems: A spectroscopic study
[ETN-88-92230] N88-22697
ELECTRON SCATTERING
Effective electron interactions due to virtual charge and spin excitations in an extended Hubbard model for Cu-O superconductors
[DE88-005971] N88-22766
ELECTRON SOURCES
Program to research laser-driven thermionic electron sources for free electron lasers
[AD-A190473] N88-22353
ELECTRONIC COUNTERMEASURES
High speed transcendental elementary function architecture in support of the Vector Wave Equation (VWE)
[AD-A189746] N88-22627
ELECTRONIC EQUIPMENT
Investigations of test methodology for the stress loading facility
[PB88-166095] N88-22049
Experimental studies on electronic properties of HgTe/CdTe and Hg sub 1-x Cd sub x Te/CdTe heterostructures and superlattices
[AD-A189826] N88-22783
ELECTRONIC FILTERS
Advanced capacitor development
[AD-A189985] N88-22276
ELECTRONS
Developments in ceramic superconducting materials N88-22229
On the acceleration of electrons and positive ions in the same direction along magnetic field lines by parallel electric fields
[IRF-PREPRINT-103] N88-22488
Improvement of plasma confinement due to electron Landau damping in tokamaks
[DE88-752339] N88-22747
Effective electron interactions due to virtual charge and spin excitations in an extended Hubbard model for Cu-O superconductors
[DE88-005971] N88-22766
ELECTROPLATING
RF properties of superconducting Pb electroplated onto Cu
[DE88-005918] N88-22765
ELECTROSTATICS
A qualitative approach to electricity
[AD-A189654] N88-22693
ELEMENTARY EXCITATIONS
First-principles calculations of quasiparticle energies at surfaces and interfaces: Semiconductor surface-state spectra and band offsets
[DE88-006340] N88-22773
ELLIPSOIDS
Periodic orbits around a satellite modelled as a triaxial ellipsoid
[AD-A190592] N88-22051
ELLIPTIC DIFFERENTIAL EQUATIONS
The inverse power method for semilinear elliptic equations
[DE88-006427] N88-22620
EMBEDDING
Embedded minimal sufaces with an infinite number of ends
[DE88-006429] N88-22680
EMISSION SPECTRA
Alkali metal diffuse band lasers
[AD-A190244] N88-22350
Sequential excitation preparation of molecular energy levels with special structural and chemical properties
[AD-A190041] N88-22718
EMISSIVITY
Measurement of emissivity of industrial surfaces using a simple method
[NASA-TT-20165] N88-22130
The thermal radiative properties of metals at high temperature
[DE88-006625] N88-22141
EMITTERS
Mathematics clinic probabilistic position-fixing
[NASA-CR-182753] N88-22672

EMULSIONS
Droplet size characteristics and energy input requirements of emulsions formed using high-intensity-pulsed electric fields
[DE88-005912] N88-22692
ENERGY CONSERVATION
Overview of 1987 moonlight project N88-22231
Wave energy flow conservation for propagation in inhomogeneous Vlasov-Maxwell equilibria
[DE88-006705] N88-22251
ENERGY CONSUMPTION
Droplet size characteristics and energy input requirements of emulsions formed using high-intensity-pulsed electric fields
[DE88-005912] N88-22692
ENERGY CONVERSION EFFICIENCY
Recent advances in photovoltaic concentrator technology
[DE88-003948] N88-22462
ENERGY DISTRIBUTION
Angular resolved energy analysis of (69)Ga+ ions from a gallium liquid metal ion source
[AERE-R-12649] N88-22760
ENERGY GAPS (SOLID STATE)
Developments in ceramic superconducting materials N88-22229
ENERGY LEVELS
Discharge excitation of the XeF C to A transition
[DE88-006448] N88-22339
Fermi level stabilization in semiconductors: Implications for implant activation efficiency
[DE88-006332] N88-22801
ENERGY OF FORMATION
Use of long-distance pair potentials in calculations of defect characteristics in metals
[TI88-701039] N88-22138
ENERGY POLICY
Technical highlights of the Alternative Fuels Utilization Program
[DE88-005064] N88-22205
ENERGY REQUIREMENTS
Droplet size characteristics and energy input requirements of emulsions formed using high-intensity-pulsed electric fields
[DE88-005912] N88-22692
ENERGY SPECTRA
Spectral measurements in a disturbed boundary layer over snow
[AD-A190217] N88-22494
Computing X-ray effects in optics
[DE88-006722] N88-22732
ENERGY STORAGE
Overview of 1987 moonlight project N88-22231
Performance evaluation of molten salt thermal storage systems
[DE87-014645] N88-22461
ENERGY TECHNOLOGY
JPRS report: Science and technology. Japan
[JPRS-JST-87-029] N88-22228
Overview of 1987 moonlight project N88-22231
ENERGY TRANSFER
Electronic energy transfer processes in the alkali/alkaline earth metal vapors
[AD-A190035] N88-22119
Molecular reaction and energy transfer rate estimation for chemical-laser analysis
[AD-A190664] N88-22126
Reactions of N2(A sup 3 sigma sup + sub u) candidates for short wavelength lasers
[DE88-007018] N88-22342
Characterization of space radiation environment in terms of the energy deposition in functionally important volumes
[DE88-005627] N88-22513
ENGINE DESIGN
Visualisation of the flow at the tip of a high speed axial flow turbine rotor: An assessment of flow visualisation techniques and the requirement of the experimental turbine
[AD-A189929] N88-22301
Continuous fiber ceramic matrix composites for heat engine components N88-22411
ENGINE INLETS
Numerical and experimental investigation of multiple shock wave/turbulent boundary layer interactions in a rectangular duct
[AD-A190772] N88-22320
ENGINE NOISE
Noise assessment of unsuppressed TF-34-GE-100A engine at Warfield ANG, Baltimore, Maryland
[AD-A189966] N88-22702
ENGINE PARTS
Small engine components test facility turbine testing cell
[NASA-TM-100887] N88-22037
Specialty three-dimensional finite element analysis codes N88-22393
Computational structural mechanics for engine structures N88-22399
Thermal-structural analyses of Space Shuttle Main Engine (SSME) hot section components N88-22404
ENGINE TESTS
Small engine components test facility turbine testing cell
[NASA-TM-100887] N88-22037
LGM-30B stage 2 disected motor test report
[AD-A190771] N88-22079
High-temperature combustor liner tests in structural component response test facility N88-22383
ENTHALPY
Evaluation of direct methane conversion to higher hydrocarbons and oxygenates
[DE88-003812] N88-22204
ENVIRONMENT EFFECTS
Assessment of crop loss from air pollutants: Meteorology-atmospheric chemistry and long range transport
[PB88-146857] N88-22448
ENVIRONMENT POLLUTION
Evaluation of existing total human exposure models
[PB88-146840] N88-22517
ENVIRONMENTAL MONITORING
Real-time environmental Arctic monitoring (R-TEAM)
[AD-A189948] N88-22508
EPINEPHRINE
A program for the study of skeletal muscle catabolism following physical trauma
[AD-A189771] N88-22521
EPITAXY
Laser evaporation studies
[AD-A189815] N88-22346
Fundamental properties and devices applications of Ge(x)Si(1-x)/Si superlattices
[AD-A190129] N88-22787
Equilibrium stability of strained epitaxial layers on a rigid substrate
[INPE-4254-PRE/1127] N88-22804
EPOXY RESINS
Eddy current nondestructive inspection of graphite epoxy using ferrite cup core probes
[AD-A189823] N88-22365
EQUATIONS OF MOTION
A three dimensional non-singular modelling of rigid manipulators
[AD-A189707] N88-22604
Singular Lagrangians. Classical dynamics and quantization. Lectures for young scientists
[TI88-701158] N88-22806
EQUATORIAL ATMOSPHERE
In-situ plasma bubble observations associated with equatorial spread-F over Natal
[INPE-4488-PRE/1252] N88-22482
EQUILIBRIUM
Wave energy flow conservation for propagation in inhomogeneous Vlasov-Maxwell equilibria
[DE88-006705] N88-22251
Equilibrium stability of strained epitaxial layers on a rigid substrate
[INPE-4254-PRE/1127] N88-22804
EQUIPMENT SPECIFICATIONS
UARS spacecraft recorder
[NASA-CR-180768] N88-22331
In situ fatigue loading stage inside scanning electron microscope N88-22419
Research sensors N88-22430
EQUIVALENCE
Constructive version of the approximation induction principle
[PB88-165477] N88-22647
EROSION
Durability testing of an iridium-plated storable rocket engine injector
[AD-A190707] N88-22078
Investigation of laser diagnostics of PACVD processes for depositing hard face coatings
[DE88-007083] N88-22176
Analysis of anomalous resistivity during the conduction phase of the plasma erosion opening switch
[DE88-006382] N88-22286
ERROR ANALYSIS
Aircraft accident report: North Star Aviation, Inc., PA-32 RT-300, N39614 and Alameda Aero Club Cessna 172, N75584, Oakland, California, March 31, 1987
[PB87-910412] N88-22021
Methodology for software reliability prediction, volume 1
[AD-A190018] N88-22571
Methodology for software reliability prediction, volume 3
[AD-A190019] N88-22572
A posterior error estimation in a finite element method for parabolic partial differential equations
[AD-A190296] N88-22636
Analysis and testing of the SURE program
[NASA-TP-2817] N88-22653
ERROR DETECTION CODES
Self-checking logic arrays
[RR-656-I] N88-22545
ERRORS
Merit of Hadamard transform active absorption spectrometer described N88-22232
An expert system for discrete component digital circuit design
[AD-A189680] N88-22274
ESTIMATES
Moving-bank multiple model adaptive estimation applied to flexible spacestructure control
[AD-A190761] N88-22071
Boundary shape identification problems in two-dimensional domains related to thermal testing of materials
[NASA-CR-181654] N88-22541
Consistent estimates of autoregressive parameters for autoregressive moving average models
[RR-663-I] N88-22564
Estimation of convolution tails
[AD-A190323] N88-22668
ESTIMATING
Empirical and hierarchical Bayes competitors of preliminary test estimators in two sample problems
[AD-A190327] N88-22670
ETCHING
Laser photodeposition and etching study
[AD-A190535] N88-22153
Calculating depletion region carrier concentrations with capacitance-voltage measurements and etching
[AD-A189630] N88-22777
EUCLIDEAN GEOMETRY
Complete minimal surfaces in R^3 of low total curvature
[DE88-006425] N88-22619
EULER EQUATIONS OF MOTION
On the prediction of highly vortical flows using an Euler equation model, part 2
[AD-A190245] N88-22305
High-resolution shock-capturing schemes for inviscid and viscous hypersonic flows
[NASA-TM-100097] N88-22651
EUROPIUM COMPOUNDS
Growth of Pb/sub 1-x/Eu/sub x/Te epitaxial layers by the liquid phase epitaxy technique
[TI88-701022] N88-22763
EUTECTIC ALLOYS
Directed-energy electron-beam processing of a hypoeutectic Cr90Ta10 alloy
[DE88-005621] N88-22157
EVALUATION
EMR (Electromagnetic Radiation) test facilities evaluation of reverberating chamber located at RADC (Rome Air Development Center), Griffiss AFB (Air Force Base), Rome, New York
[PB88-178827] N88-22048
Today's photovoltaic systems: An evaluation of their performance
[DE88-006926] N88-22457
Prediction of physical fitness: Estimated percent body fat using body circumferences versus weight-height measures
[AD-A190233] N88-22526
EVAPORATION
Superfine grain development by laser N88-22215
Hard ceramic film by laser PVD N88-22216
Evaporation characteristics of elements during vacuum arc remelting of alloy A-286 N88-22248
Laser evaporation studies
[AD-A189815] N88-22346
EXCIMER LASERS
Laser processing-status, perspectives N88-22211
Numerical modelling specific energy charcteristics of excimer KrF lasers with electron beam excitation
[DE88-701525] N88-22344
Alkali metal diffuse band lasers
[AD-A190244] N88-22350
EXCITATION
Electronic energy transfer processes in the alkali/alkaline earth metal vapors
[AD-A190035] N88-22119
Discharge excitation of the XeF C to A transition
[DE88-006448] N88-22339
Numerical modelling specific energy charcteristics of excimer KrF lasers with electron beam excitation
[DE88-701525] N88-22344
Effect of vibrational excitation on rate parameters of atmospheric reactions
[AD-A190464] N88-22477

Sequential excitation preparation of molecular energy levels with special structural and chemical properties
[AD-A190041] N88-22718
Effective electron interactions due to virtual charge and spin excitations in an extended Hubbard model for Cu-O superconductors
[DE88-005971] N88-22766
First-principles calculations of quasiparticle energies at surfaces and interfaces: Semiconductor surface-state spectra and band offsets
[DE88-006340] N88-22773

EXHAUST FLOW SIMULATION
Split-coefficient matrix solution and experimental study of axisymmetric underexpanded exhaust plumes
N88-22242

EXHAUST GASES
Investigation of aeroacoustic mechanisms by remote thermal imaging
[DE88-002612] N88-22046
An experimental investigation of rocket ramjet nozzle assembly base pressures
[AD-A189714] N88-22076
Split-coefficient matrix solution and experimental study of axisymmetric underexpanded exhaust plumes
N88-22242

EXOBIOLOGY
USSR Space Life Sciences Digest, issue 16
[NASA-CR-3922(19)] N88-22515

EXPANSION
Piston-driven, unsteady separation at a sudden expansion in a tube: Flow visualization and Laser Doppler Anemometer (LDA) measurements
[ETN-88-92104] N88-22329
String driven inflation
[DE88-006994] N88-22841
Cosmology for high energy physicists
[DE88-005705] N88-22842

EXPEDITIONS
Physical, chemical and CTD (Conductivity/Temperature/Depth) data from the Marathon 2 expedition
[AD-A189930] N88-22507

EXPERIMENT DESIGN
Short experiment study of four-wire helical antennas (half turn half wave)
[CNES-CT/DRT/TIT/AN-249-T] N88-22266
Experimental design and structural optimization
[PB88-169255] N88-22436
Experimental study on the influence of wind on acoustic pressure sensors
[ISL-R-121/86] N88-22712

EXPERT SYSTEMS
Kalman filter residual expert system
[AD-A190520] N88-22041
Characteristics of LSI-wiring expert system discussed
N88-22226
An expert system for discrete component digital circuit design
[AD-A189680] N88-22274
Inference engine for expert systems
[INPE-4465-TDL/321] N88-22590
Design and implementation of a parallel computer for expert system applications
[DE88-005286] N88-22601
Memory-based expert systems
[AD-A190203] N88-22606
Rapid prototyping of simulations in artificial intelligence environments
[DE88-004295] N88-22612

EXPLOSIVE DEVICES
Investigation of Super°Zip separation joint
[NASA-TM-4031] N88-22072

EXPLOSIVE FORMING
Characterization of an explosively consolidated rapidly solidified Fe-16Ni-9Cr-5Mo-2Cu alloy powder
[DE88-006733] N88-22162

EXPLOSIVES
Effect of moisture level in PBXW-109(E) (plastic-bonded explosive) mixes on the aging of the cured explosive
[AD-A190200] N88-22202

EXPONENTIAL FUNCTIONS
High speed transcendental elementary function architecture in support of the Vector Wave Equation (VWE)
[AD-A189746] N88-22627

EXPOSURE
Evaluation of existing total human exposure models
[PB88-146840] N88-22517

EXTENSOMETERS
Computer grading of extensometers (BS 3846)
[NPL-DMA(A)-152] N88-22560

EXTERNAL TANKS
External tank gamma ray imaging telescope study. Final review, phase 2
[NASA-CR-179320] N88-22834

EXTRATERRESTRIAL RADIATION
Characterization of space radiation environment in terms of the energy deposition in functionally important volumes
[DE88-005627] N88-22513

EXTRAVEHICULAR ACTIVITY
Design, development and evaluation of Stanford/Ames EVA prehensors
[NASA-CR-182688] N88-22540

EXTREMUM VALUES
Approximations in extreme value theory
[AD-A189817] N88-22659
Extreme value for dependent sequences via the Stein-Chen method of poisson approximation
[AD-A190325] N88-22668

EXTRUDING
Grain growth behavior of extrusion consolidated centrifugally atomized Type 304 stainless steel powder
[DE88-006788] N88-22143

EYE (ANATOMY)
Protection against laser damage to human body reviewed N88-22237
Laboratory equipment update
[AD-A189781] N88-22522

F

F REGION
In-situ plasma bubble observations associated with equatorial spread-F over Natal
[INPE-4488-PRE/1252] N88-22482
Rocket measurements of ionospheric electron temperature over Natal
[INPE-4485-PRE/1250] N88-22489

F-16 AIRCRAFT
Multivariable control law design for the AFTI/F-16 with a failed control surface using a parameter-adaptive controller
[AD-A189848] N88-22040
Subharmonic aliasing and its effects on the AFTI/F-16 digital flight control system
[AD-A190614] N88-22042

FABRICATION
Fabrication and characterization of semiconductor lasers of Pb(1-x)Sn(x)Te
[INPE-4253-PRE/1126] N88-22357
Synthesis of metastable superconductors by high dynamic pressure
[DE88-005620] N88-22764
Beam assisted fabrication of 3-5/Si monolithic devices
[AD-A189979] N88-22785
High-T(sub c) superconducting wire fabrication and testing
[DE88-005989] N88-22798
Preparation of large area NbN/AlN/NbN Josephson junctions
[DE88-006074] N88-22799

FACTORIAL DESIGN
SEARCH: An interactive computer program for optimizing two-variable, unconstrained experiments or simulation
[AD-A190593] N88-22583

FAILURE
Multivariable control law design for the AFTI/F-16 with a failed control surface using a parameter-adaptive controller
[AD-A189848] N88-22040
An investigation of the failure response of laminates under biaxial stress
[AD-A190039] N88-22090
Galvanic corrosion initiatives
[AD-A190658] N88-22155

FAILURE ANALYSIS
Investigation of Super°Zip separation joint
[NASA-TM-4031] N88-22072
Modeling failures of intermittently used machines
[AD-A190298] N88-22367
Buckling of blast loaded cylinder
[AD-A190124] N88-22376
Experiments investigating advanced materials under thermomechanical loading N88-22385
Monolithic ceramic analysis using the SCARE program
N88-22409
Fracture technology for brittle materials N88-22417

FAILURE MODES
Mode 2 fracture mechanics N88-22418

FAN BLADES
The composite blade structural analyzer (COBSTRAN)
N88-22390
Structural tailoring of advanced turboprops
N88-22400

FAR INFRARED RADIATION
Theoretical studies of Resonance Enhanced Stimulated Raman Scattering (RESRS) of frequency-doubled Alexandrite laser wavelength in cesium vapor
[NASA-CR-182870] N88-22133
Experimental studies on electronic properties of HgTe/CdTe and Hg sub 1-z Cd sub x Te/CdTe heterostructures and superlattices
[AD-A189826] N88-22783

FAST FOURIER TRANSFORMATIONS
Synthetic-aperture radars viewed as interferometers with matched filter processing of the collected data
[AD-A190608] N88-22262
Design and implementation of VLSI prime factor algorithm processor
[AD-A190483] N88-22580

FASTENERS
Thermal stress in high temperature cylindrical fasteners
[NASA-TM-100611] N88-22438

FATIGUE (MATERIALS)
Environmentally assisted crack growth in structural alloys: Perspectives and new directions
[AD-A190137] N88-22377
Lewis Structures Technology, 1988. Volume 2: Structural Mechanics
[NASA-CP-3003-VOL-2] N88-22382
Mode 2 fracture mechanics N88-22418
In situ fatigue loading stage inside scanning electron microscope N88-22419
Grain boundary oxidation and low-cycle fatigue at elevated temperatures N88-22420
Cumulative fatigue damage models N88-22422
Fatigue damage mapping N88-22423
Spectrum fatigue testing for materials characterization
[VTT-RR-502] N88-22443

FATIGUE LIFE
Life assessment of combustor liner using unified constitutive models N88-22384
Computational structural mechanics for engine structures N88-22399
Large-scale wind turbine structures N88-22429
Random Process Simulation for stochastic fatigue analysis
[NASA-TM-100464] N88-22654

FATIGUE TESTS
Bithermal fatigue of a nickel-base superalloy single crystal
[NASA-TM-100885] N88-22168
Spectrum fatigue testing for materials characterization
[VTT-RR-502] N88-22443

FAULT TOLERANCE
Methodology for software reliability prediction, volume 1
[AD-A190018] N88-22571
Methodology for software reliability prediction, volume 3
[AD-A190019] N88-22572
Exhaustive and pseudo-exhaustive testing
[AD-A190140] N88-22574
Argus reference manual
[AD-A190382] N88-22578
Simulation of fault tolerance in a hypercube arrangement of discrete processors
[AD-A189682] N88-22594
Analysis and testing of the SURE program
[NASA-TP-2817] N88-22653
A fault tolerant supervision system
[INPE-4419-TDL/307] N88-22819

FEASIBILITY ANALYSIS
Preliminary market analysis for large zeolite crystals
[NASA-CR-182882] N88-22207
Superconductivity in power engineering
[DE88-701414] N88-22776

FEEDBACK
Conditions for information capacity of the discrete-time Gaussian channel to be increased by feedback
[AD-A190317] N88-22687

FEEDBACK CONTROL
Application of eigenstructure assignment techniques in the design of a longitudinal flight control system
[AD-A189644] N88-22039
Multivariable control law design for the AFTI/F-16 with a failed control surface using a parameter-adaptive controller
[AD-A189848] N88-22040
Feedback control of distributed parameter systems with applications to large space structures
[AD-A190536] N88-22068
Approximation methods for the identification and control of distributed parameter systems
[AD-A190201] N88-22662

FERMI SURFACES
Fermi level stabilization in semiconductors: Implications for implant activation efficiency
[DE88-006332] N88-22801

FERRIC IONS
Determination of aquo-complexes of chromium and iron in chromium plating and polishing solutions by ion chromatography
[AD-A190168] N88-22148
FERRITES
Eddy current nondestructive inspection of graphite epoxy using ferrite cup core probes
[AD-A189823] N88-22365
FERROMAGNETIC MATERIALS
Excitations in magnetic low-dimensional systems: A spectroscopic study
[ETN-88-92230] N88-22697
FIBER COMPOSITES
Structure and surface characterizations of high strength carbon fibers
[AD-A189642] N88-22087
Damage models for delamination and transverse fracture
[AD-A189652] N88-22088
Fracture toughness testing of a ceramic matrix composite
[AD-A189846] N88-22089
An investigation of the failure response of laminates under biaxial stress
[AD-A190039] N88-22090
Interfacial structure-property relationships at the fiber-matrix interphase in advanced composites
[AD-A190649] N88-22093
Thermal expansion behavior of randomly oriented short carbon fiber reinforced copper composites
[NASA-TT-20175] N88-22099
Reciprocating sliding wear characteristics of copper-carbon fiber composites
[NASA-TT-20176] N88-22100
Fiber-reinforced plastic composites. Possibilities and limitations of applications as machine-construction materials
[NASA-TT-20159] N88-22102
Processing, microstructure, and mechanical properties of silicon carbide particulate reinforced aluminum alloys
[AD-A188981] N88-22136
The composite blade structural analyzer (COBSTRAN) N88-22390
Whisker-reinforced ceramic composites for heat engine components N88-22410
Nondestructive evaluation by acousto-ultrasonics N88-22412
FIBER OPTICS
Amplification of signals in fiber optics using the stimulated Raman effect
[AD-A190281] N88-22727
A 104-km unrepeatered bidirectional fiber optic demonstration link
[AD-A190282] N88-22728
Clinical measurements using fiber optic sensors
[DE88-005624] N88-22731
FIBER ORIENTATION
Thermal expansion behavior of randomly oriented short carbon fiber reinforced copper composites
[NASA-TT-20175] N88-22099
Reciprocating sliding wear characteristics of copper-carbon fiber composites
[NASA-TT-20176] N88-22100
FIELD EFFECT TRANSISTORS
Examination of temperature effects on gate-to-drain avalanche breakdown in GaAs MESFETs (Metal-Semiconductor Field Effect Transistors) by measuring light emission under RF drive
[AD-A189634] N88-22778
Modeling the effects of heavy charged particles on MOSFETs (Metal-Oxide-Semiconductor Field Effect Transistors)
[AD-A190575] N88-22792
FIELD STRENGTH
Magnet strength fluctuations in the SSC (Superconducting Super Collider) lattice. Part 2: Frequency modulation
[DE88-006491] N88-22774
FIELD THEORY (PHYSICS)
Super Virasoro algebra and solvable supersymmetric quantum field theories
[DE88-752299] N88-22681
To the field theory with a fundamental mass
[TI88-701159] N88-22807
Secondary gauge conditions in field theory
[TI88-701499] N88-22814
FIGHTER AIRCRAFT
Model selection for the multiple model adaptive algorithm for in-flight simulation
[AD-A189715] N88-22022
Multivariable control law design for the AFTI/F-16 with a failed control surface using a parameter-adaptive controller
[AD-A189848] N88-22040
Kalman filter residual expert system
[AD-A190520] N88-22041
FILLERS
Ultrasonic characterization of ceramic joints
[DE88-005844] N88-22173
FILM CONDENSATION
Dilution refrigerator with non-valve adsorption system of sup 3/He circulation
[DE88-700974] N88-22209
FILM COOLING
Film cooling effectiveness on a flat plate in high free-stream turbulence using a single row of 30 deg slant-hole injectors
[AD-A190500] N88-22816
FINES
Study of mean free path effects on growth of ultrafine metallic aerosols
[AD-A190206] N88-22149
Fine grain development by laser CVD N88-22214
Superfine grain development by laser N88-22215
FINITE DIFFERENCE THEORY
COMESH: A corner mesh finite difference code to solve multigroup diffusion equations in multidimensions
[DE88-701248] N88-22555
FINITE ELEMENT METHOD
Moving-bank multiple model adaptive estimation applied to flexible spacestructure control
[AD-A190761] N88-22071
Postbuckling delamination of a stiffened composite panel using finite element methods
[NASA-CR-182803] N88-22098
Finite element simulation of perforation of aluminum plates
[DE88-002092] N88-22362
Development of a computer code CRACK for elastic and elastoplastic fracture mechanics analysis of 2-D structures by finite element technique
[DE88-701231] N88-22370
Elasto-plastic analysis using a stress-based finite element method and an endochronic theory of plasticity
[DE88-003001] N88-22372
Finite element (MARC) solution technologies for viscoplastic analyses N88-22389
Three-dimensional inelastic approximate analysis code (MOMM) N88-22392
Specialty three-dimensional finite element analysis codes N88-22393
MHOST: An efficient finite element program for inelastic analysis of solids and structures N88-22394
Fatigue damage modeling for coated single crystal superalloys N88-22427
Development and application of the p-version of the finite element method
[AD-A190036] N88-22633
A posterior error estimation in a finite element method for parabolic partial differential equations
[AD-A190296] N88-22636
FINITE VOLUME METHOD
Mixed direct-inverse problem of transonic cascade N88-22244
Zero-lift drag predictions in supersonic flow for complex configurations N88-22246
FIRE CONTROL
Method and device for the detection and identification of a helicopter
[NASA-TT-20251] N88-22698
FIRE PREVENTION
A systems analysis of fire suppression alternatives for the US space station
[AD-A189847] N88-22064
FIRES
Heat transfer from a negatively buoyant wall jet
[NBS-GCR-88-541] N88-22208
FLAME STABILITY
Basic instability mechanisms in chemically reacting subsonic and supersonic flows
[AD-A190101] N88-22120
FLAMES
Numerical simulation of turbulent flames using vortex methods
[AD-A189813] N88-22116
FLASH BLINDNESS
A comparison of visual evoked potential and behavioral measures of flashblindness in humans
[AD-A189757] N88-22519
FLAT PLATES
Film cooling effectiveness on a flat plate in high free-stream turbulence using a single row of 30 deg slant-hole injectors
[AD-A190500] N88-22816
FLEXIBILITY
Ultrasonic characterization of ceramic joints
[DE88-005844] N88-22173
FLEXIBLE BODIES
Optimal control and identification of space structures
[AD-A190033] N88-22065
Approximation methods for the identification and control of distributed parameter systems
[AD-A190201] N88-22662
FLIGHT CHARACTERISTICS
Bifurcations in unsteady aerodynamics-implications for testing
[NASA-TM-100083] N88-22014
FLIGHT CONTROL
Application of eigenstructure assignment techniques in the design of a longitudinal flight control system
[AD-A189644] N88-22039
Multivariable control law design for the AFTI/F-16 with a failed control surface using a parameter-adaptive controller
[AD-A189848] N88-22040
Kalman filter residual expert system
[AD-A190520] N88-22041
Subharmonic aliasing and its effects on the AFTI/F-16 digital flight control system
[AD-A190614] N88-22042
Multiple model parameter adaptive control for in-flight simulation
[AD-A190568] N88-22044
FLIGHT ENVELOPES
Multiple model parameter adaptive control for in-flight simulation
[AD-A190568] N88-22044
FLIGHT INSTRUMENTS
Geometric modeling of flight information for graphical cockpit display
[AD-A190484] N88-22043
FLIGHT PATHS
Modification of the BLUEMAX 2 terrain following model to incorporate radar detection
[AD-A190594] N88-22028
Geometric modeling of flight information for graphical cockpit display
[AD-A190484] N88-22043
FLIGHT SIMULATION
Model selection for the multiple model adaptive algorithm for in-flight simulation
[AD-A189715] N88-22022
Effects of update and refresh rates on flight simulation visual displays
[NASA-TM-100415] N88-22033
Application of eigenstructure assignment techniques in the design of a longitudinal flight control system
[AD-A189644] N88-22039
Multiple model parameter adaptive control for in-flight simulation
[AD-A190568] N88-22044
FLIGHT STABILITY TESTS
Preliminary airworthiness evaluation of the UH-60A equipped with the XM-139 VOLCANO mine dispensing system
[AD-A190604] N88-22029
FLIGHT TESTS
Bifurcations in unsteady aerodynamics-implications for testing
[NASA-TM-100083] N88-22014
Real-time flight test data distribution and display
[NASA-TM-100424] N88-22050
The growth potential of corona discharges from aircraft flying in precipitation
[AD-A190507] N88-22478
FLIGHT TIME
General aviation activity and avionics survey: 1986 data
[AD-A189986] N88-22003
FLIR DETECTORS
A multiple model adaptive tracking algorithm against airborne targets
[AD-A190619] N88-22263
FLOODS
Project CODEAMA/FUNCATE (test-area of Barreirinha-AM): Field report
[INPE-4500-RPE/563] N88-22455
FLOW DISTRIBUTION
High Reynolds number, low Mach number, steady flow field calculations over a NACA 0012 airfoil using Navier-Stokes and interactive boundary layer theory
[AD-A189871] N88-22005
Transonic Navier-Stokes computations of strake-generated vortex interactions for a fighter-like configuration
[NASA-TM-100009] N88-22010
Contraction design for small low-speed wind tunnels
[NASA-CR-182747] N88-22045
Turbulent reacting flows and supersonic combustion
[AD-A189690] N88-22115
An investigation of flow structure, mixing and chemical reaction in combusting turbulent flows
[AD-A189980] N88-22117
Unsteady flow field measurements using LDV (Laser Doppler Velocimetry)
[AD-A189907] N88-22298

On the prediction of highly vortical flows using an Euler equation model, part 2
[AD-A190245] N88-22305
Interaction of a two-dimensional bluff body and incompressible jet and annulus flows
[AD-A190503] N88-22310
Cavitation inception in rectangular two-dimensional slots
[AD-A190677] N88-22318
Changes in the California current system observed off northern California during July-August 1986
[AD-A190027] N88-22510
MPD (magnetoplasmadynamic) thrust chamber flow dynamics
[AD-A189940] N88-22751

FLOW MEASUREMENT
Boundary-layer and wake measurements on a swept, circulation-control wing
[NASA-TM-89426] N88-22013
Inflow measurement made with a laser velocimeter on a helicopter model in forward flight. Volume 3: Rectangular planform blades at an advance ratio of 0.30
[NASA-TM-100543] N88-22015
Piston-driven, unsteady separation at a sudden expansion in a tube: Flow visualization and Laser Doppler Anemometer (LDA) measurements
[ETN-88-92104] N88-22329

FLOW STABILITY
The sensitivity of boundary layer instability growth rates to compliant wall properties
[AD-A190433] N88-22309

FLOW VELOCITY
An investigation of flow structure, mixing and chemical reaction in combusting turbulent flows
[AD-A189980] N88-22117

FLOW VISUALIZATION
Unsteady flow field measurements using LDV (Laser Doppler Velocimetry)
[AD-A189907] N88-22298
Visualization of flows in turbomachinery
[AD-A189927] N88-22299
Visualisation of the flow at the tip of a high speed axial flow turbine rotor
[AD-A189928] N88-22300
Visualisation of the flow at the tip of a high speed axial flow turbine rotor: An assessment of flow visualisation techniques and the requirement of the experimental turbine
[AD-A189929] N88-22301
Dense-spray structure and phenomena. Part 2: Pressure-atomized sprays
[AD-A190312] N88-22307
Interaction of a two-dimensional bluff body and incompressible jet and annulus flows
[AD-A190503] N88-22310
Chemically reacting turbulent flow
[AD-A190522] N88-22311
Numerical and experimental investigation of multiple shock wave/turbulent boundary layer interactions in a rectangular duct
[AD-A190772] N88-22320
Piston-driven, unsteady separation at a sudden expansion in a tube: Flow visualization and Laser Doppler Anemometer (LDA) measurements
[ETN-88-92104] N88-22329

FLOWMETERS
Detecting the gas bubbles in a liquid metal coolant by means of magnetic flowmeters
[TI88-701427] N88-22294

FLUID BOUNDARIES
Fluid motion in a spinning, coning cylinder via spatial eigenfunction expansion
[AD-A190758] N88-22319

FLUID DYNAMICS
Enhancement of data acquisition and numerical computation capabilities for unsteady fluid dynamics
[AD-A190115] N88-22302
Effect of freestream turbulence on a two dimensional cascade, with different surface roughness, at high Reynolds number
[AD-A190615] N88-22316
Review and assessment of the HOST turbine heat transfer program N88-22431
A physically consistent model for artificial dissipation in transonic potential flow computations
[NASA-TM-100846] N88-22652
MPD (magnetoplasmadynamic) thrust chamber flow dynamics
[AD-A189940] N88-22751

FLUID FLOW
Mixing: Stretching, breakup and chaos
[DE88-006699] N88-22327

FLUID MANAGEMENT
FLOSIN: A fluid loop analyzer for SINDA N88-22321

FLUID MECHANICS
Mixing: Stretching, breakup and chaos
[DE88-006699] N88-22327
Physical fluid mechanics in MPD thrusters
[AD-A190309] N88-22754
Research and technology
[NASA-TM-100172] N88-22851

FLUIDS
Fluids, gels and glasses under extreme conditions of pressure and temperature
[AD-A190655] N88-22125

FLUORIDES
NMR analysis of a fluorocarbon copolymer
[DE88-002364] N88-22170

FLUORINATION
A new approach to highly fluorinated lubricants
[AD-A190523] N88-22188

FLUORINE
Numerical modelling specific energy charcteristics of excimer KrF lasers with electron beam excitation
[DE88-701525] N88-22344

FLUTTER
Design of an integrated control system for flutter margin augmentation and gust load alleviation, tested on a dynamic windtunnel model
[PB88-149885] N88-22038

FLUX DENSITY
Magnetic fusion energy plasma interactive and high heat flux components. Volume 5: Technical assesement of critical issues in the steady state operation of fusion confinement devices
[DE88-006920] N88-22744

FOAMS
A three-dimensional model for the elastic properties of a foam
[DE88-006197] N88-22192

FOCUSING
Manufacturing of ultrasonic focused probes
[VTT-RR-487] N88-22368

FOKKER-PLANCK EQUATION
Memory efficient evaluations of nonlinear stochastic equations and C3 applications
[AD-A189872] N88-22569
Multigroup flux-limited asymptotic diffusion Fokker-Planck equation
[DE88-700958] N88-22615

FORCED VIBRATION
The concept of an impact resonance diagram for characterizing the nonlinear response of impact vibration
[DE88-005475] N88-22432

FORESTS
Aerodynamic aspects of the Amazon Forest
[INPE-4445-TDL/313] N88-22501

FORMALISM
Hamiltonian formalism in the model of the relativistic string with rigidity
[TI88-701503] N88-22815

FORMAT
Output formatting in Apple-soft BASIC
[DE88-701413] N88-22559

FRACTOGRAPHY
Fractography of composite delamination
[NASA-CR-182757] N88-22096
Characterization of sintered SiC by using NDE N88-22413

FRACTURE MECHANICS
Investigation of Super*Zip separation joint
[NASA-TM-4031] N88-22072
Damage models for delamination and transverse fracture
[AD-A189652] N88-22088
Fracture toughness testing of a ceramic matrix composite
[AD-A189846] N88-22089
The effective fracture toughness of aluminum at rapid heating rates
[AD-A189745] N88-22146
Stress corrosion of ceramic materials
[AD-A190501] N88-22187
A test for interfacial effects and stress transfer in ceramic matrix composites
[NASA-CR-182758] N88-22194
Crack opening and extension in inert solid propellant. An experimental study
[AD-A189808] N88-22201
Environmentally assisted crack growth in structural alloys: Perspectives and new directions
[AD-A190137] N88-22377
Lewis Structures Technology, 1988. Volume 2: Structural Mechanics
[NASA-CP-3003-VOL-2] N88-22382
Computational simulation methods for composite fracture mechanics N88-22396
Lewis Structures Technology, 1988. Volume 3: Structural Integrity Fatigue and Fracture Wind Turbines HOST
[NASA-CP-3003-VOL-3] N88-22408
Monolithic ceramic analysis using the SCARE program N88-22409
Fracture technology for brittle materials N88-22417
Mode 2 fracture mechanics N88-22418
Elevated temperature crack growth N88-22421
Large-scale wind turbine structures N88-22429
Processing defects and strength of alumina substrates
[W-10/87] N88-22441
A simplified key-curve approach for J-R-curve testing of CT specimens
[VTT-RR-503] N88-22444

FRACTURE STRENGTH
Fracture toughness testing of a ceramic matrix composite
[AD-A189846] N88-22089
Interlaminar fracture toughness of thermoplastic composites
[NASA-TM-100532] N88-22097
Postbuckling delamination of a stiffened composite panel using finite element methods
[NASA-CR-182803] N88-22098
The effective fracture toughness of aluminum at rapid heating rates
[AD-A189745] N88-22146
Fracture toughness of silicon nitride-silicon nitride joints bonded with oxynitride glass
[DE88-005548] N88-22172
Strength and microstructure of ceramics
[AD-A190712] N88-22191
Computational simulation methods for composite fracture mechanics N88-22396
Processing defects and strength of alumina substrates
[W-10/87] N88-22441
Increasing strength of graphite/epoxy bolted joints by introducing an adhesively bonded metallic insert
[FFA-TN-1987-45] N88-22442

FREDHOLM EQUATIONS
An approximation technique for solving a system of Fredholm integral equations for asymmetric detector response functions
[AD-A190577] N88-22645

FREE ELECTRON LASERS
Extension of free-electron lasers into the extreme ultraviolet
[DE88-005373] N88-22341
Program to research laser-driven thermionic electron sources for free electron lasers
[AD-A190473] N88-22353

FREE FLOW
Instruments for use in experimental studies of complex turbulent shear flow: Three component LDVs
[AD-A190526] N88-22312
Effect of freestream turbulence on a two dimensional cascade, with different surface roughness, at high Reynolds number
[AD-A190615] N88-22316
Film cooling effectiveness on a flat plate in high free-stream turbulence using a single row of 30 deg slant-hole injectors
[AD-A190500] N88-22816

FREE RADICALS
Infrared absorption spectroscopy and chemical kinetics of free radicals
[DE88-006536] N88-22112

FREQUENCY CONTROL
Investigation of boundary layer disturbances caused by periodic heating of a thin ribbon
[AD-A190572] N88-22314

FREQUENCY HOPPING
Soft decoding of recorded HF data
[FOA-C-30473-3.3] N88-22269

FREQUENCY MODULATION
Magnet strength fluctuations in the SSC (Superconducting Super Collider) lattice. Part 2: Frequency modulation
[DE88-006491] N88-22774

FREQUENCY SHIFT KEYING
The 2 FSK/QPSK (Frequency Shift Keying/Quadrature Phase Shift Keying) transmitter and receiver: Design and performance
[AD-A190028] N88-22258

FREQUENCY STABILITY
Investigation of boundary layer disturbances caused by periodic heating of a thin ribbon
[AD-A190572] N88-22314

FREQUENCY SYNTHESIZERS
Mechanisms mediating perception of complex acoustic patterns
[AD-A189765] N88-22520

FRESNEL REGION
An improved method for calculating power density in the Fresnel region of circular parabolic reflector antennas
[AD-A190569] N88-22284

FRICTION
Effect of friction and control parameters on the tracking accuracy of a target seeker
[AD-A190010] N88-22257
Traction model development
[AD-A188450] N88-22359
FRONTS (METEOROLOGY)
The effects of time-dependent winds and ocean eddies on ice motion in a marginal ice zone
[AD-A190105] N88-22511
FUEL CELLS
Recent advances in solid polymer electrolyte fuel cell technology
[DE88-005380] N88-22464
FUEL COMBUSTION
AFRAPT (Air Force Research in Aero Propulsion Technology) trainee program
[AD-A190525] N88-22123
FUEL TANKS
Development and evaluation of an airplane fuel tank ullage composition model. Volume 2: Experimental determination of airplane fuel tank ullage compositions
[AD-A190408] N88-22025
FUNCTION GENERATORS
High-voltage inverse-square function generator
[DE88-701109] N88-22270
FUNCTIONAL DESIGN SPECIFICATIONS
Using Colored Stochastic Petri Net (CS-PN) software for protocol specification, validation, and evaluation
[ENST-87C004] N88-22588
FUSELAGES
Experimental comparison of lightning simulation techniques to CV-580 airborne lightning strike measurements
[AD-A190576] N88-22496
FUSION REACTORS
Analyses and experiments on the integrity and lifetime predictions of plasma-facing components in fusion reactors
[DE87-702957] N88-22735

G

GALACTIC CLUSTERS
Multiple object redshift determinations in clusters of galaxies using OCTOPUS
[INPE-4528-PRE/1278] N88-22835
New measurements of radial velocities in clusters of galaxies
[INPE-4527-PRE/1277] N88-22845
GALAXIES
Near-infrared observations of cepheids: The distance to M33 N88-22846
GALERKIN METHOD
A posterior error estimation in a finite element method for parabolic partial differential equations
[AD-A190296] N88-22636
GALLIUM
Angular resolved energy analysis of (69)Ga+ ions from a gallium liquid metal ion source
[AERE-R-12649] N88-22760
GALLIUM ARSENIDES
Stress corrosion of ceramic materials
[AD-A190501] N88-22187
The influence of current stressing on the structure of Ag contacts to GaAs
[DE88-005988] N88-22771
Examination of temperature effects on gate-to-drain avalanche breakdown in GaAs MESFETs (Metal-Semiconductor Field Effect Transistors) by measuring light emission under RF drive
[AD-A189634] N88-22778
Autonomous control system for Czochralski growth of LEC GaAs
[AD-A189726] N88-22779
GALLIUM PHOSPHIDES
High-efficiency thin-film silicon-on-GaP solar cell for improved radiation resistance
[AD-A190268] N88-22460
GAMMA RAY ASTRONOMY
External tank gamma ray imaging telescope study. Final review, phase 2
[NASA-CR-179320] N88-22834
GAMMA RAY LASERS
SDIO/IST ultrashort wavelength laser: Novel experimental schemes for observing the Mossbauer effect in long-lived nuclear levels
[AD-A190275] N88-22351
SDIO/IST ultrashort wavelength laser. Mossbauer effect in gamma-ray lasers
[AD-A190306] N88-22352
GAMMA RAYS
Gamma-ray densitometry: Nondestructive analysis of density evolution during ceramic powder processing
[DE88-006671] N88-22198
GAS COOLED REACTORS
Basic characteristics of heat-exchanger-type steam reformer heated by high-temperature helium gas (2). Analysis by simulation model (2)
[DE87-702962] N88-22291
GAS DETECTORS
Ultrasonic oxygen sensor
[AD-A189723] N88-22537
GAS DYNAMICS
Investigation of combustion in large vortices
[AD-A190406] N88-22121
Research sensors N88-22430
GAS MIXTURES
Ultrasonic oxygen sensor
[AD-A189723] N88-22537
GAS TEMPERATURE
Research sensors N88-22430
Anomalies in the heat-capacity signatures of submonolayer adsorbates with attractive lateral interactions
[AD-A190736] N88-22817
GAS TURBINE ENGINES
Review and assessment of the HOST turbine heat transfer program N88-22431
GAS TURBINES
Research as part of the Air Force in aero propulsion technology (AFRAPT) program
[AD-A190336] N88-22036
Small engine components test facility turbine testing cell
[NASA-TM-100887] N88-22037
AFRAPT (Air Force Research in Aero Propulsion Technology) trainee program
[AD-A190525] N88-22123
Experimental determination of the coefficients of the hydraulic resistance of apertures in the rotary disks
[AD-A190627] N88-22317
Study on shaft seals for potassium turbine
[EL-891] N88-22364
GAS-GAS INTERACTIONS
Numerical and experimental investigation of multiple shock wave/turbulent boundary layer interactions in a rectangular duct
[AD-A190772] N88-22320
GAS-SOLID INTERACTIONS
Microvax networked computer system
[AD-A190308] N88-22596
GASEOUS DIFFUSION
Synthesis and analysis of novel polymers with potential for providing both high permselectivity and permeability in gas separation applications
[DE88-006533] N88-22174
GASES
Detecting the gas bubbles in a liquid metal coolant by means of magnetic flowmeters
[TI88-701427] N88-22294
Gas source MBE (Molecular Beam Epitaxy)
[AD-A189763] N88-22782
GAUGE INVARIANCE
Recent developments in the path integral approach to anomalies
[DE87-703032] N88-22616
Path integral, BRS symmetry, and string and membrane theories
[DE88-752300] N88-22810
Quantization of axial electrodynamics
[TI88-701498] N88-22813
GAUGE THEORY
Secondary gauge conditions in field theory
[TI88-701499] N88-22814
GELATION
The numerical simulation of viscous flows with change of phase and chemical reaction
[DE88-003204] N88-22292
GELS
Fluids, gels and glasses under extreme conditions of pressure and temperature
[AD-A190655] N88-22125
GEOCHEMISTRY
Advances in geochemistry and cosmochemistry: Trace element microdistributions with the synchrotron X-ray fluorescence microprobe
[DE88-006355] N88-22108
GEOGRAPHIC INFORMATION SYSTEMS
Updating of the municipal official register of real estate through a geographical information system
[INPE-4459-PRE/1238] N88-22453
Sources of digital spatial data for geographic information systems
[AD-A189788] N88-22824
Georelational data model
[INPE-4490-PRE/1254] N88-22829
GEOLOGY
Groundwater sapping valleys: Experimental studies, geological controls and implications to the interpretation of valley networks on Mars
[NASA-CR-182718] N88-22847
GEOMETRICAL OPTICS
Models for electromagnetic scattering from the sea at extremely low grazing angles
[AD-A190472] N88-22261
GEOMETRICAL THEORY OF DIFFRACTION
Models for electromagnetic scattering from the sea at extremely low grazing angles
[AD-A190472] N88-22261
GEOMETRY
Advanced probabilistic methods for quantifying the effects of various uncertainties in structural response N88-22401
Boundary shape identification problems in two-dimensional domains related to thermal testing of materials
[NASA-CR-181654] N88-22541
The elliptic Sinh-Gordon equation and the construction of toroidal soap bubbles
[DE88-006426] N88-22585
Geometric methods and the gauge structure of Berry's phase
[DE88-006538] N88-22682
GEOMORPHOLOGY
Project CODEAMA/FUNCATE (test-area of Barreirinha-AM): Field report
[INPE-4500-RPE/563] N88-22455
Bilateral symmetry elements of the Zhamanshin impact crater
[NASA-TT-20288] N88-22490
GEOPHYSICS
A hardware/software system for implementing geophysical diffraction tomography
[DE88-006411] N88-22480
Bilateral symmetry elements of the Zhamanshin impact crater
[NASA-TT-20288] N88-22490
GEOPOTENTIAL HEIGHT
Monthly mean global climatology of temperature, wind, geopotential height, and pressure for 0 - 120 km
[NASA-TM-100697] N88-22503
GEOSYNCHRONOUS ORBITS
Spacecraft trajectories
[ISBN-2-85-428166-7] N88-22054
GEOTHERMAL ENERGY UTILIZATION
Advanced geothermal technologies
[DE88-004307] N88-22463
GEOTHERMAL RESOURCES
Advanced geothermal technologies
[DE88-004307] N88-22463
GEOTHERMAL TECHNOLOGY
Advanced geothermal technologies
[DE88-004307] N88-22463
GERMANIUM
Fundamental properties and devices applications of Ge(x)Si(1-x)/Si superlattices
[AD-A190129] N88-22787
Interface formation and precursory dynamics
[AD-A190741] N88-22794
GLASS
Fluids, gels and glasses under extreme conditions of pressure and temperature
[AD-A190655] N88-22125
Fracture toughness of silicon nitride-silicon nitride joints bonded with oxynitride glass
[DE88-005548] N88-22172
Containerless glass melting N88-22222
Solar cell cover glasses for satellites N88-22225
Magnetic anomalies in the rare earth oxide superconductors GdBa2Cu3O(7-x) and YbBa2Cu3O(7-x)
[AD-A190713] N88-22793
Remarks on solid state amorphizing transformations
[DE88-006452] N88-22803
GLOVES
Design, development and evaluation of Stanford/Ames EVA prehensors
[NASA-CR-182688] N88-22540
GLUTAMINE
A program for the study of skeletal muscle catabolism following physical trauma
[AD-A189771] N88-22521
GOALS
Orbital transfer vehicle: Concept definition and system analysis study
[NASA-CR-179315] N88-22060
NASA and the challenge of ISDN: The role of satellites in an ISDN world
[NASA-CR-182749] N88-22676

GOES SATELLITES
Solar-geophysical data number 520, December 1987. Part 2: (Comprehensive reports). Data for June 1987 and miscellanea
[PB88-164207] N88-22849
GOGGLES
Advanced programming and control techniques for complex mechanical systems
[AD-A190238] N88-22349
GOLD
Ion-beam mixing and amorphization in Au/Zr bilayers
[DE88-005999] N88-22767
GOVERNMENT PROCUREMENT
Microvax networked computer system
[AD-A190308] N88-22596
GOVERNMENT/INDUSTRY RELATIONS
The impact of independent research and development regulations on companies not required to negotiate advanced independent research and development agreements
[AD-A190007] N88-22818
GRADIENTS
Trust regions and projected gradients
[DE88-005829] N88-22648
GRAIN BOUNDARIES
On rotating sphere-on-a-plate experiments and the questions of whether high angle grain boundaries melt below bulk melting temperatures
[DE88-006627] N88-22142
Investigation and synthesis of high temperature and increased stiffness RSP aluminum alloys
[AD-A190407] N88-22151
Strength and microstructure of ceramics
[AD-A190712] N88-22191
Grain boundary oxidation and low-cycle fatigue at elevated temperatures N88-22420
Interface formation and precursory dynamics
[AD-A190741] N88-22794
GRAIN SIZE
Grain growth behavior of extrusion consolidated centrifugally atomized Type 304 stainless steel powder
[DE88-006788] N88-22143
JPRS report: Science and technology. Japan
[JPRS-JST-88-002] N88-22210
Fine grain development by laser CVD N88-22214
Superfine grain development by laser N88-22215
GRAPH THEORY
The total interval of a graph
[AD-A189648] N88-22625
Structural decomposition of multiple time scale Markov processes
[AD-A189739] N88-22657
GRAPHITE
Microplasticity phenomena in graphite/magnesium metal matrix composites
[DE88-006772] N88-22086
GRAPHITE-EPOXY COMPOSITES
The buckling and vibration of composite plates using the Levy method considering shear deformation and rotary inertia
[AD-A189743] N88-22374
Increasing strength of graphite/epoxy bolted joints by introducing an adhesively bonded metallic insert
[FFA-TN-1987-45] N88-22442
GRAVIMETERS
Results of the International Comparison of Absolute Gravimeters (2nd) held in Sevres, France in June-July 1985
[AD-A189869] N88-22474
GRAVIMETRY
Results of the International Comparison of Absolute Gravimeters (2nd) held in Sevres, France in June-July 1985
[AD-A189869] N88-22474
GRAVITATION THEORY
Einstein metrics and Brans-Dicke superfields
[DE88-006992] N88-22809
String driven inflation
[DE88-006994] N88-22841
GRAVITATIONAL COLLAPSE
Hydrodynamical equations for spherical gravitational collapse in terms of a generalized theory of gravitation with higher derivatives
[DE87-703027] N88-22838
GRAVITATIONAL EFFECTS
Space experiment plan FMPT N88-22220
Amorphous semiconductors made in space N88-22221
Containerless glass melting N88-22222
GRAVITATIONAL FIELDS
Spin precession in stationary gravitational fields
[TI88-701107] N88-22470
Hydrodynamical equations for spherical gravitational collapse in terms of a generalized theory of gravitation with higher derivatives
[DE87-703027] N88-22838
GRAZING
Models for electromagnetic scattering from the sea at extremely low grazing angles
[AD-A190472] N88-22261
GRAZING INCIDENCE
Design, construction and performance of the ROSAT high resolution X-ray mirror assembly
[MPE-PREPRINT-101] N88-22836
GROUND EFFECT (AERODYNAMICS)
Model-scale sound propagation experiment
[NASA-TM-100602] N88-22709
GROUND TESTS
Description of ground motion data processing codes, volume 2
[DE88-007137] N88-22481
GROUND WATER
Groundwater sapping valleys: Experimental studies, geological controls and implications to the interpretation of valley networks on Mars
[NASA-CR-182718] N88-22847
GROUP THEORY
Lumped model generation and evaluation: Sensitivity and Lie algebraic techniques with applications to combustion
[AD-A190402] N88-22689
GROWTH
Study of mean free path effects on growth of ultrafine metallic aerosols
[AD-A190206] N88-22149
Vapor phase deposition and growth of polyimide films on copper
[AD-A189969] N88-22178
The growth potential of corona discharges from aircraft flying in precipitation
[AD-A190507] N88-22478
GUIDANCE SENSORS
Advanced guidance algorithms for homing missiles with bearings-only measurements
[AD-A190435] N88-22026
GUST ALLEVIATORS
Design of an integrated control system for flutter margin augmentation and gust load alleviation, tested on a dynamic windtunnel model
[PB88-149885] N88-22038

H

HABITS
Dietary factors related to physical fitness
[AD-A190272] N88-22527
HADRONS
Lattice QCD calculation of K yields pi nonleptonic weak transition and other hadronic weak parameters
[PREPRINT-580] N88-22717
HAFNIUM
Hafnia-rich mixed oxide ceramics of the system HfO2-ZrO2-TiO2 for heaters and heat exchangers in electrothermal thrusters: The effects of titania on selected electrical and mechanical properties of Hafnia-rich mixed oxides in the system Hafnia-Zirconia-Titania, volume 1
[NASA-CR-182800-VOL-1] N88-22197
HAMILTONIAN FUNCTIONS
Periodic orbits around a satellite modelled as a triaxial ellipsoid
[AD-A190592] N88-22051
Geometric methods and the gauge structure of Berry's phase
[DE88-006538] N88-22682
Quantization of axial electrodynamics
[TI88-701498] N88-22813
Hamiltonian formalism in the model of the relativistic string with rigidity
[TI88-701503] N88-22815
HAND (ANATOMY)
Design, development and evaluation of Stanford/Ames EVA prehensors
[NASA-CR-182688] N88-22540
HARDENING (MATERIALS)
Evolution of hardening and damage during viscoplastic deformation
[AD-A190714] N88-22381
HARDNESS
Response of aluminum alloys to erosive particle impacts
[DE88-005910] N88-22159
HARMONIC OSCILLATION
A panel method based on velocity potential to compute harmonically oscillating lift surface systems
[ETN-88-91886] N88-22290
HARMONICS
Subharmonic aliasing and its effects on the AFTI/F-16 digital flight control system
[AD-A190614] N88-22042
HASTELLOY (TRADEMARK)
Effect of strain rate on high-temperature low-cycle fatigue behavior of Hastelloy X and Hastelloy XR
[DE88-752302] N88-22140
HEAD (ANATOMY)
Basic research on flame radiation
[PB88-168372] N88-22105
Analysis of head response to torso acceleration. Volume 2: Description of data retrieval, analysis and display software
[PB88-156765] N88-22536
HEARING
Mechanisms mediating the perception of complex acoustic patterns
[AD-A190112] N88-22705
HEAT EXCHANGERS
Hafnia-rich mixed oxide ceramics of the system HfO2-ZrO2-TiO2 for heaters and heat exchangers in electrothermal thrusters: The effects of titania on selected electrical and mechanical properties of Hafnia-rich mixed oxides in the system Hafnia-Zirconia-Titania, volume 1
[NASA-CR-182800-VOL-1] N88-22197
Basic characteristics of heat-exchanger-type steam reformer heated by high-temperature helium gas (2). Analysis by simulation model (2)
[DE87-702962] N88-22291
Comparison of entropy generation and conventional design methods for heat exchangers
[AD-A190256] N88-22306
A survey of oscillating flow in Stirling engine heat exchangers
[NASA-CR-182108] N88-22322
An evaluation of nondestructive methods for ceramic heat exchanger applications
[DE88-006731] N88-22328
HEAT FLUX
Thermostructural analysis of simulated cowl lips N88-22403
Research sensors N88-22430
Magnetic fusion energy plasma interactive and high heat flux components. Volume 5: Technical assessment of critical issues in the steady state operation of fusion confinement devices
[DE88-006920] N88-22744
HEAT MEASUREMENT
Anomalies in the heat-capacity signatures of submonolayer adsorbates with attractive lateral interactions
[AD-A190736] N88-22817
HEAT OF COMBUSTION
Numerical simulation of turbulent flames using vortex methods
[AD-A189613] N88-22116
HEAT OF FORMATION
Evaluation of direct methane conversion to higher hydrocarbons and oxygenates
[DE88-003812] N88-22204
HEAT PIPES
Development of an integrated heat pipe-thermal storage system for a solar receiver
[NASA-TM-101099] N88-22458
HEAT PUMPS
Overview of 1987 moonlight project N88-22231
Application and technology requirements for heat pumps at the process industries
[DE88-006740] N88-22293
HEAT RESISTANT ALLOYS
Investigation and synthesis of high temperature and increased stiffness RSP aluminum alloys
[AD-A190407] N88-22151
High temperature oxidation and electrochemical studies related to hot corrosion
[AD-A190699] N88-22156
Characterization of HYTUF steel. Semifinished product: 160 mm dia forging block. Processor: C3I. Test Report M3-434600
[M3-434600] N88-22164
Bithermal fatigue of a nickel-base superalloy single crystal
[NASA-TM-100685] N88-22168
Life prediction modeling based on cyclic damage accumulation N88-22426
Fatigue damage modeling for coated single crystal superalloys N88-22427
HEAT SOURCES
Superfine grain development by laser N88-22215
HEAT STORAGE
Thermal analysis of heat storage canisters for a solar dynamic, space power system
[DE88-004199] N88-22075
Structural assessment of a space station solar dynamic heat receiver thermal energy storage canister N88-22406
Development of an integrated heat pipe-thermal storage system for a solar receiver
[NASA-TM-101099] N88-22458

HEAT TRANSFER
The numerical simulation of viscous flows with change of phase and chemical reaction
[DE88-003204] N88-22292
Enhancement of data acquisition and numerical computation capabilities for unsteady fluid dynamics
[AD-A190115] N88-22302
FLOSIN: A fluid loop analyzer for SINDA N88-22321
Thermal-structural analyses of Space Shuttle Main Engine (SSME) hot section components N88-22404
Review and assessment of the HOST turbine heat transfer program N88-22431
Performance evaluation of molten salt thermal storage systems
[DE87-014645] N88-22461
HEAT TRANSFER COEFFICIENTS
Heat transfer modeling of jet vane Thrust Vector Control (TVC) systems
[AD-A190106] N88-22034
HEATING
Response of aluminum alloys to erosive particle impacts
[DE88-005910] N88-22159
Investigation of boundary layer disturbances caused by periodic heating of a thin ribbon
[AD-A190572] N88-22314
HELICAL ANTENNAS
Short experiment study of four-wire helical antennas (half turn half wave)
[CNES-CT/DRT/TIT/AN-249-T] N88-22266
HELICOPTERS
Inflow measurement made with a laser velocimeter on a helicopter model in forward flight. Volume 3: Rectangular planform blades at an advance ratio of 0.30
[NASA-TM-100543] N88-22015
The effects of torque response and time delay on rotorcraft vertical axis handling qualities
[AD-A189873] N88-22023
Preliminary airworthiness evaluation of the UH-60A equipped with the XM-139 VOLCANO mine dispensing system
[AD-A190604] N88-22029
Method and device for the detection and identification of a helicopter
[NASA-TT-20251] N88-22698
Acoustic propagation in the low atmosphere. Experimental study and modeling by the radius method
[ISL-CO-247/86] N88-22713
HELIUM
Spectrographic detection of nitrogen impurity in helium
[DE88-752301] N88-22111
HELIUM FILM
Dilution refrigerator with non-valve adsorption system of sup 3/He circulation
[DE88-700974] N88-22209
HELIUM ISOTOPES
Dilution refrigerator with non-valve adsorption system of sup 3/He circulation
[DE88-700974] N88-22209
Basic characteristics of heat-exchanger-type steam reformer heated by high-temperature helium gas (2). Analysis by simulation model (2)
[DE87-702962] N88-22291
HELIUM-NEON LASERS
Particle beam alignment system for single event upset-Van de Graaf experiments
[AD-A189695] N88-22721
HERMETIC SEALS
Hermetic coating of optical fibers
[AD-A189886] N88-22177
HETEROCYCLIC COMPOUNDS
Electronic and ionic transport in polymers
[AD-A190434] N88-22185
High-performance polymeric materials
[AD-A190708] N88-22190
HETEROJUNCTIONS
First-principles calculations of quasiparticle energies at surfaces and interfaces: Semiconductor surface-state spectra and band offsets
[DE88-006340] N88-22773
Fundamental properties and devices applications of Ge(x)Si(1-x)/Si superlattices
[AD-A190129] N88-22787
HIGH ENERGY INTERACTIONS
Particle acceleration to high energies and amplification of coherent radiation by electromagnetic interactions in plasmas
[TI88-701020] N88-22737
HIGH FREQUENCIES
Soft decoding of recorded HF data
[FOA-C-30473-3.3] N88-22269
HIGH LEVEL LANGUAGES
New generation knowledge processing, volume 1
[AD-A190165] N88-22826
HIGH POWER LASERS
JPRS report: Science and technology. China
[JPRS-CST-87-043] N88-22233
Magic light high-power laser passes state certification N88-22236
Coupled high power waveguide laser research
[AD-A189800] N88-22345
Laser evaporation studies
[AD-A189815] N88-22348
HIGH PRESSURE
Fluids, gels and glasses under extreme conditions of pressure and temperature
[AD-A190655] N88-22125
Cracking tendencies of restrained welds in high strength low alloy steels under hyperbaric conditions
[AD-A190255] N88-22150
Synthesis of metastable superconductors by high dynamic pressure
[DE88-005620] N88-22764
HIGH RESOLUTION
Fluids, gels and glasses under extreme conditions of pressure and temperature
[AD-A190655] N88-22125
Design, construction and performance of the ROSAT high resolution X-ray mirror assembly
[MPE-PREPRINT-101] N88-22836
HIGH REYNOLDS NUMBER
High Reynolds number, low Mach number, steady flow field calculations over a NACA 0012 airfoil using Navier-Stokes and interactive boundary layer theory
[AD-A189871] N88-22005
Effect of freestream turbulence on a two dimensional cascade, with different surface roughness, at high Reynolds number
[AD-A190615] N88-22316
HIGH SPEED
High speed, bandpass sampling of digital communications waveforms
[AD-A189842] N88-22254
HIGH STRENGTH
Structure and surface characterizations of high strength carbon fibers
[AD-A189642] N88-22087
HIGH STRENGTH STEELS
Cracking tendencies of restrained welds in high strength low alloy steels under hyperbaric conditions
[AD-A190255] N88-22150
HIGH TEMPERATURE
Fluids, gels and glasses under extreme conditions of pressure and temperature
[AD-A190655] N88-22125
Advanced B and Al combustion kinetics over wide temperature ranges
[AD-A190752] N88-22128
Effect of strain rate on high-temperature low-cycle fatigue behavior of Hastelloy X and Hastelloy XR
[DE88-752302] N88-22140
The thermal radiative properties of metals at high temperature
[DE88-006625] N88-22141
High temperature oxidation and electrochemical studies related to hot corrosion
[AD-A190699] N88-22156
Developments in ceramic superconducting materials N88-22229
Fracture technology for brittle materials N88-22417
Elevated temperature crack growth N88-22421
Thermal stress in high temperature cylindrical fasteners
[NASA-TM-100611] N88-22438
Synthesis of metastable superconductors by high dynamic pressure
[DE88-005620] N88-22764
HIGH TEMPERATURE GASES
Basic characteristics of heat-exchanger-type steam reformer heated by high-temperature helium gas (2). Analysis by simulation model (2)
[DE87-702962] N88-22291
HIGH TEMPERATURE PLASMAS
Advanced diagnostics for reacting flows
[AD-A190485] N88-22122
HIGH TEMPERATURE PROPELLANTS
Durability testing of an iridium-plated storable rocket engine injector
[AD-A190707] N88-22078
HIGH TEMPERATURE SUPERCONDUCTORS
Thermochemistry and high temperature thermodynamic properties of rare earth-alkaline earth-copper oxide superconductors
[DE88-005976] N88-22770
High-T(sub c) superconducting wire fabrication and testing
[DE88-005989] N88-22798
High temperature superconductors in the La(sub 1+x)Ba(sub 2-x)Cu O(sub y system
[DE88-006367] N88-22802
HIGH TEMPERATURE TESTS
Unified constitutive model development for metal matrix composites at high temperature N88-22387
Examination of temperature effects on gate-to-drain avalanche breakdown in GaAs MESFETs (Metal-Semiconductor Field Effect Transistors) by measuring light emission under RF drive
[AD-A189634] N88-22778
HILBERT SPACE
Stochastic evolution equations driven by nuclear space valued martingales
[AD-A189342] N88-22677
Geometric methods and the gauge structure of Berry's phase
[DE88-006538] N88-22682
Coding capacity of generalized additive channels
[AD-A190315] N88-22685
HISTORIES
Energy from the wind
[DE88-006897] N88-22459
Marshall Space Flight Center 1960-1985: 25th anniversary report
[NASA-TM-100328] N88-22852
HOLE GEOMETRY (MECHANICS)
Life and reliability of rotating disks N88-22428
HOLOGRAPHIC INTERFEROMETRY
A review on holography, its principles and applications
[ISL-CO-242/86] N88-22338
HOLOGRAPHY
MIG-1 on-line measuring holographic microscope
[TI88-701103] N88-22332
Focused image holography abberations
[TI88-701105] N88-22333
A review on holography, its principles and applications
[ISL-CO-242/86] N88-22338
Space-variant optical systems
[AD-A189967] N88-22724
HOMING DEVICES
Advanced guidance algorithms for homing missiles with bearings-only measurements
[AD-A190435] N88-22026
HOMOGENEOUS TURBULENCE
Dense-spray structure and phenomena. Part 1. Turbulence/dispersed-phase interactions
[AD-A190606] N88-22315
HOT CORROSION
High temperature oxidation and electrochemical studies related to hot corroeion
[AD-A190699] N88-22156
Corrosion Research Center, University of Minnesota
[DE88-006681] N88-22160
High temperature corrosion of ceramics
[DE88-006567] N88-22193
HOT PRESSING
Processing, microstructure, and mechanical properties of silicon carbide particulate reinforced aluminum alloys
[AD-A189981] N88-22136
HOT-WIRE FLOWMETERS
Development of subminiature multi-sensor hot-wire probes
[NASA-TM-100052] N88-22336
HUBBLE CONSTANT
String driven inflation
[DE88-006994] N88-22841
HUMAN BEHAVIOR
Complex sound processing: An interdisciplinary approach
[AD-A189782] N88-22523
HUMAN BEINGS
Evaluation of existing total human exposure models
[PB88-146840] N88-22517
Auditory pattern memory: Mechanisms of tonal sequence discrimination by human observers
[AD-A190337] N88-22534
Extension of computer based algorithms by operator analysts
[NASA-CR-182798] N88-22575
HUMAN BODY
Anthropomorphic phantom radiation dosimetry at the NATO standard reference point at Aberdeen Proving Ground
[AD-A190508] N88-22528
HUMAN FACTORS ENGINEERING
Napping and human functioning during prolonged work
[AD-A190228] N88-22525
HUMAN PERFORMANCE
Age, alcohol, and simulated altitude: Effects on performance and breathalyzer scores
[AD-A190642] N88-22531
An evaluation of the effects of high visual taskload on the separate behaviors involved in complex monitoring performance
[AD-A190641] N88-22538

HUMIDITY
Aerodynamic aspects of the Amazon Forest
[INPE-4445-TDL/313] N88-22501
HURRICANES
Forecast of Atlantic seasonal hurricane activity for 1988 N88-22500
HYDRAULIC EQUIPMENT
A 150,000 pounds per square inch dynamic pressure calibrator
[AD-A190659] N88-22335
HYDRAULIC FLUIDS
Evaluation of the acute toxicity of a synthetic polyalphaolefin-based hydraulic fluid
[AD-A190412] N88-22184
Experimental determination of the coefficients of the hydraulic resistance of apertures in the rotary disks
[AD-A190627] N88-22317
HYDRAULIC JETS
Dense-spray structure and phenomena. Part 2: Pressure-atomized sprays
[AD-A190312] N88-22307
HYDRODYNAMICS
PLASMOR: A laser-plasma simulation code, part 2
[DE88-701289] N88-22736
Hydrodynamical equations for spherical gravitational collapse in terms of a generalized theory of gravitation with higher derivatives
[DE87-703027] N88-22638
HYDROELASTICITY
Traction model development
[AD-A188450] N88-22359
HYDROGEN
The structure of the boron-hydrogen complex in silicon
[DE88-005433] N88-22795
HYDROGEN PRODUCTION
Basic characteristics of heat-exchanger-type steam reformer heated by high-temperature helium gas (2). Analysis by simulation model (2)
[DE87-702962] N88-22291
HYDROGRAPHY
Hydrographic data from the OPTOMA (Ocean Prediction Through Observation, Modeling and Analysis) program: OPTOMA 23, 9-19 November 1986
[AD-A189868] N88-22506
Physical, chemical and CTD (Conductivity/Temperature/Depth) data from the Marathon 2 expedition
[AD-A189930] N88-22507
HYDROLOGY
Project CODEAMA/FUNCATE (test-area of Barreirinha-AM): Field report
[INPE-4500-RPE/563] N88-22455
HYDROLYSIS
On copper peroxide
[NASA-TT-20263] N88-22135
HYDROPHONES
Bodies in unsteady flow
[AD-A190416] N88-22308
HYPERCUBE MULTIPROCESSORS
Cholesky downdating on a hypercube
[DE88-006780] N88-22586
Simulation of fault tolerance in a hypercube arrangement of discrete processors
[AD-A189682] N88-22594
Implementation and performance analysis of parallel assignment algorithms on a hypercube computer
[AD-A190678] N88-22600
HYPERSONIC AIRCRAFT
Aerothermal tests of quilted dome models on a flat plate at a Mach number of 6.5
[NASA-TP-2804] N88-22325
HYPERSONIC FLOW
High-resolution shock-capturing schemes for inviscid and viscous hypersonic flows
[NASA-TM-100097] N88-22651
HYPERSONIC SPEED
Numerical study of unsteady viscous hypersonic blunt body flows with an impinging shock
[NASA-TM-100096] N88-22650
HYPERSONIC VEHICLES
Thermal stress in high temperature cylindrical fasteners
[NASA-TM-100611] N88-22438
HYPERVELOCITY GUNS
Launchability of base-driven electromagnetic projectiles
[AD-A189635] N88-22055
HYPERVELOCITY LAUNCHERS
Continuous measurements of in-bore projectile velocity
[DE88-006841] N88-22056
A chemical method for achieving acceleration of macroparticles to ultrahigh velocities
[DE88-006377] N88-22695

I

ICE
Thermal instability and heat transfer characteristics in water/ice systems
[AD-A189627] N88-22297
ICE ENVIRONMENTS
Real-time environmental Arctic monitoring (R-TEAM)
[AD-A189948] N88-22508
IDENTIFYING
On categorizing sounds
[AD-A189784] N88-22700
IGNITION
Environmental assessment for the compact ignition Tokamak
[DE88-005633] N88-22740
Transport simulations of ohmic ignition experiment: IGNITEX
[DE88-006055] N88-22757
IMAGE ANALYSIS
On the geometric interpretation of image contours
[RR-647-I-IMAG-57-LIFIA] N88-22563
IMAGE PROCESSING
Focused image holography abberations
[TI88-701105] N88-22333
Systems for ultrasonic scanning, analysis and imagery N88-22414
Satellite UV image processing
[AD-A190466] N88-22451
Method for restoration and resampling of TM sensor imagery
[INPE-4491-PRE/1255] N88-22454
A hardware/software system for implementing geophysical diffraction tomography
[DE88-006411] N88-22480
Calibration and processing of AVHRR data for temperature estimation
[INPE-4493-PRE/1257] N88-22485
Multiple-transform pipelines for image coding
[REPT-87-038] N88-22561
On the geometric interpretation of image contours
[RR-647-I-IMAG-57-LIFIA] N88-22563
Rapid feature extraction via the radon transform
[AD-A190032] N88-22573
Design and implementation of VLSI prime factor algorithm processor
[AD-A190483] N88-22580
Contour interactive extraction using image numerical treatment
[ISL-R-114/86] N88-22587
Modeling a parallel architecture for image processing
[RR-646-I] N88-22593
Finding texture boundaries in images
[AD-A190554] N88-22609
Multi-disciplinary techniques for understanding time-varying space-based imagery
[AD-A190711] N88-22610
Concurrent algorithms for a mobile robot vision system
[DE88-005850] N88-22614
Rigidity and smoothness of motion
[AD-A190555] N88-22694
ROVER: A prototype active vision system
[AD-A189246] N88-22722
IMAGE RECONSTRUCTION
Rainbow holographic image reconstructed by spatially extended white light source N88-22249
Focused image holography abberations
[TI88-701105] N88-22333
Geometric restoration of satellite image data
[AD-A190462] N88-22450
IMAGE RESOLUTION
Rainbow holographic image reconstructed by spatially extended white light source N88-22249
IMAGERY
Multi-disciplinary techniques for understanding time-varying space-based imagery
[AD-A190711] N88-22610
IMAGES
Finding texture boundaries in images
[AD-A190554] N88-22609
IMAGING TECHNIQUES
Effects of update and refresh rates on flight simulation visual displays
[NASA-TM-100415] N88-22033
Polarimetric ISAR imaging using either measured or calculated transient signatures
[AD-A190077] N88-22259
Range image segmentation and surface parameter extraction for a mobile robot
[DE87-013877] N88-22360
Systems for ultrasonic scanning, analysis and imagery N88-22414
Method for restoration and resampling of TM sensor imagery
[INPE-4491-PRE/1255] N88-22454
Comparative utilization of analog and digital processes in the treatment of MSS-LANDSAT data for studying the national parks of Brazil
[INPE-4011-TDL/240] N88-22456
IMPACT
The concept of an impact resonance diagram for characterizing the nonlinear response of impact vibration
[DE88-005475] N88-22432
IMPACT DAMAGE
Impact damage in composite laminates N88-22402
Bilateral symmetry elements of the Zhamanshin impact crater
[NASA-TT-20288] N88-22490
IMPACT LOADS
Response of aluminum alloys to erosive particle impacts
[DE88-005910] N88-22159
Impact damage in composite laminates N88-22402
IMPACT RESISTANCE
KRASH parametric sensitivity study: Transport category airplanes
[AD-A189962] N88-22024
IMPACT STRENGTH
A study of damage tolerance in curved composite panels
[AD-A190617] N88-22092
IMPACT TESTS
KRASH parametric sensitivity study: Transport category airplanes
[AD-A189962] N88-22024
Response of aluminum alloys to erosive particle impacts
[DE88-005910] N88-22159
Finite element simulation of perforation of aluminum plates
[DE88-002092] N88-22362
IMPEDANCE
Model-scale sound propagation experiment
[NASA-TM-100602] N88-22709
IMPEDANCE MATCHING
Vortices in long Josephson junctions
[AD-A190338] N88-22279
IMPURITIES
Spectrographic detection of nitrogen impurity in helium
[DE88-752301] N88-22111
Activities of As, Sb, Bi and Pb in copper mattes and their effects on impurity elimination
[TKK-V-A10(1988)] N88-22165
High temperature corrosion of ceramics
[DE88-006567] N88-22193
Long-time impurity confinement as a precursor to disruptions in ohmically heated tokamaks
[DE88-006183] N88-22742
INCLUSIONS
An evaluation of nondestructive methods for ceramic heat exchanger applications
[DE88-006731] N88-22328
INDEPENDENT VARIABLES
Comparative analysis
[AD-A190556] N88-22313
INDEXES (DOCUMENTATION)
NASA scientific and technical publications: A catalog of Special Publications, Reference Publications, Conference Publications, and Technical Papers, 1987
[NASA-SP-7063(02)] N88-22830
INDUCTION (MATHEMATICS)
Constructive version of the approximation induction principle
[PB88-165477] N88-22647
INDUSTRIES
Preliminary market analysis for large zeolite crystals
[NASA-CR-182882] N88-22207
The necessity of automation in Brazil
[INPE-4346-PRE/1183] N88-22832
INELASTIC STRESS
Experiments investigating advanced materials under thermomechanical loading N88-22385
Three-dimensional inelastic approximate analysis code (MOMM) N88-22392
Specialty three-dimensional finite element analysis codes N88-22393
MHOST: An efficient finite element program for inelastic analysis of solids and structures N88-22394
INERTIA
The buckling and vibration of composite plates using the Levy method considering shear deformation and rotary inertia
[AD-A189743] N88-22374
Napping and human functioning during prolonged work
[AD-A190228] N88-22525

INERTIAL CONFINEMENT FUSION
Activities report in laser-matter interaction
[ETN-88-92007] N88-22696
Environmental assessment for the compact ignition Tokamak
[DE88-005633] N88-22740
Magnetic fusion energy plasma interactive and high heat flux components. Volume 5: Technical assessment of critical issues in the steady state operation of fusion confinement devices
[DE88-006920] N88-22744
Rayleigh-Taylor instability in inertial confinement fusion
[TI88-701411] N88-22750
INFERENCE
Inference engine for expert systems
[INPE-4465-TDL/321] N88-22590
Statistical inference for stochastic processes
[AD-A190491] N88-22673
INFORMATION DISSEMINATION
Sigma system: Overview, prospects N88-22230
INFORMATION MANAGEMENT
Information systems for quality. Experience at the Nerviano Aeritalia plant. Avionic systems and equipment group
[ETN-88-92274] N88-22821
INFORMATION PROCESSING (BIOLOGY)
Synapses that compute motion
[AD-A190389] N88-22607
INFORMATION RETRIEVAL
Baseline observing system experiments using the AFGL global data assimilation system
[AD-A188861] N88-22062
Relationship of encoding speed and memory tests to flight training performance
[AD-A190670] N88-22539
The Scientific and Technical Information Network (STINET). Foundation for evolution
[AD-A189750] N88-22822
INFORMATION SYSTEMS
Geometric modeling of flight information for graphical cockpit display
[AD-A190484] N88-22043
Information systems for quality. Experience at the Nerviano Aeritalia plant. Avionic systems and equipment group
[ETN-88-92274] N88-22821
The Scientific and Technical Information Network (STINET). Foundation for evolution
[AD-A189750] N88-22822
Sources of digital spatial data for geographic information systems
[AD-A189788] N88-22824
Data base design and implementation
[AD-A190414] N88-22827
INFORMATION THEORY
Instrumentation for scientific computing in neural networks, information science, artificial intelligence and applied mathematics
[AD-A189981] N88-22549
Information and coding capacities of mismatched Gaussian channels
[AD-A190321] N88-22665
Information capacity of Gaussian channels
[AD-A190316] N88-22686
Coding capacity of discrete-time Gaussian and nonGaussian channels
[AD-A190318] N88-22688
INFORMATION TRANSFER
Design and implementation of VLSI prime factor algorithm processor
[AD-A190483] N88-22580
INFRARED ABSORPTION
Infrared absorption spectroscopy and chemical kinetics of free radicals
[DE88-006536] N88-22112
Infrared differential absorption lidar for vapor detection
[AD-A190600] N88-22497
INFRARED IMAGERY
Infrared-sensitive spatial light modulator
[AD-A190391] N88-22729
INFRARED LASERS
Diode laser spectroscopy of chemical moieties at surfaces
[AD-A190710] N88-22127
INFRARED PHOTOMETRY
Near-infrared observations of cepheids: The distance to M33 N88-22846
INFRARED RADIATION
Infrared differential absorption lidar for vapor detection
[AD-A190600] N88-22497
Studies of surfaces using optical sum-frequency generation
[DE88-006334] N88-22715
Dispersion measurements of microcrystals in the near ultraviolet and infrared
[DE88-006234] N88-22800
INFRARED SPECTROSCOPY
The spectroscopy and reaction kinetics of coordinatively unsaturated metal carbonyls
[AD-A190533] N88-22124
Diode laser spectroscopy of chemical moieties at surfaces
[AD-A190710] N88-22127
Excitations in magnetic low-dimensional systems: A spectroscopic study
[ETN-88-92230] N88-22697
INFRASONIC FREQUENCIES
Mechanisms mediating the perception of complex acoustic patterns
[AD-A190112] N88-22705
INHOMOGENEITY
Wave energy flow conservation for propagation in inhomogeneous Vlasov-Maxwell equilibria
[DE88-006705] N88-22251
Parametric instabilities of inhomogeneous plasma near the lower-hybrid resonance
[TI88-701201] N88-22748
INJECTORS
Durability testing of an iridium-plated storable rocket engine injector
[AD-A190707] N88-22078
Development of a laboratory test for multiport injector deposits: Approaches 1 and 2
[AD-A190697] N88-22203
Dense-spray structure and phenomena. Part 2: Pressure-atomized sprays
[AD-A190312] N88-22307
Program to research laser-driven thermionic electron sources for free electron lasers
[AD-A190473] N88-22353
Film cooling effectiveness on a flat plate in high free-stream turbulence using a single row of 30 deg slant-hole injectors
[AD-A190500] N88-22816
INSERTION
Insertions using geometric analysis and hybrid force-position control: Method and analysis
[DE87-013652] N88-22611
INSERTS
Increasing strength of graphite/epoxy bolted joints by introducing an adhesively bonded metallic insert
[FFA-TN-1987-45] N88-22442
INSPECTION
Eddy current nondestructive inspection of graphite epoxy using ferrite cup core probes
[AD-A189823] N88-22365
INSTANTONS
Recent developments in the path integral approach to anomalies
[DE87-703032] N88-22616
INTEGRAL CALCULUS
Martingale representation and the Malliavin calculus
[AD-A189721] N88-22626
INTEGRAL EQUATIONS
Global spatial periodic solutions to the Ginzburg-Landau equations
[DE88-006424] N88-22623
INTEGRALS
Recent developments in the path integral approach to anomalies
[DE87-703032] N88-22616
Remarks on the time transformation of path-integral measures
[DE87-703040] N88-22617
Path integral, BRS symmetry, and string and membrane theories
[DE88-752300] N88-22810
INTEGRATED CIRCUITS
Monolithic phase shifter study
[AD-A190213] N88-22278
Fabrication and electrical characterization of multilevel aluminum interconnects used to achieve silicon-hybrid wafer-scale integration
[AD-A190519] N88-22282
Fast analog-to-digital converter
[TI88-701488] N88-22543
Beam assisted fabrication of 3-5/Si monolithic devices
[AD-A189979] N88-22785
INTERFACE STABILITY
The influence of current stressing on the structure of Ag contacts to GaAs
[DE88-005988] N88-22771
INTERFACES
Vapor phase deposition and growth of polyimide films on copper
[AD-A189969] N88-22178
Thermal instability and heat transfer characteristics in water/ice systems
[AD-A189627] N88-22297
CK-LOG system conversion (user's manual and user interface)
[AD-A190273] N88-22577
Studies of surfaces using optical sum-frequency generation
[DE88-006334] N88-22715
Interface formation and precursory dynamics
[AD-A190741] N88-22794
INTERFACIAL ENERGY
On rotating sphere-on-a-plate experiments and the questions of whether high angle grain boundaries melt below bulk melting temperatures
[DE88-006627] N88-22142
First-principles calculations of quasiparticle energies at surfaces and interfaces: Semiconductor surface-state spectra and band offsets
[DE88-006340] N88-22773
INTERFACIAL TENSION
Methods of measurement for the evaluation of monolayer properties. Development and applications — lung surfactants
[ETN-88-92229] N88-22532
INTERFERENCE DRAG
Laser velocimeter measurements in a wing-fuselage type juncture
[NASA-TM-100588] N88-22012
INTERFEROMETERS
Synthetic-aperture radars viewed as interferometers with matched filter processing of the collected data
[AD-A190606] N88-22262
INTERFEROMETRY
Continuous measurements of in-bore projectile velocity
[DE88-006841] N88-22056
INTERLAYERS
Interlaminar fracture toughness of thermoplastic composites
[NASA-TM-100532] N88-22097
INTERNATIONAL COOPERATION
Japanese space station module N88-22224
Overview of 1987 moonlight project N88-22231
INTERPOLATION
Synthetic-aperture radars viewed as interferometers with matched filter processing of the collected data
[AD-A190606] N88-22262
Derivation of consistent surface fixed fields for use in a global NWP model
[AD-A190131] N88-22475
INTERPROCESSOR COMMUNICATION
Enhancement of data acquisition and numerical computation capabilities for unsteady fluid dynamics
[AD-A190115] N88-22302
INTERSTITIALS
Does the pipe diffusion of self-interstitials in crystals under stresses exist
[TI88-701027] N88-22762
INTERVALS
The total interval of a graph
[AD-A189648] N88-22625
INTOXICATION
Age, alcohol, and simulated altitude: Effects on performance and breathalyzer scores
[AD-A190642] N88-22531
INVERSIONS
Seismic inversion by a RMS (Root-Mean-Square) Born approximation in the space-time domain
[PB88-165402] N88-22711
INVERTERS
A high performance inverter-fed drive system of an interior permanent magnet synchronous machine
[DE88-006753] N88-22288
INVISCID FLOW
Enhanced viscous flow drag reduction using acoustic excitation
[NASA-CR-182734] N88-22295
High-resolution shock-capturing schemes for inviscid and viscous hypersonic flows
[NASA-TM-100097] N88-22651
ION BEAMS
Ion-beam mixing and amorphization in Au/Zr bilayers
[DE88-005999] N88-22767
ION EXCHANGING
Electronic and ionic transport in polymers
[AD-A190434] N88-22185
ION IMPLANTATION
Effect of P implantation on the corrosion behavior of Fe-Cr alloys
[DE88-005732] N88-22158
Ion-beam mixing and amorphization in Au/Zr bilayers
[DE88-005999] N88-22767
High density ion implanted contiguous disk bubble technology
[AD-A190169] N88-22789
ION INJECTION
Status of RF superconductivity at Argonne National Laboratory
[DE88-005913] N88-22796

ION PLATING
Structure and properties of titanium nitride and zirconium nitride thin films prepared by reactive ion plating — cutting tools
[ETN-88-92218] N88-22167
ION PROBES
Electronic and ionic transport in polymers
[AD-A190434] N88-22185
ION PROPULSION
Plasma-gas interaction studies in a hybrid plume plasma rocket
[AD-A190310] N88-22755
IONIZING RADIATION
Characterization of space radiation environment in terms of the energy deposition in functionally important volumes
[DE88-005627] N88-22513
IONOSPHERIC DISTURBANCES
Support for FY87 midlatitude electron-density calibration campaign
[AD-A190174] N88-22476
IONOSPHERIC TEMPERATURE
Support for FY87 midlatitude electron-density calibration campaign
[AD-A190174] N88-22476
IONS
Laser photoelectron spectroscopy of ions
[DE88-006860] N88-22113
Angular resolved energy analysis of (69)Ga+ ions from a gallium liquid metal ion source
[AERE-R-12649] N88-22760
IRON
Use of long-distance pair potentials in calculations of defect characteristics in metals
[TI88-701039] N88-22138
Effect of P implantation on the corrosion behavior of Fe-Cr alloys
[DE88-005732] N88-22158
ISOMORPHISM
Complexity of some problems in module algebra
[PB88-185388] N88-22648
ISOTOPIC ENRICHMENT
Vacuum-arc plasma centrifuge experiment
[INPE-4509-PRE/1263] N88-22758
ISOTROPIC MEDIA
Ultrasonic beam distortion in transversely isotropic media
[DE88-005937] N88-22699
ITERATIVE SOLUTION
Contraction design for small low-speed wind tunnels
[NASA-CR-182747] N88-22045
Smoothing technique to resolve X-ray spectra in laser nuclear fusion N88-22235
Relative orientation
[AD-A190385] N88-22449
Trust regions and projected gradients
[DE88-005829] N88-22646

J

J INTEGRAL
A simplified key-curve approach for J-R-curve testing of CT specimens
[VTT-RR-503] N88-22444
JAPANESE SPACE PROGRAM
Space utilization plans N88-22219
Space experiment plan FMPT N88-22220
Japanese space station module N88-22224
JET AIRCRAFT
AFRAPT (Air Force Research in Aero Propulsion Technology) trainee program
[AD-A190525] N88-22123
JET CONTROL
Experimental investigation of two-dimensional confined jet thrust vector control
[AD-A189645] N88-22077
JET ENGINES
Noise assessment of unsuppressed TF-34-GE-100A engine at Warfield ANG, Baltimore, Maryland
[AD-A189966] N88-22702
JET FLOW
Interaction of a two-dimensional bluff body and incompressible jet and annulus flows
[AD-A190503] N88-22310
JET MIXING FLOW
Chemically reacting turbulent flow
[AD-A190522] N88-22311
JET THRUST
Pressure measurements of impinging jet with asymmetric nozzle
[NASA-CR-182759] N88-22011
Experimental investigation of two-dimensional confined jet thrust vector control
[AD-A189645] N88-22077
JET VANES
Heat transfer modeling of jet vane Thrust Vector Control (TVC) systems
[AD-A190106] N88-22034
JOINTS (JUNCTIONS)
Fracture toughness of silicon nitride-silicon nitride joints bonded with oxynitride glass
[DE88-005548] N88-22172
Ultrasonic characterization of ceramic joints
[DE88-005844] N88-22173
Stabilization and control problems in structural dynamics
[AD-A190197] N88-22361
Increasing strength of graphite/epoxy bolted joints by introducing an adhesively bonded metallic insert
[FFA-TN-1987-45] N88-22442
A three dimensional non-singular modelling of rigid manipulators
[AD-A189707] N88-22604
JOSEPHSON JUNCTIONS
Vortices in long Josephson junctions
[AD-A190338] N88-22279
Preparation of large area NbN/AlN/NbN Josephson junctions
[DE88-006074] N88-22799
JUDGMENTS
On categorizing sounds
[AD-A189784] N88-22700
JUPITER SATELLITES
The 1985 mutual phenomena of Jupiter's satellites observed in Brazil
[INPE-4526-PRE/1276] N88-22848

K

KALMAN FILTERS
Kalman filter residual expert system
[AD-A190520] N88-22041
Moving-bank multiple model adaptive estimation applied to flexible spacestructure control
[AD-A190761] N88-22071
KINEMATICS
A three dimensional non-singular modelling of rigid manipulators
[AD-A189707] N88-22604
KINETIC ENERGY
Launchability of base-driven electromagnetic projectiles
[AD-A189635] N88-22055
Rocket measurements of ionospheric electron temperature over Natal
[INPE-4485-PRE/1250] N88-22489
KINETICS
Reactions of N2(A sup 3 sigma sup + sub u) candidates for short wavelength lasers
[DE88-007018] N88-22342
The kinetics of contact noise in NaBeta alumina
[AD-A190651] N88-22707
KNOWLEDGE
Rapid prototyping of simulations in artificial intelligence environments
[DE88-004295] N88-22612
KNOWLEDGE REPRESENTATION
Memory-based expert systems
[AD-A190203] N88-22606
KORTEWEG-DEVRIES EQUATION
Backlund transformation and the Schwarzian derivative
[AD-A190277] N88-22684
KRYPTON
Numerical modelling specific energy charcteristics of excimer KrF lasers with electron beam excitation
[DE88-701525] N88-22344
KRYPTON FLUORIDE LASERS
The development of high power KrF laser systems for plasma research by the application of stimulated Raman scattering
[ETN-88-92220] N88-22358

L

LABORATORIES
Study of lightning and lightning protection (selected pages)
[AD-A190623] N88-22498
LABORATORY EQUIPMENT
Interfacial structure-property relationships at the fiber-matrix interphase in advanced composites
[AD-A190649] N88-22093
The CRREL (Cold Regions Research and Engineering Laboratory) Hopkinson bar apparatus
[AD-A190599] N88-22380
Mechanisms mediating perception of complex acoustic patterns
[AD-A189765] N88-22520
Laboratory equipment update
[AD-A189781] N88-22522
LAGRANGE COORDINATES
Singular Lagrangians. Classical dynamics and quantization. Lectures for young scientists
[TI88-701158] N88-22806
LAMINAR BOUNDARY LAYER
Modifications to the Langley 8-foot transonic pressure tunnel for the laminar flow control experiment
[NASA-TM-4032] N88-22047
Investigation of boundary layer disturbances caused by periodic heating of a thin ribbon
[AD-A190572] N88-22314
Aerothermal tests of quilted dome models on a flat plate at a Mach number of 6.5
[NASA-TP-2804] N88-22325
LAMINAR FLOW
Duct flow nonuniformities: Effect of struts in SSME HGM II(+)
[NASA-CR-179285] N88-22296
Experiments on densely-loaded non-Newtonian slurries in laminar and turbulent pipe flows
[DE88-006209] N88-22323
LAMINAR FLOW AIRFOILS
Oscillating airfoils: Achievements and conjectures
[AD-A190490] N88-22008
LAMINAR HEAT TRANSFER
Heat transfer modeling of jet vane Thrust Vector Control (TVC) systems
[AD-A190106] N88-22034
LAMINATES
An investigation of the failure response of laminates under biaxial stress
[AD-A190039] N88-22090
Interlaminar fracture toughness of thermoplastic composites
[NASA-TM-100532] N88-22097
A system to measure damage in composite materials by the ultrasonic method
[ONERA-RT-2/7256-RY-061-R] N88-22103
Donor acceptor polymerization chemistry as a vehicle to low energy cure matrix resins
[AD-A190119] N88-22179
The buckling and vibration of composite plates using the Levy method considering shear deformation and rotary inertia
[AD-A189743] N88-22374
Impact damage in composite laminates N88-22402
LAND USE
Updating of the municipal official register of real estate through a geographical information system
[INPE-4459-PRE/1238] N88-22453
Comparative utilization of analog and digital processes in the treatment of MSS-LANDSAT data for studying the national parks of Brazil
[INPE-4011-TDL/240] N88-22456
Orbital remote sensing: An instrument for monitoring urban growth
[INPE-4456-PRE/1287] N88-22833
LANDAU DAMPING
Plasma wave radiative damping of a new type in a relativistic one-dimensional plasma
[TI88-701191] N88-22739
Improvement of plasma confinement due to electron Landau damping in tokamaks
[DE88-752339] N88-22747
LANDAU-GINZBURG EQUATIONS
Global spatial periodic solutions to the Ginzburg-Landau equations
[DE88-006424] N88-22623
LANDING GEAR
In-service measurements of SAAB SF-340 landing gear loads
[FFA-TN-1987-48] N88-22032
LANDING LOADS
In-service measurements of SAAB SF-340 landing gear loads
[FFA-TN-1987-48] N88-22032
LANTHANUM OXIDES
High temperature superconductors in the La(sub 1+x)Ba(sub 2-x)Cu O(sub y system
[DE88-006367] N88-22802
LARGE SCALE INTEGRATION
Characteristics of LSI-wiring expert system discussed N88-22226
LARGE SPACE STRUCTURES
Optimal control and identification of space structures
[AD-A190033] N88-22065
Wave propagation and dynamics of lattice structures
[AD-A190037] N88-22066
Feedback control of distributed parameter systems with applications to large space structures
[AD-A190536] N88-22068

Wave propagation and dynamics of lattice structures
[AD-A190611] N88-22069
Vibrations of structures with parametric uncertainties
[AD-A190400] N88-22378

LASER APPLICATIONS
Diode laser spectroscopy of chemical moieties at surfaces
[AD-A190710] N88-22127
Laser enhanced adhesion of copper films to sapphire substrates
[DE88-006802] N88-22144
Laser photodeposition and etching study
[AD-A190535] N88-22153
Oxide optical coatings prepared by metal-organic vapor deposition
[DE88-006809] N88-22175
JPRS report: Science and technology. Japan
[JPRS-JST-88-002] N88-22210
Laser processing-status, perspectives N88-22211
Compound ceramic processing N88-22212
Fine grain development by laser CVD N88-22214
Material surface improvement by laser N88-22217
Laser evaporation studies
[AD-A189815] N88-22346
Research on certain aspects of laser diffraction particle sizing relevant to autonomous self-diagnosing instrumentation
[AD-A190220] N88-22348
A laser-based photoacoustic spectrometer for direct breath C-13O2/C-12O2 measurement
[DE88-004915] N88-22516
Activities report in laser-matter interaction
[ETN-88-92007] N88-22696

LASER DAMAGE
Protection against laser damage to human body reviewed N88-22237
A preliminary comparison of the transient effects of single versus multiple q-switched doubled-neodymium laser pulses
[AD-A189855] N88-22347
Advanced programming and control techniques for complex mechanical systems
[AD-A190238] N88-22349
A comparison of visual evoked potential and behavioral measures of flashblindness in humans
[AD-A189757] N88-22519

LASER DOPPLER VELOCIMETERS
Laser velocimeter measurements in a wing-fuselage type juncture
[NASA-TM-100588] N88-22012
Inflow measurement made with a laser velocimeter on a helicopter model in forward flight. Volume 3: Rectangular planform blades at an advance ratio of 0.30
[NASA-TM-100543] N88-22015
Unsteady flow field measurements using LDV (Laser Doppler Velocimetry)
[AD-A189907] N88-22298
Instruments for use in experimental studies of complex turbulent shear flow: Three component LDVs
[AD-A190526] N88-22312

LASER FUSION
Smoothing technique to resolve X-ray spectra in laser nuclear fusion N88-22235
Magic light high-power laser passes state certification N88-22236

LASER HEATING
Superfine grain development by laser N88-22215
Material surface improvement by laser N88-22217

LASER INDUCED FLUORESCENCE
Turbulent reacting flows and supersonic combustion
[AD-A189690] N88-22115
Advanced diagnostics for reacting flows
[AD-A190485] N88-22122
Visualization of flows in turbomachinery
[AD-A189927] N88-22299

LASER MATERIALS
Reactions of N2(A sup 3 sigma sup + sub u) candidates for short wavelength lasers
[DE88-007018] N88-22342
Solid hosts for dye laser rods. Part 1: Criteria for choosing a host material
[DE88-006478] N88-22355

LASER MICROSCOPY
Flaw characterization in structural ceramics using scanning laser acoustic microscopy N88-22415
Nondestructive evaluation of sintered ceramics N88-22416

LASER OUTPUTS
Laser processing-status, perspectives N88-22211
Magic light high-power laser passes state certification N88-22236
A preliminary comparison of the transient effects of single versus multiple q-switched doubled-neodymium laser pulses
[AD-A189855] N88-22347
Research on certain aspects of laser diffraction particle sizing relevant to autonomous self-diagnosing instrumentation
[AD-A190220] N88-22348
Characterization of space radiation environment in terms of the energy deposition in functionally important volumes
[DE88-005627] N88-22513
Collective rotation of molecules driven by the angular momentum of light in a nematic film
[FUB-6-1986] N88-22714
Particle beam alignment system for single event upset-Van de Graaf experiments
[AD-A189695] N88-22721
Optical switching and control techniques using nonlinear optical wave mixing
[AD-A190467] N88-22730

LASER PLASMA INTERACTIONS
The development of high power KrF laser systems for plasma research by the application of stimulated Raman scattering
[ETN-88-92220] N88-22358
Activities report in laser-matter interaction
[ETN-88-92007] N88-22696

LASER PLASMAS
PLASMOR: A laser-plasma simulation code, part 2
[DE88-701289] N88-22736
Particle acceleration to high energies and amplification of coherent radiation by electromagnetic interactions in plasmas
[TI88-701020] N88-22737

LASER PUMPING
Fundamental noise processes in a laser excited optical filter
[DE88-006460] N88-22340

LASER RANGER/TRACKER
Baseline estimation from simultaneous satellite laser tracking
[NASA-CR-182750] N88-22052

LASER SPECTROSCOPY
Laser spectroscopy and dynamics of combustion intermediates
[DE88-006541] N88-22110
Infrared absorption spectroscopy and chemical kinetics of free radicals
[DE88-006536] N88-22112
Laser photoelectron spectroscopy of ions
[DE88-006860] N88-22113
The spectroscopy and reaction kinetics of coordinatively unsaturated metal carbonyls
[AD-A190533] N88-22124
Diode laser spectroscopy of chemical moieties at surfaces
[AD-A190710] N88-22127

LASER TARGET INTERACTIONS
Activities report in laser-matter interaction
[ETN-88-92007] N88-22696

LASER WEAPONS
Constellation sizing for modest directed energy platforms
[DE88-007033] N88-22343

LASER WELDING
Reduced thermal input by proper selection of YAG laser welding parameters
[DE88-000730] N88-22356

LASERS
Investigation of laser diagnostics of PACVD processes for depositing hard face coatings
[DE88-007083] N88-22176

LATTICES (MATHEMATICS)
Lattice QCD calculation of K yields pi nonleptonic weak transition and other hadronic weak parameters
[PREPRINT-580] N88-22717

LAYERS
Equilibrium stability of strained epitaxial layers on a rigid substrate
[INPE-4254-PRE/1127] N88-22804

LEAD SULFIDES
Activities of As, Sb, Bi and Pb in copper mattes and their effects on impurity elimination
[TKK-V-A10(1988)] N88-22165

LEAD TELLURIDES
Fabrication and characterization of semiconductor lasers of Pb(1-x)Sn(x)Te
[INPE-4253-PRE/1126] N88-22357
Growth of Pb/sub 1-x/Eu/sub x/Te epitaxial layers by the liquid phase epitaxy technique
[TI88-701022] N88-22763

LEADING EDGES
Thermostructural analysis of simulated cowl lips N88-22403

LEAKAGE
Visualization of flows in turbomachinery
[AD-A189927] N88-22299
Reduced thermal input by proper selection of YAG laser welding parameters
[DE88-000730] N88-22356
Study on shaft seals for potassium turbine
[EL-891] N88-22364

LEAST SQUARES METHOD
Motion sickness: Quantitative, algorithmic malaise indication in real time
[AD-A189674] N88-22518
Cholesky downdating on a hypercube
[DE88-006760] N88-22586

LEVITATION
The interaction of small particles with laser beams
[AD-A190716] N88-22354

LIAPUNOV FUNCTIONS
Markov processes applied to control, replacement and signal analysis
[AD-A190563] N88-22674

LIBRARIES
Data base design and implementation
[AD-A190414] N88-22827

LIE GROUPS
Markov processes applied to control, replacement and signal analysis
[AD-A190563] N88-22674
Lumped model generation and evaluation: Sensitivity and Lie algebraic techniques with applications to combustion
[AD-A190402] N88-22689

LIFE (DURABILITY)
In situ fatigue loading stage inside scanning electron microscope N88-22419
Cumulative fatigue damage models N88-22422
Life prediction modeling based on strainrange partitioning N88-22425
Life prediction modeling based on cyclic damage accumulation N88-22426
Fatigue damage modeling for coated single crystal superalloys N88-22427
Life and reliability of rotating disks N88-22428

LIFE SCIENCES
USSR Space Life Sciences Digest, issue 16
[NASA-CR-3922(19)] N88-22515

LIFT
Zero-lift drag predictions in supersonic flow for complex configurations N88-22246

LIFT AUGMENTATION
Performance optimization of a cruise missile using dynamic-stall induced lift augmentation
[AD-A190497] N88-22027

LIFT DEVICES
A panel method based on velocity potential to compute harmonically oscillating lift surface systems
[ETN-88-91886] N88-22290

LIGHT (VISIBLE RADIATION)
Relationship between optical transfer function and natural light field in sea or atmosphere N88-22247
Infrared-sensitive spatial light modulator
[AD-A190391] N88-22729

LIGHT EMISSION
Merit of Hadamard transform active absorption spectrometer described N88-22232

LIGHT MODULATION
Infrared-sensitive spatial light modulator
[AD-A190391] N88-22729
Research on materials and components for opto-electronic signal processing and computing
[AD-A190130] N88-22788

LIGHT SCATTERING
Research on certain aspects of laser diffraction particle sizing relevant to autonomous self-diagnosing instrumentation
[AD-A190220] N88-22348
The interaction of small particles with laser beams
[AD-A190716] N88-22354
Multiple scattering from nonspherical targets
[AD-A189939] N88-22723

LIGHT SOURCES
Rainbow holographic image reconstructed by spatially extended white light source N88-22249

LIGHT TRANSMISSION
Advanced programming and control techniques for complex mechanical systems
[AD-A190238] N88-22349

LIGHTNING
Experimental comparison of lightning simulation techniques to CV-580 airborne lightning strike measurements
[AD-A190576] N88-22496
Study of lightning and lightning protection (selected pages)
[AD-A190623] N88-22498
Proceedings of the Lightning Threat Warning Workshop
[DE88-006607] N88-22499

LIMITERS (FUSION REACTORS)
Analyses and experiments on the integrity and lifetime predictions of plasma-facing components in fusion reactors
[DE87-702957] N88-22735
LIMITS (MATHEMATICS)
The partially observed stochastic minimum principle
[AD-A189787] N88-22658
LINEAR ACCELERATORS
Status of RF superconductivity at Argonne National Laboratory
[DE88-005913] N88-22796
LINEAR ARRAYS
Space time processing, environmental-acoustic effects
[AD-A190764] N88-22708
LINEAR EQUATIONS
Pointwise stabilization for coupled quasilinear and linear wave equations
[AD-A190031] N88-22632
LINEAR TRANSFORMATIONS
Study of microcomputer-based real-time programmable optical signal processor and application
[AD-A190076] N88-22726
LINEARITY
Linear state space modeling of a turbofan engine
[AD-A190110] N88-22035
LININGS
High-temperature combustor liner tests in structural component response test facility N88-22383
Life assessment of combustor liner using unified constitutive models N88-22384
LINKAGES
A three dimensional non-singular modelling of rigid manipulators
[AD-A189707] N88-22604
LIPSCHITZ CONDITION
Detection of the number, locations and magnitudes of jumps
[AD-A190328] N88-22671
LIQUID ATOMIZATION
Dense-spray structure and phenomena. Part 2: Pressure-atomized sprays
[AD-A190312] N88-22307
LIQUID CRYSTALS
Electronic and ionic transport in polymers
[AD-A190434] N88-22185
Collective rotation of molecules driven by the angular momentum of light in a nematic film
[FUB-6-1986] N88-22714
LIQUID FLOW
Dense-spray structure and phenomena. Part 1. Turbulence/dispersed-phase interactions
[AD-A190606] N88-22315
Fluid motion in a spinning, coning cylinder via spatial eigenfunction expansion
[AD-A190758] N88-22319
LIQUID FUELS
Dense-spray structure and phenomena. Part 2: Pressure-atomized sprays
[AD-A190312] N88-22307
LIQUID METAL COOLED REACTORS
Detecting the gas bubbles in a liquid metal coolant by means of magnetic flowmeters
[TI88-701427] N88-22294
LIQUID METALS
Electrical resistivities of some compound forming liquid metal alloys
[PB88-145172] N88-22137
Angular resolved energy analysis of (69)Ga+ ions from a gallium liquid metal ion source
[AERE-R-12649] N88-22760
LIQUID PHASE EPITAXY
Growth of Pb/sub 1-x/Eu/sub x/Te epitaxial layers by the liquid phase epitaxy technique
[TI88-701022] N88-22763
LIQUID PROPELLANT ROCKET ENGINES
Durability testing of an iridium-plated storable rocket engine injector
[AD-A190707] N88-22078
LIQUID-SOLID INTERFACES
Variable-energy positron studies on liquids and liquid-solid interfaces
[DE88-006356] N88-22109
LIQUIDS
Variable-energy positron studies on liquids and liquid-solid interfaces
[DE88-006356] N88-22109
Density measurements on solids and liquids
[PB88-164934] N88-22129
Nucleation in super-saturated products
[NASA-TT-20275] N88-22134
LISP (PROGRAMMING LANGUAGE)
SimPL: A simulator for parallel LISP
[AD-A189831] N88-22566
CK-LOG system conversion (user's manual and user interface)
[AD-A190273] N88-22577
LITHIUM ALLOYS
The age hardening response of thermomechanically processed Al-Mg-Li alloys
[AD-A189870] N88-22147
LOAD DISTRIBUTION (FORCES)
Cubic spline solution of symmetric buckling problems of clamped shallow spherical shells N88-22239
LOAD TESTS
Experiments investigating advanced materials under thermomechanical loading N88-22385
MHOST: An efficient finite element program for inelastic analysis of solids and structures N88-22394
LOADS (FORCES)
Determination of the commutation and angle and load response for a continuous-current, single phase controlled rectifier
[AD-A190602] N88-22285
LOGARITHMS
High speed transcendental elementary function architecture in support of the Vector Wave Equation (VWE)
[AD-A189746] N88-22627
Research on algebraic manipulation
[AD-A190149] N88-22634
LOGIC CIRCUITS
An expert system for discrete component digital circuit design
[AD-A189680] N88-22274
Applications of optical computing to problems with symbolic computations
[AD-A189772] N88-22548
LONG WAVE RADIATION
Tropical circulations and the associated rainfall anomalies during two contrasting years
[INPE-4506-PRE/1261-REV] N88-22502
LORENTZ TRANSFORMATIONS
Spin precession in stationary gravitational fields
[TI88-701107] N88-22470
Recent developments in the path integral approach to anomalies
[DE87-703032] N88-22616
LOUVERS
Describing the source created by turbulent flow over orifices and louvers
[AD-A190254] N88-22706
LOW CARBON STEELS
Studies on hot-dip zinc-aluminum coated sheet steels
[ETN-88-92217] N88-22166
LOW FREQUENCIES
Subharmonic aliasing and its effects on the AFTI/F-16 digital flight control system
[AD-A190614] N88-22042
LOW PASS FILTERS
High speed, bandpass sampling of digital communications waveforms
[AD-A189842] N88-22254
LOW PRESSURE
Study of surface discharges
[ONERA-12/7236-PY] N88-22073
LOW SPEED WIND TUNNELS
Contraction design for small low-speed wind tunnels
[NASA-CR-182747] N88-22045
LOW TEMPERATURE ENVIRONMENTS
The CRREL (Cold Regions Research and Engineering Laboratory) Hopkinson bar apparatus
[AD-A190599] N88-22380
LOW TEMPERATURE TESTS
The CRREL (Cold Regions Research and Engineering Laboratory) Hopkinson bar apparatus
[AD-A190599] N88-22380
LUBRICANTS
A new approach to highly fluorinated lubricants
[AD-A190523] N88-22188
LUBRICATING OILS
A new method of measuring multigrade oil shear elasticity and viscosity at high shear rates
[AD-A190145] N88-22304
LUBRICATION
A new method of measuring multigrade oil shear elasticity and viscosity at high shear rates
[AD-A190145] N88-22304
Traction model development
[AD-A188450] N88-22359
LUBRICATION SYSTEMS
Traction model development
[AD-A188450] N88-22359
LUMINESCENCE
Electronic and ionic transport in polymers
[AD-A190434] N88-22185
LUMINOSITY
Hydrodynamical models of supernova SN 1987 A in the LMC
[TI88-701123] N88-22837
LUNGS
Methods of measurement for the evaluation of monolayer properties. Development and applications — lung surfactants
[ETN-88-92229] N88-22532

M

MACH NUMBER
High Reynolds number, low Mach number, steady flow field calculations over a NACA 0012 airfoil using Navier-Stokes and interactive boundary layer theory
[AD-A189871] N88-22005
MACHINE TOOLS
Fiber-reinforced plastic composites. Possibilities and limitations of applications as machine-construction materials
[NASA-TT-20159] N88-22102
MAGMA
Advanced geothermal technologies
[DE88-004307] N88-22483
MAGNESIUM
Microplasticity phenomena in graphite/magnesium metal matrix composites
[DE88-006772] N88-22086
MAGNESIUM ALLOYS
The age hardening response of thermomechanically processed Al-Mg-Li alloys
[AD-A189870] N88-22147
Corrosion and electrochemical behavior of binary magnesium alloys
[AD-A190624] N88-22154
MAGNETIC COOLING
Magnetic anomalies in the rare earth oxide superconductors GdBa2Cu3O(7-x) and YbBa2Cu3O(7-x)
[AD-A190713] N88-22793
MAGNETIC DISKS
High density ion implanted contiguous disk bubble technology
[AD-A190169] N88-22789
MAGNETIC FIELD CONFIGURATIONS
Plasmapause formation
[AERONOMICA-ACTA-A-319-1987] N88-22759
MAGNETIC FIELDS
Analysis of anomalous resistivity during the conduction phase of the plasma erosion opening switch
[DE88-006382] N88-22286
On the acceleration of electrons and positive ions in the same direction along magnetic field lines by parallel electric fields
[IRF-PREPRINT-103] N88-22488
Electrical circuit modeling of reversed field pinches
[DE88-006942] N88-22745
Parametric instabilities of inhomogeneous plasma near the lower-hybrid resonance
[TI88-701201] N88-22748
Quantization of axial electrodynamics
[TI86-701498] N88-22813
MAGNETIC MEASUREMENT
Excitations in magnetic low-dimensional systems: A spectroscopic study
[ETN-88-92230] N88-22697
MAGNETIC MIRRORS
New methods of confinement and heating of plasma in magnetic fields
[TI88-701021] N88-22738
MAGNETIC PROBES
Thin superconducting film characterization by surface acoustic waves
[AD-A190417] N88-22791
MAGNETIC PROPERTIES
A qualitative approach to electricity
[AD-A189854] N88-22693
Magnetic anomalies in the rare earth oxide superconductors GdBa2Cu3O(7-x) and YbBa2Cu3O(7-x)
[AD-A190713] N88-22793
MAGNETIC SPECTROSCOPY
Excitations in magnetic low-dimensional systems: A spectroscopic study
[ETN-88-92230] N88-22697
MAGNETOHYDRODYNAMIC FLOW
Advanced diagnostics for reacting flows
[AD-A190485] N88-22122
MPD (magnetoplasmadynamic) thrust chamber flow dynamics
[AD-A189940] N88-22751
MAGNETOHYDRODYNAMIC STABILITY
Analyses and experiments on the integrity and lifetime predictions of plasma-facing components in fusion reactors
[DE87-702957] N88-22735
MAGNETOHYDRODYNAMICS
ALEX results: A comparison of measurements from a round and a rectangular duct with 3-D code predictions
[DE88-005947] N88-22741

MAGNETOPLASMADYNAMICS
MPD (magnetoplasmadynamic) thrust chamber flow dynamics
[AD-A189940] N88-22751
Fundamental studies on MPD thrusters
[AD-A190307] N88-22753
Physical fluid mechanics in MPD thrusters
[AD-A190309] N88-22754
MPD (magnetoplasmadynamic) thruster advanced pumping system concepts
[AD-A190513] N88-22756
MAGNETOSTATIC FIELDS
Boundary element method for three-dimensional magnetostatic fields in terms of vector variables
[EL-61] N88-22649
MAGNETOSTATICS
Boundary element method for three-dimensional magnetostatic fields in terms of vector variables
[EL-61] N88-22649
MAGNETOSTRICTION
High density ion implanted contiguous disk bubble technology
[AD-A190169] N88-22789
MAN MACHINE SYSTEMS
Conflict resolution in cooperative systems
[AD-A190351] N88-22535
MAN-COMPUTER INTERFACE
Investigation into the development of computer aided design software for space based sensors
[NASA-CR-180772] N88-22552
Extension of computer based algorithms by operator analysts
[NASA-CR-182798] N88-22575
The Scientific and Technical Information Network (STINET). Foundation for evolution
[AD-A189750] N88-22822
MANAGEMENT
Napping and human functioning during prolonged work
[AD-A190228] N88-22525
MANAGEMENT SYSTEMS
GTE battery management system: State of charge indicator evaluation
[DE88-006800] N88-22272
MANDELSTAM REPRESENTATION
Secondary gauge conditions in field theory
[TI88-701499] N88-22814
MANGANESE ALLOYS
Evaporation characteristics of elements during vacuum arc remelting of alloy A-286 N88-22248
MANIPULATORS
Telerobotic operation of conventional robot manipulators
[DE88-005718] N88-22363
Design, development and evaluation of Stanford/Ames EVA prehensors
[NASA-CR-182688] N88-22540
A three dimensional non-singular modelling of rigid manipulators
[AD-A189707] N88-22604
MANNED SPACECRAFT
A systems analysis of fire suppression alternatives for the US space station
[AD-A189847] N88-22064
MANUFACTURING
Manufacturing of ultrasonic focused probes
[VTT-RR-487] N88-22368
Insertions using geometric analysis and hybrid force-position control: Method and analysis
[DE87-013652] N88-22611
Multivariate analysis and its application
[AD-A189983] N88-22661
MANY BODY PROBLEM
Corrosion Research Center, University of Minnesota
[DE88-006681] N88-22160
On new solvable many-body dynamical systems with velocity dependent forces
[PREPRINT-581] N88-22683
MAPPING
Enhanced viscous flow drag reduction using acoustic excitation
[NASA-CR-182734] N88-22295
Fatigue damage mapping N88-22423
Geometric restoration of satellite image data
[AD-A190462] N88-22450
MAPS
Relative orientation
[AD-A190385] N88-22449
PLOT3D (version-5): A computer code for drawing three dimensional graphs, maps and histograms, in single or multiple colours, for mono or stereoscopic viewing
[DE88-701410] N88-22558
Regularity of the Albanese map for nonoriented surfaces
[DE88-006428] N88-22679
MARINE ENVIRONMENTS
The corrosion resistance of an aluminum alloy coated with polysilazane derived ceramics
[AD-A190703] N88-22189
Derivation of consistent surface fixed fields for use in a global NWP model
[AD-A190131] N88-22475
Real-time environmental Arctic monitoring (R-TEAM)
[AD-A189948] N88-22508
MARKETING
High temperature materials: What's available
[AERE-R-12632] N88-22081
Preliminary market analysis for large zeolite crystals
[NASA-CR-182682] N88-22207
Function of Japan Fine Ceramics Center described N88-22227
MARKOV PROCESSES
Analysis and testing of the SURE program
[NASA-TP-2817] N88-22653
Filtering of jump processes
[AD-A189701] N88-22656
Structural decomposition of multiple time scale Markov processes
[AD-A189739] N88-22657
The partially observed stochastic minimum principle
[AD-A189787] N88-22658
Markov processes applied to control, replacement and signal analysis
[AD-A190563] N88-22674
MARS (PLANET)
Periodic orbits around a satellite modelled as a triaxial ellipsoid
[AD-A190592] N88-22051
MARS SURFACE
Groundwater sapping valleys: Experimental studies, geological controls and implications to the interpretation of valley networks on Mars
[NASA-CR-182718] N88-22847
MARTINGALES
Martingale representation and the Malliavin calculus
[AD-A189721] N88-22626
Stochastic evolution equations driven by nuclear space valued martingales
[AD-A189342] N88-22677
MASS
To the field theory with a fundamental mass
[TI88-701159] N88-22807
MASS DISTRIBUTION
Angular resolved energy analysis of (69)Ga+ ions from a gallium liquid metal ion source
[AERE-R-12649] N88-22760
MASS SPECTROMETERS
High-voltage inverse-square function generator
[DE88-701109] N88-22270
MASS TRANSFER
Mass transfer mechanisms for water adsorbed on silica gel
[DE88-005993] N88-22107
The numerical simulation of viscous flows with change of phase and chemical reaction
[DE88-003204] N88-22292
MATCHED FILTERS
Synthetic-aperture radars viewed as interferometers with matched filter processing of the collected data
[AD-A190608] N88-22262
Spatial matched processing for multipath propagation
[AD-A189790] N88-22701
MATERIAL ABSORPTION
Microwave dispersion and absorption in tissues: Molecular mechanisms
[AD-A190118] N88-22512
MATERIALS SCIENCE
The contribution of electron microscopy of materials science to society
[DE88-006341] N88-22082
MATHEMATICAL LOGIC
ONTIC: A knowledge representation system for mathematics
[AD-A190553] N88-22643
MATHEMATICAL MODELS
Linear state space modeling of a turbofan engine
[AD-A190110] N88-22035
Baseline estimation from simultaneous satellite laser tracking
[NASA-CR-182750] N88-22052
Moving-bank multiple model adaptive estimation applied to flexible spacestructure control
[AD-A190761] N88-22071
Numerical simulation of turbulent flames using vortex methods
[AD-A189813] N88-22116
Duct flow nonuniformities: Effect of struts in SSME HGM II(+)
[NASA-CR-179285] N88-22296
On the prediction of highly vortical flows using an Euler equation model, part 2
[AD-A190245] N88-22305
Numerical modelling specific energy charcteristics of excimer KrF lasers with electron beam excitation
[DE88-701525] N88-22344
Life assessment of combustor liner using unified constitutive models N88-22384
Biaxial experiments supporting the development of constitutive theories for advanced high-temperature materials N88-22386
Unified constitutive model development for metal matrix composites at high temperature N88-22387
Unified constitutive model for single crystal deformation behavior with applications N88-22388
Finite element (MARC) solution technologies for viscoplastic analyses N88-22389
Continuous fiber ceramic matrix composites for heat engine components N88-22411
Cumulative fatigue damage models N88-22422
Life prediction modeling based on strainrange partitioning N88-22425
Fatigue damage modeling for coated single crystal superalloys N88-22427
Review and assessment of the HOST turbine heat transfer program N88-22431
Atmospheric carbon dioxide and the global carbon cycle: The key uncertainties
[DE88-005059] N88-22465
A survey of denser-than-air atmospheric dispersion models
[DE88-006626] N88-22467
Description of ground motion data processing codes, volume 2
[DE88-007137] N88-22481
Proceedings of the Lightning Threat Warning Workshop
[DE88-006607] N88-22499
SEARCH: An interactive computer program for optimizing two-variable, unconstrained experiments or simulation
[AD-A190593] N88-22583
Artificial neural networks: An introduction with an annotated bibliography
[DE88-007003] N88-22603
Higher order crossings
[AD-A190489] N88-22641
Analysis and testing of the SURE program
[NASA-TP-2817] N88-22653
Statistical inference for stochastic processes
[AD-A190491] N88-22673
Lumped model generation and evaluation: Sensitivity and Lie algebraic techniques with applications to combustion
[AD-A190402] N88-22689
Model-scale sound propagation experiment
[NASA-TM-100602] N88-22709
Electrical circuit modeling of reversed field pinches
[DE88-006942] N88-22745
Plasma-gas interaction studies in a hybrid plume plasma rocket
[AD-A190310] N88-22755
A method for estimating and controlling the cost of extending technology
[AD-A190717] N88-22831
MATHEMATICAL PROGRAMMING
Tutorial on GAMS (Generalized Algebraic Modeling System): A modeling language for optimization
[AD-A189867] N88-22568
MATRICES (MATHEMATICS)
Split-coefficient matrix solution and experimental study of axisymmetric underexpanded exhaust plumes N88-22242
Sufficient matrices and the linear complementarity problem
[AD-A190429] N88-22690
MATRIX MATERIALS
Cement paste matrix composite materials center
[AD-A188657] N88-22083
Microplasticity phenomena in graphite/magnesium metal matrix composites
[DE88-006772] N88-22086
Singlet oxygen behavior in solid polymer matrices
[DE88-005171] N88-22171
Donor acceptor polymerization chemistry as a vehicle to low energy cure matrix resins
[AD-A190119] N88-22179
A test for interfacial effects and stress transfer in ceramic matrix composites
[NASA-CR-182758] N88-22194
MATRIX METHODS
Coupled bending-torsion steady-state response of pretwisted, nonuniform rotating beams using a transfer-matrix method
[NASA-TM-100596] N88-22435

MATRIX THEORY
Sufficient matrices and the linear complementarity problem
[AD-A190429] N88-22690
MAXWELL EQUATION
Wave energy flow conservation for propagation in inhomogeneous Vlasov-Maxwell equilibria
[DE88-006705] N88-22251
High speed transcendental elementary function architecture in support of the Vector Wave Equation (VWE)
[AD-A189746] N88-22627
MEAN FREE PATH
Study of mean free path effects on growth of ultrafine metallic aerosols
[AD-A190206] N88-22149
MEASURE AND INTEGRATION
Remarks on the time transformation of path-integral measures
[DE87-703040] N88-22617
MEASURING INSTRUMENTS
Density measurements on solids and liquids
[PB88-164934] N88-22129
A 150,000 pounds per square inch dynamic pressure calibrator
[AD-A190659] N88-22335
Research sensors N88-22430
Proceedings of the Lightning Threat Warning Workshop
[DE88-006807] N88-22499
MECHANICAL DEVICES
Nonlinear analysis and optimal design of dynamic mechanical systems for spacecraft application
[AD-A190644] N88-22070
MECHANICAL DRIVES
A high performance inverter-fed drive system of an interior permanent magnet synchronous machine
[DE88-006753] N88-22268
MECHANICAL MEASUREMENT
In-service measurements of SAAB SF-340 landing gear loads
[FFA-TN-1987-48] N88-22032
MECHANICAL PROPERTIES
High temperature materials: What's available
[AERE-R-12632] N88-22081
Galvanic corrosion initiatives
[AD-A190658] N88-22155
Transformation toughening of ceramics
[AD-A190399] N88-22183
Mechanical behaviour of particle filled thermoplastics
[PB88-169297] N88-22196
Hafnia-rich mixed oxide ceramics of the system HfO2-ZrO2-TiO2 for heaters and heat exchangers in electrothermal thrusters: The effects of titania on selected electrical and mechanical properties of Hafnia-rich mixed oxides in the system Hafnia-Zirconia-Titania, volume 1
[NASA-CR-182600-VOL-1] N88-22197
Developments in ceramic superconducting materials N88-22229
Features and applications of the integrated composites analyzer (ICAN) code N88-22391
Structural decomposition of multiple time scale Markov processes
[AD-A189739] N88-22657
Experimental studies on electronic properties of HgTe/CdTe and Hg sub 1-z Cd sub x Te/CdTe heterostructures and superlattices
[AD-A189826] N88-22783
Fundamental studies of the mechanical behavior of microelectronic thin film materials
[AD-A190036] N88-22786
MEDIAN (STATISTICS)
Contour interactive extraction using image numerical treatment
[ISL-R-114/86] N88-22587
MELTING
On rotating sphere-on-a-plate experiments and the questions of whether high angle grain boundaries melt below bulk melting temperatures
[DE88-006627] N88-22142
Directed-energy electron-beam processing of a hypoeutectic Cr90Ta10 alloy
[DE88-005621] N88-22157
Melt processing ceramic YBa2Cu3O(sub 6.9)
[DE88-007039] N88-22199
MEMBRANES
Synthesis and analysis of novel polymers with potential for providing both high permselectivity and permeability in gas separation applications
[DE88-006533] N88-22174
MEMORY
Relationship of encoding speed and memory tests to flight training performance
[AD-A190670] N88-22539
On categorizing sounds
[AD-A189784] N88-22700
MEMORY (COMPUTERS)
Characteristics of LSI-wiring expert system discussed N88-22226
Application of static memory for data acquisition and transmission into a computer
[T88-701491] N88-22544
MENTAL PERFORMANCE
Relationship of encoding speed and memory tests to flight training performance
[AD-A190670] N88-22539
MERCURY CADMIUM TELLURIDES
Experimental studies on electronic properties of HgTe/CdTe and Hg sub 1-z Cd sub x Te/CdTe heterostructures and superlattices
[AD-A189826] N88-22783
MESSAGE PROCESSING
Performance of data compression codes in channels with errors
[AD-A189667] N88-22253
Implementation of a distributed adaptive routing algorithm on the Intel iPSC (Intel Personal Super-Computer)
[AD-A189849] N88-22567
METAL AIR BATTERIES
Aluminum-air battery development
[DE88-006620] N88-22287
METAL FATIGUE
The growth of corner cracks under the conjoint action of high and low cycle fatigue
[AD-A190510] N88-22379
Lewis Structures Technology, 1988. Volume 3: Structural Integrity Fatigue and Fracture Wind Turbines HOST
[NASA-CP-3003-VOL-3] N88-22408
Life prediction modeling based on cyclic damage accumulation N88-22426
Fatigue damage modeling for coated single crystal superalloys N88-22427
METAL FILMS
Laser enhanced adhesion of copper films to sapphire substrates
[DE88-006802] N88-22144
Vapor phase deposition and growth of polyimide films on copper
[AD-A189969] N88-22178
Ion-beam mixing and amorphization in Au/Zr bilayers
[DE88-005999] N88-22767
METAL IONS
Determination of aquo-complexes of chromium and iron in chromium plating and polishing solutions by ion chromatography
[AD-A190168] N88-22148
METAL JOINTS
Investigation of Super*Zip separation joint
[NASA-TM-4031] N88-22072
METAL MATRIX COMPOSITES
Microplasticity phenomena in graphite/magnesium metal matrix composites
[DE88-006772] N88-22086
Drilling metal matrix composites
[AD-A190480] N88-22091
Interfacial structure-property relationships at the fiber-matrix interphase in advanced composites
[AD-A190649] N88-22093
Specimen preparation techniques for the examination of ceramic and metal-matrix composites
[DE88-005157] N88-22094
Thermal expansion behavior of randomly oriented short carbon fiber reinforced copper composites
[NASA-TT-20175] N88-22099
Reciprocating sliding wear characteristics of copper-carbon fiber composites
[NASA-TT-20176] N88-22100
Application of copper-carbon fiber composites to power semiconductor devices
[NASA-TT-20171] N88-22101
Joints in fiber-reinforced aluminum alloys
[NASA-TT-20160] N88-22104
Processing, microstructure, and mechanical properties of silicon carbide particulate reinforced aluminum alloys
[AD-A188981] N88-22136
Investigation and synthesis of high temperature and increased stiffness RSP aluminum alloys
[AD-A190407] N88-22151
Growth and deformation mechanisms of refractory alloy hybrid materials
[AD-A190492] N88-22152
Unified constitutive model development for metal matrix composites at high temperature N88-22387
METCAN: The metal matrix composite analyzer N88-22395
METAL OXIDE SEMICONDUCTORS
Two papers on a symbolic analyzer for MOS (Metal-Oxide Semiconductors) circuits
[AD-A188617] N88-22761
Modeling the effects of heavy charged particles on MOSFETs (Metal-Oxide-Semiconductor Field Effect Transistors)
[AD-A190575] N88-22792
METAL OXIDES
Compound ceramic processing N88-22212
METAL PARTICLES
Study of mean free path effects on growth of ultrafine metallic aerosols
[AD-A190206] N88-22149
METAL PLATES
The effective fracture toughness of aluminum at rapid heating rates
[AD-A189745] N88-22146
Finite element simulation of perforation of aluminum plates
[DE88-002092] N88-22362
Processing defects and strength of alumina substrates
[W-10/87] N88-22441
METAL POWDER
Grain growth behavior of extrusion consolidated centrifugally atomized Type 304 stainless steel powder
[DE88-006788] N88-22143
METAL SHEETS
Studies on hot-dip zinc-aluminum coated sheet steels
[ETN-88-92217] N88-22166
METAL SURFACES
Development of a laboratory test for multiport injector deposits: Approaches 1 and 2
[AD-A190697] N88-22203
Theory of the dissociation dynamics of small molecules on metal surfaces: Finite temperature studies
[DE88-006495] N88-22716
METAL VAPOR LASERS
Electronic energy transfer processes in the alkali/alkaline earth metal vapors
[AD-A190035] N88-22119
Alkali metal diffuse band lasers
[AD-A190244] N88-22350
METALS
Annihilation momentum density of positrons trapped at vacancy-type defects in metals and alloys
[DE88-005936] N88-22797
METASTABLE STATE
Effect of vibrational excitation on rate parameters of atmospheric reactions
[AD-A190464] N88-22477
Synthesis of metastable superconductors by high dynamic pressure
[DE88-005620] N88-22764
Magnetic anomalies in the rare earth oxide superconductors GdBa2Cu3O(7-x) and YbBa2Cu3O(7-x)
[AD-A190713] N88-22793
METEOROLOGICAL PARAMETERS
A study on electric fields and conductivity associated with electrified clouds in the region of South America
[INPE-4487-TDL/325] N88-22486
A multivariate variational objective analysis-assimilation method. Part 1: Development of the basic model
[NASA-CR-182651] N88-22491
Acoustic propagation in the low atmosphere. Experimental study and modeling by the radius method
[ISL-CO-247/86] N88-22713
METEOROLOGICAL SATELLITES
Baseline observing system experiments using the AFGL global data assimilation system
[AD-A188861] N88-22062
A multivariate variational objective analysis-assimilation method. Part 2: Case study results with and without satellite data
[NASA-CR-182653] N88-22492
METEOROLOGY
A multivariate variational objective analysis-assimilation method. Part 2: Case study results with and without satellite data
[NASA-CR-182653] N88-22492
The collection of statistics on the frequency of cloud cover over North America
[AD-A190456] N88-22495
METHANE
Evaluation of direct methane conversion to higher hydrocarbons and oxygenates
[DE88-003812] N88-22204
METHYL ALCOHOL
Technical highlights of the Alternative Fuels Utilization Program
[DE88-005064] N88-22205
METHYL COMPOUNDS
Ultraviolet absorption cross sections of methylbromide at stratospheric temperatures
[AERONOMICA-ACTA-A-320-1987] N88-22132
METRIC SPACE
Einstein metrics and Brans-Dicke superfields
[DE88-006992] N88-22809

MICROANALYSIS
Advances in geochemistry and cosmochemistry: Trace element microdistributions with the synchrotron X-ray fluorescence microprobe
[DE88-006355] N88-22108
MICROCOMPUTERS
Study of microcomputer-based real-time programmable optical signal processor and application
[AD-A190076] N88-22726
MICROCRYSTALS
Optical characterization of microcrystals
[DE88-006622] N88-22775
Dispersion measurements of microcrystals in the near ultraviolet and infrared
[DE88-006234] N88-22800
MICROELECTRONICS
JPRS report: Science and technology. Japan
[JPRS-JST-88-001] N88-22218
Nondestructive moisture measurement in microelectronics
[AD-A190515] N88-22281
The Department of Defense Superconductivity Research and Development (DSRD) options. A study of possible directions for exploitation of superconductivity in military applications
[AD-A189747] N88-22780
Fundamental studies of the mechanical behavior of microelectronic thin film materials
[AD-A190038] N88-22786
MICROMECHANICS
Microplasticity phenomena in graphite/magnesium metal matrix composites
[DE88-006772] N88-22086
Whisker-reinforced ceramic composites for heat engine components N88-22410
MICROPARTICLES
A chemical method for achieving acceleration of macroparticles to ultrahigh velocities
[DE88-006377] N88-22695
MICROPHONES
Experimental study on the influence of wind on acoustic pressure sensors
[ISL-R-121/86] N88-22712
MICROPROCESSORS
MIG-1 on-line measuring holographic microscope
[TI88-701103] N88-22332
MICROSTRIP ANTENNAS
Conformal microstrip slot antenna and antenna array
[AD-A189623] N88-22252
MICROSTRUCTURE
The contribution of electron microscopy of materials science to society
[DE88-006341] N88-22082
Processing, microstructure, and mechanical properties of silicon carbide particulate reinforced aluminum alloys
[AD-A188981] N88-22136
Segregation effects in welded stainless steels
[DE88-701224] N88-22139
The age hardening response of thermomechanically processed Al-Mg-Li alloys
[AD-A189870] N88-22147
Directed-energy electron-beam processing of a hypoeutectic Cr90Ta10 alloy
[DE88-005621] N88-22157
Transformation toughening of ceramics
[AD-A190399] N88-22183
Strength and microstructure of ceramics
[AD-A190712] N88-22191
A three-dimensional model for the elastic properties of a foam
[DE88-006197] N88-22192
High temperature corrosion of ceramics
[DE88-006567] N88-22193
The growth of corner cracks under the conjoint action of high and low cycle fatigue
[AD-A190510] N88-22379
Evolution of hardening and damage during viscoplastic deformation
[AD-A190714] N88-22381
Characterization of sintered SiC by using NDE N88-22413
MICROWAVE ATTENUATION
Microwave dispersion and absorption in tissues: Molecular mechanisms
[AD-A190118] N88-22512
MICROWAVE EMISSION
High power, high frequency radiation from beam-plasma interactions
[AD-A190207] N88-22752
MICROWAVES
Microwave sintering of alumina-SiC composites at 2.45 and 60 GHz
[DE88-006455] N88-22095
Preparing the Alcator C bolometer system for use on MTX (Microwave Tokamak Experiment)
[DE88-006724] N88-22733
MIE SCATTERING
Advanced diagnostics for reacting flows
[AD-A190485] N88-22122
MILITARY TECHNOLOGY
JPRS report: Science and technology. Japan
[JPRS-JST-87-029] N88-22228
MILLIMETER WAVES
Instrumentation for the characterization and development of millimeter wave components compatible with monolithic integration
[AD-A189724] N88-22275
MILLING MACHINES
Structure and properties of titanium nitride and zirconium nitride thin films prepared by reactive ion plating — cutting tools
[ETN-88-92218] N88-22167
MIMD (COMPUTERS)
An analysis of multiple grain CHiP architectures
[AD-A189942] N88-22570
Transformations of concurrent algorithms for highly parallel systems: A one year project summary report
[AD-A190236] N88-22576
MINERALS
An investigation of the crystalchemistry and thermochemistry of selected mineral systems
[AD-A189758] N88-22781
MINES (ORDNANCE)
Preliminary airworthiness evaluation of the UH-60A equipped with the XM-139 VOLCANO mine dispensing system
[AD-A190604] N88-22029
MINIMA
The partially observed stochastic minimum principle
[AD-A189787] N88-22658
MINIMAL SURFACES
Computer graphics tools for the study of minimal surfaces
[DE88-006421] N88-22557
Complete minimal surfaces in R^3 of low total curvature
[DE88-006425] N88-22619
Embedded minimal sufaces with an infinite number of ends
[DE88-006429] N88-22680
MINKOWSKI SPACE
To the field theory with a fundamental mass
[TI88-701159] N88-22807
Finite width corrections to the Nambu action for the Nielsen-Olesen string
[DE88-006996] N88-22812
MIRRORS
Constellation sizing for modest directed energy platforms
[DE88-007033] N88-22343
MISMATCH (ELECTRICAL)
Information and coding capacities of mismatched Gaussian channels
[AD-A190321] N88-22665
Coding capacity of generalized additive channels
[AD-A190315] N88-22685
MISSILE CONFIGURATIONS
Zero-lift drag predictions in supersonic flow for complex configurations N88-22246
MISSILE CONTROL
Advanced guidance algorithms for homing missiles with bearings-only measurements
[AD-A190435] N88-22026
Memory efficient evaluations of nonlinear stochastic equations and C3 applications
[AD-A189872] N88-22569
MISSILE TRAJECTORIES
Advanced guidance algorithms for homing missiles with bearings-only measurements
[AD-A190435] N88-22026
MISSILES
Advanced guidance algorithms for homing missiles with bearings-only measurements
[AD-A190435] N88-22026
MISSION PLANNING
Orbital transfer vehicle: Concept definition and system analysis study
[NASA-CR-179315] N88-22060
Space utilization plans N88-22219
External tank gamma ray imaging telescope study. Final review, phase 2
[NASA-CR-179320] N88-22834
MIXING
Experimental investigation of a spanwise forced mixing layer
[AD-A190136] N88-22007
Effect of moisture level in PBXW-109(E) (plastic-bonded explosive) mixes on the aging of the cured explosive
[AD-A190200] N88-22202
Mixing: Stretching, breakup and chaos
[DE88-006699] N88-22327
Optical switching and control techniques using nonlinear optical wave mixing
[AD-A190467] N88-22730
Ion-beam mixing and amorphization in Au/Zr bilayers
[DE88-005999] N88-22767
MIXING LENGTH FLOW THEORY
Turbulent reacting flows and supersonic combustion
[AD-A189690] N88-22115
An investigation of flow structure, mixing and chemical reaction in combusting turbulent flows
[AD-A189980] N88-22117
MODELS
Geometric modeling of flight information for graphical cockpit display
[AD-A190484] N88-22043
A model for nitrogen atom recombination on a silicon dioxide surface
[AD-A189843] N88-22784
Georelational data model
[INPE-4490-PRE/1254] N88-22829
MODULES
Japanese space station module N88-22224
Solar cell cover glasses for satellites N88-22225
Investigation into the development of computer aided design software for space based sensors
[NASA-CR-180772] N88-22552
Complexity of some problems in module algebra
[PB88-165386] N88-22648
MODULUS OF ELASTICITY
The age hardening response of thermomechanically processed Al-Mg-Li alloys
[AD-A189870] N88-22147
The sensitivity of boundary layer instability growth rates to compliant wall properties
[AD-A190433] N88-22309
MOISTURE CONTENT
Effect of moisture level in PBXW-109(E) (plastic-bonded explosive) mixes on the aging of the cured explosive
[AD-A190200] N88-22202
MOISTURE METERS
Nondestructive moisture measurement in microelectronics
[AD-A190515] N88-22281
MOLECULAR BEAM EPITAXY
Gas source MBE (Molecular Beam Epitaxy)
[AD-A189763] N88-22782
Beam assisted fabrication of 3-5/Si monolithic devices
[AD-A189979] N88-22785
MOLECULAR BIOLOGY
Studies of molecular biology
[DE88-005906] N88-22514
MOLECULAR COLLISIONS
Molecular reaction and energy transfer rate estimation for chemical-laser analysis
[AD-A190664] N88-22126
MOLECULAR DIFFUSION
Does the pipe diffusion of self-interstitials in crystals under stresses exist
[TI88-701027] N88-22782
MOLECULAR ENERGY LEVELS
Sequential excitation preparation of molecular energy levels with special structural and chemical properties
[AD-A190041] N88-22718
MOLECULAR EXCITATION
Molecular reaction and energy transfer rate estimation for chemical-laser analysis
[AD-A190664] N88-22126
Reactions of N2(A sup 3 sigma sup + sub u) candidates for short wavelength lasers
[DE88-007018] N88-22342
MOLECULAR INTERACTIONS
Molecular reaction and energy transfer rate estimation for chemical-laser analysis
[AD-A190664] N88-22126
MOLECULAR RELAXATION
Reactions of N2(A sup 3 sigma sup + sub u) candidates for short wavelength lasers
[DE88-007018] N88-22342
MOLECULAR ROTATION
Rotational structure and absorption cross sections from 300 to 190 K of the Schumann-Runge bands
[AERONOMICA-ACTA-A-318-1987] N88-22131
Collective rotation of molecules driven by the angular momentum of light in a nematic film
[FUB-6-1986] N88-22714
Sequential excitation preparation of molecular energy levels with special structural and chemical properties
[AD-A190041] N88-22718
MOLECULAR STRUCTURE
Sequential excitation preparation of molecular energy levels with special structural and chemical properties
[AD-A190041] N88-22718
MONITORS
Real-time environmental Arctic monitoring (R-TEAM)
[AD-A189948] N88-22508

MONOMOLECULAR FILMS
Methods of measurement for the evaluation of monolayer properties. Development and applications — lung surfactants
[ETN-88-92229] N88-22532
MONTE CARLO METHOD
Monte Carlo reliability analysis
[AD-A189972] N88-22366
MOORING
Real-time environmental Arctic monitoring (R-TEAM)
[AD-A189948] N88-22508
MORPHOLOGY
Laser enhanced adhesion of copper films to sapphire substrates
[DE88-006802] N88-22144
MOSSBAUER EFFECT
SDIO/IST ultrashort wavelength laser: Novel experimental schemes for observing the Mossbauer effect in long-lived nuclear levels
[AD-A190275] N88-22351
SDIO/IST ultrashort wavelength laser. Mossbauer effect in gamma-ray lasers
[AD-A190306] N88-22352
MOTION SICKNESS
Motion sickness: Quantitative, algorithmic malaise indication in real time
[AD-A189674] N88-22518
MOTION SIMULATION
Effects of update and refresh rates on flight simulation visual displays
[NASA-TM-100415] N88-22033
MOTORS
Performance test results: AXIAL-GAP, permanent magnet compressor motor
[DE88-006857] N88-22289
MOUNTAINS
Geometric modeling of flight information for graphical cockpit display
[AD-A190484] N88-22043
MULLITES
Superplastic flow of mullite-zirconia composites
[DE88-005905] N88-22085
MULTIPATH TRANSMISSION
Spatial matched processing for multipath propagation
[AD-A189790] N88-22701
MULTIPLEXING
Applications of optical computing to problems with symbolic computations
[AD-A189772] N88-22548
MULTIPROCESSING (COMPUTERS)
Parallel memory addressing using coincident optical pulses
[AD-A189767] N88-22547
An analysis of multiple grain CHiP architectures
[AD-A189942] N88-22570
Comparative analysis of multistage interconnection networks
[AD-A190436] N88-22598
A methodolgy, based on analytical modeling, for the design of parallel and distributed architectures for relational database query processors
[AD-A189844] N88-22825
New generation knowledge processing, volume 1
[AD-A190165] N88-22826
MULTISENSOR APPLICATIONS
Development of subminiature multi-sensor hot-wire probes
[NASA-TM-100052] N88-22336
MULTISPECTRAL BAND SCANNERS
NIMBUS-7 CZCS. Coastal Zone Color Scanner imagery for selected coastal regions. North America - Europe. South America - Africa - Antarctica. Level 2 photographic product
[NASA-CR-180755] N88-22447
MULTIVARIATE STATISTICAL ANALYSIS
A multivariate variational objective analysis-assimilation method. Part 1: Development of the basic model
[NASA-CR-182651] N88-22491
A multivariate variational objective analysis-assimilation method. Part 2: Case study results with and without satellite data
[NASA-CR-182653] N88-22492
Some comments on quadrant dependence in higher dimensions
[AD-A190329] N88-22639
Multivariate analysis and its application
[AD-A189983] N88-22661
Detection of the number, locations and magnitudes of jumps
[AD-A190328] N88-22671
MUSCLES
A program for the study of skeletal muscle catabolism following physical trauma
[AD-A189771] N88-22521
MUSCULOSKELETAL SYSTEM
A program for the study of skeletal muscle catabolism following physical trauma
[AD-A189771] N88-22521

N

N-TYPE SEMICONDUCTORS
Calculating depletion region carrier concentrations with capacitance-voltage measurements and etching
[AD-A189630] N88-22777
NASTRAN
Thermostructural analysis of simulated cowl lips
N88-22403
NAVIER-STOKES EQUATION
High Reynolds number, low Mach number, steady flow field calculations over a NACA 0012 airfoil using Navier-Stokes and interactive boundary layer theory
[AD-A189871] N88-22005
Transonic Navier-Stokes computations of strake-generated vortex interactions for a fighter-like configuration
[NASA-TM-100009] N88-22010
Random processes, turbulence and disordering fields
[AD-A190123] N88-22303
Review and assessment of the HOST turbine heat transfer program N88-22431
Numerical study of unsteady viscous hypersonic blunt body flows with an impinging shock
[NASA-TM-100096] N88-22650
High-resolution shock-capturing schemes for inviscid and viscous hypersonic flows
[NASA-TM-100097] N88-22651
NAVIGATION
The visit problem: Visibility graph-based solution
[DE88-000343] N88-22556
NEAR INFRARED RADIATION
Near-infrared observations of cepheids: The distance to M33 N88-22845
NEAR ULTRAVIOLET RADIATION
Dispersion measurements of microcrystals in the near ultraviolet and infrared
[DE88-006234] N88-22800
NECK (ANATOMY)
Basic research on flame radiation
[PB88-168372] N88-22105
Analysis of head response to torso acceleration. Volume 2: Description of data retrieval, analysis and display software
[PB88-156765] N88-22536
NEODYMIUM LASERS
A preliminary comparison of the transient effects of single versus multiple q-switched doubled-neodymium laser pulses
[AD-A189855] N88-22347
NERVOUS SYSTEM
A program for the study of skeletal muscle catabolism following physical trauma
[AD-A189771] N88-22521
NETWORK ANALYSIS
Instrumentation for the characterization and development of millimeter wave components compatible with monolithic integration
[AD-A189724] N88-22275
ECP (Electrical Circuitry Program): A proposed program for electrical circuitry analysis
[AD-A190494] N88-22280
NETWORK CONTROL
Implementation of a distributed adaptive routing algorithm on the Intel iPSC (Intel Personal Super-Computer)
[AD-A189849] N88-22567
Software structuring principles for VLSI CAD
[AD-A190386] N88-22579
NEURAL NETS
Adaptive neural network architecture
[AD-A190114] N88-22533
Instrumentation for scientific computing in neural networks, information science, artificial intelligence and applied mathematics
[AD-A189981] N88-22549
Optical Conceptual Computing and Associative Memory (OCCAM)
[AD-A190030] N88-22550
Rapid feature extraction via the radon transform
[AD-A190032] N88-22573
Artificial neural networks: An introduction with an annotated bibliography
[DE88-007003] N88-22603
Nonlinear signal processing using neural networks: Prediction and system modelling
[DE88-006479] N88-22621
NEURONS
Synapses that compute motion
[AD-A190389] N88-22607
NEUROPHYSIOLOGY
Complex sound processing: An interdisciplinary approach
[AD-A189782] N88-22523
NEUTRON IRRADIATION
Anthropomorphic phantom radiation dosimetry at the NATO standard reference point at Aberdeen Proving Ground
[AD-A190508] N88-22528
NEUTRON STARS
Generation and propagation of sound waves in a collapsing or anti-collapsing star with uniform density
[DE87-703034] N88-22839
NICKEL
Bithermal fatigue of a nickel-base superalloy single crystal
[NASA-TM-100885] N88-22168
NICKEL ALLOYS
Characterization of an explosively consolidated rapidly solidified Fe-16Ni-9Cr-5Mo-2Cu alloy powder
[DE88-006733] N88-22162
NIMBUS 7 SATELLITE
NIMBUS-7 CZCS. Coastal Zone Color Scanner imagery for selected coastal regions. North America - Europe. South America - Africa - Antarctica. Level 2 photographic product
[NASA-CR-180755] N88-22447
NIOBIUM ALLOYS
Growth and deformation mechanisms of refractory alloy hybrid materials
[AD-A190492] N88-22152
NITROGEN
Spectrographic detection of nitrogen impurity in helium
[DE88-752301] N88-22111
Reactions of N2(A sup 3 sigma sup + sub u) candidates for short wavelength lasers
[DE88-007018] N88-22342
NITROGEN ATOMS
A model for nitrogen atom recombination on a silicon dioxide surface
[AD-A189843] N88-22784
NOISE
Fundamental noise processes in a laser excited optical filter
[DE88-006460] N88-22340
NOISE (SOUND)
Auditory perception of complex sounds
[AD-A190528] N88-22529
NOISE MEASUREMENT
Experimental study on the influence of wind on acoustic pressure sensors
[ISL-R-121/86] N88-22712
NOISE POLLUTION
Noise assessment of unsuppressed TF-34-GE-100A engine at Warfield ANG, Baltimore, Maryland
[AD-A189966] N88-22702
NOISE REDUCTION
Investigation of aeroacoustic mechanisms by remote thermal imaging
[DE88-002612] N88-22046
Noise assessment of unsuppressed TF-34-GE-100A engine at Warfield ANG, Baltimore, Maryland
[AD-A189966] N88-22702
Experimental study on the influence of wind on acoustic pressure sensors
[ISL-R-121/86] N88-22712
NOISE SPECTRA
Describing the source created by turbulent flow over orifices and louvers
[AD-A190254] N88-22706
NOISE TEMPERATURE
The kinetics of contact noise in NaBeta alumina
[AD-A190651] N88-22707
NONDESTRUCTIVE TESTS
A system to measure damage in composite materials by the ultrasonic method
[ONERA-RT-2/7256-RY-061-R] N88-22103
Electromagnetic sensor arrays for nondestructive evaluation and robot control
[AD-A190210] N88-22260
Nondestructive moisture measurement in microelectronics
[AD-A190515] N88-22261
An evaluation of nondestructive methods for ceramic heat exchanger applications
[DE88-006731] N88-22328
Eddy current nondestructive inspection of graphite epoxy using ferrite cup core probes
[AD-A189823] N88-22365
Manufacturing of ultrasonic focused probes
[VTT-RR-467] N88-22368
A 3-D solid rendering of NDT data
[DE88-006199] N88-22373
Impact damage in composite laminates N88-22402

Lewis Structures Technology, 1988. Volume 3: Structural Integrity Fatigue and Fracture Wind Turbines HOST
[NASA-CP-3003-VOL-3] N88-22408
Nondestructive evaluation by acousto-ultrasonics N88-22412
Characterization of sintered SiC by using NDE N88-22413
Nondestructive evaluation of sintered ceramics N88-22416

NONISOTHERMAL PROCESSES
Bithermal fatigue: A simplified alternative to thermomechanical fatigue N88-22424

NONLINEAR EQUATIONS
Memory efficient evaluations of nonlinear stochastic equations and C3 applications
[AD-A189872] N88-22569
Almost-periodic solutions of nonlinear parabolic equations
[DE88-006423] N88-22618
Numerical solution of nonlinear algebraic equations in stiff ODE solving
[DE88-006634] N88-22622
New methods for numerical solution of one class of strongly nonlinear partial differential equations with applications
[AD-A189945] N88-22630

NONLINEAR FEEDBACK
Approximation methods for the identification and control of distributed parameter systems
[AD-A190201] N88-22662
Problems in nonlinear continuum dynamics
[AD-A190538] N88-22691

NONLINEAR FILTERS
Advanced guidance algorithms for homing missiles with bearings-only measurements
[AD-A190435] N88-22026

NONLINEAR OPTICS
Collective rotation of molecules driven by the angular momentum of light in a nematic film
[FUB-6-1986] N88-22714
Studies of surfaces using optical sum-frequency generation
[DE88-006334] N88-22715
Theory of interactions of intense light with nonlinear, inhomogeneous and periodic structures and its applications to optical bistability, optic gyroscopes, nonlinear spectroscopy, radiation protection, X-ray emission and related fields
[AD-A190040] N88-22725
Optical switching and control techniques using nonlinear optical wave mixing
[AD-A190467] N88-22730

NONLINEAR PROGRAMMING
Efficient method for structural optimization N88-22240

NONLINEAR SYSTEMS
Nonlinear analysis and optimal design of dynamic mechanical systems for spacecraft application
[AD-A190644] N88-22070
Random processes, turbulence and disordering fields
[AD-A190123] N88-22303
Buckling of blast loaded cylinder
[AD-A190124] N88-22376
The analysis of non-linear dynamic behavior (including snap-through) of postbuckled plates by simple analytical solution
[NASA-TM-89165] N88-22439
Memory efficient evaluations of nonlinear stochastic equations and C3 applications
[AD-A189872] N88-22569
Nonlinear signal processing using neural networks: Prediction and system modelling
[DE88-006479] N88-22621
Numerical methods for linear and nonlinear optimization
[AD-A190029] N88-22631
Symmetry and global bifurcation in nonlinear solid mechanics
[AD-A190521] N88-22642

NONLINEARITY
Numerical methods for linear and nonlinear optimization
[AD-A190029] N88-22631
Symmetry and global bifurcation in nonlinear solid mechanics
[AD-A190521] N88-22642
Nonlinear effects in plasma wake field acceleration
[TI88-700972] N88-22734

NORMAL DENSITY FUNCTIONS
On two-stage allocation procedures for selection problems
[AD-A190766] N88-22675

NORTH AMERICA
The collection of statistics on the frequency of cloud cover over North America
[AD-A190456] N88-22495

NORTH ATLANTIC TREATY ORGANIZATION (NATO)
Anthropomorphic phantom radiation dosimetry at the NATO standard reference point at Aberdeen Proving Ground
[AD-A190508] N88-22526

NUCLEAR EXPLOSION EFFECT
Buckling of blast loaded cylinder
[AD-A190124] N88-22376

NUCLEAR EXPLOSIONS
Characteristics of seismic sources of some Asian earthquakes and Soviet underground explosions from Gauribidanur array records
[DE88-701233] N88-22472
An approximation technique for solving a system of Fredholm integral equations for asymmetric detector response functions
[AD-A190577] N88-22645

NUCLEAR FUSION
JPRS report: Science and technology. China
[JPRS-CST-87-043] N88-22233
Smoothing technique to resolve X-ray spectra in laser nuclear fusion N88-22235
Magnetic fusion energy plasma interactive and high heat flux components. Volume 5: Technical assessment of critical issues in the steady state operation of fusion confinement devices
[DE88-006920] N88-22744

NUCLEAR HEAT
Basic characteristics of heat-exchanger-type steam reformer heated by high-temperature helium gas (2). Analysis by simulation model (2)
[DE87-702962] N88-22291

NUCLEAR MAGNETIC RESONANCE
Structure of sol-gel silica
[DE88-006870] N88-22114
Fluids, gels and glasses under extreme conditions of pressure and temperature
[AD-A190655] N88-22125
NMR analysis of a fluorocarbon copolymer
[DE88-002364] N88-22170

NUCLEAR POWER PLANTS
Small and medium power reactors 1987
[TI88-701435] N88-22720

NUCLEAR POWER REACTORS
Small and medium power reactors 1987
[TI88-701435] N88-22720

NUCLEATION
Nucleation in super-saturated products
[NASA-TT-20275] N88-22134

NUCLEI (NUCLEAR PHYSICS)
Nucleation in super-saturated products
[NASA-TT-20275] N88-22134

NUMERICAL ANALYSIS
Numerical orbit propagation methods for earth artificial satellites
[INPE-4405-RPE/556] N88-22053
Nonlinear analysis and optimal design of dynamic mechanical systems for spacecraft application
[AD-A190644] N88-22070
Numerical simulation of turbulent flames using vortex methods
[AD-A189813] N88-22116
Mode 2 fracture mechanics N88-22418
Numerical solution of nonlinear algebraic equations in stiff ODE solving
[DE88-006634] N88-22622
Numerical methods for singularly perturbed differential equations with applications
[AD-A189786] N88-22628
New methods for numerical solution of one class of strongly nonlinear partial differential equations with applications
[AD-A189945] N88-22630
Numerical methods for linear and nonlinear optimization
[AD-A190029] N88-22631
Expressing mathematical subroutines constructively
[AD-A190559] N88-22644
Numerical study of unsteady viscous hypersonic blunt body flows with an impinging shock
[NASA-TM-100096] N88-22650
Approximation methods for the identification and control of distributed parameter systems
[AD-A190201] N88-22662

NUMERICAL STABILITY
Global spatial periodic solutions to the Ginzburg-Landau equations
[DE88-006424] N88-22623
Continuity of symmetric stable processes
[AD-A190324] N88-22667

NUTRITION
Dietary factors related to physical fitness
[AD-A190272] N88-22527

O

OBESITY
Prediction of physical fitness: Estimated percent body fat using body circumferences versus weight-height measures
[AD-A190233] N88-22526

OCEAN BOTTOM
A computerized investigation using the method of images to predict the sound field in a fluid wedge overlying a slow fluid half-space
[AD-A190013] N88-22704

OCEAN CURRENTS
Ocean general circulation models: Report on proceedings of a meeting of ocean and climate modelers
[DE88-005530] N88-22504
Hydrographic data from the OPTOMA (Ocean Prediction Through Observation, Modeling and Analysis) program: OPTOMA 23, 9-19 November 1986
[AD-A189868] N88-22506
The physical oceanography of the northern Baffin Bay-Nares Strait region
[AD-A190015] N88-22509
Changes in the California current system observed off northern California during July-August 1986
[AD-A190027] N88-22510
The effects of time-dependent winds and ocean eddies on ice motion in a marginal ice zone
[AD-A190105] N88-22511

OCEAN DATA ACQUISITIONS SYSTEMS
Hydrographic data from the OPTOMA (Ocean Prediction Through Observation, Modeling and Analysis) program: OPTOMA 23, 9-19 November 1986
[AD-A189868] N88-22506

OCEAN DYNAMICS
Hydrographic data from the OPTOMA (Ocean Prediction Through Observation, Modeling and Analysis) program: OPTOMA 23, 9-19 November 1986
[AD-A189868] N88-22506
The physical oceanography of the northern Baffin Bay-Nares Strait region
[AD-A190015] N88-22509

OCEAN MODELS
Ocean general circulation models: Report on proceedings of a meeting of ocean and climate modelers
[DE88-005530] N88-22504

OCEAN SURFACE
Relationship between optical transfer function and natural light field in sea or atmosphere N88-22247
Models for electromagnetic scattering from the sea at extremely low grazing angles
[AD-A190472] N88-22261
NIMBUS-7 CZCS. Coastal Zone Color Scanner imagery for selected coastal regions. North America - Europe. South America - Africa - Antarctica. Level 2 photographic product
[NASA-CR-180755] N88-22447
Derivation of consistent surface fixed fields for use in a global NWP model
[AD-A190131] N88-22475

OCEAN TEMPERATURE
The physical oceanography of the northern Baffin Bay-Nares Strait region
[AD-A190015] N88-22509

OCEANOGRAPHIC PARAMETERS
Hydrographic data from the OPTOMA (Ocean Prediction Through Observation, Modeling and Analysis) program: OPTOMA 23, 9-19 November 1986
[AD-A189868] N88-22506
The physical oceanography of the northern Baffin Bay-Nares Strait region
[AD-A190015] N88-22509

OCEANOGRAPHY
Definition and implementation study for the Varan-S radar
[CNES-CT/DRT/TIT/RL-143-T] N88-22267
Instruments for use in experimental studies of complex turbulent shear flow: Three component LDVs
[AD-A190526] N88-22312
Ocean general circulation models: Report on proceedings of a meeting of ocean and climate modelers
[DE88-005530] N88-22504
Hydrographic data from the OPTOMA (Ocean Prediction Through Observation, Modeling and Analysis) program: OPTOMA 23, 9-19 November 1986
[AD-A189868] N88-22506

OHMIC DISSIPATION
Transport simulations of ohmic ignition experiment: IGNITEX
[DE88-006055] N88-22757

ON-LINE SYSTEMS
MIG-1 on-line measuring holographic microscope
[TI88-701103] N88-22332
Argus reference manual
[AD-A190382] N88-22578
ONBOARD EQUIPMENT
Definition and implementation study for the Varan-S radar
[CNES-CT/DRT/TIT/RL-143-T] N88-22267
OPACITY
Computer program in BASIC language for computation of spectrochemical analytical data
[DE88-701229] N88-22106
OPERATING COSTS
Requirements and cost considerations for a Combined Space Nuclear Reactor Test Facility
[DE88-006763] N88-22719
OPERATING SYSTEMS (COMPUTERS)
Sigma system: Overview, prospects N88-22230
OPERATIONS RESEARCH
SEARCH: An interactive computer program for optimizing two-variable, unconstrained experiments or simulation
[AD-A190593] N88-22583
OPERATORS (MATHEMATICS)
Coding capacity of generalized additive channels
[AD-A190315] N88-22685
OPERATORS (PERSONNEL)
Extension of computer based algorithms by operator analysts
[NASA-CR-182798] N88-22575
OPTICAL BISTABILITY
Theory of interactions of intense light with nonlinear, inhomogeneous and periodic structures and its applications to optical bistability, optic gyroscopes, nonlinear spectroscopy, radiation protection, X-ray emission and related fields
[AD-A190040] N88-22725
OPTICAL COMPUTERS
Applications of optical computing to problems with symbolic computations
[AD-A189772] N88-22548
Optical Conceptual Computing and Associative Memory (OCCAM)
[AD-A190030] N88-22550
OPTICAL DATA PROCESSING
Applications of optical computing to problems with symbolic computations
[AD-A189772] N88-22548
Optical Conceptual Computing and Associative Memory (OCCAM)
[AD-A190030] N88-22550
Space-variant optical systems
[AD-A189967] N88-22724
OPTICAL EQUIPMENT
Preliminary airworthiness evaluation of the UH-60A with Advanced Digital Optical Control System (ADOCS)
[AD-A190674] N88-22030
Applications of optical computing to problems with symbolic computations
[AD-A189772] N88-22548
OPTICAL FIBERS
Hermetic coating of optical fibers
[AD-A189886] N88-22177
Clinical measurements using fiber optic sensors
[DE88-005624] N88-22731
OPTICAL FILTERS
Fundamental noise processes in a laser excited optical filter
[DE88-006460] N88-22340
Advanced programming and control techniques for complex mechanical systems
[AD-A190238] N88-22349
OPTICAL MEASUREMENT
Ray tracing optical analysis of offset solar collector for space station solar dynamic system
[NASA-TM-100853] N88-22080
OPTICAL MEASURING INSTRUMENTS
Research on certain aspects of laser diffraction particle sizing relevant to autonomous self-diagnosing instrumentation
[AD-A190220] N88-22348
OPTICAL MEMORY (DATA STORAGE)
Rapid feature extraction via the radon transform
[AD-A190032] N88-22573
OPTICAL MICROSCOPES
MIG-1 on-line measuring holographic microscope
[TI88-701103] N88-22332
OPTICAL PATHS
Applications of optical computing to problems with symbolic computations
[AD-A189772] N88-22548
OPTICAL PROPERTIES
Oxide optical coatings prepared by metal-organic vapor deposition
[DE88-006809] N88-22175
Research on stable processible conducting polymers for electronic applications
[AD-A190246] N88-22180
A 104-km unrepeatered bidirectional fiber optic demonstration link
[AD-A190282] N88-22728
Optical characterization of microcrystals
[DE88-006622] N88-22775
OPTICAL RADAR
Infrared differential absorption lidar for vapor detection
[AD-A190600] N88-22497
OPTICAL SCANNERS
Application of new technologies to DTIC document processing
[AD-A189778] N88-22823
OPTICAL SWITCHING
Theory of interactions of intense light with nonlinear, inhomogeneous and periodic structures and its applications to optical bistability, optic gyroscopes, nonlinear spectroscopy, radiation protection, X-ray emission and related fields
[AD-A190040] N88-22725
Optical switching and control techniques using nonlinear optical wave mixing
[AD-A190467] N88-22730
OPTICAL TRANSFER FUNCTION
Relationship between optical transfer function and natural light field in sea or atmosphere N88-22247
OPTICAL WAVEGUIDES
Coupled high power waveguide laser research
[AD-A189800] N88-22345
OPTICS
Computing X-ray effects in optics
[DE88-006722] N88-22732
OPTIMAL CONTROL
Advanced guidance algorithms for homing missiles with bearings-only measurements
[AD-A190435] N88-22026
Optimal control and identification of space structures
[AD-A190033] N88-22065
The adjoint process in stochastic optimal control
[AD-A189720] N88-22605
OPTIMIZATION
Unsteady aerodynamics of a Wortmann FX-63-137 wing in a fluctuating wind field
[AD-A190128] N88-22006
Nonlinear analysis and optimal design of dynamic mechanical systems for spacecraft application
[AD-A190644] N88-22070
Efficient method for structural optimization N88-22240
Optimum signal processing in distributed sensor systems
[AD-A189443] N88-22250
Structural tailoring of high-speed turbine blades (SSME/STAEBL) N88-22398
Structural tailoring of advanced turboprops N88-22400
Experimental design and structural optimization
[PB88-169255] N88-22436
SEARCH: An interactive computer program for optimizing two-variable, unconstrained experiments or simulation
[AD-A190593] N88-22583
Numerical methods for linear and nonlinear optimization
[AD-A190029] N88-22631
Lumped model generation and evaluation: Sensitivity and Lie algebraic techniques with applications to combustion
[AD-A190402] N88-22689
Dynamical optimization techniques for the calculation of electronic structure in solids
[DE88-006010] N88-22768
ORBIT CALCULATION
Numerical orbit propagation methods for earth artificial satellites
[INPE-4405-RPE/556] N88-22053
ORBIT TRANSFER VEHICLES
Orbital transfer vehicle: Concept definition and system analysis study
[NASA-CR-179315] N88-22060
ORBITAL MECHANICS
Numerical orbit propagation methods for earth artificial satellites
[INPE-4405-RPE/556] N88-22053
Spacecraft trajectories
[ISBN-2-85-428166-7] N88-22054
ORBITAL POSITION ESTIMATION
Baseline estimation from simultaneous satellite laser tracking
[NASA-CR-182750] N88-22052
ORBITS
Periodic orbits around a satellite modelled as a triaxial ellipsoid
[AD-A190592] N88-22051
ORGANIZATIONS
NASA and the challenge of ISDN: The role of satellites in an ISDN world
[NASA-CR-182749] N88-22676
ORGANOMETALLIC COMPOUNDS
The spectroscopy and reaction kinetics of coordinatively unsaturated metal carbonyls
[AD-A190533] N88-22124
ORIFICES
Describing the source created by turbulent flow over orifices and louvers
[AD-A190254] N88-22706
OSCILLATING CYLINDERS
Experimental comparison of lightning simulation techniques to CV-580 airborne lightning strike measurements
[AD-A190576] N88-22496
OSCILLATING FLOW
Oscillating airfoils: Achievements and conjectures
[AD-A190490] N88-22008
A survey of oscillating flow in Stirling engine heat exchangers
[NASA-CR-182108] N88-22322
OSCILLATIONS
Oscillation damped movement of suspended objects
[DE88-005715] N88-22433
OUTPUT
Output formatting in Apple-soft BASIC
[DE88-701413] N88-22559
Near optimal blind deconvolution
[REPT-87-016] N88-22655
OVERVOLTAGE
The influence of current stressing on the structure of Ag contacts to GaAs
[DE88-005988] N88-22771
OXIDATION
Corrosion Research Center, University of Minnesota
[DE88-006681] N88-22160
High temperature corrosion of ceramics
[DE88-006567] N88-22193
Evaluation of direct methane conversion to higher hydrocarbons and oxygenates
[DE88-003812] N88-22204
OXIDATION-REDUCTION REACTIONS
Advanced B and Al combustion kinetics over wide temperature ranges
[AD-A190752] N88-22128
Electronic and ionic transport in polymers
[AD-A190434] N88-22185
OXIDES
Thermal conductivity of oxide ceramics
[DE88-005842] N88-22169
OXYGEN ANALYZERS
Ultrasonic oxygen sensor
[AD-A189723] N88-22537
OXYGEN PLASMA
Advanced diagnostics for reacting flows
[AD-A190485] N88-22122
OXYGEN SPECTRA
Rotational structure and absorption cross sections from 300 to 190 K of the Schumann-Runge bands
[AERONOMICA-ACTA-A-318-1987] N88-22131
OXYNITRIDES
Fracture toughness of silicon nitride-silicon nitride joints bonded with oxynitride glass
[DE88-005548] N88-22172
OZONE
Assessment of crop loss from air pollutants: Meteorology-atmospheric chemistry and long range transport
[PB88-148857] N88-22448
Surface ozone and ozonesounding results from the ABLE-2B expedition to Amazonia
[INPE-4523-PRE/1275] N88-22484

P

P WAVES
Earthquakes from peninsular India: Data from the Gauribidanur seismic array
[DE88-701232] N88-22471
PACIFIC OCEAN
Physical, chemical and CTD (Conductivity/Temperature/Depth) data from the Marathon 2 expedition
[AD-A189930] N88-22507
PACKINGS (SEALS)
Study on shaft seals for potassium turbine
[EL-691] N88-22364
PANEL METHOD (FLUID DYNAMICS)
A panel method based on velocity potential to compute harmonically oscillating lift surface systems
[ETN-88-91886] N88-22290

PANELS
Postbuckling delamination of a stiffened composite panel using finite element methods
[NASA-CR-182803] N88-22098
The effective fracture toughness of aluminum at rapid heating rates
[AD-A189745] N88-22146
PARABOLIC ANTENNAS
An improved method for calculating power density in the Fresnel region of circular parabolic reflector antennas
[AD-A190569] N88-22284
PARABOLIC DIFFERENTIAL EQUATIONS
Almost-periodic solutions of nonlinear parabolic equations
[DE88-006423] N88-22618
A posterior error estimation in a finite element method for parabolic partial differential equations
[AD-A190296] N88-22636
PARALLEL COMPUTERS
An analysis of multiple grain ChIP architectures
[AD-A189942] N88-22570
Implementation and performance analysis of parallel assignment algorithms on a hypercube computer
[AD-A190678] N88-22600
Design and implementation of a parallel computer for expert system applications
[DE88-005288] N88-22601
PARALLEL PROCESSING (COMPUTERS)
Lewis Structures Technology, 1988. Volume 3: Structural Integrity Fatigue and Fracture Wind Turbines HOST
[NASA-CP-3003-VOL-3] N88-22408
Parallel memory addressing using coincident optical pulses
[AD-A189767] N88-22547
Applications of optical computing to problems with symbolic computations
[AD-A189772] N88-22548
SimPL: A simulator for parallel LISP
[AD-A189831] N88-22566
Transformations of concurrent algorithms for highly parallel systems: A one year project summary report
[AD-A190236] N88-22576
Two-dimensional graphics tools for a transputer based display board
[NASA-TM-100820] N88-22591
Logarithmically connected, repetitive computer networks and numerical applications
[DE88-006632] N88-22592
Modeling a parallel architecture for image processing
[RR-646-I] N88-22593
Simulation of fault tolerance in a hypercube arrangement of discrete processors
[AD-A189682] N88-22594
The modeling, simulation and comparison of interconnection networks for parallel processing
[AD-A190571] N88-22599
Implementation and performance analysis of parallel assignment algorithms on a hypercube computer
[AD-A190678] N88-22600
Design and implementation of a parallel computer for expert system applications
[DE88-005288] N88-22601
A direct-execution parallel architecture for the Advanced Continuous Simulation Language (ACSL)
[NASA-CR-182809] N88-22602
Synapses that compute motion
[AD-A190389] N88-22607
Study of microcomputer-based real-time programmable optical signal processor and application
[AD-A190076] N88-22726
A methodolgy, based on analytical modeling, for the design of parallel and distributed architectures for relational database query processors
[AD-A189644] N88-22825
PARALLEL PROGRAMMING
Supercomputer environment
[AD-A190633] N88-22551
MultiScheme: A parallel processing system based on MIT (Massachusetts Institute of Technology) scheme
[AD-A190383] N88-22597
PARAMETER IDENTIFICATION
Optimal control and identification of space structures
[AD-A190033] N88-22065
A survey of oscillating flow in Stirling engine heat exchangers
[NASA-CR-182108] N88-22322
Boundary shape identification problems in two-dimensional domains related to thermal testing of materials
[NASA-CR-181654] N88-22541
Consistent estimates of autoregressive parameters for autoregressive moving average models
[RR-663-I] N88-22564
PARAMETERIZATION
Modeling failures of intermittently used machines
[AD-A190298] N88-22367
Parameterization of horizontal wind velocity variability
[AD-A190107] N88-22493
PARKS
Comparative utilization of analog and digital processes in the treatment of MSS-LANDSAT data for studying the national parks of Brazil
[INPE-4011-TDL/240] N88-22456
PARTIAL DIFFERENTIAL EQUATIONS
New methods for numerical solution of one class of strongly nonlinear partial differential equations with applications
[AD-A189945] N88-22630
PARTICLE ACCELERATION
On the acceleration of electrons and positive ions in the same direction along magnetic field lines by parallel electric fields
[IRF-PREPRINT-103] N88-22488
A chemical method for achieving acceleration of macroparticles to ultrahigh velocities
[DE88-006377] N88-22695
Particle acceleration to high energies and amplification of coherent radiation by electromagnetic interactions in plasmas
[TI88-701020] N88-22737
PARTICLE BEAMS
Particle beam alignment system for single event upset-Van de Graaf experiments
[AD-A189695] N88-22721
PARTICLE DENSITY (CONCENTRATION)
Dense-spray structure and phenomena. Part 1. Turbulence/dispersed-phase interactions
[AD-A190606] N88-22315
PARTICLE SIZE DISTRIBUTION
Transient compressible flow in porous materials
[DE88-006685] N88-22324
Research on certain aspects of laser diffraction particle sizing relevant to autonomous self-diagnosing instrumentation
[AD-A190220] N88-22348
The interaction of small particles with laser beams
[AD-A190716] N88-22354
PARTICLE THEORY
Particle cosmology comes of age
[DE88-006998] N88-22844
PARTICLE TRACKS
MIG-1 on-line measuring holographic microscope
[TI88-701103] N88-22332
PARTICLES
Mechanical behaviour of particle filled thermoplastics
[PB88-169297] N88-22196
The interaction of small particles with laser beams
[AD-A190716] N88-22354
PARTITIONS (MATHEMATICS)
Life prediction modeling based on strainrange partitioning N88-22425
PASSENGER AIRCRAFT
In-service measurements of SAAB SF-340 landing gear loads
[FFA-TN-1987-48] N88-22032
PASTES
Cement paste matrix composite materials center
[AD-A188657] N88-22083
PATTERN RECOGNITION
Range image segmentation and surface parameter extraction for a mobile robot
[DE87-013877] N88-22380
Motion sickness: Quantitative, algorithmic malaise indication in real time
[AD-A189674] N88-22518
Perception of complex auditory patterns
[AD-A190218] N88-22524
Auditory perception of complex sounds
[AD-A190528] N88-22529
Auditory pattern memory: Mechanisms of tonal sequence discrimination by human observers
[AD-A190337] N88-22534
Rapid feature extraction via the radon transform
[AD-A190032] N88-22573
Multi-disciplinary techniques for understanding time-varying space-based imagery
[AD-A190711] N88-22610
Concurrent algorithms for a mobile robot vision system
[DE88-005850] N88-22614
Multivariate analysis and its application
[AD-A189983] N88-22661
Method and device for the detection and identification of a helicopter
[NASA-TT-20251] N88-22698
Study of microcomputer-based real-time programmable optical signal processor and application
[AD-A190076] N88-22726
OCR vision system, an alternative to bar code
[DE88-003761] N88-22828
PEPTIDES
Development of polymeric films with piezoelectrical properties from polypeptides; low, odd nylons; or polyureas
[AD-A190301] N88-22181
PERCEPTION
Relationship of encoding speed and memory tests to flight training performance
[AD-A190670] N88-22539
PERFORATED PLATES
Finite element simulation of perforation of aluminum plates
[DE88-002092] N88-22362
PERFORMANCE TESTS
Development of a laboratory test for multiport injector deposits: Approaches 1 and 2
[AD-A190697] N88-22203
Performance of single and multiple system AM stereo decoder receivers
[PB88-168307] N88-22265
Performance test results: AXIAL-GAP, permanent magnet compressor motor
[DE88-006857] N88-22289
UARS spacecraft recorder
[NASA-CR-180768] N88-22331
Performance evaluation of molten salt thermal storage systems
[DE87-014845] N88-22461
Prediction of physical fitness: Estimated percent body fat using body circumferences versus weight-height measures
[AD-A190233] N88-22526
Exhaustive and pseudo-exhaustive testing
[AD-A190140] N88-22574
Model-scale sound propagation experiment
[NASA-TM-100602] N88-22709
PERIODIC FUNCTIONS
Almost-periodic solutions of nonlinear parabolic equations
[DE88-006423] N88-22618
PERIPHERAL EQUIPMENT (COMPUTERS)
Microvax networked computer system
[AD-A190308] N88-22596
PERMANENT MAGNETS
A high performance inverter-fed drive system of an interior permanent magnet synchroncus machine
[DE88-006753] N88-22288
Performance test results: AXIAL-GAP, permanent magnet compressor motor
[DE88-006857] N88-22289
PERMEABILITY
Synthesis and analysis of novel polymers with potential for providing both high permeselectivity and permeability in gas separation applications
[DE88-006533] N88-22174
PERSONAL COMPUTERS
Output formatting in Apple-soft BASIC
[DE88-701413] N88-22559
Implementation of a distributed adaptive routing algorithm on the Intel iPSC (Intel Personal Super-Computer)
[AD-A189849] N88-22567
PERSONNEL
Napping and human functioning during prolonged work
[AD-A190228] N88-22525
Prediction of physical fitness: Estimated percent body fat using body circumferences versus weight-height measures
[AD-A190233] N88-22526
An evaluation of the effects of high visual taskload on the separate behaviors involved in complex monitoring performance
[AD-A190641] N88-22538
Relationship of encoding speed and memory tests to flight training performance
[AD-A190670] N88-22539
PERT
Project Monitoring Package (PMP): A package for project activity monitoring
[DE88-701234] N88-22554
PERTURBATION
Spacecraft trajectories
[ISBN-2-85-428166-7] N88-22054
Comparative analysis
[AD-A190556] N88-22313
Effect of vibrational excitation on rate parameters of atmospheric reactions
[AD-A190464] N88-22477
Numerical methods for singularly perturbed differential equations with applications
[AD-A189786] N88-22628
Density perturbations in a rotating universe
[DE87-703036] N88-22840

PERTURBATION THEORY
Finite width corrections to the Nambu action for the Nielsen-Olesen string
[DE88-006996] N88-22812
PETRI NETS
Using Colored Stochastic Petri Net (CS-PN) software for protocol specification, validation, and evaluation
[ENST-87C004] N88-22588
The Colored Stochastic Petri Net (CS-PN) software: Application to the validation and the performance evaluation of distributed systems
[ENST-87D005] N88-22589
PETROLEUM PRODUCTS
Evaluation of the acute toxicity of a synthetic polyalphaolefin-based hydraulic fluid
[AD-A190412] N88-22184
PHASE CONTROL
Determination of the commutation and angle and load response for a continuous-current, single phase controlled rectifier
[AD-A190602] N88-22285
PHASE MODULATION
Magnet strength fluctuations in the SSC (Superconducting Super Collider) lattice. Part 2: Frequency modulation
[DE88-006491] N88-22774
PHASE SHIFT
Determination of the commutation and angle and load response for a continuous-current, single phase controlled rectifier
[AD-A190602] N88-22285
Near optimal blind deconvolution
[REPT-87-016] N88-22655
PHASE SHIFT CIRCUITS
Monolithic phase shifter study
[AD-A190213] N88-22278
PHASE SHIFT KEYING
Direct bit detection receiver noise performance analysis for 32-PSK and 64-PSK modulated signals
[AD-A190009] N88-22256
The 2 FSK/QPSK (Frequency Shift Keying/Quadrature Phase Shift Keying) transmitter and receiver: Design and performance
[AD-A190028] N88-22258
PHASE TRANSFORMATIONS
Thermal analysis of heat storage canisters for a solar dynamic, space power system
[DE88-004199] N88-22075
Directed-energy electron-beam processing of a hypoeutectic Cr90Ta10 alloy
[DE88-005821] N88-22157
Transformation toughening of ceramics
[AD-A190399] N88-22183
Synthesis of metastable superconductors by high dynamic pressure
[DE88-005620] N88-22764
Superconductivity and the tailoring of lattice parameters of the compound YBa2Cu3O(sub x)
[DE88-005904] N88-22769
An investigation of the crystalchemistry and thermochemistry of selected mineral systems
[AD-A189758] N88-22781
Remarks on solid state amorphizing transformations
[DE88-006452] N88-22803
PHOBOS
Periodic orbits around a satellite modelled as a triaxial ellipsoid
[AD-A190592] N88-22051
PHOSPHORUS POLYMERS
New phosphorus based polymer systems
[AD-A190457] N88-22186
PHOTOACOUSTIC SPECTROSCOPY
A laser-based photoacoustic spectrometer for direct breath C-13O2/C-12O2 measurement
[DE88-004915] N88-22516
PHOTOCATHODES
Stellar scintillometer atmospheric optical turbulence profiling experiment: A qualitative comparison of two identical instruments at AMOS (Air Force Maui Optical Station), 1985
[AD-A190589] N88-22479
PHOTOCHEMICAL REACTIONS
Hard ceramic film by laser PVD N88-22218
PHOTOCONDUCTORS
Infrared-sensitive spatial light modulator
[AD-A190391] N88-22729
PHOTODIODES
A 104-km unrepeatered bidirectional fiber optic demonstration link
[AD-A190262] N88-22726
PHOTOELECTROCHEMISTRY
Corrosion Research Center, University of Minnesota
[DE88-006661] N88-22160
PHOTOELECTRON SPECTROSCOPY
Laser photoelectron spectroscopy of ions
[DE88-006860] N88-22113
PHOTOGRAMMETRY
Relative orientation
[AD-A190385] N88-22449
PHOTOINTERPRETATION
Comparative utilization of analog and digital processes in the treatment of MSS-LANDSAT data for studying the national parks of Brazil
[INPE-4011-TDL/240] N88-22456
PHOTOLUMINESCENCE
Singlet oxygen behavior in solid polymer matrices
[DE88-005171] N88-22171
PHOTOMETRY
Speckle interferometry of asteroids
[NASA-CR-180438] N88-22843
PHOTONS
Cosmology for high energy physicists
[DE86-005705] N88-22842
PHOTORECEPTORS
Laboratory equipment update
[AD-A189781] N88-22522
PHOTOVOLTAIC CELLS
Recent advances in photovoltaic concentrator technology
[DE88-003948] N88-22462
PHOTOVOLTAIC CONVERSION
Today's photovoltaic systems: An evaluation of their performance
[DE88-006926] N88-22457
PHYSICAL FITNESS
Prediction of physical fitness: Estimated percent body fat using body circumferences versus weight-height measures
[AD-A190233] N88-22526
Dietary factors related to physical fitness
[AD-A190272] N88-22527
PHYSIOLOGICAL EFFECTS
Protection against laser damage to human body reviewed N88-22237
A comparison of visual evoked potential and behavioral measures of flashblindness in humans
[AD-A189757] N88-22519
Age, alcohol, and simulated altitude: Effects on performance and breathalyzer scores
[AD-A190642] N88-22531
PHYSIOLOGICAL RESPONSES
A program for the study of skeletal muscle catabolism following physical trauma
[AD-A189771] N88-22521
Complex sound processing: An interdisciplinary approach
[AD-A189782] N88-22523
PIEZOELECTRICITY
Development of polymeric films with piezoelectrical properties from polypeptides; low, odd nylons; or polyureas
[AD-A190301] N88-22181
PILOT PERFORMANCE
Aircraft accident report: North Star Aviation, Inc., PA-32 RT-300, N39614 and Alameda Aero Club Cessna 172, N75584, Oakland, California, March 31, 1987
[PB87-910412] N88-22021
Relationship of encoding speed and memory tests to flight training performance
[AD-A190670] N88-22539
PILOT TRAINING
Relationship of encoding speed and memory tests to flight training performance
[AD-A190670] N88-22539
PINCH EFFECT
Improvement of plasma confinement due to electron Landau damping in tokamaks
[DE88-752339] N88-22747
PINHOLES
Particle beam alignment system for single event upset-Van de Graaf experiments
[AD-A189695] N88-22721
PIPE FLOW
Experiments on densely-loaded non-Newtonian slurries in laminar and turbulent pipe flows
[DE88-006209] N88-22323
Piston-driven, unsteady separation at a sudden expansion in a tube: Flow visualization and Laser Doppler Anemometer (LDA) measurements
[ETN-88-92104] N88-22329
PIPELINING (COMPUTERS)
Multiple-transform pipelines for image coding
[REPT-87-038] N88-22561
PISTONS
Piston-driven, unsteady separation at a sudden expansion in a tube: Flow visualization and Laser Doppler Anemometer (LDA) measurements
[ETN-88-92104] N88-22329
PITCH (INCLINATION)
Degradation of downlink distance measurement indexes by the addition of a third tone --- tone ranging
[CNES-CT/DRT/TIT/TR-122-T] N88-22268
PLANETARY ORBITS
The 1985 mutual phenomena of Jupiter's satellites observed in Brazil
[INPE-4526-PRE/1276] N88-22848
PLASMA ACCELERATION
Nonlinear effects in plasma wake field acceleration
[TI88-700972] N88-22734
PLASMA BUBBLES
In-situ plasma bubble observations associated with equatorial spread-F over Natal
[INPE-4488-PRE/1252] N88-22482
PLASMA CONTROL
New methods of confinement and heating of plasma in magnetic fields
[TI88-701021] N88-22738
Long-time impurity confinement as a precursor to disruptions in ohmically heated tokamaks
[DE88-006183] N88-22742
Improvement of plasma confinement due to electron Landau damping in tokamaks
[DE88-752339] N88-22747
Transport simulations of ohmic ignition experiment: IGNITEX
[DE88-006055] N88-22757
PLASMA CURRENTS
Structural consequences of railgun augmentation
[DE88-007036] N88-22058
PLASMA DENSITY
Long-time impurity confinement as a precursor to disruptions in ohmically heated tokamaks
[DE88-006183] N88-22742
PLASMA DIAGNOSTICS
Advanced diagnostics for reacting flows
[AD-A190485] N88-22122
High-voltage inverse-square function generator
[DE88-701109] N88-22270
The development of high power KrF laser systems for plasma research by the application of stimulated Raman scattering
[ETN-88-92220] N88-22358
PLASMA DRIFT
Improvement of plasma confinement due to electron Landau damping in tokamaks
[DE88-752339] N88-22747
PLASMA ELECTRODES
Fundamental studies on MPD thrusters
[AD-A190307] N88-22753
PLASMA ENGINES
Fundamental studies on MPD thrusters
[AD-A190307] N88-22753
Physical fluid mechanics in MPD thrusters
[AD-A190309] N88-22754
Plasma-gas interaction studies in a hybrid plume plasma rocket
[AD-A190310] N88-22755
MPD (magnetoplasmadynamic) thruster advanced pumping system concepts
[AD-A190513] N88-22756
PLASMA EQUILIBRIUM
Nonlinear effects in plasma wake field acceleration
[TI88-700972] N88-22734
PLASMA GENERATORS
Vacuum-arc plasma centrifuge experiment
[INPE-4509-PRE/1263] N88-22758
PLASMA HEATING
New methods of confinement and heating of plasma in magnetic fields
[TI88-701021] N88-22738
Heating and confinement studies of electron cyclotron resonance heated plasmas in Heliotron E
[DE88-752312] N88-22746
Theoretical studies of the heating of toroidal plasmas with radiofrequency electromagnetic radiation
[DE88-006913] N88-22749
Plasma-gas interaction studies in a hybrid plume plasma rocket
[AD-A190310] N88-22755
PLASMA INTERACTIONS
High power, high frequency radiation from beam-plasma interactions
[AD-A190207] N88-22752
Fundamental studies on MPD thrusters
[AD-A190307] N88-22753
PLASMA JETS
Structural consequences of railgun augmentation
[DE88-007036] N88-22058
Vacuum-arc plasma centrifuge experiment
[INPE-4509-PRE/1263] N88-22758
PLASMA PHYSICS
Magic light high-power laser passes state certification N88-22236
Theoretical model of the cathode spot on a unipolar arc
[AD-A190109] N88-22277
Plasmapause formation
[AERONOMICA-ACTA-A-319-1987] N88-22759

PLASMA PROPULSION
Fundamental studies on MPD thrusters
[AD-A190307] N88-22753
Physical fluid mechanics in MPD thrusters
[AD-A190309] N88-22754
Plasma-gas interaction studies in a hybrid plume plasma rocket
[AD-A190310] N88-22755
PLASMA RADIATION
High power, high frequency radiation from beam-plasma interactions
[AD-A190207] N88-22752
PLASMA RESONANCE
Parametric instabilities of inhomogeneous plasma near the lower-hybrid resonance
[TI88-701201] N88-22748
PLASMA SPRAYING
Corrosion Research Center, University of Minnesota
[DE88-006681] N88-22160
PLASMA WAVES
Wave energy flow conservation for propagation in inhomogeneous Vlasov-Maxwell equilibria
[DE88-006705] N88-22251
Nonlinear effects in plasma wake field acceleration
[TI88-700972] N88-22734
Plasma wave radiative damping of a new type in a relativistic one-dimensional plasma
[TI88-701191] N88-22739
Parametric instabilities of inhomogeneous plasma near the lower-hybrid resonance
[TI88-701201] N88-22748
PLASMA-ELECTROMAGNETIC INTERACTION
Coordinated Auroral Experiments using Scatter And Rocket investigations (CAESAR investigations)
[MPAE-W-47-87-13] N88-22487
PLASMAPAUSE
Plasmapause formation
[AERONOMICA-ACTA-A-319-1987] N88-22759
PLASMAS (PHYSICS)
Analytic solutions to dynamic equations of plasma armature railguns
[DE88-006842] N88-22057
Analysis of anomalous resistivity during the conduction phase of the plasma erosion opening switch
[DE88-006382] N88-22286
Magnetic fusion energy plasma interactive and high heat flux components. Volume 5: Technical assessment of critical issues in the steady state operation of fusion confinement devices
[DE88-006920] N88-22744
PLASTIC DEFORMATION
Finite element (MARC) solution technologies for viscoplastic analyses N88-22389
Phenomenological modelling of rate-dependent plasticity for high strain rate problems
[DE88-006647] N88-22440
PLASTIC FLOW
Elasto-plastic analysis using a stress-based finite element method and an endochronic theory of plasticity
[DE88-003001] N88-22372
PLASTIC PROPELLANTS
Effect of moisture level in PBXW-109(E) (plastic-bonded explosive) mixes on the aging of the cured explosive
[AD-A190200] N88-22202
PLASTIC PROPERTIES
Microplasticity phenomena in graphite/magnesium metal matrix composites
[DE88-006772] N88-22086
Elasto-plastic analysis using a stress-based finite element method and an endochronic theory of plasticity
[DE88-003001] N88-22372
Measurement of the elastic-plastic surface flaw back surface topology and its relation to constraint
[DE88-006765] N88-22437
PLASTICS
Solid hosts for dye laser rods. Part 1: Criteria for choosing a host material
[DE88-006478] N88-22355
PLATE THEORY
An efficient Mindlin finite strip plate element based on assumed strain distribution N88-22407
PLATES
The analysis of non-linear dynamic behavior (including snap-through) of postbuckled plates by simple analytical solution
[NASA-TM-89165] N88-22439
Stress-intensity factors for small surface and corner cracks in plates
[NASA-TM-100599] N88-22445
PLATING
Durability testing of an iridium-plated storable rocket engine injector
[AD-A190707] N88-22076
Determination of aquo-complexes of chromium and iron in chromium plating and polishing solutions by ion chromatography
[AD-A190168] N88-22148
PLOTTING
Physical, chemical and CTD (Conductivity/Temperature/Depth) data from the Marathon 2 expedition
[AD-A189930] N88-22507
PLUMES
Split-coefficient matrix solution and experimental study of axisymmetric underexpanded exhaust plumes N88-22242
Plasma-gas interaction studies in a hybrid plume plasma rocket
[AD-A190310] N88-22755
POISSON DENSITY FUNCTIONS
Extreme value for dependent sequences via the Stein-Chen method of poisson approximation
[AD-A190325] N88-22668
POLICIES
JPRS report: Science and technology. Japan
[JPRS-JST-87-029] N88-22228
POLISHING
Determination of aquo-complexes of chromium and iron in chromium plating and polishing solutions by ion chromatography
[AD-A190168] N88-22148
POLLUTION MONITORING
Feasibility study for a 2nd generation system for airborne maritime pollution surveillance
[ETN-88-92108] N88-22466
POLLUTION TRANSPORT
Assessment of crop loss from air pollutants: Meteorology-atmospheric chemistry and long range transport
[PB88-146857] N88-22448
POLYAMIDE RESINS
Development of polymeric films with piezoelectrical properties from polypeptides; low, odd nylons; or polyureas
[AD-A190301] N88-22181
POLYCRYSTALS
Strength and microstructure of ceramics
[AD-A190712] N88-22191
POLYIMIDE RESINS
Fabrication and electrical characterization of multilevel aluminum interconnects used to achieve silicon-hybrid wafer-scale integration
[AD-A190519] N88-22282
POLYIMIDES
Vapor phase deposition and growth of polyimide films on copper
[AD-A189969] N88-22178
POLYMER CHEMISTRY
Molecular dynamics of materials possessing high energy content
[AD-A190034] N88-22118
Donor acceptor polymerization chemistry as a vehicle to low energy cure matrix resins
[AD-A190119] N88-22179
Research on stable processible conducting polymers for electronic applications
[AD-A190246] N88-22180
POLYMER MATRIX COMPOSITES
Singlet oxygen behavior in solid polymer matrices
[DE88-005171] N88-22171
Nondestructive evaluation by acousto-ultrasonics N88-22412
POLYMERIC FILMS
Research on stable processible conducting polymers for electronic applications
[AD-A190246] N88-22180
Development of polymeric films with piezoelectrical properties from polypeptides; low, odd nylons; or polyureas
[AD-A190301] N88-22181
POLYMERIZATION
Donor acceptor polymerization chemistry as a vehicle to low energy cure matrix resins
[AD-A190119] N88-22179
High-performance polymeric materials
[AD-A190706] N88-22190
POLYPEPTIDES
Development of polymeric films with piezoelectrical properties from polypeptides; low, odd nylons; or polyureas
[AD-A190301] N88-22181
POPULATION THEORY
Empirical and hierarchical Bayes competitors of preliminary test estimators in two sample problems
[AD-A190327] N88-22670
POPULATIONS
On two-stage allocation procedures for selection problems
[AD-A190766] N88-22675
POROUS MATERIALS
Molecular dynamics of materials possessing high energy content
[AD-A190034] N88-22118
Transient compressible flow in porous materials
[DE88-006685] N88-22324
POSITION (LOCATION)
Real-time environmental Arctic monitoring (R-TEAM)
[AD-A189948] N88-22508
Target localization in an inhomogeneous medium
[AD-A190008] N88-22703
POSITIVE IONS
On the acceleration of electrons and positive ions in the same direction along magnetic field lines by parallel electric fields
[IRF-PREPRINT-103] N88-22488
POSITRONS
Variable-energy positron studies on liquids and liquid-solid interfaces
[DE88-006356] N88-22109
Annihilation momentum density of positrons trapped at vacancy-type defects in metals and alloys
[DE88-005936] N88-22797
POTASSIUM
Alkali metal diffuse band lasers
[AD-A190244] N88-22350
Study on shaft seals for potassium turbine
[EL-891] N88-22364
POTENTIAL ENERGY
Molecular reaction and energy transfer rate estimation for chemical-laser analysis
[AD-A190664] N88-22126
POTENTIAL FLOW
A physically consistent model for artificial dissipation in transonic potential flow computations
[NASA-TM-100646] N88-22652
POTENTIAL THEORY
Use of long-distance pair potentials in calculations of defect characteristics in metals
[TI88-701039] N88-22138
A panel method based on velocity potential to compute harmonically oscillating lift surface systems
[ETN-88-91886] N88-22290
POWDER METALLURGY
Processing, microstructure, and mechanical properties of silicon carbide particulate reinforced aluminum alloys
[AD-A188981] N88-22136
Characterization of an explosively consolidated rapidly solidified Fe-16Ni-9Cr-5Mo-2Cu alloy powder
[DE88-006733] N88-22162
Gamma-ray densitometry: Nondestructive analysis of density evolution during ceramic powder processing
[DE88-006671] N88-22198
POWDERED ALUMINUM
Advanced B and Al combustion kinetics over wide temperature ranges
[AD-A190752] N88-22128
POWER AMPLIFIERS
Application of copper-carbon fiber composites to power semiconductor devices
[NASA-TT-20171] N88-22101
PRECESSION
Spin precession in stationary gravitational fields
[TI88-701107] N88-22470
PRECIPITATION (METEOROLOGY)
Tropical circulations and the associated rainfall anomalies during two contrasting years
[INPE-4506-PRE/1261-REV] N88-22502
PRECIPITATION HARDENING
The age hardening response of thermomechanically processed Al-Mg-Li alloys
[AD-A189870] N88-22147
PREDICTION ANALYSIS TECHNIQUES
Investigation of boundary layer disturbances caused by periodic heating of a thin ribbon
[AD-A190572] N88-22314
Whisker-reinforced ceramic composites for heat engine components N88-22410
Fracture technology for brittle materials N88-22417
Grain boundary oxidation and low-cycle fatigue at elevated temperatures N88-22420
Cumulative fatigue damage models N88-22422
Life prediction modeling based on strainrange partitioning N88-22425
Life prediction modeling based on cyclic damage accumulation N88-22426
Fatigue damage modeling for coated single crystal superalloys N88-22427
Life and reliability of rotating disks N88-22428
Review and assessment of the HOST turbine heat transfer program N88-22431
The existence of smooth densities for the prediction filtering and smoothing problems
[AD-A189865] N88-22629

PREDICTIONS
Flexiwall 3 SO: A second order predictive strategy for rapid wall adjustment in two-dimensional compressible flow
[NASA-CR-181662] N88-22018
Forecast of Atlantic seasonal hurricane activity for 1988 N88-22500
The existence of smooth densities for the prediction filtering and smoothing problems
[AD-A189865] N88-22629
PREPARATION
Specimen preparation techniques for the examination of ceramic and metal-matrix composites
[DE88-005157] N88-22094
PRESIDENTIAL REPORTS
Space shuttle accident: NASA's actions to address the Presidential Commission report
[PB88-135306] N88-22059
PRESSURE
Monthly mean global climatology of temperature, wind, geopotential height, and pressure for 0 - 120 km
[NASA-TM-100697] N88-22503
Absolute pressure derivatives of deep level defects in 3-5 semiconductors
[DE88-006318] N88-22772
PRESSURE DISTRIBUTION
High Reynolds number, low Mach number, steady flow field calculations over a NACA 0012 airfoil using Navier-Stokes and interactive boundary layer theory
[AD-A189871] N88-22005
Contraction design for small low-speed wind tunnels
[NASA-CR-182747] N88-22045
Structural consequences of railgun augmentation
[DE88-007036] N88-22058
Investigation of side-wall effects in wind tunnel with supercritical airfoil testing N88-22241
Aerothermal tests of quilted dome models on a flat plate at a Mach number of 6.5
[NASA-TP-2804] N88-22325
PRESSURE EFFECTS
Modifications to the Langley 8-foot transonic pressure tunnel for the laminar flow control experiment
[NASA-TM-4032] N88-22047
PRESSURE GRADIENTS
An experimental investigation of rocket ramjet nozzle assembly base pressures
[AD-A189714] N88-22076
ALEX results: A comparison of measurements from a round and a rectangular duct with 3-D code predictions
[DE88-005947] N88-22741
PRESSURE OSCILLATIONS
Pressure measurements of impinging jet with asymmetric nozzle
[NASA-CR-182759] N88-22011
PRESSURE SENSORS
A 150,000 pounds per square inch dynamic pressure calibrator
[AD-A190659] N88-22335
PRESSURE SUITS
Design, development and evaluation of Stanford/Ames EVA prehensors
[NASA-CR-182688] N88-22540
PRIMERS (EXPLOSIVES)
Stability of the high-temperature G-16 primer composition
[DE88-006201] N88-22206
PRINTED CIRCUITS
Fabrication and electrical characterization of multilevel aluminum interconnects used to achieve silicon-hybrid wafer-scale integration
[AD-A190519] N88-22282
PRINTERS (DATA PROCESSING)
Microvax networked computer system
[AD-A190308] N88-22506
PRINTING
Synthesis and characterization of high-T(sub c) screen-printed Y-Ba-Cu-O films on alumina
[NASA-TM-100860] N88-22805
PROBABILITY DENSITY FUNCTIONS
Filtering of jump processes
[AD-A189701] N88-22656
PROBABILITY DISTRIBUTION FUNCTIONS
Advanced probabilistic methods for quantifying the effects of various uncertainties in structural response N88-22401
Memory efficient evaluations of nonlinear stochastic equations and C3 applications
[AD-A189872] N88-22569
Some comments on quadrant dependence in higher dimensions
[AD-A190329] N88-22639
Structural decomposition of multiple time scale Markov processes
[AD-A189739] N88-22657
PROBABILITY THEORY
Multiple model parameter adaptive control for in-flight simulation
[AD-A190568] N88-22044
Probabilistic structural analysis computer code (NESSUS) N88-22397
A probabilistic approach to low-level vision
[AD-A189041] N88-22553
Mathematics clinic probabilistic position-fixing
[NASA-CR-182753] N88-22672
PROBLEM SOLVING
Comparative analysis
[AD-A190556] N88-22313
A zonal approach for the solution of coupled Euler and potential solutions of flows with complex geometries
[AD-A189752] N88-22595
Numerical solution of nonlinear algebraic equations in stiff ODE solving
[DE88-006634] N88-22622
About disequations simplification
[RR-645-I-IMAG-55-LIFIA] N88-22624
Admissible Bayes tests for structural relationship
[AD-A190326] N88-22669
PROCEDURES
Software verification using partition analysis
[AD-A190570] N88-22582
PROCESS CONTROL (INDUSTRY)
Measurement of emissivity of industrial surfaces using a simple method
[NASA-TT-20165] N88-22130
Application and technology requirements for heat pumps at the process industries
[DE88-006740] N88-22293
A fault tolerant supervision system
[INPE-4419-TDL/307] N88-22819
Information systems for quality. Experience at the Nerviano Aeritalia plant. Avionic systems and equipment group
[ETN-88-92274] N88-22821
PRODUCT DEVELOPMENT
French Multiproject Chip (MPC) activity report, 1986
[RR-650-I] N88-22273
PROGRAM VERIFICATION (COMPUTERS)
Ada (Trademark) compiler validation summary report. ALSYS: AlsyCOMP-013, V2.0 HOST: IBM PC AT. Target: IBM 370 3084Q
[AD-A189640] N88-22546
Software verification using partition analysis
[AD-A190570] N88-22582
The Colored Stochastic Petri Net (CS-PN) software: Application to the validation and the performance evaluation of distributed systems
[ENST-87D005] N88-22589
An approximation technique for solving a system of Fredholm integral equations for asymmetric detector response functions
[AD-A190577] N88-22645
PROGRAMMING LANGUAGES
Geometric modeling of flight information for graphical cockpit display
[AD-A190484] N88-22043
Output formatting in Apple-soft BASIC
[DE88-701413] N88-22559
A UNIX-based interactive VHDL (hardware description language) simulator
[AD-A189749] N88-22565
Tutorial on GAMS (Generalized Algebraic Modeling System): A modeling language for optimization
[AD-A189867] N88-22568
Argus reference manual
[AD-A190382] N88-22578
Software structuring principles for VLSI CAD
[AD-A190386] N88-22579
A direct-execution parallel architecture for the Advanced Continuous Simulation Language (ACSL)
[NASA-CR-182809] N88-22602
PROJECT MANAGEMENT
Engineering support of space shuttle experiment integration
[AD-A190135] N88-22061
Project Monitoring Package (PMP): A package for project activity monitoring
[DE88-701234] N88-22554
PROJECT PLANNING
Engineering support of space shuttle experiment integration
[AD-A190135] N88-22061
PROJECTILES
Continuous measurements of in-bore projectile velocity
[DE88-006841] N88-22056
Fluid motion in a spinning, coning cylinder via spatial eigenfunction expansion
[AD-A190758] N88-22319
PROPAGATION VELOCITY
Numerical and experimental research on propagation of elastic stress waves in conical shell under axial impulsive loading N88-22238
PROPELLANT GRAINS
Crack opening and extension in inert solid propellant. An experimental study
[AD-A189808] N88-22201
PROPELLERS
Porous wind tunnel corrections for counterrotation propeller testing
[NASA-TM-100873] N88-22019
PROPULSION
Research as part of the Air Force in aero propulsion technology (AFRAPT) program
[AD-A190336] N88-22036
AFRAPT (Air Force Research in Aero Propulsion Technology) trainee program
[AD-A190525] N88-22123
PROPULSION SYSTEM CONFIGURATIONS
Research and technology
[NASA-TM-100172] N88-22851
PROTECTION
Solar cell cover glasses for satellites N88-22225
Study of lightning and lightning protection (selected pages)
[AD-A190623] N88-22498
PROTECTIVE COATINGS
Structure and properties of titanium nitride and zirconium nitride thin films prepared by reactive ion plating — cutting tools
[ETN-88-92218] N88-22167
Investigation of laser diagnostics of PACVD processes for depositing hard face coatings
[DE88-007083] N88-22176
The corrosion resistance of an aluminum alloy coated with polysilazane derived ceramics
[AD-A190703] N88-22189
PROTEINS
Studies of molecular biology
[DE88-005906] N88-22514
PROTOCOL (COMPUTERS)
Using Colored Stochastic Petri Net (CS-PN) software for protocol specification, validation, and evaluation
[ENST-87C004] N88-22588
PROVING
Software verification using partition analysis
[AD-A190570] N88-22582
PSYCHOACOUSTICS
Mechanisms mediating perception of complex acoustic patterns
[AD-A189765] N88-22520
On categorizing sounds
[AD-A189784] N88-22700
PSYCHOLOGICAL FACTORS
On categorizing sounds
[AD-A189784] N88-22700
PSYCHOLOGICAL TESTS
Properties of some Bayesian scoring procedures for computerized adaptive tests
[AD-A189925] N88-22680
PSYCHOPHYSICS
Complex sound processing: An interdisciplinary approach
[AD-A189782] N88-22523
Finding texture boundaries in images
[AD-A190554] N88-22609
PULSE COMMUNICATION
High speed, bandpass sampling of digital communications waveforms
[AD-A189842] N88-22254
PULSE GENERATORS
High-voltage inverse-square function generator
[DE88-701109] N88-22270
PULSED LASERS
A preliminary comparison of the transient effects of single versus multiple q-switched doubled-neodymium laser pulses
[AD-A189855] N88-22347
Program to research laser-driven thermionic electron sources for free electron lasers
[AD-A190473] N88-22353
PYROTECHNICS
Stability of the high-temperature G-16 primer composition
[DE88-006201] N88-22206

Q

QUADRANTS
Some comments on quadrant dependence in higher dimensions
[AD-A190329] N88-22639

QUADRATIC EQUATIONS
Distributions of quadratic forms
[AD-A190224] N88-22663
QUADRATIC PROGRAMMING
Sufficient matrices and the linear complementarity problem
[AD-A190429] N88-22690
QUALITY CONTROL
Information systems for quality. Experience at the Nerviano Aeritalia plant. Avionic systems and equipment group
[ETN-88-92274] N88-22821
QUANTITATIVE ANALYSIS
Computer program in BASIC language for computation of spectrochemical analytical data
[DE88-701229] N88-22106
Clinical measurements using fiber optic sensors
[DE88-005624] N88-22731
QUANTUM CHROMODYNAMICS
Lattice QCD calculation of K yields pi nonleptonic weak transition and other hadronic weak parameters
[PREPRINT-580] N88-22717
QUANTUM ELECTRODYNAMICS
Quantization of axial electrodynamics
[TI88-701498] N88-22813
QUANTUM ELECTRONICS
Theory of interactions of intense light with nonlinear, inhomogeneous and periodic structures and its applications to optical bistability, optic gyroscopes, nonlinear spectroscopy, radiation protection, X-ray emission and related fields
[AD-A190040] N88-22725
QUANTUM MECHANICS
Singular Lagrangians. Classical dynamics and quantization. Lectures for young scientists
[TI88-701158] N88-22806
QUANTUM THEORY
Super Virasoro algebra and solvable supersymmetric quantum field theories
[DE88-752299] N88-22681
To the field theory with a fundamental mass
[TI88-701159] N88-22807
QUANTUM WELLS
Research on materials and components for opto-electronic signal processing and computing
[AD-A190130] N88-22788

R

RADAR
Modification of the BLUEMAX 2 terrain following model to incorporate radar detection
[AD-A190594] N88-22028
High speed transcendental elementary function architecture in support of the Vector Wave Equation (VWE)
[AD-A189746] N88-22627
RADAR CROSS SECTIONS
Modification of the BLUEMAX 2 terrain following model to incorporate radar detection
[AD-A190594] N88-22028
High speed transcendental elementary function architecture in support of the Vector Wave Equation (VWE)
[AD-A189746] N88-22627
RADAR DETECTION
Modification of the BLUEMAX 2 terrain following model to incorporate radar detection
[AD-A190594] N88-22028
RADAR MAPS
Geometric restoration of satellite image data
[AD-A190462] N88-22450
RADAR TRACKING
Modification of the BLUEMAX 2 terrain following model to incorporate radar detection
[AD-A190594] N88-22028
Polarimetric ISAR imaging using either measured or calculated transient signatures
[AD-A190077] N88-22259
RADIAL VELOCITY
New measurements of radial velocities in clusters of galaxies
[INPE-4527-PRE/1277] N88-22845
RADIANCE
Relationship between optical transfer function and natural light field in sea or atmosphere N88-22247
Calibration and processing of AVHRR data for temperature estimation
[INPE-4493-PRE/1257] N88-22485
RADIATION DETECTORS
An approximation technique for solving a system of Fredholm integral equations for asymmetric detector response functions
[AD-A190577] N88-22645
RADIATION DOSAGE
Anthropomorphic phantom radiation dosimetry at the NATO standard reference point at Aberdeen Proving Ground
[AD-A190508] N88-22528
RADIATION EFFECTS
Laser enhanced adhesion of copper films to sapphire substrates
[DE88-006802] N88-22144
The effective fracture toughness of aluminum at rapid heating rates
[AD-A189745] N88-22146
Oxide optical coatings prepared by metal-organic vapor deposition
[DE88-006809] N88-22175
A preliminary comparison of the transient effects of single versus multiple q-switched doubled-neodymium laser pulses
[AD-A189855] N88-22347
High-efficiency thin-film silicon-on-GaP solar cell for improved radiation resistance
[AD-A190268] N88-22460
Characterization of space radiation environment in terms of the energy deposition in functionally important volumes
[DE88-005627] N88-22513
A comparison of visual evoked potential and behavioral measures of flashblindness in humans
[AD-A189757] N88-22519
Computing X-ray effects in optics
[DE88-006722] N88-22732
RADIATION MEASUREMENT
An approximation technique for solving a system of Fredholm integral equations for asymmetric detector response functions
[AD-A190577] N88-22645
RADIATION PROTECTION
Theory of interactions of intense light with nonlinear, inhomogeneous and periodic structures and its applications to optical bistability, optic gyroscopes, nonlinear spectroscopy, radiation protection, X-ray emission and related fields
[AD-A190040] N88-22725
RADIATION SHIELDING
Anthropomorphic phantom radiation dosimetry at the NATO standard reference point at Aberdeen Proving Ground
[AD-A190508] N88-22528
RADIATION TOLERANCE
High-efficiency thin-film silicon-on-GaP solar cell for improved radiation resistance
[AD-A190268] N88-22460
RADIATION TRANSPORT
Multigroup flux-limited asymptotic diffusion Fokker-Planck equation
[DE88-700958] N88-22615
RADIATIVE HEAT TRANSFER
The thermal radiative properties of metals at high temperature
[DE88-006625] N88-22141
RADIO FREQUENCIES
Theoretical studies of the heating of toroidal plasmas with radiofrequency electromagnetic radiation
[DE88-006913] N88-22749
RF properties of superconducting Pb electroplated onto Cu
[DE88-005918] N88-22765
RADIOGRAPHY
Characterization of sintered SiC by using NDE N88-22413
RADIOMETERS
Investigation into the development of computer aided design software for space based sensors
[NASA-CR-180772] N88-22552
RADIOMETRIC RESOLUTION
Method for restoration and resampling of TM sensor imagery
[INPE-4491-PRE/1255] N88-22454
RADON
Rapid feature extraction via the radon transform
[AD-A190032] N88-22573
RADON ISOTOPES
Radon-222 in the Antarctic Peninsula
[INPE-4486-PRE/1251] N88-22468
RAILGUN ACCELERATORS
Analytic solutions to dynamic equations of plasma armature railguns
[DE88-006842] N88-22057
Structural consequences of railgun augmentation
[DE88-007036] N88-22058
RAIN
The growth potential of corona discharges from aircraft flying in precipitation
[AD-A190507] N88-22478
RAMAN LASERS
Theoretical studies of Resonance Enhanced Stimulated Raman Scattering (RESRS) of frequency-doubled Alexandrite laser wavelength in cesium vapor
[NASA-CR-182870] N88-22133
RAMAN SPECTRA
Theoretical studies of Resonance Enhanced Stimulated Raman Scattering (RESRS) of frequency-doubled Alexandrite laser wavelength in cesium vapor
[NASA-CR-182870] N88-22133
The development of high power KrF laser systems for plasma research by the application of stimulated Raman scattering
[ETN-88-92220] N88-22358
Amplification of signals in fiber optics using the stimulated Raman effect
[AD-A190281] N88-22727
RAMJET ENGINES
An experimental investigation of rocket ramjet nozzle assembly base pressures
[AD-A189714] N88-22076
RAMJET MISSILES
An experimental investigation of rocket ramjet nozzle assembly base pressures
[AD-A189714] N88-22076
RANDOM ACCESS MEMORY
Self-checking logic arrays
[RR-656-I] N88-22545
RANDOM NOISE
Information and coding capacities of mismatched Gaussian channels
[AD-A190321] N88-22665
Conditions for information capacity of the discrete-time Gaussian channel to be increased by feedback
[AD-A190317] N88-22687
Coding capacity of discrete-time Gaussian and nonGaussian channels
[AD-A190318] N88-22688
RANDOM PROCESSES
Thermal expansion behavior of randomly oriented short carbon fiber reinforced copper composites
[NASA-TT-20175] N88-22099
Random processes, turbulence and disordering fields
[AD-A190123] N88-22303
Random Process Simulation for stochastic fatigue analysis
[NASA-TM-100464] N88-22654
RANDOM VARIABLES
Stopping rules and observed significance levels
[AD-A190320] N88-22664
RANDOM VIBRATION
The concept of an impact resonance diagram for characterizing the nonlinear response of impact vibration
[DE88-005475] N88-22432
RANGE (EXTREMES)
MultiScheme: A parallel processing system based on MIT (Massachusetts Institute of Technology) scheme
[AD-A190383] N88-22597
RANGE FINDERS
Degradation of downlink distance measurement indexes by the addition of a third tone — tone ranging
[CNES-CT/DRT/TIT/TR-122-T] N88-22268
RANGEFINDING
Baseline estimation from simultaneous satellite laser tracking
[NASA-CR-182750] N88-22052
RANKINE CYCLE
Study on shaft seals for potassium turbine
[EL-891] N88-22364
Development of an integrated heat pipe-thermal storage system for a solar receiver
[NASA-TM-101099] N88-22458
RAPID QUENCHING (METALLURGY)
Remarks on solid state amorphizing transformations
[DE88-006452] N88-22803
RARE EARTH ELEMENTS
Thermochemistry and high temperature thermodynamic properties of rare earth-alkaline earth-copper oxide superconductors
[DE88-005976] N88-22770
RATINGS
Cetane scale evaluation and possible modification
[AD-A189730] N88-22200
RAY TRACING
Ray tracing optical analysis of offset solar collector for space station solar dynamic system
[NASA-TM-100853] N88-22080
RAYLEIGH DISTRIBUTION
Rayleigh-Taylor instability in inertial confinement fusion
[TI88-701411] N88-22750
REACTION KINETICS
Infrared absorption spectroscopy and chemical kinetics of free radicals
[DE88-006536] N88-22112

Molecular dynamics of materials possessing high energy content
[AD-A190034] N88-22118
The spectroscopy and reaction kinetics of coordinatively unsaturated metal carbonyls
[AD-A190533] N88-22124
Molecular reaction and energy transfer rate estimation for chemical-laser analysis
[AD-A190664] N88-22126
Advanced B and Al combustion kinetics over wide temperature ranges
[AD-A190752] N88-22128
High temperature oxidation and electrochemical studies related to hot corrosion
[AD-A190699] N88-22156
Effect of vibrational excitation on rate parameters of atmospheric reactions
[AD-A190464] N88-22477
Lumped model generation and evaluation: Sensitivity and Lie algebraic techniques with applications to combustion
[AD-A190402] N88-22680

REACTIVITY
Molecular dynamics of materials possessing high energy content
[AD-A190034] N88-22118

REACTOR MATERIALS
Development of a computer code CRACK for elastic and elastoplastic fracture mechanics analysis of 2-D structures by finite element technique
[DE88-701231] N88-22370

READ-ONLY MEMORY DEVICES
Self-checking logic arrays
[RR-656-I] N88-22545

REAL TIME OPERATION
Real-time flight test data distribution and display
[NASA-TM-100424] N88-22050
Real-time stressed channel simulator
[AD-A190223] N88-22067
A review on holography, its principles and applications
[ISL-CO-242/86] N88-22338
Support for FY87 midlatitude electron-density calibration campaign
[AD-A190174] N88-22476
Real-time environmental Arctic monitoring (R-TEAM)
[AD-A189948] N88-22508
Motion sickness: Quantitative, algorithmic malaise indication in real time
[AD-A189674] N88-22518
Conflict resolution in cooperative systems
[AD-A190351] N88-22535
Optical switching and control techniques using nonlinear optical wave mixing
[AD-A190467] N88-22730
A fault tolerant supervision system
[INPE-4419-TDL/307] N88-22819

RECEIVERS
Performance of single and multiple system AM stereo decoder receivers
[PB88-168307] N88-22265

RECIPROCATION
Reciprocating sliding wear characteristics of copper-carbon fiber composites
[NASA-TT-20176] N88-22100

RECOGNITION
A probabilistic approach to low-level vision
[AD-A189041] N88-22553

RECOMBINATION REACTIONS
Studies of molecular biology
[DE88-005906] N88-22514
A model for nitrogen atom recombination on a silicon dioxide surface
[AD-A189843] N88-22784

RECOMMENDATIONS
Space shuttle accident: NASA's actions to address the Presidential Commission report
[PB88-135306] N88-22059

RECRYSTALLIZATION
Fundamental studies on high temperature deformation recrystallization, and grain growth of two-phase materials
[AD-A189725] N88-22145

RECTANGLES
ALEX results: A comparison of measurements from a round and a rectangular duct with 3-D code predictions
[DE88-005947] N88-22741

RECTIFIERS
Determination of the commutation and angle and load response for a continuous-current, single phase controlled rectifier
[AD-A190602] N88-22285

RED SHIFT
Multiple object redshift determinations in clusters of galaxies using OCTOPUS
[INPE-4528-PRE/1278] N88-22835
New measurements of radial velocities in clusters of galaxies
[INPE-4527-PRE/1277] N88-22845

REENTRY SHIELDING
A model for nitrogen atom recombination on a silicon dioxide surface
[AD-A189843] N88-22784

REFERENCE ATMOSPHERES
Monthly mean global climatology of temperature, wind, geopotential height, and pressure for 0 - 120 km
[NASA-TM-100697] N88-22503

REFINING
Activities of As, Sb, Bi and Pb in copper mattes and their effects on impurity elimination
[TKK-V-A10(1988)] N88-22165

REFLECTOR ANTENNAS
An improved method for calculating power density in the Fresnel region of circular parabolic reflector antennas
[AD-A190569] N88-22284

REFLECTORS
Features and applications of the integrated composites analyzer (ICAN) code N88-22391

REFRACTION
Research on materials and components for opto-electronic signal processing and computing
[AD-A190130] N88-22788

REFRACTIVITY
Stellar scintillometer atmospheric optical turbulence profiling experiment: A qualitative comparison of two identical instruments at AMOS (Air Force Maui Optical Station), 1985
[AD-A190589] N88-22479
Spectral measurements in a disturbed boundary layer over snow
[AD-A190217] N88-22494
Dispersion measurements of microcrystals in the near ultraviolet and infrared
[DE88-006234] N88-22800

REFRACTORY COATINGS
Hermetic coating of optical fibers
[AD-A189886] N88-22177

REFRACTORY MATERIALS
High temperature materials: What's available
[AERE-R-12632] N88-22081
Fundamental studies on high temperature deformation recrystallization, and grain growth of two-phase materials
[AD-A189725] N88-22145
Biaxial experiments supporting the development of constitutive theories for advanced high-temperature materials N88-22386

REFRIGERATORS
Dilution refrigerator with non-valve adsorption system of sup 3/He circulation
[DE88-700974] N88-22209
Thin superconducting film characterization by surface acoustic waves
[AD-A190417] N88-22791

REFUELING
Development and evaluation of an airplane fuel tank ullage composition model. Volume 2: Experimental determination of airplane fuel tank ullage compositions
[AD-A190408] N88-22025

REGRESSION ANALYSIS
Modeling failures of intermittently used machines
[AD-A190298] N88-22367

REGULARITY
Regularity of the Albanese map for nonoriented surfaces
[DE88-006428] N88-22679

REGULATIONS
The impact of independent research and development regulations on companies not required to negotiate advanced independent research and development agreements
[AD-A190007] N88-22818

REINFORCED PLASTICS
Fiber-reinforced plastic composites. Possibilities and limitations of applications as machine-construction materials
[NASA-TT-20159] N88-22102

RELATIVISTIC PLASMAS
Plasma wave radiative damping of a new type in a relativistic one-dimensional plasma
[TI88-701191] N88-22739

RELATIVISTIC THEORY
Hamiltonian formalism in the model of the relativistic string with rigidity
[TI88-701503] N88-22815

RELAXATION TIME
Theoretical studies of Resonance Enhanced Stimulated Raman Scattering (RESRS) of frequency-doubled Alexandrite laser wavelength in cesium vapor
[NASA-CR-182870] N88-22133

RELIABILITY
Advanced capacitor development
[AD-A189985] N88-22276

RELIABILITY ANALYSIS
Monte Carlo reliability analysis
[AD-A189972] N88-22366
Reliability analysis within a Computer Aided Engineering (CAE) infrastructure
[NLR-MP-88059-U] N88-22369
Whisker-reinforced ceramic composites for heat engine components N88-22410
Methodology for software reliability prediction, volume 1
[AD-A190018] N88-22571
Methodology for software reliability prediction, volume 3
[AD-A190019] N88-22572
Analysis and testing of the SURE program
[NASA-TP-2817] N88-22653

RELIABILITY ENGINEERING
Comparative analysis of multistage interconnection networks
[AD-A190436] N88-22598
Information systems for quality. Experience at the Nerviano Aeritalia plant. Avionic systems and equipment group
[ETN-88-92274] N88-22821

RELIC RADIATION
A map of the cosmic background radiation at 3 millimeters
[INPE-4529-PRE/1279] N88-22850

REMOTE SENSING
Development of remote sensing techniques capable of delineating soils as an aid to soil survey
[NASA-CR-182610] N88-22452
Orbital remote sensing: An instrument for monitoring urban growth
[INPE-4456-PRE/1287] N88-22833

REMOTE SENSORS
Instrumentation to provide an active control capability for distributed parameter systems
[AD-A190043] N88-22375
Feasibility study for a 2nd generation system for airborne maritime pollution surveillance
[ETN-88-92108] N88-22466
Support for FY87 midlatitude electron-density calibration campaign
[AD-A190174] N88-22476

REPEATERS
A 104-km unrepeatered bidirectional fiber optic demonstration link
[AD-A190282] N88-22728

REPRESENTATIONS
The total interval of a graph
[AD-A189648] N88-22625

REQUIREMENTS
Large-scale wind turbine structures N88-22429
Monitoring the usage of a computer system
[DE88-004310] N88-22542
The modeling, simulation and comparison of interconnection networks for parallel processing
[AD-A190571] N88-22599

RESEARCH
Data base design and implementation
[AD-A190414] N88-22827
NASA scientific and technical publications: A catalog of Special Publications, Reference Publications, Conference Publications, and Technical Papers, 1987
[NASA-SP-7063(02)] N88-22830

RESEARCH AND DEVELOPMENT
The impact of independent research and development regulations on companies not required to negotiate advanced independent research and development agreements
[AD-A190007] N88-22818
Marshall Space Flight Center 1960-1985: 25th anniversary report
[NASA-TM-100328] N88-22852
Langley aerospace test highlights, 1987
[NASA-TM-100595] N88-22853
Space directorate research and technology accomplishments for fiscal year 1987
[NASA-TM-100607] N88-22854

RESEARCH FACILITIES
Procedures and requirements for testing in the Langley Research Center unitary plan wind tunnel
[NASA-TM-100529] N88-22016
Function of Japan Fine Ceramics Center described N88-22227
Structural dynamics branch research and accomplishments for fiscal year 1987
[NASA-TM-100279] N88-22446
Marshall Space Flight Center 1960-1985: 25th anniversary report
[NASA-TM-100328] N88-22852

RESEARCH MANAGEMENT
Engineering support of space shuttle experiment integration
[AD-A190135] N88-22061
Summary of the 1987 Gordon Research Conference on Corrosion
[AD-A189737] N88-22161
Structural dynamics branch research and accomplishments for fiscal year 1987
[NASA-TM-100279] N88-22446
The Department of Defense Superconductivity Research and Development (DSRD) options. A study of possible directions for exploitation of superconductivity in military applications
[AD-A189747] N88-22780
Space directorate research and technology accomplishments for fiscal year 1987
[NASA-TM-100607] N88-22854
RESIDUAL STRESS
Evolution of hardening and damage during viscoplastic deformation
[AD-A190714] N88-22381
RESIN MATRIX COMPOSITES
Interlaminar fracture toughness of thermoplastic composites
[NASA-TM-100532] N88-22097
Donor acceptor polymerization chemistry as a vehicle to low energy cure matrix resins
[AD-A190119] N88-22179
RESISTANCE
Experimental determination of the coefficients of the hydraulic resistance of apertures in the rotary disks
[AD-A190627] N88-22317
RESOLUTION
Conflict resolution in cooperative systems
[AD-A190351] N88-22535
RESONANCE
Theoretical studies of Resonance Enhanced Stimulated Raman Scattering (RESRS) of frequency-doubled Alexandrite laser wavelength in cesium vapor
[NASA-CR-182870] N88-22133
The concept of an impact resonance diagram for characterizing the nonlinear response of impact vibration
[DE88-005475] N88-22432
RESONANT FREQUENCIES
The concept of an impact resonance diagram for characterizing the nonlinear response of impact vibration
[DE88-005475] N88-22432
RESOURCES MANAGEMENT
Orbital remote sensing: An instrument for monitoring urban growth
[INPE-4456-PRE/1287] N88-22833
RESPIRATION
A laser-based photoacoustic spectrometer for direct breath C-13O2/C-12O2 measurement
[DE88-004915] N88-22516
RESPONSE TIME (COMPUTERS)
Computer program in BASIC language for computation of spectrochemical analytical data
[DE88-701229] N88-22106
COMESH: A corner mesh finite difference code to solve multigroup diffusion equations in multidimensions
[DE88-701248] N88-22555
REVERBERATION CHAMBERS
EMR (Electromagnetic Radiation) test facilities evaluation of reverberating chamber located at RADC (Rome Air Development Center), Griffiss AFB (Air Force Base), Rome, New York
[PB88-178827] N88-22048
REVERSE FIELD PINCH
Electrical circuit modeling of reversed field pinches
[DE88-006942] N88-22745
REYNOLDS STRESS
Development of subminiature multi-sensor hot-wire probes
[NASA-TM-100052] N88-22336
RHEOLOGY
Continual capillary viscosimetry using extrusiograph techniques
[PB88-166293] N88-22195
Experiments on densely-loaded non-Newtonian slurries in laminar and turbulent pipe flows
[DE88-006209] N88-22323
RIBBONS
Investigation of boundary layer disturbances caused by periodic heating of a thin ribbon
[AD-A190572] N88-22314
RIEMANN MANIFOLD
Markov processes applied to control, replacement and signal analysis
[AD-A190563] N88-22674
Regularity of the Albanese map for nonoriented surfaces
[DE88-006428] N88-22679
RISK
A systems analysis of fire suppression alternatives for the US space station
[AD-A189847] N88-22064
ROBOTICS
Electromagnetic sensor arrays for nondestructive evaluation and robot control
[AD-A190210] N88-22260
Range image segmentation and surface parameter extraction for a mobile robot
[DE87-013877] N88-22360
Telerobotic operation of conventional robot manipulators
[DE88-005718] N88-22363
A probabilistic approach to low-level vision
[AD-A189041] N88-22553
ROBOTS
Range image segmentation and surface parameter extraction for a mobile robot
[DE87-013877] N88-22360
Telerobotic operation of conventional robot manipulators
[DE88-005718] N88-22363
The visit problem: Visibility graph-based solution
[DE88-000343] N88-22556
Insertions using geometric analysis and hybrid force-position control: Method and analysis
[DE87-013852] N88-22611
Concurrent algorithms for a mobile robot vision system
[DE88-005850] N88-22614
ROBUSTNESS (MATHEMATICS)
Development and application of the p-version of the finite element method
[AD-A190036] N88-22633
ROCKET ENGINES
Crack opening and extension in inert solid propellant. An experimental study
[AD-A189808] N88-22201
ROCKET NOZZLES
An experimental investigation of rocket ramjet nozzle assembly base pressures
[AD-A189714] N88-22076
ROCKET SOUNDING
Coordinated Auroral Experiments using Scatter And Rocket investigations (CAESAR investigations)
[MPAE-W-47-87-13] N88-22487
RODS
Solid hosts for dye laser rods. Part 1: Criteria for choosing a host material
[DE88-006478] N88-22355
ROLLING
Mode 2 fracture mechanics N88-22418
ROOT-MEAN-SQUARE ERRORS
Seismic inversion by a RMS (Root-Mean-Square) Born approximation in the space-time domain
[PB88-165402] N88-22711
ROSAT MISSION
Design, construction and performance of the ROSAT high resolution X-ray mirror assembly
[MPE-PREPRINT-101] N88-22836
ROTATING DISKS
Life and reliability of rotating disks N88-22428
ROTATING LIQUIDS
On rotating sphere-on-a-plate experiments and the questions of whether high angle grain boundaries melt below bulk melting temperatures
[DE88-006627] N88-22142
Fluid motion in a spinning, coning cylinder via spatial eigenfunction expansion
[AD-A190758] N88-22319
ROTATION
Experimental investigation of a spanwise forced mixing layer
[AD-A190136] N88-22007
Coupled bending-torsion steady-state response of pretwisted, nonuniform rotating beams using a transfer-matrix method
[NASA-TM-100596] N88-22435
Density perturbations in a rotating universe
[DE87-703036] N88-22840
ROTOR AERODYNAMICS
Advancing-side directivity and retreating-side interactions of model rotor blade-vortex interaction noise
[NASA-TP-2784] N88-22710
ROTOR BLADES
FLAP (Force and Loads Analysis Program) code development and validation
[DE88-001131] N88-22371
ROTOR BLADES (TURBOMACHINERY)
Visualisation of the flow at the tip of a high speed axial flow turbine rotor
[AD-A189928] N88-22300
Visualisation of the flow at the tip of a high speed axial flow turbine rotor: An assessment of flow visualisation techniques and the requirement of the experimental turbine
[AD-A189929] N88-22301
Improvements to tilt rotor performance through passive blade twist control
[NASA-TM-100583] N88-22434
ROTORS
Inflow measurement made with a laser velocimeter on a helicopter model in forward flight. Volume 3: Rectangular planform blades at an advance ratio of 0.30
[NASA-TM-100543] N88-22015
Visualisation of the flow at the tip of a high speed axial flow turbine rotor
[AD-A189928] N88-22300
ROUTES
Implementation of a distributed adaptive routing algorithm on the Intel iPSC (Intel Personal Super-Computer)
[AD-A189849] N88-22567

S

S WAVES
Earthquakes from peninsular India: Data from the Gauribidanur seismic array
[DE88-701232] N88-22471
SABOT PROJECTILES
Launchability of base-driven electromagnetic projectiles
[AD-A189635] N88-22055
SAFETY
Orbital transfer vehicle: Concept definition and system analysis study
[NASA-CR-179315] N88-22060
SALINITY
Physical, chemical and CTD (Conductivity/Temperature/Depth) data from the Marathon 2 expedition
[AD-A189930] N88-22507
SAMPLING
High speed, bandpass sampling of digital communications waveforms
[AD-A189842] N88-22254
Empirical and hierarchical Bayes competitors of preliminary test estimators in two sample problems
[AD-A190327] N88-22670
SAPPHIRE
Laser enhanced adhesion of copper films to sapphire substrates
[DE88-006802] N88-22144
SATELLITE COMMUNICATION
Real-time environmental Arctic monitoring (R-TEAM)
[AD-A189948] N88-22508
SATELLITE DESIGN
Definition and implementation study for the Varan-S radar
[CNES-CT/DRT/TIT/RL-143-T] N88-22267
SATELLITE IMAGERY
Geometric restoration of satellite image data
[AD-A190462] N88-22450
Satellite UV image processing
[AD-A190466] N88-22451
Project CODEAMA/FUNCATE (test-area of Barreirinha-AM): Field report
[INPE-4500-RPE/563] N88-22455
Comparative utilization of analog and digital processes in the treatment of MSS-LANDSAT data for studying the national parks of Brazil
[INPE-4011-TDL/240] N88-22456
Calibration and processing of AVHRR data for temperature estimation
[INPE-4493-PRE/1257] N88-22485
SATELLITE NETWORKS
Degradation of downlink distance measurement indexes by the addition of a third tone — tone ranging
[CNES-CT/DRT/TIT/TR-122-T] N88-22268
SATELLITE ORBITS
Baseline estimation from simultaneous satellite laser tracking
[NASA-CR-182750] N88-22052
SATELLITE TRACKING
Baseline estimation from simultaneous satellite laser tracking
[NASA-CR-182750] N88-22052
SCALE MODELS
Model-scale sound propagation experiment
[NASA-TM-100602] N88-22709
MPD (magnetoplasmadynamic) thruster advanced pumping system concepts
[AD-A190513] N88-22756
SCANNERS
OCR vision system, an alternative to bar code
[DE88-003761] N88-22828

SCANNING
Systems for ultrasonic scanning, analysis and imagery N88-22414
Flaw characterization in structural ceramics using scanning laser acoustic microscopy N88-22415
Nondestructive evaluation of sintered ceramics N88-22416
SCATTERING
Theory of the dissociation dynamics of small molecules on metal surfaces: Finite temperature studies [DE88-006495] N88-22716
SCHOTTKY DIODES
The influence of current stressing on the structure of Ag contacts to GaAs [DE88-005988] N88-22771
SCHROEDINGER EQUATION
Geometric methods and the gauge structure of Berry's phase [DE88-006538] N88-22682
SCHWARTZ INEQUALITY
Baecklund transformation and the Schwarzian derivative [AD-A190277] N88-22684
SCINTILLATION
Stellar scintillometer atmospheric optical turbulence profiling experiment: A qualitative comparison of two identical instruments at AMOS (Air Force Maui Optical Station), 1985 [AD-A190589] N88-22479
SCINTILLATION COUNTERS
Stellar scintillometer atmospheric optical turbulence profiling experiment: A qualitative comparison of two identical instruments at AMOS (Air Force Maui Optical Station), 1985 [AD-A190589] N88-22479
SEA ICE
The effects of time-dependent winds and ocean eddies on ice motion in a marginal ice zone [AD-A190105] N88-22511
SEA WATER
Relationship between optical transfer function and natural light field in sea or atmosphere N88-22247
Physical, chemical and CTD (Conductivity/Temperature/Depth) data from the Marathon 2 expedition [AD-A189930] N88-22507
SEISMIC WAVES
Earthquakes from peninsular India: Data from the Gauribidanur seismic array [DE88-701232] N88-22471
Characteristics of seismic sources of some Asian earthquakes and Soviet underground explosions from Gauribidanur array records [DE88-701233] N88-22472
Seismic inversion by a RMS (Root-Mean-Square) Born approximation in the space-time domain [PB88-165402] N88-22711
SELECTION
Structure and surface characterizations of high strength carbon fibers [AD-A189642] N88-22087
On two-stage allocation procedures for selection problems [AD-A190766] N88-22675
SELECTIVITY
Synthesis and analysis of novel polymers with potential for providing both high permselectivity and permeability in gas separation applications [DE88-006533] N88-22174
SEMANTICS
A fully abstract semantics for event-based simulation [AD-A190560] N88-22283
Inference engine for expert systems [INPE-4465-TDL/321] N88-22590
SEMICONDUCTING FILMS
Gas source MBE (Molecular Beam Epitaxy) [AD-A189763] N88-22782
Beam assisted fabrication of 3-5/Si monolithic devices [AD-A189979] N88-22785
Fundamental properties and devices applications of Ge(x)Si(1-x)/Si superlattices [AD-A190129] N88-22787
Thin superconducting film characterization by surface acoustic waves [AD-A190417] N88-22791
SEMICONDUCTOR DEVICES
Application of copper-carbon fiber composites to power semiconductor devices [NASA-TT-20171] N88-22101
Temperature-dependent conductivity of oxygen-depleted YBCO ceramics [AD-A190340] N88-22182
Growth of Pb/sub 1-x/Eu/sub x/Te epitaxial layers by the liquid phase epitaxy technique [TI88-701022] N88-22763
SEMICONDUCTOR DIODES
Growth of Pb/sub 1-x/Eu/sub x/Te epitaxial layers by the liquid phase epitaxy technique [TI88-701022] N88-22763
SEMICONDUCTOR LASERS
Fabrication and characterization of semiconductor lasers of Pb(1-x)Sn(x)Te [INPE-4253-PRE/1128] N88-22357
SEMICONDUCTORS (MATERIALS)
Amorphous semiconductors made in space N88-22221
Pb(1-x)Sn(x)Te crystal growth in space N88-22223
Absolute pressure derivatives of deep level defects in 3-5 semiconductors [DE88-006318] N88-22772
Examination of temperature effects on gate-to-drain avalanche breakdown in GaAs MESFETs (Metal-Semiconductor Field Effect Transistors) by measuring light emission under RF drive [AD-A189634] N88-22778
Repetitive opening switches using optically activated semiconductors [AD-A190196] N88-22790
Interface formation and precursory dynamics [AD-A190741] N88-22794
Fermi level stabilization in semiconductors: Implications for implant activation efficiency [DE88-006332] N88-22801
SENSITIVITY
Shape sensitivity analysis of wing static aeroelastic characteristics [NASA-TP-2808] N88-22031
Infrared-sensitive spatial light modulator [AD-A190391] N88-22729
SENSORS
Electromagnetic sensor arrays for nondestructive evaluation and robot control [AD-A190210] N88-22260
SEPARATED FLOW
On the prediction of highly vortical flows using an Euler equation model, part 2 [AD-A190245] N88-22305
Dense-spray structure and phenomena. Part 1. Turbulence/dispersed-phase interactions [AD-A190606] N88-22315
SEPARATION
Segregation effects in welded stainless steels [DE88-701224] N88-22139
SEQUENTIAL ANALYSIS
Sequential tests for the drift of a Wiener process with a smooth prior and the heat equation [AD-A190322] N88-22638
SERIES (MATHEMATICS)
Distributions of quadratic forms [AD-A190224] N88-22663
SERVICE LIFE
MPD (magnetoplasmadynamic) thruster advanced pumping system concepts [AD-A190513] N88-22756
SHAFTS (MACHINE ELEMENTS)
Study on shaft seals for potassium turbine [EL-891] N88-22364
SHAPES
Study of mean free path effects on growth of ultrafine metallic aerosols [AD-A190206] N88-22149
SHEAR FLOW
Enhancement of data acquisition and numerical computation capabilities for unsteady fluid dynamics [AD-A190115] N88-22302
A new method of measuring multigrade oil shear elasticity and viscosity at high shear rates [AD-A190145] N88-22304
Instruments for use in experimental studies of complex turbulent shear flow: Three component LDVs [AD-A190526] N88-22312
SHEAR LAYERS
Instruments for use in experimental studies of complex turbulent shear flow: Three component LDVs [AD-A190526] N88-22312
SHEAR PROPERTIES
The buckling and vibration of composite plates using the Levy method considering shear deformation and rotary inertia [AD-A189743] N88-22374
SHEAR STRAIN
An efficient Mindlin finite strip plate element based on assumed strain distribution N88-22407
SHEAR STRESS
Bodies in unsteady flow [AD-A190416] N88-22308
SHOCK TESTS
Experimental comparison of lightning simulation techniques to CV-580 airborne lightning strike measurements [AD-A190576] N88-22496
SHOCK WAVE INTERACTION
Numerical and experimental investigation of multiple shock wave/turbulent boundary layer interactions in a rectangular duct [AD-A190772] N88-22320
Numerical study of unsteady viscous hypersonic blunt body flows with an impinging shock [NASA-TM-100096] N88-22650
High-resolution shock-capturing schemes for inviscid and viscous hypersonic flows [NASA-TM-100097] N88-22651
SHOCK WAVES
Buckling of blast loaded cylinder [AD-A190124] N88-22376
SIDE-LOOKING RADAR
Definition and implementation study for the Varan-S radar [CNES-CT/DRT/TIT/RL-143-T] N88-22267
SIDELOBES
Conformal microstrip slot antenna and antenna array [AD-A189623] N88-22252
An improved method for calculating power density in the Fresnel region of circular parabolic reflector antennas [AD-A190569] N88-22284
SIGNAL ANALYSIS
Markov processes applied to control, replacement and signal analysis [AD-A190563] N88-22674
SIGNAL DETECTION
Earthquakes from peninsular India: Data from the Gauribidanur seismic array [DE88-701232] N88-22471
Characteristics of seismic sources of some Asian earthquakes and Soviet underground explosions from Gauribidanur array records [DE88-701233] N88-22472
Study of microcomputer-based real-time programmable optical signal processor and application [AD-A190076] N88-22726
SIGNAL PROCESSING
Merit of Hadamard transform active absorption spectrometer described N88-22232
Optimum signal processing in distributed sensor systems [AD-A189443] N88-22250
Direct bit detection receiver noise performance analysis for 32-PSK and 64-PSK modulated signals [AD-A190009] N88-22256
A hardware/software system for implementing geophysical diffraction tomography [DE88-006411] N88-22480
Auditory perception of complex sounds [AD-A190528] N88-22529
Selective mechanisms in auditory and bimodal signal processing [AD-A190529] N88-22530
Auditory pattern memory: Mechanisms of tonal sequence discrimination by human observers [AD-A190337] N88-22534
Investigation into the development of computer aided design software for space based sensors [NASA-CR-180772] N88-22552
Memory efficient evaluations of nonlinear stochastic equations and C3 applications [AD-A189872] N88-22569
Design and implementation of VLSI prime factor algorithm processor [AD-A190483] N88-22580
Cholesky downdating on a hypercube [DE88-006780] N88-22586
The adjoint process in stochastic optimal control [AD-A189720] N88-22605
Nonlinear signal processing using neural networks: Prediction and system modelling [DE88-006479] N88-22621
Near optimal blind deconvolution [REPT-87-016] N88-22655
Filtering of jump processes [AD-A189701] N88-22656
The partially observed stochastic minimum principle [AD-A189787] N88-22658
Multivariate analysis and its application [AD-A189983] N88-22661
Spatial matched processing for multipath propagation [AD-A189790] N88-22701
Space time processing, environmental-acoustic effects [AD-A190764] N88-22706
Space-variant optical systems [AD-A189967] N88-22724
Infrared-sensitive spatial light modulator [AD-A190391] N88-22729
Autonomous control system for Czochralski growth of LEC GaAs [AD-A189726] N88-22779

Research on materials and components for opto-electronic signal processing and computing
[AD-A190130] N88-22788

SIGNAL RECEPTION
Target localization in an inhomogeneous medium
[AD-A190008] N88-22703

SIGNAL TO NOISE RATIOS
Direct bit detection receiver noise performance analysis for 32-PSK and 64-PSK modulated signals
[AD-A190009] N88-22256
The 2 FSK/QPSK (Frequency Shift Keying/Quadrature Phase Shift Keying) transmitter and receiver: Design and performance
[AD-A190028] N88-22258

SIGNAL TRANSMISSION
Target localization in an inhomogeneous medium
[AD-A190008] N88-22703

SIGNATURES
Polarimetric ISAR imaging using either measured or calculated transient signatures
[AD-A190077] N88-22259
Anomalies in the heat-capacity signatures of submonolayer adsorbates with attractive lateral interactions
[AD-A190736] N88-22817

SIGNS AND SYMPTOMS
Motion sickness: Quantitative, algorithmic malaise indication in real time
[AD-A189674] N88-22518

SILANES
High-performance polymeric materials
[AD-A190708] N88-22190

SILICA GEL
Mass transfer mechanisms for water adsorbed on silica gel
[DE88-005993] N88-22107
Structure of sol-gel silica
[DE88-006870] N88-22114

SILICATES
High-performance polymeric materials
[AD-A190708] N88-22190

SILICON
Fabrication and electrical characterization of multilevel aluminum interconnects used to achieve silicon-hybrid wafer-scale integration
[AD-A190519] N88-22282
High-efficiency thin-film silicon-on-GaP solar cell for improved radiation resistance
[AD-A190268] N88-22460
Fundamental properties and devices applications of Ge(x)Si(1-x)/Si superlattices
[AD-A190129] N88-22787
The structure of the boron-hydrogen complex in silicon
[DE88-005433] N88-22795

SILICON CARBIDES
Microwave sintering of alumina-SiC composites at 2.45 and 60 GHz
[DE88-006455] N88-22095
Processing, microstructure, and mechanical properties of silicon carbide particulate reinforced aluminum alloys
[AD-A186981] N88-22136
Characterization of sintered SiC by using NDE N88-22413

SILICON DIOXIDE
A model for nitrogen atom recombination on a silicon dioxide surface
[AD-A189843] N88-22784

SILICON NITRIDES
Fracture toughness of silicon nitride-silicon nitride joints bonded with oxynitride glass
[DE88-005548] N88-22172
Flaw characterization in structural ceramics using scanning laser acoustic microscopy N88-22415

SIMD (COMPUTERS)
An analysis of multiple grain CHiP architectures
[AD-A189942] N88-22570

SIMULATION
Numerical simulation of turbulent flames using vortex methods
[AD-A189813] N88-22116
A fully abstract semantics for event-based simulation
[AD-A190560] N88-22263
Finite element simulation of perforation of aluminum plates
[DE88-002092] N88-22362
Monte Carlo reliability analysis
[AD-A189972] N88-22366
Experimental comparison of lightning simulation techniques to CV-580 airborne lightning strike measurements
[AD-A190576] N88-22496
Exhaustive and pseudo-exhaustive testing
[AD-A190140] N88-22574
A direct-execution parallel architecture for the Advanced Continuous Simulation Language (ACSL)
[NASA-CR-182809] N88-22602
An approximation technique for solving a system of Fredholm integral equations for asymmetric detector response functions
[AD-A190577] N88-22645
Random Process Simulation for stochastic fatigue analysis
[NASA-TM-100464] N88-22654

SIMULATORS
The effects of torque response and time delay on rotorcraft vertical axis handling qualities
[AD-A189873] N88-22023
Development and evaluation of an airplane fuel tank ullage composition model. Volume 2: Experimental determination of airplane fuel tank ullage compositions
[AD-A190408] N88-22025
Real-time stressed channel simulator
[AD-A190223] N88-22067
A UNIX-based interactive VHDL (hardware description language) simulator
[AD-A189749] N88-22565

SINGLE CRYSTALS
Bithermal fatigue of a nickel-base superalloy single crystal
[NASA-TM-100885] N88-22168
Single crystal growth by laser CVD N88-22213
Unified constitutive model for single crystal deformation behavior with applications N88-22388
The kinetics of contact noise in NaBeta alumina
[AD-A190651] N88-22707
An investigation of the crystalchemistry and thermochemistry of selected mineral systems
[AD-A189758] N88-22781
Dispersion measurements of microcrystals in the near ultraviolet and infrared
[DE88-006234] N88-22800

SINGULARITY (MATHEMATICS)
Singular Lagrangians. Classical dynamics and quantization. Lectures for young scientists
[TI88-701158] N88-22806

SINTERING
Microwave sintering of alumina-SiC composites at 2.45 and 60 GHz
[DE88-006455] N88-22095

SITE SELECTION
Environmental assessment for the compact ignition Tokamak
[DE88-005633] N88-22740

SKIN FRICTION
Enhanced viscous flow drag reduction using acoustic excitation
[NASA-CR-182734] N88-22295

SLEEP DEPRIVATION
Napping and human functioning during prolonged work
[AD-A190228] N88-22525

SLIDING CONTACT
Traction model development
[AD-A188450] N88-22359

SLIDING FRICTION
Reciprocating sliding wear characteristics of copper-carbon fiber composites
[NASA-TT-20176] N88-22100

SLOT ANTENNAS
Conformal microstrip slot antenna and antenna array
[AD-A189623] N88-22252
Current-drive on the Versator-2 tokamak with a slotted-waveguide fast-wave coupler
[DE88-006261] N88-22743

SLOTS
Cavitation inception in rectangular two-dimensional slots
[AD-A190677] N88-22318

SLURRIES
Experiments on densely-loaded non-Newtonian slurries in laminar and turbulent pipe flows
[DE88-006209] N88-22323

SMELTING
Activities of As, Sb, Bi and Pb in copper mattes and their effects on impurity elimination
[TKK-V-A10(1988)] N88-22165

SMOOTHING
The existence of smooth densities for the prediction filtering and smoothing problems
[AD-A189865] N88-22629

SNOW COVER
Spectral measurements in a disturbed boundary layer over snow
[AD-A190217] N88-22494

SOAPS
The elliptic Sinh-Gordon equation and the construction of toroidal soap bubbles
[DE88-006426] N88-22585

SODIUM
Use of long-distance pair potentials in calculations of defect characteristics in metals
[TI88-701039] N88-22138
The kinetics of contact noise in NaBeta alumina
[AD-A190651] N88-22707

SODIUM VAPOR
Alkali metal diffuse band lasers
[AD-A190244] N88-22350

SOFTWARE ENGINEERING
Sigma system: Overview, prospects N88-22230
Investigation into the development of computer aided design software for space based sensors
[NASA-CR-180772] N88-22552
Using Colored Stochastic Petri Net (CS-PN) software for protocol specification, validation, and evaluation
[ENST-87C004] N88-22588

SOFTWARE TOOLS
Reliability analysis within a Computer Aided Engineering (CAE) infrastructure
[NLR-MP-86059-U] N88-22369
Supercomputer environment
[AD-A190633] N88-22551
A graphics editor for structured analysis with a data dictionary
[AD-A190618] N88-22584
Using Colored Stochastic Petri Net (CS-PN) software for protocol specification, validation, and evaluation
[ENST-87C004] N88-22588
The Colored Stochastic Petri Net (CS-PN) software: Application to the validation and the performance evaluation of distributed systems
[ENST-87D005] N88-22589
Two-dimensional graphics tools for a transputer based display board
[NASA-TM-100820] N88-22591
A fault tolerant supervision system
[INPE-4419-TDL/307] N88-22819

SOIL MAPPING
Development of remote sensing techniques capable of delineating soils as an aid to soil survey
[NASA-CR-182610] N88-22452

SOILS
Development of remote sensing techniques capable of delineating soils as an aid to soil survey
[NASA-CR-182610] N88-22452

SOL-GEL PROCESSES
Structure of sol-gel silica
[DE88-006870] N88-22114

SOLAR ACTIVITY
Solar-geophysical data number 520, December 1987. Part 2: (Comprehensive rsports). Data for June 1987 and miscellanea
[PB88-164207] N88-22849

SOLAR CELLS
Thermal analysis of heat storage canisters for a solar dynamic, space power system
[DE88-004199] N88-22075
Solar cell cover glasses for satellites N88-22225
High-efficiency thin-film silicon-on-GaP solar cell for improved radiation resistance
[AD-A190268] N88-22460

SOLAR COLLECTORS
Ray tracing optical analysis of offset solar collector for space station solar dynamic system
[NASA-TM-100853] N88-22080
Development of an integrated heat pipe-thermal storage system for a solar receiver
[NASA-TM-101099] N88-22458

SOLAR DYNAMIC POWER SYSTEMS
Ray tracing optical analysis of offset solar collector for space station solar dynamic system
[NASA-TM-100853] N88-22080
Structural assessment of a space station solar dynamic heat receiver thermal energy storage canister N88-22406

SOLAR GENERATORS
Thermal analysis of heat storage canisters for a solar dynamic, space power system
[DE88-004199] N88-22075

SOLAR RADIATION
Solar-geophysical data number 520, December 1987. Part 2: (Comprehensive reports). Data for June 1987 and miscellanea
[PB88-164207] N88-22849

SOLAR WIND
Plasmapause formation
[AERONOMICA-ACTA-A-319-1987] N88-22759

SOLID ELECTROLYTES
Recent advances in solid polymer electrolyte fuel cell technology
[DE88-005380] N88-22464
The kinetics of contact noise in NaBeta alumina
[AD-A190651] N88-22707

SOLID MECHANICS
Symmetry and global bifurcation in nonlinear solid mechanics
[AD-A190521] N88-22642
SOLID PROPELLANTS
Advanced B and Al combustion kinetics over wide temperature ranges
[AD-A190752] N88-22128
SOLID ROCKET PROPELLANTS
LGM-30B stage 2 disected motor test report
[AD-A190771] N88-22079
Advanced B and Al combustion kinetics over wide temperature ranges
[AD-A190752] N88-22128
Crack opening and extension in inert solid propellant. An experimental study
[AD-A189808] N88-22201
SOLID STATE DEVICES
Instrumentation for the characterization and development of millimeter wave components compatible with monolithic integration
[AD-A189724] N88-22275
SOLID SURFACES
A model for nitrogen atom recombination on a silicon dioxide surface
[AD-A189843] N88-22784
SOLIDIFICATION
Growth and deformation mechanisms of refractory alloy hybrid materials
[AD-A190492] N88-22152
Characterization of an explosively consolidated rapidly solidified Fe-16Ni-9Cr-5Mo-2Cu alloy powder
[DE88-006733] N88-22162
Remarks on solid state amorphizing transformations
[DE88-006452] N88-22803
SOLIDS
Density measurements on solids and liquids
[PB88-164934] N88-22129
A 3-D solid rendering of NDT data
[DE88-006199] N88-22373
Dynamical optimization techniques for the calculation of electronic structure in solids
[DE88-006010] N88-22768
SOLITARY WAVES
Super Virasoro algebra and solvable supersymmetric quantum field theories
[DE88-752299] N88-22681
SOLUTIONS
Almost-periodic solutions of nonlinear parabolic equations
[DE88-006423] N88-22618
SORPTION
Synthesis and analysis of novel polymers with potential for providing both high permselectivity and permeability in gas separation applications
[DE88-006533] N88-22174
SOUND FIELDS
A computerized investigation using the method of images to predict the sound field in a fluid wedge overlying a slow fluid half-space
[AD-A190013] N88-22704
SOUND TRANSMISSION
Spatial matched processing for multipath propagation
[AD-A189790] N88-22701
Target localization in an inhomogeneous medium
[AD-A190008] N88-22703
A computerized investigation using the method of images to predict the sound field in a fluid wedge overlying a slow fluid half-space
[AD-A190013] N88-22704
SOUND WAVES
Perception of complex auditory patterns
[AD-A190218] N88-22524
Mechanisms mediating the perception of complex acoustic patterns
[AD-A190112] N88-22705
Generation and propagation of sound waves in a collapsing or anti-collapsing star with uniform density
[DE87-703034] N88-22839
SOUNDING ROCKETS
In-situ plasma bubble observations associated with equatorial spread-F over Natal
[INPE-4488-PRE/1252] N88-22482
SOUNDS (TOPOGRAPHIC FEATURES)
The physical oceanography of the northern Baffin Bay-Nares Strait region
[AD-A190015] N88-22509
SOUTH AMERICA
A study on electric fields and conductivity associated with electrified clouds in the region of South America
[INPE-4487-TDL/325] N88-22486
SPACE CHARGE
Theoretical model of the cathode spot on a unipolar arc
[AD-A190109] N88-22277
SPACE FLIGHT
Langley aerospace test highlights, 1987
[NASA-TM-100595] N88-22853
SPACE POWER REACTORS
Requirements and cost considerations for a Combined Space Nuclear Reactor Test Facility
[DE88-006763] N88-22719
SPACE PROCESSING
Preliminary market analysis for large zeolite crystals
[NASA-CR-182682] N88-22207
JPRS report: Science and technology. Japan
[JPRS-JST-88-001] N88-22218
Space utilization plans N88-22219
Space experiment plan FMPT N88-22220
Amorphous semiconductors made in space N88-22221
Pb(1-x)Sn(x)Te crystal growth in space N88-22223
SPACE SHUTTLE MAIN ENGINE
Duct flow nonuniformities: Effect of struts in SSME HGM II(+)
[NASA-CR-179285] N88-22296
Advanced probabilistic methods for quantifying the effects of various uncertainties in structural response N88-22401
Thermal-structural analyses of Space Shuttle Main Engine (SSME) hot section components N88-22404
SPACE SHUTTLE MISSION 51-L
Space shuttle accident: NASA's actions to address the Presidential Commission report
[PB88-135306] N88-22059
SPACE SHUTTLE PAYLOADS
Space experiment plan FMPT N88-22220
SPACE SHUTTLES
Engineering support of space shuttle experiment integration
[AD-A190135] N88-22061
A method of atmospheric density measurements during space shuttle entry using ultraviolet-laser Rayleigh scattering
[NASA-TM-100056] N88-22337
SPACE STATION POWER SUPPLIES
Structural assessment of a space station solar dynamic heat receiver thermal energy storage canister N88-22406
SPACE STATIONS
Superconducting magnet technique for ASTROMAG on the space station
[DE88-004560] N88-22063
A systems analysis of fire suppression alternatives for the US space station
[AD-A189847] N88-22064
Ray tracing optical analysis of offset solar collector for space station solar dynamic system
[NASA-TM-100853] N88-22080
Japanese space station module N88-22224
Solar cell cover glasses for satellites N88-22225
Vibrations of structures with parametric uncertainties
[AD-A190400] N88-22378
Research and technology
[NASA-TM-100172] N88-22851
SPACE WEAPONS
Constellation sizing for modest directed energy platforms
[DE88-007033] N88-22343
SPACE-TIME FUNCTIONS
Seismic inversion by a RMS (Root-Mean-Square) Born approximation in the space-time domain
[PB88-165402] N88-22711
Einstein metrics and Brans-Dicke superfields
[DE88-006992] N88-22809
Quantization of axial electrodynamics
[TI88-701498] N88-22813
Cosmology for high energy physicists
[DE88-005705] N88-22842
SPACEBORNE EXPERIMENTS
Engineering support of space shuttle experiment integration
[AD-A190135] N88-22061
Space utilization plans N88-22219
Amorphous semiconductors made in space N88-22221
Containerless glass melting N88-22222
Pb(1-x)Sn(x)Te crystal growth in space N88-22223
Solar cell cover glasses for satellites N88-22225
SPACEBORNE TELESCOPES
Design, construction and performance of the ROSAT high resolution X-ray mirror assembly
[MPE-PREPRINT-101] N88-22836
SPACECRAFT ANTENNAS
Features and applications of the integrated composites analyzer (ICAN) code N88-22391
SPACECRAFT DESIGN
Nonlinear analysis and optimal design of dynamic mechanical systems for spacecraft application
[AD-A190644] N88-22070
Study of surface discharges
[ONERA-12/7236-PY] N88-22073
Japanese space station module N88-22224
External tank gamma ray imaging telescope study. Final review, phase 2
[NASA-CR-179320] N88-22834
SPACECRAFT GUIDANCE
Identification of a star field from a spinning satellite
[CNES-NT-120] N88-22074
SPACECRAFT INSTRUMENTS
A method of atmospheric density measurements during space shuttle entry using ultraviolet-laser Rayleigh scattering
[NASA-TM-100056] N88-22337
NIMBUS-7 CZCS. Coastal Zone Color Scanner imagery for selected coastal regions. North America - Europe. South America - Africa - Antarctica. Level 2 photographic product
[NASA-CR-180755] N88-22447
SPACECRAFT LAUNCHING
JPRS report: Science and technology. China
[JPRS-CST-87-043] N88-22233
Chronology of China's successful satellite launchings N88-22234
SPACECRAFT POWER SUPPLIES
Thermal analysis of heat storage canisters for a solar dynamic, space power system
[DE88-004199] N88-22075
Development of an integrated heat pipe-thermal storage system for a solar receiver
[NASA-TM-101099] N88-22458
SPACECRAFT REENTRY
A method of atmospheric density measurements during space shuttle entry using ultraviolet-laser Rayleigh scattering
[NASA-TM-100056] N88-22337
SPACECRAFT STABILITY
Vibrations of structures with parametric uncertainties
[AD-A190400] N88-22378
SPACECRAFT STRUCTURES
Optimal control and identification of space structures
[AD-A190033] N88-22065
Wave propagation and dynamics of lattice structures
[AD-A190037] N88-22066
SPACECRAFT TRAJECTORIES
Spacecraft trajectories
[ISBN-2-85-428166-7] N88-22054
SPACELAB
Space experiment plan FMPT N88-22220
Amorphous semiconductors made in space N88-22221
Containerless glass melting N88-22222
Pb(1-x)Sn(x)Te crystal growth in space N88-22223
SPATIAL FILTERING
Infrared-sensitive spatial light modulator
[AD-A190391] N88-22729
SPATIAL MARCHING
Split-coefficient matrix solution and experimental study of axisymmetric underexpanded exhaust plumes N88-22242
SPATIAL RESOLUTION
Method for restoration and resampling of TM sensor imagery
[INPE-4491-PRE/1255] N88-22454
Sources of digital spatial data for geographic information systems
[AD-A189788] N88-22824
SPECIFICATIONS
The effects of torque response and time delay on rotorcraft vertical axis handling qualities
[AD-A189873] N88-22023
SPECIMENS
Specimen preparation techniques for the examination of ceramic and metal-matrix composites
[DE88-005157] N88-22094
SPECKLE INTERFEROMETRY
Speckle interferometry of asteroids
[NASA-CR-180438] N88-22843
SPECTRAL METHODS
Spectrum fatigue testing for materials characterization
[VTT-RR-502] N88-22443
Development of remote sensing techniques capable of delineating soils as an aid to soil survey
[NASA-CR-182610] N88-22452
SPECTRAL RESOLUTION
Merit of Hadamard transform active absorption spectrometer described N88-22232
SPECTROGRAPHS
Mechanisms mediating perception of complex acoustic patterns
[AD-A189765] N88-22520
SPECTROSCOPIC ANALYSIS
Computer program in BASIC language for computation of spectrochemical analytical data
[DE88-701229] N88-22106

SPECTROSCOPY
Spectrographic detection of nitrogen impurity in helium
[DE88-752301] N88-22111
SPECTRUM ANALYSIS
Development of remote sensing techniques capable of delineating soils as an aid to soil survey
[NASA-CR-182610] N88-22452
Spectral measurements in a disturbed boundary layer over snow
[AD-A190217] N88-22494
Multiple object redshift determinations in clusters of galaxies using OCTOPUS
[INPE-4528-PRE/1278] N88-22835
SPEECH RECOGNITION
Perception of complex auditory patterns
[AD-A190218] N88-22524
Auditory perception of complex sounds
[AD-A190528] N88-22529
SPHERICAL COORDINATES
Adiabatic representation of three-body problem in hyperspherical coordinates. Statement of the problem
[TI88-701162] N88-22678
SPHERICAL SHELLS
Cubic spline solution of symmetric buckling problems of clamped shallow spherical shells N88-22239
SPIN
Spin precession in stationary gravitational fields
[TI88-701107] N88-22470
Effective electron interactions due to virtual charge and spin excitations in an extended Hubbard model for Cu-O superconductors
[DE88-005971] N88-22766
SPIN DYNAMICS
Fluid motion in a spinning, coning cylinder via spatial eigenfunction expansion
[AD-A190758] N88-22319
SPIN STABILIZATION
Identification of a star field from a spinning satellite
[CNES-NT-120] N88-22074
SPLINE FUNCTIONS
Cubic spline solution of symmetric buckling problems of clamped shallow spherical shells N88-22239
SPRAYERS
Dense-spray structure and phenomena. Part 2: Pressure-atomized sprays
[AD-A190312] N88-22307
SPRAYING
Dense-spray structure and phenomena. Part 1. Turbulence/dispersed-phase interactions
[AD-A190606] N88-22315
SPREAD F
In-situ plasma bubble observations associated with equatorial spread-F over Natal
[INPE-4488-PRE/1252] N88-22482
SPUTTERING
Recent advances in solid polymer electrolyte fuel cell technology
[DE88-005380] N88-22464
Preparation of large area NbN/AlN/NbN Josephson junctions
[DE88-006074] N88-22799
STABILITY
Equilibrium stability of strained epitaxial layers on a rigid substrate
[INPE-4254-PRE/1127] N88-22804
STABILIZATION
Fermi level stabilization in semiconductors: Implications for implant activation efficiency
[DE88-006332] N88-22801
STABILIZERS (FLUID DYNAMICS)
Pointwise stabilization for coupled quasilinear and linear wave equations
[AD-A190031] N88-22632
STABLE OSCILLATIONS
Oscillating airfoils: Achievements and conjectures
[AD-A190490] N88-22008
STAGE SEPARATION
Investigation of Super*Zip separation joint
[NASA-TM-4031] N88-22072
STAINLESS STEELS
Segregation effects in welded stainless steels
[DE88-701224] N88-22139
Grain growth behavior of extrusion consolidated centrifugally atomized Type 304 stainless steel powder
[DE88-006788] N88-22143
STANDARDS
Computer grading of extensometers (BS 3846)
[NPL-DMA(A)-152] N88-22560
NASA and the challenge of ISDN: The role of satellites in an ISDN world
[NASA-CR-182749] N88-22676
STAR TRACKERS
Identification of a star field from a spinning satellite
[CNES-NT-120] N88-22074
STATE VECTORS
Linear state space modeling of a turbofan engine
[AD-A190110] N88-22035
STATISTICAL ANALYSIS
General aviation activity and avionics survey: 1986 data
[AD-A189986] N88-22003
Results of the International Comparison of Absolute Gravimeters (2nd) held in Sevres, France in June-July 1985
[AD-A189869] N88-22474
The collection of statistics on the frequency of cloud cover over North America
[AD-A190456] N88-22495
Properties of some Bayesian scoring procedures for computerized adaptive tests
[AD-A189925] N88-22660
Empirical and hierarchical Bayes competitors of preliminary test estimators in two sample problems
[AD-A190327] N88-22670
STATISTICAL DISTRIBUTIONS
Grain boundary oxidation and low-cycle fatigue at elevated temperatures N88-22420
Statistical inference for stochastic processes
[AD-A190491] N88-22673
STATISTICAL MECHANICS
Memory efficient evaluations of nonlinear stochastic equations and C3 applications
[AD-A189872] N88-22569
STATISTICAL TESTS
Distributions of quadratic forms
[AD-A190224] N88-22663
Stopping rules and observed significance levels
[AD-A190320] N88-22664
Admissible Bayes tests for structural relationship
[AD-A190326] N88-22669
STEADY STATE
Coupled bending-torsion steady-state response of pretwisted, nonuniform rotating beams using a transfer-matrix method
[NASA-TM-100596] N88-22435
Magnetic fusion energy plasma interactive and high heat flux components. Volume 5: Technical assessment of critical issues in the steady state operation of fusion confinement devices
[DE88-006920] N88-22744
STEELS
Influence of temperature on the tensile strength and toughness characteristics. Material 35NCD16 ESR. Test report M5-521800
[M5-521800] N88-22163
Characterization of HYTUF steel. Semifinished product: 160 mm dia forging block. Processor: C3f. Test Report M3-434600
[M3-434600] N88-22164
STEEPEST DESCENT METHOD
Dynamical optimization techniques for the calculation of electronic structure in solids
[DE88-006010] N88-22768
STELLAR MASS
Hydrodynamical models of supernova SN 1987 A in the LMC
[TI88-701123] N88-22837
STELLAR MODELS
Hydrodynamical models of supernova SN 1987 A in the LMC
[TI88-701123] N88-22837
STEREOCHEMISTRY
New phosphorus based polymer systems
[AD-A190457] N88-22186
STEREOPHONICS
Performance of single and multiple system AM stereo decoder receivers
[PB88-168307] N88-22265
STEREOPHOTOGRAPHY
Relative orientation
[AD-A190385] N88-22449
STIFFENING
Postbuckling delamination of a stiffened composite panel using finite element methods
[NASA-CR-182803] N88-22098
STIFFNESS
Investigation and synthesis of high temperature and increased stiffness RSP aluminum alloys
[AD-A190407] N88-22151
STIFFNESS MATRIX
An efficient Mindlin finite strip plate element based on assumed strain distribution N88-22407
STIMULATION
Amplification of signals in fiber optics using the stimulated Raman effect
[AD-A190281] N88-22727
STIRLING ENGINES
A survey of oscillating flow in Stirling engine heat exchangers
[NASA-CR-182108] N88-22322
STOCHASTIC PROCESSES
Random processes, turbulence and disordering fields
[AD-A190123] N88-22303
Vibrations of structures with parametric uncertainties
[AD-A190400] N88-22378
Probabilistic structural analysis computer code (NESSUS) N88-22397
Memory efficient evaluations of nonlinear stochastic equations and C3 applications
[AD-A189872] N88-22569
Using Colored Stochastic Petri Net (CS-PN) software for protocol specification, validation, and evaluation
[ENST-87C004] N88-22588
The Colored Stochastic Petri Net (CS-PN) software: Application to the validation and the performance evaluation of distributed systems
[ENST-87D005] N88-22589
The adjoint process in stochastic optimal control
[AD-A189720] N88-22605
Martingale representation and the Malliavin calculus
[AD-A189721] N88-22626
The existence of smooth densities for the prediction filtering and smoothing problems
[AD-A189865] N88-22629
Normed Bellman equation with degenerate diffusion coefficients and its application to differential equations
[AD-A190319] N88-22637
Random Process Simulation for stochastic fatigue analysis
[NASA-TM-100464] N88-22654
The partially observed stochastic minimum principle
[AD-A189787] N88-22658
Approximations in extreme value theory
[AD-A189817] N88-22659
Stopping rules and observed significance levels
[AD-A190320] N88-22664
Estimation of convolution tails
[AD-A190323] N88-22666
Continuity of symmetric stable processes
[AD-A190324] N88-22667
Extreme value for dependent sequences via the Stein-Chen method of poisson approximation
[AD-A190325] N88-22668
Detection of the number, locations and magnitudes of jumps
[AD-A190328] N88-22671
Statistical inference for stochastic processes
[AD-A190491] N88-22673
Stochastic evolution equations driven by nuclear space valued martingales
[AD-A189342] N88-22677
Conditions for information capacity of the discrete-time Gaussian channel to be increased by feedback
[AD-A190317] N88-22687
STOPPING
Stopping rules and observed significance levels
[AD-A190320] N88-22664
STORM DAMAGE
Forecast of Atlantic seasonal hurricane activity for 1988 N88-22500
STRAIN HARDENING
Response of aluminum alloys to erosive particle impacts
[DE88-005910] N88-22159
STRAIN MEASUREMENT
Research sensors N88-22430
STRAIN RATE
Effect of strain rate on high-temperature low-cycle fatigue behavior of Hastelloy X and Hastelloy XR
[DE88-752302] N88-22140
The CRREL (Cold Regions Research and Engineering Laboratory) Hopkinson bar apparatus
[AD-A190599] N88-22380
Unified constitutive model development for metal matrix composites at high temperature N88-22387
Unified constitutive model for single crystal deformation behavior with applications N88-22388
Phenomenological modelling of rate-dependent plasticity for high strain rate problems
[DE88-006647] N88-22440
STRAKES
Transonic Navier-Stokes computations of strake-generated vortex interactions for a fighter-like configuration
[NASA-TM-100009] N88-22010
STRATOSPHERE
Ultraviolet absorption cross sections of methylbromide at stratospheric temperatures
[AERONOMICA-ACTA-A-320-1987] N88-22132
Stratospheric electric field and conductivity measurements over electrified convective clouds in the South American region, revised
[INPE-4046-PRE/1012-REV-3] N88-22483
A study on electric fields and conductivity associated with electrified clouds in the region of South America
[INPE-4487-TDL/325] N88-22486

STREAK CAMERAS
Summary and conclusions on electrooptical streak camera project
[DE88-006616] N88-22334
STRESS ANALYSIS
Efficient method for structural optimization
N88-22240
Development of a computer code CRACK for elastic and elastoplastic fracture mechanics analysis of 2-D structures by finite element technique
[DE88-701231] N88-22370
Lewis Structures Technology, 1988. Volume 2: Structural Mechanics
[NASA-CP-3003-VOL-2] N88-22382
Finite element (MARC) solution technologies for viscoplastic analyses N88-22389
Three-dimensional inelastic approximate analysis code (MOMM) N88-22392
Specialty three-dimensional finite element analysis codes N88-22393
Probabilistic structural analysis computer code (NESSUS) N88-22397
Structural tailoring of advanced turboprops
N88-22400
Thermal-structural analyses of Space Shuttle Main Engine (SSME) hot section components N88-22404
Structural assessment of a space station solar dynamic heat receiver thermal energy storage canister
N88-22406
Whisker-reinforced ceramic composites for heat engine components N88-22410
STRESS CONCENTRATION
Evolution of hardening and damage during viscoplastic deformation
[AD-A190714] N88-22381
STRESS CORROSION CRACKING
Stress corrosion of ceramic materials
[AD-A190501] N88-22187
Environmentally assisted crack growth in structural alloys: Perspectives and new directions
[AD-A190137] N88-22377
STRESS DISTRIBUTION
A test for interfacial effects and stress transfer in ceramic matrix composites
[NASA-CR-182758] N88-22194
Phenomenological modelling of rate-dependent plasticity for high strain rate problems
[DE88-006647] N88-22440
STRESS INTENSITY FACTORS
Stress-intensity factors for small surface and corner cracks in plates
[NASA-TM-100599] N88-22445
STRESS RELAXATION
Corrosion Research Center, University of Minnesota
[DE88-006681] N88-22160
STRESS TENSORS
Phenomenological modelling of rate-dependent plasticity for high strain rate problems
[DE88-006647] N88-22440
STRESS WAVES
Numerical and experimental research on propagation of elastic stress waves in conical shell under axial impulsive loading N88-22238
STRESS-STRAIN DIAGRAMS
A simplified key-curve approach for J-R-curve testing of CT specimens
[VTT-RR-503] N88-22444
STRESS-STRAIN RELATIONSHIPS
The CRREL (Cold Regions Research and Engineering Laboratory) Hopkinson bar apparatus
[AD-A190599] N88-22380
Biaxial experiments supporting the development of constitutive theories for advanced high-temperature materials N88-22386
Fatigue damage mapping N88-22423
Bithermal fatigue: A simplified alternative to thermomechanical fatigue N88-22424
STRESSES
Real-time stressed channel simulator
[AD-A190223] N88-22067
Elasto-plastic analysis using a stress-based finite element method and an endochronic theory of plasticity
[DE88-003001] N88-22372
Does the pipe diffusion of self-interstitials in crystals under stresses exist
[TI88-701027] N88-22762
STRING THEORY
Recent developments in the path integral approach to anomalies
[DE87-703032] N88-22616
Path integral, BRS symmetry, and string and membrane theories
[DE88-752300] N88-22810
Involution-dependent constants and the cancellation of divergences in the 1-loop open string amplitude
[DE88-006537] N88-22811
Finite width corrections to the Nambu action for the Nielsen-Olesen string
[DE88-006996] N88-22812
Cosmology for high energy physicists
[DE88-005705] N88-22842
STRINGS
Hamiltonian formalism in the model of the relativistic string with rigidity
[TI88-701503] N88-22815
String driven inflation
[DE88-006994] N88-22841
STRIP TRANSMISSION LINES
Conformal microstrip slot antenna and antenna array
[AD-A189623] N88-22252
STRUCTURAL ANALYSIS
Galvanic corrosion initiatives
[AD-A190658] N88-22155
Transformation toughening of ceramics
[AD-A190399] N88-22183
Developments in ceramic superconducting materials
N88-22229
JPRS report: Science and technology. China
[JPRS-CST-87-043] N88-22233
Efficient method for structural optimization
N88-22240
UARS spacecraft recorder
[NASA-CR-180768] N88-22331
Buckling of blast loaded cylinder
[AD-A190124] N88-22376
Environmentally assisted crack growth in structural alloys: Perspectives and new directions
[AD-A190137] N88-22377
Vibrations of structures with parametric uncertainties
[AD-A190400] N88-22378
The composite blade structural analyzer (COBSTRAN)
N88-22390
Three-dimensional inelastic approximate analysis code (MOMM) N88-22392
METCAN: The metal matrix composite analyzer
N88-22395
Probabilistic structural analysis computer code (NESSUS) N88-22397
Structural tailoring of high-speed turbine blades (SSME/STAEBL) N88-22398
Computational structural mechanics for engine structures N88-22399
Structural tailoring of advanced turboprops
N88-22400
Advanced probabilistic methods for quantifying the effects of various uncertainties in structural response
N88-22401
Thermostructural analysis of simulated cowl lips
N88-22403
Thermal-structural analyses of Space Shuttle Main Engine (SSME) hot section components N88-22404
Structural analyses of engine wall cooling concepts and materials N88-22405
Structural assessment of a space station solar dynamic heat receiver thermal energy storage canister
N88-22406
Whisker-reinforced ceramic composites for heat engine components N88-22410
Continuous fiber ceramic matrix composites for heat engine components N88-22411
Flaw characterization in structural ceramics using scanning laser acoustic microscopy N88-22415
Improvements to tilt rotor performance through passive blade twist control
[NASA-TM-100583] N88-22434
Experimental design and structural optimization
[PB88-169255] N88-22436
Bilateral symmetry elements of the Zhamanshin impact crater
[NASA-TT-20288] N88-22490
Structural decomposition of multiple time scale Markov processes
[AD-A189739] N88-22657
An investigation of the crystalchemistry and thermochemistry of selected mineral systems
[AD-A189758] N88-22781
Path integral, BRS symmetry, and string and membrane theories
[DE88-752300] N88-22810
Research and technology
[NASA-TM-100172] N88-22851
STRUCTURAL DESIGN
Large-scale wind turbine structures N88-22429
STRUCTURAL ENGINEERING
Stabilization and control problems in structural dynamics
[AD-A190197] N88-22361
STRUCTURAL MEMBERS
A study of damage tolerance in curved composite panels
[AD-A190617] N88-22092
STRUCTURAL PROPERTIES (GEOLOGY)
Bilateral symmetry elements of the Zhamanshin impact crater
[NASA-TT-20288] N88-22490
STRUCTURAL RELIABILITY
Crack opening and extension in inert solid propellant. An experimental study
[AD-A189808] N88-22201
STRUCTURAL STABILITY
Vibrations of structures with parametric uncertainties
[AD-A190400] N88-22378
Rigidity and smoothness of motion
[AD-A190555] N88-22694
STRUCTURAL VIBRATION
Wave propagation and dynamics of lattice structures
[AD-A190037] N88-22066
Wave propagation and dynamics of lattice structures
[AD-A190611] N88-22069
Stabilization and control problems in structural dynamics
[AD-A190197] N88-22361
Instrumentation to provide an active control capability for distributed parameter systems
[AD-A190043] N88-22375
Vibrations of structures with parametric uncertainties
[AD-A190400] N88-22378
STRUTS
Duct flow nonuniformities: Effect of struts in SSME HGM II(+)
[NASA-CR-179285] N88-22296
SUBMINIATURIZATION
Development of subminiature multi-sensor hot-wire probes
[NASA-TM-100052] N88-22336
SUBROUTINES
Expressing mathematical subroutines constructively
[AD-A190559] N88-22644
SUBSTRATES
Vapor phase deposition and growth of polyimide films on copper
[AD-A189969] N88-22178
Laser evaporation studies
[AD-A189815] N88-22346
Processing defects and strength of alumina substrates
[W-10/87] N88-22441
High-efficiency thin-film silicon-on-GaP solar cell for improved radiation resistance
[AD-A190268] N88-22460
RF properties of superconducting Pb electroplated onto Cu
[DE88-005918] N88-22765
A model for nitrogen atom recombination on a silicon dioxide surface
[AD-A189843] N88-22784
Equilibrium stability of strained epitaxial layers on a rigid substrate
[INPE-4254-PRE/1127] N88-22804
Synthesis and characterization of high-T(sub c) screen-printed Y-Ba-Cu-O films on alumina
[NASA-TM-100860] N88-22805
SUCTION
Control of laminar flow around of the wing in free-air conditions
[AD-A187479] N88-22004
SULFUR DIOXIDES
Assessment of crop loss from air pollutants: Meteorology-atmospheric chemistry and long range transport
[PB88-146857] N88-22448
SUMMARIES
Summary and conclusions on electrooptical streak camera project
[DE88-006616] N88-22334
SUPERCOMPUTERS
Supercomputer environment
[AD-A190633] N88-22551
Implementation of a distributed adaptive routing algorithm on the Intel iPSC (Intel Personal Super-Computer)
[AD-A189849] N88-22567
SUPERCONDUCTING MAGNETS
Superconducting magnet technique for ASTROMAG on the space station
[DE88-004560] N88-22063
Fluids, gels and glasses under extreme conditions of pressure and temperature
[AD-A190655] N88-22125
Magnet strength fluctuations in the SSC (Superconducting Super Collider) lattice. Part 2: Frequency modulation
[DE88-006491] N88-22774
The Department of Defense Superconductivity Research and Development (DSRD) options. A study of possible directions for exploitation of superconductivity in military applications
[AD-A189747] N88-22780

SUPERCONDUCTING SUPER COLLIDER
Magnet strength fluctuations in the SSC (Superconducting Super Collider) lattice. Part 2: Frequency modulation
[DE88-006491] N88-22774
SUPERCONDUCTIVITY
Temperature-dependent conductivity of oxygen-depleted YBCO ceramics
[AD-A190340] N88-22182
Developments in ceramic superconducting materials N88-22229
RF properties of superconducting Pb electroplated onto Cu
[DE88-005918] N88-22765
Superconductivity and the tailoring of lattice parameters of the compound YBa2Cu3O(sub x)
[DE88-005904] N88-22769
Superconductivity in power engineering
[DE88-701414] N88-22776
The Department of Defense Superconductivity Research and Development (DSRD) options. A study of possible directions for exploitation of superconductivity in military applications
[AD-A189747] N88-22780
Thin superconducting film characterization by surface acoustic waves
[AD-A190417] N88-22791
Magnetic anomalies in the rare earth oxide superconductors GdBa2Cu3O(7-x) and YbBa2Cu3O(7-x)
[AD-A190713] N88-22793
Status of RF superconductivity at Argonne National Laboratory
[DE88-005913] N88-22796
High-T(sub c) superconducting wire fabrication and testing
[DE88-005989] N88-22798
High temperature superconductors in the La(sub 1+x)Ba(sub 2-x)Cu O(sub y system
[DE88-006367] N88-22802
Synthesis and characterization of high-T(sub c) screen-printed Y-Ba-Cu-O films on alumina
[NASA-TM-100860] N88-22805
SUPERCONDUCTORS
Temperature-dependent conductivity of oxygen-depleted YBCO ceramics
[AD-A190340] N88-22182
Melt processing ceramic YBa2Cu3O(sub 6.9)
[DE88-007039] N88-22199
Function of Japan Fine Ceramics Center described N88-22227
Synthesis of metastable superconductors by high dynamic pressure
[DE88-005620] N88-22764
Effective electron interactions due to virtual charge and spin excitations in an extended Hubbard model for Cu-O superconductors
[DE88-005971] N88-22766
Superconductivity in power engineering
[DE88-701414] N88-22776
Magnetic anomalies in the rare earth oxide superconductors GdBa2Cu3O(7-x) and YbBa2Cu3O(7-x)
[AD-A190713] N88-22793
SUPERCRITICAL AIRFOILS
Investigation of side-wall effects in wind tunnel with supercritical airfoil testing N88-22241
SUPERGRAVITY
Ten dimensional N = 1 supergravity coupled to supersymmetric Yang-Mills fields in superspace
[DE87-703033] N88-22808
SUPERLATTICES
Experimental studies on electronic properties of HgTe/CdTe and Hg sub 1-z Cd sub x Te/CdTe heterostructures and superlattices
[AD-A189826] N88-22783
Fundamental properties and devices applications of Ge(x)Si(1-x)/Si superlattices
[AD-A190129] N88-22787
SUPERNOVAE
Hydrodynamical models of supernova SN 1987 A in the LMC
[TI88-701123] N88-22837
SUPERPLASTICITY
Superplastic flow of mullite-zirconia composites
[DE88-005905] N88-22085
SUPERSATURATION
Nucleation in super-saturated products
[NASA-TT-20275] N88-22134
SUPERSONIC COMBUSTION
Turbulent reacting flows and supersonic combustion
[AD-A189690] N88-22115
SUPERSONIC COMBUSTION RAMJET ENGINES
Numerical and experimental investigation of multiple shock wave/turbulent boundary layer interactions in a rectangular duct
[AD-A190772] N88-22320
SUPERSONIC FLOW
Basic instability mechanisms in chemically reacting subsonic and supersonic flows
[AD-A190101] N88-22120
JPRS report: Science and technology. China
[JPRS-CST-87-043] N88-22233
Zero-lift drag predictions in supersonic flow for complex configurations N88-22246
Numerical and experimental investigation of multiple shock wave/turbulent boundary layer interactions in a rectangular duct
[AD-A190772] N88-22320
SUPERSONIC WIND TUNNELS
Numerical and experimental investigation of multiple shock wave/turbulent boundary layer interactions in a rectangular duct
[AD-A190772] N88-22320
SURFACE CRACKS
Stress-intensity factors for small surface and corner cracks in plates
[NASA-TM-100599] N88-22445
SURFACE DEFECTS
Measurement of the elastic-plastic surface flaw back surface topology and its relation to constraint
[DE88-006765] N88-22437
SURFACE FINISHING
Specimen preparation techniques for the examination of ceramic and metal-matrix composites
[DE88-005157] N88-22094
SURFACE LAYERS
High-efficiency thin-film silicon-on-GaP solar cell for improved radiation resistance
[AD-A190268] N88-22460
Studies of surfaces using optical sum-frequency generation
[DE88-006334] N88-22715
Calculating depletion region carrier concentrations with capacitance-voltage measurements and etching
[AD-A189630] N88-22777
SURFACE PROPERTIES
Study of surface discharges
[ONERA-12/7236-PY] N88-22073
Structure of sol-gel silica
[DE88-006870] N88-22114
Measurement of emissivity of industrial surfaces using a simple method
[NASA-TT-20165] N88-22130
The thermal radiative properties of metals at high temperature
[DE88-006625] N88-22141
JPRS report: Science and technology. Japan
[JPRS-JST-88-002] N88-22210
Material surface improvement by laser N88-22217
First-principles calculations of quasiparticle energies at surfaces and interfaces: Semiconductor surface-state spectra and band offsets
[DE88-006340] N88-22773
SURFACE REACTIONS
Methods of measurement for the evaluation of monolayer properties. Development and applications — lung surfactants
[ETN-88-92229] N88-22532
SURFACE ROUGHNESS
Effect of freestream turbulence on a two dimensional cascade, with different surface roughness, at high Reynolds number
[AD-A190615] N88-22316
SURFACE STABILITY
The sensitivity of boundary layer instability growth rates to compliant wall properties
[AD-A190433] N88-22309
SURFACE TEMPERATURE
Research sensors N88-22430
SURFACE TO SURFACE MISSILES
LGM-30B stage 2 disected motor test report
[AD-A190771] N88-22079
SURFACE WAVES
Thin superconducting film characterization by surface acoustic waves
[AD-A190417] N88-22791
SURFACTANTS
Methods of measurement for the evaluation of monolayer properties. Development and applications — lung surfactants
[ETN-88-92229] N88-22532
SURGES
Molecular dynamics of materials possessing high energy content
[AD-A190034] N88-22118
Polarimetric ISAR imaging using either measured or calculated transient signatures
[AD-A190077] N88-22259
SUSPENDING (HANGING)
Oscillation damped movement of suspended objects
[DE88-005715] N88-22433
SWEPT WINGS
Boundary-layer and wake measurements on a swept, circulation-control wing
[NASA-TM-89426] N88-22013
Theoretical investigation of secondary instability of three-dimensional boundary-layer flows with application to the DFVLR-F5 model wing
[DFVLR-FB-87-44] N88-22330
SWITCHES
Analysis of anomalous resistivity during the conduction phase of the plasma erosion opening switch
[DE88-006382] N88-22286
Repetitive opening switches using optically activated semiconductors
[AD-A190196] N88-22790
SWITCHING
Optical switching and control techniques using nonlinear optical wave mixing
[AD-A190467] N88-22730
SWITCHING CIRCUITS
The modeling, simulation and comparison of interconnection networks for parallel processing
[AD-A190571] N88-22599
SYMMETRY
Symmetry and global bifurcation in nonlinear solid mechanics
[AD-A190521] N88-22642
Ten dimensional N = 1 supergravity coupled to supersymmetric Yang-Mills fields in superspace
[DE87-703033] N88-22808
Path integral, BRS symmetry, and string and membrane theories
[DE88-752300] N88-22810
SYNAPSES
Synapses that compute motion
[AD-A190389] N88-22607
SYNCHRONOUS MOTORS
A high performance inverter-fed drive system of an interior permanent magnet synchronous machine
[DE88-006753] N88-22288
SYNCHROTRON RADIATION
Advances in geochemistry and cosmochemistry: Trace element microdistributions with the synchrotron X-ray fluorescence microprobe
[DE88-006355] N88-22108
Transport simulations of ohmic ignition experiment: IGNITEX
[DE88-006055] N88-22757
SYNTHESIS (CHEMISTRY)
The combustion synthesis of boride composites
[DE88-005474] N88-22084
Research on stable processible conducting polymers for electronic applications
[AD-A190246] N88-22180
New phosphorus based polymer systems
[AD-A190457] N88-22186
A new approach to highly fluorinated lubricants
[AD-A190523] N88-22188
Evaluation of direct methane conversion to higher hydrocarbons and oxygenates
[DE88-003812] N88-22204
Synthesis of metastable superconductors by high dynamic pressure
[DE88-005620] N88-22764
Remarks on solid state amorphizing transformations
[DE88-006452] N88-22803
Synthesis and characterization of high-T(sub c) screen-printed Y-Ba-Cu-O films on alumina
[NASA-TM-100860] N88-22805
SYNTHETIC APERTURE RADAR
Synthetic-aperture radars viewed as interferometers with matched filter processing of the collected data
[AD-A190608] N88-22262
SYSTEM FAILURES
Modeling failures of intermittently used machines
[AD-A190298] N88-22367
SYSTEMS ANALYSIS
A systems analysis of fire suppression alternatives for the US space station
[AD-A189847] N88-22064
Comparative analysis
[AD-A190556] N88-22313
Monitoring the usage of a computer system
[DE88-004310] N88-22542
SYSTEMS ENGINEERING
Aluminum-air battery development
[DE88-006620] N88-22287
Designs of profiles for cascades
[NASA-TT-20161] N88-22326
Reliability analysis within a Computer Aided Engineering (CAE) infrastructure
[NLR-MP-86059-U] N88-22369
SYSTEMS INTEGRATION
Supercomputer environment
[AD-A190633] N88-22551

SYSTEMS SIMULATION
An intelligent simulation model generator
[REPT-87-053] N88-22562

T

TANDEM MIRRORS
New methods of confinement and heating of plasma in magnetic fields
[TI88-701021] N88-22738
TAPE RECORDERS
UARS spacecraft recorder
[NASA-CR-180768] N88-22331
Mechanisms mediating perception of complex acoustic patterns
[AD-A189765] N88-22520
TARGET ACQUISITION
Design and implementation of VLSI prime factor algorithm processor
[AD-A190483] N88-22580
TARGET RECOGNITION
Effect of friction and control parameters on the tracking accuracy of a target seeker
[AD-A190010] N88-22257
Polarimetric ISAR imaging using either measured or calculated transient signatures
[AD-A190077] N88-22259
Multi-disciplinary techniques for understanding time-varying space-based imagery
[AD-A190711] N88-22610
Rigidity and smoothness of motion
[AD-A190555] N88-22694
Method and device for the detection and identification of a helicopter
[NASA-TT-20251] N88-22696
TARGETS
Advanced guidance algorithms for homing missiles with bearings-only measurements
[AD-A190435] N88-22026
A multiple model adaptive tracking algorithm against airborne targets
[AD-A190619] N88-22263
TAYLOR INSTABILITY
Rayleigh-Taylor instability in inertial confinement fusion
[TI88-701411] N88-22750
TAYLOR SERIES
Efficient method for structural optimization
N88-22240
Expressing mathematical subroutines constructively
[AD-A190559] N88-22644
TECHNOLOGY ASSESSMENT
Extension of free-electron lasers into the extreme ultraviolet
[DE88-005373] N88-22341
Energy from the wind
[DE88-006897] N88-22459
A method for estimating and controlling the cost of extending technology
[AD-A190717] N88-22831
TECHNOLOGY TRANSFER
Recent advances in photovoltaic concentrator technology
[DE88-003948] N88-22482
Small and medium power reactors 1987
[TI88-701435] N88-22720
TECHNOLOGY UTILIZATION
External tank gamma ray imaging telescope study. Final review, phase 2
[NASA-CR-179320] N88-22834
TELEMETRY
Geometric restoration of satellite image data
[AD-A190462] N88-22450
TELEOPERATORS
Design, development and evaluation of Stanford/Ames EVA prehensors
[NASA-CR-182688] N88-22540
TELESCOPES
External tank gamma ray imaging telescope study. Final review, phase 2
[NASA-CR-179320] N88-22834
TEMPERATURE
Calibration and processing of AVHRR data for temperature estimation
[INPE-4493-PRE/1257] N88-22485
Monthly mean global climatology of temperature, wind, geopotential height, and pressure for 0 - 120 km
[NASA-TM-100697] N88-22503
Physical, chemical and CTD (Conductivity/Temperature/Depth) data from the Marathon 2 expedition
[AD-A189930] N88-22507
TEMPERATURE CONTROL
Advanced capacitor development
[AD-A189965] N88-22276
TEMPERATURE DEPENDENCE
Temperature-dependent conductivity of oxygen-depleted YBCO ceramics
[AD-A190340] N88-22182
TEMPERATURE DISTRIBUTION
Thermal instability and heat transfer characteristics in water/ice systems
[AD-A189627] N88-22297
TEMPERATURE EFFECTS
Corrosion Research Center, University of Minnesota
[DE88-006681] N88-22160
Influence of temperature on the tensile strength and toughness characteristics. Material 35NCD16 ESR. Test report M5-521800
[M5-521800] N88-22163
Grain boundary oxidation and low-cycle fatigue at elevated temperatures N88-22420
Examination of temperature effects on gate-to-drain avalanche breakdown in GaAs MESFETs (Metal-Semiconductor Field Effect Transistors) by measuring light emission under RF drive
[AD-A189634] N88-22778
TEMPERATURE GRADIENTS
Experiments investigating advanced materials under thermomechanical loading N88-22385
TEMPERATURE MEASUREMENT
Measurement of emissivity of industrial surfaces using a simple method
[NASA-TT-20165] N88-22130
Rocket measurements of ionospheric electron temperature over Natal
[INPE-4485-PRE/1250] N88-22489
TEMPERATURE PROFILES
Aerodynamic aspects of the Amazon Forest
[INPE-4445-TDL/313] N88-22501
TENSILE STRENGTH
The age hardening response of thermomechanically processed Al-Mg-Li alloys
[AD-A189870] N88-22147
Cracking tendencies of restrained welds in high strength low alloy steels under hyperbaric conditions
[AD-A190255] N88-22150
Influence of temperature on the tensile strength and toughness characteristics. Material 35NCD16 ESR. Test report M5-521800
[M5-521800] N88-22163
Characterization of HYTUF steel. Semifinished product: 160 mm dia forging block. Processor: C3I. Test Report M3-434800
[M3-434600] N88-22164
TENSILE TESTS
The effective fracture toughness of aluminum at rapid heating rates
[AD-A189745] N88-22146
A test for interfacial effects and stress transfer in ceramic matrix composites
[NASA-CR-182758] N88-22194
TERRAIN
Modification of the BLUEMAX 2 terrain following model to incorporate radar detection
[AD-A190594] N88-22028
The visit problem: Visibility graph-based solution
[DE88-000343] N88-22556
TERRAIN ANALYSIS
Modification of the BLUEMAX 2 terrain following model to incorporate radar detection
[AD-A190594] N88-22028
TEST CHAMBERS
Study of mean free path effects on growth of ultrafine metallic aerosols
[AD-A190206] N88-22149
TEST FACILITIES
Procedures and requirements for testing in the Langley Research Center unitary plan wind tunnel
[NASA-TM-100529] N88-22016
Small engine components test facility turbine testing cell
[NASA-TM-100887] N88-22037
Investigation of aeroacoustic mechanisms by remote thermal imaging
[DE88-002612] N88-22048
EMR (Electromagnetic Radiation) test facilities evaluation of reverberating chamber located at RADC (Rome Air Development Center), Griffiss AFB (Air Force Base), Rome, New York
[PB88-178827] N88-22048
Investigations of test methodology for the stress loading facility
[PB88-186095] N88-22049
Description of ground motion data processing codes, volume 2
[DE88-007137] N88-22481
Requirements and cost considerations for a Combined Space Nuclear Reactor Test Facility
[DE88-006763] N88-22719
Space directorate research and technology accomplishments for fiscal year 1987
[NASA-TM-100607] N88-22854
TEXTURES
Finding texture boundaries in images
[AD-A190554] N88-22609
TF-34 ENGINE
Noise assessment of unsuppressed TF-34-GE-100A engine at Warfield ANG, Baltimore, Maryland
[AD-A189966] N88-22702
THEMATIC MAPPERS (LANDSAT)
Method for restoration and resampling of TM sensor imagery
[INPE-4491-PRE/1255] N88-22454
THEOREM PROVING
About disequations simplification
[RR-645-I-IMAG-55-LIFIA] N88-22624
THERMAL ANALYSIS
Investigation of Super*Zip separation joint
[NASA-TM-4031] N88-22072
Thermal analysis of heat storage canisters for a solar dynamic, space power system
[DE88-004199] N88-22075
Boundary shape identification problems in two-dimensional domains related to thermal testing of materials
[NASA-CR-181654] N88-22541
THERMAL CONDUCTIVITY
Thermal conductivity of oxide ceramics
[DE88-005842] N88-22169
Material surface improvement by laser N88-22217
THERMAL EXPANSION
Thermal expansion behavior of randomly oriented short carbon fiber reinforced copper composites
[NASA-TT-20175] N88-22099
Features and applications of the integrated composites analyzer (ICAN) code N88-22391
Thermal stress in high temperature cylindrical fasteners
[NASA-TM-100611] N88-22438
THERMAL FATIGUE
Effect of strain rate on high-temperature low-cycle fatigue behavior of Hastelloy X and Hastelloy XR
[DE88-752302] N88-22140
Bithermal fatigue of a nickel-base superalloy single crystal
[NASA-TM-100885] N88-22168
Unified constitutive model for single crystal deformation behavior with applications N88-22398
Elevated temperature crack growth N88-22421
Bithermal fatigue: A simplified alternative to thermomechanical fatigue N88-22424
Analyses and experiments on the integrity and lifetime predictions of plasma-facing components in fusion reactors
[DE87-702957] N88-22735
THERMAL INSTABILITY
Thermal instability and heat transfer characteristics in water/ice systems
[AD-A189627] N88-22297
THERMAL MAPPING
Investigation of aeroacoustic mechanisms by remote thermal imaging
[DE88-002612] N88-22048
THERMAL PROTECTION
Aerothermal tests of quilted dome models on a flat plate at a Mach number of 6.5
[NASA-TP-2804] N88-22325
THERMAL SHOCK
Response of aluminum alloys to erosive particle impacts
[DE88-005910] N88-22159
THERMAL STABILITY
High-performance polymeric materials
[AD-A190708] N88-22190
Stability of the high-temperature G-18 primer composition
[DE88-006201] N88-22206
THERMAL STRESSES
Thermal analysis of heat storage canisters for a solar dynamic, space power system
[DE88-004199] N88-22075
Fundamental studies on high temperature deformation recrystallization, and grain growth of two-phase materials
[AD-A189725] N88-22145
A test for interfacial effects and stress transfer in ceramic matrix composites
[NASA-CR-182758] N88-22194
High-temperature combustor liner tests in structural component response test facility N88-22383
Specialty three-dimensional finite element analysis codes N88-22393
MHOST: An efficient finite element program for inelastic analysis of solids and structures N88-22394
METCAN: The metal matrix composite analyzer N88-22395

Structural tailoring of high-speed turbine blades (SSME/STAEBL) N88-22398
Thermostructural analysis of simulated cowl lips N88-22403
Thermal-structural analyses of Space Shuttle Main Engine (SSME) hot section components N88-22404
Structural analyses of engine wall cooling concepts and materials N88-22405
Elevated temperature crack growth N88-22421
Thermal stress in high temperature cylindrical fasteners
[NASA-TM-100611] N88-22438

THERMOCHEMISTRY
Thermochemistry and high temperature thermodynamic properties of rare earth-alkaline earth-copper oxide superconductors
[DE88-005976] N88-22770
An investigation of the crystalchemistry and thermochemistry of selected mineral systems
[AD-A189758] N88-22781

THERMODYNAMIC PROPERTIES
The thermal radiative properties of metals at high temperature
[DE88-006625] N88-22141
Thermochemistry and high temperature thermodynamic properties of rare earth-alkaline earth-copper oxide superconductors
[DE88-005976] N88-22770

THERMODYNAMICS
Nucleation in super-saturated products
[NASA-TT-20275] N88-22134
The age hardening response of thermomechanically processed Al-Mg-Li alloys
[AD-A189870] N88-22147
Comparison of entropy generation and conventional design methods for heat exchangers
[AD-A190256] N88-22306
Nondestructive evaluation of sintered ceramics N88-22416
Sequential tests for the drift of a Wiener process with a smooth prior and the heat equation
[AD-A190322] N88-22638

THERMOMECHANICAL TREATMENT
Experiments investigating advanced materials under thermomechanical loading N88-22385
METCAN: The metal matrix composite analyzer N88-22395

THERMONUCLEAR REACTIONS
Rayleigh-Taylor instability in inertial confinement fusion
[TI88-701411] N88-22750

THERMOPLASTIC RESINS
Interlaminar fracture toughness of thermoplastic composites
[NASA-TM-100532] N88-22097
Mechanical behaviour of particle filled thermoplastics
[PB88-169297] N88-22196

THICK FILMS
Synthesis and characterization of high-T(sub c) screen-printed Y-Ba-Cu-O films on alumina
[NASA-TM-100860] N88-22805

THICKNESS
A new method of measuring multigrade oil shear elasticity and viscosity at high shear rates
[AD-A190145] N88-22304

THIN FILMS
Structure and properties of titanium nitride and zirconium nitride thin films prepared by reactive ion plating --- cutting tools
[ETN-88-92218] N88-22167
Vapor phase deposition and growth of polyimide films on copper
[AD-A189969] N88-22178
Development of a laboratory test for multiport injector deposits: Approaches 1 and 2
[AD-A190697] N88-22203
Laser evaporation studies
[AD-A189815] N88-22346
High-efficiency thin-film silicon-on-GaP solar cell for improved radiation resistance
[AD-A190268] N88-22460
Fundamental studies of the mechanical behavior of microelectronic thin film materials
[AD-A190038] N88-22786
Thin superconducting film characterization by surface acoustic waves
[AD-A190417] N88-22791

THREAT EVALUATION
Investigations of test methodology for the stress loading facility
[PB88-166095] N88-22049

THREE BODY PROBLEM
Adiabatic representation of three-body problem in hyperspherical coordinates. Statement of the problem
[TI88-701162] N88-22678

THREE DIMENSIONAL BODIES
A three-dimensional model for the elastic properties of a foam
[DE88-006197] N88-22192
A 3-D solid rendering of NDT data
[DE88-006199] N88-22373
On the geometric interpretation of image contours
[RR-647-I-IMAG-57-LIFIA] N88-22563

THREE DIMENSIONAL BOUNDARY LAYER
Theoretical investigation of secondary instability of three-dimensional boundary-layer flows with application to the DFVLR-F5 model wing
[DFVLR-FB-87-44] N88-22330

THREE DIMENSIONAL FLOW
Experimental investigation of a spanwise forced mixing layer
[AD-A190136] N88-22007
Trends in Computational Fluid Dynamics (CFD) for aeronautical 3D steady applications: The Dutch situation
[NLR-MP-86074-U] N88-22017

THREE DIMENSIONAL MOTION
A three dimensional non-singular modelling of rigid manipulators
[AD-A189707] N88-22604
Rigidity and smoothness of motion
[AD-A190555] N88-22694

THRUST CHAMBERS
MPD (magnetoplasmadynamic) thrust chamber flow dynamics
[AD-A189940] N88-22751

THRUST VECTOR CONTROL
Pressure measurements of impinging jet with asymmetric nozzle
[NASA-CR-182759] N88-22011
Heat transfer modeling of jet vane Thrust Vector Control (TVC) systems
[AD-A190106] N88-22034
Experimental investigation of two-dimensional confined jet thrust vector control
[AD-A189845] N88-22077

THUNDERSTORMS
Stratospheric electric field and conductivity measurements over electrified convective clouds in the South American region, revised
[INPE-4046-PRE/1012-REV-3] N88-22483

TILT ROTOR AIRCRAFT
Improvements to tilt rotor performance through passive blade twist control
[NASA-TM-100583] N88-22434

TIME
CK-LOG system conversion (user's manual and user interface)
[AD-A190273] N88-22577

TIME LAG
The effects of torque response and time delay on rotorcraft vertical axis handling qualities
[AD-A189873] N88-22023

TIME OF FLIGHT SPECTROMETERS
High-voltage inverse-square function generator
[DE88-701109] N88-22270

TIME SERIES ANALYSIS
Spectral measurements in a disturbed boundary layer over snow
[AD-A190217] N88-22494
Simulation analysis of moored fluorometer time series from the Mid-Atlantic Bight
[DE88-006066] N88-22505

TIP SPEED
Visualisation of the flow at the tip of a high speed axial flow turbine rotor
[AD-A189926] N88-22300
Visualisation of the flow at the tip of a high speed axial flow turbine rotor: An assessment of flow visualisation techniques and the requirement of the experimental turbine
[AD-A189929] N88-22301

TITANIA
Hafnia-rich mixed oxide ceramics of the system HfO2-ZrO2-TiO2 for heaters and heat exchangers in electrothermal thrusters: The effects of titania on selected electrical and mechanical properties of Hafnia-rich mixed oxides in the system Hafnia-Zirconia-Titania, volume 1
[NASA-CR-182600-VOL-1] N88-22197

TITANIUM ALLOYS
Growth and deformation mechanisms of refractory alloy hybrid materials
[AD-A190492] N88-22152
Investigation of laser diagnostics of PACVD processes for depositing hard face coatings
[DE88-007083] N88-22176

TITANIUM NITRIDES
Structure and properties of titanium nitride and zirconium nitride thin films prepared by reactive ion plating --- cutting tools
[ETN-88-92218] N88-22167

TOKAMAK DEVICES
Preparing the Alcator C bolometer system for use on MTX (Microwave Tokamak Experiment)
[DE88-006724] N88-22733
Analyses and experiments on the integrity and lifetime predictions of plasma-facing components in fusion reactors
[DE87-702957] N88-22735
Environmental assessment for the compact ignition Tokamak
[DE88-005633] N88-22740
Long-time impurity confinement as a precursor to disruptions in ohmically heated tokamaks
[DE88-006183] N88-22742
Current-drive on the Versator-2 tokamak with a slotted-waveguide fast-wave coupler
[DE88-006261] N88-22743
Improvement of plasma confinement due to electron Landau damping in tokamaks
[DE88-752339] N88-22747
Transport simulations of ohmic ignition experiment: IGNITEX
[DE88-006055] N88-22757

TOLERANCES (MECHANICS)
A study of damage tolerance in curved composite panels
[AD-A190617] N88-22092

TOPOLOGY
Measurement of the elastic-plastic surface flaw back surface topology and its relation to constraint
[DE88-006765] N88-22437

TOROIDAL PLASMAS
Theoretical studies of the heating of toroidal plasmas with radiofrequency electromagnetic radiation
[DE88-006913] N88-22749

TORQUE
The effects of torque response and time delay on rotorcraft vertical axis handling qualities
[AD-A189873] N88-22023

TORQUE MOTORS
A high performance inverter-fed drive system of an interior permanent magnet synchronous machine
[DE88-006753] N88-22288

TORSION
Coupled bending-torsion steady-state response of pretwisted, nonuniform rotating beams using a transfer-matrix method
[NASA-TM-100596] N88-22435

TOUGHNESS
Fracture toughness testing of a ceramic matrix composite
[AD-A189846] N88-22089
Influence of temperature on the tensile strength and toughness characteristics. Material 35NCD16 ESR. Test report M5-521800
[M5-521800] N88-22163
Characterization of HYTUF steel. Semifinished product: 160 mm dia forging block. Processor: C3f. Test Report M3-434600
[M3-434600] N88-22164
Transformation toughening of ceramics
[AD-A190399] N88-22183

TOWED BODIES
Bodies in unsteady flow
[AD-A190416] N88-22308

TOXICITY
Evaluation of the acute toxicity of a synthetic polyalphaolefin-based hydraulic fluid
[AD-A190412] N88-22184

TRACE ELEMENTS
Advances in geochemistry and cosmochemistry: Trace element microdistributions with the synchrotron X-ray fluorescence microprobe
[DE88-006355] N88-22108

TRACKING (POSITION)
Multiple model parameter adaptive control for in-flight simulation
[AD-A190568] N88-22044
Moving-bank multiple model adaptive estimation applied to flexible spacestructure control
[AD-A190761] N88-22071
Effect of friction and control parameters on the tracking accuracy of a target seeker
[AD-A190010] N88-22257
A multiple model adaptive tracking algorithm against airborne targets
[AD-A190619] N88-22263

TRACKING FILTERS
A multiple model adaptive tracking algorithm against airborne targets
[AD-A190619] N88-22263

TRACTION
Traction model development
[AD-A188450] N88-22359

TRAJECTORY ANALYSIS
Spacecraft trajectories
[ISBN-2-85-428166-7] N88-22054
TRAJECTORY MEASUREMENT
Spacecraft trajectories
[ISBN-2-85-428166-7] N88-22054
A multiple model adaptive tracking algorithm against airborne targets
[AD-A190619] N88-22263
TRAJECTORY OPTIMIZATION
Performance optimization of a cruise missile using dynamic-stall induced lift augmentation
[AD-A190497] N88-22027
TRANSCENDENTAL FUNCTIONS
High speed transcendental elementary function architecture in support of the Vector Wave Equation (VWE)
[AD-A189746] N88-22627
TRANSDUCERS
Computer grading of extensometers (BS 3846)
[NPL-DMA(A)-152] N88-22580
TRANSFER FUNCTIONS
Coupled bending-torsion steady-state response of prewisted, nonuniform rotating beams using a transfer-matrix method
[NASA-TM-100596] N88-22435
Method for restoration and resampling of TM sensor imagery
[INPE-4491-PRE/1255] N88-22454
Experimental comparison of lightning simulation techniques to CV-580 airborne lightning strike measurements
[AD-A190576] N88-22496
TRANSFORMATIONS (MATHEMATICS)
Remarks on the time transformation of path-integral measures
[DE87-703040] N88-22617
Baecklund transformation and the Schwarzian derivative
[AD-A190277] N88-22684
Space time processing, environmental-acoustic effects
[AD-A190764] N88-22708
TRANSIENT RESPONSE
Transient compressible flow in porous materials
[DE88-006885] N88-22324
TRANSMITTER RECEIVERS
The 2 FSK/QPSK (Frequency Shift Keying/Quadrature Phase Shift Keying) transmitter and receiver: Design and performance
[AD-A190028] N88-22258
TRANSMITTERS
A 104-km unrepeatered bidirectional fiber optic demonstration link
[AD-A190282] N88-22726
TRANSONIC FLOW
Computational fluid dynamics drag prediction: Results from the Viscous Transonic Airfoil Workshop
[NASA-TM-100095] N88-22009
Mixed direct-inverse problem of transonic cascade N88-22244
A zonal approach for the solution of coupled Euler and potential solutions of flows with complex geometries
[AD-A189752] N88-22595
A physically consistent model for artificial dissipation in transonic potential flow computations
[NASA-TM-100846] N88-22652
TRANSONIC WIND TUNNELS
Modifications to the Langley 8-foot transonic pressure tunnel for the laminar flow control experiment
[NASA-TM-4032] N88-22047
TRANSPARENCE
The interaction of small particles with laser beams
[AD-A190716] N88-22354
TRANSPORT AIRCRAFT
Trends in Computational Fluid Dynamics (CFD) for aeronautical 3D steady applications: The Dutch situation
[NLR-MP-86074-U] N88-22017
KRASH parametric sensitivity study: Transport category airplanes
[AD-A189962] N88-22024
TRANSPORT PROPERTIES
Electronic and ionic transport in polymers
[AD-A190434] N88-22185
TRANSPORT THEORY
FLOSIN: A fluid loop analyzer for SINDA N88-22321
Transport simulations of ohmic ignition experiment: IGNITEX
[DE88-006055] N88-22757
TRAPPED MAGNETIC FIELDS
New methods of confinement and heating of plasma in magnetic fields
[TI66-701021] N88-22738
TRAPPED PARTICLES
Modeling the effects of heavy charged particles on MOSFETs (Metal-Oxide-Semiconductor Field Effect Transistors)
[AD-A190575] N88-22792
TRENDS
Function of Japan Fine Ceramics Center described N88-22227
Marshall Space Flight Center 1960-1985: 25th anniversary report
[NASA-TM-100328] N88-22852
TRIANGLES
Non-rigid motion and Regge calculus
[AD-A190387] N88-22640
TRIAXIAL STRESSES
Periodic orbits around a satellite modelled as a triaxial ellipsoid
[AD-A190592] N88-22051
TRIGONOMETRIC FUNCTIONS
High speed transcendental elementary function architecture in support of the Vector Wave Equation (VWE)
[AD-A189746] N88-22627
TROPICAL REGIONS
Tropical circulations and the associated rainfall anomalies during two contrasting years
[INPE-4506-PRE/1261-REV] N88-22502
TUBE CATHODES
Program to research laser-driven thermionic electron sources for free electron lasers
[AD-A190473] N88-22353
TUNABLE LASERS
Diode laser spectroscopy of chemical moieties at surfaces
[AD-A190710] N88-22127
TURBINE BLADES
Structural tailoring of high-speed turbine blades (SSME/STAEBL) N88-22398
Advanced probabilistic methods for quantifying the effects of various uncertainties in structural response N88-22401
TURBOCOMPRESSORS
Small engine components test facility turbine testing cell
[NASA-TM-100887] N88-22037
TURBOFAN ENGINES
Linear state space modeling of a turbofan engine
[AD-A190110] N88-22035
Noise assessment of unsuppressed TF-34-GE-100A engine at Warfield ANG, Baltimore, Maryland
[AD-A189966] N88-22702
TURBOMACHINERY
Visualization of flows in turbomachinery
[AD-A189927] N88-22299
TURBULENCE
Numerical simulation of turbulent flames using vortex methods
[AD-A189813] N88-22116
Basic instability mechanisms in chemically reacting subsonic and supersonic flows
[AD-A190101] N88-22120
Random processes, turbulence and disordering fields
[AD-A190123] N88-22303
Film cooling effectiveness on a flat plate in high free-stream turbulence using a single row of 30 deg slant-hole injectors
[AD-A190500] N88-22816
TURBULENCE EFFECTS
Effect of freestream turbulence on a two dimensional cascade, with different surface roughness, at high Reynolds number
[AD-A190615] N88-22316
High power, high frequency radiation from beam-plasma interactions
[AD-A190207] N88-22752
TURBULENT BOUNDARY LAYER
Enhanced viscous flow drag reduction using acoustic excitation
[NASA-CR-182734] N88-22295
Bodies in unsteady flow
[AD-A190416] N88-22308
Effect of freestream turbulence on a two dimensional cascade, with different surface roughness, at high Reynolds number
[AD-A190615] N88-22316
Numerical and experimental investigation of multiple shock wave/turbulent boundary layer interactions in a rectangular duct
[AD-A190772] N88-22320
Aerothermal tests of quilted dome models on a flat plate at a Mach number of 6.5
[NASA-TP-2804] N88-22325
TURBULENT FLOW
Turbulent reacting flows and supersonic combustion
[AD-A189690] N88-22115
An investigation of flow structure, mixing and chemical reaction in combusting turbulent flows
[AD-A189980] N88-22117
Duct flow nonuniformities: Effect of struts in SSME HGM II(+)
[NASA-CR-179285] N88-22296
Chemically reacting turbulent flow
[AD-A190522] N88-22311
Experiments on densely-loaded non-Newtonian slurries in laminar and turbulent pipe flows
[DE88-006209] N88-22323
Development of subminiature multi-sensor hot-wire probes
[NASA-TM-100052] N88-22336
Describing the source created by turbulent flow over orifices and louvers
[AD-A190254] N88-22706
TURBULENT WAKES
Effect of freestream turbulence on a two dimensional cascade, with different surface roughness, at high Reynolds number
[AD-A190615] N88-22316
TWO DIMENSIONAL BODIES
Boundary shape identification problems in two-dimensional domains related to thermal testing of materials
[NASA-CR-181654] N88-22541
Two-dimensional graphics tools for a transputer based display board
[NASA-TM-100820] N88-22591
TWO DIMENSIONAL BOUNDARY LAYER
Experimental investigation of two-dimensional confined jet thrust vector control
[AD-A189845] N88-22077
TWO DIMENSIONAL FLOW
Flexiwall 3 SO: A second order predictive strategy for rapid wall adjustment in two-dimensional compressible flow
[NASA-CR-181662] N88-22018
Effect of freestream turbulence on a two dimensional cascade, with different surface roughness, at high Reynolds number
[AD-A190615] N88-22316
TWO PHASE FLOW
Dense-spray structure and phenomena. Part 1. Turbulence/dispersed-phase interactions
[AD-A190606] N88-22315

U

U.S.S.R.
USSR Space Life Sciences Digest, issue 16
[NASA-CR-3922(19)] N88-22515
UH-60A HELICOPTER
Preliminary airworthiness evaluation of the UH-60A with Advanced Digital Optical Control System (ADOCS)
[AD-A190674] N88-22030
ULLAGE
Development and evaluation of an airplane fuel tank ullage composition model. Volume 2: Experimental determination of airplane fuel tank ullage compositions
[AD-A190406] N88-22025
ULTRASHORT PULSED LASERS
SDIO/IST ultrashort wavelength laser: Novel experimental schemes for observing the Moesbauer effect in long-lived nuclear levels
[AD-A190275] N88-22351
SDIO/IST ultrashort wavelength laser. Mossbauer effect in gamma-ray lasers
[AD-A190306] N88-22352
ULTRASONIC FLAW DETECTION
A system to measure damage in composite materials by the ultrasonic method
[ONERA-RT-2/7256-RY-061-R] N88-22103
Ultrasonic characterization of ceramic joints
[DE88-005844] N88-22173
Manufacturing of ultrasonic focused probes
[VTT-RR-487] N88-22368
Nondestructive evaluation by acousto-ultrasonics N88-22412
Characterization of sintered SiC by using NDE N88-22413
Systems for ultrasonic scanning, analysis and imagery N88-22414
ULTRASONIC TESTS
A system to measure damage in composite materials by the ultrasonic method
[ONERA-RT-2/7256-RY-061-R] N88-22103
Ultrasonic beam distortion in transversely isotropic media
[DE88-005937] N88-22699
ULTRASONICS
Ultrasonic oxygen sensor
[AD-A189723] N88-22537

ULTRAVIOLET PHOTOMETRY
Satellite UV image processing
[AD-A190466] N88-22451
ULTRAVIOLET RADIATION
Extension of free-electron lasers into the extreme ultraviolet
[DE88-005373] N88-22341
ULTRAVIOLET SPECTRA
Ultraviolet absorption cross sections of methylbromide at stratospheric temperatures
[AERONOMICA-ACTA-A-320-1987] N88-22132
ULTRAVIOLET SPECTROMETERS
Satellite UV image processing
[AD-A190466] N88-22451
UNDERGROUND EXPLOSIONS
Characteristics of seismic sources of some Asian earthquakes and Soviet underground explosions from Gauribidanur array records
[DE88-701233] N88-22472
An approximation technique for solving a system of Fredholm integral equations for asymmetric detector response functions
[AD-A190577] N88-22645
UNDERWATER ACOUSTICS
A computerized investigation using the method of images to predict the sound field in a fluid wedge overlying a slow fluid half-space
[AD-A190013] N88-22704
UNITED STATES
Aircraft accident reports, brief format, US civil and foreign aviation, issue number 10 of 1986 accidents
[PB87-916912] N88-22020
UNIVERSE
Density perturbations in a rotating universe
[DE87-703036] N88-22640
Cosmology for high energy physicists
[DE88-005705] N88-22642
UNIVERSITIES
Microvax networked computer system
[AD-A190308] N88-22596
UNSTEADY AERODYNAMICS
Unsteady aerodynamics of a Wortmann FX-63-137 wing in a fluctuating wind field
[AD-A190128] N88-22006
Bifurcations in unsteady aerodynamics-implications for testing
[NASA-TM-100083] N88-22014
UNSTEADY FLOW
Unsteady aerodynamics of a Wortmann FX-63-137 wing in a fluctuating wind field
[AD-A190128] N88-22006
Oscillating airfoils: Achievements and conjectures
[AD-A190490] N88-22008
Unsteady flow field measurements using LDV (Laser Doppler Velocimetry)
[AD-A189807] N88-22298
Enhancement of data acquisition and numerical computation capabilities for unsteady fluid dynamics
[AD-A190115] N88-22302
Bodies in unsteady flow
[AD-A190416] N88-22308
Numerical study of unsteady viscous hypersonic blunt body flows with an impinging shock
[NASA-TM-100096] N88-22650
UPGRADING
Effects of update and refresh rates on flight simulation visual displays
[NASA-TM-100415] N88-22033
UPLINKING
INPE position paper on the CCSDS standardized method of link budget computation
[INPE-4533-NTE/279] N88-22820
UPPER STAGE ROCKET ENGINES
LGM-30B stage 2 disected motor test report
[AD-A190771] N88-22079
UPWELLING WATER
Changes in the California current system observed off northern California during July-August 1986
[AD-A190027] N88-22510
URBAN DEVELOPMENT
Orbital remote sensing: An instrument for monitoring urban growth
[INPE-4456-PRE/1287] N88-22833
URBAN PLANNING
Orbital remote sensing: An instrument for monitoring urban growth
[INPE-4456-PRE/1287] N88-22833
USER MANUALS (COMPUTER PROGRAMS)
FLAP (Force and Loads Analysis Program) code development and validation
[DE88-001131] N88-22371
USER REQUIREMENTS
Real-time flight test data distribution and display
[NASA-TM-100424] N88-22050
ECP (Electrical Circuitry Program): A proposed program for electrical circuitry analysis
[AD-A190494] N88-22280
CK-LOG system conversion (user's manual and user interface)
[AD-A190273] N88-22577

V

VACUUM
Vacuum-arc plasma centrifuge experiment
[INPE-4509-PRE/1263] N88-22758
VACUUM MELTING
Evaporation characteristics of elements during vacuum arc remelting of alloy A-286 N88-22248
VACUUM PUMPS
MPD (magnetoplasmadynamic) thruster advanced pumping system concepts
[AD-A190513] N88-22756
VALLEYS
Groundwater sapping valleys: Experimental studies, geological controls and implications to the interpretation of valley networks on Mars
[NASA-CR-182718] N88-22847
VAN DE GRAAFF ACCELERATORS
Particle beam alignment system for single event upset-Van de Graaf experiments
[AD-A189695] N88-22721
VAPOR DEPOSITION
Oxide optical coatings prepared by metal-organic vapor deposition
[DE88-006809] N88-22175
Investigation of laser diagnostics of PACVD processes for depositing hard face coatings
[DE88-007083] N88-22176
Vapor phase deposition and growth of polyimide films on copper
[AD-A189969] N88-22178
JPRS report: Science and technology. Japan
[JPRS-JST-88-002] N88-22210
Single crystal growth by laser CVD N88-22213
Fine grain development by laser CVD N88-22214
Hard ceramic film by laser PVD N88-22216
Laser evaporation studies
[AD-A189815] N88-22346
Beam assisted fabrication of 3-5/Si monolithic devices
[AD-A189979] N88-22785
VAPOR PRESSURE
Study on shaft seals for potassium turbine
[EL-891] N88-22364
VAPORS
Infrared differential absorption lidar for vapor detection
[AD-A190600] N88-22497
VARIABLE PITCH PROPELLERS
The effects of torque response and time delay on rotorcraft vertical axis handling qualities
[AD-A189873] N88-22023
VARIABLE SWEEP WINGS
Influence of unsteady aerodynamic forces on dynamic response of variable sweep aircraft N88-22245
VECTOR ANALYSIS
Instrumentation for the characterization and development of millimeter wave components compatible with monolithic integration
[AD-A189724] N88-22275
Martingale representation and the Malliavin calculus
[AD-A189721] N88-22626
High speed transcendental elementary function architecture in support of the Vector Wave Equation (VWE)
[AD-A189746] N88-22627
VECTOR CURRENTS
Quantization of axial electrodynamics
[TI88-701498] N88-22813
VECTOR SPACES
The existence of smooth densities for the prediction filtering and smoothing problems
[AD-A189865] N88-22629
VELOCITY
Continuous measurements of in-bore projectile velocity
[DE88-006841] N88-22056
Analytic solutions to dynamic equations of plasma armature railguns
[DE88-006842] N88-22057
On new solvable many-body dynamical systems with velocity dependent forces
[PREPRINT-581] N88-22683
VELOCITY DISTRIBUTION
High Reynolds number, low Mach number, steady flow field calculations over a NACA 0012 airfoil using Navier-Stokes and interactive boundary layer theory
[AD-A189871] N88-22005
Unsteady aerodynamics of a Wortmann FX-63-137 wing in a fluctuating wind field
[AD-A190128] N88-22006
Boundary-layer and wake measurements on a swept, circulation-control wing
[NASA-TM-89426] N88-22013
VELOCITY MEASUREMENT
Continuous measurements of in-bore projectile velocity
[DE88-006841] N88-22056
Instruments for use in experimental studies of complex turbulent shear flow: Three component LDVs
[AD-A190526] N88-22312
New measurements of radial velocities in clusters of galaxies
[INPE-4527-PRE/1277] N88-22845
VERTICAL ORIENTATION
The effects of torque response and time delay on rotorcraft vertical axis handling qualities
[AD-A189873] N88-22023
VERY LARGE SCALE INTEGRATION
French Multiproject Chip (MPC) activity report, 1986
[RR-650-I] N88-22273
Multiple-transform pipelines for image coding
[REPT-87-038] N88-22561
Software structuring principles for VLSI CAD
[AD-A190386] N88-22579
Design and implementation of VLSI prime factor algorithm processor
[AD-A190483] N88-22580
VIBRATION
The buckling and vibration of composite plates using the Levy method considering shear deformation and rotary inertia
[AD-A189743] N88-22374
Effect of vibrational excitation on rate parameters of atmospheric reactions
[AD-A190464] N88-22477
VIBRATION DAMPING
Investigation of boundary layer disturbances caused by periodic heating of a thin ribbon
[AD-A190572] N88-22314
Instrumentation to provide an active control capability for distributed parameter systems
[AD-A190043] N88-22375
Vibrations of structures with parametric uncertainties
[AD-A190400] N88-22378
VIBRATIONAL SPECTRA
Stabilization and control problems in structural dynamics
[AD-A190197] N88-22361
Sequential excitation preparation of molecular energy levels with special structural and chemical properties
[AD-A190041] N88-22718
VINYLIDENE
NMR analysis of a fluorocarbon copolymer
[DE88-002364] N88-22170
VISCOMETRY
Continual capillary viscosimetry using extrusiograph techniques
[PB88-166293] N88-22195
VISCOPLASTICITY
Evolution of hardening and damage during viscoplastic deformation
[AD-A190714] N88-22381
Biaxial experiments supporting the development of constitutive theories for advanced high-temperature materials N88-22386
Finite element (MARC) solution technologies for viscoplastic analyses N88-22389
VISCOSITY
A new method of measuring multigrade oil shear elasticity and viscosity at high shear rates
[AD-A190145] N88-22304
VISCOUS FLOW
Computational fluid dynamics drag prediction: Results from the Viscous Transonic Airfoil Workshop
[NASA-TM-100095] N88-22009
Theoretical model and numerical solution for compressible viscous vortex cores N88-22243
The numerical simulation of viscous flows with change of phase and chemical reaction
[DE88-003204] N88-22292
Numerical study of unsteady viscous hypersonic blunt body flows with an impinging shock
[NASA-TM-100096] N88-22650
High-resolution shock-capturing schemes for inviscid and viscous hypersonic flows
[NASA-TM-100097] N88-22651
VISION
A probabilistic approach to low-level vision
[AD-A189041] N88-22553
Finding texture boundaries in images
[AD-A190554] N88-22609
ROVER: A prototype active vision system
[AD-A189246] N88-22722

VISUAL ACUITY
Laboratory equipment update
[AD-A189781] N88-22522
VISUAL DISCRIMINATION
Laboratory equipment update
[AD-A189781] N88-22522
VISUAL PERCEPTION
A comparison of visual evoked potential and behavioral measures of flashblindness in humans
[AD-A189757] N88-22519
An evaluation of the effects of high visual taskload on the separate behaviors involved in complex monitoring performance
[AD-A190641] N88-22538
VITRIFICATION
Remarks on solid state amorphizing transformations
[DE88-006452] N88-22803
VLASOV EQUATIONS
Wave energy flow conservation for propagation in inhomogeneous Vlasov-Maxwell equilibria
[DE88-006705] N88-22251
VOIDS
Flaw characterization in structural ceramics using scanning laser acoustic microscopy N88-22415
VORTEX GENERATORS
Transonic Navier-Stokes computations of strake-generated vortex interactions for a fighter-like configuration
[NASA-TM-100009] N88-22010
VORTEX SHEDDING
On the prediction of highly vortical flows using an Euler equation model, part 2
[AD-A190245] N88-22305
Bodies in unsteady flow
[AD-A190416] N88-22308
VORTICES
Experimental investigation of a spanwise forced mixing layer
[AD-A190136] N88-22007
Transonic Navier-Stokes computations of strake-generated vortex interactions for a fighter-like configuration
[NASA-TM-100009] N88-22010
Pressure measurements of impinging jet with asymmetric nozzle
[NASA-CR-182759] N88-22011
Numerical simulation of turbulent flames using vortex methods
[AD-A189813] N88-22116
Investigation of combustion in large vortices
[AD-A190406] N88-22121
Theoretical model and numerical solution for compressible viscous vortex cores N88-22243
Vortices in long Josephson junctions
[AD-A190336] N88-22279
On the prediction of highly vortical flows using an Euler equation model, part 2
[AD-A190245] N88-22305
Cavitation inception in rectangular two-dimensional slots
[AD-A190677] N88-22318
The effects of time-dependent winds and ocean eddies on ice motion in a marginal ice zone
[AD-A190105] N88-22511

W

WAFERS
Fabrication and electrical characterization of multilevel aluminum interconnects used to achieve silicon-hybrid wafer-scale integration
[AD-A190519] N88-22282
WAKES
Boundary-layer and wake measurements on a swept, circulation-control wing
[NASA-TM-89426] N88-22013
Unsteady flow field measurements using LDV (Laser Doppler Velocimetry)
[AD-A189907] N88-22298
WALL JETS
Heat transfer from a negatively buoyant wall jet
[NBS-GCR-88-541] N88-22208
WALLS
Structural analyses of engine wall cooling concepts and materials N88-22405
WASTE ENERGY UTILIZATION
Overview of 1987 moonlight project N88-22231
Application and technology requirements for heat pumps at the process industries
[DE88-006740] N88-22293
WATER
Mass transfer mechanisms for water adsorbed on silica gel
[DE88-005993] N88-22107
WATER FLOW
Changes in the California current system observed off northern California during July-August 1986
[AD-A190027] N88-22510
WATER INJECTION
Dense-spray structure and phenomena. Part 2: Pressure-atomized sprays
[AD-A190312] N88-22307
WATER POLLUTION
Feasibility study for a 2nd generation system for airborne maritime pollution surveillance
[ETN-88-92108] N88-22466
WATER RUNOFF
Groundwater sapping valleys: Experimental studies, geological controls and implications to the interpretation of valley networks on Mars
[NASA-CR-182718] N88-22847
WATER TEMPERATURE
Thermal instability and heat transfer characteristics in water/ice systems
[AD-A189627] N88-22297
WAVE DISPERSION
Plasma wave radiative damping of a new type in a relativistic one-dimensional plasma
[TI88-701191] N88-22739
WAVE EQUATIONS
High speed transcendental elementary function architecture in support of the Vector Wave Equation (VWE)
[AD-A189746] N88-22627
Pointwise stabilization for coupled quasilinear and linear wave equations
[AD-A190031] N88-22632
WAVE FUNCTIONS
To the field theory with a fundamental mass
[TI88-701159] N88-22807
WAVE PROPAGATION
Wave propagation and dynamics of lattice structures
[AD-A190037] N88-22066
Wave propagation and dynamics of lattice structures
[AD-A190611] N88-22069
Numerical and experimental research on propagation of elastic stress waves in conical shell under axial impulsive loading N88-22238
Wave energy flow conservation for propagation in inhomogeneous Vlasov-Maxwell equilibria
[DE88-006705] N88-22251
Generation and propagation of sound waves in a collapsing or anti-collapsing star with uniform density
[DE87-703034] N88-22839
WAVEGUIDE ANTENNAS
Current-drive on the Versator-2 tokamak with a slotted-waveguide fast-wave coupler
[DE88-006261] N88-22743
WAVEGUIDE LASERS
Coupled high power waveguide laser research
[AD-A189800] N88-22345
WAVELENGTHS
Theoretical studies of Resonance Enhanced Stimulated Raman Scattering (RESRS) of frequency-doubled Alexandrite laser wavelength in cesium vapor
[NASA-CR-182670] N88-22133
SDIO/IST ultrashort wavelength laser. Mossbauer effect in gamma-ray lasers
[AD-A190306] N88-22352
WEAK INTERACTIONS (FIELD THEORY)
Lattice QCD calculation of K yields pi nonleptonic weak transition and other hadronic weak parameters
[PREPRINT-580] N88-22717
WEAPONS DELIVERY
Implementation and performance analysis of parallel assignment algorithms on a hypercube computer
[AD-A190678] N88-22600
WEAR RESISTANCE
Reciprocating sliding wear characteristics of copper-carbon fiber composites
[NASA-TT-20176] N88-22100
WEATHER FORECASTING
Baseline observing system experiments using the AFGL global data assimilation system
[AD-A188861] N88-22062
Derivation of consistent surface fixed fields for use in a global NWP model
[AD-A190131] N88-22475
WEIBULL DENSITY FUNCTIONS
Modeling failures of intermittently used machines
[AD-A190298] N88-22367
WELDED JOINTS
Joints in fiber-reinforced aluminum alloys
[NASA-TT-20160] N88-22104
Cracking tendencies of restrained welds in high strength low alloy steels under hyperbaric conditions
[AD-A190255] N88-22150
Reduced thermal input by proper selection of YAG laser welding parameters
[DE88-000730] N88-22356
WELDING
Segregation effects in welded stainless steels
[DE88-701224] N88-22139
WHISKER COMPOSITES
Whisker-reinforced ceramic composites for heat engine components N88-22410
WHITE LIGHT HOLOGRAPHY
Rainbow holographic image reconstructed by spatially extended white light source N88-22249
WIND (METEOROLOGY)
Monthly mean global climatology of temperature, wind, geopotential height, and pressure for 0 - 120 km
[NASA-TM-100697] N88-22503
WIND DIRECTION
Parameterization of horizontal wind velocity variability
[AD-A190107] N88-22493
The effects of time-dependent winds and ocean eddies on ice motion in a marginal ice zone
[AD-A190105] N88-22511
WIND EFFECTS
Experimental study on the influence of wind on acoustic pressure sensors
[ISL-R-121/86] N88-22712
WIND PROFILES
Aerodynamic aspects of the Amazon Forest
[INPE-4445-TDL/313] N88-22501
WIND TUNNEL MODELS
Inflow measurement made with a laser velocimeter on a helicopter model in forward flight. Volume 3: Rectangular planform blades at an advance ratio of 0.30
[NASA-TM-100543] N88-22015
WIND TUNNEL STABILITY TESTS
Investigation of boundary layer disturbances caused by periodic heating of a thin ribbon
[AD-A190572] N88-22314
WIND TUNNEL TESTS
Procedures and requirements for testing in the Langley Research Center unitary plan wind tunnel
[NASA-TM-100529] N88-22016
Porous wind tunnel corrections for counterrotation propeller testing
[NASA-TM-100873] N88-22019
Design of an integrated control system for flutter margin augmentation and gust load alleviation, tested on a dynamic windtunnel model
[PB88-149885] N88-22038
JPRS report: Science and technology. China
[JPRS-CST-87-043] N88-22233
Investigation of side-wall effects in wind tunnel with supercritical airfoil testing N88-22241
FLAP (Force and Loads Analysis Program) code development and validation
[DE88-001131] N88-22371
Langley aerospace test highlights, 1987
[NASA-TM-100595] N88-22853
Space directorate research and technology accomplishments for fiscal year 1987
[NASA-TM-100607] N88-22854
WIND TUNNEL WALLS
Flexiwall 3 SO: A second order predictive strategy for rapid wall adjustment in two-dimensional compressible flow
[NASA-CR-181662] N88-22018
Porous wind tunnel corrections for counterrotation propeller testing
[NASA-TM-100873] N88-22019
Investigation of side-wall effects in wind tunnel with supercritical airfoil testing N88-22241
WIND TURBINES
FLAP (Force and Loads Analysis Program) code development and validation
[DE88-001131] N88-22371
Lewis Structures Technology, 1988. Volume 3: Structural Integrity Fatigue and Fracture Wind Turbines HOST
[NASA-CP-3003-VOL-3] N88-22408
Large-scale wind turbine structures N88-22429
WIND VARIATIONS
Parameterization of horizontal wind velocity variability
[AD-A190107] N88-22493
WIND VELOCITY
Unsteady aerodynamics of a Wortmann FX-63-137 wing in a fluctuating wind field
[AD-A190128] N88-22006
Parameterization of horizontal wind velocity variability
[AD-A190107] N88-22493
Describing the source created by turbulent flow over orifices and louvers
[AD-A190254] N88-22706
WINDPOWER UTILIZATION
Energy from the wind
[DE88-006897] N88-22459
WING LOADING
Shape sensitivity analysis of wing static aeroelastic characteristics
[NASA-TP-2808] N88-22031

WING PROFILES
Shape sensitivity analysis of wing static aeroelastic characteristics
[NASA-TP-2808] N88-22031
WING SPAN
Investigation of side-wall effects in wind tunnel with supercritical airfoil testing N88-22241
WINGS
Control of laminar flow around of the wing in free-air conditions
[AD-A187479] N88-22004
Unsteady aerodynamics of a Wortmann FX-63-137 wing in a fluctuating wind field
[AD-A190128] N88-22006
WIRE
High-T(sub c) superconducting wire fabrication and testing
[DE88-005989] N88-22798
WIRING
Characteristics of LSI-wiring expert system discussed N88-22226
WORDS (LANGUAGE)
Auditory perception of complex sounds
[AD-A190528] N88-22529
WORKSTATIONS
Sigma system: Overview, prospects N88-22230

X

X RAY ANALYSIS
Advances in geochemistry and cosmochemistry: Trace element microdistributions with the synchrotron X-ray fluorescence microprobe
[DE88-006355] N88-22108
X RAY DIFFRACTION
An investigation of the crystalchemistry and thermochemistry of selected mineral systems
[AD-A189758] N88-22781
X RAY FLUORESCENCE
Advances in geochemistry and cosmochemistry: Trace element microdistributions with the synchrotron X-ray fluorescence microprobe
[DE88-006355] N88-22108
X RAY SPECTRA
Smoothing technique to resolve X-ray spectra in laser nuclear fusion N88-22235
X RAY TELESCOPES
Design, construction and performance of the ROSAT high resolution X-ray mirror assembly
[MPE-PREPRINT-101] N88-22836
X RAYS
Theory of interactions of intense light with nonlinear, inhomogeneous and periodic structures and its applications to optical bistability, optic gyroscopes, nonlinear spectroscopy, radiation protection, X-ray emission and related fields
[AD-A190040] N88-22725
Computing X-ray effects in optics
[DE88-006722] N88-22732
Preparing the Alcator C bolometer system for use on MTX (Microwave Tokamak Experiment)
[DE88-006724] N88-22733
XENON FLUORIDE LASERS
Discharge excitation of the XeF C to A transition
[DE88-006448] N88-22339

Y

YAG LASERS
Laser processing-status, perspectives N88-22211
Reduced thermal input by proper selection of YAG laser welding parameters
[DE88-000730] N88-22356
YANG-MILLS FIELDS
Ten dimensional N = 1 supergravity coupled to superasymmetric Yang-Mills fields in superspace
[DE87-703033] N88-22808
YTTRIUM
Magnetic anomalies in the rare earth oxide superconductors GdBa2Cu3O(7-x) and YbBa2Cu3O(7-x)
[AD-A190713] N88-22793
Synthesis and characterization of high-T(sub c) screen-printed Y-Ba-Cu-O films on alumina
[NASA-TM-100860] N88-22805
YTTRIUM OXIDES
Melt processing ceramic YBa2Cu3O(sub 6.9)
[DE88-007039] N88-22199
Superconductivity and the tailoring of lattice parameters of the compound YBa2Cu3O(sub x)
[DE88-005904] N88-22769

Z

ZEOLITES
Preliminary market analysis for large zeolite crystals
[NASA-CR-182882] N88-22207
ZINC COATINGS
Studies on hot-dip zinc-aluminum coated sheet steels
[ETN-88-92217] N88-22166
ZIRCONIUM
Ion-beam mixing and amorphization in Au/Zr bilayers
[DE88-005999] N88-22767
ZIRCONIUM NITRIDES
Structure and properties of titanium nitride and zirconium nitride thin films prepared by reactive ion plating --- cutting tools
[ETN-88-92218] N88-22167
ZIRCONIUM OXIDES
Superplastic flow of mullite-zirconia composites
[DE88-005905] N88-22065

Typical Personal Author Index Listing

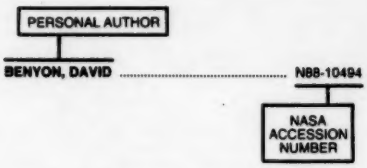

* Listings in this index are arranged alphabetically by personal author. The NASA accession number denotes the number by which the citation is identified.

A

ABDU, M. A. N88-22482
N88-22489
ABDUL-AZIZ, ALI N88-22404
ABE, STEVE N88-22414
ABRAHAO, ADRIANA N88-22453
ABRAMOF, EDUARDO N88-22357
ABSAR, SALMAN N88-22316
ACHTEMEIER, GARY L. N88-22491
N88-22492
ADAMS, J. E. N88-22265
ADDISON, VICTOR C., JR. N88-22509
AHMED, IFTIKHAR N88-22256
AHMED, M. N88-22139
AIELLO, ROBERT A. N88-22390
AKEYAMA, KENJI N88-22101
AKHTER, J. I. N88-22139
AKSAY, I. A. N88-22198
AL-BASSIOUNI, ABDEL-AZIZ M. N88-22250
ALBRECHT, A. N88-22842
ALDER, D. N88-22299
N88-22300
N88-22301
ALDRICH, J. N88-22540
ALESHIN, YU. D. N88-22332
ALLEN, J. D., JR. N88-22601
ALLEN, RALPH G. N88-22519
ALTHOFF, SUSAN L. N88-22015
ALTINOK, SADRETTIN N88-22604
ALTMAN, M. B. N88-22154
ALTSHULLER, A. P. N88-22448
AMAMCHYAN, R. G. N88-22209
AMATUNI, A. TS. N88-22734
ANDREAS, EDGAR L. N88-22494
ANGIBAULT, F. N88-22696
ANGUS, ROBERT G. N88-22525
ANKEM, S. N88-22145
ANTOLA, ANNA N88-22561
ANTONIO, C. N88-22273
APEL, E. C. N88-22340
ARAKAWA, HIDEO N88-22099
N88-22100
N88-22101
ARNAUTOW, G. N88-22474
ARORA, S. K. N88-22472
AROYAN, A. A. N88-22209
ARUTYUNYAN, M. A. N88-22209
ARYA, V. K. N88-22389
ASAY, J. R. N88-22056
ASCHENBACH, BERND N88-22836
ATLURI, S. N. N88-22445
ATTAWAY, S. W. N88-22372
ATTFIELD, J. P. N88-22602
AUGUST, RICHARD N88-22428
AURIOL, A. N88-22266
AVERY, DON E. N88-22854

B

BAAKLINI, GEORGE Y. N88-22413
N88-22416
BABCOCK, C. D. N88-22098
BAHR, A. J. N88-22260
BAILEY, D. J. N88-22542
BAILEY, J. M. N88-22289
BAILEY, MICKEY J. N88-22627
BAILLIEUL, JOHN N88-22349
BAKER, CHARLES R. N88-22665
N88-22685
N88-22686
N88-22687
N88-22688
BAKER, T. L. N88-22187
BALAS, MARK J. N88-22068
BALDWIN, T. N88-22062
BALLUFFI, R. W. N88-22142
BALSA, T. F. N88-22007
BANKS, H. T. N88-22541
BANSAL, NAROTTAM P. N88-22805
BANSIL, A. N88-22797
BARAS, JOHN N88-22658
BARBANEL, E. L. N88-22619
BARKER, JEFFREY L. N88-22511
BARNES, FRANK N88-22676
BARNETT, JOHN J. N88-22503
BARRETT, J. H. N88-22795
BARROSO, J., JR. N88-22848
BARTHELEMY, JEAN-FRANCOIS M. N88-22031
BARTO, ANDREW N88-22533
BARTOLOTTA, PAUL A. N88-22385
BARTON, CYNTHIA K. N88-22280
BASU, S. N88-22554
BASU, T. K. N88-22472
BATHER, JOHN N88-22664
BATTAGLIA, FRANCO N88-22817
BATTEEN, MARY L. N88-22510
BAUGHMAN, R. J. N88-22199
BAXTER, J. P. N88-22178
BEASLEY, MICHAEL E. N88-22510
BECKEL, C. L. N88-22126
BECKER, M. N88-22474
BECKER, MONIQUE N88-22593
BEDFORD, B. L. N88-22265
BEDNARZ, B. F. N88-22682
BEGEAL, D. R. N88-22324
BELL, JAMES H. N88-22045
BELLINI, SANDRO N88-22655
BELLUM, J. C. N88-22126
BELOVOLOV, O. V. N88-22270
BELTE, DAUMANTS N88-22029
BEMENT, LAURENCE J. N88-22072
BENAROYA, HAYM N88-22378
BENDER, GARY L. N88-22030
BENEDEK, R. N88-22768
N88-22797
BENFORD, GREGORY N88-22752
BENNETT, T. L. N88-22272
BENO, JOSEPH E. N88-22285
BENSON, KEVIN R. N88-22078
BERENS, THOMAS J. N88-22044
BERG, M. N88-22197
BERGEN, FRED D. N88-22031
BERGER, R. L. N88-22083
BERGERSON, L. D. N88-22105
BERK, H. L. N88-22251
BERMUDEZ, V. M. N88-22127
BERWEILER, WILMA N88-22441
BEYER, JAMES B. N88-22279
BHATTACHARYYA, S. K. N88-22756
BICKNELL, J. A. N88-22478
BIGIO, I. J. N88-22339
BINDON, J. N88-22299
N88-22300
N88-22301
BIRDSALL, T. G. N88-22701
BITTENCOURT, JOSE AUGUSTO N88-22758
BLACHERE, J. R. N88-22193
BLAIR, W. G. N88-22318
BLAKE, JAMES T. N88-22598
BLAKE, R. D. N88-22095
BLOSSER, MAX L. N88-22438
BLUCHER, JOSEPH N88-22136
BLUM, Y. D. N88-22189
BOCCONCELLI, ALESSANDRO N88-22508
BOCK, MARY E. N88-22683
BOEDICKER, CHRISTOPHER A. N88-22310
BOERSTOEL, J. W. N88-22017
BOES, E. C. N88-22462
BOGDANOFF, D. W. N88-22695
BOGOLYUBOV, N. N. N88-22739
BOISSIERE, P. T. N88-22383
BOLDAREV, S. T. N88-22209
BOLSHAKOV, A. E. N88-22270
BOOTH, STEVEN E. N88-22560
BORDIA, R. K. N88-22802
BORODINA, I. N. N88-22544
BOSCH, LEON ANTOON N88-22697
BOSE, B. K. N88-22288
BOULANGER, F. N88-22073
BOULANGER, YU. N88-22474
BOULDIN, D. W. N88-22601
BOWDEN, D. M. N88-22152
BOWEN, C. N88-22571
N88-22572
BOWER, J. R. N88-22328
BOWMAN, C. T. N88-22115
BOWMAN, CRAIG T. N88-22117
BOYER, J. P. N88-22073
BRABY, L. A. N88-22513
BRACKETT, D. C. N88-22695
BRADY, MICHAEL N88-22563
BRAZA, RUDY M. N88-22496
BRENNER, STEPHEN N88-22475
BREWER, DAVID N88-22419
BRININSTOOL, M. R. N88-22728
BRINKER, C. J. N88-22114
BROOKS, CUYLER W., JR. N88-22047
BROPHY, JAMES J. N88-22707
BROW, R. K. N88-22114
BROWN, K. W. N88-22400
BROWN, S. D. N88-22197
BRUCKNER, A. P. N88-22695
BRUSASCO, R. N88-22175
BRUSCHI, M. N88-22683
BRYANT, R. E. N88-22761
BUDNEY, MICHAEL D. N88-22703
BUESCHER, KEVIN L. N88-22608
BUHL, M. L. N88-22371
BULLOCK, CHARLES D. N88-22335
BURDE, E. N88-22712
BURITZ, ROBERT S. N88-22276
BURKE, A. F. N88-22271
N88-22272
BURKE, ROGER N88-22296
BURNS, MARK N88-22155
BURTSEV, V. A. N88-22344
BUTLER, J. E. N88-22127
BUTLER, P. L. N88-22601
BUZZARD, ROBERT J. N88-22418
BYERLY, RADFORD N88-22676
BYSHEVA, G. K. N88-22544

C

CAHN, DAVID F. N88-22823
CAI, LUZHONG N88-22249
CALLAHAN, M. N88-22557
N88-22680
CALS, M. P. N88-22073
CAMARANETO, GILBERTO N88-22829
CANAVAN, G. H. N88-22343
CANN, GLENN E. N88-22706
CANTOR, A. J. N88-22345
CANTWELL, BRIAN J. N88-22117
CAPELATO, H. V. N88-22835
N88-22845
CAPONE, D. W., II N88-22798
CAREY, WILLIAM M. N88-22708
CARLSON, L. W. N88-22756
CARPENTER, BARRY A. N88-22600
CARRETTA, THOMAS R. N88-22539
CARRICO, J. P. N88-22497
CARRIER, G. F. N88-22105

CARROLL, B. F. N88-22320
CARROLL, CHESTER C. N88-22602
CASASENT, DAVID N88-22610
CASATI, G. N88-22821
CASON, RANDALL W. N88-22029
CAVALCANTI, IRACEMA F. A. N88-22466
CEBECI, TUNCER N88-22006
CHADDAH, P. N88-22776
CHAMBERS, RICHARD D. N88-22188
CHAMIS, CHRISTOS C. N88-22399
CHAMPAGNE, EDWIN B. N88-22262
CHAN, JOSEPH K. N88-22257
CHAN, S. T. N88-22467
CHANDRA, SUSHIL N88-22503
CHANG-DIAZ, F. R. N88-22755
CHANG, WILLIAM S. N88-22788
CHAPMAN, GARY T. N88-22014
CHAPPELL, R. N88-22293
CHEN, E. P. N88-22362
CHEN, GOONG N88-22361
N88-22632
CHEN, I.-WEI N88-22085
CHEN, I-WEI N88-22769
CHEN, NUNKUAN N88-22236
CHEN, YUZE N88-22238
CHENG, KAIJIA N88-22236
CHENGAN, LIU N88-22615
CHERANOVSKIY, O. R. N88-22004
CHERNYSHEV, V. P. N88-22544
CHERVYAKOV, A. M. N88-22806
CHIRULLI, DONALD N88-22547
CHONACKY, N. N88-22479
CHOW, L. S. N88-22756
CHULYA, ABHISAK N88-22407
CHUNG, D. T. N88-22440
CIESLIK, S. N88-22131
CIMBALA, J. M. N88-22318
CITERLEY, R. L. N88-22823
CLARK, W. L. N88-22552
CLOUGH, R. L. N88-22171
CLOUTHIER, DENNIS J. N88-22110
CODDING, GEORGE N88-22676
COFFEY, HELEN E. N88-22849
COHEN, ARIEL N88-22723
COHEN, LEONARD D. N88-22723
COLBORN, J. A. N88-22743
COLEMAN, T. L. N88-22452
COLLINS, WILLIAM E. N88-22531
COLOMBINI, R. N88-22821
COMON, H. N88-22624
CONNELL, JOHN C., JR. N88-22569
CONWAY, TERRY L. N88-22526
N88-22527
COOMBS, DAVID J. N88-22722
COON, D. N. N88-22172
CORNIE, JAMES A. N88-22136
CORSON, MICHAEL R. N88-22721
COTTER, GLADYS A. N88-22822
COTTLE, R. W. N88-22690
COURTOIS, B. N88-22545
COURVILLE, G. E. N88-22046
COUSINS, T. N88-22528
COWLES, LISA J. N88-22005
COX, D. E. N88-22802
COYLE, J. M. N88-22636
COYLE, T. D. N88-22187
CRAWFORD, M. L. N88-22048
CRONAN, TERRY A. N88-22526
CULIK, JEROME S. N88-22460
CULPEPPER, B. T. N88-22184
CUMBERBATCH, ELLIS N88-22672
CURL, R. F. N88-22112
CURTISS, DWAYNE H. N88-22277
CZARNEK, R. N88-22201

D

DAGLE, W. R. N88-22537
DAINO, BENEDETTO N88-22714
DALE, V. H. N88-22465
DALLAQUA, RENATO SERGIO N88-22758
DALLMANN, UWE N88-22330
DALLMEYER, H. N88-22130
DALRYMPLE, T. O. N88-22432
DANDE, Y. D. N88-22776
DANIEL, RUSSELL B. N88-22645
DARDIS, WILLIAM J., III N88-22027
DASANNACHARYA, B. A. N88-22776
DASILVA, I. M. O. N88-22484
DAVIS, L. N88-22775
DAVIS, L. E. N88-22800
DAVYDOVA, T. A. N88-22748
DAWSON, D. M. N88-22091
DAY, MARK N88-22578
DEANGELIS, D. L. N88-22465
DEDES, GEORGE C. N88-22052
DEFATIMAMATTIELLOFRANCISCO, MARIA N88-22619
DEHMEL, G. N88-22487
DEHOOP, A. T. N88-22264
DELAYEN, J. R. N88-22765
DELBOSCO, EDSON N88-22758
DELFINODAVILAMASCARENHAS, NELSON N88-22454
DELLENBACK, PAUL A. N88-22348
DELORI, H. N88-22273
DELOURDESN.O.KURKDJIAN, MARIA N88-22833
DESAUSSURE, G. N88-22556
DESZOEKE, ROLAND A. N88-22507
DIBIANCA, A. N. N88-22182
DIEGLE, R. B. N88-22158
DILLON, M. P. N88-22171
DING, FU-RONG N88-22767
DIVGI, D. R. N88-22660
DIVINOMOURA, ANTONIO N88-22502
DO, CHOON H. N88-22179
DOBBS, D. L. N88-22159
DOBLMAIER, THOMAS N88-22207
DOMINGOS, HENRY N88-22281
DOMOKOS, G. N88-22303
DONALDSON, P. LYNN N88-22515
DOSANJOSFERREIRAPINTO, SERGIO N88-22455
DOSS, E. D. N88-22756
DOTSON, KELLY J. N88-22653
DOWDING, TIMOTHY J. N88-22493
DOWNING, J. P. N88-22504
DRAKE, J. B. N88-22075
DREW, CRAIG C. N88-22818
DRUMMOND, JACK N88-22843
DRYER, F. L. N88-22689
DRZAL, LAWRENCE T. N88-22093
DUBININ, I. V. N88-22270
DUFFY, STEPHEN F. N88-22410
DULIKRAVICH, GEORGE S. N88-22652
DULKE, MICHAEL F. N88-22034
DUNN, J. C. N88-22463
DURAL, GUELBIN N88-22259
DURAND, N. A. N88-22206
DURANPINTO, JOAQUIM HENRIQUE N88-22456
DURST, F. N88-22329
DUSEK, J. T. N88-22798
DUTRA, S. L. G. N88-22483
DUTTA, B. K. N88-22370
DUTTA, PIYUSH K. N88-22380
DUTTON, J. C. N88-22320
DUTTON, LINDA J. N88-22527
DYBAN, YE. P. N88-22317
DZIECIUCH, MATTHEW A. N88-22701

E

ECER, AKIN N88-22595
EGDORF, H. W. N88-22613
EIMERL, D. N88-22775
ELBAKYAN, S. S. N88-22734
ELLIOTT, J. W. N88-22710
ELLIOTT, JOE W. N88-22015
ELLIOTT, ROBERT J. N88-22605
N88-22626
N88-22629
N88-22656
N88-22658
ELLIS, GRAHAM K. N88-22591
ELLIS, J. R. N88-22386
ELLIS, JOHN C., II N88-22702
ELORANTA, EDWIN W. N88-22495
EMERIC, DARIO A. N88-22155
ENGLISH, JAMES P. N88-22181
ENGLUND, DAVID R. N88-22430
EPSTEIN, G. N88-22850
EPSTEIN, J. S. N88-22086
N88-22437
ERICKSON, G. F. N88-22355
ERMAK, D. L. N88-22467
ERTHAL, GUARACI JOSE N88-22829
ESTEFAN, R. M. N88-22203
EYDELAND, A. N88-22620

F

FAETH, G. M. N88-22307
N88-22315
FAIRBANKS, CAROLYN J. N88-22191
FALLER, J. N88-22474
FARBER, R. N88-22621
FARINELLI, TOMMY C. N88-22567
FARNETH, W. E. N88-22602
FARRELL, D. E. N88-22805
FARRELL, DENNIS N88-22380
FARRELL, M. P. N88-22465
FAURE, E. N88-22073
FAY, RICHARD R. N88-22523
FEDRO, A. J. N88-22766
FENDELL, F. E. N88-22105
FERRIS, WILLIAM F. N88-22147
FIDELSKAYA, R. P. N88-22344
FIELD, ROBERT W. N88-22718
FIGUEIRA, J. F. N88-22339
FINE, MORRIS E. N88-22151
FISCHER, THOMAS M. N88-22330
FIX, EDWARD L. N88-22518
FLAHERTY, J. E. N88-22636
FLAHERTY, JOSEPH E. N88-22628
FLEETER, SANFORD N88-22036
FLEMING, ERIC L. N88-22503
FLEMING, W. N88-22206
FLINN, J. E. N88-22143
N88-22162
FLIPPEN, R. B. N88-22802
FOKKEMA, J. T. N88-22711
FOLLMANN, DEAN A. N88-22367
FONTIJN, ARTHUR N88-22128
FOSTER, KENNETH R. N88-22512
FOURNIER, J. N88-22696
FRAIOLI, A. V. N88-22107
FRANCASENNE, EDSON LUIZ N88-22590
FREIMAN, S. W. N88-22187
FROSTENSON, NELS A. N88-22258
FU, JIE N88-22248
FUJIKAWA, K. N88-22616
FUJIKAWA, KAZUO N88-22810
FUJIMURA, KAORU N88-22735
FUJISAKI, MASATOSHI N88-22637
FUJIWARA, CHIKARA N88-22136
FUKAYA, KIYOSHI N88-22735
FYLES, PETER A. N88-22023

G

GAINER, GORDON H., JR. N88-22777
GALLAGHER, ALAN C. N88-22119
GAN, FUXI N88-22236
GANGLOFF, RICHARD P. N88-22377
GANGRADE, B. K. N88-22471
GANNON, DENNIS N88-22576
GAO, CHAO N88-22241
GARCIAFONSECA, LEILA MARIA N88-22454
GARNER, J. N88-22768
GARTLING, D. K. N88-22292
GAVELA, M. B. N88-22717
GEAR, C. W. N88-22592
GEBALLE, T. H. N88-22764
GENERAZIO, EDWARD R. N88-22414
GEORGE, THOMAS F. N88-22817
GEORGE, WILLIAM K. N88-22302
GERBER, K. N88-22104
GERBER, NATHAN N88-22319
GHONIEM, AHMED F. N88-22116
GHOSH, MALAY N88-22670
GHOSN, LOUIS N88-22418
GIBSON, J. S. N88-22065
GIELES, PAULUS MARIA CORNELIS N88-22532
GILLIES, B. B. N88-22719
GILLOTAY, D. N88-22132
GINDI, GENE R. N88-22573
GINLEY, D. S. N88-22199
GINTY, CAROL A. N88-22391
GLADDEN, HERBERT J. N88-22431
GLASS, CHRISTOPHER E. N88-22325
GLASS, G. P. N88-22112
GLASSMAN, IRVIN N88-22123
GLEZER, A. N88-22007
GMITRO, ARTHUR F. N88-22573
GODBOLE, M. J. N88-22144
GODDARD, DANIEL G. N88-22039
GODERRE, G. P. N88-22774
GODOYJUNIOR, MOACIR N88-22453
GOETTSCHING, L. N88-22326
GOETZ, DOUGLAS P. N88-22068
GOLDE, MICHAEL F. N88-22477
GOLDSTEIN, M. N88-22360
GONCHAROV, V. A. N88-22332
GONZALEZ, E. R. N88-22464
GONZALEZ, W. D. N88-22483
GOODYER, M. J. N88-22018
GORAN, WILLIAM D. N88-22824
GORETTA, K. C. N88-22798
GOSNELL, T. R. N88-22340
GOTO, T. N88-22226
GOUGH, M. P. N88-22487
GRAD, A. G. N88-22344
GRADY, JOSEPH E. N88-22402
GRAFF, G. L. N88-22198
GRAFING, PAUL N88-22207
GRAHAM, ROBERT P., JR. N88-22582
GRAMSCH, E. N88-22109

GRANATO, ENZO N88-22804
GRASSBERG, E. K. N88-22837
GRAVES, R. L. N88-22205
GRAVES, R. S. N88-22169
GRAY, CARL E., JR. N88-22435
GRAY, WILLIAM M. N88-22500
GREEN, M. A. N88-22063
GREENE, D. P. N88-22339
GREENE, KEVIN J. N88-22826
GREENSFELDER, A. P. N88-22633
GREER, WILLIS R., JR. N88-22831
GREVE, D. W. N88-22789
GREWAL, G. N88-22145
GRIMLEY, T. A. N88-22323
GRIMSHAW, JEFFREY D. N88-22041
GROSSBERG, STEPHEN N88-22549
GROSSMANN, J. M. N88-22286
GROTEN, E. N88-22474
GRUNZE, M. N88-22178
GU, SHUXIAN N88-22239
GUARISO, G. N88-22562
GUPTA, N. K. N88-22750
GUPTA, SHANTI S. N88-22675
GUSEV, L. N. N88-22544
GUSTAVSSON, ANDERS I. N88-22032
GUYOT, A. N88-22273
GUZMAN, A. N88-22789

H

HAAKINSON, E. J. N88-22265
HACHAM, AVI N88-22763
HAERTEL, HERMANN N88-22693
HALFORD, GARY R. N88-22425
HALL, C. A. N88-22056
HALL, PHILIP N88-22319
HALL, R. F. N88-22379
HALL, ROBERT J. N88-22283
HALLER, E. E. N88-22772
HALVERSON, D. C. N88-22084
HAMAKAWA, YOSHIHIRO N88-22221
HAMMOND, J. H. N88-22343
HAMMONS, KEVIN R. N88-22050
HAN, NGUEN SUAN N88-22813
N88-22815
HANOLD, R. J. N88-22463
HANSON, J. D. N88-22749
HANSON, R. K. N88-22115
N88-22122
HARACZ, RICHARD D. N88-22723
HARBACH, FRIEDRICH N88-22441
HARDIN, J. E. N88-22272
HARRIGAN, R. W. N88-22363
HARRIS, CHARLES D. N88-22047
HARRIS, STEVEN G. N88-22823
HART, R. A. N88-22345
HARTMAN, ALAN F. N88-22581
HARVEGO. E. A. N88-22719
HATFIELD, WILLIAM E. N88-22793
HAUSER, ROBERT S. N88-22580
HAVEN, BRENDA N88-22314
HAWKE, R. S. N88-22057
HAWSEY, R. A. N88-22289
HAYAKAWA, JUNJI N88-22222
HAYASHI, SHIGEYUKI N88-22213
HEALY, TIMOTHY J. N88-22642
HEARRELL, JEFFREY D. N88-22026
HEATH, M. T. N88-22586
HEDBY, GUNNAR N88-22269
HEDRICK, STEVEN D. N88-22298
HEIDENREICH, G. N88-22458
HEIDERSBACH, R. S. N88-22159
HELMS, JEFFREY H. N88-22793
HENDERSON, I. N88-22379
HENEIN, NAEIM A. N88-22200
HENKEL, C. S. N88-22586
HENRY, S. S. N88-22184
HERBEIN, DAVID S. N88-22306
HERLIHY, MAURICE N88-22578
HERMAN, H. N88-22756
HERTZBERG, A. N88-22695
HETENYI, J. N88-22195
HETZEL, F. L. N88-22105
HICKMAN, R. N88-22056
HINKLEY, J. A. N88-22097
HIRLEMAN, E. D. N88-22348
HIRSCH, JOY N88-22522
HIRSH., IRA J. N88-22529
HITZ, M. N88-22562
HO, CHIH-MING N88-22011
HOCKEY, BERNARD J. N88-22191
HOFFMAN, D. N88-22557
N88-22680
HOFFMAN, J. T. N88-22557
HOFFMAN, R. N. N88-22062
HOFGARD, JEFFERSON N88-22676
HOLBACK, B. N88-22487
HOLDER, S. L. N88-22182
HOLLAND, P. L. N88-22497
HOLST, TERRY L. N88-22009
HOMAN, C. G. N88-22055
HOOKE, LYDIA RAZRAN N88-22515
HOPKINS, DALE A. N88-22395
N88-22400
HORAUD, RADU N88-22563
HORIE, TOMOYOSHI N88-22735
HORN, BERTHOLD K. N88-22449
HOUEIX, PIERRE N88-22593
HOWE, H. C. N88-22757
HOY, GILBERT R. N88-22351
N88-22352
HSU, C. T. N88-22105
HU, YAOHE N88-22248
HUA, T. Q. N88-22741
HUANG, J. S. N88-22157
HULL, DAVID G. N88-22026
HULTQVIST, BENGT N88-22488
HUNT, G. L. N88-22272
HUNT, J. H. N88-22715
HUNT, L. ROANE N88-22325
HYMAN, CURTIS E., JR. N88-22016

I

IANOVICI, I. N88-22299
N88-22300
N88-22301
IBADOV, R. M. N88-22807
IIDA, HIROMASA N88-22735
IMAI, HIROYUKI N88-22364
IMSHENNIK, V. S. N88-22837
INGRAM, VERNON D. N88-22255
ISLER, R. C. N88-22742
ITOH, T. N88-22278
IU, KAI-KONG N88-22171
IYENGAR, S. S. N88-22556

J

JABLONSKI, F. J. N88-22848
JACKSON, B. E. N88-22716
JAGANNATHAN, V. N88-22555
JAIN, R. P. N88-22555
JALURIA, Y. N88-22208
JASINSCHI, R. N88-22640
JAYASWAL, BALHANS N88-22558
JEFFERIES, KENT S. N88-22090
JENEKHE, SAMSON A. N88-22180
JENNINGS, R. D. N88-22049
JERACKI, ROBERT J. N88-22019
JIN, B. Y. N88-22799
JO, S. C. N88-22789
JOHNSON, J. E. N88-22506
JOHNSON, MARK O. N88-22824
JOHNSON, MIKE N88-22179
JOHNSON, N. M. N88-22795
JOHNSON, PAUL N88-22578
JOHNSON, S. N88-22458
JOHNSON, STEVEN E. N88-22584
JOHNSON, W. L. N88-22803
JOHNSTON, JAMES P. N88-22312
JOHNSTON, N. J. N88-22097
JONAS, JIRI N88-22125
JONES, J. F. N88-22433
JONES, J. P. N88-22614
JONES, K. W. N88-22108
JONES, W. H. N88-22356
JORDAN, E. H. N88-22388
JOSHI, M. V. N88-22106
JOSLIN, R. D. N88-22309
JOU, C. N88-22771
JUDD, MICHAEL N88-22018
JUHASZ, ARPAD A. N88-22335
JUMPER, GEOFFREY W. N88-22816

K

KACZMAREK, H. N88-22103
KADOMTSEV, M. B. N88-22678
KADYSHEVSKIJ, V. G. N88-22807
KAKODKAR, A. N88-22370
KALAFUT, JOHN N88-22380
KALLIANPUR, G. N88-22677
KANADE, TAKEO N88-22610
KANAZAWA, I. N88-22109
KANE, DIDIER N88-22281
KANKO, MARK A. N88-22043
KANNAN, A. N88-22554
KANTOR, I. J. N88-22489
KANTZOS, PETER N88-22419
KAPINOS, V. G. N88-22138
KAPLAN, ALEXANDER E. N88-22725
KAPOOR, K. N88-22208
KARLOV, T. D. N88-22332
KARR, ALAN F. N88-22673
KASHIWAGI, TAKASHI N88-22311
KASWANDI, CAROLUS N88-22704
KATTNER, KEVIN M. N88-22792
KATZ, I. N. N88-22633
KATZ, J. D. N88-22095
KATZENELSON, JACOB N88-22579
KAUFMAN, ALBERT N88-22405
KAUFMANN, E. N. N88-22157
KAUTZ, HAROLD E. N88-22412
KAWAMURA, HIROSHI N88-22735
KAWASUMI, HIROMICHI N88-22211
N88-22217
KAYANO, MARY TOSHIE N88-22502
KEARNS, TIMOTHY G. N88-22825
KEATING, C. Y. N88-22769
KEATING, S. N88-22769
KEDDY, E. S. N88-22458
KEDEM, B. N88-22641
KEENER, EARL R. N88-22013
KEISER, J. R. N88-22159
KEITH, TOMMY E. N88-22254
KELLOGG, GARY V. N88-22033
KENIK, E. A. N88-22144
KENNEDY, J. T. N88-22345
KENNES, R. N88-22131
KERSLAKE, T. W. N88-22406
KETTERSON, J. B. N88-22799
KIDDER, STANLEY Q. N88-22492
KIKUYAMA, TOSHIHIKO N88-22220
KIM, D.-H. N88-22156
KIM, K. S. N88-22421
KIM, YOUNG SIK N88-22817
KIMMEL, E. C. N88-22184
KIMURA, TOKIO N88-22225
KING, W. C. N88-22480
KINKEAD, E. R. N88-22184
KINSEY, JAMES L. N88-22718
KIRCHHOFF, V. W. J. H. N88-22469
N88-22484
KIRK, MARTIN L. N88-22793
KIRKPATRICK, R. J. N88-22114
KISHINEVSKY, MICHAEL N88-22738
KISLIUK, MOSHE N88-22252
KLAUS, MICHAEL H. N88-22376
KLIMA, STANLEY J. N88-22416
KLOECKER, N. N88-22487
KLOPFER, G. H. N88-22650
N88-22651
KNAUSS, W. G. N88-22098
KNIGHT, KIM N88-22207
KOCH, CHRISTOF N88-22607
KOCHEL, R. CRAIG N88-22847
KODAMA, HARVEY H. N88-22565
KOEPKE, G. H. N88-22048
KOEPP, JOERG N88-22466
KOGA, TADASHI N88-22364
KOHL, H. N88-22487
KOHLMANN, MICHAEL N88-22605
N88-22626
N88-22658
KOJIMA, FUMIO N88-22541
KOLB, G. J. N88-22461
KOLOMYTKIN, V. V. N88-22762
KOMIYAMA, TORU N88-22222
KONDO, TATSUO N88-22140
KONG, C. W. N88-22178
KONO, JANIO N88-22820
KONRAD, C. H. N88-22056
KOO, JOSEPH H. N88-22348
KORENAGA, SADAYOSHI N88-22364
KOROS, W. J. N88-22174
KORTH, G. E. N88-22143
N88-22162
KOSTERLITZ, J. M. N88-22804
KOVESI-DOMOKOS, S. N88-22303
KOWALCZYK, W. N88-22648
KOWLER, E. N88-22530
KRATZKE, THOMAS M. N88-22625
KRAYNIK, A. M. N88-22192
KRILE, THOMAS F. N88-22724
KRISHNAIAH, P. R. N88-22661
KRUMBEIN, A. D. N88-22736
KRUMMERICH, MELINDA B. N88-22335
KRYDER, M. H. N88-22789
KUBENDRAN, L. R. N88-22012
KUBO, R. N88-22617
KUGAKOITI, HELIO N88-22053
KULKARNI, A. K. N88-22555
KULKARNI, P. G. N88-22106
KULL, H. J. N88-22251

KULSRUD, R. N88-22286
KUNIYA, KEIICHI N88-22099
N88-22100
N88-22101
KUO, CHU K. N88-22707
KUO, J. C. W. N88-22204
KUPPERMAN, D. S. N88-22699
KUSHNER, BRIAN G. N88-22548
KUTLER, P. N88-22650
KUZNETSOV, V. S. N88-22344
KWAK, J. F. N88-22199

L

LABARGE, W. L. N88-22024
LACKNEY, JOSEPH J. N88-22393
LADBURY, J. M. N88-22048
LAFLEN, J. H. N88-22421
LAGERQUIST, C. N88-22195
LAHDENPERA, KARI N88-22366
LAINE, R. M. N88-22189
LAMB, R. N. N88-22178
LAMBOLEY, MARCEL N88-22074
LAMBORN, MARK J. N88-22088
LANGE, R. N88-22467
LANNELONGUE, H. N88-22267
LANSINGER, JOHN M. N88-22476
LAPEDES, A. N88-22621
LARIGALDIE, S. N88-22073
LARSEN, CURTIS E. N88-22654
LASHLEE, ROBERT W., JR. N88-22071
LAVENDER, C. A. N88-22094
LAWANDY, NABIL M. N88-22133
LAWLESS, J. L. N88-22753
LAWLESS, PHILIP A. N88-22149
LAWN, BRIAN R. N88-22191
LEADER, D. R. N88-22828
LEAVENS, GARY N88-22578
LEBLANC, M. N88-22540
LEDERICH, R. J. N88-22152
LEE, CHI H. N88-22790
LEEHEY, PATRICK N88-22308
LEENEY, THOMAS A. N88-22263
LEIFER, LARRY J. N88-22540
LEMAIRE, J. N88-22759
LEMOS, FRED R. N88-22336
LENHART, S. J. N88-22189
LEONARD, C. E. N88-22289
LEONE, STEPHEN R. N88-22119
LEVETON, LAUREN B. N88-22515
LEVIN, PHILIP S. N88-22177
LEVITAN, STEVE N88-22547
LEVY, MOISES N88-22791
LEWIS, E. E. N88-22366
LI, LIXIN N88-22649
LIANG, TACHEN N88-22675
LIGRANI, PHILLIP M. N88-22336
LILIENTAL-WEBER, Z. N88-22771
LIN, BINGQIU N88-22243
LIN, SIN S. N88-22087
LISKOV, BARBARA N88-22578
LITTLE, C. N88-22373
LIU, B. N88-22182
LIU, CHENGHAI N88-22235
LIU, H. W. N88-22420
LIU, H.-T. N88-22006
LIU, WEI N88-22244
LIU, ZHISHEN N88-22247
LLOYD, W. R. N88-22437
LOCKHEAD, GREGORY R. N88-22700
LODGE, ARTHUR S. N88-22304
LOEB, ABRAHAM N88-22737
LONDON, B. D. N88-22152
LOUIE, S. G. N88-22773
LOUIS, J. F. N88-22062
LOWNDES, D. H. N88-22144
LU, ZHENGQIANG N88-22235
LUBIN, P. N88-22650
LUCAS, R. D. N88-22450
LUDWIG, GERSON OTTO N88-22758
LUEHR, H. N88-22487
LUGUERN, JEAN-PIERRE N88-22588
LUM, B. Y. N88-22084
LUND, G. N88-22835
LUNDE, STEVEN M. N88-22321
LYNN, K. G. N88-22109

M

MADORE, BARRY F. N88-22846
MAEDA, K. N88-22812
MAI, YIU-WING N88-22191
MAIANI, L. N88-22717
MAISH, A. B. N88-22462
MAITI, S. K. N88-22370
MAKIHARA, MISAKI N88-22222
MAKIMATTILA, SIMO J. N88-22166
MALIK, A. Q. N88-22139
MALIK, M. K. N88-22776
MALIK, S. N. N88-22421
MANDERS, P. J. H. M. N88-22369
MANDERSCHEID, JANE M. N88-22409
MANN, R. C. N88-22614
MANNHEIMER, R. J. N88-22323
MAPLE, M. B. N88-22764
MARBACH, H. W., JR. N88-22203
MARBLE, FRANK E. N88-22121
MARCHENKO, V. S. N88-22748
MARCONI, FRANK N88-22305
MARINAK, MARTY N88-22733
MARINHO, E. V. A. N88-22469
MARK, J. E. N88-22190
MARKOVICH, P. M. N88-22796
MARQUE, J. P. N88-22073
MARQUES, S. N88-22809
MARQUIER, M. N88-22163
MARRAFFA, LIONEL N88-22652
MARRIOTT, P. N88-22760
MARSH, BRIAN D. N88-22722
MARSHALL, D. B. N88-22183
MARTIN, MARGIE N88-22507
MARTIN, R. M. N88-22710
MARTINELLI, G. N88-22717
MARTINEZ-SANCHEZ, MANUEL N88-22754
MARTINEZ, R. N88-22612
MARTINI, PAULO ROBERTO N88-22455
MARTINSDEBARROS, PEDRO MANUEL N88-22820
MARWICK, A. D. N88-22795
MARYNICK, DENNIS S. N88-22185
MASAYTIS, V. L. N88-22490
MASSIS, T. A. N88-22206
MATHES, JAMES R., JR. N88-22022
MATOSDEMEDEIROS, VALDER N88-22485
MATSUMOTO, SHIGERU N88-22364
MATSUNAWA, AKIRA N88-22215
MATTHEWS, K. N88-22846
MATTIASSON, K. N88-22129
MATTICK, A. T. N88-22695
MAURER, R. N88-22142
MAUW, S. N88-22647
MAXWORTHY, T. N88-22329
MAZURE, A. N88-22835
N88-22845
MCALARY, CHRISTOPHER W. N88-22846
MCALLESTER, DAVID A. N88-22643
MCCALL, J. N88-22571
N88-22572
MCCARRON, E. M., III N88-22602
MCCLUNG, R. W. N88-22173
MCCLUSKEY, EDWARD J. N88-22574
MCCOOL, JOHN I. N88-22359
MCCOWN, A. W. N88-22339
MCDERMOTT, JAMES H. N88-22721
MCFALL, K. A. N88-22695
MCGAW, MICHAEL A. N88-22422
MCKAY, JACK A. N88-22721
MCKELVEY, N. N88-22571
N88-22572
MCKENZIE-CARTER, M. A. N88-22740
MCKENZIE, ROBERT L. N88-22337
MCKINNON, JOHN A. N88-22849
MCLAREN, R. A. N88-22846
MCNEELY, GERALD W. N88-22181
MCNEESE, MICHAEL D. N88-22535
MEEKS, W. H., III N88-22679
N88-22680
MEHTA, RABINDRA D. N88-22045
MEIER, G. H. N88-22161
MEIJER, J. A. N88-22137
MEISTER, JEFFREY P. N88-22392
MELHEM, RAMI N88-22547
MELIS, MATTHEW E. N88-22403
MELNICHENKO, I. A. N88-22333
MENICUCCI, D. F. N88-22457
MERRIGAN, M. A. N88-22458
MERTENS, HENRY W. N88-22531
METTING, N. F. N88-22513
MEYER, T. G. N88-22388
MICHELSEN, B. L. N88-22264
MICKELSON, M. N88-22062
MILLER, J. H., JR. N88-22182
MILLER, JAMES S. N88-22597
MIMORI, KATSUHIRO N88-22111
MIN, B. I. N88-22768
MINA, R. T. N88-22209
MINATO, A. N88-22735
MINEDA, SHINEI N88-22216
MINORIKAWA, HITOSHI N88-22101
MIRET-GOUTIER, A. N88-22771
MISCONI, N. Y. N88-22354
MISHACHEV, V. M. N88-22209
MISRA, M. N88-22066
MITTL, J. C. N88-22172
MIZE, JOHNNIE E. N88-22284
MOGILNER, A. I. N88-22294
MOLARIUS, JYRKI M. N88-22167
MONTAGNE, J.-L. N88-22651
MONTGOMERY, O. L. N88-22452
MOOERS, CHRISTOPHER N. N88-22506
N88-22510
MOORES, THOMAS J. N88-22091
MOORHEAD, PAUL E. N88-22383
MORE, J. J. N88-22646
MOROSIN, B. N88-22199
MOROZOV, S. A. N88-22294
MORRIS, PHILIP J. N88-22309
MORRISON, P. J. N88-22251
MORRISSEY, K. J. N88-22802
MORROW, T. B. N88-22323
MORSS, L. R. N88-22770
MORTARA, KARL W. N88-22652
MOSELEY, WILLIAM B. N88-22708
MOSER, L. N88-22135
MOSES, JOEL N88-22634
MOTOJIMA, O. N88-22746
MOZER, F. S. N88-22483
MUKHINA, I. YU. N88-22154
MULLIGAN, R. M. N88-22530
MUNGAL, M. G. N88-22115
MUNIR, Z. A. N88-22084
MURALIKRISHNA, P. N88-22482
N88-22489
MURPHY, H. D. N88-22463
MURTHY, PAPPU L. N. N88-22395
N88-22396
MYERS, C. W. N88-22483

N

NADEZHIN, D. K. N88-22837
NAGAO, G. N88-22811
NAGATA, JOHN I. N88-22029
NAGEL, R. T. N88-22295
NAGPAL, VINOD K. N88-22401
NAITOH, PAUL N88-22525
NAKAYAMA, MASAKI N88-22230
NAKAZAWA, S. N88-22394
NAMEKAWA, TAKASHI N88-22099
N88-22100
NARIAI, H. N88-22638
N88-22839
N88-22840
NATSIAVAS, S. N88-22098
NAVALE, A. S. N88-22559
NEHRKORN, T. N88-22062
NEIKIRK, D. P. N88-22278
NEILSON, R. M., JR. N88-22172
NEILSON, ROBERT H. N88-22186
NELLIS, W. J. N88-22784
NELSON, G. C. N88-22158
NELSON, RICHARD S. N88-22426
NEMAT-NASSER, S. N88-22440
NESEL, MICHAEL C. N88-22050
NESTERENKO, V. V. N88-22806
N88-22815
NEUGEBAUER, G. N88-22846
NEWHALL, DONALD H. N88-22335
NEWMAN, B. E. N88-22341
NEWMAN, J. C., JR. N88-22445
NEWMAN, L. A. N88-22345
NEWMAN, MICHAEL N88-22784
NEWMAN, N. N88-22771
NEWTONBANDEIRA, IRAJA N88-22357
NG, C. F. N88-22439
NI, RANDOLPH N88-22150
NICHOLS, JOSEPH W. N88-22146
NICOLAIDIS, M. N88-22545
NICOLET, M. N88-22131
NIKKI, SHIGERN N88-22788
NIKOLAEV, V. I. N88-22270
NIKOLAI, U. N88-22461
NILSSON, SOREN N88-22442
NING, CARLOS HO SHIH N88-22485
NISSLEY, DAVID M. N88-22427
NIX, WILLIAM D. N88-22786
NIXON, MARK W. N88-22434
NOGUEIRADONASCIMENTO, NELIO N88-22455
NOLAN, JOHN P. N88-22667
NOLTE, D. D. N88-22772
NORDMAN, JAMES E. N88-22279
NOTTON, M. N88-22164
NOVICK-COHEN, A. N88-22153
NOWLIN, BRENT C. N88-22037

O

OBRIEN, T. K. N88-22097
OCHS, HARRY T., III N88-22491
OCIMARMANZI, ANTONIO N88-22501
ODAY, V. M. N88-22265
OEHRLEIN, G. S. N88-22795
OELSCHLAEGEL, W. N88-22487
OGAWA, MASURO N88-22735
OGILBY, P. R. N88-22171
OHARA, TOMOYUKI N88-22455
OKAMOTO, P. R. N88-22767
OKUTOMI, MAMORU N88-22212
OKUYAMA, K. N88-22291
OLAVOFERREIRA, SUKARNO N88-22357
OLIKER, V. I. N88-22630
OLIVER, W. C. N88-22159
ONEAL, J. E. N88-22152
ONG, NAI-PHUAN N88-22783
OPHEY, LOTHAR N88-22102
ORIANI, R. A. N88-22160
OSETSKIJ, YU. N. N88-22138
OSHIDA, Y. N88-22420
OTTINGER, P. F. N88-22286
OTTINO, J. M. N88-22327
OWEN, JEFFREY E. N88-22602

P

PAILLOTIN, J. F. N88-22273
PALARDY, REAL F. N88-22374
PANDIAN, M. D. N88-22517
PANG, J. S. N88-22690
PAPPAS, JOHN A. N88-22285
PARK, D. L. N88-22719
PARK, J. T. N88-22323
PARKS, D. H. N88-22094
PARMENTIER, G. N88-22712
N88-22713
PARTANEN, JOUNI P. N88-22358
PARTHASARATHY, R. N. N88-22315
PATTON, J. N88-22156
PAUL, D. R. N88-22174
PEDRAZA, A. J. N88-22144
PENDER, C. W. N88-22552
PENDRILL, L. N88-22129
PENE, O. N88-22717
PENG, T. H. N88-22465
PENNINGER, LISA N88-22566
PEREIRA, ENIO B. N88-22468
PEREIRA, J. C. F. N88-22329
PEREZ-ABREU, V. N88-22677
PERVUSHIN, V. N. N88-22813
PETERSON, KEITH A. N88-22526
PETERSON, LAUREN M. N88-22730
PETRARCA, S. N88-22717
PETROVIC, J. J. N88-22095
PETTERSON, B. J. N88-22433
PETTIT, F. S. N88-22193
PHELPS, K. R. N88-22497
PICOLOGLOU, B. F. N88-22741
PICRAUX, S. T. N88-22158
PILCHER, JAMES O. N88-22335
PIN, F. G. N88-22360
PINSKY, MARK A. N88-22674
PINTO, I. R. C. A. N88-22483
N88-22486
PINTO, O., JR. N88-22483
PITKANEN, JORMA N88-22368
PITTS, WILLIAM H. N88-22311
PLEMMONS, R. J. N88-22586
PLOETNER, BILLY G. N88-22583
POANNOPOULOS, JOHN D. N88-22794
POGGIO, TOMASO N88-22607
POLLARD, D. L. N88-22184
POLYAKOV, P. A. N88-22739
POMERANTZ, MARTIN N88-22185
POORE, A. V. N88-22457
POST, D. N88-22201
POST, W. M. N88-22465
POWELL, B. E. N88-22379
POWERS, T. N88-22328
PRASAD, A. G. V. N88-22471
PRASAD, R. N88-22797
PREVIC, FRED H. N88-22347
N88-22519
PRIEBE, S. N88-22293
PROUST, D. N88-22835
N88-22845

Q

QIU, CHUANREN N88-22245
QUAK, D. N88-22264
QUAST, G. R. N88-22848

R

RABITZ, H. N88-22689
RABITZ, HERSCHEL N88-22596
RAGHAVAN, R. V. N88-22776
RAGNISCO, O. N88-22683
RAINES, RICHARD A. N88-22599
RAJACHANDRASEKAR, R. N88-22106
RAJESHWAR, KRISHNAN N88-22185
RAJU, I. S. N88-22445
RAMESH, M. N88-22789
RAMSTHALER, J. H. N88-22719
RANDALL, W. N88-22571
N88-22572
RAO, C. R. N88-22661
RAO, N. S. V. N88-22556
RAO, V. B. N88-22502
RATCLIFF, K. F. N88-22354
RATCLIFFE, C. A. N88-22513
RATEAU, PH. N88-22712
RAWAL, S. N88-22086
RAYCHAUDHURI, S. N88-22177
REEBER, ROBERT R. N88-22781
REED, C. B. N88-22741
REED, IRVING S. N88-22635
REED, W. C. N88-22719
REHN, L. E. N88-22767
RENARD, J. N88-22103
RENNER, ROLF H. N88-22202
RENNIE, MICHAEL W. N88-22575
REUTER, W. G. N88-22437
REYES-MOREL, P. E. N88-22769
REYNOLDS, JOHN R. N88-22185
REYNOLDS, THOMAS L. N88-22029
REYNOLDS, W. C. N88-22115
REZNICK, STEVE N88-22010
RHEE, MOON-JHONG N88-22790
RHOADES, C. E., JR. N88-22732
RICCI, WILLIAM S. N88-22091
RIDDLE, B. N88-22265
RIEDEL, HERMANN N88-22441
RIEDLING, KARL N88-22779
RILEY, W. J. N88-22182
RINNERT, K. N88-22487
RIOSNETO, ATAIR N88-22832
RIVERS, M. L. N88-22108
RO, HYEKYEONG N88-22793
ROBB, ROGER E. N88-22778
ROBBINS, ROBERT D. N88-22030
ROBERTS, D. J. N88-22613
ROBERTS, R. A. N88-22699
ROBINS, ROBERT E. N88-22450
ROBINSON, D. N. N88-22387
ROBINSON, GARY Y. N88-22782
N88-22785
ROBINSON, J. A. N88-22826
ROCCA, FABIO N88-22655
RODEAN, H. C. N88-22467
RODRIGUES, JOSE ANTONIO N88-22820
ROE, J. N. N88-22731
ROHLICEK, J. R. N88-22657
ROHRS, BRIAN R. N88-22793
ROINE, ANTTI N88-22165
ROMAGNOLI, MARCO N88-22714
ROMAN, W. C. N88-22176
ROSEN, I. G. N88-22662
ROSENBERG, NORMAN N88-22451
ROSENGREEN, A. N88-22260
ROSENTHAL, RICHARD E. N88-22568
ROTH, A. J. N88-22025
ROTH, DON J. N88-22415
ROWAN, W. L. N88-22742
ROWE, JOSEPH N88-22515
ROYER, H. N88-22338
ROYLANCE, GERALD L. N88-22644
ROZENFELD, PAWEL N88-22820
RUBINOVITZ, R. L. N88-22127
RUBINSTEIN, ROBERT N88-22398
RUFF, G. A. N88-22307
RUIZCALAVERA, LUIS P. N88-22290
RUSHTON, L. P. N88-22528
RUSK, E. T. N88-22354
RUSSELL, DAVID N88-22375
RUSSELL, S. D. N88-22727

S

SABELMAN, E. N88-22540
SAENZ, N. T. N88-22094
SAILEY, RICHARD H. N88-22015
SAKAMOTO, TATSUJI N88-22101
SAKAUE, TADASHI N88-22101
SALASALVES, DIOGENES N88-22829
SALEM, JONATHAN A. N88-22417
SALVADORSOLE, E. N88-22845
SALZMAN, D. N88-22736
SAMADANI, R. N88-22340
SAMUELS, W. D. N88-22198
SANDERS, M. L. N88-22481
SANDERS, WILLIAM A. N88-22416
SANDERSON, ARTHUR N88-22610
SANKUR, H. O. N88-22346
SANTAMATO, ENRICO N88-22714
SANTIAGO, JOSEPH M. N88-22376
SASAKI, RYU N88-22681
SASTRY, S. M. N88-22152
SATHYAMOORTHY, M. N88-22070
SATO, M. N88-22746
SAUERBREY, R. N88-22339
SAVARY, P. N88-22268
SAWANO, KIYOSHI N88-22214
SAWAOKA, AKIRA B. N88-22224
SCHANK, R. N88-22606
SCHAPERY, RICHARD A. N88-22088
SCHEIMAN, J. N88-22012
SCHERRER, R. N88-22587
SCHILLING, C. H. N88-22198
SCHIMMEL, MORRY L. N88-22072
SCHLEGEL, K. N88-22487
SCHOBER, JOSEF N88-22468
SCHOEBERL, MARK R. N88-22503
SCHOOFS, A. J. G. N88-22436
SCHROEDER, CURT N88-22061
SCHUETTLER, H. B. N88-22766
SCHULER, K. W. N88-22058
SCHULLER, I. K. N88-22799
SCHULTZ, K.-J. N88-22710
SCHWANDT, D. N88-22540
SCHWARZ, R. B. N88-22803
SCHWUTTKE, G. H. N88-22779
SCOTT, ROBERT W. N88-22492
SCOTT, T. C. N88-22692
SEDNEY, RAYMOND N88-22319
SEKHPOSYAN, E. V. N88-22734
SEKI, M. N88-22735
SELF, S. A. N88-22141
SELYAVIN, G. F. N88-22317
SEMENOV, A. L. N88-22270
SEMENOV, A. P. N88-22543
SENA, J. T. N88-22458
SENN, R. N88-22571
N88-22572
SETSER, D. W. N88-22342
SETTEMBRE, MARINA N88-22714
SETZER, ALBERTO W. N88-22468
SEUME, JORGE R. N88-22322
SHAFFER, TIMOTHY D. N88-22185
SHAFFER, WINSTON J., II N88-22702
SHAHINPOOR, M. N88-22056
N88-22057
SHANNO, DAVID F. N88-22631
SHARMA, R. D. N88-22471
SHAY, T. M. N88-22339
N88-22340
SHEN, MENGYU N88-22244
SHEN, WEI-HSIUNG N88-22669
SHEN, YUEN RON N88-22714
SHEPARD, K. W. N88-22796
SHEPHERD, J. E. N88-22324
SHER, DAVID B. N88-22553
SHERIDAN, JOSEPH G. N88-22064
SHERWOOD, C. R. N88-22504
SHEVCHENKO, O. YU. N88-22814
SHIAO, MICHAEL C. N88-22397
SHIRAKAWA, TETSUHISA N88-22219
SHOAID, K. A. N88-22139
SHOFNER, WILLIAM N88-22523
SHVETS, I. T. N88-22317
SIEBECKER, HANS N88-22698
SIEGEL, BETTE N88-22515
SIERRA, RAY N88-22177
SIMKOVICH, G. N88-22156
SIMON, GORDON N88-22638
SIMON, P. C. N88-22132
SIMON, TERRENCE W. N88-22322
SIMONS, RAINEE N. N88-22805
SIMPSON, W. A., JR. N88-22173
SINHA, BIMAL K. N88-22669
N88-22670
SISSON, W. G. N88-22692
SJOEBLOM, B. N88-22195
SKACHKOV, N. B. N88-22814
SLEIGHT, A. W. N88-22802
SLEMROD, MARSHALL N88-22691
SLOGLUND, MATS N88-22269
SMADJA, D. N88-22696
SMITH, C. H. N88-22170

SMITH, C. W. N88-22201
SMITH, J. V. N88-22108
SMITH, M. T. N88-22094
SMITH, MARK A. N88-22179
SMITH, P. N88-22339
SMITH, R. E. N88-22170
SMITH, RICHARD L. N88-22659
N88-22668
SMITH, TODD E. N88-22428
SMOOT, G. N88-22850
SNYDER, DANIEL E. N88-22535
SNYDER, LAWRENCE N88-22570
SOCIE, DARRELL N88-22423
SODRE, L. N88-22835
SOHNS, C. W. N88-22289
SOKOLOVA, O. V. N88-22543
SOLIN, JUSSI N88-22443
SOLOMON, A. D. N88-22075
SOLOMON, HERBERT N88-22663
SONG, S. N. N88-22799
SONNEFELD, MICHAEL D. N88-22258
SONNENBERGER, D. C. N88-22770
SOPOK, SAMUEL N88-22148
SORENSEN, N. R. N88-22158
SORKIN, ROBERT D. N88-22534
SPAID, FRANK W. N88-22013
SPENNY, C. H. N88-22536
SPERA, DAVID A. N88-22429
SPEYER, JASON L. N88-22026
SPICER, W. E. N88-22771
SPLETTSTOESSER, W. R. N88-22710
SPROTT, J. C. N88-22745
SPRUCK, J. N88-22585
N88-22620
SRINIVASAN, S. N88-22464
STAMNITZ, T. N88-22727
STANG, DAVID B. N88-22414
STASZAK, PAUL RUSSELL N88-22197
STAVINOHA, L. L. N88-22203
STEFKO, GEORGE L. N88-22019
STEINBERG, BERNARD N88-22252
STEKOLNIKOV, I. S. N88-22498
STENCEL, J. R. N88-22740
STERNBERG, S. N88-22530
STRADOMSKIY, M. V. N88-22317
STRIP, D. R. N88-22611
STWALLEY, WILLIAM C. N88-22350
SUBRAMANIAN, M. A. N88-22802
SUBRAMANYAM, K. N88-22639
SUGIMOTO, NOBUO N88-22232
SUSANDHI, R. N88-22554
SUTTON, S. R. N88-22108
SWANSON, D. G. N88-22749
SWANSON, PETER L. N88-22191
SWANSON, STEPHEN R. N88-22090
SWIDER, STACY E. N88-22091
SZABO, BARNA A. N88-22633
SZE, R. C. N88-22339
SZICHMAN, H. N88-22736

T

TAKAHASHI, GRANT L. N88-22262
TAKAO, MASARU N88-22808
TAKATA, HIROSHI N88-22364
TAKEDA, TETSUAKI N88-22735
TALAVERA, A. N88-22845
TALDA, TIMOTHY A. N88-22077
TALLANT, D. R. N88-22114
TALLEY, LYNNE D. N88-22507
TALLMAN, R. L. N88-22172
TANAKA, KEIKO N88-22485
TANOUE, HIROO N88-22364
TASEV, M. A. N88-22739
TAYLOR, L. M. N88-22440
TAYLOR, R. D. N88-22352
TEETER, RONALD N88-22515
TELESMAN, JACK N88-22419
TELFORD, PETER T. N88-22188
THACKRAY, RICHARD I. N88-22538
THELEN, GREGORY L. N88-22035
THOMAS, DAVID M. N88-22042
THOMAS, G. N88-22082
THOMPSON, J. R., JR. N88-22144
THOMPSON, R. L. N88-22384
N88-22406
THOMPSON, ROBERT L. N88-22389
N88-22404
N88-22407
THORN, R. J. N88-22770
THRESHER, R. W. N88-22371
THROWE, J. N88-22109
TICIANELLI, E. A. N88-22464
TIEN, T. Y. N88-22769
TIMOHOVA, M. A. N88-22154
TITTEL, F. K. N88-22339
TOBAK, MURRAY N88-22014
TONE, T. N88-22735
TONG, M. T. N88-22384
N88-22406
TOONG, TAU-YI N88-22120
TORARDI, C. C. N88-22802
TOUCHSTONE, R. M. N88-22538
TREW, R. J. N88-22275
TRIPP, DAVID E. N88-22411
TSUJI, HIROKAZU N88-22140
TUAN, PHAM DINH N88-22564
TURNER, M. S. N88-22844
TUROK, N. N88-22812
N88-22841
TURRO, NICHOLAS J. N88-22118

U

UCKAN, N. A. N88-22757
UEHARA, KAZUYA N88-22747
ULLMAN, SHIMON N88-22694
UNERTL, W. N. N88-22178
URALETS, A. YU. N88-22294
UTHE, E. E. N88-22497
UTROBIN, V. P. N88-22837

V

V.D.KWAAK, D. W. N88-22359
VAILLANT, D. N88-22267
VANDENBERG, P. M. N88-22711
VANDERBILT, DAVID P. N88-22181
VANDERLAAN, J. N88-22497
VANDERLUGT, W. N88-22137
VANDERVOOREN, J. N88-22017
VANDERWEES, A. J. N88-22017
VANDETMAREL, C. N88-22137
VANECK, TIMOTHY N88-22788
VANGELDER, P. A. N88-22038
VANNINI, M. N88-22339
VANOOSTEN, A. B. N88-22137
VANRENSEN, E. N88-22104
VANSTONE, R. H. N88-22421
VARNER, JAMES R. N88-22441
VELDMAN, A. E. P. N88-22017
VELEZ, JULIO E. N88-22040
VELSKO, S. N88-22775
VEMURI, V. N88-22603
VENKATESWARAN, V. N88-22690
VENTURINI, E. L. N88-22199
VERHOFF, VINCENT G. N88-22037
VERMOREL, J. N88-22712
N88-22713
VERNON, SUSAN N. N88-22365
VERRILLI, MICHAEL J. N88-22168
N88-22424
VIJAYAKUMAR, B. V. N88-22610
VIJAYSHANKAR, M. N. N88-22145
VILLELA, T. N88-22850
VINITSKIJ, S. I. N88-22678
VINKE, G. J. B. N88-22137
VOLLENBERG, P. H. T. N88-22196
VOLMER, M. N88-22134
VOORHEES, HARRY N88-22609
VORONOV, N. A. N88-22470
VOTTIS, P. M. N88-22055
VOZZOLA, ROBERT P. N88-22089
VYAS, K. N. N88-22554

W

WAGENER, K. B. N88-22179
WAGNER, CHARLES A. N88-22033
WAGNER, STEVEN M. N88-22274
WAKE, MASAYOSHI N88-22111
WALKER, H. F. N88-22622
WALKER, J. S. N88-22741
WALKER, K. P. N88-22388
WALKUP, JOHN F. N88-22724
WALLIN, KIM N88-22444
WALSH, F. N88-22516
WALSH, J. J. N88-22505
WALTMAN, P. N88-22630
WALUKIEWICZ, W. N88-22772
N88-22801
WANG, DAHENG N88-22238
WANG, GANCHANG N88-22236
WANG, HAN-KUN N88-22632
WANG, KANG L. N88-22787
WARDE, CARDINAL N88-22729
WARREN, RICHARD M. N88-22520
N88-22705
WARREN, W. E. N88-22192
WASHBURN, J. N88-22771
WASSUM, DONALD L. N88-22016
WATSON, CHARLES S. N88-22524
WEBER, A. N88-22134
WEBER, E. R. N88-22771
WEERTMAN, JULIA R. N88-22151
WEI, ROBERT P. N88-22377
WEILER, LUDWIG N88-22441
WEINMASTER, R. R. N88-22206
WEISBIN, C. R. N88-22360
WEISS, JOHN E. N88-22684
WEITZ, ERIC N88-22124
WELCH, B. N88-22334
WELCH, D. L. N88-22846
WELD, DANIEL S. N88-22313
WELLINGHOFF, STEPHEN T. N88-22180
WELLMAN, G. W. N88-22058
WERNER, RODNEY A. N88-22051
WERSINGER, J. M. N88-22749
WERTHNER, H. N88-22562
WESLING, TIMOTHY R. N88-22076
WEST, MICHAEL W. N88-22188
WESTPHAL, RUSSELL V. N88-22336
WETZEL, LEWIS B. N88-22261
WHETTEN, J. T. N88-22463
WHISTLER, WILLIAM N88-22252
WHITBECK, J. F. N88-22719
WHITE, C. P. N88-22289
WHITE, G. S. N88-22187
WHITE, ROBERT C. N88-22779
WHITING, LISA R. N88-22155
WICHNER, R. P. N88-22075
WIEDER, H. H. N88-22788
WIEDERHORN, S. M. N88-22187
WILDER, BRENDAN L. N88-22092
WILHELM, K. N88-22487
WILLEKENS, ERIC N88-22666
WILLIAMS, ANDREW N88-22788
WILLIAMS, ANTHONY J. N88-22280
WILLIAMS, JAMES H., JR. N88-22066
N88-22069
WILLIAMS, P. T. N88-22075
WILLIAMS, R. K. N88-22169
WILLIFORD, R. E. N88-22381
WILLMERT, K. D. N88-22070
WILLSHIRE, WILLIAM L., JR. N88-22709
WILLSKY, A. S. N88-22657
WILMORE, DOUGLAS W. N88-22521
WILSON, W. E. N88-22513
WIRTZ, G. P. N88-22197
WISNIEWSKI, HENRY L. N88-22376
WITTEN, A. J. N88-22046
N88-22480
WITTLIN, GIL N88-22024
WITTMANN, PAUL A. N88-22506
WRIGHT, A. D. N88-22371
WRIGHT, R. N. N88-22143
N88-22162
WU, X. N88-22769
WU, XIZHI N88-22638
WYGANT, J. N88-22483
WYGNANSKI, I. J. N88-22007
WYLIE, DONALD P. N88-22495

X

XIA, RENWEI N88-22240
XIE, ZUYUAN N88-22242
XU, J. N88-22769

Y

YAMADA, TOMOAKI N88-22223
YAMAKA, EIZO N88-22229
YAMANAKA, ITARU N88-22681
YAMAZAKI, YOSHIHIRO N88-22485
YAN, BINGYU N88-22237
YAN, MING N88-22245
YANG, H. Q. N88-22799
YANG, QIDE N88-22246
YANG, T. F. N88-22755
YANG, YISONG N88-22618
N88-22623
YAO, YI-CHING N88-22638
YARBROUGH, D. W. N88-22169
YASUNAGA, NOBUO N88-22216
YEE, H. C. N88-22650
N88-22651
YEN, YIN-CHAO N88-22297
YERSHOVA, T. I. N88-22154
YETTER, R. N88-22689
YIN, Y. Q. N88-22671
YING, S. C. N88-22804
YIP, PEARL W. N88-22087

YOON, C. K. N88-22085
YOST, WILLIAM A. N88-22523
YOUNG, J. F. N88-22083
YOUNG, JONATHAN D. N88-22259
YU, FRANCIS T. N88-22726
YU, MIN N88-22236
YUILLE, A. N88-22640
YUILLE, ALAN N88-22694

Z

ZAKHAROV, S. O. N88-22294
ZARETSKY, ERWIN V. N88-22428
ZARROUATI, O. N88-22054
ZENIE, ALEXANDRE N88-22588
N88-22589
ZHANG, YOUWEN N88-22249
ZHANG, ZHIMING N88-22247
ZHAO, JUNHUA N88-22248
ZHAO, YUCAI N88-22248
ZHU, JAINZHONG N88-22248
ZILBERSTEIN, GIL N88-22594
ZINKANN, G. P. N88-22796
ZIPPEL, RICHARD N88-22579
ZOLTANI, C. K. N88-22303
ZOZULYA, V. B. N88-22004
ZUSHI, H. N88-22746

Typical Corporate Source Index Listing

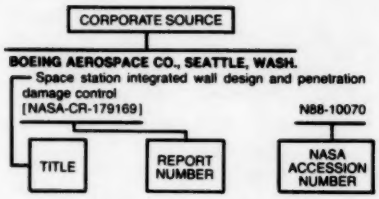

Listings in this index are arranged alphabetically by corporate source. The title of the document provides the user with a brief description of the subject matter. The report number helps to indicate the type of document cited (e.g., NASA report, translation, NASA contractor report). The NASA accession number denotes the number by which the citation is identified. The titles are arranged under each corporate source in ascending accession number order.

A

ACADEMY OF SCIENCES OF THE ARMENIAN SSR, ERIVAN.
Dilution refrigerator with non-valve adsorption system of sup 3/He circulation
[DE88-700974] N88-22209
Nonlinear effects in plasma wake field acceleration
[TI88-700972] N88-22734

ACADEMY OF SCIENCES OF THE UKRAINIAN SSR, KIEV.
Parametric instabilities of inhomogeneous plasma near the lower-hybrid resonance
[TI88-701201] N88-22748

AERITALIA S.P.A., TURIN (ITALY).
Information systems for quality. Experience at the Nerviano Aeritalia plant. Avionic systems and equipment group
[ETN-88-92274] N88-22821

AERONAUTICAL RESEARCH INST. OF SWEDEN, STOCKHOLM.
In-service measurements of SAAB SF-340 landing gear loads
[FFA-TN-1987-48] N88-22032
Increasing strength of graphite/epoxy bolted joints by introducing an adhesively bonded metallic insert
[FFA-TN-1987-45] N88-22442

AEROSPACE MEDICAL RESEARCH LABS., WRIGHT-PATTERSON AFB, OHIO.
Conflict resolution in cooperative systems
[AD-A190351] N88-22535

AEROSPACE STRUCTURES INFORMATION AND ANALYSIS CENTER, WRIGHT-PATTERSON AFB, OHIO.
Application of new technologies to DTIC document processing
[AD-A189778] N88-22823

AIR FORCE ASTROPHYSICS LAB., EDWARDS AFB, CALIF.
Durability testing of an iridium-plated storable rocket engine injector
[AD-A190707] N88-22078

AIR FORCE GEOPHYSICS LAB., HANSCOM AFB, MASS.
Results of the International Comparison of Absolute Gravimeters (2nd) held in Sevres, France in June-July 1985
[AD-A189869] N88-22474

AIR FORCE HUMAN RESOURCES LAB., BROOKS AFB, TEX.
Relationship of encoding speed and memory tests to flight training performance
[AD-A190670] N88-22539

AIR FORCE INST. OF TECH., WRIGHT-PATTERSON AFB, OHIO.
Model selection for the multiple model adaptive algorithm for in-flight simulation
[AD-A189715] N88-22022
Performance optimization of a cruise missile using dynamic-stall induced lift augmentation
[AD-A190497] N88-22027
Modification of the BLUEMAX 2 terrain following model to incorporate radar detection
[AD-A190594] N88-22028
Linear state space modeling of a turbofan engine
[AD-A190110] N88-22035
Application of eigenstructure assignment techniques in the design of a longitudinal flight control system
[AD-A189644] N88-22039
Multivariable control law design for the AFTI/F-16 with a failed control surface using a parameter-adaptive controller
[AD-A189848] N88-22040
Kalman filter residual expert system
[AD-A190520] N88-22041
Subharmonic aliasing and its effects on the AFTI/F-16 digital flight control system
[AD-A190614] N88-22042
Geometric modeling of flight information for graphical cockpit display
[AD-A190484] N88-22043
Multiple model parameter adaptive control for in-flight simulation
[AD-A190568] N88-22044
Periodic orbits around a satellite modelled as a triaxial ellipsoid
[AD-A190592] N88-22051
A systems analysis of fire suppression alternatives for the US space station
[AD-A189847] N88-22064
Moving-bank multiple model adaptive estimation applied to flexible spacestructure control
[AD-A190761] N88-22071
An experimental investigation of rocket ramjet nozzle assembly base pressures
[AD-A189714] N88-22076
Experimental investigation of two-dimensional confined jet thrust vector control
[AD-A189845] N88-22077
Fracture toughness testing of a ceramic matrix composite
[AD-A189846] N88-22089
A study of damage tolerance in curved composite panels
[AD-A190617] N88-22092
The effective fracture toughness of aluminum at rapid heating rates
[AD-A189745] N88-22146
High speed, bandpass sampling of digital communications waveforms
[AD-A189842] N88-22254
Synthetic-aperture radars viewed as interferometers with matched filter processing of the collected data
[AD-A190608] N88-22262
A multiple model adaptive tracking algorithm against airborne targets
[AD-A190619] N88-22263
An expert system for discrete component digital circuit design
[AD-A189680] N88-22274
Fabrication and electrical characterization of multilevel aluminum interconnects used to achieve silicon-hybrid wafer-scale integration
[AD-A190519] N88-22282
An improved method for calculating power density in the Fresnel region of circular parabolic reflector antennas
[AD-A190569] N88-22284
Interaction of a two-dimensional bluff body and incompressible jet and annulus flows
[AD-A190503] N88-22310
Investigation of boundary layer disturbances caused by periodic heating of a thin ribbon
[AD-A190572] N88-22314
Effect of freestream turbulence on a two dimensional cascade, with different surface roughness, at high Reynolds number
[AD-A190615] N88-22316
The buckling and vibration of composite plates using the Levy method considering shear deformation and rotary inertia
[AD-A189743] N88-22374
Experimental comparison of lightning simulation techniques to CV-580 airborne lightning strike measurements
[AD-A190578] N88-22496
Motion sickness: Quantitative, algorithmic malaise indication in real time
[AD-A189674] N88-22518
A UNIX-based interactive VHDL (hardware description language) simulator
[AD-A189749] N88-22565
Implementation of a distributed adaptive routing algorithm on the Intel iPSC (Intel Personal Super-Computer)
[AD-A189849] N88-22567
Design and implementation of VLSI prime factor algorithm processor
[AD-A190483] N88-22580
Design of an algorithm to translate nested relational algebra queries to GENESIS trace manager commands
[AD-A190502] N88-22581
Software verification using partition analysis
[AD-A190570] N88-22582
SEARCH: An interactive computer program for optimizing two-variable, unconstrained experiments or simulation
[AD-A190593] N88-22583
A graphics editor for structured analysis with a data dictionary
[AD-A190618] N88-22584
Simulation of fault tolerance in a hypercube arrangement of discrete processors
[AD-A189682] N88-22594
The modeling, simulation and comparison of interconnection networks for parallel processing
[AD-A190571] N88-22599
Implementation and performance analysis of parallel assignment algorithms on a hypercube computer
[AD-A190678] N88-22600
High speed transcendental elementary function architecture in support of the Vector Wave Equation (VWE)
[AD-A189746] N88-22627
An approximation technique for solving a system of Fredholm integral equations for asymmetric detector response functions
[AD-A190577] N88-22645
Calculating depletion region carrier concentrations with capacitance-voltage measurements and etching
[AD-A189630] N88-22777
Examination of temperature effects on gate-to-drain avalanche breakdown in GaAs MESFETs (Metal-Semiconductor Field Effect Transistors) by measuring light emission under RF drive
[AD-A189634] N88-22778
A model for nitrogen atom recombination on a silicon dioxide surface
[AD-A189643] N88-22784
Modeling the effects of heavy charged particles on MOSFETs (Metal-Oxide-Semiconductor Field Effect Transistors)
[AD-A190575] N88-22792
Film cooling effectiveness on a flat plate in high free-stream turbulence using a single row of 30 deg slant-hole injectors
[AD-A190500] N88-22816
A methodolgy, based on analytical modeling, for the design of parallel and distributed architectures for relational database query processors
[AD-A189844] N88-22825

AIR FORCE OCCUPATIONAL AND ENVIRONMENTAL HEALTH LAB., BROOKS AFB, TEX.
Noise assessment of unsuppressed TF-34-GE-100A engine at Warfield ANG, Baltimore, Maryland
[AD-A189666] N88-22702

AIR FORCE SYSTEMS COMMAND, WRIGHT-PATTERSON AFB, OHIO.
Control of laminar flow around of the wing in free-air conditions
[AD-A187479] N88-22004
Corrosion and electrochemical behavior of binary magnesium alloys
[AD-A190624] N88-22154
Experimental determination of the coefficients of the hydraulic resistance of apertures in the rotary disks
[AD-A190627] N88-22317
Study of lightning and lightning protection (selected pages)
[AD-A190623] N88-22498
AKRON UNIV., OHIO.
Unified constitutive model development for metal matrix composites at high temperature N88-22387
ALABAMA A & M UNIV., HUNTSVILLE.
Development of remote sensing techniques capable of delineating soils as an aid to soil survey
[NASA-CR-182610] N88-22452
ALABAMA UNIV., TUSCALOOSA.
A direct-execution parallel architecture for the Advanced Continuous Simulation Language (ACSL)
[NASA-CR-182809] N88-22602
ALBERTA UNIV., EDMONTON.
The adjoint process in stochastic optimal control
[AD-A189720] N88-22605
Martingale representation and the Malliavin calculus
[AD-A189721] N88-22626
The existence of smooth densities for the prediction filtering and smoothing problems
[AD-A189865] N88-22629
Filtering of jump processes
[AD-A189701] N88-22656
The partially observed stochastic minimum principle
[AD-A189787] N88-22658
ALLIED BENDIX AEROSPACE, KANSAS CITY, MO.
NMR analysis of a fluorocarbon copolymer
[DE88-002364] N88-22170
AMSTERDAM UNIV. (NETHERLANDS).
Constructive version of the approximation induction principle
[PB88-165477] N88-22647
Complexity of some problems in module algebra
[PB88-165386] N88-22648
APPLIED TECHNOLOGIES, INC., BOULDER, COLO.
Ultrasonic oxygen sensor
[AD-A189723] N88-22537
ARGONNE NATIONAL LAB., ILL.
Mass transfer mechanisms for water adsorbed on silica gel
[DE88-005993] N88-22107
Trust regions and projected gradients
[DE88-005829] N88-22646
Ultrasonic beam distortion in transversely isotropic media
[DE88-005937] N88-22699
ALEX results: A comparison of measurements from a round and a rectangular duct with 3-D code predictions
[DE88-005947] N88-22741
MPD (magnetoplasmadynamic) thruster advanced pumping system concepts
[AD-A190513] N88-22756
RF properties of superconducting Pb electroplated onto Cu
[DE88-005918] N88-22765
Effective electron interactions due to virtual charge and spin excitations in an extended Hubbard model for Cu-O superconductors
[DE88-005971] N88-22766
Ion-beam mixing and amorphization in Au/Zr bilayers
[DE88-005999] N88-22767
Dynamical optimization techniques for the calculation of electronic structure in solids
[DE88-006010] N88-22768
Thermochemistry and high temperature thermodynamic properties of rare earth-alkaline earth-copper oxide superconductors
[DE88-005976] N88-22770
Status of RF superconductivity at Argonne National Laboratory
[DE88-005913] N88-22796
Annihilation momentum density of positrons trapped at vacancy-type defects in metals and alloys
[DE88-005936] N88-22797
High-T(sub c) superconducting wire fabrication and testing
[DE88-005989] N88-22798
Preparation of large area NbN/AlN/NbN Josephson junctions
[DE88-006074] N88-22799
ARIZONA STATE UNIV., TEMPE.
Summary and conclusions on electrooptical streak camera project
[DE88-006616] N88-22334
Research on certain aspects of laser diffraction particle sizing relevant to autonomous self-diagnosing instrumentation
[AD-A190220] N88-22348
Autonomous control system for Czochralski growth of LEC GaAs
[AD-A189726] N88-22779
ARIZONA UNIV., TUCSON.
Experimental investigation of a spanwise forced mixing layer
[AD-A190136] N88-22007
Speckle interferometry of asteroids
[NASA-CR-180438] N88-22843
ARMY ARMAMENT RESEARCH AND DEVELOPMENT COMMAND, DOVER, N. J.
Determination of the commutation and angle and load response for a continuous-current, single phase controlled rectifier
[AD-A190602] N88-22295
ARMY ARMAMENT RESEARCH AND DEVELOPMENT COMMAND, WATERVLIET, N. Y.
Launchability of base-driven electromagnetic projectiles
[AD-A189635] N88-22055
Determination of aquo-complexes of chromium and iron in chromium plating and polishing solutions by ion chromatography
[AD-A190168] N88-22148
A posterior error estimation in a finite element method for parabolic partial differential equations
[AD-A190296] N88-22636
ARMY AVIATION ENGINEERING FLIGHT ACTIVITY, EDWARDS AFB, CALIF.
Preliminary airworthiness evaluation of the UH-60A equipped with the XM-139 VOLCANO mine dispensing system
[AD-A190604] N88-22029
Preliminary airworthiness evaluation of the UH-60A with Advanced Digital Optical Control System (ADOCS)
[AD-A190674] N88-22030
ARMY BELVOIR RESEARCH AND DEVELOPMENT CENTER, FORT BELVOIR, VA.
Galvanic corrosion initiatives
[AD-A190658] N88-22155
ARMY COLD REGIONS RESEARCH AND ENGINEERING LAB., HANOVER, N.H.
Thermal instability and heat transfer characteristics in water/ice systems
[AD-A189627] N88-22297
The CRREL (Cold Regions Research and Engineering Laboratory) Hopkinson bar apparatus
[AD-A190599] N88-22380
Spectral measurements in a disturbed boundary layer over snow
[AD-A190217] N88-22494
ARMY CONSTRUCTION ENGINEERING RESEARCH LAB., CHAMPAIGN, ILL.
ECP (Electrical Circuitry Program): A proposed program for electrical circuitry analysis
[AD-A190494] N88-22280
Sources of digital spatial data for geographic information systems
[AD-A189788] N88-22824
ARMY LAB. COMMAND, WATERTOWN, MASS.
Structure and surface characterizations of high strength carbon fibers
[AD-A189642] N88-22087
Drilling metal matrix composites
[AD-A190480] N88-22091
ASTROSYSTEMS INTERNATIONAL, INC., NEWARK, DEL.
High-efficiency thin-film silicon-on-GaP solar cell for improved radiation resistance
[AD-A190268] N88-22460
ATMOSPHERIC AND ENVIRONMENTAL RESEARCH, INC., CAMBRIDGE, MASS.
Baseline observing system experiments using the AFGL global data assimilation system
[AD-A188861] N88-22062
ATOMIC ENERGY RESEARCH ESTABLISHMENT, HARWELL (ENGLAND).
High temperature materials: What's available
[AERE-R-12632] N88-22081
Angular resolved energy analysis of (69)Ga+ ions from a gallium liquid metal ion source
[AERE-R-12649] N88-22760
AUBURN UNIV., ALA.
Theoretical studies of the heating of toroidal plasmas with radiofrequency electromagnetic radiation
[DE88-006913] N88-22749

B

BABCOCK AND WILCOX CO., LYNCHBURG, VA.
An evaluation of nondestructive methods for ceramic heat exchanger applications
[DE88-006731] N88-22328
BALLISTIC RESEARCH LABS., ABERDEEN PROVING GROUND, MD.
Fluid motion in a spinning, coning cylinder via spatial eigenfunction expansion
[AD-A190758] N88-22319
A 150,000 pounds per square inch dynamic pressure calibrator
[AD-A190659] N88-22335
Buckling of blast loaded cylinder
[AD-A190124] N88-22376
BATTELLE PACIFIC NORTHWEST LABS., RICHLAND, WASH.
Evolution of hardening and damage during viscoplastic deformation
[AD-A190714] N88-22381
BDM CORP., MCLEAN, VA.
Applications of optical computing to problems with symbolic computations
[AD-A189772] N88-22548
BEIJING UNIV. (CHINA).
Ion-beam mixing and amorphization in Au/Zr bilayers
[DE88-005999] N88-22767
BHABHA ATOMIC RESEARCH CENTRE, BOMBAY (INDIA).
Computer program in BASIC language for computation of spectrochemical analytical data
[DE88-701229] N88-22106
Development of a computer code CRACK for elastic and elastoplastic fracture mechanics analysis of 2-D structures by finite element technique
[DE88-701231] N88-22370
Earthquakes from peninsular India: Data from the Gauribidanur seismic array
[DE88-701232] N88-22471
Characteristics of seismic sources of some Asian earthquakes and Soviet underground explosions from Gauribidanur array records
[DE88-701233] N88-22472
Project Monitoring Package (PMP): A package for project activity monitoring
[DE88-701234] N88-22554
COMESH: A corner mesh finite difference code to solve multigroup diffusion equations in multidimensions
[DE88-701248] N88-22555
PLOT3D (version-5): A computer code for drawing three dimensional graphs, maps and histograms, in single or multiple colours, for mono or stereoscopic viewing
[DE88-701410] N88-22558
Output formatting in Apple-soft BASIC
[DE88-701413] N88-22559
Rayleigh-Taylor instability in inertial confinement fusion
[TI88-701411] N88-22750
Superconductivity in power engineering
[DE88-701414] N88-22776
BOEING AEROSPACE CO., SEATTLE, WASH.
FLOSIN: A fluid loop analyzer for SINDA N88-22321
BOEING MILITARY AIRPLANE DEVELOPMENT, SEATTLE, WASH.
Development and evaluation of an airplane fuel tank ullage composition model. Volume 2: Experimental determination of airplane fuel tank ullage compositions
[AD-A190408] N88-22025
BOHAN (WALTER A.) CO., PARK RIDGE, ILL.
NIMBUS-7 CZCS. Coastal Zone Color Scanner imagery for selected coastal regions. North America - Europe. South America - Africa - Antarctica. Level 2 photographic product
[NASA-CR-180755] N88-22447
BOSTON UNIV., MASS.
Advanced programming and control techniques for complex mechanical systems
[AD-A190238] N88-22349
Instrumentation for scientific computing in neural networks, information science, artificial intelligence and applied mathematics
[AD-A189981] N88-22549
BRADLEY UNIV., PEORIA, ILL.
Dynamical optimization techniques for the calculation of electronic structure in solids
[DE88-006010] N88-22768
BRIGHAM AND WOMEN'S HOSPITAL, BOSTON, MASS.
A program for the study of skeletal muscle catabolism following physical trauma
[AD-A189771] N88-22521
BROOKHAVEN NATIONAL LAB., UPTON, N. Y.
Advances in geochemistry and cosmochemistry: Trace element microdistributions with the synchrotron X-ray fluorescence microprobe
[DE88-006355] N88-22108

Variable-energy positron studies on liquids and liquid-solid interfaces
[DE88-006356] N88-22109
High temperature superconductors in the La(sub 1+x)Ba(sub 2-x)Cu O(sub y system
[DE88-006367] N88-22802

BROWN UNIV., PROVIDENCE, R. I.
Theoretical studies of Resonance Enhanced Stimulated Raman Scattering (RESRS) of frequency-doubled Alexandrite laser wavelength in cesium vapor
[NASA-CR-182870] N88-22133

C

CALIFORNIA INST. OF TECH., PASADENA.
Postbuckling delamination of a stiffened composite panel using finite element methods
[NASA-CR-182803] N88-22098
Investigation of combustion in large vortices
[AD-A190406] N88-22121
Remarks on solid state amorphizing transformations
[DE88-006452] N88-22803
Near-infrared observations of cepheids: The distance to M33 N88-22846

CALIFORNIA UNIV., BERKELEY.
SimPL: A simulator for parallel LISP
[AD-A189831] N88-22566
Absolute pressure derivatives of deep level defects in 3-5 semiconductors
[DE88-006318] N88-22772

CALIFORNIA UNIV., BERKELEY. LAWRENCE BERKELEY LAB.
Superconducting magnet technique for ASTROMAG on the space station
[DE88-004560] N88-22063
The contribution of electron microscopy of materials science to society
[DE88-006341] N88-22082
Studies of surfaces using optical sum-frequency generation
[DE88-006334] N88-22715
The influence of current stressing on the structure of Ag contacts to GaAs
[DE88-005988] N88-22771
Absolute pressure derivatives of deep level defects in 3-5 semiconductors
[DE88-006318] N88-22772
First-principles calculations of quasiparticle energies at surfaces and interfaces: Semiconductor surface-state spectra and band offsets
[DE88-006340] N88-22773
Optical characterization of microcrystals
[DE88-006622] N88-22775
Fermi level stabilization in semiconductors: Implications for implant activation efficiency
[DE88-006332] N88-22801

CALIFORNIA UNIV., DAVIS.
The combustion synthesis of boride composites
[DE88-005474] N88-22084
Numerical methods for linear and nonlinear optimization
[AD-A190029] N88-22631

CALIFORNIA UNIV., IRVINE.
High power, high frequency radiation from beam-plasma interactions
[AD-A190207] N88-22752

CALIFORNIA UNIV., LOS ANGELES.
Optimal control and identification of space structures
[AD-A190033] N88-22065
Magnetic fusion energy plasma interactive and high heat flux components. Volume 5: Technical assessment of critical issues in the steady state operation of fusion confinement devices
[DE88-006920] N88-22744
Fundamental properties and devices applications of Ge(x)Si(1-x)/Si superlattices
[AD-A190129] N88-22787

CALIFORNIA UNIV., SAN DIEGO.
Baecklund transformation and the Schwarzian derivative
[AD-A190277] N88-22684
Research on materials and components for opto-electronic signal processing and computing
[AD-A190130] N88-22788

CALIFORNIA UNIV., SAN DIEGO, LA JOLLA.
Phenomenological modelling of rate-dependent plasticity for high strain rate problems
[DE88-006647] N88-22440
Synthesis of metastable superconductors by high dynamic pressure
[DE88-005620] N88-22764

CARNEGIE-MELLON UNIV., PITTSBURGH, PA.
Multi-disciplinary techniques for understanding time-varying space-based imagery
[AD-A190711] N88-22610
Fundamental studies on MPD thrusters
[AD-A190307] N88-22753
Two papers on a symbolic analyzer for MOS (Metal-Oxide Semiconductors) circuits
[AD-A188617] N88-22761
High density ion implanted contiguous disk bubble technology
[AD-A190169] N88-22789

CENTER FOR NAVAL ANALYSES, ALEXANDRIA, VA.
Modeling failures of intermittently used machines
[AD-A190298] N88-22367
Properties of some Bayesian scoring procedures for computerized adaptive tests
[AD-A189925] N88-22660

CENTRAL INST. FOR THE DEAF, ST. LOUIS, MO.
Auditory perception of complex sounds
[AD-A190528] N88-22529

CENTRE D'ESSAIS AERONAUTIQUE TOULOUSE (FRANCE).
Influence of temperature on the tensile strength and toughness characteristics. Material 35NCD16 ESR. Test report M5-521800
[M5-521800] N88-22163
Characterization of HYTUF steel. Semifinished product: 160 mm dia forging block. Processor: C3f. Test Report M3-434600
[M3-434600] N88-22164

CENTRE NATIONAL D'ETUDES SPATIALES, TOULOUSE (FRANCE).
Spacecraft trajectories
[ISBN-2-85-428166-7] N88-22054
Identification of a star field from a spinning satellite
[CNES-NT-120] N88-22074
Short experiment study of four-wire helical antennas (half turn half wave)
[CNES-CT/DRT/TIT/AN-249-T] N88-22266
Definition and implementation study for the Varan-S radar
[CNES-CT/DRT/TIT/RL-143-T] N88-22267
Degradation of downlink distance measurement indexes by the addition of a third tone
[CNES-CT/DRT/TIT/TR-122-T] N88-22268

CHICAGO UNIV., ILL.
Advances in geochemistry and cosmochemistry: Trace element microdistributions with the synchrotron X-ray fluorescence microprobe
[DE88-006355] N88-22108
Particle cosmology comes of age
[DE88-006998] N88-22844

CHINA NUCLEAR INFORMATION CENTRE, BEIJING.
Multigroup flux-limited asymptotic diffusion Fokker-Planck equation
[DE88-700958] N88-22615

CINCINNATI UNIV., OHIO.
High-performance polymeric materials
[AD-A190708] N88-22190

CLARKSON UNIV., POTSDAM, N.Y.
Nonlinear analysis and optimal design of dynamic mechanical systems for spacecraft application
[AD-A190644] N88-22070
Nondestructive moisture measurement in microelectronics
[AD-A190515] N88-22281

CLEVELAND STATE UNIV., OHIO.
Computational simulation methods for composite fracture mechanics N88-22396
Whisker-reinforced ceramic composites for heat engine components N88-22410
Continuous fiber ceramic matrix composites for heat engine components N88-22411

COLORADO STATE UNIV., FORT COLLINS.
Forecast of Atlantic seasonal hurricane activity for 1988 N88-22500
Gas source MBE (Molecular Beam Epitaxy)
[AD-A189763] N88-22782
Beam assisted fabrication of 3-5/Si monolithic devices
[AD-A189979] N88-22785

COLORADO UNIV., BOULDER.
Laser photoelectron spectroscopy of ions
[DE88-006860] N88-22113
Electronic energy transfer processes in the alkali/alkaline earth metal vapors
[AD-A190035] N88-22119
NASA and the challenge of ISDN: The role of satellites in an ISDN world
[NASA-CR-182749] N88-22676

COLUMBIA UNIV., NEW YORK, N.Y.
Molecular dynamics of materials possessing high energy content
[AD-A190034] N88-22118

CONSIGLIO NAZIONALE DELLE RICERCHE, FLORENCE (ITALY).
Discharge excitation of the XeF C to A transition
[DE88-006448] N88-22339

CORNELL UNIV., ITHACA, N.Y.
Symmetry and global bifurcation in nonlinear solid mechanics
[AD-A190521] N88-22642

D

DEFENCE RESEARCH ESTABLISHMENT, OTTAWA. (ONTARIO).
Anthropomorphic phantom radiation dosimetry at the NATO standard reference point at Aberdeen Proving Ground
[AD-A190508] N88-22528

DEFENSE TECHNICAL INFORMATION CENTER, ALEXANDRIA, VA.
The Scientific and Technical Information Network (STINET). Foundation for evolution
[AD-A189750] N88-22622

DEPARTMENT OF ENERGY, IDAHO FALLS, IDAHO.
Application and technology requirements for heat pumps at the process industries
[DE88-006740] N88-22293

DEPARTMENT OF ENERGY, WASHINGTON, D. C.
Energy from the wind
[DE88-006897] N88-22459
Northern lights: The economic and practical potential of imported power from Canada
[DE88-006026] N88-22473

DEPARTMENT OF THE AIR FORCE, WASHINGTON, D.C.
Feedback control of distributed parameter systems with applications to large space structures
[AD-A190536] N88-22068

DEUTSCHE FORSCHUNGS- UND VERSUCHSANSTALT FUER LUFT- UND RAUMFAHRT, COLOGNE (WEST GERMANY).
Performance evaluation of molten salt thermal storage systems
[DE87-014645] N88-22461

DEUTSCHE FORSCHUNGS- UND VERSUCHSANSTALT FUER LUFT- UND RAUMFAHRT, GOETTINGEN (WEST GERMANY).
Theoretical investigation of secondary instability of three-dimensional boundary-layer flows with application to the DFVLR-F5 model wing
[DFVLR-FB-87-44] N88-22330

DORNIER-WERKE G.M.B.H., FRIEDRICHSHAFEN (WEST GERMANY).
Feasibility study for a 2nd generation system for airborne maritime pollution surveillance
[ETN-88-92108] N88-22466

DOUGLAS AIRCRAFT CO., INC., LONG BEACH, CALIF.
Oscillating airfoils: Achievements and conjectures
[AD-A190490] N88-22008

DREXEL UNIV., PHILADELPHIA, PA.
Multiple scattering from nonspherical targets
[AD-A189939] N88-22723

DU PONT DE NEMOURS (E. I.) AND CO., AIKEN, S.C.
OCR vision system, an alternative to bar code
[DE88-003761] N88-22828

DU PONT DE NEMOURS (E. I.) AND CO., WILMINGTON, DEL.
High temperature superconductors in the La(sub 1+x)Ba(sub 2-x)Cu O(sub y system
[DE88-006367] N88-22802

DUKE UNIV., DURHAM, N. C.
Comparative analysis of multistage interconnection networks
[AD-A190436] N88-22598
On categorizing sounds
[AD-A189784] N88-22700

DURHAM UNIV. (ENGLAND).
A new approach to highly fluorinated lubricants
[AD-A190523] N88-22188

E

ECOLE NATIONALE SUPERIEURE DES TELECOMMUNICATIONS, PARIS (FRANCE).
Using Colored Stochastic Petri Net (CS-PN) software for protocol specification, validation, and evaluation
[ENST-87C004] N88-22588
The Colored Stochastic Petri Net (CS-PN) software: Application to the validation and the performance evaluation of distributed systems
[ENST-87D005] N88-22589

ECOLE POLYTECHNIQUE, PALAISEAU (FRANCE).
Activities report in laser-matter interaction
[ETN-88-92007] N88-22696

EDGERTON, GERMESHAUSEN AND GRIER, INC., IDAHO FALLS, IDAHO.
Microplasticity phenomena in graphite/magnesium metal matrix composites
[DE88-006772] N88-22086

Grain growth behavior of extrusion consolidated centrifugally atomized Type 304 stainless steel powder
[DE88-006788] N88-22143
Characterization of an explosively consolidated rapidly solidified Fe-16Ni-9Cr-5Mo-2Cu alloy powder
[DE88-006733] N88-22162
Fracture toughness of silicon nitride-silicon nitride joints bonded with oxynitride glass
[DE88-005548] N88-22172
Status of electric vehicle simulation programs at the INEL: Summer 1987
[DE88-006745] N88-22271
GTE battery management system: State of charge indicator evaluation
[DE88-006800] N88-22272
Application and technology requirements for heat pumps at the process industries
[DE88-006740] N88-22293
Measurement of the elastic-plastic surface flaw back surface topology and its relation to constraint
[DE88-006765] N88-22437
Requirements and cost considerations for a Combined Space Nuclear Reactor Test Facility
[DE88-006763] N88-22719
Environmental assessment for the compact ignition Tokamak
[DE88-005633] N88-22740

ELECTROTECHNICAL LAB., IBARAKI (JAPAN).
Study on shaft seals for potassium turbine
[EL-891] N88-22364

ELTECH SYSTEMS, INC., FAIRPORT HARBOR, OHIO.
Aluminum-air battery development
[DE88-006620] N88-22287

EMORY UNIV., ATLANTA, GA.
New methods for numerical solution of one class of strongly nonlinear partial differential equations with applications
[AD-A189945] N88-22630

ENGINEERING SCIENCE SOFTWARE, INC., SMITHFIELD, R.I.
Unified constitutive model for single crystal deformation behavior with applications N88-22388

ENVIRONMENTAL PROTECTION AGENCY, RESEARCH TRIANGLE PARK, N.C.
Assessment of crop loss from air pollutants: Meteorology-atmospheric chemistry and long range transport
[PB88-146857] N88-22448

ENVIRONMENTAL RESEARCH INST. OF MICHIGAN, ANN ARBOR.
Optical switching and control techniques using nonlinear optical wave mixing
[AD-A190467] N88-22730

ERLANGEN-NUREMBERG UNIV. (WEST GERMANY).
Piston-driven, unsteady separation at a sudden expansion in a tube: Flow visualization and Laser Doppler Anemometer (LDA) measurements
[ETN-88-92104] N88-22329

F

FEDERAL AVIATION ADMINISTRATION, WASHINGTON, D.C.
Age, alcohol, and simulated altitude: Effects on performance and breathalyzer scores
[AD-A190642] N88-22531
An evaluation of the effects of high visual taskload on the separate behaviors involved in complex monitoring performance
[AD-A190641] N88-22536

FERMI NATIONAL ACCELERATOR LAB., BATAVIA, ILL.
Einstein metrics and Brans-Dicke superfields
[DE88-006992] N88-22809
Finite width corrections to the Nambu action for the Nielsen-Olesen string
[DE88-006996] N88-22812
String driven inflation
[DE88-006994] N88-22841
Cosmology for high energy physicists
[DE88-005705] N88-22842
Particle cosmology comes of age
[DE88-006998] N88-22844

FLORIDA UNIV., GAINESVILLE.
Donor acceptor polymerization chemistry as a vehicle to low energy cure matrix resins
[AD-A190119] N88-22179
The interaction of small particles with laser beams
[AD-A190716] N88-22354

FLOW RESEARCH, INC., KENT, WASH.
Unsteady aerodynamics of a Wortmann FX-63-137 wing in a fluctuating wind field
[AD-A190128] N88-22006

FONDAZIONE UGO BORDONI, ROME (ITALY).
Collective rotation of molecules driven by the angular momentum of light in a nematic film
[FUB-6-1986] N88-22714

FRAUNHOFER INST. FUER WERKSTOFFMECHANIK, FREIBURG (WEST GERMANY).
Processing defects and strength of alumina substrates
[W-10/87] N88-22441

G

GENERAL ACCOUNTING OFFICE, WASHINGTON, D. C.
Space shuttle accident: NASA's actions to address the Presidential Commission report
[PB88-135306] N88-22059

GENERAL ELECTRIC CO., EVENDALE, OHIO.
Elevated temperature crack growth N88-22421

GENERAL ELECTRIC CO., SCHENECTADY, N.Y.
A high performance inverter-fed drive system of an interior permanent magnet synchronous machine
[DE88-006753] N88-22288

GEORGIA UNIV., ATHENS.
Effective electron interactions due to virtual charge and spin excitations in an extended Hubbard model for Cu-O superconductors
[DE88-005971] N88-22766

GOSUDARSTVENNYI KOMITET PO ISPOLZOVANIYU ATOMNOI ENERGII, MOSCOW (USSR).
Use of long-distance pair potentials in calculations of defect characteristics in metals
[TI88-701039] N88-22138
High-voltage inverse-square function generator
[DE88-701109] N88-22270
MIG-1 on-line measuring holographic microscope
[TI88-701103] N88-22332
Focused image holography abberations
[TI88-701105] N88-22333
Spin precession in stationary gravitational fields
[TI88-701107] N88-22470
Fast analog-to-digital converter
[TI88-701488] N88-22543
Application of static memory for data acquisition and transmission into a computer
[TI88-701491] N88-22544
Does the pipe diffusion of self-interstitials in crystals under stresses exist
[TI88-701027] N88-22762
Hydrodynamical models of supernova SN 1987 A in the LMC
[TI88-701123] N88-22837

GOSUDARSTVENNYI KOMITET PO ISPOLZOVANIYU ATOMNOI ENERGII, OBNINSK (USSR).
Detecting the gas bubbles in a liquid metal coolant by means of magnetic flowmeters
[TI88-701427] N88-22294

GRENOBLE-1 UNIV. (FRANCE).
French Multiproject Chip (MPC) activity report, 1986
[RR-650-I] N88-22273
Self-checking logic arrays
[RR-656-I] N88-22545
On the geometric interpretation of image contours
[RR-647-I-IMAG-57-LIFIA] N88-22563
Consistent estimates of autoregressive parameters for autoregressive moving average models
[RR-663-I] N88-22564
Modeling a parallel architecture for image processing
[RR-646-I] N88-22593
About disequations simplification
[RR-645-I-IMAG-55-LIFIA] N88-22624

GRONINGEN RIJKSUNIVERSITEIT (NETHERLANDS).
Electrical resistivities of some compound forming liquid metal alloys
[PB88-145172] N88-22137

GRUMMAN AEROSPACE CORP., BETHPAGE, N.Y.
On the prediction of highly vortical flows using an Euler equation model, part 2
[AD-A190245] N88-22305

H

HELSINKI UNIV. OF TECHNOLOGY, ESPOO (FINLAND).
Activities of As, Sb, Bi and Pb in copper mattes and their effects on impurity elimination
[TKK-V-A10(1988)] N88-22165
Studies on hot-dip zinc-aluminum coated sheet steels
[ETN-88-92217] N88-22166
Structure and properties of titanium nitride and zirconium nitride thin films prepared by reactive ion plating
[ETN-88-92218] N88-22167
The development of high power KrF laser systems for plasma research by the application of stimulated Raman scattering
[ETN-88-92220] N88-22358
Boundary element method for three-dimensional magnetostatic fields in terms of vector variables
[EL-61] N88-22649

HIROSHIMA UNIV., TAKEHARA (JAPAN).
Recent developments in the path integral approach to anomalies
[DE87-703032] N88-22616
Remarks on the time transformation of path-integral measures
[DE87-703040] N88-22617
Super Virasoro algebra and solvable supersymmetric quantum field theories
[DE88-752299] N88-22681
Ten dimensional N = 1 supergravity coupled to supersymmetric Yang-Mills fields in superspace
[DE87-703033] N88-22808
Path integral, BRS symmetry, and string and membrane theories
[DE88-752300] N88-22810
Hydrodynamical equations for spherical gravitational collapse in terms of a generalized theory of gravitation with higher derivatives
[DE87-703027] N88-22838
Generation and propagation of sound waves in a collapsing or anti-collapsing star with uniform density
[DE87-703034] N88-22839
Density perturbations in a rotating universe
[DE87-703036] N88-22840

HONEYWELL, INC., BLOOMINGTON, MINN.
Research on stable processible conducting polymers for electronic applications
[AD-A190245] N88-22180

HUGHES AIRCRAFT CO., EL SEGUNDO, CALIF.
Advanced capacitor development
[AD-A189985] N88-22276

I

ILLINOIS STATE WATER SURVEY, CHAMPAIGN.
A multivariate variational objective analysis-assimilation method. Part 1: Development of the basic model
[NASA-CR-182651] N88-22491
A multivariate variational objective analysis-assimilation method. Part 2: Case study results with and without satellite data
[NASA-CR-182653] N88-22492

ILLINOIS UNIV., URBANA.
Cement paste matrix composite materials center
[AD-A188657] N88-22083
Structure of sol-gel silica
[DE88-006870] N88-22114
Fluids, gels and glasses under extreme conditions of pressure and temperature
[AD-A190655] N88-22125
Numerical and experimental investigation of multiple shock wave/turbulent boundary layer interactions in a rectangular duct
[AD-A190772] N88-22320
Supercomputer environment
[AD-A190633] N88-22551
Logarithmically connected, repetitive computer networks and numerical applications
[DE88-006832] N88-22592
Representation, analysis and design of multirate discrete-time control systems
[AD-A190499] N88-22608
The total interval of a graph
[AD-A189648] N88-22625
ALEX results: A comparison of measurements from a round and a rectangular duct with 3-D code predictions
[DE88-005947] N88-22741

ILLINOIS UNIV., URBANA-CHAMPAIGN.
Hafnia-rich mixed oxide ceramics of the system HfO2-ZrO2-TiO2 for heaters and heat exchangers in electrothermal thrusters: The effects of titania on selected electrical and mechanical properties of Hafnia-rich mixed oxides in the system Hafnia-Zirconia-Titania, volume 1
[NASA-CR-182800-VOL-1] N88-22197
Fatigue damage mapping N88-22423

INDIAN INST. OF TECH., KANPUR.
Annihilation momentum density of positrons trapped at vacancy-type defects in metals and alloys
[DE88-005936] N88-22797

INDIANA UNIV., BLOOMINGTON.
Perception of complex auditory patterns
[AD-A190218] N88-22524
Transformations of concurrent algorithms for highly parallel systems: A one year project summary report
[AD-A190236] N88-22576

INDIANA UNIV.-PURDUE UNIV., INDIANAPOLIS.
A zonal approach for the solution of coupled Euler and potential solutions of flows with complex geometries
[AD-A189752] N88-22595

INSTITUT D'AERONOMIE SPATIALE DE BELGIQUE, BRUSSELS.
Rotational structure and absorption cross sections from 300 to 190 K of the Schumann-Runge bands
[AERONOMICA-ACTA-A-316-1987] N88-22131
Ultraviolet absorption cross sections of methylbromide at stratospheric temperatures
[AERONOMICA-ACTA-A-320-1987] N88-22132
Plasmapause formation
[AERONOMICA-ACTA-A-319-1987] N88-22759
INSTITUT FRANCO-ALLEMAND DE RECHERCHES, ST. LOUIS (FRANCE).
A review on holography, its principles and applications
[ISL-CO-242/86] N88-22338
Contour interactive extraction using image numerical treatment
[ISL-R-114/86] N88-22587
Experimental study on the influence of wind on acoustic pressure sensors
[ISL-R-121/86] N88-22712
Acoustic propagation in the low atmosphere. Experimental study and modeling by the radius method
[ISL-CO-247/86] N88-22713
INSTITUTO DE PESQUISAS ESPACIAIS, SAO JOSE DOS CAMPOS (BRAZIL).
Numerical orbit propagation methods for earth artificial satellites
[INPE-4405-RPE/556] N88-22053
Fabrication and characterization of semiconductor lasers of Pb(1-x)Sn(x)Te
[INPE-4253-PRE/1126] N88-22357
Updating of the municipal official register of real estate through a geographical information system
[INPE-4459-PRE/1238] N88-22453
Method for restoration and resampling of TM sensor imagery
[INPE-4491-PRE/1255] N88-22454
Project CODEAMA/FUNCATE (test-area of Barreirinha-AM): Field report
[INPE-4500-RPE/563] N88-22455
Comparative utilization of analog and digital processes in the treatment of MSS-LANDSAT data for studying the national parks of Brazil
[INPE-4011-TDL/240] N88-22456
Radon-222 in the Antarctic Peninsula
[INPE-4486-PRE/1251] N88-22468
Surface CO results from the ABLE-2B expedition to Amazonia
[INPE-4501-PRE/1258] N88-22469
In-situ plasma bubble observations associated with equatorial spread-F over Natal
[INPE-4488-PRE/1252] N88-22482
Stratospheric electric field and conductivity measurements over electrified convective clouds in the South American region, revised
[INPE-4046-PRE/1012-REV-3] N88-22483
Surface ozone and ozonesounding results from the ABLE-2B expedition to Amazonia
[INPE-4523-PRE/1275] N88-22484
Calibration and processing of AVHRR data for temperature estimation
[INPE-4493-PRE/1257] N88-22485
A study on electric fields and conductivity associated with electrified clouds in the region of South America
[INPE-4487-TDL/325] N88-22486
Rocket measurements of ionospheric electron temperature over Natal
[INPE-4485-PRE/1250] N88-22489
Aerodynamic aspects of the Amazon Forest
[INPE-4445-TDL/313] N88-22501
Tropical circulations and the associated rainfall anomalies during two contrasting years
[INPE-4506-PRE/1261-REV] N88-22502
Inference engine for expert systems
[INPE-4465-TDL/321] N88-22590
Vacuum-arc plasma centrifuge experiment
[INPE-4509-PRE/1263] N88-22758
Equilibrium stability of strained epitaxial layers on a rigid substrate
[INPE-4254-PRE/1127] N88-22804
A fault tolerant supervision system
[INPE-4419-TDL/307] N88-22819
INPE position paper on the CCSDS standardized method of link budget computation
[INPE-4533-NTE/279] N88-22820
Georelational data model
[INPE-4490-PRE/1254] N88-22829
The necessity of automation in Brazil
[INPE-4346-PRE/1183] N88-22832
Orbital remote sensing: An instrument for monitoring urban growth
[INPE-4456-PRE/1267] N88-22833
Multiple object redshift determinations in clusters of galaxies using OCTOPUS
[INPE-4528-PRE/1278] N88-22835
New measurements of radial velocities in clusters of galaxies
[INPE-4527-PRE/1277] N88-22845
The 1985 mutual phenomena of Jupiter's satellites observed in Brazil
[INPE-4526-PRE/1276] N88-22848
A map of the cosmic background radiaton at 3 millimeters
[INPE-4529-PRE/1279] N88-22850
INSTITUTO NACIONAL DE TECNICA AEROESPACIAL, ESTEBAN TERRADAS, TORREJON DE ARDOZ (SPAIN).
A panel method based on velocity potential to compute harmonically oscillating lift surface systems
[ETN-88-91886] N88-22290
INTERNATIONAL ATOMIC ENERGY AGENCY, VIENNA (AUSTRIA).
Small and medium power reactors 1987
[TI88-701435] N88-22720
INTERNATIONAL BUSINESS MACHINES CORP., YORKTOWN HEIGHTS, N. Y.
The structure of the boron-hydrogen complex in silicon
[DE88-005433] N88-22795
IOWA UNIV., IOWA CITY.
Alkali metal diffuse band lasers
[AD-A190244] N88-22350
ISRAEL ATOMIC ENERGY COMMISSION, YAVNEH.
PLASMOR: A laser-plasma simulation code, part 2
[DE88-701289] N88-22736
Particle acceleration to high energies and amplification of coherent radiation by electromagnetic interactions in plasmas
[TI88-701020] N88-22737
New methods of confinement and heating of plasma in magnetic fields
[TI88-701021] N88-22738
Growth of Pb/sub 1-x/Eu/sub x/Te epitaxial layers by the liquid phase epitaxy technique
[TI88-701022] N88-22763
ISRAEL OCEANOGRAPHIC AND LIMNOLOGICAL RESEARCH LTD., HAIFA.
Derivation of consistent surface fixed fields for use in a global NWP model
[AD-A190131] N88-22475

J

JAPAN ATOMIC ENERGY RESEARCH INST., TOKYO.
Effect of strain rate on high-temperature low-cycle fatigue behavior of Hastelloy X and Hastelloy XR
[DE88-752302] N88-22140
Basic characteristics of heat-exchanger-type steam reformer heated by high-temperature helium gas (2). Analysis by simulation model (2)
[DE87-702962] N88-22291
Analyses and experiments on the integrity and lifetime predictions of plasma-facing components in fusion reactors
[DE87-702957] N88-22735
Improvement of plasma confinement due to electron Landau damping in tokamaks
[DE88-752339] N88-22747
JAYCOR, VIENNA, VA.
CK-LOG system conversion (user's manual and user interface)
[AD-A190273] N88-22577
Data base design and implementation
[AD-A190414] N88-22827
JET PROPULSION LAB., CALIFORNIA INST. OF TECH., PASADENA.
Extension of computer based algorithms by operator analysts
[NASA-CR-182798] N88-22575
Mathematics clinic probabilistic position-fixing
[NASA-CR-182753] N88-22672
JOHNS HOPKINS UNIV., BALTIMORE, MD.
Random processes, turbulence and disordering fields
[AD-A190123] N88-22303
Statistical inference for stochastic processes
[AD-A190491] N88-22673
JOINT INST. FOR NUCLEAR RESEARCH, DUBNA (USSR).
Adiabatic representation of three-body problem in hyperspherical coordinates. Statement of the problem
[TI88-701162] N88-22678
Plasma wave radiative damping of a new type in a relativistic one-dimensional plasma
[TI88-701191] N88-22739
Singular Lagrangians. Classical dynamics and quantization. Lectures for young scientists
[TI88-701158] N88-22806
To the field theory with a fundamental mass
[TI88-701159] N88-22807

Quantization of axial electrodynamics
[TI88-701498] N88-22813
Secondary gauge conditions in field theory
[TI88-701499] N88-22814
Hamiltonian formalism in the model of the relativistic string with rigidity
[TI88-701503] N88-22815
JOINT PUBLICATIONS RESEARCH SERVICE, ARLINGTON, VA.
JPRS report: Science and technology. Japan
[JPRS-JST-88-002] N88-22210
Laser processing-status, perspectives N88-22211
Compound ceramic processing N88-22212
Single crystal growth by laser CVD N88-22213
Fine grain development by laser CVD N88-22214
Superfine grain development by laser N88-22215
Hard ceramic film by laser PVD N88-22216
Material surface improvement by laser N88-22217
JPRS report: Science and technology. Japan
[JPRS-JST-88-001] N88-22218
Space utilization plans N88-22219
Space experiment plan FMPT N88-22220
Amorphous semiconductors made in space N88-22221
Containerless glass melting N88-22222
Pb(1-x)Sn(x)Te crystal growth in space N88-22223
Japanese space station module N88-22224
Solar cell cover glasses for satellites N88-22225
Characteristics of LSI-wiring expert system discussed N88-22226
Function of Japan Fine Ceramics Center described N88-22227
JPRS report: Science and technology. Japan
[JPRS-JST-87-029] N88-22228
Developments in ceramic superconducting materials N88-22229
Sigma system: Overview, prospects N88-22230
Overview of 1987 moonlight project N88-22231
Merit of Hadamard transform active absorption spectrometer described N88-22232
JPRS report: Science and technology. China
[JPRS-CST-87-043] N88-22233
Chronology of China's successful satellite launchings N88-22234
Smoothing technique to resolve X-ray spectra in laser nuclear fusion N88-22235
Magic light high-power laser passes state certification N88-22236
Protection against laser damage to human body reviewed N88-22237
Numerical and experimental research on propagation of elastic stress waves in conical shell under axial impulsive loading N88-22238
Cubic spline solution of symmetric buckling problems of clamped shallow spherical shells N88-22239
Efficient method for structural optimization N88-22240
Investigation of side-wall effects in wind tunnel with supercritical airfoil testing N88-22241
Split-coefficient matrix solution and experimental study of axisymmetric underexpanded exhaust plumes N88-22242
Theoretical model and numerical solution for compressible viscous vortex cores N88-22243
Mixed direct-inverse problem of transonic cascade N88-22244
Influence of unsteady aerodynamic forces on dynamic response of variable sweep aircraft N88-22245
Zero-lift drag predictions in supersonic flow for complex configurations N88-22246
Relationship between optical transfer function and natural light field in sea or atmosphere N88-22247
Evaporation characteristics of elements during vacuum arc remelting of alloy A-286 N88-22248
Rainbow holographic image reconstructed by spatially extended white light source N88-22249

K

KANSAS STATE UNIV., MANHATTAN.
Reactions of N2(A sup 3 sigma sup + sub u) candidates for short wavelength lasers
[DE88-007018] N88-22342
KENTUCKY UNIV., LEXINGTON.
Laser spectroscopy and dynamics of combustion intermediates
[DE88-006541] N88-22110
KIRUNA GEOPHYSICAL INST. (SWEDEN).
On the acceleration of electrons and positive ions in the same direction along magnetic field lines by parallel electric fields
[IRF-PREPRINT-103] N88-22488

KRUG INTERNATIONAL, SAN ANTONIO, TEX.
A preliminary comparison of the transient effects of single versus multiple q-switched doubled-neodymium laser pulses
[AD-A189855] N88-22347
A comparison of visual evoked potential and behavioral measures of flashblindness in humans
[AD-A189757] N88-22519
KTECH CORP., ALBUQUERQUE, N. MEX.
Continuous measurements of in-bore projectile velocity
[DE88-006841] N88-22056
KYOTO UNIV., UJI (JAPAN).
Heating and confinement studies of electron cyclotron resonance heated plasmas in Heliotron E
[DE88-752312] N88-22746

L

LAWRENCE LIVERMORE NATIONAL LAB., CALIF.
Analytic solutions to dynamic equations of plasma armature railguns
[DE88-006842] N88-22057
The combustion synthesis of boride composites
[DE88-005474] N88-22084
Directed-energy electron-beam processing of a hypoeutectic Cr90Ta10 alloy
[DE88-005621] N88-22157
Oxide optical coatings prepared by metal-organic vapor deposition
[DE88-006809] N88-22175
The concept of an impact resonance diagram for characterizing the nonlinear response of impact vibration
[DE88-005475] N88-22432
A survey of denser-than-air atmospheric dispersion models
[DE88-006626] N88-22467
Proceedings of the Lightning Threat Warning Workshop
[DE88-006607] N88-22499
Artificial neural networks: An introduction with an annotated bibliography
[DE88-007003] N88-22603
Clinical measurements using fiber optic sensors
[DE88-005624] N88-22731
Computing X-ray effects in optics
[DE88-006722] N88-22732
Preparing the Alcator C bolometer system for use on MTX (Microwave Tokamak Experiment)
[DE88-006724] N88-22733
Synthesis of metastable superconductors by high dynamic pressure
[DE88-005620] N88-22764
Dispersion measurements of microcrystals in the near ultraviolet and infrared
[DE88-006234] N88-22800
LEHIGH UNIV., BETHLEHEM, PA.
Environmentally assisted crack growth in structural alloys: Perspectives and new directions
[AD-A190137] N88-22377
LOCKHEED-CALIFORNIA CO., BURBANK.
KRASH parametric sensitivity study: Transport category airplanes
[AD-A189962] N88-22024
LOCKHEED ENGINEERING AND MANAGEMENT SERVICES CO., INC., WASHINGTON, D.C.
USSR Space Life Sciences Digest, issue 16
[NASA-CR-3922(19)] N88-22515
LOCKHEED MISSILES AND SPACE CO., HUNTSVILLE, ALA.
Duct flow nonuniformities: Effect of struts in SSME HGM II(+)
[NASA-CR-179285] N88-22296
LOS ALAMOS NATIONAL LAB., N. MEX.
Microwave sintering of alumina-SiC composites at 2.45 and 60 GHz
[DE88-006455] N88-22095
Discharge excitation of the XeF C to A transition
[DE88-006448] N88-22339
Fundamental noise processes in a laser excited optical filter
[DE88-006460] N88-22340
Extension of free-electron lasers into the extreme ultraviolet
[DE88-005373] N88-22341
Constellation sizing for modest directed energy platforms
[DE88-007033] N88-22343
Solid hosts for dye laser rods. Part 1: Criteria for choosing a host material
[DE88-006478] N88-22355
Advanced geothermal technologies
[DE88-004307] N88-22463
Recent advances in solid polymer electrolyte fuel cell technology
[DE88-005380] N88-22464
Monitoring the usage of a computer system
[DE88-004310] N88-22542
Rapid prototyping of simulations in artificial intelligence environments
[DE88-004295] N88-22612
Discrete event simulation in the artificial intelligence environment
[DE88-004296] N88-22613
Nonlinear signal processing using neural networks: Prediction and system modelling
[DE88-006479] N88-22621
Remarks on solid state amorphizing transformations
[DE88-006452] N88-22803
LOUISIANA STATE UNIV., BATON ROUGE.
The visit problem: Visibility graph-based solution
[DE88-000343] N88-22556
LOYOLA UNIV., CHICAGO, ILL.
Complex sound processing: An interdisciplinary approach
[AD-A189782] N88-22523

M

MAINE UNIV., ORONO.
Vapor phase deposition and growth of polyimide films on copper
[AD-A189969] N88-22178
MANCHESTER UNIV. (ENGLAND).
The growth potential of corona discharges from aircraft flying in precipitation
[AD-A190507] N88-22478
MARC ANALYSIS RESEARCH CORP., PALO ALTO, CALIF.
MHOST: An efficient finite element program for inelastic analysis of solids and structures N88-22394
MARTIN MARIETTA AEROSPACE, DENVER, COLO.
Microplasticity phenomena in graphite/magnesium metal matrix composites
[DE88-006772] N88-22086
MARTIN MARIETTA CORP., BETHESDA, MD.
Orbital transfer vehicle: Concept definition and system analysis study
[NASA-CR-179315] N88-22060
External tank gamma ray imaging telescope study. Final review, phase 2
[NASA-CR-179320] N88-22834
MARYLAND UNIV., COLLEGE PARK.
Fundamental studies on high temperature deformation recrystallization, and grain growth of two-phase materials
[AD-A189725] N88-22145
Higher order crossings
[AD-A190489] N88-22641
Repetitive opening switches using optically activated semiconductors
[AD-A190196] N88-22790
MASSACHUSETTS INST. OF TECH., CAMBRIDGE.
Numerical simulation of turbulent flames using vortex methods
[AD-A189613] N88-22116
Basic instability mechanisms in chemically reacting subsonic and supersonic flows
[AD-A190101] N88-22120
Processing, microstructure, and mechanical properties of silicon carbide particulate reinforced aluminum alloys
[AD-A189861] N88-22136
On rotating sphere-on-a-plate experiments and the questions of whether high angle grain boundaries melt below bulk melting temperatures
[DE88-006627] N88-22142
Cracking tendencies of restrained welds in high strength low alloy steels under hyperbaric conditions
[AD-A190255] N88-22150
A fully abstract semantics for event-based simulation
[AD-A190560] N88-22283
Comparison of entropy generation and conventional design methods for heat exchangers
[AD-A190256] N88-22306
Bodies in unsteady flow
[AD-A190416] N88-22308
Comparative analysis
[AD-A190556] N88-22313
Relative orientation
[AD-A190385] N88-22449
Argus reference manual
[AD-A190382] N88-22578
Software structuring principles for VLSI CAD
[AD-A190386] N88-22579
MultiScheme: A parallel processing system based on MIT (Massachusetts Institute of Technology) scheme
[AD-A190383] N88-22597
Synapses that compute motion
[AD-A190389] N88-22607
Finding texture boundaries in images
[AD-A190554] N88-22609
Research on algebraic manipulation
[AD-A190149] N88-22634
Non-rigid motion and Regge calculus
[AD-A190387] N88-22640
ONTIC: A knowledge representation system for mathematics
[AD-A190553] N88-22643
Expressing mathematical subroutines constructively
[AD-A190559] N88-22644
Structural decomposition of multiple time scale Markov processes
[AD-A189739] N88-22657
Rigidity and smoothness of motion
[AD-A190555] N88-22694
Describing the source created by turbulent flow over orifices and louvers
[AD-A190254] N88-22706
Sequential excitation preparation of molecular energy levels with special structural and chemical properties
[AD-A190041] N88-22718
Infrared-sensitive spatial light modulator
[AD-A190391] N88-22729
Current-drive on the Versator-2 tokamak with a slotted-waveguide fast-wave coupler
[DE88-006261] N88-22743
Physical fluid mechanics in MPD thrusters
[AD-A190309] N88-22754
Plasma-gas interaction studies in a hybrid plume plasma rocket
[AD-A190310] N88-22755
Interface formation and precursory dynamics
[AD-A190741] N88-22794
MASSACHUSETTS UNIV., AMHERST.
Mixing: Stretching, breakup and chaos
[DE88-006699] N88-22327
Adaptive neural network architecture
[AD-A190114] N88-22533
Computer graphics tools for the study of minimal surfaces
[DE88-006421] N88-22557
The elliptic Sinh-Gordon equation and the construction of toroidal soap bubbles
[DE88-006426] N88-22585
Almost-periodic solutions of nonlinear parabolic equations
[DE88-006423] N88-22618
Complete minimal surfaces in R^3 of low total curvature
[DE88-006425] N88-22619
The inverse power method for semilinear elliptic equations
[DE88-006427] N88-22620
Global spatial periodic solutions to the Ginzburg-Landau equations
[DE88-006424] N88-22623
Regularity of the Albanese map for nonoriented surfaces
[DE88-006428] N88-22679
Embedded minimal sufaces with an infinite number of ends
[DE88-006429] N88-22680
MAX-PLANCK-INST. FUER AERONOMIE, KATLENBURG-LINDAU (WEST GERMANY).
Coordinated Auroral Experiments using Scatter And Rocket investigations (CAESAR investigations)
[MPAE-W-47-87-13] N88-22487
MAX-PLANCK-INST. FUER METALLFORSCHUNG, STUTTGART (WEST GERMANY).
On rotating sphere-on-a-plate experiments and the questions of whether high angle grain boundaries melt below bulk melting temperatures
[DE88-006627] N88-22142
MAX-PLANCK-INST. FUER PHYSIK UND ASTROPHYSIK, GARCHING (WEST GERMANY).
Design, construction and performance of the ROSAT high resolution X-ray mirror assembly
[MPE-PREPRINT-101] N88-22836
MCDONNELL-DOUGLAS RESEARCH LABS., ST. LOUIS, MO.
Growth and deformation mechanisms of refractory alloy hybrid materials
[AD-A190492] N88-22152
MICHIGAN STATE UNIV., EAST LANSING.
Interfacial structure-property relationships at the fiber-matrix interphase in advanced composites
[AD-A190649] N88-22093
MICHIGAN UNIV., ANN ARBOR.
Superplastic flow of mullite-zirconia composites
[DE88-005905] N88-22085
Dense-spray structure and phenomena. Part 2: Pressure-atomized sprays
[AD-A190312] N88-22307
Dense-spray structure and phenomena. Part 1. Turbulence/dispersed-phase interactions
[AD-A190606] N88-22315

Spatial matched processing for multipath propagation
[AD-A189790] N88-22701
Superconductivity and the tailoring of lattice parameters of the compound YBa2Cu3O(sub x)
[DE88-005904] N88-22769

MIDWEST RESEARCH INST., GOLDEN, COLO.
FLAP (Force and Loads Analysis Program) code development and validation
[DE88-001131] N88-22371

MINNESOTA UNIV., MINNEAPOLIS.
Corrosion Research Center, University of Minnesota
[DE88-006681] N88-22160
A survey of oscillating flow in Stirling engine heat exchangers
[NASA-CR-182108] N88-22322

MOBIL RESEARCH AND DEVELOPMENT CORP., PAULSBORO, N.J.
Evaluation of direct methane conversion to higher hydrocarbons and oxygenates
[DE88-003812] N88-22204

MOUND LAB., MIAMISBURG, OHIO.
Reduced thermal input by proper selection of YAG laser welding parameters
[DE88-000730] N88-22356

MRC BEARINGS-SKF AEROSPACE, KING OF PRUSSIA, PA.
Traction model development
[AD-A188450] N88-22359

N

NATIONAL AERONAUTICS AND SPACE ADMINISTRATION, WASHINGTON, D.C.
Thermal expansion behavior of randomly oriented short carbon fiber reinforced copper composites
[NASA-TT-20175] N88-22099
Reciprocating sliding wear characteristics of copper-carbon fiber composites
[NASA-TT-20176] N88-22100
Application of copper-carbon fiber composites to power semiconductor devices
[NASA-TT-20171] N88-22101
Fiber-reinforced plastic composites. Possibilities and limitations of applications as machine-construction materials
[NASA-TT-20159] N88-22102
Joints in fiber-reinforced aluminum alloys
[NASA-TT-20160] N88-22104
Measurement of emissivity of industrial surfaces using a simple method
[NASA-TT-20165] N88-22130
Nucleation in super-saturated products
[NASA-TT-20275] N88-22134
On copper peroxide
[NASA-TT-20263] N88-22135
Designs of profiles for cascades
[NASA-TT-20161] N88-22326
Bilateral symmetry elements of the Zhamanshin impact crater
[NASA-TT-20288] N88-22490
Method and device for the detection and identification of a helicopter
[NASA-TT-20251] N88-22698
NASA scientific and technical publications: A catalog of Special Publications, Reference Publications, Conference Publications, and Technical Papers, 1987
[NASA-SP-7063(02)] N88-22830

NATIONAL AERONAUTICS AND SPACE ADMINISTRATION. AMES RESEARCH CENTER, MOFFETT FIELD, CALIF.
Computational fluid dynamics drag prediction: Results from the Viscous Transonic Airfoil Workshop
[NASA-TM-100095] N88-22009
Transonic Navier-Stokes computations of strake-generated vortex interactions for a fighter-like configuration
[NASA-TM-100009] N88-22010
Boundary-layer and wake measurements on a swept, circulation-control wing
[NASA-TM-89426] N88-22013
Bifurcations in unsteady aerodynamics-implications for testing
[NASA-TM-100083] N88-22014
Real-time flight test data distribution and display
[NASA-TM-100424] N88-22050
Development of subminiature multi-sensor hot-wire probes
[NASA-TM-100052] N88-22336
A method of atmospheric density measurements during space shuttle entry using ultraviolet-laser Rayleigh scattering
[NASA-TM-100056] N88-22337
Numerical study of unsteady viscous hypersonic blunt body flows with an impinging shock
[NASA-TM-100096] N88-22650
High-resolution shock-capturing schemes for inviscid and viscous hypersonic flows
[NASA-TM-100097] N88-22651

NATIONAL AERONAUTICS AND SPACE ADMINISTRATION. GODDARD SPACE FLIGHT CENTER, GREENBELT, MD.
Monthly mean global climatology of temperature, wind, geopotential height, and pressure for 0 - 120 km
[NASA-TM-100697] N88-22503

NATIONAL AERONAUTICS AND SPACE ADMINISTRATION. HUGH L. DRYDEN FLIGHT RESEARCH CENTER, EDWARDS, CALIF.
Effects of update and refresh rates on flight simulation visual displays
[NASA-TM-100415] N88-22033

NATIONAL AERONAUTICS AND SPACE ADMINISTRATION. LYNDON B. JOHNSON SPACE CENTER, HOUSTON, TEX.
Random Process Simulation for stochastic fatigue analysis
[NASA-TM-100464] N88-22654

NATIONAL AERONAUTICS AND SPACE ADMINISTRATION. LANGLEY RESEARCH CENTER, HAMPTON, VA.
Laser velocimeter measurements in a wing-fuselage type juncture
[NASA-TM-100588] N88-22012
Inflow measurement made with a laser velocimeter on a helicopter model in forward flight. Volume 3: Rectangular planform blades at an advance ratio of 0.30
[NASA-TM-100543] N88-22015
Procedures and requirements for testing in the Langley Research Center unitary plan wind tunnel
[NASA-TM-100529] N88-22016
Shape sensitivity analysis of wing static aeroelastic characteristics
[NASA-TP-2808] N88-22031
Modifications to the Langley 8-foot transonic pressure tunnel for the laminar flow control experiment
[NASA-TM-4032] N88-22047
Investigation of Super*Zip separation joint
[NASA-TM-4031] N88-22072
Interlaminar fracture toughness of thermoplastic composites
[NASA-TM-100532] N88-22097
Aerothermal tests of quilted dome models on a flat plate at a Mach number of 6.5
[NASA-TP-2804] N88-22325
Improvements to tilt rotor performance through passive blade twist control
[NASA-TM-100583] N88-22434
Coupled bending-torsion steady-state response of pretwisted, nonuniform rotating beams using a transfer-matrix method
[NASA-TM-100596] N88-22435
Thermal stress in high temperature cylindrical fasteners
[NASA-TM-100611] N88-22438
The analysis of non-linear dynamic behavior (including snap-through) of postbuckled plates by simple analytical solution
[NASA-TM-89165] N88-22439
Stress-intensity factors for small surface and corner cracks in plates
[NASA-TM-100599] N88-22445
Boundary shape identification problems in two-dimensional domains related to thermal testing of materials
[NASA-CR-181654] N88-22541
Analysis and testing of the SURE program
[NASA-TP-2817] N88-22653
Model-scale sound propagation experiment
[NASA-TM-100602] N88-22709
Advancing-side directivity and retreating-side interactions of model rotor blade-vortex interaction noise
[NASA-TP-2784] N88-22710
Langley aerospace test highlights, 1987
[NASA-TM-100595] N88-22853
Space directorate research and technology accomplishments for fiscal year 1987
[NASA-TM-100607] N88-22854

NATIONAL AERONAUTICS AND SPACE ADMINISTRATION. LEWIS RESEARCH CENTER, CLEVELAND, OHIO.
Porous wind tunnel corrections for counterrotation propeller testing
[NASA-TM-100873] N88-22019
Small engine components test facility turbine testing cell
[NASA-TM-100887] N88-22037
Ray tracing optical analysis of offset solar collector for space station solar dynamic system
[NASA-TM-100853] N88-22080
Bithermal fatigue of a nickel-base superalloy single crystal
[NASA-TM-100885] N88-22168
Lewis Structures Technology, 1988. Volume 2: Structural Mechanics
[NASA-CP-3003-VOL-2] N88-22382
High-temperature combustor liner tests in structural component response test facility N88-22383
Life assessment of combustor liner using unified constitutive models N88-22384
Experiments investigating advanced materials under thermomechanical loading N88-22385
Biaxial experiments supporting the development of constitutive theories for advanced high-temperature materials N88-22386
Finite element (MARC) solution technologies for viscoplastic analyses N88-22389
The composite blade structural analyzer (COBSTRAN) N88-22390
Features and applications of the integrated composites analyzer (ICAN) code N88-22391
METCAN: The metal matrix composite analyzer N88-22395
Computational structural mechanics for engine structures N88-22399
Structural tailoring of advanced turboprops N88-22400
Impact damage in composite laminates N88-22402
Thermostructural analysis of simulated cowl lips N88-22403
Thermal-structural analyses of Space Shuttle Main Engine (SSME) hot section components N88-22404
Structural assessment of a space station solar dynamic heat receiver thermal energy storage canister N88-22406
An efficient Mindlin finite strip plate element based on assumed strain distribution N88-22407
Lewis Structures Technology, 1988. Volume 3: Structural Integrity Fatigue and Fracture Wind Turbines HOST
[NASA-CP-3003-VOL-3] N88-22408
Monolithic ceramic analysis using the SCARE program N88-22409
Nondestructive evaluation by acousto-ultrasonics N88-22412
Characterization of sintered SiC by using NDE N88-22413
Systems for ultrasonic scanning, analysis and imagery N88-22414
Flaw characterization in structural ceramics using scanning laser acoustic microscopy N88-22415
Nondestructive evaluation of sintered ceramics N88-22416
Fracture technology for brittle materials N88-22417
Mode 2 fracture mechanics N88-22418
In situ fatigue loading stage inside scanning electron microscope N88-22419
Cumulative fatigue damage models N88-22422
Bithermal fatigue: A simplified alternative to thermomechanical fatigue N88-22424
Life prediction modeling based on strainrange partitioning N88-22425
Life and reliability of rotating disks N88-22428
Large-scale wind turbine structures N88-22429
Research sensors N88-22430
Review and assessment of the HOST turbine heat transfer program N88-22431
Structural dynamics branch research and accomplishments for fiscal year 1987
[NASA-TM-100279] N88-22446
Development of an integrated heat pipe-thermal storage system for a solar receiver
[NASA-TM-101099] N88-22458
Two-dimensional graphics tools for a transputer based display board
[NASA-TM-100820] N88-22591
A physically consistent model for artificial dissipation in transonic potential flow computations
[NASA-TM-100846] N88-22652
Synthesis and characterization of high-T(sub c) screen-printed Y-Ba-Cu-O films on alumina
[NASA-TM-100860] N88-22805
Research and technology
[NASA-TM-100172] N88-22851

NATIONAL AERONAUTICS AND SPACE ADMINISTRATION. MARSHALL SPACE FLIGHT CENTER, HUNTSVILLE, ALA.
Marshall Space Flight Center 1960-1985: 25th anniversary report
[NASA-TM-100328] N88-22852

NATIONAL AEROSPACE LAB., AMSTERDAM (NETHERLANDS).
Trends in Computational Fluid Dynamics (CFD) for aeronautical 3D steady applications: The Dutch situation
[NLR-MP-86074-U] N88-22017
Design of an integrated control system for flutter margin augmentation and gust load alleviation, tested on a dynamic windtunnel model
[PB88-149885] N88-22038

Reliability analysis within a Computer Aided Engineering (CAE) infrastructure
[NLR-MP-86059-U] N88-22369

NATIONAL BUREAU OF STANDARDS, BOULDER, COLO.

EMR (Electromagnetic Radiation) test facilities evaluation of reverberating chamber located at RADC (Rome Air Development Center), Griffiss AFB (Air Force Base), Rome, New York
[PB88-178827] N88-22048

NATIONAL BUREAU OF STANDARDS, GAITHERSBURG, MD.

Stress corrosion of ceramic materials
[AD-A190501] N88-22187

Strength and microstructure of ceramics
[AD-A190712] N88-22191

Chemically reacting turbulent flow
[AD-A190522] N88-22311

NATIONAL COMPUTING CENTRE LTD., MANCHESTER (ENGLAND).

Ada (Trademark) compiler validation summary report. ALSYS: AlsyCOMP-013, V2.0 HOST: IBM PC AT. Target: IBM 370 3084Q
[AD-A189640] N88-22546

NATIONAL GEOPHYSICAL DATA CENTER, BOULDER, COLO.

Solar-geophysical data number 520, December 1987. Part 2: (Comprehensive reports). Data for June 1987 and miscellanea
[PB88-164207] N88-22849

NATIONAL LAB. FOR HIGH ENERGY PHYSICS, OHO (JAPAN).

Spectrographic detection of nitrogen impurity in helium
[DE88-752301] N88-22111

NATIONAL PHYSICAL LAB., TEDDINGTON (ENGLAND).

Computer grading of extensometers (BS 3846)
[NPL-DMA(A)-152] N88-22560

NATIONAL TELECOMMUNICATIONS AND INFORMATION ADMINISTRATION, BOULDER, COLO.

Investigations of test methodology for the stress loading facility
[PB88-168095] N88-22049

Performance of single and multiple system AM stereo decoder receivers
[PB88-168307] N88-22265

NATIONAL TRANSPORTATION SAFETY BOARD, WASHINGTON, D. C.

Aircraft accident reports, brief format, US civil and foreign aviation, issue number 10 of 1986 accidents
[PB87-916912] N88-22020

Aircraft accident report: North Star Aviation, Inc., PA-32 RT-300, N39514 and Alameda Aero Club Cessna 172, N75584, Oakland, California, March 31, 1987
[PB87-910412] N88-22021

NAUCHNO-ISSLEDOVATELSKIJ INST. EHLEKTROFIZICHESKOJ APPARATURY, LENINGRAD (USSR).

Numerical modelling specific energy charcteristics of excimer KrF lasers with electron beam excitation
[DE88-701525] N88-22344

NAVAL HEALTH RESEARCH CENTER, SAN DIEGO, CALIF.

Napping and human functioning during prolonged work
[AD-A190228] N88-22525

Prediction of physical fitness: Estimated percent body fat using body circumferences versus weight-height measures
[AD-A190233] N88-22526

Dietary factors related to physical fitness
[AD-A190272] N88-22527

NAVAL OCEAN SYSTEMS CENTER, SAN DIEGO, CALIF.

Amplification of signals in fiber optics using the stimulated Raman effect
[AD-A190281] N88-22727

A 104-km unrepeatered bidirectional fiber optic demonstration link
[AD-A190282] N88-22728

NAVAL POSTGRADUATE SCHOOL, MONTEREY, CALIF.

High Reynolds number, low Mach number, steady flow field calculations over a NACA 0012 airfoil using Navier-Stokes and interactive boundary layer theory
[AD-A189871] N88-22005

The effects of torque response and time delay on rotorcraft vertical axis handling qualities
[AD-A189873] N88-22023

Heat transfer modeling of jet vane Thrust Vector Control (TVC) systems
[AD-A190108] N88-22034

The age hardening response of thermomechanically processed Al-Mg-Li alloys
[AD-A189870] N88-22147

Optimum signal processing in distributed sensor systems
[AD-A189443] N88-22250

Strategies in the topological approach to electromagnetic interference control
[AD-A189874] N88-22255

Direct bit detection receiver noise performance analysis for 32-PSK and 64-PSK modulated signals
[AD-A190009] N88-22256

Effect of friction and control parameters on the tracking accuracy of a target seeker
[AD-A190010] N88-22257

The 2 FSK/QPSK (Frequency Shift Keying/Quadrature Phase Shift Keying) transmitter and receiver: Design and performance
[AD-A190026] N88-22258

Theoretical model of the cathode spot on a unipolar arc
[AD-A190109] N88-22277

Unsteady flow field measurements using LDV (Laser Doppler Velocimetry)
[AD-A189907] N88-22298

Parameterization of horizontal wind velocity variability
[AD-A190107] N88-22493

Hydrographic data from the OPTOMA (Ocean Prediction Through Observation, Modeling and Analysis) program: OPTOMA 23, 9-19 November 1986
[AD-A189868] N88-22506

The physical oceanography of the northern Baffin Bay-Nares Strait region
[AD-A190015] N88-22509

Changes in the California current system observed off northern California during July-August 1986
[AD-A190027] N88-22510

The effects of time-dependent winds and ocean eddies on ice motion in a marginal ice zone
[AD-A190105] N88-22511

Tutorial on GAMS (Generalized Algebraic Modeling System): A modeling language for optimization
[AD-A189867] N88-22565

Memory efficient evaluations of nonlinear stochastic equations and C3 applications
[AD-A189872] N88-22569

A three dimensional non-singular modelling of rigid manipulators
[AD-A189707] N88-22604

Target localization in an inhomogeneous medium
[AD-A190008] N88-22703

A computerized investigation using the method of images to predict the sound field in a fluid wedge overlying a slow fluid half-space
[AD-A190013] N88-22704

The impact of independent research and development regulations on companies not required to negotiate advanced independent research and development agreements
[AD-A190007] N88-22818

A method for estimating and controlling the cost of extending technology
[AD-A190717] N88-22831

NAVAL RESEARCH LAB., WASHINGTON, D.C.

Diode laser spectroscopy of chemical moieties at surfaces
[AD-A190710] N88-22127

Models for electromagnetic scattering from the sea at extremely low grazing angles
[AD-A190472] N88-22261

Analysis of anomalous resistivity during the conduction phase of the plasma erosion opening switch
[DE88-006382] N88-22286

NAVAL SURFACE WEAPONS CENTER, SILVER SPRING, MD.

Effect of moisture level in PBXW-109(E) (plastic-bonded explosive) mixes on the aging of the cured explosive
[AD-A190200] N88-22202

Eddy current nondestructive inspection of graphite epoxy using ferrite cup core probes
[AD-A189823] N88-22365

NAVAL UNDERWATER SYSTEMS CENTER, NEW LONDON, CONN.

Space time processing, environmental-acoustic effects
[AD-A190764] N88-22708

NEVADA UNIV., LAS VEGAS.

Evaluation of existing total human exposure models
[PB88-146840] N88-22517

NEW MEXICO UNIV., ALBUQUERQUE.

Continuous measurements of in-bore projectile velocity
[DE88-006841] N88-22056

Analytic solutions to dynamic equations of plasma armature railguns
[DE88-006842] N88-22057

Molecular reaction and energy transfer rate estimation for chemical-laser analysis
[AD-A190664] N88-22126

Singlet oxygen behavior in solid polymer matrices
[DE88-005171] N88-22171

Telerobotic operation of conventional robot manipulators
[DE88-005718] N88-22363

NORTH CAROLINA STATE UNIV., RALEIGH.

Instrumentation for the characterization and development of millimeter wave components compatible with monolithic integration
[AD-A189724] N88-22275

Enhanced viscous flow drag reduction using acoustic excitation
[NASA-CR-182734] N88-22295

Cholesky downdating on a hypercube
[DE88-006780] N88-22586

NORTH CAROLINA UNIV., CHAPEL HILL.

Temperature-dependent conductivity of oxygen-depleted YBCO ceramics
[AD-A190340] N88-22182

Normed Bellman equation with degenerate diffusion coefficients and its application to differential equations
[AD-A190319] N88-22637

Sequential tests for the drift of a Wiener process with a smooth prior and the heat equation
[AD-A190322] N88-22638

Approximations in extreme value theory
[AD-A189817] N88-22659

Stopping rules and observed significance levels
[AD-A190320] N88-22664

Information and coding capacities of mismatched Gaussian channels
[AD-A190321] N88-22665

Estimation of convolution tails
[AD-A190323] N88-22666

Continuity of symmetric stable processes
[AD-A190324] N88-22667

Extreme value for dependent sequences via the Stein-Chen method of poisson approximation
[AD-A190325] N88-22668

Stochastic evolution equations driven by nuclear space valued martingales
[AD-A189342] N88-22677

Coding capacity of generalized additive channels
[AD-A190315] N88-22685

Information capacity of Gaussian channels
[AD-A190316] N88-22686

Conditions for information capacity of the discrete-time Gaussian channel to be increased by feedback
[AD-A190317] N88-22687

Coding capacity of discrete-time Gaussian and nonGaussian channels
[AD-A190318] N88-22688

An investigation of the crystalchemistry and thermochemistry of selected mineral systems
[AD-A189758] N88-22781

Magnetic anomalies in the rare earth oxide superconductors GdBa2Cu3O(7-x) and YbBa2Cu3O(7-x)
[AD-A190713] N88-22793

NORTHEASTERN UNIV., BOSTON, MASS.

Annihilation momentum density of positrons trapped at vacancy-type defects in metals and alloys
[DE88-005936] N88-22797

NORTHROP SERVICES, INC., DAYTON, OHIO.

Evaluation of the acute toxicity of a synthetic polyalphaolefin-based hydraulic fluid
[AD-A190412] N88-22184

NORTHWEST RESEARCH ASSOCIATES, INC., BELLEVUE, WASH.

Geometric restoration of satellite image data
[AD-A190462] N88-22450

Satellite UV image processing
[AD-A190466] N88-22451

Support for FY87 midlatitude electron-density calibration campaign
[AD-A190174] N88-22476

NORTHWESTERN UNIV., EVANSTON, ILL.

The spectroscopy and reaction kinetics of coordinatively unsaturated metal carbonyls
[AD-A190533] N88-22124

Investigation and synthesis of high temperature and increased stiffness RSP aluminum alloys
[AD-A190407] N88-22151

Monte Carlo reliability analysis
[AD-A189972] N88-22366

Markov processes applied to control, replacement and signal analysis
[AD-A190563] N88-22674

Preparation of large area NbN/AlN/NbN Josephson junctions
[DE88-006074] N88-22799

O

OAK RIDGE GASEOUS DIFFUSION PLANT, TENN.
Performance test results: AXIAL-GAP, permanent magnet compressor motor
[DE88-006857] N88-22289

OAK RIDGE NATIONAL LAB., TENN.
Investigation of aeroacoustic mechanisms by remote thermal imaging
[DE88-002612] N88-22046
Thermal analysis of heat storage canisters for a solar dynamic, space power system
[DE88-004199] N88-22075
Laser enhanced adhesion of copper films to sapphire substrates
[DE88-006802] N88-22144
Response of aluminum alloys to erosive particle impacts
[DE88-005910] N88-22159
Thermal conductivity of oxide ceramics
[DE88-005842] N88-22169
Ultrasonic characterization of ceramic joints
[DE88-005844] N88-22173
Technical highlights of the Alternative Fuels Utilization Program
[DE88-005064] N88-22205
Performance test results: AXIAL-GAP, permanent magnet compressor motor
[DE88-006857] N88-22289
Range image segmentation and surface parameter extraction for a mobile robot
[DE87-013877] N88-22360
Atmospheric carbon dioxide and the global carbon cycle: The key uncertainties
[DE88-005059] N88-22465
A hardware/software system for implementing geophysical diffraction tomography
[DE88-006411] N88-22480
The visit problem: Visibility graph-based solution
[DE88-000343] N88-22556
Cholesky downdating on a hypercube
[DE88-006780] N88-22586
Design and implementation of a parallel computer for expert system applications
[DE88-005288] N88-22601
Concurrent algorithms for a mobile robot vision system
[DE88-005850] N88-22614
Droplet size characteristics and energy input requirements of emulsions formed using high-intensity-pulsed electric fields
[DE88-005912] N88-22692
Long-time impurity confinement as a precursor to disruptions in ohmically heated tokamaks
[DE88-006183] N88-22742
Transport simulations of ohmic ignition experiment: IGNITEX
[DE88-006055] N88-22757
The structure of the boron-hydrogen complex in silicon
[DE88-005433] N88-22795

OFFICE NATIONAL D'ETUDES ET DE RECHERCHES AEROSPATIALES, PARIS (FRANCE).
Study of surface discharges
[ONERA-12/7236-PY] N88-22073
A system to measure damage in composite materials by the ultrasonic method
[ONERA-RT-2/7256-RY-061-R] N88-22103

OFFICE OF THE DEPUTY UNDER SECRETARY OF DEFENSE FOR RESEARCH AND DEVELOPMENT (RESEARCH AND ADVANCED TECHNOLOGY), WASHINGTON, D.C.
The Department of Defense Superconductivity Research and Development (DSRD) options. A study of possible directions for exploitation of superconductivity in military applications
[AD-A189747] N88-22780

OGDEN AIR LOGISTICS CENTER, HILL AFB, UTAH.
LGM-30B stage 2 disected motor test report
[AD-A190771] N88-22079

OHIO STATE UNIV., COLUMBUS.
Baseline estimation from simultaneous satellite laser tracking
[NASA-CR-182750] N88-22052
Polarimetric ISAR imaging using either measured or calculated transient signatures
[AD-A190077] N88-22259

OLD DOMINION UNIV., NORFOLK, VA.
SDIO/IST ultrashort wavelength laser: Novel experimental schemes for observing the Mossbauer effect in long-lived nuclear levels
[AD-A190275] N88-22351
SDIO/IST ultrashort wavelength laser. Mossbauer effect in gamma-ray lasers
[AD-A190306] N88-22352

OREGON STATE UNIV., CORVALLIS.
Physical, chemical and CTD (Conductivity/Temperature/Depth) data from the Marathon 2 expedition
[AD-A189930] N88-22507

P

PACIFIC NORTHWEST LABS., RICHLAND, WASH.
Specimen preparation techniques for the examination of ceramic and metal-matrix composites
[DE88-005157] N88-22094
Gamma-ray densitometry: Nondestructive analysis of density evolution during ceramic powder processing
[DE88-006671] N88-22196
Ocean general circulation models: Report on proceedings of a meeting of ocean and climate modelers
[DE88-005530] N88-22504
Characterization of space radiation environment in terms of the energy deposition in functionally important volumes
[DE88-005627] N88-22513

PAKISTAN INST. OF NUCLEAR SCIENCE AND TECHNOLOGY, ISLAMABAD.
Segregation effects in welded stainless steels
[DE88-701224] N88-22139

PENNSYLVANIA STATE UNIV., UNIVERSITY PARK.
High temperature oxidation and electrochemical studies related to hot corrosion
[AD-A190899] N88-22156
The sensitivity of boundary layer instability growth rates to compliant wall properties
[AD-A190433] N88-22309
Cavitation inception in rectangular two-dimensional slots
[AD-A190677] N88-22318
Stabilization and control problems in structural dynamics
[AD-A190197] N88-22361
Pointwise stabilization for coupled quasilinear and linear wave equations
[AD-A190031] N88-22632
Study of microcomputer-based real-time programmable optical signal processor and application
[AD-A190076] N88-22726

PENNSYLVANIA UNIV., PHILADELPHIA.
Conformal microstrip slot antenna and antenna array
[AD-A189623] N88-22252
Microwave dispersion and absorption in tissues: Molecular mechanisms
[AD-A190118] N88-22512

PHYSICAL SCIENCES, INC., ALEXANDRIA, VA.
Particle beam alignment system for single event upset-Van de Graaf experiments
[AD-A189695] N88-22721

PITTSBURGH UNIV., PA.
High temperature corrosion of ceramics
[DE88-006567] N88-22193
Effect of vibrational excitation on rate parameters of atmospheric reactions
[AD-A190464] N88-22477
Parallel memory addressing using coincident optical pulses
[AD-A189767] N88-22547
Some comments on quadrant dependence in higher dimensions
[AD-A190329] N88-22639
Multivariate analysis and its application
[AD-A189983] N88-22661
Admissible Bayes tests for structural relationship
[AD-A190326] N88-22669
Empirical and hierarchical Bayes competitors of preliminary test estimators in two sample problems
[AD-A190327] N88-22670
Detection of the number, locations and magnitudes of jumps
[AD-A190328] N88-22671

POLITECNICO DI MILANO (ITALY).
Multiple-transform pipelines for image coding
[REPT-87-038] N88-22561
An intelligent simulation model generator
[REPT-87-053] N88-22562
Near optimal blind deconvolution
[REPT-87-016] N88-22655

PORTSMOUTH POLYTECHNIC (ENGLAND).
The growth of corner cracks under the conjoint action of high and low cycle fatigue
[AD-A190510] N88-22379

PRATT AND WHITNEY AIRCRAFT, EAST HARTFORD, CONN.
Life prediction modeling based on cyclic damage accumulation N88-22426
Fatigue damage modeling for coated single crystal superalloys N88-22427

PRINCETON UNIV., N. J.
AFRAPT (Air Force Research in Aero Propulsion Technology) trainee program
[AD-A190525] N88-22123
Microvax networked computer system
[AD-A190308] N88-22596
Lumped model generation and evaluation: Sensitivity and Lie algebraic techniques with applications to combustion
[AD-A190402] N88-22689
Environmental assessment for the compact ignition Tokamak
[DE88-005633] N88-22740
Experimental studies on electronic properties of HgTe/CdTe and Hg sub 1-z Cd sub x Te/CdTe heterostructures and superlattices
[AD-A189826] N88-22783

PURDUE UNIV., WEST LAFAYETTE, IND.
Research as part of the Air Force in aero propulsion technology (AFRAPT) program
[AD-A190336] N88-22036
Auditory pattern memory: Mechanisms of tonal sequence discrimination by human observers
[AD-A190337] N88-22534
On two-stage allocation procedures for selection problems
[AD-A190766] N88-22675
Theory of interactions of intense light with nonlinear, inhomogeneous and periodic structures and its applications to optical bistability, optic gyroscopes, nonlinear spectroscopy, radiation protection, X-ray emission and related fields
[AD-A190040] N88-22725

R

R AND D ASSOCIATES, ALEXANDRIA, VA.
MPD (magnetoplasmadynamic) thrust chamber flow dynamics
[AD-A189940] N88-22751

RCA AEROSPACE AND DEFENSE, CAMDEN, N.J.
UARS spacecraft recorder
[NASA-CR-180768] N88-22331

RENSSELAER POLYTECHNIC INST., TROY, N.Y.
Advanced B and Al combustion kinetics over wide temperature ranges
[AD-A190752] N88-22128
Laser photodeposition and etching study
[AD-A190535] N88-22153
Numerical methods for singularly perturbed differential equations with applications
[AD-A189786] N88-22626
Problems in nonlinear continuum dynamics
[AD-A190538] N88-22691

RESEARCH INST. OF NATIONAL DEFENCE, LINKOEPING (SWEDEN).
Soft decoding of recorded HF data
[FOA-C-30473-3.3] N88-22269

RESEARCH TRIANGLE INST., RESEARCH TRIANGLE PARK, N.C.
Study of mean free path effects on growth of ultrafine metallic aerosols
[AD-A190206] N88-22149

RHODE ISLAND UNIV., KINGSTON.
Summary of the 1987 Gordon Research Conference on Corrosion
[AD-A189737] N88-22161

RICE UNIV., HOUSTON, TEX.
Infrared absorption spectroscopy and chemical kinetics of free radicals
[DE88-006536] N88-22112
Discharge excitation of the XeF C to A transition
[DE88-006448] N88-22339

ROCHESTER UNIV., N. Y.
Studies of molecular biology
[DE88-005906] N88-22514
A probabilistic approach to low-level vision
[AD-A189041] N88-22553
Theory of the dissociation dynamics of small molecules on metal surfaces: Finite temperature studies
[DE88-006495] N88-22716
ROVER: A prototype active vision system
[AD-A189246] N88-22722

ROCKWELL INTERNATIONAL CORP., CANOGA PARK, CALIF.
Requirements and cost considerations for a Combined Space Nuclear Reactor Test Facility
[DE88-006763] N88-22719

ROCKWELL INTERNATIONAL CORP., THOUSAND OAKS, CALIF.
Transformation toughening of ceramics
[AD-A190399] N88-22183
Laser evaporation studies
[AD-A189815] N88-22346

ROME AIR DEVELOPMENT CENTER, GRIFFISS AFB, N.Y.
Stellar scintillometer atmospheric optical turbulence profiling experiment: A qualitative comparison of two identical instruments at AMOS (Air Force Maui Optical Station), 1985
[AD-A190589] N88-22479
ROME UNIV. (ITALY).
On new solvable many-body dynamical systems with velocity dependent forces
[PREPRINT-581] N88-22683
Lattice QCD calculation of K yields pi nonleptonic weak transition and other hadronic weak parameters
[PREPRINT-580] N88-22717
RUTGERS - THE STATE UNIV., NEW BRUNSWICK, N. J.
Heat transfer from a negatively buoyant wall jet
[NBS-GCR-88-541] N88-22208
Selective mechanisms in auditory and bimodal signal processing
[AD-A190529] N88-22530

S

SAINT ANDREW'S UNIV. (SCOTLAND).
Discharge excitation of the XeF C to A transition
[DE88-006448] N88-22339
SALFORD UNIV. (ENGLAND).
Angular resolved energy analysis of (69)Ga+ ions from a gallium liquid metal ion source
[AERE-R-12649] N88-22760
SANDIA NATIONAL LABS., ALBUQUERQUE, N. MEX.
Continuous measurements of in-bore projectile velocity
[DE88-006841] N88-22056
Structural consequences of railgun augmentation
[DE88-007036] N88-22058
Structure of sol-gel silica
[DE88-006870] N88-22114
Effect of P implantation on the corrosion behavior of Fe-Cr alloys
[DE88-005732] N88-22158
Singlet oxygen behavior in solid polymer matrices
[DE88-005171] N88-22171
A three-dimensional model for the elastic properties of a foam
[DE88-006197] N88-22192
Melt processing ceramic YBa2Cu3O(sub 6.9)
[DE88-007039] N88-22199
Stability of the high-temperature G-16 primer composition
[DE88-006201] N88-22206
The numerical simulation of viscous flows with change of phase and chemical reaction
[DE88-003204] N88-22292
Transient compressible flow in porous materials
[DE88-006685] N88-22324
Finite element simulation of perforation of aluminum plates
[DE88-002092] N88-22362
Telerobotic operation of conventional robot manipulators
[DE88-005718] N88-22363
Elasto-plastic analysis using a stress-based finite element method and an endochronic theory of plasticity
[DE88-003001] N88-22372
A 3-D solid rendering of NDT data
[DE88-006199] N88-22373
Oscillation damped movement of suspended objects
[DE88-005715] N88-22433
Phenomenological modelling of rate-dependent plasticity for high strain rate problems
[DE88-006647] N88-22440
Today's photovoltaic systems: An evaluation of their performance
[DE88-006926] N88-22457
Performance evaluation of molten salt thermal storage systems
[DE87-014645] N88-22461
Recent advances in photovoltaic concentrator technology
[DE88-003948] N88-22462
Advanced geothermal technologies
[DE88-004307] N88-22483
Description of ground motion data processing codes, volume 2
[DE88-007137] N88-22481
Insertions using geometric analysis and hybrid force-position control: Method and analysis
[DE87-013652] N88-22611
SAO PAULO UNIV., SAO CARLOS (BRAZIL).
Recent advances in solid polymer electrolyte fuel cell technology
[DE88-005380] N88-22464
SCIENCE APPLICATIONS INTERNATIONAL CORP., SAN DIEGO, CALIF.
Performance of data compression codes in channels with errors
[AD-A189667] N88-22253
Methodology for software reliability prediction, volume 1
[AD-A190018] N88-22571
Methodology for software reliability prediction, volume 3
[AD-A190019] N88-22572
SOUTHAMPTON UNIV. (ENGLAND).
Flexiwall 3 SO: A second order predictive strategy for rapid wall adjustment in two-dimensional compressible flow
[NASA-CR-181662] N88-22018
SOUTHERN RESEARCH INST., BIRMINGHAM, ALA.
Development of polymeric films with piezoelectrical properties from polypeptides; low, odd nylons; or polyureas
[AD-A190301] N88-22181
SOUTHWEST RESEARCH INST., SAN ANTONIO, TEX.
Development of a laboratory test for multiport injector deposits: Approaches 1 and 2
[AD-A190697] N88-22203
Experiments on densely-loaded non-Newtonian slurries in laminar and turbulent pipe flows
[DE88-006209] N88-22323
SPACE DATA CORP., TEMPE, ARIZ.
Engineering support of space shuttle experiment integration
[AD-A190135] N88-22061
SPECTRAN CORP., STURBRIDGE, MASS.
Hermetic coating of optical fibers
[AD-A189886] N88-22177
SRI INTERNATIONAL CORP., MENLO PARK, CALIF.
The corrosion resistance of an aluminum alloy coated with polysilazane derived ceramics
[AD-A190703] N88-22189
Electromagnetic sensor arrays for nondestructive evaluation and robot control
[AD-A190210] N88-22260
Infrared differential absorption lidar for vapor detection
[AD-A190600] N88-22497
STANFORD UNIV., CALIF.
Contraction design for small low-speed wind tunnels
[NASA-CR-182747] N88-22045
Turbulent reacting flows and supersonic combustion
[AD-A189690] N88-22115
An investigation of flow structure, mixing and chemical reaction in combusting turbulent flows
[AD-A189980] N88-22117
Advanced diagnostics for reacting flows
[AD-A190485] N88-22122
The thermal radiative properties of metals at high temperature
[DE88-006625] N88-22141
Instruments for use in experimental studies of complex turbulent shear flow: Three component LDVs
[AD-A190526] N88-22312
Design, development and evaluation of Stanford/Ames EVA prehensors
[NASA-CR-182688] N88-22540
Exhaustive and pseudo-exhaustive testing
[AD-A190140] N88-22574
Distributions of quadratic forms
[AD-A190224] N88-22663
Sufficient matrices and the linear complementarity problem
[AD-A190429] N88-22690
Synthesis of metastable superconductors by high dynamic pressure
[DE88-005620] N88-22764
The influence of current stressing on the structure of Ag contacts to GaAs
[DE88-005988] N88-22771
Fundamental studies of the mechanical behavior of microelectronic thin film materials
[AD-A190038] N88-22786
STATE UNIV. OF NEW YORK, ALBANY.
Enhancement of data acquisition and numerical computation capabilities for unsteady fluid dynamics
[AD-A190115] N88-22302
STATE UNIV. OF NEW YORK, BUFFALO.
Anomalies in the heat-capacity signatures of submonolayer adsorbates with attractive lateral interactions
[AD-A190736] N88-22817
SVERDRUP TECHNOLOGY, INC., CLEVELAND, OHIO.
Three-dimensional inelastic approximate analysis code (MOMM) N88-22392
Specialty three-dimensional finite element analysis codes N88-22393
Probabilistic structural analysis computer code (NESSUS) N88-22397
Structural tailoring of high-speed turbine blades (SSME/STAEBL) N88-22398
Advanced probabilistic methods for quantifying the effects of various uncertainties in structural response N88-22401
Structural analyses of engine wall cooling concepts and materials N88-22405
SWEDISH INST. FOR MATERIALS TESTING, BORAS.
Density measurements on solids and liquids
[PB88-164934] N88-22129
Continual capillary viscosimetry using extrusiograph techniques
[PB88-166293] N88-22195
SYRACUSE UNIV., N. Y.
Grain boundary oxidation and low-cycle fatigue at elevated temperatures N88-22420
New generation knowledge processing, volume 1
[AD-A190165] N88-22826

T

TCS, INC., SAN DIEGO, CALIF.
Real-time stressed channel simulator
[AD-A190223] N88-22067
TECHNICAL RESEARCH CENTRE OF FINLAND, ESPOO.
Manufacturing of ultrasonic focused probes
[VTT-RR-487] N88-22368
Spectrum fatigue testing for materials characterization
[VTT-RR-502] N88-22443
A simplified key-curve approach for J-R-curve testing of CT specimens
[VTT-RR-503] N88-22444
TECHNION - ISRAEL INST. OF TECH., HAIFA.
Visualization of flows in turbomachinery
[AD-A189927] N88-22299
Visualisation of the flow at the tip of a high speed axial flow turbine rotor
[AD-A189928] N88-22300
Visualisation of the flow at the tip of a high speed axial flow turbine rotor: An assessment of flow visualisation techniques and the requirement of the experimental turbine
[AD-A189929] N88-22301
TECHNISCHE HOGESCHOOL, DELFT (NETHERLANDS).
Electromagnetic compatability: An introduction to the theory of interference and shielding, 3rd revised edition
[PB88-165410] N88-22264
Seismic inversion by a RMS (Root-Mean-Square) Born approximation in the space-time domain
[PB88-165402] N88-22711
TECHNISCHE HOGESCHOOL, EINDHOVEN (NETHERLANDS).
Mechanical behaviour of particle filled thermoplastics
[PB88-169297] N88-22196
Experimental design and structural optimization
[PB88-169255] N88-22436
Methods of measurement for the evaluation of monolayer properties. Development and applications
[ETN-88-92229] N88-22532
Excitations in magnetic low-dimensional systems: A spectroscopic study
[ETN-88-92230] N88-22697
TENNESSEE SPACE LABS., INC., MANCHESTER.
Investigation into the development of computer aided design software for space based sensors
[NASA-CR-180772] N88-22552
TENNESSEE UNIV., KNOXVILLE.
Laser enhanced adhesion of copper films to sapphire substrates
[DE88-006802] N88-22144
Performance test results: AXIAL-GAP, permanent magnet compressor motor
[DE88-006857] N88-22289
A hardware/software system for implementing geophysical diffraction tomography
[DE88-006411] N88-22480
Design and implementation of a parallel computer for expert system applications
[DE88-005288] N88-22601
TEXAS A&M UNIV., COLLEGE STATION.
Damage models for delamination and transverse fracture
[AD-A189652] N88-22068
TEXAS ACCELERATOR CENTER, THE WOODLANDS.
Magnet strength fluctuations in the SSC (Superconducting Super Collider) lattice. Part 2: Frequency modulation
[DE88-006491] N88-22774
TEXAS CHRISTIAN UNIV., FORT WORTH.
New phosphorus based polymer systems
[AD-A190457] N88-22186
TEXAS TECHNOLOGICAL UNIV., LUBBOCK.
Space-variant optical systems
[AD-A189967] N88-22724

TEXAS UNIV., ARLINGTON.
Electronic and ionic transport in polymers
[AD-A190434] N88-22185
TEXAS UNIV., AUSTIN.
Advanced guidance algorithms for homing missiles with bearings-only measurements
[AD-A190435] N88-22026
Synthesis and analysis of novel polymers with potential for providing both high permselectivity and permeability in gas separation applications
[DE88-006533] N88-22174
Wave energy flow conservation for propagation in inhomogeneous Vlasov-Maxwell equilibria
[DE88-006705] N88-22251
Monolithic phase shifter study
[AD-A190213] N88-22278
Geometric methods and the gauge structure of Berry's phase
[DE88-006538] N88-22682
Long-time impurity confinement as a precursor to disruptions in ohmically heated tokamaks
[DE88-006183] N88-22742
Involution-dependent constants and the cancellation of divergences in the 1-loop open string amplitude
[DE88-006537] N88-22811
THERMO ELECTRON CORP., WALTHAM, MASS.
Program to research laser-driven thermionic electron sources for free electron lasers
[AD-A190473] N88-22353
TOKYO UNIV. (JAPAN).
Finite width corrections to the Nambu action for the Nielsen-Olesen string
[DE88-006996] N88-22812
TRACER TECHNOLOGIES, INC., SOMERVILLE, MASS.
A laser-based photoacoustic spectrometer for direct breath C-13O2/C-12O2 measurement
[DE88-004915] N88-22516
TRANSPORTATION SYSTEMS CENTER, CAMBRIDGE, MASS.
General aviation activity and avionics survey: 1986 data
[AD-A189986] N88-22003
Analysis of head response to torso acceleration. Volume 2: Description of data retrieval, analysis and display software
[PB88-156765] N88-22536
TRW SPACE TECHNOLOGY LABS., REDONDO BEACH, CALIF.
Basic research on flame radiation
[PB88-168372] N88-22105

U

UNIDYNAMICS/PHOENIX, ARIZ.
Stability of the high-temperature G-16 primer composition
[DE88-006201] N88-22206
UNITED TECHNOLOGIES RESEARCH CENTER, EAST HARTFORD, CONN.
Investigation of laser diagnostics of PACVD processes for depositing hard face coatings
[DE88-007083] N88-22176
Coupled high power waveguide laser research
[AD-A189800] N88-22345
UNIVERSITY OF NORTHERN ILLINOIS, DE KALB.
Effective electron interactions due to virtual charge and spin excitations in an extended Hubbard model for Cu-O superconductors
[DE88-005971] N88-22766
UNIVERSITY OF SOUTH FLORIDA, ST. PETERSBURG.
Simulation analysis of moored fluorometer time series from the Mid-Atlantic Bight
[DE88-006066] N88-22505
UNIVERSITY OF SOUTHERN CALIFORNIA, LOS ANGELES.
Pressure measurements of impinging jet with asymmetric nozzle
[NASA-CR-182759] N88-22011
The algebraic structure of convolutional codes
[AD-A190280] N88-22635
Approximation methods for the identification and control of distributed parameter systems
[AD-A190201] N88-22662
UNIVERSITY OF SOUTHERN ILLINOIS, CARBONDALE.
Groundwater sapping valleys: Experimental studies, geological controls and implications to the interpretation of valley networks on Mars
[NASA-CR-182718] N88-22647
UTAH STATE UNIV., LOGAN.
Numerical solution of nonlinear algebraic equations in stiff ODE solving
[DE88-006634] N88-22622
UTAH UNIV., SALT LAKE CITY.
An investigation of the failure response of laminates under biaxial stress
[AD-A190039] N88-22090
Fractography of composite delamination
[NASA-CR-182757] N88-22096
A test for interfacial effects and stress transfer in ceramic matrix composites
[NASA-CR-182758] N88-22194
The kinetics of contact noise in NaBeta alumina
[AD-A190651] N88-22707

V

VERAC, INC., SAN DIEGO, CALIF.
Optical Conceptual Computing and Associative Memory (OCCAM)
[AD-A190030] N88-22550
VIRGINIA POLYTECHNIC INST. AND STATE UNIV., BLACKSBURG.
Crack opening and extension in inert solid propellant. An experimental study
[AD-A189808] N88-22201
VIRGINIA UNIV., CHARLOTTESVILLE.
High temperature superconductors in the La(sub 1+x)Ba(sub 2-x)Cu O(sub y system
[DE88-006367] N88-22802

W

WASHINGTON UNIV., SEATTLE.
Gamma-ray densitometry: Nondestructive analysis of density evolution during ceramic powder processing
[DE88-006671] N88-22198
An analysis of multiple grain ChIP architectures
[AD-A189942] N88-22570
A chemical method for achieving acceleration of macroparticles to ultrahigh velocities
[DE88-006377] N88-22695
WASHINGTON UNIV., ST. LOUIS, MO.
Development and application of the p-version of the finite element method
[AD-A190036] N88-22633
WAYNE STATE UNIV., DETROIT, MICH.
Cetane scale evaluation and possible modification
[AD-A189730] N88-22200
WEA, CAMBRIDGE, MASS.
Wave propagation and dynamics of lattice structures
[AD-A190037] N88-22066
Wave propagation and dynamics of lattice structures
[AD-A190611] N88-22069
WEIDLINGER ASSOCIATES, NEW YORK, N.Y.
Vibrations of structures with parametric uncertainties
[AD-A190400] N88-22378
WISCONSIN UNIV., MADISON.
Vortices in long Josephson junctions
[AD-A190338] N88-22279
A new method of measuring multigrade oil shear elasticity and viscosity at high shear rates
[AD-A190145] N88-22304
Instrumentation to provide an active control capability for distributed parameter systems
[AD-A190043] N88-22375
The collection of statistics on the frequency of cloud cover over North America
[AD-A190456] N88-22495
Electrical circuit modeling of reversed field pinches
[DE88-006942] N88-22745
Thin superconducting film characterization by surface acoustic waves
[AD-A190417] N88-22791
WISCONSIN UNIV., MILWAUKEE.
Mechanisms mediating perception of complex acoustic patterns
[AD-A189765] N88-22520
Mechanisms mediating the perception of complex acoustic patterns
[AD-A190112] N88-22705
WOODS HOLE OCEANOGRAPHIC INSTITUTION, MASS.
Real-time environmental Arctic monitoring (R-TEAM)
[AD-A189948] N88-22508
WORCESTER POLYTECHNIC INST., MASS.
Preliminary market analysis for large zeolite crystals
[NASA-CR-182882] N88-22207

X

XEROX CORP., PALO ALTO, CALIF.
A qualitative approach to electricity
[AD-A189854] N88-22693
XEROX PALO ALTO RESEARCH CENTER, CALIF.
The structure of the boron-hydrogen complex in silicon
[DE88-005433] N88-22795

Y

YALE UNIV., NEW HAVEN, CONN.
Laboratory equipment update
[AD-A189781] N88-22522
Rapid feature extraction via the radon transform
[AD-A190032] N88-22573
Memory-based expert systems
[AD-A190203] N88-22606

Typical Contract Number Index Listing

Listings in this index are arranged alphanumerically by contract number. Under each contract number the NASA accession numbers denoting documents that have been produced as a result of research done under that contract are arranged in ascending order. The NASA accession number denotes the number by which the citation is identified.

AF AFOSR-0066-87 ..... N88-22475
AF AFOSR-0115-86 ..... N88-22090
AF AFOSR-0147-86 ..... N88-22576
AF AFOSR-0178-84 ..... N88-22350
AF AFOSR-0179-86 ..... N88-22153
AF AFOSR-0190-84 ..... N88-22755
AF AFOSR-0239-85 ..... N88-22691
AF AFOSR-0286-84 ..... N88-22121
AF AFOSR-0302-84 ..... N88-22534
AF AFOSR-0337-84 ..... N88-22524
AF AFOSR-0344-85 ..... N88-22573
AF AFOSR-0359-84 ..... N88-22790
AF AFOSR-0373-83 ..... N88-22120
AF AFOSR-0381-85 ..... N88-22718
AF PROJ. 2304 ..... N88-22639
AF PROJ. 2306 ..... N88-22191
AF PROJ. 2308 ..... N88-22315
AF PROJ. 5730 ..... N88-22756
AF-AFOSR-ISSA-00008-86 ..... N88-22311
AF-AFOSR-ISSA-00012-85 ..... N86-22311
AF-AFOSR-0006-85 ..... N88-22725
AF-AFOSR-0015-87 ..... N88-22595
AF-AFOSR-0019-86 ..... N88-22128
AF-AFOSR-0021-87 ..... N88-22596
AF-AFOSR-0025-86 ..... N88-22279
AF-AFOSR-0027-83 ..... N88-22190
AF-AFOSR-0028-87 ..... N88-22782
AF-AFOSR-0029-82 ..... N88-22673
AF-AFOSR-0033-83 ..... N88-22753
AF-AFOSR-0036-86 ..... N88-22278
AF-AFOSR-0040-84 ..... N88-22118
AF-AFOSR-0045-87 ..... N88-22125
AF-AFOSR-0051-86 ..... N88-22786
AF-AFOSR-0054-87 ..... N88-22523
AF-AFOSR-0056-87 ..... N88-22122
AF-AFOSR-0068-84 ..... N88-22088
AF-AFOSR-0068-86 ..... N88-22684
AF-AFOSR-0076-84 ..... N88-22070
AF-AFOSR-0083-83 ..... N88-22478
AF-AFOSR-0084-82 ..... N88-22188
AF-AFOSR-0098-87 ..... N88-22794
AF-AFOSR-0119-86 ..... N88-22754
AF-AFOSR-0124-83 ..... N88-22068
AF-AFOSR-0156-85 ..... N88-22628
AF-AFOSR-0170-86 ..... N88-22631
AF-AFOSR-0185-86 ..... N88-22642
AF-AFOSR-0187-82 ..... N88-22641
AF-AFOSR-0187-84 ..... N88-22348
AF-AFOSR-0189-82 ..... N88-22674
AF-AFOSR-0206-83 ..... N88-22530
AF-AFOSR-0209-86 ..... N88-22302
AF-AFOSR-0233-82 ..... N88-22752
AF-AFOSR-0239-84 ..... N88-22610
AF-AFOSR-0244-85 ..... N88-22307
AF-AFOSR-0253-85 ..... N88-22361
N88-22632
AF-AFOSR-0254-86 ..... N88-22375
AF-AFOSR-0258-82 ..... N88-22657
AF-AFOSR-0259-85 ..... N88-22635
AF-AFOSR-0260-85 ..... N88-22705
AF-AFOSR-0260-86 ..... N88-22533
AF-AFOSR-0262-86 ..... N88-22275
AF-AFOSR-0264-85 ..... N88-22634
AF-AFOSR-0264-86 ..... N88-22726
AF-AFOSR-0272-84 ..... N88-22119
AF-AFOSR-0273-86 ..... N88-22349
AF-AFOSR-0276-86 ..... N88-22312
AF-AFOSR-0282-86 ..... N88-22549
AF-AFOSR-0285-84 ..... N88-22630
AF-AFOSR-0286-86 ..... N88-22093
AF-AFOSR-0292-85 ..... N88-22123
AF-AFOSR-0302-85 ..... N88-22700
AF-AFOSR-0304-86 ..... N88-22520
AF-AFOSR-0305-86 ..... N88-22036
AF-AFOSR-0308-85 ..... N88-22299
N88-22300
N88-22301
AF-AFOSR-0308-86 ..... N88-22522
AF-AFOSR-0309-84 ..... N88-22065
AF-AFOSR-0314-87 ..... N88-22161
AF-AFOSR-0315-82 ..... N88-22633
AF-AFOSR-0324-86 ..... N88-22007
AF-AFOSR-0332-86 ..... N88-22605
N88-22626
N88-22629
N88-22656
N88-22658
AF-AFOSR-0335-84 ..... N88-22529
AF-AFOSR-0337-85 ..... N88-22151
AF-AFOSR-0340-84 ..... N88-22366
AF-AFOSR-0341-84 ..... N88-22789
AF-AFOSR-0346-85 ..... N88-22689
AF-AFOSR-0350-84 ..... N88-22791
AF-AFOSR-0356-84 ..... N88-22116
AF-AFOSR-0367-85 ..... N88-22145
AF-AFOSR-0371-84 ..... N88-22026
AF-AFOSR-0372-83 ..... N88-22124
AF-AFOSR-0373-84 ..... N88-22117
AF-AFOSR-0382-84 ..... N88-22724
AF-AFOSR-0389-84 ..... N88-22788
AF-AFOSR-0393-84 ..... N88-22662
AFOSR-ISSA-87-0034 ..... N88-22191
ARPA ORDER 4871 ..... N88-22566
ARPA ORDER 4952 ..... N88-22730
ARPA ORDER 9099 ..... N88-22779
BMFT-03-M-2008-5 ..... N88-22441
CIRM-PROANTAR-9503 ..... N88-22468
CIRM-PROANTAR-9586 ..... N88-22468
CIRM-PROANTAR-9618 ..... N88-22468
DA PROJ. CM5-1 ..... N88-22253
DA PROJ. F61-543 ..... N88-22181
DA PROJ. RR0-4206 ..... N88-22693
DA PROJ. RS3-4-A-52 ..... N88-22181
DA PROJ. 1L1-61102-AH-43 ..... N88-22303
DAAG29-79-D-1002 ..... N88-22781
DAAG29-84-K-0032 ..... N88-22783
DAAG29-84-K-0046 ..... N88-22304
DAAG29-84-K-0164 ..... N88-22200
DAAG29-84-K-0174 ..... N88-22136
DAAK11-82-C-0158 ..... N88-22497
DAAK11-84-C-0010 ..... N88-22723
DAAK70-85-E-0054 ..... N88-22203
DAAL03-86-K-0052 ..... N88-22783
DACA76-85-C-0001 ..... N88-22553
N88-22722
DACA76-85-C-0010 ..... N88-22607
N88-22609
DACA76-85-C-0100 ..... N88-22449
DAMD17-81-C-1201 ..... N88-22521
DE-AC02-76CH-00016 ..... N88-22108
N88-22109
N88-22602
DE-AC02-76CH-03000 ..... N88-22809
N88-22812
N88-22841
N88-22842
N88-22844
DE-AC02-78ET-51013 ..... N88-22743
DE-AC02-83CH-10093 ..... N88-22371
DE-AC03-76SF-00098 ..... N88-22063
N88-22082
N88-22715
N88-22771
N88-22772
N88-22773
N88-22801
DE-AC04-76DP-00053 ..... N88-22356
DE-AC04-76DP-00613 ..... N88-22170
DE-AC04-76DP-00789 ..... N88-22056
N88-22057
N88-22058
N88-22114
N88-22158
N88-22171
N88-22192
N88-22199
N88-22206
N88-22292
N88-22324
N88-22362
N88-22363
N88-22372
N88-22373
N88-22433
N88-22440
N88-22457
N88-22461
N88-22462
N88-22481
N88-22611
DE-AC05-84OR-21400 ..... N88-22046
N88-22075
N88-22144
N88-22159
N88-22169
N88-22173
N88-22205
N88-22360
N88-22465
N88-22480
N88-22556
N88-22586
N88-22601
N88-22614
N88-22692
N88-22742
N88-22757
N88-22795
DE-AC05-84OT-21400 ..... N88-22289
DE-AC06-76RL-01830 ..... N88-22094
N88-22196
N88-22504
N88-22513
DE-AC07-76ID-01570 ..... N88-22086
N88-22143
N88-22162
N88-22172
N88-22271
N88-22272
N88-22288
N88-22293
N88-22326
N88-22437
N88-22719
N88-22740
DE-AC09-76SR-00001 ..... N88-22828
DE-AC22-86PC-90009 ..... N88-22204
DE-AI09-79DP-40092 ..... N88-22286
DE-FG02-84ER-45117 ..... N88-22193
DE-FG02-84ER-45173 ..... N88-22160
DE-FG02-85ER-13333 ..... N88-22327
DE-FG02-85ER-53198 ..... N88-22745
DE-FG02-85ER-60281 ..... N88-22514
DE-FG02-85ER-60344 ..... N88-22516
DE-FG02-86ER-13560 ..... N88-22176
DE-FG02-86ER-25015 ..... N88-22557
N88-22585
N88-22618
N88-22619
N88-22620
N88-22623
N88-22679
N88-22680
DE-FG02-86ER-25018 ..... N88-22622
DE-FG02-87ER-13895 ..... N88-22113
DE-FG02-87ER-13744 ..... N88-22716
DE-FG02-87ER-25026 ..... N88-22592

DE-FG02-87ER-45302 ..... N88-22085
N88-22769
DE-FG02-87ER-45310 ..... N88-22142
DE-FG03-85ER-51069 ..... N88-22744
DE-FG03-86ER45230 ..... N88-22764
DE-FG05-80ET-53088 ..... N88-22251
DE-FG05-85ER-13439 ..... N88-22112
DE-FG05-85ER-40200 ..... N88-22682
N88-22811
DE-FG05-85ER-53206 ..... N88-22749
DE-FG05-85ER-80265 ..... N88-22505
DE-FG05-86ER-13507 ..... N88-22174
DE-FG05-86ER-13544 ..... N88-22110
DE-FG05-87ER-40374 ..... N88-22774
DE-FG06-85ER-13382 ..... N88-22695
DE-FG22-86PC-90962 ..... N88-22323
DFG-DU-101/7-1,2 ..... N88-22329
DRET-85-053 ..... N88-22713
DRET-86-001 ..... N88-22073
DTFA03-84-C-0004 ..... N88-22024
EPA-R-812189 ..... N88-22517
FC-85-563 ..... N88-22131
FINEP 537/CT N88-22483
FINEP-537/CT N88-22468
N88-22469
N88-22484
N88-22489
FINEP-539/CT N88-22482
F04611-85-C-0096 ..... N88-22201
F08635-84-K-0209 ..... N88-22729
F19628-83-C-0156 ..... N88-22061
F19628-84-K-0005 ..... N88-22477
F19628-84-K-0021 ..... N88-22252
F19628-86-C-0141 ..... N88-22062
F19628-87-C-0003 ..... N88-22450
N88-22451
N88-22476
F29601-84-K-0036 ..... N88-22126
F30602-81-C-0206 ..... N88-22281
F30602-83-C-0118 ..... N88-22571
N88-22572
F30602-84-C-0199 ..... N88-22177
F30602-84-K-0001 ..... N88-22826
F33615-84-C-0600 ..... N88-22347
N88-22519
F33615-84-C-2424 ..... N88-22278
F33615-84-C-2431 ..... N88-22025
F33615-84-C-3216 ..... N88-22823
F33615-84-C-5028 ..... N88-22359
F33615-84-K-1520 ..... N88-22761
F33615-85-C-0532 ..... N88-22184
F33615-85-C-5093 ..... N88-22179
F33615-86-C-2658 ..... N88-22460
F33615-86-C-4503 ..... N88-22537
F49620-82-K-0010 ..... N88-22606
F49620-84-C-0009 ..... N88-22378
F49620-84-C-0017 ..... N88-22149
F49620-84-C-0067 ..... N88-22730
F49620-84-C-0091 ..... N88-22346
F49620-84-K-0011 ..... N88-22260
F49620-85-C-0008 ..... N88-22661
N88-22669
N88-22670
N88-22671
F49620-85-C-0106 ..... N88-22345
F49620-85-C-0115 ..... N88-22305
F49620-85-C-0116 ..... N88-22379
F49620-85-C-0117 ..... N88-22354
F49620-85-C-0143 ..... N88-22183
F49620-85-C-0144 ..... N88-22637
N88-22638
N88-22659
N88-22664
N88-22666
N88-22667
N88-22668
N88-22677
F49620-85-C-0148 ..... N88-22066
N88-22069
F49620-86-C-0012 ..... N88-22779
F49620-86-C-0030 ..... N88-22548
F49620-86-C-0070 ..... N88-22550
F49620-86-C-0108 ..... N88-22152
F49620-86-C-0117 ..... N88-22751
F49620-86-C-0136 ..... N88-22551
F49620-86-K-0021 ..... N88-22785
F49620-86-K-0022 ..... N88-22115
F49620-87-C-0004 ..... N88-22008
F49620-87-C-0023 ..... N88-22083
F49620-87-C-0031 ..... N88-22381
GRI-5086-260-1415 ..... N88-22105
NAGW-707 ..... N88-22847
NAGW-867 ..... N88-22843
NAGW-1105 ..... N88-22676
NAG1-654 ..... N88-22295
NAG1-705 ..... N88-22096
NAG1-819 ..... N88-22011
NAG2-444 ..... N88-22194
NAG3-348 ..... N88-22420
NAG3-379 ..... N88-22387
NAG3-465 ..... N88-22423
NAG3-495 ..... N88-22197
NAG3-512 ..... N88-22388
NAG3-550 ..... N88-22395
NAG3-598 ..... N88-22322
NAG3-24105 ..... N88-22397
NAG5-526 ..... N88-22133
NAG8-059 ..... N88-22491
N88-22492
NAG8-093 ..... N88-22602
NAG8-619 ..... N88-22207
NAG13-3 ..... N88-22452
NASW-4292 ..... N88-22515
NASW-4307 ..... N88-22099
N88-22100
N88-22101
N88-22102
N88-22104
N88-22130
N88-22134
N88-22135
N88-22326
N88-22490
N88-22698
NAS1-18107 ..... N88-22541
NAS3-2410S N88-22414
NAS3-23288 ..... N88-22426
NAS3-23698 ..... N88-22394
NAS3-23939 ..... N88-22388
N88-22427
NAS3-23940 ..... N88-22421
NAS3-23941 ..... N88-22400
NAS3-24105 ..... N88-22384
N88-22428
NAS5-29079 ..... N88-22447
NAS5-29186 ..... N88-22331
NAS5-30061 ..... N88-22552
NAS7-918 ..... N88-22575
N88-22672
NAS8-36108 ..... N88-22060
NAS8-36394 ..... N88-22834
NAS8-37359 ..... N88-22296
NB83NADA4047 ..... N88-22208
NCC2-294 ..... N88-22045
NCC2-295 ..... N88-22540
NCC3-24 ..... N88-22414
NCC3-46 ..... N88-22418
NCC3-81 ..... N88-22410
N88-22411
NSF ATM-80-02097 ..... N88-22483
NSF DCR-85-03662 ..... N88-22578
NSF DCR-86-02958 ..... N88-22722
NSF DMS-84-0623 ..... N88-22690
NSF DMS-86-06964 ..... N88-22675
NSF OCE-83-16930 ..... N88-22507
NSG-1483 ..... N88-22098
NSG-5265 ..... N88-22052
NSG7-172 ..... N88-22018
N00014-76-C-0816 ..... N88-22182
N88-22793
N00014-78-C-0392 ..... N88-22512
N00014-78-C-0696 ..... N88-22308
N00014-79-C-0632 ..... N88-22186
N00014-80-C-0622 ..... N88-22579
N00014-82-K-0193 ..... N88-22553
N00014-82-K-0603 ..... N88-22707
N00014-83-C-0333 ..... N88-22353
N00014-83-C-0694 ..... N88-22006
N00014-83-C-2255 ..... N88-22721
N00014-83-K-0107 ..... N88-22377
N00014-83-K-0125 ..... N88-22578
N88-22597
N00014-84-C-0149 ..... N88-22608
N00014-84-C-0167 ..... N88-22675
N00014-84-C-0218 ..... N88-22507
N00014-84-C-0392 ..... N88-22189
N00014-84-C-0699 ..... N88-22180
N00014-84-K-0099 ..... N88-22597
N00014-85-C-0008 ..... N88-22639
N00014-85-C-0668 ..... N88-22189
N00014-85-C-0688 ..... N88-22693
N00014-85-K-0124 ..... N88-22283
N88-22313
N88-22449
N88-22607
N88-22609
N88-22640
N88-22644
N88-22694
N00014-85-K-0328 ..... N88-22570
N00014-85-K-0343 ..... N88-22690
N00014-85-K-0555 ..... N88-22787
N00014-85-K-0570 ..... N88-22625
N00014-85-K-0600 ..... N88-22574
N00014-85-K-0641 ..... N88-22178
N00014-85-K-0665 ..... N88-22320
N00014-86-C-0135 ..... N88-22508
N00014-86-C-2352 ..... N88-22577
N88-22627
N00014-86-C-2356 ..... N88-22351
N88-22352
N00014-86-F-0022 ..... N88-22187
N00014-86-F-0049 ..... N88-22849
N00014-86-K-0039 ..... N88-22665
N88-22685
N88-22686
N88-22687
N88-22688
N00014-86-K-0043 ..... N88-22817
N00014-86-K-0133 ..... N88-22156
N00014-86-K-0156 ..... N88-22663
N00014-86-K-0180 ..... N88-22579
N88-22643
N88-22644
N00014-86-K-0202 ..... N88-22259
N00014-86-K-0608 ..... N88-22182
N00014-86-K-0769 ..... N88-22185
N00014-87-C-0001 ..... N88-22367
N88-22660
N00014-87-C-0133 ..... N88-22067
N00014-87-K-0436 ..... N88-22495
N00024-85-C-6041 ..... N88-22309
N88-22318
N00039-84-C-0087 ..... N88-22566
N00228-85-G-3262 ..... N88-22150
N88-22306
N88-22706
N62269-84-C-0268 ..... N88-22181
N66001-85-D-0029 ..... N88-22253
PROJ. RR0-4108 ..... N88-22512
STPA-85-95-004 ..... N88-22103
STPA-198/CO N88-22164
STU-84-4563 ..... N88-22032
W-31-109-ENG-38 ..... N88-22646
N88-22770
N88-22796
N88-22797
N88-22798
N88-22799
W-7405-ENG-36 ..... N88-22095
N88-22339
N88-22340
N88-22341
N88-22343
N88-22355
N88-22458
N88-22463
N88-22464
N88-22542
N88-22612
N88-22613
N88-22621
N88-22803
W-7405-ENG-48 ..... N88-22084
N88-22141
N88-22157
N88-22175
N88-22287
N88-22334
N88-22342
N88-22432
N88-22467
N88-22499
N88-22603
N88-22731
N88-22732
N88-22733
N88-22764
N88-22775
N88-22800
W-31109-ENG-38 ..... N88-22107
N88-22699
N88-22741
N88-22765
N88-22766
N88-22767
N88-22768
176-10-05-70 ..... N88-22854
307-51-00 ..... N88-22805
474-12-10 ..... N88-22080
505-33-1B N88-22591
505-40-4 ..... N88-22337
505-60-01 ..... N88-22010
N88-22014
505-60-21 ..... N88-22012
505-60-31 ..... N88-22336
505-60-31-03 ..... N88-22047
505-61-01-02 ..... N88-22018

505-61-01-07 ..... N88-22435
505-61-51 ..... N88-22013
505-61-51-06 ..... N88-22710
505-61-51-10 ..... N88-22015
505-61-71-01 ..... N88-22016
505-62-21 ..... N88-22652
505-62-38 ..... N88-22037
505-63-1B N88-22382
N88-22408
N88-22446
505-63-01-01 ..... N88-22097
505-63-01-05 ..... N88-22445
505-63-11-02 ..... N88-22439
505-63-51-01 ..... N88-22434
505-63-91-02 ..... N88-22709
505-66-21-01 ..... N88-22653
505-90-21-01 ..... N88-22541
506-40-21-01 ..... N88-22325
506-43-31-04 ..... N88-22438
506-43-41-01 ..... N88-22031
545-03-01 ..... N88-22019
586-01-11 ..... N88-22322
922-22-08 ..... N88-22033
928-24-00-02 ..... N88-22072

Typical Report Number Index Listing

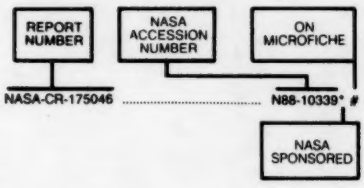

Listings in this index are arranged alphanumerically by report number. The NASA accession number denotes the number by which the citation is identified. An asterisk (*) indicates that the item is a NASA report. A pound sign (#) indicates that the item is available on microfiche.

A-87098 ..... N88-22013* #
A-87288 ..... N88-22010* #
A-88045 ..... N88-22336* #
A-88058 ..... N88-22337* #
A-88076 ..... N88-22014* #
A-88142 ..... N88-22009* #
A-88147 ..... N88-22650* #
A-88148 ..... N88-22651* #

AAMRL-TR-87-053 ..... N88-22184 #
AAMRL-TR-87-066 ..... N88-22535 #

ACARS-123187 ..... N88-22452* #

AD-A187479 ..... N88-22004 #
AD-A188450 ..... N88-22359 #
AD-A188617 ..... N88-22761 #
AD-A188657 ..... N88-22083 #
AD-A188861 ..... N88-22062 #
AD-A188981 ..... N88-22136 #
AD-A189041 ..... N88-22553 #
AD-A189246 ..... N88-22722 #
AD-A189342 ..... N88-22677 #
AD-A189443 ..... N88-22250 #
AD-A189623 ..... N88-22252 #
AD-A189627 ..... N88-22297 #
AD-A189630 ..... N88-22777 #
AD-A189634 ..... N88-22778 #
AD-A189635 ..... N88-22055 #
AD-A189640 ..... N88-22546 #
AD-A189642 ..... N88-22087 #
AD-A189644 ..... N88-22039 #
AD-A189648 ..... N88-22625 #
AD-A189652 ..... N88-22068 #
AD-A189667 ..... N88-22253 #
AD-A189674 ..... N88-22518 #
AD-A189680 ..... N88-22274 #
AD-A189682 ..... N88-22594 #
AD-A189690 ..... N88-22115 #
AD-A189695 ..... N88-22721 #
AD-A189701 ..... N88-22656 #
AD-A189707 ..... N88-22604 #
AD-A189714 ..... N88-22076 #
AD-A189715 ..... N88-22022 #
AD-A189720 ..... N88-22605 #
AD-A189721 ..... N88-22626 #
AD-A189723 ..... N88-22537 #
AD-A189724 ..... N88-22275 #
AD-A189725 ..... N88-22145 #
AD-A189726 ..... N88-22779 #
AD-A189730 ..... N88-22200 #
AD-A189737 ..... N88-22161 #
AD-A189739 ..... N88-22657 #
AD-A189743 ..... N88-22374 #
AD-A189745 ..... N88-22146 #
AD-A189746 ..... N88-22627 #
AD-A189747 ..... N88-22780 #
AD-A189749 ..... N88-22565 #
AD-A189750 ..... N88-22822 #
AD-A189752 ..... N88-22595 #
AD-A189757 ..... N88-22519 #
AD-A189758 ..... N88-22781 #
AD-A189763 ..... N88-22782 #
AD-A189765 ..... N88-22520 #
AD-A189767 ..... N88-22547 #
AD-A189771 ..... N88-22521 #
AD-A189772 ..... N88-22548 #
AD-A189778 ..... N88-22823 #
AD-A189781 ..... N88-22522 #
AD-A189782 ..... N88-22523 #
AD-A189784 ..... N88-22700 #
AD-A189786 ..... N88-22628 #
AD-A189787 ..... N88-22658 #
AD-A189788 ..... N88-22824 #
AD-A189790 ..... N88-22701 #
AD-A189800 ..... N88-22345 #
AD-A189808 ..... N88-22201 #
AD-A189813 ..... N88-22116 #
AD-A189815 ..... N88-22346 #
AD-A189817 ..... N88-22659 #
AD-A189823 ..... N88-22365 #
AD-A189826 ..... N88-22783 #
AD-A189831 ..... N88-22566 #
AD-A189842 ..... N88-22254 #
AD-A189843 ..... N88-22784 #
AD-A189844 ..... N88-22825 #
AD-A189845 ..... N88-22077 #
AD-A189846 ..... N88-22089 #
AD-A189847 ..... N88-22064 #
AD-A189848 ..... N88-22040 #
AD-A189849 ..... N88-22567 #
AD-A189854 ..... N88-22693 #
AD-A189855 ..... N88-22347 #
AD-A189865 ..... N88-22629 #
AD-A189867 ..... N88-22568 #
AD-A189868 ..... N88-22506 #
AD-A189869 ..... N88-22474 #
AD-A189870 ..... N88-22147 #
AD-A189871 ..... N88-22005 #
AD-A189872 ..... N88-22569 #
AD-A189873 ..... N88-22023 #
AD-A189874 ..... N88-22255 #
AD-A189886 ..... N88-22177 #
AD-A189907 ..... N88-22298 #
AD-A189925 ..... N88-22660 #
AD-A189927 ..... N88-22299 #
AD-A189928 ..... N88-22300 #
AD-A189929 ..... N88-22301 #
AD-A189930 ..... N88-22507 #
AD-A189939 ..... N88-22723 #
AD-A189940 ..... N88-22751 #
AD-A189942 ..... N88-22570 #
AD-A189945 ..... N88-22630 #
AD-A189948 ..... N88-22508 #
AD-A189962 ..... N88-22024 #
AD-A189966 ..... N88-22702 #
AD-A189967 ..... N88-22724 #
AD-A189969 ..... N88-22178 #
AD-A189972 ..... N88-22366 #
AD-A189979 ..... N88-22785 #
AD-A189980 ..... N88-22117 #
AD-A189981 ..... N88-22549 #
AD-A189983 ..... N88-22661 #
AD-A189985 ..... N88-22276 #
AD-A189986 ..... N88-22003 #
AD-A190007 ..... N88-22818 #
AD-A190008 ..... N88-22703 #
AD-A190009 ..... N88-22256 #
AD-A190010 ..... N88-22257 #
AD-A190013 ..... N88-22704 #
AD-A190015 ..... N88-22509 #
AD-A190018 ..... N88-22571 #
AD-A190019 ..... N88-22572 #
AD-A190027 ..... N88-22510 #
AD-A190028 ..... N88-22258 #
AD-A190029 ..... N88-22631 #
AD-A190030 ..... N88-22550 #
AD-A190031 ..... N88-22632 #
AD-A190032 ..... N88-22573 #
AD-A190033 ..... N88-22065 #
AD-A190034 ..... N88-22118 #
AD-A190035 ..... N88-22119 #
AD-A190036 ..... N88-22633 #
AD-A190037 ..... N88-22066 #
AD-A190038 ..... N88-22786 #
AD-A190039 ..... N88-22090 #
AD-A190040 ..... N88-22725 #
AD-A190041 ..... N88-22718 #
AD-A190043 ..... N88-22375 #
AD-A190076 ..... N88-22726 #
AD-A190077 ..... N88-22259 #
AD-A190101 ..... N88-22120 #
AD-A190105 ..... N88-22511 #
AD-A190106 ..... N88-22034 #
AD-A190107 ..... N88-22493 #
AD-A190109 ..... N88-22277 #
AD-A190110 ..... N88-22035 #
AD-A190112 ..... N88-22705 #
AD-A190114 ..... N88-22533 #
AD-A190115 ..... N88-22302 #
AD-A190118 ..... N88-22512 #
AD-A190119 ..... N88-22179 #
AD-A190123 ..... N88-22303 #
AD-A190124 ..... N88-22376 #
AD-A190128 ..... N88-22006 #
AD-A190129 ..... N88-22787 #
AD-A190130 ..... N88-22788 #
AD-A190131 ..... N88-22475 #
AD-A190135 ..... N88-22061 #
AD-A190136 ..... N88-22007 #
AD-A190137 ..... N88-22377 #
AD-A190140 ..... N88-22574 #
AD-A190145 ..... N88-22304 #
AD-A190149 ..... N88-22634 #
AD-A190165 ..... N88-22826 #
AD-A190168 ..... N88-22148 #
AD-A190169 ..... N88-22789 #
AD-A190173 ..... N88-22575* #
AD-A190174 ..... N88-22476 #
AD-A190196 ..... N88-22790 #
AD-A190197 ..... N88-22361 #
AD-A190200 ..... N88-22202 #
AD-A190201 ..... N88-22662 #
AD-A190203 ..... N88-22606 #
AD-A190206 ..... N88-22149 #
AD-A190207 ..... N88-22752 #
AD-A190210 ..... N88-22260 #
AD-A190213 ..... N88-22278 #
AD-A190217 ..... N88-22494 #
AD-A190218 ..... N88-22524 #
AD-A190220 ..... N88-22348 #
AD-A190223 ..... N88-22067 #
AD-A190224 ..... N88-22663 #
AD-A190228 ..... N88-22525 #
AD-A190233 ..... N88-22526 #
AD-A190236 ..... N88-22576 #
AD-A190238 ..... N88-22349 #
AD-A190244 ..... N88-22350 #
AD-A190245 ..... N88-22305 #
AD-A190246 ..... N88-22180 #
AD-A190254 ..... N88-22706 #
AD-A190255 ..... N88-22150 #
AD-A190256 ..... N88-22306 #
AD-A190268 ..... N88-22460 #
AD-A190272 ..... N88-22527 #
AD-A190273 ..... N88-22577 #
AD-A190275 ..... N88-22351 #
AD-A190277 ..... N88-22684 #
AD-A190280 ..... N88-22635 #
AD-A190281 ..... N88-22727 #
AD-A190282 ..... N88-22728 #
AD-A190296 ..... N88-22636 #
AD-A190298 ..... N88-22367 #
AD-A190301 ..... N88-22181 #
AD-A190306 ..... N88-22352 #
AD-A190307 ..... N88-22753 #
AD-A190308 ..... N88-22596 #
AD-A190309 ..... N88-22754 #
AD-A190310 ..... N88-22755 #
AD-A190312 ..... N88-22307 #
AD-A190315 ..... N88-22685 #
AD-A190316 ..... N88-22686 #
AD-A190317 ..... N88-22687 #
AD-A190318 ..... N88-22688 #
AD-A190319 ..... N88-22637 #
AD-A190320 ..... N88-22664 #
AD-A190321 ..... N88-22665 #

AD-A190322 ..... N88-22638 #
AD-A190323 ..... N88-22666 #
AD-A190324 ..... N88-22667 #
AD-A190325 ..... N88-22668 #
AD-A190326 ..... N88-22669 #
AD-A190327 ..... N88-22670 #
AD-A190328 ..... N88-22671 #
AD-A190329 ..... N88-22639 #
AD-A190336 ..... N88-22036 #
AD-A190337 ..... N88-22534 #
AD-A190338 ..... N88-22279 #
AD-A190340 ..... N88-22182 #
AD-A190351 ..... N88-22535 #
AD-A190382 ..... N88-22578 #
AD-A190383 ..... N88-22597 #
AD-A190385 ..... N88-22449 #
AD-A190386 ..... N88-22579 #
AD-A190387 ..... N88-22640 #
AD-A190389 ..... N88-22607 #
AD-A190391 ..... N88-22720 #
AD-A190397 ..... N88-22672* #
AD-A190399 ..... N88-22183 #
AD-A190400 ..... N88-22378 #
AD-A190402 ..... N88-22689 #
AD-A190406 ..... N88-22121 #
AD-A190407 ..... N88-22151 #
AD-A190408 ..... N88-22025 #
AD-A190412 ..... N88-22184 #
AD-A190414 ..... N88-22827 #
AD-A190416 ..... N88-22308 #
AD-A190417 ..... N88-22791 #
AD-A190429 ..... N88-22690 #
AD-A190433 ..... N88-22309 #
AD-A190434 ..... N88-22185 #
AD-A190435 ..... N88-22026 #
AD-A190436 ..... N88-22598 #
AD-A190456 ..... N88-22495 #
AD-A190457 ..... N88-22186 #
AD-A190462 ..... N88-22450 #
AD-A190464 ..... N88-22477 #
AD-A190466 ..... N88-22451 #
AD-A190467 ..... N88-22730 #
AD-A190472 ..... N88-22261 #
AD-A190473 ..... N88-22353 #
AD-A190480 ..... N88-22091 #
AD-A190483 ..... N88-22580 #
AD-A190484 ..... N88-22043 #
AD-A190485 ..... N88-22122 #
AD-A190489 ..... N88-22641 #
AD-A190490 ..... N88-22008 #
AD-A190491 ..... N88-22673 #
AD-A190492 ..... N88-22152 #
AD-A190494 ..... N88-22280 #
AD-A190497 ..... N88-22027 #
AD-A190499 ..... N88-22608 #
AD-A190500 ..... N88-22816 #
AD-A190501 ..... N88-22187 #
AD-A190502 ..... N88-22581 #
AD-A190503 ..... N88-22310 #
AD-A190507 ..... N88-22478 #
AD-A190508 ..... N88-22528 #
AD-A190510 ..... N88-22379 #
AD-A190513 ..... N88-22756 #
AD-A190515 ..... N88-22281 #
AD-A190519 ..... N88-22282 #
AD-A190520 ..... N88-22041 #
AD-A190521 ..... N88-22642 #
AD-A190522 ..... N88-22311 #
AD-A190523 ..... N88-22188 #
AD-A190525 ..... N88-22123 #
AD-A190526 ..... N88-22312 #
AD-A190528 ..... N88-22529 #
AD-A190529 ..... N88-22530 #
AD-A190533 ..... N88-22124 #
AD-A190535 ..... N88-22153 #
AD-A190536 ..... N88-22068 #
AD-A190538 ..... N88-22691 #
AD-A190553 ..... N88-22643 #
AD-A190554 ..... N88-22609 #
AD-A190555 ..... N88-22694 #
AD-A190556 ..... N88-22313 #
AD-A190559 ..... N88-22644 #
AD-A190560 ..... N88-22283 #
AD-A190563 ..... N88-22674 #
AD-A190568 ..... N88-22044 #
AD-A190569 ..... N88-22284 #
AD-A190570 ..... N88-22582 #
AD-A190571 ..... N88-22599 #
AD-A190572 ..... N88-22314 #
AD-A190575 ..... N88-22792 #
AD-A190576 ..... N88-22496 #
AD-A190577 ..... N88-22645 #
AD-A190589 ..... N88-22479 #
AD-A190592 ..... N88-22051 #
AD-A190593 ..... N88-22583 #
AD-A190594 ..... N88-22028 #
AD-A190599 ..... N88-22380 #
AD-A190600 ..... N88-22497 #
AD-A190602 ..... N88-22285 #
AD-A190604 ..... N88-22029 #
AD-A190606 ..... N88-22315 #
AD-A190608 ..... N88-22262 #
AD-A190611 ..... N88-22069 #
AD-A190614 ..... N88-22042 #
AD-A190615 ..... N88-22316 #
AD-A190617 ..... N88-22092 #
AD-A190618 ..... N88-22584 #
AD-A190619 ..... N88-22263 #
AD-A190623 ..... N88-22496 #
AD-A190624 ..... N88-22154 #
AD-A190627 ..... N88-22317 #
AD-A190633 ..... N88-22551 #
AD-A190641 ..... N88-22538 #
AD-A190642 ..... N88-22531 #
AD-A190644 ..... N88-22070 #
AD-A190649 ..... N88-22093 #
AD-A190651 ..... N88-22707 #
AD-A190655 ..... N88-22125 #
AD-A190658 ..... N88-22155 #
AD-A190659 ..... N88-22335 #
AD-A190664 ..... N88-22126 #
AD-A190670 ..... N88-22539 #
AD-A190674 ..... N88-22030 #
AD-A190677 ..... N88-22318 #
AD-A190678 ..... N88-22600 #
AD-A190697 ..... N88-22203 #
AD-A190699 ..... N88-22156 #
AD-A190703 ..... N88-22189 #
AD-A190707 ..... N88-22078 #
AD-A190708 ..... N88-22190 #
AD-A190710 ..... N88-22127 #
AD-A190711 ..... N88-22610 #
AD-A190712 ..... N88-22191 #
AD-A190713 ..... N88-22793 #
AD-A190714 ..... N88-22381 #
AD-A190716 ..... N88-22354 #
AD-A190717 ..... N88-22831 #
AD-A190736 ..... N88-22817 #
AD-A190741 ..... N88-22794 #
AD-A190752 ..... N88-22128 #
AD-A190758 ..... N88-22319 #
AD-A190761 ..... N88-22071 #
AD-A190764 ..... N88-22708 #
AD-A190766 ..... N88-22675 #
AD-A190771 ..... N88-22079 #
AD-A190772 ..... N88-22320 #

AD-E500947 ..... N88-22535 #
AD-E801596 ..... N88-22449 #
AD-E801596 ..... N88-22578 #
AD-E801596 ..... N88-22579 #
AD-E801596 ..... N88-22597 #
AD-E801596 ..... N88-22607 #
AD-E801596 ..... N88-22640 #
AD-E801596 ..... N88-22729 #

AERE-R-12632 ..... N88-22081 #
AERE-R-12649 ..... N88-22760 #

AERONOMICA-ACTA-A-318-1987 ..... N88-22131 #
AERONOMICA-ACTA-A-319-1987 ..... N88-22759 #
AERONOMICA-ACTA-A-320-1987 ..... N88-22132 #

AFAL-TR-87-043 ..... N88-22201 #
AFAL-TR-87-061 ..... N88-22078 #
AFAL-TR-87-067 ..... N88-22756 #

AFATL-TR-87-32 ..... N88-22729 #

AFGL-TR-87-0114 ..... N88-22474 #
AFGL-TR-87-0253 ..... N88-22061 #
AFGL-TR-87-0262 ..... N88-22477 #
AFGL-TR-87-0270 ..... N88-22450 #
AFGL-TR-87-0271 ..... N88-22451 #
AFGL-TR-87-0299 ..... N88-22476 #
AFGL-TR-87-0327 ..... N88-22062 #

AFHRL-TP-87-49 ..... N88-22539 #

AFIT/CS/ENG/87-1 ..... N88-22825 #

AFIT/GA/AA/87D-8 ..... N88-22051 #
AFIT/GA/AA/87D-9 ..... N88-22076 #
AFIT/GA/AA/87D-10 ..... N88-22035 #
AFIT/GA/AA/88M-3 ..... N88-22092 #

AFIT/GAE/AA/87D-2 ..... N88-22310 #
AFIT/GAE/AA/87D-5 ..... N88-22064 #
AFIT/GAE/AA/87D-7 ..... N88-22816 #
AFIT/GAE/AA/87D-14 ..... N88-22146 #
AFIT/GAE/AA/87D-16 ..... N88-22374 #
AFIT/GAE/AA/87D-22 ..... N88-22077 #
AFIT/GAE/AA/87D-24 ..... N88-22089 #
AFIT/GAE/AA/87S-1 ..... N88-22027 #
AFIT/GAE/AA/87S-2 ..... N88-22039 #
AFIT/GAE/AA/88M-1 ..... N88-22316 #
AFIT/GAE/AA/88M-2 ..... N88-22314 #

AFIT/GCE/ENG/87-2 ..... N88-22600 #
AFIT/GCE/ENG/87D-4 ..... N88-22041 #
AFIT/GCE/ENG/87D-5 ..... N88-22580 #
AFIT/GCE/ENG/87D-6 ..... N88-22043 #
AFIT/GCE/ENG/87D-8 ..... N88-22599 #

AFIT/GCS/ENG/87D-11 ..... N88-22567 #
AFIT/GCS/ENG/87D-13 ..... N88-22581 #
AFIT/GCS/ENG/87D-28 ..... N88-22274 #

AFIT/GCS/MA/88M-02 ..... N88-22582 #

AFIT/GE/ENG/87D-3 ..... N88-22627 #
AFIT/GE/ENG/87D-5 ..... N88-22496 #
AFIT/GE/ENG/87D-18 ..... N88-22518 #
AFIT/GE/ENG/87D-28 ..... N88-22584 #
AFIT/GE/ENG/87D-31 ..... N88-22254 #
AFIT/GE/ENG/87D-33 ..... N88-22565 #
AFIT/GE/ENG/87D-36 ..... N88-22071 #
AFIT/GE/ENG/87D-37 ..... N88-22263 #
AFIT/GE/ENG/87D-40 ..... N88-22022 #
AFIT/GE/ENG/87D-50 ..... N88-22784 #
AFIT/GE/ENG/87D-65 ..... N88-22282 #
AFIT/GE/ENG/87D-66 ..... N88-22042 #
AFIT/GE/ENG/87D-69 ..... N88-22040 #
AFIT/GE/ENG/87D-73 ..... N88-22778 #
AFIT/GE/ENG/88M-3 ..... N88-22044 #
AFIT/GE/ENG/88M-6 ..... N88-22264 #

AFIT/GEP/ENP/87D-8 ..... N88-22777 #

AFIT/GEP/GNE/88M-4 ..... N88-22792 #

AFIT/GNE/ENG/88M-3 ..... N88-22645 #

AFIT/GSO/ENG/87D-1 ..... N88-22594 #

AFIT/GST/ENS/88M-5 ..... N88-22028 #
AFIT/GST/ENS/88M-9 ..... N88-22583 #

AFOSR-87-1013TR ..... N88-22664 #
AFOSR-87-1430TR ..... N88-22705 #
AFOSR-87-1636TR ..... N88-22520 #
AFOSR-87-1726TR ..... N88-22522 #
AFOSR-87-1729TR ..... N88-22630 #
AFOSR-87-1732TR ..... N88-22161 #
AFOSR-87-1734TR ..... N88-22378 #
AFOSR-87-1736TR ..... N88-22350 #
AFOSR-87-1737TR ..... N88-22576 #
AFOSR-87-1738TR ..... N88-22635 #
AFOSR-87-1739TR ..... N88-22278 #
AFOSR-87-1740TR ..... N88-22149 #
AFOSR-87-1742TR ..... N88-22782 #
AFOSR-87-1743TR ..... N88-22548 #
AFOSR-87-1745TR ..... N88-22606 #
AFOSR-87-1747TR ..... N88-22345 #
AFOSR-87-1752TR ..... N88-22260 #
AFOSR-87-1755TR ..... N88-22642 #
AFOSR-87-1756TR ..... N88-22610 #
AFOSR-87-1758TR-PT-1 ..... N88-22315 #
AFOSR-87-1759TR ..... N88-22755 #
AFOSR-87-1760TR ..... N88-22754 #
AFOSR-87-1761TR ..... N88-22311 #
AFOSR-87-1762TR ..... N88-22188 #
AFOSR-87-1763TR ..... N88-22036 #
AFOSR-87-1765TR ..... N88-22153 #
AFOSR-87-1766TR ..... N88-22123 #
AFOSR-87-1768TR ..... N88-22641 #
AFOSR-87-1769TR ..... N88-22691 #
AFOSR-87-1770TR ..... N88-22312 #
AFOSR-87-1772TR ..... N88-22529 #
AFOSR-87-1773TR ..... N88-22530 #
AFOSR-87-1775TR ..... N88-22534 #
AFOSR-87-1777TR ..... N88-22069 #
AFOSR-87-1779TR ..... N88-22008 #
AFOSR-87-1780TR ..... N88-22093 #
AFOSR-87-1781TR ..... N88-22478 #
AFOSR-87-1781TR ..... N88-22524 #
AFOSR-87-1785TR ..... N88-22124 #
AFOSR-87-1788TR ..... N88-22302 #
AFOSR-87-1789TR ..... N88-22533 #
AFOSR-87-1795TR ..... N88-22684 #
AFOSR-87-1796TR ..... N88-22349 #
AFOSR-87-1799TR ..... N88-22361 #
AFOSR-87-1802TR ..... N88-22726 #
AFOSR-87-1817TR ..... N88-22637 #
AFOSR-87-1828TR ..... N88-22628 #
AFOSR-87-1829TR ..... N88-22752 #
AFOSR-87-1830TR ..... N88-22122 #
AFOSR-87-1845TR ..... N88-22626 #

AFOSR-87-1846TR ..... N88-22605 #
AFOSR-87-1847TR ..... N88-22629 #
AFOSR-87-1848TR ..... N88-22659 #
AFOSR-87-1851TR ..... N88-22666 #
AFOSR-87-1852TR ..... N88-22657 #
AFOSR-87-1853TR ..... N88-22116 #
AFOSR-87-1854TR ..... N88-22183 #
AFOSR-87-1860TR ..... N88-22724 #
AFOSR-87-1876TR ..... N88-22668 #
AFOSR-87-1878TR ..... N88-22636 #
AFOSR-87-1880TR ..... N88-22788 #
AFOSR-87-1883TR ..... N88-22751 #
AFOSR-87-1889TR ..... N88-22120 #
AFOSR-87-1890TR ..... N88-22117 #
AFOSR-87-1891TR ..... N88-22689 #
AFOSR-87-1896TR ..... N88-22348 #
AFOSR-87-1897TR ..... N88-22791 #
AFOSR-87-1899TR ..... N88-22115 #
AFOSR-87-1902TR ..... N88-22083 #
AFOSR-87-1903TR ..... N88-22007 #
AFOSR-87-1910TR-PT-2 ..... N88-22305 #
AFOSR-87-1912TR ..... N88-22700 #
AFOSR-87-1914TR ..... N88-22677 #
AFOSR-87-1928TR ..... N88-22346 #
AFOSR-87-1930TR ..... N88-22656 #
AFOSR-87-1931TR ..... N88-22523 #
AFOSR-87-1939TR ..... N88-22658 #
AFOSR-87-1955TR ..... N88-22667 #
AFOSR-87-1958TR ..... N88-22596 #
AFOSR-87-1959TR ..... N88-22669 #
AFOSR-87-1960TR ..... N88-22670 #
AFOSR-87-1961TR ..... N88-22671 #
AFOSR-87-1962TR ..... N88-22026 #
AFOSR-87-1966TR ..... N88-22549 #
AFOSR-87-1967TR ..... N88-22661 #
AFOSR-87-1968TR ..... N88-22551 #
AFOSR-87-1980TR ..... N88-22662 #
AFOSR-87-1995TR ..... N88-22790 #
AFOSR-87-2007TR ..... N88-22381 #
AFOSR-87-2008TR ..... N88-22070 #
AFOSR-87-2009TR-PT-2 ..... N88-22307 #
AFOSR-87-2011TR ..... N88-22190 #
AFOSR-87-2012TR ..... N88-22753 #
AFOSR-87-2015TR ..... N88-22674 #
AFOSR-87-2016TR ..... N88-22673 #
AFOSR-87-2034TR ..... N88-22068 #
AFOSR-87-2039TR ..... N88-22634 #
AFOSR-87-2040TR ..... N88-22152 #
AFOSR-87-2041TR ..... N88-22191 #
AFOSR-87-2042TR ..... N88-22279 #
AFOSR-87-2043TR ..... N88-22354 #
AFOSR-87-2044TR ..... N88-22789 #
AFOSR-88-0033TR ..... N88-22275 #
AFOSR-88-0055TR ..... N88-22145 #
AFOSR-88-0056TR ..... N88-22794 #
AFOSR-88-0062TR ..... N88-22066 #
AFOSR-88-0095TR ..... N88-22730 #
AFOSR-88-0129TR ..... N88-22088 #
AFOSR-88-0146TR ..... N88-22632 #
AFOSR-88-0148TR ..... N88-22550 #
AFOSR-88-0149TR ..... N88-22633 #
AFOSR-88-0158TR ..... N88-22125 #
AFOSR-88-0161TR ..... N88-22786 #
AFOSR-88-0162TR ..... N88-22725 #
AFOSR-88-0164TR ..... N88-22375 #
AFOSR-88-0166TR ..... N88-22718 #
AFOSR-88-0167TR ..... N88-22119 #
AFOSR-88-0168TR ..... N88-22118 #
AFOSR-88-0170TR ..... N88-22128 #
AFOSR-88-0172TR ..... N88-22573 #
AFOSR-88-0173TR ..... N88-22065 #
AFOSR-88-0174TR ..... N88-22631 #
AFOSR-88-0193TR ..... N88-22779 #
AFOSR-88-0194TR ..... N88-22090 #

AFWAL-TR-86-1160 ..... N88-22262 #
AFWAL-TR-86-2073 ..... N88-22276 #
AFWAL-TR-87-1167 ..... N88-22761 #
AFWAL-TR-87-2060-VOL-2 ..... N88-22025 #
AFWAL-TR-87-2070 ..... N88-22460 #
AFWAL-TR-87-4079 ..... N88-22359 #
AFWAL-TR-87-4093 ..... N88-22179 #
AFWAL-TR-87-4130 ..... N88-22379 #

AFWL-TR-85-57 ..... N88-22126 #

AI-M-951 ..... N88-22313 #
AI-M-966 ..... N88-22283 #
AI-M-973 ..... N88-22607 #
AI-M-989 ..... N88-22694 #
AI-M-994 ..... N88-22449 #
AI-M-996 ..... N88-22640 #
AI-M-999 ..... N88-22644 #
AI-M-1008 ..... N88-22579 #

AI-TR-968 ..... N88-22609 #
AI-TR-979 ..... N88-22643 #

AIAA-88-2216 ..... N88-22050* #
AIAA-88-2963 ..... N88-22037* #

ALGO-PUB-0097 ..... N88-22575* #

ANL/MCS-TM-107 ..... N88-22646 #

ARCCB-MR-87036 ..... N88-22055 #

ARCCB-TR-87034 ..... N88-22148 #
ARCCB-TR-87037 ..... N88-22636 #

ARFSD-TR-87010 ..... N88-22285 #

ARL/PSU/TR-87-013 ..... N88-22318 #
ARL/PSU/TR-87-014 ..... N88-22309 #

ARO-20010.5-MS ..... N88-22781 #
ARO-20815.7-EG ..... N88-22304 #
ARO-21015.4-PH ..... N88-22783 #
ARO-21397.2-EG ..... N88-22200 #
ARO-21530.1-MS ..... N88-22136 #
ARO-23975.3-PH ..... N88-22783 #

ASIAC-887.1A ..... N88-22823 #

AVSCOM-TM-88-B-006 ..... N88-22015* #
AVSCOM-TM-88-B-010 ..... N88-22434* #

AVSCOM-TR-87-B-3 ..... N88-22710* #

BARC-1344 ..... N88-22106 #
BARC-1346 ..... N88-22370 #
BARC-1347 ..... N88-22471 #
BARC-1348 ..... N88-22472 #
BARC-1349 ..... N88-22554 #
BARC-1367 ..... N88-22555 #
BARC-1369 ..... N88-22558 #
BARC-1372 ..... N88-22750 #
BARC-1374 ..... N88-22559 #
BARC-1376 ..... N88-22776 #

BDX-613-3804 ..... N88-22170 #

BER-424-17 ..... N88-22602* #

BNL-40744 ..... N88-22109 #
BNL-40757 ..... N88-22802 #
BNL-40762 ..... N88-22108 #

BRDEC-2460 ..... N88-22155 #

BRL-IMR-886 ..... N88-22319 #

BRL-TR-2813 ..... N88-22319 #
BRL-TR-2856 ..... N88-22335 #
BRL-TR-2861 ..... N88-22303 #
BRL-TR-2863 ..... N88-22376 #

B8731726 ..... N88-22017 #
B8733100 ..... N88-22369 #

CERL-TR-E-88/03 ..... N88-22280 #

CERL-TR-N-88/01 ..... N88-22824 #

CESAR-88/06 ..... N88-22614 #

CMU-CS-87-106 ..... N88-22761 #

CNES-CT/DRT/TIT/AN-249-T ..... N88-22266 #

CNES-CT/DRT/TIT/RL-143-T ..... N88-22267 #

CNES-CT/DRT/TIT/TR-122-T ..... N88-22268 #

CNES-NT-120 ..... N88-22074 #

CNIC-00047 ..... N88-22615 #

CONF-870102-32 ..... N88-22719 #
CONF-870422-11 ..... N88-22769 #
CONF-870691-11 ..... N88-22699 #
CONF-870797-13 ..... N88-22844 #
CONF-870799-5 ..... N88-22775 #
CONF-870856-4 ..... N88-22328 #
CONF-870873-26 ..... N88-22799 #
CONF-870878-5 ..... N88-22198 #
CONF-870955-3 ..... N88-22796 #
CONF-870955-4 ..... N88-22765 #
CONF-871007-86 ..... N88-22740 #
CONF-871007-88 ..... N88-22757 #
CONF-871007-90 ..... N88-22741 #
CONF-871027-45 ..... N88-22158 #
CONF-871036-10 ..... N88-22692 #
CONF-871065-2 ..... N88-22288 #
CONF-871124-80 ..... N88-22772 #
CONF-871124-85 ..... N88-22802 #
CONF-871124-89 ..... N88-22801 #
CONF-871124-92 ..... N88-22767 #
CONF-871124-93 ..... N88-22114 #
CONF-871125-22 ..... N88-22144 #
CONF-871126-11 ..... N88-22766 #
CONF-871167-2 ..... N88-22798 #
CONF-871189-2 ..... N88-22085 #
CONF-871204-4 ..... N88-22485 #
CONF-871234-13 ..... N88-22107 #
CONF-871254-4 ..... N88-22339 #
CONF-871254-5-PT-1 ..... N88-22355 #
CONF-871254-6 ..... N88-22340 #
CONF-871266-1 ..... N88-22773 #
CONF-871273-1 ..... N88-22771 #
CONF-880110-22 ..... N88-22764 #
CONF-880117-1 ..... N88-22586 #
CONF-880118-2 ..... N88-22095 #
CONF-880160-3 ..... N88-22373 #
CONF-880163-1-VUGRAPHS ..... N88-22742 #
CONF-880164-1 ..... N88-22341 #
CONF-880212-4 ..... N88-22483 #
CONF-880314-2 ..... N88-22159 #
CONF-880358-1 ..... N88-22162 #
CONF-880408-2 ..... N88-22199 #
CONF-880420-1 ..... N88-22461 #
CONF-880424-2 ..... N88-22556 #
CONF-880424-3 ..... N88-22611 #
CONF-880424-4 ..... N88-22360 #
CONF-880424-8 ..... N88-22363 #
CONF-880424-9 ..... N88-22433 #
CONF-880438-1 ..... N88-22362 #
CONF-880438-2 ..... N88-22292 #
CONF-880438-3 ..... N88-22372 #
CONF-880438-5 ..... N88-22440 #
CONF-880445-1 ..... N88-22170 #
CONF-880455-3 ..... N88-22612 #
CONF-880455-4 ..... N88-22613 #
CONF-880456-1 ..... N88-22542 #
CONF-880457-1 ..... N88-22462 #
CONF-880457-2 ..... N88-22075 #
CONF-880458-1 ..... N88-22628 #
CONF-880461-1 ..... N88-22046 #
CONF-880462-1 ..... N88-22601 #
CONF-880462-2 ..... N88-22614 #
CONF-880462-3 ..... N88-22480 #
CONF-880468-1 ..... N88-22464 #
CONF-880469-1 ..... N88-22432 #
CONF-880473-1 ..... N88-22206 #
CONF-880475-1 ..... N88-22192 #
CONF-880478-1 ..... N88-22057 #
CONF-880478-3 ..... N88-22056 #
CONF-880478-4 ..... N88-22058 #
CONF-8704270-1 ..... N88-22173 #
CONF-8704271-1 ..... N88-22172 #
CONF-8705226-4 ..... N88-22768 #
CONF-8706103-7 ..... N88-22797 #
CONF-8706130-4 ..... N88-22621 #
CONF-8706187-1 ..... N88-22327 #
CONF-8706254-1 ..... N88-22458* #
CONF-8706274-1 ..... N88-22731 #
CONF-8706276-1 ..... N88-22171 #
CONF-8706277-1 ..... N88-22109 #
CONF-8707141-4 ..... N88-22842 #
CONF-8707147-SUMM ..... N88-22504 #
CONF-8708104-7 ..... N88-22803 #
CONF-8708110-32 ..... N88-22800 #
CONF-8708180-8 ..... N88-22108 #
CONF-8708213-2 ..... N88-22086 #
CONF-8708213-3 ..... N88-22437 #
CONF-8708220-1 ..... N88-22646 #
CONF-8709162-SUMM ..... N88-22499 #
CONF-8709178-1 ..... N88-22356 #
CONF-8709239-1 ..... N88-22082 #
CONF-8709248-1 ..... N88-22293 #
CONF-8710116-6 ..... N88-22169 #
CONF-8710116-7 ..... N88-22205 #
CONF-8710165-10 ..... N88-22175 #
CONF-8710216-3 ..... N88-22084 #
CONF-8710241-11 ..... N88-22063 #
CONF-8710253-1 ..... N88-22094 #
CONF-8710288-1 ..... N88-22157 #
CONF-8711114-5 ..... N88-22770 #
CONF-8711149-1 ..... N88-22513 #
CONF-8711157-1 ..... N88-22795 #

CRC-TR-87-13 ..... N88-22574 #

CRDEC-CR-88005 ..... N88-22723 #
CRDEC-CR-88039 ..... N88-22497 #

CRM-87-111 ..... N88-22367 #
CRM-87-161 ..... N88-22660 #

CRREL-SR-87-24 ..... N88-22380 #

CRREL-87-21 ..... N88-22494 #
CRREL-87-22 ..... N88-22297 #

CSL-TN-87-331 ..... N88-22574 #

DC-101 ..... N88-22606 #

DE87-013652 ..... N88-22611 #
DE87-013877 ..... N88-22360 #
DE87-014645 ..... N88-22461 #
DE87-702957 ..... N88-22735 #
DE87-702962 ..... N88-22291 #
DE87-703027 ..... N88-22838 #
DE87-703032 ..... N88-22616 #
DE87-703033 ..... N88-22808 #
DE87-703034 ..... N88-22839 #
DE87-703036 ..... N88-22840 #
DE87-703040 ..... N88-22617 #
DE88-000343 ..... N88-22556 #
DE88-000730 ..... N88-22356 #
DE88-001131 ..... N88-22371 #
DE88-002092 ..... N88-22362 #
DE88-002364 ..... N88-22170 #
DE88-002612 ..... N88-22046 #
DE88-003001 ..... N88-22372 #
DE88-003153 ..... N88-22456* #
DE88-003204 ..... N88-22292 #
DE88-003761 ..... N88-22828 #
DE88-003812 ..... N88-22204 #
DE88-003948 ..... N88-22462 #
DE88-004199 ..... N88-22075 #
DE88-004295 ..... N88-22612 #
DE88-004296 ..... N88-22613 #
DE88-004307 ..... N88-22463 #
DE88-004310 ..... N88-22542 #
DE88-004560 ..... N88-22063 #
DE88-004915 ..... N88-22516 #
DE88-005059 ..... N88-22465 #
DE88-005064 ..... N88-22205 #
DE88-005157 ..... N88-22094 #
DE88-005171 ..... N88-22171 #
DE88-005268 ..... N88-22601 #
DE88-005373 ..... N88-22341 #
DE88-005380 ..... N88-22464 #
DE88-005433 ..... N88-22795 #
DE88-005474 ..... N88-22084 #
DE88-005475 ..... N88-22432 #
DE88-005530 ..... N88-22504 #
DE88-005548 ..... N88-22172 #
DE88-005620 ..... N88-22764 #
DE88-005621 ..... N88-22157 #
DE88-005624 ..... N88-22731 #
DE88-005627 ..... N88-22513 #
DE88-005633 ..... N88-22740 #
DE88-005705 ..... N88-22842 #
DE88-005715 ..... N88-22433 #
DE88-005718 ..... N88-22363 #
DE88-005732 ..... N88-22158 #
DE88-005829 ..... N88-22646 #
DE88-005842 ..... N88-22169 #
DE88-005844 ..... N88-22173 #
DE88-005850 ..... N88-22614 #
DE88-005904 ..... N88-22769 #
DE88-005905 ..... N88-22065 #
DE88-005906 ..... N88-22514 #
DE88-005910 ..... N88-22159 #
DE88-005912 ..... N88-22692 #
DE88-005913 ..... N88-22796 #
DE88-005918 ..... N88-22765 #
DE88-005936 ..... N88-22797 #
DE88-005937 ..... N88-22699 #
DE88-005947 ..... N88-22741 #
DE88-005971 ..... N88-22766 #
DE88-005976 ..... N88-22770 #
DE88-005988 ..... N88-22771 #
DE88-005989 ..... N88-22798 #
DE88-005993 ..... N88-22107 #
DE88-005999 ..... N88-22767 #
DE88-006010 ..... N88-22768 #
DE88-006026 ..... N88-22473 #
DE88-006055 ..... N88-22757 #
DE88-006066 ..... N88-22505 #
DE88-006074 ..... N88-22799 #
DE88-006183 ..... N88-22742 #
DE88-006197 ..... N88-22192 #
DE88-006199 ..... N88-22373 #
DE88-006201 ..... N88-22206 #
DE88-006209 ..... N88-22323 #
DE88-006234 ..... N88-22800 #
DE88-006261 ..... N88-22743 #
DE88-006318 ..... N88-22772 #
DE88-006332 ..... N88-22801 #
DE88-006334 ..... N88-22715 #
DE88-006340 ..... N88-22773 #
DE88-006341 ..... N88-22082 #
DE88-006355 ..... N88-22108 #
DE88-006356 ..... N88-22109 #
DE88-006367 ..... N88-22802 #
DE88-006377 ..... N88-22695 #
DE88-006382 ..... N88-22286 #
DE88-006411 ..... N88-22480 #
DE88-006421 ..... N88-22557 #
DE88-006423 ..... N88-22618 #
DE88-006424 ..... N88-22623 #
DE88-006425 ..... N88-22619 #
DE88-006426 ..... N88-22585 #
DE88-006427 ..... N88-22620 #
DE88-006428 ..... N88-22679 #
DE88-006429 ..... N88-22680 #
DE88-006448 ..... N88-22339 #
DE88-006452 ..... N88-22803 #
DE88-006455 ..... N88-22095 #
DE88-006460 ..... N88-22340 #
DE88-006478 ..... N88-22355 #
DE88-006479 ..... N88-22621 #
DE88-006491 ..... N88-22774 #
DE88-006495 ..... N88-22716 #
DE88-006533 ..... N88-22174 #
DE88-006536 ..... N88-22112 #
DE88-006537 ..... N88-22811 #
DE88-006538 ..... N88-22682 #
DE88-006541 ..... N88-22110 #
DE88-006567 ..... N88-22193 #
DE88-006607 ..... N88-22499 #
DE88-006616 ..... N88-22334 #
DE88-006620 ..... N88-22287 #
DE88-006622 ..... N88-22775 #
DE88-006625 ..... N88-22141 #
DE88-006626 ..... N88-22467 #
DE88-006627 ..... N88-22142 #
DE88-006632 ..... N88-22592 #
DE88-006634 ..... N88-22622 #
DE88-006647 ..... N88-22440 #
DE88-006671 ..... N88-22198 #
DE88-006681 ..... N88-22160 #
DE88-006685 ..... N88-22324 #
DE88-006699 ..... N88-22327 #
DE88-006705 ..... N88-22251 #
DE88-006722 ..... N88-22732 #
DE88-006724 ..... N88-22733 #
DE88-006731 ..... N88-22328 #
DE88-006733 ..... N88-22162 #
DE88-006740 ..... N88-22293 #
DE88-006745 ..... N88-22271 #
DE88-006753 ..... N88-22268 #
DE88-006763 ..... N88-22719 #
DE88-006765 ..... N88-22437 #
DE88-006772 ..... N88-22086 #
DE88-006780 ..... N88-22586 #
DE88-006788 ..... N88-22143 #
DE88-006800 ..... N88-22272 #
DE88-006802 ..... N88-22144 #
DE88-006809 ..... N88-22175 #
DE88-006841 ..... N88-22056 #
DE88-006842 ..... N88-22057 #
DE88-006857 ..... N88-22289 #
DE88-006860 ..... N88-22113 #
DE88-006870 ..... N88-22114 #
DE88-006897 ..... N88-22459 #
DE88-006913 ..... N88-22749 #
DE88-006920 ..... N88-22744 #
DE88-006926 ..... N88-22457 #
DE88-006942 ..... N88-22745 #
DE88-006992 ..... N88-22809 #
DE88-006994 ..... N88-22841 #
DE88-006996 ..... N88-22812 #
DE88-006998 ..... N88-22844 #
DE88-007003 ..... N88-22603 #
DE88-007018 ..... N88-22342 #
DE88-007033 ..... N88-22343 #
DE88-007036 ..... N88-22058 #
DE88-007039 ..... N88-22199 #
DE88-007083 ..... N88-22176 #
DE88-007137 ..... N88-22481 #
DE88-700958 ..... N88-22615 #
DE88-700974 ..... N88-22209 #
DE88-701109 ..... N88-22270 #
DE88-701224 ..... N88-22139 #
DE88-701229 ..... N88-22106 #
DE88-701231 ..... N88-22370 #
DE88-701232 ..... N88-22471 #
DE88-701233 ..... N88-22472 #
DE88-701234 ..... N88-22554 #
DE88-701248 ..... N88-22555 #
DE88-701289 ..... N88-22736 #
DE88-701410 ..... N88-22558 #
DE88-701413 ..... N88-22559 #
DE88-701414 ..... N88-22776 #
DE88-701525 ..... N88-22344 #
DE88-752299 ..... N88-22681 #
DE88-752300 ..... N88-22810 #
DE88-752301 ..... N88-22111 #
DE88-752302 ..... N88-22140 #
DE88-752312 ..... N88-22746 #
DE88-752339 ..... N88-22747 #

DFVLR-FB-87-44 ..... N88-22330 #

DOE/CE-0189 ..... N88-22459 #

DOE/ER-13382/T1 ..... N88-22695 #
DOE/ER-13439/3 ..... N88-22112 #
DOE/ER-13507/2 ..... N88-22174 #
DOE/ER-13544/T1 ..... N88-22110 #
DOE/ER-13560/2 ..... N88-22176 #
DOE/ER-13695 ..... N88-22113 #
DOE/ER-13744/2 ..... N88-22716 #
DOE/ER-25015/2 ..... N88-22557 #
DOE/ER-25015/3 ..... N88-22680 #
DOE/ER-25015/4 ..... N88-22679 #
DOE/ER-25015/5 ..... N88-22620 #
DOE/ER-25015/6 ..... N88-22585 #
DOE/ER-25015/7 ..... N88-22619 #
DOE/ER-25015/8 ..... N88-22623 #
DOE/ER-25015/9 ..... N88-22618 #
DOE/ER-25018/2 ..... N88-22622 #
DOE/ER-25026/18 ..... N88-22592 #
DOE/ER-40200/126 ..... N88-22811 #
DOE/ER-40200/127 ..... N88-22682 #
DOE/ER-40374/4-PT-2 ..... N88-22774 #
DOE/ER-45117/3 ..... N88-22193 #
DOE/ER-45173/4 ..... N88-22160 #
DOE/ER-45310/6 ..... N88-22142 #
DOE/ER-53198/117 ..... N88-22745 #
DOE/ER-53206/10 ..... N88-22749 #
DOE/ER-60261/3 ..... N88-22514 #
DOE/ER-60285/T1 ..... N88-22505 #
DOE/ER-60344/1 ..... N88-22516 #

DOE/ET-51013/242 ..... N88-22743 #
DOE/ET-53088/309 ..... N88-22251 #

DOE/PC-90009/3 ..... N88-22204 #
DOE/PC-90962/T5 ..... N88-22323 #

DOE/PE-0079 ..... N88-22473 #

DOT-HS-807-158-VOL-2 ..... N88-22536 #

DOT-TSC-FAA-87-5 ..... N88-22003 #

DOT-TSC-NHTSA-86-6-VOL-2 ..... N88-22536 #

DOT/FAA/AM-88/1 ..... N88-22538 #
DOT/FAA/AM-88/2 ..... N88-22531 #

DOT/FAA/CT-87/13 ..... N88-22024 #

DP-MS-87-132 ..... N88-22828 #

DR-3 ..... N88-22060* #

DREO-968 ..... N88-22528 #

DTIC/TR-88/5 ..... N88-22822 #

D180-30344-2-VOL-2 ..... N88-22025 #

E-3740 ..... N88-22851* #
E-3920 ..... N88-22446* #
E-3970-VOL-2 ..... N88-22382* #
E-3970-VOL-3 ..... N88-22408* #
E-4010 ..... N88-22591* #
E-4040 ..... N88-22652* #
E-4056 ..... N88-22080* #
E-4069 ..... N88-22805* #
E-4099 ..... N88-22019* #
E-4118 ..... N88-22168* #
E-4120 ..... N88-22037* #

EFI-935(86)-86 ..... N88-22734 #
EFI-937(88)-86 ..... N88-22209 #

EGG-EP-7780 ..... N88-22272 #
EGG-EP-7946 ..... N88-22271 #

EGG-M-02087 ..... N88-22086 #
EGG-M-02287 ..... N88-22437 #
EGG-M-04787 ..... N88-22268 #
EGG-M-08086 ..... N88-22172 #
EGG-M-08687 ..... N88-22328 #
EGG-M-12587 ..... N88-22162 #
EGG-M-25786 ..... N88-22719 #
EGG-M-26787 ..... N88-22293 #
EGG-M-33387 ..... N88-22740 #

EGG-SCM-7219 ..... N88-22143 #

EL-61 ..... N88-22649 #
EL-891 ..... N88-22364 #

ENST-87C004 ..... N88-22586 #
ENST-87D005 ..... N88-22589 #

EPA-600/D-87-366 ..... N88-22448 #
EPA-600/4-87-044 ..... N88-22517 #

ERIM-175900-12-F ..... N88-22730 #

ESL-718048-6 ..... N88-22259 #

ETN-87-98751 ..... N88-22326* #
ETN-88-91803 ..... N88-22054
ETN-88-91871 ..... N88-22714 #
ETN-88-91886 ..... N88-22290 #
ETN-88-91989 ..... N88-22073 #
ETN-88-91990 ..... N88-22103 #
ETN-88-91991 ..... N88-22163 #
ETN-88-91992 ..... N88-22164 #
ETN-88-92007 ..... N88-22696 #
ETN-88-92014 ..... N88-22587 #
ETN-88-92015 ..... N88-22712 #
ETN-88-92016 ..... N88-22338 #
ETN-88-92018 ..... N88-22713 #
ETN-88-92024 ..... N88-22266 #
ETN-88-92026 ..... N88-22074 #
ETN-88-92030 ..... N88-22267 #
ETN-88-92031 ..... N88-22268 #
ETN-88-92076 ..... N88-22560
ETN-88-92083 ..... N88-22487 #
ETN-88-92086 ..... N88-22836
ETN-88-92101 ..... N88-22441 #
ETN-88-92104 ..... N88-22329 #
ETN-88-92108 ..... N88-22466 #
ETN-88-92113 ..... N88-22330 #
ETN-88-92172 ..... N88-22588 #
ETN-88-92175 ..... N88-22589 #
ETN-88-92197 ..... N88-22488 #
ETN-88-92198 ..... N88-22442 #
ETN-88-92199 ..... N88-22032 #
ETN-88-92206 ..... N88-22269 #
ETN-88-92210 ..... N88-22131 #
ETN-88-92211 ..... N88-22759 #
ETN-88-92212 ..... N88-22132 #
ETN-88-92213 ..... N88-22368 #
ETN-88-92214 ..... N88-22443 #
ETN-88-92215 ..... N88-22444 #
ETN-88-92216 ..... N88-22165 #
ETN-88-92217 ..... N88-22166 #
ETN-88-92218 ..... N88-22167 #
ETN-88-92219 ..... N88-22649 #
ETN-88-92220 ..... N88-22358 #
ETN-88-92223 ..... N88-22369 #
ETN-88-92225 ..... N88-22017 #
ETN-88-92229 ..... N88-22532 #
ETN-88-92230 ..... N88-22697 #
ETN-88-92269 ..... N88-22717 #
ETN-88-92270 ..... N88-22683 #
ETN-88-92271 ..... N88-22655
ETN-88-92272 ..... N88-22561
ETN-88-92273 ..... N88-22562
ETN-88-92274 ..... N88-22821 #
ETN-88-92278 ..... N88-22624 #
ETN-88-92279 ..... N88-22563 #
ETN-88-92281 ..... N88-22273 #
ETN-88-92284 ..... N88-22593 #
ETN-88-92285 ..... N88-22545 #
ETN-88-92286 ..... N88-22564 #

FAA-MS-87-5 ..... N88-22003 #

FEI-1820 ..... N88-22294 #

FFA-TN-1987-45 ..... N88-22442 #
FFA-TN-1987-48 ..... N88-22032 #

FLOW-RR-431 ..... N88-22006 #

FNAL/C-87/206-A ..... N88-22842 #
FNAL/C-87/228-A ..... N88-22844 #

FNAL/PUB-87/209-A ..... N88-22812 #
FNAL/PUB-87/215-A ..... N88-22841 #
FNAL/PUB-88/18-A ..... N88-22809 #

FOA-C-30473-3.3 ..... N88-22269 #

FTD-ID(RS)T-0004-88 ..... N88-22498 #
FTD-ID(RS)T-1042-87 ..... N88-22004 #
FTD-ID(RS)T-1334-87 ..... N88-22317 #
FTD-ID(RS)T-1384-87 ..... N88-22154 #

FUB-6-1986 ..... N88-22714 #

FVI-87-07 ..... N88-22648 #
FVI-87-09 ..... N88-22647 #

GALCIT-SM-87-19 ..... N88-22098* #

GAO/NSIAD-88-30BR ..... N88-22059 #

GRI-88/0003 ..... N88-22105 #

H-1439 ..... N88-22033* #
H-1454 ..... N88-22050* #

HL87/1155 ..... N88-22081 #
HL87/1163 ..... N88-22760 #

IA-1422 ..... N88-22737 #
IA-1424 ..... N88-22738 #
IA-1428 ..... N88-22763 #
IA-1432-PT-2 ..... N88-22736 #

IADBL/3 ..... N88-22350 #

IAE-4324/11 ..... N88-22762 #
IAE-4376/11 ..... N88-22138 #

IAEA-TECDOC-445 ..... N88-22720 #

IAPCM-0004 ..... N88-22615 #

ICASE-88-23 ..... N88-22541* #

ICOMP-88-4 ..... N88-22591* #
ICOMP-88-6 ..... N88-22652* #

IFSR-309 ..... N88-22251 #

INPE-4011-TDL/240 ..... N88-22456 #
INPE-4046-PRE/1012-REV-3 ..... N88-22483 #
INPE-4253-PRE/1126 ..... N88-22357 #
INPE-4254-PRE/1127 ..... N88-22804 #
INPE-4346-PRE/1183 ..... N88-22832 #
INPE-4405-RPE/556 ..... N88-22053 #
INPE-4419-TDL/307 ..... N88-22819 #
INPE-4445-TDL/313 ..... N88-22501 #
INPE-4456-PRE/1287 ..... N88-22833 #
INPE-4459-PRE/1238 ..... N88-22453 #
INPE-4465-TDL/321 ..... N88-22590 #
INPE-4485-PRE/1250 ..... N88-22489 #
INPE-4486-PRE/1251 ..... N88-22468 #
INPE-4487-TDL/325 ..... N88-22486 #
INPE-4488-PRE/1252 ..... N88-22482 #
INPE-4490-PRE/1254 ..... N88-22829 #
INPE-4491-PRE/1255 ..... N88-22454 #
INPE-4493-PRE/1257 ..... N88-22485 #
INPE-4500-RPE/563 ..... N88-22455 #
INPE-4501-PRE/1258 ..... N88-22469 #
INPE-4506-PRE/1261-REV ..... N88-22502 #
INPE-4509-PRE/1263 ..... N88-22758 #
INPE-4523-PRE/1275 ..... N88-22484 #
INPE-4526-PRE/1276 ..... N88-22848 #
INPE-4527-PRE/1277 ..... N88-22845 #
INPE-4528-PRE/1278 ..... N88-22835 #
INPE-4529-PRE/1279 ..... N88-22850 #
INPE-4533-NTE/279 ..... N88-22820 #

IRF-PREPRINT-103 ..... N88-22488 #

IRL87-0001 ..... N88-22693 #

ISBN-2-85-428166-7 ..... N88-22054
ISBN-9-51-382645-7 ..... N88-22444 #
ISBN-9-51-382912-X ..... N88-22368 #
ISBN-9-51-382988-X ..... N88-22443 #
ISBN-9-51-666253-6 ..... N88-22649 #
ISBN-9-51-754289-5 ..... N88-22165 #
ISBN-90-71382-19-2 ..... N88-22436 #
ISBN-91-7848-060-4 ..... N88-22195 #
ISBN-91-7848-062-0 ..... N88-22129 #

ISFM-87-148 ..... N88-22377 #

ISL-CO-242/86 ..... N88-22338 #
ISL-CO-247/86 ..... N88-22713 #

ISL-R-114/86 ..... N88-22587 #
ISL-R-121/86 ..... N88-22712 #

ISSN-0001-6845 ..... N88-22649 #
ISSN-0038-0911 ..... N88-22849 #
ISSN-0065-3713 ..... N88-22131 #
ISSN-0065-3713 ..... N88-22132 #
ISSN-0065-3713 ..... N88-22759 #
ISSN-0143-7313 ..... N88-22560
ISSN-0171-1342 ..... N88-22330 #
ISSN-0284-1711 ..... N88-22488 #
ISSN-0347-3708 ..... N88-22269 #
ISSN-0358-5077 ..... N88-22368 #
ISSN-0358-5077 ..... N88-22443 #
ISSN-0358-5077 ..... N88-22444 #
ISSN-0366-9106 ..... N88-22364 #
ISSN-0751-1337 ..... N88-22588 #
ISSN-0751-1345 ..... N88-22589 #
ISSN-0784-3577 ..... N88-22165 #

ITEF-4(1987) ..... N88-22332 #
ITEF-12(1987) ..... N88-22333 #
ITEF-15(1987) ..... N88-22470 #
ITEF-24(1987) ..... N88-22270 #
ITEF-59(1987) ..... N88-22543 #
ITEF-156(1987) ..... N88-22544 #

ITEP-57(1987) ..... N88-22837 #

JAERI-M-86-176 ..... N88-22735 #
JAERI-M-87-007 ..... N88-22291 #
JAERI-M-87-152 ..... N88-22140 #
JAERI-M-87-180 ..... N88-22747 #

JIAA-TR-84 ..... N88-22045* #

JINR-E-2-87-279 ..... N88-22813 #
JINR-E-2-87-368 ..... N88-22814 #

JINR-R-2-86-323 ..... N88-22806 #
JINR-R-2-86-830 ..... N88-22807 #
JINR-R-2-87-363 ..... N88-22815 #
JINR-R-4-86-696 ..... N88-22678 #
JINR-R-17-87-128 ..... N88-22739 #

JPL-D-462 ..... N88-22672* #
JPL-D-4624 ..... N88-22575* #

JPRS-CST-87-043 ..... N88-22233 #

JPRS-JST-87-029 ..... N88-22228 #
JPRS-JST-88-001 ..... N88-22218 #
JPRS-JST-88-002 ..... N88-22210 #

K/ETAC-51 ..... N88-22289 #

KEK-87-6 ..... N88-22111 #

KIYI-86-17 ..... N88-22748 #

L-16346 ..... N88-22325* #
L-16354 ..... N88-22710* #
L-16387 ..... N88-22047* #
L-16398 ..... N88-22072* #
L-16413 ..... N88-22653* #
L-16418 ..... N88-22031* #

LA-UR-87-2662 ..... N88-22621 #
LA-UR-87-3950 ..... N88-22458* #
LA-UR-87-4103 ..... N88-22542 #
LA-UR-87-4125 ..... N88-22483 #
LA-UR-87-4255 ..... N88-22612 #
LA-UR-87-4256 ..... N88-22613 #
LA-UR-88-51 ..... N88-22341 #
LA-UR-88-100 ..... N88-22464 #
LA-UR-88-414-PT-1 ..... N88-22355 #
LA-UR-88-573 ..... N88-22340 #
LA-UR-88-588 ..... N88-22803 #
LA-UR-88-597 ..... N88-22095 #
LA-UR-88-656 ..... N88-22339 #

LA-11238-MS ..... N88-22343 #

LBL-23599 ..... N88-22772 #
LBL-23600 ..... N88-22801 #
LBL-23993 ..... N88-22063 #
LBL-24049 ..... N88-22082 #
LBL-24467 ..... N88-22773 #
LBL-24490 ..... N88-22771 #
LBL-24692 ..... N88-22715 #

LC-79-640375 ..... N88-22849 #

LIDS-P-1711 ..... N88-22657 #

LISS-18 ..... N88-22686 #
LISS-19 ..... N88-22685 #
LISS-20 ..... N88-22685 #
LISS-21 ..... N88-22688 #
LISS-22 ..... N88-22687 #

LMSC-HEC-TR-F225800 ..... N88-22296* #

LR-31114 ..... N88-22024 #

MAQCP-NR-528(87) ..... N88-22079 #

MCR-87-2600 ..... N88-22060* #
MDC-K0535 ..... N88-22008 #
MDC-QA002 ..... N88-22152 #
MIT/LCS/TR-400 ..... N88-22578 #
MIT/LCS/TR-402 ..... N88-22597 #
MLM-3456(OP) ..... N88-22356 #
MM-5034-87-11 ..... N88-22088 #
MPAE-W-47-87-13 ..... N88-22487 #
MPE-PREPRINT-101 ..... N88-22836
MTL-TR-11-1 ..... N88-22091 #
MTL-TR-87-49 ..... N88-22087 #
MW-87-P-10 ..... N88-22278 #
M3-434600 ..... N88-22164 #
M5-521800 ..... N88-22163 #
NAS 1.15:4031 ..... N88-22072* #
NAS 1.15:4032 ..... N88-22047* #
NAS 1.15:89165 ..... N88-22439* #
NAS 1.15:89426 ..... N88-22013* #
NAS 1.15:100009 ..... N88-22010* #
NAS 1.15:100052 ..... N88-22336* #
NAS 1.15:100056 ..... N88-22337* #
NAS 1.15:100083 ..... N88-22014* #
NAS 1.15:100095 ..... N88-22009* #
NAS 1.15:100096 ..... N88-22650* #
NAS 1.15:100097 ..... N88-22651* #
NAS 1.15:100172 ..... N88-22851* #
NAS 1.15:100279 ..... N88-22446* #
NAS 1.15:100328 ..... N88-22852* #
NAS 1.15:100415 ..... N88-22033* #
NAS 1.15:100424 ..... N88-22050* #
NAS 1.15:100464 ..... N88-22654* #
NAS 1.15:100529 ..... N88-22016* #
NAS 1.15:100532 ..... N88-22097* #
NAS 1.15:100543 ..... N88-22015* #
NAS 1.15:100583 ..... N88-22434* #
NAS 1.15:100588 ..... N88-22012* #
NAS 1.15:100595 ..... N88-22853* #
NAS 1.15:100596 ..... N88-22435* #
NAS 1.15:100599 ..... N88-22445* #
NAS 1.15:100602 ..... N88-22709* #
NAS 1.15:100607 ..... N88-22854* #
NAS 1.15:100611 ..... N88-22438* #
NAS 1.15:100697 ..... N88-22503* #
NAS 1.15:100820 ..... N88-22591* #
NAS 1.15:100846 ..... N88-22652* #
NAS 1.15:100853 ..... N88-22080* #
NAS 1.15:100860 ..... N88-22805* #
NAS 1.15:100873 ..... N88-22019* #
NAS 1.15:100885 ..... N88-22168* #
NAS 1.15:100887 ..... N88-22037* #
NAS 1.15:101099 ..... N88-22458* #
NAS 1.21:7063(02) ..... N88-22830* #
NAS 1.26:3922(19) ..... N88-22515* #
NAS 1.26:179285 ..... N88-22296* #
NAS 1.26:179315 ..... N88-22060* #
NAS 1.26:179320 ..... N88-22834* #
NAS 1.26:180438 ..... N88-22843* #
NAS 1.26:180755 ..... N88-22447* #
NAS 1.26:180768 ..... N88-22331* #
NAS 1.26:180772 ..... N88-22552* #
NAS 1.26:181654 ..... N88-22541* #
NAS 1.26:181662 ..... N88-22018* #
NAS 1.26:182108 ..... N88-22322* #
NAS 1.26:182610 ..... N88-22452* #
NAS 1.26:182651 ..... N88-22491* #
NAS 1.26:182653 ..... N88-22492* #
NAS 1.26:182688 ..... N88-22540* #
NAS 1.26:182718 ..... N88-22847* #
NAS 1.26:182734 ..... N88-22295* #
NAS 1.26:182747 ..... N88-22045* #
NAS 1.26:182749 ..... N88-22676* #
NAS 1.26:182750 ..... N88-22052* #
NAS 1.26:182753 ..... N88-22672* #
NAS 1.26:182757 ..... N88-22096* #
NAS 1.26:182758 ..... N88-22194* #
NAS 1.26:182759 ..... N88-22011* #
NAS 1.26:182798 ..... N88-22575* #
NAS 1.26:182800-VOL-1 ..... N88-22197* #
NAS 1.26:182803 ..... N88-22098* #
NAS 1.26:182809 ..... N88-22602* #
NAS 1.26:182870 ..... N88-22133* #
NAS 1.26:182882 ..... N88-22207* #
NAS 1.55:3003-VOL-2 ..... N88-22382* #
NAS 1.55:3003-VOL-3 ..... N88-22408* #
NAS 1.60:2784 ..... N88-22710* #
NAS 1.60:2804 ..... N88-22325* #
NAS 1.60:2808 ..... N88-22031* #
NAS 1.60:2817 ..... N88-22653* #
NAS 1.77:20159 ..... N88-22102* #
NAS 1.77:20160 ..... N88-22104* #
NAS 1.77:20161 ..... N88-22326* #
NAS 1.77:20165 ..... N88-22130* #
NAS 1.77:20171 ..... N88-22101* #
NAS 1.77:20175 ..... N88-22099* #
NAS 1.77:20176 ..... N88-22100* #
NAS 1.77:20251 ..... N88-22698* #
NAS 1.77:20263 ..... N88-22135* #
NAS 1.77:20275 ..... N88-22134* #
NAS 1.77:20288 ..... N88-22490* #
NASA-CP-3003-VOL-2 ..... N88-22382* #
NASA-CP-3003-VOL-3 ..... N88-22408* #
NASA-CR-3922(19) ..... N88-22515* #
NASA-CR-179285 ..... N88-22296* #
NASA-CR-179315 ..... N88-22060* #
NASA-CR-179320 ..... N88-22834* #
NASA-CR-180438 ..... N88-22843* #
NASA-CR-180755 ..... N88-22447* #
NASA-CR-180768 ..... N88-22331* #
NASA-CR-180772 ..... N88-22552* #
NASA-CR-181654 ..... N88-22541* #
NASA-CR-181662 ..... N88-22018* #
NASA-CR-182108 ..... N88-22322* #
NASA-CR-182610 ..... N88-22452* #
NASA-CR-182651 ..... N88-22491* #
NASA-CR-182653 ..... N88-22492* #
NASA-CR-182688 ..... N88-22540* #
NASA-CR-182718 ..... N88-22847* #
NASA-CR-182734 ..... N88-22295* #
NASA-CR-182747 ..... N88-22045* #
NASA-CR-182749 ..... N88-22676* #
NASA-CR-182750 ..... N88-22052* #
NASA-CR-182753 ..... N88-22672* #
NASA-CR-182757 ..... N88-22096* #
NASA-CR-182758 ..... N88-22194* #
NASA-CR-182759 ..... N88-22011* #
NASA-CR-182798 ..... N88-22575* #
NASA-CR-182800-VOL-1 ..... N88-22197* #
NASA-CR-182803 ..... N88-22098* #
NASA-CR-182809 ..... N88-22602* #
NASA-CR-182870 ..... N88-22133* #
NASA-CR-182882 ..... N88-22207* #
NASA-SP-7063(02) ..... N88-22830* #
NASA-TM-4031 ..... N88-22072* #
NASA-TM-4032 ..... N88-22047* #
NASA-TM-89165 ..... N88-22439* #
NASA-TM-89426 ..... N88-22013* #
NASA-TM-100009 ..... N88-22010* #
NASA-TM-100052 ..... N88-22336* #
NASA-TM-100056 ..... N88-22337* #
NASA-TM-100083 ..... N88-22014* #
NASA-TM-100095 ..... N88-22009* #
NASA-TM-100096 ..... N88-22650* #
NASA-TM-100097 ..... N88-22651* #
NASA-TM-100172 ..... N88-22851* #
NASA-TM-100279 ..... N88-22446* #
NASA-TM-100328 ..... N88-22852* #
NASA-TM-100415 ..... N88-22033* #
NASA-TM-100424 ..... N88-22050* #
NASA-TM-100464 ..... N88-22654* #
NASA-TM-100529 ..... N88-22016* #
NASA-TM-100532 ..... N88-22097* #
NASA-TM-100543 ..... N88-22015* #
NASA-TM-100583 ..... N88-22434* #
NASA-TM-100588 ..... N88-22012* #
NASA-TM-100595 ..... N88-22853* #
NASA-TM-100596 ..... N88-22435* #
NASA-TM-100599 ..... N88-22445* #
NASA-TM-100602 ..... N88-22709* #
NASA-TM-100607 ..... N88-22854* #
NASA-TM-100611 ..... N88-22438* #
NASA-TM-100697 ..... N88-22503* #
NASA-TM-100820 ..... N88-22591* #
NASA-TM-100846 ..... N88-22652* #
NASA-TM-100853 ..... N88-22080* #
NASA-TM-100860 ..... N88-22805* #
NASA-TM-100873 ..... N88-22019* #
NASA-TM-100885 ..... N88-22168* #
NASA-TM-100887 ..... N88-22037* #
NASA-TM-101099 ..... N88-22458* #
NASA-TP-2784 ..... N88-22710* #
NASA-TP-2804 ..... N88-22325* #
NASA-TP-2808 ..... N88-22031* #
NASA-TP-2817 ..... N88-22653* #
NASA-TT-20159 ..... N88-22102* #
NASA-TT-20160 ..... N88-22104* #
NASA-TT-20161 ..... N88-22326* #
NASA-TT-20165 ..... N88-22130* #
NASA-TT-20171 ..... N88-22101* #
NASA-TT-20175 ..... N88-22099* #
NASA-TT-20176 ..... N88-22100* #
NASA-TT-20251 ..... N88-22698* #
NASA-TT-20263 ..... N88-22135* #
NASA-TT-20275 ..... N88-22134* #
NASA-TT-20288 ..... N88-22490* #
NBS-GCR-88-541 ..... N88-22208 #
NBSIR-87/3080 ..... N88-22048 #
NHRC-87-21 ..... N88-22525 #
NHRC-87-25 ..... N88-22526 #
NHRC-87-28 ..... N88-22527 #
NIIEFA-P-K-0733 ..... N88-22344 #
NLR-MP-86034-U ..... N88-22038 #
NLR-MP-86059-U ..... N88-22369 #
NLR-MP-86074-U ..... N88-22017 #
NMRI-87-55 ..... N88-22184 #
NOSC/TD-1166 ..... N88-22253 #
NOSC/TR-1185 ..... N88-22728 #
NOSC/TR-1196 ..... N88-22727 #
NPL-DMA(A)-152 ..... N88-22560
NPS-54-88-002 ..... N88-22831 #
NPS-62-88-009 ..... N88-22255 #
NPS-68-87-008 ..... N88-22509 #
NPS-68-88-001 ..... N88-22506 #
NPS-68-88-002 ..... N88-22510 #
NPS55-88-001 ..... N88-22568 #
NRL-MR-6098 ..... N88-22261 #
NRL-MR-6149 ..... N88-22286 #
NSWC/TR-86-104 ..... N88-22202 #
NSWC/TR-87-148 ..... N88-22365 #
NTIA-87-223 ..... N88-22265 #
NTIA-87-228 ..... N88-22049 #
NTSB/AAB-87/12 ..... N88-22020 #
NTSB/AAR-87/09 ..... N88-22021 #
NUSC-TR-8077 ..... N88-22708 #
NWRA-CR-R019 ..... N88-22450 #
NWRA-CR-87-R016 ..... N88-22451 #
NWRA-CR-87-R018 ..... N88-22476 #
ONERA-RT-2/7256-RY-061-R ..... N88-22103 #
ONERA-12/7236-PY ..... N88-22073 #
ORNL/TM-10617 ..... N88-22757 #
OSU-384 ..... N88-22052* #
PB87-910412 ..... N88-22021 #
PB87-916912 ..... N88-22020 #
PB88-135306 ..... N88-22059 #
PB88-145172 ..... N88-22137 #
PB88-146840 ..... N88-22517 #
PB88-146857 ..... N88-22448 #
PB88-149885 ..... N88-22038 #
PB88-156765 ..... N88-22536 #
PB88-164207 ..... N88-22849 #
PB88-164934 ..... N88-22129 #
PB88-165386 ..... N88-22648 #
PB88-165402 ..... N88-22711 #
PB88-165410 ..... N88-22264 #
PB88-165477 ..... N88-22647 #
PB88-166095 ..... N88-22049 #
PB88-166293 ..... N88-22195 #
PB88-168307 ..... N88-22265 #
PB88-168372 ..... N88-22105 #
PB88-169255 ..... N88-22436 #
PB88-169297 ..... N88-22196 #
PB88-178827 ..... N88-22048 #
PFC/RR-87-20 ..... N88-22743 #
PINSTECH/NPD-121 ..... N88-22139 #
PNL-SA-15056 ..... N88-22513 #

PNL-SA-15115 ..... N88-22094 #
PNL-SA-15179 ..... N88-22198 #
PNL-SA-15557 ..... N88-22504 #

PPLK-R-15 ..... N88-22746 #

PREPRINT-580 ..... N88-22717 #
PREPRINT-581 ..... N88-22683 #

PSI-9898 ..... N88-22721 #

PTR-87-6 ..... N88-22351 #

R-088-87 ..... N88-22550 #

RADC-TR-87-165-VOL-1 ..... N88-22826 #
RADC-TR-87-171-VOL-1 ..... N88-22571 #
RADC-TR-87-171-VOL-2 ..... N88-22572 #
RADC-TR-87-200 ..... N88-22177 #
RADC-TR-87-209 ..... N88-22252 #
RADC-TR-87-210 ..... N88-22281 #
RADC-TR-87-245 ..... N88-22479 #

RDA-TR-144200 ..... N88-22751 #

REPT-1-52097 ..... N88-22753 #
REPT-87-016 ..... N88-22655
REPT-87-038 ..... N88-22561
REPT-87-053 ..... N88-22562
REPT-88B0092 ..... N88-22503* #
REPT-314-50 ..... N88-22050* #
REPT-314-60 ..... N88-22050* #
REPT-1987-23 ..... N88-22264 #
REPT-1987-26 ..... N88-22711 #
REPT-23111-07367 ..... N88-22381 #
REPT-87144-2 ..... N88-22308 #
REPT-080043-1-M ..... N88-22701 #

RPL-69005 ..... N88-22756 #

RR-645-I-IMAG-55-LIFIA ..... N88-22624 #
RR-646-I ..... N88-22593 #
RR-647-I-IMAG-57-LIFIA ..... N88-22563 #
RR-650-I ..... N88-22273 #
RR-656-I ..... N88-22545 #
RR-663-I ..... N88-22564 #

RRK-86-23 ..... N88-22838 #
RRK-86-32 ..... N88-22616 #
RRK-86-33 ..... N88-22808 #
RRK-86-34 ..... N88-22839 #
RRK-86-36 ..... N88-22840 #
RRK-86-40 ..... N88-22617 #
RRK-87-20 ..... N88-22810 #
RRK-87-21 ..... N88-22681 #

S-576 ..... N88-22654* #

SAND-83-1788 ..... N88-22324 #
SAND-87-0611C ..... N88-22292 #
SAND-87-0988C ..... N88-22362 #
SAND-87-1176-VOL-2 ..... N88-22481 #
SAND-87-1196C ..... N88-22158 #
SAND-87-1218C ..... N88-22372 #
SAND-87-1497C ..... N88-22461 #
SAND-87-1503C ..... N88-22114 #
SAND-87-1835C ..... N88-22363 #
SAND-87-1942C ..... N88-22611 #
SAND-87-2123C ..... N88-22058 #
SAND-87-2191C ..... N88-22206 #
SAND-87-2192C ..... N88-22433 #
SAND-87-2315C ..... N88-22056 #
SAND-87-2316C ..... N88-22057 #
SAND-87-2319C ..... N88-22171 #
SAND-87-2585 ..... N88-22457 #
SAND-87-3065C ..... N88-22192 #
SAND-87-3078C ..... N88-22462 #
SAND-88-0240C ..... N88-22440 #
SAND-88-0378C ..... N88-22373 #
SAND-88-0486C ..... N88-22199 #

SC5411.FR ..... N88-22346 #
SC5444.AR ..... N88-22183 #

SDC-TM-3309 ..... N88-22061 #

SERI/TR-217-3125 ..... N88-22371 #

SGD-520-PT-2 ..... N88-22849 #

SORI-EAS-87-554 ..... N88-22181 #

SP-RAPP-187-21 ..... N88-22129 #
SP-RAPP-1987:19 ..... N88-22195 #

SR-1 ..... N88-22475 #
SR-3 ..... N88-22062 #

SU-SOL-87-15 ..... N88-22690 #

SWRI-4765/1 ..... N88-22203 #

TCS-TP-87-059 ..... N88-22067 #

TE4327-20-88 ..... N88-22353 #

TI88-700972 ..... N88-22734 #
TI88-701020 ..... N88-22737 #
TI88-701021 ..... N88-22738 #
TI88-701022 ..... N88-22763 #
TI88-701027 ..... N88-22762 #
TI88-701039 ..... N88-22138 #
TI88-701103 ..... N88-22332 #
TI88-701105 ..... N88-22333 #
TI88-701107 ..... N88-22470 #
TI88-701123 ..... N88-22837 #
TI88-701158 ..... N88-22806 #
TI88-701159 ..... N88-22807 #
TI88-701162 ..... N88-22678 #
TI88-701191 ..... N88-22739 #
TI88-701201 ..... N88-22748 #
TI88-701411 ..... N88-22750 #
TI88-701427 ..... N88-22294 #
TI88-701435 ..... N88-22720 #
TI88-701488 ..... N88-22543 #
TI88-701491 ..... N88-22544 #
TI88-701498 ..... N88-22813 #
TI88-701499 ..... N88-22814 #
TI88-701503 ..... N88-22815 #

TKK-V-A10(1988) ..... N88-22165 #

TM-27 ..... N88-22575* #
TM-29 ..... N88-22672* #
TM-121 ..... N88-22701 #

TR-3 ..... N88-22793 #
TR-4 ..... N88-22178 #
TR-15-ONR ..... N88-22707 #
TR-29 ..... N88-22182 #
TR-87-27 ..... N88-22671 #
TR-87-31 ..... N88-22669 #
TR-87-32 ..... N88-22639 #
TR-87-34 ..... N88-22670 #
TR-87-53 ..... N88-22675 #
TR-87-213 ..... N88-22668 #
TR-200 ..... N88-22667 #
TR-204 ..... N88-22677 #
TR-205 ..... N88-22659 #
TR-206 ..... N88-22666 #
TR-209 ..... N88-22664 #
TR-211 ..... N88-22637 #
TR-212 ..... N88-22638 #
TR-219 ..... N88-22722 #
TR-232 ..... N88-22553 #
TR-398 ..... N88-22663 #
TR-683 ..... N88-22721 #

TRW-S/N-48027 ..... N88-22105 #

UBUFFALO/DC/88/TR-63 ..... N88-22817 #

UCID-21140 ..... N88-22733 #
UCID-21313 ..... N88-22603 #
UCID-21340 ..... N88-22732 #

UCLA/PPG-1125-VOL-5 ..... N88-22744 #

UCRL-21009-PT-3 ..... N88-22342 #
UCRL-21017 ..... N88-22334 #
UCRL-21018-VOL-1 ..... N88-22287 #
UCRL-21021 ..... N88-22141 #
UCRL-21024 ..... N88-22467 #
UCRL-96102 ..... N88-22800 #
UCRL-96109 ..... N88-22775 #
UCRL-96370 ..... N88-22157 #
UCRL-96861 ..... N88-22084 #
UCRL-97240 ..... N88-22432 #
UCRL-97399 ..... N88-22175 #
UCRL-97816 ..... N88-22731 #
UCRL-98108 ..... N88-22764 #

UH-IBPD-002-87(1987)-PT-2 ..... N88-22774 #

UILU-ACT-86 ..... N88-22625 #

UILU-ENG-88-1706 ..... N88-22592 #
UILU-ENG-88-2202 ..... N88-22625 #
UILU-ENG-88-2211 ..... N88-22608 #
UILU-ENG-88-4001 ..... N88-22320 #

UIUCDCS-R-88-1402 ..... N88-22592 #

USAAVSCOM-TM-88-B-002 ..... N88-22097* #

USAFOEHL-87-184EH0441LNA ..... N88-22702 #

USAFSAM-TR-87-15 ..... N88-22347 #
USAFSAM-TR-87-21 ..... N88-22519 #
USAFSAM-TR-87-31 ..... N88-22537 #

UTAP-86/87 ..... N88-22812 #

UTRC/R87-927184 ..... N88-22345 #

VTT-RR-487 ..... N88-22368 #
VTT-RR-502 ..... N88-22443 #
VTT-RR-503 ..... N88-22444 #

W-10/87 ..... N88-22441 #

WHOI-87-50 ..... N88-22508 #

FEDERAL REGIONAL DEPOSITORY LIBRARIES

ALABAMA

AUBURN UNIV. AT MONTGOMERY LIBRARY
Documents Department
Montgomery, AL 36193
(205) 271-9650

UNIV. OF ALABAMA LIBRARY
Documents Dept.-Box S
University, AL 35486
(205) 348-6046

ARIZONA

DEPT. OF LIBRARY, ARCHIVES AND PUBLIC RECORDS
Third Floor—State Cap.
1700 West Washington
Phoenix, AZ 85007
(602) 255-4121

UNIVERSITY OF ARIZONA LIB.
Government Documents Dept.
Tucson, AZ 85721
(602) 621-6433

ARKANSAS

ARKANSAS STATE LIBRARY
One Capitol Mall
Little Rock, AR 72201
(501) 371-2326

CALIFORNIA

CALIFORNIA STATE LIBRARY
Govt. Publications Section
P.O. Box 2037
Sacramento, CA 95809
(916) 324-4863

COLORADO

UNIV OF COLORADO LIB.
Government Pub. Division
Campus Box 184
Boulder, CO 80309
(303) 492-8834

DENVER PUBLIC LIBRARY
Govt. Pub. Department
1357 Broadway
Denver, CO 80203
(303) 571-2131

CONNECTICUT

CONNECTICUT STATE LIBRARY
Government Documents Unit
231 Capitol Avenue
Hartford, CT 06106
(203) 566-7029

FLORIDA

UNIV. OF FLORIDA LIBRARIES
Library West
Documents Department
Gainesville, FL 32611
(904) 392-0367

GEORGIA

UNIV. OF GEORGIA LIBRARIES
Government Reference Dept.
Athens, GA 30602
(404) 542-8949

HAWAII

UNIV. OF HAWAII LIBRARY
Govt. Documents Collection
2550 The Mall
Honolulu, HI 96822
(808) 948-8230

IDAHO

UNIV. OF IDAHO LIBRARY
Documents Section
Moscow, ID 83843
(208) 885-6344

ILLINOIS

ILLINOIS STATE LIBRARY
Information Services Branch
Centennial Building
Springfield, IL 62756
(217) 782-5185

INDIANA

INDIANA STATE LIBRARY
Serials Documents Section
140 North Senate Avenue
Indianapolis, IN 46204
(317) 232-3686

IOWA

UNIV. OF IOWA LIBRARIES
Govt. Documents Department
Iowa City, IA 52242
(319) 353-3318

KANSAS

UNIVERSITY OF KANSAS
Doc. Collect—Spencer Lib.
Lawrence, KS 66045-2800
(913) 864-4662

KENTUCKY

UNIV. OF KENTUCKY LIBRARIES
Govt. Pub. Department
Lexington, KY 40506-0039
(606) 257-3139

LOUISIANA

LOUISIANA STATE UNIVERSITY
Middleton Library
Govt. Docs. Dept.
Baton Rouge, LA 70803
(504) 388-2570

LOUISIANA TECHNICAL UNIV. LIBRARY
Documents Department
Ruston, LA 71272-0046
(318) 257-4962

MAINE

UNIVERSITY OF MAINE
Raymond H. Fogler Library
Tri-State Regional Documents Depository
Orono, ME 04469
(207) 581-1680

MARYLAND

UNIVERSITY OF MARYLAND
McKeldin Lib.—Doc. Div.
College Park, MD 20742
(301) 454-3034

MASSACHUSETTS

BOSTON PUBLIC LIBRARY
Government Docs. Dept.
Boston, MA 02117
(617) 536-5400 ext.226

MICHIGAN

DETROIT PUBLIC LIBRARY
Sociology Department
5201 Woodward Avenue
Detroit, MI 48202-4093
(313) 833-1409

MICHIGAN STATE LIBRARY
P.O. Box 30007
Lansing, MI 48909
(517) 373-1593

MINNESOTA

UNIVERSITY OF MINNESOTA
Government Pubs. Division
409 Wilson Library
309 19th Avenue South
Minneapolis, MN 55455
(612) 373-7870

MISSISSIPPI

UNIV. OF MISSISSIPPI LIB.
Documents Department
University, MS 38677
(601) 232-5857

MONTANA

UNIV. OF MONTANA
Mansfield Library
Documents Division
Missoula, MT 59812
(406) 243-6700

NEBRASKA

UNIVERSITY OF NEBRASKA - LINCOLN
Love Library
Documents Department
Lincoln, NE 68588-0410
(402) 472-2562

NEVADA

UNIVERSITY OF NEVADA LIB.
Govt. Pub. Department
Reno, NV 89557-0044
(702) 784-6579

NEW JERSEY

NEWARK PUBLIC LIBRARY
5 Washington Street
Newark, NJ 07101-0630
(201) 733-7812

NEW MEXICO

UNIVERSITY OF NEW MEXICO
Zimmerman Library
Government Pub. Dept.
Albuquerque, NM 87131
(505) 277-5441

NEW MEXICO STATE LIBRARY
Reference Department
325 Don Gaspar Avenue
Santa Fe, NM 87503
(505) 827-3826

NEW YORK

NEW YORK STATE LIBRARY
Empire State Plaza
Albany, NY 12230
(518) 474-5563

NORTH CAROLINA

UNIVERSITY OF NORTH CAROLINA AT CHAPEL HILL
Davis Library
BA/SS Documents Division
Chapel Hill, NC 27515
(919) 962-1151

NORTH DAKOTA

UNIVERSITY OF NORTH DAKOTA
Chester Fritz Library
Documents Department
Grand Forks, ND 58202
(701) 777-4629
In cooperation with North Dakota State Univ. Library

OHIO

STATE LIBRARY OF OHIO
Documents Department
65 South Front Street
Columbus, OH 43266-0334
(614) 462-7051

OKLAHOMA

OKLAHOMA DEPT. OF LIB.
Government Documents
200 NE 18th Street
Oklahoma City, OK 73105
(405) 521-2502, ext. 252

OKLAHOMA STATE UNIV. LIB.
Documents Department
Stillwater, OK 74078
(405) 624-6546

OREGON

PORTLAND STATE UNIV. LIB.
Documents Department
P.O. Box 1151
Portland, OR 97207
(503) 229-3673

PENNSYLVANIA

STATE LIBRARY OF PENN.
Government Pub. Section
P.O. Box 1601
Harrisburg, PA 17105
(717) 787-3752

TEXAS

TEXAS STATE LIBRARY
Public Services Department
P.O. Box 12927—Cap. Sta.
Austin, TX 78711
(512) 475-2996

TEXAS TECH. UNIV. LIBRARY
Govt. Documents Department
Lubbock, TX 79409
(806) 742-2268

UTAH

UTAH STATE UNIVERSITY
Merrill Library, U.M.C. 30
Logan, UT 84322
(801) 750-2682

VIRGINIA

UNIVERSITY OF VIRGINIA
Alderman Lib.—Public Doc.
Charlottesville, VA 22903-2498
(804) 924-3133

WASHINGTON

WASHINGTON STATE LIBRARY
Documents Section
Olympia, WA 98504
(206) 753-4027

WEST VIRGINIA

WEST VIRGINIA UNIV. LIB.
Documents Department
Morgantown, WV 26506-6069
(304) 293-3640

WISCONSIN

MILWAUKEE PUBLIC LIBRARY
814 West Wisconsin Avenue
Milwaukee, WI 53233
(414) 278-3065

ST. HIST LIB. OF WISCONSIN
Government Pub. Section
816 State Street
Madison, WI 53706
(608) 262-4347

WYOMING

WYOMING STATE LIBRARY
Supreme Ct. & Library Bld.
Cheyenne, WY 82002
(307) 777-5919

National Aeronautics and
Space Administration
Code NTT-4
Washington, D.C.
20546

Official Business
Penalty for Private Use, $300

SPECIAL FOURTH-CLASS RATE
POSTAGE & FEES PAID
NASA
PERMIT No. G 27

NASA
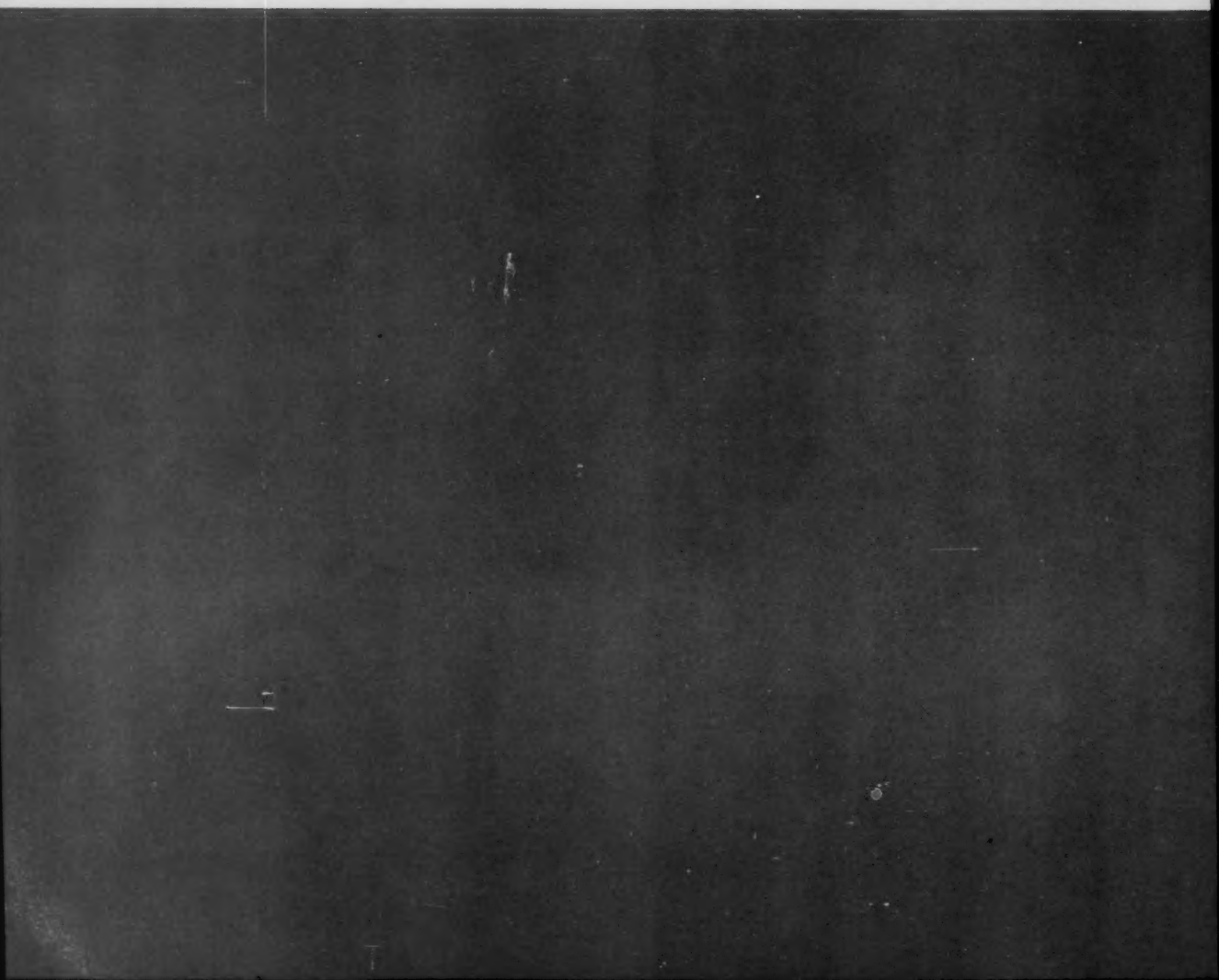
POSTMASTER: If Undeliverable (Section 158
Postal Manual) Do Not Return